

RMIS View/Print Document Cover Sheet

This document was retrieved from the Documentation and Records Management (DRM) ISEARCH System. It is intended for Information only and may not be the most recent or updated version. Contact a Document Service Center (see Hanford Info for locations) if you need additional retrieval information.

Accession #: D196080859

Document #: SD-RTG-SARP-001

Title/Desc:

RTG TRANSPORTATION SYSTEM SARP DOCKET NO 94-6-9904
[VOL I] [SEC 1 OF 4]

Pages: 301

This document was too large to scan as a whole document, therefore it required breaking into smaller sections.

Document number: SD-RTG-SARP-001

Section 1 of 4

Title: RADIOISOTOPE THERMOELECTRIC GENERATOR
TRANSPORTATION SYSTEM SAFETY ANALYSIS REPORT
FOR PACKAGING

Date: 4/18/96 Revision: 0

Originator: FERRELL PC

Co: WHC

Recipient: _____

Co: _____

References: EDT-613639

APR 18 1996

ENGINEERING DATA TRANSMITTAL

Page 1 of 1
1. DOT No 613639

2. To: (Receiving Organization) Distribution	3. From: (Originating Organization) Packaging Engineering	4. Related EDT No.: NA
5. Proj./Prog./Dept./Div.: RTG Packaging/B4100/XJ10A	6. Con. Emp.: P. C. Ferrell	7. Purchase Order No.: NA
8. Originator Remarks: This document is being transmitted to DOE-EN and Lawrence Livermore National Laboratory for final review under Docket No. 94-G-9904. Once the document is determined to be acceptable, DOE-EM will issue a Certificate of Compliance (CoC). This document is cleared for Public Release.		9. Equip./Component No.: NA
		10. System/Shop/Facility: 427
11. Receiver Remarks:		12. Major Assn. Div. No.: NA
		13. Permit/Permit Application No.: NA
		14. Required Response Date: 04/19/96

15. DATA TRANSMITTED					(1)	(2)	(3)	(4)
(a) Item No	(b) Document/Drawing No	(c) Sheet No	(d) Rev No	(e) Title or Description of Data Transmitted	Approval Designator	Reason for Transmittal	Orig. Major Disposition	Recomm. or Disposition
1	WHC-SD-RTG-SARP-001	A11	0	Radioisotope Thermoelectric Generator Transportation System Safety Analysis Report for Packaging Vol 1 + 2	SQ	1,2	1	1

16. KEY					
Approval Designator (F)	Reason for Transmittal (R)			Disposition (D) & (6)	
1. S, Q, D or NA (See WHC-CM 2-5, Sec 7.2.7)	1. Approval	4. Review	5. Post Review	1. Approved	4. Rejected w/comment
	2. Release	3. Final Review	6. Draft (Receipt Acknow. Required)	2. Approved w/comments	5. Rejected w/comment
	3. Information	6. Draft (Receipt Acknow. Required)		3. Disapproved w/comment	6. Receipt acknowledged

17. SIGNATURE DISTRIBUTION (See Approval Designator for required signatories)											
Reason	Date	(1) Name	(2) Signature	(3) Date	(4) Title	(5) Name	(6) Signature	(7) Date	(8) Title	Rev. No.	Disp.
1	/	Con. Emp.: PC Ferrell	<i>PC Ferrell</i>	4/16/96	41-21						
1	/	Con. Emp.: JG Flato	<i>JG Flato</i>	4/16/96	61-11						
1	/	SA: NE Flato	<i>NE Flato</i>	4/16/96	82-11						
1	/	Safety: Our normally	<i>Our normally</i>	4/16/96	21						
		Env.									
1	/	DL Becker	<i>DL Becker</i>	4/16/96	61-21						
1	/	W Birkland	<i>W Birkland</i>	4/16/96	82-08						

18. P. C. Ferrell Signature of ECT Originator	19. Authorized Representative Date for Receiving Organization	20. J. B. Ferrell Signature of Manager Date	21. DOE APPROVAL (if required) Ctrl. No. 1) Approved 2) Approved w/comments 3) Disapproved w/comments
--	---	--	--

Radioisotope Thermoelectric Generator Transportation System Safety Analysis Report for Packaging

(Volumes I and II)

P. C. Farrell

Westinghouse Hanford Company, Richland, WA 99352
U.S. Department of Energy Contract DE-AC06-87RL10930

EDT/ECN: 613639 UC: 513
Org Code: B4100 Charge Code: XJ10A
BAR Code: AF7010200 Total Pages: 976

Key Words: RTG, General Purpose Heat Source, Package, Inner Containment Vessel, Outer Containment Vessel, Shielding Criticality

Abstract: This SARP describes the RTG Transportation System Package, a Type B(U) packaging system that is used to transport an RTG or similar payload. The payload, which is included in this SARP, is a generic, enveloping payload that specifically encompasses the General Purpose Heat Source (GPHS) RTG payload. The package consists of two independent containment systems mounted on a shock isolation transport skid and transported within an exclusive-use trailer.

TRADEMARK DISCLAIMER. Reference herein to any specific commercial product, process, or service by trade name, trademark, manufacturer, or otherwise, does not necessarily constitute or imply its endorsement, recommendation, or favoring by the United States Government or any agency thereof or its contractors or subcontractors.

Printed in the United States of America. To obtain copies of this document, contact: WMC/SCS Document Control Services, P.O. Box 1970, Mailstop M-08, Richland WA 99352, phone (509) 372-2420; fax (509) 376-4909.

V.L. Birkland 4/16/96
Release Approval Date



Release Stamp

Approved for Public Release

Radioisotope Thermoelectric Generator Transportation System Safety Analysis Report for Packaging

Docket No. 94-6-9904

Prepared for the U.S. Department of Energy
Office of Environmental Restoration and
Waste Management



Westinghouse
Hanford Company Richland, Washington

Management and Operations Contractor for the
U.S. Department of Energy under Contract DE-AC06-87RL10830

Approved for Public Release

LIST OF EFFECTIVE PAGES

Page	Rev	Comment	Page	Rev	Comment
1-iii - i-vii	0	TOC	3.6.1-1 - 3.6.1-2	0	
1-viii - 1-ix	0	Acronyms	3.6.2-1 - 3.6.2-30	0	
1-1 - 1-12	0		3.6.3-1 - 3.6.3-4	0	
1.3.0-1	0		3.6.4-1 - 3.6.4-16	0	
1.3.1-1	0		3.6.5-1 - 3.6.6-145	0	
1.3.2-1 - 1.3.2-17	0		3.6.6-1 - 3.6.7-15	0	
1.3.3-1 - 1.3.3-3	0		3.6.7-1 - 3.6.7-19	0	
2-1 - 2-92	0		4-1 - 4-21	0	
2.10.0-1	0		4.5.0-1	0	
2.10.1-1 - 2.10.1-2	0		4.5.1-1	0	
2.10.2-1 - 2.10.2-29	0		4.5.2-1 - 4.5.2-41	0	
2.10.3-1 - 2.10.3-29	0		5-1 - 5-21	0	
2.10.4-1 - 2.10.4-2	0		5.5.0-1	0	
2.10.5-1 - 2.10.5-28	0		5.5.1-1	0	
2.10.6-1 - 2.10.6-5	0		5.5.2-1 - 5.5.2-14	0	
2.10.7-1 - 2.10.7-5	0		5.5.3-1 - 5.5.3-16	0	
2.10.8-1 - 2.10.8-49	0		6-1 - 6-27	0	
2.10.9-1 - 2.10.9-4	0		6.6.0-1	0	
2.10.10-1	0		6.6.1-1	0	
2.10.11-1 - 2.10.11-7	0		6.6.2-1 - 6.6.2-11	0	
2.10.12-1 - 2.10.12-68	0		7-1 - 7-6	0	
2.10.13-1 - 2.10.13-11	0		7.4-1	0	
2.10.14-1 - 2.10.14-2	0		8-1 - 8-12	0	
2.10.15-1 - 2.10.15-120	0		8.3-1	0	
3-1 - 3-54	0		9-1 - 9-12	0	
3.6.0-1	0		9.4-1	0	

CONTENTS

1.0	GENERAL INFORMATION	1-1
1.1	INTRODUCTION	1-1
1.2	PACKAGE DESCRIPTION	1-1
1.2.1	Packaging	1-1
1.2.2	Operational Features	1-6
1.2.3	Contents of Packaging	1-6
1.3	APPENDIX	1.3.0-1
1.3.1	References	1.3.1-1
1.3.2	General Arrangement Drawings	1.3.2-1
1.3.3	GPHS RTG Interface Control Drawing	1.3.3-1
2.0	STRUCTURAL EVALUATION	2-1
2.1	STRUCTURAL DESIGN	2-1
2.1.1	Discussion	2-1
2.1.2	Design Criteria	2-4
2.2	WEIGHTS AND CENTER OF GRAVITY	2-10
2.3	MECHANICAL PROPERTIES OF MATERIALS	2-11
2.4	GENERAL STANDARDS FOR ALL PACKAGES	2-19
2.4.1	Minimum Package Size	2-19
2.4.2	Temper-Indicating Feature	2-19
2.4.3	Positive Closure	2-19
2.4.4	Chemical and Galvanic Reactions	2-19
2.5	LIFTING AND TIEDOWN STANDARDS FOR ALL PACKAGES	2-20
2.5.1	Lifting Devices	2-20
2.5.2	Tiedown Devices	2-28
2.6	NORMAL CONDITIONS OF TRANSPORT	2-39
2.6.1	Heat	2-40
2.6.2	Cold	2-60
2.6.3	Reduced External Pressure	2-51
2.6.4	Increased External Pressure	2-51
2.6.5	Vibration	2-51
2.6.6	Water Spray	2-62
2.6.7	Free Drop	2-62
2.6.8	Corner Drop	2-63
2.6.9	Compression	2-64
2.6.10	Penetration	2-66
2.7	HYPOTHETICAL ACCIDENT CONDITIONS	2-67
2.7.1	Free Drop	2-67
2.7.2	Puncture	2-61
2.7.3	Thermal	2-64
2.7.4	Immersion	2-82
2.7.5	Immersion--All Packages	2-82
2.7.6	Summary of Damage	2-87
2.8	SPECIAL FORM	2-92
2.9	FUEL RODS	2-92
2.10	APPENDIX	2.10.0-1

CONTENTS (cont'd)

2.10.1	References	2.10.1-1
2.10.2	ICV Two-Dimensional (Axisymmetric) ANSYS Model	2.10.2-1
2.10.3	OCV Head and Fin Model	2.10.3-1
2.10.4	Fin-to-OCV Head Weld Properties ANSYS Model	2.10.4-1
2.10.5	OCV Head ANSYS Model for Tiedown Analysis	2.10.5-1
2.10.6	Blattner O-ring Performance Test Data	2.10.6-1
2.10.7	Summary of Thermal Load Cases and Results	2.10.7-1
2.10.8	OCV Two-Dimensional (Axisymmetric) ANSYS Model	2.10.8-1
2.10.9	RTG Transportation System Package Certification Test Plan	2.10.9-1
2.10.10	Certification Drop Test Procedure for the RTG Transportation System Package	2.10.10-1
2.10.11	Structural Development Test Program	2.10.11-1
2.10.12	ICV Three-Dimensional ANSYS Model	2.10.12-1
2.10.13	OCV Three-Dimensional ANSYS Model	2.10.13-1
2.10.14	O-ring Seal Compression Measurements	2.10.14-1
2.10.15	Summary of Damage from Certification Testing	2.10.15-1
3.0	THERMAL EVALUATION	3-1
3.1	DISCUSSION	3-1
3.2	SUMMARY OF THERMAL PROPERTIES OF MATERIALS	3-4
3.3	TECHNICAL SPECIFICATIONS OF COMPONENTS	3-9
3.4	THERMAL EVALUATION FOR NORMAL CONDITIONS OF TRANSPORT	3-10
3.4.1	Thermal Model	3-11
3.4.2	Maximum Temperatures	3-21
3.4.3	Minimum Temperatures	3-24
3.4.4	Maximum Internal Pressures	3-24
3.4.5	Maximum Thermal Stresses	3-26
3.4.6	Temperatures For Operational Conditions	3-25
3.4.7	Evaluation of Package Performance for Normal Conditions of Transport	3-30
3.5	HYPOTHETICAL ACCIDENT THERMAL EVALUATION	3-30
3.5.1	Thermal Model	3-31
3.5.2	Package Conditions and Environment	3-35
3.5.3	Package Temperatures	3-45
3.5.4	Maximum Internal Pressures	3-47
3.5.5	Maximum Thermal Stresses	3-54
3.5.6	Evaluation of Package Performance for the Thermal Hypothetical Accident Conditions	3-54
3.6	APPENDIX	3.6.0-1
3.6.1	References	3.6.1-1
3.6.2	Thermal Modeling Details	3.6.2-1

CONTENTS (cont'd)

3.6.3	Performance Of Rigid Polyurethane Foam Under Fire Accident Conditions	3.6.3-1
3.6.4	SINDA Output For Normal Conditions Of Transport	3.6.4-1
3.6.5	SINDA Output For Hypothetical Accident Conditions Of Transport	3.6.5-1
3.6.6	Miscellaneous Calculations	3.6.6-1
3.6.7	Listing of 2-D Computer Model	3.6.7-1
4.0	CONTAINMENT	4-1
4.1	CONTAINMENT BOUNDARY	4-1
4.1.1	Containment Vessel	4-1
4.1.2	Containment Penetrations	4-4
4.1.3	Seals and Welds	4-10
4.1.4	Closures	4-15
4.2	REQUIREMENTS FOR NORMAL CONDITIONS OF TRANSPORT	4-15
4.2.1	Containment of Radioactive Material	4-15
4.2.2	Pressurization of Containment Vessel	4-16
4.2.3	Containment Criterion	4-16
4.3	CONTAINMENT REQUIREMENTS FOR HYPOTHETICAL ACCIDENT CONDITIONS	4-16
4.3.1	Fission Gas Products	4-16
4.3.2	Containment of Radioactive Materials	4-17
4.3.3	Containment Criterion	4-19
4.4	SPECIAL REQUIREMENTS	4-21
4.5	APPENDIX	4.5.0-1
4.5.1	References	4.5.1-1
4.5.2	Teledyne Test Reports HPG5-DST-238 and HPG3-DST-1000	4.5.2-1
5.0	SHIELDING EVALUATION	5-1
5.1	DISCUSSION AND RESULTS	5-1
5.2	SOURCE SPECIFICATION	5-2
5.3	MODEL SPECIFICATION	5-16
5.3.1	Regulatory Normal Conditions of Transport Model	5-16
5.3.2	Regulatory Hypothetical Accident Condition Model	5-16
5.4	SHIELDING EVALUATION	5-16
5.4.1	Gamma Shielding Analyses	5-21
5.4.2	Neutron Shielding Analyses	5-21
5.4.3	Uncertainties in the Shielding Analysis Models	5-21
5.5	APPENDIX	5.5.0-1
5.5.1	References	5.5.1-1
5.5.2	Gamma Shielding Analyses MCNP Input Files	5.5.2-1
5.5.3	Neutron Shielding Analyses MCNP Input Files	5.5.3-1

CONTENTS (con't'd)

6.0	CRITICALITY EVALUATION	6-1
6.1	DISCUSSION AND RESULTS	6-1
6.2	PACKAGE FUEL LOADING	6-2
6.3	MODEL SPECIFICATION	6-2
6.3.1	Description of Computational Model	6-2
6.3.2	Package Regional Densities	6-18
6.4	CRITICALITY CALCULATIONS	6-18
6.4.1	Calculation Method	6-18
6.4.2	Fuel/Moderator Loading Optimization	6-18
6.4.3	Criticality Results	6-19
6.5	CRITICAL BENCHMARK EXPERIMENTS	6-22
6.5.1	Benchmark Experiments and Applicability	6-22
6.5.2	Details of Benchmark Calculations	6-22
6.5.3	Results of Benchmark Calculations	6-25
6.6	APPENDIX	6.6.0-1
6.6.1	References	6.6.1-1
6.6.2	MCNP Code Input Listings	6.6.2-1
7.0	OPERATING PROCEDURES	7-1
7.1	PROCEDURES FOR LOADING THE PACKAGE	7-1
7.1.1	General Information	7-1
7.1.2	Opening the Empty Package	7-2
7.1.3	Payload Installation	7-2
7.1.4	Closure of the Inner Containment Vessel (ICV)	7-3
7.1.5	Closure of the Outer Containment Vessel (OCV)	7-3
7.1.6	Installation of the Impact Limiter and Final Preparations for Shipment	7-4
7.2	PROCEDURES FOR UNLOADING THE PACKAGE	7-6
7.2.1	Opening the Package	7-6
7.2.2	Payload Removal	7-6
7.3	PREPARATION OF AN EMPTY PACKAGE FOR TRANSPORT	7-6
7.4	REFERENCES	7-4-1
8.0	ACCEPTANCE TESTS AND MAINTENANCE PROGRAM	8-1
8.1	ACCEPTANCE TESTS	8-1
8.1.1	Visual Inspection	8-1
8.1.2	Structural and Pressure Tests	8-1
8.1.3	Leakage Rate Tests	8-2
8.1.4	Component Tests	8-6
8.1.5	Tests for Shielding Integrity	8-7
8.1.6	Thermal Acceptance Tests	8-7

CONTENTS (cont'd)

8.2	MAINTENANCE PROGRAM	8-7
8.2.1	Structural and Pressure Tests	8-7
8.2.2	Leakage Rate Tests	8-7
8.2.3	Subsystems Maintenance	8-11
8.2.4	Valves, Rupture Discs, and Gaskets on the Containment Vessel	8-12
8.2.5	Shielding	8-12
8.2.6	Thermal	8-12
8.3	REFERENCES	8-3-1
9.0	QUALITY ASSURANCE	9-1
9.1	INTRODUCTION	9-1
9.2	SCOPE	9-1
9.3	QUALITY ASSURANCE PLAN	9-2
9.3.1	Quality Element 1.0, Organization	9-2
9.3.2	Quality Element 2.0, Quality Assurance Program	9-4
9.3.3	Quality Element 3.0, Package Design Control	9-5
9.3.4	Quality Element 4.0, Procurement Document Control	9-6
9.3.5	Quality Element 5.0, Instructions, Procedures, and Drawings	9-7
9.3.6	Quality Element 6.0, Document Control	9-7
9.3.7	Quality Element 7.0, Control of Purchased Material, Equipment and Services	9-7
9.3.8	Quality Element 8.0, Identification and Control of Material, Parts and Components	9-8
9.3.9	Quality Element 9.0, Control of Special Processes	9-8
9.3.10	Quality Element 10.0, Inspection	9-8
9.3.11	Quality Element 11.0, Test Control	9-8
9.3.12	Quality Element 12.0, Control of Measuring and Test Equipment	9-8
9.3.13	Quality Element 13.0, Handling, Storage, and Shipping Control	9-9
9.3.14	Quality Element 14.0, Inspection, Test, and Operating Status	9-10
9.3.15	Quality Element 15.0, Nonconforming Materials, Parts, or Components	9-10
9.3.16	Quality Element 16.0, Corrective Action	9-10
9.3.17	Quality Element 17.0, Quality Assurance Records	9-11
9.3.18	Quality Element 18.0, Audits	9-12
9.4	REFERENCES	9-4-1

LIST OF ACRONYMS

ABS	Acrylonitrile Butadiene Styrene
AISI	American Iron and Steel Institute
AMS	Aerospace Materials Specification
ANSI	American National Standards Institute
ASME B&PV	American Society of Mechanical Engineers Boiler and Pressure Vessel Code
ASTM	American Society for Testing and Materials
BTU	British Thermal Unit
CCW	counterclockwise
CFR	Code of Federal Regulations
CG	Center of Gravity
CI	Curies
CTA	Certification Test Article
DOE	U.S. Department of Energy
DOT	U.S. Department of Transportation
EAOA	Engineering Applications Quality Assurance
EAS&SOA	Engineering Applications and Support Quality Assurance
EB	Electron Beam
ENDF	Evaluated Nuclear Data Files
ETG	Electrically Heated Thermoelectric Generator
GPHS	General Purpose Heat Source
GTAW	Gas Tungsten Arc Weld
HAC	Hypothetical Accident Conditions
HF	Hot Face
IAEA	International Atomic Energy Agency
ICV	Inner Containment Vessel
ID	Inside Diameter
LANL	Los Alamos National Laboratory
MCNP	Monte Carlo Neutron Photon
MNOP	Maximum Normal Operating Pressure
MSLD	Mass Spectrometer Leak Detector
NASA	National Aeronautics and Space Administration
NIST	National Institute for Science and Technology
NCR	Nonconformance Report
NCT	Normal Conditions of Transport
NPT	National Pipe Thread
NRC	Nuclear Regulatory Commission
OCV	Outer Containment Vessel
OD	Outsider Diameter
PC	Personal Computer
PSIA	Pounds per Square Inch Absolute
PSIG	Pounds per Square Inch Gage
PVC	Polyvinyl Chloride
QA	Quality Assurance
QAP	Quality Assurance Program
QAPI	Quality Assurance Plan Index
QAPP	Quality Assurance Program Plan
RFO	Request For Quote
RTG	Radioisotope Thermoelectric Generator
RTV	Room Temperature Vulcanizing

LIST OF ACRONYMS (cont'd)

SARP	Safety Analysis Report for Packaging
SST	Safe, Secure Transporter
STP	Standard Temperature and Pressure
TGA	Thermogravimetric Analysis
UN	United Nations
UNC	United Nations Course
UNF	United Nations Fine
WHC	Westinghouse Hartford Company

1.0 GENERAL INFORMATION

1.1 INTRODUCTION

The Radioisotope Thermoelectric Generator (RTG) Transportation System Package is a Type B(U) packaging system that is used to transport a RTG or similar payload. The payload, which is included in this Safety Analysis Report for Packaging (SARP), is a generic, enveloping payload that specifically encompasses the General Purpose Heat Source (GPHS) RTG payload. The payload is classified as Fissile Class (H) and contains sufficient quantities of plutonium to warrant the special requirements of 10 CFR 71.63¹ ("*Special Requirements for Plutonium Shipments*").

The RTG Transportation System Package consists of two independent containment systems. The package is mounted on its own shock-isolation transport skid (for shock and vibration protection of the payload) and is transported within an exclusive-use trailer. Up to two packages may be shipped within one trailer, depending on payload heatload and plutonium content. For operational protection of the payload, an active cooling system is provided for the package. In accordance with 10 CFR 71.51(b), the cooling system is not required to be active for the RTG Transportation System Package to successfully comply with the activity release limits of 10 CFR 71.51(e). The packaging and its individual components are shown in the General Arrangement Drawings in Appendix 1.3.2. The packaging model name is RTG Package.

1.2 PACKAGE DESCRIPTION

1.2.1 Packaging

The RTG Transportation System Package consists of a packaging (with a removable impact limiter) and a payload. The packaging stands approximately 77 in. high, with a maximum diameter (of the impact limiter) of 70 in. The gross weight of each package, with impact limiter and payload, is approximately 9,800 pounds. Each packaging consists of two separate containment vessels: an inner containment vessel (ICV) and an outer containment vessel (OCV). The containment structures are fabricated from AISI Type 304L stainless steel. Each containment vessel consists of a bell-shaped structure attached to a heavy base with high-strength alloy steel closure bolts. Each bell assembly consists of a cylindrical shell with a standard American Society of Mechanical Engineers (ASME) torispherical head at the top and a bolting flange at the bottom. Leaktight sealing of each level of containment is effected with butyl O-ring seals in a face seal configuration between the bolting flange and base. Each containment vessel uses an inner O-ring for containment and an outer O-ring for leakage rate checking. The major containment boundary components of each vessel are the bell, base, and containment O-ring.

Each containment vessel is equipped with a helium fill (primary vent) port; the ICV also has a secondary vent port. These ports are used to establish a pressurized (19 ± 1 psia) helium atmosphere inside each packaging containment boundary at the time of loading. In addition, each containment vessel is equipped with a leakage rate test port. These test ports, which access the volume between the containment O-ring and the leakage rate test O-ring, verify leak tightness, via helium leakage rate testing, of each level of containment after assembly. All ports are sealed with brass cap screws fitted with butyl Parker Stat-O-Seals[®]. Vent ports, which penetrate containment, are leakage rate checked before shipment. Electrical feed-through connectors are

¹Stat-O-Seal is a registered trademark of the Parker Hannifin Corporation.

used to monitor the RTG payload during transport. To provide the required level of leak tightness, the electrical feed-throughs use D.G. O'Brien Series 107 sealed electrical connector assemblies that are welded into the ICV and OCV base. The containment vessels are designed to withstand all pressure buildups that may occur during normal conditions of transport (NCT) and hypothetical accident conditions (HAC). No pressure relief systems for the containment boundaries are provided.

No neutron absorbing materials other than the packaging steel walls are required for compliance with 10 CFR 71. However, for normal handling purposes, a water-glycol solution is used, in the OCV cooling jacket, that acts as a neutron absorber to reduce worker radiation exposure. Other means of heat dissipation include the following:

- High emissivity surface treatments on the inner and outer surfaces of the ICV and the inner surface of the OCV
- A dimensionally-controlled gap between the ICV and OCV bells
- A helium cover gas within the containment vessel cavities.

The packaging has a removable impact limiter at the bottom end. The impact limiter is comprised of two densities of fire-resistant, polyurethane foam fully encased in a AISI Type 304 stainless steel shell. A chemo-metal thermal shield is incorporated in the impact limiter, adjacent to the bottom of the OCV base. The impact limiter shell is equipped with plastic melt-out plugs for pressure relief if off-gassing of the foam occurs during the HAC fire event. The impact limiter also has drain tubes that drain any potential condensate from the cooling jacket. The impact limiter includes an integral bolting ring and is attached to the base of the OCV with 1-in. diameter high-strength Inconel bolts. The bolt shanks are necked down to 0.806 in. in diameter to allow them to stretch rather than break on impact. The steel shell is painted white to achieve low solar absorptivity.

The payload cavity is approximately 57 in. (maximum height at centerline) by 34 in. in diameter. Each payload has its own shipping rack assembly, which attaches to the base of the ICV. The shipping rack assembly includes a 33-in. diameter AISI Type 304 stainless steel barrier plate, elevated from the ICV base, to segregate any heat-producing elements of the payload from the ICV containment seal and electrical feed-through connector. The shipping rack assembly may also include additional payload support structure, fabricated from AISI Type 304 stainless steel. The shipping rack assembly will remain in place when subjected to the regulatory test requirements of 10 CFR 71.71 and 71.73. Payloads attach through the shipping rack assembly as opposed to directly to it. This arrangement permits the payloads to break free during HAC events without compromising shipping rack assembly retention.

The package is secured to its transport skid with a pair of tiedown straps that pass over the top of the locally-reinforced OCV bell at right angles to one another. Consequently, there are no tiedown devices that are an integral part of the packaging. Lifting the package is accomplished via three OCV fins, which double as lifting lugs. ICV bell lifting is accomplished by a single lift point centered in the ICV head. A personnel barrier is provided at the center of the OCV head to satisfy the exclusive use shipment temperature limitation (180 °F) for accessible surfaces per 10 CFR 71.43(g).

An exploded view of the cask assembly is presented in Figure 1.2.1-1. Additional detail of the two containment vessels is provided in Sections 1.2.1.1 (OCV) and 1.2.1.2 (ICV).

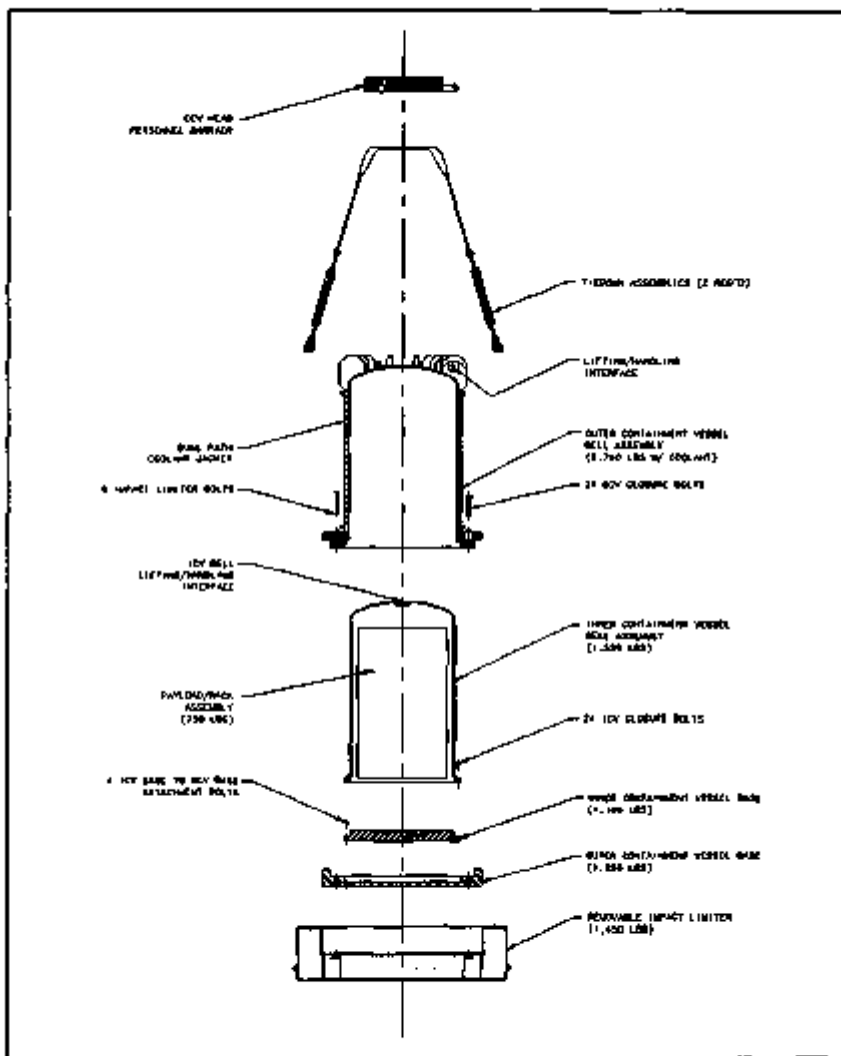


FIGURE 1.2.1-1. RTG Packaging Exploded View.

1.2.1.1 Outer Containment Vessel (OCV). The OCV consists of a AISI Type 304L stainless steel base (63.25 in. O.D., 3.50-in. thickness in the seal area), to which an AISI Type 304L stainless steel bell assembly is attached by 24, 1 1/8-in., ASTM-A320, Grade L43 bolts (identified as cap screws on the drawings in Appendix 1.3.2). The bell flange fits within a 2.40-in.-deep counterbore in the base, sized to limit motion in an accident so the closure bolts cannot be loaded in direct shear. The seal between the bell flange and the base is achieved by using two concentrically arranged butyl rubber O-ring face seals. The inner containment seal has a nominal diameter of 0.393 in.; the outer test seal has a nominal diameter of 0.275 in. The bell is made of a cylindrical shell, 35.88-in. I.D., welded to an ASME torispherical head, both having a wall thickness of 0.50 in. The head includes 0.25-in. thick doubler strips that locally strengthen the head at the location of the tie-down straps. Twenty-four 0.25-in.-thick fins are attached to the head around the knuckle region, three of which are slightly shorter and have holes for lifting the loaded package. The fins provide a degree of impact cushioning in a top-down impact, as well as some heat rejection capability during transport. The overall height of the OCV, including the fins, is 68 in. Located on the upper side of the bell bolting flange is a thermal shield. The thermal shield is a hollow structure (which is filled with fiberglass insulation to protect the sealing area from HAC fire temperatures) and fabricated from 0.38-in. and 0.25-in. thick AISI Type 304L plate material. Closure and impact limiter bolt heads are accessed through tubes running through the thermal shield.

Located within a recessed hole in the OCV base is the electrical feed-through assembly, which provides a means to continuously monitor the RTG payload during transport. The electrical feed-through assembly consists of a D.G. O'Brien Series 107 electrical connector mounted in an AISI type 316L stainless steel sleeve. This sleeve is welded to the OCV base. From the D.G. O'Brien connector, wiring is routed to a contact housing plate (polyethamide Ultem 1000[™]), which is located on the top surface of the OCV base. Because it passes through the containment boundary, the D.G. O'Brien connector and sleeve form part of the boundary. In addition, the gold-plated, carbon steel electrical pins and the glass seals surrounding the pins are part of the OCV containment boundary. Once installed, the electrical feed-through portion of the containment boundary is never broken; therefore, leakage rate testing at the time of shipment is not required.

The only port that passes through the OCV containment boundary is a vent port, located in the base, through which air is evacuated from and helium is backfilled through the annulus between the ICV and OCV. A test port is located between the two O-ring seals for leakage rate testing. Vent and test port plugs are made of brass and sealed using a butyl Parker Star-O-Seal[®]. Each plug is protected by a brass cap sealed with a Teflon[™] weather gasket.

Located on the outside of the OCV is a coolant jacket, extending from the top of the thermal shield to the bottom of the fins. It consists of two parallel spiral passages, each having a cross section of 2 in. long by 1 in. in the radial direction. The cooling system uses a 70% water/30% propylene glycol solution, and is designed such that either or both of the cooling paths may be used to protect the package payloads from excessive heat buildup during handling and transportation operations. The coolant jacket incorporates a pressure relief device to preclude an over-pressure condition if a cooling system malfunction occurs. During normal transportation, two redundant chilling systems are connected to the coolant jacket, one to each coolant loop. However, for purposes of the evaluation of compliance with 10 CFR 71.51(b), the coolant jacket is assumed to be drained and dry, with no active cooling in effect, when it is conservative for evaluation purposes.

[™]Ultem-1000 is a registered trademark of General Electric Plastics.

[™]Teflon is a registered trademark of the E.I. duPont de Nemours Company.

The interior of the OCV bell is painted flat black to enhance radiative heat transfer from the ICV. Eight nonmetallic contact buttons that help protect the paint during handling operations are located near the bottom inside surface of the OCV bell. The exterior of the OCV bell is painted white to achieve low solar absorptivity.

1.2.1.2 Inner Containment Vessel (ICV). The ICV consists of a AISI Type 304L stainless steel base (38.94 in. O.D., 3.47 in. thick), to which an AISI Type 304L stainless steel bell assembly is attached by 24, 3/4-in., ASTM-A540, Grade B23, Class 1 bolts. The seal between the bell flange and the base is achieved by using two concentrically arranged butyl rubber O-ring face seals. The inner seal, which is the containment seal, is a single, 0.275-in. nominal diameter butyl rubber O-ring seal. The test seal is a single, 0.275-in. nominal diameter butyl rubber O-ring seal and is located outboard of the containment seal. The bell is made of a cylindrical shell, 34-in. I.D. and 0.75-in. thick, and an ASME torispherical head that is 0.38-in. thick. At the top center of the head, a 2-in.-thick plate is located, which is drilled and tapped to accept a 0.75-in. swivel lifting eye (not present during transport). The overall ICV assembly height is approximately 62.63 in. Both the inside and outside of the bell are painted flat black to enhance radiative heat transfer. There is a radial gap from 0.03 in. minimum to 0.25 in. maximum between the ICV outside diameter and the OCV inside diameter. The axial gap between the ICV and OCV heads is from 0.06 in. minimum to 0.50 in. maximum. This axial gap is sized to ensure that, under HAC events that load the package in an axial direction, contact will first occur between the two heads rather than between the ICV and OCV flanges. The ICV base fits within a counterbore in the OCV base and is attached by four 1/4-in. bolts. These bolts constrain the two containment vessels to act together during transportation so that more accurate monitoring of the normal shock and vibration response of the RTG payloads can be obtained. The bolts have no regulatory structural significance and will fail at inertia loads well under 10 g's.

Located within a stainless steel mounting receptacle on the ICV base is the ICV electrical feed-through assembly which, together with the OCV electrical feed-through assembly, is used to provide continuous monitoring of the RTG payload. The electrical feed-through assembly consists of a D.G. O'Brien Series 107 electrical connector mounted in an AISI Type 316L stainless steel sleeve that is welded to the AISI Type 304L stainless steel ICV mounting receptacle. An insulating sleeve, used to thermally protect the electrical feed-through assembly, surrounds the mounting receptacle. Below the D.G. O'Brien connector, wiring is routed to a spring loaded plunger mounting plate (polyetherimide Ultem 1000[®]) that interfaces with the OCV contact housing plate. Because it passes through the containment boundary, the D.G. O'Brien connector and stainless steel sleeve form part of the containment boundary. In addition, the gold-plated carbon steel electrical pins and the glass seals surrounding the pins are part of the ICV containment boundary. As with the OCV, the electrical feed-through portion of the containment boundary is never broken.

Two ICV vent ports, which penetrate the ICV containment boundary and are used during the helium purge process, and one ICV seal leakage rate test port, are located in the bell flange. The ports are similar in design to the previously discussed OCV ports. One of the vent ports connects to a 0.38-in.-diameter, stainless steel riser tube that transports the fill gas from the flange to the top of the ICV interior cavity. This tube allows for more uniform helium insertion into the payload cavity and precludes direct helium impingement onto the payload. Vent and test port plugs are made of brass and sealed using a butyl Parker Stat-O-Seal[®].

The RTG payloads are attached to the ICV base through a shipping rack assembly for positive restraint during normal shipping and handling operations. The shipping rack assembly attaches directly to the ICV base with four 3/4-10 unified national coarse (UNC) bolts, and is totally independent of the payload attachment. The shipping rack assembly includes a 33-in.-diameter, 0.38-in.-thick, AISI Type 304 stainless steel barrier plate. The barrier plate will keep any heat-producing debris, which could conceivably result from payload breakup during a HAC free drop,

away from the ICV seal area and electrical feed-through assembly. This, in turn, will ensure that the ICV containment seal and electrical feed-through assembly will never exceed their maximum allowable temperature limits. The lower surface of the barrier plate is insulated for added thermal protection. To further protect the seals from smaller sized debris (if any), a debris shield is located at the internal junction of the ICV bell and base. Although the debris shield is not intended to form a seal, vent ports are designed to access both sides of the shield, thus ensuring the presence of helium adjacent to the containment O-ring during leakage rate checking. Geometric and structural details of the GPHS shipping rack assembly are provided in Appendix 1.3.2.

1.2.2 Operational Features

For normal transportation operations, one or two packages, along with their shock-mounted transport skid(s) and auxiliary cooling systems (if required), are carried in a single, exclusive-use trailer. The transport skids are equipped with channels for removal from the trailer by fork truck. During transport, in addition to direct monitoring of the payloads via the electrical feed-throughs, package coolant temperature may be actively monitored to ensure that payload temperature limits are not exceeded. Additionally, transportation induced shock and vibration may be measured. Passive shock indicators attached to the package(s) would determine if payload acceleration limits have been exceeded during transport. Accelerometers may also be mounted on the package(s) to actively monitor vibrations to ensure that payload operational limits are not exceeded.

Active cooling is provided for the payload by a 70% water/30% propylene glycol mixture circulating through the package OCV cooling jacket. The recirculated coolant is conditioned by two trailer-mounted auxiliary chiller units. Each unit serves one cooling loop, with either cooling loop being capable of protecting the operational integrity of the payload. Thus, the cooling system is completely redundant. For two package shipments, each auxiliary chiller services one cooling loop of each package.

The ICV bell is typically nested within the OCV bell for loading and unloading purposes. That is, the two containment vessel bells are connected via special spacer blocks and lifted or lowered together. This configuration allows active cooling of the entire assembly, including the payload, during loading and unloading operations. Each spacer block used for the nesting operation attaches to the OCV bell using two closure bolt holes and to the ICV bell using one tapped attachment hole (refer to Section G-G of General Arrangement Drawing Number H-9-5003).

For assembly purposes, alignment pins are provided to ensure correct installation of the packaging components (i.e., the ICV and OCV bells with their respective bases, the ICV within the OCV, and the OCV within the impact limiter). The ICV base is attached to the OCV base with four 1/4-in. diameter bolts so that the entire package assembly acts as essentially a rigid body for vibration monitoring purposes.

1.2.3 Contents of Packaging

The payloads to be accommodated by the RTG Transportation System Packaging are typically RTGs. The RTGs use a radioactive heat source (^{238}Pu) to generate electricity. The packaging design is also compatible with other similar payloads that serve only as heat sources. Governing characteristics for a generic, enveloping payload are summarized in Table 1.2.3-1. Limits on selected initial isotopic content for the ^{238}Pu fuel are listed in Table 1.2.3-4. Plutonium-238 initial fuel properties and associated gamma and neutron spectra are provided in Tables 5-3, 5-4, and 5-5 of Section 5.0. Adequacy of the packaging design to accommodate the generic enveloping payload definition is established in the remainder of the SARP.

The GPHS RTG is the specific payload that is the primary driver for the design of the RTG Transportation System Packaging. Consequently, characteristics corresponding to that specific payload are also covered in detail in the remainder of the SARP. General Arrangement Drawing Number H-9-5005, which is included in Appendix 1.3.2, illustrates the GPHS RTG mounted in the RTG Transportation System Package. Interface details for the GPHS RTG are given in interface control drawings, which are also included as Appendix 1.3.3. The key characteristics of the GPHS RTG payload, which directly influence the packaging design, are summarized in Table 1.2.3-2. By comparison with Table 1.2.3-1, it is apparent that the GPHS RTG payload is enveloped by the generic payload definition. The main components of the GPHS RTG are shown in Figure 1.2.3-1.

The GPHS housing is constructed of ASTM Type 2219 aluminum. Excluding the lower end wiring and converter support ring assembly hardware used for attachment to the GPHS shipping rack assembly, the GPHS RTG weighs 123.5 pounds. The total weight of the GPHS RTG, including the interface hardware, is 200 pounds.

The GPHS RTG payload is bolted to the ICV base plate via four 3/4-10 UNC by 8-in.-long bolts that pass through both the converter support ring and shipping rack assembly. Because the shipping rack assembly is also attached directly to the ICV base by another payload independent set of bolts, payload attachment bolts can fall in a HAC event without compromising retention of the shipping rack assembly. Although the packaging design basis requires that the shipping rack assembly remains in place, it is conservatively assumed that the GPHS RTG payload can break away from its mounts and the RTG itself can break up during a HAC event.

The GPHS RTG contains plutonium fuel in the form of PuO_2 , which is sintered into pellets. Each fuel pellet is a right circular cylinder with rounded edges and a density of 9.6 g/cm³. The properties for the fuel pellets used in the GPHS RTG are provided in Tables 1.2.3-3 and 1.2.3-4. Each fuel pellet is clad with an iridium shell that contains a vent that allows helium produced during the decay of the ²³⁹Pu to escape. The iridium-clad pellets are 1.085 in. long by 1.084 in. in diameter. Two of the clad pellets (also known as fueled clads) are encapsulated in a graphite impact shell and two of these impact shells are enclosed in a reentry member called an aeroshell. The aeroshell arrangement is shown in Figure 1.2.3-2. The aeroshell is designed to survive atmospheric reentry and is the smallest size of heat-generating fragment that could arise from the break-up of the GPHS RTG under a HAC impact. A series of tests were performed to verify the aeroshell's structural integrity².

The maximum specified heat-generating capacity of each aeroshell is 250 W (82.5 W per fueled clad, four fueled clads per aeroshell). The GPHS RTG contains 18 aeroshells that are stacked along the axial center line of the RTG. Hence, the maximum GPHS RTG internal heat load is 4,500 W.

TABLE 1.2.3-1. Generic Payload Definition.

Parameter	Enveloping definition
Number of payloads per package	No specific control; limited by maximum allowed heat load, weight, and PuO ₂ content per package
Number of packages per trailer	1 or 2; limited by maximum allowed heat load and PuO ₂ content per package
Payload weight (w/o shipping rack assembly) per package	625 pound maximum
Heat load per package	4,500 W maximum
Heat load per trailer	6,000 W maximum
Size of heat-producing sources used within the payload	Minimum dimension for smallest possible post-accident, heat-producing source shall be greater than 1 in. (i.e., difference between barrier plus OD and ICV ID)
Maximum PuO ₂ content per package	11,304 g; 142,000 Ci
Maximum PuO ₂ content per trailer	12,560 g; 157,800 Ci
Maximum neutron emission rate for fueled clad	6000 n/s-g ²³⁸ Pu
Cooling fins (if any) that protrude from body of payload	Must be structurally bounded by fin representation used for structural certification testing, i.e., <ul style="list-style-type: none"> * Fin material no stronger than A-36 steel * Fins no thicker than 1/4 in. * Fin corners with included angle no less than 90°
Initial payload internal inert gas charge per package (assumed to communicate with ICV cavity)	Initial charge to consist of a maximum of 0.0135 lb-moles
Gas generation rate from within the payload per package	2.06 x 10 ⁻⁴ cm ³ /sec maximum at STP (assumed to communicate with ICV cavity)
Off-gas because of cabling and other payload specific auxiliaries external to the payload housing, per package	No more than the amount possible from complete decomposition of 2 pounds of Silicone rubber
Minimum distance between adjacent packages within the trailer, centerline to centerline	9.5 ft.

TABLE 1.2.3-2. GPHS RTG Payload Definition.

Parameter	GPHS RTG payload definition
Maximum number per package	1
Maximum number per trailer	1
Payload weight (w/o shipping rack assembly) per package	200 pound maximum
Heat output per package	4,500 W maximum
Heat output per trailer	4,500 W maximum
Size of heat-producing sources used within the payload	Minimum dimension for smallest possible postaccident, heat-producing source is 2.091 in. i.e., minimum dimension of an aeroshell assembly)
Maximum PuO ₂ content per package	11,304 g; 142,000 Ci
Maximum PuO ₂ content per trailer	11,304 g; 142,000 Ci
Maximum neutron emission rate per package	6,000 n/s-g ²³⁹ Pu (5.14 x 10 ⁷ n/s, total)
Maximum fissile material content per package (²³⁹ Pu, ²⁴¹ Pu and ²⁴¹ Pu)	8,980 g
Cooling fins that protrude from body of payload	<ul style="list-style-type: none"> • Material is ASTM 2219 aluminum • Fins are 0.015 in. thick at tip, 0.056 in. thick at root • Fins use 90° corners
Initial payload internal inert gas charge per package (assumed to communicate with ICV cavity)	Initial charge to consist of 0.565 ft ³ (16 L) of inert gas at STP, equivalent to 1.67 x 10 ⁻⁴ lb-moles. With this initial charge, payload internal pressure equalizes to 25 psia.
Gas generation rate from within the payload per package	2.06 x 10 ⁻³ cm ³ /sec maximum at STP (assumed to communicate with ICV cavity)
Off-gas because of cabling and other payload specific auxiliaries external to the payload housing, per package	The dominant components that can off-gas are two, approximately 80-in.-long cable assemblies that include less than one pound of silicone rubber insulation each

GPHS - RTG

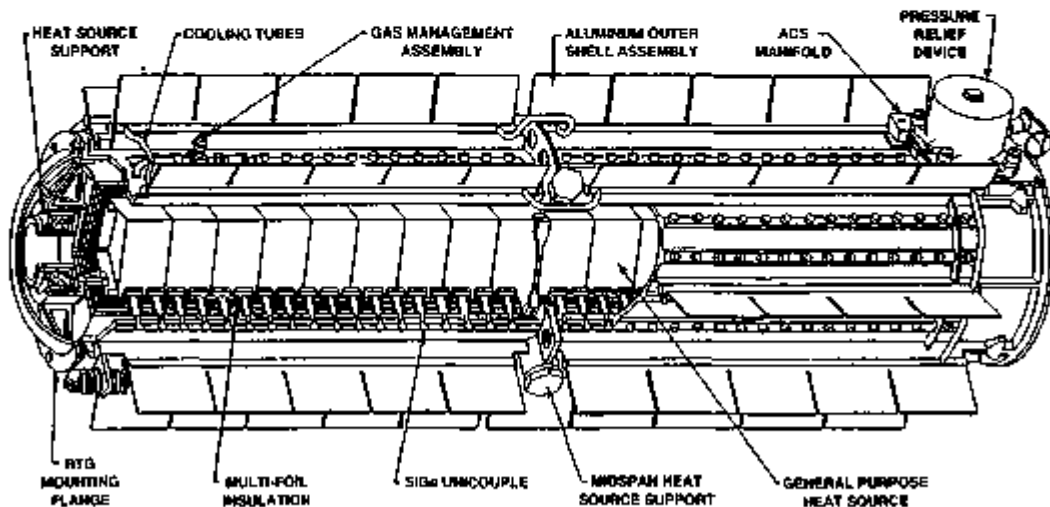


FIGURE 1.2.3-1. GPHS RTG Payload Configuration.

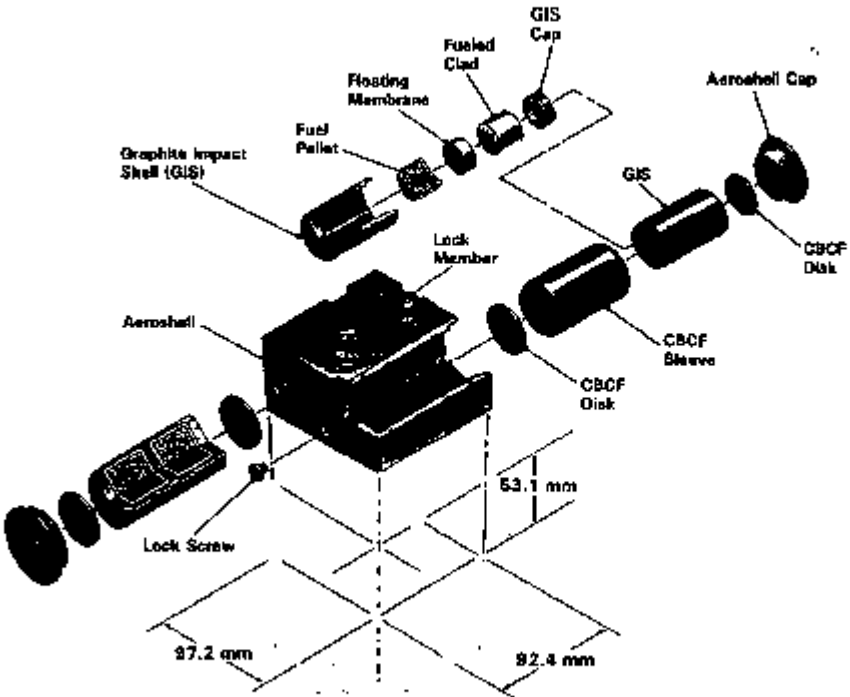


FIGURE 1.2.3-2. GPHS Fuel Arrangement.

TABLE 1.2.3-3. Fuel Pellet Properties of the GPHS RTG.

Fuel pellet property (excluding cladding)	GPHS fuel pellet
Diameter (cm)	2.7534
Length (cm)	2.7559
Fuel Volume (cm ³)	16.409
Density (g PuO ₂ /cm ³)	9.6
Weight (g)	157
Thermal Power (W)	82.5
Activity (Ci)	1,990
Specific Activity (Ci/g)	12.6

TABLE 1.2.3-4. Plutonium Fuel Initial Isotopic Limits for Generic and GPHS Payloads.

²³⁹ Pu content	80 to 85 mol - % of total plutonium
²⁴⁰ Pu content	≤ 0.0001 mol - % of total plutonium
²⁴¹ Pu content	< 20 mol - % of total plutonium
¹⁸ O content	> 99.99 mol - % of total oxygen

1.3 APPENDIX

The following is a list of appendices contained within this section:

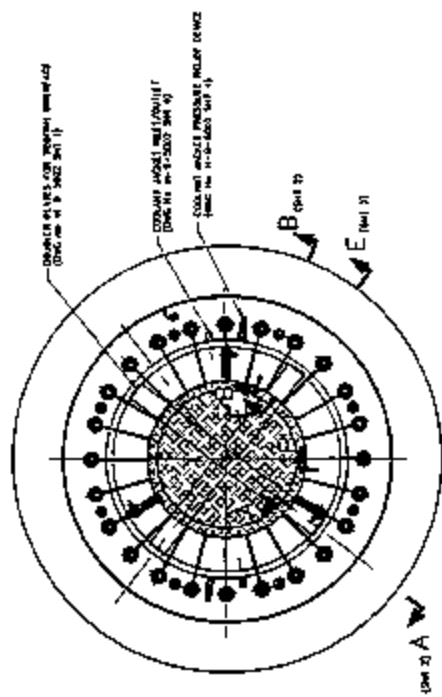
- 1.3.1 References
- 1.3.2 General Arrangement Drawings
- 1.3.3 GPHS RTG Interface Control Drawing

1.3.1 References

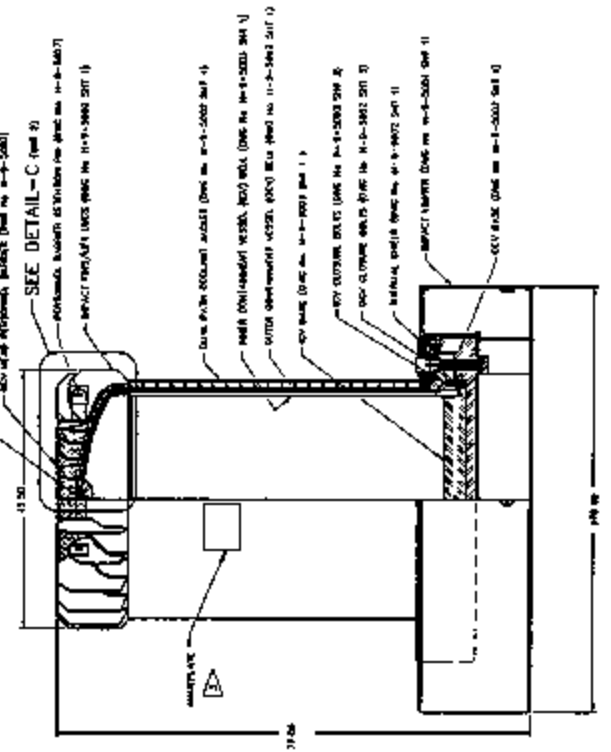
1. 10 CFR 71, 1993, "Packaging and Transportation of Radioactive Materials," *Code of Federal Regulations*, as amended.
2. DOE, 1988, "Physical Protection of Special Nuclear Material and Vital Equipment," Department of Energy Order 5632.2A. U.S. Department of Energy, Washington, D.C.
3. *General Purpose Heat Source Safety Verification Programs:*
 - a. *Edge-on Flyer Plate Test*, LA-10872-MS, March 1987.
 - b. *SVT-1 through SVT-6*, LA-10353-MS, June 1985.
 - c. *SVT-7 through SVT-10*, LA-10408-MS, September 1985.
 - d. *SVT-11 through SVT-12*, LA-10710-MS, May 1986.
 - e. *Bullet/Fragment Test Series*, LA-10364-MS, May 1985.
 - f. *Explosion Overpressure Test Series*, LA-10897-MS, September 1986.

1.3.2 General Arrangement Drawings

<u>Drawing Number</u>	<u>Title</u>	<u>Number of sheets</u>
H-9-5000	General Notes, RTG Transportation Package	1
H-9-5001	General Assembly and Details, RTG Transportation Package	2
H-9-5002	Assembly and Details, Outer Containment Vessel (OCV), RTG Transportation Package	6
H-9-5003	Assembly and Details, Inner Containment Vessel (ICV), RTG Transportation Package	4
H-9-5004	Assembly and Details, Impact Limiter, RTG Transportation Package	1
H-9-5005	GPHS RTG Shipping Configuration, RTG Transportation Package	2
H-9-5007	RTG OCV Head Personnel Barrier, RTG Transportation Package	1



PLAN
F (cont'd)



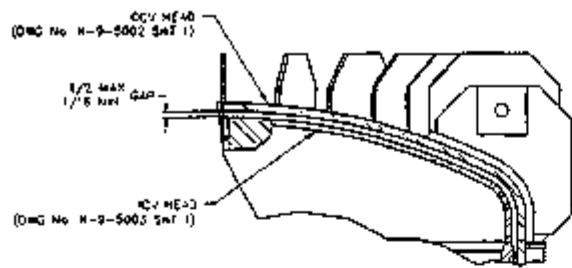
ELEVATION

FOR GENERAL NOTES AND FLAG NOTES
SEE DRAWING No. H-9-3000.

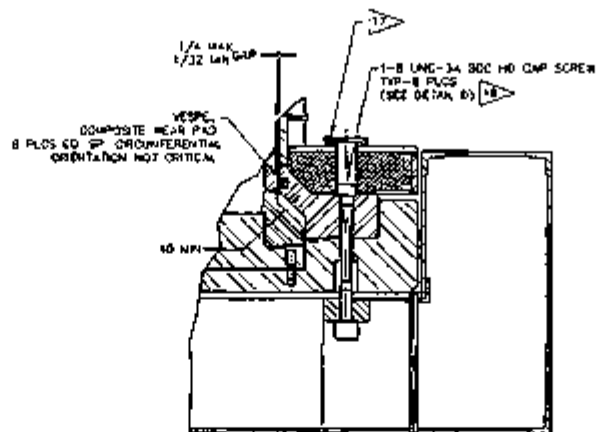


DOCUMENT NUMBER, WMC-SD-RTG-54RP-001
PAGE NUMBER, 1.3.2-3

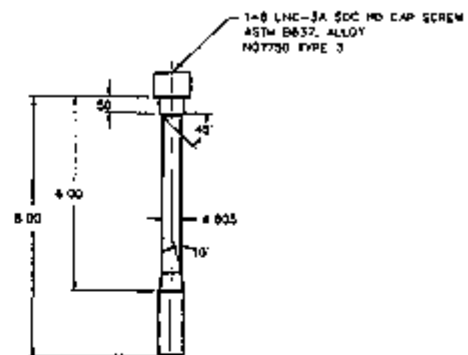
REVISIONS		DATE		BY		CHKD		APP'D		TITLE		SCALE		SHEET NO.		TOTAL SHEETS	
U.S. DEPARTMENT OF DEFENSE ARMY RESEARCH OFFICE-DURHAM RESEARCH TRIANGLE PARK, N.C. 27709-5000 WMC-SD-RTG-54RP-001 GENERAL ASSEMBLY AND DETAILS												7	437	5010	H-9-3001	8	



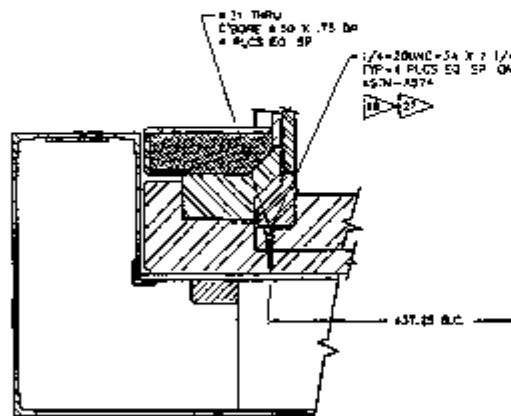
DETAIL-C (SHT 1)



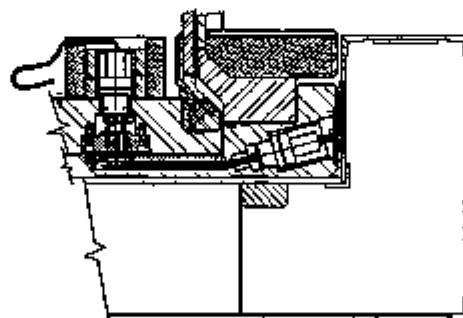
SECTION B-B (SHT 1)
IMPACT LIMITER ATTACHMENT BOLT



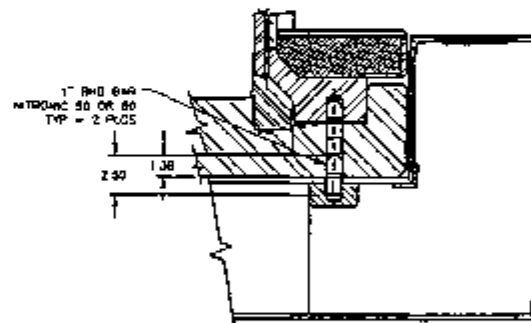
DETAIL D
IMPACT LIMITER BOLT



SECTION A-A (SHT 1)
OCY-OCY BASE ATTACHMENT BOLT

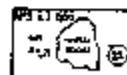


SECTION E-E (SHT 1)
FEED-THRU



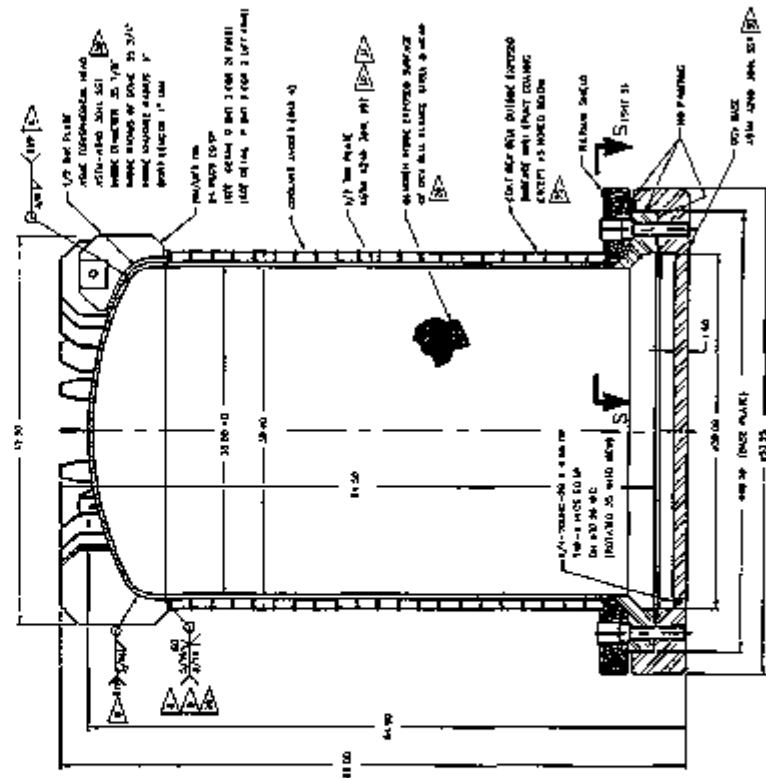
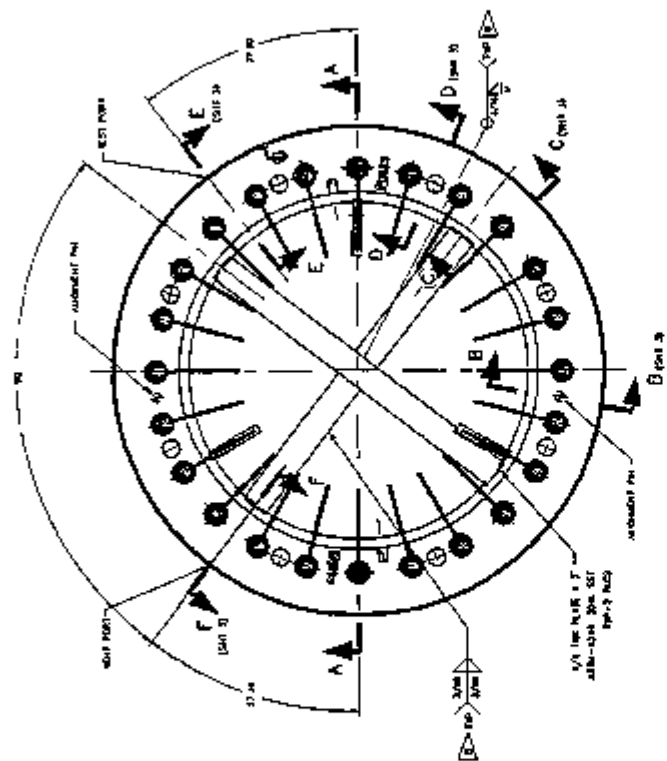
SECTION F-F (SHT 1)
OCY-IMPACT LIMITER ADJUSTMENT PIN

FOR GENERAL NOTES AND FLAG NOTES
SEE DRAWING No. H-9-5000.



DOCUMENT NUMBER, WHC-3D-RTG-SARP-001
PAGE NUMBER, 1.3.2-4

U.S. DEPARTMENT OF DEFENSE Defense Operations Office		RTG TRANSPORTATION PACKAGE GENERAL ASSEMBLY AND DETAILS	
REV	DATE	BY	CHKD
1	427	5010	H-9-5001
GENERAL ASSEMBLY AND DETAILS		PAGE NUMBER, 1.3.2-4	



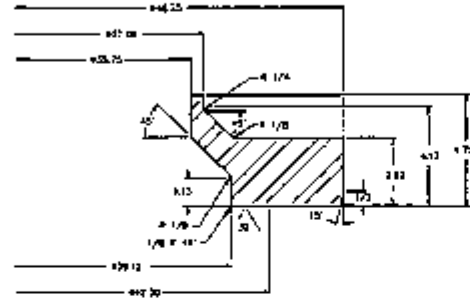
FOR GENERAL NOTES AND FLAG NOTES
SEE DRAWING No H-9-5000



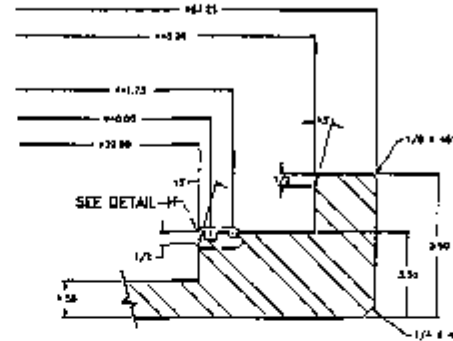
DOCUMENT NUMBER, WNC-50-RTG-SARP-001
PAGE NUMBER, 132-5
Rev. 0

NO.	REV.	DATE	BY	CHKD.	DESCRIPTION
1					
2					
3					
4					
5					
6					
7					
8					
9					
10					
11					
12					
13					
14					
15					
16					
17					
18					
19					
20					
21					
22					
23					
24					
25					
26					
27					
28					
29					
30					
31					
32					
33					
34					
35					
36					
37					
38					
39					
40					
41					
42					
43					
44					
45					
46					
47					
48					
49					
50					

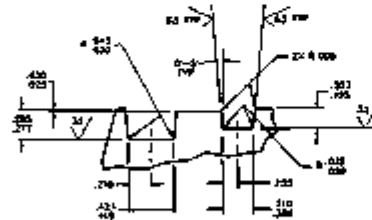
U.S. GOVERNMENT OF OCEAR	
RTG TRANSP PKG	
OUTER CONTAINMENT VESSEL (OCV)	
ASSY AND DET	
NO. 627	5010 H-9-5002



OCV BELL FLANGE DETAIL
MTC 1291-1332 SEE B37



OCV BASE DETAIL



DETAIL-H
DIMENSIONS

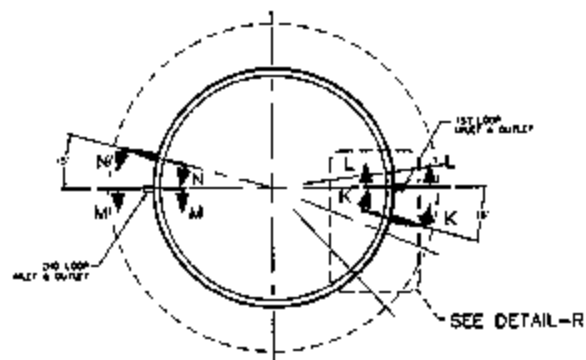
FOR GENERAL NOTES AND FLAG NOTES
SEE DRAWING No. H-9-5000.



DOCUMENT NUMBER, MHC-SD-RTG-SARP-00T
PAGE NUMBER, 1.3.2-8
REV. 0

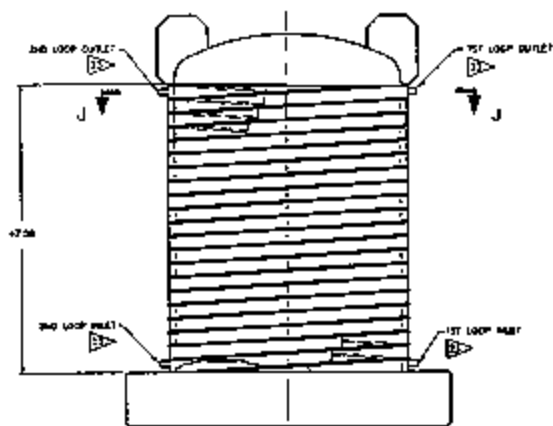
NO.	REV.	DATE	DESCRIPTION
1			
2			
3			
4			
5			
6			
7			
8			
9			
10			
11			
12			
13			
14			
15			
16			
17			
18			
19			
20			
21			
22			
23			
24			
25			
26			
27			
28			
29			
30			
31			
32			
33			
34			
35			
36			
37			
38			
39			
40			
41			
42			
43			
44			
45			
46			
47			
48			
49			
50			

U.S. DEPARTMENT OF ENERGY			
Nuclear Energy Research Administration			
RTG TRANSFER PKG OUTER CONTAINMENT VESSEL (OCV) ASSY AND DET			
DATE	NO. OF SHEETS	TOTAL SHEETS	REV. NO.
8/27/80	5010	H-9-5002	0

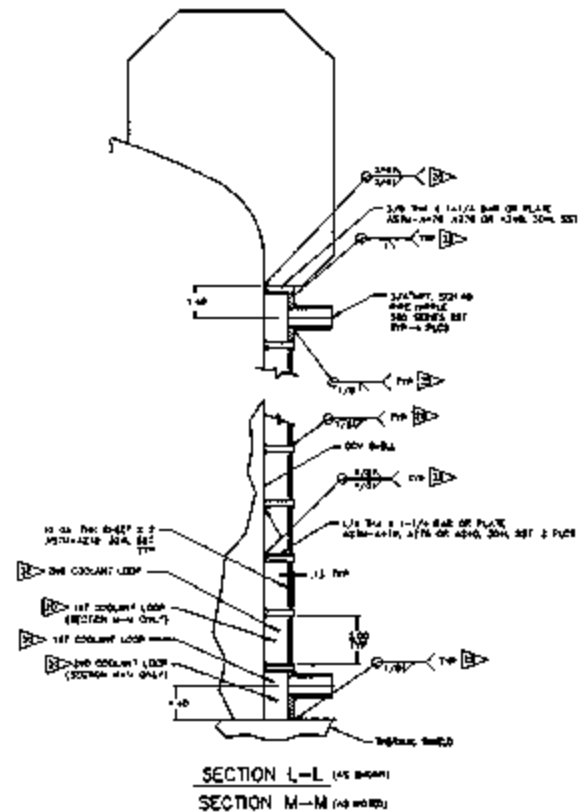


SECTION J-J

(VIEW ROTATED 73° CW FROM ELEVATION VIEW - 3-7-4)

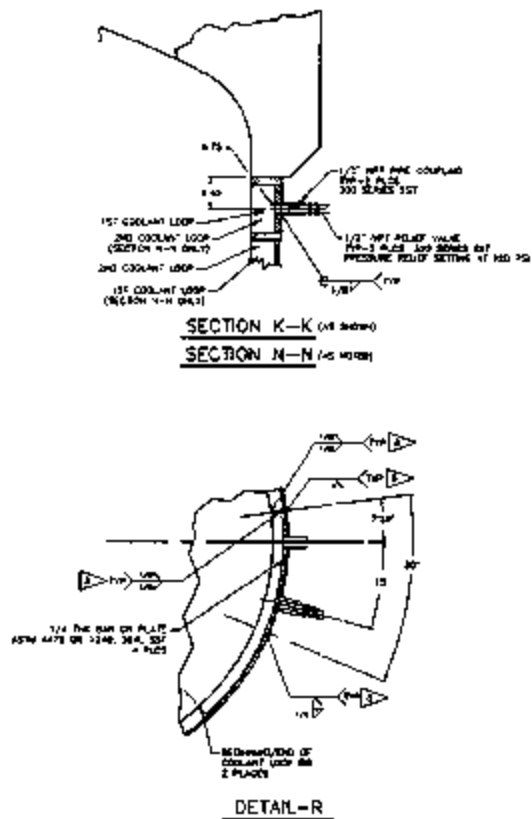


(VIEW ROTATED 73° CW FROM ELEVATION VIEW - 3-7-4)



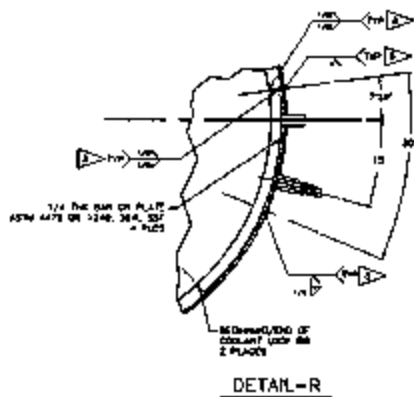
SECTION L-L (AS SHOWN)

SECTION M-M (AS SHOWN)



SECTION K-K (AS SHOWN)

SECTION N-N (AS SHOWN)



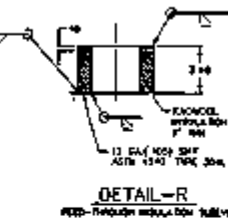
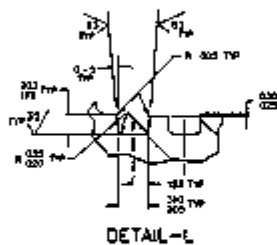
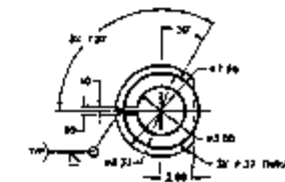
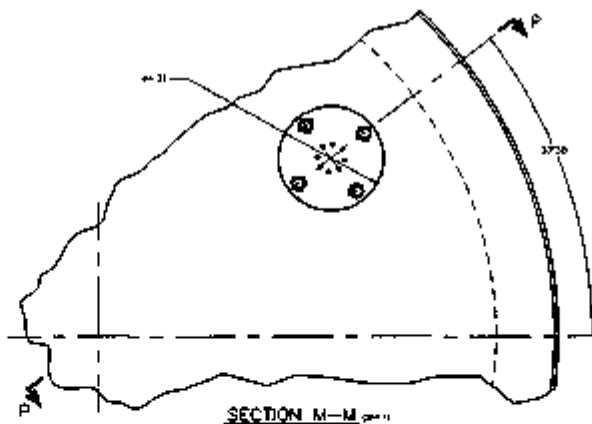
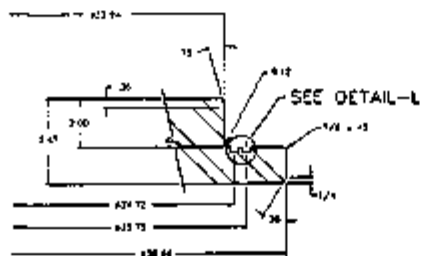
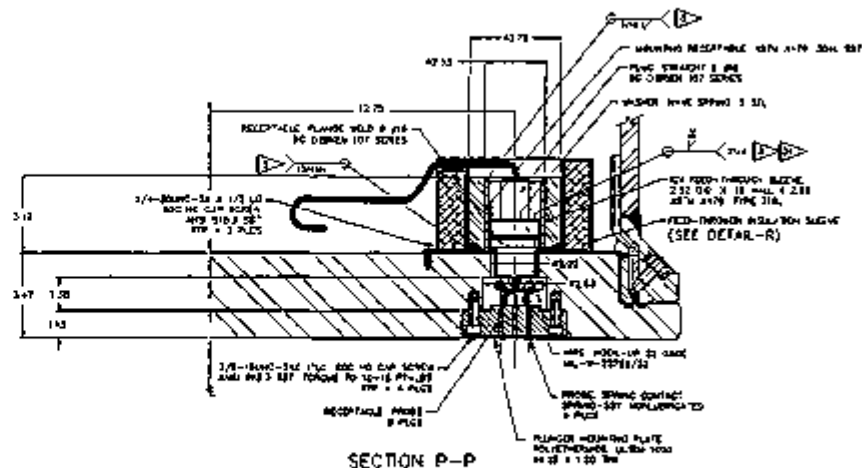
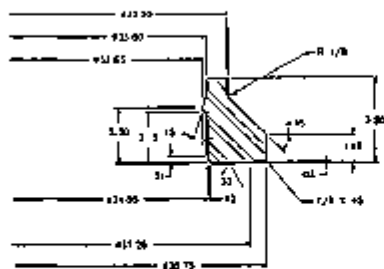
DETAIL-R

FOR GENERAL NOTES AND FLAG NOTES
SEE DRAWING No. H-9-5000.

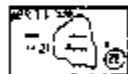


DOCUMENT NUMBER, WDC-SD-RTG-SAMP-001
PAGE NUMBER, 1.3.2-3

NO. OF SHEETS		DATE		BY		CHKD		APP'D		TITL		DWTG		SCALE	
1											RTG TRANSP PKG OUTER CONTAINMENT VESSEL (OCV) ASSY AND DET				
											WDC-SD-RTG-SAMP-001				
											1.3.2-3				
											APR 11 1966				
											RTG TRANSP PKG OUTER CONTAINMENT VESSEL (OCV) ASSY AND DET				
											WDC-SD-RTG-SAMP-001				
											1.3.2-3				



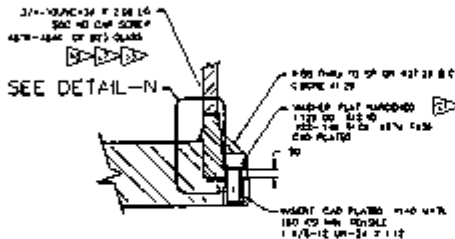
FOR GENERAL NOTES AND FLAG NOTES
 SEE DRAWING No. H-9-3000.



DOCUMENT NUMBER, W40-50-RTG-SAPP-001
 PAGE NUMBER, 1.3.2-11
 Rev. 0

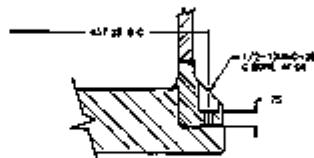
U.S. DEPARTMENT OF ENERGY			
Nuclear Energy Research and Development Administration			
RTG TRANSF PKG			
INNER CONTAINMENT VESSEL (ICV)			
ASSY AND DET			
REV	DATE	BY	CHKD
1	427 5010	H-9-3003	10

REV		DATE		BY		CHKD	
1	427	5010	H-9-3003	10			



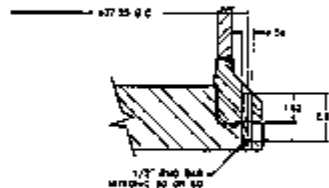
SECTION F-F (SHF 1)

CLOSURE BOLT
TYPE-24 PL



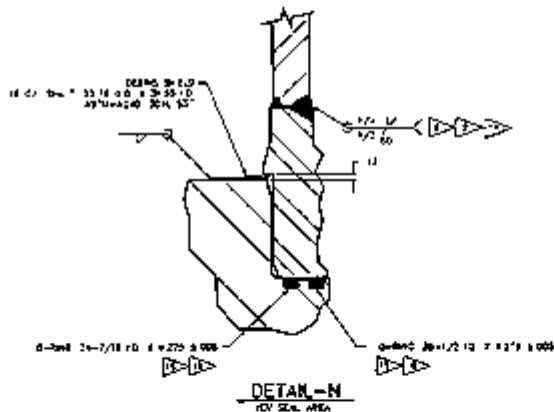
SECTION G-G (SHF 1)

PROOF RING ATTACHMENT HOLE
TYPE-2 PLCS



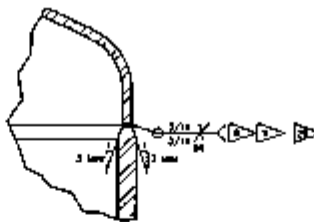
SECTION C-C (SHF 1)

ATTACHMENT PIN
TYPE-2 PLCS



DETAIL-N

KEY SEAL AREA



DETAIL-J

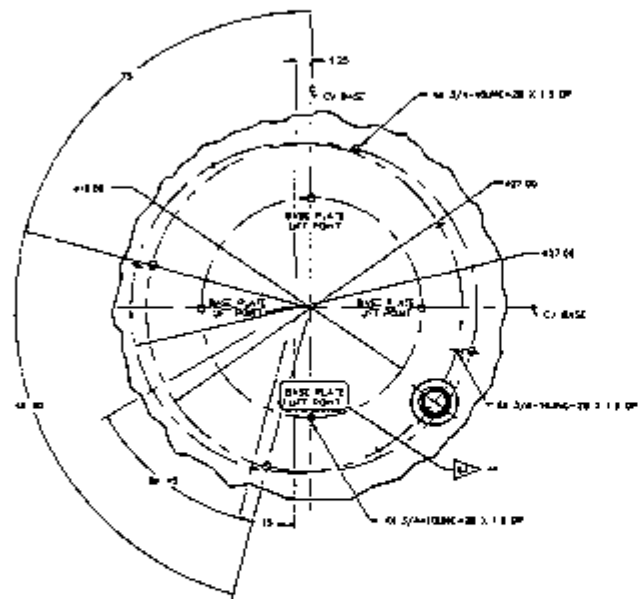
(SHF 1)

FOR GENERAL NOTES AND FLAG NOTES
SEE DRAWING No. H-9-5000.

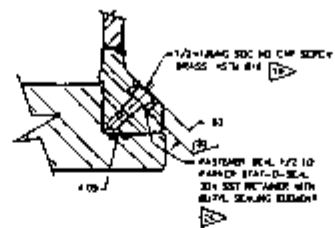


DOCUMENT NUMBER: WAC-SD-RTG-SARP-001
PAGE NUMBER: 132-12 Rev. 0

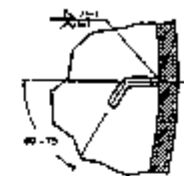
41 SCHEMATIC OF ENERGY					
RTG TRANSF PKG					
INNER CONTAINMENT VESSEL (ICV)					
ASSY AND DET					
427 5010 H-9-5003 1 0					
1 2 3 4 5 6 7 8 9 10 11 12					
10-8-83					



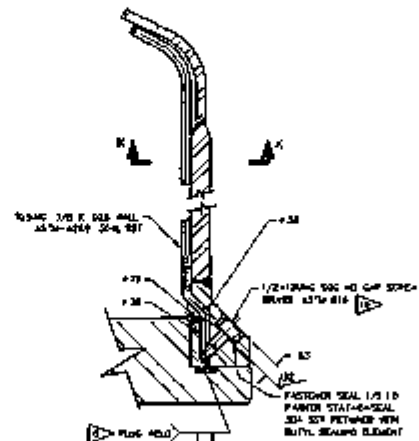
SECTION B-B (REV 1)
AND MAINING SOLT HOLES



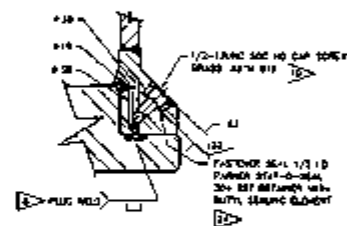
SECTION D-D (REV 1)
MAIN CONTAINMENT VESSEL PORT



SECTION K-K

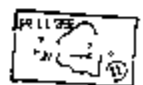


SECTION E-E (REV 1)
MAIN CONTAINMENT VESSEL PORT



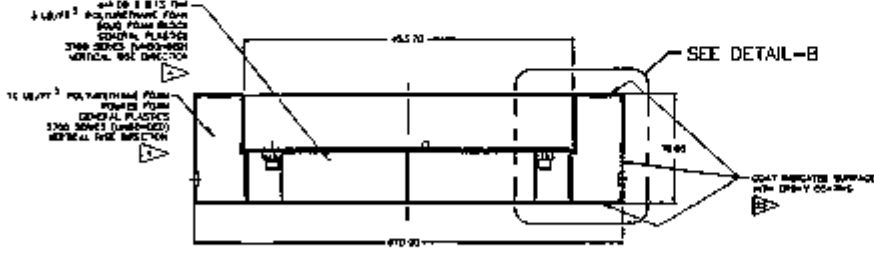
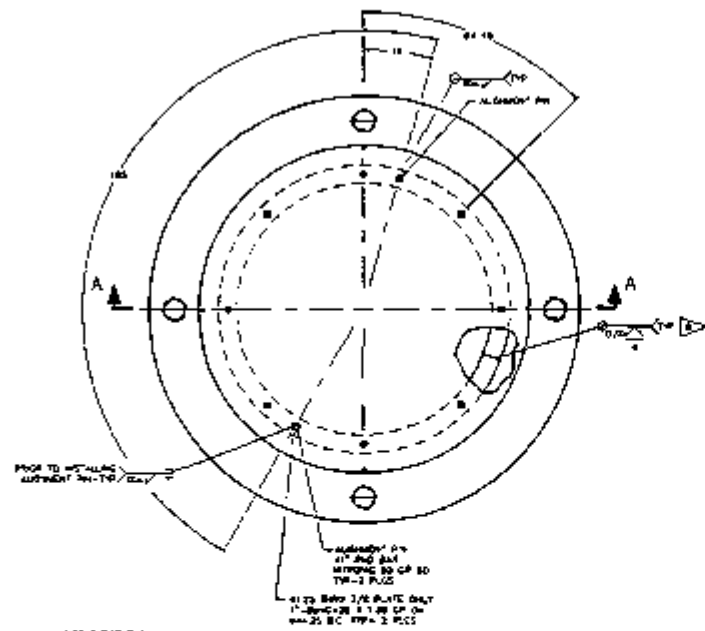
SECTION H-H (REV 0)
MAIN CONTAINMENT VESSEL VERT PORT

FOR GENERAL NOTES AND FLAG NOTES
SEE DRAWING No. H-9-5000.

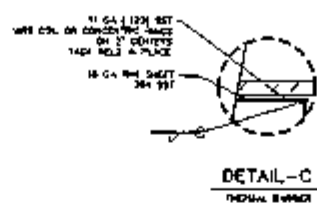


DOCUMENT NUMBER: 98C-SO-RTG-SARP-001
PAGE NUMBER: 1.3.2-13
Rev. 0

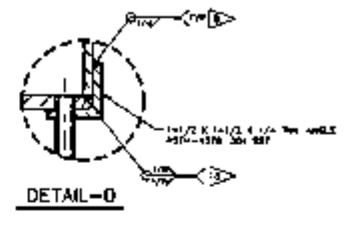
NO. 1	NO. 2	NO. 3	NO. 4	NO. 5	NO. 6	NO. 7	NO. 8	NO. 9	NO. 10	NO. 11	NO. 12	NO. 13	NO. 14	NO. 15	NO. 16	NO. 17	NO. 18	NO. 19	NO. 20
RTG TRANSP PKG INNER CONTAINMENT VESSEL (ICV) ASSY AND DET										427 5016 H-Q-5003 15000									



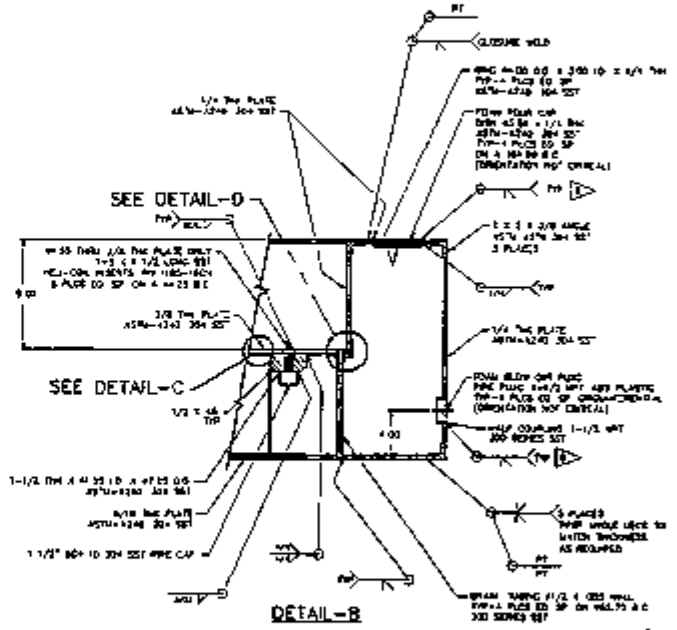
SECTION A-A



DETAIL-C
THERMAL BARRIER

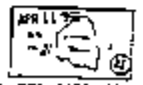


DETAIL-D



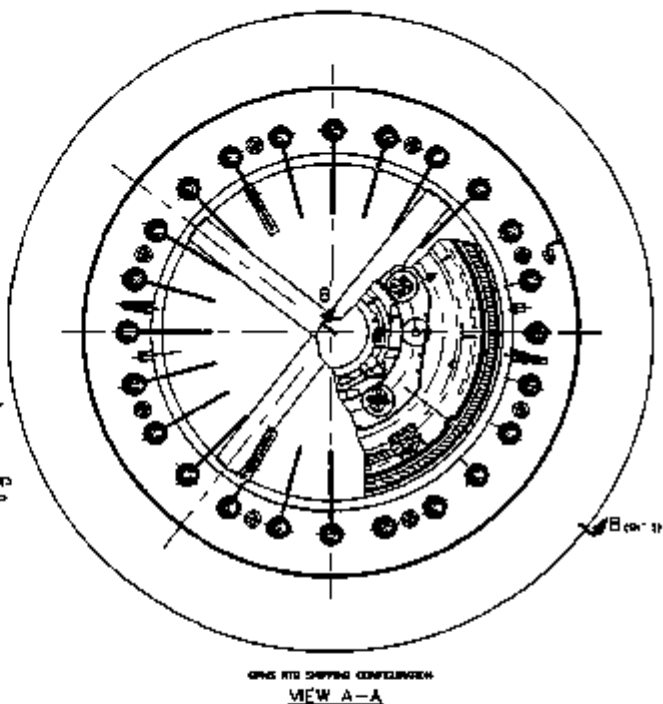
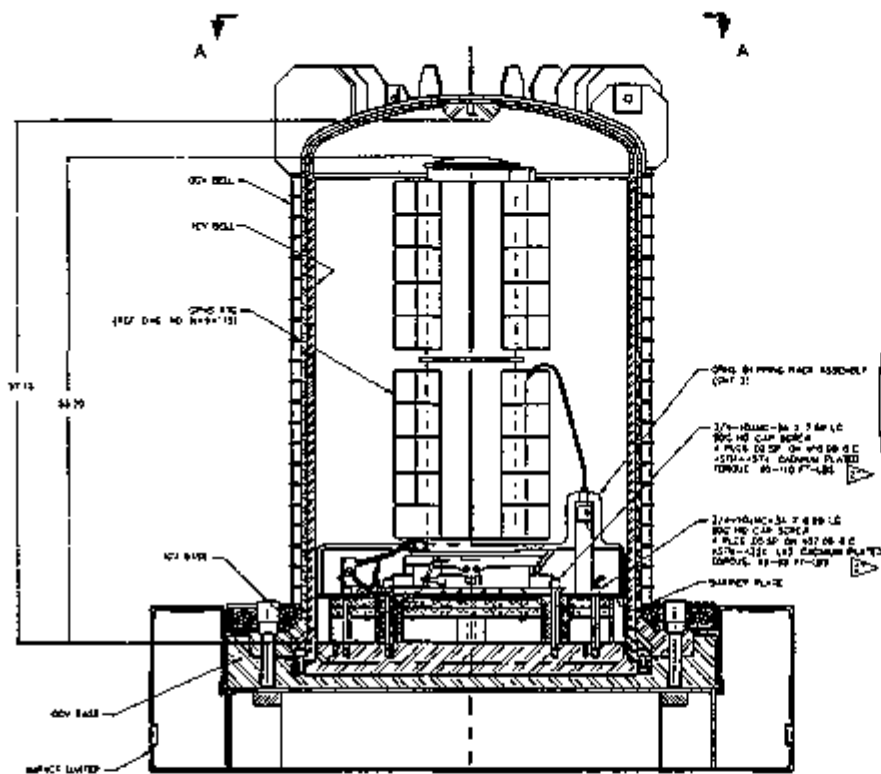
DETAIL-B

FOR GENERAL NOTES AND FLAG NOTES
SEE DRAWING No. H-9-5000.

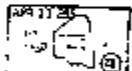


DOCUMENT NUMBER, WMC-80-RTG-SARP-001
PAGE NUMBER, 1,3,3-14
Rev. 0

41 DEPARTMENT OF HIGHWAY TRANSPORTATION RTG TRANSPORTATION PACKAGE IMPACT LIMITER ASSY AND DET		427 5010 H-9-5004 8
---	--	---------------------



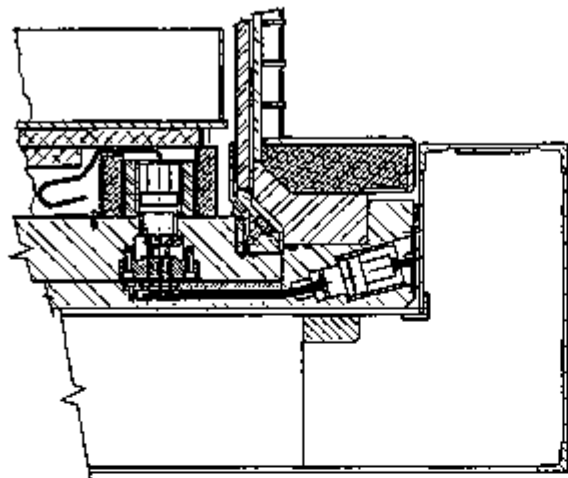
FOR GENERAL NOTES AND FLAG NOTES
SEE DRAWING No. H-9-5000.



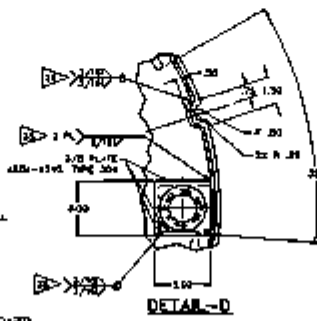
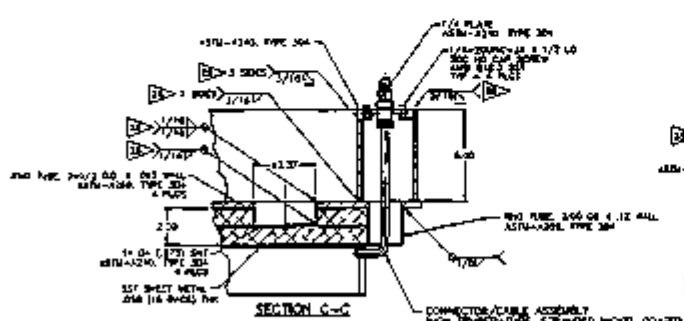
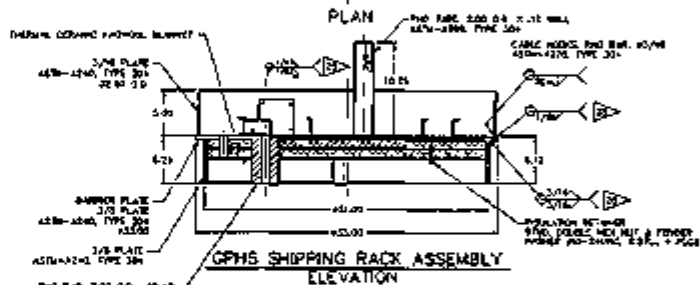
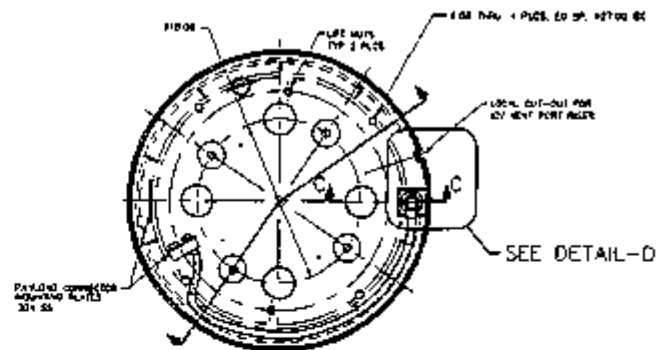
DOCUMENT NUMBER, WAC-50-RIG-SARP-001
PAGE NUMBER, 1.1-15

REV. NO.	DESCRIPTION	DATE	BY	CHKD.	APP. NO.

U.S. GOVERNMENT OF COURTESY Atomic Energy Commission Washington, D.C. 20545	
RTG TRANSPORTATION PACKAGE GPHS RTG SHIPPING CONFIGURATION	
FORM 1127	9010 H-9-5000



SECTION B-B (part 1)



CONNECTOR/CABLE ASSEMBLY FROM TEMPERATURE TREATED NICKEL COATED COPPER CLUTCH WITH ABRASIVE POLISHING OF NICKEL AND STEEL PARTS.

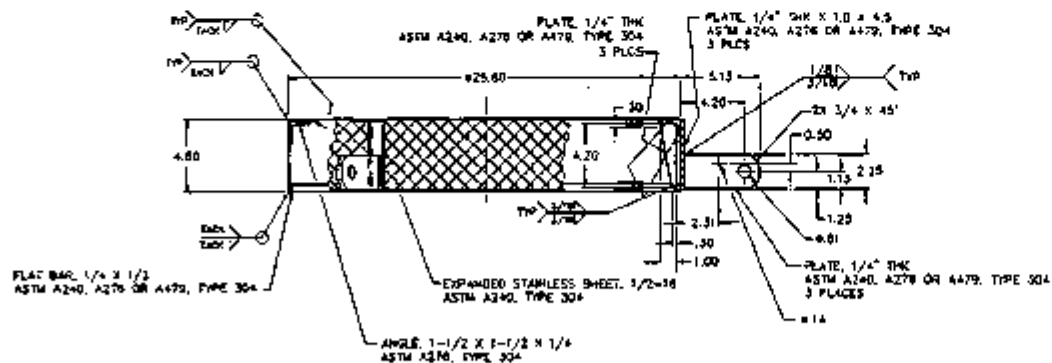
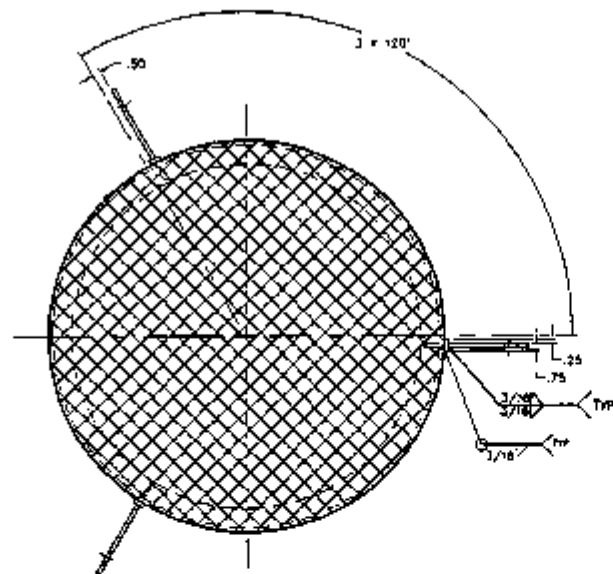
FOR GENERAL NOTES AND FLAG NOTES SEE DRAWING NO. H-8-5000.



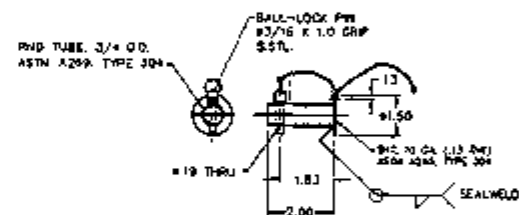
DOCUMENT NUMBER: WNC-SO-RTG-SARP-001
PAGE NUMBER: 1,3,2-15

NO.	REV.	DATE	BY	CHKD.	DESCRIPTION

U.S. DEPARTMENT OF COMMERCE					
RTG TRANSPORTATION PACKAGE					
GPS SHIPPING CONFIGURATION					
FIG NO.	5010	H-8-5005	0		

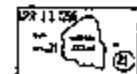


RTG OCY HEAD PERSONNEL BARRIER



PERSONNEL BARRIER RETENTION PIN

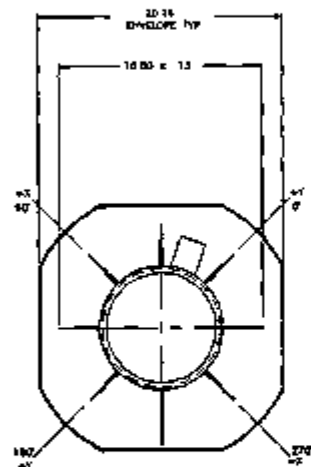
FOR GENERAL NOTES AND FLAG NOTES
SEE DRAWING No. H-9-5000.



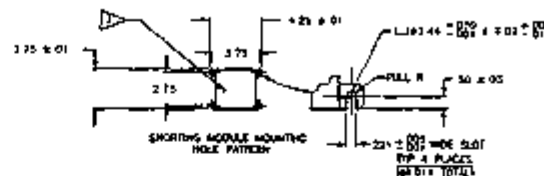
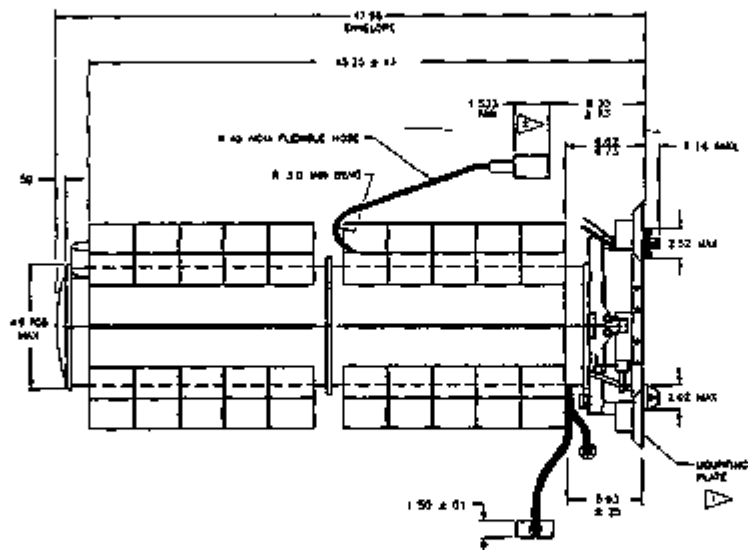
DOCUMENT NUMBER, WHC-50-RTG-SARP-001
PAGE NUMBER, 1.52-17

NO.	DATE	BY	CHKD	APP'D	DESCRIPTION
1	10/11/56
2

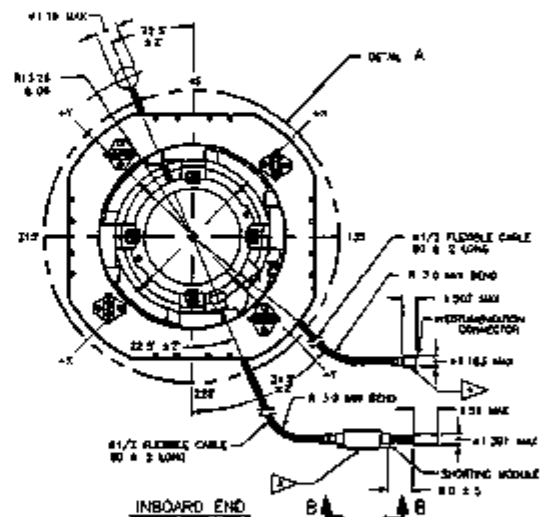
U.S. DEPARTMENT OF ENERGY Atomic Energy Commission	RTG TRANSPORTATION PACKAGE RTG OCY HEAD PERSONNEL BARRIER
427	5010 H-9-5007
1	10/11/56



OUTBOARD END



VIEW B-B



INBOARD END

NOTES

- ▽ DPMS RACK ASSEMBLY INTERFACE
- ▽ GAS CONNECTOR INTERFACE
- ▽ SHORTHING MODULE INTERFACE
- ▽ INSTRUMENTATION CONNECTOR INTERFACE

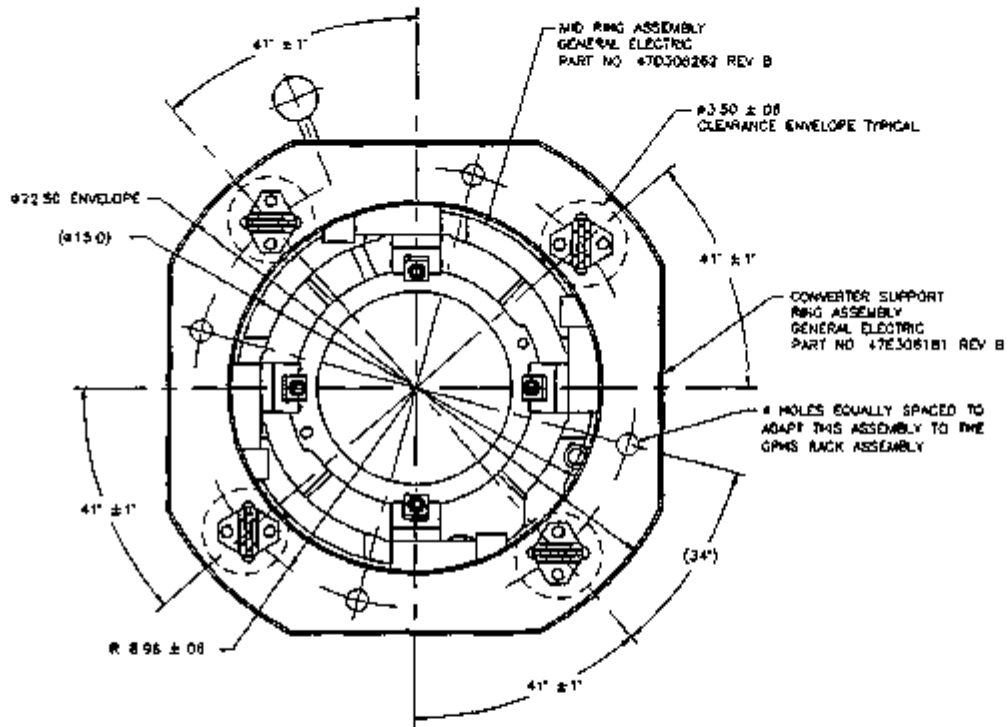
THE TWO CABLES INTERFACE WITH DUMMY CONNECTORS SHOWN ON G.E. DRAWING 47E305501 10 & S NS3113-18-A AND MS3113-14-A.



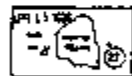
DOCUMENT NUMBER WHC-50-RTC-SARP-001
PAGE NUMBER, 133-2
REV. 0

DATE	BY	CHKD	APP'D	U.S. DEPARTMENT OF ENERGY
				OPHS
				INTERFACE CONTROL DRAWING
				F 477 0010 H-9-119

H-9-119 1.3.2.0



DETAIL A



DOCUMENT NUMBER, WHC-SD-RTQ-SAMP-001
PAGE NUMBER, 132-3

U.S. DEPARTMENT OF ENERGY Health, Safety, and Environment WHC-SD-RTQ-SAMP-001		GPHS INTERFACE CONTROL DRAWING	
F 437 5010	H-9-119		

H-9-119

1.3.3 GPHS RTG Interface Control Drawing

<u>Drawing Number</u>	<u>Title</u>	<u>Number of sheets</u>
H-9-110	GPHS Interface Control Drawing	2

2.0 STRUCTURAL EVALUATION

This section presents evaluations that demonstrate that the RTG Transportation System Package meets all applicable structural criteria. The package consists of an outer containment vessel (OCV), an inner containment vessel (ICV), an impact limiter, and payloads with associated shipping rack assemblies. Normal conditions of transport (NCT) and hypothetical accident condition (HAC) evaluations, using analytic and experimental techniques, are performed to address 10 CFR 71¹ performance requirements. Analytic demonstration techniques comply with the methodology presented in NRC Regulatory Guide 7.6². With the exception of the free drop event, the NCT events are handled analytically. For the HAC events, fire and immersion are handled analytically, and the other events by a combination of analysis, half-scale development testing, and full-scale certification testing.

Experience with previous packaging designs is taken advantage of to the fullest extent possible. Thus, the temperature dependent physical properties and intumescent³ of the polyurethane foam used in the impact limiter are taken from the manufacturer's extensive data base⁴. Nuclear Packaging's TRUPACT-II development program demonstrated the impact absorbing and thermal insulating properties of polyurethane foam. Butyl rubber O-ring performance characteristics have been established by test and are detailed in Appendix 2.10.6. Properties of AISI Type 304L stainless steel, used almost exclusively for packaging structural components, are well documented over a wide range of temperatures in the ASME Boiler and Pressure Vessel (B&PV) Code⁵.

A full series of NCT free drop, HAC 30-ft free drop, and HAC 40-in. puncture drop tests were successfully run with the package remaining leaktight (an integrated leakage rate of less than 1.0×10^{-7} cc/sec, air). The test plan is given in Appendix 2.10.9 and the test procedure in Appendix 2.10.10.

2.1 STRUCTURAL DESIGN

2.1.1 Discussion

This packaging will safely transport Radioisotope Thermoelectric Generators (RTG). The RTG payloads provide highly reliable power sources for use in deep space and terrestrial missions. The packaging consists of three major component subassemblies: (1) an OCV, which provides a primary containment boundary, (2) an ICV, which provides a secondary containment boundary, and (3) an impact limiter, which cushions impact under the HAC drop events, as well as providing insulation for the seal area from the HAC fire temperatures. The ICV and OCV assemblies constitute independent containments as required by 10 CFR 71.63 for shipments containing more than 20 curies (Ci) of plutonium.

³Intumescent is the property of this family of foams that describes their ability to increase their volume as they melt in the presence of flame, thus filling voids left by punctures or tears in the impact limiter sheathing, and providing reliable thermal insulation, even after damage.

2.1.1.1 Outer Containment Vessel (OCV). The OCV consists of an AISI Type 304L stainless steel base to which a Type 304L stainless steel ball assembly is attached by 24, 1 1/4-in., ASTM A320-L43 alloy steel closure bolts. The closure bolts engage hardened steel inserts that are threaded into the OCV base. The ball flange fits within a counterbore in the base sized to limit motion in an accident so that the attaching bolts cannot be loaded in direct shear. The ball is made of a cylindrical shell welded to an American Society of Mechanical Engineers (ASME) torispherical head, both having a wall thickness of 0.60 in. Twenty-four 0.25-in.-thick energy absorbing fins are attached to the head approximately at the knuckle region. Three of the fins have reinforced holes for lifting the entire package.

The seal between the ball flange and the base is effected by use of two concentrically arranged butyl rubber O-ring face seals. The inner containment seal has a nominal diameter of 0.393 in., and the outer noncontainment test seal has a nominal diameter of 0.275 in. A vent port is located in the base, through which air is evacuated from the annulus between the ICV and OCV and through which helium is backfilled. There is also a noncontainment test port located between the two O-ring seals for leakage rate testing the containment seal. Vent and test port plugs are made of brass and sealed using butyl O-rings. Port covers with Teflon[®] seals are used outboard of the plugs and provide an enclosure to retain any leakage per 10 CFR 71.43(e). One electrical feed-through connector is located in the base plate. The device consists of a Type 316L stainless steel body, electrical conductor pins, and a glass-sealing material between the body and the pins. The body is firmly held in place in the base plate by a surrounding structure, and is attached to the base plate material with a gas tungsten arc weld. Outside the OCV containment, a removable plug is used to connect the electrical feed-through connector to the recording equipment. Between the ICV and OCV bases, permanent wire connections are used in conjunction with a spring-loaded pin contact assembly to complete the electrical feed-through circuit between the two vessels. See Figure 2.3-1 for a schematic of the electrical feed-through components.

Located on the outside of the OCV cylindrical area is a coolant jacket consisting of two identical, parallel spiral passages. The passages are constructed of Type 304L and are integrally welded to the OCV shell. Two pressure relief valves, one for each coolant loop, are set for 50 psf and will release excessive pressure that may develop in the coolant jacket because of abnormal system operation. During normal transportation operations, two redundant chilling systems will be connected to the coolant jacket, one to each cooling loop. However, for purposes of the evaluation of compliance with 10 FR 71, the coolant jacket will be assumed to be drained and dry with no active cooling in effect. A thermal shield is located between the lower end of the cooling jacket and the OCV flange consisting of a hollow structure with a 3/8-in. thick top plate and filled with insulation. This feature will protect the flange from puncture and the elastomer seals from the fire peak transient temperatures. The interior of the OCV ball is painted flat black to enhance radiative heat transfer from the ICV. The outside of the OCV ball is painted white to achieve low solar absorptivity while retaining a relatively high emissivity.

2.1.1.2 Inner Containment Vessel (ICV). The ICV consists of an AISI Type 304L stainless steel base, to which a Type 304L stainless steel ball is attached by 24, 3/4-in., ASTM A540-B23 alloy steel closure bolts. The closure bolts engage hardened steel inserts that are threaded into the ICV base. The ball is made of a cylindrical shell, with a 0.75-in.-wall thickness, and an ASME torispherical head that is 0.36 inch thick. At the top center of the head is a block which is drilled and tapped to accept a lifting eye. Both the inside and outside of the ball are painted flat black to enhance radiative heat transfer. A radial gap of 1/32 in. minimum and 1/4 in. maximum exists between the ICV outside diameter and the OCV inside diameter. The gap between the ICV and OCV heads is from 1/16 in. minimum to 1/2 in. maximum, and is sized to ensure that under HAC events, contact will first occur between the two heads rather than between the ICV and OCV

flanges. This feature avoids direct loading of the OCV flange by the ICV in a HAC drop. The ICV fits within a counterbore in the OCV base and is located there by two alignment pins and attached by four 1/4-in diameter, A-574 bolts.

Containment sealing between the bell flange and base is effected by use of two concentrically arranged, 0.275-in nominal diameter butyl rubber O-ring face seals. As with the OCV, the inner O-ring seal provides the containment boundary and the outer O-ring supports leakage rate testing. Two vent ports through the containment boundary (used during the helium purge process), and one O-ring seal leakage rate test port (noncontainment) are located in the bell flange. Vent and test port plugs are made of brass and sealed using butyl O-rings. One electrical feed-through connector, of identical construction to the corresponding OCV component, is located in the base plate. As with the OCV, the electrical feed through body is firmly held in place in the base plate by surrounding structure and is attached to the base plate material with a gas tungsten arc weld. Inside the ICV containment, a removable plug is used to connect the electrical feed-through connector to the temperature measuring devices mounted on the payload. See Figure 2-3-1 for a schematic of the electrical feed-through component.

Payload specific shipping rack assemblies are securely fastened to the ICV base using ASTM A320 L43 alloy steel bolts, and are designed to remain in place during a HAC drop event and prevent proximity of payload heat sources to the seal area. The shipping rack assembly for the General Purpose Heat Source (GPHS) RTG is attached using four 8-in long, 3/4-in bolts. The length of these bolts, coupled with limited clearance between the shipping rack assembly and ICV wall, exclude the potential for direct shear forces. The payload is fastened to the ICV base using bolts that pass through the shipping rack assembly, thus payload inertia loads are not transmitted to the shipping rack assembly or its attaching bolts. The payload bolts are allowed to fail in a HAC drop event without compromising the shipping rack assembly-to-base attachment. The GPHS RTG is attached using four 3/4-in, ASTM A-574 bolts. The shipping rack assembly for all payloads includes a 3/8 in thick, 33-in O D stainless steel barrier plate. The small, 0.50 in radial gap between the shipping rack and ICV wall will not allow payload heat sources to relocate below the shipping rack assembly. To further protect the ICV containment seal from smaller size debris, if any, a stainless steel debris shield is located at the internal junction of the ICV bell and base.

2.1.1.3 Impact Limiter. The impact limiter is a AISI Type 304 stainless steel shell, 70 in in O D, and 18 in tall, with a 53.75-in diameter central pocket on the top, 9 in deep, into which fits the OCV base. The plate at the bottom of the impact limiter is 0.31 in thick. The plate forming the bottom of the pocket is 0.38 in thick. The inner and outer cylindrical walls and top annular section are 0.26 in thick. All corner joints are reinforced with Type 304 stainless steel angles.

A 1.5-in-thick bolting ring just beneath the pocket bottom is used to attach the impact limiter to the OCV, and contains threaded holes that have stainless steel Helix-coil inserts. Eight 1-in-diameter ASTM B637, Alloy N07750 Type 3 bolts, with a shank diameter reduced to 0.805 in to better absorb energy by stretching, attach the impact limiter to the package. Direct shear in the bolts is precluded by the relatively long bolts and extra hole clearance in the mating OCV base.

The cavity within the impact limiter is filled with rigid polyurethane structural foam of 3 lb/ft³ and 12 lb/ft³ densities. For the center portion, out to a diameter of 41 in, 3 lb/ft³ density is used. A sheet metal thermal shield is incorporated in the structure between the center pocket bottom plate and the foam. For the remainder, 12 lb/ft³ foam is used. To ensure that structural performance will not vary over time, the foam is not bonded to the shell structure. The foam serves the dual purpose of limiting impact loads from drop and puncture events, and providing thermal insulation during the HAC fire event. Thermal melt out plugs are provided to vent gas that may be produced by the foam during the HAC fire. Drain tubes, which pass through the impact

limiter, are provided to conduct any condensate from the OCV surface to a collection pan located beneath the package.

2.1.1.4 Manufacturing. Standard methods are used to fabricate these components, in accordance with NUREGs CR-3019⁷ and CR-3854⁸. All heads are standard ASME torispherical head designs. All vessel bell joints and transitions in thickness, such as from the 0.75-in.-thick ICV wall to the 0.38-in.-thick ICV head, are in accordance with the ASME B&PV Code. All circumferential and longitudinal welds used in the ICV and OCV containment boundary bells are full penetration and radiograph inspected. Certain containment boundary welds, such as those associated with vent port and electrical feed-through penetrations that see little structural loading, are inspected by liquid penetrant, as allowed by NuReg CR-3019. All structurally significant noncontainment welds are liquid penetrant inspected.

Polyurethane foam installation techniques used for the impact limiter are the same as those employed in many other radioactive shipping packagings. These foam installation techniques are discussed in Sections 2.3 and 8.1.4.1.

2.1.2 Design Criteria

The package meets regulatory requirements by a combination of analysis and test. The acceptance criteria for analytic assessments is in accordance with Regulatory Guide 7.8 as supplemented by Section III of the ASME B&PV Code. Load combinations are in accordance with Regulatory Guide 7.8⁹. Full-scale prototypical hardware is also tested by subjecting it to several free drop and puncture orientations. The following post-test acceptance criteria is used:

- A demonstration of leaktight containment boundaries (less than 1×10^7 scc/sec leakage rate, air, per ANSI N14.5¹⁰)
- A demonstration that seal area geometry still provides adequate compression on a minimum diameter O-ring seal for all worst-case HAC scenarios, including a subsequent fire.

Package deformations resulting from structural testing must be such that deformed geometry assumptions used in shielding, criticality, and thermal analyses are not invalidated. Furthermore, the shipping rack assembly must remain attached to the ICV base and the impact limiter must remain attached to the OCV. For the NCT 4-ft free drop case, the acceptance criteria selected for the package is that the ability of the package to adequately survive a subsequent HAC sequence (i.e., maintain two leaktight containment boundaries) is not compromised.

2.1.2.1 Allowable Stresses. Mechanical properties of the materials of construction, such as yield strength, S_y , ultimate strength, S_u , and allowable strength, S_m , are listed in Tables 2.3-1 and 2.3-2. All analytical assessments made herein use these properties and the allowable stresses listed below in Table 2.1.2-1.

TABLE 2 1 2-1 Allowable Stress Limits

Stress category	NCT	HAC
General Primary Membrane Stress Intensity	S_m	Lesser of $2.4S_m$ or $0.7S_y$
Local Primary Membrane Stress Intensity	$1.8S_m$	Lesser of $3.6S_m$ or S_y
Primary Membrane + Bending Stress Intensity	$1.5S_m$	Lesser of $3.6S_m$ or S_y
Range of Primary + Secondary Stress Intensity	$3.0S_m$	Not applicable
Pure Shear Stress	$0.6S_m$	$0.42S_y$
Fastener Membrane Stress	Lesser of $2.0S_m$ or S_t	Lesser of S_t or $0.7S_y$
Fastener Membrane + Bending Stress	Lesser of $3.0S_m$ or S_t	S_t^*
Bearing Stress	S_r	S_y for seal surfaces, S_t elsewhere
Peak	Per Section 2 1 2 2 2	

*Stress limits on the containment fasteners are predicated by containment criteria delineated in Section 4 0, Containment, i.e., no yielding allowed for closure bolts used with face seals

2 1 2 1 1 Lifting A minimum safety factor of three against yield consistent with 10 CFR 71 45(a) must be present on any lifting attachment that is a structural part of the package

2 1 2 1 2 Tiedowns Under the simultaneous action of the 10g longitudinal, 6g lateral, and 2g vertical body forces, the stresses in the package must not exceed material yield strengths, consistent with 10 CFR 71 45(b). Although this section does not apply to the RTG Transportation System Package, which has no integral tiedown devices as part of the licensed package, tiedown evaluations are conservatively included which consider tiedown interface loads with the package

2 1 2 1 3 Normal Conditions of Transport and Hypothetical Accident Conditions Regulatory Guide 7 6 is used in the assessment of the package components for both the NCT and the HAC. A tabulated summary of allowable stresses used for package structures is presented in Table 2 1 2-1. These data are consistent with Regulatory Guide 7 6 and Section NB-3000 and Appendix F of the ASME B&PV Code, Section III

2 1 2 1 4 Buckling Usage of Regulatory Guide 7 6 design criteria is dependent on linearly elastic structural response. Nonlinear phenomena such as buckling would preclude using Regulatory Guide 7 6 as a basis for evaluating containment structure integrity as determined by theoretical analysis. Buckling assessments are required only under the following conditions:

- Structural evaluation is by theoretical analysis, using Regulatory Guide 7 6 as the design basis
- Applied loadings could potentially produce buckling

For the RTG Transportation System Package, there are only three structural assessments for

which a buckling analysis would be relevant. The valid load cases are Sections 2 6 4, 2 6 9, and 2 7 5.

To assess the potential for buckling in these load cases, the relevant geometric components of the package containment structure will be evaluated separately. There are two containment boundaries in the package where buckling analysis is appropriate. These are the bell assemblies of both the ICV and the OCV. Each assembly comprises a cylindrical shell topped with a torispherically dished head.

For the torispherical heads, ASME B&PV Code, Section III, Subsection NE will be applied. For the cylindrical shells, the methodology of ASME B&PV Code Case N-284¹² will be applied.

The four basic steps involved in the application of ASME B&PV Code Case N-284 are summarized below:

- 1 Theoretical Elastic buckling stresses are determined for hoop and axial compression and in-plane shear loadings using classical theory.
- 2 Capacity reduction factors are applied that account for the difference between classical theory and predicted instability stresses for fabricated shells.
- 3 Plasticity reduction factors are applied for those cases where elastically determined buckling stresses are above the proportional limit.
- 4 Elastic and inelastic buckling checks that employ an appropriate factor of safety and applicable interaction equations are made using worst case applied compressive and in-plane shear stresses.

Consistent with Regulatory Guide 7 6 philosophy, factors of safety corresponding to ASME B&PV Code Level A and D Service conditions are employed for NCT (Section 2 6) and HAC (Section 2 7) loadings, respectively. The applicable factors of safety are 2 0 for NCT and 1 34 for HAC, as specified in ASME B&PV Code Case N-284.

2 1 2 2 Miscellaneous Structural Failure Modes: This subsection addresses the potential structural failure modes of brittle fracture and fatigue. Bolted joint designs are also shown to develop the full strength of the bolt before tearout from the base material.

2 1 2 2 1 Brittle Fracture: All packaging structural components are made from ductile materials. All containment boundary vessels are made from AISI Type 304L stainless steel; the impact limiter shell is made from AISI Type 304 stainless steel. Because Type 304/304L stainless steel does not undergo a ductile-to-brittle transition in the temperature range of interest (down to -40 °F), brittle fracture is precluded. The materials used for bolts in the package (ASTM-A320, Grade 43 for the OCV closure and shipping rack attachment, ASTM-A540, Grade B23 Class 1 for the ICV closure and ASTM B637 Alloy N07750, Type 3 for the impact limiter attachment) are expressly designed for cold-temperature service. Section 5 of NuReg/CR-1615¹³ states, "Bolts are generally not considered as fracture-critical components because multiple load paths exist and because bolted systems are designed to be redundant. In other words, failure of one or more bolts can be tolerated since failure normally does not lead to penetration or rupture of the container." The nominal factor of safety on the closure bolts is large and will be discussed later. Thus, brittle fracture of packaging components is of no concern.

2.1.2.2.2 Fatigue.

2.1.2.2.2.1 Normal Operating Cycles. Normal operating cycles do not present a fatigue concern for package components. This is because none of the components exhibit significant stress concentrations, and by satisfying the allowable limit for range of primary plus secondary stress intensity for NCT (3.0S_m), the allowable fatigue stress limit for the expected number of operating cycles will automatically be satisfied.

The maximum number of operating cycles is conservatively estimated to be 1,000 over a package life span of 20 years, or one complete load/unload cycle about every 7 days. A cycle is defined as the loading of the highest heat payload, arriving at thermal and pressure equilibrium, and unloading, thereby returning to ambient pressure and temperature, without active cooling. In practice, this would never be allowed, because without active cooling the payload would be damaged and would result in a significant economic loss.

From the ASME B&PV Code, Section III, Appendix I, Figure I-9.2.1 (included as Figure 2.1.2-11, and Table I-9.1 of the Code, the fatigue allowable alternating stress intensity amplitude, S_a, for 1,000 cycles is 119,000 psi. When corrected for the ratio of elastic moduli (essentially a temperature correction), the fatigue allowable for the warmest part of the package (conservatively, 350 °F, for the ICV head per Table 2.10.7.1-2 of the temperature summary of Appendix 2.10.7 becomes:

$$S_a = 119,000 \left[\frac{26.8(10)^9}{28.3(10)^9} \right] = 112,700 \text{ psi}$$

The nonfatigue allowable stress intensity range, from the ASME B&PV Code, Section III, Division 1, Subsection NB-3222.2, however, is 3.0S_m. Interpolating values of S_m from Table 2.3-1 for the temperature of 350 °F above, the resulting allowable stress intensity range is 3.0S_m = 48,750 psi. The maximum allowable alternating stress intensity is one-half of this range, or 24,375 psi. Thus, because of the absence of significant stress concentrations, the fatigue allowable alternating stress intensity will not govern the package design.

2.1.2.2.2.2 Normal Vibration Over the Road. Fatigue concerns associated with normal vibration over the road are addressed in Section 2.6.5.

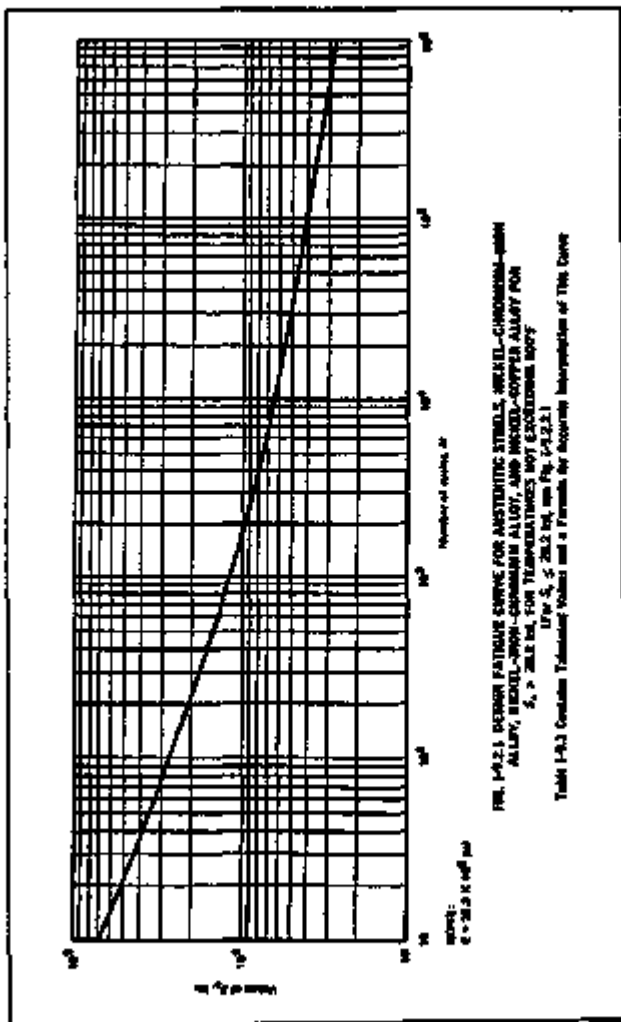


FIGURE 2.1.2-1. ASME B&PV Code, Section III, Appendix I, Figure 1.8.2.1.

2.1.2.2.2.3 Bolt Tearout from Base Material. The bolting materials (ASTM A320 L43 and ASTM A540 Gr B23, Class 1 alloy steel and ASTM B637, Alloy NO7750 Type 3) are inherently stronger than the material into which they thread (ASTM Type 304 or 304L). However, the full strength of the bolt is developed by the engaged length of thread and/or use of replaceable threaded inserts. According to Table 2.1.2-1, the highest allowable stress limit on containment closure bolts is the yield point, S_y . It is also shown that the full tensile yield strength of the ICV and OCV closure bolts is developed by the shear yield strength of the bolt, insert, and base material threads.

Calculations for the shipping rack assembly attachment bolts will be shown as an example. The bolts are 3/4-10 UNC-3A, but class 2A will be conservatively assumed for both internal and external threads. The bolts are 8 in. long, and the shipping rack assembly height is 5.25 in. Therefore, the engaged thread length is 0.75 in. From the article *Strength of Threads* by Raymond Boucher¹⁶, the corresponding ICV base hole threads will have a shear area of 1.7225 in.² per in. of engagement. For a 0.75-in. engagement, the area is 1.2919 in.². For Type 304L, the base material shear strength will be 60% of the tensile strength, or $0.6 \times 70,000 = 42,000$ psi. The shear-out load for the threads will be as follows:

$$S \times A = 54,260 \text{ lb}$$

Where: $S = 42,000$ psi
 $A = 1.2919$ in.²

The tensile stress area of the bolt is 0.330 in.². The tensile strength of the A320 L43 bolting material is 125,000 psi, and the tensile failure load of the bolt is given below.

$$F \times A = 41,250 \text{ lb}$$

where: $F = 125,000$ psi
 $A = 0.330$ in.²

Thus, the bolt ultimate failure load is less than the thread strip-out load, and the full strength of the bolt is therefore developed. Table 2.1.2.2.3-1 summarizes the results for the bolts that are important to containment. Closure bolt yield checks utilize the same approach as above, but are based on the tensile yield strength of the particular bolt material. In addition, since the minimum tensile strength of the thread inserts is 160,000 psi, which is essentially at (for ICVI or above) (for OCV) the closure bolt material strength, shear-out is governed by bolt strength. Consequently, shear-out calculations for the ICV and OCV closure bolts use bolt external thread shear area and shear strength rather than insert internal thread shear area and shear strength.

The inserts for the ICV and OCV are firmly mounted against a shoulder in the base. The insert outer thread pitch diameters (1-5/8-12 UN for the OCV and 1-1/8-12 UNF for the ICV) are considerably larger than the bolt clearance holes in the base material above the insert, and thus, a margin against strip-out is ensured on the insert external threads. For purposes of determining shear-out force for the impact limiter bolts, the threaded inserts are conservatively ignored.

TABLE 2 1 2 2 3-1 Comparison of Bolt Tensile Strength and Pull-out Forces

Bolt identification	Bolt size & material	Thread stress area per in	Engaged length (in)	Bolt tensile failure force (lb)	Thread shear-out force (lb)
Barner plate attachment (ultimate)	3/4-10 x 6 A320, L43	1.7225*	0.75	41,250	54,258
Impact limiter attachment (ultimate)	1-8 x 8.0 B637, Alloy NO7750 Type 3	2.3256*	1.47	61,430†	143,560
ICV closure (ultimate)	3/4-10 x 2.0 A540, Gr 823 Class 1	1.217*	1.02	54,450	122,893
ICV closure (yield)	3/4-10 x 2.0 A540, Gr 823 Class 1	1.217*	1.02	49,500	111,721
OCV closure (ultimate)	1X-7 x 6 A320, L43	2.1098†	1.52	119,050	240,517
OCV closure (yield)	1X-7 x 6 A320, L43	2.1098†	1.52	100,002	202,034

*Hole internal thread

†Bolt external thread

‡Based on 0.806 in diameter and 160,000 psi minimum ultimate strength for the bolt.

The 1/4-20 UNC bolts that attach the ICV and OCV base plates together and the 3/4-10 UNC bolts that attach the payload to the ICV base are not required to survive a HAC drop. Because the bolt is seen to be the limiting component in all bolted joints, no further reference is made to engaged thread capacity in the Safety Analysis Report for Packaging (SARP).

To ensure full seating between the ICV and OCV closure bolts and threads, a one-time torque value which is in excess of the value specified for normal use will be applied to the bolted joint during the manufacturing process. This will reduce the possibility of closure bolt torque loss in HAC drop and puncture events. For the ICV, this value is 300 ft-lb, and for the OCV, 1,500 ft-lb. The formula governing the relationship between bolt torque and tensile force is introduced in Section 2.6.1.2.1.

2.2 WEIGHTS AND CENTER OF GRAVITY

The weight of the empty package is 8,850 pounds. The maximum weight of the payload, including the shipping rack assembly, is 750 pounds, which includes a margin for possible future increases in payload weight. The component breakdown is given in Table 2.2-1. The reference for center of gravity is the bottom surface of the impact limiter.

TABLE 2.2-1. RTG Transportation System Package Component Weights.

Component	Weight (lb)	CG (in.)
Inner containment vessel bell	1,550	40.8
Inner containment vessel base	1,100	12.1
Outer containment vessel bell (with cooling water)	2,700	37.8
Outer containment vessel base	1,850	10.9
Impact limiter	1,650	7.8
Maximum payload and shipping rack	750	40.0
Maximum payload	525	49.0
Maximum shipping rack	225	19.0

The total weight and center of gravity location used for calculations is 9,600 pounds and 25.2 in. above the bottom surface of the impact limiter. The radial center of gravity is on the package centerline, because of symmetry.

2.3 MECHANICAL PROPERTIES OF MATERIALS

The structural materials used in the package are as follows:

- AISI Type 304L austenitic stainless steel (OCV, ICV containment boundaries)
- AISI Type 304 austenitic stainless steel (impact limiter shell, payload shipping rack assembly)
- ASTM-A320, Grade L43, bolts (heat treated alloy steel, cadmium plated)
- ASTM-A540, Grade B23, Class 1 bolts (heat-treated alloy steel), cadmium plated (ICV bolts)
- ASTM-B16 brass (vent and test port plugs)
- D. G. O'Brien electrical feed-through receptacle, 107 Series, part No. 1070018-112 (ICV and OCV electrical feed-through)
- ASTM A479 Type 316L electrical feed-through sleeve
- AISI 4130 hardened thread insert (OCV and ICV), cadmium plated
- ASTM B837, Alloy N07750 Type 3 impact limiter attachment bolts

- AMS7245 stainless steel *Heli-coil*^{®**} threaded inserts (for impact limiter attachment bolts).

Other nonstructural materials used are as follows:

- 3 lb/ft³ and 12 lb/ft³ polyurethane foam (General Plastics 3700 series)
- Fiberglass insulation in the thermal shield
- Ceramic fiber insulation in the shipping rack assemblies
- Du Pont Vespel^{®***} (OCV ball alignment pads)
- Butyl O-rings for ICV and OCV containment seals
- Teflon[®] gaskets (OCV vent and test port plug covers)
- Austenitic stainless steel (coolant jacket pressure relief valves)
- Nitronic 50 or 60 alignment pins (nitrided austenitic stainless steel)
- ABS plastic (impact limiter pressure relief plugs)
- Miscellaneous steel fasteners.

Nonstructural materials associated with the instrumentation feed-through are as follows (see Figure 2.3-1):

- Plug, D. G. O'Brien 107 Series, part No. 1071063-118
- Connector, Deutsch part No. DB050-14-18PX-069
- Polythamide resin, G. E. Plastics Ultem-1000[®]
- Electrical cable, Belden part No. 85164, including Du Pont Tefzel^{®****} insulation
- Conductor wire, MIL-W-22759/32, Alpha Wire Corporation
- Rubber gasket, ASTM D2000-75E-Type 5C
- Contact pins, ASTM B301, nickel and gold plated
- Contact probe and spring, Interconnect Devices part Nos. R5CR and S6H18.70
- Electrical feed-through cable, flexible standard nickel-coated copper conductor with en

^{**}*Heli-coil* is a registered trademark of Emhart Fastening Technologies.

^{***}*Vespel* is a registered trademark of the E.I. duPont de Nemours Company.

^{****}*Tefzel* is a registered trademark of the E.I. duPont de Nemours Company.

Inorganic insulation of mica and glass fiber.

The Packaging General Arrangement Drawings presented in Appendix 4.3.2 identify these materials and their uses. The schematic shown in Figure 2.3-1 identifies the locations of the electrical feed-through components.

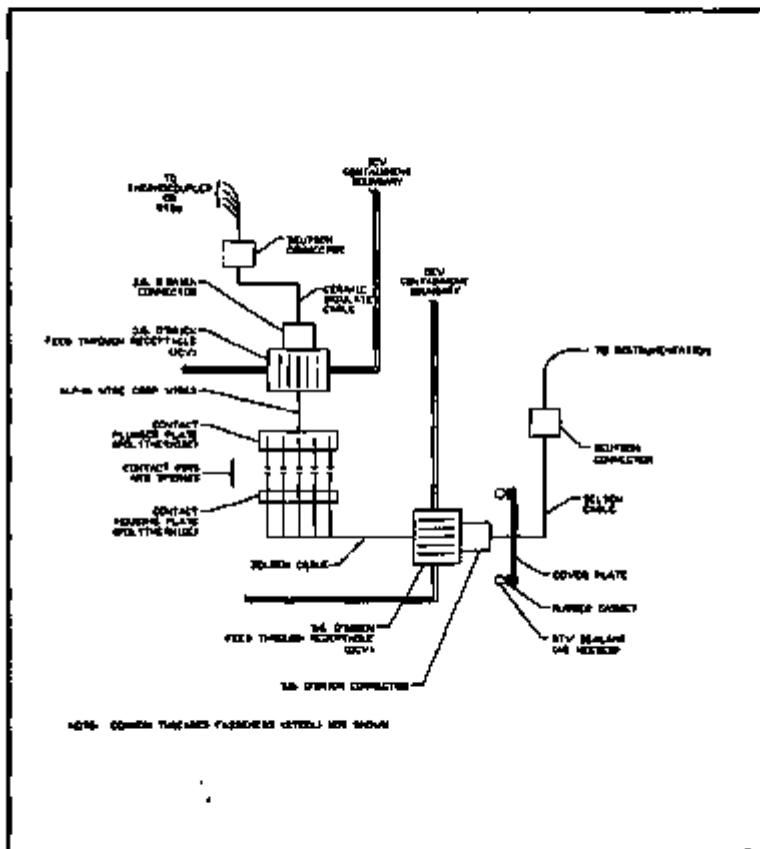


FIGURE 2.3-1. Electrical Feed-through Materials Schematic.

The following tables present the properties of the structural materials used in the package.

The following tables present the properties of the structural materials used in the package. Material properties are linearly interpolated or extrapolated from these values as necessary. For the analysis of the impact limiter shell (in Section 2.6.2, material properties for Type 304L are conservatively used in place of properties of Type 304 stainless steel. No properties are given for the materials used for the brass vent and test port plugs or for the electrical feed-through assemblies, since these components are not structurally analyzed. They see only negligible loads, even in the HAC drop and puncture events.

TABLE 2.3-1. Mechanical Properties of AISI Type 304L Stainless Steel.

Steel material specification	Temperature (°F)	Yield strength S_y (ksi)	Ultimate strength S_u (ksi)	Allowable strength S_w (ksi)	Elastic modulus 110^3 psi	Coefficient of thermal expansion (10^{-6} in/in/°F)
AISI Type 304L ASTM A240 ASTM A479 ASTM A269 ASTM A312 ASTM A276	70	--	--	--	28.3	6.48
	100	25.0	70.0	16.7	--	6.65
	200	21.3	66.2	16.7	27.6	6.79
	300	19.1	60.9	16.7	27.0	6.90
	400	17.5	58.5	15.8	26.5	6.19
	500	16.3	57.8	14.8	26.8	6.37
	600	15.5	57.0	14.0	25.3	6.53
	700	14.8	56.2	13.5	24.6	6.69
	800	14.4	55.5	13.0	24.1	6.82
	900	13.8	53.8	--	23.5	--
	1000	13.3	50.8	--	--	10.3
	1100	12.5	46.8	--	22.1	--
	1200	--	--	--	--	10.4
1300	10.1	31.4	--	20.5	--	

*Properties for temperatures through 1000 °F are taken from the ASME B&PV Code, Section II, Part D, Table Y-1; for higher temperatures, values from Ref. 26 are used, reduced by 2,500 psi to provide a smooth transition from the ASME data for lower temperatures.

*Properties for temperatures through 1000 °F are taken from the ASME B&PV Code, Section II, Part D, Table U; for higher temperature, values from Ref. 24 are used.

*Properties for temperatures through 800 °F are taken from the ASME B&PV Code, Section II, Part D, Table 2A.

*Properties for temperatures through 800 °F are taken from the ASME B&PV Code, Section II, Part D, Table TM-1, Material Group G; for higher temperatures, values from Ref. 26 are used.

*Properties for temperatures through 800 °F are taken from the ASME B&PV Code, Section II, Part D, Table TE-1; for higher temperatures, values from Ref. 25 are used. The value shown is mean from 70 °F.

Notes: (1) Values given for S_y , S_u , and S_w at 100 °F apply from -20 to 100 °F.

(2) Stainless Steel Density is 0.29 lb/in³.

(3) Poisson's Ratio is 0.3.

(4) ASTM A351 CF3 casting material may be used for the containment boundaries as an alternate material because minimum ultimate, yield, and allowable strengths equal or slightly exceed the tabulated values.

TABLE 2 3-2 Mechanical Properties of ASTM A320, Grade L43, Bolting Material

Bolting material specification	Temperature (°F)	Yield ^a strength S _y (ksi)	Ultimate ^b strength S _u (ksi)	Allowable ^c strength S _a (ksi)	Elastic ^d modulus (10 ⁶ psi)	Coefficient ^e of thermal expansion (10 ⁻⁶ in/in/°F)
ASTM-A320 Grade L43	70	--	--	--	27.8	6.20
	100	105.0	125.0	35.0	--	6.27
	200	99.0	--	33.0	27.1	6.54
	300	95.7	--	31.9	26.7	6.78
	400	91.8	--	30.6	26.1	6.98
	500	86.5	--	29.5	25.7	7.16

^aASME B&PV Code, Section II, Part D, Table Y-1^bASME B&PV Code, Section II, Part D, Table Y-1^cASME B&PV Code, Section II, Part D, Table 4^dASME B&PV Code, Section II, Part D, Table TM 1, Material Group B^eASME B&PV Code, Section II, Part D, Table TE 1, Material Group E The value shown is mean from 70 °F

TABLE 2 3-3 Mechanical Properties of ASTM-A540, Grade B23, Class 1, Bolting Material

Bolting material specification	Temperature (°F)	Yield ^a strength S _y (ksi)	Ultimate ^b strength S _u (ksi)	Allowable ^c strength S _a (ksi)	Elastic ^d modulus (10 ⁶ psi)	Coefficient ^e of thermal expansion (10 ⁻⁶ in/in/°F)
ASTM-A540 Grade B23 Class 1	70	--	--	--	27.8	6.20
	100	150.0	185.0	50.0	--	6.27
	200	140.1	--	47.8	27.1	6.54
	300	136.3	--	46.2	26.7	6.78
	400	131.7	--	44.8	26.1	6.98
	500	127.7	--	43.4	25.7	7.16

^aASME B&PV Code, Section II, Part D, Table Y-1^bASME B&PV Code, Section II, Part D, Table Y-1^cASME B&PV Code, Section II, Part D, Table 4^dASME B&PV Code, Section II, Part D, Table TM-1, Material Group B^eASME B&PV Code, Section II, Part D, Table TE-1, Material Group E The value shown is mean from 70 °F

The energy-absorbing foam used in the removable impact limiter is a closed cell polyurethane foam. The nominal densities used are 3 lb/ft³ for foam located directly beneath the OCV base plate, and 12 lb/ft³ in the remainder of the impact limiter. This type of material has been used extensively and successfully in transportation packages for a number of years. Examples are Nuclear Packaging's 125 B-1 (NRC Docket 71-9200), 10 142-1 (NRC Docket 71-9208), PAS-1TM (NRC Docket 71-9184), TRUPACT-1TM (NRC Docket 71-8218), as well as Chem Nuclear System's 1-13C 11TM (NRC Docket 71-9152).

The polyurethane foam's energy-absorbing characteristics have been amply demonstrated via comprehensive testing programs. Compression testing over a wide range of densities (3 to 25 lb/ft³) and temperatures (-20 to 300 °F) has been performed. Additionally, the intrinsic properties have been verified by fire testing of appropriately encapsulated foam samples^{*****} (General Plastics Last-A-Foam^{*****}).

Detailed stress-strain relationships for the polyurethane foam are not required for analysis, because analytic assessments are not performed for the NCT and HAC free drop or HAC puncture events. However, because package performance is demonstrated by testing, and performance is a function of foam properties, stress-strain characteristics and installation techniques for the foam are carefully controlled. Foam installation consists of the following two steps:

1. The 3 lb/ft³ nominal density foam is pre-cast as a solid slab and is then placed into the impact limiter.
2. The 12 lb/ft³ nominal density foam is poured into the impact limiter as a liquid, which then solidifies to fill all voids in the impact limiter not already filled by the 3 lb/ft³ foam.

The polyurethane foam stress-strain relationships are carefully controlled, regardless of whether the foam is pre-fabricated or poured in situ. For both foams, the direction of rise on curing is controlled to be parallel to the axis of the package. At the time the foam is originally poured, samples are retained and tested to certify foam compressive strength, and stress-strain plots are developed from the test results.

Table 2.3-4 provides the strength data used to judge acceptance of the tested foam samples. Nominally expected compressive strengths for the 3 and 12 lb/ft³ foams in both parallel and perpendicular to rise directions are presented. The 3 lb/ft³ foam plays only a minor role in packaging response, and its acceptance is controlled based on room temperature (72 to 78°F) strengths. Recognizing the more significant role played by the 12 lb/ft³ foam and the strong dependence of polyurethane foam strength on temperature (strength significantly increases with decreasing temperature), acceptance of 12 lb/ft³ foam is based on strength at worst case temperature extremes. Thus, retained sample testing for 12 lb/ft³ foam is performed at both cold (-20 to -25 °F) and hot (160 to 165 °F) conditions.

To be acceptable, measured strength for individual samples of 3 lb/ft³ foam must fall within 15% of the nominal strengths in Table 2.3-4. When averaged, the strength for all samples of 3 lb/ft³ foam must fall within 10% of tabulated nominals. For the 12 lb/ft³ foam, acceptance at cold temperatures is based on measured strengths for individual samples being no more than 15% greater than tabulated nominals. The average cold strength for all samples of 12 lb/ft³ foam must be no more than 10% above nominals. At hot conditions, measured strengths for individual samples of 12 lb/ft³ foam must be at least 85% of tabulated nominals. The average hot strength for all 12 lb/ft³ samples must be at least 80% of nominals.

*****Last-A-Foam is a registered trademark of the General Plastics Company.

TABLE 2.3-4 Nominal Compressive Strengths of Polyurethane Foam

Direction of rise	Parallel			Perpendicular			
	Nominal foam density	3 lb/ft ³	12 lb/ft ³	3 lb/ft ³	12 lb/ft ³		
Test Temperature	72 to 78 °F	-20 to -25 °F	160 to 165 °F	72 to 78 °F	-20 to -25 °F	160 to 165 °F	
Strain	10 %	59	635	327	54	606	331
	40 %	62	803	425	51	785	427
	70 %	97	2,577	1,171	88	2,894	1,260

Figure 2.3-2 graphically presents a comparison of the foam strength used in the Structural Certification Test Article impact limiter (15-1/2 lb/ft³, perpendicular to rise, 75 °F foam) with the acceptance controls placed on corresponding production limiter foam (12 lb/ft³, perpendicular to rise, -20 and 160 °F foam). The strength of the foam used in the structures testing was at or above that which would exist in a production unit limiter in cold conditions. Thus, impact accelerations experienced during structural testing clearly envelope those that could ever occur for a production unit. The other temperature extrema is handled by extrapolation and is detailed in Section 2.7.3.1.1. For hot conditions, foam strength is assumed to be the average hot strength shown in Figure 2.3-2.

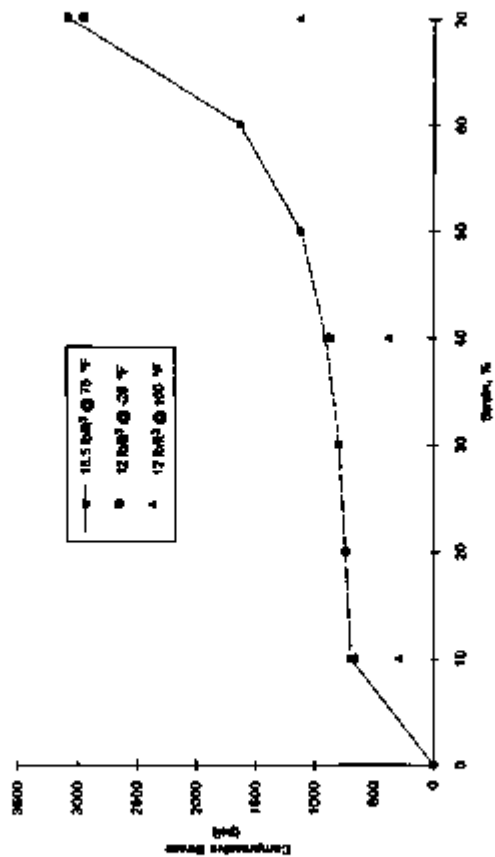


FIGURE 2.3-2. Comparison of Average Foam Strength Properties.

2.4 GENERAL STANDARDS FOR ALL PACKAGES

This section demonstrates that the general standards for all packages are met:

2.4.1 Minimum Package Size

The minimum dimension of the package is 39.4 in. over the GCV coolant jacket outer diameter. Thus, the requirement of 10 CFR 71.43(a) is satisfied.

2.4.2 Tamper-Indicating Feature

A tamper-indicating device is included in the form of a lockwire across one impact limiter attachment bolt tube. Breakage or detachment of this wire will provide evidence of possible unauthorized access to the package because all impact limiter attachment bolts must be removed to gain access to either the GCV cavity or vent port plug.

2.4.3 Positive Closure

The package cannot be opened unintentionally. The GCV ball is attached by 24, 1 1/4-in. closure bolts, and the ICV by 24, 3/4-in. closure bolts. Complete removal of all bolts from a given vessel is necessary before a ball may be removed. Notably, removal of all eight 1.0-in. impact limiter attachment bolts is also required before removal of the GCV ball.

2.4.4 Chemical and Galvanic Reactions

The materials of construction used in the packaging will not have significant reactions with the payload, air, or water. Essentially all of these materials have been used previously in radioactive material packaging without incident.

The payloads are thermoelectric generators using radioisotope fuel in oxide form. These devices are designed to perform many years in space or in terrestrial missions, and contain no liquids and only inert gas. The materials of construction are common structural materials. Thus, no corrosive agents exist in the payloads. Further, these payloads present no source of volatiles that could affect the butyl rubber O-ring containment seals. Therefore, no reaction between the payload and any part of the packaging will occur.

Both packaging containment boundaries are constructed exclusively of AISI Type 304L stainless steel, which is highly corrosion resistant to most environments. The weld material and processes have been selected per the ASME B&PV Code to provide as good or better material properties as the base material, including corrosion resistance. The base material and weld material have about the same electrochemical potential, minimizing any galvanic corrosion that could occur. The material is also not subject to corrosion from the glycol/water coolant mixture used in the GCV coolant jacket. Noncontainment structures such as the shipping rack assemblies and the impact limiter shell are made from AISI Type 304 stainless steels.

The polyurethane foam that is used in the impact limiter has the same chemical makeup relative to corrosion as that which has been successfully used in a number of transportation packages, such as the NuPac 125-B²³ and the CNSI 1-13C II²⁴. These and other packagings using this foam have had a long and successful record of performance, demonstrating that the foam does

not cause any adverse conditions on the packaging. The polyurethane foam is a closed cell foam that is low in free halogens. The foam material is sealed with plastic pipe caps inside a dry cavity in the impact limiter. For these reasons, no significant corrosion will occur because of the polyurethane foam.

Brass fittings used in the packaging are corrosion resistant. Brass material is slightly anodic to the stainless steel. Any damage that could occur to the brass is easily detectable because the fittings are all removed and handled each time the packaging is loaded or unloaded.

All threaded fasteners used in the packaging are made from cadmium-plated alloy steel except the impact limiter attachment bolts, which are made of Inconel. The compatibility of cadmium, Inconel and austenitic stainless steels in transport of nuclear materials has been clearly established in previous designs, such as the NuPac 125-B Cask.

Aluminum is used only for the payload and is not a material of packaging construction. Aluminum is only present within the ICV in an atmosphere of dry helium, thus, no possibility of corrosion involving aluminum exists.

2.5 LIFTING AND TIEDOWN STANDARDS FOR ALL PACKAGES

2.5.1 Lifting Devices

The following two types of lifting devices are used on the RTG Transportation System Package:

1. A standard lifting eye, bolted to the top of the ICV, for lifting the ICV bell only. The lifting eye is removed during transport.
2. Three fins provided with holes, on the top of the OCV, for lifting either the OCV bell or the entire licensed package, including the payload. Nonlicensed hardware, such as support struts, will not be lifted with the package.

2.5.1.1 Inner Containment Vessel Bell Lifting

2.5.1.1.1 Lifting Forces. The weight of the ICV bell is 1,550 pounds, but for conservatism, a value of 1,800 pounds will be used in the analysis. The ICV bell lift point is labeled "Lift Lift Only," to preclude lifting anything but the bell.

2.5.1.1.2 Stress Calculations. To determine the lifting adequacy of the ICV bell, four modes of failure will be examined: (1) Torispherical Head Material Yield, (2) Lift Block Weld Shear, (3) Lifting Eye Thread Strip-out, and (4) Lifting Eye Failure.

To ensure that any possible lifting overload does not damage the containment boundary (per 10 CFR 71.45(a)), the design is such that the minimum margin of safety occurs for the lifting eye mounting hole thread strip-out. That is, if the lifting system is overloaded, the lifting eye mounting hole threads will fail before any other component of the package fails. The lifting eye itself will fail before the mounting hole threads, but it is not a part of the licensed package to which this requirement applies.

The temperature of the ICV head, which is applicable to all of the failure modes above, is 338 °F from Appendix 2.10.7, Table 2.10.7.1-2 (thermal node 200). However, a value of 350 °F

will be conservatively used. From Table 2.3-1, $S_y = 18,300$ psi and $S_u = 59,700$ psi.

(1) Torispherical Head Material Yield

To determine the stresses in the ICV head, a simple finite element model was used. The model is a two dimensional (2-D) representation of the entire ICV, including base, and is described in Appendix 2.10.2. For the present application, the base elements were excluded, and the lower flange of the bell was restrained. The lifting load of 1,600 pounds was applied upward at the center of the top of the ICV bell. The maximum resultant stress intensity (including bending) was 1,906 psi at the junction between the shell and lifting block, element 153. The margin of safety given below.

$$M.S. = \frac{18,300}{3(1,906)} - 1 = +2.20$$

To determine the applied load at which the head fails, assume a failure defined as the primary local membrane stress intensity P_1 (without bending) exceeding the ultimate strength in tension. For the given loading of 1,600 pounds, the maximum primary local membrane stress intensity is 709 psi, likewise in element 153. The ratio is given below.

$$\frac{\text{Failure Load}}{59,700 \text{ psi}} = \frac{1,600 \text{ lb}}{709 \text{ psi}} \Rightarrow \text{Failure Load} = 134,725 \text{ lb}$$

(2) Lift Block Weld Shear

The ICV lift block has an outside diameter of 6 in., the ICV wall is 0.375 in. thick, and the weld is full penetration. The shear area is $(6.0)(0.375)\pi = 7.07 \text{ in.}^2$. Assuming full weld properties, the weld shear strengths are as follows:

$$\begin{aligned} \text{Shear yield} &= (0.6)(18,300) = 10,980 \text{ psi} \\ \text{Shear ultimate} &= (0.6)(59,700) = 35,820 \text{ psi} \end{aligned}$$

The shear stress in the weld is:

$$\frac{1,600}{7.07} = 226 \text{ psi}$$

The margin of safety is:

$$M.S. = \frac{10,980}{3(226)} - 1 = +Large$$

The failure load is the ultimate shear strength times the area, or $(7.07)(35,820) = 253,247$ pounds

(3) Lifting Eye Thread Strip out

The lifting eye will use a 3/4-10UNC-2A thread, with a 1-in. engagement. From the article *Strength of Threads* by Raymond Boucher, the corresponding bolt hole will have a shear area of 1.7225 in² per in. of engagement. The shear stress in the threads will be

$$\frac{1,600}{1.7225} = 929 \text{ psi}$$

the margin of safety, using the same shear yield of 10,980 psi is

$$M.S. = \frac{10,980}{3(929)} - 1 = +2.84$$

The failure load, using the shear ultimate strength, is $(35,820)(1.7225) = 61,700$ pounds

(4) Lifting Eye Failure

Although it is not a part of the licensed package, the ICV lifting eye will be treated here because of importance in lifting. The ICV lifting eye will be a swivel eye from American Drill Bushing Co., part No. 23102, with a catalog rating of 7,000 pounds. A factor of safety of five is included in this rating, so that the ultimate failure load will be at least

$$(5)(7,000) = 35,000 \text{ lb}$$

The margin of safety on ultimate is (using a load multiplication factor of five instead of three)

$$M.S. = \frac{35,000}{5(11,600)} - 1 = +3.38$$

Thus, each mode of failure has a minimum safety factor in excess of three on yield (or five on ultimate in the case of the ICV lifting eye), and the first element of the licensed package to fail in the event of an overload is the screw thread of the ICV lifting block. The ICV lifting eye itself, however, will fail first before the failure of any packaging component, as shown in the table below.

TABLE 2.6.1.1.2-1. ICV Bell Lifting Failure Mode Hierarchy.

Failure mode	Ultimate failure load (lb)
Eyebolt breakage	35,000
Thread strip-out	81,700
Head failure	134,725
Weld shear	253,247

2.5.1.2 Outer Containment Vessel Lifting

2.5.1.2.1 Lifting Forces. The OCV lifting devices must lift the entire package, including the payload, ICV, OCV, and impact limiter. These components weigh a maximum of 9,600 pounds. Three evenly spaced fins are provided with 0.88-in. diameter holes for attachment of lifting hardware. The area surrounding the lifting hole is reinforced on both sides with 0.39-in.-thick plates. The fins are 0.25-in. thick and are fastened using 3/16-in. fillet welds along both sides to a 0.75-in.-wide, 0.50-in. thick doubler plate, which is in turn fastened using 3/8-in. fillet welds to the OCV head, in a region that spans the knuckle area. The doubler plate protects the OCV head (containment boundary) in the event of a lifting overload, as described in Section 2.5.1.2.2. A lifting cable angle to the horizontal of at least 60° is operationally imposed. The maximum load per cable is:

$$F_{max} = \frac{9,600}{3(\sin 60^\circ)} = 3,696 \text{ lb}$$

A value of 3,600 pounds will be conservatively used in all calculations.

2.5.1.2.2 Stress Calculations. The lifting of the OCV will consider three failure modes: (1) Torispherical Head Material Yield, (2) Lift Hole Bearing Yield, and (3) Fin Weld Shear Yield.

To ensure that any possible lifting overload does not damage the containment boundary (per 10 CFR 71.45(a)), the design is such that the minimum margin of safety occurs for the failure of the fin-to-doubler weld. That is, if the lifting system is overloaded, the stronger doubler-to-OCV head weld will remain undamaged, and the weaker fin-to-doubler weld will fail, thus protecting the containment boundary.

From Appendix 2.10.7, Table 2.10.7.1-2, the temperature of the OCV head (no active cooling) in the region of the fin weld (thermal node 304) is 237 °F. A value of 250 °F will be conservatively used. For this temperature, from Table 2.3-1 the yield strength S_y is 20,200 psi, and the ultimate strength S_u is 63,550 psi. The corresponding shear strengths are:

$$\begin{aligned} \text{Shear yield} &= (0.6)(20,200) = 12,120 \text{ psi} \\ \text{Shear ultimate} &= (0.8)(63,550) = 38,130 \text{ psi} \end{aligned}$$

From Appendix 2.10.7, Table 2.10.7.1-2, the temperature of the fin near the lifting hole (thermal node 305) is 158 °F. A value of 175 °F will be conservatively used. For this

temperature, from Table 2.3-3 the yield strength S_y is 22,225 psi and the ultimate strength S_u is 67,150 psi.

(1) Torispherical Head Material Yield

The stresses in the OCY torispherical head due to lifting with the lift fins were examined using a finite element model. The model is described in Appendix 2.10.3. Because three lift fins are used, a 1/3 symmetry portion of the OCY bell was modeled, with the lift fin located in the center of the segment. To simplify the model, the doubler plate was not included. Instead, the fin was modeled as directly attached to the OCY head. The action of the doubler plate is to distribute fin lifting loads over a slightly larger area of the OCY head, and thus, to omit the doubler conservatively increased OCY head stress. A lifting cable unit force of 1 pound was applied to the fin at an angle of 80° to the horizontal in the plane of the fin. The resulting maximum stress intensity (including bending) is 1.472 psi per pound of load, or for the maximum lifting cable load of 3,800 pounds, the maximum stress is $(1.472)(3,800) = 6,994$ psi. For a yield strength of 20,200 psi, the margin of safety is:

$$M.S. = \frac{20,200}{6,994} - 1 = +0.12$$

To determine the applied load at which the head fails, assume a failure defined as the primary local membrane stress intensity S_p (without bending) exceeding the ultimate strength in tension. From the model, the maximum primary local membrane stress is 0.434 psi per pound of load, or 1,649 psi for the 3,800-pound maximum cable load. Therefore, the ratio:

$$\frac{\text{Failure Load}}{63,650 \text{ psi}} = \frac{3,800 \text{ lb}}{1,649 \text{ psi}} \rightarrow \text{Failure Load} = 148,448 \text{ lb}$$

(2) Lift Hole Bearing Yield

The lifting cable will be attached to the lift fins by means of a shackle (or equivalent) that passes through a 0.86-in. diameter hole in each lift fin. The pin that passes through the hole will be at least 0.75 in. in diameter. Because of the 0.38-in.-thick reinforcements on each side of the 0.26-in.-thick fin, the length of the hole will be 1 in. The bearing area is found from the product of pin diameter and hole length, and for the maximum lifting cable load of 3,800 pounds, the bearing stress is:

$$\frac{3,800}{10.75(1.0)} = 5,087 \text{ psi}$$

A conservative approach is to assume the bearing yield is identical to the tensile yield. The yield strength at the temperature of the fin is 22,225 psi, and the margin of safety is:

$$M.S. = \frac{22,225}{3(5,067)} - 1 = -0.48$$

The failure load for the hole bearing mode of failure can be found from the ratio:

$$\frac{\text{Failure Load}}{87,150 \text{ psi}} = \frac{3,800 \text{ lb}}{5,067 \text{ psi}} \rightarrow \text{Failure Load} = 50,358 \text{ lb}$$

(3) Fin Weld Shear

The fin weld is a 0.188-in. fillet weld on both sides of the fin along the line of contact with the OCY head. Because the fin is loaded in its own plane, the weld is loaded by direct shear and a torsion around its centroid. To determine the area properties of the weld, it was modeled using a finite element analysis program using 24 elements, from which the centroidal position of each element and the element length was obtained. These values were then used to calculate the area, centroid, polar moment of inertia, and other properties necessary for the calculation of weld stress as shown below. These property calculations are treated in Appendix 2.10.4. Table 2.5.1.2.2-1 summarizes the relevant properties and dimensions, with reference to Figure 2.5.1.2.2-1:

TABLE 2.5.1.2.2-1. Fin Weld Physical Properties on Each Side of the Fin.

Property or Dimension	Value	Unit
Weld length	9.48	in.
x-centroid	3.83	in.
y-centroid	4.26	in.
J, Polar Moment of Inertia	84.59	in. ⁴ per in. of weld width
c (upper)	4.54	in.
c (lower)	4.76	in.
θ (upper)	67.63	degrees
θ (lower)	26.32	degrees
Perpendicular distance	1.83	in.

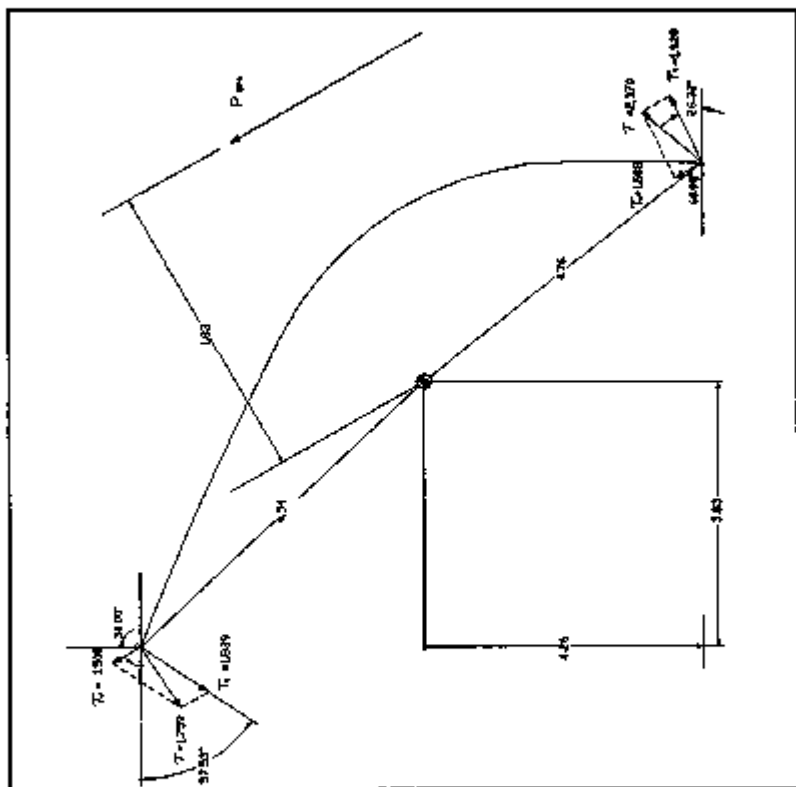


FIGURE 2.3.1.2.2-1. Magnitude and Direction of Stresses for Both Ends of the Fin Weld.

Because the shear area of a fillet weld is 0.707 times the weld leg dimension, the actual area and moment of inertia are as follows:

$$A = (9.48)(2)(0.188)(0.707) = 2.52 \text{ in}^2$$

$$J = (64.59)(2)(0.188)(0.707) = 17.17 \text{ in}^4$$

There will be two kinds of shear stress on the weld. One will be a uniform shear because of the cable load directed along the line of action of the cable. The other will be a torsional shear, acting perpendicular to the radius from the centroid. From Table 2.5.1.2.2.1 and Figure 2.5.1.2.2-1 above, the perpendicular distance from the line of action of the cable to the weld centroid is 1.83 in, and the moment, therefore, is

$$T = (3,800)(1.83) = 6,954 \text{ in-lb}$$

where 3,800 pounds is the cable load. The torsional shear stress at the upper end is

$$\tau_t = \frac{Tc}{J} = 1,839 \text{ psi}$$

where

$$\begin{aligned} T &= 6,954 \text{ in-lb} \\ c &= 4.54 \text{ in} \\ J &= 17.17 \text{ in}^4 \end{aligned}$$

At the lower end, the torsional shear stress is 1,928 psi, where 4.78 in is substituted for c in the above equation. The uniform shear stress is

$$\tau_v = \frac{F}{A} = 1,508 \text{ psi}$$

where

$$\begin{aligned} F &= 3,800 \text{ lb} \\ A &= 2.52 \text{ in}^2 \end{aligned}$$

Figure 2.5.1.2.2-1 shows the magnitude and direction of these stresses for both the upper and lower ends of the weld. Combining by vectorial methods, the resultant stress at the top is 1,759 psi, and 2,370 psi at the bottom. Thus, the maximum stress occurs at the bottom. Using a weld shear yield strength of 12,120 psi, the minimum margin of safety is

$$M.S. = \frac{12,120}{3(2,370)} - 1 = +0.70$$

Using a weld shear ultimate strength of 36,130 psi, the cable load at which the weld will fail can be found from the following ratio:

$$\frac{\text{Failure Load}}{38,130 \text{ psi}} = \frac{3,600 \text{ lb}}{2,370 \text{ psi}} \rightarrow \text{Failure Load} = 61,137 \text{ lb}$$

Thus, all failure modes have positive margins of safety using a load factor of three. The hole bearing and fin weld ultimate failure loads are comparable in value and will occur well before the spherpherical head failure, as shown in Table 2.5.1.2.2 below, affording complete protection to the containment boundary.

Table 2.5.1.2.2 OCV Lifting Failure Mode Hierarchy

Failure mode	Ultimate failure load (lb)
Hole bearing	50,354
Fin weld shear	61,137
Head failure	146,446

2.5.2 Tiedown Devices

The RTG transportation system trailer comes up to two packages. Each package will be fastened to a shock and vibration isolated trailer skid. The upper surface of the trailer skid, on which the package (impact limiter) rests, is a platform that is suspended by shock and vibration isolators. A socket is formed on the top of the platform by a ring made from steel bar into which the impact limiter fits, and which serves the purpose of reacting chocking loads. The package is secured to the trailer skid by two flat, 3 in.-wide flexible metal mesh straps, passing over the top of the package at right angles, and attaching to the platform at its diagonal corners. This configuration is shown in Figure 2.5.2-1. Inertial loads are assumed to act through the package center of gravity. The worst case loads will be found from the maximum payload condition, where total weight is 8,600 pounds and center of gravity location is 25.2 in. above the platform.

Because no tiedown devices are a part of the licensed package, the requirements of 10 CFR 71.45 do not apply. However, in the interest of completeness, the interface loads and resulting stresses will be determined. Inertial loads of 10g longitudinal, 5g lateral, and 2g vertically upward will be applied simultaneously. Friction between the package and straps is included in the calculations to show that an assumption of zero for friction is conservative.

2.5.2.1 Tiedown Forces. The geometry of the package strap tiedown is shown in Figures 2.5.2.1-1 and 2.5.2.1-2. The plane of the second figure is parallel to the (longitudinal) direction of motion, thus the straps, which are oriented at 45° to the direction of motion, are represented by their projections onto this plane. As shown in the first figure, the strap makes an angle with the package vertical wall in the plane of the strap. The interface between the straps and the package is modeled by assuming that each strap passes over frictionless pulleys at the top corners, with friction applied at one point in the top center of the package. To find total strap tension, the portion due to each inertial load will be found separately, and finally added.

Let X, Y, and Z represent the 10g, 5g, and 2g inertial forces, respectively. Referring to Figure 2.5.2.1-2, summing moments about point A gives

$$WGL_1 + 2L_2 \sin 45^\circ [-T_s - F + (T_s + F) - (T_s + F) \sin \theta] - 2L_2 (T_s + F) \cos \theta = 0$$

or:

$$T_s = \frac{WGL_1}{2(L_2 \{\sin 45^\circ\} \{\sin \theta\} + L_2 \{\cos \theta\})} - F = 18,991 \text{ lb}$$

where: T_s = strap tension due to the longitudinal load
 W = the weight of the package, 9,800 lb
 θ = the strap angle to the vertical, 24.5°, see Figure 2.5.2.1-1
 F = friction reaction force ($F = 0$ for maximum strap load)
 L_1 = the height of the center of gravity, 26.2 in.
 L_2 = a moment arm, 68.35 in., see Figures 2.5.2.1-1 and 2.5.2.1-2
 L_3 = a moment arm, found from:

$$L_3 = \frac{A_{\text{impact}}}{\text{radius}} + \frac{A_{\text{knuckle}}}{\text{radius}} = 47.97 \text{ in.}$$

where: Radius of impact limiter is 35 in.

Radius to contact of strap on knuckle is 18.35 in., see Figures 2.5.2.1-1 and 2.5.2.1-2.

Because of package symmetry, the same calculation can be used for the lateral direction by substituting the inertia force Y for X , resulting in:

$$T_y = 8,498 \text{ lb}$$

where T_y = strap tension because of the lateral load. Summing forces vertically:

$$WZ = 4T_y \{\cos \theta\}$$

from which $T_y = 5,275$ pounds, where W and θ have the same values as before. It is clear that the strap tension forces are maximized by setting the friction force, F , to zero. If this is done, strap forces completely cancel when summed in the horizontal direction. Therefore, horizontal inertia loads are reacted solely by the ring mounted on the skid by the bottom of the impact limiter. The checking forces are as follows:

$$H_x = 19,600IX = 98,000 \text{ lb}$$

$$H_y = 19,600IY = 48,000 \text{ lb}$$

where: H_x = the longitudinal checking load
 H_y = the lateral checking load

Note also that $H_z = 0$ (no checking force from vertical inertia load). The total strap load is a linear

sum of T_x , T_y , and T_z , or $T_c = 18,991 + 9,496 + 5,275 = 33,762$ pounds. The two checking loads must be combined by vector summation:

$$H_c = \sqrt{(96.000)^2 + (48.000)^2} = 107,331 \text{ lb}$$

For conservatism, the stress calculations on the licensed hardware will be carried out using $T = 35,000$ pounds and $H = 110,000$ pounds.

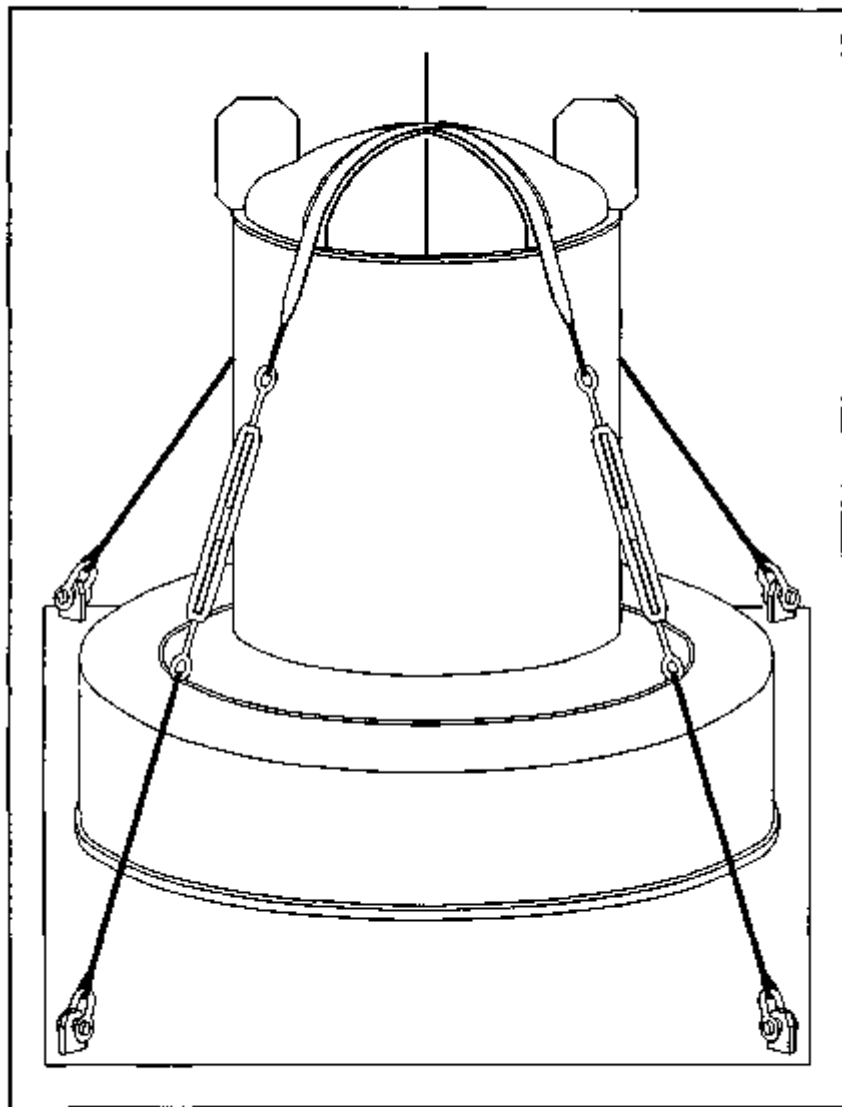


FIGURE 2.5.2-1. Packaging Tiedown General Arrangement.

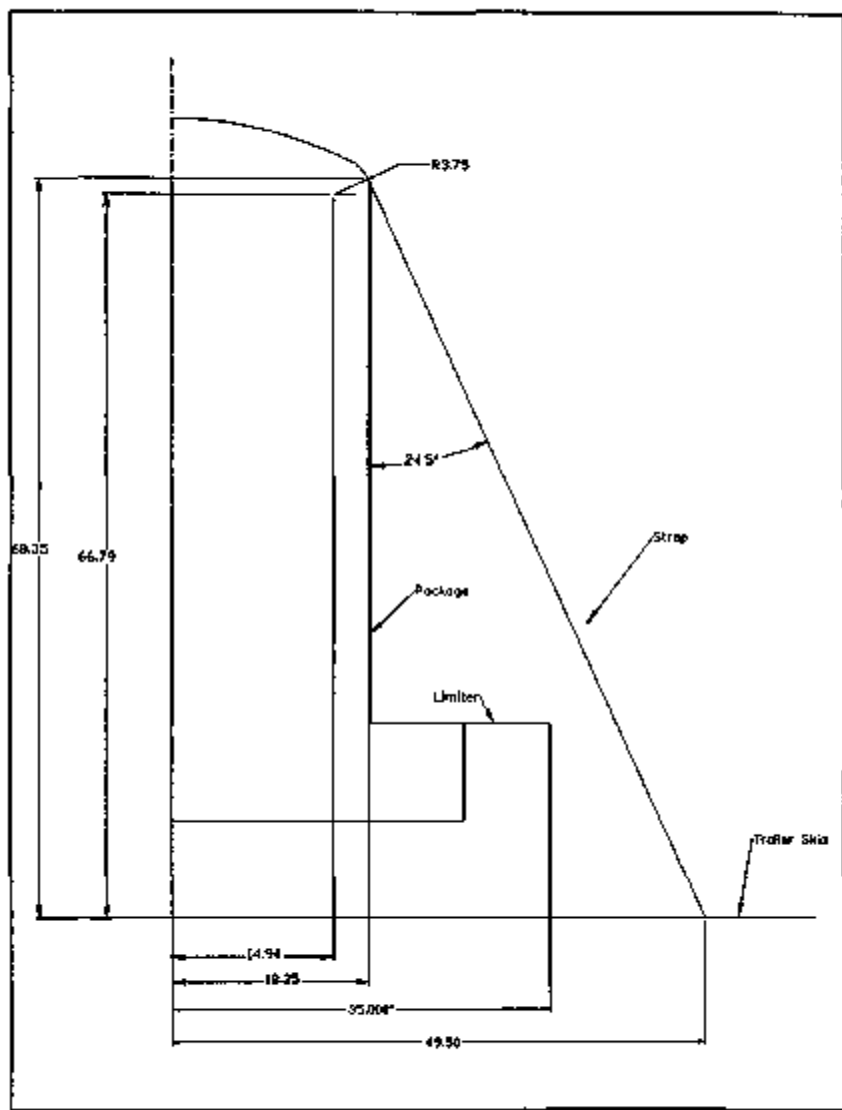


FIGURE 2.5.2.1-1. Package Tiedown Geometric Parameters.

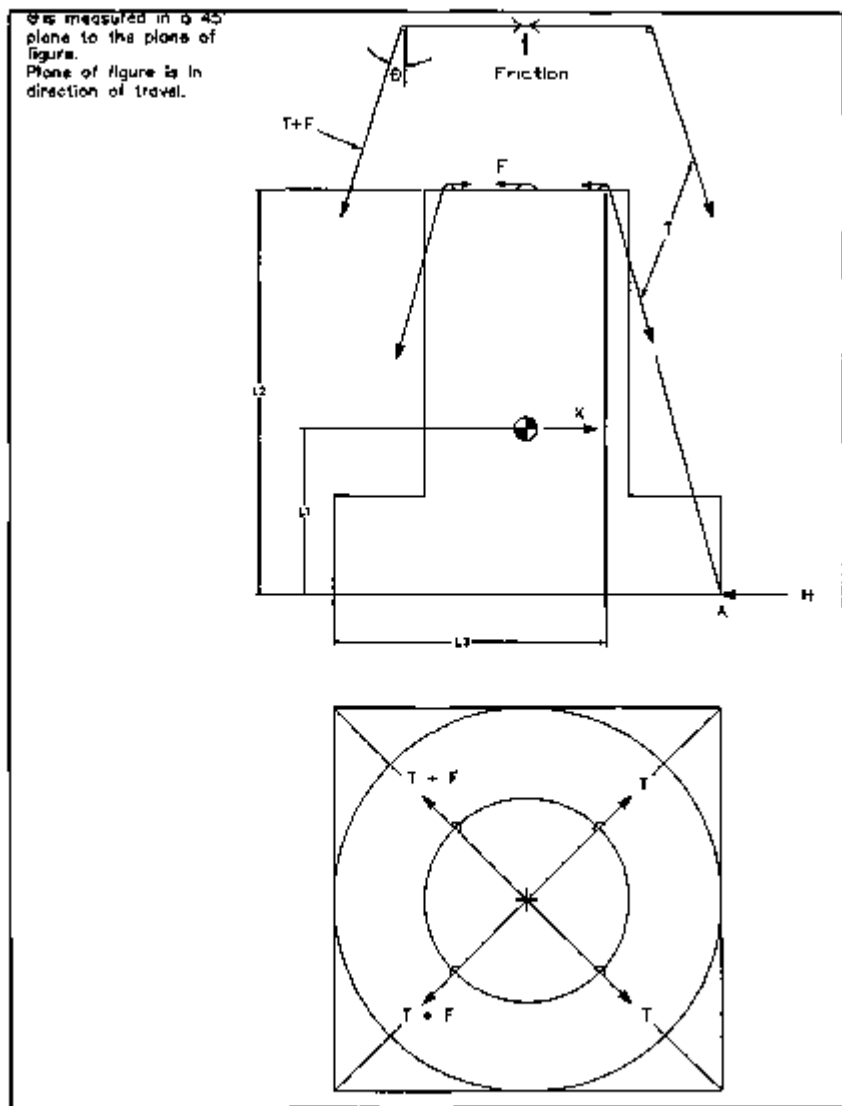


FIGURE 2.5.2.1-2. Package Tiedown Forces.

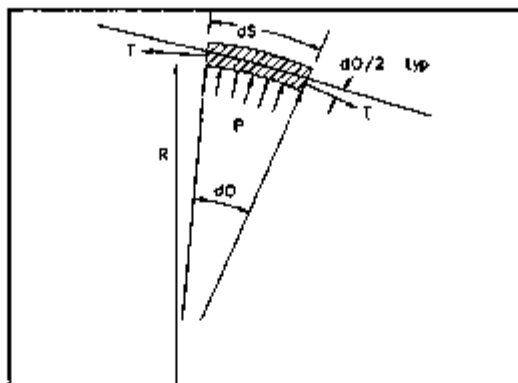


FIGURE 2.5.2.2-1 Tiedown Doubler Differential Segment

2.5.2.2 Stresses in the Package Due to Tiedown Forces: The two tiedown straps are 3-in.-wide flexible metal straps, and pass over the OCV head, crossing in the middle. Because of a tensile load in the straps, they exert a pressure on the torispherical head that results in stresses in the head and sidewall, as determined from the following considerations.

Figure 2.5.2.2-1 depicts a small segment of strap of length dS , subtending the angle $d\theta$, with a constant radius R . There is a uniform tension in the strap, T , which is reacted by a pressure on the concave side, P . For a strap width, w , the sum of forces in the radial direction gives the following:

$$(Pw)dS = 2T \left[\sin \left(\frac{d\theta}{2} \right) \right]$$

Note that $dS = R d\theta$ and for small θ

$$\sin \left(\frac{d\theta}{2} \right) \approx \frac{d\theta}{2}$$

Substituting these values and simplifying

$$P = \frac{T}{wR}$$

Thus, for constant tension and width, the pressure beneath a strap is inversely proportional to the bend radius. The tiedown strap passes over the following two radii:

1. The 0.50 in. thick torispherical head with 0.25 in. thick doubler, having an outside radius of

$$36.26 + 0.26 = 36.50 \text{ in}$$

2. The knuckle and doubler, having a combined outside radius of 3.75 in

The two pressures applied to the package are then (assuming $T = 35,000 \text{ lb}$ and $w = 3.0 \text{ in}$)

$$P_1 = \frac{T}{wR} = 319.6 \text{ psi}$$

where $R = 36.50 \text{ in}$, and

$$P_2 = \frac{T}{wR} = 3.111 \text{ psi}$$

where $R = 3.75 \text{ in}$

A finite element model was constructed of a quarter section of the OCV head, including a portion of the cylindrical side wall, as shown in Figure 2.10.5-1, Appendix 2.10.5. The head thickness was 0.50 in, and a 3 in.-wide doubler plate of 0.25-in. thickness was added to cover the area beneath each strap, starting at the top of the coolant jacket on one side and continuing over to the top of the coolant jacket on the other side. Displacements on the lower edge of the cylindrical sidewall portion were set to zero, and appropriate displacement constraints were used to enforce circumferential symmetry. Details of the model are given in Appendix 2.10.5.

The maximum stress intensity of 19,051 psi occurs in the shell material because of bending, and is located beneath the strap in the knuckle, near the transition to the cylindrical wall. From Appendix 2.10.7, Table 2.10.7.1-2, the temperature of the head in this region (thermal node 304) is 237 °F, but a value of 250 °F will conservatively be used. From Table 2.3-1, the yield strength of AISI Type 304L at this temperature is 20,200 psi. The margin of safety is

$$M.S. = \frac{20,200}{19,051} - 1 = +0.06$$

The stresses in the impact limiter due to bedown forces will be considered under three possible failure modes (referring to Figure 2.5.2.2-2): (1) top plate yield, (2) side wall yield, (3) base plate yield.

For the purposes of this analysis, the impact limiter foam will conservatively be assumed to have negligible properties. The load from the package must be reacted by the 1-in. high bar at the top of the trailer skid that forms a ring around the bottom of the impact limiter. The load path, shown in Figure 2.5.2.2.2, is from the OCV baseplate to the pocket structure into which the OCV fits, then to the impact limiter top plate, through the side walls, into the impact limiter base, and out to the ring. The impact limiter pocket structure, which fits closely around the OCV baseplate, has no appreciable stress. The pocket sidewalls are significantly more flexible than the impact limiter top plate, which will carry the reaction load. Material strength values of Type 304L will be conservatively used in place of the higher Type 304 values.

(1) Impact Limiter Top Plate

An approximation to the stress in the impact limiter top plate may be obtained by considering it as an infinite plate loaded in-plane by the chocking load of 110,000 pounds. In *Theory of Elasticity*¹⁶, Article 42, Equation 75, the following formulations for principal stress are given, for a point directly ahead of the load at the inside radius of a plate loaded in-plane

$$\sigma_r = - \frac{P(3+\mu)}{4\pi r^2}$$

$$\sigma_\theta = \frac{P(1-\mu)}{4\pi r^2}$$

By substituting the quantities

- $\mu = 0.3$ (Poisson's ratio)
- $r = 27.125$ in
- $P = 110,000$ lb
- $t = 0.25$ -in thick

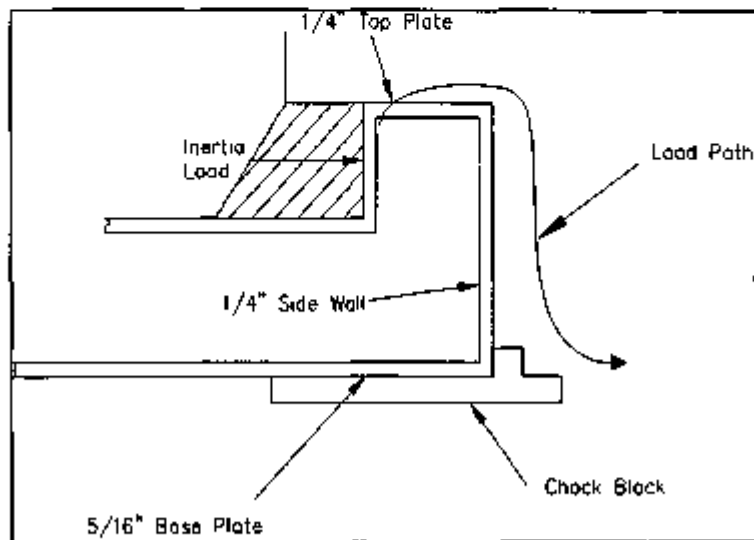


FIGURE 2.5.2.2-2 Tiedown Loading of the Impact Limiter

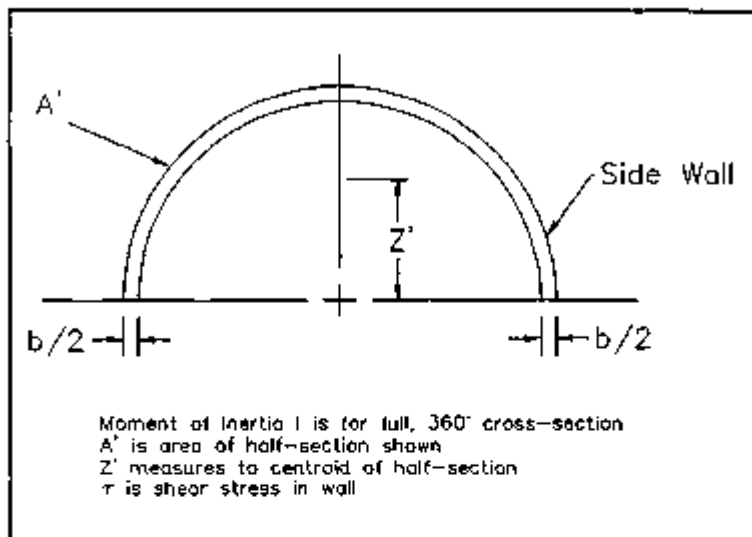


FIGURE 2.5.2.2-3. Impact Limiter Shell Analysis Parameters.

then:

$$\sigma_r = -4,258 \text{ psi} = \sigma_{min}$$

$$\sigma_a = 904 \text{ psi} = \sigma_{max}$$

Stress intensity (SI) equals twice the maximum shear stress, or:

$$SI = 2\tau_{max} = (\sigma_{max} - \sigma_{min}) = 904 - (-4,258) = 5,163 \text{ psi}$$

From Appendix 2.10.7, Table 2.10.7.1-2, the temperature of the top plate (thermal node 408) is 153 °F, but a value of 160 °F will be conservatively used. From Table 2.3-1, the yield strength of AISI Type 304L at this temperature is 22,780 psi. The margin of safety is:

$$M.S. = \frac{22,780}{5,163} - 1 = +3.41$$

12) Impact Limiter Side Wall

The shear stress in the side wall per pound of chocking load will be examined. According to Young²⁰, page 85, Equation 2:

$$\tau = \frac{VA'z'}{Ib}$$

where the dimensional parameters are identified in Figure 2.5.2.2-3.

For the present case, $V = 110,000$ pounds. The outer diameter of the wall is 70 in., and the thickness is 0.25 in. The moment of inertia is:

$$I = \frac{\pi}{64} [(70.0)^4 - (69.5)^4] = 33,315 \text{ in.}^4$$

The parameter b for a hollow section is the sum of two wall thicknesses or the following:

$$b = (2)(0.25) = 0.50$$

The quantity A' is the area of the section on one side of the neutral axis. Therefore:

$$A' = \frac{(0.50)\pi}{4} [(70.0)^2 - (69.5)^2] = 27.39 \text{ in.}^2$$

The quantity z' is the distance from the neutral axis to the centroid of the area A' . Using Table 1, Case 22, of *Roark's Formulas for Stress and Strain* for this case (half of a circular thin ring), $z' = 22.20$ in. Substituting these values into the above formula for shear stress provides the following:

$$\tau_{\text{max}} = \frac{(110,000)(27.39)(22.20)}{(33,315)(0.50)} = 4,015 \text{ psi}$$

Stress intensity is equal to twice the maximum shear or the following:

$$S^I = 2\tau_{\text{max}} = (2)(4,015) = 8,030 \text{ psi}$$

From Appendix 2.10.7, Table 2.10.7.1-2, the temperature of the sidewall (thermal node 406) is 123 °F, but a value of 140 °F will be conservatively used. From Table 2.3-1, the yield strength is 23,520 psi. The margin of safety is:

$$M.S. = \frac{23,520}{8,031} - 1 = +1.93$$

(3) Impact Limiter Base Plate

The impact limiter base plate must bear in plane against the reaction ring on the trailer stud because the plate is 0.31 in. thick and the diameter 70.0 in., the projected area is

$$A = (70)(0.31) = 21.7 \text{ in}^2$$

The compressive stress is

$$\sigma_c = \frac{110,000}{21.7} = 5,069 \text{ psi}$$

A conservative approach is to assume the bearing yield is identical to the tensile yield. From Appendix 2.10.7, Table 2.10.7.1-2, the temperature of the base plate (thermal node 410) is 132 °F, but a value of 140 °F will be conservatively used. From Table 2.3-1, the yield strength is 23,520 psi. The margin of safety is

$$M.S. = \frac{23,520}{8,069} - 1 = +3.64$$

Thus, all margins relating to tie-down loads are positive.

2.6 NORMAL CONDITIONS OF TRANSPORT

When subjected to Normal Conditions of Transport (NCT), as specified in 10 CFR 71.71, the package meets the performance requirements specified in Subpart E of 10 CFR 71, as documented in the following subsections. With the exception of NCT free drop, the primary proof of performance is via analysis. The NRC Regulatory Guide 7.6 criteria is shown to be met for all analytical evaluations presented in this section. The specific issues of brittle fracture, fogging, and shear out of bolted fasteners are analytically addressed in Section 2.1.2.2 and shown not to be limiting for the package. The ability of the butyl O-ring containment seals to remain leaktight at NCT temperature extremes is demonstrated with reference to performance testing, documented in Appendix 2.10.6.

Qualification of the RTG Transportation System Package for the NCT free drop test requirements of 10 CFR 71.71 was accomplished via a comprehensive certification test program. Previously, an engineering development test program using a half-scale prototype model was also undertaken.

Full scale certification testing demonstrated package effectiveness in meeting all NCT free drop requirements. The certification test program showed that no reduction in effectiveness of the package results from any NCT free drop. Further, the NCT free drop certification test sequence demonstrated that the ability of the package to adequately survive a subsequent HAC free drop and

puncture test sequence was not compromised. Certification testing results show that NCT free drop package deformations are insignificant relative to NCT thermal, shielding, and cruciality performance. The NCT free drop testing is discussed in Section 2.8.7.

2.6.1 Heat

The NCT thermal analyses, presented in Section 3.0, provide package component temperatures for several combinations of payload and environment. The principal case examined is the worst case of maximum payload heat load (the GPHS RTG, which generates 4,600 W of thermal power) and insulation, maximum external temperature, and without active cooling. For this principal case, active cooling is not considered, and the coolant jacket is drained of coolant, per 10 CFR 71.51(b). A case involving the maximum heat load and minimum ambient temperature without insulation, and a case where active cooling is present were also examined to establish the entire range of stress states experienced by the package in typical usage. These load cases are summarized in Table 2.6.1-1.

TABLE 2.6.1-1. NCT and Normal Operational Load Combinations.

Condition	Case 1	Case 2	Case 3
Solar	Full solar	No solar	Full solar
Ambient temperature	100 °F	-40 °F	100 °F
Payload	GPHS	GPHS	GPHS
Cooling	No active cooling	No active cooling	Active cooling (both loops)

2.6.1.1 Summary of Temperatures and Pressures. The stress analyses to follow use the temperatures and pressures listed in Appendix 2.10.7 for the cases listed in Table 2.6.1-1. These values result from the thermal analyses described in Section 3.0. The baseline for pressure is the package initial loading configuration, with the chiller providing 40 °F coolant to both loops, 70 °F ambient temperature, and no insulation. For that case, the steady state pressure internal to the ICV is 20 psia; the pressure internal to the ICV/OCV annulus is also 20 psia. These pressures are controlled as described in Sections 8.2.2.2 and 8.2.2.5.

A summary of vessel operational gas temperatures is given in Table 2.6.1.1-1, taken directly from the results given in Section 3.0 and summarized in Appendix 2.10.7, Table 2.10.7.1-5. For purposes of structural analysis, the pressures shown in Table 2.6.1.1-2 have been adjusted from those calculated in Section 3.0 (summarized in Table 2.10.7.1-5) to form a conservatively large net pressure differential for each containment vessel. This is accomplished by rounding applicable internal pressures upward and the external pressures downward. The pressure external to the ICV and internal to the OCV is listed as two different values, even though it must nominally be a single value, because the lower value forms a larger net pressure differential for the ICV, and the higher value forms a larger net pressure differential for the OCV. The ICV internal pressures given in the table have been further adjusted upward to account for other sources of gas pressure described in the next section. The OCV minimum external pressure is 3.5 psia, in anticipation of Section 2.6.3.

For example, Case 1 pressures are determined as follows. From Appendix 2.10.7, Table 2.10.7.1-6, the calculated ICV internal pressure, based on the amount of helium gas placed within the ICV and its temperature, is 24.4 psia. From Section 2.6.1.1.1, the additional pressure is

determined as 5.3 psia, or a sum of 29.7 psia. Then, for conservatism, this value is rounded upward to 30.0 psia, and is listed in Table 2.6.1.1-2. Next, from Appendix 2.10.7, Table 2.10.7.1-5, the calculated OCV internal pressure, based on the amount of helium gas placed within the OCV and its temperature, is 26.3 psia. This value is rounded downward to 20.0 psia to form a conservatively large net differential pressure of 30.0 - 20.0 = 10.0 psid for the ICV, and rounded upward to 30.0 psia to form a conservatively large net differential pressure of 30.0 - 3.6 = 26.6 psid for the OCV. Cases 2 and 3 are handled in a similar manner. For simplicity in the analyses that follow, Case 1 pressure differentials (10 psid for the ICV and 26.6 psid for the OCV) will be used in place of the lower Case 2 and 3 pressure differentials.

TABLE 2.6.1.1-1. Summary of NCT and Normal Operational Internal Gas Temperatures.

Location	Case 1 full solar 100 °F ambient no cooling	Case 2 no solar -40 °F ambient no cooling	Case 3 full solar 100 °F ambient active cooling
ICV Internal Gas Temperature (°F)	354	256	213
OCV Internal Gas Temperature (°F)	285	165	115

TABLE 2.6.1.1-2. Summary of NCT and Normal Operational Internal Gas Pressures.

Location	Case 1 full solar 100 °F ambient no cooling	Case 2 no solar -40 °F ambient no cooling	Case 3 full solar 100 °F ambient active cooling
ICV internal gas pressure (psia)	30	27	26
ICV external gas pressure (psia)	20	19	18
OCV internal gas pressure (psia)	30	24	22
OCV external gas pressure (psia)	3.6	3.6	3.6

2.6.1.1.1 Sources of Pressure. The baseline vessel internal pressures were defined in Section 2.6.1.1. These initial equilibrium pressures will increase or decrease as the gas temperatures change under varying nonoperational (i.e., regulatory) conditions, and such changes are reflected in the pressures listed in Table 2.10.7.1-5. Additionally, there are two potential sources of gas within the ICV which, over time, could possibly cause a slight increase in total pressure: (1) Leakage from the payload initial gas charge and (2) Decay of heat source radionuclides.

The first source, leakage from the payload initial gas charge, could arise because of payload pressure boundary failure, in which case the payload internal gas would escape into the package cavity and increase the ICV pressure. However, as will now be demonstrated, the potential pressure increase is relatively small.

According to Table 1.2.3-2, the amount of gas within the GPHS payload, which could be added to the gas already inside the ICV, is 18 L (0.555 ft³) at STP. Because one lb-mole of any

gas occupies 369 ft³ at STP^{**}, the amount of gas within the GPHS is:

$$n = \frac{0.588}{369} = 1.57(10)^{-4} \text{ lb-mole}$$

The corresponding amount of gas within the generic payload, per Table 1.2.3-1, is 0.0136 lb-mole, which, as the higher value, forms the basis for all further calculations.

The other source of gas that could accumulate over time is the helium resulting from the decay of the radioactive heat source. The maximum helium gas generation rate for all of the radioactive material within the GPHS payload is $2.06(10)^{-4}$ standard cm³/sec. This may be converted to 0.038 ft³ in 60 days. Converting to lb-moles is:

$$n = \frac{0.038}{369} = 1.06(10)^{-4} \text{ lb-mole}$$

This would be added to the gas already in the cavity in 60 days.

The perfect gas law will determine the partial pressure resulting from the two added amounts. To do this requires knowing V, the cavity void volume with the payload installed. Because releasing a given amount of gas into a smaller volume will result in a higher pressure, an underestimation of void volume is conservative. Such an estimate can be formed by ignoring the void volume of the torispherical head and the void volume below the shipping rack assembly, and simply subtracting the basic cylindrical volume of the GPHS RTG payload from the remaining volume of the ICV, taking ICV volume from the top of the shipping rack assembly to the top of the cylindrical section:

$$V = \frac{\pi}{4} [(34.0)^2 (51.5 - 5.25) - (9.7)^2 (47.95)] = 38,448 \text{ in.}^3 = 22.25 \text{ ft}^3$$

where: ICV inner diameter = 34.0 in.
 ICV cylindrical length = 51.5 in.
 GPHS RTG basic diameter = 9.7 in.
 GPHS RTG length = 47.95 in.
 Shipping rack assembly height = 5.25 in.

The pressure differential due to the two additional sources now is:

$$p = \frac{n_1 + n_2 RT}{V} = 6.3 \text{ psia}$$

**Standard conditions are 14.7 psia and 32 °F.

where $n_1 = 0.0135(10^3)$ lb/mole
 $n_2 = 1.08(10^4)$ lb/mole
 $V = 22.25$ ft³
 $R = 10.74$ psia-ft³/lb-mole-°R
 $T = 814$ °R (354 °F, from Table 2.6.1.1-1)

2.6.1.2 Differential Thermal Expansion A radial and axial clearance is maintained between the ICV bell and the OCV bell. The variation of this clearance because of differential thermal expansion will now be examined.

Both the radial and axial thermal expansion of each vessel will be dominated by the temperature of the cylindrical walls, which are thermally modeled in each case by four nodes: 210 to 240 in the ICV, and 310 to 340 in the OCV. As shown in Figure 3.4.1-2, nodes 210/310 are located 6.88 in. below the top of the coolant jacket. The corresponding measurements for the other node pairs are: nodes 220/320, 20.58 in.; nodes 230/330, 34.30 in.; and nodes 240/340, 43.88 in. The radial differential thermal expansion between the two vessels is found by subtracting the radial thermal expansion of the OCV from that of the ICV at each of the four elevations discussed above. The residual radial clearance is found by subtracting this result from the initial minimum manufactured clearance. Temperatures are taken from Section 3.6.4. For example, for Case 3, the temperature for node 210 is 151 °F, and for node 310, 64 °F. The outside diameter of the ICV is 35.5 in., and the inside diameter of the OCV is 36.88 in. From Table 2.3-1, the coefficient of thermal expansion for Type 304L at temperatures of 151 °F and 64 °F are $8.67(10^{-6})$ in./in./°F and $8.44(10^{-6})$ in./in./°F, respectively. The minimum initial radial clearance is 1/32 in. The residual radial clearance, therefore, is

$$RC_{res} = 0.031 - 0.5[35.5(151 - 70)(8.67(10^{-6})) - 36.88(64 - 70)(8.44(10^{-6}))] = 0.018 \text{ in.}$$

Residual radial clearances at other locations and for all load cases are presented in Table 2.6.1.2-1.

The axial differential thermal expansion between the two vessels is found by subtracting the axial thermal expansion of the OCV from that of the ICV using the average temperature of the four stations described above. (Average temperature is valid because each node represents about equal lengths of vessel shell.) The residual axial clearance is found by subtracting this result from the initial minimum manufactured clearance. For example, for Case 3, the temperatures of nodes 210 to 240 are 151, 134, 118, and 78 °F, respectively, and the average is 120 °F. The temperatures of nodes 310 to 340 are 64, 59, 54, and 49 °F, respectively, and the average is 55 °F. From Table 2.3-1, the coefficient of thermal expansion for Type 304L at temperatures of 120 °F and 55 °F are $8.60(10^{-6})$ in./in./°F and $8.42(10^{-6})$ in./in./°F, respectively. The OCV inside height, 52.9 in., may be conservatively used for both vessels. The minimum initial axial clearance is 1/16 in. The residual axial clearance, therefore, is

$$AC_{res} = 0.062 - 62.9[(120 - 70)(8.60(10^{-6})) - (55 - 70)(8.42(10^{-6}))] = 0.028 \text{ in.}$$

Residual axial clearances for all load cases are presented in Table 2.6.1.2-1.

TABLE 2.6.1.2-1. Summary of NCT and Normal Operational Differential Expansions.

Parameter	Case 1 full solar 100 °F ambient, no cooling	Case 2 no solar -40 °F ambient, no cooling	Case 3 full solar 100 °F ambient, active cooling
Residual axial clearance (in.)	0.039	0.038	0.028
Residual radial clearance (in.)			
Elevation 210/310	0.024	0.022	0.018
Elevation 220/320	0.024	0.022	0.020
Elevation 230/330	0.024	0.022	0.021
Elevation 240/340	0.028	0.028	0.027

Thus, a positive clearance is maintained between the ICV and OCV bells under NCT and normal operational conditions. The relative differential thermal expansion between the closure bolts and vessel flanges is treated in the next section.

2.6.1.2.1 Bolt Thermal Expansion. As noted in Section 2.3, the bolting material used for the OCV and ICV containment assembly closure bolts (ASTM-A320, Grade L43 and ASTM-A540, Grade B23, Class 1) has a different coefficient of thermal expansion than the material used for the vessel flanges (AISI Type 304L). As the temperature of the vessels changes from the initial conditions, this leads to variations in bolt pre-load because of different amounts of thermal expansion/contraction in the bolt and in the joint material. Because the expansion coefficient of AISI Type 304L in the joint is greater than that of the bolt, an increase in joint temperature will normally mean an increase in bolt clamping force and bolt stress. A decrease in joint temperature will normally mean a decrease in bolt clamping force and bolt stress. In the analyses to follow, the actual temperatures of the bolt and joint, as calculated in Section 3.0 (and as summarized in Appendix 2.10.7) are used. From Shigley, *Mechanical Engineering Design*²¹, the initial pre-load force in the bolts, resulting from assembly torque, is:

$$F_p = \frac{T}{Kd}$$

where: T = bolt torque, in.-lb
 K = 0.186, friction torque coefficient for cadmium plated threads²²
 d = nominal bolt diameter, in.

Table 2.6.1.2.1-1 lists the bolt parameters along with pre-load force for the ICV and OCV closure bolts.

TABLE 2.6.1.2.1-1. Closure Bolt Parameters and Pre-load Force.

Location	d (in.)	Stress area (in. ²)	Length*(in.)	Torque (ft-lb)	Pre-load force (lb)
ICV	0.75	0.3300	1.49	250	21,505
OCV	1.25	0.9524	5.19	300	15,484

*Grip length, defined as the length from the head to the midpoint of the engaged threads.

The finite element models described in the last section (see Appendices 2.10.2 for the ICV and 2.10.8 for the OCV model) include a model of the closure bolts as spars. They are given an initial stretch so that under nominal conditions (zero net pressure and uniform reference temperature of 70 °F) the load in the bolts is equal to the pre-load force values given in the table above. During model postprocessing, the resultant force in the spar is extracted. Because in the 2-D model a single spar must represent all of the bolts, the force in each bolt may be found as:

$$F_b = \frac{2nF_s}{n}$$

where:
 F_b = force in each bolt, lb
 F_s = force in model spar, lb/radian
 n = number of bolts.

Based on a tensile stress area of A_s , the stress in the bolt is:

$$\sigma_b = \frac{F_b}{A_s}$$

The allowable bolt stress for NCT is $2S_u$, based on the ASME B&PV Code, Section III, Article NB-3232.1, and is found from bolt temperature and Tables 2.3-2 and 2.3-3. The margin of safety is:

$$M.S. = \frac{2S_u}{\sigma_b} - 1$$

The following table summarizes load, stress, temperature, allowable, and margin of safety for the closure vessel bolts for each case in Table 2.6.1-1.

TABLE 2.6.1.2.1-2. Closure Bolt Load, Stress, and Margin of Safety.

Load case	Bolt location	Bolt load (lb)	Bolt stress (psi)	Bolt temp. (°F) ^a	$2S_u$ Allowable (psi)	Margin of safety
1	ICV	23,417	70,861	217	95,056	+0.34
	OCV	23,390	24,559	210	65,760	+1.68
2	ICV	21,446	64,985	70	100,000	+0.54
	OCV	14,833	15,674	61	70,000	+3.49
3	ICV	21,746	65,897	85	100,000	+0.62
	OCV	16,291	17,095	86	70,000	+3.08

^aThe closure bolts were not explicitly modeled in the 2-D NCT thermal analysis. The bolt temperatures listed are those of the respective bolting flanges, i.e., thermal node 250 for the ICV and thermal node 350 for the OCV, and are taken from Tables 2.10.7.1-2, -3, and -4.

According to Reference 23, the preload force may vary by up to $\pm 30\%$ for a given applied torque value. Therefore, Case 1 (the case having the lowest bolt margin of safety) was rerun, using a pre-stretch in the element representing the bolts of 130% of the nominal value. This case represents the maximum possible load in the bolts. The results are shown in Table 2.6.1.2.1-3, where the relatively large margins of safety demonstrate that the bolt stress is still well below yield, even when conservatively accounting for a large scatter in bolt preload force.

TABLE 2.6.1.2.1-3. Closure Bolt Load and Stress Considering Preload Force Variation.

Load case	Bolt location	Bolt load (lb)	Bolt stress (psi)	Bolt temp. (°F)	Yield strength (psi)	Margin of safety on yield
1	ICV	29,856	89,867	217	139,280	0.55
	OCV	27,904	28,299	210	98,670	2.37

Thus, a positive margin of safety is maintained under NCT and normal operational conditions for all closure bolts.

2.6.1.3 Stress Calculations. The axisymmetric finite element models of the ICV and OCV already introduced in Section 2.6.1.2 are used to determine the stress in both containment vessels because of the combined effects of differential thermal expansion and pressure loads. To aid in the classification of stress, the cases of Table 2.6.1-1 are broken down into several load cases as shown in Table 2.6.1.3-1. The internal pressure-only cases (ICV-P and OCV-P) are run to allow primary (pressure) stresses to be considered independently of secondary (thermal) stresses. Classification of stress intensities is per Table NB-3217-1 of the ASME B&PV Code. According to Table NB-3217-1, pressure-induced membrane stresses in the knuckle portion of the torispherical heads are classified as local membrane stresses, and bending stresses in the knuckle are classified as secondary stresses. The cases ICV-A and OCV-A aid in consideration of the total range of stress by including the period during payload assembly operations during which the annulus between the vessels is evacuated before helium backfill.

TABLE 2.6.1.3-1. Containment Vessel Stress Analysis Load Cases.

	Load case No.	Description
ICV cases	ICV-P	10 psi net internal pressure only, uniform 70 °F
	ICV-1	10 psi net internal pressure, case 1 ^a temperatures
	ICV-2	10 psi net internal pressure, case 2 temperatures
	ICV-3	10 psi net internal pressure, case 3 temperatures
	ICV-A	20 psi net internal pressure, loading transient temperatures ^b
OCV cases	OCV-P	26.5 psi net internal pressure only, uniform 70 °F
	OCV-1	26.5 psi net internal pressure, case 1 temperatures
	OCV-2	26.5 psi net internal pressure, case 2 temperatures
	OCV-3	26.5 psi net internal pressure, case 3 temperatures
	OCV-A	14.7 psi net ext. pressure, loading transient temperatures ^b

^aCases 1, 2, and 3 are defined in Table 2.6.1-1.

^bLoad cases ICV-A and OCV-A correspond to the point during package assembly when the ICV/OCV annulus is evacuated before backfill.

Temperatures for each case are taken from Appendix 2.10.7 and temperature-dependant modul of elasticity and thermal expansion coefficients are used as given in Section 2.3. Finite element model plots are shown in Figures 2.10.2-1 (ICV) and 2.10.8-1 (OCV). Stress intensity results are summarized in Tables 2.6.1.3-2 and 2.6.1.3-3.

For each load case listed above, the stress location, classification, stress value, allowable, and margin of safety are listed. The minimum margin of safety is +2.83 (case OCV-3). The allowables shown in the tables are based on the design criteria given in Table 2.1.2-1 and properties given in Table 2.3-1.

Membrane and bending stresses, resulting from the pressure-only cases (without thermal effect), are insignificant. The only cases of interest are the combined pressure and thermal cases, where the maximum membrane and bending stress intensity occurs in or near the ICV and OCV head knuckle regions.

TABLE 2.6.1.3-2. Summary of ICV Stress Intensities and Margins of Safety.

Case No.	Stress location	Stress category	Maximum stress intensity (psi)	Allowable stress intensity (psi) ^a	Margin of safety
	Head crown midshell	P_n	1,041 (elem 145)	15,700 (S_m)	> +10
ICV-P	Head Crown, shell surface	$P_1 + P_2$	1,855 (elem 145)	25,050 ($1.5S_u$)	> +10
	Knuckle midshell	P_2	1,093 (elem 144)	25,050 ($1.5S_u$)	> +10
	Knuckle shell surface	$P_1 + P_2 + Q$	2,110 (elem 144)	50,100 ($3.0S_u$)	> +10
ICV-1	Knuckle shell surface	$P_1 + P_2 + Q$	3,139 (elem 145)	46,750 ($3.0S_u$)	> +10
ICV-2	Knuckle shell surface	$P_1 + P_2 + Q$	3,535 (elem 145)	50,100 ($3.0S_u$)	> +10
ICV-3	Knuckle shell surface	$P_1 + P_2 + Q$	2,716 (elem 145)	50,100 ($3.0S_u$)	> +10
ICV-A	Knuckle shell surface	$P_1 + P_2 + Q$	4,646 (elem 144)	50,100 ($3.0S_u$)	> +10

^aAllowable stress intensity based on temperatures of applicable stress location, given in Appendix 2.10.7.1. For case ICV-1, the maximum temperature is 338 °F, but 350 °F will be conservatively assumed for all locations. For Cases ICV-2, ICV-3, ICV-A and ICV-P, temperatures are below 300 °F, but 300 °F is conservatively used for all locations.

TABLE 2.6.1.3-3. Summary of OCV Stress Intensities and Margins of Safety.

Case No.	Stress location	Stress category ^{2,3,4}	Maximum stress intensity (psi)	Allowable stress intensity (psi) ⁵	Margin of safety
	Head crown midshell	P_m	1,085 (item 121)	16,700 (S_m)	> +10
OCV-P	Head crown shell surface	$P_t + P_b$	1,667 (item 122)	25,050 ($1.5S_m$)	> +10
	Knuckle mid-shell	P_L	1,840 (item 119)	25,050 ($1.5S_m$)	> +10
	Knuckle shell surface	$P_L + P_b + Q$	3,522 (item 119)	50,100 ($3.0S_m$)	> +10
OCV-1	Knuckle shell surface	$P_L + P_b + Q$	7,585 (item 118)	50,100 ($3.0S_m$)	+5.61
OCV-2	Knuckle shell surface	$P_L + P_b + Q$	9,002 (item 116)	50,100 ($3.0S_m$)	+4.57
OCV-3	Knuckle shell surface	$P_L + P_b + Q$	12,733 (item 117)	50,100 ($3.0S_m$)	+2.93
OCV-A	Knuckle midshell	$P_L + P_b + Q$	7,287 (item 117)	50,100 ($3.0S_m$)	+5.88

⁵Allowable stress intensity based on temperatures given in Appendix 2.10.7.1. All temperatures are below 300 °F, but 300 °F is conservatively used for all locations.

2.6.1.4 Comparison With Allowable Stresses. As discussed in Section 2.1.2, stress limits are in accordance with Regulatory Guide 7.6, and load combinations are in accordance with Regulatory Guide 7.6. From Table 2.3-1, the S_m value for AISI Type 304L stainless steel used in both vessels is 16,700 psi up to 300 °F, and is 16,250 psi at the conservative maximum of 350 °F. From Table 2.1.2-1, the allowable stress intensity limits under NCT are S_m for general primary membrane stress intensities (P_m), $1.5S_m$ for local primary membrane stress intensities (P_L), $1.5S_m$ for primary membrane (general or local) plus primary bending stress intensities ($P_L + P_b$), and $3.0S_m$ for the range of primary plus secondary stress intensities ($P_L + P_b + Q$). Minimum margins of safety, all of which are positive, are presented in Tables 2.6.1.3-2 and 2.6.1.3-3. Thus, the design criteria are satisfied.

2.6.1.5 Range of Primary Plus Secondary Stress Intensities. Per Regulatory Guide 7.6, Paragraph C.4, the maximum range of primary plus secondary stress intensity under NCT must be less than $3.0S_m$. This limitation on stress intensity range applies to the entire history of NCT loadings, and not just to the stress intensities from each individual load transient. To evaluate the maximum range, examination was made of the various load cases, including both regulatory and worst-case operational, and the maximum stress intensity arising from the worst-case load case was determined. To conservatively bound the maximum stress intensity range, the difference between the worst-case maximum stress intensity and the nominal (70 °F, no stress) condition was doubled, to account for a maximum possible stress reversal.

From Tables 2.6.1.3-2 and 2.6.1.3-3, the worst case is OCV-3, with a stress intensity of 12,733 psi. Doubling this value results in a maximum range for primary and secondary stress

intensity of 25,466 psi. As discussed in Section 2.6.1.4, the value of S_u for AISI Type 304L stainless steel is 16,700 psi for case OCY-3, because the peak temperature is less than 300 °F. The margin of safety for the range of primary plus secondary stress intensity is as follows:

$$M.S. = \frac{3S_u}{\sigma_1} - 1 = +0.97$$

where: $S_u = 16,700$ psi
 $\sigma_1 = 25,466$ psi.

2.6.2 Cold

The cold NCT consists of exposing the RTG Transportation System Package to a steady-state ambient temperature of -40 °F. Insulation and payload internal decay heat are assumed to be negligible. These conditions will result in a uniform temperature throughout the package of -40 °F.

The effect on the two containment vessels will be negligible. The only containment structural component not comprised of ASTM-A240, Type 304L, stainless steel are the ASTM-A320, Grade L43 OCY closure bolts and the ASTM-A540, Grade B23, Class 1 ICV closure bolts. Both materials have the same coefficient of thermal expansion, which is less than that for the Type 304L structural material. Hence, a reduction in temperature from that at which the closure bolts were installed will result in some loss of pre-load in the closure system. The pre-load loss is easily determined from the two-dimensional, axisymmetric finite element models, assuming a bolt installation temperature of 70 °F.

The ICV model is described in Appendix 2.10.2. No net pressure is assumed for the cold NCT analysis. As previously described in Section 2.6.1.2.1, the closure bolt is modeled as a spar, and for this analysis is given an initial stretch that results in 70% of the pre-load applied to the bolt at assembly, or $(0.7)(21,505) = 15,054$ (see Table 2.6.1.2.1-1). Then, setting all the temperatures in the model to -40 °F results in a spar load of 68,680 lb/radian, using material properties extrapolated from the values shown in Tables 2.3-1 and 2.3-3. This can be converted into load per closure bolt as before, resulting in:

$$F_b = \frac{2\pi F_s}{n} = 15,336 \text{ lb}$$

where: F_b = load per bolt, lb
 F_s = spar load, 68,680 lb/radian
 n = 24 bolts.

Because F_b is positive, a residual closure force will exist in the ICV closure system at -40 °F. This will correspondingly ensure that a residual compression remains on the ICV O-ring seals.

The OCY model is described in Appendix 2.10.8. The bolt pre-load used is conservatively taken as $(0.7)(15,484) = 10,839$ lb (see Table 2.6.1.2.1-1). Following the same procedure as for the ICV, the spar load at -40 °F is 1.6,385 pounds. The conversion to load per closure bolt is given below:

$$F_b = \frac{2nF_c}{n} = 4,284 \text{ lb}$$

where F_b = load per bolt, lb
 F_c = spar load, 16,365 lbf/radian
 n = 24 bolts

Because F_b is positive, a residual closure force will exist in the OCV closure system at -40 °F. This will correspondingly ensure that a residual compression remains on the OCV O-ring seals.

Because all other containment structural components are fabricated from the same material and are at a uniform temperature, differential expansion stresses are not a concern. Brittle fracture concerns are addressed in Section 2.1.2.2.1, and O-ring sealing performance at -40 °F is discussed in Section 4.0.

2.6.3 Reduced External Pressure

The effect of a reduced external pressure of 3.5 psia has been examined in Section 2.6.1 where, in anticipation of this requirement, pressure external to the OCV was set to 3.5 psia. The internal pressure of the OCV was conservatively rounded upward to 30 psia, yielding a conservative net pressure differential of $30 - 3.5 = 26.5$ psid (see Section 2.6.1.1). This pressure was used with the most unfavorable temperature conditions, and margins of safety were positive as shown in Table 2.6.1.3.3. Therefore, reduced external pressure is not a concern.

2.6.4 Increased External Pressure

The effect of an increased external pressure of 20 psia is negligible for the RTG Transportation System Package. As discussed in Section 2.6.1.1, the pressure within the OCV was conservatively rounded downward to 18.0 psia, as shown for case 3. The effect of the increased external pressure on the OCV would be a $20.0 - 18.0 = 2.0$ psig external pressure. However, the OCV can withstand a full vacuum (zero psia internal, 14.7 psia external pressure), because this load is applied during the process of assembly of the payload into the package, just before helium backfill of the annulus. Margins of safety for this case (Case OCV-A) were shown to be positive in Table 2.6.1.3.3. Therefore, increased external pressure is not a concern.

2.6.5 Vibration

The effects of the vibration normally incident to transportation are shown to be insignificant. To protect the relatively delicate payloads from harmful effects of shock and vibration, the package is mounted on shock isolators having a natural frequency much lower than the lowest natural frequency of any package component, including payloads. For this reason, the package behaves essentially as a rigid body and responds to the vibratory inertia loads in a quasi-static manner. Because these resulting inertia loads are so small, they create no significant level of plating stress.

2.6.6.1 Vibratory Response Analysis. The RTG Transportation System will consist of a package, as defined in Section 1.0, in addition to an exclusive-use trailer and a shock-isolated skid. To protect the RTG payloads from the effects of over-the-road vibration, the isolated natural frequency of the package and skid will be about 2.5 Hz. Because the lowest natural frequencies of the package components are on the order of 200 Hz, it is possible to treat the package and shock isolation skid as a single degree of freedom, spring-mass system, and inertial response loading may be applied to the package quasi-statically.

Draft ANSI Standard N14.23²² identifies peak truck trailer vibration inputs. Table 2 of ANSI N14.23 shows peak vibration accelerations of a trailer bed as a function of package and decdown system natural frequency. For the frequency range 0 to 5 Hz, and conservatively assuming a light CFR, Table 2 gives peak accelerations (99% level) of 2g in the vertical direction, and 0.1g in both the lateral and longitudinal directions.

2.6.6.2 Calculation of Alternating Stresses. Section 6.2 of ANSI N14.23 states that the fatigue effects of random vibration can be approximated by using 75% of the constant-amplitude stress. Therefore, the fatigue stress, S_w , on the vessel can be found by applying 75% of the peak acceleration as a constant body force. The vertical acceleration to be applied is given below:

$$2(0.75) = 1.5 g$$

Because this is virtually identical to the force of gravity itself, and the package is quite rigid, (designed to withstand several hundred g's in impact scenarios), the stresses resulting from this load will be insignificant. A similar conclusion can be reached for the 0.1g lateral and longitudinal loads. A further, significant conservatism is afforded by the fact that, while the values from ANSI N14.23 reflect 3% damping, the isolators used will impart at least 10% damping. This will further reduce the vibrational response of the package.

2.6.6 Water Spray

The materials of construction used for the package are such that the water spray test identified in 10 CFR 71.71(c)(5) will have a negligible effect on the package.

2.6.7 Free Drop

The maximum weight of the RTG Transportation System Package is less than 11,000 pounds. Subpart F of 10 CFR 71 requires a determination of the effect of dropping a package of this weight from a height of 4 ft onto a flat, horizontal, essentially unyielding surface, striking the surface in a position for which maximum damage is expected. Physical testing of a full scale prototype was used to address this 4-ft free drop requirement. Two full-scale prototypes, called certification test articles (CTA-1 and CTA-2), were used during the drop testing program. The first test article (CTA-1) experienced two failures during the first drop test series. The package was subsequently modified and a second test article (CTA-2) was fabricated. All of the 4-ft free drop tests performed on CTA-1 were repeated on CTA-2. Only CTA-1 had active and passive accelerometers. The accelerometer data is included for information only.

The drop orientations for which maximum damage can be assumed are discussed in Appendix 2.10.9.1. These orientations are as follows:

- Bottom-down near-vertical oblique drop
- Bottom-down center of gravity over struck corner
- Side-slakedown drop
- Bottom-down flat end drop
- Top-down flat end drop.

The NCT 4-ft free drops are significant only in the sense that they must not compromise the ability of the package to successfully undergo subsequent 30-ft HAC free drops. Accordingly, for certification testing, each of the above NCT free drops was followed by a HAC free drop impact in the same orientation and impacting at the same initial point of contact.

The results of the NCT free drops on package performance are negligible, particularly in comparison to the results of the HAC free drops. Only CTA-1 was outfitted with active and passive accelerometers as described in Appendix 2.10.15.4.3. Table 2.6.7-1 gives the results for peak acceleration at the c.g. of the package and the status of the passive accelerometers (whether tripped or not) for the NCT free drops that were conducted using CTA-1. Observed containment boundary deformations as a result of the NCT free drops using both CTA-1 and CTA-2 were essentially the same and negligible. The peak acceleration values were less than the corresponding values obtained from the HAC, 30-ft free drops, discussed in Section 2.7.B. More detailed descriptions of the damage for each NCT free drop are recorded, including photographs, in Appendix 2.10.15.

TABLE 2.6.7-1. NCT Free Drop Impact Limiter Deformations and Package Center of Gravity Peak Accelerations for CTA-1.

Drop No.	Description	Impact limiter deformation (in.)	Peak accel. (g)	Passive accel. status		
				200 g	300 g	400 g
1	Near vertical	Negligible	53	No trip	No trip	No trip
2	CG over corner	1.1	69	No trip	No trip	No trip
3	Side-slakedown	1.9	56	No trip	No trip	No trip
4	Bottom down	Negligible	170	Trip	No trip	No trip
5	Top down	Pin damage only	90	No trip	No trip	No trip

With negligible containment boundary deformations and small impact limiter deformations, it is clear that NCT free drops do not substantially reduce the effectiveness of the packaging, either directly as a result of the 4-ft free drops, or indirectly, by compromising the ability of the package to withstand a subsequent HAC sequence. Observed NCT freedrop deformations are modest and completely consistent with NCT thermal shielding and criticality evaluations.

2.6.8 Corner Drop

This test does not apply to the package, because the package weight is in excess of 100 kg (220 pounds) and the materials of construction do not include wood or fiberboard.

2.6.9 Compression

It can be demonstrated that a pressure on the top and bottom of the package equal to five times the package weight produces small stresses. Per 10 CFR 71.71(c)(9), a uniform pressure of the greater of 1.85 psi, or a pressure equivalent to the weight of five packages, shall be applied to the top and bottom of the package. The package weight is 9,600 pounds. The vertically projected area is given below:

$$A = \frac{\pi}{4} D^2 = 1,068 \text{ in.}^2$$

where: D = OCV shell outside diameter = 36.88 in.

The pressure created by five packages is:

$$p = \frac{5(9,600)}{1,068} = 44.9 \text{ psi}$$

This clearly exceeds 1.85 psi and becomes controlling. In the analysis, a conservative value of 50 psi will be used.

Using the same finite element model for the OCV as that used in Section 2.6.1, the stresses in the OCV bell because of the application of 50 psi can be found. The pressure was assumed to be applied uniformly to the OCV torispherical head area, and the bottom of the package is vertically fixed, in order to react the compressive load. Internal pressure is conservatively assumed to be zero. Temperatures from Case 1 are included in the analysis, taken from Section 3.6.4. The maximum local membrane stress intensity is 7,626 psi, classified as P_1 because it occurs in the OCV head knuckle area. Similarly, the maximum sum of membrane plus bending stress is 8,331 psi at the same location, but classified as a $P_2 + P_3 + Q$ (secondary) stress, once again, because of its location in the knuckle. From Tables 2.1.2-1 and 2.3-1, the allowable for P_1 is 25,050 psi, and for $P_2 + P_3 + Q$ the limit is 50,100 psi, for temperatures lower than 300 °F. For the OCV head, the maximum temperature is below 300 °F. The margin of safety on local membrane stress is:

$$M.S. = \frac{25,050}{7,626} - 1 = +2.25$$

The margin of safety on the sum of local membrane and bending stress in the knuckle is given below:

$$M.S. = \frac{50,100}{8,331} - 1 = +5.01$$

To confirm structural stability, a buckling analysis is performed on the OCV for the maximum anticipated compression load of 150 psi (1,068 in.²) = 63,400 pounds. For analysis purposes, the

stiffening effects of the cooling jacket are conservatively ignored. Additionally, an elevated temperature of 350 °F is conservatively assumed. For the basic OCY shell, the axial and hoop compressive stresses associated with the 53,400 pound external load are calculated below:

$$\sigma_a = \frac{P}{2\pi R t} = 934.5 \text{ psi}$$

$$\sigma_h = \mu \sigma_a = 280.4 \text{ psi}$$

where: σ_a = axial compressive stress
 σ_h = hoop compressive stress (at restrained ends of cylindrical shell)
 R = shell mean radius = 18.19 in.
 t = shell thickness = 0.50 in.
 P = external load = 53,400 lb
 μ = Poisson's ratio = 0.3.

At these low stress magnitudes, resulting plasticity reduction factors from Section 1510 of ASME B&PV Code Case N-284 are equal to unity. Hence, inelastic buckling checks are not required. Consequently, the buckling analysis requires only a determination of theoretical buckling stress values. The results can then be compared to the above actual, calculated stress values, with capacity reduction factors and appropriate factors of safety (FS = 2.0 for NCT) applied. If the theoretical buckling stresses are greater than the adjusted actual stress values, then buckling will not occur.

From Section 1511 of Code Case N-284, the appropriate capacity reduction values are determined to be as follows:

$$a_{ax} \text{ (axial compression)} = 0.207$$

$$a_{hx} \text{ (hoop compression)} = 0.800$$

from which adjusted actual stress values can be determined:

$$\sigma_{ax} = \frac{\sigma_a \times FS}{a_{ax}} = 9,029 \text{ psi}$$

$$\sigma_{hx} = \frac{\sigma_h \times FS}{a_{hx}} = 701 \text{ psi}$$

From Section 1712 of Code Case N-284, the theoretical buckling values for an effective OCY free length of 58 in. are determined to be as follows:

$$\sigma_{\text{axial}} \text{ (axial compression)} = 444,314 \text{ psi}$$

$$\sigma_{\text{hoop}} \text{ (hoop compression)} = 37,725 \text{ psi}$$

Comparison of results indicates:

$$M.S. \text{ (axial)} = \frac{444,814}{9,026} - 1 = +Large$$

$$M.S. \text{ (hoop)} = \frac{37,725}{701.0} - 1 = +Large$$

Consequently, buckling of the OCV shell will not occur.

The buckling analysis of the OCV torispherical head follows the procedure outlined in Section 2.7.5 for HAC, except that the 150% increase in allowable stress is not applied. Therefore, an allowable pressure for NCT can be obtained by dividing the value of 140 psig obtained for HAC by the factor of 1.5 as follows:

$$P_s = \frac{140}{1.5} = 93 \text{ psi}$$

Thus, the margin of safety is:

$$M.S. = \frac{P_s}{P} - 1 = \frac{93}{50} - 1 = +0.86$$

Thus, the margins of safety on buckling are all positive.

2.6.10 Penetration

The 40-in. drop of a 13-pound, spherically headed, 1.25-in.-diameter steel bar is of negligible consequence to the package. This is because the package has been designed to minimize the consequences associated with the much more limiting case of a 40-in. drop of the entire package onto a puncture bar (see Section 2.7.2). The containment boundary is a smooth, curved steel surface, without any fragile features that could be damaged by the bar. The vent and test port plugs and electrical feed-through assemblies are protected by the impact limiter. Some slight denting of the coolant jacket (0.14 in. thick) or the impact limiter (0.25 in. thick) outer shells might possibly occur, but would have no effect on package operation or effectiveness. Thus, no damage of any consequence will result from this test.

2.7 HYPOTHETICAL ACCIDENT CONDITIONS

The RTG Transportation System Package, when subjected to the sequence of HAC events specified in 10 CFR 71.75, must meet the performance requirements specified in Subpart E of 10 CFR 71. With the exception of the Thermal and Immersion tests, the primary proof of performance for HAC is via the use of full-scale testing. These requirements, as specifically related to the objectives of the certification test program, may be summarized as follows:

1. **No loss of containment:** Leaktightness of both containment boundaries (i.e., less than 1×10^{-7} std cc/sec air) will be maintained throughout the sequence of tests (see Section 4.0). Additionally, no deformations will be induced that would lead to degradation of containment under the subsequent HAC fire event (see Section 2.7.3).
2. **Maintenance of adequate biological shielding capability:** The ability of the package system to satisfy the post-HAC dose rate criterion of 1.000 mrem/hr at 1-m from the package will not be compromised (see Section 5.0).
3. **Maintenance of subcritical payload:** No post-test conditions will exist that would result in a transformation of any payload into a supercritical state (see Section 5.0).

For additional details regarding the structural certification testing performed, see Appendix 2.10.9. Results of the certification free drop testing are presented in Appendix 2.10.15 and summarized in Section 2.7.2.3. Analyses are presented where necessary to supplement or expand on the test results. The HAC Thermal and Immersion tests are addressed herein by analysis.

2.7.1 Free Drop

Subpart F of 10 CFR 71 requires that a 30-ft HAC free drop be considered for the RTG Transportation System Package. The free drop is to be onto a flat, horizontal, essentially unyielding surface, and the package is to strike the surface in a position for which maximum damage is expected. The ability of the package to adequately withstand this specified HAC free drop condition is demonstrated by testing a full-scale prototypical package. Section 3.0 of Appendix 2.10.9 presents the configuration details of the Certification Test Articles (CTAs).

As noted in Appendix 2.10.15, two CTAs were used. The first CTA experienced two failures during testing. The package design was subsequently modified and a second CTA was fabricated. All of the 4-ft and 30-ft free drop tests performed on the first CTA (CTA-1) were repeated on the second CTA (CTA-2).

2.7.1.1 Identification of Worst-Case Drop Conditions. For both the NCT and HAC free drops, it is required that the package strike the essentially unyielding surface "in a position for which maximum damage is expected." Because of the relatively high structural strength of the package containment vessels, the possibility of any impact-induced structural deformation being great enough to adversely affect shielding capability and/or criticality control is considered to be negligible. Results of the half-scale developmental free drop testing affirm this conclusion (see Appendix 2.10.11). Therefore, in determining which free drop orientations would satisfy the regulatory "worst damage" requirement, attention was focused predominantly on the issue of containment. A detailed discussion of free drop test rationale is given in Appendix 2.10.9 and is summarized below.

Loss of containment could potentially occur either directly as a result of free drop impact

loading, or indirectly, because of impact-induced damage that might lead to degradation of sealing capability in the subsequent HAC fire event.

For the first case (direct damage), the following possibilities must be considered:

1. Loss of sealing capability because of seal area structural deformations.
Seal area structural deformations might arise from impact forces that could bend the OCV flange and distort the seal area surfaces. HAC free drop orientations in which the impact force must first pass through the OCV flange before being distributed throughout the rest of the package present such a possibility. Variations in free drop orientation entail variations in both impact force and in the extent of the OCV flange that absorbs the force. A center of gravity-over-impacted corner drop represents large impact forces (because no energy is converted to package rotation) and simultaneously represents a case where the total force must pass through a small portion of the OCV flange. Other orientations are also identified that could impart distorting forces to the OCV flange seal areas. One is a bottom-down drop where, because of the stiffness of the impact limiter in this particular orientation, the greatest overall impact forces are expected. However, because the entire OCV flange is essentially evenly loaded, less potential for flange bending is expected. Another is a side-slakedown drop, where even though the impact is directed at the relatively strong edge of the flange, some potential for flange distortion exists.
2. Loss of sealing capability of the electrical feed-through connectors.
The seal between the electrical feed-through body and the electrical pins would be affected primarily by inertia forces along the axis of the pins. The bottom-down drop mentioned above, in which maximum overall impact forces are expected, would subject the electrical feed-through pins to worst-case forces along their axes, since the ICV electrical feed-through orientation is parallel to the drop axis. Impact forces are also applied both perpendicular and oblique to electrical feed-through pin axes in the c.g.-over-corner and side-slakedown drops mentioned above.
3. Rupture of containment.
The only potential for rupture of containment shells in a HAC free drop would arise from payload-vessel interaction. Therefore, a simulated payload was included during free drop testing, which besides properly simulating the weight and c.g. of the worst-case payload, also incorporated conservatively strong, square-cornered fins. Further, the top of the simulated payload that faces the ICV head is an open-ended, 14 in. O.D., 0.50-in.-thick steel pipe. The worst case interaction of payload and ICV head would occur in a top-down drop, because the ICV head is 0.37-in. thick, whereas the ICV sidewall is 0.76-in. thick.
4. Separation of either or both ball assemblies from their respective bases (i.e., closure bolt failure). The only likely HAC free drop orientation that could induce a separation loading on the closure bolts and lead to physical separation of a ball from a base would be a side-slakedown impact. All other impact orientations would have the effect of driving the base onto the ball, or vice versa. This effect is included in the side-slakedown orientation discussed above. Because of flange and baseplate design, no closure bolt shear load is possible in any orientation.

The thermal analysis for the HAC fire event depends on the insulating presence of the impact limiter and shipping rack assembly to protect the containment seals for the duration of the fire. Consequently, the following must also be considered to determine worst-case free drop orientations:

6. **Loss of impact limiter.**
In a bottom-down, near vertical free drop, separation loads on some of the limiter attachment bolts can occur. The initial impact forces at the outside edge of the limiter, using the rear corner of the package as a fulcrum, cause tensile reaction forces on the limiter attachments on the far side of the package. These forces are maximized for a package free drop of 10" from the vertical using a circumferential orientation that places an impact limiter attachment bolt 180° from the point of impact.
6. **Excessive impact limiter damage.**
Maximum impact limiter deformation can be expected for the e.g. over impacted corner orientation, because considerable "stroke" is required before significant amounts of polyurethane foam are mobilized to absorb the free drop kinetic energy. The same effect would be found in the side-slakedown free drop, though to a somewhat lesser extent, because of energy dissipation in the top end fins. Both cases can be addressed by the free drop orientations discussed above.
7. **Separation of payload shipping rack assembly from inner vessel base.**
The top-down and side-slakedown free drops impose maximum tensile and shear loads on the shipping rack assembly-to-ICV base attachments and on the payload attachments. These free drops thus demonstrate shipping rack assembly retention.

2.7.1.2 Pressure. In addition to package orientation, test pressures and temperatures must also be selected to complete the definition of the conditions existing at the time of a HAC 30-ft free drop test. The maximum package normal operational internal pressure, conservatively taken to be 30 psia (see Section 2.6.1.1), is insignificant from a structural standpoint (see Tables 2.6.1.3-2, Case ICV-P, and 2.6.1.3-3, Case OCY-P). Therefore, full-scale structural certification testing was performed with the package certification test article (CTA) interior filled with air at the ambient atmospheric pressure.

2.7.1.3 Adjustments for Ambient Temperature. In going from regulatory maximum temperatures (maximum payload heat generation, 100 °F ambient temperature, no active cooling, with solar loading applied) to the regulatory minimum (-20 °F ambient, no payload heat, no solar loading), the strength of the impact limiter increases more rapidly than that of structural components, primarily because of the influence of the polyurethane foam. See Section 2.3 for a discussion on the temperature-dependent nature of the mechanical strength of polyurethane foam.

Thus, maximum structural effects because of impact reaction loading can generally be expected at minimum temperature conditions, where loads will be greatest relative to containment component structural strength. Because of its relatively lower strength at higher temperatures, the impact limiter will undergo the greatest deformations at maximum temperature conditions. Because certification testing was carried out at the prevailing ambient temperature, adjustments were made to conservatively account for the variation in impact limiter reaction loads and deformations over the anticipated operational temperature range.

For the low temperature extrema, at which maximum impact loads were expected, the impact limiter was artificially stiffened to match worst-case production unit impact limiter characteristics at -20 °F. To accomplish this, polyurethane foam at a higher density than the nominal value of 12 lb/ft³ was used in the impact limiter. As explained in Section 2.3, the mechanical strength of polyurethane foam increases in proportion to its density. As also explained in that section, the mechanical strength of the foam increases in proportion to a decrease in its temperature. It was therefore possible to select a foam density that would be as stiff at ambient (test) temperature as the production unit (12 lb/ft³) would be at its minimum operational temperature of -20 °F. The substitute density is approximately 15.5 lb/ft³. A comparison of the

mechanical properties of the two foams is given in Figure 2.3-2. The data for the 15.5 lb/ft³ test foam is the average strength of the foam actually used in the CTA impact limiter in the perpendicular to rise orientation at room temperature. The corresponding data for production unit foam (from Table 2.3-4) is for high-limit strength, 12 lb/ft³ density, and -20 °F. Note that this procedure conservatively overestimates impact effects on the containment structures, because the relative strength of the structure is less at the test temperature than it would be at the -20 °F temperature for which impact loads were simulated.

To conservatively account for the effects of increased temperature on impact limiter deformations, a simplified analytical approach is used to determine impact limiter response to various temperature conditions. For this analysis, total energy absorption of the impact limiter is divided into the strain energy arising from deformation of the stainless steel outer shell and strain energy arising from deformation of the polyurethane foam. The approach is described in Section 4.1.3.2 of Appendix 2.10.9. This methodology will establish worst case impact limiter deformations that will correspond to the highest environmental and payload temperatures at the time of the HAC free drop.

2.7.1.4 Identification of Specific Drop Tests to be Performed. Based on the above general discussions, five specific HAC 30-ft free drop tests have been selected for inclusion in the certification test program. Although only a single worst case HAC 30-ft drop is required by the Regulations, all five tests will be performed to ensure that the most vulnerable package features are subjected to worst case loads/deformations. The free drop tests were performed in the following order:

1. Bottom-down near-vertical oblique free drop, at 10° from the vertical, with an impact limiter attachment bolt located 180° away from the point of impact. Addresses impact limiter retention.
2. Bottom-down e. g. over impacted corner, with the electrical feed-through oriented at the point of impact (0°). Addresses localized seal area structural deformations, specifically including electrical feed-through location; also impact limiter maximum deflections.
3. Bottom-down flat end free drop. Addresses seal area structural deformations; ICV electrical feed-through connector pins parallel to their axes; maximum overall impact levels.
4. Side-slid-down free drop, with electrical feed-through oriented at 90° from the point of impact. Package axis at 13° to horizontal with fins contacting ground first. Addresses seal area structural deformations; closure bolt rupture; ICV electrical feed-through connector pins, perpendicular to their axes; separation of shipping rack assembly from ICV baseplate and impact limiter damage.
5. Top-down flat end drop. Addresses separation of shipping rack assembly from ICV baseplate; rupture of containment because of interaction with loose payload.

These free drop orientations are shown schematically in Figure 1 of Appendix 2.10.9.2. Rationale for the choice of drop angles for free drop Nos. 1 and 3 is given in Section 4.1 of Appendix 2.10.9.1. These drops will be preceded by the same series of NCT free drops from a height of 4-ft, as described in Section 2.6.7.

2.7.1.5 Summary of Results from Free Drop Tests. The discussion of the results of HAC free drops is combined with that of HAC puncture drops and is presented in Section 2.7.2.3.

2.7.2 Puncture

Subpart F of 10 CFR 71 requires that a 40-in. free drop of the RTG Transportation System Package onto the upper end of a solid, vertical, cylindrical, mild steel (puncture) bar mounted on a horizontal, essentially unyielding surface be considered. The puncture bar must be 8 in. in diameter, with the top surface horizontal and its edge rounded to a radius of not more than 0.25 in. The package must be oriented in a position for which maximum damage is expected, and the length of the puncture bar is to be such that maximum damage will occur. The minimum length of the puncture bar must be 8 in.

The ability of the package to adequately withstand this specified puncture condition was demonstrated by testing two full-scale package CTAs. Before the puncture tests, the CTAs were subjected to the full range of NCT and HAC 4- and 30-ft drops. Puncture tests were typically directed through the center of gravity at the regions of the package damaged by the preceding 30-ft free drops. This is consistent with 10 CFR 71.73(a), which requires that puncture be considered subsequent to the HAC free drop condition.

2.7.2.1 Identification of Worst-Case Puncture Conditions. To properly select a worst-case set of puncture conditions, items that would potentially compromise the integrity of the package must be clearly identified. The primary item to be addressed is the potential for loss of containment. Such a possible failure mode could arise directly, because of the actual puncture bar impact on the containment components, or indirectly, by inducing damage that would compromise the ability of the package containment seals or electrical feed-through connectors to survive the subsequent HAC fire event. Accordingly, the following worst-case possibilities were identified:

1. **Loss of sealing capability because of seal area structural deformations.**
Structural deformations in the seal area could arise from puncture impacts on the impact limiter where the puncture bar is aimed at the OCV flange region. Other orientations with potential to cause seal area deformations would be impacts on the side of the OCV wall and on the top of the OCV thermal shield. In each case, direct impact between the puncture bar and the OCV flange is impossible because of the presence of intervening structure, i.e., the impact limiter, the coolant jacket, or the thermal shield. For the worst-case interaction with the impact limiter, the puncture bar should impact directly on previous free drop damage.
2. **Loss of sealing capability of the electrical feed-through connectors.**
Loss of sealing capability of the electrical feed-through connectors would be unlikely to occur unless the puncture bar contacted at or near the electrical feed-through connector itself. The ICV electrical feed-through connector is well protected by surrounding structure and is not susceptible to damage from the puncture bar. The electrical feed-through OCV connector is protected by the impact limiter side thickness. As long as the puncture bar cannot penetrate the impact limiter shell, no damage to the electrical feed-through connector can accrue from a puncture event. Prevention of penetration can be demonstrated by a puncture aimed at the side of the impact limiter.
3. **Rupture of containment.**
The only portion of the OCV bell not protected by either the fins, the thermal shield, or the cooling jacket is the top of the OCV torispherical head. Therefore, rupture of containment is unlikely. This can be demonstrated by a near vertical, top down puncture drop on the region of the OCV head not covered by doubler plates, and by oblique impact of the bar on the coolant jacket ribs.
4. **Separation of either or both bell assemblies from their respective base plates.**
Separation of either or both bell assemblies from their respective base plates is also

considered unlikely to arise because of a puncture event, because no puncture bar impact orientation could produce a significant separation load on the CTA closure bolts. Additionally, puncture impacts entail significantly reduced energy compared to the HAC free drops, and would therefore be much less likely to induce closure separation.

5. Loss of thermal protection

Loss of thermal protection would occur if the impact limiter was separated from the package. The limiter would be subjected to worst-case pry-off forces in a top-down free drop, where the puncture bar contacts the outer top surface of the impact limiter.

On a smaller scale, loss of thermal protection could occur because of penetration of the puncture bar through the impact limiter in the seal region, thus opening up a thermal path to the seals or electrical feed-through connectors. Deep penetration of the puncture bar could result in tear out of foam as the package rotates off the bar. Likewise, engagement of the puncture bar onto the thermal shield could render it ineffective in providing a thermal barrier for the HAC fire event.

2.7.2.2. Identification of Puncture Tests to be Specifically Performed. Considering the discussions provided above, eleven specific puncture tests were selected. As noted in Section 2.7.1, two CTAs were used during the course of the package certification testing effort. Nine punctures were performed on CTA-1. For CTA-2, four of these punctures were repeated and two new punctures were performed. The selected puncture orientations are shown schematically in Figure 6 of Appendix 2.10.9.1 and Figure 2 of Appendix 2.10.9.2. Although only a single worst-case, 40-in drop onto a puncture bar is required by the Regulations, all eleven tests were performed to ensure that the most vulnerable package features are actually subjected to worst-case puncture bar impacts. All puncture drops (except Nos. 7, 8, and 9 for CTA-1 and No. 7 for CTA-2) were performed with the puncture bar oriented toward the package c.g., because this maximized impact damage to the CTA. As with the free drop tests, all puncture tests were performed at the prevailing ambient temperature and without pressure in the containment vessels.

For punctures on the impact limiter, the impacted surface will generally be aligned to be at an angle to the puncture bar. As demonstrated in the half scale engineering development tests, Appendix 2.10.11, as well as certification testing of the TRUPACT II, NRC Docket 71-S218, this will tend to maximize the potential for rupture of the impact limiter shell, as well as consequent tear-out of foams as the package rotates off the puncture bar.

A summary of planned HAC puncture tests is as follows:

1. Impact on the previous c.g. over impacted corner 30-ft free drop damage. The orientation of the electrical feed through area also corresponds to this damage. Addresses seal area structural deformations, and loss of thermal protection because of excessive impact limiter damage.
2. Impact on the bottom surface of the impact limiter near the outer edge of the region backed by the lower density foam. Addresses loss of thermal protection because of excessive impact limiter damage.
3. Side impact on the impact limiter, puncture bar axis directed at the OCV vent port feature. Addresses seal area structural deformations and loss of thermal protection because of excessive impact limiter damage.
4. Impact on the side surface (coolant pocket) of the package, just above OCV thermal shield, oriented to correspond to the electrical feed-through location. Addresses seal

area structural deformations.

5. Oblique impact on the side surface (coolant jacket), package oriented top down with its axis at 45° to the puncture bar axis. Impact point will be 45° CCW from the electrical feed-through location, viewed from finned end. Addresses damage that may occur because of puncture impact on coolant jacket ribs.
6. Top-down, near-vertical, package oriented at 9° to the vertical axis. The impact point is located 225° CCW from the electrical feed-through, viewed from above. The impact point is as close as possible to the center of the OCV head, while not contacting the region that is reinforced by the over-the-top doubler plates. The drop height will be measured from the position of the personnel barrier, but for conservatism, the barrier will not be present. Addresses potential for rupture of the OCV head.
7. Top-down package orientation, impact on the top surface of the impact limiter. Impact point is at 150° CCW from the electrical feed-through, in alignment with an impact limiter attachment bolt. Addresses loss of thermal protection because of loss of impact limiter.
8. Top-down package orientation, impact on the top surface of the thermal shield, with the puncture bar axis at 30° to package axis, aimed at the corner between the thermal shield and the coolant jacket. Initial contact of edge of puncture bar to be 1 in. inboard of the outer edge of the thermal shield, equidistant between two OCV closure bolt tubes. Addresses seal area structural deformations; loss of thermal protection because of thermal shield damage.
9. Top-down package orientation, impact directly on an impact limiter attachment bolt access tube. Addresses potential for distortion of the OCV flange due to the transmission of impact force through the tube.
10. Side impact on impact limiter through the package e.g., edge of puncture bar aligned with the impact limiter lower corner joint weld seam. This will subject the weld to shearing loads since the impact limiter corner angle is somewhat stiffer than the sidewall.
11. Side impact on impact limiter through the package e.g., edge of puncture bar aligned with center of one of the plastic melt plugs. This will subject this weld area to a shearing load and will try to rupture the impact limiter side wall.

More detail concerning certification drop testing is found in Appendix 2.10.9.

2.7.2.3 Results of Free Drop and Puncture Tests. Testing of two full-size certification test articles indicates that the package can withstand the HAC free drop and puncture events. The first acceptance criterion, that of a leaktight condition (1×10^{-7} cc/sec, air or less), was met by the OCV and ICV of the second certification test article (CTA-2). Leakage rate tests performed on both the containment boundary butyl O-ring seals and the remainder of the containment boundary (including the electrical feed-through) after the NCT free drops and HAC free drops and punctures demonstrate that the leaktight criterion was satisfied by both the ICV and OCV.

In addition to leakage rate testing, measurements of compression of the containment O-rings subsequent to the complete test sequence was made (see Appendix 2.10.14). These measurements demonstrated minimal reduction in O-ring compression because of the combination

of all NCT and HAC free drop and HAC puncture events. These measured reductions in compression were added to the calculated reductions in O-ring compression because of thermal distortion. For the worst-case configuration, the maximum measured compression reduction was assumed to occur at the same location as the maximum calculated reduction because of thermal distortion, and the two values were added. For both the ICV and OCY, resultant minimum O-ring compressions did not fall below the minimum value used in qualifying the O-ring material. These material tests (see Appendix 2.10.5) demonstrated the ability of the butyl material used for the containment O-rings (Finliner Rubber compound RR0405-70) to maintain a leaktight seal at lower values of compression and at higher temperatures than are predicted for the HAC fire event. The thermal analysis assumptions regarding the extent of impact limiter deformation and the observed retention of the limiter and shipping rack assembly (that insulate the seal areas) were validated. Thus, leaktight boundaries will be maintained after the sequence of NCT free drops, HAC free drops and punctures, and the HAC fire event.

The second acceptance criterion, maintenance of adequate biological shielding capability (see Section 2.7), is met because the worst case reconfigured and concentrated radioactive material may be placed in contact with the thinnest portion of the containment boundaries (the torispherical heads) without exceeding the applicable limits of 1,000 mrem/hr at a distance of 1-m.

The third acceptance criterion, maintenance of subcritical payload, is also met, because similarly reconfigured and concentrated payload, when optimally moderated, remains in a subcritical condition (see Section 6.0). Both of the latter two acceptance criteria are completely unaffected by any permanent deformations of the package containment boundaries that could result from HAC free drops and punctures.

2.7.3 Thermal

During the HAC event sequence, the package will be exposed to fire conditions as described in 10 CFR 71.73(b)(3). This will increase the temperature and pressure of the gas within the ICV and the gas within the annulus between the ICV and OCY. The most critical stress state will occur at the highest package temperature, because the material allowables will be lowest at that time. The maximum gas pressure will be assumed to coincide with the peak temperatures of the package. This ensures the conservatism of the analysis. Furthermore, the maximum possible amount of decomposition gas from the electrical cable insulation included with the payload will be assumed to be added to the gas already within the ICV. Finally, to ensure the minimum required amount of O-ring seal compression is maintained, the thermal expansion stresses in the closure bolts will be examined to ensure they do not exceed yield as a result of the HAC fire temperatures. Thermal distortions of the adjacent seal surfaces are quantified in Section 4.0, again to ensure that sufficient compression remains for leaktight seals.

2.7.3.1 Summary of Pressures and Temperatures. The stress and deformation analyses in this section use the temperatures listed in Section 3.6.5. Because the 30-ft free drop must precede the fire in the prescribed HAC sequence, the possibility of payload structural failure and release of the heat-producing modules has been considered. A review of payload structural design identified the GPHS RTG as possessing a potential for reconfiguration in certain 30-ft free drop orientations. Analysis of the GPHS RTG by its manufacturer (General Electric) established that the minimum size component containing a heat source that could possibly result from the reconfiguration would be the rectangular aeroshells. These components, which are 97.2 mm by 92.4 mm by 53.1 mm, are designed to withstand atmospheric re-entry. Because the worst-case reconfiguration of the GPHS RTG is conservatively assumed (i.e., release of all aeroshells into the ICV), and because the GPHS RTG represents the highest heat payload, consideration of the other payloads is unnecessary.

2.7.3.1.1 Packaging Temperatures. The temperatures listed result from an analysis where conservative assumptions are used concerning the post-HAC reconfiguration of both the packaging and the GPHS RTG payload. According to 10 CFR 71, post-HAC fire ambient temperature is identical to pre-HAC fire temperature (i.e., either -20 or 100 °F), insulation is zero, and no active cooling is assumed. HAC fire temperatures will be a function of the external package deformation, principally of the impact limiter, and of the reconfiguration of the payload internal to the package.

2.7.3.1.1.1 Packaging External Deformation Effects. The post-HAC free drop packaging reconfiguration of greatest interest will primarily involve deformations to the polyurethane foam-filled impact limiter on the bottom end of the package. This is because the impact limiter acts as a thermal insulator in the seal area during the HAC fire event, and thus provides an additional level of protection for the containment seals. Maximum impact limiter deformations in the vicinity of the closure seal flanges because of 30-ft free drops and subsequent 40-in. puncture bar impacts could be expected to arise from two free drop orientations:

- Bottom-down oblique orientation, with the package center of gravity over the impacted corner (CTA-2 test No. 4).
- Side slakedown impact, defined for the package as the near-simultaneous impact of the top-and fins and the bottom-and impact limiter (CTA-2 test No. 12).

Accordingly, both configurations have been evaluated for thermal response in the HAC fire. The effect of char and void space formation are included as detailed in Appendix 3.6.3. Thermal analysis described in Section 3.6.2 indicates that the highest seal temperatures resulted from side slakedown impact damage. Consequently, all analyses use this package reconfiguration geometry. Further, worst-case impact limiter deformations will arise from initial conditions that produce the highest temperatures for the polyurethane foam in the impact limiter (i.e., foam temperatures arising from maximum payload heat, combined with the maximum regulatory ambient temperature of 100 °F and regulatory solar loading). Determination of worst-case impact limiter deformations that would be expected at maximum foam temperatures was accomplished by analytical modification of the ambient temperature impact results obtained from the certification drop testing. The amount of foam exposed by the puncture bar in CTA-2 Test No. 16 was approximately 12.7 in². This area is quite small relative to the area of the impact limiter and, because of the intumescent behavior of the polyurethane foam material (see Reference 10 of chapter 3), the opening will be effectively closed during the HAC fire event. Using the approach detailed in Section 4.1.3.2 of Appendix 2.10.9, the impact limiter deformations for each of the two orientations above at maximum temperature conditions are calculated as follows.

As discussed in Section 2.7.1.3, the impact limiter foam strength for use in the free drop tests (at ambient temperature) was selected to have a value slightly in excess of the maximum strength of the production unit foam when at a temperature of -20 °F. The measured post-impact deflections of the impact limiter represent minimum values. The corresponding maximum deflections are functions only of the minimum deflections and of the maximum pre-impact foam temperatures. As described above, these pre-impact conditions correspond to maximum payload heat, 100 °F ambient, and regulatory insolation, without active cooling (i.e., Case 1 of Section 2.8.1). These foam temperatures are given in Section 3.6.4. For purposes of calculation, a volume-weighted average temperature will be used. This is conservative for maximum deflection, because the foam that actually crushes is located in the outer portions of the impact limiter, where temperatures are below the average value.

Each nodal temperature in the impact limiter foam region corresponds to an annular volume. The volume-weighted temperature is found by multiplying each nodal temperature by its corresponding annular volume, summing all such products, and dividing the sum by the total foam

volume. Only the stronger, 12 lb/ft³ foam is included, because the 3 lb/ft³ foam is not active in the two orientations of interest defined above. Figure 2.7.3.1.1.1-1 illustrates the correspondence of node number to location in the model, and the dimensions from which each annulus volume can be calculated. For example, the annulus corresponding to thermal node Nos. 431, 432, and 433 has an o.d. of 59.3 in., an i.d. of 54.2 in., and a thickness of 3.04 in. The volume is given below:

$$\frac{\pi}{4}(59.3^2 - 54.2^2)(3.04) = 1382 \text{ in.}^3$$

The total volume of 12 lb/ft³ foam is 34,110 in.³. Using the method just described, and impact limiter foam temperatures from Section 3.6.4, the maximum pre-impact, volume-weighted temperature of the 12 lb/ft³ foam is 162 °F. A value of 160 °F will be conservatively used. Given the pre-impact maximum foam temperature, it is now possible to determine the foam plateau crush strength. From Table 2.3-4, the lower-limit crush strength at a strain of 25% (the approximate plateau), perpendicular to rise, and at a temperature of 160 °F is 341 psi. (This value represents the minimum for the average of all samples and is equal to 90% of the table values.) From Figure 2.3-2, the plateau strength (also at 25% strain) of the foam used in the CTA was 755 psi.

A. Side Drop Damage

Although the side drop crush deflection of the impact limiter was not uniform over the limiter length, the maximum value will be used over the entire length of the limiter. This conservatively accounts for additional puncture drop damage. From Section 2.7.6 the maximum radial deflection

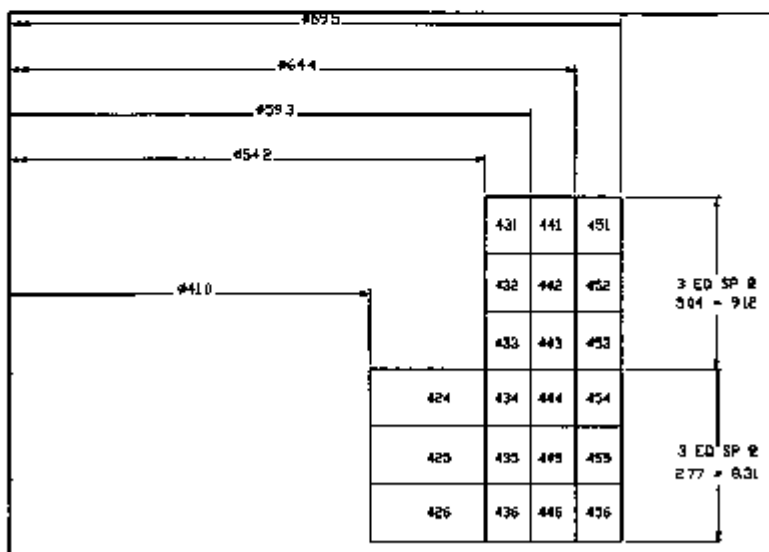


FIGURE 2.7.3.1.1.1-1. Impact Limiter Foam Thermal Node Relationships.

from the fourth HAC-free drop (CTA-2 test No. 12, side-slutdown) was 4 in. This value resulted from the full series of HAC free drop and puncture events. The first step in the modification of this value to reflect maximum temperature is to determine the energy absorbed by the impact limiter shell, from which the average force per unit length of the crumpled impact limiter shell can be derived. The energy absorbed by the impact limiter shell is given below.

$W_s =$ total drop kinetic energy - W_f , where W_f is the energy absorbed by the foam.

W_f is equal to the product of crushed foam volume and foam plateau strength. The crushed volume is given below:

$$V = l \left[\frac{1}{2} (R)^2 (2\theta - \sin 2\theta) \right] = 1,634 \text{ in.}^3$$

where: l is 17.438 in. (length of foam in impact limiter)
 R is 34.75 in. (outside radius of foam in impact limiter)
 θ is half the included angle of the impact surface, found from:

$$\theta = \cos^{-1} \left(\frac{R - \delta}{R} \right) = 27.76^\circ$$

where: δ is the radial crush deflection, 4 in.

The crush footprint area is given below:

$$A = 2lR\sin\theta = 564.5 \text{ in.}^2$$

The energy absorbed by the foam is then 1,158,170 in.-lb, which is the product of the plateau strength of the test foam of 756 psi and the crushed volume of 1,534 in.³ found above. The energy absorbed by the impact limiter shell is given below:

$$W_s = (M)(360 + \delta) - W_f = 2,338(10^6) \text{ in.-lb}$$

where: M is package weight, 9,600 lb
 δ is 4.0 in.
 W_f is 1,158,170 in.-lb.

The average force per unit length of the impact limiter shell is:

$$f = \frac{W_s}{A} = 4,138 \text{ lb/in.}$$

This value corresponds to ambient test temperature. It must be adjusted to reflect maximum temperature conditions. From Appendix 2.10.7, Table 2.10.7.1-2, the average temperature of the

active parts of the impact limiter shell (nodes 406, 408, and 410) will be conservatively taken as 150 °F. From Table 2.3-1, the ratio of yield strength of the shell material at 150 °F to the strength at ambient temperature (75 °F) is 0.926, where ASTM Type 304L data is used in place of ASTM Type 304 data. The force per unit length of the impact limiter shell at maximum temperature conditions is given below:

$$f = 0.926(4,138) = 3,832 \text{ lb/in.}$$

The following equation can now be solved for the radial crush deflection, δ , at maximum temperature conditions:

$$M(360-\delta) = fA(\delta) + sV(\delta)$$

where: M is 9,600 lb
 f is 3,832 lb/in.
 s is 341 psi (12 lb/ft² foam crush strength at maximum temperature conditions)
 $A(\delta)$ is footprint area, a function of δ , same as shown above
 $V(\delta)$ is crushed volume, a function of δ , same as shown above.

Solving iteratively, the maximum crush deflection, δ , is 5.9 in.

B. C.G. Over Corner Damage

This type of damage results from the c.g. over corner orientation. From Section 2.7.6, the maximum deflection along the line of crush from the second HAC free drop (CTA-2 test No. 6, c.g. over corner) was 5.5 in. This value resulted from the full series of HAC free drop and puncture events. As in the case of radial damage, the force per unit length of impact limiter shell must first be calculated.

The damaged volume in this case is an ungula of a right circular cylinder. Figure 2.7.3.1.1.1-2 shows the definition of the crush, δ , as well as the pertinent angles of the ungula. The volume is found from the following series of calculations:

$$\theta = \cos^{-1} \left(\frac{R - 1.24\delta}{R} \right) = 38.51^\circ$$

$$\begin{aligned} H &= 1.7\delta = 9.35 \text{ in.} \\ c &= R - 1.24\delta = 27.93 \text{ in.} \\ a &= R \sin \theta = 20.87 \text{ in.} \end{aligned}$$

$$V = \frac{H \left[aR^2 - \frac{1}{3}a^3 - R^2c\theta \right]}{R - c} = 728 \text{ in.}^3$$

where: θ = half the included angle of the ungula on the impact limiter base

H = the height of the ungula on the outer cylindrical surface

c and a are intermediate parameters

R = impact limiter foam radius, 34.75 in.

V = crushed volume, in.³

δ = 5.5 in.

$$1.7 = \frac{1}{\sin 36^\circ}$$

$$1.24 = \frac{1}{\sin 54^\circ}$$

The footprint area of contact is the upper surface (partial ellipse) of the ungula. It is found from the following:

$$A = \frac{\pi(1.7R)^2}{2} - R \left[(1.7R - 2.1\delta) \left[1 - \left(\frac{1.7R - 2.1\delta}{1.7R} \right)^2 \right]^{0.5} + 1.7R \sin^{-1} \left[\frac{1.7R - 2.1\delta}{1.7R} \right] \right] = 326 \text{ in.}^2$$

R and δ are as described above. The energy absorbed by the foam is then 548,640 in.-lb, which is the product of the plateau strength of the test foam of 755 psi and the crushed volume of 728 in.³ found above. The energy absorbed by the impact limiter shell is given below:

$$W_s = (M)(360 + \delta) - W_f = 2.959(10^6) \text{ in.-lb}$$

where: M = package weight, 8,600 lb

δ = 5.5 in.

W_f = 548,640 in.-lb

The average force per unit length of the impact limiter shell is given below:

$$f = \frac{W_s}{A} = 9.105 \text{ lb/in.}$$

As for the side drop damage, this value will be adjusted to reflect a conservative impact limiter shell temperature of 150 °F. The result is $0.826(9.105) = 7.531$ (lb/in). The following equation can now be solved for the maximum c.p. over corner crush deflection at maximum temperature conditions:

$$M(360 + \delta) = M(\delta) + sV(\delta)$$

These parameters are as defined above. Solving iteratively, the maximum crush deflection, δ , is 5.1 in.

The radial crush damage represents the most conservative case with respect to seal area

temperatures, and is therefore used for all HAC thermal analyses. The thermal analyses also incorporate thermal shield damage, which is modeled as a 5-in. diameter impression with a depth equal to one-half of the fiberglass insulation thickness, or 1.3 in., which is conservatively greater than the actual damage described in Section 2.7.6.2.

2.7.3.1.1.2 Payload Reconfiguration Effects: For the post-HAC free drop payload reconfiguration, the worst case will conservatively be taken as release of all 18 aeroshells from a GPHS RTG into the ICV. Though the free drop orientations assumed for worst-case impact limiter damage do not induce the largest impact loadings on the package, it will be conservatively assumed that all aeroshells will be released into the interior of the package independent of free drop orientation. Consequently, worst case thermal response of the packaging will depend on the post-impact distribution of the aeroshells. This will hinge in turn on the post-impact orientation of the package.

There are only two credible orientations that the package may come to rest on the regulatory flat, essentially unyielding surface, following the HAC free drop and puncture bar tests. These are as follows: (1) upright, resting on the impact limiter, and (2) on its side, resting simultaneously on the side of the impact limiter and the upper and ICV torispherical head/lid assembly. All other orientations would be unstable. Both orientations are evaluated to determine the effect of payload reconfiguration on maximum seal temperature and differential thermal distortion in the seal area. Though an upright package would not normally leave the bottom of the impact limiter exposed to the HAC fire, the entire impact limiter will conservatively be subjected to the HAC fire.

To conservatively estimate the effects of heat transfer from the aeroshells to the package structure, the following assumptions will be made for post free drop aeroshell distribution:

- For the package bottom down orientation, the aeroshells will be distributed uniformly around the perimeter of the shipping rack barrier plate, in positions nearest the ICV seal region; this distribution will be referred to as "circumferential."
- With the package on its side, the aeroshells will be distributed axially along one side of the package, extending from the top of the vertical portion of the shipping rack barrier plate to the juncture with the ICV torispherical head; this distribution will be referred to as "axial."

In addition to these two cases, an extremely conservative, unstable post-free drop orientation will be evaluated. Although there is no credible basis for such a case, it will be assumed that all aeroshells will collect in one corner at the lower end of the ICV, and on top of the shipping rack (with some aeroshells in contact with the ICV wall above the shipping rack barrier plate), in as compact a mass as the random orientation of their geometries will allow. Simplified scale model testing indicated that the resulting mass of aeroshells would exhibit an approximately 50% void volume. This distribution will be referred to as "corner (or unguled)." This arbitrary geometric assumption will tend to concentrate the aeroshell heat generation into a minimum volume, thus artificially intensifying the effects of payload reconfiguration on seal temperatures and seal area thermal expansion/distortion.

For additional conservatism, all HAC thermal analysis cases will assume that the GPHS RTG structure has also broken off its mount, and has come to rest in a position that either partially or completely blocks radiative and convective heat transfer from the aeroshells into the interior of the package (depending on final package orientation).

2.7.3.1.1.3 Combined Effects For even greater conservatism, it will be assumed that the reconfigured payload, the impact limiter damage, and the thermal shield damage will be circumferentially coincident during the HAC fire.

The effects of maximum seal area differential thermal expansion and HAC free drop-induced seal area deformations (if any) will also occur simultaneously at the same location on the containment seal for each containment vessel. The compounding of conservative assumptions will ensure that the worst-case reduction in seal compression during the entire course of the HAC sequence will never result in residual seal compressions less than those confirmed as acceptable by prior testing. See Section 4.3.2 for additional detail.

A summary of thermal HAC load cases is given in Table 2.7.3.1.1.3-1. All load cases combine maximum HAC free drop and puncture damage with the HAC fire event. The HAC load cases evaluated comply with the load combination requirements of 10 CFR 71 and Regulatory Guide 7.8 by imposing minimum and maximum ambient temperature conditions (-20 and 100 °F, respectively) with package temperatures arising from maximum payload heat generation. Zero payload heat generation and minimum ambient temperature result in essentially uniform package component temperatures. The structural and containment effects of this load case are insignificant and are not included in the summary table. The nonregulatory combination of minimum ambient-maximum payload temperatures was also imposed. This latter load case was evaluated because of greater potential for inducing maximum differential thermal expansions in the package components. Consistent with 10 CFR 71, solar loading is ignored before, during, and after the HAC fire.

TABLE 2.7.3.1.1.3-1 Summary of Thermal HAC Load Cases

Condition	Case 1	Case 2	Case 3	Case 4	Case 5	Case 6
Ambient temperature (°F)	100	-20	100	-20	100	-20
Damaged payload configuration	Circum.	Circum.	Axial	Axial	Corner	Corner
Damaged impact limiter configuration	Side crush	Side crush	Side crush	Side crush	Side crush	Side crush

2.7.3.1.2 Sources of Pressure Internal pressure arising from the HAC fire has been developed by the perfect gas law, and includes decomposition gas of the electrical cable insulation. As discussed in Section 2.6.1.1, the pressure within the ICV under NCT will result from the following:

- The initial charge of helium, 20 psia in each vessel at the time of loading
- Possible leakage from the GPHS RTG initial charge
- Decay of heat source radionuclides

The resulting pressure was calculated to be 29.7 psia at the no-coolant condition gas temperature of 354 °F. The potential off-gas from the thermal decomposition of the GPHS RTG payload electrical cable insulation under the HAC fire must be added to this pressure. Electrical cable off-gas was not added under NCT because the cable is "baked out" before use.

The GPHS RTG payload electrical cable insulation is a silicone rubber, containing silicon, oxygen, and hydrogen. The decomposition products will be inert silicon dioxide and hydrogen gas.

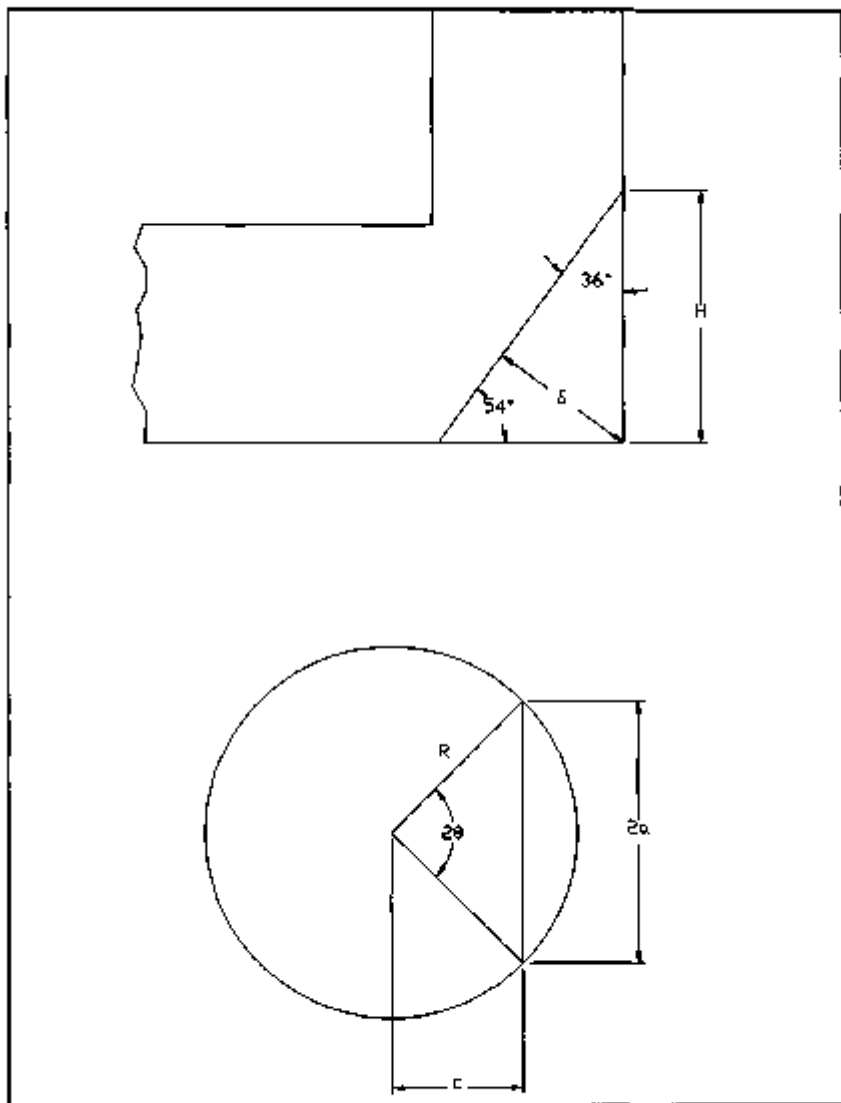


FIGURE 2.7.3.1.1.1-2. Impact Limber Crush Relationships.

H₂. Each of the two 80.0-in. long electrical cables contains one pound of rubber for a total of two pounds, all of which is assumed to decompose. The basic building block of the compound will be a monomer consisting of one silicon atom, one oxygen, and two hydrogen. The weight of one lb-mole of the monomer can be found from the following breakdown:

$$\begin{aligned} 1 \times 28 &= 28 \text{ lb of silicon (Si) per lb-mole of monomer} \\ 1 \times 16 &= 16 \text{ lb of oxygen (O) per lb-mole of monomer} \\ 2 \times 1 &= 2 \text{ lb of hydrogen (H) per lb-mole of monomer} \end{aligned}$$

This gives a sum of $28 + 16 + 2 = 46$ lb per lb-mole of monomer. Because there are 2 pounds of rubber, there are:

$$\frac{2}{46} = 0.043 \text{ lb-mole of rubber present in the ICV}$$

Because it takes 2 lb-moles of hydrogen to make one lb-mole of H₂, there is one lb-mole of H₂ per lb-mole of rubber, or the following:

$$1 \times 0.043 = 0.043 \text{ lb-mole of H}_2 \text{ gas that will be released in the worst case.}$$

From Appendix 2.10.7, Table 2.10.7.2-2, HAC case 5, the maximum ICV gas temperature from the worst-case reconfiguration assumption is 840 °F. From the perfect gas law, the pressure of the added gas is given below:

$$p = \frac{nRT}{V} = 27.0 \text{ psia}$$

where:

- $n = 0.043$ lb-mole
- $R = 10.74$ psia-ft³/lb-mole-°R
- $T = 840 + 460 = 1300$ °R
- $V = 22.25$ ft³ from Section 2.6.1.1.1.

In Section 2.6.1.1, the existing gas in the ICV under NCT had a pressure of 29.7 psia at a temperature of 354 °F. When raised to a temperature of 840 °F, the pressure can be found from the ratio of absolute temperatures to be as follows:

$$p_{HAC} = p_{NCT} \frac{(840+460)}{(354+460)} = 47.4 \text{ psia}$$

where:

- p_{HAC} = the HAC ICV partial pressure
- p_{NCT} = the NCT ICV pressure, 29.7 psia.

The total pressure within the ICV during the HAC event is the sum of the pressure of the pre-existing gas and the off-gas:

$$p_{tot} = 47.4 + 27.0 = 74.4 \text{ psia.}$$

In Section 2.6.1.3, the gas in the OCV under NCT had a pressure of 26.3 psia at 285 °F. When raised to 852 °F (OCV internal gas temperature for HAC case 5, Table 2.10.7.2-2), the OCV pressure can be found from the ratio of absolute temperatures to be as follows:

$$p_{HAC} = p_{NCT} \frac{1852 + 460}{1285 + 460} = 46.3 \text{ psia}$$

where: p_{HAC} is the HAC OCV pressure
 p_{NCT} is the NCT OCV pressure, 26.3 psia

Off-gassing is not a concern in the OCV, because no component generates gas during the HAC fire. Pressure external to the OCV is atmospheric ambient, or 14.7 psia. A summary of HAC load cases and resulting maximum containment vessel gas temperatures is presented in Table 2.7.3.1.2-1. Corresponding vessel pressures are summarized in Table 2.7.3.1.2-2.

For conservatism, the maximum pressure differentials of the ICV and OCV, augmented by 10%, will be used to evaluate each vessel in all HAC load cases. For the ICV, this will be $(74.4 - 46.3)(1.1) = 30.9$ psid, and for the OCV this will be $(46.3 - 14.7)(1.1) = 34.8$ psid.

TABLE 2.7.3.1.2-1. Summary of HAC Containment Vessel Gas Temperatures.

Condition	Case 1	Case 2	Case 3	Case 4	Case 5	Case 6
Ambient temperature (°F)	100	-20	100	-20	100	-20
Damaged payload configuration	Circum.	Circum.	Axial	Axial	Corner	Corner
ICV internal gas temperature (°F)	836	778	747	684	840	762
OCV internal gas temperature (°F)	849	798	851	796	852	799

TABLE 2.7.3.1.2-2. Summary of HAC Containment Vessel Pressures.

Condition	Case 1	Case 2	Case 3	Case 4	Case 5	Case 6
ICV internal gas pressure (psia)	74.3	72.2	71.0	68.7	74.1	72.3
OCV internal gas pressure (psia)	46.2	44.3	46.3	44.4	46.3	44.4
ICV external gas pressure (psia)	46.2	44.3	46.3	44.4	46.3	44.4
OCV external gas pressure (psia)	14.7	14.7	14.7	14.7	14.7	14.7

2.7.3.2. Thermal Expansion. The containment vessel HAC relative differential expansion analysis is similar to that for the NCT, which was covered in Section 2.6.1.2. Much of that section is repeated here, with appropriate substitutions reflecting any differences between the NCT and HAC cases.

A radial and axial clearance is maintained between both the ICV and OCV bell during the HAC fire event, and thus, no vessel loading because of relative differential thermal expansion will occur. This is because the OCV reaches higher temperatures and expands away from the ICV. When a steady state condition has been reached after the HAC fire, however, the relative

temperature difference is reversed, and the ICV becomes the warmer of the two vessels. Because, after the top-down HAC free drop, the heads of the two vessels are likely to be in contact, the fact that the OCV is cooler than the ICV indicates an axial interference will exist between the vessels. However, the interference is small, as will now be demonstrated. Further, because the interference occurs in the center of the heads, little force is transferred to the vessel walls or seal areas.

Both the radial and axial thermal expansion of each vessel will be dominated by the temperature of the cylindrical walls, which are thermally modeled in each case by four nodes: 210 to 240 in the ICV, and 310 to 340 in the OCV. As shown in Figure 3.4.1-2, nodes 210 and 310 are located 5.86 in. below the top of the coolant jacket. The corresponding measurements for the other node pairs are as follows: nodes 220 and 320, 20.58 in.; nodes 230 and 330, 34.30 in.; and nodes 240 and 340, 43.86 in. A third dimension is added by the inclusion of four circumferential segments, A through D, each having identical nodal geometric relationships. The radial differential thermal expansion between the two vessels is found by subtracting the radial thermal expansion of the OCV from that of the ICV at each of the four elevations discussed above. The residual radial clearance is found by subtracting this result from the initial minimum manufactured clearance. The single temperature value corresponding to each elevation is a weighted average of the temperatures from each circumferential segment, using temperatures from Section 3.5.5. The weighting factor is based on the size of the angular segments, as given in Table 2.7.3.2-1.

TABLE 2.7.3.2-1. Segment Weighing Factors.

Segment	HAC cases 1, 2, 5, and 6		HAC cases 3 and 4	
	Included angle (°)	Factor	Included angle (°)	Factor
A	22.5	0.125	15	0.083
B	45	0.250	30	0.167
C	67.5	0.375	90	0.500
D	45	0.250	45	0.250

For example, for HAC case 6 (unguided rubble configuration, -20 °F ambient, post-HAC fire steady state), the segment sizes are (see Figure 3.5.2-3): 22.5°, 45°, 67.5°, and 45° for segments A through D, respectively. The half-symmetry total angle is 180°. The segment A weighing factor is therefore 22.5/180 = 0.125. The other three weighing factors for segments B, C, and D are 0.25, 0.375, and 0.25, respectively. From Section 3.5.5, the temperatures of segments A through D at the node 240 (ICV) elevation are 443, 337, 186, and 153 °F, respectively. The weighted average temperature is given below:

$$T_{\text{avg}} = 0.125(443) + 0.25(337) + 0.375(186) + 0.25(153) = 240 \text{ °F} \quad (\text{ICV})$$

The corresponding temperatures for the OCV at node 340 elevation are 307, 236, 129, and 123 °F. The weighted average temperature for the OCV is given below:

$$T_{\text{avg}} = 0.125(307) + 0.25(236) + 0.375(129) + 0.25(123) = 177 \text{ °F} \quad (\text{OCV})$$

From Table 2.3-1, the coefficient of thermal expansion for Type 304L at temperatures of

240 °F and 177 °F are $8.67(10^{-6})$ and $8.73(10^{-6})$ in/in/°F, respectively. The nominal outside diameter of the ICV is 35.5 in, and the nominal inside diameter of the OCV is 35.88 in. The minimum initial manufactured radial clearance is 1/32 in. The residual radial clearance is given below:

$$AC_{rr} = 0.031 - 0.6[35.5(240 - 70)8.67(10^{-6}) - 35.88(177 - 70)8.73(10^{-6})] = 0.021 \text{ in}$$

Residual radial clearances at other locations and for all HAC load cases are presented in Table 2.7.3.2-3.

The axial thermal differential expansion between the two vessels is found by subtracting the axial thermal expansion of the OCV from that of the ICV using the average temperature of the four stations together with the four segments described above. The average of the four stations in one segment is a straight average, and the average of the four segments uses weighted inputs as described above. For example, for HAC case 6 (same post-HAC fire steady state condition as above), the temperatures and resulting averages are given in Table 2.7.3.2-2.

TABLE 2.7.3.2-2 HAC Case 6 (Post-HAC Fire Steady State) Temperature Averages, °F

ICV segments					OCV segments				
Nodes	A	B	C	D	Nodes	A	B	C	D
210	185	192	191	188	310	149	140	145	142
220	222	208	193	187	320	174	162	148	143
230	341	272	171	178	330	276	218	132	132
240	443	337	185	153	340	307	238	129	123
Segment averages	300	262	180	177	Segment averages	226	191	139	135
Weighting factor	0.125	0.25	0.375	0.25	Weighting factor	0.125	0.25	0.375	0.25
Overall ICV average temperature				212	Overall OCV average temperature				162

From Table 2.3.1, the coefficient of thermal expansion for Type 304L at 212 and 162 °F are $8.81(10^{-6})$ and $8.70(10^{-6})$ in/in/°F, respectively. The OCV inside height of 62.9 in may be conservatively used as a length for both vessels. The minimum initial axial manufactured clearance is 1/16 in. The maximum potential axial interference is given below:

$$AC_{ax} = 0.0 - 62.9[(212 - 70)8.81(10^{-6}) - (162 - 70)8.70(10^{-6})] = -0.029 \text{ in}$$

Residual axial clearances for all HAC load cases are presented in Table 2.7.3.2-3.

TABLE 2.7.3.2-3. Summary of HAC Differential Expansions.

Condition	Case 1	Case 2	Case 3	Case 4	Case 5	Case 6
Residual axial clearance (in.)	-0.026	-0.028	-0.018	-0.018	-0.028	-0.029
Residual radial clearance (in.)						
Elevation 210 and 310	0.025	0.024	0.026	0.025	0.025	0.024
Elevation 220 and 320	0.025	0.024	0.026	0.025	0.025	0.024
Elevation 230 and 330	0.024	0.023	0.026	0.024	0.024	0.023
Elevation 240 and 340	0.021	0.021	0.030	0.030	0.022	0.021

The worst-case radial condition is a clearance reduction of 32% (HAC case 6, elevation 240 and 340), and the worst case axial condition is a clearance reduction of 47% (also HAC case 6).

The HAC bolt differential expansion and stress analysis is very similar to that for the NCT. Much of that section is repeated here, with appropriate substitutions reflecting any differences between the NCT and HAC cases. The differential thermal stress values were determined from the ANSYS finite element models of the ICV and OCV presented in Appendices 2.10.12 and 2.10.8 respectively. Because of the potential for payload reconfiguration and subsequent nonaxisymmetric thermal loading, the ICV was modeled as a half-symmetry three-dimensional (3-D) representation. A 2-D OCV model is considered adequate for the HAC cases primarily because the controlling thermal condition for the OCV is radiation from the HAC fire, which is assumed to be totally engulfing and constitutes a uniform radiative input of relatively large magnitude. In addition, unlike the ICV, the OCV does not have concentrated heat sources applied directly to its interior. As further confirmation of the adequacy of an axisymmetric model, a 3-D model of the OCV was made for the segment of the OCV where the impact limiter damage and damaged payload coincide, and where flange distortion is greatest. As detailed in Appendix 2.10.13, the 2-D representation is conservative for both the OCV closure bolt load and flange distortion. For each HAC case of Table 2.7.3.1.1.3-1, temperatures from the thermal analysis of Section 3.6.5 are applied to the structural finite element models, allowing the determination of thermal stress and distortion. In each HAC case, distortions are referenced to room temperature (70 °F), and the pressure established in Section 2.7.3.1.2 is included.

As noted in Section 2.3 the bolting material used for the containment assembly closure bolts (ASTM-A320, Grade L43 or ASTM A540, Grade B23, Class 1) has a different coefficient of thermal expansion than the material used for the vessel flanges (Type 304L). As the temperature of the vessels changes from the initial conditions, this leads to variations in closure bolt pre-load because of different amounts of thermal expansion/contraction in both the bolt and flange material. Because the expansion coefficient of Type 304L in the flange is greater than that of the closure bolt, an increase in flange material temperature will normally mean an increase in closure bolt clamping force and stress. A decrease in flange material temperature will normally mean a decrease in closure bolt clamping force and stress. In the analyses to follow, the actual temperatures of the closure bolts and flanges, as listed in Section 3.6.5 are used. The initial pre-load force in the closure bolts, because of assembly torque, is given below:

$$F_i = \frac{T}{Kd}$$

where: T = closure bolt torque, in.-lb
 K = 0.188, friction torque coefficient for cadmium plated threads²
 d = nominal closure bolt diameter, in.

Table 2.7.3.2-4 lists the closure bolt parameters along with pre-load force for the ICV and OCV closure bolts.

TABLE 2.7.3.2-4. Closure Bolt Parameters and Pre-load Force.

Location	d (in.)	Stress area (in. ²)	Length ^a (in.)	Torque (ft-lb)	Pre-load force (lb)
ICV	0.75	0.3300	1.49	250	21,505
OCV	1.25	0.9524	5.19	300	15,484

^aGrip length, defined as the length from the head to the midpoint of the threads.

The finite element models of the containment assemblies described in Appendices 2.10.12 and 2.10.6 include a model of the closure bolts as spars. They are given an initial stretch such that under nominal conditions (zero net pressure and uniform temperature) the load in the closure bolts is equal to the pre-load force values given in Table 2.7.3.2-4. During model post-processing, the resultant force in the spar is extracted. For the OCV, 2-D model, a single spar must represent all of the closure bolts. In this case, the force in each closure bolt is found from the following:

$$F_b = \frac{2\pi F_s}{n}$$

where: F_b = the individual closure bolt force, lb
 F_s = the spar load, lb/radian
 n = the number of closure bolts.

For the ICV 3-D model, the closure bolts are modeled individually, and their force may be directly extracted. In both cases, the stress in each closure bolt is given below:

$$\sigma_b = \frac{F_b}{A_s}$$

where: F_b = closure bolt force, lb
 A_s = stress area of closure bolt, in.²

The margin of safety is:

$$M.S. = -\frac{S_{ax}}{\sigma_y} - 1$$

The allowable stress, S_{ax} , for HAC is the lesser of S_y or $0.75S_u$, based on the ASME B&PV Code, Section III, Appendix F-1335.1, and is found from closure bolt temperature and Table 2.3-2. Table 2.7.3.2-6 summarizes load, stress, temperature, allowable, and margin of safety for the closure bolts for each HAC case in Table 2.7.3.1.1.3-1. As can be seen in Table 2.7.3.2-6, a positive margin of safety is maintained during HAC events for all closure bolts. Seal area distortions are addressed in Section 4.3.2 and are shown to remain within the limits necessary to ensure leaktight containment boundaries.

TABLE 2.7.3.2-6. Closure Bolt Load, Stress and Margin of Safety.

Case number	Bolt location	Bolt load (lb)	Bolt stress (psi)	Bolt temperature (°F)	Allowable bolt stress (psi)	Margin of safety
1	ICV	23,856	72,594	262	115,500	+0.59
	OCV	66,911	76,255	342	87,500	+0.25
2	ICV	22,588	68,448	154	115,500	+0.68
	OCV	70,987	74,536	242	87,500	+0.17
3	ICV	24,636	74,652	284	115,500	+0.55
	OCV	66,856	76,197	368	87,500	+0.25
4	ICV	23,201	70,306	159	115,500	+0.64
	OCV	70,880	74,423	273	87,500	+0.18
5	ICV	23,986	72,712	267	115,500	+0.58
	OCV	68,730	72,165	343	87,500	+0.21
6	ICV	22,672	68,400	166	115,500	+0.69
	OCV	72,655	76,286	243	87,500	+0.15

^aBecause the ICV thermal model did not specifically include closure bolts, the closure bolt temperature for structural purposes is conservatively taken as the temperature of the ICV flange (thermal node 250) at the warmest circumferential location. The OCV closure bolts were explicitly modeled, and their temperatures listed above correspond to the warmer of thermal node 353 (shank portion of bolt) or thermal node 355 (thread portion of bolt, again at the warmest circumferential location). The transient location is the time at which peak wall temperature occurs: 30 minutes after the start of the HAC fire for the OCV and 40 minutes for the ICV.

According to Reference 23, the preload force may vary by up to $\pm 30\%$ for a given applied torque value. Therefore, the cases having the lowest bolt margin of safety (Case 3 for the ICV and Case 6 for the OCV) were rerun, using a pre-stretch in the elements representing the bolts of 130% of the nominal value. This represents the maximum possible load in the bolts. The results are shown in Table 2.7.3.2-6, where the relatively large margins of safety demonstrate that the bolt stress is still well below yield, even when accounting for a large scatter in the bolt preload force.

Table 2.7.3.2-6. Closure Bolt Load and Stress Considering Pretold Force Variation (HAC)

Load case (HAC)	Bolt location	Bolt load (lb)	Bolt stress (psi)	Bolt temp. (°F)	Yield strength (psi)	Margin of safety on yield
5	ICV	30,866	93,594	264	137,028	+0.46
6	OCV	65,740	72,178	243	87,561	+0.35

2.7.3.3 Stress Calculations. Allowable stress limits for HAC events are available from Table 2.1.2-1 and are based on ASME B&PV Code, Appendix F (Service Level D) limits. Per that table, closure bolt stresses and primary stresses in the vessel structures resulting from the HAC thermal event must be determined and shown to remain within stated allowable limits. As indicated by Table 2.1.2-1, there are no limits applicable for secondary stresses resulting from HAC events. Consequently, thermally induced secondary stresses do not need to be quantified.

The closure bolt thermal distortion stresses (including pre-load and pressure effects) have been calculated in the preceding section and were shown to remain within allowable limits. The remainder of this section, therefore, focuses on vessel primary stresses, i.e., those resulting from worst case internal pressures occurring during the HAC thermal event.

The finite element model results for internal pressure only (NCT load cases ICV-P and OCV-P from Section 2.6.1.3) will be scaled to derive the primary stress under HAC events. These two NCT load cases used 10 psid internal pressure and 26.5 psid internal pressure, respectively, and thus, the results for the HAC maximum pressure is found by scaling the ratios of the HAC pressure differential developed in Section 2.7.3.1.2:

$$\frac{30.9}{10.0} = 3.09 \text{ for the ICV}$$

and,

$$\frac{34.8}{26.5} = 1.313 \text{ for the OCV}$$

Tables 2.7.3.3-1 and 2.7.3.3-2 summarize the stress results for membrane and membrane plus bending stress for the ICV and OCV. The worst-case containment boundary temperatures correspond to HAC case 3. The peak ICV is 1190 °F at thermal node 210, and the peak OCV is 1249 °F at thermal node 304. Temperatures are taken from Section 3.6.5 and are conservatively rounded up to 1200 °F for the ICV and to 1300 °F for the OCV.

TABLE 2.7.3.3-1. Summary of ICV Stress Intensities and Margins of Safety.

Case No.	Stress location	Stress category	Maximum stress intensity (psi)	Temp. (°F)	Allowable stress intensity (psi)	Margin of safety
ICV-P	Head crown midshell	P_m	3,217 (elem 145)	1,200	27,405 (0.7 S_u)	+7.52
	Head crown shell surface	$P_L + P_m$	8,041 (elem 145)	1,200	39,150 (S_u)	+5.48
	Knuckle midshell	P_L	3,377 (elem 144)	1,200	39,150 (S_u)	> +10

TABLE 2.7.3.3-2. Summary of OCV Stress Intensities and Margins of Safety.

Case No.	Stress location	Stress category	Maximum stress intensity (psi)	Temp. (°F)	Allowable stress intensity (psi)	Margin of safety
OCV-P	Head crown midshell	P_m	1,425 (elem 121)	1,300	21,990 (0.7 S_u)	> +10
	Head crown shell surface	$P_L + P_m$	2,189 (elem 122)	1,300	31,400 (S_u)	> +10
	Knuckle midshell	P_L	2,418 (elem 119)	1,300	31,400 (S_u)	> +10

2.7.3.4 Comparison with Allowable Stresses. As discussed in Section 2.1.2 stress limits are in accordance with Regulatory Guide 7.6, and load combinations are in accordance with Regulatory Guide 7.8. From Table 2.1.2-1, for HAC, the allowable stress intensity for primary membrane stress is the lesser of $2.4S_m$ or $0.7S_u$. For both vessels, the value of $0.7S_u$ is the lesser, and is listed as the allowable stress intensity at temperature for P_m in the tables above. From Table 2.1.2-1, the allowable stress intensity for both primary membrane plus bending stress ($P_L + P_m$) and local primary membrane stress (P_L) is the lesser of $3.6S_m$ or S_u . For both vessels, S_u is the lesser, and is listed as the allowable stress at temperature for ($P_L + P_m$) and P_L in the tables above. For both vessels, the critical stress locations are in the head, where temperatures are the greatest. Minimum margins of safety are presented in the last column of Tables 2.7.3.3-1 and 2.7.3.3-2, and all margins of safety are positive. Thus, the design criteria are satisfied.

Closure bolt, bell flange, and base responses to the HAC thermal event have also been studied to ensure that the leaktight capability of the ICV and OCV containment O-rings is not compromised. Closure bolt stresses were addressed in Section 2.7.3.2. Section 4.3.2 addresses maximum seal area distortions and residual compressions for the ICV and OCV containment O-rings. Figures 2.10.12-12 and 2.10.8-13 present worst-case stress intensities in the vicinity of the O-rings for the ICV and OCV. Based on the following observations relating to those analyses, it is concluded that the HAC thermal event will not compromise the leaktight capability of the O-rings. First, the closure bolts remain elastic for all potential worst-case HAC thermal events (see Section 2.7.3.2). This ensures that a positive clamping force will always exist between mating bell flanges and bases. Second, O-ring seal area distortions and corresponding residual compressions for containment O-rings remain within the limits necessary to ensure O-ring leaktight performance (see Section 4.3.2). Third, although there are no limits placed on HAC secondary

stresses (see Section 2.7.3.3), a review of Figures 2.10.9-13 and 2.10.12-12 indicate that secondary stresses caused by the HAC thermal event remain within corresponding NCT allowable limits.

2.7.4 Immersion

The criticality evaluation presented in Section 6.0 assumes optimum hydrogenous moderation of the contents. Thus, the effects and consequences of water in-leakage are conservatively addressed.

2.7.5 Immersion - all Packages

For the RTG Transportation System Package, the effect of immersing an undamaged specimen in 50 ft of water is equivalent to imposing an external pressure of 21 psig on the OCV. Although the effect of immersion on package temperatures is expected to be equivalent to that of active cooling of the package, the component temperatures used are conservatively taken from NCT case 1 of Table 2.6.1-1, which lists maximum regulatory temperatures.

Initial acceptance tests will give assurance that the OCV will withstand the 21 psig HAC external pressure. Specifically, the Fabrication Verification Leak Test subjects the OCV boundary to a full internal vacuum, or the equivalent of a 14.7 psig external pressure. A 14.7 psig external pressure can therefore be considered to be a minimum acceptable condition for external pressure as confirmed by testing. Per ASME B&PV Code Case N-284, the factor of safety for NCT is 2.0, whereas for HAC the applicable factor of safety is 1.34. This difference in factors of safety implies that, for HAC, an acceptable external pressure would be a minimum of $(14.7)(2.0/1.34) = 21.9$ psig.

To confirm structural stability, buckling analyses are performed on the relevant structural containment components of both the OCV and ICV. The results of these analyses, which demonstrate large margins of safety, indicate that buckling will not occur.

The immersion pressure differential is formed by conservatively assuming an internal pressure of zero, and therefore, a pressure of 21 psig is applied externally to both vessel cylindrical shells. The ICV cylindrical shell has a smaller diameter, shorter length and a greater wall thickness than that of the OCV. Therefore, it will be less vulnerable to structural instability than the shell of the OCV, and an indication of structural stability in the OCV shell automatically implies structural stability in the ICV shell under the same applied external pressure loading and at the same temperature.

The OCV shell is assumed to be 350 °F, which is conservatively higher than the temperature for both the ICV and OCV shells, considering the maximum wall temperature from Table 2.10.7.1-2 of Appendix 2.10.7. For the basic OCV shell, the hoop and axial compressive stresses associated with the 21 psig external pressure are calculated below:

$$\sigma_c = \frac{PR}{2t} = 362.0 \text{ psi}$$

$$\sigma_p = \frac{PR}{t} = 764.0 \text{ psi}$$

where: σ_h = hoop compressive stress
 σ_p = axial compressive stress
 P = external pressure = 21 psig
 R = shell mean radius = 18.18 in.
 t = shell thickness = 0.50 in.

Residual plasticity reduction factors from Section 1510 of ASME B5PV Code Case N-264 are equal to unity. Hence, inelastic buckling checks are not required. Consequently, all that the buckling analysis entails is determination of theoretical buckling stress values. The results can then be compared to the above actual, calculated stress values, with capacity reduction factors and appropriate factors of safety (FS = 1.34 for HAC) applied. If the theoretical buckling stresses are greater than the adjusted actual stress values, then buckling will not occur.

From Section 1511 of Code Case N-264, the appropriate capacity reduction values are determined to be as follows:

$$\sigma_{ax} \text{ (axial compression)} = 0.207$$

$$\sigma_{hx} \text{ (hoop compression)} = 0.800$$

Adjusted actual stress values are determined as follows:

$$\sigma_{pa} = \frac{\sigma_p \times FS}{\sigma_{ax}} = 2,472.9 \text{ psi}$$

$$\sigma_{ha} = \frac{\sigma_p \times FS}{\sigma_{hx}} = 1,279.7 \text{ psi}$$

where: σ_{pa} = adjusted axial compressive stress

σ_{ha} = adjusted hoop compressive stress.

From Section 1712 of Code Case N-264, the theoretical buckling values for an effective OCV shell free length of 56 in. are determined to be as follows:

$$\sigma_{axt} \text{ (axial compression)} = 444,914 \text{ psi}$$

$$\sigma_{hxt} \text{ (hoop compression)} = 37,725 \text{ psi}$$

Comparison of results indicates the following:

$$M.S. \text{ (axial compression)} = \frac{444,914}{2,159.8} - 1 = + \text{ Large}$$

$$M.S. \text{ (hoop compression)} = \frac{37,725}{1,278.7} - 1 = + \text{ Large}$$

Consequently, buckling of the OCV shell will not occur.

The buckling analysis of the torispherical heads is based on the ASME B&PV Code, Section III, Subsection NE, Paragraph NE-3133.4(e). This section applies for Design Condition and Level A and B loadings. Because the pressure loading due to immersion can be classified as Level D, the allowable buckling stress and, therefore, the allowable pressure, can be increased by 150% per Paragraph NE-3222.2. The basic calculational procedure is outlined below:

1. Calculate factor A using the following formula:

$$A = \frac{0.125}{(R/T)}$$

where: R = crown inside radius
 T = head thickness

2. Read value of factor B from Figure 2.7.6-1 (Figure VII-1102-4 of the above-referenced Code section)
3. Calculate the maximum allowable pressure, P_a , using the following formula:

The dimensions for the ICV and OCV heads are summarized in Table 2.7.5-1.

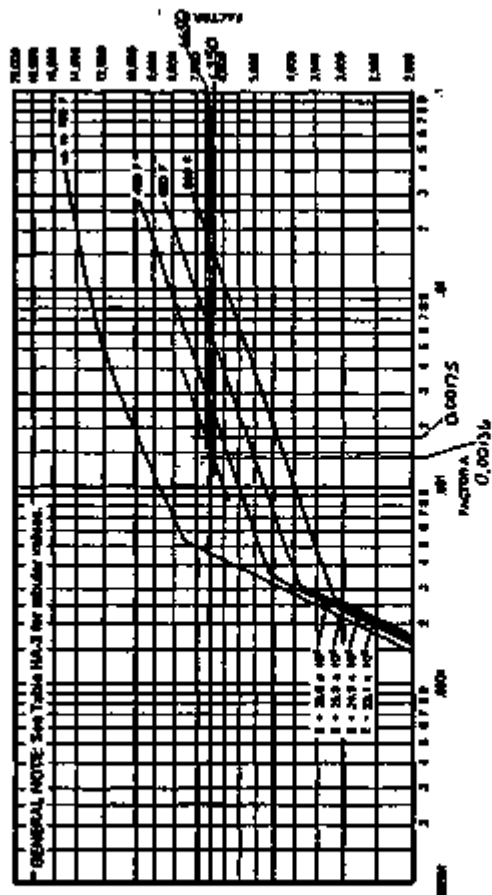


FIG. HA-3 CHART FOR DETERMINING SHELL THICKNESS OF COMPONENTS UNDER EXTERNAL PRESSURE WHEN CONSTRUCTED OF AUSTENITIC STEEL (304-316 MAXIMUM CARBON, TYPE 304L DROTE (1))

FIGURE 2.7.5-1. ASME B&PV Code, Section III, Part D, Figure HA-3.

$$P_s = \frac{1.50B}{(R/T)}$$

TABLE 2.7.5-1. Torispherical Head Geometric Parameters.

Vessel	Inside radius (in.)	Thickness (in.)	R/T
ICV	35.00	0.38	92.10
OCV	36.76	0.60	71.60

The allowable pressure for the ICV torispherical head will now be calculated per the procedure outlined above.

$$1. A = \frac{0.125}{(R/T)} = \frac{0.125}{92.10} = 0.00136$$

or

$$2. B = 6,350 \text{ (see Figure 2.7.6-1)}$$

Note: The ICV maximum head temperature is taken as 350 °F (conservatively in excess of the value given for thermal node 200 from Table 2.10.7.1-2, Appendix 2.10.7). The corresponding value for "B" is interpolated between temperature curves labeled "400 °F" and "up to 100 °F."

$$3. P_s = \frac{1.50B}{(R/T)} = \frac{(1.50)(6,350)}{92.10} = 103.4 \text{ psi}$$

Thus, the margin of safety for the ICV torispherical head is given below:

$$M.S. = \frac{P_s}{P} - 1 = \frac{103.4}{21.0} - 1 = 3.92$$

Following the same procedure for the OCV head yields the following results:

1. $A = 0.00176$
2. $B = 6,650$

The OCV maximum head temperature is taken as 350 °F (conservatively in excess of the value given for thermal node 300 from Table 2.10.7.1-2, Appendix 2.10.7). The corresponding value for B is interpolated between temperature curves labeled "400 °F" and "up to 100 °F."

3. $P_s = 140 \text{ psi}$

The margin of safety for the OCV torispherical head is given below:

The margins of safety on buckling are all positive.

$$M.S. = \frac{F_2}{P} - 1 = \frac{140.0}{21.0} - 1 = + 5.67$$

2.7.6 Summary of Damage

Two full-scale prototypes of the package were subjected to a series of NCT 4-ft free drops, HAC 30-in. free drops, and HAC 40-in. puncture drops. The two drop test series are described in Appendix 2.10.9 and summarized in Sections 2.7.1 and 2.7.2. A description of the first and second Certification Test Articles (CTA-1 and CTA-2), the simulated payload, and the drop pad, and details of test results, are given in Appendix 2.10.15. Subsequent to all tests, the CTA was leak-tight, having an integrated leakage rate of less than $1(10^7)$ acc/sec, air, for both ICV and OCV. The following paragraphs summarize the results of the drop testing.

2.7.6.1 Summary of Free Drop Damage. A series of five free drops was performed from a height of 4 ft followed by the same series from 30 ft. As a result of problems encountered during the first certification test series (which used CTA-1), a new certification test article, designated CTA-2, was fabricated. All of the 4-ft and 30-ft free drops were repeated with CTA-2 and these results are summarized in the following paragraphs. The results of the 4-ft drops (corresponding to NCT) are described in Section 2.6.7. In general, the only criteria for the 4-ft free drops is that the damage not compromise the ability of the package to survive subsequent 30-ft free drops. This was true in each case. The package deformations resulting from the 30-ft free drops were scaled-up versions of the damage resulting from 4-ft free drops, and subsequent to all testing (including punctures), the success criteria of Section 2.7 were satisfied as follows:

1. Containment was maintained. The second certification test consisted of a series of four sets of tests as described in Appendix 2.10.15. After each set of tests, the OCV and ICV O-ring seals were leakage rate tested and no detectable leakage was found. At the end of all of the drop tests, the entire OCV and ICV containment boundaries (sum of the leakage rates for the seals and for the structural boundary) were leakage rate tested. The final containment boundary leakage rate of the CTA-2 vessels was $4.35(10^4)$ acc/sec (air) for the OCV and $8.3(10^4)$ acc/sec (air) for the ICV, which are less than the maximum leakage rate for a definition of leak tightness of $1(10^7)$ acc/sec (air).*** Additionally, the deformations in the seal area of each vessel were below levels which would, when added to thermal distortions resulting from the HAC fire event, compromise the ability of the seals to maintain leak tight containment. The evaluation of seal area distortions and the relationship to containment is discussed in Section 4.3.2.
2. Biological shielding was maintained, as demonstrated by the relatively small overall deformations of CTA-2, and the extremely conservative assumptions made in the shielding analysis of Section 5.0.
3. A subcritical payload was maintained, as demonstrated by the relatively small overall deformations of CTA-2, and the extremely conservative assumptions made in the criticality analysis of Section 6.0.

*** The leakage rates measured by the mass spectrometer leak detector were in terms of helium and were 1.13×10^{-4} acc/sec for the OCV and 2.15×10^{-4} acc/sec for the ICV, and were converted to a leak rate of air by dividing the helium rate by 2.6.

Specific results of HAC free drop testing follows. After each HAC free drop, the OCV closure bolts exhibited average residual torques that varied from 223 to 252 ft-lb. Drope are identified in Section 2.7.1.4. Photographs are presented in Appendix 2.10.15.

1. The bottom-down, near-vertical free drop (CTA-2 test No. 2) was intended to demonstrate impact limiter retention by developing a large separation moment between the impact limiter and the package body. The angle of impact with the ground and the circumferential orientation of the package to the impact point was designed to maximize limiter attachment bolt forces. External limiter deformations were small. The result of this free drop was complete retention of the limiter with no visible change in position on the package body. Two of the eight impact limiter attachment bolt torques, however, fell to negligible or zero values. This is considered acceptable, since the purpose of the attachment bolts is to retain the position of the impact limiter, which was achieved. Examination of the attachment bolts subsequent to testing showed small amounts of deformation and stretching (<0.025 in.), particularly in the "necked down" region of the bolt shank. This feature was included specifically to enhance the bolts' ability to absorb energy without failure.
2. The bottom-down, e.g. over corner free drop (CTA-2 test No. 5) caused the impact limiter corner to crush 5.5 inches, which extrapolates to 6.1 in. in the warm foam condition (this calculation is carried out in Section 2.7.3.1.1.1(B)). Because the original distance of foam along the line of crush is 11 in., the localized maximum uniaxial foam strain, in the worst case, would be $6.1/11 = 55\%$. This is acceptable and demonstrates the ability of the impact limiter to protect the package from bottoming-out when all of the free drop energy is directed at the impact limiter's weakest corner.
3. The side-sladdown free drop (CTA-2 test No. 12) was oriented to impart the maximum impact to the side of the impact limiter and the package baseplate region. It caused the impact limiter to crush radially inward a distance of 4 in. at the top of the impact limiter, tapering down to a negligible amount at the bottom of the impact limiter. This was extrapolated to a value of 5.9 in. in the warm foam condition, conservatively assuming the same maximum deformation at both the top and bottom of the impact limiter. (This calculation is carried out in Section 2.7.3.1.1.1(A)). Because the original distance of foam along a radius is 7.85 in., the localized maximum uniaxial foam strain, in the worst case, would be $5.9/7.85 = 77\%$.

This is acceptable and demonstrates the ability of the impact limiter to protect the package from bottoming-out in severe sladdown conditions.

The package also sustained damage in a region at the top of the coolant jacket due to primary impact. The top rib of the coolant jacket was deformed radially inward 1.25 in., which included some OCV and ICV sidewall deformation. This is acceptable because the OCV boundary remained leaktight.

4. The bottom end down free drop (CTA-2 test No. 8) had the potential for producing the highest impact decelerations. Impact limiter deformations were negligible as this drop caused a flattening of the previous deformations that protruded from the bottom of the impact limiter.
5. The top end down free drop (CTA-2 test No. 13) demonstrated the ability of the top end of the package to absorb the full impact energy of the free drop. The fins deformed until the top of the OCV head contacted the impact surface. The final diameter of the resulting flat on the top end was approximately 15 in.

2.7.6.2 Summary of Puncture Damage. A series of eleven puncture drops was performed from a height of 40 in. As noted in Section 2.7.6, two certification test articles (CTA-1 and CTA-2) were used during certification testing of the package. Nine puncture drops were performed on CTA-1. Six puncture drops were performed on CTA-2; four were repeated from the first test and two new puncture drops were added. The effect of the puncture damage on the acceptance criteria of Section 2.7 has already been included in the discussion in Section 2.7.6.1. Specific results of HAC puncture damage follows. The puncture drops are identified in Section 2.7.2.2. Photographs are presented in Appendix 2.10.15.

1. The first puncture (CTA-2 test No. 3) demonstrated that the puncture bar, contacting the impact limiter in the most unfavorable orientation, could not dislodge the impact limiter from the package. The package was oriented top end down, and the 60-in.-long puncture bar was used. Contact occurred on the top surface of the impact limiter, near its outside edge. The circumferential position, as viewed from the top of the CTA, was 75° cw from the electrical feed-through, adjacent to impact limiter attachment bolt No. 7. (This was the only impact limiter attachment bolt that exhibited no residual torque.) Because of the package orientation, the puncture bar did not align with the package c.g. The resulting dent was only 0.3 in. deep, and no evidence of overall impact limiter movement relative to the package was noted.
2. The second puncture (CTA-2 test No. 6) was directly on the damage created by the o.g. over bottom limiter corner free drop. The puncture bar, therefore, contacted the impact limiter through the CTA-2 c.g. This puncture drop demonstrated that a puncture on previously compacted foam would neither penetrate the impact limiter shell nor compromise the integrity of the seal area, through which the line of force traveled. The puncture bar did not penetrate the impact limiter shell and the depth of indentation was 1.7 in.
3. The third puncture (CTA-2 test No. 9) demonstrated that a puncture on the side of the impact limiter at the lower corner joint weld seam would not rupture the weld. The puncture dent depth, measured from the side of the impact limiter, was approximately 3.5 in. No evidence of incipient ripping of the impact limiter shell was noted.
4. The fourth puncture (CTA-2 test No. 14) demonstrated the ability of the OCV sidewall and coolant jacket to absorb the entire drop energy without rupture, buckling, or deleterious deformations in the seal area. The CTA-2 was placed horizontally over the puncture bar at the c.g. The dent depth (measured from the outer diameter of the coolant jacket ribs) was 1 in. The OCV sidewall deformed approximately 0.37 in.
5. The fifth puncture (CTA-2 test No. 16) showed that the package torispherical heads could absorb the entire drop energy without rupture, buckling, or penetration. The CTA-2 was oriented at 3° from the vertical so that the puncture bar would just contact the unreinforced area of the OCV head. The drop height was 45 in., which was the distance between the OCV head and the puncture bar. The drop height was increased to simulate the presence of the OCV head personnel barrier. The resulting dent was 1-1/4 in. deep, with a similar depth in the ICV head.
6. The sixth puncture (CTA-2 test No. 18) showed that the puncture would only rupture a small amount of the impact limiter side wall when the impact was directed at the plastic melt plug. The melt plug holder weld failed and allowed the impact limiter shell to tear, exposing about 12.7 sq. in. of foam. The effect of this amount of exposed foam is insignificant and is evaluated in Section 3.6.2.4 of Appendix 3.6.2, Chapter 3.0.
7. The second puncture (CTA-1 test No. 12) demonstrated that the bottom impact limiter shell

could prevent penetration of the puncture bar, even under the unfavorable shearing conditions set up by impacting the impact limiter on the low-density foam, but just adjacent to the high-density foam. Further, the corner of the puncture bar contacted the impact limiter shell at an angle. Initial impact was 20 in. from the impact limiter center, or within 1 in. of the junction between the high- and low-density foams. Because the line of force was through the c.g., all of the drop energy was available for deformation. The resulting dent was 2.6 in. deep, and no evidence of incipient ripping of the impact limiter shell was noted.

8. The third puncture performed on CTA-1 (CTA-1 test No. 13) demonstrated that a puncture on the impact limiter side shell adjacent to virgin high-density foam would not penetrate the shell. Also, because the line of force was directed through one of the OCV vent ports to the c.g., this puncture demonstrated that the vent ports located in the OCV base were not vulnerable to punctures. The puncture dent depth, measured from the side of the impact limiter, was 3 in. No evidence of incipient ripping of the impact limiter shell was noted.
9. The fifth puncture performed on CTA-1 (CTA-1 test No. 15) demonstrated the ability of the OCV sidewall and coolant jacket to absorb an oblique impact with the puncture bar, and to prove that the coolant jacket ribs, if ripped off, could not cause a breach of the OCV sidewall. The puncture bar contacted the package at an angle of 45° and aligned with the c.g. The maximum depth of the resulting dent (measured from the outer diameter of the coolant jacket ribs) was 1.5 in., with some deformation of the OCV sidewall. The ICV sidewall deformed 0.22 in.
10. The eighth puncture performed on CTA-1 (CTA-1 test No. 18) demonstrated that oblique impact of the OCV thermal shield with the puncture bar would not cause deformations in excess of those assumed in the thermal analysis. The long puncture bar was again used, and contacted the top of the OCV thermal shield 1 in. inboard from its outside edge. The package was oriented at 30° from the vertical. The resulting dent was just under 1.3 in. deep at its center, and of lesser depth elsewhere. For the analysis, a more conservative dent of 8 in. in diameter with a uniform depth of 1.3 in. was assumed.
11. The ninth puncture performed on CTA-1 (CTA-1 test No. 19) showed that direct impact on an impact limiter bolt access tube could not impart deleterious deformations to the OCV bolting flange. The package was oriented with axis vertical, and centered on an impact limiter bolt access tube. The 80-in.-long puncture bar was used. Portions of two adjacent OCV closure bolt access tubes were also impacted. Also, one of the coolant jacket nipples was crushed by secondary impact with the puncture bar.

2.7.6.3 Electrical Feed-through. The electrical feed-through located in the OCV and ICV remained leaktight after the full series of free drop and puncture events. (The electrical feed-throughs were leakage rate tested as a part of the vessel boundaries.) Because the OCV electrical feed-through is mounted at an orientation that is nearly perpendicular to that of the ICV electrical feed-through, it was possible to test the electrical feed-through structurally at several orientations to the principal impact load. In other words, the electrical feed-through pins were tested under conditions of peak impact load in orientations parallel to their axes, normal to their axes, and at several orientations in between. Further, it was demonstrated that the puncture bar could not penetrate the impact limiter shell or cause direct or indirect damage to the electrical feed-through devices.

2.7.6.4 Payload Interaction and Payload Rack Performance. During both the drop test series, the simulated payload interacted structurally with the ICV and the shipping rack assembly. The simulated payload broke free as the four payload attachment bolts pulled through the payload base. This allowed the payload to strike the inside of the ICV wall and head. Two of the payload fins crushed down to the rigid payload body. Three other fins were also damaged. The simulated

payload fins were of a stronger design and made from a stronger material than any of the actual payload fins. Interaction also occurred between the top of the simulated payload and the ICV head. The end of the main structural member of the simulated payload (a 14 in. o.d., 0.5 in. wall thickness steel pipe) struck the ICV lifting block, leaving a dent in the pipe that was 4.5 in. long and 0.5 in. deep. The ability of the ICV to withstand interaction forces with a loose, worst-case payload in a 30 ft HAC drop is thus demonstrated.

Damage to the shipping rack assembly was negligible. The shipping rack assembly barrier plate was deformed slightly (less than 1/16 in.) due to the loose simulated payload. The rack remained substantially in place without contacting the ICV wall. The ceramic fiber insulation located beneath the barrier plate also remained in place. The insulated sleeve that surrounds the ICV electrical feed-through mounting receptacle sustained no damage.

Because prototypical attachment bolts were used, the simulated payload was capable of applying the maximum amount of force to the mounting interface, which is the shipping rack assembly. These interface loads consisted of compression (toward the ICV baseplate) and traction in the plane of the shipping rack assembly barrier plate. Tension loads were not applied, because the simulated payload attachment bolts pass through the shipping rack assembly and attach directly to the ICV baseplate. The ability of the shipping rack assembly to protect the closure seals and electrical feed-through devices both structurally and thermally was thus demonstrated.

2.7.6.5 Measurements

2.7.6.5.1 Closure Bolt Removal Torque. None of the OCV or ICV closure bolts suffered a loss of pre-load because of the testing. A complete record of residual torques due to the entire series of free drop and puncture events for CTA-2 is given in Appendix 2.10.15.4.4. Before any drop testing, a study using CTA-2 demonstrated that removal torque could be as low as 50% of the assembly torque. With that test in mind, it is noted that the minimum removal torque after the full series of tests was well over 50% of the original application torque for both the OCV and ICV closure bolts.

The average OCV closure bolt removal torques varied from a low of 223 ft-lb to a high of 252 ft-lb. The assembly torque was 300 ft-lb. It is noted that several OCV closure bolts exhibited a removal torque of the full value of 300 ft-lb. The average ICV closure bolt removal torques varied from a low of 178 ft-lb to a high of 208 ft-lb. The assembly torque was 260 ft-lb. Measurements before and after the test series indicated there was no change in length in either the ICV or OCV closure bolts.

2.7.6.5.2 Seal Area Measurements. To perform properly, the containment vessel closure seals are dependent, in part, upon sufficient compression. Compression of the seals is a direct function of the space that the seal is forced (by surrounding metal) to occupy. During drop testing, permanent deformations of the flanges near the seals could change the relationship of the flanges to each other and thus change the seal compression. These measurements are discussed in greater detail in Appendix 2.10.14.

The maximum change in seal compression was a decrease of 0.005 in. for the OCV containment (0.393 nominal diameter) O-ring seal, and 0.001 in. for the ICV containment (0.275 nominal diameter) O-ring seal. These values are used in the analysis of containment in Section 4.3.2.

2.7.6.6 Measured Accelerations. During the first series of free drop tests, CTA-1 was instrumented with active and passive accelerometers. Details regarding placement and instrumentation parameters are given in the test procedure, Appendix 2.10.15. Passive

accelerometers were clustered as near as possible to the c.g. on one side of the CTA-1, and consisted of omni-directional trip indicators of 200, 300, and 400 g capacity. The active accelerometers were of the piezoresistive type, with a capacity of ± 750 g. The raw signals were recorded on analog tape and digitally filtered at 300Hz. This filtering frequency preserved a small degree of "ringing", which affords confidence that the full height of the original impact pulse is not lost. Thus, listed peaks are somewhat conservative. In cases of redundant measurements, the maximum reading is shown.

TABLE 2.7.6.0-1. Accelerometer Measurements (CTA-1).

Test No.	Active Accelerometer Peak Measurements		Passive Accelerometer Status		
	c.g. acceleration (gs)	Angular acceleration (rad/sec ²)	200 g	300 g	400 g
6	275	2.25	Trip	Trip	Trip
7	269	Negligible	Trip	No trip	No trip
8	295	2.78	Trip	Trip	Trip
9	260	Negligible	Trip	Trip	Trip
10	240	Negligible	Trip	Trip	No trip

2.8 SPECIAL FORM

This section does not apply, because special form is not claimed.

2.9 FUEL RODS

This section does not apply, because fuel rods will not be shipped in this package.

2.10 APPENDIX

The following is a list of appendices contained within this section:

- 2.10.1 References
- 2.10.2 ICV Two-Dimensional (Axisymmetric) ANSYS Model
- 2.10.3 OCV Head and Fin ANSYS Model for Lifting Analysis
- 2.10.4 OCV Fin-to-Head Weld Properties ANSYS Model for Lifting Analysis
- 2.10.5 OCV Head ANSYS Model for Tiedown Analysis
- 2.10.6 Elastomer O-ring Performance Test Data
- 2.10.7 Summary of Thermal Load Cases and Results
- 2.10.8 OCV Two-Dimensional (Axisymmetric) ANSYS Model
- 2.10.9 RTG Transportation System Package Certification Test Plan
- 2.10.10 Certification Drop Test Procedure for the RTG Package
- 2.10.11 Half-Scale Structural Development Test Report
- 2.10.12 ICV Three-Dimensional ANSYS Model
- 2.10.13 OCV Three-Dimensional ANSYS Model
- 2.10.14 O-Ring Seal Compression Measurements
- 2.10.15 Summary of Damage from Certification Testing

2.10.1 References

1. 10 CFR 71, 1993, "Packaging and Transportation of Radioactive Materials," *Code of Federal Regulations*, as amended.
2. Regulatory Guide (Reg Guide) 7.6, 1978, *Design Criteria for the Structural Analysis of Shipping Cask Containment Vessels*, Rev. 1.
3. "General Plastics Last-A-Foam" FR-3700 for Crash & Fire Protection of Nuclear Material Shipping Containers," 1992, General Plastics Manufacturing Co., Tacoma, Washington.
4. "Safety Analysis Report for the TRUPACT-II Shipping Package," NRC Docket Number 71-7218, Nuclear Packaging, Inc., Federal Way, Washington.
5. American Society of Mechanical Engineers (ASME) Boiler and Pressure Vessel (B&PV) Code.
6. ANSI, 1987, *American National Standard for Radioactive Materials--Leakage Tests on Packages for Shipment* ANSI Standard N14.5, American National Standards Institute, New York, New York.
7. NUREG CR-3019, 1985, *Recommended Welding Criteria for Use in the Fabrication of Shipping Containers for Radioactive Material*.
8. NUREG CR-3864, 1986, *Fabrication Criteria for Shipping Containers*.
9. Regulatory Guide (Reg Guide) 7.6, 1989, *Load Combinations for the Structural Analysis of Shipping Casks for Radioactive Material*, Rev. 1.
10. ASME B&PV Code Case N-284, 1980, *Metal Containment Shell Buckling Design Methods*, Section III, Division 1, Class MC.
11. NUREG/CR-1816, 1981, *Recommendations for Protecting Against Failure by Brittle Fracture in Ferritic Steel Shipping Containers Up to Four Inches Thick*.
12. ASME B&PV Code Case N-47-23, Class 1 Components in Elevated Temperature Service.
13. *Safety Analysis Report for the NuPac 125-B Fuel Shipping Cask*, NRC Docket No. 71-9200, Nuclear Packaging, Inc., Federal Way, Washington.
14. *Safety Analysis Report for the NuPac 10-142 Shipping Cask*, NRC Docket No. 71-9208, Nuclear Packaging, Inc., Federal Way, Washington.
15. *Safety Analysis Report for the NuPac PAS-1 Shipping Cask*, NRC Docket No. 71-9184, Nuclear Packaging, Inc., Federal Way, Washington.
16. *Safety Analysis Report for the CNSI 1-13C II Shipping Cask*, NRC Docket No. 71-8152, Chem-Nuclear Systems, Inc., Columbia, South Carolina.
17. *Parker O-Ring Handbook*, ORD 5700, Parker Seal O-Ring Division, Lexington, Kentucky.
18. Boucher, R., 1961, "Strength of Threads," *Product Engineering*, 1961.

19. Timoshenko, S., and J. Goodier, *Theory of Elasticity*, 3rd Edition, McGraw-Hill, New York, New York.
20. Young, W. C., *Roark's Formulas for Stress and Strain*, 6th Edition, McGraw-Hill, New York, New York.
21. Shigley, J. E., and L. D. Mitchell, *Mechanical Engineering Design*, 4th Edition, McGraw-Hill, New York, New York.
22. ANSI, 1980, *Design Basis for Resistance to Shock and Vibration of Radioactive Material Packages Greater Than One Ton in Truck Transport*, Standard N-14.23, American National Standards Institute, New York, New York.
23. Bickford, J., *An Introduction to the Design and Behavior of Bolted Joints*, Marcel Dekker, New York, New York.
24. Baily, B., *STRAIN, A Computerized Database Program*, Lawrence Livermore National Laboratory.
25. Stala, J. M., *Applied Finite Element Modeling*, Marcel Dekker, New York, New York.

2.10.2 ICV Two-Dimensional (Axisymmetric) ANSYS Model

2.10.2.1 Description The 2-D ICV model is an axisymmetric finite element model of the entire ICV. It consists of a base and a bell, connected by a bolt element and a gap element. It is used to evaluate containment vessel stresses and closure bolt stresses under NCT. (The model used for HAC is 3-D and is described in Appendix 2.10.12.) The applied loading takes the form of internal gas pressure, nodal temperatures, and initial closure bolt pre-load. The model is used for the ICV analysis cases given in Table 2.6.1.3-1, as well as the ICV bell lifting analysis of Section 2.5.1.2. The model layout is shown in Figure 2.10.2-1.

2.10.2.2 Construction The model consists of four element types:

1. To model the ICV containment boundary, isoparametric 2-D elements are used for both the 3.47 in. thick base and ICV flange. This element type is also used in the ICV bell wall, with a quantity of four through the wall thickness, up to a height of 11.725 in. above the datum (the bottom of the base).
2. For the remainder of the ICV bell, axisymmetric shells, located at the section midplane, are used. The shell thicknesses are 0.75 in. in the wall, 0.375 in. in the torispherical head, and in the area of the lifting block. 2 in. To join shell and isoparametric elements, an embedded shell element is used, having 1/10th of the bending stiffness of the adjacent shell element. See Reference 25, Chapter 9.
3. A single 2-D spar (element 156, nodes 52 and 104) was used to represent all of the closure bolts. The property of closure bolt area was entered on a per-radian basis by first multiplying the equivalent area of each bolt by the total bolt quantity (24) and then dividing by 2π . Since the threads extend all the way to the bolt head, the closure bolt area is based on the minimum thread area and is equal to 0.330 in² per bolt. The bolt element was given an initial strain to achieve the desired closure bolt pre-load force at 70 °F in the absence of other loads (per Table 2.6.1.2.1-1).
4. A gap is used between the ICV base and flange at the closure bolt location to react to the bolt loads. Because this concedes with a step machined in the flange lower surface, no other gap elements were necessary.

Node and element plots of key portions of the model are given in Figures 2.10.2-2 through 2.10.2-7. An interpreted ANSYS input listing is given in Table 2.10.2-1.

2.10.2.3 Material Properties The modulus of elasticity and coefficient of thermal expansion varied with temperature according to the data in Tables 2.3.1 and 2.3-2. Poisson's ratio is 0.3.

2.10.2.4 Constraints The bottom center node of the ICV base was fixed in all coordinate directions, but the rest of the base was allowed to deflect as determined by the loading. The top center of the ICV was restrained in a radial direction to ensure axisymmetry. The hoop direction of all nodes was restrained. The top center node was also restrained from rotation about the hoop axis.

2.10.2.5 Applied Loading All ICV surfaces subject to internal pressure had a constant pressure applied. Nodal temperature loading was applied using temperatures resulting from thermal model output. Because there were fewer thermal model nodes than structural model nodes, interpolation of thermal model temperatures was required. Temperatures in the ICV base were set as follows: nodes 1 to 20 used the average of thermal nodes 260 and 261, nodes 21 to 30 used the average of thermal nodes 262 and 263, and nodes 31 to 58 used the average of thermal nodes 264, 265.

and 266. The ICV flange temperature was set using thermal node 250. In the wall region above the ICV flange, the temperatures of structural nodes that corresponded exactly in location to the thermal model counterparts were set directly; the temperatures of structural nodes that fell in between thermal nodes were established using linear interpolation. Because the closure bolt was not modeled thermally, in the structural model it took the temperatures of the ICV flange and base at its attachment nodes. The reference temperature was 70 °F.

The ICV base and closure bolts were not used in the lifting analysis. The lower flange nodes (96 to 101) were fixed in the axial direction, and a vertical force of 1,600 pounds was applied to the center of the ICV head. For lifting, nodal temperatures corresponding to NCT case 1 were used. No pressure loading was used.

2.10.2.6 Results. Worst-case ICV lifting stress intensity occurs in the head and is shown in Figure 2.10.2.8. The worst-case containment boundary stresses occur for NCT case ICV-2 (see Section 2.6.1.3) and are shown in Figure 2.10.2-9 through 2.10.2-11. The worst-case ICV flange stress intensity is for NCT case ICV-1 and is shown in Figure 2.10.2-12.

APPENDIX 2.10.2
REVISED ANSYS COMPUTER OUTPUT

STATIC ANALYSIS (NAME= 0)

LINEAR ANALYSIS - NO NON-LINEAR PROPERTIES

REFERENCE TEMPERATURE= 70.000 (TEMP)

UNIFORM TEMPERATURE = -40.000 (TEMP)

****ANALYSIS OPTIONS (KEY VALUES) (IF ANY) ****

NO STATIC INTERPOLATION/EXTRAPOLATION (KEY(5)=0)

SMALL DEFLECTION SOLUTION (KEY(4)=0)

NO STRESS STIFFENING (KEY(8)=0)

USE INITIAL-STIFFNESS NEWTON-RAPHSON SOLUTION PROCEDURE (KEY(9)=3)

3D-CORE NAVI-FRONT EQUATION SOLVER (KEY(10)=0)

LIST ELEMENT TYPES FROM 1 TO 20 BY 1

NO.	STIF	KEYOFF VALUES								IMPR	
1	42	0	0	1	0	0	0	0	0	0	ISOPNL, STRESS SOLID, 2-D
2	57	0	0	0	0	0	0	0	0	0	PLASTIC ANISY. CONIC SHELL
3	1	0	0	0	0	0	0	0	0	0	SPAR, 2-D
4	12	0	0	0	0	0	0	0	0	0	INTERFACE ELEM. 2-D

LIST ALL REAL SETS

REAL CONSTANT SET 1 ITEMS 1 TO 6	0.75000	0.00000E+00	0.00000E+00	0.00000E+00	0.00000E+00	0.00000E+00
REAL CONSTANT SET 2 ITEMS 1 TO 4	0.37500	0.00000E+00	0.00000E+00	0.00000E+00	0.00000E+00	0.00000E+00
REAL CONSTANT SET 3 ITEMS 1 TO 6	1.2600	0.26810E-02	0.00000E+00	0.00000E+00	0.00000E+00	0.00000E+00
REAL CONSTANT SET 4 ITEMS 1 TO 6	0.00000E+00	0.95540E+00	0.00000E+00	0.00000E+00	0.00000E+00	0.00000E+00
REAL CONSTANT SET 5 ITEMS 1 TO 4	2.0000	0.00000E+00	0.00000E+00	0.00000E+00	0.00000E+00	0.00000E+00
REAL CONSTANT SET 6 ITEMS 1 TO 4	0.34800	0.00000E+00	0.00000E+00	0.00000E+00	0.00000E+00	0.00000E+00

LIST ALL COORDINATE SYSTEMS

SYSTEM	TYPE	CENTER	PARAMETER	DIR1	DIR2	DIR3
0	0 (CARTESIAN)	0.000	0.000	0.000	0.000	0.000
1	1 (CYLINDRICAL)	0.000	0.000	0.000	1.000	0.000
2	2 (SPHERICAL)	0.000	0.000	0.000	1.000	1.000
11	1 (CYLINDRICAL)	0.000	27.220	0.000	1.000	0.000
12	1 (CYLINDRICAL)	14.940	56.370	0.000	1.000	1.000

SYSTEM	ORIENTATION VECTORS (X,Y,Z)					
0	1.00	0.00	0.00	0.00	1.00	0.00
1	1.00	0.00	0.00	0.00	1.00	0.00
2	1.00	0.00	0.00	0.00	1.00	0.00
11	1.00	0.00	0.00	0.00	1.00	0.00
12	1.00	0.00	0.00	0.00	1.00	0.00

CPS TYPE	XC	YC	ZC	THICK	FWTZ	THHZ
11	1	0.00000E+00	27.220	0.00000E+00	0.000	0.000
12	1	14.940	56.370	0.00000E+00	0.000	0.000

LIST ALL SELECTED ELEMENTS. (LIST NAMES)

ELEM NAT TYP REL ESYE MORDER

1	1	1	1	0	1	6	7	2
2	1	1	1	0	2	7	8	3
3	1	1	1	0	3	8	9	4
4	1	1	1	0	4	9	10	5
5	1	1	1	0	5	10	11	6
6	1	1	1	0	6	11	12	7
7	1	1	1	0	7	12	13	8
8	1	1	1	0	8	13	14	9
9	1	1	1	0	9	14	15	10
10	1	1	1	0	10	15	16	11
11	1	1	1	0	11	16	17	12
12	1	1	1	0	12	17	18	13
13	1	1	1	0	13	18	19	14
14	1	1	1	0	14	19	20	15
15	1	1	1	0	15	20	21	16
16	1	1	1	0	16	21	22	17
17	1	1	1	0	17	22	23	18
18	1	1	1	0	18	23	24	19
19	1	1	1	0	19	24	25	20
20	1	1	1	0	20	25	26	21
21	1	1	1	0	21	26	27	22
22	1	1	1	0	22	27	28	23
23	1	1	1	0	23	28	29	24
24	1	1	1	0	24	29	30	25
25	1	1	1	0	25	30	31	26
26	1	1	1	0	26	31	32	27
27	1	1	1	0	27	32	33	28
28	1	1	1	0	28	33	34	29
29	1	1	1	0	29	34	35	30
30	1	1	1	0	30	35	36	31
31	1	1	1	0	31	36	37	32
32	1	1	1	0	32	37	38	33
33	1	1	1	0	33	38	39	34
34	1	1	1	0	34	39	40	35
35	1	1	1	0	35	40	41	36
36	1	1	1	0	36	41	42	37
37	1	1	1	0	37	42	43	38
38	1	1	1	0	38	43	44	39
39	1	1	1	0	39	44	45	40
40	1	1	1	0	40	45	46	41
41	1	1	1	0	41	46	47	42
42	1	1	1	0	42	47	48	43
43	1	1	1	0	43	48	49	44
44	1	1	1	0	44	49	50	45
45	1	1	1	0	45	50	51	46
46	1	1	1	0	46	51	52	47
47	1	1	1	0	47	52	53	48
48	1	1	1	0	48	53	54	49
49	1	1	1	0	49	54	55	50
50	1	1	1	0	50	55	56	51
51	1	1	1	0	51	56	57	52
52	1	1	1	0	52	57	58	53
53	1	1	1	0	53	58	59	54
54	1	1	1	0	54	59	60	55
55	1	1	1	0	55	60	61	56
56	1	1	1	0	56	61	62	57
57	1	1	1	0	57	62	63	58
58	1	1	1	0	58	63	64	59
59	1	1	1	0	59	64	65	60
60	1	1	1	0	60	65	66	61
61	1	1	1	0	61	66	67	62
62	1	1	1	0	62	67	68	63
63	1	1	1	0	63	68	69	64
64	1	1	1	0	64	69	70	65
65	1	1	1	0	65	70	71	66
66	1	1	1	0	66	71	72	67
67	1	1	1	0	67	72	73	68
68	1	1	1	0	68	73	74	69
69	1	1	1	0	69	74	75	70
70	1	1	1	0	70	75	76	71
71	1	1	1	0	71	76	77	72
72	1	1	1	0	72	77	78	73
73	1	1	1	0	73	78	79	74
74	1	1	1	0	74	79	80	75
75	1	1	1	0	75	80	81	76
76	1	1	1	0	76	81	82	77
77	1	1	1	0	77	82	83	78
78	1	1	1	0	78	83	84	79
79	1	1	1	0	79	84	85	80
80	1	1	1	0	80	85	86	81
81	1	1	1	0	81	86	87	82
82	1	1	1	0	82	87	88	83
83	1	1	1	0	83	88	89	84
84	1	1	1	0	84	89	90	85
85	1	1	1	0	85	90	91	86
86	1	1	1	0	86	91	92	87
87	1	1	1	0	87	92	93	88
88	1	1	1	0	88	93	94	89
89	1	1	1	0	89	94	95	90
90	1	1	1	0	90	95	96	91
91	1	1	1	0	91	96	97	92
92	1	1	1	0	92	97	98	93
93	1	1	1	0	93	98	99	94
94	1	1	1	0	94	99	100	95
95	1	1	1	0	95	100	101	96
96	1	1	1	0	96	101	102	97
97	1	1	1	0	97	102	103	98
98	1	1	1	0	98	103	104	99
99	1	1	1	0	99	104	105	100
100	1	1	1	0	100	105	106	101
101	1	1	1	0	101	106	107	102
102	1	1	1	0	102	107	108	103
103	1	1	1	0	103	108	109	104
104	1	1	1	0	104	109	110	105
105	1	1	1	0	105	110	111	106
106	1	1	1	0	106	111	112	107
107	1	1	1	0	107	112	113	108
108	1	1	1	0	108	113	114	109
109	1	1	1	0	109	114	115	110
110	1	1	1	0	110	115	116	111
111	1	1	1	0	111	116	117	112
112	1	1	1	0	112	117	118	113
113	1	1	1	0	113	118	119	114
114	1	1	1	0	114	119	120	115
115	1	1	1	0	115	120	121	116
116	1	1	1	0	116	121	122	117
117	1	1	1	0	117	122	123	118
118	1	1	1	0	118	123	124	119
119	1	1	1	0	119	124	125	120
120	1	1	1	0	120	125	126	121
121	1	1	1	0	121	126	127	122
122	1	1	1	0	122	127	128	123
123	1	1	1	0	123	128	129	124
124	1	1	1	0	124	129	130	125
125	1	1	1	0	125	130	131	126
126	1	1	1	0	126	131	132	127
127	1	1	1	0	127	132	133	128
128	1	1	1	0	128	133	134	129
129	1	1	1	0	129	134	135	130
130	1	1	1	0	130	135	136	131
131	1	1	1	0	131	136	137	132
132	1	1	1	0	132	137	138	133
133	1	1	1	0	133	138	139	134
134	1	1	1	0	134	139	140	135
135	1	1	1	0	135	140	141	136
136	1	1	1	0	136	141	142	137
137	1	1	1	0	137	142	143	138
138	1	1	1	0	138	143	144	139
139	1	1	1	0	139	144	145	140
140	1	1	1	0	140	145	146	141
141	1	1	1	0	141	146	147	142
142	1	1	1	0	142	147	148	143
143	1	1	1	0	143	148	149	144
144	1	1	1	0	144	149	150	145
145	1	1	1	0	145	150	151	146
146	1	1	1	0	146	151	152	147
147	1	1	1	0	147	152	153	148
148	1	1	1	0	148	153	154	149
149	1	1	1	0	149	154	155	150
150	1	1	1	0	150	155	156	151

66	1	1	1	0	132	133	136	137
67	1	1	1	0	133	134	139	138
68	1	1	1	0	134	135	140	139
69	1	1	1	0	134	137	142	141
70	1	1	1	0	137	138	143	142
71	1	1	1	0	138	139	144	143
72	1	1	1	0	139	140	145	144
73	1	1	1	0	141	142	147	145
74	1	1	1	0	142	143	148	147
75	1	1	1	0	143	144	149	148
76	1	1	1	0	144	145	150	149
77	1	1	1	0	146	147	152	151
78	1	1	1	0	147	148	153	152
79	1	1	1	0	148	149	154	153
80	1	1	1	0	149	150	155	154

ELEM	MAT	TYF	REL	ESYS	NODES			
81	1	1	1	0	151	152	157	154
82	1	1	1	0	152	153	158	157
83	1	1	1	0	153	154	159	158
84	1	1	1	0	154	155	160	159
85	1	1	1	0	156	157	162	161
86	1	1	1	0	157	158	163	162
87	1	1	1	0	158	159	164	163
88	1	1	1	0	159	160	165	164
89	1	1	1	0	161	162	167	166
90	1	1	1	0	162	163	168	167
91	1	1	1	0	163	164	169	168
92	1	1	1	0	164	165	170	169
93	1	1	1	0	166	167	172	171
94	1	1	1	0	167	168	173	172
95	1	1	1	0	168	169	174	173
96	1	1	1	0	169	170	175	174
97	1	1	1	0	171	172	177	176
98	1	1	1	0	172	173	178	177
99	1	1	1	0	173	174	179	178
100	1	1	1	0	174	175	180	179

ELEM	MAT	TYF	REL	ESYS	NODES			
101	1	1	1	0	95	121	126	126
102	1	2	6	0	173	178		
103	1	2	1	0	178	201		
104	1	2	1	0	201	202		
105	1	2	1	0	202	203		
106	1	2	1	0	203	204		
107	1	2	1	0	204	205		
108	1	2	1	0	205	206		
109	1	2	1	0	206	207		
110	1	2	1	0	207	208		
111	1	2	1	0	208	209		
112	1	2	1	0	209	210		
113	1	2	1	0	210	211		
114	1	2	1	0	211	212		
115	1	2	1	0	212	213		
116	1	2	1	0	213	214		
117	1	2	1	0	214	215		
118	1	2	1	0	215	216		
119	1	2	1	0	216	217		
120	1	2	1	0	217	218		

ELEM	MAT	TYF	REL	ESYS	NODES	
121	1	2	1	0	218	219
122	1	2	1	0	219	220
123	1	2	1	0	220	221
124	1	2	1	0	221	222
125	1	2	1	0	222	223
126	1	2	1	0	223	224
127	1	2	1	0	224	225
128	1	2	1	0	225	226
129	1	2	1	0	226	227
130	1	2	1	0	227	228

131	1	2	1	0	230	239
132	1	2	1	0	239	250
133	1	2	1	0	230	251
134	1	2	1	0	231	252
135	1	2	1	0	232	253
136	1	2	1	0	233	254
137	1	2	1	0	234	255
138	1	2	1	0	235	256
139	1	2	2	0	236	237
140	1	2	2	0	237	238

ELEM	INT	TRP	REL	EDTS	NONE	
141	1	2	2	0	238	239
142	1	2	2	0	239	240
143	1	2	2	0	240	241
144	1	2	2	0	241	242
145	1	2	2	0	242	243
146	1	2	2	0	243	244
147	1	2	2	0	244	245
148	1	2	2	0	245	246
149	1	2	2	0	246	247
150	1	2	2	0	247	248
151	1	2	2	0	248	249
152	1	2	2	0	249	250
153	1	2	2	0	250	251
154	1	2	2	0	251	252
155	1	2	3	0	252	253
156	2	3	3	0	52	104
157	2	4	4	0	43	97
158	2	4	4	0	53	99

LIST ALL INJECTRO NONE 0375- 0

None	X	Y	Z	TRWY	TRWZ	TRCZ
1	0.00000E+00	0.00000E+00	0.00000E+00	0.00	0.00	0.00
2	0.00000E+00	0.86750	0.00000E+00	0.00	0.00	0.00
3	0.00000E+00	1.73500	0.00000E+00	0.00	0.00	0.00
4	0.00000E+00	2.60250	0.00000E+00	0.00	0.00	0.00
5	0.00000E+00	3.47000	0.00000E+00	0.00	0.00	0.00
6	3.50000	0.00000E+00	0.00000E+00	0.00	0.00	0.00
7	3.50000	0.86750	0.00000E+00	0.00	0.00	0.00
8	3.50000	1.73500	0.00000E+00	0.00	0.00	0.00
9	3.50000	2.60250	0.00000E+00	0.00	0.00	0.00
10	3.50000	3.47000	0.00000E+00	0.00	0.00	0.00
11	7.00000	0.00000E+00	0.00000E+00	0.00	0.00	0.00
12	7.00000	0.86750	0.00000E+00	0.00	0.00	0.00
13	7.00000	1.73500	0.00000E+00	0.00	0.00	0.00
14	7.00000	2.60250	0.00000E+00	0.00	0.00	0.00
15	7.00000	3.47000	0.00000E+00	0.00	0.00	0.00
16	9.87500	0.00000E+00	0.00000E+00	0.00	0.00	0.00
17	9.87500	0.86750	0.00000E+00	0.00	0.00	0.00
18	9.87500	1.73500	0.00000E+00	0.00	0.00	0.00
19	9.87500	2.60250	0.00000E+00	0.00	0.00	0.00
20	9.87500	3.47000	0.00000E+00	0.00	0.00	0.00
None	X	Y	Z	TRWY	TRWZ	TRCZ
21	12.750	0.00000E+00	0.00000E+00	0.00	0.00	0.00
22	12.750	0.86750	0.00000E+00	0.00	0.00	0.00
23	12.750	1.73500	0.00000E+00	0.00	0.00	0.00
24	12.750	2.60250	0.00000E+00	0.00	0.00	0.00
25	12.750	3.47000	0.00000E+00	0.00	0.00	0.00
26	14.325	0.00000E+00	0.00000E+00	0.00	0.00	0.00
27	14.325	0.86750	0.00000E+00	0.00	0.00	0.00
28	14.325	1.73500	0.00000E+00	0.00	0.00	0.00
29	14.325	2.60250	0.00000E+00	0.00	0.00	0.00
30	14.325	3.47000	0.00000E+00	0.00	0.00	0.00
31	15.900	0.00000E+00	0.00000E+00	0.00	0.00	0.00
32	15.900	0.86750	0.00000E+00	0.00	0.00	0.00
33	15.900	1.73500	0.00000E+00	0.00	0.00	0.00
34	15.900	2.60250	0.00000E+00	0.00	0.00	0.00
35	15.900	3.47000	0.00000E+00	0.00	0.00	0.00
36	16.970	0.00000E+00	0.00000E+00	0.00	0.00	0.00

37	16.978	0.86750	0.00000E+00	0.00	0.00	0.00
38	16.978	1.4700	0.00000E+00	0.00	0.00	0.00
39	16.978	2.0725	0.00000E+00	0.00	0.00	0.00
40	16.978	2.6750	0.00000E+00	0.00	0.00	0.00

NODE	X	Y	Z	THX1	THY1	THZ1
41	17.340	0.00000E+00	0.00000E+00	0.00	0.00	0.00
42	17.340	0.86750	0.00000E+00	0.00	0.00	0.00
43	17.340	1.4700	0.00000E+00	0.00	0.00	0.00
44	17.873	0.00000E+00	0.00000E+00	0.00	0.00	0.00
47	17.873	0.86750	0.00000E+00	0.00	0.00	0.00
48	17.873	1.4700	0.00000E+00	0.00	0.00	0.00
51	18.625	0.00000E+00	0.00000E+00	0.00	0.00	0.00
52	18.625	0.38000	0.00000E+00	0.00	0.00	0.00
53	18.625	1.4700	0.00000E+00	0.00	0.00	0.00
56	19.480	0.00000E+00	0.00000E+00	0.00	0.00	0.00
57	19.480	0.38000	0.00000E+00	0.00	0.00	0.00
58	19.480	1.4700	0.00000E+00	0.00	0.00	0.00
65	16.815	2.6750	0.00000E+00	0.00	0.00	0.00
66	17.880	1.4700	0.00000E+00	0.00	0.00	0.00
67	17.340	1.4700	0.00000E+00	0.00	0.00	0.00
68	17.873	1.4700	0.00000E+00	0.00	0.00	0.00
69	18.625	1.4700	0.00000E+00	0.00	0.00	0.00
100	19.373	1.4700	0.00000E+00	0.00	0.00	0.00
101	17.880	2.0700	0.00000E+00	0.00	0.00	0.00
102	17.340	2.0700	0.00000E+00	0.00	0.00	0.00

NODE	X	Y	Z	THX2	THY2	THZ2
103	17.873	2.0700	0.00000E+00	0.00	0.00	0.00
104	18.625	2.0700	0.00000E+00	0.00	0.00	0.00
105	19.373	2.0700	0.00000E+00	0.00	0.00	0.00
106	17.880	2.6200	0.00000E+00	0.00	0.00	0.00
107	17.994	2.6200	0.00000E+00	0.00	0.00	0.00
108	18.108	2.6200	0.00000E+00	0.00	0.00	0.00
109	18.221	2.6200	0.00000E+00	0.00	0.00	0.00
110	19.373	2.6200	0.00000E+00	0.00	0.00	0.00
111	17.000	3.9657	0.00000E+00	0.00	0.00	0.00
112	17.458	3.8004	0.00000E+00	0.00	0.00	0.00
113	17.817	3.8542	0.00000E+00	0.00	0.00	0.00
114	18.373	3.1079	0.00000E+00	0.00	0.00	0.00
115	18.833	3.1617	0.00000E+00	0.00	0.00	0.00
116	17.000	3.2733	0.00000E+00	0.00	0.00	0.00
117	17.323	3.3808	0.00000E+00	0.00	0.00	0.00
118	17.646	3.4883	0.00000E+00	0.00	0.00	0.00
119	17.969	3.5958	0.00000E+00	0.00	0.00	0.00
120	18.292	3.7033	0.00000E+00	0.00	0.00	0.00
121	17.000	3.6000	0.00000E+00	0.00	0.00	0.00
122	17.308	3.7613	0.00000E+00	0.00	0.00	0.00

NODE	X	Y	Z	THX3	THY3	THZ3
123	17.373	3.9223	0.00000E+00	0.00	0.00	0.00
124	17.563	4.0836	0.00000E+00	0.00	0.00	0.00
125	17.750	4.2450	0.00000E+00	0.00	0.00	0.00
126	18.879	3.7799	0.00000E+00	0.00	0.00	0.00
127	17.000	3.9829	0.00000E+00	0.00	0.00	0.00
128	17.383	4.2804	0.00000E+00	0.00	0.00	0.00
129	17.536	4.4284	0.00000E+00	0.00	0.00	0.00
130	17.750	4.6373	0.00000E+00	0.00	0.00	0.00
131	17.000	4.6480	0.00000E+00	0.00	0.00	0.00
132	17.188	4.6823	0.00000E+00	0.00	0.00	0.00
133	17.373	4.7430	0.00000E+00	0.00	0.00	0.00
134	17.563	4.8875	0.00000E+00	0.00	0.00	0.00
135	17.750	5.0340	0.00000E+00	0.00	0.00	0.00
136	17.000	5.0150	0.00000E+00	0.00	0.00	0.00
137	17.188	5.1180	0.00000E+00	0.00	0.00	0.00
138	17.373	5.2950	0.00000E+00	0.00	0.00	0.00
139	17.563	5.3880	0.00000E+00	0.00	0.00	0.00
140	17.750	5.3950	0.00000E+00	0.00	0.00	0.00
141	17.000	5.3780	0.00000E+00	0.00	0.00	0.00
142	17.188	5.4175	0.00000E+00	0.00	0.00	0.00

NODE	X	Y	Z	THX4	THY4	THZ4
143	17.373	5.6450	0.00000E+00	0.00	0.00	0.00
144	17.563	5.7125	0.00000E+00	0.00	0.00	0.00

145	17.750	3.7688	0.00000E+00	0.00	0.00	0.00
146	17.000	6.1258	0.00000E+00	0.00	0.00	0.00
147	17.188	6.1258	0.00000E+00	0.00	0.00	0.00
148	17.375	6.1258	0.00000E+00	0.00	0.00	0.00
149	17.563	6.1258	0.00000E+00	0.00	0.00	0.00
150	17.750	6.1258	0.00000E+00	0.00	0.00	0.00
151	17.000	7.0583	0.00000E+00	0.00	0.00	0.00
152	17.188	7.0583	0.00000E+00	0.00	0.00	0.00
153	17.375	7.0583	0.00000E+00	0.00	0.00	0.00
154	17.563	7.0583	0.00000E+00	0.00	0.00	0.00
155	17.750	7.0583	0.00000E+00	0.00	0.00	0.00
156	17.000	7.9917	0.00000E+00	0.00	0.00	0.00
157	17.188	7.9917	0.00000E+00	0.00	0.00	0.00
158	17.375	7.9917	0.00000E+00	0.00	0.00	0.00
159	17.563	7.9917	0.00000E+00	0.00	0.00	0.00
160	17.750	7.9917	0.00000E+00	0.00	0.00	0.00
161	17.000	8.9250	0.00000E+00	0.00	0.00	0.00
162	17.188	8.9250	0.00000E+00	0.00	0.00	0.00

MODE	X	Y	Z	THX1	THY2	THZ2
163	17.375	9.8550	0.00000E+00	0.00	0.00	0.00
164	17.563	9.8550	0.00000E+00	0.00	0.00	0.00
165	17.750	9.8550	0.00000E+00	0.00	0.00	0.00
166	17.000	9.8583	0.00000E+00	0.00	0.00	0.00
167	17.188	9.8583	0.00000E+00	0.00	0.00	0.00
168	17.375	9.8583	0.00000E+00	0.00	0.00	0.00
169	17.563	9.8583	0.00000E+00	0.00	0.00	0.00
170	17.750	9.8583	0.00000E+00	0.00	0.00	0.00
171	17.000	10.792	0.00000E+00	0.00	0.00	0.00
172	17.188	10.792	0.00000E+00	0.00	0.00	0.00
173	17.375	10.792	0.00000E+00	0.00	0.00	0.00
174	17.563	10.792	0.00000E+00	0.00	0.00	0.00
175	17.750	10.792	0.00000E+00	0.00	0.00	0.00
176	17.000	11.725	0.00000E+00	0.00	0.00	0.00
177	17.188	11.725	0.00000E+00	0.00	0.00	0.00
178	17.375	11.725	0.00000E+00	0.00	0.00	0.00
179	17.563	11.725	0.00000E+00	0.00	0.00	0.00
180	17.750	11.725	0.00000E+00	0.00	0.00	0.00
201	17.375	11.689	0.00000E+00	0.00	0.00	0.00
202	17.375	11.684	0.00000E+00	0.00	0.00	0.00

MODE	X	Y	Z	THX1	THY2	THZ2
203	17.375	16.419	0.00000E+00	0.00	0.00	0.00
204	17.375	15.583	0.00000E+00	0.00	0.00	0.00
209	17.375	14.544	0.00000E+00	0.00	0.00	0.00
206	17.375	17.512	0.00000E+00	0.00	0.00	0.00
207	17.375	18.477	0.00000E+00	0.00	0.00	0.00
208	17.375	19.441	0.00000E+00	0.00	0.00	0.00
209	17.375	20.406	0.00000E+00	0.00	0.00	0.00
210	17.375	21.370	0.00000E+00	0.00	0.00	0.00
211	17.375	22.334	0.00000E+00	0.00	0.00	0.00
212	17.375	24.654	0.00000E+00	0.00	0.00	0.00
213	17.375	25.599	0.00000E+00	0.00	0.00	0.00
214	17.375	26.738	0.00000E+00	0.00	0.00	0.00
215	17.375	28.079	0.00000E+00	0.00	0.00	0.00
216	17.375	29.418	0.00000E+00	0.00	0.00	0.00
217	17.375	30.755	0.00000E+00	0.00	0.00	0.00
218	17.375	32.096	0.00000E+00	0.00	0.00	0.00
219	17.375	33.438	0.00000E+00	0.00	0.00	0.00
220	17.375	34.779	0.00000E+00	0.00	0.00	0.00
221	17.375	36.118	0.00000E+00	0.00	0.00	0.00
222	17.375	37.458	0.00000E+00	0.00	0.00	0.00

MODE	X	Y	Z	THX1	THY2	THZ2
223	17.375	38.798	0.00000E+00	0.00	0.00	0.00
224	17.375	40.138	0.00000E+00	0.00	0.00	0.00
225	17.375	41.478	0.00000E+00	0.00	0.00	0.00
226	17.375	42.818	0.00000E+00	0.00	0.00	0.00
227	17.375	44.158	0.00000E+00	0.00	0.00	0.00
228	17.375	45.498	0.00000E+00	0.00	0.00	0.00
229	17.375	46.838	0.00000E+00	0.00	0.00	0.00
230	17.375	48.178	0.00000E+00	0.00	0.00	0.00
231	17.375	49.517	0.00000E+00	0.00	0.00	0.00
232	17.375	50.857	0.00000E+00	0.00	0.00	0.00

233	17.375	51.870	0.0000E+00	0.00	0.00	4.00
234	17.375	52.837	0.0000E+00	0.00	0.00	0.00
235	17.375	53.808	0.0000E+00	0.00	0.00	0.00
236	17.375	53.970	0.0000E+00	0.00	0.00	0.00
237	17.375	55.170	0.0000E+00	0.00	0.00	0.00
238	17.377	56.370	0.0000E+00	0.00	0.00	0.00
239	17.379	56.980	0.0000E+00	0.00	0.00	4.50
240	17.146	57.498	0.0000E+00	0.00	0.00	0.00
241	16.850	57.860	0.0000E+00	0.00	0.00	0.00
242	16.498	58.244	0.0000E+00	0.00	0.00	0.00
NODE	T	T	Z	TINZ	TMINZ	
243	16.857	58.538	0.0000E+00	0.00	0.00	0.00
244	14.881	59.243	0.0000E+00	0.00	0.00	0.00
245	13.018	59.915	0.0000E+00	0.00	0.00	0.00
246	11.485	60.495	0.0000E+00	0.00	0.00	0.00
247	9.8866	60.999	0.0000E+00	0.00	0.00	0.00
248	8.2561	61.428	0.0000E+00	0.00	0.00	0.00
249	6.6272	61.788	0.0000E+00	0.00	0.00	0.00
250	4.9834	62.055	0.0000E+00	0.00	0.00	0.00
251	3.3284	62.251	0.0000E+00	0.00	0.00	0.00
252	1.6661	62.369	0.0000E+00	0.00	0.00	0.00
253	0.1371E-09	62.485	0.0000E+00	0.00	0.00	0.00

LIST ALL MATERIALS PROPERTY= ALL

PROPERTY TABLE MAT= 1 MIN. POINTS= 2
 TEMPERATURE DATA TEMPERATURE DATA
 -9999.D 0.30000 9999.D 0.30000

PROPERTY TABLE EK MAT= 1 MIN. POINTS= 75
 TEMPERATURE DATA TEMPERATURE DATA
 -40.000 0.2900E+00 70.000 0.2038E+00
 100.00 0.2810E+00 200.00 0.2746E+00
 300.00 0.2700E+00 400.00 0.2658E+00
 500.00 0.2580E+00 600.00 0.2510E+00
 700.00 0.2480E+00 800.00 0.2380E+00
 900.00 0.2330E+00 1000.D 0.2250E+00
 1100.0 0.2210E+00 1200.D 0.2150E+00
 1300.0 0.2050E+00

PROPERTY TABLE ALPX MAT= 1 MIN. POINTS= 15
 TEMPERATURE DATA TEMPERATURE DATA
 -40.000 0.8130E-05 70.000 0.8460E-05
 100.00 0.8510E-05 200.00 0.8790E-05
 300.00 0.9000E-05 400.00 0.9190E-05
 500.00 0.9370E-05 600.00 0.9530E-05
 700.00 0.9690E-05 800.00 0.9820E-05
 900.00 0.1006E-04 1000.0 0.1030E-04
 1100.0 0.1033E-04 1200.0 0.1060E-04
 1300.0 0.1065E-04

PROPERTY TABLE EK MAT= 2 MIN. POINTS= 7
 TEMPERATURE DATA TEMPERATURE DATA
 -40.000 0.2840E+00 70.000 0.2780E+00
 100.00 0.2760E+00 200.00 0.2700E+00
 300.00 0.2670E+00 400.00 0.2610E+00
 500.00 0.2570E+00

PROPERTY TABLE ALPX MAT= 2 MIN. POINTS= 7
 TEMPERATURE DATA TEMPERATURE DATA
 -40.000 0.9940E-05 70.000 0.9500E-05
 100.00 0.9270E-05 200.00 0.8510E-05
 300.00 0.7800E-05 400.00 0.6800E-05
 500.00 0.7760E-05

TIME= 0.0000E+00 NITER= -5
 LSTEP= 1STEP= -1 ITER= 0

UNIFORM TEMPERATURE= -40.000 (TREF= 70.000)
 BOUNDARY CONDITIONS STOPPED DUE TO STATIC CONVERGENCE OPTION
 PLASTIC CONVERG. CRITERION= 0.0100
 CREEP OPTIMUM CRITERION= 0.1000
 LARGE DEPL. CONVERG. CRITERION= 0.001000
 DISPLACEMENT LIMIT= 0.0000E+00

MPRINT= 00000 MPRINT= 5 REACTION PRINT FREQ= 0000
 DISP. POST DATA FREQ= 5 REACT. POST DATA FREQ= 5

ELEMENT PRINT		AMP POST DATA		FREQUENCIES		
TYPE	STIFF	STRESS	FORCE	STRESS	DATA	FORCE
	MOD.	PRINT	PRINT	DATA	LEVEL	DATA
1	12	00000	00000	3	3	5
2	11	00000	00000	5	3	5
3	1	00000	00000	1	3	5
4	12	00000	00000	5	3	5

LOADS INPUT FILE= 26 LOADS OUTPUT FILE= 23

ALL ANALYSIS DATA WILL BE WRITTEN ONTO FILE?

LIST DISPLACEMENTS FOR ALL SELECTED MODES

MODE	LABEL	DISP	DISP
1	UZ	0.00000000E+00	0.00000000E+00
2	UZ	0.00000000E+00	0.00000000E+00
3	UZ	0.00000000E+00	0.00000000E+00
4	UZ	0.00000000E+00	0.00000000E+00
5	UZ	0.00000000E+00	0.00000000E+00
6	UZ	0.00000000E+00	0.00000000E+00
7	UZ	0.00000000E+00	0.00000000E+00
8	UZ	0.00000000E+00	0.00000000E+00
9	UZ	0.00000000E+00	0.00000000E+00
10	UZ	0.00000000E+00	0.00000000E+00
11	UZ	0.00000000E+00	0.00000000E+00
12	UZ	0.00000000E+00	0.00000000E+00
13	UZ	0.00000000E+00	0.00000000E+00
14	UZ	0.00000000E+00	0.00000000E+00
15	UZ	0.00000000E+00	0.00000000E+00
16	UZ	0.00000000E+00	0.00000000E+00
17	UZ	0.00000000E+00	0.00000000E+00
18	UZ	0.00000000E+00	0.00000000E+00
19	UZ	0.00000000E+00	0.00000000E+00
20	UZ	0.00000000E+00	0.00000000E+00

MODE	LABEL	DISP	DISP
21	UZ	0.00000000E+00	0.00000000E+00
22	UZ	0.00000000E+00	0.00000000E+00
23	UZ	0.00000000E+00	0.00000000E+00
24	UZ	0.00000000E+00	0.00000000E+00
25	UZ	0.00000000E+00	0.00000000E+00
26	UZ	0.00000000E+00	0.00000000E+00
27	UZ	0.00000000E+00	0.00000000E+00
28	UZ	0.00000000E+00	0.00000000E+00
29	UZ	0.00000000E+00	0.00000000E+00
30	UZ	0.00000000E+00	0.00000000E+00
31	UZ	0.00000000E+00	0.00000000E+00
32	UZ	0.00000000E+00	0.00000000E+00
33	UZ	0.00000000E+00	0.00000000E+00
34	UZ	0.00000000E+00	0.00000000E+00
35	UZ	0.00000000E+00	0.00000000E+00
36	UZ	0.00000000E+00	0.00000000E+00
37	UZ	0.00000000E+00	0.00000000E+00
38	UZ	0.00000000E+00	0.00000000E+00
39	UZ	0.00000000E+00	0.00000000E+00
40	UZ	0.00000000E+00	0.00000000E+00

MODE	LABEL	DISP	DISP
41	UZ	0.00000000E+00	0.00000000E+00
42	UZ	0.00000000E+00	0.00000000E+00
43	UZ	0.00000000E+00	0.00000000E+00
44	UZ	0.00000000E+00	0.00000000E+00
45	UZ	0.00000000E+00	0.00000000E+00
46	UZ	0.00000000E+00	0.00000000E+00
47	UZ	0.00000000E+00	0.00000000E+00
48	UZ	0.00000000E+00	0.00000000E+00
49	UZ	0.00000000E+00	0.00000000E+00
50	UZ	0.00000000E+00	0.00000000E+00
51	UZ	0.00000000E+00	0.00000000E+00
52	UZ	0.00000000E+00	0.00000000E+00
53	UZ	0.00000000E+00	0.00000000E+00
54	UZ	0.00000000E+00	0.00000000E+00
55	UZ	0.00000000E+00	0.00000000E+00
56	UZ	0.00000000E+00	0.00000000E+00
57	UZ	0.00000000E+00	0.00000000E+00
58	UZ	0.00000000E+00	0.00000000E+00

95 UZ	0.00000000E+00	0.00000000E+00
96 UZ	0.00000000E+00	0.00000000E+00
97 UZ	0.00000000E+00	0.00000000E+00
98 UZ	0.00000000E+00	0.00000000E+00
99 UZ	0.00000000E+00	0.00000000E+00
100 UZ	0.00000000E+00	0.00000000E+00
101 UZ	0.00000000E+00	0.00000000E+00
102 UZ	0.00000000E+00	0.00000000E+00

MODE LABEL	D1SP	C01SP
103 UZ	0.00000000E+00	0.00000000E+00
104 UZ	0.00000000E+00	0.00000000E+00
105 UZ	0.00000000E+00	0.00000000E+00
106 UZ	0.00000000E+00	0.00000000E+00
107 UZ	0.00000000E+00	0.00000000E+00
108 UZ	0.00000000E+00	0.00000000E+00
109 UZ	0.00000000E+00	0.00000000E+00
110 UZ	0.00000000E+00	0.00000000E+00
111 UZ	0.00000000E+00	0.00000000E+00
112 UZ	0.00000000E+00	0.00000000E+00
113 UZ	0.00000000E+00	0.00000000E+00
114 UZ	0.00000000E+00	0.00000000E+00
115 UZ	0.00000000E+00	0.00000000E+00
116 UZ	0.00000000E+00	0.00000000E+00
117 UZ	0.00000000E+00	0.00000000E+00
118 UZ	0.00000000E+00	0.00000000E+00
119 UZ	0.00000000E+00	0.00000000E+00
120 UZ	0.00000000E+00	0.00000000E+00
121 UZ	0.00000000E+00	0.00000000E+00
122 UZ	0.00000000E+00	0.00000000E+00

MODE LABEL	D1SP	C01SP
123 UZ	0.00000000E+00	0.00000000E+00
124 UZ	0.00000000E+00	0.00000000E+00
125 UZ	0.00000000E+00	0.00000000E+00
126 UZ	0.00000000E+00	0.00000000E+00
127 UZ	0.00000000E+00	0.00000000E+00
128 UZ	0.00000000E+00	0.00000000E+00
129 UZ	0.00000000E+00	0.00000000E+00
130 UZ	0.00000000E+00	0.00000000E+00
131 UZ	0.00000000E+00	0.00000000E+00
132 UZ	0.00000000E+00	0.00000000E+00
133 UZ	0.00000000E+00	0.00000000E+00
134 UZ	0.00000000E+00	0.00000000E+00
135 UZ	0.00000000E+00	0.00000000E+00
136 UZ	0.00000000E+00	0.00000000E+00
137 UZ	0.00000000E+00	0.00000000E+00
138 UZ	0.00000000E+00	0.00000000E+00
139 UZ	0.00000000E+00	0.00000000E+00
140 UZ	0.00000000E+00	0.00000000E+00
141 UZ	0.00000000E+00	0.00000000E+00
142 UZ	0.00000000E+00	0.00000000E+00

MODE LABEL	D1SP	C01SP
143 UZ	0.00000000E+00	0.00000000E+00
144 UZ	0.00000000E+00	0.00000000E+00
145 UZ	0.00000000E+00	0.00000000E+00
146 UZ	0.00000000E+00	0.00000000E+00
147 UZ	0.00000000E+00	0.00000000E+00
148 UZ	0.00000000E+00	0.00000000E+00
149 UZ	0.00000000E+00	0.00000000E+00
150 UZ	0.00000000E+00	0.00000000E+00
151 UZ	0.00000000E+00	0.00000000E+00
152 UZ	0.00000000E+00	0.00000000E+00
153 UZ	0.00000000E+00	0.00000000E+00
154 UZ	0.00000000E+00	0.00000000E+00
155 UZ	0.00000000E+00	0.00000000E+00
156 UZ	0.00000000E+00	0.00000000E+00
157 UZ	0.00000000E+00	0.00000000E+00
158 UZ	0.00000000E+00	0.00000000E+00
159 UZ	0.00000000E+00	0.00000000E+00
160 UZ	0.00000000E+00	0.00000000E+00
161 UZ	0.00000000E+00	0.00000000E+00
162 UZ	0.00000000E+00	0.00000000E+00

MODE	LABEL	DISP	CDISP
163	UR	0.00000000E+00	0.00000000E+00
164	UR	0.00000000E+00	0.00000000E+00
165	UR	0.00000000E+00	0.00000000E+00
166	UR	0.00000000E+00	0.00000000E+00
167	UR	0.00000000E+00	0.00000000E+00
168	UR	0.00000000E+00	0.00000000E+00
169	UR	0.00000000E+00	0.00000000E+00
170	UR	0.00000000E+00	0.00000000E+00
171	UR	0.00000000E+00	0.00000000E+00
172	UR	0.00000000E+00	0.00000000E+00
173	UR	0.00000000E+00	0.00000000E+00
174	UR	0.00000000E+00	0.00000000E+00
175	UR	0.00000000E+00	0.00000000E+00
176	UR	0.00000000E+00	0.00000000E+00
177	UR	0.00000000E+00	0.00000000E+00
178	UR	0.00000000E+00	0.00000000E+00
179	UR	0.00000000E+00	0.00000000E+00
180	UR	0.00000000E+00	0.00000000E+00
201	UR	0.00000000E+00	0.00000000E+00
202	UR	0.00000000E+00	0.00000000E+00

MODE	LABEL	DISP	CDISP
203	UR	0.00000000E+00	0.00000000E+00
204	UR	0.00000000E+00	0.00000000E+00
205	UR	0.00000000E+00	0.00000000E+00
206	UR	0.00000000E+00	0.00000000E+00
207	UR	0.00000000E+00	0.00000000E+00
208	UR	0.00000000E+00	0.00000000E+00
209	UR	0.00000000E+00	0.00000000E+00
210	UR	0.00000000E+00	0.00000000E+00
211	UR	0.00000000E+00	0.00000000E+00
212	UR	0.00000000E+00	0.00000000E+00
213	UR	0.00000000E+00	0.00000000E+00
214	UR	0.00000000E+00	0.00000000E+00
215	UR	0.00000000E+00	0.00000000E+00
216	UR	0.00000000E+00	0.00000000E+00
217	UR	0.00000000E+00	0.00000000E+00
218	UR	0.00000000E+00	0.00000000E+00
219	UR	0.00000000E+00	0.00000000E+00
220	UR	0.00000000E+00	0.00000000E+00
221	UR	0.00000000E+00	0.00000000E+00
222	UR	0.00000000E+00	0.00000000E+00

MODE	LABEL	DISP	CDISP
223	UR	0.00000000E+00	0.00000000E+00
224	UR	0.00000000E+00	0.00000000E+00
225	UR	0.00000000E+00	0.00000000E+00
226	UR	0.00000000E+00	0.00000000E+00
227	UR	0.00000000E+00	0.00000000E+00
228	UR	0.00000000E+00	0.00000000E+00
229	UR	0.00000000E+00	0.00000000E+00
230	UR	0.00000000E+00	0.00000000E+00
231	UR	0.00000000E+00	0.00000000E+00
232	UR	0.00000000E+00	0.00000000E+00
233	UR	0.00000000E+00	0.00000000E+00
234	UR	0.00000000E+00	0.00000000E+00
235	UR	0.00000000E+00	0.00000000E+00
236	UR	0.00000000E+00	0.00000000E+00
237	UR	0.00000000E+00	0.00000000E+00
238	UR	0.00000000E+00	0.00000000E+00
239	UR	0.00000000E+00	0.00000000E+00
240	UR	0.00000000E+00	0.00000000E+00
241	UR	0.00000000E+00	0.00000000E+00
242	UR	0.00000000E+00	0.00000000E+00

MODE	LABEL	DISP	CDISP
243	UR	0.00000000E+00	0.00000000E+00
244	UR	0.00000000E+00	0.00000000E+00
245	UR	0.00000000E+00	0.00000000E+00
246	UR	0.00000000E+00	0.00000000E+00
247	UR	0.00000000E+00	0.00000000E+00
248	UR	0.00000000E+00	0.00000000E+00

249 MZ 0.00000000E+00 0.00000000E+00
 250 MZ 0.00000000E+00 0.00000000E+00
 251 MZ 0.00000000E+00 0.00000000E+00
 252 MZ 0.00000000E+00 0.00000000E+00
 253 MZ 0.00000000E+00 0.00000000E+00
 1 UR 0.00000000E+00 0.00000000E+00
 5 UR 0.00000000E+00 0.00000000E+00
 253 UR 0.00000000E+00 0.00000000E+00
 1 UR 0.00000000E+00 0.00000000E+00
 253 NOT2 0.00000000E+00 0.00000000E+00

LIST ELEMENT PARAMETERS FOR ALL SELECTED ELEMENTS

ELEM	FACE	VALUE(S)	FACE NODES
4	3	10.0000000	10 9
8	3	10.0000000	15 10
12	3	10.0000000	20 15
16	3	10.0000000	25 20
20	3	10.0000000	30 25
24	3	10.0000000	35 30
28	3	10.0000000	40 35
27	2	10.0000000	35 39
28	2	10.0000000	39 40
29	2	10.0000000	40 38
37	1	10.0000000	95 97
37	4	10.0000000	101 97
41	4	10.0000000	105 101
45	4	10.0000000	111 106
49	4	10.0000000	116 111
53	4	10.0000000	121 116
101	1	10.0000000	95 121
101	4	10.0000000	126 99
61	4	10.0000000	131 126
65	4	10.0000000	136 131
ELEM	FACE	VALUE(S)	FACE NODES
69	4	10.0000000	141 136
73	4	10.0000000	146 141
77	4	10.0000000	151 146
81	4	10.0000000	156 151
85	4	10.0000000	161 156
89	4	10.0000000	166 161
93	4	10.0000000	171 166
97	4	10.0000000	176 171
103	1	10.0000000	178 201
104	1	10.0000000	201 202
105	1	10.0000000	202 203
106	1	10.0000000	203 204
107	1	10.0000000	204 205
108	1	10.0000000	205 206
109	1	10.0000000	206 207
110	1	10.0000000	207 208
111	1	10.0000000	208 209
112	1	10.0000000	209 210
113	1	10.0000000	210 211
114	1	10.0000000	211 212
ELEM	FACE	VALUE(S)	FACE NODES
115	1	10.0000000	212 213
116	1	10.0000000	213 214
117	1	10.0000000	214 215
118	1	10.0000000	215 216
119	1	10.0000000	216 217
120	1	10.0000000	217 218
121	1	10.0000000	218 219
122	1	10.0000000	219 220
123	1	10.0000000	220 221
124	1	10.0000000	221 222
125	1	10.0000000	222 223
126	1	10.0000000	223 224
127	1	10.0000000	224 225
128	1	10.0000000	225 226
129	1	10.0000000	226 227
130	1	10.0000000	227 228

131	1	10.000000	0.0000000E+00	228	229
132	1	10.000000	0.0000000E+00	229	230
133	1	10.000000	0.0000000E+00	230	231
134	1	10.000000	0.0000000E+00	231	232
ELEM FACE VALUE(S) FACE NUMBER					
135	1	10.000000	0.0000000E+00	232	233
136	1	10.000000	0.0000000E+00	233	234
137	1	10.000000	0.0000000E+00	234	235
138	1	10.000000	0.0000000E+00	235	236
139	1	10.000000	0.0000000E+00	236	237
140	1	10.000000	0.0000000E+00	237	238
141	1	10.000000	0.0000000E+00	238	239
142	1	10.000000	0.0000000E+00	239	240
143	1	10.000000	0.0000000E+00	240	241
144	1	10.000000	0.0000000E+00	241	242
145	1	10.000000	0.0000000E+00	242	243
146	1	10.000000	0.0000000E+00	243	244
147	1	10.000000	0.0000000E+00	244	245
148	1	10.000000	0.0000000E+00	245	246
149	1	10.000000	0.0000000E+00	246	247
150	1	10.000000	0.0000000E+00	247	248
151	1	10.000000	0.0000000E+00	248	249
152	1	10.000000	0.0000000E+00	249	250
153	1	10.000000	0.0000000E+00	250	251
154	1	10.000000	0.0000000E+00	251	252
ELEM FACE VALUE(S) FACE NUMBER					
155	1	10.000000	0.0000000E+00	252	253

LIST ELEMENT CONNECTIONS FOR ALL SELECTED ELEMENTS

LIST TEMPERATURES FOR ALL SELECTED NODES

NODE	TEMPERATURE	FLUXES
1	321.59	0.00000E+00
2	221.59	0.00000E+00
3	221.59	0.00000E+00
4	221.59	0.00000E+00
5	221.59	0.00000E+00
6	221.59	0.00000E+00
7	221.59	0.00000E+00
8	221.59	0.00000E+00
9	221.59	0.00000E+00
10	221.59	0.00000E+00
11	221.59	0.00000E+00
12	221.59	0.00000E+00
13	221.59	0.00000E+00
14	221.59	0.00000E+00
15	221.59	0.00000E+00
16	221.59	0.00000E+00
17	221.59	0.00000E+00
18	221.59	0.00000E+00
19	221.59	0.00000E+00
20	221.59	0.00000E+00
NODE TEMPERATURE FLUXES		
21	220.44	0.00000E+00
22	220.44	0.00000E+00
23	220.44	0.00000E+00
24	220.44	0.00000E+00
25	220.44	0.00000E+00
26	220.44	0.00000E+00
27	220.44	0.00000E+00
28	220.44	0.00000E+00
29	220.44	0.00000E+00
30	220.44	0.00000E+00
31	218.20	0.00000E+00
32	218.20	0.00000E+00
33	218.20	0.00000E+00
34	218.20	0.00000E+00
35	218.20	0.00000E+00
36	218.20	0.00000E+00
37	218.20	0.00000E+00

38	218.20	0.00000E+00
39	218.20	0.00000E+00
40	218.20	0.00000E+00
NO#E TEMPERATURE FLUENCE		
41	218.20	0.00000E+00
42	218.20	0.00000E+00
43	218.20	0.00000E+00
44	218.20	0.00000E+00
47	218.20	0.00000E+00
48	218.20	0.00000E+00
51	218.20	0.00000E+00
52	218.20	0.00000E+00
53	218.20	0.00000E+00
56	218.20	0.00000E+00
57	218.20	0.00000E+00
58	218.20	0.00000E+00
95	218.91	0.00000E+00
96	218.91	0.00000E+00
97	218.91	0.00000E+00
98	218.91	0.00000E+00
99	218.91	0.00000E+00
100	218.91	0.00000E+00
101	218.91	0.00000E+00
102	218.91	0.00000E+00
NO#E TEMPERATURE FLUENCE		
103	218.91	0.00000E+00
104	218.91	0.00000E+00
105	218.91	0.00000E+00
106	218.91	0.00000E+00
107	218.91	0.00000E+00
108	218.91	0.00000E+00
109	218.91	0.00000E+00
110	218.91	0.00000E+00
111	218.91	0.00000E+00
112	218.91	0.00000E+00
113	218.91	0.00000E+00
114	218.91	0.00000E+00
115	218.91	0.00000E+00
116	218.91	0.00000E+00
117	218.91	0.00000E+00
118	218.91	0.00000E+00
119	218.91	0.00000E+00
120	218.91	0.00000E+00
121	218.91	0.00000E+00
122	218.91	0.00000E+00
NO#E TEMPERATURE FLUENCE		
123	218.91	0.00000E+00
124	218.91	0.00000E+00
125	218.91	0.00000E+00
126	221.22	0.00000E+00
127	221.22	0.00000E+00
128	221.22	0.00000E+00
129	221.22	0.00000E+00
130	221.22	0.00000E+00
131	225.53	0.00000E+00
132	225.53	0.00000E+00
133	225.53	0.00000E+00
134	225.53	0.00000E+00
135	225.53	0.00000E+00
136	225.53	0.00000E+00
137	225.53	0.00000E+00
138	225.53	0.00000E+00
139	225.53	0.00000E+00
140	225.53	0.00000E+00
141	228.13	0.00000E+00
142	228.13	0.00000E+00
NO#E TEMPERATURE FLUENCE		
143	228.13	0.00000E+00
144	228.13	0.00000E+00
145	228.13	0.00000E+00

144	230.66	0.00000E+00
147	230.64	0.00000E+00
148	230.64	0.00000E+00
149	230.64	0.00000E+00
150	230.66	0.00000E+00
151	234.03	0.00000E+00
152	234.03	0.00000E+00
153	234.03	0.00000E+00
154	234.03	0.00000E+00
155	234.03	0.00000E+00
156	237.61	0.00000E+00
157	237.61	0.00000E+00
158	237.61	0.00000E+00
159	237.61	0.00000E+00
160	237.61	0.00000E+00
161	241.20	0.00000E+00
162	241.20	0.00000E+00

NODE	TEMPERATURE	FLUXENCE
163	241.20	0.00000E+00
164	241.20	0.00000E+00
165	241.20	0.00000E+00
166	244.78	0.00000E+00
167	244.78	0.00000E+00
168	244.78	0.00000E+00
169	244.78	0.00000E+00
170	244.78	0.00000E+00
171	248.37	0.00000E+00
172	248.37	0.00000E+00
173	248.37	0.00000E+00
174	248.37	0.00000E+00
175	248.37	0.00000E+00
176	251.95	0.00000E+00
177	251.95	0.00000E+00
178	251.95	0.00000E+00
179	251.95	0.00000E+00
180	251.95	0.00000E+00
201	290.25	0.00000E+00
202	290.24	0.00000E+00

NODE	TEMPERATURE	FLUXENCE
203	265.14	0.00000E+00
204	269.54	0.00000E+00
205	273.93	0.00000E+00
206	278.33	0.00000E+00
207	282.73	0.00000E+00
208	287.13	0.00000E+00
209	291.52	0.00000E+00
210	295.92	0.00000E+00
211	299.28	0.00000E+00
212	302.63	0.00000E+00
213	305.99	0.00000E+00
214	309.34	0.00000E+00
215	312.70	0.00000E+00
216	316.06	0.00000E+00
217	319.41	0.00000E+00
218	322.76	0.00000E+00
219	326.11	0.00000E+00
220	329.47	0.00000E+00
221	332.84	0.00000E+00
222	336.20	0.00000E+00

NODE	TEMPERATURE	FLUXENCE
223	339.55	0.00000E+00
224	342.90	0.00000E+00
225	346.26	0.00000E+00
226	349.61	0.00000E+00
227	352.97	0.00000E+00
228	356.32	0.00000E+00
229	359.67	0.00000E+00
230	363.02	0.00000E+00
231	366.37	0.00000E+00
232	369.72	0.00000E+00
233	373.07	0.00000E+00

234	325.37	0.00000E+00
235	321.63	0.00000E+00
236	319.87	0.00000E+00
237	318.12	0.00000E+00
238	316.36	0.00000E+00
239	314.60	0.00000E+00
240	312.84	0.00000E+00
241	311.09	0.00000E+00
242	309.33	0.00000E+00

NODE	TEMPERATURE	FLUENCE
243	307.57	0.00000E+00
244	312.70	0.00000E+00
245	317.82	0.00000E+00
246	322.95	0.00000E+00
247	328.08	0.00000E+00
248	333.20	0.00000E+00
249	338.32	0.00000E+00
250	343.45	0.00000E+00
251	348.57	0.00000E+00
252	353.70	0.00000E+00
253	358.82	0.00000E+00

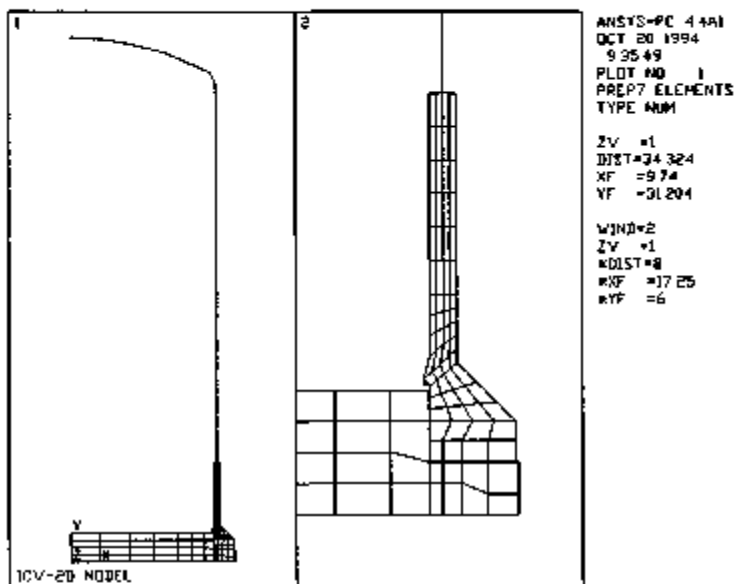


FIGURE 2.10.2-1.

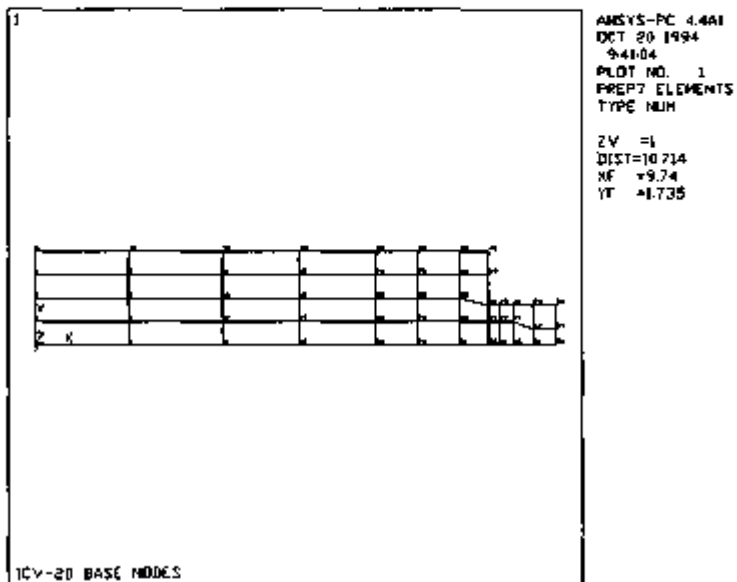


FIGURE 2.10.2-2.

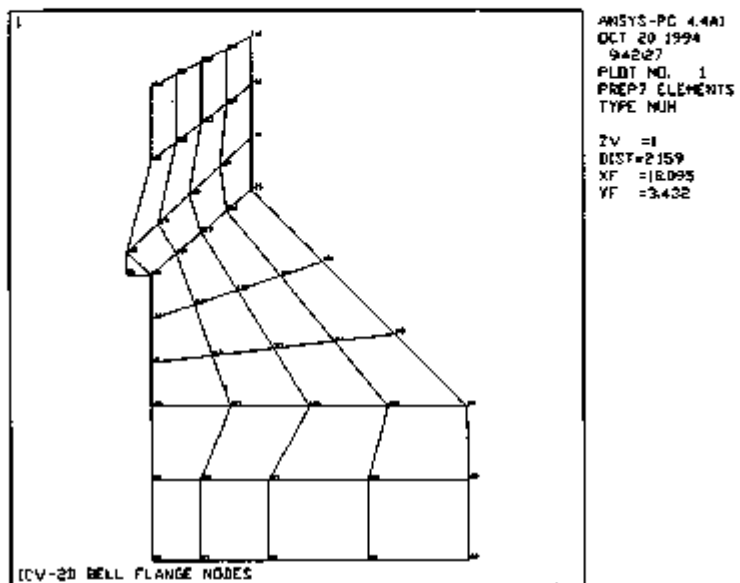


FIGURE 2.10.2-3.

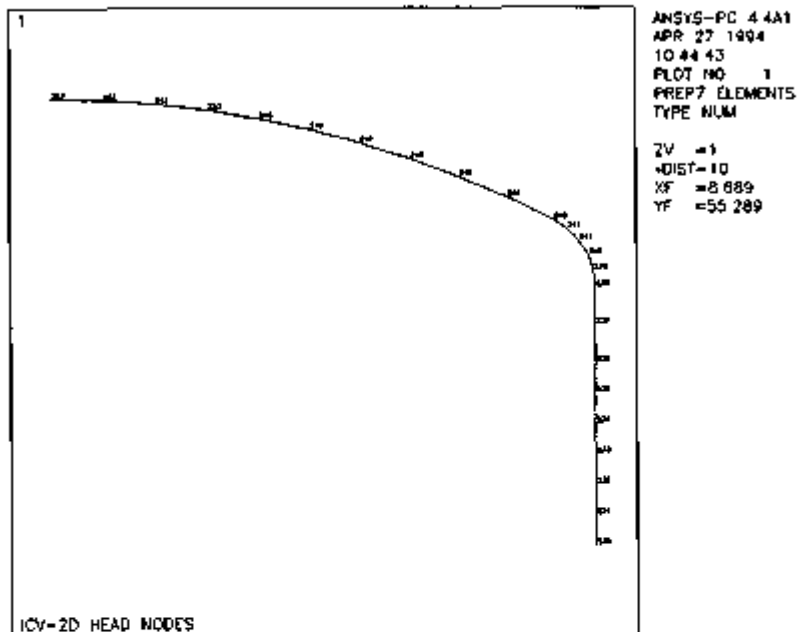


FIGURE 2.10.2-4

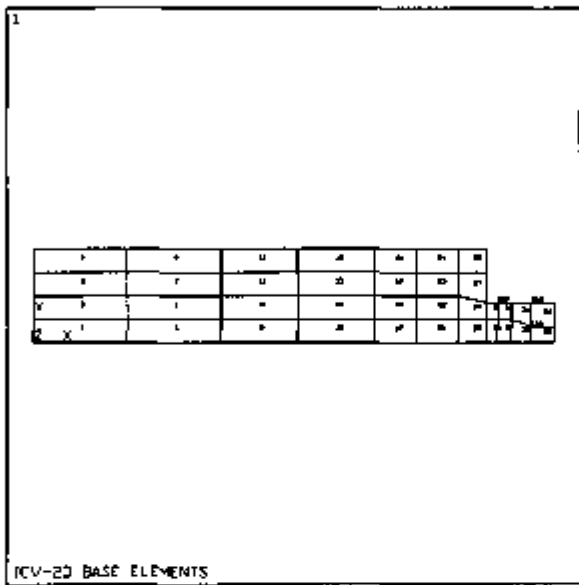


FIGURE 2.10.2-6.

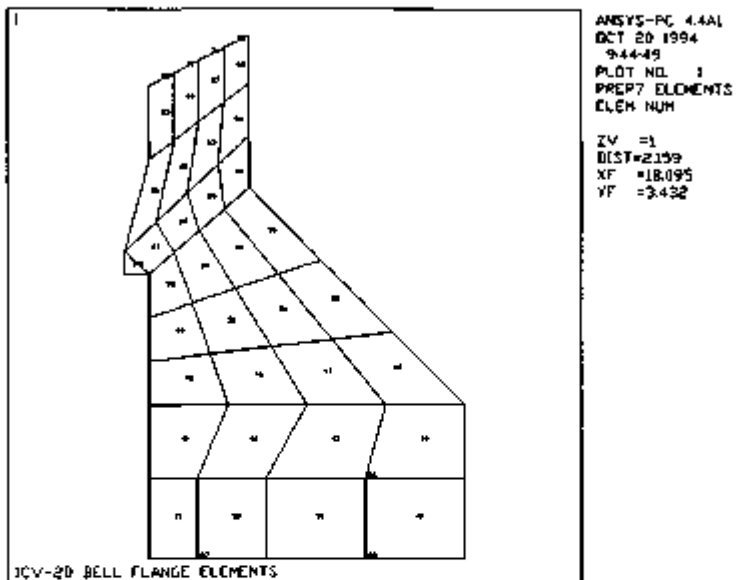


FIGURE 2.10.2-6.

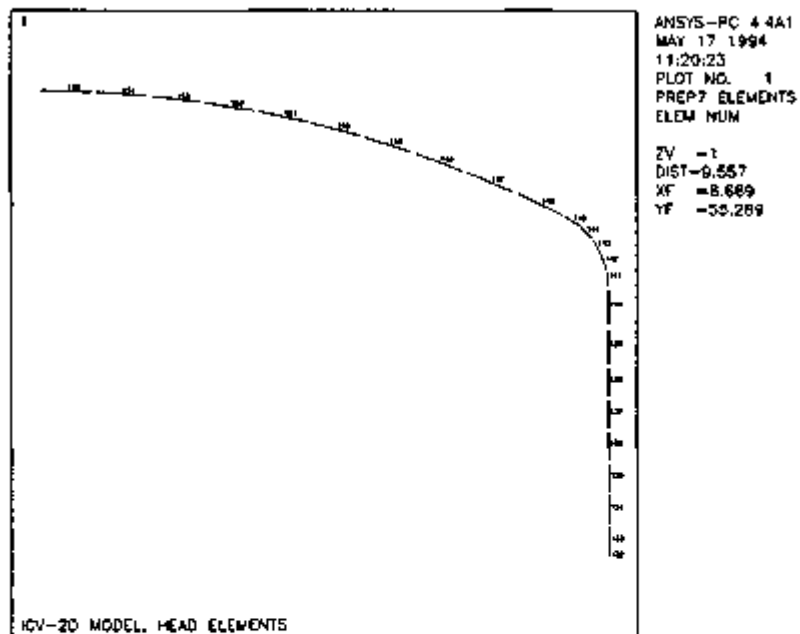


FIGURE 2.10.2-7.

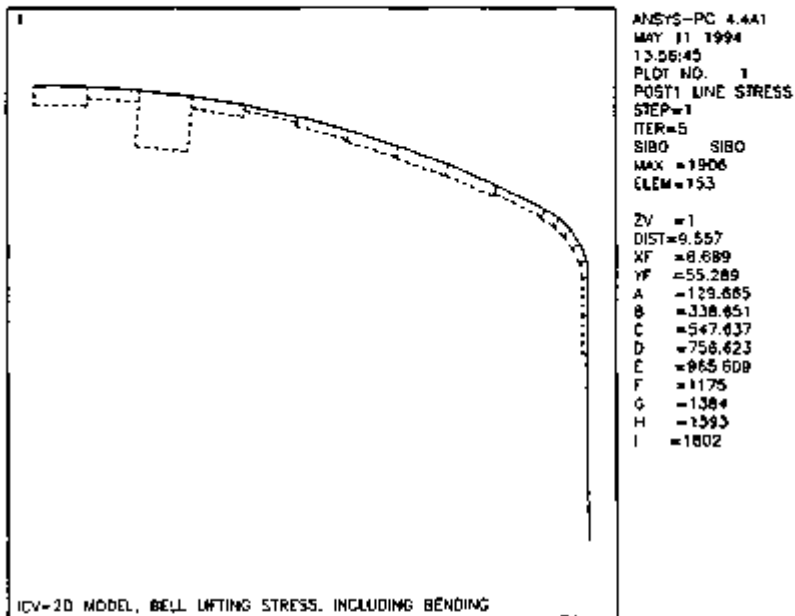


FIGURE 2.10.2-8.

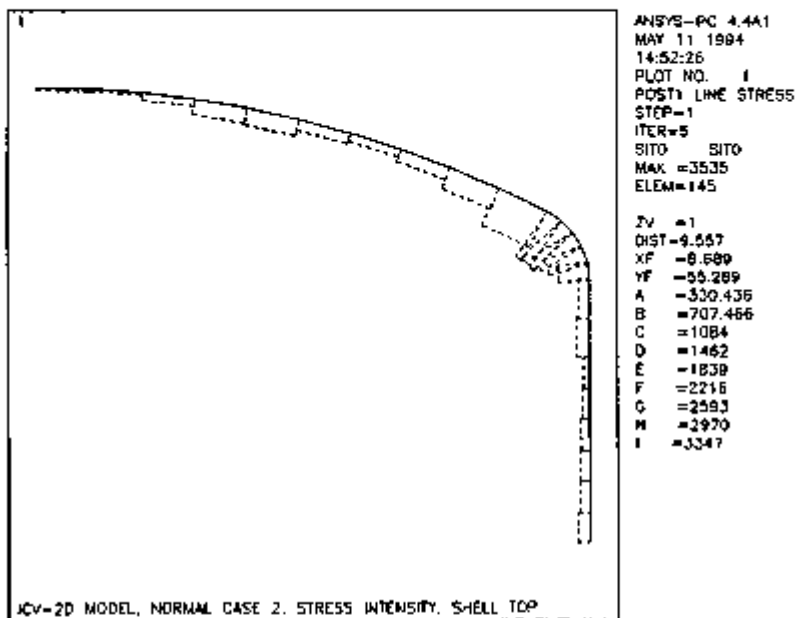


FIGURE 2.10.2-8.

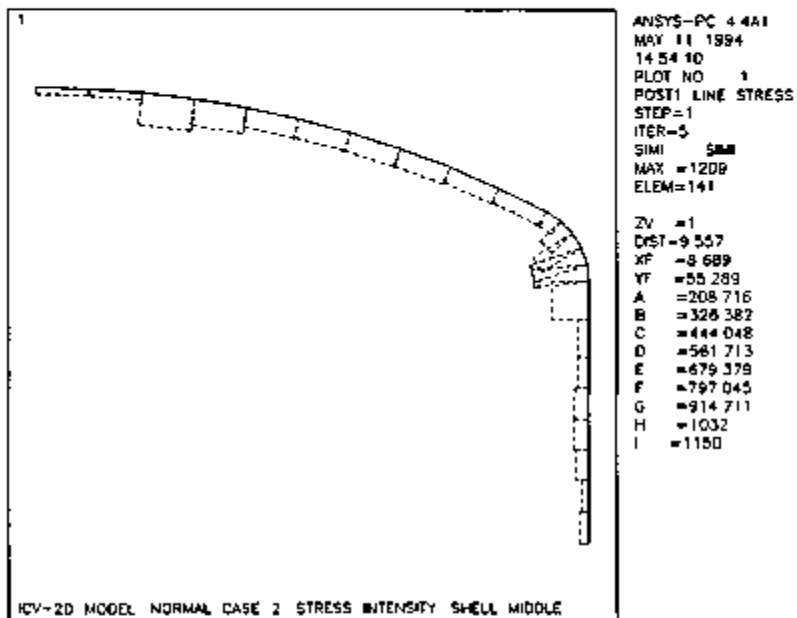


FIGURE 2.10.2-10.

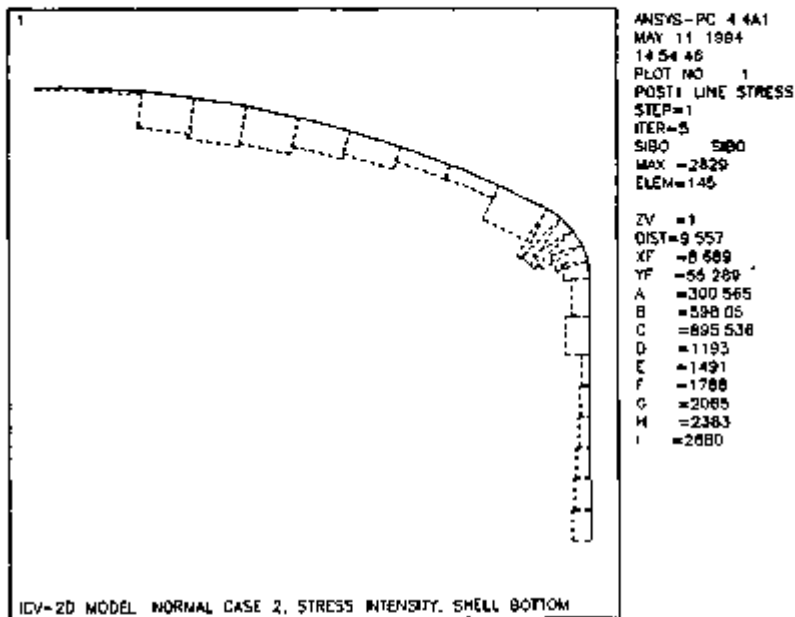


FIGURE 2.10.2-11.

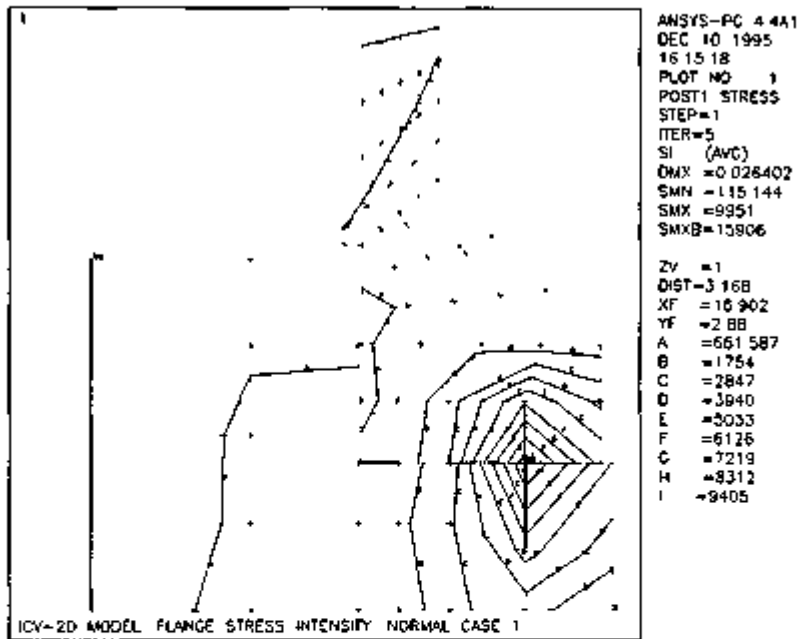


FIGURE 2 10 2-12

2.10.3 OCV Head and Fin Model

2.10.3.1 Description. The OCV head and fin model is a 3-D finite element model of a one-third symmetry segment of the upper portion of the OCV, used to evaluate lifting stresses in the OCV head. Other stresses related to lifting the package using the OCV fins are evaluated in Section 2.5.1.2. The extent of the model is 120° with a single lifting fin in the center. To simplify the model, the doubler plate between the fin and the OCV head was not modeled. Instead, the fin was modeled as directly attached to the OCV head. The action of the doubler plate is to distribute fin-lifting loads over a slightly larger area of the OCV head, and thus, to omit the doubler plate conservatively increased OCV head stress. The fin is therefore connected at a right angle directly to the OCV head. The lower edge of the model ends in the OCV wall a short distance above the OCV flange, because flange details are irrelevant to this analysis. The coolant jacket is also not modeled for the same reason. The lifting load is applied directly to a node located at the fin hole center, and the fin hole itself is not modeled. Bearing stress at the lift hole and stresses in the fin weld are analyzed using classical methods in Section 2.5.1.2. The weld properties are found with the aid of a small finite element model documented in Appendix 2.10.4. The model layout is shown in Figure 2.10.3-1.

2.10.3.2 Construction. The model is constructed of quadrilateral shell elements of two thicknesses: 0.50 in. for the OCV wall, and 0.25 in. for the fin. The fin hole reinforcement is conservatively ignored. The model extends from its lower edge just above the OCV flange up to the center of the top of the OCV head. The highest row of nodes is actually located at a small radius from the center to simplify modeling. No stress or strain discontinuities occur. Node and element plots of key portions of the model are given in Figures 2.10.3-2 through 2.10.3-6. An interpreted ANSYS input listing is given in Table 2.10.3-1.

2.10.3.3 Material Properties. A modulus of elasticity of 27,18(10)⁸ psi was used, corresponding to 270 °F, which represents overall head temperature. Poisson's ratio was 0.3.

2.10.3.4 Constraints. Nodes along the cut edges were constrained in the one linear and two rotational degrees of freedom required to ensure symmetry of the model. The nodes along the bottom were fixed in all six degrees of freedom, as appropriate to the lifting case. This edge was far enough away from the area of interest around the fin that constraint details were relatively unimportant.

2.10.3.5 Applied Loading. Two loads were applied to the fin in its own plane at the location of the fin hole center, node 756. Their vector sum was a unit load along the line of action of the cable, which is at 60° to the horizontal. Pressure internal to the OCV was not used. Nodal temperatures were not used.

2.10.3.6 Results. A plot of maximum stress intensity in the OCV head is shown in Figures 2.10.3-7 and 2.10.3-8, and for the OCV wall bottom in Figure 2.10.3-9. The full value of stress is found by multiplying the stress result shown here with the cable load, as detailed in Section 2.5.1.2.

TABLE 2.10.3-1. Interpreted ANSYS Input Listing.

```

STATIC ANALYSIS (NAME= D)
LINEAR ANALYSIS - NO NON-LINEAR PROPERTIES
REFERENCE TEMPERATURE= 0.800 (TEMP)
UNIFORM TEMPERATURE = 0.800 (TEMP)
*****ANALYSIS OPTIONS (KEY VALUES) (IF ANY) *****
NO STATIC INTERPOLATION/EXTRAPOLATION (KEY(3)=0)
SMALL DEFLECTION SOLUTION (KEY(4)=0)
NO STRESS STIFFENING (KEY(6)=0)
USE LINEAR SOLUTION PROCEDURE (KEY(9)=0)
IN-CORE WAVE-FRONT EQUATION SOLVER (KEY(10)=0)
LIST ELEMENT TYPES FROM 1 TO 20 BY 1
NO. STIP KEYOPT VALUES INOPR
1 43 0 0 0 0 0 0 0 0 0 0 QUAD, FLAT SHELL
LIST ALL REAL SETS
REAL CONSTANT SET 1 ITEMS 1 TO 10
0.50000 0.00000E+00 0.00000E+00 0.00000E+00 0.00000E+00 0.00000E+00 0.00000E+00
0.00000E+00 0.00000E+00 0.00000E+00 0.00000E+00 0.00000E+00 0.00000E+00 0.00000E+00
0.00000E+00 0.00000E+00 0.00000E+00 0.00000E+00 0.00000E+00 0.00000E+00 0.00000E+00
REAL CONSTANT SET 2 ITEMS 1 TO 10
0.25000 0.00000E+00 0.00000E+00 0.00000E+00 0.00000E+00 0.00000E+00 0.00000E+00
0.00000E+00 0.00000E+00 0.00000E+00 0.00000E+00 0.00000E+00 0.00000E+00 0.00000E+00
0.00000E+00 0.00000E+00 0.00000E+00 0.00000E+00 0.00000E+00 0.00000E+00 0.00000E+00
LIST ALL COORDINATE SYSTEMS
SYSTEM TYPE CENTER PARAMETERS 6/ING KEYS
0 0 (CARTESIAN) 0.000 0.000 0.000 0.000 0.000 0.000 0 0
1 1 (CYLINDRICAL) 0.000 0.000 0.000 1.000 0.000 0 0
2 2 (SPHERICAL) 0.000 0.000 0.000 1.000 1.000 0 0
11 1 (CYLINDRICAL) 0.000 25.15# 0.000 1.000 1.000 0 0
12 1 (CYLINDRICAL) 14.940 54.29# 0.000 1.000 1.000 0 0
13 1 (CYLINDRICAL) 0.000 0.000 0.000 1.000 1.000 0 0
SYSTEM ORIENTATION VECTORS (#,1,2)
0 1.00 0.00 0.00 0.00 1.00 0.00 0.00 0.00 1.00
1 1.00 0.00 0.00 0.00 1.00 0.00 0.00 0.00 1.00
2 1.00 0.00 0.00 0.00 1.00 0.00 0.00 0.00 1.00
11 1.00 0.00 0.00 0.00 1.00 0.00 0.00 0.00 1.00
12 1.00 0.00 0.00 0.00 1.00 0.00 0.00 0.00 1.00
13 1.00 0.00 0.00 0.00 1.00 0.00 0.00 1.00 0.00
ELEM TYPE XC TC ZC TREF FRTZ THICK
11 1 0.00000E+00 25.15# 0.00000E+00 0.000 0.000 0.000
12 1 14.940 54.29# 0.00000E+00 0.000 0.000 0.000
13 1 0.00000E+00 0.00000E+00 0.00000E+00 0.000 0.000 -90.000
LIST ALL SELECTED KEYPOINTS, DELT= 0
PT. X,Y,Z LOCATION NODE ELEM ESIZE
1 18.1900 53.3800 0.00000E+00 221 0
2 18.1900 54.2900 0.00000E+00 220 0
3 15.4200 57.1800 0.00000E+00 214 0
4 15.0000 58.7200 0.00000E+00 211 0
5 15.0000 60.5600 0.00000E+00 444 0
6 15.0000 62.5600 0.00000E+00 448 0
7 19.2500 62.5600 0.00000E+00 450 0
8 21.2500 60.5600 0.00000E+00 454 0
9 21.2500 54.4300 0.00000E+00 456 0
10 20.0000 53.3800 0.00000E+00 462 0
11 16.9400 54.4300 0.00000E+00 0 0

```

LIST ALL SELECTOR LINE SEGMENTS.

SEG. NO.	KEYPT	DIRECTION		DIV	SPACING	NODES/ELEM	
1	1	0.0000	-1.0000	0.0000	1	1.0000	-1 -1
	2	0.0000	1.0000	0.0000			0 0
2	2	-0.0000	0.0000	0.0000	4	1.0000	215 219
	2	0.0011	-1.0000	0.0000			0 0
3	4	-0.0020	0.0000	0.0000	3	1.0000	212 213
	3	0.0002	-0.4575	0.0000			0 0
4	4	0.0000	-1.0000	0.0000	4	1.0000	445 447
	5	0.0000	1.0000	0.0000			0 0
5	5	-0.7071	-0.7071	0.0000	2	1.0000	649 649
	6	0.7071	0.7071	0.0000			0 0
6	6	-1.0000	0.0000	0.0000	4	1.0000	451 453
	7	1.0000	0.0000	0.0000			0 0
7	7	-0.7071	0.7071	0.0000	2	1.0000	455 455
	8	0.7071	-0.7071	0.0000			0 0
8	8	0.0000	1.0000	0.0000	6	1.0000	457 461
	9	0.0000	-1.0000	0.0000			0 0
9	9	0.7071	0.7071	0.0000	2	1.0000	463 463
	10	-0.7071	-0.7071	0.0000			0 0
10	10	1.0000	0.0000	0.0000	2	1.0000	464 464
	11	-1.0000	0.0000	0.0000			0 0

LIST NO.	ALL KEYPNTS/LINE	SELECTED AREAS.				NODES		ELEMENTS		MAT REL TYP ELEM			
		1	2	3	4	465	510	301	368	1	2	1	0
1		1	2	3	4								
		5	6	7	8								
		9	ID										

LIST ALL SELECTED ELEMENTS. (LIST NODES)

ELEM	MAT	TYP	REL	ELEM	NODES			
1	1	1	1	0	2	3	43	42
2	1	1	1	0	3	4	44	43
3	1	1	1	0	4	5	45	44
4	1	1	1	0	5	6	46	45
5	1	1	1	0	6	7	47	46
6	1	1	1	0	7	8	48	47
7	1	1	1	0	8	9	49	48
8	1	1	1	0	9	10	50	49
9	1	1	1	0	10	11	51	50
10	1	1	1	0	11	12	52	51
11	1	1	1	0	12	13	53	52
12	1	1	1	0	13	14	54	53
13	1	1	1	0	14	15	55	54
14	1	1	1	0	15	16	56	55
15	1	1	1	0	16	17	57	56
16	1	1	1	0	17	18	58	57
17	1	1	1	0	18	19	59	58
18	1	1	1	0	19	20	60	59
19	1	1	1	0	20	21	61	60
20	1	1	1	0	21	22	62	61

ELEM	MAT	TYP	REL	ELEM	NODES			
21	1	1	1	0	22	23	63	62
22	1	1	1	0	23	24	64	63
23	1	1	1	0	24	25	65	64
24	1	1	1	0	25	26	66	65
25	1	1	1	0	26	27	67	66
26	1	1	1	0	27	28	68	67
27	1	1	1	0	28	29	69	68
28	1	1	1	0	29	30	70	69
29	1	1	1	0	30	31	71	70
30	1	1	1	0	31	32	72	71
31	1	1	1	0	42	43	83	82
32	1	1	1	0	43	44	84	83
33	1	1	1	0	44	45	85	84
34	1	1	1	0	45	46	86	85
35	1	1	1	0	46	47	87	86
36	1	1	1	0	47	48	88	87
37	1	1	1	0	48	49	89	88
38	1	1	1	0	49	50	90	89

39	1	1	1	0	50	51	91	90
40	1	1	1	0	51	52	92	91
ELEM	MAT	TYP	REL	ESYS	MODES			
41	1	1	1	0	52	53	93	92
42	1	1	1	0	53	54	94	93
43	1	1	1	0	54	55	95	94
44	1	1	1	0	55	56	96	95
45	1	1	1	0	56	57	97	96
46	1	1	1	0	57	58	98	97
47	1	1	1	0	58	59	99	98
48	1	1	1	0	59	60	100	99
49	1	1	1	0	60	61	101	100
50	1	1	1	0	61	62	102	101
51	1	1	1	0	62	63	103	102
52	1	1	1	0	63	64	104	103
53	1	1	1	0	64	65	105	104
54	1	1	1	0	65	66	106	105
55	1	1	1	0	66	67	107	106
56	1	1	1	0	67	68	108	107
57	1	1	1	0	68	69	109	108
58	1	1	1	0	69	70	110	109
59	1	1	1	0	70	71	111	110
60	1	1	1	0	71	72	112	111

ELEM	MAT	TYP	REL	ESYS	MODES			
61	1	1	1	0	82	83	123	122
62	1	1	1	0	83	84	124	123
63	1	1	1	0	84	85	125	124
64	1	1	1	0	85	86	126	125
65	1	1	1	0	86	87	127	126
66	1	1	1	0	87	88	128	127
67	1	1	1	0	88	89	129	128
68	1	1	1	0	89	90	130	129
69	1	1	1	0	90	91	131	130
70	1	1	1	0	91	92	132	131
71	1	1	1	0	92	93	133	132
72	1	1	1	0	93	94	134	133
73	1	1	1	0	94	95	135	134
74	1	1	1	0	95	96	136	135
75	1	1	1	0	96	97	137	136
76	1	1	1	0	97	98	138	137
77	1	1	1	0	98	99	139	138
78	1	1	1	0	99	100	140	139
79	1	1	1	0	100	101	141	140
80	1	1	1	0	101	102	142	141

ELEM	MAT	TYP	REL	ESYS	MODES			
81	1	1	1	0	102	103	143	142
82	1	1	1	0	103	104	144	143
83	1	1	1	0	104	105	145	144
84	1	1	1	0	105	106	146	145
85	1	1	1	0	106	107	147	146
86	1	1	1	0	107	108	148	147
87	1	1	1	0	108	109	149	148
88	1	1	1	0	109	110	150	149
89	1	1	1	0	110	111	151	150
90	1	1	1	0	111	112	152	151
91	1	1	1	0	112	113	153	152
92	1	1	1	0	113	114	154	153
93	1	1	1	0	114	115	155	154
94	1	1	1	0	115	116	156	155
95	1	1	1	0	116	117	157	156
96	1	1	1	0	117	118	158	157
97	1	1	1	0	118	119	159	158
98	1	1	1	0	119	120	160	159
99	1	1	1	0	120	121	161	160
100	1	1	1	0	121	122	162	161

ELEM	MAT	TYP	REL	ESYS	MODES			
101	1	1	1	0	133	134	173	172
102	1	1	1	0	133	134	174	173

903	1	1	1	0	134	135	175	174
904	1	1	1	0	133	134	176	179
905	1	1	1	0	135	137	177	176
906	1	1	1	0	137	138	178	177
907	1	1	1	0	138	139	179	176
908	1	1	1	0	139	140	180	179
909	1	1	1	0	140	141	181	180
910	1	1	1	0	141	142	182	181
911	1	1	1	0	142	143	183	182
912	1	1	1	0	143	144	184	183
913	1	1	1	0	144	145	185	184
914	1	1	1	0	143	144	184	185
915	1	1	1	0	146	147	187	186
916	1	1	1	0	147	148	188	187
917	1	1	1	0	148	149	189	188
918	1	1	1	0	149	150	190	189
919	1	1	1	0	150	151	191	190
920	1	1	1	0	151	152	192	191

ELEM	MAT	TRP	REL	ESTS	NODES
121	1	1	1	0	162 163 205 202
122	1	1	1	0	161 164 204 203
123	1	1	1	0	164 165 205 204
124	1	1	1	0	161 166 206 205
125	1	1	1	0	165 167 207 206
126	1	1	1	0	167 168 208 207
127	1	1	1	0	168 169 209 208
128	1	1	1	0	169 170 210 209
129	1	1	1	0	170 171 211 210
130	1	1	1	0	171 172 212 211
131	1	1	1	0	172 173 213 212
132	1	1	1	0	173 174 214 213
133	1	1	1	0	174 175 215 214
134	1	1	1	0	173 176 216 215
135	1	1	1	0	176 177 217 216
136	1	1	1	0	177 178 218 217
137	1	1	1	0	178 179 219 218
138	1	1	1	0	179 180 220 219
139	1	1	1	0	180 181 221 220
140	1	1	1	0	181 182 222 221

ELEM	MAT	TRP	REL	ESTS	NODES
141	1	1	1	0	182 183 223 222
142	1	1	1	0	183 184 224 223
143	1	1	1	0	184 185 225 224
144	1	1	1	0	185 186 226 225
145	1	1	1	0	186 187 227 226
146	1	1	1	0	187 188 228 227
147	1	1	1	0	188 189 229 228
148	1	1	1	0	189 190 230 229
149	1	1	1	0	190 191 231 230
150	1	1	1	0	191 192 232 231
151	1	1	1	0	202 203 243 242
152	1	1	1	0	203 204 244 243
153	1	1	1	0	204 205 245 244
154	1	1	1	0	205 206 246 245
155	1	1	1	0	206 207 247 246
156	1	1	1	0	207 208 248 247
157	1	1	1	0	208 209 249 248
158	1	1	1	0	209 210 250 249
159	1	1	1	0	210 211 251 250
160	1	1	1	0	211 212 252 251

ELEM	MAT	TRP	REL	ESTS	NODES
161	1	1	1	0	212 213 253 252
162	1	1	1	0	213 214 254 253
163	1	1	1	0	214 215 255 254
164	1	1	1	0	215 216 256 255
165	1	1	1	0	216 217 257 256
166	1	1	1	0	217 218 258 257
167	1	1	1	0	218 219 259 258
168	1	1	1	0	219 220 260 259
169	1	1	1	0	220 221 261 260

170	1	1	1	0	221	222	262	261
171	1	1	1	0	222	223	263	262
172	1	1	1	0	223	224	264	263
173	1	1	1	0	224	225	265	264
174	1	1	1	0	225	226	266	265
175	1	1	1	0	226	227	267	266
176	1	1	1	0	227	228	268	267
177	1	1	1	0	228	229	269	268
178	1	1	1	0	229	230	270	269
179	1	1	1	0	230	231	271	270
180	1	1	1	0	231	232	272	271

ELEM	MAT	TPP	REL	ESYS	NODES			
181	1	1	1	0	242	243	283	282
182	1	1	1	0	243	244	284	283
183	1	1	1	0	244	245	285	284
184	1	1	1	0	245	246	286	285
185	1	1	1	0	246	247	287	286
186	1	1	1	0	247	248	288	287
187	1	1	1	0	248	249	289	288
188	1	1	1	0	249	250	290	289
189	1	1	1	0	250	251	291	290
190	1	1	1	0	251	252	292	291
191	1	1	1	0	252	253	293	292
192	1	1	1	0	253	254	294	293
193	1	1	1	0	254	255	295	294
194	1	1	1	0	255	256	296	295
195	1	1	1	0	256	257	297	296
196	1	1	1	0	257	258	298	297
197	1	1	1	0	258	259	299	298
198	1	1	1	0	259	260	300	299
199	1	1	1	0	260	261	301	300
200	1	1	1	0	261	262	302	301

ELEM	MAT	TPP	REL	ESYS	NODES			
201	1	1	1	0	262	263	303	302
202	1	1	1	0	263	264	304	303
203	1	1	1	0	264	265	305	304
204	1	1	1	0	265	266	306	305
205	1	1	1	0	266	267	307	306
206	1	1	1	0	267	268	308	307
207	1	1	1	0	268	269	309	308
208	1	1	1	0	269	270	310	309
209	1	1	1	0	270	271	311	310
210	1	1	1	0	271	272	312	311
211	1	1	1	0	272	273	313	312
212	1	1	1	0	273	274	314	313
213	1	1	1	0	274	275	315	314
214	1	1	1	0	275	276	316	315
215	1	1	1	0	276	277	317	316
216	1	1	1	0	277	278	318	317
217	1	1	1	0	278	279	319	318
218	1	1	1	0	279	280	320	319
219	1	1	1	0	280	281	321	320
220	1	1	1	0	281	282	322	321

ELEM	MAT	TPP	REL	ESYS	NODES			
221	1	1	1	0	282	283	323	322
222	1	1	1	0	283	284	324	323
223	1	1	1	0	284	285	325	324
224	1	1	1	0	285	286	326	325
225	1	1	1	0	286	287	327	326
226	1	1	1	0	287	288	328	327
227	1	1	1	0	288	289	329	328
228	1	1	1	0	289	290	330	329
229	1	1	1	0	290	291	331	330
230	1	1	1	0	291	292	332	331
231	1	1	1	0	292	293	333	332
232	1	1	1	0	293	294	334	333
233	1	1	1	0	294	295	335	334
234	1	1	1	0	295	296	336	335
235	1	1	1	0	296	297	337	336
236	1	1	1	0	297	298	338	337
237	1	1	1	0	298	299	339	338
238	1	1	1	0	299	300	340	339
239	1	1	1	0	300	301	341	340
240	1	1	1	0	301	302	342	341
241	1	1	1	0	302	303	343	342
242	1	1	1	0	303	304	344	343
243	1	1	1	0	304	305	345	344
244	1	1	1	0	305	306	346	345
245	1	1	1	0	306	307	347	346
246	1	1	1	0	307	308	348	347

237	1	1	1	0	306	309	349	348
238	1	1	1	0	309	310	350	349
239	1	1	1	0	310	311	351	350
348	1	1	1	0	311	312	352	351

BLDN	MAT	TYP	REL	EXYS	MODES			
------	-----	-----	-----	------	-------	--	--	--

241	1	1	1	0	322	323	363	362
242	1	1	1	0	323	324	364	363
243	1	1	1	0	324	325	365	364
244	1	1	1	0	325	326	366	365
245	1	1	1	0	326	327	367	366
246	1	1	1	0	327	328	368	367
247	1	1	1	0	328	329	369	368
248	1	1	1	0	329	330	370	369
249	1	1	1	0	330	331	371	370
250	1	1	1	0	331	332	372	371
251	1	1	1	0	332	333	373	372
252	1	1	1	0	333	334	374	373
253	1	1	1	0	334	335	375	374
254	1	1	1	0	335	336	376	375
255	1	1	1	0	336	337	377	376
256	1	1	1	0	337	338	378	377
257	1	1	1	0	338	339	379	378
258	1	1	1	0	339	340	380	379
259	1	1	1	0	340	341	381	380
260	1	1	1	0	341	342	382	381

BLDN	MAT	TYP	REL	EXYS	MODES			
------	-----	-----	-----	------	-------	--	--	--

261	1	1	1	0	342	343	383	382
262	1	1	1	0	343	344	384	383
263	1	1	1	0	344	345	385	384
264	1	1	1	0	345	346	386	385
265	1	1	1	0	346	347	387	386
266	1	1	1	0	347	348	388	387
267	1	1	1	0	348	349	389	388
268	1	1	1	0	349	350	390	389
269	1	1	1	0	350	351	391	390
270	1	1	1	0	351	352	392	391
271	1	1	1	0	352	353	402	401
272	1	1	1	0	353	354	404	403
273	1	1	1	0	354	355	405	404
274	1	1	1	0	355	356	406	405
275	1	1	1	0	356	357	407	406
276	1	1	1	0	357	358	408	407
277	1	1	1	0	358	359	409	408
278	1	1	1	0	359	360	410	409
279	1	1	1	0	360	370	410	409
279	1	1	1	0	370	371	411	410
280	1	1	1	0	371	372	412	411

BLDN	MAT	TYP	REL	EXYS	MODES			
------	-----	-----	-----	------	-------	--	--	--

281	1	1	1	0	372	373	413	412
282	1	1	1	0	373	374	414	413
283	1	1	1	0	374	375	415	414
284	1	1	1	0	375	376	416	415
285	1	1	1	0	376	377	417	416
286	1	1	1	0	377	378	418	417
287	1	1	1	0	378	379	419	418
288	1	1	1	0	379	380	420	419
289	1	1	1	0	380	381	421	420
290	1	1	1	0	381	382	422	421
291	1	1	1	0	382	383	423	422
292	1	1	1	0	383	384	424	423
293	1	1	1	0	384	385	425	424
294	1	1	1	0	385	386	426	425
295	1	1	1	0	386	387	427	426
296	1	1	1	0	387	388	428	427
297	1	1	1	0	388	389	429	428
298	1	1	1	0	389	390	430	429
299	1	1	1	0	390	391	431	430
300	1	1	1	0	391	392	432	431

ELEM	MAT	TYP	REL	ESYS	MODE1	MODE2	MODE3	MODE4
301	1	1	2	0	211	645	676	212
302	1	1	2	0	445	446	475	474
303	1	1	2	0	446	447	475	475
304	1	1	2	0	447	444	449	476
305	1	1	2	0	476	475	473	212
306	1	1	2	0	475	495	473	473
307	1	1	2	0	475	476	491	495
308	1	1	2	0	212	473	473	212
309	1	1	2	0	476	449	455	491
310	1	1	2	0	449	448	431	486
311	1	1	2	0	473	495	304	473
312	1	1	2	0	212	472	471	214
313	1	1	2	0	495	436	304	364
314	1	1	2	0	495	491	492	496
315	1	1	2	0	473	304	309	471
316	1	1	2	0	491	488	489	492
317	1	1	2	0	214	471	470	212
318	1	1	2	0	688	651	652	689
319	1	1	2	0	304	496	497	389
320	1	1	2	0	471	509	510	470

ELEM	MAT	TYP	REL	ESYS	MODE1	MODE2	MODE3	MODE4
321	1	1	2	0	215	470	469	216
322	1	1	2	0	496	492	493	497
323	1	1	2	0	216	469	468	217
324	1	1	2	0	492	489	490	498
325	1	1	2	0	308	497	498	510
326	1	1	2	0	470	810	306	449
327	1	1	2	0	217	668	467	218
328	1	1	2	0	489	432	433	490
329	1	1	2	0	218	467	666	219
330	1	1	2	0	220	219	466	465
331	1	1	2	0	221	220	465	664
332	1	1	2	0	469	306	507	468
333	1	1	2	0	498	505	510	510
334	1	1	2	0	505	506	510	510
335	1	1	2	0	497	494	496	496
336	1	1	2	0	468	307	308	467
337	1	1	2	0	508	466	467	467
338	1	1	2	0	487	464	465	465
339	1	1	2	0	465	466	500	487
340	1	1	2	0	497	473	477	494

ELEM	MAT	TYP	REL	ESYS	MODE1	MODE2	MODE3	MODE4
341	1	1	2	0	493	490	477	477
342	1	1	2	0	490	486	592	595
343	1	1	2	0	506	505	502	503
344	1	1	2	0	490	453	477	477
345	1	1	2	0	486	464	487	487
346	1	1	2	0	466	508	499	580
347	1	1	2	0	506	503	501	587
348	1	1	2	0	307	301	499	588
349	1	1	2	0	486	462	444	444
350	1	1	2	0	487	300	485	486
351	1	1	2	0	499	485	300	380
352	1	1	2	0	464	485	443	442
353	1	1	2	0	494	479	480	382
354	1	1	2	0	433	430	433	477
355	1	1	2	0	302	480	481	383
356	1	1	2	0	303	481	482	381
357	1	1	2	0	489	381	482	433
358	1	1	2	0	499	483	484	485
359	1	1	2	0	494	477	478	479
360	1	1	2	0	483	484	484	443

ELEM	MAT	TYP	REL	ESYS	MODE1	MODE2	MODE3	MODE4
361	1	1	2	0	484	483	441	456
362	1	1	2	0	483	482	440	441
363	1	1	2	0	477	433	434	478
364	1	1	2	0	482	481	439	440
365	1	1	2	0	481	480	438	439

344	1	1	2	0	478	457	479	479
347	1	1	2	0	480	479	457	455
348	1	1	2	0	478	494	487	457

LIST ALL SELECTED NODE DATA

MODE	X	Y	Z	TRX1	TRX2	TRX3
2	0.46484	41.128	1.1516	-90.00	-30.00	90.00
3	1.3288	41.852	2.3016	-90.00	-30.00	90.00
4	1.9910	40.929	3.4484	-90.00	-30.00	90.00
5	2.6804	40.758	4.5908	-90.00	-30.00	90.00
6	3.3862	40.538	5.7262	-90.00	-30.00	90.00
7	3.9975	40.269	6.8546	-90.00	-30.00	90.00
8	4.5054	39.953	7.9753	-90.00	-30.00	90.00
9	5.0240	39.589	9.0814	-90.00	-30.00	90.00
10	5.5754	39.178	10.177	-90.00	-30.00	90.00
11	6.1599	38.721	11.259	-90.00	-30.00	90.00
12	7.0790	38.249	12.321	-90.00	-30.00	90.00
13	7.6496	37.737	13.358	-90.00	-30.00	90.00
14	8.2110	37.186	14.222	-90.00	-30.00	90.00
15	8.4619	36.868	14.457	-90.00	-30.00	90.00
16	8.6797	36.463	15.034	-90.00	-30.00	90.00
17	8.8570	35.987	15.341	-90.00	-30.00	90.00
18	8.9879	35.453	15.569	-90.00	-30.00	90.00
19	9.0681	34.881	15.706	-90.00	-30.00	90.00
20	9.0950	34.290	15.753	-90.00	-30.00	90.00
21	9.0950	33.380	15.753	-90.00	-30.00	90.00

MODE	X	Y	Z	TRX1	TRX2	TRX3
22	9.0950	32.242	15.753	-90.00	-30.00	90.00
23	9.0950	30.871	15.753	-90.00	-30.00	90.00
24	9.0950	48.335	15.753	-90.00	-30.00	90.00
25	9.0950	47.560	15.753	-90.00	-30.00	90.00
26	9.0950	45.527	15.753	-90.00	-30.00	90.00
27	9.0950	43.192	15.753	-90.00	-30.00	90.00
28	9.0950	40.509	15.753	-90.00	-30.00	90.00
29	9.0950	37.427	15.753	-90.00	-30.00	90.00
30	9.0950	33.887	15.753	-90.00	-30.00	90.00
31	9.0950	29.821	15.753	-90.00	-30.00	90.00
32	9.0950	25.150	15.753	-90.00	-30.00	90.00
42	0.94026	61.125	0.94026	0.00	0.00	0.00
43	1.8792	41.052	1.8792	0.00	0.00	0.00
44	2.8156	40.929	2.8156	0.00	0.00	0.00
45	3.7482	40.798	3.7482	0.00	0.00	0.00
46	4.6756	40.538	4.6756	0.00	0.00	0.00
47	5.5987	40.269	5.5987	0.00	0.00	0.00
48	6.5181	39.953	6.5181	0.00	0.00	0.00
49	7.4147	39.589	7.4147	0.00	0.00	0.00
50	8.3091	39.178	8.3091	0.00	0.00	0.00

MODE	X	Y	Z	TRX1	TRX2	TRX3
51	9.0922	38.721	9.1022	0.00	0.00	0.00
52	10.011	38.249	10.011	0.00	0.00	0.00
53	10.818	37.737	10.818	0.00	0.00	0.00
54	11.612	37.186	11.612	0.00	0.00	0.00
55	11.967	36.868	11.967	0.00	0.00	0.00
56	12.275	36.443	12.275	0.00	0.00	0.00
57	12.526	35.987	12.526	0.00	0.00	0.00
58	12.711	35.453	12.711	0.00	0.00	0.00
59	12.826	34.881	12.826	0.00	0.00	0.00
60	12.862	34.290	12.862	0.00	0.00	0.00
61	12.862	33.380	12.862	0.00	0.00	0.00
62	12.862	32.212	12.862	0.00	0.00	0.00
63	12.862	30.871	12.862	0.00	0.00	0.00
64	12.862	49.335	12.862	0.00	0.00	0.00
65	12.862	47.560	12.862	0.00	0.00	0.00
66	12.862	45.527	12.862	0.00	0.00	0.00
67	12.862	43.192	12.862	0.00	0.00	0.00
68	12.862	40.509	12.862	0.00	0.00	0.00
69	12.862	37.427	12.862	0.00	0.00	0.00
70	12.862	33.887	12.862	0.00	0.00	0.00

MODE	X	Y	Z	TRX1	TRX2	TRX3
71	12.862	29.821	12.862	0.00	0.00	0.00
72	12.862	25.150	12.862	0.00	0.00	0.00

82	1.1516	41.125	9.66486	0.00	0.00	0.00
83	2.3016	41.852	1.3258	0.00	0.00	0.00
84	3.4484	60.929	1.9910	0.00	0.00	0.00
85	4.5904	60.734	1.4584	0.00	0.00	0.00
86	5.7285	60.335	7.3965	0.00	0.00	0.00
87	6.8644	60.269	3.7573	0.00	0.00	0.00
88	7.9933	59.953	4.4654	0.00	0.00	0.00
89	9.0611	50.580	5.2630	0.00	0.00	0.00
90	10.177	50.178	3.8754	0.00	0.00	0.00
91	11.258	50.721	6.4999	0.00	0.00	0.00
92	12.361	50.249	7.0790	0.00	0.00	0.00
93	13.250	57.737	7.6696	0.00	0.00	0.00
94	14.222	57.184	3.2110	0.00	0.00	0.00
95	14.657	56.868	8.4619	0.00	0.00	0.00
96	15.034	56.463	8.4797	0.00	0.00	0.00
97	15.341	55.987	8.8570	0.00	0.00	0.00
98	15.548	55.473	8.9879	0.00	0.00	0.00
99	15.704	54.967	9.0481	0.00	0.00	0.00

MODE	X	Y	Z	TRX1	TRX2	TRX3
100	15.753	54.290	9.0950	0.00	0.00	0.00
101	15.753	53.380	9.0950	0.00	0.00	0.00
102	15.753	52.212	9.0950	0.00	0.00	0.00
103	15.753	50.871	9.0950	0.00	0.00	0.00
104	15.753	49.330	9.0950	0.00	0.00	0.00
105	15.753	47.560	9.0950	0.00	0.00	0.00
106	15.753	45.327	9.0950	0.00	0.00	0.00
107	15.753	43.192	9.0950	0.00	0.00	0.00
108	15.753	40.800	9.0950	0.00	0.00	0.00
109	15.753	37.427	9.0950	0.00	0.00	0.00
110	15.753	33.667	9.0950	0.00	0.00	0.00
111	15.753	29.801	9.0950	0.00	0.00	0.00
112	15.753	25.150	9.0950	0.00	0.00	0.00
122	1.2495	61.785	0.45479	0.00	0.00	0.00
123	2.4974	61.052	0.90996	0.00	0.00	0.00
124	3.7418	60.929	1.36419	0.00	0.00	0.00
125	4.9811	60.750	1.8130	0.00	0.00	0.00
126	6.2256	60.534	2.2616	0.00	0.00	0.00
127	7.4776	60.269	2.7071	0.00	0.00	0.00
128	8.6815	59.953	3.1489	0.00	0.00	0.00

MODE	X	Y	Z	TRX1	TRX2	TRX3
129	9.8534	59.580	3.5864	0.00	0.00	0.00
130	11.042	59.178	4.0190	0.00	0.00	0.00
131	12.214	58.721	4.4462	0.00	0.00	0.00
132	13.364	58.249	4.8623	0.00	0.00	0.00
133	14.577	57.737	5.2526	0.00	0.00	0.00
134	15.432	57.186	5.6167	0.00	0.00	0.00
135	15.965	56.868	5.7883	0.00	0.00	0.00
136	16.212	56.463	5.9373	0.00	0.00	0.00
137	16.646	55.987	6.0505	0.00	0.00	0.00
138	16.892	55.453	6.1481	0.00	0.00	0.00
139	17.043	54.981	6.2830	0.00	0.00	0.00
140	17.093	54.490	6.2213	0.00	0.00	0.00
141	17.093	53.395	6.2213	0.00	0.00	0.00
142	17.093	52.213	6.2213	0.00	0.00	0.00
143	17.093	50.871	6.2213	0.00	0.00	0.00
144	17.093	49.330	6.2213	0.00	0.00	0.00
145	17.093	47.560	6.2213	0.00	0.00	0.00
146	17.093	45.327	6.2213	0.00	0.00	0.00
147	17.093	43.192	6.2213	0.00	0.00	0.00
148	17.093	40.800	6.2213	0.00	0.00	0.00

MODE	X	Y	Z	TRX1	TRX2	TRX3
149	17.093	37.427	6.2213	0.00	0.00	0.00
150	17.093	35.887	6.2213	0.00	0.00	0.00
151	17.093	29.801	6.2213	0.00	0.00	0.00
152	17.093	25.150	6.2213	0.00	0.00	0.00
162	1.3095	61.125	0.23998	0.00	0.00	0.00
163	2.6173	61.852	0.46149	0.00	0.00	0.00
164	3.9214	60.929	0.69145	0.00	0.00	0.00
165	5.2202	60.734	0.92047	0.00	0.00	0.00
166	6.5119	60.538	1.1482	0.00	0.00	0.00
167	7.7967	60.290	1.3764	0.00	0.00	0.00
168	9.0669	59.953	1.5987	0.00	0.00	0.00
169	10.327	50.580	1.8209	0.00	0.00	0.00

170	11.572	59.178	2.0465	0.00	0.00	0.00
171	12.602	58.721	2.2576	0.00	0.00	0.00
172	13.943	58.259	2.4385	0.00	0.00	0.00
173	15.047	57.787	2.6867	0.00	0.00	0.00
174	16.172	57.184	2.8514	0.00	0.00	0.00
175	16.667	56.866	2.9368	0.00	0.00	0.00
176	17.096	56.463	3.0144	0.00	0.00	0.00
177	17.443	55.987	3.0760	0.00	0.00	0.00

MODE	K	Y	Z	TKXT	TWZ2	TWZ3
178	17.708	55.453	3.1315	0.00	0.00	0.00
179	17.867	54.881	3.1493	0.00	0.00	0.00
180	17.914	54.290	3.1587	0.00	0.00	0.00
181	17.914	53.389	3.1587	0.00	0.00	0.00
182	17.914	52.212	3.1587	0.00	0.00	0.00
183	17.914	50.871	3.1587	0.00	0.00	0.00
184	17.914	49.330	3.1587	0.00	0.00	0.00
185	17.914	47.568	3.1587	0.00	0.00	0.00
186	17.914	45.527	3.1587	0.00	0.00	0.00
187	17.914	43.192	3.1587	0.00	0.00	0.00
188	17.914	40.509	3.1587	0.00	0.00	0.00
189	17.914	37.427	3.1587	0.00	0.00	0.00
190	17.914	33.887	3.1587	0.00	0.00	0.00
191	17.914	29.821	3.1587	0.00	0.00	0.00
192	17.914	25.134	3.1587	0.00	0.00	0.00
202	1.3299	61.125	0.23181E+09	0.00	0.00	0.00
203	2.6378	61.052	0.23180E+09	0.00	0.00	0.00
204	3.9619	60.929	0.23178E+09	0.00	0.00	0.00
205	5.3008	60.738	0.23174E+09	0.00	0.00	0.00
206	6.6124	60.538	0.23168E+09	0.00	0.00	0.00

MODE	X	Y	Z	TKXT	TWZ2	TWZ3
207	7.9750	60.269	0.23164E+09	0.00	0.00	0.00
208	9.2667	59.953	0.23161E+09	0.00	0.00	0.00
209	10.664	59.589	0.23159E+09	0.00	0.00	0.00
210	11.751	59.178	0.23156E+09	0.00	0.00	0.00
211	13.008	58.721	0.23154E+09	0.00	0.00	0.00
212	14.158	58.219	0.23152E+09	0.00	0.00	0.00
213	15.209	57.737	0.23150E+09	0.00	0.00	0.00
214	16.422	57.184	0.23148E+09	0.00	0.00	0.00
215	16.924	56.868	0.23146E+09	0.00	0.00	0.00
216	17.759	56.463	0.23144E+09	0.00	0.00	0.00
217	17.714	55.987	0.23142E+09	0.00	0.00	0.00
218	17.914	55.453	0.23140E+09	0.00	0.00	0.00
219	18.136	54.881	0.23138E+09	0.00	0.00	0.00
220	18.190	54.290	0.23136E+09	0.00	0.00	0.00
221	18.190	53.389	0.23134E+09	0.00	0.00	0.00
222	18.190	52.212	0.23132E+09	0.00	0.00	0.00
223	18.190	50.871	0.23130E+09	0.00	0.00	0.00
224	18.190	49.334	0.23128E+09	0.00	0.00	0.00
225	18.190	47.568	0.23126E+09	0.00	0.00	0.00
226	18.190	45.527	0.23124E+09	0.00	0.00	0.00

MODE	X	Y	Z	TKXT	TWZ2	TWZ3
227	18.190	43.192	0.23122E+09	0.00	0.00	0.00
228	18.190	40.509	0.23120E+09	0.00	0.00	0.00
229	18.190	37.427	0.23118E+09	0.00	0.00	0.00
230	18.190	33.887	0.23116E+09	0.00	0.00	0.00
231	18.190	29.821	0.23114E+09	0.00	0.00	0.00
232	18.190	25.130	0.23112E+09	0.00	0.00	0.00
242	1.3095	61.125	-0.23098	0.00	0.00	0.00
243	2.6173	61.082	-0.46149	0.00	0.00	0.00
244	3.9214	60.929	-0.69165	0.00	0.00	0.00
245	5.2802	60.738	-0.92067	0.00	0.00	0.00
246	6.5719	60.538	-1.14882	0.00	0.00	0.00
247	7.7967	60.269	-1.3754	0.00	0.00	0.00
248	9.0668	59.953	-1.5987	0.00	0.00	0.00
249	10.3227	59.589	-1.8209	0.00	0.00	0.00
250	11.372	59.178	-2.0425	0.00	0.00	0.00
251	12.802	58.721	-2.2576	0.00	0.00	0.00
252	13.943	58.219	-2.4385	0.00	0.00	0.00
253	15.067	57.737	-2.6567	0.00	0.00	0.00
254	16.172	57.184	-2.8514	0.00	0.00	0.00
255	16.667	56.866	-2.9368	0.00	0.00	0.00

MODE	X	Y	Z	THXZ	THYZ	TRXZ
254	17.996	56.463	-3.0144	0.00	0.00	0.00
257	17.949	35.987	-3.0768	0.00	0.00	0.00
258	17.903	35.453	-3.1213	0.00	0.00	0.00
259	17.841	24.881	-3.1623	0.00	0.00	0.00
260	17.914	54.900	-3.1587	0.00	0.00	0.00
261	17.914	43.380	-3.1547	0.00	0.00	0.00
262	17.914	52.212	-3.1587	0.00	0.00	0.00
263	17.914	90.871	-3.1547	0.00	0.00	0.00
264	17.914	49.330	-3.1587	0.00	0.00	0.00
265	17.914	47.560	-3.1587	0.00	0.00	0.00
266	17.914	45.527	-3.1587	0.00	0.00	0.00
267	17.914	43.192	-3.1547	0.00	0.00	0.00
268	17.914	40.509	-3.1587	0.00	0.00	0.00
269	17.914	37.427	-3.1547	0.00	0.00	0.00
270	17.914	33.887	-3.1587	0.00	0.00	0.00
271	17.914	29.821	-3.1547	0.00	0.00	0.00
272	17.914	25.150	-3.1587	0.00	0.00	0.00
282	1.8695	61.125	-0.49479	0.00	0.00	0.00
283	2.4774	61.853	-0.90896	0.00	0.00	0.00
284	3.7418	60.929	-1.5619	0.00	0.00	0.00
MODE	X	Y	Z	THXZ	THYZ	TRXZ
285	4.9811	60.738	-1.8158	0.00	0.00	0.00
286	6.2134	60.538	-2.2616	0.00	0.00	0.00
287	7.4378	60.269	-2.7071	0.00	0.00	0.00
288	8.6575	59.981	-3.1489	0.00	0.00	0.00
289	9.8536	59.589	-3.5864	0.00	0.00	0.00
290	11.042	59.178	-4.0198	0.00	0.00	0.00
291	12.216	58.721	-4.4462	0.00	0.00	0.00
292	13.384	58.219	-4.8623	0.00	0.00	0.00
293	14.537	57.737	-5.2526	0.00	0.00	0.00
294	15.632	57.184	-5.6147	0.00	0.00	0.00
295	15.905	56.668	-5.7835	0.00	0.00	0.00
296	16.212	56.163	-5.9172	0.00	0.00	0.00
297	16.646	55.997	-6.0595	0.00	0.00	0.00
298	16.892	55.453	-6.1481	0.00	0.00	0.00
299	17.163	54.881	-6.2050	0.00	0.00	0.00
300	17.598	54.298	-6.2313	0.00	0.00	0.00
301	17.993	53.709	-6.2213	0.00	0.00	0.00
302	17.093	52.212	-6.2213	0.00	0.00	0.00
303	17.093	50.871	-6.2213	0.00	0.00	0.00
304	17.093	49.330	-6.2213	0.00	0.00	0.00
MODE	X	Y	Z	THXZ	THYZ	TRXZ
305	17.093	47.560	-6.2213	0.00	0.00	0.00
306	17.093	45.527	-6.2213	0.00	0.00	0.00
307	17.093	43.192	-6.2213	0.00	0.00	0.00
308	17.093	40.509	-6.2213	0.00	0.00	0.00
309	17.093	37.427	-6.2213	0.00	0.00	0.00
310	17.093	33.887	-6.2213	0.00	0.00	0.00
311	17.093	29.821	-6.2213	0.00	0.00	0.00
312	17.093	25.150	-6.2213	0.00	0.00	0.00
322	1.1516	61.125	-0.66486	0.00	0.00	0.00
323	2.3916	61.052	-1.3288	0.00	0.00	0.00
324	3.6484	60.929	-1.9930	0.00	0.00	0.00
325	4.9986	60.738	-2.6504	0.00	0.00	0.00
326	6.2961	60.538	-3.3062	0.00	0.00	0.00
327	7.6046	60.349	-3.9575	0.00	0.00	0.00
328	8.9233	59.955	-4.6084	0.00	0.00	0.00
329	9.8811	59.589	-5.2430	0.00	0.00	0.00
330	10.177	59.178	-5.8754	0.00	0.00	0.00
331	11.254	58.721	-6.4999	0.00	0.00	0.00
332	12.261	58.219	-7.0900	0.00	0.00	0.00
333	13.250	57.737	-7.6496	0.00	0.00	0.00
MODE	X	Y	Z	THXZ	THYZ	TRXZ
334	14.222	57.184	-8.2190	0.00	0.00	0.00
335	14.487	56.668	-8.4879	0.00	0.00	0.00
336	15.034	56.463	-8.6797	0.00	0.00	0.00
337	15.341	55.987	-8.8570	0.00	0.00	0.00
338	15.506	55.453	-8.9879	0.00	0.00	0.00
339	15.786	54.881	-9.0851	0.00	0.00	0.00
340	15.793	54.298	-9.0990	0.00	0.00	0.00
341	15.733	53.709	-9.0950	0.00	0.00	0.00
342	15.753	52.212	-9.0950	0.00	0.00	0.00

343	15.753	30.871	-9.0950	0.00	0.00	0.00
344	15.753	49.239	-9.0950	0.00	0.00	0.00
342	15.753	47.444	-9.0950	0.00	0.00	0.00
346	15.753	45.527	-9.0950	0.00	0.00	0.00
347	15.753	43.192	-9.0950	0.00	0.00	0.00
348	15.753	40.589	-9.0950	0.00	0.00	0.00
349	15.753	37.427	-9.0950	0.00	0.00	0.00
350	15.753	33.687	-9.0950	0.00	0.00	0.00
351	15.753	29.824	-9.0950	0.00	0.00	0.00
352	15.753	25.159	-9.0950	0.00	0.00	0.00
362	0.94026	61.125	-0.94026	0.00	0.00	0.00

MODE	K	T	Z	THX1	THX2	THX3
363	1.8792	61.052	-1.8792	0.00	0.00	0.00
364	2.8186	60.929	-2.8186	0.00	0.00	0.00
365	3.7582	60.796	-3.7582	0.00	0.00	0.00
366	4.6976	60.538	-4.6976	0.00	0.00	0.00
367	5.5967	60.297	-5.5967	0.00	0.00	0.00
368	6.3407	59.953	-6.3407	0.00	0.00	0.00
369	7.0347	59.589	-7.0347	0.00	0.00	0.00
370	8.3094	59.178	-8.3094	0.00	0.00	0.00
371	9.1922	58.721	-9.1922	0.00	0.00	0.00
372	10.011	58.269	-10.011	0.00	0.00	0.00
373	10.818	57.737	-10.818	0.00	0.00	0.00
374	11.612	57.186	-11.612	0.00	0.00	0.00
375	11.967	56.606	-11.967	0.00	0.00	0.00
376	12.275	56.003	-12.275	0.00	0.00	0.00
377	12.536	55.987	-12.536	0.00	0.00	0.00
378	12.711	55.453	-12.711	0.00	0.00	0.00
379	12.824	54.881	-12.824	0.00	0.00	0.00
380	12.862	54.299	-12.862	0.00	0.00	0.00
381	12.862	53.389	-12.862	0.00	0.00	0.00
382	12.862	52.217	-12.862	0.00	0.00	0.00

MODE	K	T	Z	THX1	THX2	THX3
393	12.862	50.871	-12.862	0.00	0.00	0.00
394	12.862	49.239	-12.862	0.00	0.00	0.00
395	12.862	47.568	-12.862	0.00	0.00	0.00
396	12.862	45.527	-12.862	0.00	0.00	0.00
387	12.862	43.192	-12.862	0.00	0.00	0.00
388	12.862	40.589	-12.862	0.00	0.00	0.00
389	12.862	37.427	-12.862	0.00	0.00	0.00
390	12.862	33.287	-12.862	0.00	0.00	0.00
391	12.862	29.824	-12.862	0.00	0.00	0.00
392	12.862	25.159	-12.862	0.00	0.00	0.00
402	0.66486	61.125	-1.7516	90.00	-30.00	-90.00
403	1.3288	61.052	-2.3016	90.00	-30.00	-90.00
404	1.9928	60.929	-3.3484	90.00	-30.00	-90.00
405	2.6568	60.756	-4.3960	90.00	-30.00	-90.00
406	3.3062	60.538	-5.7365	90.00	-30.00	-90.00
407	3.9579	60.297	-6.8946	90.00	-30.00	-90.00
408	4.6054	59.953	-7.9723	90.00	-30.00	-90.00
409	5.2430	59.589	-9.0811	90.00	-30.00	-90.00
410	5.8754	59.178	-10.1977	90.00	-30.00	-90.00
411	6.4999	58.721	-11.3590	90.00	-30.00	-90.00

MODE	K	T	Z	THX1	THX2	THX3
412	7.0790	58.269	-12.261	90.00	-30.00	-90.00
413	7.6496	57.737	-13.250	90.00	-30.00	-90.00
414	8.2110	57.186	-14.322	90.00	-30.00	-90.00
415	8.4419	56.606	-14.637	90.00	-30.00	-90.00
416	8.6797	56.003	-15.094	90.00	-30.00	-90.00
417	8.8870	55.987	-15.341	90.00	-30.00	-90.00
418	8.9879	55.453	-15.568	90.00	-30.00	-90.00
419	9.0681	54.881	-15.706	90.00	-30.00	-90.00
420	9.0950	54.299	-15.793	90.00	-30.00	-90.00
421	9.0950	53.389	-15.753	90.00	-30.00	-90.00
422	9.0950	52.212	-15.753	90.00	-30.00	-90.00
423	9.0950	50.871	-15.753	90.00	-30.00	-90.00
424	9.0950	49.239	-15.753	90.00	-30.00	-90.00
425	9.0950	47.560	-15.753	90.00	-30.00	-90.00
426	9.0950	45.527	-15.753	90.00	-30.00	-90.00
427	9.0950	43.192	-15.753	90.00	-30.00	-90.00
428	9.0950	40.500	-15.753	90.00	-30.00	-90.00
429	9.0950	37.427	-15.753	90.00	-30.00	-90.00

430	9.9990	33.897	-13.753	90.00	-30.00	-90.00
431	9.9990	29.871	-13.753	90.00	-30.00	-90.00
NO08	X	Y	Z	TW01	TW02	TW03
432	9.9990	25.150	-13.753	90.00	-30.00	-90.00
444	13.000	40.380	0.00000E+00	0.00	0.00	0.00
445	13.000	59.165	0.00000E+00	0.00	0.00	0.00
446	13.000	59.610	0.00000E+00	0.00	0.00	0.00
447	13.000	60.855	0.00000E+00	0.00	0.00	0.00
448	13.000	62.300	0.00000E+00	0.00	0.00	0.00
449	14.000	61.500	0.00000E+00	0.00	0.00	0.00
450	19.250	62.300	0.00000E+00	0.00	0.00	0.00
451	16.063	62.500	0.00000E+00	0.00	0.00	0.00
452	17.125	62.300	0.00000E+00	0.00	0.00	0.00
453	18.188	62.500	0.00000E+00	0.00	0.00	0.00
454	21.250	60.500	0.00000E+00	0.00	0.00	0.00
455	20.250	61.500	0.00000E+00	0.00	0.00	0.00
456	21.250	54.630	0.00000E+00	0.00	0.00	0.00
457	21.250	59.322	0.00000E+00	0.00	0.00	0.00
458	21.250	58.363	0.00000E+00	0.00	0.00	0.00
459	21.250	57.560	0.00000E+00	0.00	0.00	0.00
460	21.250	54.557	0.00000E+00	0.00	0.00	0.00
461	21.250	53.408	0.00000E+00	0.00	0.00	0.00
462	20.000	53.380	0.00000E+00	0.00	0.00	0.00
NO09	X	Y	Z	TW01	TW02	TW03
463	20.623	54.005	0.00000E+00	0.00	0.00	0.00
464	19.005	53.380	0.00000E+00	0.00	0.00	0.00
465	18.704	54.273	0.00000E+00	0.00	0.00	0.00
466	18.762	53.001	0.00000E+00	0.00	0.00	0.00
467	18.452	52.584	0.00000E+00	0.00	0.00	0.00
468	18.119	54.265	0.00000E+00	0.00	0.00	0.00
469	17.805	50.862	0.00000E+00	0.00	0.00	0.00
470	17.297	57.433	0.00000E+00	0.00	0.00	0.00
471	16.618	57.998	0.00000E+00	0.00	0.00	0.00
472	15.764	58.423	0.00000E+00	0.00	0.00	0.00
473	14.902	58.908	0.00000E+00	0.00	0.00	0.00
474	13.828	59.045	0.00000E+00	0.00	0.00	0.00
475	14.134	59.495	0.00000E+00	0.00	0.00	0.00
476	14.103	60.377	0.00000E+00	0.00	0.00	0.00
477	19.267	60.768	0.00000E+00	0.00	0.00	0.00
478	20.429	60.215	0.00000E+00	0.00	0.00	0.00
479	20.036	59.500	0.00000E+00	0.00	0.00	0.00
480	20.758	58.504	0.00000E+00	0.00	0.00	0.00
481	20.266	57.540	0.00000E+00	0.00	0.00	0.00
482	20.354	56.381	0.00000E+00	0.00	0.00	0.00
NO09	X	Y	Z	TW01	TW02	TW03
483	20.443	55.620	0.00000E+00	0.00	0.00	0.00
484	20.523	54.976	0.00000E+00	0.00	0.00	0.00
485	19.959	54.502	0.00000E+00	0.00	0.00	0.00
486	19.649	54.011	0.00000E+00	0.00	0.00	0.00
487	19.236	54.293	0.00000E+00	0.00	0.00	0.00
488	18.701	61.446	0.00000E+00	0.00	0.00	0.00
489	17.008	61.000	0.00000E+00	0.00	0.00	0.00
490	17.953	61.279	0.00000E+00	0.00	0.00	0.00
491	15.469	60.461	0.00000E+00	0.00	0.00	0.00
492	14.812	60.438	0.00000E+00	0.00	0.00	0.00
493	17.035	60.305	0.00000E+00	0.00	0.00	0.00
494	18.799	59.416	0.00000E+00	0.00	0.00	0.00
495	15.478	59.576	0.00000E+00	0.00	0.00	0.00
496	16.671	59.287	0.00000E+00	0.00	0.00	0.00
497	17.667	59.483	0.00000E+00	0.00	0.00	0.00
498	18.078	58.787	0.00000E+00	0.00	0.00	0.00
499	19.634	55.580	0.00000E+00	0.00	0.00	0.00
500	19.334	54.799	0.00000E+00	0.00	0.00	0.00
501	19.528	58.495	0.00000E+00	0.00	0.00	0.00
502	19.185	58.422	0.00000E+00	0.00	0.00	0.00
NO08	X	Y	Z	TW01	TW02	TW03
503	19.357	57.480	0.00000E+00	0.00	0.00	0.00
504	16.154	58.977	0.00000E+00	0.00	0.00	0.00
505	18.471	58.254	0.00000E+00	0.00	0.00	0.00
506	18.451	57.341	0.00000E+00	0.00	0.00	0.00
507	18.783	56.366	0.00000E+00	0.00	0.00	0.00
508	19.013	55.617	0.00000E+00	0.00	0.00	0.00

308	17.068	58.708	0.08800E+08	0.80	8.00	8.00
310	17.785	59.082	0.08800E+08	0.80	8.00	8.00

LIST ALL MATERIALS PROPERTY= ALL

PROPERTY TABLE EX	MAT=	1	MIN. POINTS=	2
TEMPERATURE	DATA	TEMPERATURE	DATA	
-9999.0	0.27180E+08	9999.8	8.27180E+08	

PROPERTY TABLE MUY	MAT=	1	MIN. POINTS=	2
TEMPERATURE	DATA	TEMPERATURE	DATA	
-9999.0	0.30000	9999.8	8.30000	
TIME=	0.80000E+00	HITTER=	1	

UNIFORM TEMPERATURE= 0.000 (TREF= 8.000)

PLASTIC CONVERG. CRITERION= 0.0180

CREEP OPTIMUM CRITERION= 0.1000

LARGE DEFL. CONVERG. CRITERION= 0.001000

DISPLACEMENT LIMIT= 0.80000E+00

MPRINT= 99900 NPOST= 1 REACTION PRINT FREQ= 99900
DISP. POST DATA FREQ= 1 REACT. POST DATA FREQ= 1

ELEMENT PRINT AND POST DATA FREQUENCIES

TYPE	STIFF	STRESS	FORCE	STRESS	DATA	FORCE
	NO.	PRINT	PRINT	DATA	LEVEL	DATA
1	43	99900	99908	1	3	1

LOADS INPUT FILE= 26 LOADS OUTPUT FILE= 23

ALL ANALYSIS DATA WILL BE WRITTEN ONTO FILE27

LIST DISPLACEMENTS FOR ALL SELECTED NODES

NODE	LABEL	DISP	DIR
32	UX	0.00000000E+00	0.00000000E+00
43	ROTX	0.00000000E+00	0.00000000E+00
32	UY	0.00000000E+00	0.00000000E+00
43	UT	0.00000000E+00	0.00000000E+00
32	ROTY	0.00000000E+00	0.00000000E+00
43	ROTY	0.00000000E+00	0.00000000E+00
72	UX	0.00000000E+00	0.00000000E+00
72	UT	0.00000000E+00	0.00000000E+00
72	UZ	0.00000000E+00	0.00000000E+00
72	ROTX	0.00000000E+00	0.00000000E+00
72	ROTY	0.00000000E+00	0.00000000E+00
72	ROTZ	0.00000000E+00	0.00000000E+00
112	UX	0.00000000E+00	0.00000000E+00
112	UT	0.00000000E+00	0.00000000E+00
112	UZ	0.00000000E+00	0.00000000E+00
112	ROTX	0.00000000E+00	0.00000000E+00
112	ROTY	0.00000000E+00	0.00000000E+00
118	ROTX	0.00000000E+00	0.00000000E+00
152	UX	0.00000000E+00	0.00000000E+00
152	UY	0.00000000E+00	0.00000000E+00

NODE	LABEL	DISP	DIR
152	UZ	0.00000000E+00	0.00000000E+00
152	ROTX	0.00000000E+00	0.00000000E+00
152	ROTY	0.00000000E+00	0.00000000E+00
152	ROTZ	0.00000000E+00	0.00000000E+00
192	UX	0.00000000E+00	0.00000000E+00
192	UY	0.00000000E+00	0.00000000E+00
192	UZ	0.00000000E+00	0.00000000E+00
192	ROTX	0.00000000E+00	0.00000000E+00
192	ROTY	0.00000000E+00	0.00000000E+00
192	ROTZ	0.00000000E+00	0.00000000E+00
232	UX	0.00000000E+00	0.00000000E+00
232	UY	0.00000000E+00	0.00000000E+00
232	UZ	0.00000000E+00	0.00000000E+00
232	ROTX	0.00000000E+00	0.00000000E+00
232	ROTY	0.00000000E+00	0.00000000E+00
232	ROTZ	0.00000000E+00	0.00000000E+00
272	UX	0.00000000E+00	0.00000000E+00
272	UY	0.00000000E+00	0.00000000E+00

272 UZ	D.00000000E+00	0.00000000E+00
272 ROTX	D.00000000E+00	0.00000000E+00
MODE LABEL	D15P	C01P
372 ROTY	D.00000000E+00	0.00000000E+00
272 ROTZ	D.00000000E+00	0.00000000E+00
312 UX	D.00000000E+00	0.00000000E+00
312 UY	D.00000000E+00	0.00000000E+00
312 UZ	D.00000000E+00	0.00000000E+00
312 ROTX	D.00000000E+00	0.00000000E+00
312 ROTY	D.00000000E+00	0.00000000E+00
312 ROTZ	D.00000000E+00	0.00000000E+00
352 UX	D.00000000E+00	0.00000000E+00
352 UY	D.00000000E+00	0.00000000E+00
352 UZ	D.00000000E+00	0.00000000E+00
352 ROTX	D.00000000E+00	0.00000000E+00
352 ROTY	D.00000000E+00	0.00000000E+00
352 ROTZ	D.00000000E+00	0.00000000E+00
392 UX	D.00000000E+00	0.00000000E+00
392 UY	D.00000000E+00	0.00000000E+00
392 UZ	D.00000000E+00	0.00000000E+00
392 ROTX	D.00000000E+00	0.00000000E+00
392 ROTY	D.00000000E+00	0.00000000E+00
392 ROTZ	D.00000000E+00	0.00000000E+00
MODE LABEL	D15P	C01P
432 UX	D.00000000E+00	0.00000000E+00
432 ROTY	D.00000000E+00	0.00000000E+00
432 UZ	D.00000000E+00	0.00000000E+00
431 UT	D.00000000E+00	0.00000000E+00
2 UT	D.00000000E+00	0.00000000E+00
3 UT	D.00000000E+00	0.00000000E+00
4 UT	D.00000000E+00	0.00000000E+00
5 UT	D.00000000E+00	0.00000000E+00
6 UT	D.00000000E+00	0.00000000E+00
7 UT	D.00000000E+00	0.00000000E+00
8 UT	D.00000000E+00	0.00000000E+00
9 UT	D.00000000E+00	0.00000000E+00
10 UT	D.00000000E+00	0.00000000E+00
11 UT	D.00000000E+00	0.00000000E+00
12 UT	D.00000000E+00	0.00000000E+00
13 UT	D.00000000E+00	0.00000000E+00
14 UT	D.00000000E+00	0.00000000E+00
15 UT	D.00000000E+00	0.00000000E+00
16 UT	D.00000000E+00	0.00000000E+00
17 UT	D.00000000E+00	0.00000000E+00
MODE LABEL	D15P	C01P
18 UT	D.00000000E+00	0.00000000E+00
19 UT	D.00000000E+00	0.00000000E+00
20 UT	D.00000000E+00	0.00000000E+00
21 UT	D.00000000E+00	0.00000000E+00
22 UT	D.00000000E+00	0.00000000E+00
23 UT	D.00000000E+00	0.00000000E+00
24 UT	D.00000000E+00	0.00000000E+00
25 UT	D.00000000E+00	0.00000000E+00
26 UT	D.00000000E+00	0.00000000E+00
27 UT	D.00000000E+00	0.00000000E+00
28 UT	D.00000000E+00	0.00000000E+00
29 UT	D.00000000E+00	0.00000000E+00
30 UT	D.00000000E+00	0.00000000E+00
31 UT	D.00000000E+00	0.00000000E+00
32 UT	D.00000000E+00	0.00000000E+00
482 UT	D.00000000E+00	0.00000000E+00
483 UT	D.00000000E+00	0.00000000E+00
484 UT	D.00000000E+00	0.00000000E+00
485 UT	D.00000000E+00	0.00000000E+00
486 UT	D.00000000E+00	0.00000000E+00
MODE LABEL	D15P	C01P
487 UT	D.00000000E+00	0.00000000E+00
488 UT	D.00000000E+00	0.00000000E+00
489 UT	D.00000000E+00	0.00000000E+00
410 UT	D.00000000E+00	0.00000000E+00
411 UT	D.00000000E+00	0.00000000E+00
412 UT	D.00000000E+00	0.00000000E+00

413 UT	0.00000000E+00	0.00000000E+00
414 UT	0.00000000E+00	0.00000000E+00
415 UT	0.00000000E+00	0.00000000E+00
416 UT	0.00000000E+00	0.00000000E+00
417 UT	0.00000000E+00	0.00000000E+00
418 UT	0.00000000E+00	0.00000000E+00
419 UT	0.00000000E+00	0.00000000E+00
420 UT	0.00000000E+00	0.00000000E+00
421 UT	0.00000000E+00	0.00000000E+00
422 UT	0.00000000E+00	0.00000000E+00
423 UT	0.00000000E+00	0.00000000E+00
424 UT	0.00000000E+00	0.00000000E+00
425 UT	0.00000000E+00	0.00000000E+00
426 UT	0.00000000E+00	0.00000000E+00

MODE LABEL	DISP	DISP
427 UT	0.00000000E+00	0.00000000E+00
428 UT	0.00000000E+00	0.00000000E+00
429 UT	0.00000000E+00	0.00000000E+00
430 UT	0.00000000E+00	0.00000000E+00
2 RGTX	0.00000000E+00	0.00000000E+00
3 RGTX	0.00000000E+00	0.00000000E+00
4 RGTX	0.00000000E+00	0.00000000E+00
5 RGTX	0.00000000E+00	0.00000000E+00
6 RGTX	0.00000000E+00	0.00000000E+00
7 RGTX	0.00000000E+00	0.00000000E+00
8 RGTX	0.00000000E+00	0.00000000E+00
9 RGTX	0.00000000E+00	0.00000000E+00
10 RGTX	0.00000000E+00	0.00000000E+00
11 RGTX	0.00000000E+00	0.00000000E+00
12 RGTX	0.00000000E+00	0.00000000E+00
13 RGTX	0.00000000E+00	0.00000000E+00
14 RGTX	0.00000000E+00	0.00000000E+00
15 RGTX	0.00000000E+00	0.00000000E+00
16 RGTX	0.00000000E+00	0.00000000E+00
17 RGTX	0.00000000E+00	0.00000000E+00

MODE LABEL	DISP	DISP
18 RGTX	0.00000000E+00	0.00000000E+00
19 RGTX	0.00000000E+00	0.00000000E+00
20 RGTX	0.00000000E+00	0.00000000E+00
21 RGTX	0.00000000E+00	0.00000000E+00
22 RGTX	0.00000000E+00	0.00000000E+00
23 RGTX	0.00000000E+00	0.00000000E+00
24 RGTX	0.00000000E+00	0.00000000E+00
25 RGTX	0.00000000E+00	0.00000000E+00
26 RGTX	0.00000000E+00	0.00000000E+00
27 RGTX	0.00000000E+00	0.00000000E+00
28 RGTX	0.00000000E+00	0.00000000E+00
29 RGTX	0.00000000E+00	0.00000000E+00
30 RGTX	0.00000000E+00	0.00000000E+00
31 RGTX	0.00000000E+00	0.00000000E+00
32 RGTX	0.00000000E+00	0.00000000E+00
402 RGTX	0.00000000E+00	0.00000000E+00
403 RGTX	0.00000000E+00	0.00000000E+00
404 RGTX	0.00000000E+00	0.00000000E+00
405 RGTX	0.00000000E+00	0.00000000E+00
606 RGTX	0.00000000E+00	0.00000000E+00

MODE LABEL	DISP	DISP
407 RGTX	0.00000000E+00	0.00000000E+00
408 RGTX	0.00000000E+00	0.00000000E+00
409 RGTX	0.00000000E+00	0.00000000E+00
410 RGTX	0.00000000E+00	0.00000000E+00
411 RGTX	0.00000000E+00	0.00000000E+00
412 RGTX	0.00000000E+00	0.00000000E+00
413 RGTX	0.00000000E+00	0.00000000E+00
414 RGTX	0.00000000E+00	0.00000000E+00
415 RGTX	0.00000000E+00	0.00000000E+00
416 RGTX	0.00000000E+00	0.00000000E+00
417 RGTX	0.00000000E+00	0.00000000E+00
418 RGTX	0.00000000E+00	0.00000000E+00
419 RGTX	0.00000000E+00	0.00000000E+00
420 RGTX	0.00000000E+00	0.00000000E+00
421 RGTX	0.00000000E+00	0.00000000E+00
422 RGTX	0.00000000E+00	0.00000000E+00

```

427 RT7K 0.00000000E+00 0.00000000E+00
428 RT7K 0.00000000E+00 0.00000000E+00
429 RT7K 0.00000000E+00 0.00000000E+00
426 RT7K 0.00000000E+00 0.00000000E+00

MODE LABEL      B1SP      C1SP
427 RT7K 0.00000000E+00 0.00000000E+00
428 RT7K 0.00000000E+00 0.00000000E+00
429 RT7K 0.00000000E+00 0.00000000E+00
426 RT7K 0.00000000E+00 0.00000000E+00
2  RT2  0.00000000E+00 0.00000000E+00
3  RT2  0.00000000E+00 0.00000000E+00
4  RT2  0.00000000E+00 0.00000000E+00
9  RT2  0.00000000E+00 0.00000000E+00
8  RT2  0.00000000E+00 0.00000000E+00
7  RT2  0.00000000E+00 0.00000000E+00
6  RT2  0.00000000E+00 0.00000000E+00
5  RT2  0.00000000E+00 0.00000000E+00
14 RT2  0.00000000E+00 0.00000000E+00
11 RT2  0.00000000E+00 0.00000000E+00
12 RT2  0.00000000E+00 0.00000000E+00
13 RT2  0.00000000E+00 0.00000000E+00
14 RT2  0.00000000E+00 0.00000000E+00
15 RT2  0.00000000E+00 0.00000000E+00
16 RT2  0.00000000E+00 0.00000000E+00
17 RT2  0.00000000E+00 0.00000000E+00

MODE LABEL      B1SP      C1SP
18 RT2  0.00000000E+00 0.00000000E+00
19 RT2  0.00000000E+00 0.00000000E+00
20 RT2  0.00000000E+00 0.00000000E+00
21 RT2  0.00000000E+00 0.00000000E+00
22 RT2  0.00000000E+00 0.00000000E+00
23 RT2  0.00000000E+00 0.00000000E+00
24 RT2  0.00000000E+00 0.00000000E+00
25 RT2  0.00000000E+00 0.00000000E+00
26 RT2  0.00000000E+00 0.00000000E+00
27 RT2  0.00000000E+00 0.00000000E+00
28 RT2  0.00000000E+00 0.00000000E+00
29 RT2  0.00000000E+00 0.00000000E+00
30 RT2  0.00000000E+00 0.00000000E+00
31 RT2  0.00000000E+00 0.00000000E+00
32 RT2  0.00000000E+00 0.00000000E+00
402 RT2  0.00000000E+00 0.00000000E+00
403 RT2  0.00000000E+00 0.00000000E+00
404 RT2  0.00000000E+00 0.00000000E+00
405 RT2  0.00000000E+00 0.00000000E+00
406 RT2  0.00000000E+00 0.00000000E+00

MODE LABEL      B1SP      C1SP
407 RT2  0.00000000E+00 0.00000000E+00
408 RT2  0.00000000E+00 0.00000000E+00
409 RT2  0.00000000E+00 0.00000000E+00
410 RT2  0.00000000E+00 0.00000000E+00
411 RT2  0.00000000E+00 0.00000000E+00
412 RT2  0.00000000E+00 0.00000000E+00
413 RT2  0.00000000E+00 0.00000000E+00
414 RT2  0.00000000E+00 0.00000000E+00
415 RT2  0.00000000E+00 0.00000000E+00
416 RT2  0.00000000E+00 0.00000000E+00
417 RT2  0.00000000E+00 0.00000000E+00
418 RT2  0.00000000E+00 0.00000000E+00
419 RT2  0.00000000E+00 0.00000000E+00
420 RT2  0.00000000E+00 0.00000000E+00
421 RT2  0.00000000E+00 0.00000000E+00
422 RT2  0.00000000E+00 0.00000000E+00
423 RT2  0.00000000E+00 0.00000000E+00
424 RT2  0.00000000E+00 0.00000000E+00
425 RT2  0.00000000E+00 0.00000000E+00

MODE LABEL      B1SP      C1SP
427 RT2  0.00000000E+00 0.00000000E+00
428 RT2  0.00000000E+00 0.00000000E+00
429 RT2  0.00000000E+00 0.00000000E+00
430 RT2  0.00000000E+00 0.00000000E+00

```

431 ROTZ 0.0000000E+00 0.0000000E+00
432 ROTZ 0.0000000E+00 0.0000000E+00
LIST FORCES FOR ALL SELECTED MODES

MODE	LABEL	FRIDE	EFORCE
489	FY	0.0000000E+00	0.0000000E+00
489	FZ	-0.3600000E+00	0.0000000E+00

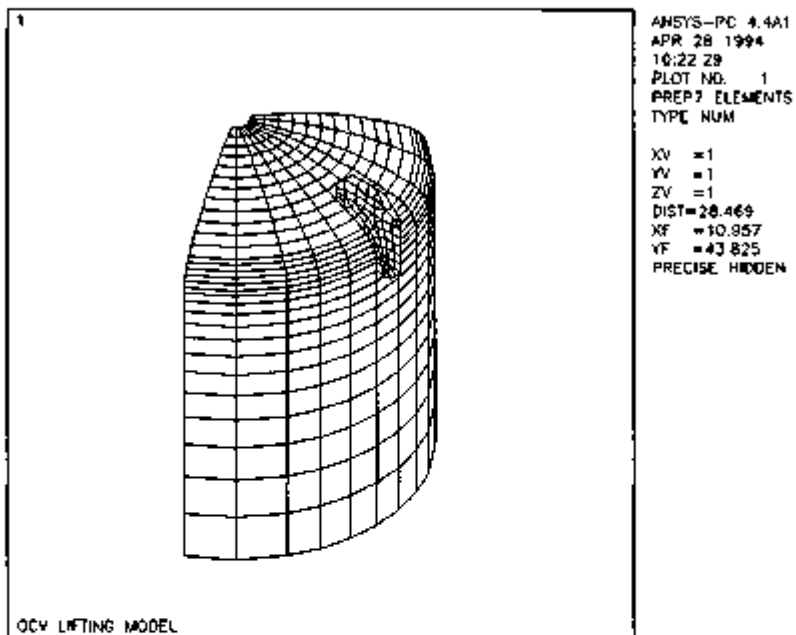


FIGURE 2.10.3-1.

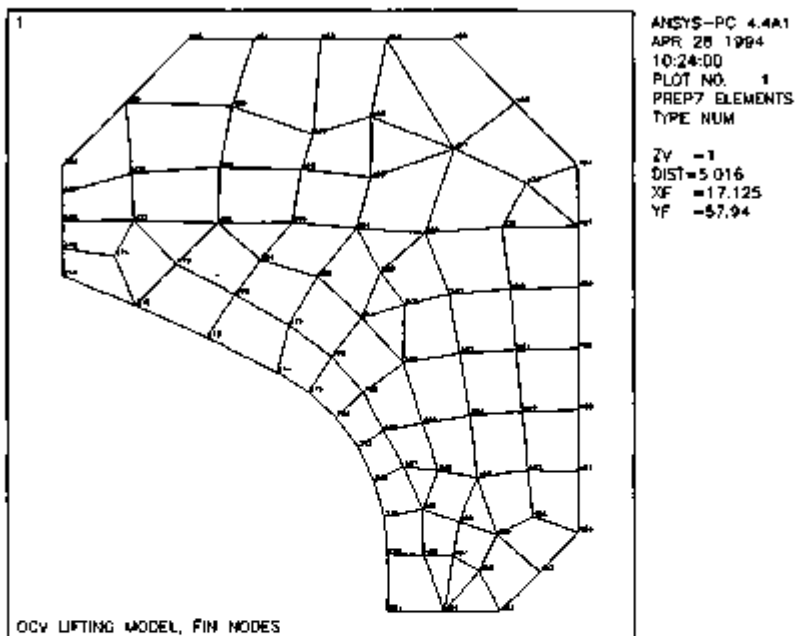


FIGURE 2.10.3-2.

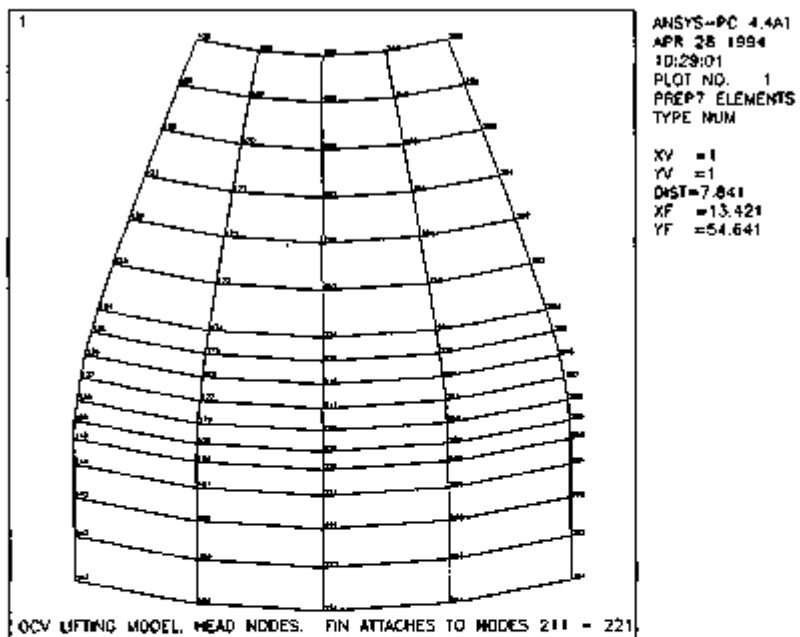


FIGURE 2.10.3-3.

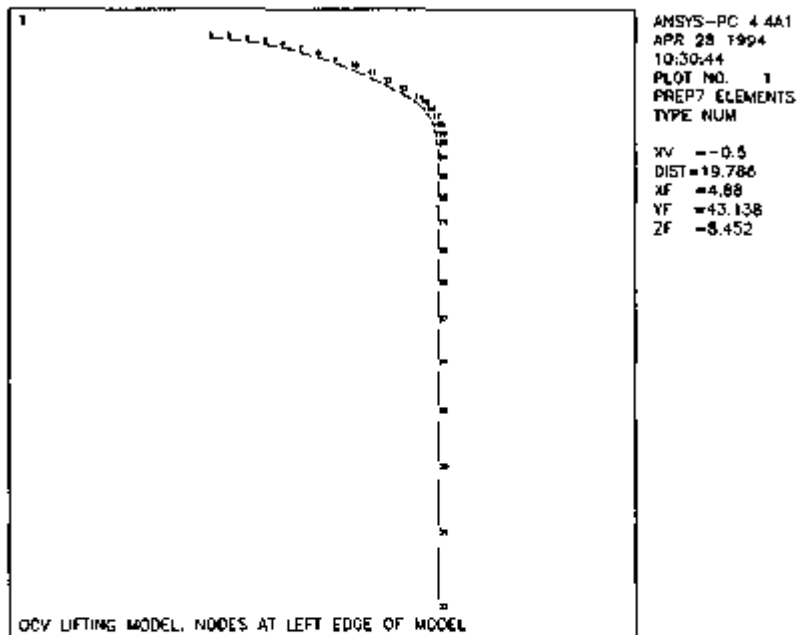


FIGURE 2.10.3-4.

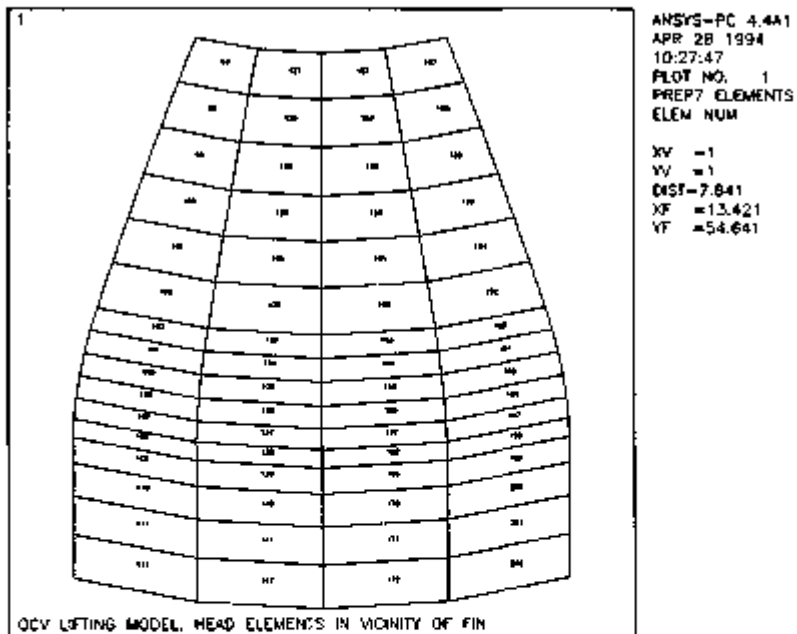


FIGURE 2.10.3-6.

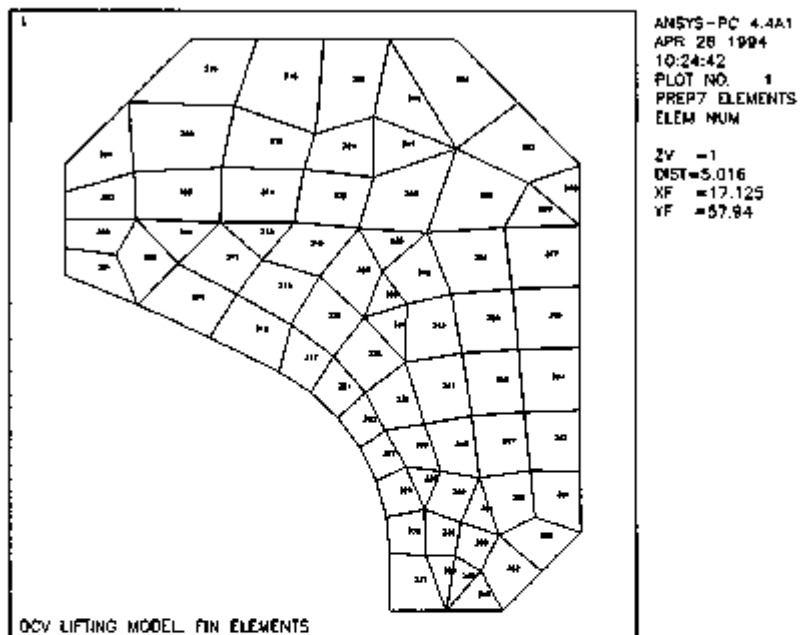


FIGURE 2.10.3-6.

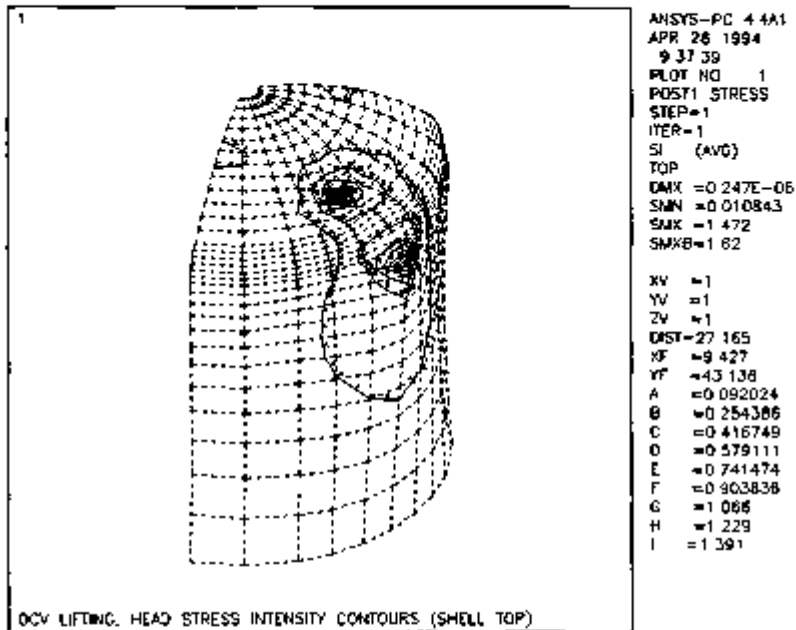


FIGURE 2.10.3-7.

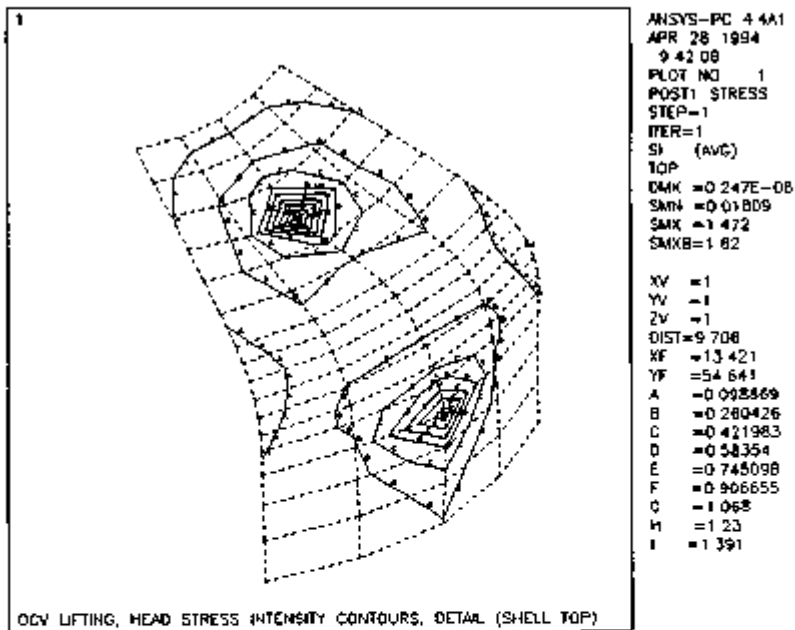


FIGURE 2.10.3-8.

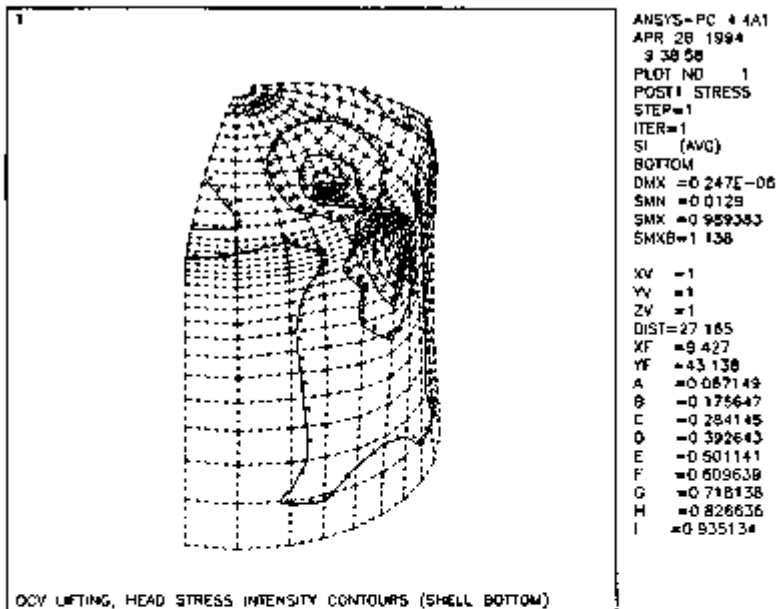


FIGURE 2.10.3-6.

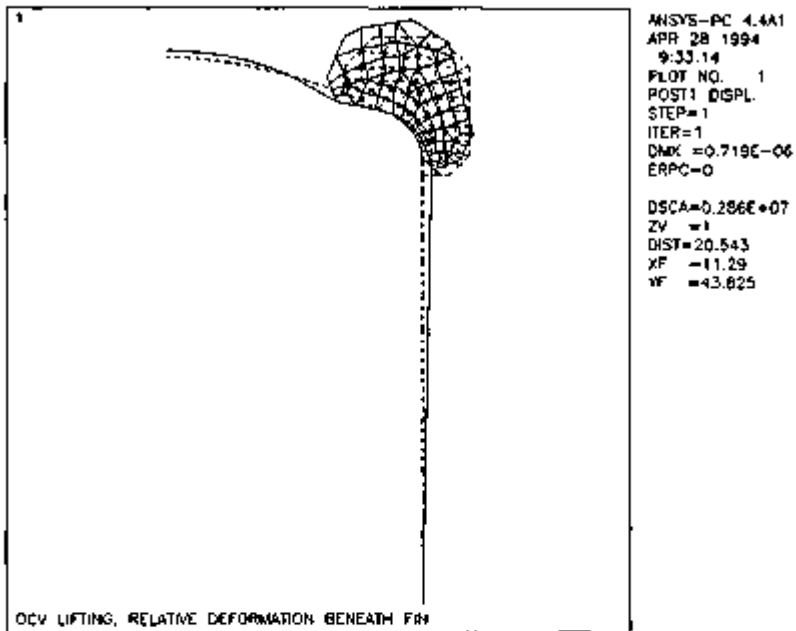


FIGURE 2.10.3-10.

2.10.4 Fin-to-OCV Head Weld Properties ANSYS Model

2.10.4.1 Description

This 3-D model of the fin-to-OCV head weld is used only to determine the centroid and moment of inertia of the weld for use in weld stress calculations. It is modeled as a strip of 24 elements along the contour of the OCV head. Centroidal locations of the centers of each element relative to the global origin and length of each element were used in a spreadsheet to arrive at the overall centroid and length of the weld. The spreadsheet also calculated other parameters necessary to the calculation of maximum weld stress: the distances from the weld centroid to the extreme ends of the weld, the moment arm from the line of action of the lifting force to the weld centroid, and the angles to the horizontal of the maximum weld stresses. These parameters are summarized in Table 2.6.1.2.2-1 and illustrated in Figure 2.6.1.2.2-1.

2.10.4.2 Construction. Two rows of 25 nodes were used to model the fin-to-OCV head weld from bottom to top, with each row separated by a nominal distance to form quadrilateral elements. The finite element output consisted of element centroidal locations and element area. The element length along the weld was found by dividing the element area by width. A plot of node locations is given in Figure 2.10.4-1.

2.10.4.3 Material Properties. Not used.

2.10.4.4 Constraints. All nodes completely constrained.

2.10.4.5 Applied Loads. None.

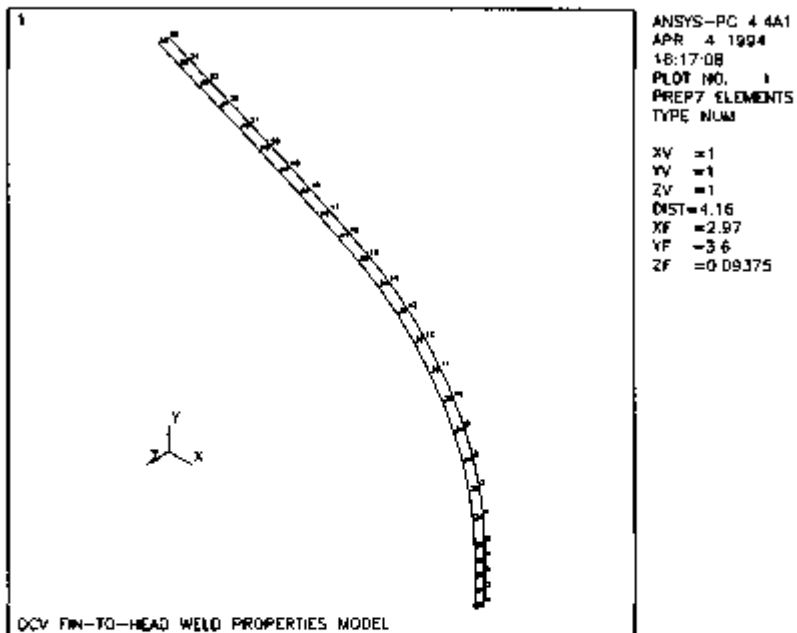


FIGURE 2.10.4-1.

2.10.5 OCV Head ANSYS Model for Tiedown Analysis

2.10.5.1 Description. The OCV head tiedown model is a 3-D model of a one-quarter symmetry segment of the upper portion of the OCV used to evaluate tiedown stresses in the OCV head. The extent of the model is 90° with a 3-in.-wide, 0.25-in.-thick doubler plate extending from the center of the head, over the knuckle radius, and to the top of the water jacket. The lower edge of the model ends in the wall a short distance above the OCV flange, because flange details are irrelevant to this analysis. The water jacket and fins are also not modeled, as they have little effect on tiedown induced head stress. The model layout is shown in Figure 2.10.5-1.

2.10.5.2 Construction. The model is constructed of quadrilateral shell elements of two thicknesses: 0.5 in. for the OCV wall and 0.75 in. (equal to the sum of the head and doubler thicknesses) in the area of the doubler strip. The doubler strip is bounded by nodes 489, 264, 361 (at the top center), 276, and 502. A model node plot is given in Figure 2.10.5-2 and an element plot in Figure 2.10.5-3. An interpreted ANSYS input listing is given in Table 2.10.5-1.

2.10.5.3 Material Properties. A modulus of elasticity of 27.1×10^6 psi was used, corresponding to 270 °F, which represents overall head temperature. Poisson's ratio was 0.3.

2.10.5.4 Constraints. Nodes along the cut edges were constrained in the one linear and two rotational degrees of freedom required to ensure symmetry of the model. The node at the exact top center of the OCV head was restrained to have no radial displacement. The nodes along the bottom were fixed in all six degrees of freedom, as appropriate to the tiedown case. This edge was far enough away from the area of interest (the knuckle) that constraint details were relatively unimportant.

2.10.5.5 Applied Loading. Pressure loading was applied to the top surface of the doubler plate to simulate the load from the tiedown strap. As discussed in Section 2.5.2.2, two pressures were used to model the tiedown strap loads. Besides tiedown strap tension, the magnitude of pressure also depended on the radius of the body beneath the strap. Therefore, one value of pressure (319.6 psi) was applied from the OCV head center down to the top of the knuckle ledge (defined by nodes 266, 273, 274, and 276), and the second value of pressure (3,111 psi) was applied in the knuckle region down to the point where the strap leaves the OCV surface (defined by nodes 201, 202, 203, and 196). Pressure internal to the OCV was conservatively ignored. Node temperatures were not used.

2.10.5.6 Results. Stress intensity because of applied strap loads are shown in Figures 2.10.5-4 through 2.10.5-6.

TABLE 2.10.6-1. Interpreted ANSYS Input Listing.

```

STATIC ANALYSIS (KANT=0)
LINEAR ANALYSIS - NO NON-LINEAR PROPERTIES
REFERENCE TEMPERATURE= 0.000 (TRUE)
UNIFORM TEMPERATURE = 0.000 (TRUE)
*****ANALYSIS OPTIONS (KEY VALUES) (IF ANY) *****
NO STATIC INTERPOLATION/EXTRAPOLATION (KAY(3)=0)
SMALL DEFLECTION SOLUTION (KAY(6)=0)
NO STRESS STIFFENING (KAY(8)=0)
USE LINEAR SOLUTION PROCEDURE (KAY(9)=0)
IN-CORE WAVE-FRONT EQUATION SOLVER (KAY(10)=0)
LIST ELEMENT TYPES FROM 1 TO 20 BY 1
NO. STIF      KEYOPT VALUES      IMPR
1  63  0  0  0  0  0  0  0  0  0  0  QUAD, PLAT, SHELL
LIST ALL REAL SETS
REAL CONSTANT SET 1 ITEMS 1 TO 10
0.24000      0.00000E+00  0.00000E+00  0.00000E+00  0.00000E+00  0.00000E+00
0.00000E+00  0.00000E+00  0.00000E+00  0.00000E+00  0.00000E+00  0.00000E+00
0.00000E+00  0.00000E+00  0.00000E+00  0.00000E+00  0.00000E+00  0.00000E+00
REAL CONSTANT SET 2 ITEMS 1 TO 10
0.25000      0.00000E+00  0.00000E+00  0.00000E+00  0.00000E+00  0.00000E+00
0.00000E+00  0.00000E+00  0.00000E+00  0.00000E+00  0.00000E+00  0.00000E+00
0.00000E+00  0.00000E+00  0.00000E+00  0.00000E+00  0.00000E+00  0.00000E+00
REAL CONSTANT SET 3 ITEMS 1 TO 10
0.75000      0.00000E+00  0.00000E+00  0.00000E+00  0.00000E+00  0.00000E+00
0.00000E+00  0.00000E+00  0.00000E+00  0.00000E+00  0.00000E+00  0.00000E+00
0.00000E+00  0.00000E+00  0.00000E+00  0.00000E+00  0.00000E+00  0.00000E+00
LIST ALL COORDINATE SYSTEMS
SYSTEM TYPE      CENTER      PARAMETERS      BING KEYS
0 0 (CARTESIAN)      0.000      0.000      0.000      1.000      0.000      0 0
1 1 (CYLINDRICAL)      0.000      0.000      0.000      1.000      0.000      0 0
2 2 (SPHERICAL)      0.000      0.000      0.000      1.000      1.000      0 0
11 1 (CYLINDRICAL)      0.000      0.000      0.000      1.000      1.000      0 0
12 1 (CYLINDRICAL)      14.910      29.270      0.000      1.000      1.000      0 0
13 3 (TOROIDAL)      0.000      29.270      0.000      14.910      1.000      0 0
14 5 (TOROIDAL)      0.000      29.270      0.000      14.910      1.000      0 0
SYSTEM      ORIENTATION VECTORS (K, Y, Z)
0      1.00  0.00  0.00  0.00  1.00  0.00  0.00  0.00  1.00
1      1.00  0.00  0.00  0.00  1.00  0.00  0.00  0.00  1.00
2      1.00  0.00  0.00  0.00  1.00  0.00  0.00  0.00  1.00
11     1.00  0.00  0.00  0.00  0.00 -1.00  0.00  1.00  0.00
12     1.00  0.00  0.00  0.00  1.00  0.00  0.00  0.00  1.00
13     1.00  0.00  0.00  0.00  0.00 -1.00  0.00  1.00  0.00
14     1.00  0.00  0.00  0.00  0.00 -1.00  0.00  1.00  0.00
CYS TYPE      XC      YC      ZC      TB1Y      TB2Z      TB3Z
11 1 0.00000E+00  0.00000E+00  0.00000E+00  0.000      0.000      -90.000
12 1 14.910      29.270      0.00000E+00  0.000      0.000      0.000
13 3 0.00000E+00  29.270      0.00000E+00  0.000      0.000      -90.000
14 5 0.00000E+00  29.270      0.00000E+00  0.000      0.000      -90.000
LIST ALL SELECTED KEYPOINTS. 0KEYS= 0
PT.      X, Y, Z LOCATION      MODE      ELEM      ESIZE
5  12,1900      29.2700      0.000000E+00      515      0
LIST ALL SELECTED LINE SEGMENTS.
    
```

SEC. NO.	KEYPT	DIRECTION	DIV	SPACING	NODES/ELEM
23	25	0.9983 -0.0587 0.0000	3	1.0000	362 363
	2	-1.0000 0.0000 0.0000			0 0
27	2	0.0000 0.0000 -1.0000	3	1.0000	364 365
	19	0.0000 -0.0587 -0.9983			0 0
48	31	-0.7065 0.0418 0.7064	8	1.0000	266 272
	32	0.6389 -0.4316 -0.6309			0 0
49	32	0.6398 0.0000 0.7685	3	1.0000	276 278
	36	-0.7685 0.0000 -0.6398			0 0
50	37	-0.7064 0.0418 0.7065	8	1.0000	277 283
	36	0.6389 -0.4316 -0.6309			0 0
51	31	0.0084 0.0294 0.9994	3	1.0000	284 285
	37	-0.9994 0.0294 -0.0084			0 0
52	31	0.9983 -0.0587 0.0000	3	1.0000	362 363
	38	-1.0000 0.0000 0.0000			0 0
53	38	0.0000 0.0000 1.0000	3	1.0000	364 365
	37	0.0000 -0.0587 -0.9983			0 0
54	32	-0.6316 0.4499 0.6315	3	1.0000	369 378
	39	0.2972 -0.9074 -0.2971			0 0
55	39	0.6457 0.0000 0.7636	3	1.0000	282 283
	40	-0.7636 0.0000 -0.6457			0 0

SEC. NO.	KEYPT	DIRECTION	DIV	SPACING	NODES/ELEM
56	34	-0.6316 0.4499 0.6316	3	1.0000	371 372
	40	0.2971 -0.9074 -0.2972			0 0
57	41	-0.7065 0.0418 0.7064	8	1.0000	266 272
	42	0.6389 -0.4316 -0.6309			0 0
58	42	0.6398 0.0000 0.7685	3	1.0000	276 278
	43	-0.7685 0.0000 -0.6398			0 0
59	44	-0.7064 0.0418 0.7065	8	1.0000	277 283
	43	0.6389 -0.4316 -0.6309			0 0
60	41	0.0084 0.0294 0.9994	3	1.0000	284 285
	44	-0.9994 0.0294 -0.0084			0 0
61	41	0.9983 -0.0587 0.0000	3	1.0000	362 363
	45	-1.0000 0.0000 0.0000			0 0
62	45	0.0000 0.0000 1.0000	3	1.0000	364 365
	44	0.0000 -0.0587 -0.9983			0 0
63	42	-0.6316 0.4499 0.6315	3	1.0000	369 378
	46	0.2972 -0.9074 -0.2971			0 0
64	44	0.6457 0.0000 0.7636	3	1.0000	282 283
	47	-0.7636 0.0000 -0.6457			0 0
65	45	-0.6316 0.4499 0.6316	3	1.0000	371 372
	47	0.2971 -0.9074 -0.2972			0 0

SEC. NO.	KEYPT	DIRECTION	DIV	SPACING	NODES/ELEM
66	48	-0.0195 -0.9998 -0.0136	2	1.0000	521 521
	49	-0.3078 0.9084 0.2830			0 0
67	50	-0.7630 0.0000 -0.6464	3	1.0000	505 504
	48	0.6464 0.0000 0.7630			0 0
68	50	0.0136 -0.9998 0.0115	2	1.0000	526 526
	51	-0.2830 0.9084 0.3078			0 0
69	49	0.6457 0.0000 0.7636	3	1.0000	282 283
	51	-0.7636 0.0000 -0.6457			0 0

LIST NO.	ALL KEYPPTS/LINE	SECTION AREAS	NODES	ELEMENTS	MAT REL	TRP	EQYS
1	17 24 25 27		505 514	472 489	1 1 1	0	
2	3 4 5 17 33		322 525	490 499	1 1 1	0	
3	3 44 45 36						
4	3 17 27 26		327 528	500 509	1 1 1	0	
	65 43 46 35						
5	26 27 9 8		538 538	506 515	1 1 1	0	
	46 47 31 37						
6	11 12 13 14		0 0	0 0	0 0 0	0	
	13 14 15 16						
7	21 22 23 24		0 0	0 0	0 0 0	0	
	17 18 19 20						
8	28 29 20 19		286 299	328 291	1 1 1	0	
	21 31 24 32						
9	3 28 29 29		310 328	252 284	1 1 1	0	
	24 21 0 25						
9	7 28 19 19		343 360	283 314	1 1 1	0	
	29 26 0 30						

NO.	2	3	26	19	344	348	315	321	1	1	1	0
	0	25	32	27								
NO.	POINTS	A	IN	SEC.	MODES		ELEMENTS		NAT	NEL	TPP	ESYS
11	29	30	24	28	373	376	322	338	1	1	1	0
12	33	35	34	31								
12	3	4	33	29	379	386	331	343	1	1	1	0
13	2	36	33	23								
13	24	26	6	7	387	396	346	368	1	1	1	0
14	34	37	10	20								
	-	-	-	-	558	635	516	646	1	1	1	0
	4	8	12	47								
	48	39	38	44								

LIST ALL SELECTED ELEMENTS. (LIST NAMES)

ELEM	NAT	TPP	NEL	ESYS	MODES
225	1	1	3	0	286 284 284 286
229	1	1	3	0	287 286 286 287
230	1	1	3	0	288 287 287 288
231	1	1	3	0	289 288 288 289
232	1	1	3	0	290 289 289 290
233	1	1	3	0	291 290 290 291
234	1	1	3	0	292 291 291 292
235	1	1	3	0	293 292 292 293
236	1	1	3	0	294 293 293 294
237	1	1	3	0	295 294 294 295
238	1	1	3	0	296 295 295 296
239	1	1	3	0	297 296 296 297
240	1	1	3	0	298 297 297 298
241	1	1	3	0	299 298 298 299
242	1	1	3	0	300 299 299 300
243	1	1	3	0	301 300 300 301
244	1	1	3	0	302 301 301 302
245	1	1	3	0	303 302 302 303
246	1	1	3	0	304 303 303 304
247	1	1	3	0	305 304 304 305

ELEM	NAT	TPP	NEL	ESYS	MODES
248	1	1	3	0	306 305 305 306
249	1	1	3	0	307 306 306 307
250	1	1	3	0	308 307 307 308
251	1	1	3	0	309 308 308 309
252	1	1	1	0	310 309 309 310
253	1	1	1	0	311 310 310 311
254	1	1	1	0	312 311 311 312
255	1	1	1	0	313 312 312 313
256	1	1	1	0	314 313 313 314
257	1	1	1	0	315 314 314 315
258	1	1	1	0	316 315 315 316
259	1	1	1	0	317 316 316 317
260	1	1	1	0	318 317 317 318
261	1	1	1	0	319 318 318 319
262	1	1	1	0	320 319 319 320
263	1	1	1	0	321 320 320 321
264	1	1	1	0	322 321 321 322
265	1	1	1	0	323 322 322 323
266	1	1	1	0	324 323 323 324
267	1	1	1	0	325 324 324 325

ELEM	NAT	TPP	NEL	ESYS	MODES
268	1	1	1	0	326 325 325 326
269	1	1	1	0	327 326 326 327
270	1	1	1	0	328 327 327 328
271	1	1	1	0	329 328 328 329
272	1	1	1	0	330 329 329 330
273	1	1	1	0	331 330 330 331
274	1	1	1	0	332 331 331 332
275	1	1	1	0	333 332 332 333
276	1	1	1	0	334 333 333 334
277	1	1	1	0	335 334 334 335
278	1	1	1	0	336 335 335 336

279	1	1	1	D	321	270	271	318
280	1	1	1	D	316	313	306	307
281	1	1	1	D	318	271	272	315
282	1	1	1	D	315	272	268	304
283	1	1	1	D	331	332	343	342
284	1	1	1	D	332	333	344	343
285	1	1	1	D	331	342	341	330
286	1	1	1	D	333	273	283	344
287	1	1	1	D	330	341	346	329

ELER	MAT	TPP	REL	EXTS	NODES			
288	1	1	1	D	342	343	352	351
289	1	1	1	D	343	344	345	352
290	1	1	1	D	342	351	350	341
291	1	1	1	D	344	283	282	345
292	1	1	1	D	341	350	339	340
293	1	1	1	D	351	352	353	354
294	1	1	1	D	352	343	344	355
295	1	1	1	D	351	354	353	350
296	1	1	1	D	344	282	281	344
297	1	1	1	D	350	351	336	339
298	1	1	1	D	354	359	357	354
299	1	1	1	D	355	344	347	350
300	1	1	1	D	354	357	354	353
301	1	1	1	D	346	281	280	347
302	1	1	1	D	350	356	337	330
303	1	1	1	D	357	359	366	360
304	1	1	1	D	356	357	340	340
305	1	1	1	D	359	347	346	340
306	1	1	1	D	358	356	360	340
307	1	1	1	D	347	280	279	340

ELER	MAT	TPP	REL	EXTS	NODES			
308	1	1	1	D	356	358	336	337
309	1	1	1	D	360	348	349	358
310	1	1	1	D	348	279	278	349
311	1	1	1	D	350	349	335	336
312	1	1	1	D	334	335	349	349
313	1	1	1	D	340	278	277	334
314	1	1	1	D	277	276	334	334
315	1	1	3	D	361	363	366	364
316	1	1	3	D	364	366	368	365
317	1	1	3	D	363	362	367	366
318	1	1	3	D	368	366	367	367
319	1	1	3	D	365	368	285	276
320	1	1	3	D	362	284	284	367
321	1	1	3	D	368	367	284	285
322	1	1	3	D	373	274	265	369
323	1	1	3	D	374	373	369	370
324	1	1	3	D	292	374	370	281
325	1	1	3	D	375	275	274	373
326	1	1	3	D	376	379	373	374
327	1	1	3	D	203	374	374	282

ELER	MAT	TPP	REL	EXTS	NODES			
328	1	1	3	D	371	273	275	375
329	1	1	3	D	372	371	375	376
330	1	1	3	D	196	372	376	203
331	1	1	1	D	379	309	300	377
332	1	1	1	D	380	379	377	378
333	1	1	1	D	284	380	378	382
334	1	1	1	D	381	308	307	379
335	1	1	1	D	382	381	379	380
336	1	1	1	D	205	382	380	204
337	1	1	1	D	383	307	308	381
338	1	1	1	D	384	385	381	382
339	1	1	1	D	206	384	382	205
340	1	1	1	D	385	306	307	383
341	1	1	1	D	386	385	383	384
342	1	1	1	D	207	384	384	206
343	1	1	1	D	369	265	306	385

344	1	1	1	0	370	368	306	306
345	1	1	1	0	201	370	146	287
346	1	1	1	0	389	333	273	371
347	1	1	1	0	380	389	371	372

ELEM	MAT	TYP	REL	ESYS	MODES			
348	1	1	1	0	197	390	372	196
349	1	1	1	0	291	332	333	389
350	1	1	1	0	382	391	389	390
351	1	1	1	0	198	392	390	197
352	1	1	1	0	293	331	332	391
353	1	1	1	0	394	393	391	192
354	1	1	1	0	199	394	392	198
355	1	1	1	0	395	330	331	398
356	1	1	1	0	396	395	395	394
357	1	1	1	0	200	396	394	199
358	1	1	1	0	387	329	330	395
359	1	1	1	0	388	387	395	396
360	1	1	1	0	194	388	394	200
472	1	1	3	0	505	504	487	489
473	1	1	1	0	506	505	489	490
474	1	1	1	0	507	506	490	491
475	1	1	1	0	508	507	491	492
476	1	1	1	0	509	508	492	493
477	1	1	1	0	495	509	492	486
478	1	1	3	0	510	503	504	505

ELEM	MAT	TYP	REL	ESYS	MODES			
479	1	1	1	0	511	510	505	506
480	1	1	1	0	512	511	506	507
481	1	1	1	0	513	512	507	508
482	1	1	1	0	514	513	508	509
483	1	1	1	0	496	514	509	495
484	1	1	3	0	512	497	508	510
485	1	1	1	0	501	502	510	511
486	1	1	1	0	500	501	511	512
487	1	1	1	0	499	500	512	513
488	1	1	1	0	498	499	513	514
489	1	1	1	0	496	496	514	496
490	1	1	1	0	522	284	181	516
491	1	1	1	0	517	522	516	515
492	1	1	1	0	523	286	284	522
493	1	1	1	0	518	523	522	517
494	1	1	1	0	524	286	283	523
495	1	1	1	0	519	524	523	518
496	1	1	1	0	525	287	284	524
497	1	1	1	0	520	525	524	519
498	1	1	1	0	521	281	287	525

ELEM	MAT	TYP	REL	ESYS	MODES			
499	1	1	1	0	487	521	525	528
500	1	1	3	0	527	202	201	521
501	1	1	3	0	504	527	531	487
502	1	1	3	0	528	203	202	527
503	1	1	3	0	503	528	527	504
504	1	1	3	0	526	194	203	528
505	1	1	3	0	487	526	528	505
506	1	1	1	0	529	197	196	526
507	1	1	1	0	530	526	526	487
508	1	1	1	0	534	198	197	535
509	1	1	1	0	531	534	533	530
510	1	1	1	0	537	199	198	534
511	1	1	1	0	532	537	534	531
512	1	1	1	0	538	200	199	537
513	1	1	1	0	533	538	537	532
514	1	1	1	0	534	194	200	538
515	1	1	1	0	529	534	538	533
516	1	1	1	0	538	951	532	531
517	1	1	1	0	549	950	531	530
518	1	1	1	0	951	552	543	532

ELBN	MA1	TYP	REL	ESTS	NODES
519	1	1	1	0	548 549 560 570
520	1	1	1	0	547 548 579 578
521	1	1	1	0	544 547 578 562
522	1	1	1	0	552 545 557 563
523	1	1	1	0	539 544 562 544
524	1	1	1	0	579 580 643 643
525	1	1	1	0	581 582 630 640
526	1	1	1	0	581 640 641 580
527	1	1	1	0	582 563 637 630
528	1	1	1	0	588 642 643 643
529	1	1	1	0	589 641 642 642
530	1	1	1	0	578 579 634 633
531	1	1	1	0	579 643 644 644
532	1	1	1	0	578 633 634 548
533	1	1	1	0	579 644 645 634
534	1	1	1	0	543 544 637 637
535	1	1	1	0	627 641 640 640
536	1	1	1	0	543 557 594 544
537	1	1	1	0	625 640 638 638
538	1	1	1	0	643 642 630 631

ELBN	MA1	TYP	REL	ESTS	NODES
539	1	1	1	0	643 631 632 644
540	1	1	1	0	544 562 561 543
541	1	1	1	0	642 641 629 630
542	1	1	1	0	637 637 638 638
543	1	1	1	0	626 627 640 640
544	1	1	1	0	627 628 641 641
545	1	1	1	0	628 636 640 640
546	1	1	1	0	638 639 641 641
547	1	1	1	0	644 632 622 645
548	1	1	1	0	624 625 638 638
549	1	1	1	0	634 634 635 635
550	1	1	1	0	634 643 644 634
551	1	1	1	0	638 639 648 624
552	1	1	1	0	637 564 647 639
553	1	1	1	0	622 644 645 645
554	1	1	1	0	631 638 618 619
555	1	1	1	0	627 615 616 628
556	1	1	1	0	627 626 614 615
557	1	1	1	0	630 629 617 618
558	1	1	1	0	631 619 620 632

ELBN	MA1	TYP	REL	ESTS	NODES
559	1	1	1	0	629 628 616 617
560	1	1	1	0	542 644 603 561
561	1	1	1	0	625 625 613 614
562	1	1	1	0	632 628 621 622
563	1	1	1	0	633 635 623 604
564	1	1	1	0	639 647 608 608
565	1	1	1	0	629 624 612 613
566	1	1	1	0	635 646 647 647
567	1	1	1	0	622 621 594 644
568	1	1	1	0	635 647 633 635
569	1	1	1	0	614 613 601 573
570	1	1	1	0	624 608 606 612
571	1	1	1	0	616 573 484 637
572	1	1	1	0	615 614 611 601
573	1	1	1	0	618 617 484 484
574	1	1	1	0	619 630 496 495
575	1	1	1	0	619 635 488 488
576	1	1	1	0	646 594 592 647
577	1	1	1	0	628 638 592 621
578	1	1	1	0	621 595 594 594

ELBN	MA1	TYP	REL	ESTS	NODES
579	1	1	1	0	634 633 630 611
580	1	1	1	0	608 607 605 606
581	1	1	1	0	635 633 632 623

582	1	1	1	0	544	545	405	607
583	1	1	1	0	544	554	555	545
584	1	1	1	0	594	593	591	592
585	1	1	1	0	447	448	654	453
586	1	1	1	0	543	541	540	542
587	1	1	1	0	403	540	541	541
588	1	1	1	0	404	423	442	443
589	1	1	1	0	411	400	401	401
590	1	1	1	0	413	412	609	610
591	1	1	1	0	457	453	454	454
592	1	1	1	0	401	400	572	573
593	1	1	1	0	467	592	590	468
594	1	1	1	0	593	400	493	591
595	1	1	1	0	573	572	490	494
596	1	1	1	0	458	456	453	453
597	1	1	1	0	411	599	600	600
598	1	1	1	0	454	440	440	455

ELEM	MAT	TYP	REL	EGTS	NODES			
599	1	1	1	0	412	404	596	600
600	1	1	1	0	592	591	589	590
601	1	1	1	0	411	410	598	599
602	1	1	1	0	450	452	455	455
603	1	1	1	0	400	599	571	572
604	1	1	1	0	468	590	588	609
605	1	1	1	0	447	450	455	455
606	1	1	1	0	423	452	451	462
607	1	1	1	0	591	493	492	589
608	1	1	1	0	403	402	595	595
609	1	1	1	0	572	571	499	499
610	1	1	1	0	410	440	597	598
611	1	1	1	0	451	452	450	450
612	1	1	1	0	403	402	539	540
613	1	1	1	0	590	589	587	588
614	1	1	1	0	405	505	504	505
615	1	1	1	0	599	598	570	571
616	1	1	1	0	449	588	586	450
617	1	1	1	0	565	583	534	544
618	1	1	1	0	506	451	450	450

ELEM	MAT	TYP	REL	EGTS	NODES			
619	1	1	1	0	540	599	541	542
620	1	1	1	0	509	492	491	507
621	1	1	1	0	571	570	560	499
622	1	1	1	0	409	596	584	597
623	1	1	1	0	578	577	549	570
624	1	1	1	0	580	487	585	584
625	1	1	1	0	451	576	492	492
626	1	1	1	0	590	505	503	504
627	1	1	1	0	402	576	577	590
628	1	1	1	0	579	569	501	500
629	1	1	1	0	547	491	490	585
630	1	1	1	0	451	586	575	576
631	1	1	1	0	193	544	547	603
632	1	1	1	0	597	594	540	540
633	1	1	1	0	584	585	574	575
634	1	1	1	0	544	554	553	567
635	1	1	1	0	559	558	540	541
636	1	1	1	0	569	568	502	501
637	1	1	1	0	525	490	489	574
638	1	1	1	0	599	577	577	588

ELEM	MAT	TYP	REL	EGTS	NODES			
639	1	1	1	0	584	583	532	531
640	1	1	1	0	576	575	519	518
641	1	1	1	0	576	518	517	577
642	1	1	1	0	584	531	530	544
643	1	1	1	0	545	567	533	532
644	1	1	1	0	575	574	520	519
645	1	1	1	0	547	553	529	530
646	1	1	1	0	558	517	515	540

647	1	1	1	0	548	538	497	502
648	1	1	1	0	574	489	487	520

LIST ALL SELECTED HOME DESIG= D

MODE	X	Y	Z	TWOY	THRY	FOUR
182	17.894	30.505	8.52877E-11	0.00	-90.00	0.00
194	0.18014E+09	30.505	-17.894	90.00	0.00	-90.00
196	11.547	30.505	-13.670	90.00	-40.19	-90.00
197	9.3221	30.505	-13.190	90.00	-32.15	-90.00
198	7.3103	30.505	-16.332	90.00	-24.11	-90.00
199	4.9548	30.505	-17.194	90.00	-16.08	-90.00
200	2.5420	30.505	-17.748	90.00	-8.04	-90.00
201	13.670	30.505	-11.547	90.00	-49.81	-90.00
202	13.002	30.505	-12.294	90.00	-46.40	-90.00
203	12.294	30.505	-13.002	90.00	-43.40	-90.00
204	17.718	30.505	-2.5020	90.00	-81.96	-90.00
205	17.194	30.505	-4.9548	90.00	-73.92	-90.00
206	16.332	30.505	-7.3103	90.00	-65.89	-90.00
207	15.190	30.505	-9.3221	90.00	-57.85	-90.00
208	2.1133	33.938	0.80000E+05	0.00	-90.00	0.00
209	12.042	32.042	-18.291	90.00	-59.25	-90.00
210	9.4784	33.807	-1.3547	90.00	-66.85	-90.00
217	4.8383	33.573	-2.7865	90.00	-68.68	-90.00
248	5.1855	33.253	-4.0436	90.00	-56.70	-90.00
269	7.4861	34.882	-5.3790	90.00	-54.34	-90.00

MODE	X	Y	Z	TWOY	THRY	FOUR
270	8.7003	34.266	-6.6761	90.00	-52.78	-90.00
271	10.075	33.632	-7.9481	90.00	-51.67	-90.00
272	11.333	32.903	-9.2183	90.00	-50.67	-90.00
273	10.501	32.041	-12.026	90.00	-39.75	-90.00
274	11.962	32.042	-11.232	90.00	-46.75	-90.00
275	11.252	32.042	-11.962	90.00	-43.25	-90.00
276	0.14003E+09	33.938	-2.1133	90.00	0.00	-90.00
277	1.3367	33.807	-3.4704	90.00	-21.25	-90.00
278	2.7003	33.573	-4.8203	90.00	-29.31	-90.00
279	4.0436	33.258	-6.1595	90.00	-33.30	-90.00
280	5.3790	32.802	-7.4861	90.00	-35.66	-90.00
281	6.6761	34.266	-8.7903	90.00	-37.23	-90.00
282	7.9481	33.632	-10.075	90.00	-38.31	-90.00
283	9.2183	32.903	-11.333	90.00	-39.19	-90.00
284	1.0315	33.938	-1.0572	90.00	-68.00	-90.00
285	1.0572	33.938	-1.0315	90.00	-38.00	-90.00
286	3.1400	33.784	-2.3749	90.00	-52.90	-90.00
287	4.4404	33.535	-3.6842	90.00	-56.32	-90.00
288	5.7295	33.190	-4.9821	90.00	-48.99	-90.00
289	7.0043	34.752	-6.2656	90.00	-48.19	-90.00

MODE	X	Y	Z	TWOY	THRY	FOUR
290	8.2618	34.220	-7.5316	90.00	-47.65	-90.00
291	9.4990	33.597	-8.7771	90.00	-47.26	-90.00
292	10.773	32.862	-9.9991	90.00	-44.97	-90.00
293	2.3749	33.784	-3.1400	90.00	-37.19	-90.00
294	3.6842	33.535	-4.4404	90.00	-39.68	-90.00
295	4.9821	33.190	-5.7295	90.00	-41.81	-90.00
296	6.2636	34.752	-7.0043	90.00	-41.81	-90.00
297	7.5316	34.220	-8.2618	90.00	-42.35	-90.00
298	8.7771	33.597	-9.4990	90.00	-42.75	-90.00
299	9.9991	32.862	-10.773	90.00	-43.61	-90.00
300	16.422	32.842	0.11270E+10	0.00	-90.00	0.00
301	14.097	33.121	-0.31917E+08	0.00	-90.00	0.00
302	11.709	34.815	-0.50703E+08	0.00	-90.00	0.00
303	9.4254	34.744	-0.34933E+08	0.00	-90.00	0.00
304	7.0174	35.309	-0.49850E+08	0.00	-90.00	0.00
305	4.5762	35.788	-0.30854E+08	0.00	-90.00	0.00
306	13.957	32.842	-8.8833	90.00	-58.28	-90.00
307	15.020	32.842	-8.6408	90.00	-66.15	-90.00
308	15.794	32.842	-4.4991	90.00	-74.10	-90.00
309	16.264	32.842	-2.2713	90.00	-82.07	-90.00

MODE	X	Y	Z	THY1	THY2	THXZ
310	14.047	33.986	-2.8834	90.00	-81.83	-90.00
311	11.850	33.945	-1.8334	90.00	-81.21	-90.00
312	9.5495	34.672	-1.5130	90.00	-81.02	-90.00
313	7.3263	35.310	-1.4212	90.00	-77.32	-90.00
314	5.4663	33.304	-1.6205	90.00	-75.27	-90.00
315	15.394	32.469	-7.3333	90.00	-58.71	-90.00
316	13.260	32.367	-5.7752	90.00	-64.46	-90.00
317	15.825	33.004	-3.9428	90.00	-74.06	-90.00
318	10.948	33.676	-6.4852	90.00	-59.34	-90.00
319	11.443	33.408	-4.9922	90.00	-66.65	-90.00
320	12.165	33.694	-3.5653	90.00	-73.67	-90.00
321	9.5141	34.289	-5.4320	90.00	-60.19	-90.00
322	10.870	34.304	-4.2834	90.00	-67.25	-90.00
323	10.479	34.333	-2.9634	90.00	-76.23	-90.00
324	8.2187	34.747	-4.6825	90.00	-68.71	-90.00
325	8.4340	34.821	-3.3133	90.00	-67.38	-90.00
326	8.8410	34.803	-2.5667	90.00	-73.81	-90.00
327	7.1451	35.085	-3.7399	90.00	-62.37	-90.00
328	6.8807	35.324	-2.8142	90.00	-67.76	-90.00
329	9.43990E+10	34.042	-16.422	90.00	0.00	-90.00

MODE	X	Y	Z	THY1	THY2	THXZ
330	2.2713	32.042	-16.264	90.00	-7.35	-90.00
331	4.4991	32.042	-15.794	90.00	-15.90	-90.00
332	6.6400	32.042	-15.020	90.00	-23.85	-90.00
333	8.6833	32.042	-13.957	90.00	-31.89	-90.00
334	0.26780E+08	35.781	-3.9621	90.00	0.00	-90.00
335	0.46980E+08	35.530	-5.8202	90.00	0.00	-90.00
336	0.46948E+08	35.184	-7.4229	90.00	0.00	-90.00
337	0.67896E+08	34.764	-9.4254	90.00	0.00	-90.00
338	0.46182E+08	34.213	-11.203	90.00	0.00	-90.00
339	0.33332E+08	33.590	-12.950	90.00	0.00	-90.00
340	0.34228E+08	32.878	-14.664	90.00	0.00	-90.00
341	2.8721	32.927	-14.405	90.00	-8.19	-90.00
342	4.8607	32.928	-13.973	90.00	-16.28	-90.00
343	5.9052	32.922	-13.314	90.00	-23.32	-90.00
344	7.6133	32.925	-12.408	90.00	-31.34	-90.00
345	4.6172	33.422	-11.085	90.00	-38.95	-90.00
346	9.3389	34.214	-9.7190	90.00	-25.23	-90.00
347	4.3939	34.709	-8.4893	90.00	-27.57	-90.00
348	3.8210	35.121	-7.3067	90.00	-22.46	-90.00
349	3.4692	35.511	-5.7302	90.00	-14.38	-90.00

MODE	X	Y	Z	THY1	THY2	THXZ
350	3.8904	33.639	-12.682	90.00	-6.48	-90.00
351	3.6464	33.628	-12.324	90.00	-16.48	-90.00
352	5.2182	33.490	-11.795	90.00	-23.87	-90.00
353	7.6658	34.234	-11.006	90.00	-8.61	-90.00
354	3.1601	34.214	-18.734	90.00	-15.44	-90.00
355	4.5401	34.148	-18.446	90.00	-23.28	-90.00
356	1.5373	34.719	-9.3941	90.00	-9.29	-90.00
357	2.4494	34.595	-9.5970	90.00	-15.49	-90.00
358	1.4387	33.140	-7.3889	90.00	-18.60	-90.00
359	3.6286	34.565	-9.3992	90.00	-21.09	-90.00
360	2.5482	34.855	-8.4423	90.00	-16.38	-90.00
361	0.14027E+09	35.008	0.80000E+00	0.00	-90.00	0.00
362	1.4894	33.972	0.80000E+00	0.00	-90.00	0.00
363	0.70484	35.993	0.00000E+00	0.00	-90.00	0.00
364	0.53636E+09	33.905	-0.78486	90.00	0.00	-90.00
365	0.34817E+09	33.972	-1.4894	90.00	0.00	-90.00
366	0.63482	35.990	-0.68311	90.00	-45.23	-90.00
367	1.1998	35.923	-0.68776	90.00	-48.16	-90.00
368	0.70412	35.974	-7.1793	90.00	-30.04	-90.00
369	12.990	31.790	-10.876	90.00	-58.04	-90.00

MODE	X	Y	Z	THY1	THY2	THXZ
370	13.251	31.295	-11.236	90.00	-49.92	-90.00
371	10.874	31.790	-12.890	90.00	-39.04	-90.00
372	11.254	31.215	-15.351	90.00	-40.86	-90.00
373	12.308	31.731	-11.683	90.00	-44.89	-90.00
374	12.481	31.223	-11.973	90.00	-44.04	-90.00
375	11.463	31.731	-12.308	90.00	-43.31	-90.00
376	11.572	31.223	-12.681	90.00	-43.36	-90.00

377	16.942	31.718	0.99794E-11	9.00	-90.00	0.00
378	17.450	31.715	0.80643E-11	9.00	-90.00	0.00
379	16.776	31.712	-2.3513	90.00	-82.02	-90.00
380	17.378	31.711	-6.4310	90.00	-81.99	-90.00
381	16.286	31.713	-4.6584	90.00	-74.04	-90.00
382	14.738	31.218	-4.8198	90.00	-73.98	-90.00
383	15.480	31.713	-6.8764	90.00	-66.05	-90.00
384	15.933	31.218	-7.1079	90.00	-65.96	-90.00
385	14.374	31.712	-8.9623	90.00	-58.04	-90.00
386	14.787	31.217	-9.2620	90.00	-57.94	-90.00
387	0.18942E-09	31.719	-14.942	90.00	0.00	-90.00
388	0.18938E-09	31.215	-17.430	90.00	0.00	-90.00
389	8.9643	31.712	-14.374	90.00	-31.94	-90.00

MODE	K	T	Z	THY1	THY2	TMO2
590	9.2620	31.217	-14.787	90.00	-32.04	-90.00
591	4.8764	31.713	-13.480	90.00	-27.95	-90.00
592	7.1079	31.218	-15.933	90.00	-24.04	-90.00
593	4.8384	31.713	-16.286	90.00	-13.96	-90.00
594	4.8198	31.218	-14.789	90.00	-16.02	-90.00
595	2.3513	31.712	-16.776	90.00	-7.98	-90.00
596	2.3310	31.217	-17.438	90.00	-5.01	-90.00
487	13.480	25.150	-11.757	90.00	-49.73	-90.00
488	13.880	25.480	-11.757	90.00	-49.73	-90.00
489	13.880	27.430	-11.757	90.00	-49.73	-90.00
490	13.880	27.180	-11.757	90.00	-49.73	-90.00
491	13.880	24.135	-11.757	90.00	-49.73	-90.00
492	13.880	25.480	-11.757	90.00	-49.73	-90.00
493	13.880	24.465	-11.757	90.00	-49.73	-90.00
494	11.757	23.880	-13.880	90.00	-40.27	-90.00
495	13.211	23.480	-12.503	90.00	-44.58	-90.00
496	12.503	23.880	-13.211	90.00	-43.42	-90.00
497	11.757	25.150	-13.880	90.00	-40.27	-90.00
498	11.757	24.945	-13.880	90.00	-40.27	-90.00
499	11.757	25.480	-13.880	90.00	-40.27	-90.00

MODE	K	T	Z	THY1	THY2	TMO2
590	11.757	25.125	-13.880	90.00	-40.27	-90.00
591	11.757	27.180	-13.880	90.00	-40.27	-90.00
592	11.757	27.430	-13.880	90.00	-40.27	-90.00
593	12.508	25.150	-13.211	90.00	-43.42	-90.00
594	13.211	25.150	-12.503	90.00	-44.58	-90.00
595	13.212	27.430	-12.504	90.00	-44.58	-90.00
596	13.212	27.180	-12.503	90.00	-44.58	-90.00
597	13.212	26.935	-12.508	90.00	-44.58	-90.00
598	13.212	25.094	-12.503	90.00	-44.58	-90.00
599	13.212	24.465	-12.503	90.00	-44.58	-90.00
510	12.304	27.430	-13.212	90.00	-43.42	-90.00
511	12.503	27.180	-13.212	90.00	-43.42	-90.00
512	12.308	26.125	-13.212	90.00	-43.42	-90.00
513	12.583	25.999	-13.212	90.00	-43.42	-90.00
514	12.308	24.045	-13.212	90.00	-43.42	-90.00
515	18.190	25.959	0.22102E+16	8.00	-90.00	0.00
516	18.886	25.564	0.31732E-11	8.00	-90.00	0.00
217	18.211	25.150	-2.5424	90.00	-57.95	-90.00
416	17.476	25.150	-3.0445	90.00	-73.48	-90.00
519	16.397	25.150	-7.4451	90.00	-65.84	-90.00

MODE	K	T	Z	THY1	THY2	TMO2
520	15.330	25.958	-9.6968	90.00	-57.70	-90.00
521	13.889	25.564	-11.481	90.00	-49.77	-90.00
522	17.986	25.965	-2.5309	90.00	-81.96	-90.00
523	17.378	25.568	-5.8126	90.00	-73.91	-90.00
524	14.505	25.965	-7.3959	90.00	-65.86	-90.00
525	15.307	25.865	-9.6333	90.00	-57.82	-90.00
526	11.681	25.964	-13.805	90.00	-40.23	-90.00
527	13.139	25.964	-12.429	90.00	-46.99	-90.00
528	12.429	25.964	-13.139	90.00	-43.41	-90.00
529	0.18493E-09	25.958	-18.190	90.00	0.00	-90.00
530	9.6968	25.950	-19.390	90.00	-32.21	-90.00
531	7.4531	25.930	-14.297	90.00	-24.18	-90.00
532	5.0445	25.959	-17.476	90.00	-16.11	-90.00
533	2.5424	25.958	-18.811	90.00	-8.05	-90.00
534	0.31732E-09	25.964	-18.886	90.00	0.00	-90.00

531	0.4331	29.063	-13.367	00.00	-32.10	-90.00
536	7.3959	29.905	-16.540	00.00	-24.14	-90.00
537	5.0126	29.063	-17.370	00.00	-16.09	-90.00
538	2.5306	29.905	-17.940	00.00	-1.04	-90.00
539	10.190	95.000	0.00000E+00	0.00	-90.00	0.00

MODE	K	T	Z	THTK	THTZ	THTZ
540	18.190	27.909	0.00000E+00	0.00	-90.00	0.00
541	18.190	24.393	0.00000E+00	0.00	-90.00	0.00
542	18.190	24.489	0.00000E+00	0.00	-90.00	0.00
543	19.190	21.928	0.00000E+00	0.00	-90.00	0.00
544	18.190	18.063	0.00000E+00	0.00	-90.00	0.00
543	0.12932E+09	15.000	-15.190	00.00	0.00	-90.00
545	17.844	15.000	-3.5496	00.00	-79.73	-90.00
547	14.810	15.000	-9.3627	00.00	-67.50	-90.00
548	15.126	15.000	-10.167	00.00	-34.25	-90.00
549	12.662	15.000	-12.662	00.00	-45.00	-90.00
550	10.107	15.000	-13.126	00.00	-23.71	-90.00
551	4.0627	15.000	-16.810	00.00	-22.50	-90.00
552	3.5496	15.000	-17.844	00.00	-11.25	-90.00
553	0.17994E+09	27.909	-18.190	00.00	0.00	-90.00
554	0.17372E+09	24.393	-18.190	00.00	0.00	-90.00
555	0.16597E+09	24.405	-18.190	00.00	0.00	-90.00
556	0.15632E+09	21.928	-18.190	00.00	0.00	-90.00
557	0.14430E+09	18.063	-18.190	00.00	0.00	-90.00
558	16.117	27.473	-1.6285	00.00	-84.05	-90.00
559	16.957	25.977	-2.2091	00.00	-83.05	-90.00

MODE	J	Y	Z	THTK	THTZ	THTZ
560	18.096	24.117	-1.0689	00.00	-84.17	-90.00
561	18.044	21.959	-1.3090	00.00	-82.73	-90.00
562	17.639	18.056	-3.7970	00.00	-70.72	-90.00
563	5.5429	18.311	-17.842	00.00	-14.25	-90.00
564	2.6996	21.603	-17.909	00.00	-5.34	-90.00
565	2.1181	23.904	-18.064	00.00	-6.69	-90.00
566	2.1162	25.906	-18.067	00.00	-6.67	-90.00
567	2.2975	27.457	-18.068	00.00	-7.24	-90.00
568	0.6850	27.766	-18.270	00.00	-32.92	-90.00
569	10.289	24.543	-13.021	00.00	-34.33	-90.00
570	10.611	25.564	-14.774	00.00	-35.69	-90.00
571	10.842	24.722	-14.604	00.00	-36.59	-90.00
572	10.946	23.846	-14.530	00.00	-37.08	-90.00
573	10.944	22.878	-14.329	00.00	-36.99	-90.00
574	15.253	27.848	-9.9412	00.00	-56.87	-90.00
575	16.440	27.336	-7.7859	00.00	-64.66	-90.00
576	17.437	27.113	-5.1794	00.00	-73.46	-90.00
577	17.906	27.384	-3.2044	00.00	-79.29	-90.00
578	16.746	24.001	-7.1094	00.00	-67.01	-90.00
579	14.945	24.290	-10.370	00.00	-55.24	-90.00

MODE	J	Y	Z	THTK	THTZ	THTZ
580	12.429	17.087	-13.282	00.00	-43.10	-90.00
581	9.7361	17.536	-13.345	00.00	-42.36	-90.00
582	6.8977	17.701	-16.832	00.00	-22.26	-90.00
583	6.0756	27.331	-17.370	00.00	-14.89	-90.00
584	7.4251	24.906	-14.646	00.00	-24.09	-90.00
585	15.006	26.599	-10.241	00.00	-35.56	-90.00
586	15.952	25.732	-8.7421	00.00	-61.28	-90.00
587	14.760	25.551	-10.618	00.00	-34.29	-90.00
588	15.509	24.638	-9.5052	00.00	-50.50	-90.00
589	14.567	24.601	-10.804	00.00	-33.21	-90.00
590	15.203	24.027	-9.9648	00.00	-56.70	-90.00
591	14.345	23.681	-11.120	00.00	-52.31	-90.00
592	14.917	23.183	-10.470	00.00	-55.09	-90.00
593	14.231	22.901	-11.390	00.00	-51.40	-90.00
594	14.587	22.441	-10.866	00.00	-53.31	-90.00
595	4.8095	25.317	-17.695	00.00	-13.30	-90.00
596	4.1917	24.525	-17.113	00.00	-19.91	-90.00
597	3.7823	25.257	-15.892	00.00	-26.00	-90.00
598	9.5502	24.716	-15.442	00.00	-31.67	-90.00
599	10.044	24.285	-15.144	00.00	-33.51	-90.00

NODE	X	Y	Z	TOUT	TINT	TIME
480	19.285	23.441	-15.095	90.00	-34.42	-90.00
481	19.795	23.802	-15.044	90.00	-34.89	-90.00
482	17.597	24.748	-4.4084	90.00	-75.32	-90.00
483	17.844	23.434	-3.9383	90.00	-78.81	-90.00
484	17.506	21.628	-4.9438	90.00	-74.23	-90.00
485	5.9691	23.720	-17.752	90.00	-32.60	-90.00
486	5.6418	25.302	-17.287	90.00	-30.13	-90.00
487	4.1893	22.215	-17.781	90.00	-33.21	-90.00
488	5.8029	22.857	-17.538	90.00	-37.61	-90.00
489	7.6693	24.226	-16.496	90.00	-34.92	-90.00
510	8.7965	25.595	-15.953	90.00	-30.71	-90.00
511	9.5408	23.175	-13.487	90.00	-31.61	-90.00
512	7.0340	22.770	-16.775	90.00	-32.75	-90.00
513	8.8322	23.304	-16.258	90.00	-36.80	-90.00
514	9.1715	25.887	-15.789	90.00	-30.28	-90.00
515	10.084	21.864	-15.128	90.00	-33.47	-90.00
516	10.958	21.889	-14.535	90.00	-37.81	-90.00
517	11.784	21.626	-13.872	90.00	-40.30	-90.00
518	12.521	21.936	-13.195	90.00	-43.50	-90.00
519	13.199	21.932	-12.521	90.00	-46.50	-90.00

NODE	X	Y	Z	TOUT	TINT	TIME
620	13.906	22.810	-11.844	90.00	-49.37	-90.00
621	14.183	22.290	-11.389	90.00	-51.24	-90.00
622	14.310	21.631	-11.229	90.00	-51.88	-90.00
623	17.092	22.992	-6.4234	90.00	-60.99	-90.00
624	6.6492	21.575	-16.951	90.00	-21.44	-90.00
625	7.9581	21.897	-16.358	90.00	-24.88	-90.00
626	9.1344	21.008	-15.738	90.00	-30.14	-90.00
627	10.098	20.803	-15.158	90.00	-33.72	-90.00
628	11.038	21.032	-14.498	90.00	-37.35	-90.00
629	11.757	20.872	-13.838	90.00	-40.27	-90.00
630	12.831	20.879	-13.184	90.00	-43.54	-90.00
631	13.283	20.851	-12.428	90.00	-46.81	-90.00
632	15.530	20.946	-11.695	90.00	-49.98	-90.00
633	14.481	20.433	-7.5234	90.00	-66.24	-90.00
634	15.591	20.287	-9.5781	90.00	-58.99	-90.00
635	16.471	21.941	-7.7197	90.00	-64.89	-90.00
636	15.733	21.512	-9.1296	90.00	-58.87	-90.00
637	4.7010	20.289	-17.572	90.00	-14.98	-90.00
638	6.7079	20.805	-16.088	90.00	-21.64	-90.00
639	5.1199	21.194	-17.453	90.00	-14.35	-90.00

NODE	X	Y	Z	TOUT	TINT	TIME
640	9.3031	19.712	-19.851	90.00	-30.78	-90.00
641	11.283	19.923	-14.268	90.00	-38.34	-90.00
642	12.496	19.852	-13.219	90.00	-43.39	-90.00
643	13.470	19.642	-12.224	90.00	-47.78	-90.00
644	14.587	19.958	-11.326	90.00	-51.46	-90.00
645	14.708	20.791	-10.714	90.00	-53.61	-90.00
646	14.990	21.781	-10.385	90.00	-55.69	-90.00
647	15.354	22.612	-9.4278	90.00	-58.78	-90.00
648	15.777	23.543	-9.0533	90.00	-60.15	-90.00
649	16.034	24.128	-8.4268	90.00	-61.70	-90.00
650	16.328	24.372	-8.0145	90.00	-63.05	-90.00
651	16.887	25.317	-6.8368	90.00	-67.92	-90.00
652	16.621	25.718	-7.5982	90.00	-64.83	-90.00
653	16.245	22.888	-8.8843	90.00	-63.26	-90.00
654	16.180	23.326	-8.3114	90.00	-62.81	-90.00
655	14.268	23.725	-8.7385	90.00	-63.42	-90.00

LIST ALL MATERIALS PROPERTY= ALL

PROPERTY TABLE EN MAT= 1 MIN. POINTS= 2
 TEMPERATURE DATA TEMPERATURE DATA
 TYPPE= 0 0.27180E+08 9999.0 0.37180E+08
 TIME= 0.00000E+00 BILTER= 1
 UNIFORM TEMPERATURE= 0.000 (TREF= 0.000)
 PLASTIC CONVERG. CRITERION= 0.0100
 CREEP OPTIMUM. CRITERION= 0.0000
 LARGE DEFL. CONVERG. CRITERION= 0.001000
 DISPLACEMENT LIMIT= 0.00000E+00

NPRINT= 0900 APOST= 1 REACTION PRINT FREQ= 0900
 DISP. POST DATA FREQ= 1 REACT. POST DATA FREQ= 1

ELEMENT	PRINT	REP	POST	DATA	FREQUENCIES
TYPE	UNIT	STRESS	FORCE	STRESS	DATA
	NO.	PRINT	PRINT	DATA	LEVEL
		1	2	3	4
1	63	0900	0900	1	3

LOADS INPUT FILE= 26 LOADS OUTPUT FILE= 23

ALL ANALYSIS DATA WILL BE WRITTEN ONTO FILE? 7

LIST DISPLACEMENTS FOR ALL SELECTED NODES

NODE	LABEL	DISP	CDISP
182	UT	8.00000000E+00	0.00000000E+00
284	UT	8.00000000E+00	0.00000000E+00
300	UT	0.00000000E+00	0.00000000E+00
301	UT	8.00000000E+00	0.00000000E+00
302	UT	0.00000000E+00	0.00000000E+00
308	UT	0.00000000E+00	0.00000000E+00
304	UT	0.00000000E+00	0.00000000E+00
309	UT	0.00000000E+00	0.00000000E+00
344	RTZ	0.00000000E+00	0.00000000E+00
348	UT	0.00000000E+00	0.00000000E+00
363	MY	0.00000000E+00	0.00000000E+00
377	MY	0.00000000E+00	0.00000000E+00
378	MY	0.00000000E+00	0.00000000E+00
395	MY	0.00000000E+00	0.00000000E+00
516	MY	0.00000000E+00	0.00000000E+00
597	RTZ	0.00000000E+00	0.00000000E+00
540	MY	0.00000000E+00	0.00000000E+00
541	MY	0.00000000E+00	0.00000000E+00
542	UT	0.00000000E+00	0.00000000E+00
543	UT	0.00000000E+00	0.00000000E+00

NODE	LABEL	DISP	CDISP
544	UT	0.00000000E+00	0.00000000E+00
182	RTX	0.00000000E+00	0.00000000E+00
284	RTX	8.00000000E+00	0.00000000E+00
300	RTX	0.00000000E+00	0.00000000E+00
301	RTX	0.00000000E+00	0.00000000E+00
302	RTX	0.00000000E+00	0.00000000E+00
308	RTX	0.00000000E+00	0.00000000E+00
304	RTX	0.00000000E+00	0.00000000E+00
309	RTX	0.00000000E+00	0.00000000E+00
344	RTX	0.00000000E+00	0.00000000E+00
348	RTX	0.00000000E+00	0.00000000E+00
363	RTX	0.00000000E+00	0.00000000E+00
377	RTX	0.00000000E+00	0.00000000E+00
378	RTX	0.00000000E+00	0.00000000E+00
395	RTX	0.00000000E+00	0.00000000E+00
516	RTX	0.00000000E+00	0.00000000E+00
597	RTX	0.00000000E+00	0.00000000E+00
540	RTX	0.00000000E+00	0.00000000E+00
541	RTX	0.00000000E+00	0.00000000E+00
542	RTX	0.00000000E+00	0.00000000E+00

NODE	LABEL	DISP	CDISP
543	RTX	0.00000000E+00	0.00000000E+00
544	RTX	0.00000000E+00	0.00000000E+00
182	RTZ	0.00000000E+00	0.00000000E+00
284	RTZ	0.00000000E+00	0.00000000E+00
300	RTZ	0.00000000E+00	0.00000000E+00
301	RTZ	0.00000000E+00	0.00000000E+00
302	RTZ	0.00000000E+00	0.00000000E+00
308	RTZ	0.00000000E+00	0.00000000E+00
304	RTZ	0.00000000E+00	0.00000000E+00
309	RTZ	0.00000000E+00	0.00000000E+00
344	RTZ	0.00000000E+00	0.00000000E+00
348	RTZ	0.00000000E+00	0.00000000E+00
363	RTZ	0.00000000E+00	0.00000000E+00
377	RTZ	0.00000000E+00	0.00000000E+00
378	RTZ	0.00000000E+00	0.00000000E+00

NODE	LABEL	DISP	CDISP
528	RD1Z	0.00000000E+00	0.00000000E+00
529	RD1Z	0.00000000E+00	0.00000000E+00
534	RD1Z	0.00000000E+00	0.00000000E+00
535	WC	0.00000000E+00	0.00000000E+00
539	WY	0.00000000E+00	0.00000000E+00
539	WZ	0.00000000E+00	0.00000000E+00
539	RD1N	0.00000000E+00	0.00000000E+00
539	RD1Y	0.00000000E+00	0.00000000E+00
539	RD1Z	0.00000000E+00	0.00000000E+00
543	UN	0.00000000E+00	0.00000000E+00
543	UY	0.00000000E+00	0.00000000E+00
543	UZ	0.00000000E+00	0.00000000E+00
543	RD1X	0.00000000E+00	0.00000000E+00
543	RD1Y	0.00000000E+00	0.00000000E+00
543	RD1Z	0.00000000E+00	0.00000000E+00
544	UN	0.00000000E+00	0.00000000E+00
544	UY	0.00000000E+00	0.00000000E+00
544	UZ	0.00000000E+00	0.00000000E+00
544	RD1X	0.00000000E+00	0.00000000E+00
544	RD1Y	0.00000000E+00	0.00000000E+00

NODE	LABEL	DISP	CDISP
544	RD1Z	0.00000000E+00	0.00000000E+00
547	UN	0.00000000E+00	0.00000000E+00
547	UY	0.00000000E+00	0.00000000E+00
547	UZ	0.00000000E+00	0.00000000E+00
547	RD1X	0.00000000E+00	0.00000000E+00
547	RD1Y	0.00000000E+00	0.00000000E+00
547	RD1Z	0.00000000E+00	0.00000000E+00
548	WC	0.00000000E+00	0.00000000E+00
548	WY	0.00000000E+00	0.00000000E+00
548	WZ	0.00000000E+00	0.00000000E+00
548	RD1N	0.00000000E+00	0.00000000E+00
548	RD1Y	0.00000000E+00	0.00000000E+00
548	RD1Z	0.00000000E+00	0.00000000E+00
549	UN	0.00000000E+00	0.00000000E+00
549	UY	0.00000000E+00	0.00000000E+00
549	UZ	0.00000000E+00	0.00000000E+00
549	RD1N	0.00000000E+00	0.00000000E+00
549	RD1Y	0.00000000E+00	0.00000000E+00
549	RD1Z	0.00000000E+00	0.00000000E+00
550	WC	0.00000000E+00	0.00000000E+00

NODE	LABEL	DISP	CDISP
550	WY	0.00000000E+00	0.00000000E+00
550	WZ	0.00000000E+00	0.00000000E+00
550	RD1X	0.00000000E+00	0.00000000E+00
550	RD1Y	0.00000000E+00	0.00000000E+00
550	RD1Z	0.00000000E+00	0.00000000E+00
551	UX	0.00000000E+00	0.00000000E+00
551	UY	0.00000000E+00	0.00000000E+00
551	UZ	0.00000000E+00	0.00000000E+00
551	RD1X	0.00000000E+00	0.00000000E+00
551	RD1Y	0.00000000E+00	0.00000000E+00
551	RD1Z	0.00000000E+00	0.00000000E+00
552	UX	0.00000000E+00	0.00000000E+00
552	UY	0.00000000E+00	0.00000000E+00
552	UZ	0.00000000E+00	0.00000000E+00
552	RD1X	0.00000000E+00	0.00000000E+00
552	RD1Y	0.00000000E+00	0.00000000E+00
552	RD1Z	0.00000000E+00	0.00000000E+00
561	UX	0.00000000E+00	0.00000000E+00

LIST ELEMENT PREPARERS FOR ALL SELECTOR ELEMENTS

ELEM	FACE	VALUE(S)	FACE	NODES
283	1	0.00000000E+00	331	332 343 342
284	1	0.00000000E+00	332	333 344 343
285	1	0.00000000E+00	331	342 341 330
286	1	0.00000000E+00	333	273 283 344
287	1	0.00000000E+00	330	341 348 329
288	1	0.00000000E+00	342	343 352 251
289	1	0.00000000E+00	343	344 345 352

298	1	0.00000000E+00	0.00000000E+00	342	351	358	341
291	1	0.00000000E+00	0.00000000E+00	344	283	302	345
292	1	0.00000000E+00	0.00000000E+00	341	350	339	340
293	1	0.00000000E+00	0.00000000E+00	351	352	355	354
294	1	0.00000000E+00	0.00000000E+00	312	345	346	355
295	1	0.00000000E+00	0.00000000E+00	351	354	353	350
296	1	0.00000000E+00	0.00000000E+00	345	282	281	344
297	1	0.00000000E+00	0.00000000E+00	350	353	330	339
298	1	0.00000000E+00	0.00000000E+00	355	359	357	354
299	1	0.00000000E+00	0.00000000E+00	355	346	347	359
300	1	0.00000000E+00	0.00000000E+00	354	357	354	353
301	1	0.00000000E+00	0.00000000E+00	346	281	280	347
302	1	0.00000000E+00	0.00000000E+00	353	356	337	338

ELEM	FACE	VALUE(S)	FACE NUMBER
303	1	0.00000000E+00	337 329 340 360
304	1	0.00000000E+00	356 357 360 368
305	1	0.00000000E+00	359 347 348 349
306	1	0.00000000E+00	358 356 340 360
307	1	0.00000000E+00	347 280 279 340
308	1	0.00000000E+00	356 358 355 337
309	1	0.00000000E+00	360 348 349 358
310	1	0.00000000E+00	348 379 278 349
311	1	0.00000000E+00	358 349 331 354
312	1	0.00000000E+00	334 335 349 349
313	1	0.00000000E+00	349 278 277 334
314	1	0.00000000E+00	277 276 334 334
306	1	0.00000000E+00	535 197 196 524
307	1	0.00000000E+00	530 535 525 497
308	1	0.00000000E+00	536 198 197 538
309	1	0.00000000E+00	531 536 535 539
310	1	0.00000000E+00	337 199 198 536
311	1	0.00000000E+00	532 537 535 537
312	1	0.00000000E+00	358 280 197 537
313	1	0.00000000E+00	533 538 337 532

ELEM	FACE	VALUE(S)	FACE NUMBER
314	1	0.00000000E+00	534 194 280 538
318	1	0.00000000E+00	529 534 538 533
315	1	0.00000000E+00	351 343 346 364
316	1	0.00000000E+00	364 366 365 363
317	1	0.00000000E+00	363 362 367 366
318	1	0.00000000E+00	368 364 367 367
319	1	0.00000000E+00	365 368 285 276
320	1	0.00000000E+00	362 264 284 367
321	1	0.00000000E+00	368 367 284 285
472	1	0.00000000E+00	585 584 487 489
473	1	0.00000000E+00	586 585 489 490
474	1	0.00000000E+00	587 586 490 491
475	1	0.00000000E+00	588 587 491 492
476	1	0.00000000E+00	589 588 492 493
477	1	0.00000000E+00	590 589 493 494
478	1	0.00000000E+00	510 585 594 502
479	1	0.00000000E+00	511 510 585 504
480	1	0.00000000E+00	512 511 586 507
481	1	0.00000000E+00	513 512 587 508
482	1	0.00000000E+00	514 513 588 509

ELEM	FACE	VALUE(S)	FACE NUMBER
483	1	0.00000000E+00	486 514 589 495
484	1	0.00000000E+00	587 487 583 510
485	1	0.00000000E+00	581 582 518 511
486	1	0.00000000E+00	580 581 511 512
487	1	0.00000000E+00	499 580 512 513
488	1	0.00000000E+00	498 499 513 514
489	1	0.00000000E+00	494 499 514 506
490	1	0.00000000E+00	522 284 182 514
491	1	0.00000000E+00	517 522 516 522
492	1	0.00000000E+00	523 285 284 522
493	1	0.00000000E+00	518 523 522 517
484	1	0.00000000E+00	524 285 285 523
495	1	0.00000000E+00	519 524 523 518
496	1	0.00000000E+00	525 287 286 524
497	1	0.00000000E+00	526 525 524 519

496	1	0.00000000E+00	0.00000000E+00	521	201	207	525
499	1	0.00000000E+00	0.00000000E+00	487	521	525	520
500	1	0.00000000E+00	0.00000000E+00	527	202	201	521
501	1	0.00000000E+00	0.00000000E+00	504	527	521	487
502	1	0.00000000E+00	0.00000000E+00	528	203	202	527
ELN#	FACE	VALUE (\$)	VALUE (\$)	FACE NODES			
503	1	0.00000000E+00	0.00000000E+00	503	520	527	504
504	1	0.00000000E+00	0.00000000E+00	524	104	203	520
505	1	0.00000000E+00	0.00000000E+00	497	526	520	503
528	1	0.00000000E+00	0.00000000E+00	204	204	204	204
529	1	0.00000000E+00	0.00000000E+00	207	204	204	207
530	1	0.00000000E+00	0.00000000E+00	200	207	207	200
531	1	0.00000000E+00	0.00000000E+00	209	200	200	209
532	1	0.00000000E+00	0.00000000E+00	290	209	209	270
533	1	0.00000000E+00	0.00000000E+00	291	200	270	271
534	1	0.00000000E+00	0.00000000E+00	292	291	271	272
535	1	0.00000000E+00	0.00000000E+00	274	292	272	265
536	1	0.00000000E+00	0.00000000E+00	293	292	284	284
537	1	0.00000000E+00	0.00000000E+00	294	293	285	287
538	1	0.00000000E+00	0.00000000E+00	295	294	287	288
539	1	0.00000000E+00	0.00000000E+00	296	295	288	289
540	1	0.00000000E+00	0.00000000E+00	297	296	289	290
541	1	0.00000000E+00	0.00000000E+00	298	297	290	291
542	1	0.00000000E+00	0.00000000E+00	299	298	291	292
543	1	0.00000000E+00	0.00000000E+00	275	290	292	274
544	1	0.00000000E+00	0.00000000E+00	277	276	285	293
ELN#	FACE	VALUE (\$)	VALUE (\$)	FACE NODES			
545	1	0.00000000E+00	0.00000000E+00	278	277	293	294
546	1	0.00000000E+00	0.00000000E+00	279	278	294	295
547	1	0.00000000E+00	0.00000000E+00	280	279	295	296
548	1	0.00000000E+00	0.00000000E+00	281	280	296	297
549	1	0.00000000E+00	0.00000000E+00	282	281	297	298
550	1	0.00000000E+00	0.00000000E+00	283	282	298	299
551	1	0.00000000E+00	0.00000000E+00	273	283	299	274
552	1	0.00000000E+00	0.00000000E+00	285	284	296	286
553	1	0.00000000E+00	0.00000000E+00	282	285	311	311
554	1	0.00000000E+00	0.00000000E+00	283	284	313	312
555	1	0.00000000E+00	0.00000000E+00	281	282	311	310
556	1	0.00000000E+00	0.00000000E+00	280	281	310	309
557	1	0.00000000E+00	0.00000000E+00	284	285	314	313
558	1	0.00000000E+00	0.00000000E+00	285	284	267	314
559	1	0.00000000E+00	0.00000000E+00	326	312	313	313
560	1	0.00000000E+00	0.00000000E+00	312	326	323	311
561	1	0.00000000E+00	0.00000000E+00	314	267	328	313
562	1	0.00000000E+00	0.00000000E+00	313	528	325	326
563	1	0.00000000E+00	0.00000000E+00	323	326	311	311
564	1	0.00000000E+00	0.00000000E+00	311	328	317	310
ELN#	FACE	VALUE (\$)	VALUE (\$)	FACE NODES			
565	1	0.00000000E+00	0.00000000E+00	318	317	308	309
566	1	0.00000000E+00	0.00000000E+00	367	327	324	328
567	1	0.00000000E+00	0.00000000E+00	356	325	323	323
568	1	0.00000000E+00	0.00000000E+00	357	326	328	328
569	1	0.00000000E+00	0.00000000E+00	267	268	327	327
570	1	0.00000000E+00	0.00000000E+00	323	322	319	320
571	1	0.00000000E+00	0.00000000E+00	327	324	325	325
572	1	0.00000000E+00	0.00000000E+00	320	319	316	317
573	1	0.00000000E+00	0.00000000E+00	325	324	321	322
574	1	0.00000000E+00	0.00000000E+00	327	340	269	324
575	1	0.00000000E+00	0.00000000E+00	317	336	307	308
576	1	0.00000000E+00	0.00000000E+00	323	321	318	319
577	1	0.00000000E+00	0.00000000E+00	324	269	270	321
578	1	0.00000000E+00	0.00000000E+00	319	318	315	316
579	1	0.00000000E+00	0.00000000E+00	321	270	271	318
580	1	0.00000000E+00	0.00000000E+00	316	315	306	307
581	1	0.00000000E+00	0.00000000E+00	318	271	272	315
582	1	0.00000000E+00	0.00000000E+00	315	272	265	306
583	1	0.00000000E+00	0.00000000E+00	373	274	269	369
584	1	0.00000000E+00	0.00000000E+00	374	275	269	370

ELEM	FACE	VALUE(S)	FACE	MODES
324	1	0.00000000E+00	0.00000000E+00	302 374 370 201
325	1	0.00000000E+00	0.00000000E+00	375 273 274 373
326	1	0.00000000E+00	0.00000000E+00	374 375 373 374
327	1	0.00000000E+00	0.00000000E+00	303 376 374 202
328	1	0.00000000E+00	0.00000000E+00	371 375 295 375
329	1	0.00000000E+00	0.00000000E+00	372 371 375 376
330	1	0.00000000E+00	0.00000000E+00	194 372 376 203
331	1	0.00000000E+00	0.00000000E+00	379 309 300 377
332	1	0.00000000E+00	0.00000000E+00	300 379 377 378
333	1	0.00000000E+00	0.00000000E+00	204 380 378 182
334	1	0.00000000E+00	0.00000000E+00	381 380 309 379
335	1	0.00000000E+00	0.00000000E+00	382 381 379 380
336	1	0.00000000E+00	0.00000000E+00	205 382 380 204
337	1	0.00000000E+00	0.00000000E+00	383 382 308 381
338	1	0.00000000E+00	0.00000000E+00	384 383 381 382
339	1	0.00000000E+00	0.00000000E+00	384 384 382 383
340	1	0.00000000E+00	0.00000000E+00	385 384 383 384
341	1	0.00000000E+00	0.00000000E+00	385 385 384 385
342	1	0.00000000E+00	0.00000000E+00	387 386 384 386
343	1	0.00000000E+00	0.00000000E+00	389 389 386 388

ELEM	FACE	VALUE(S)	FACE	MODES
344	1	0.00000000E+00	0.00000000E+00	370 389 385 386
345	1	0.00000000E+00	0.00000000E+00	281 378 386 207
346	1	0.00000000E+00	0.00000000E+00	389 333 373 371
347	1	0.00000000E+00	0.00000000E+00	390 389 371 372
348	1	0.00000000E+00	0.00000000E+00	197 390 372 196
349	1	0.00000000E+00	0.00000000E+00	391 332 333 389
350	1	0.00000000E+00	0.00000000E+00	392 391 389 390
351	1	0.00000000E+00	0.00000000E+00	198 392 390 197
352	1	0.00000000E+00	0.00000000E+00	393 331 332 391
353	1	0.00000000E+00	0.00000000E+00	394 393 391 392
354	1	0.00000000E+00	0.00000000E+00	399 394 392 198
355	1	0.00000000E+00	0.00000000E+00	395 330 331 393
356	1	0.00000000E+00	0.00000000E+00	396 393 393 394
357	1	0.00000000E+00	0.00000000E+00	206 394 393 399
358	1	0.00000000E+00	0.00000000E+00	397 394 393 395
359	1	0.00000000E+00	0.00000000E+00	388 387 389 386
360	1	0.00000000E+00	0.00000000E+00	194 388 396 200
361	1	0.00000000E+00	0.00000000E+00	390 351 383 341
362	1	0.00000000E+00	0.00000000E+00	349 350 381 380
363	1	0.00000000E+00	0.00000000E+00	391 352 383 382

ELEM	FACE	VALUE(S)	FACE	MODES
519	1	0.00000000E+00	0.00000000E+00	548 549 580 579
520	1	0.00000000E+00	0.00000000E+00	547 548 379 378
521	1	0.00000000E+00	0.00000000E+00	546 547 578 562
522	1	0.00000000E+00	0.00000000E+00	552 543 587 563
523	1	0.00000000E+00	0.00000000E+00	539 544 562 544
524	1	0.00000000E+00	0.00000000E+00	579 580 643 643
525	1	0.00000000E+00	0.00000000E+00	581 582 680 640
526	1	0.00000000E+00	0.00000000E+00	581 642 641 590
527	1	0.00000000E+00	0.00000000E+00	582 643 687 688
528	1	0.00000000E+00	0.00000000E+00	580 642 643 642
529	1	0.00000000E+00	0.00000000E+00	580 641 642 642
530	1	0.00000000E+00	0.00000000E+00	578 679 684 633
531	1	0.00000000E+00	0.00000000E+00	579 643 644 644
532	1	0.00000000E+00	0.00000000E+00	578 683 684 682
533	1	0.00000000E+00	0.00000000E+00	579 644 645 634
534	1	0.00000000E+00	0.00000000E+00	563 564 637 637
535	1	0.00000000E+00	0.00000000E+00	637 641 640 640
536	1	0.00000000E+00	0.00000000E+00	563 557 384 384
537	1	0.00000000E+00	0.00000000E+00	625 640 638 638
538	1	0.00000000E+00	0.00000000E+00	643 642 630 631

ELEM	FACE	VALUE(S)	FACE	MODES
539	1	0.00000000E+00	0.00000000E+00	643 631 633 644
540	1	0.00000000E+00	0.00000000E+00	544 562 561 543
541	1	0.00000000E+00	0.00000000E+00	642 641 689 630
542	1	0.00000000E+00	0.00000000E+00	637 638 638 638
543	1	0.00000000E+00	0.00000000E+00	634 637 641 640
544	1	0.00000000E+00	0.00000000E+00	637 638 641 641
545	1	0.00000000E+00	0.00000000E+00	625 636 640 640

544	1	0.00000000E+00	0.00000000E+00	428	427	641	641
547	1	0.00000000E+00	0.00000000E+00	444	432	622	645
548	1	0.00000000E+00	0.00000000E+00	424	429	630	630
549	1	0.00000000E+00	0.00000000E+00	434	434	635	633
550	1	0.00000000E+00	0.00000000E+00	434	424	644	636
551	1	0.00000000E+00	0.00000000E+00	438	430	608	634
552	1	0.00000000E+00	0.00000000E+00	437	564	607	639
553	1	0.00000000E+00	0.00000000E+00	432	444	645	643
554	1	0.00000000E+00	0.00000000E+00	431	430	610	639
555	1	0.00000000E+00	0.00000000E+00	427	415	614	628
556	1	0.00000000E+00	0.00000000E+00	427	424	614	615
557	1	0.00000000E+00	0.00000000E+00	430	429	617	618
558	1	0.00000000E+00	0.00000000E+00	431	419	620	632

ELER	FACE	VALUE(S)	FACE NODES				
559	1	0.00000000E+00	0.00000000E+00	429	628	616	617
560	1	0.00000000E+00	0.00000000E+00	562	604	603	561
561	1	0.00000000E+00	0.00000000E+00	426	425	613	614
562	1	0.00000000E+00	0.00000000E+00	632	620	621	622
563	1	0.00000000E+00	0.00000000E+00	433	435	623	604
564	1	0.00000000E+00	0.00000000E+00	439	407	600	600
565	1	0.00000000E+00	0.00000000E+00	421	424	612	613
566	1	0.00000000E+00	0.00000000E+00	454	464	647	647
567	1	0.00000000E+00	0.00000000E+00	422	421	594	644
568	1	0.00000000E+00	0.00000000E+00	434	467	453	635
569	1	0.00000000E+00	0.00000000E+00	416	415	601	635
570	1	0.00000000E+00	0.00000000E+00	424	406	404	612
571	1	0.00000000E+00	0.00000000E+00	416	573	404	617
572	1	0.00000000E+00	0.00000000E+00	615	614	611	601
573	1	0.00000000E+00	0.00000000E+00	418	417	494	404
574	1	0.00000000E+00	0.00000000E+00	619	618	494	495
575	1	0.00000000E+00	0.00000000E+00	619	498	480	620
576	1	0.00000000E+00	0.00000000E+00	646	594	592	647
577	1	0.00000000E+00	0.00000000E+00	420	406	593	621
578	1	0.00000000E+00	0.00000000E+00	621	593	594	594

ELER	FACE	VALUE(S)	FACE NODES				
579	1	0.00000000E+00	0.00000000E+00	414	413	610	611
580	1	0.00000000E+00	0.00000000E+00	406	407	400	606
581	1	0.00000000E+00	0.00000000E+00	435	453	652	625
582	1	0.00000000E+00	0.00000000E+00	544	545	605	607
583	1	0.00000000E+00	0.00000000E+00	544	534	555	565
584	1	0.00000000E+00	0.00000000E+00	594	593	591	592
585	1	0.00000000E+00	0.00000000E+00	447	446	454	653
586	1	0.00000000E+00	0.00000000E+00	543	541	540	542
587	1	0.00000000E+00	0.00000000E+00	403	540	541	541
588	1	0.00000000E+00	0.00000000E+00	404	403	402	603
589	1	0.00000000E+00	0.00000000E+00	611	400	601	601
590	1	0.00000000E+00	0.00000000E+00	613	612	609	610
591	1	0.00000000E+00	0.00000000E+00	452	453	454	654
592	1	0.00000000E+00	0.00000000E+00	401	400	572	573
593	1	0.00000000E+00	0.00000000E+00	447	592	590	640
594	1	0.00000000E+00	0.00000000E+00	593	495	495	591
595	1	0.00000000E+00	0.00000000E+00	373	372	490	494
596	1	0.00000000E+00	0.00000000E+00	652	654	653	653
597	1	0.00000000E+00	0.00000000E+00	611	1	590	600
598	1	0.00000000E+00	0.00000000E+00	454	448	649	655

ELER	FACE	VALUE(S)	FACE NODES				
599	1	0.00000000E+00	0.00000000E+00	412	406	594	400
600	1	0.00000000E+00	0.00000000E+00	592	591	589	590
601	1	0.00000000E+00	0.00000000E+00	611	610	590	590
602	1	0.00000000E+00	0.00000000E+00	450	452	655	655
603	1	0.00000000E+00	0.00000000E+00	400	599	571	572
604	1	0.00000000E+00	0.00000000E+00	448	500	580	640
605	1	0.00000000E+00	0.00000000E+00	449	450	655	655
606	1	0.00000000E+00	0.00000000E+00	423	452	651	602
607	1	0.00000000E+00	0.00000000E+00	591	493	492	589
608	1	0.00000000E+00	0.00000000E+00	406	405	595	594
609	1	0.00000000E+00	0.00000000E+00	572	571	499	490
610	1	0.00000000E+00	0.00000000E+00	410	409	597	594
611	1	0.00000000E+00	0.00000000E+00	621	452	650	650
612	1	0.00000000E+00	0.00000000E+00	402	402	590	580
613	1	0.00000000E+00	0.00000000E+00	590	589	587	588

616	1	0.00000000E+00	0.00000000E+00	402	565	566	595
615	1	0.00000000E+00	0.00000000E+00	199	596	570	571
616	1	0.00000000E+00	0.00000000E+00	449	588	586	650
617	1	0.00000000E+00	0.00000000E+00	545	555	554	544
618	1	0.00000000E+00	0.00000000E+00	186	651	650	650
ELEM	FACE	VALUE (\$)		FACE NODES			
619	1	0.00000000E+00	0.00000000E+00	568	559	561	562
620	1	0.00000000E+00	0.00000000E+00	389	482	481	587
621	1	0.00000000E+00	0.00000000E+00	571	578	590	499
622	1	0.00000000E+00	0.00000000E+00	689	596	586	597
623	1	0.00000000E+00	0.00000000E+00	578	597	549	578
624	1	0.00000000E+00	0.00000000E+00	365	587	585	585
625	1	0.00000000E+00	0.00000000E+00	651	576	682	682
626	1	0.00000000E+00	0.00000000E+00	596	595	585	586
627	1	0.00000000E+00	0.00000000E+00	692	578	577	559
628	1	0.00000000E+00	0.00000000E+00	370	569	561	560
629	1	0.00000000E+00	0.00000000E+00	187	491	490	583
630	1	0.00000000E+00	0.00000000E+00	651	586	575	575
631	1	0.00000000E+00	0.00000000E+00	598	366	367	583
632	1	0.00000000E+00	0.00000000E+00	587	584	568	569
633	1	0.00000000E+00	0.00000000E+00	386	383	574	575
634	1	0.00000000E+00	0.00000000E+00	566	554	553	547
635	1	0.00000000E+00	0.00000000E+00	559	558	548	541
636	1	0.00000000E+00	0.00000000E+00	569	548	562	501
637	1	0.00000000E+00	0.00000000E+00	380	498	489	576
638	1	0.00000000E+00	0.00000000E+00	559	577	517	558
ELEM	FACE	VALUE (\$)		FACE NODES			
639	1	0.00000000E+00	0.00000000E+00	584	585	532	551
640	1	0.00000000E+00	0.00000000E+00	576	575	519	518
641	1	0.00000000E+00	0.00000000E+00	576	518	517	577
642	1	0.00000000E+00	0.00000000E+00	586	573	530	560
643	1	0.00000000E+00	0.00000000E+00	583	567	533	532
644	1	0.00000000E+00	0.00000000E+00	575	576	520	519
645	1	0.00000000E+00	0.00000000E+00	567	553	529	533
646	1	0.00000000E+00	0.00000000E+00	555	517	515	540
647	1	0.00000000E+00	0.00000000E+00	368	310	497	582
648	1	0.00000000E+00	0.00000000E+00	574	489	487	520
228	2	319.633248	0.00000000E+00	286	284	264	266
229	2	319.633248	0.00000000E+00	267	266	266	267
230	2	319.633248	0.00000000E+00	288	287	267	266
231	2	319.633248	0.00000000E+00	289	288	268	269
232	2	319.633248	0.00000000E+00	290	289	269	270
233	2	319.633248	0.00000000E+00	291	290	270	271
234	2	319.633248	0.00000000E+00	292	291	271	272
235	2	319.633248	0.00000000E+00	274	292	272	265
236	2	319.633248	0.00000000E+00	293	293	286	286
237	2	319.633248	0.00000000E+00	294	293	286	287
ELEM	FACE	VALUE (\$)		FACE NODES			
238	2	319.633248	0.00000000E+00	295	294	287	288
239	2	319.633248	0.00000000E+00	296	295	288	289
240	2	319.633248	0.00000000E+00	297	296	289	290
241	2	319.633248	0.00000000E+00	298	297	290	291
242	2	319.633248	0.00000000E+00	299	298	291	292
243	2	319.633248	0.00000000E+00	275	299	292	274
244	2	319.633248	0.00000000E+00	277	276	285	293
245	2	319.633248	0.00000000E+00	278	277	295	294
246	2	319.633248	0.00000000E+00	279	278	296	295
247	2	319.633248	0.00000000E+00	280	279	295	294
248	2	319.633248	0.00000000E+00	281	280	296	297
249	2	319.633248	0.00000000E+00	282	281	297	298
250	2	319.633248	0.00000000E+00	283	282	298	299
251	2	319.633248	0.00000000E+00	273	283	299	275
315	2	319.633248	0.00000000E+00	361	363	368	364
316	2	319.633248	0.00000000E+00	366	366	365	365
317	2	319.633248	0.00000000E+00	363	362	367	366
318	2	319.633248	0.00000000E+00	368	366	367	367
319	2	319.633248	0.00000000E+00	365	368	285	276
320	2	319.633248	0.00000000E+00	362	364	284	367

ELM	FACE	VALUE(S)		FACE	VALUES		
321	2	319.633268	0.00000000E+00	365	367	284	283
322	2	3111.13113	0.00000000E+00	373	274	265	369
323	2	3111.13115	0.00000000E+00	374	373	389	370
324	2	3111.13115	0.00000000E+00	202	374	370	291
325	2	3111.13115	0.00000000E+00	375	275	274	373
326	2	3111.13113	0.00000000E+00	376	273	373	374
327	2	3111.13115	0.00000000E+00	203	376	374	362
328	2	3111.13113	0.00000000E+00	371	273	273	375
329	2	3111.13115	0.00000000E+00	372	371	375	376
330	2	3111.13113	0.00000000E+00	196	373	376	285

LIST ELEMENT CONNECTIONS FOR ALL SELECTED ELEMENTS

LIST SOLID MODEL BOUNDARY CONDITIONS (LABEL = APEF)
ON ALL SELECTED AREAS

AREA	PRESSURE	SIXON	SIXIN	SIXRO	SLOPE
1	0.000E+00	0	0	0.000E+00	0.000E+00
2	0.000E+00	0	0	0.000E+00	0.000E+00
3	0.000E+00	0	0	0.000E+00	0.000E+00
4	0.000E+00	0	0	0.000E+00	0.000E+00
7	0.000E+00	0	0	0.000E+00	0.000E+00
8	0.000E+00	0	0	0.000E+00	0.000E+00
9	0.000E+00	0	0	0.000E+00	0.000E+00
10	0.000E+00	0	0	0.000E+00	0.000E+00
11	0.000E+00	0	0	0.000E+00	0.000E+00
12	0.000E+00	0	0	0.000E+00	0.000E+00
13	0.000E+00	0	0	0.000E+00	0.000E+00
14	0.000E+00	0	0	0.000E+00	0.000E+00

LIST SOLID MODEL BOUNDARY CONDITIONS (LABEL = ACVF)
ON ALL SELECTED AREAS

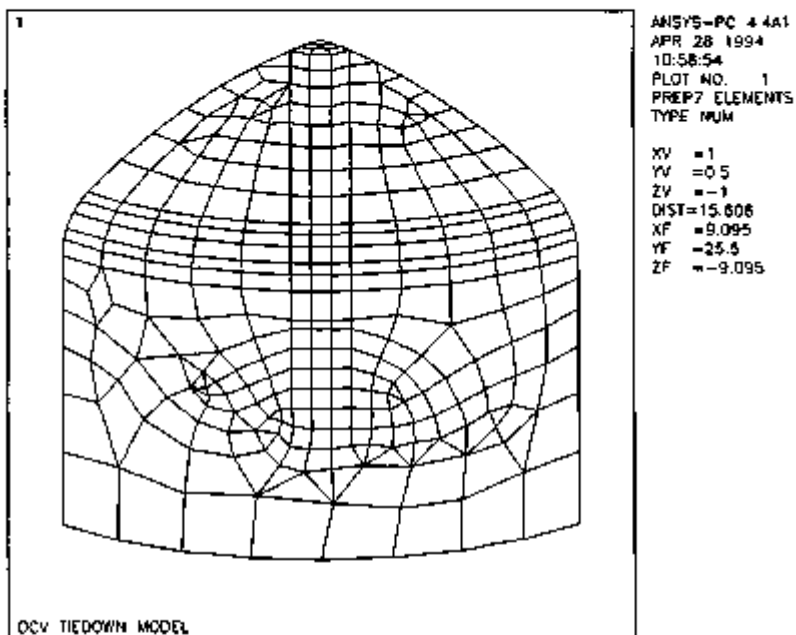


FIGURE 2.10.5-1.

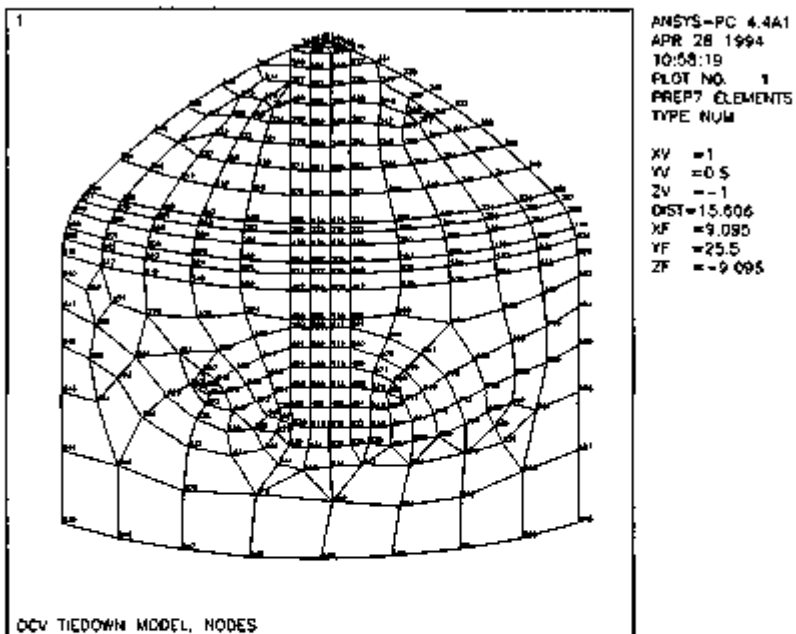


FIGURE 2.10.5-2.

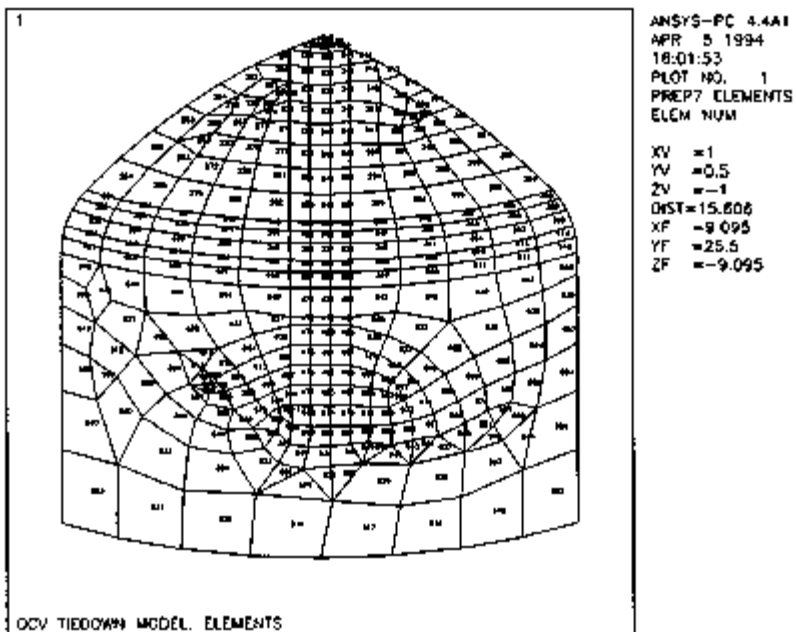


FIGURE 2.10.6-3.

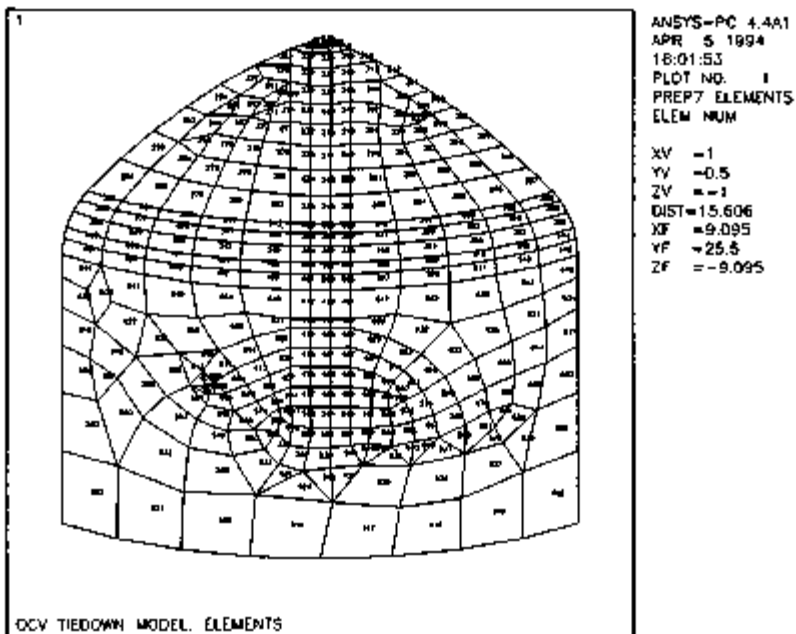


FIGURE 2.10.5-4.

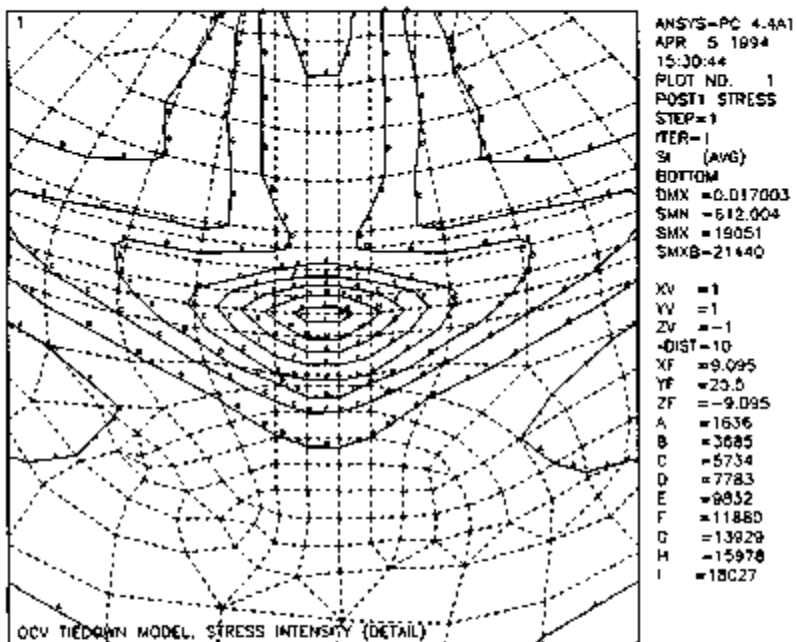


FIGURE 2.10.5-5.

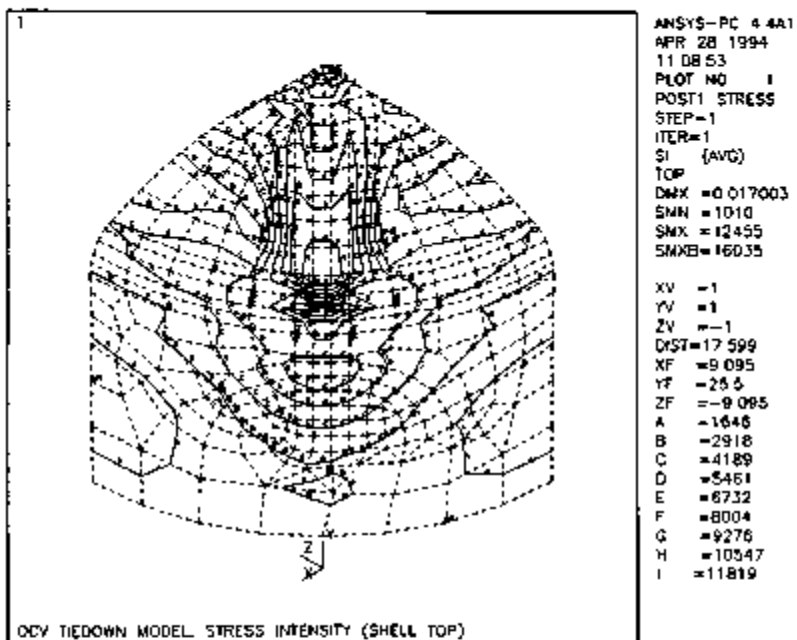


FIGURE 2.10.5-9.

2.10.6 Elastomer O-ring Performance Test Data

Radioisotope Thermoelectric Generator Transportation System Packaging O-Ring Material Thermal Validation Test Report

1.0 INTRODUCTION

The Radioisotope Thermoelectric Generator (RTG) Transportation System packaging uses elastomeric O-rings for the primary containment boundary seals. These O-rings are required to maintain leaktight containment (i.e., part of an integrated leakage rate of less than 1.0×10^{-7} acc/sec, air) under normal conditions of transport (NCT) and hypothetical accident conditions (HAC), as set forth in 10 CFR 71. (The foregoing definition of the term "leaktight" is assumed in the balance of this report.) The tests described herein were performed to demonstrate the ability of the elastomer material to perform adequately under the conditions of compression, temperature, and time at temperature that are predicted to occur in the RTG packaging under both NCT and HAC.

2.0 PURPOSE

These tests were performed to demonstrate the ability of the elastomer material to provide a leaktight seal under specific conditions of compression, temperature, and time at temperature. The material used in the tests, Butyl compound RR0405-70, manufactured by Rainier Rubber of Seattle, Washington, is identical to that used in the full-scale packaging seals.

3.0 TEST DESCRIPTION

Sample O-rings made of the subject Butyl material were tested in a test fixture constructed to test four different compressions during one sequence. The fixture consists of an inner plate with three concentric O-ring grooves of different depths on each side. Each side is then assembled by bolting a circular plate on each side with shims between each side plate and the inner plate sized to give the desired compression on the O-rings (see 4.1, Discussion of Compression Ranges). The outer O-rings have a higher compression and the center O-rings are in place to allow the inner/outer O-rings to be tested. The center O-rings have a considerably higher compression (21%) to assure sealing under all conditions. All O-rings had a nominal cross-section diameter of 0.275 in. Leakage rate testing was performed on the spaces between the outer/center and inner/center O-rings via ports through the outer plates. The fixture was placed within an environmental test chamber and brought to uniform temperatures for specified times. The test consisted of an initial low temperature segment at -40 °F, followed by a 360 °F segment for 24 hours, then continuing at 350 °F for 144 hours, followed by a final low-temperature segment at -20 °F. Upon initial assembly and the end of each low-temperature segment, the O-rings were tested for leaktight conditions using standard helium mass spectrometer leakage rate testing equipment. At the end of each high-temperature segment, a vacuum test was performed using the mass spectrometer to achieve a pressure low enough to perform a test (less than 0.2 mbar). Details are given in the following section.

4.0 TEST PARAMETERS

This section will discuss the calculation of O-ring specimen compression in the fixture, followed by test temperature/time specifications.

4.1 DISCUSSION OF COMPRESSION RANGES

With the O-rings installed in the accommodation grooves of the center plate, the compression condition is a function of the space available for the cross-section to occupy. This space is controlled by the depth of the groove and the shims installed. Shims are installed inboard and outboard of the three concentric grooves between each of eight bolts on each side.

The test fixture is shown on Packaging Technology, Inc. (PacTec) drawing D-AA-314. The fixture dimensions are listed in Table 4.1-1.

Table 4.1-1. Test Fixture Dimensions.

Feature	Dimension (in.) left side*	Dimension (in.) right side*
Outer O-ring groove depth (x)	.2053	.2075
Center O-ring groove depth (y)	.175	.175
Inner O-ring groove depth (z)	.200	.2033
Shim thickness (t L, R) (t)	.044	.031
Average outer O-ring cross-section (Dmo)	.2770	.2776
Average center O-ring cross-section (Dmc)	.2772	.2773
Average inner O-ring cross-section (Dmi)	.2773	.2774

* Left and right sides are delineated by the installation into the environmental chamber viewed facing the unit door.

The values of compression in the test fixture will now be calculated. The space available for the O-ring to occupy is equal to the sum of the groove depth plus the shim thickness, or (x) or (Z) to (t).

The compression of the outer O-ring is then

$$C_1 = \frac{D_{out} - [x + t]}{D_{ms}} \quad] = \text{Left, Right}$$

for the left side, outer O-ring:

$$X_{ms} = .2053$$

$$D_{mo}(\text{left}) = .2770$$

$$C_{out} = .044$$

$$C_{compression} = \frac{2770 - (2063 \cdot .044)}{2770}$$

$$= .10 (10\%)$$

Using the same method as described above, the compression values for a completely full test fixture are listed in Table 4.1-2.

Table 4.1-2. Compression Values (%).

Location	Left	Right
Outer	10%	14%
Center	21%	21%
Inner	12%	15.5%

4.2 TEST CONDITIONS

Before being subjected to test conditions, the fixture was assembled with the proper O-ring and the center and outer seals. (The inner O-rings were not available at this time.) This pair of specimens, at compressions of 10% (left side) and 14% (right side) was tested at the temperatures and time durations shown in Table 4.2-1.

Table 4.2-1. Temperature/Time Segment Test Parameters.

Test Segment	Temperature (°F)	Time duration (hr)	Test Type
Initial assembly	Ambient	Immediate upon assembly	Helium
Low-temperature (1)	-40	Immediate upon stabilization	Helium
High-temperature (1)	380	24	High vacuum*
High-temperature (2)	380	144	High vacuum*
Low-temperature (2)	-20	Immediate upon stabilization	Helium

*Less than 0.2 mbar.

5.0 EQUIPMENT

5.1 TEST HARDWARE AND EQUIPMENT

The fixture used for the O-ring testing is shown in PacTec drawing D-AA-314. The test was conducted in an environmental test chamber capable of accommodating the fixture, cooling it to -40 °F, and warming it to 380 °F. Helium-based leakage rate test equipment with a minimum sensitivity of 2×10^{-9} acc/sec. was used to establish O-ring leakage rates at temperatures throughout the test range.

6.2 TEST SPECIMEN

The O-ring test specimens were made from Rainier Rubber Butyl compound RR0405-70. The O-ring cross-sectional diameter was nominally 0.275 in. The cross-sectional diameter was measured in 4 quadrants before and after testing. Each O-ring test specimen contained at least one production-quality splice. Actual dimensions for each O-ring test specimen are given in Table 4.1-1. As inner O-rings were not available at the time of the test, only outer O-rings (10% and 14% compression) were installed.

6.3 LEAKAGE MEASUREMENT

Leakage rate test equipment, equipment operational calibration, and connection to the test fixture was the responsibility of Nondestructive Examination (NDE) technicians. Leakage rate tests were performed in accordance with WHC-CM-4-38, Nondestructive Examination Procedures, NDT-LT-8000, Appendix A and the Helium Mass Spectrometer Test - Tracer Probe and Hood Techniques method described in the American Society of Mechanical Engineers (ASME) Boiler and Pressure Vessel Code, Section V, Article 10, Appendix V.

6.4 TEMPERATURE MEASUREMENT

Temperature measurement data was recorded and printed using a six-thermocouple data logger system.

6.5 HEATING AND COOLING

An electric resistance, heated oven was used for heating and cooling the test fixture. Bottled CO₂ gas was used for the cooling function.

6.0 RESULTS

Detailed test results are provided in Reference 1. The test results are summarized in Table 6-1. The specimens were leakage rate tested against an acceptance criteria of 1×10^{-7} sec/sec (slr). All O-ring tests were satisfactory and the O-rings did not show any sign of failure over the entire test sequence.

Table 6-1. Summary of Test Results.

O-ring	Compression (%)	Test Temperature	Leaktight per criteria?
Left (outer)	10	-40 °F then 380 °F for 8 hr. then 350 °F for 144 hr. then -20 °F	Yes
Right (outer)	14		Yes

Subsequent to testing, minor changes in durometer were noted, and the O-rings took a compression set, as shown by the post-test cross-sectional diameter measurements of Table 6-2. These changes had no apparent effect on the ability of the O-ring to maintain leaktight integrity for

the range of temperatures and durations tested.

Table 6-2. O-ring Specimen Measurement Data.

O-ring Location	Measurement Sequence B: before test A: after test	Cross-sectional Diameter Axial Direction (in.)	O-ring Inside Diameter (in.)	Hardness (durometer)
Left (outer)	B	.2770	12.98	67
Left (outer)	A	.2380	12.71	66
Right (outer)	B	.2776	12.98	68
Right (outer)	A	.2500	12.70	64

7.0 CONCLUSIONS

The Butyl O-ring material to be used in the RTG Transportation System Packaging has been demonstrated to be satisfactory at compression values as low as 10% and at the temperatures and durations listed in Table 6-1, including pre-test segments at -40 °F, and post-test segments at -20 °F.

8.0 REFERENCES

1. *Radioisotope Thermoelectric Generator Transportation System Packaging O-ring Material Thermal Validation Test Report for Face Seal Test Fixture, WHC-SD-RTG-TRP-010.*

2.10.7 Summary of Thermal Load Cases and Results

This appendix summarizes key temperature results from Sections 3.6.4 and 3.6.5 for use in Chapter 2.0 and 4.0. Nodes are identified in Figures 3.4.1-2, details A through D.

2.10.7.1 Normal Conditions of Transport.

TABLE 2.10.7.1-1. Regulatory NCT and Operational Conditions Load Cases.

Condition	Case 1	Case 2	Case 3
Solar	Full solar	No solar	Full solar
Ambient temperature	100 °F	-40 °F	100 °F
Payload	Maximum heat	Maximum heat	Maximum heat
Cooling	No active cooling	No active cooling	Active cooling (both loops)

TABLE 2.10.7.1-2. Regulatory Normal Conditions of Transport Load Case 1 Results.

Package component	Model node number	Temperature °F
Ambient air	1	100
OCV top	300 / 304	267 / 237
Coolant jacket	326	238
OCV sidewall	320	284
OCV base	360	220
ICV top	200 / 204	338 / 308
ICV sidewall	220	329
ICV base	261	222
OCV main seals	350	210
ICV main seals	250	219
OCV fin	305	158
Impact limiter shell	406 / 408 / 410	153 / 123 / 132
Impact limiter foam	421 / 455	203 / 128

TABLE 2.10.7.1-3. Regulatory Normal Conditions of Transport Load Case 2 Results.

Package component	Model node number	Temperature °F
Ambient air	1	-40
OCV top	300 / 304	148 / 105
Coolant jacket	328	115
OCV sidewall	320	165
OCV base	360	74
ICV top	200 / 204	245 / 203
ICV sidewall	220	220
ICV base	261	76
OCV main seals	350	61
ICV main seals	250	73
ICV fin	305	12
Impact limiter shell	406 / 408 / 410	-13 / -34 / -23
Impact limiter foam	421 / 455	65 / -28

TABLE 2.10.7.1-4. Operational Conditions Load Case 3 Results.

Package component	Model node number	Temperature °F
Ambient air	1	100
Coolant fluid	901	40
OCV top	300 / 304	222 / 178
Coolant jacket	328	46
OCV sidewall	320	59
OCV base	360	67
ICV top	200 / 204	275 / 231
ICV sidewall	220	134
ICV base	261	67
OCV main seals	350	85
ICV main seals	250	83
OCV fin	305	135
Impact limiter shell	406 / 408 / 410	122 / 119 / 116
Impact limiter foam	421 / 455	91 / 117

TABLE 2 10 7 1 5 Summary of NCT Gas Temperatures

Condition	Case 1 full solar 100 °F ambient no cooling	Case 2 no solar -40 °F ambient no cooling	Case 3 full solar 100 °F ambient active cooling
ICV internal gas temperature (°F)	364	266	213
OCV internal gas temperature (°F)	285	165	115

TABLE 2 10 7 1-6 Summary of NCT Gas Pressures
(excluding payload gas generation)

Condition	Case 1 full solar 100 °F ambient no cooling	Case 2 no solar -40 °F ambient no cooling	Case 3 full solar 100 °F ambient active cooling
ICV internal gas temperature (psia)	24.4	21.5	20.2
OCV internal gas temperature (psia)	26.3	22.1	20.3

2.10.7.2 Hypothetical Accident Conditions.

TABLE 2.10.7.2-1. Load Cases for the Hypothetical Accident Condition Analyses.

Case	Pre-hypothetical accident conditions	Post-hypothetical accident conditions
1	<p>a. Undamaged payload, 4,500 W maximum decay heat load.</p> <p>b. Undamaged package, upright position, adiabatic bottom conditions.</p> <p>c. Cooling jacket drained</p> <p>d. Steady state conditions with 100 °F still air; no solar.</p>	<p>a. Circumferential distribution of heat-source modules on barrier plate, 4,500 W total.</p> <p>b. Side drop impact limiter damage; package upright, all surfaces exposed to ambient.</p> <p>c. Cooling jacket drained.</p> <p>d. 1475 °F fire for 30 minutes, followed by ambient air at 100 °F; no solar during and after fire.</p>
2	<p>Same as load case No. 1 except:</p> <p>d. Steady state conditions with -20 °F still air; no solar.</p>	<p>Same as load case No. 1 except:</p> <p>d. 1475 °F fire for 30 minutes, followed by ambient air at -20 °F; no solar during and after fire.</p>
3	<p>Same as load case No. 1.</p>	<p>Same as load case No. 1, except:</p> <p>a. Axial distribution of heat-source modules along ICV wall above rubble dam; 4,500 W total</p> <p>b. Side drop impact limiter damage; package on its side, all surfaces exposed.</p>
4	<p>Same as load case No. 2.</p>	<p>Same as load case No. 3, except:</p> <p>d. 1475 °F fire for 30 minutes, followed by ambient air at -20 °F; no solar during and after fire.</p>
5	<p>Same as load case No. 1.</p>	<p>Same as load case No. 1, except:</p> <p>a. Ungula shaped rubble pile of heat source modules on barrier plate; 4,500 W total.</p> <p>b. Side drop impact limiter damage; package at 45° angle of repose, all surfaces exposed.</p>
6	<p>Same as load case No. 2.</p>	<p>Same as load case No. 5, except:</p> <p>d. 1475 °F fire for 30 minutes, followed by ambient air at -20 °F; no solar during and after fire.</p>

TABLE 2.10.7.2-2. Summary of HAC Peak Temperatures.

Condition	Case 1	Case 2	Case 3	Case 4	Case 5	Case 6
ICV internal gas temperature (°F)	836	779	747	684	840	782
OCV internal gas temperature (°F)	848	790	851	798	852	789

TABLE 2.10.7.2-3. Summary of HAC Pressures (excluding gas generation).

Condition	Case 1	Case 2	Case 3	Case 4	Case 5	Case 6
ICV internal gas pressure (psia)	38.9	37.2	36.2	34.3	39.0	37.3
OCV internal gas pressure (psia)	45.2	44.3	46.2	44.4	46.3	44.4

2.10.8 OCV Two-Dimensional (Axisymmetric) ANSYS Model

2.10.8.1 Description. The 2-D, OCV model is an axisymmetric finite element model of the entire OCV. It consists of a base and a bell, connected by a bolt element and flange interface gap elements. It is used to evaluate containment vessel stresses and closure bolt stresses under NCT and closure bolt stresses and residual O-ring compression under HAC. Further use of the model is made to determine stresses in the torispherical head under NCT compression loads. The containment bell, the bolting flange, the thermal shield, and the coolant jacket are fully modeled. The fins, which are only significant to lifting analyses, are not modeled. The shutdown strap doublers, which are only significant to the shutdown analysis, are also not included. The applied loading takes the form of internal gas pressure, nodal temperatures, and initial closure bolt pre-load. Certain node locations were chosen to coincide with the nodes found in the SINDA thermal models described in Section 3. The relative displacement of two coincident nodes, one belonging to the OCV base structure and one to the bell at the location of the containment O-ring, are used to determine the change in O-ring compression because of the applied conditions. The model layout is shown in Figure 2.10.8-1. The model is used for the OCV analysis for the NCT load cases given in Table 2.6.1.3-1, the HAC load cases given in Table 2.7.3.1.1.3-1, and the compression analysis of Section 2.8.9.

2.10.8.2 Construction. The model consists of five element types:

1. To model the containment boundary near the OCV flange, 2-D isoparametric elements are used. This element type is used to a distance of 5.50 in. above the bottom of the OCV flange (this level corresponds to the top of the thermal shield). The entire OCV base is also modeled with this element type.
2. For the remainder of the containment vessel, for the thermal shield, and for the coolant jacket, axisymmetric shells are used, located at the section midplane. To join shell and isoparametric elements, embedded elements are used, having 1/10th the bending stiffness of the adjacent shell elements (see Reference 25, Chapter 9). The containment shell elements are 0.50 in. thick, the thermal shield contains elements of 0.25 and 0.375 in. in thickness, and the coolant jacket contains elements of 0.135 and 0.25 in. in thickness.
3. A single 2-D spar (element 100, nodes 16 and 120) was used to represent all of the closure bolts. The property of bolt area was entered on a per-radian basis. It was calculated by first multiplying the standard area of each closure bolt by the total bolt quantity (24) and then dividing by 2π . The standard area of each bolt was a length-weighted average of shank area and thread area and is equal to 1.10 in.². The bolt element was also given an initial strain to achieve the desired closure bolt pre-load force at 70 °F, in the absence of other applied loads, per Table 2.8.1.2.1-1.
4. A single 2-D beam (element 101) was used to represent the closure bolt access tubes. The properties of tube area and moment of inertia were entered on a per-radian basis. They were calculated by first multiplying the standard area and moment of inertia of each tube by the total tube quantity (24) and then dividing by 2π . To accomplish moment transfer between the beam element and the 2-D isoparametric elements of the flange, an embedded element, having 1/10th of the area and moment of inertia of the tube element, was used.
6. Four gaps are used between the OCV base and OCV flange (located at flange nodes 1, 11, 18, 21, and 26) to react the closure bolt loads and to model the propensity of the OCV flange to pivot about its outside edge because of thermal distortion.

Model node and element plots of key portions of the model are given in Figures 2.10.8-2

through 2.10.B-7. An interpreted ANSYS input listing is given in Table 2.10.8-1.

2.10.8.3 Material Properties. The modulus of elasticity and coefficient of thermal expansion varied with temperature according to the data in Tables 2.3-1 and 2.3-2. Poisson's ratio was 0.3.

2.10.8.4 Constraints. The bottom center node of the OCV base was fixed in all coordinate directions. In addition, one other node at the OCV base center and the node at the center of the OCV head were fixed in the radial direction, and all nodes are fixed in the hoop direction, consistent with axisymmetry. The top center node was also restrained from rotation about the hoop axis. For the compression analysis, the lower edge of the OCV flange is fixed in the axial direction.

2.10.8.6 Applied Loading. All surfaces subject to internal pressure had a constant pressure applied. Nodal temperature loading was applied using temperatures resulting from NCT thermal model output. Because there were fewer thermal model nodes than structural model nodes, interpolation of NCT thermal model temperatures was required. Temperatures in the OCV base were set as follows: nodes 155 to 162 are set to thermal node 360; nodes 149 and 150 are set to thermal node 362; nodes 143 and 144 are set to thermal node 364; nodes 119 to 140 and 163 are set to the average of thermal nodes 368 and 367; and nodes 101 to 118 are set to the average of thermal nodes 368 and 369. The rectangular portion of the OCV flange used thermal nodes 350, 352, 364, and 356, and the angled portion used thermal node 344. The thermal shield used thermal nodes 345 to 347. The closure bolt temperature was set using thermal model node 363 for the upper shank and node 355 for the lower threads. In the region above the OCV flange where shell elements were used, the temperatures of structural nodes that corresponded exactly to the thermal model counterparts were set directly, and the temperatures of structural nodes which fall in between thermal nodes were established using linear interpolation. The reference was 70 °F.

For the compression load case, the applied loading was 50 psi on the torispherical head and knuckle, using temperatures from NCT case 1, and no internal pressure.

2.10.8.6 Results. A plot of stress intensity corresponding to the analysis described in Section 2.8.9 is shown in Figure 2.10.8-8. Worst-case containment boundary stresses for NCT loadings (see Section 2.8.1.3) are shown in Figures 2.10.8-9 through 2.10.8-11, and a corresponding plot of stress intensity in the OCV flange is shown in Figure 2.10.8-12. A plot of worst-case OCV flange stress intensity for HAC loadings is shown in Figure 2.10.8-13. Closure bolt stress results are given in Sections 2.8.1.2.1 and 2.7.3.2. Relative thermal distortion of the containment O-ring seal area is discussed in Section 4.3.2.

2.10.8.7 Refined Model. A refined version of the model was also developed, and is shown in Figure 2.10.8-14. The refinement occurs in the flange-to-base interface region, where the number of gap elements is increased from four to 17. The position of the outermost gap, at the flange pry point, is unchanged. The increased density of gaps serves the purpose of more accurately calculating the bolt loads and the thermal distortion at the containment O-ring in the worst-case HAC fire event. Gap elements have a zero (or negligible) stiffness when open, and a stiffness when closed that represents the "bearing" of the surfaces in contact. In the HAC fire event, the OCV ball flange rotates a small amount by pivoting about the pry point at the outside edge of the flange, loading the closure bolts. The prying force creates a contact stress in the flange and base material that causes the pry point to increase to an area. The area extends until the prying load can be supported without exceeding the yield strength of the material. This is accomplished in the modeling process by decreasing the closed stiffness of the interface gap elements such that the flange and base portions of the model "pass through" each other under load, allowing more gap elements to come in contact, and thus modeling the actual contact area. A plot of the distorted

model under HAC fire conditions is shown in Figure 2.10.8-15. The area in contact is calculated based on the number of gaps in contact. The model was run, using decreased gap stiffness values, until the sum of closed gap forces (the prying force) could be supported on the contact area (located in between the closed gaps) without exceeding the yield strength of 304L at a conservative temperature of 150 °F. The use of yield strength conservatively ignores strain hardening. The overall effect of this refinement is to increase conservatively the opening between the flange and base at the containment O-ring, thus decreasing seal compression. To increase conservatism further in the analysis of seal opening, a run was made using only 70% of the nominal bolt preload force. An additional run was made focusing on maximum bolt load, using 130% of nominal bolt preload force.

Other aspects of the refined model are identical to those described in Sections 2.10.8.1 through 2.10.8.5 above. An interpreted ANSYS input listing is given in Table 2.10.8-2.

TABLE 2.10.B-1. Interpreted ANSYS Input Listing.

```

STATIC ANALYSIS (KANT=0)
LINEAR ANALYSIS - NO NON-LINEAR PROPERTIES
REFERENCE TEMPERATURE= 70.000 (TEMP)
UNIFORM TEMPERATURE = -40.000 (TEMP)

*****ANALYSIS OPTIONS (KEY VALUES) (IF ANY) *****
NO STATIC INTERPOLATION/EXTRAPOLATION (KANT(3)=0)
SMALL DEFLECTION SOLUTION (KAY(4)=0)
NO STRESS STIFFENING (KRY(8)=0)
USE INITIAL-STIFFNESS NEWTON-RAPHSON SOLUTION PROCEDURE (KAY(9)=3)
7H-CORE MOVE-FRONT EXHAUSTION SOLVER (KAY(10)=0)
LIST ELEMENT TYPES FROM 1 TO 20 BY 1
NO. STIF KEYOPT VALUES INCR
1 42 0 0 1 0 0 0 0 0 0 100PAR, STRESS SCALD, 2-0
2 31 0 0 0 0 0 0 0 0 0 PLASTIC AXISYM. CONIC SHELL
3 1 0 0 0 0 0 0 0 0 0 SPAR, 2-0
4 3 0 0 0 0 0 0 0 0 0 ELASTIC BEAM, 2-D
5 12 0 0 0 0 0 0 0 0 0 INTERFACE ELEM. 2-0

LIST ALL REAL SETS
REAL CONSTANT SET 2 ITERS 1 TO 4
0.30000 0.00000E+00 0.00000E+00 0.00000E+00 0.00000E+00 0.00000E+00
REAL CONSTANT SET 3 ITERS 1 TO 4
4.2020 0.04140E-03 0.00000E+00 0.00000E+00 0.00000E+00 0.00000E+00
REAL CONSTANT SET 4 ITERS 1 TO 4
3.4260 3.4330 2.5000 2.0000 0.00000E+00 0.00000E+00
REAL CONSTANT SET 5 ITERS 1 TO 4
0.00000E+00 0.79100E+10 0.00000E+00 0.00000E+00 0.00000E+00 0.00000E+00
REAL CONSTANT SET 21 ITERS 1 TO 4
0.37500 0.00000E+00 0.00000E+00 0.00000E+00 0.00000E+00 0.00000E+00
REAL CONSTANT SET 22 ITERS 1 TO 4
0.25000 0.00000E+00 0.00000E+00 0.00000E+00 0.00000E+00 0.00000E+00
REAL CONSTANT SET 23 ITERS 1 TO 4
0.13500 0.00000E+00 0.00000E+00 0.00000E+00 0.00000E+00 0.00000E+00
REAL CONSTANT SET 24 ITERS 1 TO 4
0.23200 0.00000E+00 0.00000E+00 0.00000E+00 0.00000E+00 0.00000E+00
REAL CONSTANT SET 25 ITERS 1 TO 4
0.34260 0.34330 0.25000 2.0000 0.00000E+00 0.00000E+00
REAL CONSTANT SET 26 ITERS 1 TO 4
0.11000 0.00000E+00 0.00000E+00 0.00000E+00 0.00000E+00 0.00000E+00
LIST ALL COORDINATE SYSTEMS
SYSTEM TYPE CENTER PARAMETERS SING KTY3
0 0 (CARTESIAN) 0.000 0.000 0.000 0.000 0.000 0 0
1 1 (CYLINDRICAL) 0.000 0.000 0.000 1.000 0.000 0 0
2 2 (SPHERICAL) 0.000 0.000 0.000 1.000 1.000 0 0
11 1 (CYLINDRICAL) 0.000 25.750 0.000 1.000 1.000 0 0
12 1 (CYLINDRICAL) 14.940 54.250 0.000 1.000 1.000 0 0

```

SYSTEM	ORIENTATION VECTORS (X, Y, Z)								
0	1.00	0.00	0.00	0.00	1.00	0.00	0.00	0.00	1.00
1	1.00	0.00	0.00	0.00	1.00	0.00	0.00	0.00	1.00
2	1.00	0.00	0.00	0.00	1.00	0.00	0.00	0.00	1.00
11	1.00	0.00	0.00	0.00	1.00	0.00	0.00	0.00	1.00
12	1.00	0.00	0.00	0.00	1.00	0.00	0.00	0.00	1.00
ESTR TYPE	XC	YC	ZC	TXCY	TKYZ	TKYZ	TKYZ	TKYZ	TKYZ
11	0.00000E+00	25.130	0.00000E+00	0.000	0.000	0.000	0.000	0.000	0.000
12	14.948	54.290	0.00000E+00	0.000	0.000	0.000	0.000	0.000	0.000

LIST ALL SELECTED ELEMENTS. (LIST NUMBER)

ELEM	MAT	TYP	REL	ESYS	NUMBER
1	1	1	1	0	1
2	1	1	1	0	2
3	1	1	1	0	3
4	1	1	1	0	4
5	1	1	1	0	5
6	1	1	1	0	6
7	1	1	1	0	7
8	1	1	1	0	8
9	1	1	1	0	9
10	1	1	1	0	10
11	1	1	1	0	11
12	1	1	1	0	12
13	1	1	1	0	13
14	1	1	1	0	14
15	1	1	1	0	15
16	1	1	1	0	16
17	1	1	1	0	17
18	1	1	1	0	18
19	1	1	1	0	19
20	1	1	1	0	20
21	1	1	1	0	21
22	1	1	1	0	22
23	1	1	1	0	23
24	1	1	1	0	24

ELEM	MAT	TYP	REL	ESYS	NUMBER
25	1	1	1	0	25
26	1	1	1	0	26
27	1	1	1	0	27
28	1	1	1	0	28
29	1	1	1	0	29
30	1	1	1	0	30
31	1	1	1	0	31
32	1	1	1	0	32
33	1	1	1	0	33
34	1	1	1	0	34
35	1	1	1	0	35
36	1	1	1	0	36
37	1	1	1	0	37
38	1	1	1	0	38
39	1	1	1	0	39
40	1	1	1	0	40

ELEM	MAT	TYP	REL	ESYS	NUMBER
41	1	1	1	0	41
42	1	1	1	0	42
43	1	1	1	0	43
44	1	1	1	0	44
45	1	1	1	0	45
46	1	1	1	0	46
47	1	1	1	0	47
48	1	1	1	0	48
49	1	1	1	0	49
50	1	1	1	0	50
51	1	1	1	0	51
52	1	1	1	0	52
53	1	1	1	0	53
54	1	1	1	0	54
55	1	1	1	0	55
56	1	1	1	0	56
57	1	1	1	0	57
58	1	1	1	0	58
59	1	1	1	0	59

80	1	1	1	0	132	133	140	139
83	1	1	1	0	136	137	144	143
84	1	1	1	0	137	138	143	144
85	1	1	1	0	138	139	146	145
86	1	1	1	0	139	140	147	146
89	1	1	1	0	143	144	151	150

ELEM	MAT	TYP	REL	ENTG	NODES			
70	1	1	1	0	144	145	152	151
73	1	1	1	0	150	151	158	157
76	1	1	1	0	151	152	159	158
81	1	1	1	0	157	158	165	164
82	1	1	1	0	158	159	166	165
87	1	1	1	0	164	165	172	171
88	1	1	1	0	165	166	173	172
93	1	1	1	0	125	118	178	126
94	1	1	1	0	118	119	178	178
95	1	2	2	0	49	53		
96	1	2	2	0	53	55		
97	1	2	2	0	23	27		
98	1	2	2	0	57	59		
99	1	2	2	0	50	41		
100	1	2	2	0	61	43		
101	1	2	2	0	43	45		
102	1	2	2	0	45	67		
103	1	2	2	0	67	69		
104	1	2	2	0	69	71		
105	1	2	2	0	71	73		

ELEM	MAT	TYP	REL	ENTG	NODES			
106	1	2	2	0	73	75		
107	1	2	2	0	75	77		
108	1	2	2	0	77	79		
109	1	2	2	0	81	83		
110	1	2	2	0	79	81		
111	1	2	2	0	85	85		
112	1	2	2	0	85	87		
113	1	2	2	0	87	86		
114	1	2	2	0	89	91		
115	1	2	2	0	91	93		
116	1	2	2	0	93	180		
117	1	2	2	0	180	181		
118	1	2	2	0	181	182		
119	1	2	2	0	182	183		
120	1	2	2	0	183	184		
121	1	2	2	0	184	185		
122	1	2	2	0	185	186		
123	1	2	2	0	186	187		
124	1	2	2	0	187	188		
125	1	2	2	0	93	94		

ELEM	MAT	TYP	REL	ENTG	NODES			
126	1	2	2	0	95	96		
127	1	2	2	0	97	98		
128	1	2	2	0	99	40		
129	1	2	2	0	41	42		
130	1	2	2	0	43	44		
131	1	2	2	0	45	46		
132	1	2	2	0	47	48		
133	1	2	2	0	49	70		
134	1	2	2	0	71	72		
135	1	2	2	0	73	74		
136	1	2	2	0	75	76		
137	1	2	2	0	77	78		
138	1	2	2	0	79	80		
139	1	2	2	0	81	82		
140	1	2	2	0	83	84		
141	1	2	2	0	85	86		
142	1	2	2	0	87	88		
143	1	2	2	0	89	90		

144	1	2	23	0	91	92
145	1	2	23	0	93	94

BLIN	MAT	TYP	REL	ESTS	NODES	
------	-----	-----	-----	------	-------	--

146	1	2	23	0	61	54
147	1	2	23	0	34	34
148	1	2	23	0	56	58
149	1	2	23	0	36	60
150	1	2	23	0	60	62
151	1	2	23	0	62	64
152	1	2	23	0	64	66
153	1	2	23	0	66	68
154	1	2	23	0	68	70
155	1	2	23	0	70	72
156	1	2	23	0	72	74
157	1	2	23	0	74	76
158	1	2	23	0	76	78
159	1	2	23	0	78	80
160	1	2	23	0	80	82
161	1	2	23	0	82	84
162	1	2	23	0	84	86
163	1	2	23	0	86	88
164	1	2	23	0	88	90
165	1	2	23	0	90	92

BLIN	MAT	TYP	REL	ESTS	NODES	
------	-----	-----	-----	------	-------	--

166	1	2	23	0	92	94
167	1	2	21	0	49	41
168	1	2	21	0	41	33
169	1	2	21	0	31	24
170	1	2	21	0	24	17
171	1	2	22	0	5	17
172	1	2	24	0	46	49
173	1	2	26	0	90	5
174	1	4	6	0	75	11
175	1	4	25	0	94	15
176	2	3	3	0	124	15
177	2	5	5	0	140	21
178	2	5	5	0	133	16
179	2	5	5	0	126	11
180	2	5	5	0	178	1

LIST ALL SELECTED NODE INSTS= 0

NODE	X	Y	Z	TEXT	INFX	INFXZ
1	23.991	0.00000E+00	0.00000E+00	0.00	0.00	0.00
2	24.125	0.50000E+00	0.00000E+00	0.00	0.00	0.00
3	24.125	1.4180	0.00000E+00	0.00	0.00	0.00
4	24.125	2.1150	0.00000E+00	0.00	0.00	0.00
5	24.125	2.8200	0.00000E+00	0.00	0.00	0.00
6	23.125	0.00000E+00	0.00000E+00	0.00	0.00	0.00
7	23.125	0.78900	0.00000E+00	0.00	0.00	0.00
8	23.125	1.6100	0.00000E+00	0.00	0.00	0.00
9	23.125	2.1150	0.00000E+00	0.00	0.00	0.00
10	23.125	2.8200	0.00000E+00	0.00	0.00	0.00
11	22.125	0.00000E+00	0.00000E+00	0.00	0.00	0.00
12	23.125	0.78900	0.00000E+00	0.00	0.00	0.00
13	22.125	1.6100	0.00000E+00	0.00	0.00	0.00
14	22.125	2.1150	0.00000E+00	0.00	0.00	0.00
15	22.125	2.8200	0.00000E+00	0.00	0.00	0.00
16	20.875	0.00000E+00	0.00000E+00	0.00	0.00	0.00
17	20.875	0.70500	0.00000E+00	0.00	0.00	0.00
18	20.875	1.4180	0.00000E+00	0.00	0.00	0.00
19	20.875	2.1150	0.00000E+00	0.00	0.00	0.00
20	20.875	2.8200	0.00000E+00	0.00	0.00	0.00
NODE	X	Y	Z	TEXT	INFX	INFXZ
21	20.000	0.00000E+00	0.00000E+00	0.00	0.00	0.00
22	19.540	1.1300	0.00000E+00	0.00	0.00	0.00
23	19.643	1.6913	0.00000E+00	0.00	0.00	0.00
24	19.727	2.2567	0.00000E+00	0.00	0.00	0.00

25	19.810	2.5288	0.00000E+00	0.00	0.00	0.00
26	19.560	0.00000E+00	0.00000E+00	0.00	0.00	0.00
27	18.775	1.9725	0.00000E+00	0.00	0.00	0.00
28	18.984	2.4804	0.00000E+00	0.00	0.00	0.00
29	19.155	2.8255	0.00000E+00	0.00	0.00	0.00
30	19.373	3.2547	0.00000E+00	0.00	0.00	0.00
31	22.125	5.6328	0.00000E+00	0.00	0.00	0.00
32	17.875	3.8150	0.00000E+00	0.00	0.00	0.00
33	18.229	3.1479	0.00000E+00	0.00	0.00	0.00
34	18.583	3.4804	0.00000E+00	0.00	0.00	0.00
35	18.937	3.8133	0.00000E+00	0.00	0.00	0.00
36	25.438	5.6320	0.00000E+00	0.00	0.00	0.00
37	26.436	2.4288	0.00000E+00	0.00	0.00	0.00
38	17.875	3.8150	0.00000E+00	0.00	0.00	0.00
39	18.185	3.8175	0.00000E+00	0.00	0.00	0.00
40	18.500	4.1388	0.00000E+00	0.00	0.00	0.00

MODE	X	Y	Z	TWT1	TWT2	TWT3
41	19.508	3.6328	0.00000E+00	0.00	0.00	0.00
42	17.875	4.7588	0.00000E+00	0.00	0.00	0.00
43	18.184	4.7588	0.00000E+00	0.00	0.00	0.00
44	18.500	4.7588	0.00000E+00	0.00	0.00	0.00
45	17.940	4.7658	0.00000E+00	0.00	0.00	0.00
46	18.190	4.9458	0.00000E+00	0.00	0.00	0.00
47	18.448	4.9458	0.00000E+00	0.00	0.00	0.00
48	17.960	5.6328	0.00000E+00	0.00	0.00	0.00
49	18.190	5.6328	0.00000E+00	0.00	0.00	0.00
50	18.440	5.6328	0.00000E+00	0.00	0.00	0.00
51	18.190	7.7928	0.00000E+00	0.00	0.00	0.00
52	19.508	7.7928	0.00000E+00	0.00	0.00	0.00
53	18.190	10.042	0.00000E+00	0.00	0.00	0.00
54	19.508	10.042	0.00000E+00	0.00	0.00	0.00
55	18.190	12.292	0.00000E+00	0.00	0.00	0.00
56	19.508	12.292	0.00000E+00	0.00	0.00	0.00
57	18.190	14.542	0.00000E+00	0.00	0.00	0.00
58	19.508	14.542	0.00000E+00	0.00	0.00	0.00
59	18.190	16.792	0.00000E+00	0.00	0.00	0.00
60	19.508	16.792	0.00000E+00	0.00	0.00	0.00

MODE	X	Y	Z	TWT1	TWT2	TWT3
63	18.190	19.042	0.00000E+00	0.00	0.00	0.00
64	19.508	19.042	0.00000E+00	0.00	0.00	0.00
65	18.190	21.292	0.00000E+00	0.00	0.00	0.00
66	19.508	21.292	0.00000E+00	0.00	0.00	0.00
67	18.190	23.542	0.00000E+00	0.00	0.00	0.00
68	19.508	23.542	0.00000E+00	0.00	0.00	0.00
69	18.190	25.792	0.00000E+00	0.00	0.00	0.00
70	19.508	25.792	0.00000E+00	0.00	0.00	0.00
71	18.190	28.042	0.00000E+00	0.00	0.00	0.00
72	19.508	28.042	0.00000E+00	0.00	0.00	0.00
73	18.190	30.292	0.00000E+00	0.00	0.00	0.00
74	19.508	30.292	0.00000E+00	0.00	0.00	0.00
75	18.190	32.542	0.00000E+00	0.00	0.00	0.00
76	19.508	32.542	0.00000E+00	0.00	0.00	0.00
77	18.190	34.792	0.00000E+00	0.00	0.00	0.00
78	19.508	34.792	0.00000E+00	0.00	0.00	0.00
79	18.190	37.042	0.00000E+00	0.00	0.00	0.00
80	19.508	37.042	0.00000E+00	0.00	0.00	0.00
81	18.190	39.292	0.00000E+00	0.00	0.00	0.00
82	19.508	39.292	0.00000E+00	0.00	0.00	0.00

MODE	X	Y	Z	TWT1	TWT2	TWT3
83	18.190	41.542	0.00000E+00	0.00	0.00	0.00
84	19.508	41.542	0.00000E+00	0.00	0.00	0.00
85	18.190	43.792	0.00000E+00	0.00	0.00	0.00
86	19.508	43.792	0.00000E+00	0.00	0.00	0.00
87	18.190	46.042	0.00000E+00	0.00	0.00	0.00
88	19.508	46.042	0.00000E+00	0.00	0.00	0.00
89	18.190	48.292	0.00000E+00	0.00	0.00	0.00
90	19.508	48.292	0.00000E+00	0.00	0.00	0.00
91	18.190	50.542	0.00000E+00	0.00	0.00	0.00
92	19.508	50.542	0.00000E+00	0.00	0.00	0.00
93	18.190	52.790	0.00000E+00	0.00	0.00	0.00
94	19.504	52.790	0.00000E+00	0.00	0.00	0.00

181	26.625	-3.5000	0.00000E+00	0.00	0.00	0.00
182	26.625	-2.7500	0.00000E+00	0.00	0.00	0.00
183	26.625	-2.0000	0.00000E+00	0.00	0.00	0.00
184	26.625	-1.0000	0.00000E+00	0.00	0.00	0.00
185	26.625	0.00000E+00	0.00000E+00	0.00	0.00	0.00
186	26.625	1.2500	0.00000E+00	0.00	0.00	0.00
187	26.625	2.0000	0.00000E+00	0.00	0.00	0.00
188	26.327	-3.5000	0.00000E+00	0.00	0.00	0.00
MODE	X	Y	Z	THX1	THX2	THX3
189	25.327	-2.7500	0.00000E+00	0.00	0.00	0.00
110	25.327	-2.0000	0.00000E+00	0.00	0.00	0.00
111	25.327	-1.0000	0.00000E+00	0.00	0.00	0.00
112	25.327	0.00000E+00	0.00000E+00	0.00	0.00	0.00
113	25.327	1.2500	0.00000E+00	0.00	0.00	0.00
114	25.327	2.0000	0.00000E+00	0.00	0.00	0.00
115	24.150	-3.5000	0.00000E+00	0.00	0.00	0.00
116	24.150	-2.7500	0.00000E+00	0.00	0.00	0.00
117	24.150	-2.0000	0.00000E+00	0.00	0.00	0.00
118	24.150	-1.0000	0.00000E+00	0.00	0.00	0.00
119	24.150	0.00000E+00	0.00000E+00	0.00	0.00	0.00
120	24.150	1.2500	0.00000E+00	0.00	0.00	0.00
121	24.150	2.0000	0.00000E+00	0.00	0.00	0.00
122	22.125	-3.5000	0.00000E+00	0.00	0.00	0.00
123	22.125	-3.0000	0.00000E+00	0.00	0.00	0.00
124	22.125	-2.3700	0.00000E+00	0.00	0.00	0.00
125	22.125	-1.0000	0.00000E+00	0.00	0.00	0.00
126	22.125	0.00000E+00	0.00000E+00	0.00	0.00	0.00
129	20.875	-3.5000	0.00000E+00	0.00	0.00	0.00
130	20.875	-2.7500	0.00000E+00	0.00	0.00	0.00
MODE	X	Y	Z	THX1	THX2	THX3
131	20.875	-2.0000	0.00000E+00	0.00	0.00	0.00
132	20.875	-1.0000	0.00000E+00	0.00	0.00	0.00
133	20.875	0.00000E+00	0.00000E+00	0.00	0.00	0.00
134	20.000	-3.5000	0.00000E+00	0.00	0.00	0.00
137	20.000	-2.7500	0.00000E+00	0.00	0.00	0.00
138	20.000	-2.0000	0.00000E+00	0.00	0.00	0.00
139	20.000	-1.0000	0.00000E+00	0.00	0.00	0.00
140	20.000	0.00000E+00	0.00000E+00	0.00	0.00	0.00
143	19.545	-3.5000	0.00000E+00	0.00	0.00	0.00
144	19.545	-2.7500	0.00000E+00	0.00	0.00	0.00
145	19.545	-2.0000	0.00000E+00	0.00	0.00	0.00
146	19.545	-1.0000	0.00000E+00	0.00	0.00	0.00
147	19.545	0.00000E+00	0.00000E+00	0.00	0.00	0.00
150	14.659	-3.5000	0.00000E+00	0.00	0.00	0.00
151	14.659	-2.7500	0.00000E+00	0.00	0.00	0.00
152	14.659	-2.0000	0.00000E+00	0.00	0.00	0.00
157	9.7726	-3.5000	0.00000E+00	0.00	0.00	0.00
158	9.7726	-2.7500	0.00000E+00	0.00	0.00	0.00
159	9.7726	-2.0000	0.00000E+00	0.00	0.00	0.00
164	4.5664	-3.5000	0.00000E+00	0.00	0.00	0.00
MODE	X	Y	Z	THX1	THX2	THX3
165	4.5664	-2.7500	0.00000E+00	0.00	0.00	0.00
166	4.5664	-2.0000	0.00000E+00	0.00	0.00	0.00
171	0.20000E+03	-3.5000	0.00000E+00	0.00	0.00	0.00
172	0.20000E+03	-2.7500	0.00000E+00	0.00	0.00	0.00
173	0.20000E+03	-2.0000	0.00000E+00	0.00	0.00	0.00
178	23.991	0.00000E+00	0.00000E+00	0.00	0.00	0.00
180	18.100	54.200	0.00000E+00	0.00	0.00	0.00
181	18.000	55.170	0.00000E+00	0.00	0.00	0.00
182	17.773	55.945	0.00000E+00	0.00	0.00	0.00
183	17.180	56.673	0.00000E+00	0.00	0.00	0.00
184	16.423	57.162	0.00000E+00	0.00	0.00	0.00
185	13.323	58.800	0.00000E+00	0.00	0.00	0.00
186	8.4473	60.143	0.00000E+00	0.00	0.00	0.00
187	4.2537	60.867	0.00000E+00	0.00	0.00	0.00
188	0.14827E+09	61.750	0.00000E+00	0.00	0.00	0.00

LIST ALL MATERIALS PROPERTY= ALL

PROPERTY TABLE MDT= 1 NUM. POINTS= 2
 TEMPERATURE DATA TEMPERATURE DATA
 -9999.0 0.39600 9999.0 0.30000

PROPERTY TABLE EN MDT= 1 NUM. POINTS= 15
 TEMPERATURE DATA TEMPERATURE DATA
 -40.000 0.29900E+08 70.000 0.26500E+08
 100.00 0.28100E+08 200.00 0.27400E+08
 300.00 0.27800E+08 400.00 0.26400E+08
 500.00 0.25900E+08 600.00 0.25900E+08
 700.00 0.24800E+08 800.00 0.24100E+08
 900.00 0.23500E+08 1000.0 0.22300E+08
 1100.0 0.22100E+08 1200.0 0.21900E+08
 1300.0 0.20500E+08

PROPERTY TABLE ALPX MDT= 1 NUM. POINTS= 15
 TEMPERATURE DATA TEMPERATURE DATA
 -40.000 0.01300E-05 70.000 0.04400E-05
 100.00 0.02300E-05 200.00 0.07900E-05
 300.00 0.09000E-05 400.00 0.09100E-05
 500.00 0.01700E-05 600.00 0.02500E-05
 700.00 0.09400E-05 800.00 0.08200E-05
 900.00 0.10060E-04 1000.0 0.08500E-04
 1100.0 0.10350E-04 1200.0 0.10400E-04
 1300.0 0.10450E-04

PROPERTY TABLE EK MDT= 2 NUM. POINTS= 7
 TEMPERATURE DATA TEMPERATURE DATA
 -40.000 0.28400E+08 70.000 0.27900E+08
 100.00 0.27800E+08 200.00 0.27100E+08
 300.00 0.26700E+08 400.00 0.26100E+08
 500.00 0.25700E+08

PROPERTY TABLE ALPX MDT= 2 NUM. POINTS= 7
 TEMPERATURE DATA TEMPERATURE DATA
 -40.000 0.59400E-05 70.000 0.68000E-05
 100.00 0.42700E-05 200.00 0.65400E-05
 300.00 0.47800E-05 400.00 0.66800E-05
 500.00 0.71400E-05

TOL= 0.00000E+00 NITER= -5
 KTEMP= LSTEP= -1 ITER= 0

UNIFORM TEMPERATURE= -40.000 (TREF= 70.000)
 BOUNDARY CONDITIONS STOPPED DUE TO STATIC CONVERGENCE OPTION
 PLASTIC CONVERG. CRITERION= 0.0100
 CREEP OPTIMUM. CRITERION= 0.1000
 LARGE DEFL. CONVERG. CRITERION= 0.001000
 DISPLACEMENT LIMIT= 0.00000E+00

MPRINT= 99900 MPOST= 5 REACTION PRINT FREQ= 99900
 DISP. POST DATA FREQ= 5 REACT. POST DATA FREQ= 5

ELEMENT PRINT AND POST DATA PARAMETERS

TYPE	STIFF	STRESS	FORCE	STRESS	DATA	FORCE	DATA
	MG.	PRINT	PRINT	DATA	DATA	DATA	DATA
1	42	99900	99900	5	5	5	5
2	51	99900	99900	5	5	5	5
3	1	99900	99900	5	5	5	5
4	3	99900	99900	5	5	5	5
5	12	99900	99900	5	5	5	5

LOADS INPUT FILE= 26 LOADS OUTPUT FILE= 25

ALL ANALYSIS DATA WILL BE WRITTEN ONTO FILE2?

LIST DISPLACEMENTS FOR ALL SELECTED NODES

NODE	LABEL	DISP	DISP
1	UZ	0.00000000E+00	0.00000000E+00
2	UZ	0.00000000E+00	0.00000000E+00
3	UZ	0.00000000E+00	0.00000000E+00
4	UZ	0.00000000E+00	0.00000000E+00
5	UZ	0.00000000E+00	0.00000000E+00
6	UZ	0.00000000E+00	0.00000000E+00

7	UZ	0.00000000E+00	0.00000000E+00
8	UZ	0.00000000E+00	0.00000000E+00
9	UZ	0.00000000E+00	0.00000000E+00
10	UZ	0.00000000E+00	0.00000000E+00
11	UZ	0.00000000E+00	0.00000000E+00
12	UZ	0.00000000E+00	0.00000000E+00
13	UZ	0.00000000E+00	0.00000000E+00
14	UZ	0.00000000E+00	0.00000000E+00
15	UZ	0.00000000E+00	0.00000000E+00
16	UZ	0.00000000E+00	0.00000000E+00
17	UZ	0.00000000E+00	0.00000000E+00
18	UZ	0.00000000E+00	0.00000000E+00
19	UZ	0.00000000E+00	0.00000000E+00
20	UZ	0.00000000E+00	0.00000000E+00

MODE	LABEL	BISF	CSISF
21	UZ	0.00000000E+00	0.00000000E+00
22	UZ	0.00000000E+00	0.00000000E+00
23	UZ	0.00000000E+00	0.00000000E+00
24	UZ	0.00000000E+00	0.00000000E+00
25	UZ	0.00000000E+00	0.00000000E+00
26	UZ	0.00000000E+00	0.00000000E+00
27	UZ	0.00000000E+00	0.00000000E+00
28	UZ	0.00000000E+00	0.00000000E+00
29	UZ	0.00000000E+00	0.00000000E+00
30	UZ	0.00000000E+00	0.00000000E+00
31	UZ	0.00000000E+00	0.00000000E+00
32	UZ	0.00000000E+00	0.00000000E+00
33	UZ	0.00000000E+00	0.00000000E+00
34	UZ	0.00000000E+00	0.00000000E+00
35	UZ	0.00000000E+00	0.00000000E+00
36	UZ	0.00000000E+00	0.00000000E+00
37	UZ	0.00000000E+00	0.00000000E+00
38	UZ	0.00000000E+00	0.00000000E+00
39	UZ	0.00000000E+00	0.00000000E+00
40	UZ	0.00000000E+00	0.00000000E+00

MODE	LABEL	BISF	CSISF
41	UZ	0.00000000E+00	0.00000000E+00
42	UZ	0.00000000E+00	0.00000000E+00
43	UZ	0.00000000E+00	0.00000000E+00
44	UZ	0.00000000E+00	0.00000000E+00
45	UZ	0.00000000E+00	0.00000000E+00
46	UZ	0.00000000E+00	0.00000000E+00
47	UZ	0.00000000E+00	0.00000000E+00
48	UZ	0.00000000E+00	0.00000000E+00
49	UZ	0.00000000E+00	0.00000000E+00
50	UZ	0.00000000E+00	0.00000000E+00
51	UZ	0.00000000E+00	0.00000000E+00
52	UZ	0.00000000E+00	0.00000000E+00
53	UZ	0.00000000E+00	0.00000000E+00
54	UZ	0.00000000E+00	0.00000000E+00
55	UZ	0.00000000E+00	0.00000000E+00
56	UZ	0.00000000E+00	0.00000000E+00
57	UZ	0.00000000E+00	0.00000000E+00
58	UZ	0.00000000E+00	0.00000000E+00
59	UZ	0.00000000E+00	0.00000000E+00
60	UZ	0.00000000E+00	0.00000000E+00
61	UZ	0.00000000E+00	0.00000000E+00
62	UZ	0.00000000E+00	0.00000000E+00

MODE	LABEL	BISF	CSISF
63	UZ	0.00000000E+00	0.00000000E+00
64	UZ	0.00000000E+00	0.00000000E+00
65	UZ	0.00000000E+00	0.00000000E+00
66	UZ	0.00000000E+00	0.00000000E+00
67	UZ	0.00000000E+00	0.00000000E+00
68	UZ	0.00000000E+00	0.00000000E+00
69	UZ	0.00000000E+00	0.00000000E+00
70	UZ	0.00000000E+00	0.00000000E+00
71	UZ	0.00000000E+00	0.00000000E+00
72	UZ	0.00000000E+00	0.00000000E+00
73	UZ	0.00000000E+00	0.00000000E+00
74	UZ	0.00000000E+00	0.00000000E+00
75	UZ	0.00000000E+00	0.00000000E+00
76	UZ	0.00000000E+00	0.00000000E+00

77	WZ	0.00000000E+00	0.00000000E+00
78	WZ	0.00000000E+00	0.00000000E+00
79	WZ	0.00000000E+00	0.00000000E+00
80	WZ	0.00000000E+00	0.00000000E+00
81	WZ	0.00000000E+00	0.00000000E+00
82	WZ	0.00000000E+00	0.00000000E+00
NAME LABEL DISP DISP			
83	WZ	0.00000000E+00	0.00000000E+00
84	WZ	0.00000000E+00	0.00000000E+00
85	WZ	0.00000000E+00	0.00000000E+00
86	WZ	0.00000000E+00	0.00000000E+00
87	WZ	0.00000000E+00	0.00000000E+00
88	WZ	0.00000000E+00	0.00000000E+00
89	WZ	0.00000000E+00	0.00000000E+00
90	WZ	0.00000000E+00	0.00000000E+00
91	WZ	0.00000000E+00	0.00000000E+00
92	WZ	0.00000000E+00	0.00000000E+00
93	WZ	0.00000000E+00	0.00000000E+00
94	WZ	0.00000000E+00	0.00000000E+00
95	WZ	0.00000000E+00	0.00000000E+00
96	WZ	0.00000000E+00	0.00000000E+00
97	WZ	0.00000000E+00	0.00000000E+00
98	WZ	0.00000000E+00	0.00000000E+00
99	WZ	0.00000000E+00	0.00000000E+00
100	WZ	0.00000000E+00	0.00000000E+00
NAME LABEL DISP DISP			
109	WZ	0.00000000E+00	0.00000000E+00
110	WZ	0.00000000E+00	0.00000000E+00
111	WZ	0.00000000E+00	0.00000000E+00
112	WZ	0.00000000E+00	0.00000000E+00
113	WZ	0.00000000E+00	0.00000000E+00
114	WZ	0.00000000E+00	0.00000000E+00
115	WZ	0.00000000E+00	0.00000000E+00
116	WZ	0.00000000E+00	0.00000000E+00
117	WZ	0.00000000E+00	0.00000000E+00
118	WZ	0.00000000E+00	0.00000000E+00
119	WZ	0.00000000E+00	0.00000000E+00
120	WZ	0.00000000E+00	0.00000000E+00
121	WZ	0.00000000E+00	0.00000000E+00
122	WZ	0.00000000E+00	0.00000000E+00
123	WZ	0.00000000E+00	0.00000000E+00
124	WZ	0.00000000E+00	0.00000000E+00
125	WZ	0.00000000E+00	0.00000000E+00
126	WZ	0.00000000E+00	0.00000000E+00
127	WZ	0.00000000E+00	0.00000000E+00
128	WZ	0.00000000E+00	0.00000000E+00
129	WZ	0.00000000E+00	0.00000000E+00
130	WZ	0.00000000E+00	0.00000000E+00
NAME LABEL DISP DISP			
131	WZ	0.00000000E+00	0.00000000E+00
132	WZ	0.00000000E+00	0.00000000E+00
133	WZ	0.00000000E+00	0.00000000E+00
134	WZ	0.00000000E+00	0.00000000E+00
135	WZ	0.00000000E+00	0.00000000E+00
136	WZ	0.00000000E+00	0.00000000E+00
137	WZ	0.00000000E+00	0.00000000E+00
138	WZ	0.00000000E+00	0.00000000E+00
139	WZ	0.00000000E+00	0.00000000E+00
140	WZ	0.00000000E+00	0.00000000E+00
141	WZ	0.00000000E+00	0.00000000E+00
142	WZ	0.00000000E+00	0.00000000E+00
143	WZ	0.00000000E+00	0.00000000E+00
144	WZ	0.00000000E+00	0.00000000E+00
145	WZ	0.00000000E+00	0.00000000E+00
146	WZ	0.00000000E+00	0.00000000E+00
147	WZ	0.00000000E+00	0.00000000E+00
150	WZ	0.00000000E+00	0.00000000E+00
151	WZ	0.00000000E+00	0.00000000E+00
152	WZ	0.00000000E+00	0.00000000E+00
153	WZ	0.00000000E+00	0.00000000E+00
154	WZ	0.00000000E+00	0.00000000E+00
155	WZ	0.00000000E+00	0.00000000E+00
156	WZ	0.00000000E+00	0.00000000E+00

NODE LABEL	DIST	EDIST
165 UE	0.00000000E+00	0.00000000E+00
166 UE	0.00000000E+00	0.00000000E+00
171 UE	0.00000000E+00	0.00000000E+00
172 UE	0.00000000E+00	0.00000000E+00
173 UE	0.00000000E+00	0.00000000E+00
176 UE	0.00000000E+00	0.00000000E+00
180 UE	0.00000000E+00	0.00000000E+00
181 UE	0.00000000E+00	0.00000000E+00
182 UE	0.00000000E+00	0.00000000E+00
183 UE	0.00000000E+00	0.00000000E+00
184 UE	0.00000000E+00	0.00000000E+00
185 UE	0.00000000E+00	0.00000000E+00
186 UE	0.00000000E+00	0.00000000E+00
187 UE	0.00000000E+00	0.00000000E+00
188 UE	0.00000000E+00	0.00000000E+00
171 UX	0.00000000E+00	0.00000000E+00
172 UX	0.00000000E+00	0.00000000E+00
173 UX	0.00000000E+00	0.00000000E+00
188 UX	0.00000000E+00	0.00000000E+00
185 EQ12	0.00000000E+00	0.00000000E+00

NODE LABEL	DIST	EDIST
171 UF	0.00000000E+00	0.00000000E+00

LIST ELEMENT PRESSURES FOR ALL SELECTED ELEMENTS

ELEM	FACE	VALUE(S)	FACE NODES
75	1	26.5000000	49 53
96	1	26.5000000	53 55
77	1	26.5000000	75 57
98	1	26.5000000	57 59
99	1	26.5000000	59 61
100	1	26.5000000	61 63
101	1	26.5000000	63 65
102	1	26.5000000	65 67
103	1	26.5000000	67 69
104	1	26.5000000	69 71
105	1	26.5000000	71 73
106	1	26.5000000	73 75
107	1	26.5000000	75 77
108	1	26.5000000	77 79
109	1	26.5000000	79 81
110	1	26.5000000	81 83
111	1	26.5000000	83 85
112	1	26.5000000	85 87
113	1	26.5000000	87 89
114	1	26.5000000	89 91

ELEM	FACE	VALUE(S)	FACE NODES
115	1	26.5000000	91 93
116	1	26.5000000	93 95
117	1	26.5000000	95 97
118	1	26.5000000	97 99
119	1	26.5000000	99 101
120	1	26.5000000	101 103
121	1	26.5000000	103 105
122	1	26.5000000	105 107
123	1	26.5000000	107 109
124	1	26.5000000	109 111
65	3	26.5000000	146 148
66	3	26.5000000	147 149
70	2	26.5000000	145 152
76	2	26.5000000	152 159
82	2	26.5000000	159 166
88	2	26.5000000	166 173
17	4	26.5000000	22 26
18	4	26.5000000	27 22
21	4	26.5000000	32 27
26	4	26.5000000	38 32

ELEM	FACE	VOLUME(1)		FACE NUMBER
27	4	29.5000000	0.0000000E+00	42 38
29	4	29.5000000	0.0000000E+00	43 42
31	4	29.5000000	0.0000000E+00	44 45

LIST ELEMENT CONNECTIONS FOR ALL SELECTED ELEMENTS

LIST ELEMENT TEMPERATURES FOR ALL SELECTED ELEMENTS

ELEMENT	TEMPERATURES			
176	207.09000	210.16000	0.0000000E+00	0.0000000E+00
	0.0000000E+00	0.0000000E+00	0.0000000E+00	0.0000000E+00
	0.0000000E+00	0.0000000E+00		

LIST TEMPERATURES FOR ALL SELECTED NODES

NODE	TEMPERATURE	FLUENCE
1	207.30	0.00000E+00
2	207.30	0.00000E+00
3	208.96	0.00000E+00
4	208.59	0.00000E+00
5	208.59	0.00000E+00
6	209.30	0.00000E+00
7	209.30	0.00000E+00
8	206.54	0.00000E+00
9	206.59	0.00000E+00
10	206.59	0.00000E+00
11	209.30	0.00000E+00
12	209.30	0.00000E+00
13	206.94	0.00000E+00
14	206.95	0.00000E+00
15	206.59	0.00000E+00
16	209.30	0.00000E+00
17	209.30	0.00000E+00
18	209.69	0.00000E+00
19	209.37	0.00000E+00
20	209.37	0.00000E+00

NODE	TEMPERATURE	FLUENCE
21	209.80	0.00000E+00
22	209.80	0.00000E+00
23	209.80	0.00000E+00
24	209.57	0.00000E+00
25	209.57	0.00000E+00
26	209.80	0.00000E+00
27	212.54	0.00000E+00
28	212.54	0.00000E+00
29	212.54	0.00000E+00
30	212.54	0.00000E+00
31	182.05	0.00000E+00
32	212.54	0.00000E+00
33	212.54	0.00000E+00
34	212.54	0.00000E+00
35	212.54	0.00000E+00
36	190.09	0.00000E+00
37	201.61	0.00000E+00
38	178.54	0.00000E+00
39	212.34	0.00000E+00
40	212.54	0.00000E+00

NODE	TEMPERATURE	FLUENCE
41	220.96	0.00000E+00
42	220.96	0.00000E+00
43	220.96	0.00000E+00
44	220.96	0.00000E+00
45	220.96	0.00000E+00
46	220.96	0.00000E+00
47	220.96	0.00000E+00
48	220.96	0.00000E+00
49	220.96	0.00000E+00
50	220.96	0.00000E+00
51	220.96	0.00000E+00
52	173.94	0.00000E+00
53	220.37	0.00000E+00
54	213.94	0.00000E+00

57	229.33	0.00000E+00
58	214.36	0.00000E+00
59	243.29	0.00000E+00
60	215.61	0.00000E+00
61	247.24	0.00000E+00
62	246.85	0.00000E+00

NODE	TEMPERATURE	FLUXENCE
63	251.20	0.00000E+00
64	218.09	0.00000E+00
65	256.68	0.00000E+00
66	223.85	0.00000E+00
67	262.16	0.00000E+00
68	227.62	0.00000E+00
69	257.64	0.00000E+00
70	222.38	0.00000E+00
71	273.11	0.00000E+00
72	237.94	0.00000E+00
73	276.59	0.00000E+00
74	241.91	0.00000E+00
75	284.07	0.00000E+00
76	246.67	0.00000E+00
77	284.03	0.00000E+00
78	246.59	0.00000E+00
79	283.59	0.00000E+00
80	246.51	0.00000E+00
81	283.94	0.00000E+00
82	246.43	0.00000E+00

NODE	TEMPERATURE	FLUXENCE
83	283.92	0.00000E+00
84	246.36	0.00000E+00
85	283.88	0.00000E+00
86	246.28	0.00000E+00
87	283.84	0.00000E+00
88	246.26	0.00000E+00
89	283.86	0.00000E+00
90	246.12	0.00000E+00
91	283.76	0.00000E+00
92	246.84	0.00000E+00
93	283.72	0.00000E+00
94	245.96	0.00000E+00
101	208.89	0.00000E+00
102	208.89	0.00000E+00
103	208.89	0.00000E+00
104	208.89	0.00000E+00
105	208.89	0.00000E+00
106	208.89	0.00000E+00
107	208.89	0.00000E+00
108	208.89	0.00000E+00

NODE	TEMPERATURE	FLUXENCE
109	208.89	0.00000E+00
110	208.89	0.00000E+00
111	208.89	0.00000E+00
112	208.89	0.00000E+00
113	208.89	0.00000E+00
114	208.89	0.00000E+00
115	208.89	0.00000E+00
116	208.89	0.00000E+00
117	208.89	0.00000E+00
118	208.89	0.00000E+00
119	208.89	0.00000E+00
120	208.89	0.00000E+00
121	208.89	0.00000E+00
122	218.29	0.00000E+00
123	218.29	0.00000E+00
124	218.29	0.00000E+00
125	218.29	0.00000E+00
126	218.29	0.00000E+00
129	218.29	0.00000E+00
130	218.29	0.00000E+00

NODE	TEMPERATURE	FLUXDNC
131	210.29	0.00000E+00
132	210.29	0.00000E+00
133	210.29	0.00000E+00
134	210.29	0.00000E+00
137	210.29	0.00000E+00
138	210.29	0.00000E+00
139	210.29	0.00000E+00
140	210.29	0.00000E+00
143	210.29	0.00000E+00
144	210.29	0.00000E+00
145	210.29	0.00000E+00
146	210.29	0.00000E+00
147	210.29	0.00000E+00
150	215.70	0.00000E+00
151	215.70	0.00000E+00
152	215.70	0.00000E+00
157	218.74	0.00000E+00
158	218.74	0.00000E+00
159	218.74	0.00000E+00
164	220.18	0.00000E+00

NODE	TEMPERATURE	FLUXDNC
165	220.18	0.00000E+00
166	220.18	0.00000E+00
171	220.18	0.00000E+00
172	220.18	0.00000E+00
173	220.18	0.00000E+00
178	236.61	0.00000E+00
180	236.61	0.00000E+00
181	236.61	0.00000E+00
182	236.61	0.00000E+00
183	236.61	0.00000E+00
184	236.61	0.00000E+00
185	267.43	0.00000E+00
186	267.43	0.00000E+00
187	267.43	0.00000E+00
189	267.43	0.00000E+00

12 1 (CYLINDRICAL) 14.940 54.290 0.000 1.000 1.000 0 0

SYSTEM

ORIENTATION VECTORS (X, Y, Z)

	X	Y	Z	X	Y	Z	X	Y	Z
0	1.00	0.00	0.00	0.00	1.00	0.00	0.00	0.00	1.00
1	1.00	0.00	0.00	0.00	1.00	0.00	0.00	0.00	1.00
2	1.00	0.00	0.00	0.00	1.00	0.00	0.00	0.00	1.00
11	1.00	0.00	0.00	0.00	1.00	0.00	0.00	0.00	1.00
12	1.00	0.00	0.00	0.00	1.00	0.00	0.00	0.00	1.00

SYSTEM TYPE	XC	YC	ZC	INER	INTZ	THICK
11	1	0.00000E+00	25.150	0.00000E+00	0.000	0.000
12	1	14.940	54.290	0.00000E+00	0.000	0.000

LIST ALL SELECTED ELEMENTS. (LIST NAMES)

ELEM	MAT	TYP	REL	ESYS	NODES		
3	1	1	1	0	3	4	9
4	1	1	1	0	4	5	10
5	1	1	1	0	5	9	14
6	1	1	1	0	6	10	14
11	1	1	1	0	11	14	19
12	1	1	1	0	12	15	20
15	1	1	1	0	15	19	24
16	1	1	1	0	16	20	24
18	1	1	1	0	18	21	27
19	1	1	1	0	19	22	27
20	1	1	1	0	20	23	27
21	1	1	1	0	21	24	27
22	1	1	1	0	22	25	30
23	1	1	1	0	23	26	33
24	1	1	1	0	24	27	33
25	1	1	1	0	25	28	34
26	1	1	1	0	26	29	34
27	1	1	1	0	27	30	35
28	1	1	1	0	28	31	35
29	1	1	1	0	29	32	36
30	1	1	1	0	30	33	36
31	1	1	1	0	31	34	39
32	1	1	1	0	32	35	39
33	1	1	1	0	33	36	42
34	1	1	1	0	34	37	42
35	1	1	1	0	35	38	43
36	1	1	1	0	36	39	43
37	1	1	1	0	37	40	44
38	1	1	1	0	38	41	44
39	1	1	1	0	39	42	45
40	1	1	1	0	40	43	45

ELEM	MAT	TYP	REL	ESYS	NODES		
30	1	1	1	0	43	44	47
31	1	1	1	0	45	45	49
32	1	1	1	0	46	47	49
33	1	4	1	0	101	102	109
34	1	4	1	0	102	103	110
35	1	4	1	0	103	104	111
36	1	4	1	0	104	105	112
37	1	4	1	0	105	106	113
38	1	4	1	0	106	107	114
39	1	4	1	0	106	107	116
40	1	4	1	0	109	110	117
41	1	4	1	0	110	111	119
43	1	4	1	0	112	113	120
44	1	4	1	0	113	114	121
51	1	6	1	0	122	123	129
52	1	6	1	0	123	124	131
57	1	6	1	0	129	130	137
58	1	6	1	0	130	131	139
63	1	4	1	0	136	137	144
64	1	4	1	0	137	138	145

ELEM	MAT	TYP	REL	ESYS	NODES		
60	1	4	1	0	143	144	151
70	1	6	1	0	144	145	152
75	1	4	1	0	150	151	158
76	1	6	1	0	151	152	159
81	1	4	1	0	157	158	165
82	1	6	1	0	159	159	164
87	1	4	1	0	164	165	172
88	1	6	1	0	165	166	173
95	1	2	2	0	49	53	
96	1	2	2	0	53	55	
97	1	2	2	0	55	57	
98	1	2	2	0	57	59	

99	1	2	2	0	59	61
100	1	2	2	0	61	63
101	1	2	2	0	63	65
102	1	2	2	0	65	67
103	1	2	2	0	67	69
104	1	2	2	0	69	71
105	1	2	2	0	71	73
106	1	2	2	0	73	75

ELEM	MAT	TYP	REL	ESTS	NODES	
------	-----	-----	-----	------	-------	--

107	1	2	2	0	75	77
108	1	2	2	0	77	79
109	1	2	2	0	79	81
110	1	2	2	0	81	83
111	1	2	2	0	83	85
112	1	2	2	0	85	87
113	1	2	2	0	87	89
114	1	2	2	0	89	91
115	1	2	2	0	91	93
116	1	2	2	0	93	100
117	1	2	2	0	100	121
118	1	2	2	0	101	122
119	1	2	2	0	102	123
120	1	2	2	0	103	124
121	1	2	2	0	104	125
122	1	2	2	0	100	126
123	1	2	2	0	106	127
124	1	2	2	0	107	128
125	1	2	22	0	53	54
126	1	2	22	0	53	54

ELEM	MAT	TYP	REL	ESTS	NODES	
------	-----	-----	-----	------	-------	--

127	1	2	22	0	57	58
128	1	2	22	0	59	60
129	1	2	22	0	61	62
130	1	2	22	0	63	64
131	1	2	22	0	65	66
132	1	2	22	0	67	68
133	1	2	22	0	69	70
134	1	2	22	0	71	72
135	1	2	22	0	73	74
136	1	2	22	0	75	76
137	1	2	22	0	77	78
138	1	2	22	0	79	80
139	1	2	22	0	81	82
140	1	2	22	0	83	84
141	1	2	22	0	85	86
142	1	2	22	0	87	88
143	1	2	22	0	89	90
144	1	2	22	0	91	92
145	1	2	21	0	93	94
146	1	2	23	0	41	94

ELEM	MAT	TYP	REL	ESTS	NODES	
------	-----	-----	-----	------	-------	--

147	1	2	23	0	54	54
148	1	2	23	0	56	58
149	1	2	23	0	58	60
150	1	2	23	0	60	62
151	1	2	23	0	62	64
152	1	2	23	0	64	66
153	1	2	23	0	66	68
154	1	2	23	0	68	70
155	1	2	23	0	70	72
156	1	2	23	0	72	74
157	1	2	23	0	74	76
158	1	2	23	0	76	78
159	1	2	23	0	78	80
160	1	2	23	0	80	82
161	1	2	23	0	82	84
162	1	2	23	0	84	86
163	1	2	23	0	86	88

164	1	2	23	0	98	98
165	1	2	23	0	98	92
166	1	2	23	0	92	94

ELEM	HAZ	TYP	REL	EXYS	NODES	
167	1	2	21	0	49	41
168	1	2	21	0	41	31
169	1	2	21	0	31	36
170	1	2	21	0	36	37
171	1	2	22	0	5	37
172	1	2	24	0	46	49
173	1	2	26	0	10	5
174	1	4	4	0	13	31
175	1	4	25	0	14	12
176	2	3	3	0	124	15
177	1	1	1	0	201	221 232 202
178	1	1	1	0	202	222 223 203
179	1	1	1	0	203	223 224 204
180	1	1	1	0	204	224 225 205
181	1	1	1	0	205	225 226 206
182	1	1	1	0	206	226 227 207
183	1	1	1	0	207	227 228 208
184	1	1	1	0	208	228 229 209
185	1	1	1	0	209	229 230 210
186	1	1	1	0	210	230 231 211

ELEM	HAZ	TYP	REL	EXYS	NODES	
187	1	1	1	0	211	231 232 212
188	1	1	1	0	212	232 233 213
189	1	1	1	0	213	233 234 214
190	1	1	1	0	214	234 235 215
191	1	1	1	0	215	235 236 216
192	1	1	1	0	216	236 237 217
193	1	1	1	0	231	241 222 222
194	1	1	1	0	222	241 242 242
195	1	1	1	0	222	242 223 223
196	1	1	1	0	223	242 224 224
197	1	1	1	0	224	242 243 243
198	1	1	1	0	224	243 225 225
199	1	1	1	0	225	243 226 226
200	1	1	1	0	226	243 244 244
201	1	1	1	0	226	244 227 227
202	1	1	1	0	227	244 228 228
203	1	1	1	0	228	244 245 245
204	1	1	1	0	228	245 229 229
205	1	1	1	0	229	245 230 230
206	1	1	1	0	230	245 246 246

ELEM	HAZ	TYP	REL	EXYS	NODES	
207	1	1	1	0	230	246 231 231
208	1	1	1	0	231	246 232 232
209	1	1	1	0	232	246 247 247
210	1	1	1	0	232	247 233 233
211	1	1	1	0	233	247 234 234
212	1	1	1	0	234	247 248 248
213	1	1	1	0	234	248 235 235
214	1	1	1	0	235	248 236 236
215	1	1	1	0	236	248 22 22
216	1	1	1	0	236	22 237 237
217	1	1	1	0	241	3 242 242
218	1	1	1	0	242	3 8 8
219	1	1	1	0	242	8 243 243
220	1	1	1	0	243	8 244 244
221	1	1	1	0	244	8 13 13
222	1	1	1	0	244	13 245 245
223	1	1	1	0	245	13 246 246
224	1	1	1	0	246	13 14 14
225	1	1	1	0	246	14 247 247
226	1	1	1	0	247	14 248 248

ELEM	HAZ	TYP	REL	EXYS	NODES	
------	-----	-----	-----	------	-------	--

227	1	1	1	0	300	301	302	303
228	1	6	1	0	301	302	322	321
229	1	6	1	0	302	303	323	322
230	1	6	1	0	303	304	324	323
231	1	6	1	0	304	305	325	324
232	1	6	1	0	305	306	326	325
233	1	6	1	0	306	307	327	326
234	1	6	1	0	307	308	328	327
235	1	4	1	0	308	309	329	328
236	1	6	1	0	309	310	330	329
237	1	4	1	0	310	311	331	330
238	1	6	1	0	311	312	332	331
239	1	4	1	0	312	313	333	332
240	1	6	1	0	313	314	334	333
241	1	4	1	0	314	315	335	334
242	1	6	1	0	315	316	336	335
243	1	6	1	0	316	317	337	336
244	1	6	1	0	321	301	119	119
245	1	6	1	0	321	341	322	322
246	1	6	1	0	322	341	342	342

ELIN	MAT	TYP	REL	ESYS	MEMBER			
247	1	4	1	0	322	342	323	323
248	1	6	1	0	323	342	324	324
249	1	6	1	0	324	342	343	343
250	1	4	1	0	324	343	325	325
251	1	6	1	0	325	343	326	326
252	1	4	1	0	326	343	344	344
253	1	4	1	0	326	344	327	327
254	1	6	1	0	327	344	328	328
255	1	6	1	0	328	344	345	345
256	1	4	1	0	328	345	329	329
257	1	6	1	0	329	345	330	330
258	1	4	1	0	330	345	346	346
259	1	6	1	0	330	346	331	331
260	1	4	1	0	331	346	332	332
261	1	6	1	0	332	346	347	347
262	1	6	1	0	332	347	333	333
263	1	6	1	0	347	333	334	334
264	1	4	1	0	347	334	335	348
265	1	6	1	0	348	335	336	336
266	1	4	1	0	348	336	337	349

ELIN	MAT	TYP	REL	ESYS	MEMBER			
267	1	6	1	0	341	111	321	321
268	1	6	1	0	321	111	112	112
269	1	4	1	0	321	112	110	110
270	1	6	1	0	117	341	342	342
271	1	4	1	0	117	342	343	352
272	1	6	1	0	352	343	344	126
273	1	6	1	0	116	344	345	345
274	1	6	1	0	124	345	346	346
275	1	6	1	0	124	346	131	131
276	1	6	1	0	131	346	347	347
277	1	6	1	0	131	347	348	130
278	1	6	1	0	138	348	349	145
279	1	6	1	0	116	117	352	351
280	1	6	1	0	115	116	351	350
281	1	6	1	0	351	352	126	123
282	1	6	1	0	350	131	122	122
283	2	8	4	0	301	201		
284	2	5	6	0	302	202		
285	2	8	4	0	303	203		
286	2	5	6	0	304	204		

ELIN	MAT	TYP	REL	ESYS	MEMBER			
287	2	8	6	0	305	205		
288	2	5	6	0	306	206		
289	2	8	6	0	307	207		
290	2	5	6	0	308	208		

291	2	5	4	0	309	209
292	2	5	4	0	310	210
293	2	5	4	0	311	211
294	2	5	4	0	312	212
295	2	5	4	0	313	213
296	2	5	4	0	314	214
297	2	5	4	0	315	215
298	2	5	4	0	316	216
299	2	5	4	0	317	217

LIST ALL SELECTED NODE DISTS = 0

NODE	X	Y	Z	THX1	THY1	THZ1
2	24.125	1.4100	0.00000E+00	0.00	0.00	0.00
4	24.125	2.1150	0.00000E+00	0.00	0.00	0.00
5	24.125	2.8200	0.00000E+00	0.00	0.00	0.00
9	23.125	1.4100	0.00000E+00	0.00	0.00	0.00
10	23.125	2.1150	0.00000E+00	0.00	0.00	0.00
12	23.125	2.8200	0.00000E+00	0.00	0.00	0.00
14	22.125	2.1150	0.00000E+00	0.00	0.00	0.00
15	22.125	2.8200	0.00000E+00	0.00	0.00	0.00
18	20.875	1.4100	0.00000E+00	0.00	0.00	0.00
19	20.875	2.1150	0.00000E+00	0.00	0.00	0.00
20	20.875	2.8200	0.00000E+00	0.00	0.00	0.00
22	19.540	1.1300	0.00000E+00	0.00	0.00	0.00
23	19.543	1.6933	0.00000E+00	0.00	0.00	0.00
24	19.727	2.2567	0.00000E+00	0.00	0.00	0.00
25	19.810	2.8200	0.00000E+00	0.00	0.00	0.00
27	18.710	1.9725	0.00000E+00	0.00	0.00	0.00
28	18.936	2.4006	0.00000E+00	0.00	0.00	0.00
29	19.155	2.8286	0.00000E+00	0.00	0.00	0.00
30	19.375	3.2567	0.00000E+00	0.00	0.00	0.00

NODE	X	Y	Z	THX1	THY1	THZ1
31	22.125	5.6340	0.00000E+00	0.00	0.00	0.00
32	17.875	2.8150	0.00000E+00	0.00	0.00	0.00
33	18.329	3.1078	0.00000E+00	0.00	0.00	0.00
34	18.583	3.4006	0.00000E+00	0.00	0.00	0.00
35	18.537	3.6933	0.00000E+00	0.00	0.00	0.00
36	26.430	5.6320	0.00000E+00	0.00	0.00	0.00
37	26.434	2.8200	0.00000E+00	0.00	0.00	0.00
38	17.875	3.5050	0.00000E+00	0.00	0.00	0.00
39	18.184	3.8175	0.00000E+00	0.00	0.00	0.00
40	18.540	4.1300	0.00000E+00	0.00	0.00	0.00
41	19.540	5.6320	0.00000E+00	0.00	0.00	0.00
42	17.875	4.7500	0.00000E+00	0.00	0.00	0.00
43	18.186	4.7500	0.00000E+00	0.00	0.00	0.00
44	18.540	4.7500	0.00000E+00	0.00	0.00	0.00
45	17.940	4.9450	0.00000E+00	0.00	0.00	0.00
46	18.159	4.9450	0.00000E+00	0.00	0.00	0.00
47	18.448	4.9450	0.00000E+00	0.00	0.00	0.00
48	17.940	5.6320	0.00000E+00	0.00	0.00	0.00
49	18.199	5.6320	0.00000E+00	0.00	0.00	0.00
50	18.448	5.6320	0.00000E+00	0.00	0.00	0.00

NODE	X	Y	Z	THX1	THY1	THZ1
53	18.199	7.7920	0.00000E+00	0.00	0.00	0.00
54	19.540	7.7920	0.00000E+00	0.00	0.00	0.00
55	18.199	10.042	0.00000E+00	0.00	0.00	0.00
56	19.500	10.042	0.00000E+00	0.00	0.00	0.00
57	18.199	12.292	0.00000E+00	0.00	0.00	0.00
58	19.500	12.292	0.00000E+00	0.00	0.00	0.00
59	18.199	14.542	0.00000E+00	0.00	0.00	0.00
60	19.500	14.542	0.00000E+00	0.00	0.00	0.00
61	18.199	16.792	0.00000E+00	0.00	0.00	0.00
62	19.500	16.792	0.00000E+00	0.00	0.00	0.00
63	18.199	19.042	0.00000E+00	0.00	0.00	0.00
64	19.500	19.042	0.00000E+00	0.00	0.00	0.00
65	18.199	21.292	0.00000E+00	0.00	0.00	0.00
66	19.500	21.292	0.00000E+00	0.00	0.00	0.00
67	18.199	23.542	0.00000E+00	0.00	0.00	0.00
68	19.500	23.542	0.00000E+00	0.00	0.00	0.00

69	18.190	25.792	0.00000E+00	0.00	0.00	0.00
70	19.508	25.792	0.00000E+00	0.00	0.00	0.00
71	18.190	28.042	0.00000E+00	0.00	0.00	0.00
72	19.508	28.042	0.00000E+00	0.00	0.00	0.00

MODE	X	Y	Z	TWR1	TWR2	TWR3
73	18.190	30.292	0.00000E+00	0.00	0.00	0.00
74	19.508	30.292	0.00000E+00	0.00	0.00	0.00
75	18.190	32.842	0.00000E+00	0.00	0.00	0.00
76	19.508	32.842	0.00000E+00	0.00	0.00	0.00
77	18.190	34.792	0.00000E+00	0.00	0.00	0.00
78	19.508	34.792	0.00000E+00	0.00	0.00	0.00
79	18.190	37.042	0.00000E+00	0.00	0.00	0.00
80	19.508	37.042	0.00000E+00	0.00	0.00	0.00
81	18.190	39.292	0.00000E+00	0.00	0.00	0.00
82	19.508	39.292	0.00000E+00	0.00	0.00	0.00
83	18.190	41.542	0.00000E+00	0.00	0.00	0.00
84	19.508	41.542	0.00000E+00	0.00	0.00	0.00
85	18.190	43.792	0.00000E+00	0.00	0.00	0.00
86	19.508	43.792	0.00000E+00	0.00	0.00	0.00
87	18.190	46.042	0.00000E+00	0.00	0.00	0.00
88	19.508	46.042	0.00000E+00	0.00	0.00	0.00
89	18.190	48.292	0.00000E+00	0.00	0.00	0.00
90	19.508	48.292	0.00000E+00	0.00	0.00	0.00
91	18.190	50.542	0.00000E+00	0.00	0.00	0.00
92	19.508	50.542	0.00000E+00	0.00	0.00	0.00

MODE	X	Y	Z	TWR1	TWR2	TWR3
93	18.190	52.790	0.00000E+00	0.00	0.00	0.00
94	19.508	52.790	0.00000E+00	0.00	0.00	0.00
101	26.625	-3.5000	0.00000E+00	0.00	0.00	0.00
102	26.625	-2.7500	0.00000E+00	0.00	0.00	0.00
103	26.625	-2.0000	0.00000E+00	0.00	0.00	0.00
104	26.625	-1.0000	0.00000E+00	0.00	0.00	0.00
105	26.625	0.00000E+00	0.00000E+00	0.00	0.00	0.00
106	26.625	1.2500	0.00000E+00	0.00	0.00	0.00
107	26.625	2.4300	0.00000E+00	0.00	0.00	0.00
108	26.625	-3.5000	0.00000E+00	0.00	0.00	0.00
109	26.625	-2.7500	0.00000E+00	0.00	0.00	0.00
110	26.625	-2.0000	0.00000E+00	0.00	0.00	0.00
111	26.625	-1.0000	0.00000E+00	0.00	0.00	0.00
112	26.625	0.00000E+00	0.00000E+00	0.00	0.00	0.00
113	26.625	1.2500	0.00000E+00	0.00	0.00	0.00
114	26.625	2.4300	0.00000E+00	0.00	0.00	0.00
115	26.625	-3.5000	0.00000E+00	0.00	0.00	0.00
116	26.625	-2.7500	0.00000E+00	0.00	0.00	0.00
117	26.625	-2.0000	0.00000E+00	0.00	0.00	0.00
118	26.625	-1.0000	0.00000E+00	0.00	0.00	0.00

MODE	X	Y	Z	TWR1	TWR2	TWR3
119	24.150	0.00000E+00	0.00000E+00	0.00	0.00	0.00
120	24.150	1.2500	0.00000E+00	0.00	0.00	0.00
121	24.150	2.4300	0.00000E+00	0.00	0.00	0.00
122	22.125	-3.5000	0.00000E+00	0.00	0.00	0.00
123	22.125	-3.0000	0.00000E+00	0.00	0.00	0.00
124	22.125	-2.3700	0.00000E+00	0.00	0.00	0.00
129	20.875	-3.5000	0.00000E+00	0.00	0.00	0.00
130	20.875	-2.7500	0.00000E+00	0.00	0.00	0.00
131	20.875	-2.0000	0.00000E+00	0.00	0.00	0.00
136	20.000	-3.5000	0.00000E+00	0.00	0.00	0.00
137	20.000	-2.7500	0.00000E+00	0.00	0.00	0.00
138	20.000	-2.0000	0.00000E+00	0.00	0.00	0.00
143	19.545	-3.5000	0.00000E+00	0.00	0.00	0.00
144	19.545	-2.7500	0.00000E+00	0.00	0.00	0.00
145	19.545	-2.0000	0.00000E+00	0.00	0.00	0.00
150	14.059	-3.5000	0.00000E+00	0.00	0.00	0.00
151	14.059	-2.7500	0.00000E+00	0.00	0.00	0.00
152	14.059	-2.0000	0.00000E+00	0.00	0.00	0.00
157	9.7726	-3.5000	0.00000E+00	0.00	0.00	0.00
158	9.7726	-2.7500	0.00000E+00	0.00	0.00	0.00

MODE	X	Y	Z	TWR1	TWR2	TWR3
159	9.7726	-2.0000	0.00000E+00	0.00	0.00	0.00
164	4.8864	-3.5000	0.00000E+00	0.00	0.00	0.00

148	4.8844	-2.7500	0.00000E+00	0.00	0.00	0.00
166	4.8844	-2.8000	0.00000E+00	0.00	0.00	0.00
171	0.20000E+03	-3.5000	0.00000E+00	0.00	0.00	0.00
172	0.20000E+03	-2.7500	0.00000E+00	0.00	0.00	0.00
173	0.20000E+03	-2.0000	0.00000E+00	0.00	0.00	0.00
180	10.790	54.890	0.00000E+00	0.00	0.00	0.00
181	18.040	55.170	0.00000E+00	0.00	0.00	0.00
182	17.713	55.905	0.00000E+00	0.00	0.00	0.00
183	17.958	56.673	0.00000E+00	0.00	0.00	0.00
184	16.423	57.182	0.00000E+00	0.00	0.00	0.00
188	12.823	58.899	0.00000E+00	0.00	0.00	0.00
186	0.4473	60.163	0.00000E+00	0.00	0.00	0.00
187	4.25370	60.897	0.00000E+00	0.00	0.00	0.00
188	0.140270	61.150	0.00000E+00	0.00	0.00	0.00
201	23.991	0.00000E+00	0.00000E+00	0.00	0.00	0.00
202	23.990	0.00000E+00	0.00000E+00	0.00	0.00	0.00
203	23.623	0.00000E+00	0.00000E+00	0.00	0.00	0.00
204	23.379	0.00000E+00	0.00000E+00	0.00	0.00	0.00

MODE	X	Y	Z	THX	THY	THZ
205	23.125	0.00000E+00	0.00000E+00	0.00	0.00	0.00
206	22.878	0.00000E+00	0.00000E+00	0.00	0.00	0.00
207	22.623	0.00000E+00	0.00000E+00	0.00	0.00	0.00
208	22.375	0.00000E+00	0.00000E+00	0.00	0.00	0.00
209	22.123	0.00000E+00	0.00000E+00	0.00	0.00	0.00
210	21.873	0.00000E+00	0.00000E+00	0.00	0.00	0.00
211	21.500	0.00000E+00	0.00000E+00	0.00	0.00	0.00
212	21.188	0.00000E+00	0.00000E+00	0.00	0.00	0.00
213	20.873	0.00000E+00	0.00000E+00	0.00	0.00	0.00
214	20.546	0.00000E+00	0.00000E+00	0.00	0.00	0.00
215	20.218	0.00000E+00	0.00000E+00	0.00	0.00	0.00
216	20.000	0.00000E+00	0.00000E+00	0.00	0.00	0.00
217	19.560	0.00000E+00	0.00000E+00	0.00	0.00	0.00
221	24.858	0.25000	0.00000E+00	0.00	0.00	0.00
222	23.623	0.27575	0.00000E+00	0.00	0.00	0.00
223	23.597	0.30150	0.00000E+00	0.00	0.00	0.00
224	23.358	0.32725	0.00000E+00	0.00	0.00	0.00
225	23.125	0.35300	0.00000E+00	0.00	0.00	0.00
226	22.873	0.35300	0.00000E+00	0.00	0.00	0.00
227	22.623	0.35300	0.00000E+00	0.00	0.00	0.00

MODE	Y	Y	Z	THY	THZ	THZ
228	22.379	0.33300	0.00000E+00	0.00	0.00	0.00
229	22.125	0.33300	0.00000E+00	0.00	0.00	0.00
230	21.873	0.33300	0.00000E+00	0.00	0.00	0.00
231	21.500	0.33300	0.00000E+00	0.00	0.00	0.00
232	21.188	0.33300	0.00000E+00	0.00	0.00	0.00
233	20.873	0.33300	0.00000E+00	0.00	0.00	0.00
234	20.546	0.40600	0.00000E+00	0.00	0.00	0.00
235	20.218	0.43900	0.00000E+00	0.00	0.00	0.00
256	19.880	0.51200	0.00000E+00	0.00	0.00	0.00
257	19.560	0.56500	0.00000E+00	0.00	0.00	0.00
261	24.125	0.34000	0.00000E+00	0.00	0.00	0.00
262	23.623	0.48250	0.00000E+00	0.00	0.00	0.00
263	23.125	0.79500	0.00000E+00	0.00	0.00	0.00
264	22.623	0.79500	0.00000E+00	0.00	0.00	0.00
265	22.125	0.79500	0.00000E+00	0.00	0.00	0.00
266	21.500	0.79500	0.00000E+00	0.00	0.00	0.00
267	20.873	0.79500	0.00000E+00	0.00	0.00	0.00
268	20.218	0.91750	0.00000E+00	0.00	0.00	0.00
301	23.991	0.00000E+00	0.00000E+00	0.00	0.00	0.00
302	23.800	0.00000E+00	0.00000E+00	0.00	0.00	0.00

MODE	X	Y	Z	THX	THY	THZ
303	23.623	0.00000E+00	0.00000E+00	0.00	0.00	0.00
304	23.375	0.00000E+00	0.00000E+00	0.00	0.00	0.00
305	23.125	0.00000E+00	0.00000E+00	0.00	0.00	0.00
306	22.873	0.00000E+00	0.00000E+00	0.00	0.00	0.00
307	22.623	0.00000E+00	0.00000E+00	0.00	0.00	0.00
308	22.375	0.00000E+00	0.00000E+00	0.00	0.00	0.00
309	22.125	0.00000E+00	0.00000E+00	0.00	0.00	0.00
310	21.873	0.00000E+00	0.00000E+00	0.00	0.00	0.00
311	21.500	0.00000E+00	0.00000E+00	0.00	0.00	0.00
312	21.188	0.00000E+00	0.00000E+00	0.00	0.00	0.00

313	20.875	0.0000E+00	0.0000E+00	0.00	0.00	0.00
314	20.544	0.0000E+00	0.0000E+00	0.00	0.00	0.00
315	20.210	0.0000E+00	0.0000E+00	0.00	0.00	0.00
316	20.000	0.0000E+00	0.0000E+00	0.00	0.00	0.00
317	19.540	0.0000E+00	0.0000E+00	0.00	0.00	0.00
321	24.150	-0.50000	0.0000E+00	0.00	0.00	0.00
322	23.800	-0.50000	0.0000E+00	0.00	0.00	0.00
323	23.625	-0.50000	0.0000E+00	0.00	0.00	0.00
334	23.375	-0.50000	0.0000E+00	0.00	0.00	0.00
325	23.125	-0.50000	0.0000E+00	0.00	0.00	0.00

NODE	X	Y	Z	TRXZ	TRYZ	TRXZ
326	22.875	-0.50000	0.0000E+00	0.00	0.00	0.00
327	22.625	-0.50000	0.0000E+00	0.00	0.00	0.00
328	22.375	-0.50000	0.0000E+00	0.00	0.00	0.00
329	22.125	-0.50000	0.0000E+00	0.00	0.00	0.00
330	21.875	-0.50000	0.0000E+00	0.00	0.00	0.00
331	21.500	-0.50000	0.0000E+00	0.00	0.00	0.00
332	21.100	-0.50000	0.0000E+00	0.00	0.00	0.00
333	20.875	-0.50000	0.0000E+00	0.00	0.00	0.00
334	20.544	-0.50000	0.0000E+00	0.00	0.00	0.00
335	20.210	-0.50000	0.0000E+00	0.00	0.00	0.00
336	20.000	-0.50000	0.0000E+00	0.00	0.00	0.00
337	19.540	-0.50000	0.0000E+00	0.00	0.00	0.00
341	24.150	-1.00000	0.0000E+00	0.00	0.00	0.00
342	23.830	-1.00000	0.0000E+00	0.00	0.00	0.00
343	23.125	-1.00000	0.0000E+00	0.00	0.00	0.00
344	22.625	-1.00000	0.0000E+00	0.00	0.00	0.00
345	22.125	-1.00000	0.0000E+00	0.00	0.00	0.00
346	21.500	-1.00000	0.0000E+00	0.00	0.00	0.00
347	20.875	-1.00000	0.0000E+00	0.00	0.00	0.00
348	20.000	-1.00000	0.0000E+00	0.00	0.00	0.00

NODE	X	Y	Z	TRXZ	TRYZ	TRXZ
349	19.545	-1.00000	0.0000E+00	0.00	0.00	0.00
350	23.137	-3.50000	0.0000E+00	0.00	0.00	0.00
351	23.137	-2.87500	0.0000E+00	0.00	0.00	0.00
352	23.137	-2.18500	0.0000E+00	0.00	0.00	0.00

LIST ALL MATERIALS PROPERTY= ALL

PROPERTY TABLE MARY MAT= 1 NUM. POINTS= 2
 TEMPERATURE DATA TEMPERATURE DATA
 -9999.0 0.30000 9999.0 0.30000

PROPERTY TABLE BX MAT= 1 NUM. POINTS= 15
 TEMPERATURE DATA TEMPERATURE DATA
 -40.000 0.28900E+08 70.000 0.28300E+08
 100.00 0.28100E+08 200.00 0.27600E+08
 300.00 0.27800E+08 400.00 0.26500E+08
 500.00 0.25800E+08 600.00 0.25300E+08
 700.00 0.24800E+08 800.00 0.24100E+08
 900.00 0.23900E+08 1000.0 0.23200E+08
 1100.0 0.22400E+08 1200.0 0.21300E+08
 1300.0 0.20500E+08

PROPERTY TABLE ALPH MAT= 1 NUM. POINTS= 15
 TEMPERATURE DATA TEMPERATURE DATA
 -40.000 0.81500E-05 70.000 0.81600E-05
 100.00 0.82500E-05 200.00 0.82700E-05
 300.00 0.80800E-05 400.00 0.81900E-05
 500.00 0.83700E-05 600.00 0.84300E-05
 700.00 8.9600E-05 800.00 8.98200E-05
 900.00 0.10060E-04 1000.0 0.10300E-04
 1100.0 0.10350E-04 1200.0 0.10400E-04
 1300.0 0.10490E-04

PROPERTY TABLE EX MAT= 2 NUM. POINTS= 7
 TEMPERATURE DATA TEMPERATURE DATA
 -40.000 8.28400E+05 70.000 8.27900E+05
 100.00 8.27600E+05 200.00 8.27100E+05
 300.00 8.26700E+05 400.00 8.26100E+05
 500.00 8.25700E+05

PROPERTY TABLE ALPH MAT= 2 MIN. POINT= 7
 TEMPERATURE DATA TEMPERATURE DATA
 -40.00 0.51400E+05 70.00 0.42800E+05
 00.00 0.62700E+05 200.00 0.23400E+05
 300.00 0.57000E+05 400.00 0.49000E+05
 500.00 0.71000E+05

TIME= 0.00000E+00 ITER= 10
 ETAP= LSTP= -1 ITER= 0

UNIFORM TEMPERATURE= 70.000 (TIME= 70.000)
 BOUNDARY CONDITIONS STEPPED DUE TO STATIC CONVERGENCE OPTION
 PLASTIC CONVERG. CRITERION= 0.0100
 CREEP OPTIMUM. CRITERION= 0.1000
 LARGE DEFL. CONVERG. CRITERION= 0.501000
 DISPLACEMENT LIMIT= 0.00000E+00

NPRINT= 9990 NPOST= 10 REACTION PRINT FREQ= 9990
 Q1SP. POST DATA FREQ= 10 REACT. POST DATA FREQ= 10

ELEMENT PRINT AND POST DATA FREQUENCIES

TYPE	STIFF	STRESS	FORCE	STRESS	DATA	DATA	FORCE
NO.	PRINT	PRINT	DATA	LEVEL	DATA		DATA
1	42	99900	99900	10	3		10
2	51	99900	99900	10	3		10
3	1	99900	99900	10	3		10
4	3	99900	99900	10	3		10
5	12	99900	99900	10	3		10
6	42	99900	99900	10	3		10

LOADS INPUT FILE= 20 LOADS OUTPUT FILE= 23

ALL ANALYSIS DATA WILL BE WRITTEN INTO FILE27

LIST DISPLACEMENTS FOR ALL SELECTED NODES

NODE	LABEL	DISP	CDISP
3	U2	0.00000000E+00	0.00000000E+00
4	U2	0.00000000E+00	0.00000000E+00
5	U2	0.00000000E+00	0.00000000E+00
8	U2	0.00000000E+00	0.00000000E+00
9	U2	0.00000000E+00	0.00000000E+00
10	U2	0.00000000E+00	0.00000000E+00
13	U2	0.00000000E+00	0.00000000E+00
14	U2	0.00000000E+00	0.00000000E+00
15	U2	0.00000000E+00	0.00000000E+00
16	U2	0.00000000E+00	0.00000000E+00
19	U2	0.00000000E+00	0.00000000E+00
20	U2	0.00000000E+00	0.00000000E+00
22	U2	0.00000000E+00	0.00000000E+00
23	U2	0.00000000E+00	0.00000000E+00
24	U2	0.00000000E+00	0.00000000E+00
25	U2	0.00000000E+00	0.00000000E+00
27	U2	0.00000000E+00	0.00000000E+00
28	U2	0.00000000E+00	0.00000000E+00
29	U2	0.00000000E+00	0.00000000E+00
30	U2	0.00000000E+00	0.00000000E+00

NODE	LABEL	DISP	CDISP
31	U2	0.00000000E+00	0.00000000E+00
32	U2	0.00000000E+00	0.00000000E+00
33	U2	0.00000000E+00	0.00000000E+00
34	U2	0.00000000E+00	0.00000000E+00
35	U2	0.00000000E+00	0.00000000E+00
36	U2	0.00000000E+00	0.00000000E+00
37	U2	0.00000000E+00	0.00000000E+00
38	U2	0.00000000E+00	0.00000000E+00
39	U2	0.00000000E+00	0.00000000E+00
40	U2	0.00000000E+00	0.00000000E+00
41	U2	0.00000000E+00	0.00000000E+00
42	U2	0.00000000E+00	0.00000000E+00
43	U2	0.00000000E+00	0.00000000E+00
44	U2	0.00000000E+00	0.00000000E+00
45	U2	0.00000000E+00	0.00000000E+00
46	U2	0.00000000E+00	0.00000000E+00

```

47 UZ 0.00000000E+00 0.00000000E+00
48 UZ 0.00000000E+00 0.00000000E+00
49 UZ 0.00000000E+00 0.00000000E+00
50 UZ 0.00000000E+00 0.00000000E+00

NODE LABEL D1# C1#P
53 UZ 0.00000000E+00 0.00000000E+00
54 UZ 0.00000000E+00 0.00000000E+00
55 UZ 0.00000000E+00 0.00000000E+00
56 UZ 0.00000000E+00 0.00000000E+00
57 UZ 0.00000000E+00 0.00000000E+00
58 UZ 0.00000000E+00 0.00000000E+00
59 UZ 0.00000000E+00 0.00000000E+00
60 UZ 0.00000000E+00 0.00000000E+00
61 UZ 0.00000000E+00 0.00000000E+00
62 UZ 0.00000000E+00 0.00000000E+00
63 UZ 0.00000000E+00 0.00000000E+00
64 UZ 0.00000000E+00 0.00000000E+00
65 UZ 0.00000000E+00 0.00000000E+00
66 UZ 0.00000000E+00 0.00000000E+00
67 UZ 0.00000000E+00 0.00000000E+00
68 UZ 0.00000000E+00 0.00000000E+00
69 UZ 0.00000000E+00 0.00000000E+00
70 UZ 0.00000000E+00 0.00000000E+00
71 UZ 0.00000000E+00 0.00000000E+00
72 UZ 0.00000000E+00 0.00000000E+00

NODE LABEL D1# C1#P
73 UZ 0.00000000E+00 0.00000000E+00
74 UZ 0.00000000E+00 0.00000000E+00
75 UZ 0.00000000E+00 0.00000000E+00
76 UZ 0.00000000E+00 0.00000000E+00
77 UZ 0.00000000E+00 0.00000000E+00
78 UZ 0.00000000E+00 0.00000000E+00
79 UZ 0.00000000E+00 0.00000000E+00
80 UZ 0.00000000E+00 0.00000000E+00
81 UZ 0.00000000E+00 0.00000000E+00
82 UZ 0.00000000E+00 0.00000000E+00
83 UZ 0.00000000E+00 0.00000000E+00
84 UZ 0.00000000E+00 0.00000000E+00
85 UZ 0.00000000E+00 0.00000000E+00
86 UZ 0.00000000E+00 0.00000000E+00
87 UZ 0.00000000E+00 0.00000000E+00
88 UZ 0.00000000E+00 0.00000000E+00
89 UZ 0.00000000E+00 0.00000000E+00
90 UZ 0.00000000E+00 0.00000000E+00
91 UZ 0.00000000E+00 0.00000000E+00
92 UZ 0.00000000E+00 0.00000000E+00

NODE LABEL D1# C1#P
93 UZ 0.00000000E+00 0.00000000E+00
94 UZ 0.00000000E+00 0.00000000E+00
101 UZ 0.00000000E+00 0.00000000E+00
102 UZ 0.00000000E+00 0.00000000E+00
103 UZ 0.00000000E+00 0.00000000E+00
104 UZ 0.00000000E+00 0.00000000E+00
105 UZ 0.00000000E+00 0.00000000E+00
106 UZ 0.00000000E+00 0.00000000E+00
107 UZ 0.00000000E+00 0.00000000E+00
108 UZ 0.00000000E+00 0.00000000E+00
109 UZ 0.00000000E+00 0.00000000E+00
110 UZ 0.00000000E+00 0.00000000E+00
111 UZ 0.00000000E+00 0.00000000E+00
112 UZ 0.00000000E+00 0.00000000E+00
113 UZ 0.00000000E+00 0.00000000E+00
114 UZ 0.00000000E+00 0.00000000E+00
115 UZ 0.00000000E+00 0.00000000E+00
116 UZ 0.00000000E+00 0.00000000E+00
117 UZ 0.00000000E+00 0.00000000E+00
118 UZ 0.00000000E+00 0.00000000E+00

NODE LABEL D1# C1#P
119 UZ 0.00000000E+00 0.00000000E+00
120 UZ 0.00000000E+00 0.00000000E+00

```

121	UR	0.00000000E+00	0.00000000E+00
122	UR	0.00000000E+00	0.00000000E+00
123	UR	0.00000000E+00	0.00000000E+00
124	UR	0.00000000E+00	0.00000000E+00
129	UR	0.00000000E+00	0.00000000E+00
130	UR	0.00000000E+00	0.00000000E+00
131	UR	0.00000000E+00	0.00000000E+00
136	UR	0.00000000E+00	0.00000000E+00
137	UR	0.00000000E+00	0.00000000E+00
138	UR	0.00000000E+00	0.00000000E+00
143	UR	0.00000000E+00	0.00000000E+00
144	UR	0.00000000E+00	0.00000000E+00
145	UR	0.00000000E+00	0.00000000E+00
150	UR	0.00000000E+00	0.00000000E+00
151	UR	0.00000000E+00	0.00000000E+00
152	UR	0.00000000E+00	0.00000000E+00
157	UR	0.00000000E+00	0.00000000E+00
158	UR	0.00000000E+00	0.00000000E+00

NODE	LABEL	BISP	CBISP
159	UR	0.00000000E+00	0.00000000E+00
164	UR	0.00000000E+00	0.00000000E+00
165	UR	0.00000000E+00	0.00000000E+00
166	UR	0.00000000E+00	0.00000000E+00
171	UR	0.00000000E+00	0.00000000E+00
172	UR	0.00000000E+00	0.00000000E+00
173	UR	0.00000000E+00	0.00000000E+00
180	UR	0.00000000E+00	0.00000000E+00
181	UR	0.00000000E+00	0.00000000E+00
182	UR	0.00000000E+00	0.00000000E+00
183	UR	0.00000000E+00	0.00000000E+00
194	UR	0.00000000E+00	0.00000000E+00
185	UR	0.00000000E+00	0.00000000E+00
196	UR	0.00000000E+00	0.00000000E+00
197	UR	0.00000000E+00	0.00000000E+00
198	UR	0.00000000E+00	0.00000000E+00
201	UR	0.00000000E+00	0.00000000E+00
202	UR	0.00000000E+00	0.00000000E+00
203	UR	0.00000000E+00	0.00000000E+00
204	UR	0.00000000E+00	0.00000000E+00

NODE	LABEL	BISP	CBISP
205	UR	0.00000000E+00	0.00000000E+00
206	UR	0.00000000E+00	0.00000000E+00
207	UR	0.00000000E+00	0.00000000E+00
208	UR	0.00000000E+00	0.00000000E+00
209	UR	0.00000000E+00	0.00000000E+00
210	UR	0.00000000E+00	0.00000000E+00
211	UR	0.00000000E+00	0.00000000E+00
212	UR	0.00000000E+00	0.00000000E+00
213	UR	0.00000000E+00	0.00000000E+00
214	UR	0.00000000E+00	0.00000000E+00
215	UR	0.00000000E+00	0.00000000E+00
216	UR	0.00000000E+00	0.00000000E+00
217	UR	0.00000000E+00	0.00000000E+00
221	UR	0.00000000E+00	0.00000000E+00
222	UR	0.00000000E+00	0.00000000E+00
223	UR	0.00000000E+00	0.00000000E+00
224	UR	0.00000000E+00	0.00000000E+00
225	UR	0.00000000E+00	0.00000000E+00
226	UR	0.00000000E+00	0.00000000E+00
227	UR	0.00000000E+00	0.00000000E+00

NODE	LABEL	BISP	CBISP
228	UR	0.00000000E+00	0.00000000E+00
229	UR	0.00000000E+00	0.00000000E+00
230	UR	0.00000000E+00	0.00000000E+00
231	UR	0.00000000E+00	0.00000000E+00
232	UR	0.00000000E+00	0.00000000E+00
233	UR	0.00000000E+00	0.00000000E+00
234	UR	0.00000000E+00	0.00000000E+00
235	UR	0.00000000E+00	0.00000000E+00
236	UR	0.00000000E+00	0.00000000E+00
237	UR	0.00000000E+00	0.00000000E+00

241	UZ	0.00000000E+00	0.00000000E+00
242	UZ	0.00000000E+00	0.00000000E+00
243	UZ	0.00000000E+00	0.00000000E+00
244	UZ	0.00000000E+00	0.00000000E+00
245	UZ	0.00000000E+00	0.00000000E+00
246	UZ	0.00000000E+00	0.00000000E+00
247	UZ	0.00000000E+00	0.00000000E+00
248	UZ	0.00000000E+00	0.00000000E+00
301	UZ	0.00000000E+00	0.00000000E+00
302	UZ	0.00000000E+00	0.00000000E+00

NODE	LABEL	DISP	DISP
303	UZ	0.00000000E+00	0.00000000E+00
304	UZ	0.00000000E+00	0.00000000E+00
305	UZ	0.00000000E+00	0.00000000E+00
306	UZ	0.00000000E+00	0.00000000E+00
307	UZ	0.00000000E+00	0.00000000E+00
308	UZ	0.00000000E+00	0.00000000E+00
309	UZ	0.00000000E+00	0.00000000E+00
310	UZ	0.00000000E+00	0.00000000E+00
311	UZ	0.00000000E+00	0.00000000E+00
312	UZ	0.00000000E+00	0.00000000E+00
313	UZ	0.00000000E+00	0.00000000E+00
314	UZ	0.00000000E+00	0.00000000E+00
315	UZ	0.00000000E+00	0.00000000E+00
316	UZ	0.00000000E+00	0.00000000E+00
317	UZ	0.00000000E+00	0.00000000E+00
321	UZ	0.00000000E+00	0.00000000E+00
322	UZ	0.00000000E+00	0.00000000E+00
323	UZ	0.00000000E+00	0.00000000E+00
324	UZ	0.00000000E+00	0.00000000E+00
325	UZ	0.00000000E+00	0.00000000E+00

NODE	LABEL	DISP	DISP
326	UZ	0.00000000E+00	0.00000000E+00
327	UZ	0.00000000E+00	0.00000000E+00
328	UZ	0.00000000E+00	0.00000000E+00
329	UZ	0.00000000E+00	0.00000000E+00
330	UZ	0.00000000E+00	0.00000000E+00
331	UZ	0.00000000E+00	0.00000000E+00
332	UZ	0.00000000E+00	0.00000000E+00
333	UZ	0.00000000E+00	0.00000000E+00
334	UZ	0.00000000E+00	0.00000000E+00
335	UZ	0.00000000E+00	0.00000000E+00
336	UZ	0.00000000E+00	0.00000000E+00
337	UZ	0.00000000E+00	0.00000000E+00
341	UZ	0.00000000E+00	0.00000000E+00
342	UZ	0.00000000E+00	0.00000000E+00
343	UZ	0.00000000E+00	0.00000000E+00
344	UZ	0.00000000E+00	0.00000000E+00
345	UZ	0.00000000E+00	0.00000000E+00
346	UZ	0.00000000E+00	0.00000000E+00
347	UZ	0.00000000E+00	0.00000000E+00
348	UZ	0.00000000E+00	0.00000000E+00

NODE	LABEL	DISP	DISP
349	UZ	0.00000000E+00	0.00000000E+00
350	UZ	0.00000000E+00	0.00000000E+00
351	UZ	0.00000000E+00	0.00000000E+00
352	UZ	0.00000000E+00	0.00000000E+00
171	UN	0.00000000E+00	0.00000000E+00
172	UN	0.00000000E+00	0.00000000E+00
173	UN	0.00000000E+00	0.00000000E+00
189	UN	0.00000000E+00	0.00000000E+00
189	ROTZ	0.00000000E+00	0.00000000E+00
171	UN	0.00000000E+00	0.00000000E+00

LIST ELEMENT PRESSURES FOR ALL SELECTED ELEMENTS

ELEM	FACE	VALUE(S)	FACE	NODES
99	1	34.7995000	0.00000000E+00	49 53
96	1	34.7995000	0.00000000E+00	53 57
97	1	34.7995000	0.00000000E+00	55 57
98	1	34.7995000	0.00000000E+00	57 59

99	1	34.7998000	0.00000000E+00	59	61
100	1	34.7998000	0.00000000E+00	61	63
101	1	34.7998000	0.00000000E+00	63	65
102	1	34.7998000	0.00000000E+00	65	67
103	1	34.7998000	0.00000000E+00	67	69
104	1	34.7998000	0.00000000E+00	69	71
105	1	34.7998000	0.00000000E+00	71	73
106	1	34.7998000	0.00000000E+00	73	75
107	1	34.7998000	0.00000000E+00	75	77
108	1	34.7998000	0.00000000E+00	77	79
109	1	34.7998000	0.00000000E+00	79	81
110	1	34.7998000	0.00000000E+00	81	83
111	1	34.7998000	0.00000000E+00	83	85
112	1	34.7998000	0.00000000E+00	85	87
113	1	34.7998000	0.00000000E+00	87	89
114	1	34.7998000	0.00000000E+00	89	91

ELEM	FACE	VALUE(S)	FACE NODES		
115	1	34.7998000	0.00000000E+00	91	93
116	1	34.7998000	0.00000000E+00	93	100
117	1	34.7998000	0.00000000E+00	100	101
118	1	34.7998000	0.00000000E+00	101	102
119	1	34.7998000	0.00000000E+00	102	103
120	1	34.7998000	0.00000000E+00	103	104
121	1	34.7998000	0.00000000E+00	104	105
122	1	34.7998000	0.00000000E+00	105	106
123	1	34.7998000	0.00000000E+00	106	107
124	1	34.7998000	0.00000000E+00	107	108
70	2	34.7998000	0.00000000E+00	145	152
74	2	34.7998000	0.00000000E+00	152	159
82	2	34.7998000	0.00000000E+00	159	166
86	2	34.7998000	0.00000000E+00	166	173
278	3	34.7998000	0.00000000E+00	349	349
266	3	34.7998000	0.00000000E+00	337	349
243	2	34.7998000	0.00000000E+00	317	337
192	3	34.7998000	0.00000000E+00	237	217
214	2	34.7998000	0.00000000E+00	22	237
18	4	34.7998000	0.00000000E+00	27	22

ELEM	FACE	VALUE(S)	FACE NODES		
21	4	34.7998000	0.00000000E+00	32	27
26	4	34.7998000	0.00000000E+00	38	34
27	4	34.7998000	0.00000000E+00	42	38
39	4	34.7998000	0.00000000E+00	43	42
31	4	34.7998000	0.00000000E+00	48	45
192	4	34.7998000	0.00000000E+00	217	216
243	1	34.7998000	0.00000000E+00	316	317

LIST ELEMENT CONNECTIONS FOR ALL SELECTED ELEMENTS

LIST TEMPERATURES FOR ALL SELECTED MODES

MODE	TEMPERATURE	FLUENCE
3	180.28	0.00000E+00
4	203.81	0.00000E+00
5	203.81	0.00000E+00
8	180.28	0.00000E+00
9	203.81	0.00000E+00
10	203.81	0.00000E+00
13	180.28	0.00000E+00
14	203.81	0.00000E+00
15	203.81	0.00000E+00
18	174.96	0.00000E+00
19	184.77	0.00000E+00
20	194.77	0.00000E+00
22	153.35	0.00000E+00
23	174.84	0.00000E+00
24	184.77	0.00000E+00
26	194.77	0.00000E+00
27	243.17	0.00000E+00
28	243.17	0.00000E+00
29	243.17	0.00000E+00
30	243.17	0.00000E+00

NODE	TEMPERATURE	FLUENCE
31	1250.3	0.00000E+00
32	243.17	0.00000E+00
33	243.17	0.00000E+00
34	243.17	0.00000E+00
35	243.17	0.00000E+00
36	987.05	0.00000E+00
37	435.48	0.00000E+00
38	243.17	0.00000E+00
39	243.17	0.00000E+00
40	243.17	0.00000E+00
41	772.95	0.00000E+00
42	538.16	0.00000E+00
43	538.16	0.00000E+00
44	538.16	0.00000E+00
45	538.16	0.00000E+00
46	538.16	0.00000E+00
47	538.16	0.00000E+00
48	538.16	0.00000E+00
49	538.16	0.00000E+00
50	538.16	0.00000E+00

NODE	TEMPERATURE	FLUENCE
53	710.35	0.00000E+00
54	772.95	0.00000E+00
55	882.93	0.00000E+00
56	772.95	0.00000E+00
57	882.60	0.00000E+00
58	877.56	0.00000E+00
59	882.65	0.00000E+00
60	952.17	0.00000E+00
61	882.60	0.00000E+00
62	1056.8	0.00000E+00
63	882.74	0.00000E+00
64	1191.4	0.00000E+00
65	884.31	0.00000E+00
66	1195.8	0.00000E+00
67	925.28	0.00000E+00
68	1198.5	0.00000E+00
69	827.45	0.00000E+00
70	1202.1	0.00000E+00
71	829.02	0.00000E+00
72	1205.7	0.00000E+00

NODE	TEMPERATURE	FLUENCE
73	890.59	0.00000E+00
74	1209.2	0.00000E+00
75	891.16	0.00000E+00
76	1212.8	0.00000E+00
77	891.73	0.00000E+00
78	1215.8	0.00000E+00
79	892.30	0.00000E+00
80	1214.8	0.00000E+00
81	896.87	0.00000E+00
82	1215.7	0.00000E+00
83	896.44	0.00000E+00
84	1216.7	0.00000E+00
85	900.01	0.00000E+00
86	1217.7	0.00000E+00
87	901.58	0.00000E+00
88	1218.7	0.00000E+00
89	903.15	0.00000E+00
90	1219.7	0.00000E+00
91	904.72	0.00000E+00
92	1220.7	0.00000E+00

NODE	TEMPERATURE	FLUENCE
93	906.29	0.00000E+00
94	1221.6	0.00000E+00
101	144.81	0.00000E+00
102	144.81	0.00000E+00
103	144.81	0.00000E+00
104	144.81	0.00000E+00
105	144.81	0.00000E+00

106	144.81	D.0000E+00
107	144.81	D.0000E+00
108	144.81	D.0000E+00
109	144.81	D.0000E+00
110	144.81	D.0000E+00
111	144.81	D.0000E+00
112	144.81	D.0000E+00
113	144.81	D.0000E+00
114	144.81	D.0000E+00
115	144.81	D.0000E+00
116	144.81	D.0000E+00

NODE	TEMPERATURE	FLUENCE
119	144.81	D.0000E+00
120	144.81	D.0000E+00
121	144.81	D.0000E+00
122	111.00	D.0000E+00
123	111.00	D.0000E+00
124	111.00	D.0000E+00
127	111.00	D.0000E+00
130	111.00	D.0000E+00
131	111.00	D.0000E+00
134	111.00	D.0000E+00
137	111.00	D.0000E+00
138	111.00	D.0000E+00
143	111.00	D.0000E+00
144	111.00	D.0000E+00
145	111.00	D.0000E+00
150	93.893	D.0000E+00
151	93.893	D.0000E+00
152	93.893	D.0000E+00
157	94.837	D.0000E+00
158	94.837	D.0000E+00

NODE	TEMPERATURE	FLUENCE
159	94.837	D.0000E+00
164	93.051	D.0000E+00
165	93.051	D.0000E+00
166	93.051	D.0000E+00
171	93.051	D.0000E+00
172	93.051	D.0000E+00
173	93.051	D.0000E+00
180	1219.1	D.0000E+00
181	1219.1	D.0000E+00
182	1219.1	D.0000E+00
183	1219.1	D.0000E+00
184	1219.1	D.0000E+00
185	1219.0	D.0000E+00
186	1219.9	D.0000E+00
187	1219.9	D.0000E+00
188	1219.9	D.0000E+00
201	156.76	D.0000E+00
202	156.76	D.0000E+00
203	156.76	D.0000E+00
204	156.76	D.0000E+00

NODE	TEMPERATURE	FLUENCE
205	156.76	D.0000E+00
206	156.76	D.0000E+00
207	156.76	D.0000E+00
208	156.76	D.0000E+00
209	156.76	D.0000E+00
210	153.35	D.0000E+00
211	153.35	D.0000E+00
212	153.35	D.0000E+00
213	153.35	D.0000E+00
214	153.35	D.0000E+00
215	153.35	D.0000E+00
216	153.35	D.0000E+00
217	153.35	D.0000E+00
221	156.76	D.0000E+00
222	156.76	D.0000E+00

223	156.74	0.00000E+00
224	156.74	0.00000E+00
225	156.74	0.00000E+00
226	156.74	0.00000E+00
227	156.74	0.00000E+00

NODE	TEMPERATURE	FLUX[CF]
228	156.76	0.00000E+00
229	156.74	0.00000E+00
230	153.35	0.00000E+00
231	153.35	0.00000E+00
232	153.35	0.00000E+00
233	153.35	0.00000E+00
234	153.35	0.00000E+00
235	153.35	0.00000E+00
236	153.35	0.00000E+00
237	153.35	0.00000E+00
241	156.74	0.00000E+00
242	156.74	0.00000E+00
243	156.74	0.00000E+00
244	156.74	0.00000E+00
245	156.74	0.00000E+00
246	153.35	0.00000E+00
247	153.35	0.00000E+00
248	153.35	0.00000E+00
301	111.00	0.00000E+00
302	111.00	0.00000E+00

NODE	TEMPERATURE	FLUX[CF]
303	111.00	0.00000E+00
304	111.00	0.00000E+00
305	111.00	0.00000E+00
306	111.00	0.00000E+00
307	111.00	0.00000E+00
308	111.00	0.00000E+00
309	111.00	0.00000E+00
310	111.00	0.00000E+00
311	111.00	0.00000E+00
312	111.00	0.00000E+00
313	111.00	0.00000E+00
314	111.00	0.00000E+00
315	111.00	0.00000E+00
316	111.00	0.00000E+00
317	111.00	0.00000E+00
321	111.00	0.00000E+00
322	111.00	0.00000E+00
323	111.00	0.00000E+00
324	111.00	0.00000E+00
325	111.00	0.00000E+00

NODE	TEMPERATURE	FLUX[CF]
326	111.00	0.00000E+00
327	111.00	0.00000E+00
328	111.00	0.00000E+00
329	111.00	0.00000E+00
330	111.00	0.00000E+00
331	111.00	0.00000E+00
332	111.00	0.00000E+00
333	111.00	0.00000E+00
334	111.00	0.00000E+00
335	111.00	0.00000E+00
336	111.00	0.00000E+00
337	111.00	0.00000E+00
341	111.00	0.00000E+00
342	111.00	0.00000E+00
343	111.00	0.00000E+00
344	111.00	0.00000E+00
345	111.00	0.00000E+00
346	111.00	0.00000E+00
347	111.00	0.00000E+00
348	111.00	0.00000E+00

NODE	TEMPERATURE	FLUX[CF]
349	111.00	0.00000E+00

350	111.06	0.00000E+00
351	111.06	0.00000E+00
352	111.06	0.00000E+00

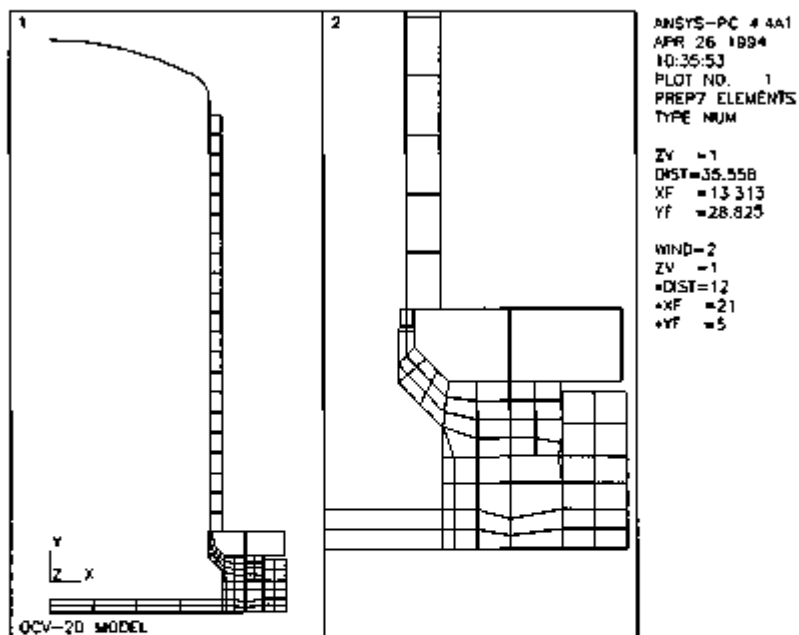


FIGURE 2.10.8-1.

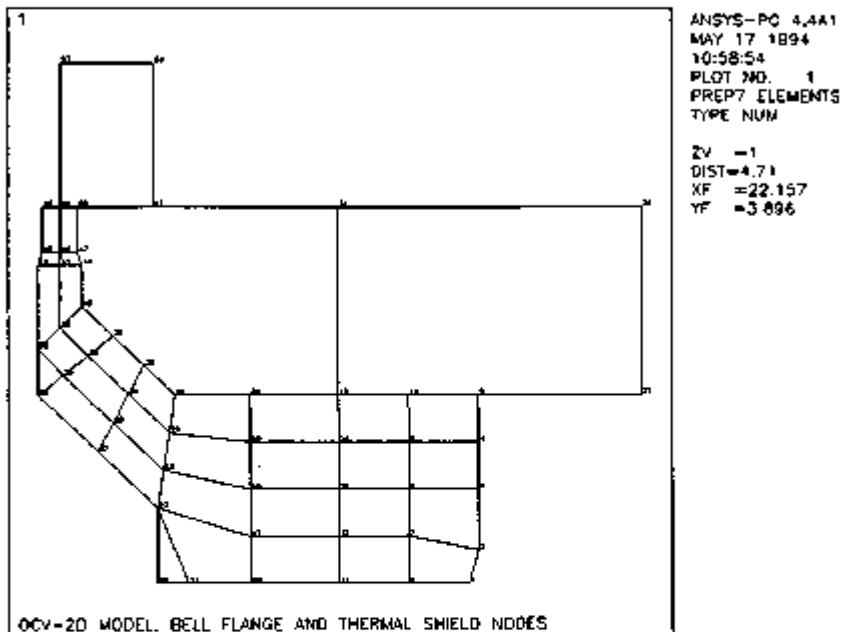


FIGURE 2.10.8-2.

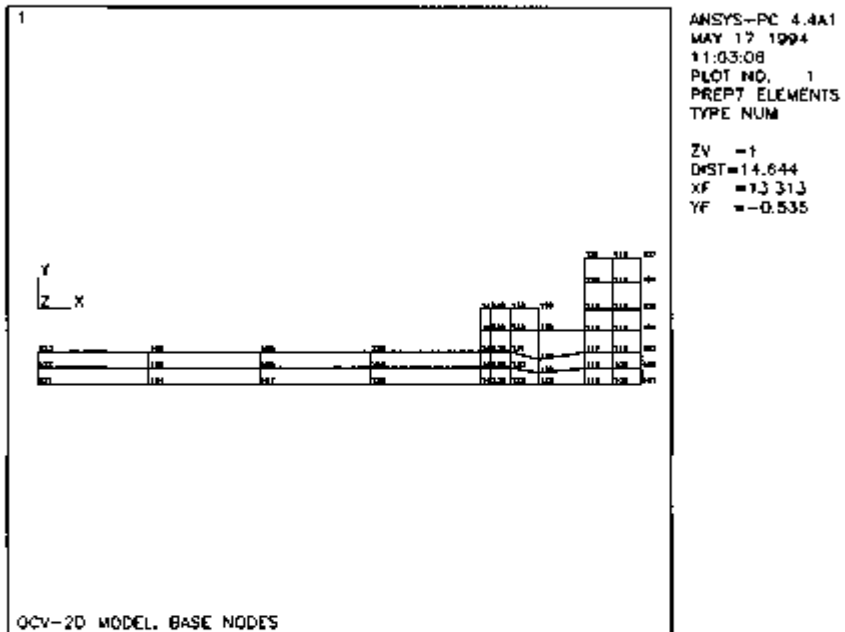


FIGURE 2.10.8-3.

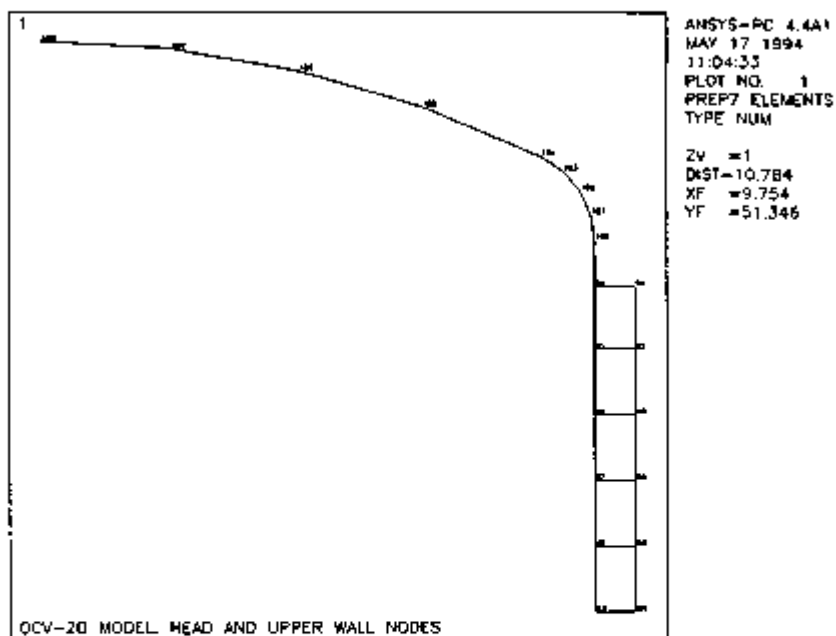


FIGURE 2.10.8-4.

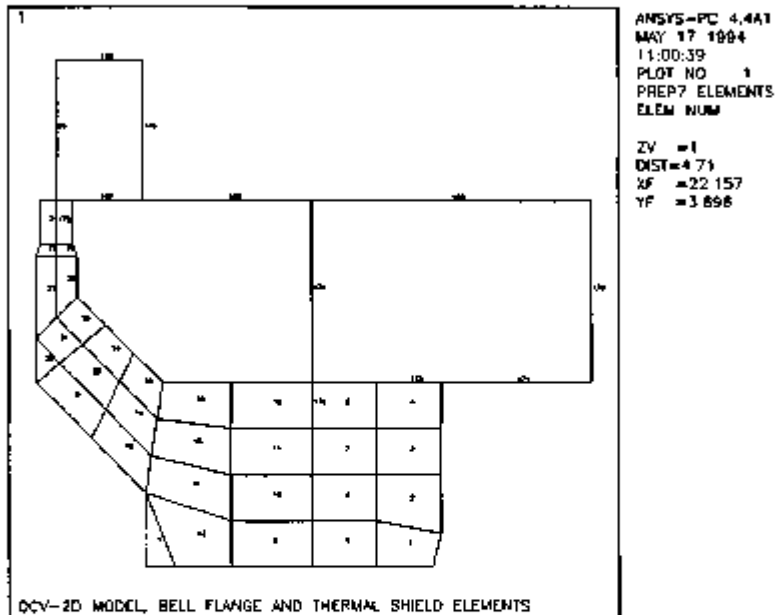


FIGURE 2.10.8-5.

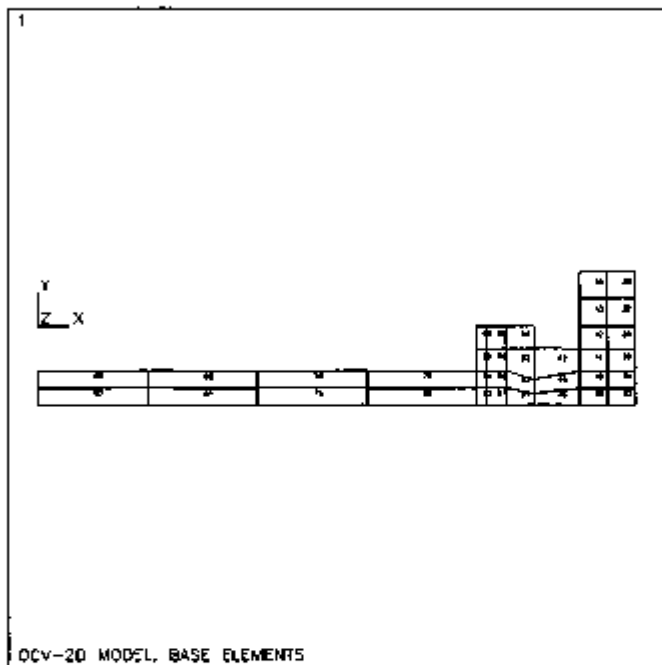


FIGURE 2.10.8-6.

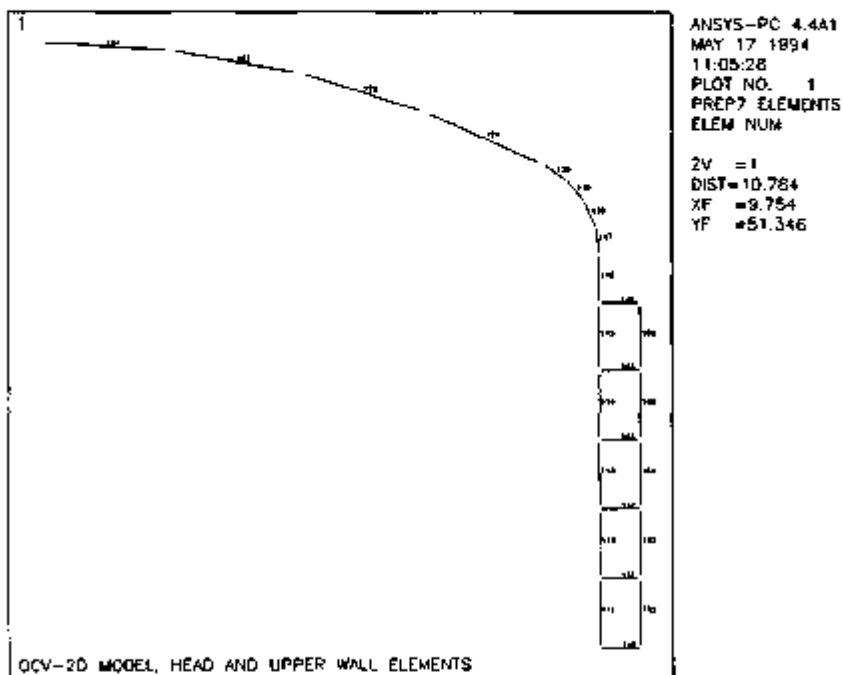


FIGURE 2.10.B-7.

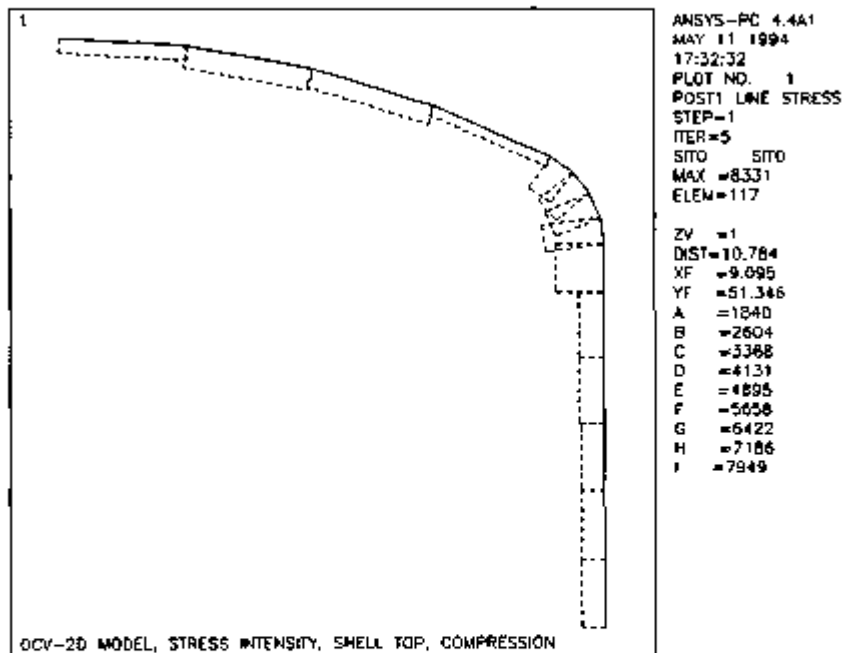


FIGURE 2.10.B-8.

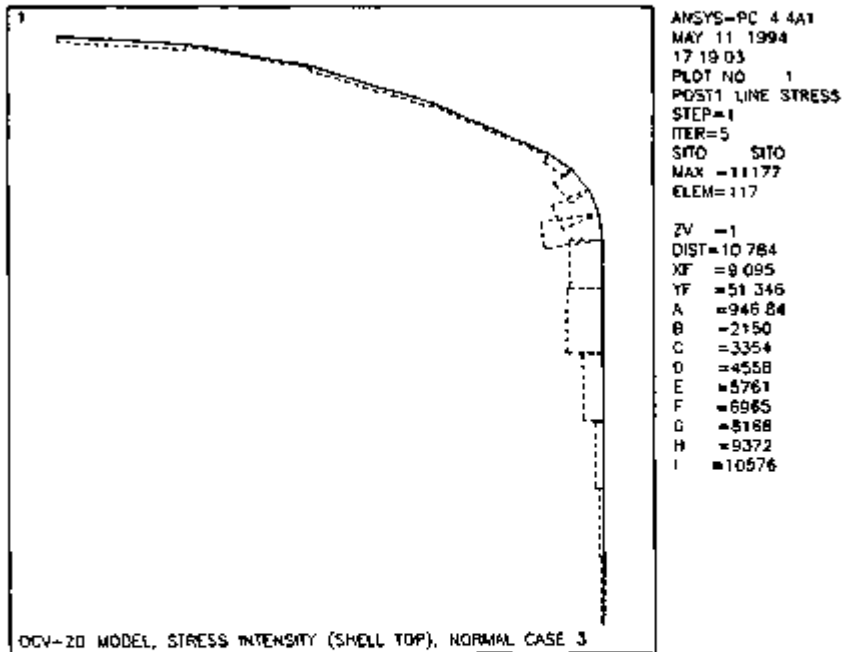


FIGURE 2.10.B-9.

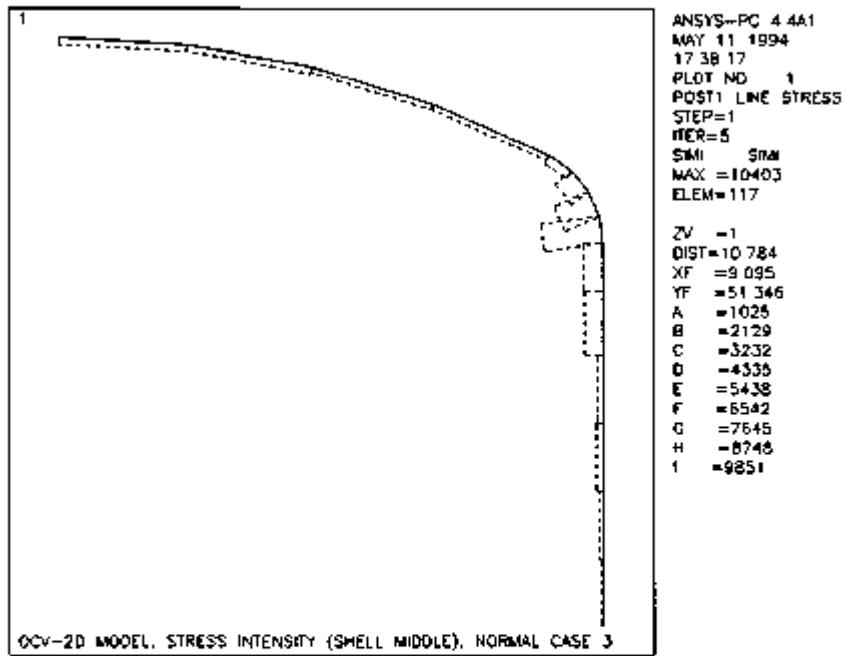


FIGURE 2.10.8-10.

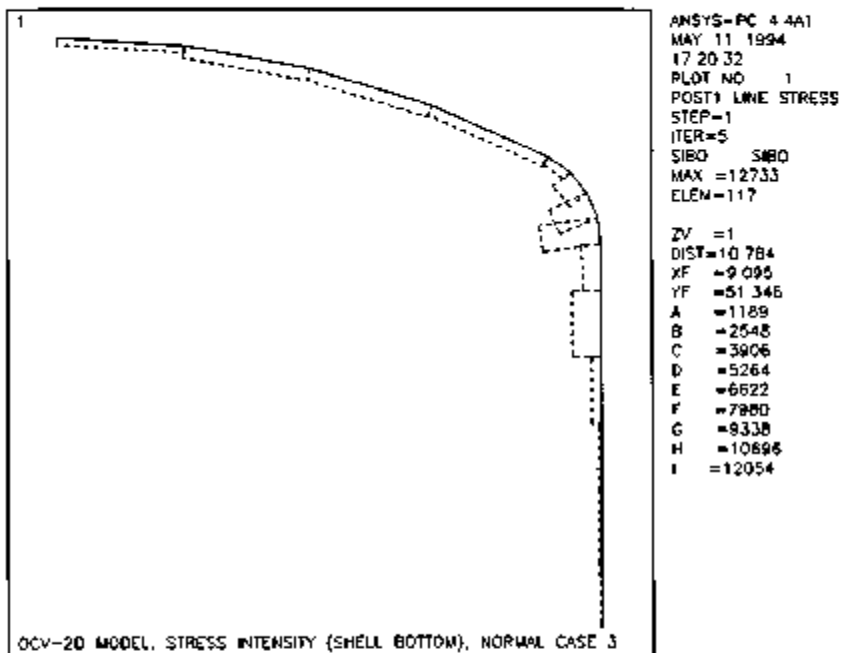


FIGURE 2.10.8-11.

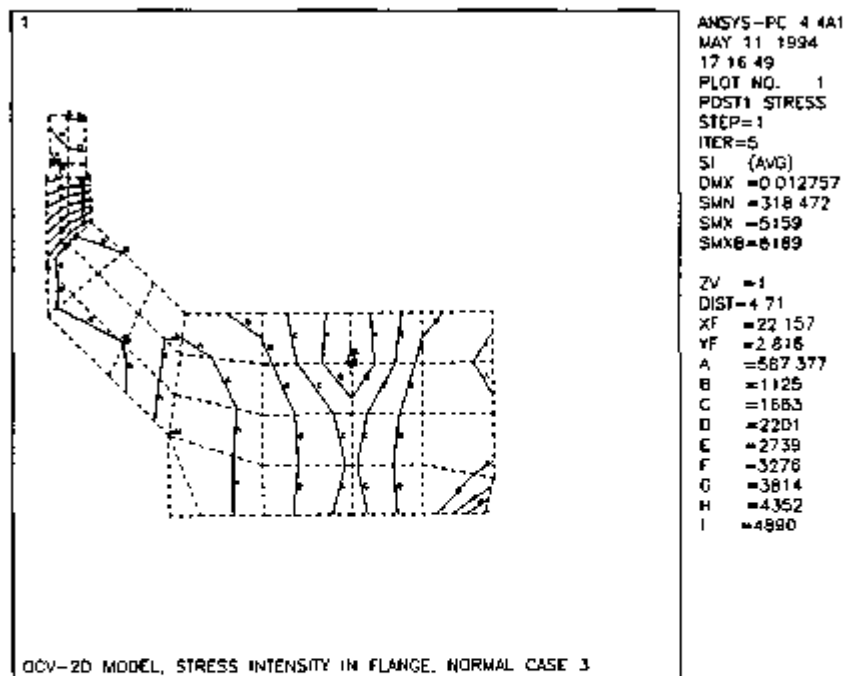


FIGURE 2.10.8-12.

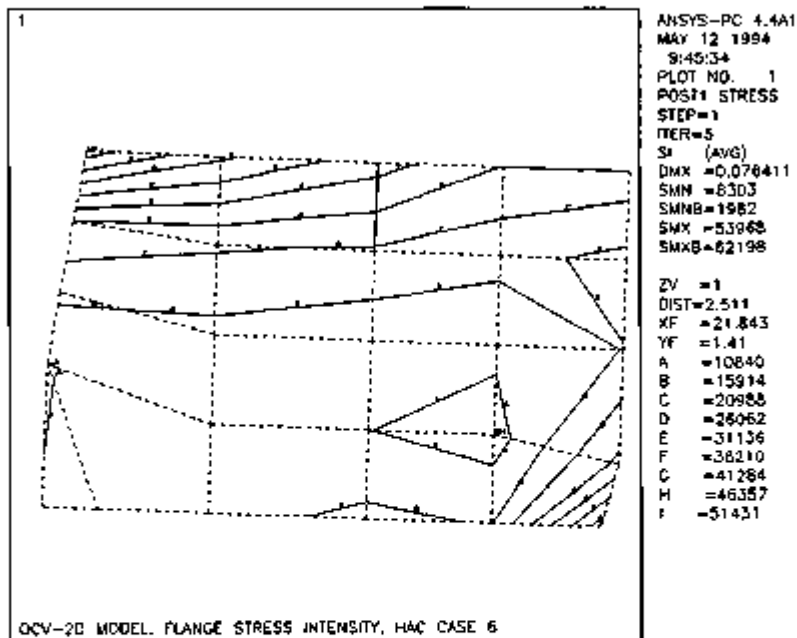


FIGURE 2.10.B-13.

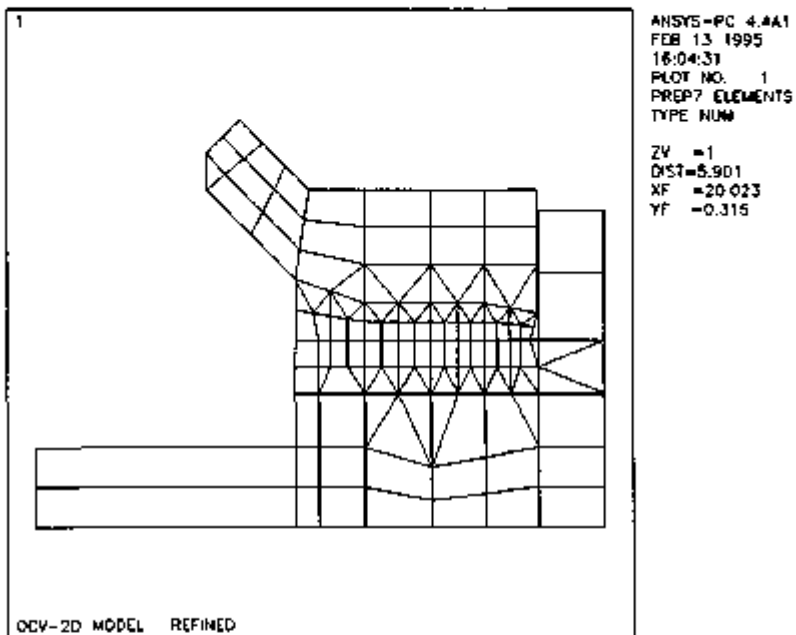


FIGURE 2.10.8-14.

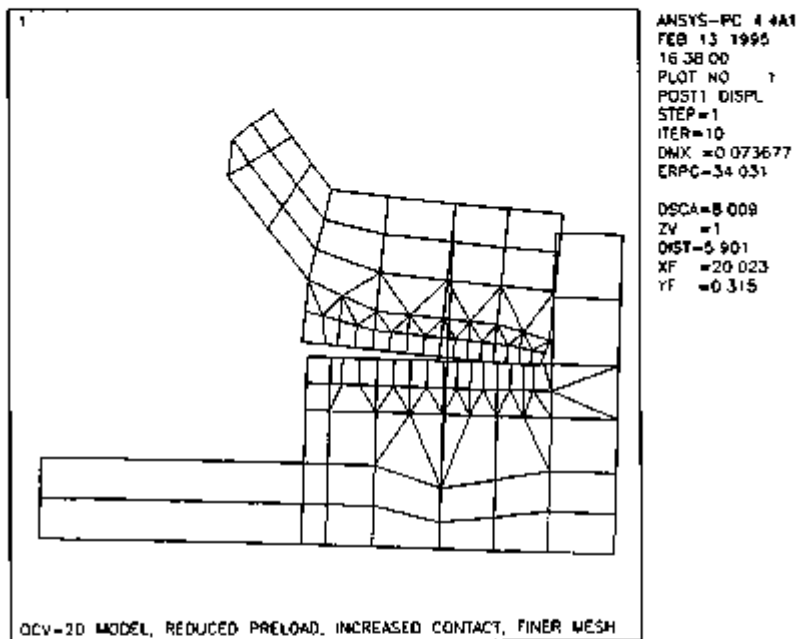


FIGURE 2.10.8-15.

2 10 9 RTG Transportation System Package Certification Test Plan

2 10 9 1 First Certification Test Series The RTG Transportation System Certification Test Plan for the first certification test series is included in its entirety in document WHC-SD-RTG-TP-009. The first certification test article (CTA-1) was used during this drop test series.

2 10 9 2 Second Certification Test Series The RTG Transportation System Certification Test Plan for the second certification test series is included in its entirety in document WHC-SD-RTG-TP-018, Rev. 1. The second certification test article (CTA-2) was used during this drop test series.

2 10 9 3 Simulated Payload Attached are a fabrication drawing of the simulated payload configuration (Figure 2 10 9 3-3) and sketches of the simulated payload and the GPHS payload within the package (Figures 2 10 9 3-1 and 2 10 9 3-2, respectively). For visual comparison purposes, superimposed on the GPHS payload is an outline of the simulated payload. The cg marks on each figure indicate the cg of the payload (without rack). The following weight and center of gravity information table is provided as additional information to aid in the comparison of simulated and real payloads.

Table 2 10 9 3-1 Simulated Payload Comparisons

Payload	Payload shipping rack weight (lb)	Payload weight w/o shipping rack (lb)	Total weight of payload plus shipping rack (lb)	Height of payload cg above banner plate (in.)	Height of payload plus rack cg above ICV base plate (in.)
Simulated	225	570	795	26.9	24.5
GPHS	225	200	425	17.5	13.4

As shown, the weight of the simulated payload conservatively envelopes the weight of the GPHS RTG payload. With a packaging weight and cg (excluding payload and shipping rack) of 8,850 pounds and 9.98 in. above the ICV base plate per Table 2 2-1, the overall cg of the package only varies by 1.05 in. between the simulated and GPHS payload configurations (11.18 and 10.14 in. above ICV base plate, respectively). This slight cg variation has negligible effect on package response to HAC free drop and puncture events.

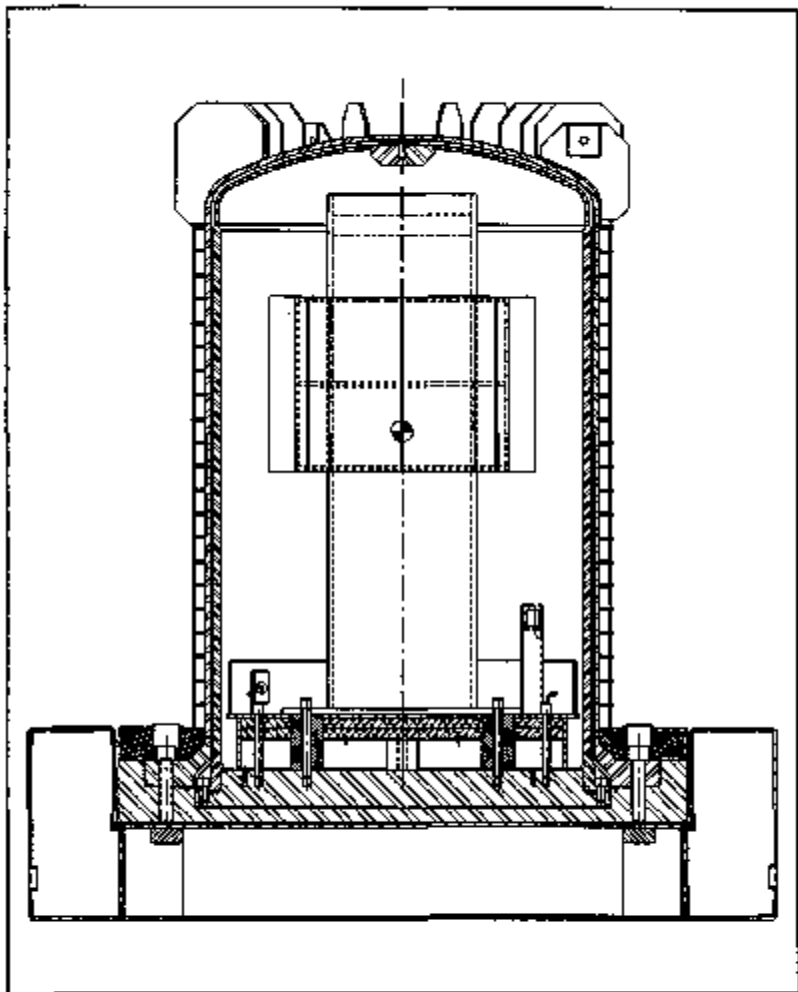


FIGURE 2.10.9.3-1. Simulated Payload Within the RTG Shipping Package.

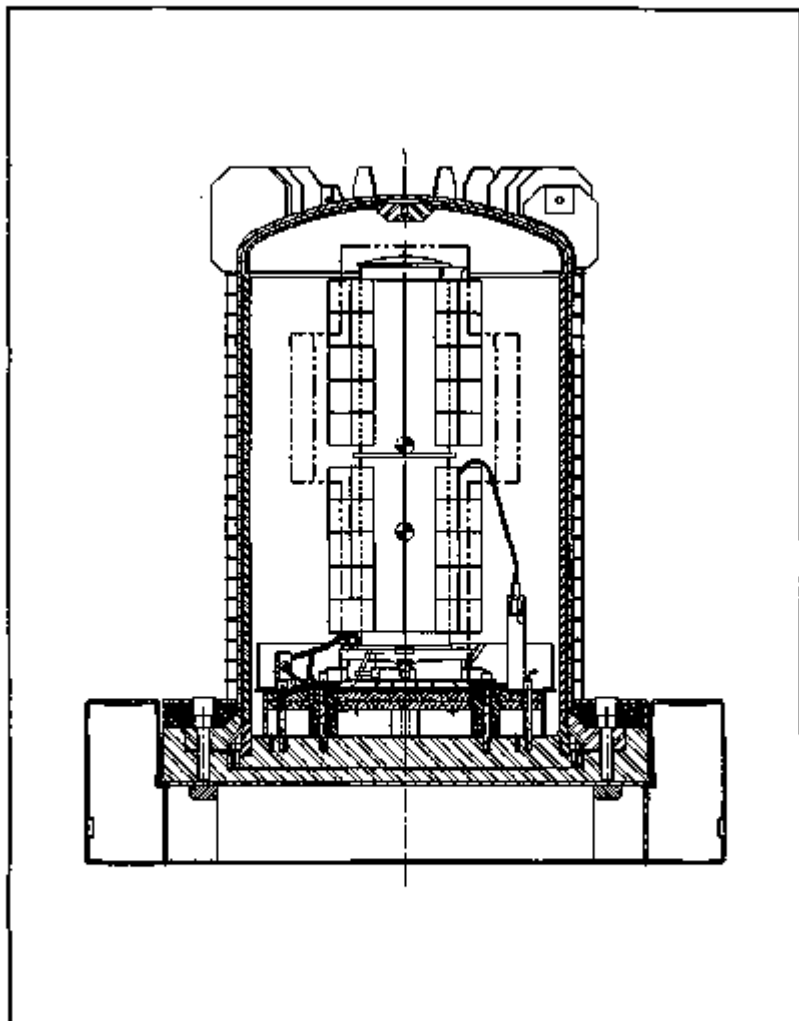


FIGURE 2.10.9.3-2. GPHS/Simulated Payload Within RTG Package.

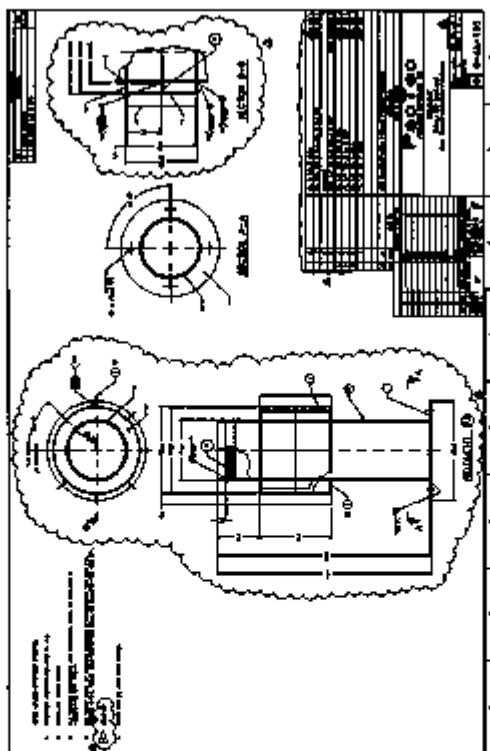


FIGURE 2.10.9.3-3.

BEST COPY AVAILABLE

2.10.10 Certification Drop Test Procedure for the RTG Transportation System Package

The test procedure for Drop Testing of the RTG Transportation System Package Prototype is included in its entirety in document WHC-SD-RTG-TC-003 for CTA-1 and WHC-SD-RTG-TC-015, Rev. 1 for CTA-2.

2.10.11 Structural Development Test Program

As a part of the design process, structural design development testing was performed in February 1992.

2.10.11.1 Test Objectives.

2.10.11.1.1 Primary. (1) To confirm impact limiter design (dimensions, materials, attachments), or to guide design refinements, as necessary. (2) To confirm OCV head fin design, or to guide design refinements, as necessary.

2.10.11.1.2 Secondary. (1) To investigate OCV seal area response (establish amount of permanent deformations at sealing surfaces or in closure bolts, if any.)

2.10.11.2 Test Hardware. A half-scale simulation of the package was used in the test program (see Figure 2.10.11.2-1). Components related to test objectives were duplicated to a degree of accuracy considered appropriate for purposes of design concept verification. For instance, components related to primary objectives (impact limiter and OCV head fins) were scaled precisely. Secondary objective components (OCV seal flange and base plate, and closure bolts) were scaled with accuracy sufficient to allow a broad determination of overall structural response.

2.10.11.2.1 Impact Limiter. The impact limiter geometry was precisely scaled. The primary impact absorption material was polyurethane foam. The density of the foam directly beneath the OCV was 3 lb/ft³, with the remainder being 12 lb/ft³. The impact limiter outer shell incorporated 11 gage (0.12 in. thick) carbon steel sheet metal on one half-segment, and 13 gage (0.09-in. thickness) carbon steel sheet metal on the other half-segment. These gages were intended to conservatively scale 1/4 in. and 3/16 in. thick plate, respectively. Testing was conducted on both half segments in order to gauge the effects of shell thickness on impact limiter response.

Eight 3/8-in. diameter impact limiter attachment bolts were used to represent the 3/4-in. diameter bolts of the actual package. This was somewhat conservative, because the scaled-up tensile stress area of the 3/8-in. diameter bolts is $4 \times 0.0775 \text{ in.}^2 = 0.310 \text{ in.}^2$, which is less than the 0.334 in.² tensile stress area of a standard 3/4 in. diameter bolt. The half-scale impact limiter attachment bolts were torqued to 150 in-lb, resulting in an equivalent pre-load on a stress basis to the actual anticipated full-scale impact limiter bolt pre-load of 100 ft-lb.

2.10.11.2.2 Outer Containment Vessel. The OCV components, particularly in the seal area, were closely simulated to allow a determination of seal response to the regulatory test events. The OCV flange and base plate geometries in the seal region were accurately scaled, except that actual O-ring seal grooves were not incorporated. The vessel ball was also accurately represented, except that the cooling jacket was not included (its weight was lumped into the scale payload mass). The OCV head thickness was 3/8 in., whereas the actual full-scale thickness will be 1/2 in. This conservatively simulated the combined OCV and ICV head thicknesses: $1/2 \times (1/2 + 3/8) = 7/16 \text{ in.}$, where the full-scale ICV head thickness is 3/8 in.

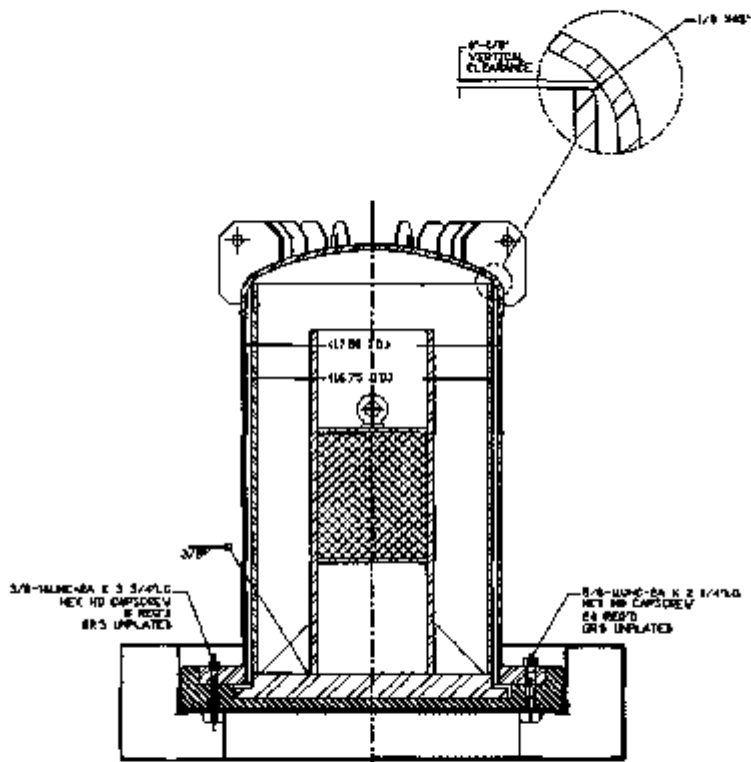


FIGURE 2.10.11.2-1. RTG HgM Scale Test Article.

The OCV head fins were precisely scaled. The only difference was that all 24 of the half-scale fins had 3/4-in. diameter holes in them (to simulate shackle holes for lifting purposes), whereas the actual package will have 3/4-in. diameter lifting holes in only three of its fins.

Twenty-four, 5/8-in. diameter OCV closure bolts were used to represent the 1-1/4 in. diameter closure bolts of the actual package. This was somewhat conservative, since the scaled-up tensile stress area of the 5/8-in. diameter bolts is $4 \times 0.226 \text{ in.}^2 = 0.904 \text{ in.}^2$, which is less than the 0.989 in.² tensile stress area of a standard 1 1/4 inch diameter bolt. The half-scale closure bolts were torqued to 300 in.-lb, resulting in an equivalent pre-load on a stress basis to two-thirds of the actual anticipated full-scale OCV closure bolt pre-load of 300 ft.-lb.

The OCV thermal shield was not simulated on the half-scale test article. Because the thermal shield acts to stiffen the OCV flange, its absence tended to conservatively maximize any deformation effects that might occur in the OCV seal region. The overall geometry of the OCV flange, as well as the offset of the OCV wall from the closure bolt circle, were only roughly approximated.

2.10.11.2.3 Inner Containment Vessel. The ICV geometry was approximated with a simple welded plate and shell assembly. This structure was intended to simulate the response of an actual ICV relative to the OCV for the regulatory test events. Accordingly, the ICV base plate was positioned within the OCV base plate in the same manner as will occur in the actual package. Clearance between the top of the ICV head and the OCV head and between the sides of the ICV and OCV was adjusted to allow realistic relative impacts between the ICV and OCV. The ICV base plate and bell thicknesses were both scaled exactly.

2.10.11.2.4 Other Features. The total weight of the half-scale test package assembly, including simulated payload, was 1,170 pounds, which represents a full-scale weight of $8 \times 1,170 \text{ pounds} = 9,360 \text{ pounds}$. The center of gravity of the assembly was 11.5 in. from the base of the impact limiter, representing a full-scale distance of $2 \times 11.5 \text{ in.} = 23 \text{ in.}$

The payload assumed was the maximum-weight RTG, equal to 620 pounds, including shipping rack. Additionally, package weight not directly simulated on the half-scale model (e.g., the cooling jacket) was lumped into the payload weight. The overall package weight and c.g. was obtained by a segment of steel pipe, welded vertically to the ICV base plate, and partially filled with lead balls.

The OCV and ICV half-scale test assemblies were both fabricated of carbon steel, instead of the stainless steel that will be used on the actual package. This was conservative, particularly for puncture tests, because carbon steel is less ductile than stainless steel, and would tend to rupture or tear more readily than would actual package materials.

For each drop test, three passive accelerometers were installed on the half-scale test article at the elevation of the c.g. These accelerometers indicated impact accelerations of 200g, 300g, and 400g, corresponding to full-scale values of 100g, 150g, and 200g, respectively.

2.10.11.3 Test Sequence. All testing was done at the prevailing ambient temperature, which was generally around 60 °F. The development test program consisted of two separate phases, an initial phase, and a follow-up phase. Generally, the follow-up phase incorporated design refinements in the half-scale test package that arose from knowledge gained from the test results of the initial phase.

2.10.11.3.1 Initial Phase. The first round of half-scale structural development testing consisted of the following tests:

- Six NCT free drops of 4 ft
- Five HAC free drops of 30 ft
- Six HAC puncture drops of 40 in.

Drop orientations ranged from flat end drops to flat side drops (defined for the RTG Transportation System Package as simultaneous impact on the OCV head fins and the impact limiter) and several orientations in between. Drop orientations were selected on the following bases:

- To maximize impact loading and consequent structural deformations, particularly in the OCV seal region
- To maximize separation loading on the OCV closure bolts and the impact limiter attachment bolts
- To maximize impact limiter deflections to ensure that sufficient crush depth will be available to preclude "bottoming out" on the package structure beneath the impact limiter, as well as to provide a residual thermal barrier against the HAC fire event
- To maximize HAC puncture bar damage to the impact limiter to ensure no loss of thermal barrier integrity.

Each HAC free drop impact occurred at the same point of impact and at the same orientation as a prior NCT free drop impact. This ensures that no NCT drop compromises the ability of the package to sustain a similarly-oriented HAC drop at the same impact location.

2.10.11.3.2 Follow-Up Phase. The follow-up testing was conducted to address specific issues unearthed during the initial phase of testing. This phase consisted of the following tests:

- One HAC free drop of 30 ft
- Five HAC puncture drops of 40 in.

Particular issues covered by the additional testing (see Section 2.10.11.4 below) included the following:

- Evaluate impact limiter outer bottom shell modification to reduce puncture bar penetration
- Evaluate impact limiter attachment bolt modification to preclude bolt breakage
- Evaluate effects of lubrication on closure and impact limiter attachment bolt pre-load retention.

Specifically, the carbon steel bottom plate of the impact limiter was replaced with 11 gage stainless steel to improve puncture resistance. Also, the impact limiter attachment bolts were "necked down" in the unthreaded shaft region to allow greater straining (energy absorption) during impact events and prevent fracture. Finally, all bolts (OCV closure and impact limiter attachment) were lubricated before installation to reduce torsional stress and induce more axial (pre-load) strain in the bolts.

2.10.11.4 Significant Results of Initial Test Phases.**2.10.11.4.1 Normal Conditions of Transport 4-Foot Free Drops.**

1. Deformations were limited to OCV head flange and impact limiter; no permanent deformation was visually detected in the OCV seal region.
2. The impact limiter was retained for all drops, and no foam was exposed.
3. Positive residual torques existed for all bolts (OCV closure and impact limiter attachment) at the conclusion of the NCT free drops.
4. Accelerations were limited to 300g (150g full scale) for all NCT free drops.
5. Accelerations were less than 200g (100g full scale) for NCT side drops.

2.10.11.4.2 Hypothetical Accident Condition 30-Foot Free Drops.

1. All significant deformations were limited to OCV head flange and impact limiter.
2. The impact limiter was retained for all drops, and no foam was exposed.
3. For the near-vertical drop (10° angle), three impact limiter attachment bolts broke; no other drop orientations resulted in broken bolts.
4. Positive residual torques existed for all bolts (OCV closure and impact limiter attachment) at the conclusion of all other HAC free drops.
5. A minimum residual impact limiter foam thickness of about 2 in. (4 in. in full scale) remained after all HAC free drops (e.g. over corner and side drop resulted in the greatest impact limiter deformation); this is considered sufficient for protection against the HAC fire event.
6. Insignificant permanent deformation occurred in the OCV seal region (see Section 2.10.11.6).
7. Accelerations exceeded 400g (200g full scale) for all except the top end drop (consistent with 300g design basis assumed for actual package).
8. Acceleration was between 300 and 400g (150 and 200g full scale) for the top end drop.

2.10.11.4.3 Hypothetical Accident Condition 40-In. Puncture Drops.

1. Containment vessels were not punctured; modest (<1 in. deep), fully acceptable local deformation occurred on OCV ball after direct impact of puncture bar.
2. Impact limiter bottom plate (both thicknesses) ruptured, and "bottoming out" of puncture bar on OCV base plate occurred.
3. Impact limiter 11-gauge cylindrical sidewall exhibited minor, fully acceptable, crescent-shaped tear.

4. For the side puncture drop, one OCV closure bolt (the one nearest the impact point) lost all pre-load; adjacent closure bolts retained pre-load torques of more than 250 in-lb (of the initial 300 in-lb pre-load torque).
5. Positive residual torques existed for all bolts (OCV closure and impact limiter attachment) at the conclusion of all other HAC puncture drops.
6. Maximum acceleration was less than 200g (100g full scale) for all puncture tests.

2.10.11.5 Significant Results of Follow-Up Test Phase

2.10.11.5.1 Hypothetical Accident Condition 30 Foot Free Drops.

1. Repetition of the near-vertical HAC free drop, with modified impact limiter attachment bolts installed, resulted in bolt stretch (and loss of all pre-load on one attachment bolt), but no breakage; design refinement is considered successful.
2. Minimum residual pre-load on all OCV closure bolts was greater than for previous similar drop, probably because of lubrication of bolts.
3. Accelerations exceeded 400g (200g full scale).

2.10.11.5.2 Hypothetical Accident Condition 40-in. Puncture Drops.

1. Modified impact limiter bottom shell reduced puncture bar penetration, but did not preclude it entirely; resulting puncture damage was considered minor from a HAC fire barrier standpoint, because of the intumescent character of the foam.
2. No accelerometers tripped for any of the follow-up HAC puncture tests.

2.10.11.6 Conclusions. In general, the structural development test program was considered to be very successful. The basic structural design being used has been sound. Both the removable foam impact limiter and particularly the OCV head fire performed well in reducing impact loads. No significant deformations were observed that would lead to loss of containment, excessive loss of shielding, or which would preclude acceptable package performance in a subsequent HAC fire event.

As a result of the developmental testing, the following design refinements have been made to the RTG Transportation System Package:

1. Use of stainless steel instead of carbon steel for the impact limiter shell
2. Use of 1/4-in. thick plate on the top and outer cylindrical side surfaces, and 5/16-in. thick plate on the bottom surface of the impact limiter
3. Addition of 2 in. of height to the impact limiter (7 in. increased to 9 in.)
4. "Necking down" impact limiter attachment bolts
5. Minor OCV base plate design change to allow for longer effective length on OCV closure bolts
6. Cadmium plating of all bolts

7. Incorporate thermal barrier interior to limiter, adjacent to OCV base.

Items 1 and 2 will improve impact limiter puncture resistance, and item 3 will increase the residual foam depth after HAC impact. Although performance in these categories was deemed adequate subsequent to the follow-up testing, these design refinements will provide an additional comfort margin in the design.

Item 4 results in improved impact limiter attachment bolt performance, as discussed in Section 2.10.11.3.2. Item 5 allows greater axial stretch of the OCV closure bolts under pre-load, providing more margin against an excessive loss of pre-load during handling and operation. Item 6 will provide permanent lubrication for all bolts; again, the result will be improved retention of initial pre-load.

Item 7 is a backup thermal feature that may not be ultimately retained. The decision will be based on the results of the full-scale certification puncture tests.

RMIS View/Print Document Cover Sheet

This document was retrieved from the Documentation and Records Management (DRM) ISEARCH System. It is intended for Information only and may not be the most recent or updated version. Contact a Document Service Center (see Hanford Info for locations) if you need additional retrieval information.

Accession #: D196080875

Document #: SD-RTG-SARP-001

Title/Desc:

RTG TRANSPORTATION SYSTEM SARP DOCKET NO 94-6-9904
[VOL I] [SEC 2 OF 4]

Pages: 203

This document was too large to scan as a whole document,
therefore it required breaking into smaller sections.

Document number: SD-RTG-SARP-001

Section 2 of 4

Title: RADIOISOTOPE THERMOELECTRIC GENERATOR
TRANSPORTATION SYSTEM SAFETY ANALYSIS REPORT
FOR PACKAGING

Date: 4/18/96 Revision: 0

Originator: FERRILL PC

Co: WHC

Recipient: _____

Co: _____

References: EDT-613639

2.10.12 ICV Three-Dimensional ANSYS Model

2.10.12.1 Description. The 3-D ICV finite element model employs half symmetry to address nonaxisymmetric RTG heat-producing debris potentially resulting from the HAC 30-ft free drop. It consists of a base and a bell, connected by bolt elements and gap elements. The plane of symmetry bisects an arc between two closure bolts. Impact limiter damage and heat-producing debris are both conservatively assumed to be centered on the plane of symmetry, halfway between two closure bolts.

The model helps evaluate closure bolt stresses and O-ring residual compression for the ICV under HAC. (The model used for NCT is 2-D and is described in Appendix 2.10.2.1. The applied loading takes the form of internal gas pressure, nodal temperatures, and initial closure bolt pre-load. Certain node locations were chosen to coincide with the nodes found in the SINDA thermal models described in Section 3.0. The relative displacement of two coincident nodes, one belonging to the ICV base structure and one to the ICV bell at the inside diameter of the ICV flange, are used with linear extrapolation to determine the change in O-ring compression from the applied conditions. The model is used for ICV analysis for the HAC load cases given in Table 2.7.3.1, 1.3-1. The model layout is shown in Figure 2.10.12-1.

2.10.12.2 Construction. The model consists of four element types:

1. To model the region around the ICV flange and base, 3-D isoparametric solid elements were used. The nodal pattern was repeated in the circumferential direction every 15° of arc, incrementing node numbers by 30 each time.
2. For the center of the ICV base and for the ICV wall and head, quadrilateral shell elements were used. In the ICV base, the thickness was 3.47 in., in the ICV wall, 0.75 in., and in the ICV head, 0.375 in. (The lifting block was not modeled because it was located far from regions of interest.) To join shell and isoparametric elements, embedded elements are used, having 1/10th the bending stiffness of the adjacent shell elements (see Reference 25, Chapter 8).
3. A 3-D spar element was used to model each closure bolt. The half-symmetry model used had 13 closure bolts with a pre-load force corresponding to a torque of 250 ft-lb. The bolt element was given an initial strain to achieve the desired closure bolt pre-load force at 70 °F, without other applied loads.
4. Gap elements were used between nodes 25 and 403 (and at every corresponding location circumferentially) for a total of 13 between the ICV base and flange. Every such gap corresponds to a closure bolt location. Because the bolt/gap radial location coincides with a step machined in the flange lower surface, no other gap elements on the contact face proved to be necessary. Three additional gaps are also used in the radial direction at 0°, 90°, and 180° to locate the ICV bell horizontally with respect to the ICV base. These gaps have a small "open stiffness" for model stability and a nominal gap size of 0.03 in., which is the nominal centered radial clearance between the ICV bell I.D. and the ICV base O.D.

Node and element plots of key portions of the model are given in Figures 2.10.12-2 through 2.10.12-11. An interpreted ANSYS input listing is given in Table 2.10.12-1.

2.10.12.3 Material Properties. The modulus of elasticity and coefficient of thermal expansion varied with temperature according to the data in Tables 2.3-1 and 2.3-2. Poisson's ratio is 0.3.

2.10.12.4 Constraints. The node at the center of the ICV base is fixed in all six degrees of

freedom, but the rest of the ICV base was allowed to deflect as determined by the applied loading. Nodes along the cut edges were constrained in the one linear and two rotational degrees of freedom required to ensure symmetry of the model.

2.10.12.5 Applied Loading. All ICV surfaces subject to internal pressure had a constant pressure applied. Nodal temperature loading was applied using temperatures resulting from the 3-D thermal model output for each HAC configuration assumption. Each HAC thermal model was composed of six segments: one centered on 0°, one centered on 180°, and four segments in between (two on each side). The centers of the HAC thermal model segments corresponded (with one exception) to a circumferential location of nodes in the structural model. (In one case, the center of a HAC thermal model segment fell on 101.25°, but a location of 105° was assumed in the structural model.) Circumferential interpolation was used to set the nodal temperatures of structural locations that fell in between the centers of the HAC thermal model segments. Some interpolation was also used within each circumferential location to fully define the temperatures of the structural model. Because the closure bolts were not modeled thermally in the structural model, it took the temperatures of the ICV flange and base at its attachment nodes. The reference was 70 °F.

2.10.12.6 Results. A plot of ICV flange stress intensity for the HAC event analysis is given in Figure 2.10.12-12. Other results are given in Sections 2.7.3.2 and 4.3.2.

0.00000E+00 0.00000E+00 0.00000E+00 0.00000E+00 0.00000E+00 0.00000E+00
0.00000E+00 0.00000E+00 0.00000E+00 0.00000E+00 0.00000E+00 0.00000E+00

REAL CONSTANT SET 42 ITEMS 1 TO 18

0.25000E+10 -0.20000E+07 0.00000E+00 0.00000E+00 0.00000E+00 0.00000E+00
0.00000E+00 0.00000E+00 0.00000E+00 0.00000E+00 0.00000E+00 0.00000E+00
0.00000E+00 0.00000E+00 0.00000E+00 0.00000E+00 0.00000E+00 0.00000E+00

REAL CONSTANT SET 43 ITEMS 1 TO 18

0.35000E+10 0.20000E+01 0.00000E+00 0.00000E+00 0.00000E+00 0.00000E+00
0.00000E+00 0.00000E+00 0.00000E+00 0.00000E+00 0.00000E+00 0.00000E+00
0.00000E+00 0.00000E+00 0.00000E+00 0.00000E+00 0.00000E+00 0.00000E+00

REAL CONSTANT SET 44 ITEMS 1 TO 18

0.25000E+10 0.30000E+01 0.00000E+00 0.00000E+00 0.00000E+00 0.00000E+00
0.00000E+00 0.00000E+00 0.00000E+00 0.00000E+00 0.00000E+00 0.00000E+00
0.00000E+00 0.00000E+00 0.00000E+00 0.00000E+00 0.00000E+00 0.00000E+00

LIST ALL COORDINATE SYSTEMS

SYSTEM	ORIENTATION VECTORS (X,Y,Z)
0	1.00 0.00 0.00 0.00 1.00 0.00 0.00 0.00 1.00
1	1.00 0.00 0.00 0.00 1.00 0.00 0.00 0.00 1.00
2	1.00 0.00 0.00 0.00 1.00 0.00 0.00 0.00 1.00
11	1.00 0.00 0.00 0.00 1.00 0.00 -1.00 0.00 1.00
12	1.00 0.00 0.00 0.00 1.00 0.00 0.00 0.00 1.00
13	1.00 0.00 0.00 0.00 1.00 0.00 0.00 0.00 1.00
15	1.00 0.00 0.00 0.00 1.00 0.00 -1.00 0.00 1.00

SYSTEM ORIENTATION VECTORS (X,Y,Z)

SYSTEM	ORIENTATION VECTORS (X,Y,Z)
0	1.00 0.00 0.00 0.00 1.00 0.00 0.00 0.00 1.00
7	1.00 0.00 0.00 0.00 1.00 0.00 0.00 0.00 1.00
2	1.00 0.00 0.00 0.00 1.00 0.00 0.00 0.00 1.00
11	1.00 0.00 0.00 0.00 1.00 0.00 -1.00 0.00 1.00
12	1.00 0.00 0.00 0.00 1.00 0.00 0.00 0.00 1.00
13	1.00 0.00 0.00 0.00 1.00 0.00 0.00 0.00 1.00
15	1.00 0.00 0.00 0.00 1.00 0.00 -1.00 0.00 1.00

COORD. TYPE	XC	YC	ZC	THX1	THX2	THX3
11	0.00000E+00	0.00000E+00	0.00000E+00	0.000	0.000	-90.000
12	0.00000E+00	27.252	0.00000E+00	0.000	0.000	0.000
13	14.937	54.397	0.00000E+00	0.000	0.000	0.000
15	0.16000E+01	0.00000E+00	0.00000E+00	0.000	0.000	-90.000

LIST ALL SELECTED ELEMENTS. (LIST MORE)

ELEM	MAT	TYP	REL	ESYS	NODES
1	1	6	23	0	391 151 181 390
2	1	6	23	0	390 181 211 396
3	1	6	23	0	392 121 151 391
4	1	6	23	0	396 211 241 397
5	1	6	23	0	121 122 152 151
6	1	6	23	0	151 152 182 181
7	1	6	23	0	181 182 212 211
8	1	6	23	0	211 212 242 241
9	1	6	23	0	393 91 121 398
10	1	6	23	0	91 92 122 121
11	1	6	23	0	397 241 271 396
12	1	6	23	0	241 242 272 271
13	1	6	23	0	92 98 128 122
14	1	6	23	0	122 123 153 152
15	1	6	23	0	152 153 183 182
16	1	6	23	0	182 183 213 212
17	1	6	23	0	212 213 243 242
18	1	6	23	0	242 243 273 272
19	1	6	23	0	394 61 91 393
20	1	6	23	0	61 62 92 91

ELEM	MAT	TYP	REL	ESYS	NODES
21	1	6	23	0	62 63 93 92
22	1	6	23	0	395 271 301 399
23	1	6	23	0	271 272 302 301
24	1	6	23	0	272 273 303 302
25	1	6	24	0	63 71 101 93

26	1	6	24	0	93	101	131	123				
27	1	6	24	0	123	121	149	133				
28	1	6	24	0	153	141	181	159				
29	1	4	24	0	183	151	211	213				
30	1	4	24	0	213	221	251	243				
31	1	6	24	0	243	251	281	273				
32	1	6	24	0	273	281	311	303				
33	1	5	1	0	43	71	72	67	99	101	102	97
34	1	5	1	0	93	101	102	97	123	131	132	127
35	1	5	1	0	123	131	132	127	153	161	162	157
36	1	5	1	0	153	161	162	157	183	191	192	187
37	1	5	1	0	183	191	192	187	213	221	222	217
38	1	5	1	0	213	221	222	217	243	251	252	247
39	1	5	1	0	243	251	252	247	273	281	282	277
40	1	5	1	0	273	281	282	277	303	311	312	307

ELEM MAT TYP REL EBYS

MODE

41	1	5	1	0	45	70	71	65	95	100	101	93
42	1	5	1	0	95	100	101	95	125	130	131	123
43	1	5	1	0	125	130	131	123	155	160	161	153
44	1	5	1	0	155	160	161	153	185	190	191	183
45	1	5	1	0	185	190	191	183	215	220	221	213
46	1	5	1	0	215	220	221	213	245	250	251	243
47	1	5	1	0	245	250	251	243	275	280	281	273
48	1	5	1	0	275	280	281	273	305	310	311	303
49	1	4	23	0	295	31	61	594				
50	1	4	23	0	31	32	62	61				
51	1	4	23	0	32	33	63	62				
52	1	4	24	0	33	41	71	65				
53	1	4	23	0	399	301	331	400				
54	1	4	23	0	301	302	332	331				
55	1	4	23	0	302	303	333	332				
56	1	4	24	0	303	311	341	333				
57	1	4	23	0	303	311	342	307	333	344	342	337
58	1	4	23	0	307	310	341	308	343	341	341	335
59	1	5	1	0	33	41	42	37	43	71	72	67
60	1	5	1	0	35	40	41	38	69	76	71	63

ELEM MAT TYP REL EBYS

MODE

61	1	5	1	0	37	42	43	38	67	72	73	68
62	1	5	1	0	47	72	73	68	97	102	103	98
63	1	5	1	0	97	102	103	98	127	132	133	128
64	1	5	1	0	127	132	133	128	157	162	163	158
65	1	5	1	0	157	162	163	158	187	192	193	188
66	1	5	1	0	187	192	193	188	217	222	223	218
67	1	5	1	0	217	222	223	218	247	252	253	248
68	1	5	1	0	247	252	253	248	277	282	283	278
69	1	5	1	0	277	282	283	278	307	312	313	308
70	1	5	1	0	307	312	313	308	337	342	343	338
71	1	5	1	0	42	46	49	43	78	79	79	73
72	1	5	1	0	72	78	79	73	102	106	109	105
73	1	5	1	0	102	106	109	105	132	136	139	133
74	1	5	1	0	132	136	139	133	158	162	165	153
75	1	5	1	0	162	166	169	163	192	196	199	193
76	1	5	1	0	192	196	199	193	222	226	229	223
77	1	5	1	0	222	226	229	223	252	256	259	253
78	1	5	1	0	252	256	259	253	282	286	289	283
79	1	5	1	0	282	286	289	283	312	316	319	313
80	1	5	1	0	312	316	319	313	342	346	349	343

ELEM MAT TYP REL EBYS

MODE

81	1	5	1	0	311	317	318	312	341	347	348	342
82	1	5	1	0	281	287	288	282	311	317	318	312
83	1	5	1	0	281	287	288	282	281	287	288	282
84	1	5	1	0	221	227	228	222	251	257	258	252
85	1	5	1	0	191	197	198	192	221	227	228	222
86	1	5	1	0	161	167	168	162	191	197	198	192
87	1	5	1	0	131	137	138	132	161	167	168	162
88	1	5	1	0	101	107	108	102	131	137	138	132
89	1	5	1	0	71	77	78	72	101	107	108	102
90	1	5	1	0	41	47	48	42	71	77	78	72

91	1	5	1	0	41	46	47	47	71	74	77	77
92	1	5	1	0	71	74	77	77	101	104	107	107
93	1	5	1	0	101	106	107	107	131	134	137	137
94	1	5	1	0	131	136	137	137	161	164	167	167
95	1	5	1	0	161	166	167	167	191	194	197	197
96	1	5	1	0	191	196	197	197	221	224	227	227
97	1	5	1	0	221	226	227	227	251	254	257	257
98	1	5	1	0	251	256	257	257	281	284	287	287
99	1	5	1	0	281	286	287	287	311	314	317	317
100	1	5	1	0	311	316	317	317	341	344	347	347

ELEN MAT TYP REL ESTS

NODES

101	1	5	1	0	40	43	46	61	70	75	76	71
102	1	5	1	0	70	75	76	73	100	103	106	101
103	1	5	1	0	100	105	106	104	130	135	136	131
104	1	5	1	0	130	135	136	131	160	163	166	161
105	1	5	1	0	160	165	166	164	190	195	196	191
106	1	5	1	0	190	195	196	194	220	225	226	221
107	1	5	1	0	220	225	226	221	250	255	256	251
108	1	5	1	0	250	255	256	254	280	285	286	281
109	1	5	1	0	280	285	286	284	310	315	316	311
110	1	5	1	0	310	315	316	314	340	345	346	341
111	1	5	1	0	34	39	40	35	64	69	70	65
112	1	5	1	0	64	69	70	65	94	99	100	95
113	1	5	1	0	94	99	100	95	124	129	130	125
114	1	5	1	0	124	129	130	125	154	159	160	155
115	1	5	1	0	154	159	160	155	184	189	190	185
116	1	5	1	0	184	189	190	185	214	219	220	215
117	1	5	1	0	214	219	220	215	244	249	250	245
118	1	5	1	0	244	249	250	245	274	279	280	275
119	1	5	1	0	274	279	280	275	304	309	310	305
120	1	5	1	0	304	309	310	305	334	339	340	335

ELEN MAT TYP REL ESTS

NODES

121	1	5	1	0	39	44	45	40	69	74	75	70
122	1	5	1	0	69	74	75	70	99	104	105	100
123	1	5	1	0	99	104	105	100	129	134	135	130
124	1	5	1	0	129	134	135	130	159	164	165	160
125	1	5	1	0	159	164	165	160	189	194	195	190
126	1	5	1	0	189	194	195	190	219	224	225	220
127	1	5	1	0	219	224	225	220	249	254	255	250
128	1	5	1	0	249	254	255	250	279	284	285	280
129	1	5	1	0	279	284	285	280	309	314	315	310
130	1	5	1	0	309	314	315	310	339	344	345	340
131	1	6	23	0	395	1	31	31				
132	1	6	23	0	1	2	32	31				
133	1	6	23	0	2	3	33	32				
134	1	6	23	0	400	331	361	361				
135	1	6	23	0	331	332	362	361				
136	1	6	23	0	332	333	363	362				
137	1	6	24	0	3	11	41	33				
138	1	6	24	0	333	341	371	365				
139	1	5	1	0	342	345	349	345	372	378	379	373
140	1	5	1	0	337	342	343	339	367	372	373	368

ELEN MAT TYP REL ESTS

NODES

141	1	5	1	0	333	341	342	337	365	371	372	367
142	1	5	1	0	341	347	348	342	371	377	378	373
143	1	5	1	0	341	344	347	347	371	376	377	372
144	1	5	1	0	335	348	341	335	365	370	371	363
145	1	5	1	0	334	339	348	335	364	369	370	365
146	1	5	1	0	348	345	344	341	370	375	376	371
147	1	5	1	0	339	344	345	340	369	374	375	370
148	1	5	1	0	12	10	10	13	42	48	49	43
149	1	5	1	0	7	12	13	8	37	42	43	38
150	1	5	1	0	3	11	12	7	33	41	42	37
151	1	5	1	0	11	17	18	12	41	47	48	42
152	1	5	1	0	11	16	17	17	41	46	47	42
153	1	5	1	0	5	10	11	3	35	40	41	36
154	1	5	1	0	4	9	10	5	34	39	40	35
155	1	5	1	0	10	15	16	11	40	45	46	41

756	1	5	1	0	9	16	15	10	39	64	85	40
157	1	5	1	0	14	20	21	15	44	90	51	45
198	1	5	1	0	13	21	22	16	45	51	52	46
199	1	5	1	0	44	50	51	43	74	80	81	75
160	1	5	1	0	43	51	52	44	75	81	82	76

ELEM JAN TYP REL ESTS

MOSES

161	1	5	1	0	74	80	81	75	104	110	111	105
162	1	5	1	0	75	81	82	76	105	111	112	106
163	1	5	1	0	104	110	111	105	134	140	141	133
164	1	5	1	0	105	111	112	106	135	141	142	136
166	1	5	1	0	134	140	141	135	164	170	171	160
166	1	5	1	0	135	141	142	136	165	171	172	166
167	1	5	1	0	164	170	171	165	194	200	201	198
168	1	5	1	0	165	171	172	166	195	201	202	199
169	1	5	1	0	194	200	201	195	224	230	231	228
170	1	5	1	0	195	201	202	196	225	231	232	229
171	1	5	1	0	224	230	231	225	254	260	261	255
172	1	5	1	0	225	231	232	226	255	261	262	256
173	1	5	1	0	254	260	261	255	284	290	291	285
174	1	5	1	0	255	261	262	256	285	291	292	286
175	1	5	1	0	284	290	291	285	314	320	321	318
176	1	5	1	0	285	291	292	286	315	321	322	319
177	1	5	1	0	314	320	321	315	344	350	351	348
178	1	5	1	0	315	321	322	316	345	351	352	349
179	1	5	1	0	344	350	351	345	374	380	381	375
180	1	5	1	0	345	351	352	346	375	381	382	376

ELEM JAN TYP REL ESTS

MOSES

181	1	5	1	0	20	23	24	21	50	53	54	51
182	1	5	1	0	21	24	25	22	51	54	55	52
183	1	5	1	0	50	53	54	51	80	83	84	81
184	1	5	1	0	51	54	55	52	81	84	85	82
185	1	5	1	0	80	83	84	81	110	113	114	111
186	1	5	1	0	81	84	85	82	111	114	115	112
187	1	5	1	0	110	113	114	111	140	143	144	141
188	1	5	1	0	111	114	115	112	141	144	145	142
189	1	5	1	0	140	143	144	141	170	173	174	171
190	1	5	1	0	141	144	145	142	171	174	175	172
191	1	5	1	0	170	173	174	171	200	203	204	201
192	1	5	1	0	171	174	175	172	201	204	205	202
193	1	5	1	0	200	203	204	201	230	233	234	231
194	1	5	1	0	201	204	205	202	231	234	235	232
195	1	5	1	0	230	233	234	231	260	263	264	261
196	1	5	1	0	231	234	235	232	261	264	265	262
197	1	5	1	0	260	263	264	261	290	293	294	291
198	1	5	1	0	261	264	265	262	291	294	295	292
199	1	5	1	0	290	293	294	291	320	323	324	321
200	1	5	1	0	291	294	295	292	321	324	325	322

ELEM JAN TYP REL ESTS

MOSES

201	1	5	1	0	320	323	324	321	350	353	354	351
202	1	5	1	0	321	324	325	322	351	354	355	352
203	1	5	1	0	350	353	354	351	380	383	384	381
204	1	5	1	0	351	354	355	352	381	384	385	382
205	2	4	43	0	32	423						
206	2	4	43	0	33	423						
207	2	4	43	0	33	423						
208	2	4	43	0	115	493						
209	2	4	43	0	175	553						
210	2	4	43	0	295	673						
211	2	3	3	0	54	437						
212	2	3	3	0	354	737						
213	2	3	3	0	114	497						
214	2	3	3	0	174	557						
215	2	3	3	0	254	617						
216	2	3	3	0	294	677						
217	1	5	1	0	23	26	27	24	53	56	57	54
218	1	5	1	0	24	27	28	25	54	57	58	55
219	1	5	1	0	53	56	57	54	83	86	87	84
220	1	5	1	0	54	57	58	55	84	87	88	85

ELBN	MAT	TYP	REL	ESTS	NODES											
221	1	5	1	0	85	86	87	84	115	116	117	114				
222	1	5	1	0	84	87	88	85	114	117	118	115				
223	1	5	1	0	117	118	117	114	145	146	147	144				
224	1	5	1	0	114	117	118	115	144	147	148	145				
225	1	5	1	0	143	146	147	144	175	176	177	174				
226	1	5	1	0	144	147	148	145	174	177	178	175				
227	1	5	1	0	173	176	177	174	203	204	207	204				
228	1	5	1	0	174	177	178	175	204	207	208	205				
229	1	5	1	0	203	206	207	204	233	236	237	234				
230	1	5	1	0	204	207	208	205	234	237	238	235				
231	1	5	1	0	233	236	237	234	263	266	267	264				
232	1	5	1	0	234	237	238	235	264	267	268	265				
233	1	5	1	0	263	266	267	264	293	294	297	294				
234	1	5	1	0	264	267	268	265	294	297	298	295				
235	1	5	1	0	293	296	297	294	323	326	327	324				
236	1	5	1	0	294	297	298	295	324	327	328	325				
237	1	5	1	0	323	326	327	324	353	356	357	354				
238	1	5	1	0	324	327	328	325	354	357	358	355				
239	1	5	1	0	353	356	357	354	383	386	387	384				
240	1	5	1	0	354	357	358	355	384	387	388	385				

ELBN	MAT	TYP	REL	ESTS	NODES											
241	1	7	1	0	403	404	408	407	433	434	438	437				
242	1	7	1	0	402	403	407	404	432	433	437	436				
243	1	7	1	0	407	408	412	411	437	438	442	441				
244	1	7	1	0	404	407	411	410	436	437	441	440				
245	1	7	1	0	433	434	438	437	463	464	468	467				
246	1	7	1	0	463	464	468	467	493	494	498	497				
247	1	7	1	0	432	433	437	436	462	463	467	466				
248	1	7	1	0	462	463	467	466	492	493	497	496				
249	1	7	1	0	437	438	442	441	467	468	472	471				
250	1	7	1	0	436	437	441	440	466	467	471	470				
251	1	7	1	0	407	408	412	411	497	498	502	501				
252	1	7	1	0	406	407	411	410	496	497	501	500				
253	1	7	1	0	497	498	502	501	523	524	528	527				
254	1	7	1	0	523	524	528	527	553	554	558	557				
255	1	7	1	0	492	493	497	496	522	523	527	526				
256	1	7	1	0	522	523	527	526	552	553	557	556				
257	1	7	1	0	497	498	502	501	527	528	532	531				
258	1	7	1	0	496	497	501	500	526	527	531	530				
259	1	7	1	0	527	528	532	531	557	558	562	561				
260	1	7	1	0	526	527	531	530	556	557	561	560				

ELBN	MAT	TYP	REL	ESTS	NODES											
261	1	7	1	0	553	554	558	557	583	584	588	587				
262	1	7	1	0	583	584	588	587	613	614	618	617				
263	1	7	1	0	552	553	557	556	582	583	587	586				
264	1	7	1	0	582	583	587	586	612	613	617	616				
265	1	7	1	0	557	558	562	561	587	588	592	591				
266	1	7	1	0	554	557	561	560	586	587	591	590				
267	1	7	1	0	587	588	592	591	617	618	622	621				
268	1	7	1	0	584	587	591	590	616	617	621	620				
269	1	7	1	0	617	618	622	621	643	644	648	647				
270	1	7	1	0	643	644	648	647	673	674	678	677				
271	1	7	1	0	612	613	617	616	642	643	647	646				
272	1	7	1	0	642	643	647	646	672	673	677	676				
273	1	7	1	0	617	618	622	621	647	648	652	651				
274	1	7	1	0	616	617	621	620	646	647	651	650				
275	1	7	1	0	647	648	652	651	677	678	682	681				
276	1	7	1	0	646	647	651	650	676	677	681	680				
277	1	7	1	0	673	674	678	677	703	704	708	707				
278	1	7	1	0	703	704	708	707	733	734	738	737				
279	1	7	1	0	672	673	677	676	702	703	707	706				
280	1	7	1	0	702	703	707	706	732	733	737	736				

ELBN	MAT	TYP	REL	ESTS	NODES							
281	1	7	1	0	677	678	682	681	707	708	712	711
282	1	7	1	0	676	677	681	680	706	707	711	710

283	1	7	1	0	707	708	710	711	737	738	742	761
284	1	7	1	0	708	707	711	710	736	737	761	740
285	1	7	1	0	723	734	738	737	768	764	768	767
286	1	7	1	0	732	733	737	736	762	763	767	766
287	1	7	1	0	737	738	742	741	767	766	772	771
288	1	7	1	0	736	737	741	740	766	767	771	770
289	1	7	1	0	401	402	406	408	431	432	436	435
290	1	7	1	0	431	432	436	435	461	462	464	465
291	1	7	1	0	405	406	410	409	435	436	440	439
292	1	7	1	0	435	436	440	439	463	464	470	469
293	1	7	1	0	441	442	446	445	491	492	496	495
294	1	7	1	0	465	466	470	469	495	496	500	499
295	1	7	1	0	491	492	496	495	521	522	526	525
296	1	7	1	0	495	496	500	499	525	526	530	529
297	1	7	1	0	521	522	526	525	551	552	554	555
298	1	7	1	0	525	526	530	529	555	556	560	559
299	1	7	1	0	551	552	556	555	581	582	586	585
300	1	7	1	0	555	556	560	559	585	586	590	589

ELEN MAT TYP REL ESYS

MODES

301	1	7	1	0	581	582	586	585	611	612	616	615
302	1	7	1	0	585	586	590	589	615	616	620	619
303	1	7	1	0	611	612	616	615	641	642	646	645
304	1	7	1	0	615	616	620	619	645	646	650	649
305	1	7	1	0	641	642	646	645	671	672	676	675
306	1	7	1	0	645	646	650	649	675	676	680	679
307	1	7	1	0	671	672	676	675	701	702	706	705
308	1	7	1	0	675	676	680	679	705	706	710	709
309	1	7	1	0	701	702	706	705	731	732	736	735
310	1	7	1	0	731	732	736	735	761	762	766	765
311	1	7	1	0	705	706	710	709	735	736	740	739
312	1	7	1	0	735	736	740	739	765	766	770	769
313	1	7	1	0	411	412	416	415	441	442	446	445
314	1	7	1	0	410	411	415	414	440	441	445	444
315	1	7	1	0	409	410	414	413	439	440	444	443
316	1	7	1	0	441	442	446	445	471	472	476	475
317	1	7	1	0	440	441	445	444	470	471	475	474
318	1	7	1	0	439	440	444	443	469	470	474	473
319	1	7	1	0	471	472	476	475	501	502	506	505
320	1	7	1	0	470	471	475	474	500	501	505	504

ELEN MAT TYP REL ESYS

MODES

321	1	7	1	0	449	470	474	473	499	500	504	503
322	1	7	1	0	501	502	506	505	531	532	536	535
323	1	7	1	0	500	501	505	504	530	531	535	534
324	1	7	1	0	499	500	504	503	529	530	534	533
325	1	7	1	0	531	532	536	535	561	562	566	565
326	1	7	1	0	530	531	535	534	560	561	565	564
327	1	7	1	0	529	530	534	533	559	560	564	563
328	1	7	1	0	561	562	566	565	591	592	596	595
329	1	7	1	0	560	561	565	564	590	591	595	594
330	1	7	1	0	559	560	564	563	589	590	594	593
331	1	7	1	0	591	592	596	595	621	622	626	625
332	1	7	1	0	590	591	595	594	620	621	625	624
333	1	7	1	0	589	590	594	593	619	620	624	623
334	1	7	1	0	621	622	626	625	651	652	656	655
335	1	7	1	0	620	621	625	624	650	651	655	654
336	1	7	1	0	619	620	624	623	649	650	654	653
337	1	7	1	0	617	618	622	621	647	648	652	651
338	1	7	1	0	651	652	656	655	680	681	685	684
339	1	7	1	0	649	650	654	653	679	680	684	683
340	1	7	1	0	681	682	686	685	711	712	716	715

ELEN MAT TYP REL ESYS

MODES

341	1	7	1	0	685	686	690	689	719	720	724	723
342	1	7	1	0	679	680	684	683	709	710	714	713
343	1	7	1	0	711	712	716	715	741	742	746	745
344	1	7	1	0	741	742	746	745	771	772	776	775
345	1	7	1	0	710	711	715	714	740	741	745	744
346	1	7	1	0	740	741	745	744	770	771	775	774
347	1	7	1	0	709	710	714	713	739	740	744	743

346	1	7	1	0	739	740	744	743	749	770	774	773
349	1	7	1	0	475	476	480	479	445	444	450	449
350	1	7	1	0	474	475	479	478	444	445	449	448
351	1	7	1	0	473	474	478	477	443	444	448	447
352	1	7	1	0	445	446	450	449	475	476	480	479
353	1	7	1	0	444	445	449	448	474	475	479	478
354	1	7	1	0	443	444	448	447	473	474	478	477
355	1	7	1	0	479	478	480	479	501	500	510	509
356	1	7	1	0	474	475	479	478	504	503	509	508
357	1	7	1	0	473	474	478	477	500	504	508	507
358	1	7	1	0	505	506	510	509	535	536	540	539
359	1	7	1	0	504	505	509	508	534	535	539	538
360	1	7	1	0	503	504	508	507	533	534	538	537

ELEM MAT TYP REL ESTS

NODES

361	1	7	1	0	535	536	540	539	565	566	570	569
362	1	7	1	0	534	535	539	538	564	565	569	568
363	1	7	1	0	533	534	538	537	563	564	568	567
364	1	7	1	0	565	566	570	569	599	596	600	599
365	1	7	1	0	564	565	569	568	594	599	599	598
366	1	7	1	0	563	564	568	567	593	598	598	597
367	1	7	1	0	599	596	600	599	629	624	630	629
368	1	7	1	0	594	595	599	598	624	625	629	628
369	1	7	1	0	593	594	598	597	623	625	629	627
370	1	7	1	0	625	626	630	629	655	656	660	659
371	1	7	1	0	624	625	629	628	654	655	659	658
372	1	7	1	0	623	624	628	627	653	654	658	657
373	1	7	1	0	655	656	660	659	685	686	690	689
374	1	7	1	0	654	655	659	658	684	685	689	688
375	1	7	1	0	653	654	658	657	683	684	688	687
376	1	7	1	0	685	686	690	689	715	716	720	719
377	1	7	1	0	684	685	689	688	714	715	719	718
378	1	7	1	0	683	684	688	687	713	714	718	717
379	1	7	1	0	715	716	720	719	745	746	750	749
380	1	7	1	0	714	715	719	718	775	776	780	779

ELEM MAT TYP REL ESTS

NODES

381	1	7	1	0	714	715	719	718	744	745	749	748
382	1	7	1	0	744	745	749	748	774	775	779	778
383	1	7	1	0	743	744	748	747	773	774	778	777
384	1	7	1	0	743	744	748	747	773	774	778	777
385	1	8	22	0	748	778	784	754				
386	1	8	22	0	718	748	754	724				
387	1	8	22	0	688	718	724	694				
388	1	8	22	0	658	688	694	664				
389	1	8	22	0	628	658	664	634				
390	1	8	22	0	598	628	634	604				
391	1	8	22	0	568	598	604	574				
392	1	8	22	0	538	568	574	544				
393	1	8	22	0	508	538	544	514				
394	1	8	22	0	478	508	514	484				
395	1	8	22	0	448	478	484	454				
396	1	8	22	0	418	448	454	424				
397	1	7	1	0	789	790	794	793	779	780	786	785
398	1	7	1	0	748	749	753	754	778	779	785	784
399	1	7	1	0	718	719	724	725	749	750	756	755
400	1	7	1	0	718	719	725	724	748	749	755	754

ELEM MAT TYP REL ESTS

NODES

401	1	7	1	0	889	890	896	895	719	720	726	725
402	1	7	1	0	888	889	895	894	718	719	725	724
403	1	7	1	0	889	890	896	895	889	890	896	895
404	1	7	1	0	888	889	895	894	888	889	895	894
405	1	7	1	0	829	830	836	835	659	660	666	665
406	1	7	1	0	828	829	835	834	658	659	665	664
407	1	7	1	0	599	600	606	605	629	630	636	635
408	1	7	1	0	598	599	605	604	628	629	635	634
409	1	7	1	0	569	570	576	575	599	600	606	605
410	1	7	1	0	568	569	575	574	598	599	605	604
411	1	7	1	0	539	540	546	545	569	570	576	575
412	1	7	1	0	538	539	545	544	568	569	575	574

643	1	7	1	0	500	510	514	515	539	540	544	545
644	1	7	1	0	500	509	515	514	538	539	543	544
645	1	7	1	0	470	480	484	485	509	510	516	515
646	1	7	1	0	470	479	485	484	508	509	515	514
647	1	7	1	0	449	450	454	455	479	480	486	485
648	1	7	1	0	419	420	424	425	449	450	456	455
649	1	7	1	0	410	419	425	424	448	449	455	454
650	1	7	1	0	448	449	453	454	478	479	485	484

ELEM MAT TYP REL EBY8

NOD88

621	1	7	1	0	417	418	424	423	447	448	454	453
622	1	7	1	0	421	417	425	422	451	447	453	452
623	1	7	1	0	447	448	454	453	477	478	484	483
624	1	7	1	0	451	447	453	452	481	477	483	482
625	1	7	1	0	477	478	484	483	507	508	514	513
626	1	7	1	0	481	477	483	482	511	507	513	512
627	1	7	1	0	507	508	514	513	537	538	544	543
628	1	7	1	0	511	507	513	512	541	537	543	542
629	1	7	1	0	537	538	544	543	567	568	574	573
630	1	7	1	0	541	537	543	542	571	567	573	572
631	1	7	1	0	567	568	574	573	597	598	604	603
632	1	7	1	0	571	567	573	572	601	597	603	602
633	1	7	1	0	597	598	604	603	627	628	634	633
634	1	7	1	0	601	597	603	602	631	627	633	632
635	1	7	1	0	627	628	634	633	657	658	664	663
636	1	7	1	0	631	627	633	632	661	657	663	662
637	1	7	1	0	657	658	664	663	687	688	694	693
638	1	7	1	0	661	657	663	662	691	687	693	692
639	1	7	1	0	687	688	694	693	717	718	724	723
640	1	7	1	0	691	687	693	692	721	717	723	722

ELEM MAT TYP REL EBY8

NOD85

641	1	7	1	0	717	718	724	723	747	748	754	753
642	1	7	1	0	721	717	725	722	751	747	753	752
643	1	7	1	0	751	747	753	752	781	777	783	782
644	1	7	1	0	747	748	754	753	777	778	784	783
645	1	2	2	0	794	794	1161	1131				
646	1	2	2	0	824	834	851	801				
647	1	2	2	0	854	864	881	831				
648	1	2	2	0	724	734	1131	1101				
649	1	2	2	0	434	514	891	851				
650	1	2	2	0	694	724	1101	1071				
651	1	2	2	0	914	944	921	891				
652	1	2	2	0	544	574	951	921				
653	1	2	2	0	974	984	991	951				
654	1	2	2	0	604	634	1011	981				
655	1	2	2	0	634	664	1041	1011				
656	1	2	2	0	664	694	1071	1041				
657	1	2	2	0	809	831	852	802				
658	1	2	2	0	831	861	882	832				
659	1	2	2	0	882	852	883	883				
660	1	2	2	0	852	862	863	853				

ELEM MAT TYP REL EBY8

NOD85

661	1	2	2	0	861	891	892	862				
662	1	2	2	0	882	892	893	883				
663	1	2	2	0	883	893	894	884				
664	1	2	2	0	853	863	864	854				
665	1	2	2	0	863	893	894	864				
666	1	2	2	0	891	921	922	892				
667	1	2	2	0	892	922	923	893				
668	1	2	2	0	893	923	924	894				
669	1	2	2	0	884	854	895	885				
670	1	2	2	0	854	864	865	855				
671	1	2	2	0	864	894	895	865				
672	1	2	2	0	894	924	925	895				
673	1	2	2	0	885	835	836	886				
674	1	2	2	0	835	865	866	836				
675	1	2	2	0	865	895	896	866				
676	1	2	2	0	895	925	926	896				
677	1	2	2	0	921	951	952	922				

478	1	2	2	0	922	932	933	923
479	1	2	2	0	923	933	934	924
480	1	2	2	0	924	934	935	925

ELEM	MAT	TYP	REL	ENTS	NODES			
481	1	2	2	0	925	935	934	926
482	1	2	2	0	926	936	937	927
483	1	2	2	0	934	944	947	937
484	1	2	2	0	936	946	947	937
485	1	2	2	0	946	926	927	937
486	1	2	2	0	926	934	937	927
487	1	2	2	0	951	981	982	932
488	1	2	2	0	952	982	983	933
489	1	2	2	0	953	983	984	934
490	1	2	2	0	954	984	985	935
491	1	2	2	0	955	985	986	936
492	1	2	2	0	956	986	987	937
493	1	2	2	0	981	911	912	982
494	1	2	2	0	982	912	913	983
495	1	2	2	0	983	913	914	984
496	1	2	2	0	984	914	915	985
497	1	2	2	0	985	915	914	986
498	1	2	2	0	986	916	917	987
499	1	2	2	0	916	944	947	917
500	1	2	2	0	915	945	946	916

ELEM	MAT	TYP	REL	KEYS	NODES			
501	1	2	2	0	916	944	945	915
502	1	2	2	0	915	943	944	914
503	1	2	2	0	912	942	943	913
504	1	2	2	0	911	941	942	912
505	1	2	2	0	944	976	977	947
506	1	2	2	0	945	975	976	946
507	1	2	2	0	944	974	975	945
508	1	2	2	0	943	973	974	944
509	1	2	2	0	942	972	973	943
510	1	2	2	0	941	971	972	942
511	1	2	2	0	976	916	917	977
512	1	2	2	0	975	915	916	976
513	1	2	2	0	974	914	915	975
514	1	2	2	0	973	913	914	974
515	1	2	2	0	972	912	913	973
516	1	2	2	0	971	911	912	972
517	1	2	2	0	916	936	937	917
518	1	2	2	0	915	935	936	916
519	1	2	2	0	916	934	935	916
520	1	2	2	0	913	933	934	914

ELEM	MAT	TYP	REL	ENTS	NODES			
521	1	2	2	0	912	932	933	913
522	1	2	2	0	911	931	932	912
523	1	2	2	0	934	966	967	937
524	1	2	2	0	935	965	966	936
525	1	2	2	0	934	964	965	935
526	1	2	2	0	933	963	964	934
527	1	2	2	0	932	962	963	933
528	1	2	2	0	931	961	962	932
537	2	4	41	0	329	709		
538	2	4	41	0	268	643		
539	2	4	41	0	209	588		
548	2	4	41	0	149	523		
541	2	4	41	0	88	463		
542	2	4	42	0	389	763		
543	2	4	42	0	29	403		
546	2	4	44	0	17	406		
549	2	4	44	0	377	768		
576	2	4	43	0	997	595		
571	1	2	2	0	807	837	838	808
572	1	2	2	0	806	836	839	807

ELEM	MAT	TYP	REL	ENTS	NODES			
------	-----	-----	-----	------	-------	--	--	--

475	1	9	21	0	809	839	860	810
474	1	9	21	0	810	840	841	811
475	1	9	21	0	811	841	842	812
476	1	9	21	0	812	842	843	813
477	1	9	21	0	813	843	844	814
478	1	9	21	0	814	844	845	815
479	1	9	21	0	815	845	846	816
480	1	9	21	0	816	846	847	817
481	1	2	2	0	837	867	868	838
482	1	2	2	0	838	868	869	839
483	1	9	21	0	839	869	870	840
484	1	9	21	0	840	870	871	841
485	1	9	21	0	841	871	872	842
486	1	9	21	0	842	872	873	843
487	1	9	21	0	843	873	874	844
488	1	9	21	0	844	874	875	845
489	1	9	21	0	845	875	876	846
490	1	9	21	0	846	876	877	847
491	1	2	2	0	867	897	898	868
492	1	2	2	0	868	898	899	869

ELBN	MAT	TYP	REL	ESTB	MODES
493	1	9	21	0	869 899 900 870
494	1	9	21	0	870 900 901 871
495	1	9	21	0	871 901 902 872
496	1	9	21	0	872 902 903 873
497	1	9	21	0	873 903 904 874
498	1	9	21	0	874 904 905 875
499	1	9	21	0	875 905 906 876
700	1	9	21	0	876 906 907 877
701	1	2	2	0	897 927 928 898
702	1	2	2	0	898 928 929 899
703	1	9	21	0	899 929 930 900
704	1	9	21	0	900 930 931 901
705	1	9	21	0	901 931 932 902
706	1	9	21	0	902 932 933 903
707	1	9	21	0	903 933 934 904
708	1	9	21	0	904 934 935 905
709	1	9	21	0	905 935 936 906
710	1	9	21	0	906 936 937 907
711	1	2	2	0	927 957 958 928
712	1	2	2	0	928 958 959 929

ELBN	MAT	TYP	REL	ESTB	MODES
713	1	9	21	0	929 959 960 930
714	1	9	21	0	930 960 961 931
715	1	9	21	0	931 961 962 932
716	1	9	21	0	932 962 963 933
717	1	9	21	0	933 963 964 934
718	1	9	21	0	934 964 965 935
719	1	9	21	0	935 965 966 936
720	1	9	21	0	936 966 967 937
721	1	2	2	0	957 987 988 958
722	1	2	2	0	958 988 989 959
723	1	9	21	0	959 989 990 960
724	1	9	21	0	960 990 991 961
725	1	9	21	0	961 991 992 962
726	1	9	21	0	962 992 993 963
727	1	9	21	0	963 993 994 964
728	1	9	21	0	964 994 995 965
729	1	9	21	0	965 995 996 966
730	1	9	21	0	966 996 997 967
731	1	2	2	0	987 1017 1018 988
732	1	2	2	0	988 1018 1019 989

ELBN	MAT	TYP	REL	ESTB	MODES
733	1	9	21	0	989 1019 1020 990
734	1	9	21	0	990 1020 1021 991
735	1	9	21	0	991 1021 1022 992
736	1	9	21	0	992 1022 1023 993

737	↑	P	21	0	893	1023	1024	994
738	↑	Q	21	0	894	1024	1025	998
739	↑	P	21	0	895	1025	1026	996
740	↑	Q	21	0	896	1026	1027	997
741	↑	Z	2	0	1017	1047	1048	1018
742	↑	Z	2	0	1018	1048	1049	1019
743	↑	P	21	0	1019	1049	1050	1020
744	↑	P	21	0	1020	1050	1051	1021
745	↑	P	21	0	1021	1051	1052	1022
746	↑	Q	21	0	1022	1052	1053	1023
747	↑	P	21	0	1023	1053	1054	1024
748	↑	Q	21	0	1024	1054	1055	1025
749	↑	P	21	0	1025	1055	1056	1026
750	↑	Q	21	0	1026	1056	1057	1027
751	↑	Z	2	0	1047	1077	1078	1048
752	↑	Z	2	0	1048	1078	1079	1049

ELEM	MAP	TRP	REL	ESTD	MODES			
753	↑	P	21	0	1049	1079	1080	1050
754	↑	Q	21	0	1050	1080	1081	1051
755	↑	P	21	0	1051	1081	1082	1052
756	↑	P	21	0	1052	1082	1083	1053
757	↑	P	21	0	1053	1083	1084	1054
758	↑	P	21	0	1054	1084	1085	1055
759	↑	Q	21	0	1055	1085	1086	1056
760	↑	P	21	0	1056	1086	1087	1057
761	↑	Z	2	0	1077	1107	1108	1078
762	↑	Z	2	0	1078	1108	1109	1079
763	↑	Q	21	0	1079	1109	1110	1080
764	↑	P	21	0	1080	1110	1111	1081
765	↑	P	21	0	1081	1111	1112	1082
766	↑	P	21	0	1082	1112	1113	1083
767	↑	P	21	0	1083	1113	1114	1084
768	↑	P	21	0	1084	1114	1115	1085
769	↑	Q	21	0	1085	1115	1116	1086
770	↑	P	21	0	1086	1116	1117	1087
771	↑	Z	2	0	1107	1137	1138	1108
772	↑	Z	2	0	1108	1138	1139	1109

ELEM	MAP	TRP	REL	ESTD	MODES			
773	↑	Q	21	0	1109	1139	1140	1110
774	↑	Q	21	0	1110	1140	1141	1111
775	↑	Q	21	0	1111	1141	1142	1112
776	↑	P	21	0	1112	1142	1143	1113
777	↑	Q	21	0	1113	1143	1144	1114
778	↑	P	21	0	1114	1144	1145	1115
779	↑	P	21	0	1115	1145	1146	1116
780	↑	Q	21	0	1116	1146	1147	1117
781	↑	Z	2	0	1137	1167	1168	1138
782	↑	Z	2	0	1138	1168	1169	1139
783	↑	P	21	0	1139	1169	1170	1140
784	↑	P	21	0	1140	1170	1171	1141
785	↑	P	21	0	1141	1171	1172	1142
786	↑	P	21	0	1142	1172	1173	1143
787	↑	P	21	0	1143	1173	1174	1144
788	↑	P	21	0	1144	1174	1175	1145
789	↑	P	21	0	1145	1175	1176	1146
790	↑	Q	21	0	1146	1176	1177	1147
791	↑	P	21	0	847	847	848	848
792	↑	P	21	0	847	877	878	848

ELEM	MAP	TRP	REL	ESTD	MODES			
793	↑	Q	21	0	877	907	908	848
794	↑	P	21	0	907	937	938	849
795	↑	P	21	0	937	967	968	850
796	↑	P	21	0	967	997	998	851
797	↑	Q	21	0	997	1027	1028	852
798	↑	P	21	0	1027	1057	1058	853
799	↑	Q	21	0	1057	1087	1088	854
800	↑	P	21	0	1087	1117	1118	855
801	↑	Q	21	0	1117	1147	1148	856

805	1	2	1	0	1347	1177	548	548
805	2	3	3	0	84	467		
805	2	3	3	0	144	527		
805	2	3	3	0	204	587		
806	2	3	3	0	264	647		
807	2	3	3	0	324	707		
808	2	3	4	0	24	407		
809	2	3	4	0	324	767		

LIST ALL SELECTED NODE DATA= 0

NODE	X	Y	Z	THX1	THY2	THZ2
1	4.0800	1.7350	0.67604E-11	0.00	0.00	0.00
2	9.3750	1.7350	0.67604E-11	0.00	0.00	0.00
3	12.750	1.7350	0.67604E-11	0.00	0.00	0.00
4	12.750	0.60000E+00	0.10000E-20	0.00	0.00	0.00
5	12.750	0.84500	0.32025E-11	0.00	0.00	0.00
7	12.750	2.5950	0.10111E-10	0.00	0.00	0.00
8	12.750	3.4700	0.13521E-10	0.00	0.00	0.00
9	15.900	0.60000E+00	0.10000E-20	0.00	0.00	0.00
10	15.900	0.84500	0.32025E-11	0.00	0.00	0.00
11	15.900	1.7350	0.67604E-11	0.00	0.00	0.00
12	15.900	2.5950	0.10111E-10	0.00	0.00	0.00
13	15.900	3.4700	0.13521E-10	0.00	0.00	0.00
14	16.970	0.60000E+00	0.00000E+00	0.00	0.00	0.00
15	16.970	0.84500	0.32025E-11	0.00	0.00	0.00
16	16.970	1.4700	0.57279E-11	0.00	0.00	0.00
17	16.970	2.0700	0.80658E-11	0.00	0.00	0.00
18	16.970	2.6200	0.10209E-10	0.00	0.00	0.00
19	16.970	3.4700	0.13521E-10	0.00	0.00	0.00
20	17.813	0.60000E+00	0.00000E+00	0.00	0.00	0.00
21	17.813	0.84500	0.32025E-11	0.00	0.00	0.00

NODE	X	Y	Z	THX1	THY2	THZ2
22	17.813	1.4700	0.57279E-11	0.00	0.00	0.00
23	18.425	0.60000E+00	0.00000E+00	0.00	0.00	0.00
24	18.425	0.84500	0.32025E-11	0.00	0.00	0.00
25	18.425	1.4690	0.57240E-11	0.00	0.00	0.00
26	19.470	0.60000E+00	0.10000E-20	0.00	0.00	0.00
27	19.470	0.84500	0.32025E-11	0.00	0.00	0.00
28	19.470	1.4700	0.57279E-11	0.00	0.00	0.00
31	5.7954	1.7350	-1.5929	0.00	0.00	0.00
32	9.0354	1.7350	-2.4264	0.00	0.00	0.00
33	12.514	1.7350	-3.2999	0.00	0.00	0.00
34	12.514	0.12058E-10	-3.2999	0.00	0.00	0.00
35	12.514	0.84500	-3.2999	0.00	0.00	0.00
37	12.514	2.5950	-3.2999	0.00	0.00	0.00
38	12.514	3.4700	-3.2999	0.00	0.00	0.00
39	15.350	0.16035E-10	-4.1152	0.00	0.00	0.00
40	15.350	0.84500	-4.1152	0.00	0.00	0.00
41	15.350	1.7350	-4.1152	0.00	0.00	0.00
42	15.350	2.5950	-4.1152	0.00	0.00	0.00
43	15.350	3.4700	-4.1152	0.00	0.00	0.00
44	16.392	0.17114E-10	-4.3922	0.00	0.00	0.00

NODE	X	Y	Z	THX1	THY2	THZ2
45	16.392	0.84500	-4.3922	0.00	0.00	0.00
46	16.392	1.4700	-4.3922	0.00	0.00	0.00
47	16.392	2.0700	-4.3922	0.00	0.00	0.00
48	16.392	2.6200	-4.3922	0.00	0.00	0.00
49	16.392	3.4700	-4.3922	0.00	0.00	0.00
50	17.206	0.17064E-10	-6.6303	0.00	0.00	0.00
51	17.206	0.84500	-6.6303	0.00	0.00	0.00
52	17.206	1.4700	-6.6303	0.00	0.00	0.00
53	17.990	0.18783E-10	-6.8205	0.00	0.00	0.00
54	17.990	0.30000	-6.8205	0.00	0.00	0.00
55	17.990	1.4490	-6.8205	0.00	0.00	0.00
56	18.807	0.19635E-10	-5.0392	0.00	0.00	0.00
57	18.807	0.30000	-5.0392	0.00	0.00	0.00
58	18.807	1.4700	-5.0392	0.00	0.00	0.00
61	3.1562	1.7350	-7.0000	0.00	0.00	0.00
62	8.1990	1.7350	-4.6475	0.00	0.00	0.00
63	11.042	1.7350	-6.3750	0.00	0.00	0.00

66	11.042	0.24804E-18	-6.3750	0.00	0.00	0.00
67	11.042	0.86500	-6.3750	0.00	0.00	0.00
67	11.042	2.5980	-6.3750	0.00	0.00	0.00
MODE	X	Y	Z	TH0Y	TH1Z	TH2Z
68	11.042	3.4700	-6.3750	0.00	0.00	0.00
69	13.770	0.30977E-10	-7.9500	0.00	0.00	0.00
70	13.770	0.84500	-7.9500	0.00	0.00	0.00
71	13.770	1.7350	-7.9500	0.00	0.00	0.00
72	13.770	2.5950	-7.9500	0.00	0.00	0.00
73	13.770	3.4700	-7.9500	0.00	0.00	0.00
74	14.696	0.33042E-10	-8.4850	0.00	0.00	0.00
75	14.696	0.84500	-8.4850	0.00	0.00	0.00
76	14.696	1.4700	-8.4850	0.00	0.00	0.00
77	14.696	2.8700	-8.4850	0.00	0.00	0.00
78	14.696	2.4200	-8.4850	0.00	0.00	0.00
79	14.696	3.4700	-8.4850	0.00	0.00	0.00
80	13.427	0.34704E-10	-8.9045	0.00	0.00	0.00
81	13.427	0.86500	-8.9045	0.00	0.00	0.00
82	13.427	1.4700	-8.9045	0.00	0.00	0.00
83	16.130	0.36288E-10	-9.5125	0.00	0.00	0.00
84	16.130	0.58000	-9.5125	0.00	0.00	0.00
85	16.130	1.4400	-9.5125	0.00	0.00	0.00
86	16.862	0.37932E-10	-9.7350	0.00	0.00	0.00
87	16.862	0.58000	-9.7350	0.00	0.00	0.00
MODE	X	Y	Z	TH0Y	TH1Z	TH2Z
88	16.862	1.4700	-9.7350	0.00	0.00	0.00
89	4.2486	1.7350	-4.2428	0.00	0.00	0.00
90	6.6291	1.7300	-6.6291	0.00	0.00	0.00
92	9.0156	1.7350	-9.0156	0.00	0.00	0.00
94	9.0156	0.35129E-10	-9.0156	0.00	0.00	0.00
95	9.0156	0.84500	-9.0156	0.00	0.00	0.00
97	9.0156	2.5950	-9.0156	0.00	0.00	0.00
98	9.0156	3.4700	-9.0156	0.00	0.00	0.00
99	11.243	0.43800E-10	-11.243	0.00	0.00	0.00
100	11.243	0.84500	-11.243	0.00	0.00	0.00
101	11.243	1.7350	-11.243	0.00	0.00	0.00
102	11.243	2.5950	-11.243	0.00	0.00	0.00
103	11.243	3.4700	-11.243	0.00	0.00	0.00
104	12.000	0.46768E-10	-12.000	0.00	0.00	0.00
105	12.000	0.84500	-12.000	0.00	0.00	0.00
106	12.000	1.4700	-12.000	0.00	0.00	0.00
107	12.000	2.0700	-12.000	0.00	0.00	0.00
108	12.000	2.6200	-12.000	0.00	0.00	0.00
109	12.000	3.4700	-12.000	0.00	0.00	0.00
110	12.596	0.49079E-10	-12.596	0.00	0.00	0.00
MODE	X	Y	Z	TH0Y	TH1Z	TH2Z
111	12.596	0.84500	-12.596	0.00	0.00	0.00
112	12.596	1.4700	-12.596	0.00	0.00	0.00
113	13.170	0.51310E-10	-13.170	0.00	0.00	0.00
114	13.170	0.93000	-13.170	0.00	0.00	0.00
115	13.170	1.4690	-13.170	0.00	0.00	0.00
116	13.767	0.53645E-10	-13.767	0.00	0.00	0.00
117	13.767	0.93000	-13.767	0.00	0.00	0.00
118	13.767	1.4700	-13.767	0.00	0.00	0.00
121	5.0400	1.7350	-5.0962	0.00	0.00	0.00
122	4.6875	1.7350	-8.1190	0.00	0.00	0.00
123	6.3750	1.7350	-11.042	0.00	0.00	0.00
124	6.3750	0.43026E-10	-11.042	0.00	0.00	0.00
125	6.3750	0.84500	-11.042	0.00	0.00	0.00
127	6.3750	2.5950	-11.042	0.00	0.00	0.00
128	6.3750	3.4700	-11.042	0.00	0.00	0.00
129	7.9500	0.33654E-10	-13.770	0.00	0.00	0.00
130	7.9500	0.84500	-13.770	0.00	0.00	0.00
131	7.9500	1.7350	-13.770	0.00	0.00	0.00
132	7.9500	2.5950	-13.770	0.00	0.00	0.00
133	7.9500	3.4700	-13.770	0.00	0.00	0.00
MODE	X	Y	Z	TH0Y	TH1Z	TH2Z
134	8.4850	0.57963E-10	-14.696	0.00	0.00	0.00
135	8.4850	0.84500	-14.696	0.00	0.00	0.00
136	8.4850	1.4700	-14.696	0.00	0.00	0.00

137	8.4858	2.8700	-14.696	0.00	0.00	0.00
138	8.4858	2.6200	-14.696	0.00	0.00	0.00
139	8.4858	3.4700	-14.696	0.00	0.00	0.00
140	8.9045	0.68109E-10	-19.427	0.00	0.00	0.00
141	8.9045	0.04500	-19.427	0.00	0.00	0.00
142	9.3125	1.4700	-16.430	0.00	0.00	0.00
143	9.3125	0.62809E-10	-16.430	0.00	0.00	0.00
144	9.3125	0.58000	-16.430	0.00	0.00	0.00
145	9.3125	1.4490	-16.430	0.00	0.00	0.00
146	9.7350	0.65701E-10	-16.662	0.00	0.00	0.00
147	9.7350	0.58000	-16.662	0.00	0.00	0.00
148	9.7350	1.6700	-16.662	0.00	0.00	0.00
151	1.9529	1.7350	-9.0536	0.00	0.00	0.00
152	2.4264	1.7350	-9.0536	0.00	0.00	0.00
153	3.2999	1.7350	-12.316	0.00	0.00	0.00
154	3.2999	0.47988E-10	-12.316	0.00	0.00	0.00
155	3.2999	0.04500	-12.316	0.00	0.00	0.00

NAME	X	Y	Z	THX1	THX2	THX3
157	3.2999	2.5950	-12.316	0.00	0.00	0.00
158	3.2999	3.4700	-12.316	0.00	0.00	0.00
159	4.1152	0.59643E-10	-19.358	0.00	0.00	0.00
160	4.1152	0.04500	-19.358	0.00	0.00	0.00
161	4.1152	1.7350	-19.358	0.00	0.00	0.00
162	4.1152	2.5950	-19.358	0.00	0.00	0.00
163	4.1152	3.4700	-19.358	0.00	0.00	0.00
164	4.3922	0.63870E-10	-16.392	0.00	0.00	0.00
165	4.3922	0.04500	-16.392	0.00	0.00	0.00
166	4.3922	1.4700	-16.392	0.00	0.00	0.00
167	4.3922	2.8700	-16.392	0.00	0.00	0.00
168	4.3922	2.6200	-16.392	0.00	0.00	0.00
169	4.3922	3.4700	-16.392	0.00	0.00	0.00
170	4.6183	0.67043E-10	-17.206	0.00	0.00	0.00
171	4.6183	0.04500	-17.206	0.00	0.00	0.00
172	4.6183	1.4700	-17.206	0.00	0.00	0.00
173	4.6285	0.70099E-10	-17.990	0.00	0.00	0.00
174	4.6285	0.58000	-17.990	0.00	0.00	0.00
175	4.6285	1.4690	-17.990	0.00	0.00	0.00
176	5.0392	0.73208E-10	-18.807	0.00	0.00	0.00

NAME	X	Y	Z	THX1	THX2	THX3
177	5.0392	0.58000	-18.807	0.00	0.00	0.00
178	5.0392	1.4700	-18.807	0.00	0.00	0.00
181	0.45680E-10	1.7350	-6.0900	0.00	0.00	0.00
182	0.34938E-10	1.7350	-9.3750	0.00	0.00	0.00
183	0.45680E-10	1.7350	-12.750	0.00	0.00	0.00
184	0.45680E-10	0.49680E-10	-12.750	0.00	0.00	0.00
185	0.45680E-10	0.04500	-12.750	0.00	0.00	0.00
187	0.45680E-10	2.5950	-12.750	0.00	0.00	0.00
188	0.45680E-10	3.4700	-12.750	0.00	0.00	0.00
189	0.61954E-10	0.61954E-10	-15.980	0.00	0.00	0.00
190	0.61954E-10	0.04500	-15.980	0.00	0.00	0.00
191	0.61954E-10	1.7350	-15.980	0.00	0.00	0.00
192	0.61954E-10	2.5950	-15.980	0.00	0.00	0.00
193	0.61954E-10	3.4700	-15.980	0.00	0.00	0.00
194	0.66124E-10	0.66124E-10	-18.978	0.00	0.00	0.00
195	0.66124E-10	0.04500	-18.978	0.00	0.00	0.00
196	0.66124E-10	1.4700	-18.978	0.00	0.00	0.00
197	0.66124E-10	2.0780	-18.978	0.00	0.00	0.00
198	0.66124E-10	2.8290	-18.978	0.00	0.00	0.00
199	0.66124E-10	3.4700	-18.978	0.00	0.00	0.00

NAME	X	Y	Z	THX1	THX2	THX3
200	0.69408E-10	0.69408E-10	-17.813	0.00	0.00	0.00
201	0.69408E-10	0.04500	-17.813	0.00	0.00	0.00
202	0.69408E-10	1.4700	-17.813	0.00	0.00	0.00
203	0.72572E-10	0.72572E-10	-18.625	0.00	0.00	0.00
204	0.72572E-10	0.58000	-18.625	0.00	0.00	0.00
205	0.72572E-10	1.4490	-18.625	0.00	0.00	0.00
206	0.75869E-10	0.75869E-10	-19.478	0.00	0.00	0.00
207	0.75869E-10	0.58000	-19.478	0.00	0.00	0.00
208	0.75869E-10	1.4700	-19.478	0.00	0.00	0.00
211	-1.3529	1.7350	-9.0536	0.00	0.00	0.00
212	-2.4264	1.7350	-9.0536	0.00	0.00	0.00

213	-3.2999	1.7390	-12.336	0.00	0.00	0.00
214	-3.2999	0.47988E+10	-12.336	0.00	0.00	0.00
215	-3.2999	0.84500	-12.336	0.00	0.00	0.00
217	-3.2999	2.5990	-12.336	0.00	0.00	0.00
218	-3.2999	3.4700	-12.336	0.00	0.00	0.00
219	-4.1152	0.59843E+10	-15.358	0.00	0.00	0.00
220	-4.1152	0.84500	-15.358	0.00	0.00	0.00
221	-4.1152	1.7390	-15.358	0.00	0.00	0.00
222	-4.1152	2.5990	-15.358	0.00	0.00	0.00
MODE	K	T	Z	TH0Y	TH0Z	TH0Z
223	-4.1152	3.4700	-15.358	0.00	0.00	0.00
224	-4.3922	0.63870E+10	-16.392	0.00	0.00	0.00
225	-4.3922	0.84500	-16.392	0.00	0.00	0.00
226	-4.3922	1.4700	-16.392	0.00	0.00	0.00
227	-4.3922	2.0700	-16.392	0.00	0.00	0.00
228	-4.3922	2.6900	-16.392	0.00	0.00	0.00
229	-4.3922	3.4700	-16.392	0.00	0.00	0.00
230	-4.6103	0.67043E+10	-17.236	0.00	0.00	0.00
231	-4.6103	0.84500	-17.236	0.00	0.00	0.00
232	-4.6103	1.4700	-17.236	0.00	0.00	0.00
233	-4.6205	0.70099E+10	-17.990	0.00	0.00	0.00
234	-4.6205	0.58000	-17.990	0.00	0.00	0.00
235	-4.6205	1.4490	-17.990	0.00	0.00	0.00
236	-5.0392	0.73280E+10	-18.807	0.00	0.00	0.00
237	-5.0392	0.58000	-18.807	0.00	0.00	0.00
238	-5.0392	1.4700	-18.807	0.00	0.00	0.00
241	-3.0000	1.7390	-5.3962	0.00	0.00	0.00
242	-4.4475	1.7390	-8.1190	0.00	0.00	0.00
243	-4.3790	1.7390	-11.042	0.00	0.00	0.00
244	-6.3750	0.43028E+10	-11.042	0.00	0.00	0.00
MODE	K	T	Z	TH0Y	TH0Z	TH0Z
245	-6.3750	0.84500	-11.042	0.00	0.00	0.00
247	-6.3750	2.5990	-11.042	0.00	0.00	0.00
248	-6.3750	3.4700	-11.042	0.00	0.00	0.00
249	-7.9500	0.5464E+10	-13.770	0.00	0.00	0.00
250	-7.9500	0.84500	-13.770	0.00	0.00	0.00
251	-7.9500	1.7390	-13.770	0.00	0.00	0.00
252	-7.9500	2.5990	-13.770	0.00	0.00	0.00
253	-7.9500	3.4700	-13.770	0.00	0.00	0.00
254	-8.4450	0.57269E+10	-14.696	0.00	0.00	0.00
255	-8.4450	0.84500	-14.696	0.00	0.00	0.00
256	-8.4450	1.4700	-14.696	0.00	0.00	0.00
257	-8.4450	2.0700	-14.696	0.00	0.00	0.00
258	-8.4450	2.6200	-14.696	0.00	0.00	0.00
259	-8.4450	3.4700	-14.696	0.00	0.00	0.00
260	-8.9063	0.60109E+10	-15.427	0.00	0.00	0.00
261	-8.9063	0.84500	-15.427	0.00	0.00	0.00
262	-8.9063	1.4700	-15.427	0.00	0.00	0.00
263	-9.3125	0.62869E+10	-16.130	0.00	0.00	0.00
264	-9.3125	0.38000	-16.130	0.00	0.00	0.00
265	-9.3125	1.4490	-16.130	0.00	0.00	0.00
MODE	K	T	Z	TH0Y	TH0Z	TH0Z
266	-9.7350	0.65701E+10	-16.862	0.00	0.00	0.00
267	-9.7350	0.58000	-16.862	0.00	0.00	0.00
268	-9.7350	1.4700	-16.862	0.00	0.00	0.00
271	-4.2626	1.7390	-4.2626	0.00	0.00	0.00
272	-6.6291	1.7390	-6.6291	0.00	0.00	0.00
273	-9.0154	1.7390	-9.0154	0.00	0.00	0.00
274	-9.0154	0.35129E+10	-9.0154	0.00	0.00	0.00
275	-9.0154	0.84300	-9.0154	0.00	0.00	0.00
277	-9.0154	2.5950	-9.0154	0.00	0.00	0.00
278	-9.0154	3.4700	-9.0154	0.00	0.00	0.00
279	-11.243	0.43808E+10	-11.243	0.00	0.00	0.00
280	-11.243	0.84500	-11.243	0.00	0.00	0.00
281	-11.243	1.7390	-11.243	0.00	0.00	0.00
282	-11.243	2.5950	-11.243	0.00	0.00	0.00
283	-11.243	3.4700	-11.243	0.00	0.00	0.00
284	-12.000	0.60754E+10	-12.000	0.00	0.00	0.00
285	-12.000	0.84500	-12.000	0.00	0.00	0.00
286	-12.000	1.4700	-12.000	0.00	0.00	0.00
287	-12.000	2.8700	-12.000	0.00	0.00	0.00

295	-12.000	2.6298	-12.000	0.00	0.00	0.00
MODE	K	Y	Z	THW	THZ	THOZ
299	-12.596	3.4799	-12.000	0.00	0.00	0.00
299	-12.596	0.49079E-10	-12.596	0.00	0.00	0.00
291	-12.596	0.84500	-12.596	0.00	0.00	0.00
292	-12.596	1.4799	-12.596	0.00	0.00	0.00
293	-12.170	0.51316E-10	-12.170	0.00	0.00	0.00
294	-13.170	0.58000	-13.170	0.00	0.00	0.00
295	-13.170	1.4699	-13.170	0.00	0.00	0.00
296	-13.767	0.32443E-10	-13.767	0.00	0.00	0.00
297	-13.767	0.58000	-13.767	0.00	0.00	0.00
298	-13.767	1.4700	-13.767	0.00	0.00	0.00
301	-5.1962	1.7350	-5.0000	0.00	0.00	0.00
302	-6.1990	1.7350	-6.6875	0.00	0.00	0.00
303	-11.042	1.7350	-6.3750	0.00	0.00	0.00
304	-11.042	0.36040E-10	-6.3750	0.00	0.00	0.00
305	-11.042	0.64500	-6.3750	0.00	0.00	0.00
307	-11.042	2.5950	-6.3750	0.00	0.00	0.00
308	-11.042	3.4700	-6.3750	0.00	0.00	0.00
309	-13.770	0.30977E-10	-7.9500	0.00	0.00	0.00
310	-13.770	0.64500	-7.9500	0.00	0.00	0.00
311	-13.770	1.7350	-7.9900	0.00	0.00	0.00
MODE	M	Y	Z	THW	THZ	THOZ
312	-13.770	2.5950	-7.9500	0.00	0.00	0.00
313	-13.770	3.4799	-7.9500	0.00	0.00	0.00
314	-14.606	0.33062E-10	-8.4850	0.00	0.00	0.00
315	-14.606	0.84500	-8.4850	0.00	0.00	0.00
316	-14.606	1.4799	-8.4850	0.00	0.00	0.00
317	-14.606	2.0799	-8.4850	0.00	0.00	0.00
318	-14.606	3.4399	-8.4850	0.00	0.00	0.00
319	-14.606	3.4799	-8.4850	0.00	0.00	0.00
320	-15.427	0.34794E-10	-8.9065	0.00	0.00	0.00
321	-15.427	0.64500	-8.9065	0.00	0.00	0.00
322	-15.427	1.4799	-8.9065	0.00	0.00	0.00
323	-16.130	0.36296E-10	-9.3125	0.00	0.00	0.00
324	-16.130	0.58000	-9.3125	0.00	0.00	0.00
325	-16.130	1.4699	-9.3125	0.00	0.00	0.00
326	-16.862	0.37952E-10	-9.7350	0.00	0.00	0.00
327	-16.862	0.58000	-9.7350	0.00	0.00	0.00
328	-16.862	1.4700	-9.7350	0.00	0.00	0.00
331	-5.7994	1.7350	-4.5529	0.00	0.00	0.00
332	-9.0556	1.7350	-2.4264	0.00	0.00	0.00
333	-12.116	1.7350	-3.2999	0.00	0.00	0.00
MODE	K	Y	Z	THW	THZ	THOZ
334	-12.316	0.12850E-10	-3.2999	0.00	0.00	0.00
335	-12.316	0.64500	-3.2999	0.00	0.00	0.00
337	-12.316	2.5950	-3.2999	0.00	0.00	0.00
339	-12.316	3.4700	-3.2999	0.00	0.00	0.00
339	-15.358	0.14035E-10	-4.1152	0.00	0.00	0.00
340	-15.358	0.64500	-4.1152	0.00	0.00	0.00
341	-15.358	1.7350	-4.1152	0.00	0.00	0.00
342	-16.358	2.5950	-4.1152	0.00	0.00	0.00
343	-16.358	3.4799	-4.1152	0.00	0.00	0.00
344	-16.392	0.37116E-10	-4.3922	0.00	0.00	0.00
345	-16.392	0.64500	-4.3922	0.00	0.00	0.00
346	-16.392	1.4700	-4.3922	0.00	0.00	0.00
347	-16.392	2.0700	-4.3922	0.00	0.00	0.00
348	-16.392	2.6200	-4.3922	0.00	0.00	0.00
349	-16.392	3.4700	-4.3922	0.00	0.00	0.00
350	-17.206	0.17964E-10	-4.6103	0.00	0.00	0.00
351	-17.206	0.84500	-4.6103	0.00	0.00	0.00
352	-17.206	1.4700	-4.6103	0.00	0.00	0.00
353	-17.999	0.10703E-10	-4.6205	0.00	0.00	0.00
354	-17.999	0.58000	-4.6205	0.00	0.00	0.00
MODE	X	Y	Z	THW	THZ	THOZ
355	-17.999	1.4699	-4.6205	0.00	0.00	0.00
356	-18.807	0.19435E-10	-5.0392	0.00	0.00	0.00
357	-18.807	0.58000	-5.0392	0.00	0.00	0.00
358	-18.807	1.4700	-5.0392	0.00	0.00	0.00
361	-6.0000	1.7350	-0.10912E-07	0.00	0.00	0.00

362	-9.3790	1.7350	-0.26429E-07	0.00	0.00	0.00
363	-12.750	1.7350	-0.22644E-07	0.00	0.00	0.00
364	-12.750	0.87090E-10	-0.10090E-29	0.00	0.00	0.00
365	-12.750	0.84500	-0.12349E-02	0.00	0.00	0.00
367	-12.750	2.9950	-0.22942E-07	0.00	0.00	0.00
368	-12.750	1.4700	-0.22329E-02	0.00	0.00	0.00
369	-15.900	0.10001E-10	0.10000E-29	0.00	0.00	0.00
370	-15.900	0.84500	-0.27871E-02	0.00	0.00	0.00
371	-15.900	1.7350	-0.27840E-07	0.00	0.00	0.00
372	-15.900	2.9950	-0.27865E-02	0.00	0.00	0.00
373	-15.900	3.4700	-0.27861E-07	0.00	0.00	0.00
376	-16.970	0.11502E-10	-0.29950E-02	0.00	0.00	0.00
375	-16.970	0.84500	-0.299747E-02	0.00	0.00	0.00
376	-16.970	1.4700	-0.29965E-02	0.00	0.00	0.00
377	-16.970	2.0700	-0.29942E-02	0.00	0.00	0.00

MODE	H	T	Z	TWRZ	TWRZ	TWRZ
378	-16.970	2.6200	-0.299740E-02	0.00	0.00	0.00
379	-16.970	3.4700	-0.299737E-02	0.00	0.00	0.00
380	-17.813	0.12100E-10	-0.21200E-02	0.00	0.00	0.00
381	-17.813	0.84500	-0.31225E-02	0.00	0.00	0.00
382	-17.813	1.4700	-0.31223E-02	0.00	0.00	0.00
383	-18.625	0.12722E-10	-0.32652E-02	0.00	0.00	0.00
384	-18.625	0.58000	-0.32649E-02	0.00	0.00	0.00
385	-18.625	1.4400	-0.32644E-02	0.00	0.00	0.00
386	-19.470	0.13300E-10	0.10000E-29	0.00	0.00	0.00
387	-19.470	0.58000	-0.34131E-02	0.00	0.00	0.00
388	-19.470	1.4700	-0.341280E-02	0.00	0.00	0.00
390	0.00000E+00	1.7350	0.67604E-11	0.00	0.00	0.00
391	1.0000	1.7350	0.67604E-11	0.00	0.00	0.00
392	2.0000	1.7350	0.67604E-11	0.00	0.00	0.00
393	3.0000	1.7350	0.67604E-11	0.00	0.00	0.00
394	4.0000	1.7350	0.67604E-11	0.00	0.00	0.00
395	5.0000	1.7350	0.67604E-11	0.00	0.00	0.00
396	-1.0000	1.7350	-0.17664E-08	0.00	0.00	0.00
397	-2.0000	1.7350	-0.34999E-08	0.00	0.00	0.00
398	-3.0000	1.7350	-0.52528E-08	0.00	0.00	0.00

MODE	X	T	Z	TWRZ	TWRZ	TWRZ
399	-4.0000	1.7350	-0.70057E-08	0.00	0.00	0.00
400	-5.0000	1.7350	-0.87590E-08	0.00	0.00	0.00
401	17.000	1.4700	0.57279E-11	0.00	0.00	0.00
402	17.813	1.4700	0.57279E-11	0.00	0.00	0.00
403	18.625	1.4700	0.57279E-11	0.00	0.00	0.00
404	19.375	1.4700	0.57279E-11	0.00	0.00	0.00
405	17.800	2.0700	0.80659E-11	0.00	0.00	0.00
406	17.813	2.0700	0.80659E-11	0.00	0.00	0.00
407	18.625	2.0700	0.80659E-11	0.00	0.00	0.00
408	19.375	2.0700	0.80659E-11	0.00	0.00	0.00
409	17.800	2.6200	0.10020E-10	0.00	0.00	0.00
410	17.813	2.6200	0.10020E-10	0.00	0.00	0.00
411	18.625	2.6200	0.10020E-10	0.00	0.00	0.00
412	19.375	2.6200	0.10020E-10	0.00	0.00	0.00
413	17.800	3.0450	0.11669E-10	0.00	0.00	0.00
416	17.831	3.0450	0.11669E-10	0.00	0.00	0.00
415	18.643	3.0450	0.11671E-10	0.00	0.00	0.00
416	18.545	3.4325	0.13979E-10	0.00	0.00	0.00
417	17.800	3.4700	0.13521E-10	0.00	0.00	0.00
418	17.250	3.7200	0.14527E-10	0.00	0.00	0.00

MODE	H	T	Z	TWRZ	TWRZ	TWRZ
419	17.500	3.9867	0.15534E-10	0.00	0.00	0.00
420	17.750	4.2450	0.16541E-10	0.00	0.00	0.00
421	16.889	3.4700	0.13521E-10	0.00	0.00	0.00
422	17.800	4.8200	0.18761E-10	0.00	0.00	0.00
423	17.189	4.8200	0.18761E-10	0.00	0.00	0.00
424	17.375	4.8200	0.18761E-10	0.00	0.00	0.00
425	17.542	4.8200	0.18761E-10	0.00	0.00	0.00
426	17.750	4.8200	0.18761E-10	0.00	0.00	0.00
431	16.421	1.4700	-4.3999	0.00	0.00	0.00
432	17.286	1.4700	-4.4010	0.00	0.00	0.00
433	17.999	1.4700	-4.3999	0.00	0.00	0.00
434	18.715	1.4700	-5.0144	0.00	0.00	0.00
435	16.421	2.0700	-4.3999	0.00	0.00	0.00

436	17,286	2,0788	+4,8103	0.00	0.00	0.00
437	17,990	2,0788	+4,8208	0.00	0.00	0.00
438	18,715	2,0788	+5,0146	0.00	0.00	0.00
439	18,421	2,6288	+4,3990	0.00	0.00	0.00
440	17,206	2,6288	+4,6102	0.00	0.00	0.00
441	17,990	2,6288	+4,8205	0.00	0.00	0.00
442	18,715	2,6288	+5,0146	0.00	0.00	0.00

MODE	M	Y	Z	THY1	THY2	THO2
443	16,429	3,0434	-4,3990	0.00	0.00	0.00
444	16,954	3,1762	-4,5374	0.00	0.00	0.00
445	17,447	3,3033	-4,6759	0.00	0.00	0.00
446	17,990	3,4325	-4,8043	0.00	0.00	0.00
447	18,421	3,4786	-4,9399	0.00	0.00	0.00
448	16,662	3,7281	-4,4644	0.00	0.00	0.00
449	16,904	3,8867	-4,5293	0.00	0.00	0.00
450	17,145	4,2654	-4,8948	0.00	0.00	0.00
451	16,281	3,4786	-4,5626	0.00	0.00	0.00
452	16,421	4,8288	-4,3999	0.00	0.00	0.00
453	16,608	4,8288	-4,4485	0.00	0.00	0.00
454	16,785	4,8288	-4,4970	0.00	0.00	0.00
455	16,964	4,8288	-4,5455	0.00	0.00	0.00
456	17,145	4,8288	-4,5940	0.00	0.00	0.00
457	14,722	1,4788	-8,5008	0.00	0.00	0.00
458	15,134	1,4788	-8,5062	0.00	0.00	0.00
459	15,430	1,4788	-9,3125	0.00	0.00	0.00
460	16,779	1,4788	-9,6875	0.00	0.00	0.00
461	14,722	2,0788	-8,5008	0.00	0.00	0.00
462	15,426	2,0788	-8,9062	0.00	0.00	0.00

MODE	M	Y	Z	THY1	THY2	THO2
467	16,130	2,0788	-9,3125	0.00	0.00	0.00
468	16,779	2,0788	-9,6875	0.00	0.00	0.00
469	14,722	2,6288	-8,3000	0.00	0.00	0.00
470	15,426	2,6288	-8,9062	0.00	0.00	0.00
471	16,130	2,6288	-9,3125	0.00	0.00	0.00
472	16,779	2,6288	-9,6875	0.00	0.00	0.00
473	14,722	3,0430	-8,3000	0.00	0.00	0.00
474	15,183	3,1762	-8,7655	0.00	0.00	0.00
475	15,643	3,3033	-9,0312	0.00	0.00	0.00
476	16,076	3,4325	-9,2912	0.00	0.00	0.00
477	14,722	3,4788	-8,3000	0.00	0.00	0.00
478	15,939	3,7283	-8,5250	0.00	0.00	0.00
479	15,155	3,9867	-8,7500	0.00	0.00	0.00
480	15,372	4,2436	-8,8750	0.00	0.00	0.00
481	14,597	3,4788	-8,4275	0.00	0.00	0.00
482	14,722	4,8288	-8,3000	0.00	0.00	0.00
483	14,886	4,8288	-8,5937	0.00	0.00	0.00
484	15,047	4,8288	-8,6675	0.00	0.00	0.00
485	15,210	4,8288	-8,7612	0.00	0.00	0.00
486	15,372	4,8288	-8,8750	0.00	0.00	0.00

MODE	X	Y	Z	THY1	THY2	THO2
491	12,821	1,4700	-12,821	0.00	0.00	0.00
492	12,595	1,4700	-12,595	0.00	0.00	0.00
493	13,170	1,4700	-13,170	0.00	0.00	0.00
494	13,780	1,4700	-13,700	0.00	0.00	0.00
495	12,821	2,0700	-12,821	0.00	0.00	0.00
496	12,595	2,0700	-12,595	0.00	0.00	0.00
497	13,170	2,0700	-13,170	0.00	0.00	0.00
498	13,780	2,0700	-13,700	0.00	0.00	0.00
499	12,821	2,6308	-12,821	0.00	0.00	0.00
500	12,595	2,6308	-12,595	0.00	0.00	0.00
501	13,170	2,6308	-13,170	0.00	0.00	0.00
502	13,780	2,6308	-13,700	0.00	0.00	0.00
503	12,821	3,0690	-12,821	0.00	0.00	0.00
504	12,596	3,1762	-12,596	0.00	0.00	0.00
505	12,772	3,3033	-12,772	0.00	0.00	0.00
506	13,126	3,4325	-13,126	0.00	0.00	0.00
507	12,821	3,4788	-12,821	0.00	0.00	0.00
508	12,196	3,7283	-12,196	0.00	0.00	0.00
509	12,374	3,9867	-12,374	0.00	0.00	0.00
510	12,551	4,2436	-12,551	0.00	0.00	0.00

MODE	X	Y	Z	TWOY	THRY	THRY
511	11.918	3.4700	-11.918	0.00	0.00	0.00
512	12.021	4.8200	-12.021	0.00	0.00	0.00
513	12.153	4.8200	-12.153	0.00	0.00	0.00
514	12.286	4.8200	-12.286	0.00	0.00	0.00
515	12.419	4.8200	-12.419	0.00	0.00	0.00
516	12.551	4.8200	-12.551	0.00	0.00	0.00
517	0.3008	1.6700	-16.722	0.00	0.00	0.00
518	0.3008	1.6700	-17.426	0.00	0.00	0.00
519	9.3123	1.6700	-16.130	0.00	0.00	0.00
520	9.6875	1.6700	-16.779	0.00	0.00	0.00
521	8.5860	2.0700	-16.722	0.00	0.00	0.00
522	8.9843	2.0700	-15.426	0.00	0.00	0.00
523	9.3123	2.0700	-16.130	0.00	0.00	0.00
524	9.6875	2.0700	-16.779	0.00	0.00	0.00
525	8.5860	2.4200	-16.722	0.00	0.00	0.00
526	8.9843	2.4200	-15.426	0.00	0.00	0.00
527	9.3123	2.4200	-16.130	0.00	0.00	0.00
528	9.6875	2.4200	-16.779	0.00	0.00	0.00
529	8.5860	2.8200	-16.722	0.00	0.00	0.00
530	8.9843	2.8200	-15.426	0.00	0.00	0.00
531	9.3123	2.8200	-16.130	0.00	0.00	0.00
532	9.6875	2.8200	-16.779	0.00	0.00	0.00
533	8.5860	3.0450	-16.722	0.00	0.00	0.00
534	8.7656	3.1742	-15.183	0.00	0.00	0.00

MODE	X	Y	Z	TWOY	THRY	THRY
535	9.0313	3.3033	-15.843	0.00	0.00	0.00
536	9.3913	3.4325	-16.896	0.00	0.00	0.00
537	8.5860	3.4700	-16.722	0.00	0.00	0.00
538	8.6250	3.7833	-16.990	0.00	0.00	0.00
539	8.7580	3.9847	-15.183	0.00	0.00	0.00
540	8.8750	4.2450	-15.372	0.00	0.00	0.00
541	8.4278	3.4700	-16.597	0.00	0.00	0.00
542	8.5860	4.8200	-16.722	0.00	0.00	0.00
543	8.5938	4.8200	-16.885	0.00	0.00	0.00
544	8.4075	4.8200	-15.647	0.00	0.00	0.00
545	8.7813	4.8200	-15.210	0.00	0.00	0.00
546	8.8750	4.8200	-15.372	0.00	0.00	0.00
551	4.3999	1.6700	-16.421	0.00	0.00	0.00
552	4.6302	1.6700	-17.286	0.00	0.00	0.00
553	4.8200	1.6700	-17.990	0.00	0.00	0.00
554	5.0346	1.6700	-18.715	0.00	0.00	0.00
555	4.3999	2.0700	-16.421	0.00	0.00	0.00
556	4.6302	2.0700	-17.286	0.00	0.00	0.00
557	4.8200	2.0700	-17.990	0.00	0.00	0.00
558	5.0346	2.0700	-18.715	0.00	0.00	0.00

MODE	X	Y	Z	TWOY	THRY	THRY
559	4.3999	2.4200	-16.421	0.00	0.00	0.00
560	4.6302	2.4200	-17.286	0.00	0.00	0.00
561	4.8200	2.4200	-17.990	0.00	0.00	0.00
562	5.0346	2.4200	-18.715	0.00	0.00	0.00
563	4.3999	3.0450	-16.421	0.00	0.00	0.00
564	4.5374	3.1742	-16.956	0.00	0.00	0.00
565	4.6749	3.3033	-17.447	0.00	0.00	0.00
566	4.8043	3.4325	-17.938	0.00	0.00	0.00
567	4.3999	3.6700	-16.421	0.00	0.00	0.00
568	4.4646	3.7200	-16.462	0.00	0.00	0.00
569	4.5293	3.9847	-16.984	0.00	0.00	0.00
570	4.5940	4.2650	-17.143	0.00	0.00	0.00
571	4.3626	3.4700	-16.281	0.00	0.00	0.00
572	4.3999	4.8200	-16.421	0.00	0.00	0.00
573	4.4485	4.8200	-16.682	0.00	0.00	0.00
574	4.4970	4.8200	-16.943	0.00	0.00	0.00
575	4.5456	4.8200	-16.564	0.00	0.00	0.00
576	4.5940	4.8200	-17.145	0.00	0.00	0.00
581	0.46240E-10	1.4700	-17.000	0.00	0.00	0.00
582	0.49106E-10	1.4700	-17.812	0.00	0.00	0.00

MODE	X	Y	Z	TWOY	THRY	THRY
583	0.72572E-10	1.4700	-18.625	0.00	0.00	0.00
584	0.75495E-10	1.4700	-19.375	0.00	0.00	0.00
585	0.44240E-10	2.0700	-17.000	0.00	0.00	0.00
586	0.49606E-10	2.0700	-17.812	0.00	0.00	0.00
587	0.72572E-10	3.0700	-18.625	0.00	0.00	0.00
588	0.75495E-10	2.0700	-19.375	0.00	0.00	0.00
589	0.44240E-10	3.6200	-17.000	0.00	0.00	0.00

590	0.69406E-10	2.6280	-17.812	0.00	0.00	0.00
591	0.72572E-10	2.6280	-18.625	0.00	0.00	0.00
592	0.73496E-10	2.6280	-19.375	0.00	0.00	0.00
593	0.86240E-10	3.0650	-17.000	0.00	0.00	0.00
594	0.88511E-10	3.1742	-17.531	0.00	0.00	0.00
595	0.70581E-10	3.3633	-18.062	0.00	0.00	0.00
596	0.72329E-10	3.4325	-18.562	0.00	0.00	0.00
597	0.64840E-10	3.4780	-17.000	0.00	0.00	0.00
598	0.67219E-10	3.7203	-17.250	0.00	0.00	0.00
599	0.68188E-10	3.9867	-17.500	0.00	0.00	0.00
600	0.69163E-10	4.2650	-17.750	0.00	0.00	0.00
601	0.65679E-10	3.4780	-16.885	0.00	0.00	0.00
602	0.66240E-10	4.8200	-17.000	0.00	0.00	0.00

NODE	Y	Z	THX1	THX2	THX3
603	0.66979E-10	4.8200	-17.950	0.00	0.00
604	0.67702E-10	4.8200	-17.375	0.00	0.00
605	0.68432E-10	4.8200	-17.563	0.00	0.00
606	0.69163E-10	4.8200	-17.750	0.00	0.00
611	-4.3999	1.4700	-16.421	0.00	0.00
612	-4.6102	1.4700	-17.806	0.00	0.00
613	-4.8208	1.4700	-17.990	0.00	0.00
614	-5.0146	1.4700	-18.795	0.00	0.00
615	-4.3999	2.0700	-16.421	0.00	0.00
616	-4.6102	2.0700	-17.206	0.00	0.00
617	-4.8208	2.0700	-17.990	0.00	0.00
618	-5.0146	2.0700	-18.795	0.00	0.00
619	-4.3999	2.6280	-16.421	0.00	0.00
620	-4.6102	2.6280	-17.206	0.00	0.00
621	-4.8208	2.6280	-17.990	0.00	0.00
622	-5.0146	2.6280	-18.795	0.00	0.00
623	-4.3999	3.0650	-16.421	0.00	0.00
624	-4.6102	3.1742	-16.994	0.00	0.00
625	-4.6769	3.3033	-17.447	0.00	0.00
626	-4.8043	3.4325	-17.930	0.00	0.00

NODE	X	Y	Z	THX1	THX2	THX3
627	-4.3999	3.6700	-16.421	0.00	0.00	0.00
628	-4.6646	3.7203	-16.662	0.00	0.00	0.00
629	-4.9293	3.9867	-14.904	0.00	0.00	0.00
630	-4.9940	4.2599	-17.145	0.00	0.00	0.00
631	-4.3626	3.4780	-14.281	0.00	0.00	0.00
632	-4.3999	4.8200	-16.421	0.00	0.00	0.00
633	-4.6646	4.8200	-16.662	0.00	0.00	0.00
634	-4.9778	4.8200	-14.793	0.00	0.00	0.00
635	-4.9635	4.8200	-16.964	0.00	0.00	0.00
636	-4.9048	4.8200	-17.145	0.00	0.00	0.00
641	-8.5000	1.4700	-14.722	0.00	0.00	0.00
642	-8.5062	1.4700	-15.426	0.00	0.00	0.00
643	-9.3125	1.4700	-16.130	0.00	0.00	0.00
644	-9.6875	1.4700	-16.779	0.00	0.00	0.00
645	-8.5000	3.0700	-14.722	0.00	0.00	0.00
646	-8.5062	3.0700	-15.426	0.00	0.00	0.00
647	-9.3125	3.0700	-14.130	0.00	0.00	0.00
648	-9.6875	3.0700	-16.779	0.00	0.00	0.00
649	-8.5000	2.6280	-14.722	0.00	0.00	0.00
650	-8.5062	2.6280	-15.426	0.00	0.00	0.00

NODE	X	Y	Z	THX1	THX2	THX3
651	-9.3125	2.6200	-16.130	0.00	0.00	0.00
652	-9.6875	2.6200	-16.779	0.00	0.00	0.00
653	-8.5000	3.0650	-14.722	0.00	0.00	0.00
654	-8.7654	3.1742	-15.183	0.00	0.00	0.00
655	-9.0312	3.3033	-15.643	0.00	0.00	0.00
656	-9.2812	3.4325	-16.076	0.00	0.00	0.00
657	-8.5000	3.4780	-14.722	0.00	0.00	0.00
658	-8.6210	3.7203	-14.998	0.00	0.00	0.00
659	-8.7580	3.9867	-15.195	0.00	0.00	0.00
660	-8.8790	4.2650	-13.372	0.00	0.00	0.00
661	-8.1375	3.4700	-14.597	0.00	0.00	0.00
662	-8.5060	4.8200	-14.722	0.00	0.00	0.00
663	-8.5937	4.8200	-14.885	0.00	0.00	0.00
664	-8.6875	4.8200	-15.047	0.00	0.00	0.00
665	-8.7812	4.8200	-15.210	0.00	0.00	0.00

444	-8,0750	4,8280	-15,1472	0.00	0.00	0.00	0.00
471	-12,0211	1,4760	-12,0211	0.00	0.00	0.00	0.00
472	-12,1591	1,4760	-12,1591	0.00	0.00	0.00	0.00
473	-13,1170	1,4760	-13,1170	0.00	0.00	0.00	0.00
474	-13,1700	1,4760	-13,1700	0.00	0.00	0.00	0.00
484	-13,0511	3,0780	-13,0511	0.00	0.00	0.00	0.00
485	-13,1596	3,0780	-13,1596	0.00	0.00	0.00	0.00
486	-13,1708	3,0780	-13,1708	0.00	0.00	0.00	0.00
487	-12,0211	3,4295	-12,0211	0.00	0.00	0.00	0.00
488	-12,1596	3,4295	-12,1596	0.00	0.00	0.00	0.00
489	-12,1708	3,4295	-12,1708	0.00	0.00	0.00	0.00
490	-12,3314	4,4240	-12,3314	0.00	0.00	0.00	0.00
491	-12,3426	4,4240	-12,3426	0.00	0.00	0.00	0.00
492	-11,0144	1,6260	-11,0144	0.00	0.00	0.00	0.00
493	-11,0256	1,6260	-11,0256	0.00	0.00	0.00	0.00
494	-12,2680	4,8280	-12,2680	0.00	0.00	0.00	0.00
505	-13,419	4,8280	-13,419	0.00	0.00	0.00	0.00
506	-12,551	4,8280	-12,551	0.00	0.00	0.00	0.00
701	-14,722	1,4270	-14,722	0.00	0.00	0.00	0.00
702	-15,436	1,4270	-15,436	0.00	0.00	0.00	0.00
703	-16,150	1,4270	-16,150	0.00	0.00	0.00	0.00
704	-16,779	1,4270	-16,779	0.00	0.00	0.00	0.00
705	-14,722	2,0700	-14,722	0.00	0.00	0.00	0.00
706	-15,443	2,0700	-15,443	0.00	0.00	0.00	0.00
707	-14,158	2,0700	-14,158	0.00	0.00	0.00	0.00
708	-14,639	3,7285	-14,639	0.00	0.00	0.00	0.00
709	-16,779	2,4830	-16,779	0.00	0.00	0.00	0.00
710	-17,125	2,4830	-17,125	0.00	0.00	0.00	0.00
711	-14,722	2,4830	-14,722	0.00	0.00	0.00	0.00
712	-14,779	2,5200	-14,779	0.00	0.00	0.00	0.00
713	-14,722	3,0490	-14,722	0.00	0.00	0.00	0.00
714	-15,163	3,1742	-15,163	0.00	0.00	0.00	0.00
715	-15,443	3,3005	-15,443	0.00	0.00	0.00	0.00
716	-14,078	3,4325	-14,078	0.00	0.00	0.00	0.00
717	-14,722	3,4708	-14,722	0.00	0.00	0.00	0.00
718	-14,639	3,7285	-14,639	0.00	0.00	0.00	0.00
719	-15,155	3,9667	-15,155	0.00	0.00	0.00	0.00
720	-15,372	4,3490	-15,372	0.00	0.00	0.00	0.00
721	-14,587	3,4708	-14,587	0.00	0.00	0.00	0.00
722	-14,722	4,0300	-14,722	0.00	0.00	0.00	0.00
723	-14,885	4,0300	-14,885	0.00	0.00	0.00	0.00
724	-15,417	4,0300	-15,417	0.00	0.00	0.00	0.00
725	-15,417	4,0300	-15,417	0.00	0.00	0.00	0.00
726	-15,417	4,0300	-15,417	0.00	0.00	0.00	0.00
727	-15,417	4,0300	-15,417	0.00	0.00	0.00	0.00
728	-15,417	4,0300	-15,417	0.00	0.00	0.00	0.00
729	-15,417	4,0300	-15,417	0.00	0.00	0.00	0.00
730	-15,417	4,0300	-15,417	0.00	0.00	0.00	0.00
731	-15,417	4,0300	-15,417	0.00	0.00	0.00	0.00
732	-14,708	1,4708	-14,708	0.00	0.00	0.00	0.00
733	-14,715	1,4708	-14,715	0.00	0.00	0.00	0.00
734	-14,421	2,0700	-14,421	0.00	0.00	0.00	0.00
735	-17,208	2,0700	-17,208	0.00	0.00	0.00	0.00
736	-16,421	2,0700	-16,421	0.00	0.00	0.00	0.00
737	-17,098	2,0700	-17,098	0.00	0.00	0.00	0.00
738	-16,715	2,0700	-16,715	0.00	0.00	0.00	0.00
739	-16,421	2,0700	-16,421	0.00	0.00	0.00	0.00
740	-17,028	2,4830	-17,028	0.00	0.00	0.00	0.00
741	-17,098	2,4830	-17,098	0.00	0.00	0.00	0.00
742	-18,113	2,4830	-18,113	0.00	0.00	0.00	0.00
743	-17,098	2,4830	-17,098	0.00	0.00	0.00	0.00
744	-18,113	2,4830	-18,113	0.00	0.00	0.00	0.00
745	-18,113	2,4830	-18,113	0.00	0.00	0.00	0.00
746	-18,113	2,4830	-18,113	0.00	0.00	0.00	0.00
747	-18,113	2,4830	-18,113	0.00	0.00	0.00	0.00
748	-18,113	2,4830	-18,113	0.00	0.00	0.00	0.00
749	-18,113	2,4830	-18,113	0.00	0.00	0.00	0.00
750	-18,113	2,4830	-18,113	0.00	0.00	0.00	0.00
751	-18,113	2,4830	-18,113	0.00	0.00	0.00	0.00
752	-18,113	2,4830	-18,113	0.00	0.00	0.00	0.00
753	-18,113	2,4830	-18,113	0.00	0.00	0.00	0.00
754	-18,113	2,4830	-18,113	0.00	0.00	0.00	0.00
755	-18,113	2,4830	-18,113	0.00	0.00	0.00	0.00
756	-18,113	2,4830	-18,113	0.00	0.00	0.00	0.00
757	-18,113	2,4830	-18,113	0.00	0.00	0.00	0.00
758	-18,113	2,4830	-18,113	0.00	0.00	0.00	0.00
759	-18,113	2,4830	-18,113	0.00	0.00	0.00	0.00
760	-18,113	2,4830	-18,113	0.00	0.00	0.00	0.00
761	-18,113	2,4830	-18,113	0.00	0.00	0.00	0.00
762	-18,113	2,4830	-18,113	0.00	0.00	0.00	0.00
763	-18,113	2,4830	-18,113	0.00	0.00	0.00	0.00
764	-18,113	2,4830	-18,113	0.00	0.00	0.00	0.00
765	-18,113	2,4830	-18,113	0.00	0.00	0.00	0.00
766	-18,113	2,4830	-18,113	0.00	0.00	0.00	0.00
767	-18,113	2,4830	-18,113	0.00	0.00	0.00	0.00
768	-18,113	2,4830	-18,113	0.00	0.00	0.00	0.00
769	-18,113	2,4830	-18,113	0.00	0.00	0.00	0.00
770	-18,113	2,4830	-18,113	0.00	0.00	0.00	0.00
771	-18,113	2,4830	-18,113	0.00	0.00	0.00	0.00
772	-18,113	2,4830	-18,113	0.00	0.00	0.00	0.00
773	-18,113	2,4830	-18,113	0.00	0.00	0.00	0.00
774	-18,113	2,4830	-18,113	0.00	0.00	0.00	0.00
775	-18,113	2,4830	-18,113	0.00	0.00	0.00	0.00
776	-18,113	2,4830	-18,113	0.00	0.00	0.00	0.00
777	-18,113	2,4830	-18,113	0.00	0.00	0.00	0.00
778	-18,113	2,4830	-18,113	0.00	0.00	0.00	0.00
779	-18,113	2,4830	-18,113	0.00	0.00	0.00	0.00
780	-18,113	2,4830	-18,113	0.00	0.00	0.00	0.00
781	-18,113	2,4830	-18,113	0.00	0.00	0.00	0.00
782	-18,113	2,4830	-18,113	0.00	0.00	0.00	0.00
783	-18,113	2,4830	-18,113	0.00	0.00	0.00	0.00
784	-18,113	2,4830	-18,113	0.00	0.00	0.00	0.00
785	-18,113	2,4830	-18,113	0.00	0.00	0.00	0.00
786	-18,113	2,4830	-18,113	0.00	0.00	0.00	0.00
787	-18,113	2,4830	-18,113	0.00	0.00	0.00	0.00
788	-18,113	2,4830	-18,113	0.00	0.00	0.00	0.00
789	-18,113	2,4830	-18,113	0.00	0.00	0.00	0.00
790	-18,113	2,4830	-18,113	0.00	0.00	0.00	0.00
791	-18,113	2,4830	-18,113	0.00	0.00	0.00	0.00
792	-18,113	2,4830	-18,113	0.00	0.00	0.00	0.00
793	-18,113	2,4830	-18,113	0.00	0.00	0.00	0.00
794	-18,113	2,4830	-18,113	0.00	0.00	0.00	0.00
795	-18,113	2,4830	-18,113	0.00	0.00	0.00	0.00
796	-18,113	2,4830	-18,113	0.00	0.00	0.00	0.00
797	-18,113	2,4830	-18,113	0.00	0.00	0.00	0.00
798	-18,113	2,4830	-18,113	0.00	0.00	0.00	0.00
799	-18,113	2,4830	-18,113	0.00	0.00	0.00	0.00
800	-18,113	2,4830	-18,113	0.00	0.00	0.00	0.00

744	-16.934	3.1763	-4.5374	0.00	0.00	0.00
745	-17.447	3.3833	-4.6749	0.00	0.00	0.00
746	-17.930	3.4325	-4.8043	0.00	0.00	0.00
747	-16.421	3.4700	-4.3999	0.00	0.00	0.00
748	-16.942	3.7283	-4.6446	0.00	0.00	0.00
749	-16.904	3.9867	-4.9293	0.00	0.00	0.00
750	-17.343	4.2450	-4.9948	0.00	0.00	0.00
751	-16.881	4.4930	-4.5625	0.00	0.00	0.00
752	-16.431	4.4930	-4.3999	0.00	0.00	0.00
753	-16.402	4.8206	-4.6446	0.00	0.00	0.00
754	-16.783	4.8206	-4.4970	0.00	0.00	0.00
755	-16.944	4.8206	-4.5455	0.00	0.00	0.00
756	-17.343	4.8206	-4.9948	0.00	0.00	0.00
761	-17.000	1.4700	-0.29797E-07	0.00	0.00	0.00
762	-17.813	1.4700	-0.31232E-07	0.00	0.00	0.00
763	-18.625	1.4700	-0.32666E-07	0.00	0.00	0.00
764	-19.375	1.4700	-0.33941E-07	0.00	0.00	0.00
766	-17.000	2.8700	-0.29795E-07	0.00	0.00	0.00
766	-17.813	2.8700	-0.31219E-07	0.00	0.00	0.00

NODE	X	Y	Z	THX1	THY2	THZ2
767	-18.625	2.8700	-0.32666E-07	0.00	0.00	0.00
768	-19.375	2.8700	-0.33939E-07	0.00	0.00	0.00
769	-17.000	2.8200	-0.29793E-07	0.00	0.00	0.00
770	-17.813	2.8200	-0.31117E-07	0.00	0.00	0.00
771	-18.625	2.8200	-0.32442E-07	0.00	0.00	0.00
772	-19.375	2.8200	-0.33937E-07	0.00	0.00	0.00
773	-17.000	3.8450	-0.29791E-07	0.00	0.00	0.00
774	-17.813	3.1742	-0.30722E-07	0.00	0.00	0.00
775	-18.663	3.3633	-0.31653E-07	0.00	0.00	0.00
776	-18.963	3.4325	-0.32579E-07	0.00	0.00	0.00
777	-17.000	3.4700	-0.29798E-07	0.00	0.00	0.00
778	-17.250	3.7283	-0.30227E-07	0.00	0.00	0.00
779	-17.500	3.9867	-0.30664E-07	0.00	0.00	0.00
780	-17.750	4.2450	-0.31191E-07	0.00	0.00	0.00
781	-16.885	3.4700	-0.29534E-07	0.00	0.00	0.00
782	-17.000	4.8206	-0.29784E-07	0.00	0.00	0.00
783	-17.188	4.8206	-0.30113E-07	0.00	0.00	0.00
784	-17.375	4.8206	-0.30442E-07	0.00	0.00	0.00
785	-17.562	4.8206	-0.30770E-07	0.00	0.00	0.00
786	-17.750	4.8206	-0.31099E-07	0.00	0.00	0.00

NODE	X	Y	Z	THX1	THY2	THZ2
801	17.375	6.0950	0.23756E-10	0.00	0.00	0.00
802	17.375	8.8950	0.34699E-10	0.00	0.00	0.00
803	17.375	11.695	0.45570E-10	0.00	0.00	0.00
804	17.375	14.532	0.46419E-10	0.00	0.00	0.00
805	17.375	21.378	0.83268E-10	0.00	0.00	0.00
806	17.375	34.779	0.13848E-09	0.00	0.00	0.00
807	17.375	48.179	0.18799E-09	0.00	0.00	0.00
808	17.375	52.278	0.20367E-09	0.00	0.00	0.00
809	17.375	56.378	0.21959E-09	0.00	0.00	0.00
810	17.283	57.038	0.22223E-09	0.00	0.00	0.00
811	17.014	57.468	0.22499E-09	0.00	0.00	0.00
812	16.595	58.199	0.22660E-09	0.00	0.00	0.00
813	14.049	58.537	0.22809E-09	0.00	0.00	0.00
814	13.015	59.914	0.23346E-09	0.00	0.00	0.00
815	9.8680	60.999	0.23708E-09	0.00	0.00	0.00
816	6.6882	61.780	0.24073E-09	0.00	0.00	0.00
817	3.3288	62.752	0.24437E-09	0.00	0.00	0.00
818	0.80806E+00	63.430	0.24830E-09	0.00	0.00	0.00
831	16.783	8.8950	-4.4970	0.00	0.00	0.00
832	16.783	8.8950	-4.4970	0.00	0.00	0.00

NODE	X	Y	Z	THX1	THY2	THZ2
833	16.783	11.695	-4.4970	0.00	0.00	0.00
834	16.783	14.532	-4.4970	0.00	0.00	0.00
835	16.783	21.378	-4.4970	0.00	0.00	0.00
836	16.783	34.779	-4.4970	0.00	0.00	0.00
837	16.783	48.179	-4.4970	0.00	0.00	0.00
838	16.783	52.279	-4.4970	0.00	0.00	0.00
839	16.783	56.379	-4.4970	0.00	0.00	0.00
840	16.694	57.030	-4.4732	0.00	0.00	0.00
841	16.437	57.460	-4.4482	0.00	0.00	0.00

962	4.2950	56.195	-16.829	0.00	0.00	0.00
963	4.1938	56.837	-15.302	0.00	0.00	0.00
964	3.3684	59.914	-12.572	0.00	0.00	0.00
965	X	Y	Z	TRV1	TRV2	TRV3
966	3.3333	60.999	-9.3289	0.00	0.00	0.00
966	1.7150	61.780	-6.4805	0.00	0.00	0.00
967	0.86136	62.252	-3.2146	0.00	0.00	0.00
961	0.67782E-10	6.0990	-17.375	0.00	0.00	0.00
962	0.67782E-10	8.8950	-17.375	0.00	0.00	0.00
963	0.67782E-10	11.695	-17.375	0.00	0.00	0.00
964	0.67782E-10	16.333	-17.375	0.00	0.00	0.00
965	0.67782E-10	21.370	-17.375	0.00	0.00	0.00
966	0.67782E-10	24.370	-17.375	0.00	0.00	0.00
967	0.67782E-10	46.370	-17.375	0.00	0.00	0.00
968	0.67782E-10	82.270	-17.375	0.00	0.00	0.00
969	0.67782E-10	94.370	-17.375	0.00	0.00	0.00
968	0.67344E-10	57.090	-17.283	0.00	0.00	0.00
991	0.66395E-10	57.640	-17.816	0.00	0.00	0.00
992	0.64661E-10	58.195	-16.595	0.00	0.00	0.00
993	0.62535E-10	58.537	-14.849	0.00	0.00	0.00
994	0.50714E-10	59.914	-13.815	0.00	0.00	0.00
995	0.38439E-10	60.999	-9.8680	0.00	0.00	0.00
996	0.25819E-10	61.780	-6.6280	0.00	0.00	0.00
997	0.12960E-10	62.252	-3.3280	0.00	0.00	0.00

965	X	Y	Z	TRV1	TRV2	TRV3
1011	-4.4978	8.8950	-16.783	0.00	0.00	0.00
1012	-4.4978	8.8950	-16.783	0.00	0.00	0.00
1013	-4.4978	11.695	-16.783	0.00	0.00	0.00
1014	-4.4978	16.333	-16.783	0.00	0.00	0.00
1015	-4.4978	21.370	-16.783	0.00	0.00	0.00
1016	-4.4978	24.370	-16.783	0.00	0.00	0.00
1017	-4.4978	46.370	-16.783	0.00	0.00	0.00
1018	-4.4978	52.270	-16.783	0.00	0.00	0.00
1019	-4.4978	54.370	-16.783	0.00	0.00	0.00
1020	-4.4752	57.090	-16.694	0.00	0.00	0.00
1021	-4.4043	57.640	-16.637	0.00	0.00	0.00
1022	-4.2950	58.195	-16.829	0.00	0.00	0.00
1023	-4.1938	58.537	-15.502	0.00	0.00	0.00
1024	-3.3686	59.914	-12.572	0.00	0.00	0.00
1025	-3.3333	60.999	-9.3289	0.00	0.00	0.00
1026	-1.7150	61.780	-6.4805	0.00	0.00	0.00
1027	-0.86136	62.252	-3.2146	0.00	0.00	0.00
1041	-8.6875	6.0990	-15.867	0.00	0.00	0.00
1042	-8.6875	8.8950	-15.867	0.00	0.00	0.00
1043	-8.6875	11.695	-15.867	0.00	0.00	0.00

1044	X	Y	Z	TRV1	TRV2	TRV3
1044	-8.6875	16.333	-15.867	0.00	0.00	0.00
1045	-8.6875	21.370	-15.867	0.00	0.00	0.00
1044	-8.6875	24.370	-15.867	0.00	0.00	0.00
1047	-8.6875	46.370	-15.867	0.00	0.00	0.00
1048	-8.6875	52.270	-15.867	0.00	0.00	0.00
1049	-8.6875	54.370	-15.867	0.00	0.00	0.00
1050	-8.6414	57.090	-14.668	0.00	0.00	0.00
1051	-8.5082	57.640	-14.737	0.00	0.00	0.00
1052	-8.3973	58.195	-14.371	0.00	0.00	0.00
1053	-8.0245	58.537	-13.899	0.00	0.00	0.00
1054	-6.5977	59.914	-11.372	0.00	0.00	0.00
1055	-6.5925	60.999	-8.5434	0.00	0.00	0.00
1056	-3.3731	61.780	-5.7389	0.00	0.00	0.00
1057	-1.6644	62.252	-2.8822	0.00	0.00	0.00
1071	-12.286	6.0990	-12.286	0.00	0.00	0.00
1072	-12.286	8.8950	-12.286	0.00	0.00	0.00
1073	-12.286	11.695	-12.286	0.00	0.00	0.00
1074	-12.286	16.333	-12.286	0.00	0.00	0.00
1075	-12.286	21.370	-12.286	0.00	0.00	0.00
1076	-12.286	24.370	-12.286	0.00	0.00	0.00

1077	X	Y	Z	TRV1	TRV2	TRV3
1077	-12.286	46.370	-12.286	0.00	0.00	0.00
1078	-12.286	52.270	-12.286	0.00	0.00	0.00
1079	-12.286	56.370	-12.286	0.00	0.00	0.00

1080	-12.221	57.090	-12.221	0.00	0.00	0.00
1081	-12.032	57.640	-12.032	0.00	0.00	0.00
1082	-11.734	58.195	-11.734	0.00	0.00	0.00
1083	-11.348	58.737	-11.348	0.00	0.00	0.00
1084	-9.2032	59.214	-9.2032	0.00	0.00	0.00
1085	-6.9794	60.999	-6.9794	0.00	0.00	0.00
1086	-4.6855	61.780	-4.6855	0.00	0.00	0.00
1087	-2.3533	62.252	-2.3533	0.00	0.00	0.00
1101	-19.047	6.8950	-8.6875	0.00	0.00	0.00
1102	-19.047	6.8950	-8.6875	0.00	0.00	0.00
1103	-19.047	11.695	-8.6875	0.00	0.00	0.00
1104	-15.847	15.332	-8.6875	0.00	0.00	0.00
1105	-15.847	21.378	-8.6875	0.00	0.00	0.00
1106	-15.847	34.779	-8.6875	0.00	0.00	0.00
1107	-15.847	45.178	-8.6875	0.00	0.00	0.00
1108	-15.847	52.270	-8.6875	0.00	0.00	0.00
1109	-15.847	56.378	-8.6875	0.00	0.00	0.00

4000	X	Y	Z	TMX1	TMX2	TMX3
1110	-14.048	57.090	-8.6416	0.00	0.00	0.00
1111	-14.737	57.640	-8.5082	0.00	0.00	0.00
1112	-14.371	58.195	-8.2972	0.00	0.00	0.00
1113	-13.899	58.737	-8.0345	0.00	0.00	0.00
1114	-11.272	59.214	-6.5077	0.00	0.00	0.00
1115	-8.5434	60.999	-4.9325	0.00	0.00	0.00
1116	-5.7385	61.780	-3.3121	0.00	0.00	0.00
1117	-2.8922	62.252	-1.6640	0.00	0.00	0.00
1131	-16.783	6.8950	-4.4970	0.00	0.00	0.00
1132	-16.783	8.8998	-4.4970	0.00	0.00	0.00
1133	-16.783	11.665	-4.4970	0.00	0.00	0.00
1134	-16.783	15.332	-4.4970	0.00	0.00	0.00
1135	-16.783	21.378	-4.4970	0.00	0.00	0.00
1136	-16.783	34.779	-4.4970	0.00	0.00	0.00
1137	-16.783	45.178	-4.4970	0.00	0.00	0.00
1138	-16.783	52.270	-4.4970	0.00	0.00	0.00
1139	-16.783	56.378	-4.4970	0.00	0.00	0.00
1140	-16.694	57.090	-4.4732	0.00	0.00	0.00
1141	-16.437	57.640	-4.4462	0.00	0.00	0.00
1142	-16.029	58.195	-4.2950	0.00	0.00	0.00

4000	X	Y	Z	TMX1	TMX2	TMX3
1143	-15.362	58.737	-4.1538	0.00	0.00	0.00
1144	-12.572	59.214	-3.3286	0.00	0.00	0.00
1145	-9.5289	60.999	-2.3533	0.00	0.00	0.00
1146	-6.4085	61.780	-1.7190	0.00	0.00	0.00
1147	-2.2148	62.252	-0.88136	0.00	0.00	0.00
1161	-17.375	6.8950	-0.30437E-07	0.00	0.00	0.00
1162	-17.375	8.8950	-0.30438E-07	0.00	0.00	0.00
1163	-17.375	11.695	-0.30415E-07	0.00	0.00	0.00
1164	-17.375	16.332	-0.30394E-07	0.00	0.00	0.00
1168	-17.375	21.378	-0.30377E-07	0.00	0.00	0.00
1166	-17.375	34.779	-0.30259E-07	0.00	0.00	0.00
1167	-17.375	48.170	-0.30234E-07	0.00	0.00	0.00
1168	-17.375	52.270	-0.30257E-07	0.00	0.00	0.00
1169	-17.375	56.378	-0.30241E-07	0.00	0.00	0.00
1170	-17.283	57.090	-0.30677E-07	0.00	0.00	0.00
1171	-17.016	57.640	-0.29687E-07	0.00	0.00	0.00
1172	-16.935	58.193	-0.28846E-07	0.00	0.00	0.00
1173	-16.049	58.737	-0.27908E-07	0.00	0.00	0.00
1174	-13.095	59.214	-0.22848E-07	0.00	0.00	0.00
1175	-9.8630	60.999	-0.17057E-07	0.00	0.00	0.00

4000	X	Y	Z	TMX1	TMX2	TMX3
1176	-6.4252	61.780	-0.11176E-07	0.00	0.00	0.00
1177	-3.3280	62.252	-0.55949E-08	0.00	0.00	0.00

LIST ALL MATERIALS PROPERTY= ALL

PROPERTY TABLE MXT MAT= 1 NUM. POINTS= 2
 TEMPERATURE DATA TEMPERATURE DATA
 -9999.0 0.30000 9999.0 0.30000

PROPERTY TABLE EK MAT= 1 NUM. POINTS= 15
 TEMPERATURE DATA TEMPERATURE DATA

-40.000	0.39900E+06	70.000	0.26300E+06
100.00	0.28100E+06	200.00	0.27600E+06
300.00	0.37000E+06	400.00	0.26500E+06
500.00	0.25800E+06	600.00	0.25100E+06
700.00	0.34800E+06	800.00	0.26100E+06
900.00	0.23500E+06	1000.0	0.22200E+06
1100.0	0.22100E+06	1200.0	0.21300E+06
1300.0	0.20700E+06		

PROPERTY TABLE ALPH MAT= 1 NUM. POINTS= 13
 TEMPERATURE DATA TEMPERATURE DATA

-40.000	0.81300E-05	70.000	0.86600E-05
100.00	0.82100E-05	200.00	0.87900E-05
300.00	0.90000E-05	400.00	0.91900E-05
500.00	0.93700E-05	600.00	0.95300E-05
700.00	0.96900E-05	800.00	0.98200E-05
900.00	0.10060E-04	1000.0	0.10300E-04
1100.0	0.10750E-04	1200.0	0.10400E-04
1300.0	0.10450E-04		

PROPERTY TABLE EX MAT= 2 NUM. POINTS= 7
 TEMPERATURE DATA TEMPERATURE DATA

-40.000	0.29400E+06	70.000	0.27800E+06
100.00	0.27600E+06	200.00	0.27100E+06
300.00	0.26700E+06	400.00	0.26100E+06
500.00	0.25700E+06		

PROPERTY TABLE ALPH MAT= 2 NUM. POINTS= 7
 TEMPERATURE DATA TEMPERATURE DATA

-40.000	0.59600E-05	70.000	0.62000E-05
100.00	0.62700E-05	200.00	0.65400E-05
300.00	0.67900E-05	400.00	0.69600E-05
500.00	0.71600E-05		

LIST ALL COUPLED SETS
 TIME= 0.00000E+00 NITER= -5
 KTRW= 1370= -1 ITR= 0

UNIFORM TEMPERATURE= 70.000 (TIME= 70.000)

PRINT REACTION FORCES WITH NO ELEMENT FORCES (KRF=2)
 SOLVARY CONDITIONS STEPPED DUE TO STATIC CONVERGENCE OPTION
 PLASTIC CONVERG. CRITERION= 0.0100
 CREEP OPTION, CRITERION= 0.0000
 LARGE DEFL. CONVERG. CRITERION= 0.001000
 DISPLACEMENT LIMIT= 0.00000E+00

NPRINT= 99900 NFRONT= 5 REACTION PRINT FREQ= 99900
 DISP. POST DATA FREQ= 5 REACT. POST DATA FREQ= 5

ELEMENT PRINT AND POST DATA FREQUENCIES						
TYPE	STIFF	STRESS	FORCE	STRESS	DATA	FORCE
	NO.	PRINT	PRINT	DATA	LEVEL	DATA
2	63	99900	99900	5	3	5
3	8	99900	99900	5	3	5
4	52	99900	99900	5	3	5
5	45	99900	99900	5	3	5
6	63	99900	99900	5	3	5
7	45	99900	99900	5	3	5
8	63	99900	99900	5	3	5
9	45	99900	99900	5	3	5

LOADS INPUT FILE= 26 LOADS OUTPUT FILE= 25

ALL ANALYSIS DATA WILL BE WRITTEN OUTO FILE27

LIST DISPLACEMENTS FOR ALL SELECTED NODES

NODE LABEL	DISP	EDTRW
1177 EDTH	0.00000000E+00	0.00000000E+00
1177 IZ	0.00000000E+00	0.00000000E+00
1176 EDTH	0.00000000E+00	0.00000000E+00
1176 IZ	0.00000000E+00	0.00000000E+00
1175 EDTH	0.00000000E+00	0.00000000E+00

1173	UZ	0.00000000E+00	0.00000000E+00
1174	RD7H	0.00000000E+00	0.00000000E+00
1174	UZ	0.00000000E+00	0.00000000E+00
1173	RD7H	0.00000000E+00	0.00000000E+00
1173	UZ	0.00000000E+00	0.00000000E+00
1172	RD7H	0.00000000E+00	0.00000000E+00
1172	UZ	0.00000000E+00	0.00000000E+00
1171	RD7H	0.00000000E+00	0.00000000E+00
1171	UZ	0.00000000E+00	0.00000000E+00
1170	RD7H	0.00000000E+00	0.00000000E+00
1170	UZ	0.00000000E+00	0.00000000E+00
1169	RD7H	0.00000000E+00	0.00000000E+00
1169	UZ	0.00000000E+00	0.00000000E+00
1168	RD7H	0.00000000E+00	0.00000000E+00
1168	UZ	0.00000000E+00	0.00000000E+00

MODE	LABEL	D1#P	D21#P
1167	RD7H	0.00000000E+00	0.00000000E+00
1167	UZ	0.00000000E+00	0.00000000E+00
1166	RD7H	0.00000000E+00	0.00000000E+00
1166	UZ	0.00000000E+00	0.00000000E+00
1165	RD7H	0.00000000E+00	0.00000000E+00
1165	UZ	0.00000000E+00	0.00000000E+00
1164	RD7H	0.00000000E+00	0.00000000E+00
1164	UZ	0.00000000E+00	0.00000000E+00
1163	RD7H	0.00000000E+00	0.00000000E+00
1163	UZ	0.00000000E+00	0.00000000E+00
1162	RD7H	0.00000000E+00	0.00000000E+00
1162	UZ	0.00000000E+00	0.00000000E+00
1161	RD7H	0.00000000E+00	0.00000000E+00
1161	UZ	0.00000000E+00	0.00000000E+00
390	RD7H	0.00000000E+00	0.00000000E+00
318	RD7H	0.00000000E+00	0.00000000E+00
318	UZ	0.00000000E+00	0.00000000E+00
290	UP	0.00000000E+00	0.00000000E+00
290	UP	0.00000000E+00	0.00000000E+00
317	RD7H	0.00000000E+00	0.00000000E+00

MODE	LABEL	D1#P	D21#P
316	RD7H	0.00000000E+00	0.00000000E+00
316	RD7H	0.00000000E+00	0.00000000E+00
314	RD7H	0.00000000E+00	0.00000000E+00
313	RD7H	0.00000000E+00	0.00000000E+00
312	RD7H	0.00000000E+00	0.00000000E+00
311	RD7H	0.00000000E+00	0.00000000E+00
310	RD7H	0.00000000E+00	0.00000000E+00
309	RD7H	0.00000000E+00	0.00000000E+00
308	RD7H	0.00000000E+00	0.00000000E+00
307	RD7H	0.00000000E+00	0.00000000E+00
306	RD7H	0.00000000E+00	0.00000000E+00
305	RD7H	0.00000000E+00	0.00000000E+00
304	RD7H	0.00000000E+00	0.00000000E+00
303	RD7H	0.00000000E+00	0.00000000E+00
302	RD7H	0.00000000E+00	0.00000000E+00
301	RD7H	0.00000000E+00	0.00000000E+00
298	RD7H	0.00000000E+00	0.00000000E+00
295	RD7H	0.00000000E+00	0.00000000E+00
294	RD7H	0.00000000E+00	0.00000000E+00
293	RD7H	0.00000000E+00	0.00000000E+00

MODE	LABEL	D1#P	D21#P
292	RD7H	0.00000000E+00	0.00000000E+00
281	RD7H	0.00000000E+00	0.00000000E+00
280	RD7H	0.00000000E+00	0.00000000E+00
279	RD7H	0.00000000E+00	0.00000000E+00
278	RD7H	0.00000000E+00	0.00000000E+00
277	RD7H	0.00000000E+00	0.00000000E+00
276	RD7H	0.00000000E+00	0.00000000E+00
275	RD7H	0.00000000E+00	0.00000000E+00
274	RD7H	0.00000000E+00	0.00000000E+00
273	RD7H	0.00000000E+00	0.00000000E+00
272	RD7H	0.00000000E+00	0.00000000E+00
271	RD7H	0.00000000E+00	0.00000000E+00
270	RD7H	0.00000000E+00	0.00000000E+00

```

789 NGTK 0.00000000E+00 0.00000000E+00
790 NGTK 0.00000000E+00 0.00000000E+00
791 NGTK 0.00000000E+00 0.00000000E+00
792 NGTK 0.00000000E+00 0.00000000E+00
793 NGTK 0.00000000E+00 0.00000000E+00
794 NGTK 0.00000000E+00 0.00000000E+00
795 NGTK 0.00000000E+00 0.00000000E+00

MODE LABEL      DISP      CDISP
762 NGTK 0.00000000E+00 0.00000000E+00
763 NGTK 0.00000000E+00 0.00000000E+00
426 NGTK 0.00000000E+00 0.00000000E+00
425 NGTK 0.00000000E+00 0.00000000E+00
424 NGTK 0.00000000E+00 0.00000000E+00
423 NGTK 0.00000000E+00 0.00000000E+00
422 NGTK 0.00000000E+00 0.00000000E+00
421 NGTK 0.00000000E+00 0.00000000E+00
420 NGTK 0.00000000E+00 0.00000000E+00
419 NGTK 0.00000000E+00 0.00000000E+00
418 NGTK 0.00000000E+00 0.00000000E+00
417 NGTK 0.00000000E+00 0.00000000E+00
416 NGTK 0.00000000E+00 0.00000000E+00
415 NGTK 0.00000000E+00 0.00000000E+00
414 NGTK 0.00000000E+00 0.00000000E+00
413 NGTK 0.00000000E+00 0.00000000E+00
412 NGTK 0.00000000E+00 0.00000000E+00
411 NGTK 0.00000000E+00 0.00000000E+00
410 NGTK 0.00000000E+00 0.00000000E+00
409 NGTK 0.00000000E+00 0.00000000E+00

MODE LABEL      DISP      CDISP
408 NGTK 0.00000000E+00 0.00000000E+00
407 NGTK 0.00000000E+00 0.00000000E+00
406 NGTK 0.00000000E+00 0.00000000E+00
405 NGTK 0.00000000E+00 0.00000000E+00
404 NGTK 0.00000000E+00 0.00000000E+00
403 NGTK 0.00000000E+00 0.00000000E+00
402 NGTK 0.00000000E+00 0.00000000E+00
401 NGTK 0.00000000E+00 0.00000000E+00
400 NGTK 0.00000000E+00 0.00000000E+00
399 NGTK 0.00000000E+00 0.00000000E+00
398 NGTK 0.00000000E+00 0.00000000E+00
397 NGTK 0.00000000E+00 0.00000000E+00
396 NGTK 0.00000000E+00 0.00000000E+00
395 NGTK 0.00000000E+00 0.00000000E+00
394 NGTK 0.00000000E+00 0.00000000E+00
393 NGTK 0.00000000E+00 0.00000000E+00
392 NGTK 0.00000000E+00 0.00000000E+00
391 NGTK 0.00000000E+00 0.00000000E+00
390 NGTK 0.00000000E+00 0.00000000E+00
389 NGTK 0.00000000E+00 0.00000000E+00

MODE LABEL      DISP      CDISP
387 NGTK 0.00000000E+00 0.00000000E+00
386 NGTK 0.00000000E+00 0.00000000E+00
385 NGTK 0.00000000E+00 0.00000000E+00
384 NGTK 0.00000000E+00 0.00000000E+00
383 NGTK 0.00000000E+00 0.00000000E+00
382 NGTK 0.00000000E+00 0.00000000E+00
381 NGTK 0.00000000E+00 0.00000000E+00
380 NGTK 0.00000000E+00 0.00000000E+00
379 NGTK 0.00000000E+00 0.00000000E+00
378 NGTK 0.00000000E+00 0.00000000E+00
377 NGTK 0.00000000E+00 0.00000000E+00
376 NGTK 0.00000000E+00 0.00000000E+00
375 NGTK 0.00000000E+00 0.00000000E+00
817 UR 0.00000000E+00 0.00000000E+00
816 UR 0.00000000E+00 0.00000000E+00
815 UR 0.00000000E+00 0.00000000E+00
814 UR 0.00000000E+00 0.00000000E+00
813 UR 0.00000000E+00 0.00000000E+00
812 UR 0.00000000E+00 0.00000000E+00
811 UR 0.00000000E+00 0.00000000E+00

```

MODE	LABEL	D1SP	C01SP
810	UZ	0.08800000E+00	0.80000000E+00
809	UZ	0.08800000E+00	0.80000000E+00
808	UZ	0.08800000E+00	0.80000000E+00
807	UZ	0.08800000E+00	0.80000000E+00
806	UZ	0.08800000E+00	0.80000000E+00
805	UZ	0.08800000E+00	0.80000000E+00
804	UZ	0.08800000E+00	0.80000000E+00
803	UZ	0.08800000E+00	0.80000000E+00
802	UZ	0.08800000E+00	0.80000000E+00
801	UZ	0.08800000E+00	0.80000000E+00
798	UZ	0.08800000E+00	0.80000000E+00
797	UZ	0.80000000E+00	0.00000000E+00
796	UZ	0.80000000E+00	0.00000000E+00
795	UZ	0.80000000E+00	0.00000000E+00
794	UZ	0.80000000E+00	0.00000000E+00
793	UZ	0.80000000E+00	0.00000000E+00
792	UZ	0.80000000E+00	0.00000000E+00
791	UZ	0.80000000E+00	0.00000000E+00
789	UZ	0.80000000E+00	0.00000000E+00
779	UZ	0.80000000E+00	0.00000000E+00
778	UZ	0.80000000E+00	0.00000000E+00
777	UZ	0.80000000E+00	0.00000000E+00

MODE	LABEL	D1SP	C01SP
776	UZ	0.80000000E+00	0.80000000E+00
775	UZ	0.80000000E+00	0.80000000E+00
774	UZ	0.80000000E+00	0.80000000E+00
773	UZ	0.80000000E+00	0.80000000E+00
772	UZ	0.80000000E+00	0.80000000E+00
771	UZ	0.80000000E+00	0.80000000E+00
770	UZ	0.80000000E+00	0.80000000E+00
769	UZ	0.08800000E+00	0.80000000E+00
768	UZ	0.08800000E+00	0.80000000E+00
767	UZ	0.08800000E+00	0.80000000E+00
766	UZ	0.08800000E+00	0.80000000E+00
765	UZ	0.08800000E+00	0.80000000E+00
764	UZ	0.08800000E+00	0.80000000E+00
763	UZ	0.08800000E+00	0.80000000E+00
762	UZ	0.08800000E+00	0.80000000E+00
761	UZ	0.08800000E+00	0.80000000E+00
424	UZ	0.00000000E+00	0.08800000E+00
425	UZ	0.00000000E+00	0.08800000E+00
426	UZ	0.00000000E+00	0.08800000E+00
423	UZ	0.00000000E+00	0.08800000E+00

MODE	LABEL	D1SP	C01SP
422	UZ	0.00000000E+00	0.08800000E+00
421	UZ	0.00000000E+00	0.08800000E+00
420	UZ	0.00000000E+00	0.08800000E+00
419	UZ	0.00000000E+00	0.08800000E+00
418	UZ	0.00000000E+00	0.08800000E+00
417	UZ	0.00000000E+00	0.08800000E+00
416	UZ	0.00000000E+00	0.08800000E+00
374	MOX	0.00000000E+00	0.00000000E+00
415	UZ	0.00000000E+00	0.00000000E+00
414	UZ	0.08800000E+00	0.08800000E+00
413	UZ	0.08800000E+00	0.08800000E+00
412	UZ	0.08800000E+00	0.08800000E+00
411	UZ	0.08800000E+00	0.08800000E+00
410	UZ	0.08800000E+00	0.08800000E+00
409	UZ	0.08800000E+00	0.08800000E+00
408	UZ	0.08800000E+00	0.08800000E+00
407	UZ	0.08800000E+00	0.08800000E+00
406	UZ	0.08800000E+00	0.08800000E+00
405	UZ	0.08800000E+00	0.08800000E+00
404	UZ	0.08800000E+00	0.08800000E+00

MODE	LABEL	D1SP	C01SP
403	UZ	0.00000000E+00	0.00000000E+00
402	UZ	0.00000000E+00	0.00000000E+00
401	UZ	0.00000000E+00	0.00000000E+00
400	UZ	0.00000000E+00	0.00000000E+00
399	UZ	0.00000000E+00	0.00000000E+00
398	UZ	0.00000000E+00	0.00000000E+00
397	UZ	0.00000000E+00	0.00000000E+00

396 UZ	0.00000000E+00	0.00000000E+00
397 UZ	0.00000000E+00	0.00000000E+00
398 UZ	0.00000000E+00	0.00000000E+00
399 UZ	0.00000000E+00	0.00000000E+00
400 UZ	0.00000000E+00	0.00000000E+00
401 UZ	0.00000000E+00	0.00000000E+00
402 UZ	0.00000000E+00	0.00000000E+00
403 UZ	0.00000000E+00	0.00000000E+00
404 UZ	0.00000000E+00	0.00000000E+00
405 UZ	0.00000000E+00	0.00000000E+00
406 UZ	0.00000000E+00	0.00000000E+00
407 UZ	0.00000000E+00	0.00000000E+00
408 UZ	0.00000000E+00	0.00000000E+00
409 UZ	0.00000000E+00	0.00000000E+00
410 UZ	0.00000000E+00	0.00000000E+00

MODE LABEL	P1BP	CD1BP
382 UZ	0.00000000E+00	0.00000000E+00
381 UZ	0.00000000E+00	0.00000000E+00
380 UZ	0.00000000E+00	0.00000000E+00
379 UZ	0.00000000E+00	0.00000000E+00
378 UZ	0.00000000E+00	0.00000000E+00
377 UZ	0.00000000E+00	0.00000000E+00
376 UZ	0.00000000E+00	0.00000000E+00
375 UZ	0.00000000E+00	0.00000000E+00
374 UZ	0.00000000E+00	0.00000000E+00
373 UZ	0.00000000E+00	0.00000000E+00
372 UZ	0.00000000E+00	0.00000000E+00
371 UZ	0.00000000E+00	0.00000000E+00
370 UZ	0.00000000E+00	0.00000000E+00
369 UZ	0.00000000E+00	0.00000000E+00
368 UZ	0.00000000E+00	0.00000000E+00
367 UZ	0.00000000E+00	0.00000000E+00
366 UZ	0.00000000E+00	0.00000000E+00
365 UZ	0.00000000E+00	0.00000000E+00
364 UZ	0.00000000E+00	0.00000000E+00
363 UZ	0.00000000E+00	0.00000000E+00
362 UZ	0.00000000E+00	0.00000000E+00

MODE LABEL	P1BP	CD1BP
361 UZ	0.00000000E+00	0.00000000E+00
36 UZ	0.00000000E+00	0.00000000E+00
37 UZ	0.00000000E+00	0.00000000E+00
26 UZ	0.00000000E+00	0.00000000E+00
25 UZ	0.00000000E+00	0.00000000E+00
24 UZ	0.00000000E+00	0.00000000E+00
23 UZ	0.00000000E+00	0.00000000E+00
22 UZ	0.00000000E+00	0.00000000E+00
21 UZ	0.00000000E+00	0.00000000E+00
20 UZ	0.00000000E+00	0.00000000E+00
19 UZ	0.00000000E+00	0.00000000E+00
18 UZ	0.00000000E+00	0.00000000E+00
17 UZ	0.00000000E+00	0.00000000E+00
16 UZ	0.00000000E+00	0.00000000E+00
15 UZ	0.00000000E+00	0.00000000E+00
14 UZ	0.00000000E+00	0.00000000E+00
13 UZ	0.00000000E+00	0.00000000E+00
12 UZ	0.00000000E+00	0.00000000E+00
11 UZ	0.00000000E+00	0.00000000E+00
10 UZ	0.00000000E+00	0.00000000E+00

MODE LABEL	P1BP	CD1BP
9 UZ	0.00000000E+00	0.00000000E+00
8 UZ	0.00000000E+00	0.00000000E+00
7 UZ	0.00000000E+00	0.00000000E+00
6 UZ	0.00000000E+00	0.00000000E+00
5 UZ	0.00000000E+00	0.00000000E+00
4 UZ	0.00000000E+00	0.00000000E+00
3 UZ	0.00000000E+00	0.00000000E+00
373 ROTX	0.00000000E+00	0.00000000E+00
372 ROTX	0.00000000E+00	0.00000000E+00
371 ROTX	0.00000000E+00	0.00000000E+00
370 ROTX	0.00000000E+00	0.00000000E+00
369 ROTX	0.00000000E+00	0.00000000E+00
368 ROTX	0.00000000E+00	0.00000000E+00
367 ROTX	0.00000000E+00	0.00000000E+00
366 ROTX	0.00000000E+00	0.00000000E+00
365 ROTX	0.00000000E+00	0.00000000E+00
364 ROTX	0.00000000E+00	0.00000000E+00


```

343 ROTZ 0.00000000E+00 0.00000000E+00
342 ROTX 0.00000000E+00 0.00000000E+00
341 ROTY 0.00000000E+00 0.00000000E+00
28 ROTZ 0.00000000E+00 0.00000000E+00
27 ROTX 0.00000000E+00 0.00000000E+00

NODE LABEL BISP CDISP
26 ROTX 0.00000000E+00 0.00000000E+00
25 ROTX 0.00000000E+00 0.00000000E+00
24 ROTX 0.00000000E+00 0.00000000E+00
23 ROTX 0.00000000E+00 0.00000000E+00
22 ROTX 0.00000000E+00 0.00000000E+00
21 ROTX 0.00000000E+00 0.00000000E+00
20 ROTX 0.00000000E+00 0.00000000E+00
19 ROTX 0.00000000E+00 0.00000000E+00
18 ROTX 0.00000000E+00 0.00000000E+00
17 ROTX 0.00000000E+00 0.00000000E+00
16 ROTX 0.00000000E+00 0.00000000E+00
15 ROTX 0.00000000E+00 0.00000000E+00
14 ROTX 0.00000000E+00 0.00000000E+00
13 ROTX 0.00000000E+00 0.00000000E+00
12 ROTX 0.00000000E+00 0.00000000E+00
11 ROTX 0.00000000E+00 0.00000000E+00
10 ROTX 0.00000000E+00 0.00000000E+00
9 ROTX 0.00000000E+00 0.00000000E+00
8 ROTX 0.00000000E+00 0.00000000E+00
7 ROTX 0.00000000E+00 0.00000000E+00

NODE LABEL BISP CDISP
5 ROTX 0.00000000E+00 0.00000000E+00
4 ROTX 0.00000000E+00 0.00000000E+00
3 ROTX 0.00000000E+00 0.00000000E+00
1 UZ 0.00000000E+00 0.00000000E+00
2 UZ 0.00000000E+00 0.00000000E+00
1 ROTX 0.00000000E+00 0.00000000E+00
2 ROTX 0.00000000E+00 0.00000000E+00
1 ROTY 0.00000000E+00 0.00000000E+00
2 ROTY 0.00000000E+00 0.00000000E+00
3 ROTY 0.00000000E+00 0.00000000E+00
4 ROTY 0.00000000E+00 0.00000000E+00
5 ROTY 0.00000000E+00 0.00000000E+00
6 ROTY 0.00000000E+00 0.00000000E+00
7 ROTY 0.00000000E+00 0.00000000E+00
8 ROTY 0.00000000E+00 0.00000000E+00
9 ROTY 0.00000000E+00 0.00000000E+00
10 ROTY 0.00000000E+00 0.00000000E+00
11 ROTY 0.00000000E+00 0.00000000E+00
12 ROTY 0.00000000E+00 0.00000000E+00
13 ROTY 0.00000000E+00 0.00000000E+00
14 ROTY 0.00000000E+00 0.00000000E+00

NODE LABEL BISP CDISP
15 ROTY 0.00000000E+00 0.00000000E+00
16 ROTY 0.00000000E+00 0.00000000E+00
17 ROTY 0.00000000E+00 0.00000000E+00
18 ROTY 0.00000000E+00 0.00000000E+00
19 ROTY 0.00000000E+00 0.00000000E+00
20 ROTY 0.00000000E+00 0.00000000E+00
21 ROTY 0.00000000E+00 0.00000000E+00
22 ROTY 0.00000000E+00 0.00000000E+00
23 ROTY 0.00000000E+00 0.00000000E+00
24 ROTY 0.00000000E+00 0.00000000E+00
25 ROTY 0.00000000E+00 0.00000000E+00
26 ROTY 0.00000000E+00 0.00000000E+00
27 ROTY 0.00000000E+00 0.00000000E+00
28 ROTY 0.00000000E+00 0.00000000E+00
349 ROTY 0.00000000E+00 0.00000000E+00
348 ROTY 0.00000000E+00 0.00000000E+00
347 ROTY 0.00000000E+00 0.00000000E+00

NODE LABEL BISP CDISP
346 ROTY 0.00000000E+00 0.00000000E+00

```

```

369 RSTY 0.00000000E+00 0.00000000E+00
370 RSTY 0.00000000E+00 0.00000000E+00
371 RSTY 0.00000000E+00 0.00000000E+00
372 RSTY 0.00000000E+00 0.00000000E+00
373 RSTY 0.00000000E+00 0.00000000E+00
374 RSTY 0.00000000E+00 0.00000000E+00
375 RSTY 0.00000000E+00 0.00000000E+00
376 RSTY 0.00000000E+00 0.00000000E+00
377 RSTY 0.00000000E+00 0.00000000E+00
378 RSTY 0.00000000E+00 0.00000000E+00
379 RSTY 0.00000000E+00 0.00000000E+00
380 RSTY 0.00000000E+00 0.00000000E+00
381 RSTY 0.00000000E+00 0.00000000E+00
382 RSTY 0.00000000E+00 0.00000000E+00
383 RSTY 0.00000000E+00 0.00000000E+00
384 RSTY 0.00000000E+00 0.00000000E+00
385 RSTY 0.00000000E+00 0.00000000E+00
386 RSTY 0.00000000E+00 0.00000000E+00
387 RSTY 0.00000000E+00 0.00000000E+00

MODE LABEL      D:SP      C:SP
388 RSTY 0.00000000E+00 0.00000000E+00
389 RSTY 0.00000000E+00 0.00000000E+00
390 RSTY 0.00000000E+00 0.00000000E+00
391 RSTY 0.00000000E+00 0.00000000E+00
392 RSTY 0.00000000E+00 0.00000000E+00
393 RSTY 0.00000000E+00 0.00000000E+00
394 RSTY 0.00000000E+00 0.00000000E+00
395 RSTY 0.00000000E+00 0.00000000E+00
396 RSTY 0.00000000E+00 0.00000000E+00
397 RSTY 0.00000000E+00 0.00000000E+00
398 RSTY 0.00000000E+00 0.00000000E+00
399 RSTY 0.00000000E+00 0.00000000E+00
400 RSTY 0.00000000E+00 0.00000000E+00
401 RSTY 0.00000000E+00 0.00000000E+00
402 RSTY 0.00000000E+00 0.00000000E+00
403 RSTY 0.00000000E+00 0.00000000E+00
404 RSTY 0.00000000E+00 0.00000000E+00
405 RSTY 0.00000000E+00 0.00000000E+00
406 RSTY 0.00000000E+00 0.00000000E+00
407 RSTY 0.00000000E+00 0.00000000E+00
408 RSTY 0.00000000E+00 0.00000000E+00

MODE LABEL      D:SP      C:SP
409 RSTY 0.00000000E+00 0.00000000E+00
410 RSTY 0.00000000E+00 0.00000000E+00
411 RSTY 0.00000000E+00 0.00000000E+00
412 RSTY 0.00000000E+00 0.00000000E+00
413 RSTY 0.00000000E+00 0.00000000E+00
414 RSTY 0.00000000E+00 0.00000000E+00
415 RSTY 0.00000000E+00 0.00000000E+00
416 RSTY 0.00000000E+00 0.00000000E+00
417 RSTY 0.00000000E+00 0.00000000E+00
418 RSTY 0.00000000E+00 0.00000000E+00
419 RSTY 0.00000000E+00 0.00000000E+00
420 RSTY 0.00000000E+00 0.00000000E+00
421 RSTY 0.00000000E+00 0.00000000E+00
422 RSTY 0.00000000E+00 0.00000000E+00
423 RSTY 0.00000000E+00 0.00000000E+00
424 RSTY 0.00000000E+00 0.00000000E+00
425 RSTY 0.00000000E+00 0.00000000E+00
426 RSTY 0.00000000E+00 0.00000000E+00
761 RSTY 0.00000000E+00 0.00000000E+00
762 RSTY 0.00000000E+00 0.00000000E+00

MODE LABEL      D:SP      C:SP
763 RSTY 0.00000000E+00 0.00000000E+00
764 RSTY 0.00000000E+00 0.00000000E+00
765 RSTY 0.00000000E+00 0.00000000E+00
766 RSTY 0.00000000E+00 0.00000000E+00
767 RSTY 0.00000000E+00 0.00000000E+00
768 RSTY 0.00000000E+00 0.00000000E+00
769 RSTY 0.00000000E+00 0.00000000E+00
770 RSTY 0.00000000E+00 0.00000000E+00
771 RSTY 0.00000000E+00 0.00000000E+00

```

772	ROTY	0.00000000E+00	0.00000000E+00
773	ROTY	0.00000000E+00	0.00000000E+00
774	ROTY	0.00000000E+00	0.00000000E+00
775	ROTY	0.00000000E+00	0.00000000E+00
776	ROTY	0.00000000E+00	0.00000000E+00
777	ROTY	0.00000000E+00	0.00000000E+00
778	ROTY	0.00000000E+00	0.00000000E+00
779	ROTY	0.00000000E+00	0.00000000E+00
780	ROTY	0.00000000E+00	0.00000000E+00
781	ROTY	0.00000000E+00	0.00000000E+00
782	ROTY	0.00000000E+00	0.00000000E+00

NODE	LABEL	DISP	CRISP
783	ROTY	0.00000000E+00	0.00000000E+00
784	ROTY	0.00000000E+00	0.00000000E+00
785	ROTY	0.00000000E+00	0.00000000E+00
786	ROTY	0.00000000E+00	0.00000000E+00
881	ROTY	0.00000000E+00	0.00000000E+00
882	ROTY	0.00000000E+00	0.00000000E+00
883	ROTY	0.00000000E+00	0.00000000E+00
884	ROTY	0.00000000E+00	0.00000000E+00
885	ROTY	0.00000000E+00	0.00000000E+00
886	ROTY	0.00000000E+00	0.00000000E+00
887	ROTY	0.00000000E+00	0.00000000E+00
888	ROTY	0.00000000E+00	0.00000000E+00
889	ROTY	0.00000000E+00	0.00000000E+00
810	ROTY	0.00000000E+00	0.00000000E+00
811	ROTY	0.00000000E+00	0.00000000E+00
812	ROTY	0.00000000E+00	0.00000000E+00
813	ROTY	0.00000000E+00	0.00000000E+00
814	ROTY	0.00000000E+00	0.00000000E+00
815	ROTY	0.00000000E+00	0.00000000E+00
816	ROTY	0.00000000E+00	0.00000000E+00

NODE	LABEL	DISP	CRISP
817	ROTY	0.00000000E+00	0.00000000E+00
818	ROTY	0.00000000E+00	0.00000000E+00
1161	ROTY	0.00000000E+00	0.00000000E+00
1162	ROTY	0.00000000E+00	0.00000000E+00
1163	ROTY	0.00000000E+00	0.00000000E+00
1164	ROTY	0.00000000E+00	0.00000000E+00
1165	ROTY	0.00000000E+00	0.00000000E+00
1166	ROTY	0.00000000E+00	0.00000000E+00
1167	ROTY	0.00000000E+00	0.00000000E+00
1168	ROTY	0.00000000E+00	0.00000000E+00
1169	ROTY	0.00000000E+00	0.00000000E+00
1170	ROTY	0.00000000E+00	0.00000000E+00
1171	ROTY	0.00000000E+00	0.00000000E+00
1172	ROTY	0.00000000E+00	0.00000000E+00
1173	ROTY	0.00000000E+00	0.00000000E+00
1174	ROTY	0.00000000E+00	0.00000000E+00
1175	ROTY	0.00000000E+00	0.00000000E+00
1176	ROTY	0.00000000E+00	0.00000000E+00
1177	ROTY	0.00000000E+00	0.00000000E+00

LIST ELEMENT PROPERTIES FOR ALL SELECTED ELEMENTS

ELEM	RADE	VALUE(S)	FALSE MODES
443	2	30.8999605	747 751 781 777
442	2	30.8999605	717 721 751 747
448	2	30.8999605	667 691 721 717
438	2	30.8999605	657 641 691 687
436	2	30.8999605	627 631 641 657
436	2	30.8999605	597 601 631 627
432	2	30.8999605	567 571 601 597
430	2	30.8999605	537 541 571 567
428	2	30.8999605	507 511 541 537
426	2	30.8999605	477 481 511 507
424	2	30.8999605	447 451 481 477
422	2	30.8999605	417 421 451 447
445	1	30.8999605	754 784 1101 1131
446	1	30.8999605	424 454 851 801
447	1	30.8999605	494 484 821 831
448	1	30.8999605	724 754 1131 1101

649	1	30.899605	0.00000000E+00	484	894	899	861
650	1	30.899605	0.00000000E+00	604	724	1101	1071
651	1	30.899608	0.00000000E+00	514	544	921	891
652	1	30.899605	0.00000000E+00	514	574	951	921

ELEM	FACE	VALUE (B)	FACE MODES
631	1	30.899608	0.00000000E+00
634	1	30.899605	0.00000000E+00
639	1	30.899608	0.00000000E+00
636	1	30.899605	0.00000000E+00
637	1	30.899608	0.00000000E+00
638	1	30.899605	0.00000000E+00
639	1	30.899608	0.00000000E+00
640	1	30.899605	0.00000000E+00
641	1	30.899608	0.00000000E+00
642	1	30.899605	0.00000000E+00
643	1	30.899605	0.00000000E+00
644	1	30.899605	0.00000000E+00
645	1	30.899608	0.00000000E+00
646	1	30.899605	0.00000000E+00
647	1	30.899605	0.00000000E+00
648	1	30.899605	0.00000000E+00
649	1	30.899605	0.00000000E+00
648	1	30.899605	0.00000000E+00
647	1	30.899605	0.00000000E+00
646	1	30.899605	0.00000000E+00
645	1	30.899605	0.00000000E+00
644	1	30.899605	0.00000000E+00
643	1	30.899605	0.00000000E+00
642	1	30.899605	0.00000000E+00
641	1	30.899605	0.00000000E+00
640	1	30.899605	0.00000000E+00
639	1	30.899605	0.00000000E+00
638	1	30.899605	0.00000000E+00
637	1	30.899605	0.00000000E+00
636	1	30.899605	0.00000000E+00
635	1	30.899605	0.00000000E+00
634	1	30.899605	0.00000000E+00
633	1	30.899605	0.00000000E+00
632	1	30.899605	0.00000000E+00
631	1	30.899605	0.00000000E+00

ELEM	FACE	VALUE (B)	FACE MODES
473	1	30.899605	0.00000000E+00
474	1	30.899605	0.00000000E+00
475	1	30.899605	0.00000000E+00
476	1	30.899605	0.00000000E+00
477	1	30.899605	0.00000000E+00
478	1	30.899605	0.00000000E+00
479	1	30.899605	0.00000000E+00
480	1	30.899605	0.00000000E+00
481	1	30.899608	0.00000000E+00
482	1	30.899605	0.00000000E+00
483	1	30.899605	0.00000000E+00
484	1	30.899605	0.00000000E+00
485	1	30.899605	0.00000000E+00
486	1	30.899605	0.00000000E+00
487	1	30.899605	0.00000000E+00
488	1	30.899605	0.00000000E+00
489	1	30.899608	0.00000000E+00
490	1	30.899605	0.00000000E+00
491	1	30.899605	0.00000000E+00
492	1	30.899605	0.00000000E+00

ELEM	FACE	VALUE (B)	FACE MODES
493	1	30.899605	0.00000000E+00
494	1	30.899605	0.00000000E+00
495	1	30.899605	0.00000000E+00
496	1	30.899605	0.00000000E+00
497	1	30.899605	0.00000000E+00
498	1	30.899605	0.00000000E+00
499	1	30.899605	0.00000000E+00
500	1	30.899605	0.00000000E+00
501	1	30.899605	0.00000000E+00
502	1	30.899605	0.00000000E+00
503	1	30.899605	0.00000000E+00
504	1	30.899605	0.00000000E+00
505	1	30.899605	0.00000000E+00
506	1	30.899605	0.00000000E+00
507	1	30.899605	0.00000000E+00
508	1	30.899605	0.00000000E+00
509	1	30.899605	0.00000000E+00
510	1	30.899605	0.00000000E+00
511	1	30.899605	0.00000000E+00
512	1	30.899605	0.00000000E+00

ELEM	FACE	VALUE (B)	FACE MODES
513	1	30.899605	0.00000000E+00
514	1	30.899605	0.00000000E+00

515	1	30.8999605	0.00000000E+00	1072	1102	1103	1073
516	1	30.8999605	0.00000000E+00	1071	1101	1102	1072
517	1	30.8999605	0.00000000E+00	1106	1136	1137	1107
518	1	30.8999605	0.00000000E+00	1105	1135	1136	1106
519	1	30.8999605	0.00000000E+00	1104	1134	1135	1105
520	1	30.8999605	0.00000000E+00	1103	1133	1134	1104
521	1	30.8999605	0.00000000E+00	1102	1132	1133	1103
522	1	30.8999605	0.00000000E+00	1101	1131	1132	1102
523	1	30.8999607	0.00000000E+00	1136	1166	1167	1137
524	1	30.8999605	0.00000000E+00	1135	1165	1166	1136
525	1	30.8999605	0.00000000E+00	1134	1164	1165	1135
526	1	30.8999605	0.00000000E+00	1133	1163	1164	1134
527	1	30.8999605	0.00000000E+00	1132	1162	1163	1133
528	1	30.8999605	0.00000000E+00	1131	1161	1162	1132
802	1	30.8999605	0.00000000E+00	1167	1197	818	818
891	1	30.8999605	0.00000000E+00	1117	1147	818	818
890	1	30.8999605	0.00000000E+00	1087	1117	818	818
799	1	30.8999605	0.00000000E+00	1057	1087	818	818

ELEM	FACE	VALUE(%)	FACE NODES				
796	1	30.8999605	0.00000000E+00	1027	1057	818	818
797	1	30.8999605	0.00000000E+00	997	1027	818	818
796	1	30.8999605	0.00000000E+00	967	997	818	818
795	1	30.8999605	0.00000000E+00	937	967	818	818
794	1	30.8999605	0.00000000E+00	907	937	818	818
793	1	30.8999605	0.00000000E+00	877	907	818	818
792	1	30.8999605	0.00000000E+00	847	877	818	818
791	1	30.8999605	0.00000000E+00	817	847	818	818
790	1	30.8999605	0.00000000E+00	1146	1176	1177	1147
789	1	30.8999605	0.00000000E+00	1145	1175	1176	1146
788	1	30.8999605	0.00000000E+00	1144	1174	1175	1145
787	1	30.8999605	0.00000000E+00	1143	1173	1174	1144
786	1	30.8999605	0.00000000E+00	1142	1172	1173	1143
785	1	30.8999605	0.00000000E+00	1141	1171	1172	1142
784	1	30.8999605	0.00000000E+00	1140	1170	1171	1141
783	1	30.8999605	0.00000000E+00	1139	1169	1170	1140
782	1	30.8999605	0.00000000E+00	1138	1168	1169	1139
781	1	30.8999605	0.00000000E+00	1137	1167	1168	1138
780	1	30.8999605	0.00000000E+00	1116	1146	1147	1117
779	1	30.8999605	0.00000000E+00	1115	1145	1146	1116

ELEM	FACE	VALUE(%)	FACE NODES				
778	1	30.8999605	0.00000000E+00	1114	1144	1145	1115
777	1	30.8999605	0.00000000E+00	1113	1143	1144	1114
776	1	30.8999605	0.00000000E+00	1112	1142	1143	1113
775	1	30.8999605	0.00000000E+00	1111	1141	1142	1112
774	1	30.8999605	0.00000000E+00	1110	1140	1141	1111
773	1	30.8999605	0.00000000E+00	1109	1139	1140	1110
772	1	30.8999605	0.00000000E+00	1108	1138	1139	1109
771	1	30.8999605	0.00000000E+00	1107	1137	1138	1108
770	1	30.8999605	0.00000000E+00	1086	1116	1117	1087
769	1	30.8999605	0.00000000E+00	1085	1115	1116	1086
768	1	30.8999605	0.00000000E+00	1084	1114	1115	1085
767	1	30.8999605	0.00000000E+00	1083	1113	1114	1084
766	1	30.8999605	0.00000000E+00	1082	1112	1113	1083
765	1	30.8999605	0.00000000E+00	1081	1111	1112	1082
764	1	30.8999605	0.00000000E+00	1080	1110	1111	1081
763	1	30.8999605	0.00000000E+00	1079	1109	1110	1080
762	1	30.8999605	0.00000000E+00	1078	1108	1109	1079
761	1	30.8999605	0.00000000E+00	1077	1107	1108	1078
760	1	30.8999605	0.00000000E+00	1056	1086	1087	1057
759	1	30.8999605	0.00000000E+00	1055	1085	1086	1056

ELEM	FACE	VALUE(%)	FACE NODES				
758	1	30.8999605	0.00000000E+00	1054	1084	1085	1055
757	1	30.8999605	0.00000000E+00	1023	1053	1054	1024
756	1	30.8999605	0.00000000E+00	1022	1052	1053	1023
755	1	30.8999605	0.00000000E+00	1051	1081	1082	1052
754	1	30.8999605	0.00000000E+00	1050	1080	1081	1051
753	1	30.8999605	0.00000000E+00	1049	1079	1080	1050
752	1	30.8999605	0.00000000E+00	1048	1078	1079	1049
751	1	30.8999605	0.00000000E+00	1047	1077	1078	1048
750	1	30.8999605	0.00000000E+00	1026	1056	1057	1027
749	1	30.8999605	0.00000000E+00	1025	1055	1056	1026

748	1	30.8996481	0.00000000E+00	1824	1854	1855	1825
747	1	30.8996482	0.00000000E+00	1823	1853	1854	1824
746	1	30.8996483	0.00000000E+00	1822	1852	1853	1823
745	1	30.8996485	0.00000000E+00	1821	1851	1852	1822
744	1	30.8996481	0.00000000E+00	1820	1850	1851	1821
743	1	30.8996485	0.00000000E+00	1819	1849	1850	1820
742	1	30.8996481	0.00000000E+00	1818	1848	1849	1819
741	1	30.8996485	0.00000000E+00	1817	1847	1848	1818
740	1	30.8996481	0.00000000E+00	996	1826	1827	997
739	1	30.8996485	0.00000000E+00	995	1825	1826	996

ELEM	FACE	VALUE (I)	FACE NUMBER
738	1	30.8996481	994 1824 1825 995
737	1	30.8996485	993 1823 1824 994
736	1	30.8996484	992 1822 1823 993
735	1	30.8996485	991 1821 1822 992
734	1	30.8996408	990 1820 1821 991
733	1	30.8996408	989 1819 1820 990
732	1	30.8996405	988 1818 1819 989
731	1	30.8996408	987 1817 1818 988
730	1	30.8996405	986 996 997 987
729	1	30.8996405	985 995 996 986
728	1	30.8996405	984 994 995 985
727	1	30.8996408	983 993 994 984
726	1	30.8996405	982 992 993 983
725	1	30.8996405	981 991 992 982
724	1	30.8996405	980 990 991 981
723	1	30.8996409	999 989 990 980
722	1	30.8996405	998 988 989 979
721	1	30.8996407	997 987 988 978
720	1	30.8996405	996 986 987 977
719	1	30.8996405	995 985 986 984

ELEM	FACE	VALUE (I)	FACE NUMBER
718	1	30.8996405	994 964 965 935
717	1	30.8996408	993 963 964 934
716	1	30.8996405	992 962 963 933
715	1	30.8996405	991 961 962 932
714	1	30.8996405	990 960 961 931
713	1	30.8996405	929 959 960 930
712	1	30.8996485	928 958 959 929
711	1	30.8996405	927 957 958 928
710	1	30.8996485	926 956 957 987
709	1	30.8996485	925 955 956 986
708	1	30.8996485	924 954 955 988
707	1	30.8996485	923 953 954 984
706	1	30.8996485	922 952 953 983
705	1	30.8996485	921 951 952 982
704	1	30.8996485	920 950 951 981
703	1	30.8996485	899 929 950 980
702	1	30.8996488	898 928 929 899
701	1	30.8996484	897 927 928 898
700	1	30.8996488	876 906 987 877
699	1	30.8996485	875 905 986 876

ELEM	FACE	VALUE (I)	FACE NUMBER
698	1	30.8996485	874 904 985 875
697	1	30.8996485	873 903 984 874
696	1	30.8996485	872 902 983 873
695	1	30.8996481	871 901 982 872
694	1	30.8996485	870 900 981 871
693	1	30.8996481	869 899 980 870
692	1	30.8996485	868 898 899 869
691	1	30.8996481	867 897 898 868
690	1	30.8996485	866 896 897 867
689	1	30.8996481	843 873 874 844
688	1	30.8996485	844 874 875 843
687	1	30.8996481	843 873 874 844
686	1	30.8996485	842 872 873 843
685	1	30.8996485	841 871 872 842
684	1	30.8996481	840 870 871 841
683	1	30.8996485	839 869 870 840
682	1	30.8996481	838 868 869 839
681	1	30.8996481	817 867 868 838

680	1	30.8999605	0.00000000E+00	818	846	867	817
679	1	30.8999608	0.00000000E+00	875	865	846	816
ELMN	FACE	VALUE(S)		FACE	MODE		
678	1	30.8999605	0.00000000E+00	814	846	845	815
677	1	30.8999608	0.00000000E+00	873	843	844	814
676	1	30.8999605	0.00000000E+00	812	842	843	813
675	1	30.8999608	0.00000000E+00	871	841	842	812
674	1	30.8999605	0.00000000E+00	870	840	841	811
673	1	30.8999607	0.00000000E+00	869	839	840	810
672	1	30.8999605	0.00000000E+00	868	838	839	809
671	1	30.8999605	0.00000000E+00	907	837	838	808
1	2	30.8999605	0.00000000E+00	841	831	832	807
2	2	30.8999605	0.00000000E+00	894	831	832	806
3	2	30.8999605	0.00000000E+00	852	821	821	805
4	2	30.8999605	0.00000000E+00	896	821	821	807
5	2	30.8999605	0.00000000E+00	831	822	822	804
6	2	30.8999605	0.00000000E+00	851	822	822	804
7	2	30.8999605	0.00000000E+00	881	822	822	811
8	2	30.8999605	0.00000000E+00	211	822	822	841
9	2	30.8999605	0.00000000E+00	853	81	121	392
10	2	30.8999605	0.00000000E+00	81	82	122	121
11	2	30.8999605	0.00000000E+00	307	241	271	390
12	2	30.8999605	0.00000000E+00	241	242	272	271
ELMN	FACE	VALUE(S)		FACE	MODE		
13	2	30.8999605	0.00000000E+00	92	83	123	122
14	2	30.8999607	0.00000000E+00	122	123	153	152
15	2	30.8999605	0.00000000E+00	153	153	183	182
16	2	30.8999605	0.00000000E+00	182	183	213	212
17	2	30.8999605	0.00000000E+00	212	213	243	242
18	2	30.8999605	0.00000000E+00	242	243	273	272
19	2	30.8999605	0.00000000E+00	294	41	91	393
20	2	30.8999605	0.00000000E+00	41	42	92	91
21	2	30.8999605	0.00000000E+00	62	63	93	92
22	2	30.8999605	0.00000000E+00	396	271	301	390
23	2	30.8999605	0.00000000E+00	271	272	302	301
24	2	30.8999605	0.00000000E+00	272	273	303	302
49	2	30.8999605	0.00000000E+00	395	31	61	394
50	2	30.8999605	0.00000000E+00	31	32	62	61
51	2	30.8999605	0.00000000E+00	32	33	63	62
52	2	30.8999605	0.00000000E+00	309	381	351	400
53	2	30.8999605	0.00000000E+00	381	382	332	331
54	2	30.8999605	0.00000000E+00	382	383	333	332
134	2	30.8999605	0.00000000E+00	395	1	31	31
132	2	30.8999605	0.00000000E+00	1	2	32	31
ELMN	FACE	VALUE(S)		FACE	MODE		
133	2	30.8999605	0.00000000E+00	2	3	33	32
134	2	30.8999605	0.00000000E+00	480	331	341	341
135	2	30.8999605	0.00000000E+00	331	332	342	341
136	2	30.8999605	0.00000000E+00	332	333	343	342
61	4	30.8999605	0.00000000E+00	38	63	73	68
62	4	30.8999605	0.00000000E+00	68	73	103	98
63	4	30.8999605	0.00000000E+00	98	103	133	128
64	4	30.8999605	0.00000000E+00	128	133	163	158
65	4	30.8999605	0.00000000E+00	158	163	193	188
66	4	30.8999605	0.00000000E+00	188	193	223	218
67	4	30.8999605	0.00000000E+00	218	223	253	248
68	4	30.8999605	0.00000000E+00	248	253	283	278
69	4	30.8999605	0.00000000E+00	278	283	313	308
70	4	30.8999605	0.00000000E+00	308	313	343	338
71	4	30.8999605	0.00000000E+00	43	49	79	72
72	4	30.8999605	0.00000000E+00	73	79	109	103
73	4	30.8999605	0.00000000E+00	103	109	139	133
74	4	30.8999605	0.00000000E+00	133	139	169	163
75	4	30.8999605	0.00000000E+00	163	169	199	193
76	4	30.8999605	0.00000000E+00	193	199	229	223
ELMN	FACE	VALUE(S)		FACE	MODE		
77	4	30.8999605	0.00000000E+00	223	229	259	253
78	4	30.8999605	0.00000000E+00	253	259	289	283
79	4	30.8999605	0.00000000E+00	283	289	319	313
80	4	30.8999605	0.00000000E+00	313	319	349	343

139	4	30.8996482	0.00000000E+00	343	349	379	373
140	4	30.8996485	0.00000000E+00	336	343	373	340
140	4	30.8996482	0.00000000E+00	18	19	49	43
149	4	30.8996485	0.00000000E+00	8	13	43	36
71	3	30.8996408	0.00000000E+00	49	48	76	70
72	3	30.8996405	0.00000000E+00	79	78	108	109
73	3	30.8996405	0.00000000E+00	109	108	138	139
74	3	30.8996405	0.00000000E+00	139	138	168	169
75	3	30.8996405	0.00000000E+00	169	168	198	199
76	3	30.8996405	0.00000000E+00	199	198	228	229
77	3	30.8996402	0.00000000E+00	229	228	258	259
78	3	30.8996405	0.00000000E+00	259	258	288	289
79	3	30.8996405	0.00000000E+00	289	288	318	319
80	3	30.8996408	0.00000000E+00	319	318	348	349
443	3	30.8996405	0.00000000E+00	731	733	762	761
442	3	30.8996405	0.00000000E+00	721	722	752	751

ELEM	FACE	VALUE(I)	FACE NODES
440	3	30.8996405	691 692 722 721
440	5	30.8996405	661 662 691 691
434	3	30.8996405	631 632 662 661
434	5	30.8996405	601 602 631 631
433	3	30.8996408	571 572 602 601
430	3	30.8996405	541 542 572 571
428	3	30.8996405	511 512 542 541
426	3	30.8996405	481 482 512 511
139	3	30.8996402	349 348 378 379
62	5	30.8996485	651 652 682 681
148	3	30.8996481	19 18 48 49
422	5	30.8996485	421 422 452 451
318	5	30.8996481	489 413 443 439
318	3	30.8996485	439 443 473 469
321	5	30.8996481	469 473 503 499
324	3	30.8996425	499 503 533 529
327	5	30.8996425	529 533 563 559
330	3	30.8996425	559 563 593 589
333	5	30.8996425	589 593 623 619
336	5	30.8996425	619 623 653 649

ELEM	FACE	VALUE(I)	FACE NODES
339	3	30.8996405	649 653 683 679
342	3	30.8996489	679 683 713 709
347	5	30.8996485	709 713 743 739
346	3	30.8996482	739 743 773 769
321	3	30.8996482	611 617 647 643
356	3	30.8996485	643 647 677 673
357	3	30.8996485	673 677 707 703
340	3	30.8996485	583 587 617 613
343	3	30.8996485	613 617 647 643
346	3	30.8996485	643 647 677 673
369	3	30.8996485	677 681 711 707
372	3	30.8996485	707 711 741 737
375	3	30.8996485	737 741 771 767
378	3	30.8996485	767 771 801 797
383	3	30.8996485	797 801 831 827
384	3	30.8996485	827 831 861 857
289	3	30.8999908	601 605 635 631
298	3	30.8999908	631 635 665 661
291	3	30.8999908	665 669 699 695
292	3	30.8999908	695 699 729 725

ELEM	FACE	VALUE(I)	FACE NODES
293	3	30.8999908	725 729 759 755
294	3	30.8999908	755 759 789 785
295	3	30.8999908	785 789 815 811
297	3	30.8999908	815 819 845 841
298	3	30.8999908	845 849 875 871
299	3	30.8999908	871 875 901 897
300	3	30.8999908	901 905 931 927
301	3	30.8999908	927 931 957 953
302	3	30.8999908	953 957 983 979
303	3	30.8999908	979 983 1005 1001
304	3	30.8999908	1001 1005 1031 1027

305	5	30.8999908	0.08000008E+00	641	645	675	671
306	5	30.8999908	0.08000008E+00	645	649	679	675
307	5	30.8999908	0.08000008E+00	671	675	701	701
308	5	30.8999908	0.08000008E+00	675	679	709	706
309	5	30.8999908	0.08000008E+00	701	705	735	731
310	5	30.8999908	0.08000008E+00	731	735	765	761
311	5	30.8999908	0.08000008E+00	765	769	739	735
312	5	30.8999908	0.08000008E+00	735	739	769	765
ELEM	FACE	VALUE(S)		FACE NODES			
81	1	30.8999908	0.08000008E+00	370	377	347	348
82	3	30.8999908	0.08000008E+00	280	287	317	318
83	1	30.8999908	0.08000008E+00	250	257	287	288
84	3	30.8999908	0.08000008E+00	220	227	257	258
85	1	30.8999908	0.08000008E+00	190	197	227	228
86	3	30.8999908	0.08000008E+00	160	167	197	198
87	1	30.8999908	0.08000008E+00	130	137	167	168
88	3	30.8999908	0.08000008E+00	100	107	137	138
89	1	30.8999908	0.08000008E+00	70	77	107	108
90	3	30.8999908	0.08000008E+00	40	47	77	78
91	1	30.8999908	0.08000008E+00	47	46	76	77
92	3	30.8999908	0.08000008E+00	77	76	106	107
93	1	30.8999908	0.08000008E+00	107	106	136	137
94	3	30.8999908	0.08000008E+00	137	136	166	167
95	1	30.8999908	0.08000008E+00	167	166	196	197
96	3	30.8999908	0.08000008E+00	197	196	226	227
97	1	30.8999908	0.08000008E+00	227	226	256	257
98	3	30.8999908	0.08000008E+00	257	256	286	287
99	1	30.8999908	0.08000008E+00	287	286	316	317
100	3	30.8999908	0.08000008E+00	317	316	346	347
ELEM	FACE	VALUE(S)		FACE NODES			
142	1	30.8999908	0.08000008E+00	346	347	377	378
143	3	30.8999908	0.08000008E+00	347	344	376	377
151	1	30.8999908	0.08000008E+00	18	17	47	48
152	3	30.8999908	0.08000008E+00	17	14	44	47

LIST ELEMENT CONVECTIONS FOR ALL SELECTED ELEMENTS

LIST TEMPERATURES FOR ALL SELECTED NODES

NODE	TEMPERATURE	FLUXDCE
1	204.84	0.00000E+00
2	210.48	0.00000E+00
3	214.11	0.00000E+00
4	214.11	0.00000E+00
5	214.11	0.00000E+00
7	214.11	0.00000E+00
8	214.11	0.00000E+00
9	220.42	0.00000E+00
10	220.42	0.00000E+00
11	220.42	0.00000E+00
12	220.42	0.00000E+00
13	220.42	0.00000E+00
14	220.42	0.00000E+00
15	220.42	0.00000E+00
16	220.42	0.00000E+00
17	220.42	0.00000E+00
18	220.42	0.00000E+00
19	220.42	0.00000E+00
20	220.42	0.00000E+00
21	220.42	0.00000E+00
NODE	TEMPERATURE	FLUXDCE
22	220.42	0.00000E+00
23	220.42	0.00000E+00
24	220.42	0.00000E+00
25	220.42	0.00000E+00
26	220.42	0.00000E+00
27	220.42	0.00000E+00
28	220.42	0.00000E+00
31	204.56	0.00000E+00
32	209.50	0.00000E+00
33	212.44	0.00000E+00

34	212.44	0.00000E+00
35	212.44	0.00000E+00
37	212.44	0.00000E+00
38	212.44	0.00000E+00
39	219.57	0.00000E+00
40	219.57	0.00000E+00
41	219.57	0.00000E+00
42	219.57	0.00000E+00
43	219.57	0.00000E+00
44	219.57	0.00000E+00

NODE	TEMPERATURE	FLUXENCE
45	219.57	0.00000E+00
46	219.57	0.00000E+00
47	219.57	0.00000E+00
48	219.57	0.00000E+00
49	219.57	0.00000E+00
50	219.57	0.00000E+00
51	219.57	0.00000E+00
52	219.57	0.00000E+00
53	219.57	0.00000E+00
54	219.57	0.00000E+00
55	219.57	0.00000E+00
56	219.57	0.00000E+00
57	219.57	0.00000E+00
58	219.57	0.00000E+00
61	210.77	0.00000E+00
62	210.77	0.00000E+00
63	210.77	0.00000E+00
64	210.77	0.00000E+00
65	210.77	0.00000E+00
67	210.77	0.00000E+00

NODE	TEMPERATURE	FLUXENCE
68	218.71	0.00000E+00
69	218.71	0.00000E+00
70	218.71	0.00000E+00
71	218.71	0.00000E+00
72	218.71	0.00000E+00
73	218.71	0.00000E+00
74	218.71	0.00000E+00
75	218.71	0.00000E+00
76	218.71	0.00000E+00
77	218.71	0.00000E+00
78	218.71	0.00000E+00
79	218.71	0.00000E+00
80	218.71	0.00000E+00
81	218.71	0.00000E+00
82	218.71	0.00000E+00
83	218.71	0.00000E+00
84	218.71	0.00000E+00
85	218.71	0.00000E+00
86	218.71	0.00000E+00
87	218.71	0.00000E+00

NODE	TEMPERATURE	FLUXENCE
88	217.85	0.00000E+00
91	209.90	0.00000E+00
92	207.95	0.00000E+00
93	209.90	0.00000E+00
94	209.90	0.00000E+00
95	209.90	0.00000E+00
96	209.90	0.00000E+00
97	209.90	0.00000E+00
98	217.85	0.00000E+00
99	217.85	0.00000E+00
100	217.85	0.00000E+00
101	217.85	0.00000E+00
102	217.85	0.00000E+00
103	217.85	0.00000E+00
104	217.85	0.00000E+00
105	217.85	0.00000E+00
106	217.85	0.00000E+00
107	217.85	0.00000E+00
108	217.85	0.00000E+00

109	217.85	0.00098E+00
110	217.85	0.00098E+00

NODE	TEMPERATURE	FLUXDNC
111	217.85	0.00098E+00
112	217.86	0.00098E+00
113	217.85	0.00098E+00
114	217.85	0.00098E+00
115	217.85	0.00098E+00
116	217.85	0.00098E+00
117	217.85	0.00098E+00
118	217.85	0.00098E+00
121	205.95	0.00098E+00
122	207.49	0.00098E+00
123	209.04	0.00098E+00
124	209.04	0.00098E+00
125	209.04	0.00098E+00
127	209.04	0.00098E+00
128	209.04	0.00098E+00
129	217.81	0.00098E+00
130	217.81	0.00098E+00
131	217.81	0.00098E+00
132	217.81	0.00098E+00
133	217.81	0.00098E+00

NODE	TEMPERATURE	FLUXDNC
134	217.81	0.00098E+00
135	217.81	0.00098E+00
136	217.81	0.00098E+00
137	217.81	0.00098E+00
138	217.81	0.00098E+00
139	217.81	0.00098E+00
140	217.81	0.00098E+00
141	217.81	0.00098E+00
142	217.81	0.00098E+00
143	217.81	0.00098E+00
144	217.81	0.00098E+00
145	217.81	0.00098E+00
146	217.81	0.00098E+00
147	217.81	0.00098E+00
148	217.81	0.00098E+00
151	205.91	0.00098E+00
152	207.44	0.00098E+00
153	208.98	0.00098E+00
154	208.98	0.00098E+00
155	208.98	0.00098E+00

NODE	TEMPERATURE	FLUXDNC
157	208.98	0.00098E+00
158	208.98	0.00098E+00
159	217.76	0.00098E+00
160	217.76	0.00098E+00
161	217.76	0.00098E+00
162	217.76	0.00098E+00
163	217.76	0.00098E+00
164	217.76	0.00098E+00
165	217.76	0.00098E+00
166	217.76	0.00098E+00
167	217.76	0.00098E+00
168	217.76	0.00098E+00
169	217.76	0.00098E+00
170	217.76	0.00098E+00
171	217.76	0.00098E+00
172	217.76	0.00098E+00
173	217.76	0.00098E+00
174	217.76	0.00098E+00
175	217.76	0.00098E+00
176	217.76	0.00098E+00

NODE	TEMPERATURE	FLUXDNC
177	217.75	0.00098E+00
178	217.75	0.00098E+00
181	205.96	0.00098E+00
182	207.19	0.00098E+00

183	266.92	0.00000E+00
184	266.92	0.00000E+00
185	266.92	0.00000E+00
187	266.92	0.00000E+00
186	266.92	0.00000E+00
189	217.72	0.00000E+00
190	217.72	0.00000E+00
191	217.72	0.00000E+00
192	217.72	0.00000E+00
193	217.72	0.00000E+00
194	217.72	0.00000E+00
195	217.72	0.00000E+00
196	217.72	0.00000E+00
197	217.72	0.00000E+00
198	217.72	0.00000E+00
199	217.72	0.00000E+00

NODE	TEMPERATURE	FLUENCE
200	217.72	0.00000E+00
201	217.72	0.00000E+00
202	217.72	0.00000E+00
203	217.72	0.00000E+00
204	217.72	0.00000E+00
205	217.72	0.00000E+00
206	217.72	0.00000E+00
207	217.72	0.00000E+00
208	217.72	0.00000E+00
211	205.82	0.00000E+00
212	207.34	0.00000E+00
213	208.87	0.00000E+00
214	208.87	0.00000E+00
215	208.87	0.00000E+00
217	208.87	0.00000E+00
218	208.87	0.00000E+00
219	217.67	0.00000E+00
220	217.67	0.00000E+00
221	217.67	0.00000E+00
222	217.67	0.00000E+00

NODE	TEMPERATURE	FLUENCE
223	217.67	0.00000E+00
224	217.67	0.00000E+00
225	217.67	0.00000E+00
226	217.67	0.00000E+00
227	217.67	0.00000E+00
228	217.67	0.00000E+00
229	217.67	0.00000E+00
230	217.67	0.00000E+00
231	217.67	0.00000E+00
232	217.67	0.00000E+00
233	217.67	0.00000E+00
234	217.67	0.00000E+00
235	217.67	0.00000E+00
236	217.67	0.00000E+00
237	217.67	0.00000E+00
238	217.67	0.00000E+00
241	205.81	0.00000E+00
242	207.33	0.00000E+00
243	208.85	0.00000E+00
244	208.86	0.00000E+00

NODE	TEMPERATURE	FLUENCE
245	208.86	0.00000E+00
247	208.86	0.00000E+00
248	208.86	0.00000E+00
249	217.67	0.00000E+00
250	217.67	0.00000E+00
251	217.67	0.00000E+00
252	217.67	0.00000E+00
253	217.67	0.00000E+00
254	217.67	0.00000E+00
255	217.67	0.00000E+00
256	217.67	0.00000E+00
257	217.67	0.00000E+00

288	217.67	0.00000E+00
289	217.67	0.00000E+00
290	217.67	0.00000E+00
291	217.67	0.00000E+00
292	217.67	0.00000E+00
293	217.67	0.00000E+00
294	217.67	0.00000E+00
295	217.67	0.00000E+00

MODE	TEMPERATURE	FLUENCE
296	217.67	0.00000E+00
297	217.67	0.00000E+00
298	217.67	0.00000E+00
299	209.81	0.00000E+00
300	207.32	0.00000E+00
301	208.86	0.00000E+00
302	208.86	0.00000E+00
303	208.86	0.00000E+00
304	208.86	0.00000E+00
305	208.86	0.00000E+00
306	208.86	0.00000E+00
307	208.86	0.00000E+00
308	208.86	0.00000E+00
309	217.67	0.00000E+00
310	217.67	0.00000E+00
311	217.67	0.00000E+00

MODE	TEMPERATURE	FLUENCE
312	217.67	0.00000E+00
313	217.67	0.00000E+00
314	217.67	0.00000E+00
315	217.67	0.00000E+00
316	217.67	0.00000E+00
317	217.67	0.00000E+00
318	217.67	0.00000E+00
319	217.67	0.00000E+00
320	217.67	0.00000E+00
321	217.67	0.00000E+00
322	217.67	0.00000E+00
323	217.67	0.00000E+00
324	217.67	0.00000E+00
325	217.67	0.00000E+00
326	217.67	0.00000E+00
327	217.67	0.00000E+00
328	217.67	0.00000E+00
329	209.79	0.00000E+00
330	207.31	0.00000E+00
331	208.83	0.00000E+00

MODE	TEMPERATURE	FLUENCE
332	217.67	0.00000E+00
333	217.67	0.00000E+00
334	217.67	0.00000E+00
335	217.67	0.00000E+00
336	217.67	0.00000E+00
337	217.67	0.00000E+00
338	217.67	0.00000E+00
339	217.67	0.00000E+00
340	217.67	0.00000E+00
341	217.67	0.00000E+00
342	217.67	0.00000E+00
343	217.67	0.00000E+00
344	217.67	0.00000E+00
345	217.67	0.00000E+00
346	217.67	0.00000E+00
347	217.67	0.00000E+00
348	217.67	0.00000E+00
349	217.67	0.00000E+00
350	217.67	0.00000E+00
351	217.67	0.00000E+00
352	217.67	0.00000E+00
353	217.67	0.00000E+00
354	217.67	0.00000E+00
355	208.83	0.00000E+00

NODE	TEMPERATURE	FLUXW
354	208.83	0.0000E+00
355	208.83	0.0000E+00
357	208.83	0.0000E+00
390	208.83	0.0000E+00
399	217.67	0.0000E+00
348	217.67	0.0000E+00
341	217.67	0.0000E+00
342	217.67	0.0000E+00
343	217.67	0.0000E+00
344	217.67	0.0000E+00
345	217.67	0.0000E+00
346	217.67	0.0000E+00
347	217.67	0.0000E+00
348	217.67	0.0000E+00
349	217.67	0.0000E+00
398	217.67	0.0000E+00
351	217.67	0.0000E+00
392	217.67	0.0000E+00
353	217.67	0.0000E+00
354	217.67	0.0000E+00

NODE	TEMPERATURE	FLUXW
355	217.67	0.0000E+00
356	217.67	0.0000E+00
357	217.67	0.0000E+00
358	217.67	0.0000E+00
341	202.79	0.0000E+00
342	207.30	0.0000E+00
343	208.82	0.0000E+00
344	208.82	0.0000E+00
345	208.82	0.0000E+00
347	208.82	0.0000E+00
348	208.82	0.0000E+00
349	217.67	0.0000E+00
378	217.67	0.0000E+00
371	217.67	0.0000E+00
372	217.67	0.0000E+00
373	217.67	0.0000E+00
374	217.67	0.0000E+00
375	217.67	0.0000E+00
376	217.67	0.0000E+00
377	217.67	0.0000E+00

NODE	TEMPERATURE	FLUXW
378	217.67	0.0000E+00
379	217.67	0.0000E+00
380	217.67	0.0000E+00
381	217.67	0.0000E+00
382	217.67	0.0000E+00
383	217.67	0.0000E+00
384	217.67	0.0000E+00
385	217.67	0.0000E+00
386	217.67	0.0000E+00
387	217.67	0.0000E+00
388	217.67	0.0000E+00
390	206.31	0.0000E+00
391	206.31	0.0000E+00
392	206.31	0.0000E+00
393	206.31	0.0000E+00
394	206.31	0.0000E+00
395	206.31	0.0000E+00
396	206.31	0.0000E+00
397	206.31	0.0000E+00
398	206.31	0.0000E+00

NODE	TEMPERATURE	FLUXW
399	206.31	0.0000E+00
400	206.31	0.0000E+00
401	251.76	0.0000E+00
402	251.76	0.0000E+00
403	251.76	0.0000E+00
404	251.76	0.0000E+00

405	251.74	0.00000E+00
406	251.70	0.00000E+00
407	251.74	0.00000E+00
408	251.70	0.00000E+00
409	251.70	0.00000E+00
410	251.74	0.00000E+00
411	251.70	0.00000E+00
412	251.74	0.00000E+00
413	251.70	0.00000E+00
414	251.74	0.00000E+00
415	251.70	0.00000E+00
416	251.74	0.00000E+00
417	251.70	0.00000E+00
418	251.74	0.00000E+00

NODE	TEMPERATURE	FLUXANCE
419	251.70	0.00000E+00
420	251.70	0.00000E+00
421	251.70	0.00000E+00
422	345.70	0.00000E+00
423	345.70	0.00000E+00
424	345.70	0.00000E+00
425	345.70	0.00000E+00
426	345.70	0.00000E+00
431	251.30	0.00000E+00
432	251.30	0.00000E+00
433	251.30	0.00000E+00
434	251.30	0.00000E+00
435	251.30	0.00000E+00
436	251.30	0.00000E+00
437	251.30	0.00000E+00
438	251.30	0.00000E+00
439	251.30	0.00000E+00
440	251.30	0.00000E+00
441	251.30	0.00000E+00
442	251.30	0.00000E+00

NODE	TEMPERATURE	FLUXANCE
443	251.30	0.00000E+00
444	251.30	0.00000E+00
445	251.30	0.00000E+00
446	251.30	0.00000E+00
447	251.30	0.00000E+00
448	251.30	0.00000E+00
449	251.30	0.00000E+00
450	251.30	0.00000E+00
451	251.30	0.00000E+00
452	346.61	0.00000E+00
453	346.61	0.00000E+00
454	346.61	0.00000E+00
455	346.61	0.00000E+00
456	346.61	0.00000E+00
461	250.84	0.00000E+00
462	250.84	0.00000E+00
463	250.84	0.00000E+00
464	250.84	0.00000E+00
465	250.84	0.00000E+00
466	250.84	0.00000E+00

NODE	TEMPERATURE	FLUXANCE
467	250.84	0.00000E+00
468	250.84	0.00000E+00
469	250.84	0.00000E+00
470	250.84	0.00000E+00
471	250.84	0.00000E+00
472	250.84	0.00000E+00
473	250.84	0.00000E+00
474	250.84	0.00000E+00
475	250.84	0.00000E+00
476	250.84	0.00000E+00
477	250.84	0.00000E+00
478	250.84	0.00000E+00
479	250.84	0.00000E+00
480	250.84	0.00000E+00

481	250.84	0.00000E+00
482	247.52	0.00000E+00
483	247.52	0.00000E+00
484	247.52	0.00000E+00
485	247.52	0.00000E+00
486	247.52	0.00000E+00

MODE	TEMPERATURE	FLUENCE
491	250.36	0.00000E+00
492	250.36	0.00000E+00
493	250.36	0.00000E+00
494	250.36	0.00000E+00
495	250.36	0.00000E+00
496	250.36	0.00000E+00
497	250.36	0.00000E+00
498	250.36	0.00000E+00
499	250.36	0.00000E+00
500	250.36	0.00000E+00
501	250.36	0.00000E+00
502	250.36	0.00000E+00
503	250.36	0.00000E+00
504	250.36	0.00000E+00
505	250.36	0.00000E+00
506	250.36	0.00000E+00
507	250.36	0.00000E+00
508	250.36	0.00000E+00
509	250.36	0.00000E+00
510	250.36	0.00000E+00

MODE	TEMPERATURE	FLUENCE
511	250.36	0.00000E+00
512	248.43	0.00000E+00
513	248.43	0.00000E+00
514	248.43	0.00000E+00
515	248.43	0.00000E+00
516	248.43	0.00000E+00
521	250.32	0.00000E+00
522	250.32	0.00000E+00
523	250.32	0.00000E+00
524	250.32	0.00000E+00
525	250.32	0.00000E+00
526	250.32	0.00000E+00
527	250.32	0.00000E+00
528	250.32	0.00000E+00
529	250.32	0.00000E+00
530	250.32	0.00000E+00
531	250.32	0.00000E+00
532	250.32	0.00000E+00
533	250.32	0.00000E+00
534	250.32	0.00000E+00

MODE	TEMPERATURE	FLUENCE
535	250.27	0.00000E+00
536	250.27	0.00000E+00
537	250.27	0.00000E+00
538	250.27	0.00000E+00
539	250.27	0.00000E+00
540	250.27	0.00000E+00
541	250.27	0.00000E+00
542	248.28	0.00000E+00
543	248.28	0.00000E+00
544	248.28	0.00000E+00
545	248.28	0.00000E+00
546	248.28	0.00000E+00
547	250.27	0.00000E+00
548	250.27	0.00000E+00
549	250.27	0.00000E+00
550	250.27	0.00000E+00
551	250.27	0.00000E+00
552	250.27	0.00000E+00
553	250.27	0.00000E+00
554	250.27	0.00000E+00
555	250.27	0.00000E+00
556	250.27	0.00000E+00
557	250.27	0.00000E+00
558	250.27	0.00000E+00

MODE	TEMPERATURE	FLUENCE
------	-------------	---------

537	250.27	0.00000E+00
540	250.27	0.00000E+00
541	250.27	0.00000E+00
542	250.27	0.00000E+00
543	250.27	0.00000E+00
544	250.27	0.00000E+00
565	250.27	0.00000E+00
566	250.27	0.00000E+00
567	250.27	0.00000E+00
568	250.27	0.00000E+00
569	250.27	0.00000E+00
570	250.27	0.00000E+00
571	250.27	0.00000E+00
572	348.13	0.00000E+00
573	348.13	0.00000E+00
574	348.13	0.00000E+00
575	348.13	0.00000E+00
576	348.13	0.00000E+00
581	250.21	0.00000E+00
582	250.21	0.00000E+00

NODE	TEMPERATURE	FLUENCE
583	250.21	0.00000E+00
584	250.21	0.00000E+00
585	250.21	0.00000E+00
586	250.21	0.00000E+00
587	250.21	0.00000E+00
588	250.21	0.00000E+00
589	250.21	0.00000E+00
590	250.21	0.00000E+00
591	250.21	0.00000E+00
592	250.21	0.00000E+00
593	250.21	0.00000E+00
594	250.21	0.00000E+00
595	250.21	0.00000E+00
596	250.21	0.00000E+00
597	250.21	0.00000E+00
598	250.21	0.00000E+00
599	250.21	0.00000E+00
600	250.21	0.00000E+00
601	250.21	0.00000E+00
602	347.98	0.00000E+00

NODE	TEMPERATURE	FLUENCE
603	347.98	0.00000E+00
604	347.98	0.00000E+00
605	347.98	0.00000E+00
606	347.98	0.00000E+00
611	250.15	0.00000E+00
612	250.15	0.00000E+00
613	250.15	0.00000E+00
614	250.15	0.00000E+00
615	250.15	0.00000E+00
616	250.15	0.00000E+00
617	250.15	0.00000E+00
618	250.15	0.00000E+00
619	250.15	0.00000E+00
620	250.15	0.00000E+00
621	250.15	0.00000E+00
622	250.15	0.00000E+00
623	250.15	0.00000E+00
624	250.15	0.00000E+00
625	250.15	0.00000E+00
626	250.15	0.00000E+00

NODE	TEMPERATURE	FLUENCE
627	250.15	0.00000E+00
628	250.15	0.00000E+00
629	250.15	0.00000E+00
630	250.15	0.00000E+00
631	250.15	0.00000E+00
632	347.83	0.00000E+00
633	347.83	0.00000E+00
634	347.83	0.00000E+00

435	347.83	0.0000E+00
436	347.83	0.0000E+00
441	250.16	0.0000E+00
442	250.16	0.0000E+00
443	250.16	0.0000E+00
444	250.16	0.0000E+00
445	250.16	0.0000E+00
446	250.16	0.0000E+00
447	250.16	0.0000E+00
448	250.16	0.0000E+00
449	250.16	0.0000E+00
450	250.16	0.0000E+00

MODE	TEMPERATURE	FLUENCE
451	250.16	0.0000E+00
452	250.16	0.0000E+00
453	250.16	0.0000E+00
454	250.16	0.0000E+00
455	250.16	0.0000E+00
456	250.16	0.0000E+00
457	250.16	0.0000E+00
458	250.16	0.0000E+00
459	250.16	0.0000E+00
460	250.16	0.0000E+00
461	250.16	0.0000E+00
462	347.88	0.0000E+00
463	347.88	0.0000E+00
464	347.88	0.0000E+00
465	347.88	0.0000E+00
466	347.88	0.0000E+00
471	250.17	0.0000E+00
472	250.17	0.0000E+00
473	250.17	0.0000E+00
474	250.17	0.0000E+00

MODE	TEMPERATURE	FLUENCE
475	250.17	0.0000E+00
476	250.17	0.0000E+00
477	250.17	0.0000E+00
478	250.17	0.0000E+00
479	250.17	0.0000E+00
480	250.17	0.0000E+00
481	250.17	0.0000E+00
482	250.17	0.0000E+00
483	250.17	0.0000E+00
484	250.17	0.0000E+00
485	250.17	0.0000E+00
486	250.17	0.0000E+00
487	250.17	0.0000E+00
488	250.17	0.0000E+00
489	250.17	0.0000E+00
490	250.17	0.0000E+00
491	250.17	0.0000E+00
492	347.93	0.0000E+00
493	347.93	0.0000E+00
494	347.93	0.0000E+00

MODE	TEMPERATURE	FLUENCE
495	347.93	0.0000E+00
496	347.93	0.0000E+00
501	250.19	0.0000E+00
502	250.19	0.0000E+00
503	250.19	0.0000E+00
504	250.19	0.0000E+00
505	250.19	0.0000E+00
506	250.19	0.0000E+00
507	250.19	0.0000E+00
508	250.19	0.0000E+00
509	250.19	0.0000E+00
510	250.19	0.0000E+00
511	250.19	0.0000E+00
512	250.19	0.0000E+00
513	250.19	0.0000E+00
514	250.19	0.0000E+00

715	258.19	0.00000E+00
716	258.19	0.00000E+00
717	258.19	0.00000E+00
718	258.19	0.00000E+00

NODE	TEMPERATURE	FLUENCE
719	250.19	0.00000E+00
720	250.19	0.00000E+00
721	250.19	0.00000E+00
722	347.96	0.00000E+00
723	347.96	0.00000E+00
724	347.96	0.00000E+00
725	347.96	0.00000E+00
726	347.96	0.00000E+00
731	258.29	0.00000E+00
732	258.29	0.00000E+00
733	258.29	0.00000E+00
734	258.29	0.00000E+00
735	258.29	0.00000E+00
736	258.29	0.00000E+00
737	258.29	0.00000E+00
738	258.29	0.00000E+00
739	258.29	0.00000E+00
740	258.29	0.00000E+00
741	258.29	0.00000E+00
742	258.29	0.00000E+00

NODE	TEMPERATURE	FLUENCE
743	250.20	0.00000E+00
744	250.20	0.00000E+00
745	250.20	0.00000E+00
746	250.20	0.00000E+00
747	250.20	0.00000E+00
748	258.20	0.00000E+00
749	258.20	0.00000E+00
750	258.20	0.00000E+00
751	258.20	0.00000E+00
752	348.00	0.00000E+00
753	348.00	0.00000E+00
754	348.00	0.00000E+00
755	348.00	0.00000E+00
756	348.00	0.00000E+00
757	258.21	0.00000E+00
758	258.21	0.00000E+00
759	258.21	0.00000E+00
760	258.21	0.00000E+00
761	258.21	0.00000E+00
762	258.21	0.00000E+00
763	258.21	0.00000E+00
764	258.21	0.00000E+00
765	258.21	0.00000E+00
766	258.21	0.00000E+00

NODE	TEMPERATURE	FLUENCE
767	258.21	0.00000E+00
768	258.21	0.00000E+00
769	258.21	0.00000E+00
770	258.21	0.00000E+00
771	258.21	0.00000E+00
772	258.21	0.00000E+00
773	258.21	0.00000E+00
774	258.21	0.00000E+00
775	258.21	0.00000E+00
776	258.21	0.00000E+00
777	258.21	0.00000E+00
778	258.21	0.00000E+00
779	258.21	0.00000E+00
780	258.21	0.00000E+00
781	258.21	0.00000E+00
782	348.89	0.00000E+00
783	348.89	0.00000E+00
784	348.89	0.00000E+00
785	348.89	0.00000E+00
786	348.89	0.00000E+00

NODE	TEMPERATURE	FLUENCE
801	439.65	0.00000E+00
802	471.63	0.00000E+00

803	703.68	0.00000E+00
804	734.41	0.00000E+00
805	765.22	0.00000E+00
806	795.95	0.00000E+00
807	812.97	0.00000E+00
808	812.97	0.00000E+00
809	992.32	0.00000E+00
810	992.32	0.00000E+00
811	992.32	0.00000E+00
812	992.32	0.00000E+00
813	992.32	0.00000E+00
814	992.32	0.00000E+00
815	997.75	0.00000E+00
816	997.75	0.00000E+00
817	997.75	0.00000E+00
818	997.75	0.00000E+00
821	441.92	0.00000E+00
832	573.06	0.00000E+00

NODE	TEMPERATURE	FLUENCE
833	704.20	0.00000E+00
834	725.61	0.00000E+00
835	747.01	0.00000E+00
836	794.43	0.00000E+00
837	813.31	0.00000E+00
838	813.31	0.00000E+00
839	992.26	0.00000E+00
840	992.26	0.00000E+00
841	992.26	0.00000E+00
842	992.26	0.00000E+00
843	992.26	0.00000E+00
844	992.26	0.00000E+00
845	997.43	0.00000E+00
846	997.43	0.00000E+00
847	997.43	0.00000E+00
848	444.20	0.00000E+00
849	574.50	0.00000E+00
853	704.81	0.00000E+00
864	736.80	0.00000E+00
865	768.80	0.00000E+00

NODE	TEMPERATURE	FLUENCE
866	794.94	0.00000E+00
867	813.64	0.00000E+00
868	813.64	0.00000E+00
869	992.70	0.00000E+00
870	992.70	0.00000E+00
871	992.70	0.00000E+00
872	992.70	0.00000E+00
873	992.70	0.00000E+00
874	992.70	0.00000E+00
875	997.15	0.00000E+00
876	997.15	0.00000E+00
877	997.15	0.00000E+00
891	446.47	0.00000E+00
892	575.96	0.00000E+00
893	705.41	0.00000E+00
894	738.00	0.00000E+00
895	770.59	0.00000E+00
896	793.44	0.00000E+00
897	813.95	0.00000E+00
898	813.95	0.00000E+00

NODE	TEMPERATURE	FLUENCE
899	992.13	0.00000E+00
900	992.13	0.00000E+00
901	992.13	0.00000E+00
902	992.13	0.00000E+00
903	992.13	0.00000E+00
904	992.13	0.00000E+00
905	994.82	0.00000E+00
906	996.85	0.00000E+00
907	996.85	0.00000E+00
921	446.23	0.00000E+00

922	879.34	0.00000E+00
923	704.49	0.00000E+00
924	735.34	0.00000E+00
925	766.26	0.00000E+00
926	776.21	0.00000E+00
927	816.60	0.00000E+00
928	816.60	0.00000E+00
929	963.26	0.00000E+00
930	963.26	0.00000E+00
931	963.26	0.00000E+00

NODE	TEMPERATURE	FLUX[CI]
932	963.26	0.00000E+00
933	963.26	0.00000E+00
934	963.26	0.00000E+00
935	991.51	0.00000E+00
936	991.51	0.00000E+00
937	991.51	0.00000E+00
951	445.99	0.00000E+00
952	574.78	0.00000E+00
953	763.57	0.00000E+00
954	752.72	0.00000E+00
955	761.88	0.00000E+00
956	796.97	0.00000E+00
957	818.82	0.00000E+00
958	818.82	0.00000E+00
959	974.43	0.00000E+00
960	974.43	0.00000E+00
961	974.43	0.00000E+00
962	974.43	0.00000E+00
963	974.43	0.00000E+00
964	974.43	0.00000E+00

NODE	TEMPERATURE	FLUX[CE]
965	986.16	0.00000E+00
966	986.16	0.00000E+00
967	986.16	0.00000E+00
981	445.74	0.00000E+00
982	574.20	0.00000E+00
983	703.65	0.00000E+00
984	730.09	0.00000E+00
985	757.53	0.00000E+00
986	797.71	0.00000E+00
987	821.23	0.00000E+00
988	821.23	0.00000E+00
989	965.59	0.00000E+00
990	965.59	0.00000E+00
991	965.59	0.00000E+00
992	965.59	0.00000E+00
993	965.59	0.00000E+00
994	965.59	0.00000E+00
995	965.59	0.00000E+00
996	965.59	0.00000E+00
997	965.59	0.00000E+00

NODE	TEMPERATURE	FLUX[CE]
1011	445.90	0.00000E+00
1012	573.61	0.00000E+00
1013	701.73	0.00000E+00
1014	727.45	0.00000E+00
1015	753.17	0.00000E+00
1016	798.50	0.00000E+00
1017	823.65	0.00000E+00
1018	823.65	0.00000E+00
1019	956.74	0.00000E+00
1020	956.74	0.00000E+00
1021	956.74	0.00000E+00
1022	956.74	0.00000E+00
1023	956.74	0.00000E+00
1024	956.74	0.00000E+00
1025	973.48	0.00000E+00
1026	973.48	0.00000E+00
1027	973.48	0.00000E+00
1041	445.90	0.00000E+00

1042	573.85	0.00000E+00
1043	702.11	0.00000E+00

NODE	TEMPERATURE	FLUENCE
1044	728.58	0.00000E+00
1045	755.04	0.00000E+00
1046	798.74	0.00000E+00
1047	823.93	0.00000E+00
1048	823.93	0.00000E+00
1049	956.91	0.00000E+00
1050	956.91	0.00000E+00
1051	956.91	0.00000E+00
1052	956.91	0.00000E+00
1053	956.91	0.00000E+00
1054	956.91	0.00000E+00
1055	973.47	0.00000E+00
1056	973.47	0.00000E+00
1057	973.47	0.00000E+00
1071	448.48	0.00000E+00
1072	574.89	0.00000E+00
1073	702.49	0.00000E+00
1074	729.79	0.00000E+00
1075	756.91	0.00000E+00
1076	798.96	0.00000E+00

NODE	TEMPERATURE	FLUENCE
1077	824.21	0.00000E+00
1078	824.21	0.00000E+00
1079	957.07	0.00000E+00
1080	957.07	0.00000E+00
1081	957.07	0.00000E+00
1082	957.07	0.00000E+00
1083	957.07	0.00000E+00
1084	957.07	0.00000E+00
1085	973.46	0.00000E+00
1086	973.46	0.00000E+00
1101	645.78	0.00000E+00
1102	574.32	0.00000E+00
1103	782.87	0.00000E+00
1104	730.83	0.00000E+00
1105	756.79	0.00000E+00
1106	799.23	0.00000E+00
1107	824.48	0.00000E+00
1108	824.48	0.00000E+00
1109	957.24	0.00000E+00

NODE	TEMPERATURE	FLUENCE
1110	957.24	0.00000E+00
1111	957.24	0.00000E+00
1112	957.24	0.00000E+00
1113	957.24	0.00000E+00
1114	957.24	0.00000E+00
1115	973.46	0.00000E+00
1116	973.46	0.00000E+00
1117	973.46	0.00000E+00
1131	448.87	0.00000E+00
1132	574.56	0.00000E+00
1133	703.25	0.00000E+00
1134	731.95	0.00000E+00
1135	768.66	0.00000E+00
1136	799.67	0.00000E+00
1137	824.76	0.00000E+00
1138	824.76	0.00000E+00
1139	957.48	0.00000E+00
1140	957.48	0.00000E+00
1141	957.48	0.00000E+00
1142	957.48	0.00000E+00

NODE	TEMPERATURE	FLUENCE
1143	957.48	0.00000E+00
1144	957.48	0.00000E+00
1145	973.48	0.00000E+00
1146	973.45	0.00000E+00

1167	975.43	0.09800E+08
1181	448.96	0.09800E+08
1162	574.79	0.09000E+09
1163	708.63	0.09000E+09
1164	733.08	0.09000E+09
1165	752.53	0.09800E+08
1164	799.71	0.09800E+08
1167	825.04	0.09800E+08
1168	828.04	0.09800E+08
1169	957.57	0.09800E+08
1170	997.57	0.09000E+09
1171	957.57	0.09000E+09
1172	917.57	0.09000E+09
1173	957.57	0.09000E+09
1174	997.57	0.09000E+09
1175	975.44	0.09000E+09
- NODE TEMPERATURE FLUXES		
1176	975.44	0.09000E+09
1177	975.44	0.09000E+09

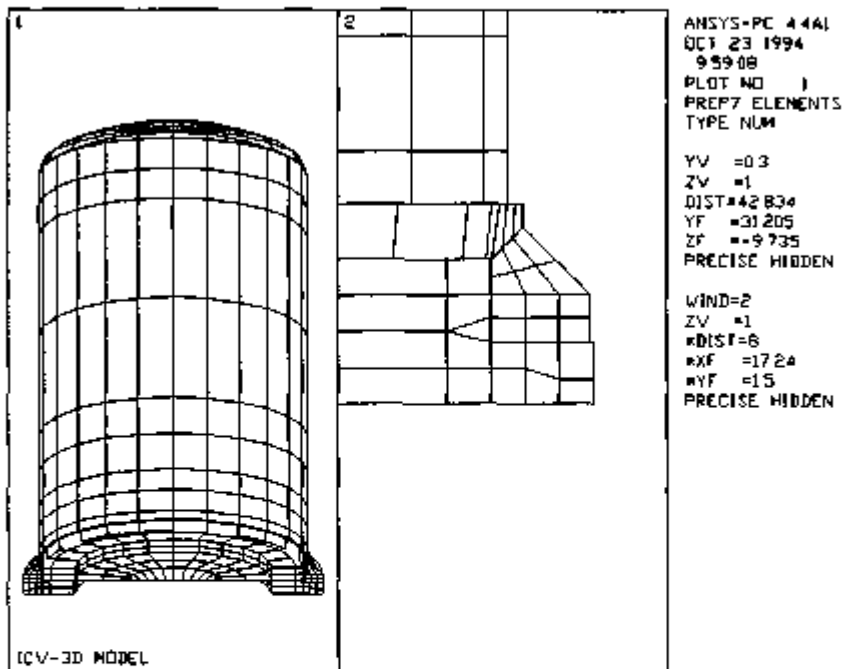


FIGURE 2.10.12-1

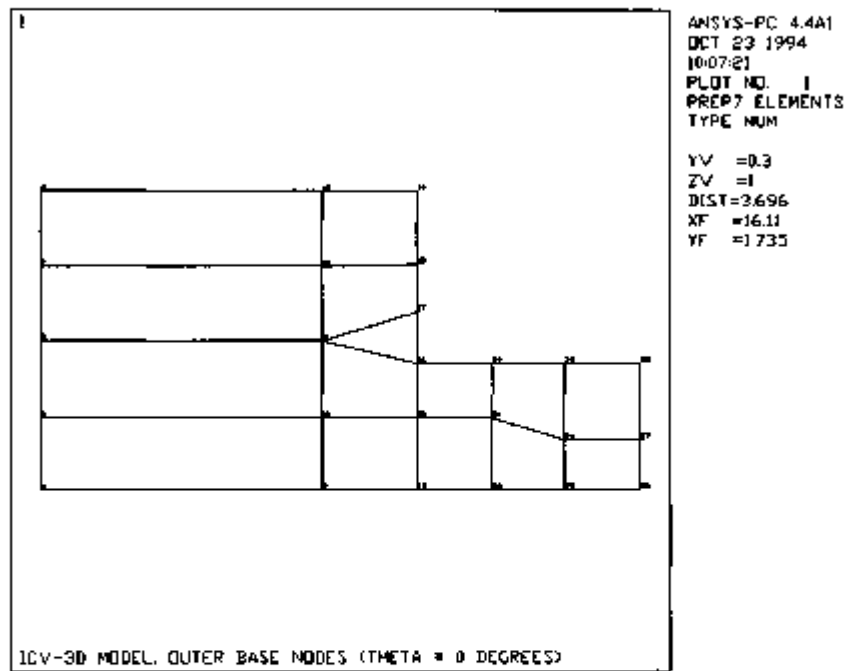


FIGURE 2.10.12-2.

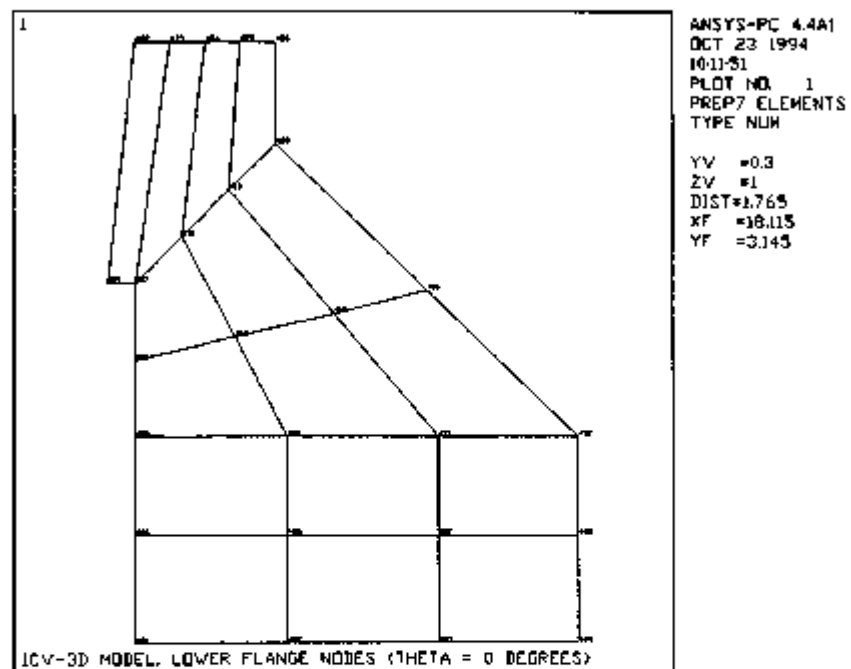


FIGURE 2.10.12-3.

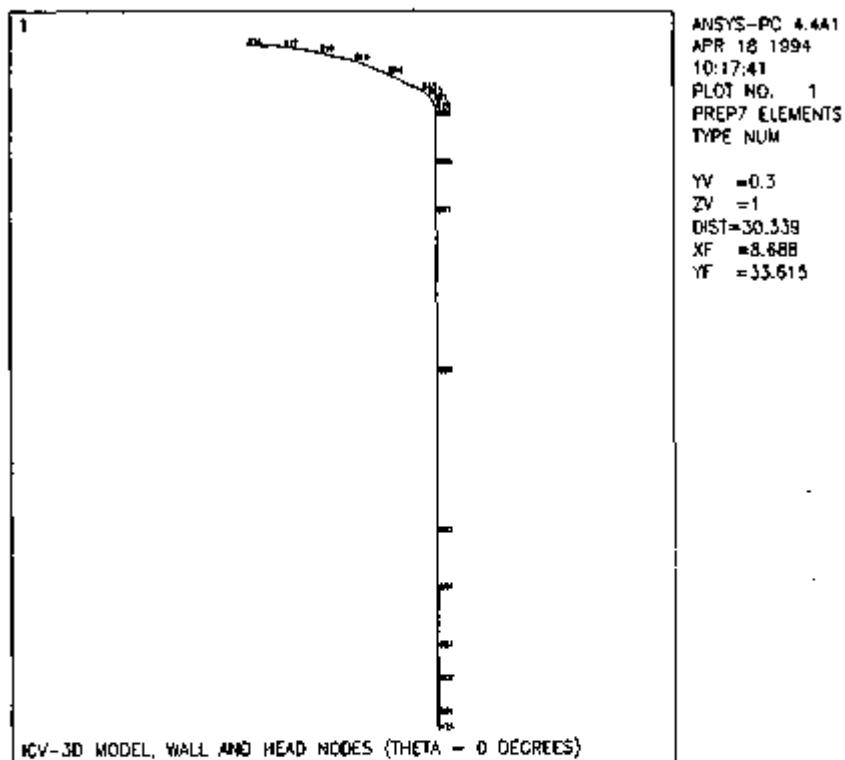


FIGURE 2.10.12-4.

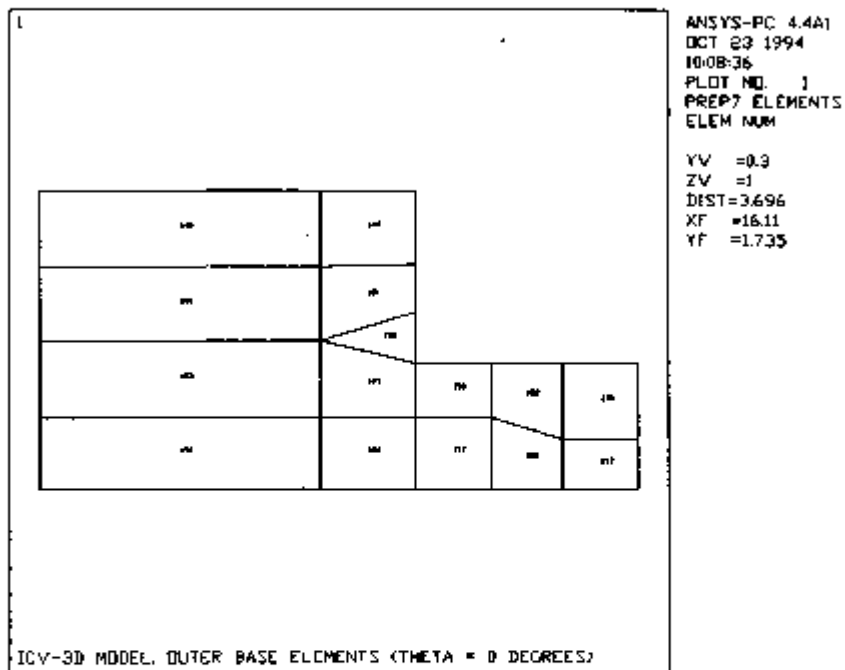


FIGURE 2.10.12-5.

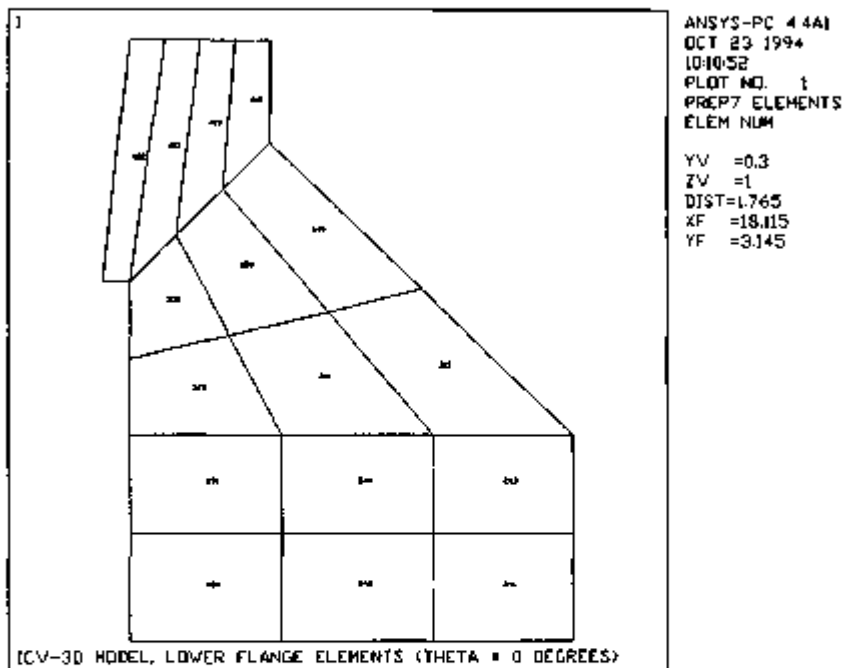


FIGURE 2.10.12-6.

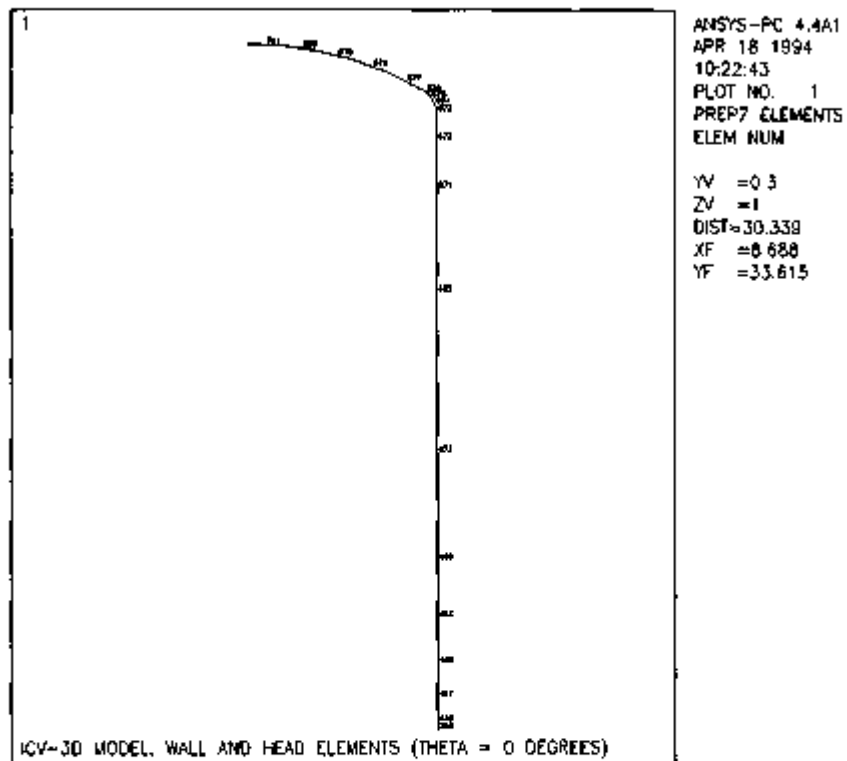


FIGURE 2.10.12-7.

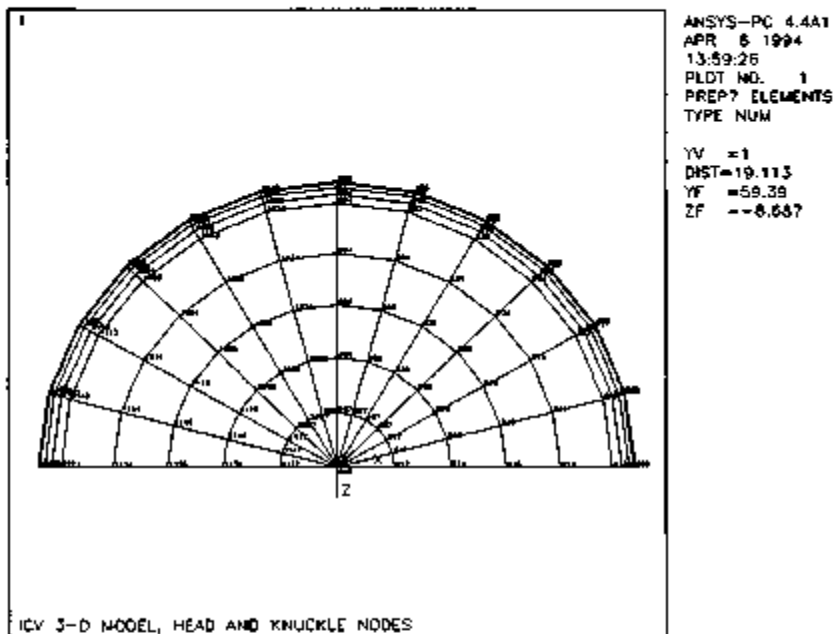


FIGURE 2.10.12-8.

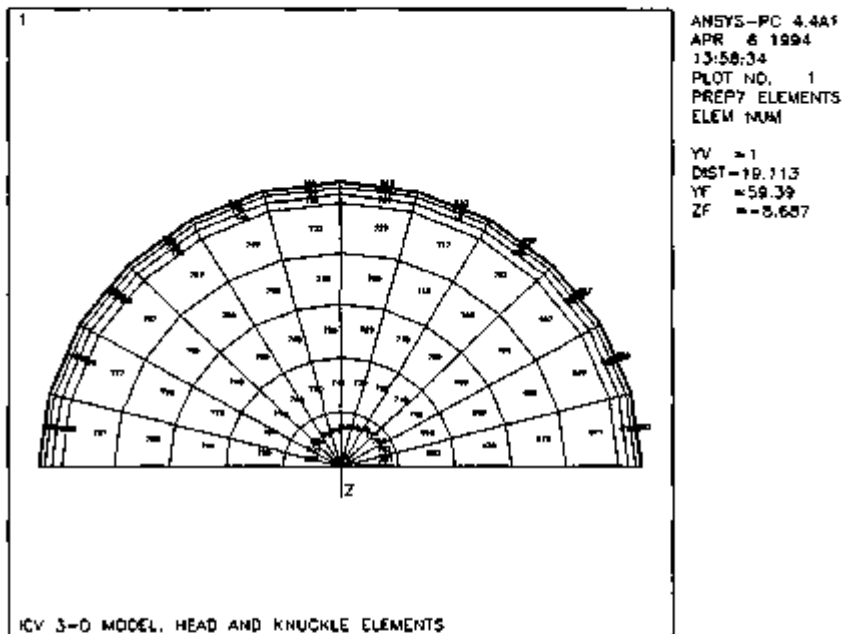


FIGURE 2.10.12-8.

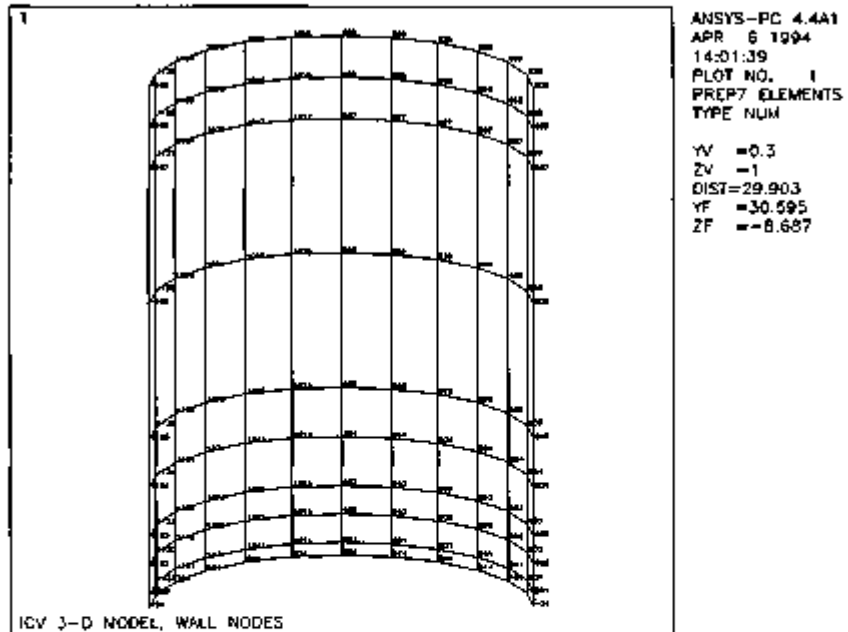


FIGURE 2.10.12-10.

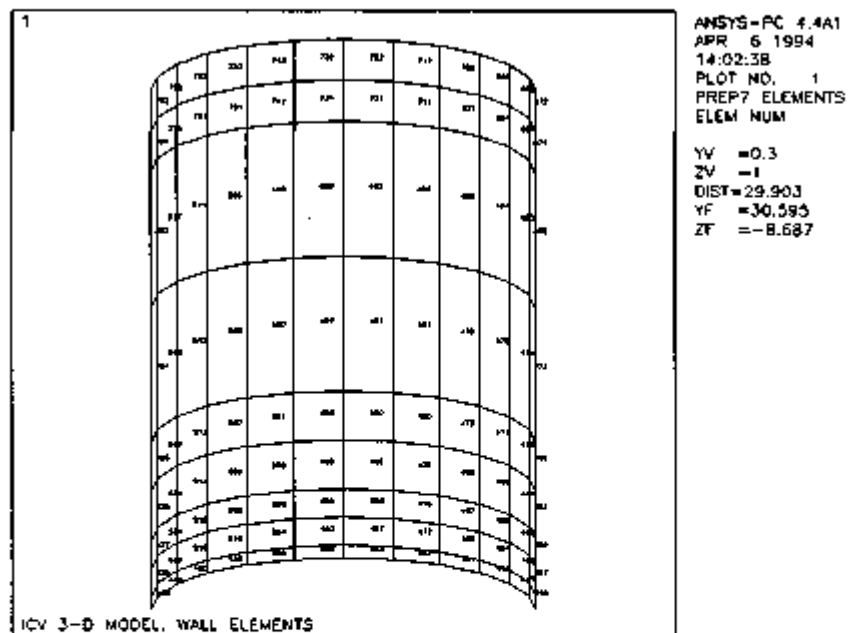


FIGURE 2.10.12-11.

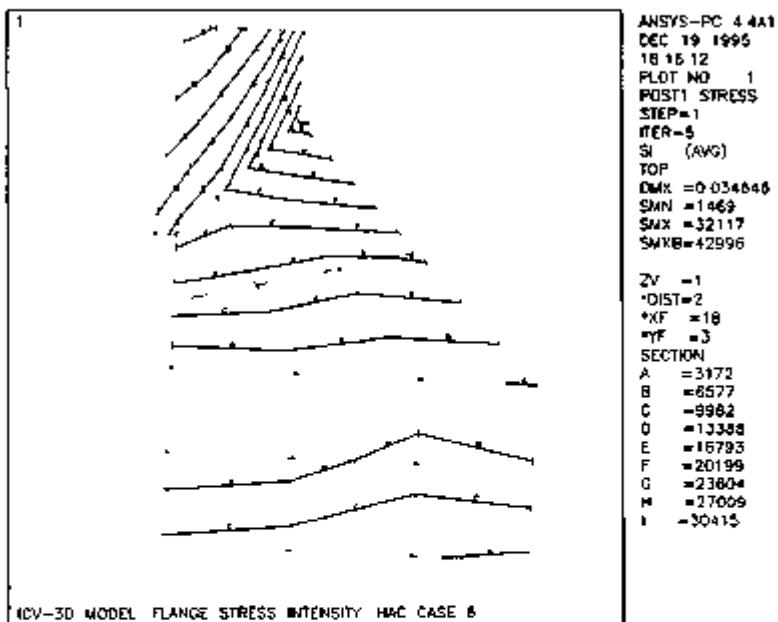


FIGURE 2 10 12-12

2.10.13 OCV Three-Dimensional ANSYS Model

A 3-D model of the OCV was developed to validate the use of a 2-D OCV model (see Section 2.10.8) for evaluation of HAC events. The primary issue to be investigated was the significance of circumferential variations of temperature caused by payload reconfiguration. A secondary issue, the nonsymmetry introduced in the OCV base because of the electrical feed-through penetration, was also addressed by the 3-D model. By comparing results obtained from the 3-D model with those obtained from a corresponding 2-D model, use of the 2-D OCV model for evaluation of HAC events is justified.

2.10.13.1 Description. The 3-D OCV model is a partial representation of the OCV. It includes a 30° segment of the OCV assembly, including base, flange, wall, thermal shield, coolant jacket, and the two closure bolts contained within the segment. This segment begins at the point of maximum heat load (where impact limiter side impact damage coincides with the axial distribution of the damaged payload), and ends at the angular location where the circumferential temperature gradient is essentially zero (about 30° from the maximum heat location). In this manner, the segment can be treated as an isolated structure for both thermal and structural purposes. The OCV head is not modeled; the OCV wall and thermal shield terminate at an elevation of 38.13 in. from the bottom of the OCV base. This geometry was chosen because the axial temperature gradients become essentially zero at this location, and that it is sufficiently far removed from the seal area that distortion effects above this point will have an insignificant effect on OCV containment.

The electrical feed-through geometry was inserted into the finite element model to evaluate its effects on thermal distortion in the containment seal area. The cutout for the electrical feed-through plug was modeled as a 2.59-in. constant diameter cylindrical void, extending horizontally from the outside diameter of the OCV base to a point directly under the containment seal, at a distance of 0.18 in. below the sealing surface. This approximation is conservative because the electrical feed-through cutout maximum diameter of 2.55 in. actually extends for a length of only 3.98 in., and not all the way to the OCV containment seal location. The remaining electrical feed-through cutout has smaller diameters. Also, the actual electrical feed-through cutout is drilled at an angle into the OCV base, taking the cutout location much further below the containment seal location than is used in the ANSYS model.

The electrical feed-through contact plate cutout was modeled as a 8.62 in. long by 2.73 in. wide by 1.00 in. deep rectangular void in the upper surface of the inside portion of the OCV base (the portion where the ICV base contacts the OCV base). This approximation is conservative because the actual contact plate cutout is 1.00 in. deep only over a 7.96 in. long by 1.41 in. wide area, and the remainder of the contact plate cutout is only 0.53 in. deep. No actual electrical feed-through components were included in the ANSYS model, because their structural effects would be negligible. The finite element model (applicable to both the thermal and structural analyses) is shown in Figures 2.10.13-1 through 2.10.13-3.

The detailed OCV analysis consisted of the following four parts.

1. A SINDA finite difference transient thermal evaluation, using a detailed 3-D OCV model, as documented in Section 3.5.2.4.
2. An ANSYS finite element equivalent static thermal evaluation, using SINDA results and a partial 3-D OCV model, as explained above. Using ANSYS, the SINDA results were expanded into the finer mesh finite element model to obtain a more accurate temperature distribution at the OCV seal location and in the area of the electrical feed-through components.

3. An ANSYS 3-D finite element static structural evaluation, using the refined temperature distribution, along with maximum OCV internal pressure, to evaluate the effects of pressure and thermal distortion in the OCV seal area.
4. A corresponding ANSYS 2-D axisymmetric finite element static structural evaluation using temperatures at the hottest circumferential position from the 3-D thermal model along with maximum OCV internal pressure. Model construction is detailed in Section 2.10.8.

2.10.13.2 Construction. For both the ANSYS 3-D thermal and structural models, the same basic types of finite elements were used.

1. The base, flange, and shell portions of the OCV were modeled with 20-node quadratic (isoparametric brick elements). On surfaces where contact elements were applied (i.e., between the OCV flange and base sealing surfaces), the midside nodes of the brick elements were removed to allow accurate representation of the force-deflection characteristics of the contact elements used in the structural model. Additionally, midside nodes were removed from brick element edges that were normal to the closure bolt elements and in direct contact with bolt attachment nodes to linearize bolt interactions with these elements.
2. The OCV thermal shield and coolant jacket were modeled with 4-node linear shell elements for the thermal analysis. For the structural analysis, these elements were converted to 8-node quadratic elements. Reduced-strength shell elements were embedded in the brick elements at the interfaces of bricks and shells to carry rotational displacements between the two types of elements in the structural analysis.
3. Line elements (conducting rods for the thermal model and spar elements for the structural model) were used to represent the closure bolts. The structural closure bolt elements were pre-loaded by applying the appropriate prestrain to achieve a 14,500-pound OCV closure bolt pre-load. This prestrain was applied before any thermal or pressure loadings were imposed on the structural model.
4. For the structural model, 5-node, 3-D surface contact elements were used to accurately simulate contact or separation of the OCV flange and base sealing surfaces under the influence of all applied loadings.

2.10.13.3 Material Properties. The thermal conductivity of the OCV stainless steel structural elements and alloy steel closure bolts varied as a function of temperature according to the data in Table 3.2-1 of Section 3. The modulus of elasticity and coefficient of thermal expansion varied with temperature according to Tables 2.3-1 and 2.3-2. Poisson's ratio was 0.3.

2.10.13.4 Boundary Conditions. A representative thermal loading corresponding to HAC load case 3 was used for evaluation. This particular case was selected because it provides a relatively large temperature difference between the OCV shell and flange, a significant circumferential temperature gradient, and relatively high OCV O-ring seal temperatures.

2.10.13.4.1 Thermal Model. The worst-case temperatures and temperature gradients in and around the OCV containment seal area occur at the period of time corresponding to the end of the HAC fire event (i.e., 30 minutes from the start of the event). Therefore, thermal conditions occurring at this time were evaluated to determine worst-case OCV containment seal temperatures and seal area distortions.

At all boundaries (external surfaces) of the ANSYS thermal model, except the 0 and 30° surfaces (which were assumed to be symmetry surfaces, and therefore adiabatic), external heat

fluxes from the SINDA model were applied as surface loads. Because each surface node of the SINDA model represents a discrete area, the flux values were divided by the appropriate areas, and the resulting flux densities were imposed directly on the equivalent surface areas of the ANSYS model. Because the SINDA results were derived from a transient analysis, an instantaneous heat flux imbalance was incurred, because of material specific heat effects (heat lost in raising material temperatures). To account for this effect in the ANSYS static analysis, these heat losses were modeled as heat sinks in the model interior. Each interior SINDA node represents a specific volume of material. Therefore, for the ANSYS evaluation, the internal heat loss at each SINDA node was divided by the corresponding volume, and the result was directly applied over the equivalent volume of the finite element model as a volumetric heat sink. In this manner, a static heat flux balance was achieved over the domain of the finite element model. To the interior of this domain were added temperatures derived at interior nodes of the SINDA model. In areas of high heat flux, additional ANSYS initial nodal temperatures were derived by linear interpolation of SINDA internal and external node temperatures. The resulting ANSYS model was then run in a static thermal analysis to accurately determine the remainder of the finite element model nodal temperature values. These temperatures were then transposed into the ANSYS structural model as loads for the structural thermal distortion analysis.

2.10.13.4.2 Structural Model. The thermal analysis nodal temperatures, as described in the above section, along with a representative internal pressure loading of 39.7 psia, were applied to the ANSYS structural model. A reference of 70 °F was used to derive thermal distortion effects. The 0 and 30° surfaces were assumed to be symmetry boundaries, and appropriate displacement constraints were applied accordingly. Additionally, to achieve static stability, a single axial zero-displacement constraint was applied at the center of the bottom surface of the finite element model base.

Resulting closure bolt loads and distortions (sealing surface separation) at the location of the OCV containment seal were determined for comparison with the corresponding 2-D model of the OCV.

2.10.13.5 Analysis Results and Comparison with 2-D ANSYS Model. Both 3-D and 2-D models were run using representative inputs as discussed above. Results of the 3-D thermal analysis, in the form of temperature contours, are shown in Figures 2.10.13-4 through 2.10.13-6.

Results of the 3-D structural analysis indicate the maximum relative displacement between OCV flange and base seal surfaces at the location of the OCV containment seal is 0.022 in., and is essentially constant around the circumference of the 30° model segment. The results also indicate that the presence of the electrical feed-through in the OCV base is of little significance. In general, this is because OCV flange twist is the dominant displacement mode that affects seal compression. OCV base distortions, in contrast, are relatively small. The OCV seal area distortion pattern (with displacements scaled by a factor of 26) is shown in Figure 2.10.13-7. The maximum closure bolt load was 48,795 pounds. Results from the corresponding 2-D model were a relative displacement

between flange and base at the containment seal location of 0.018 in., and a closure bolt load of 42,938 pounds. The good agreement of results between 3-D and 2-D models justified use of the 2-D model for the OCV.

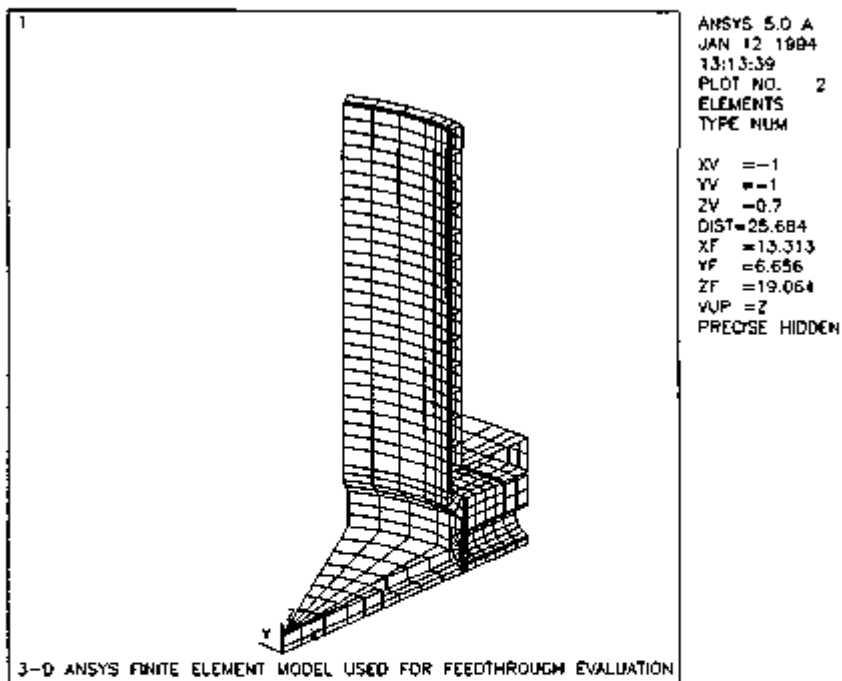


FIGURE 2.10.13-1.

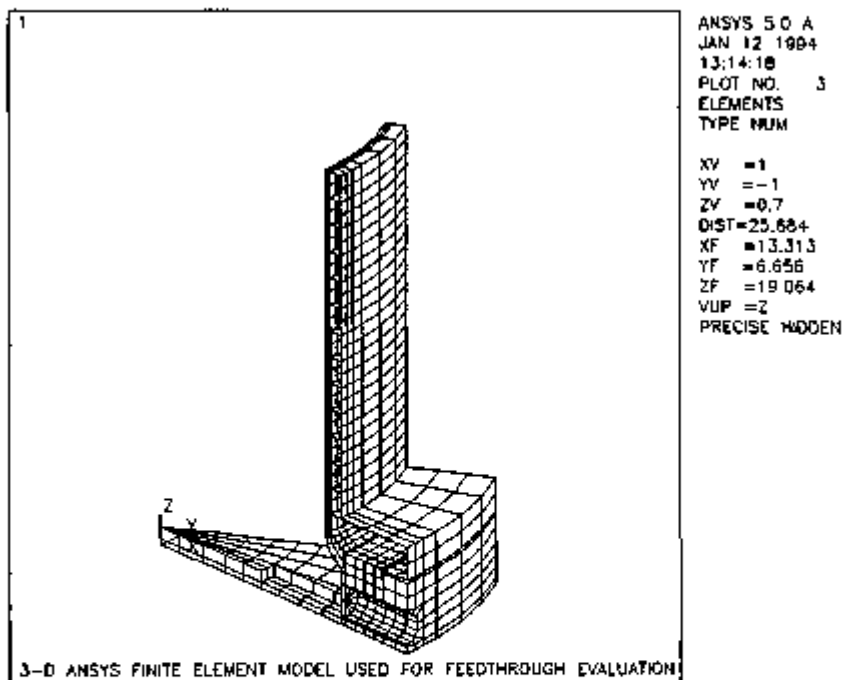


FIGURE 2.10.13-2.

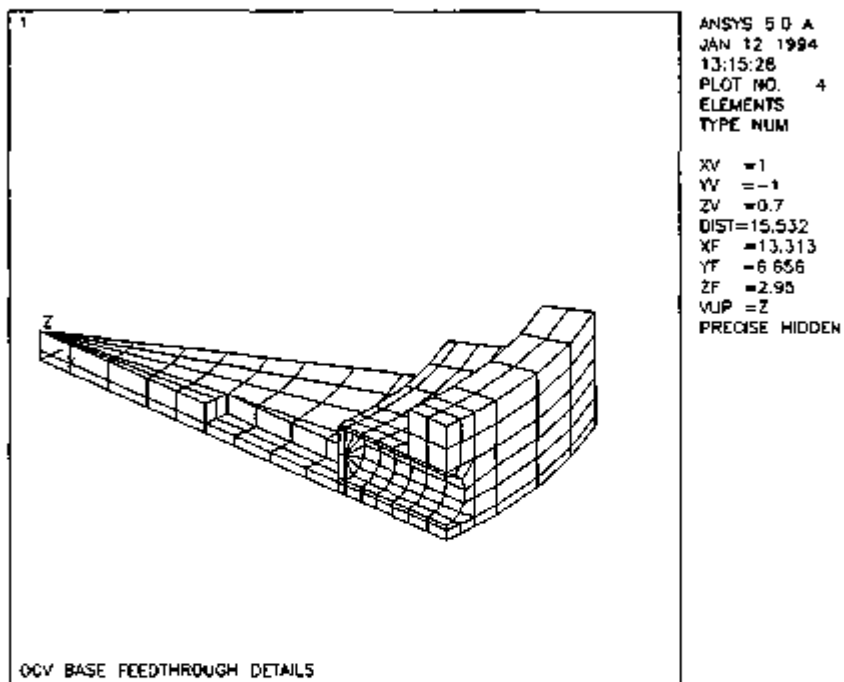


FIGURE 2.10.13-3.

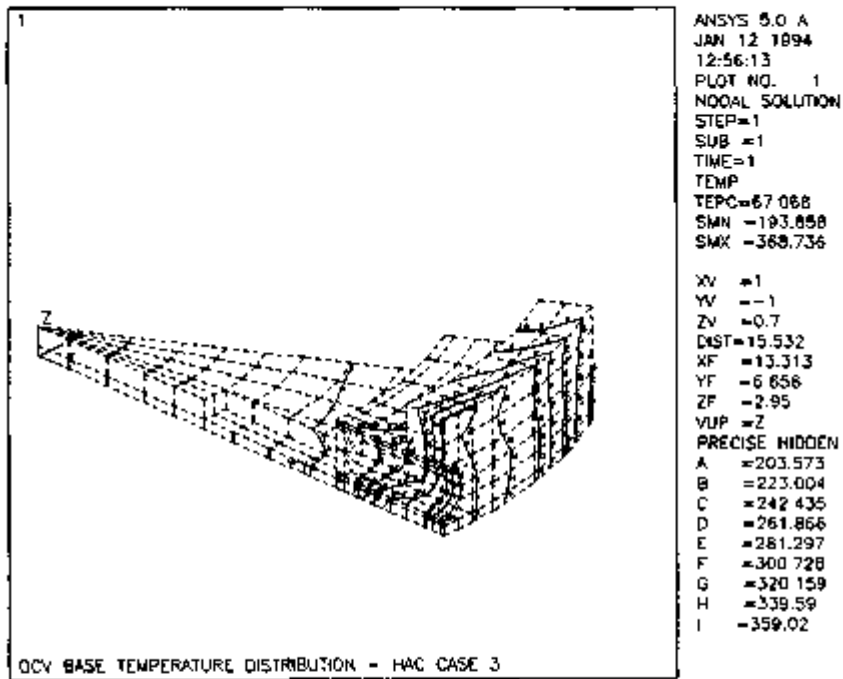


FIGURE 2.10.13-4.

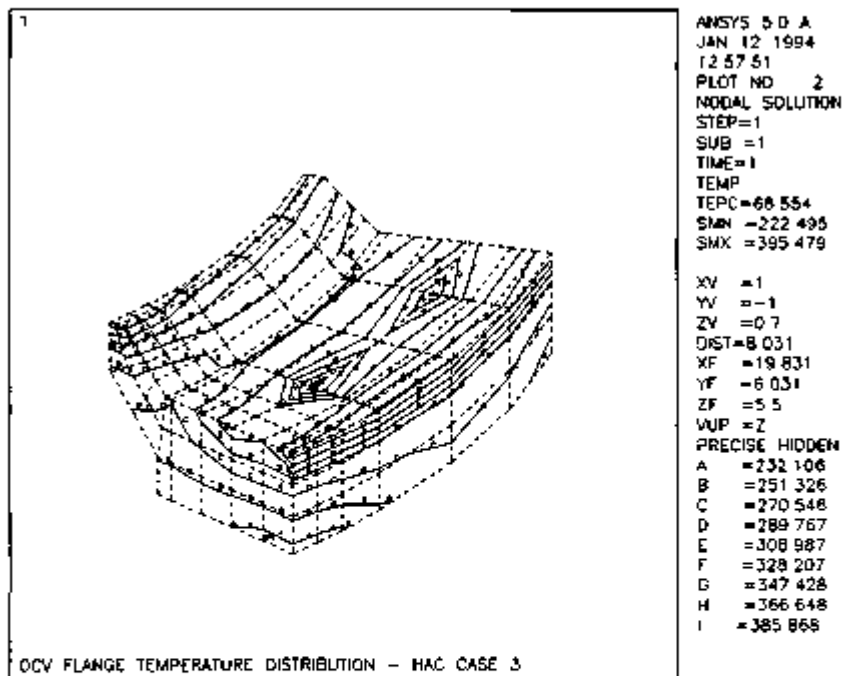


FIGURE 2.10.13-5

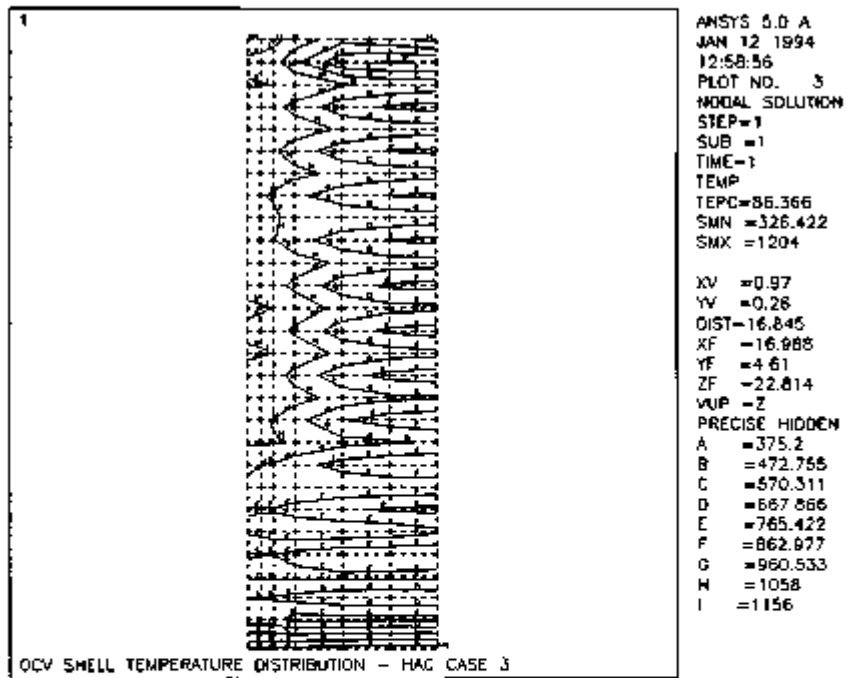


FIGURE 2.10.13-8.

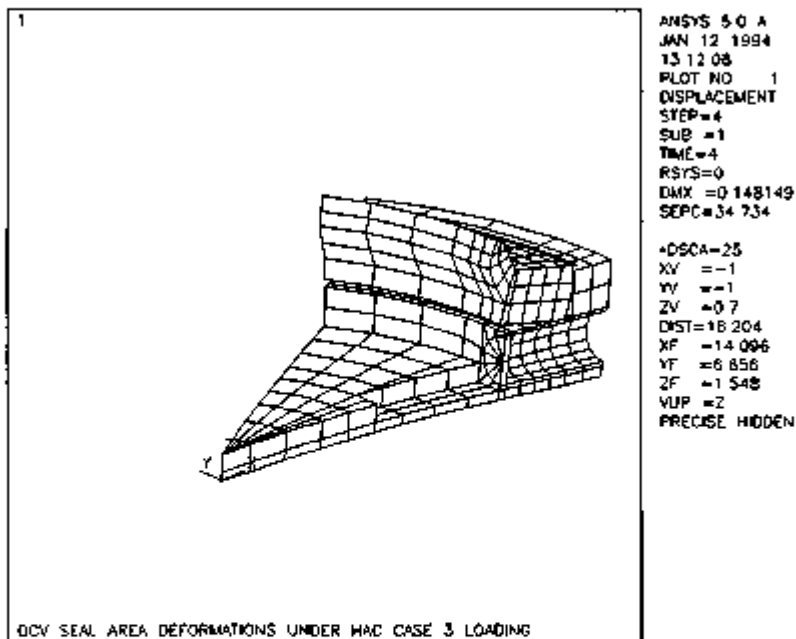


FIGURE 2.10.13-7.

2.10.14 O-ring Seal Compression Measurements

The RTG Transportation System Package uses elastomeric, face-type O-rings as containment seals. The ability of these O-ring seals to function is dependent on the degree of compression afforded by the containment seal area mating surfaces. In the HAC fire event, thermal distortions of the mating surfaces can cause a reduction in O-ring compression. To demonstrate that the combined effects of the HAC 30-ft. free drop, the 40-in. puncture drop, and the HAC fire event do not reduce the O-ring compression below acceptable levels, the compression O-ring reduction due to drop event-related flange distortion is summed with the calculated O-ring compression reduction due to HAC fire event thermal distortion. For this reason, an evaluation of drop event flange distortion and potential reduction in O-ring compression must be made. These calculations are more fully discussed in Section 4.0. Data was collected before and after the entire drop event series.

The O-ring compression is directly related to the axial dimension of the space it is forced to occupy. This axial dimension is created by the relative positions of the bottom of the O-ring groove in the vessel base and the flat ball flange. Nominally, the dimension is simply equal to the O-ring groove depth, as long as the flange is tightly mated to the base. Reduction of O-ring compression can only occur from relative distortion between the groove bottom and the flange surface. The method described below focuses on the space available for the O-ring to occupy. Measurements were taken in accordance with PacTec procedure TP-004, and are recorded on data sheets contained in Appendix 2.10.15.5.

The direct compression method preserves a record of the space available for the O-ring seal to occupy by assembling a soft metal replica of the elastomer O-ring into the O-ring groove. The replica had an initial dimension larger than the groove depth (but not necessarily equal to the O-ring). Subsequent to assembly into the groove, it had a dimension equal to the space available for the O-ring to occupy plus an insignificant amount of elastic springback (less than 2% of its diameter). The elastic springback was present in equal amounts in both pre- and post-test measurements, and thus, had no effect on net measurements. The O-ring replicas were common copper tubing. Nominal 1/4-in. tubing was used for both of the closure seal grooves on the ICV, and nominal 1/4- and 5/16-in. tubing was used to measure the small and large O-ring grooves, respectively, of the OCV. The replicas were of one piece, with a small gap (about 1 to 2 in.) where the ends met. The gap was placed midway between two measurement points. Measurements were made in eight locations on each replica for each of the four O-ring grooves. One measurement was taken at the circumferential position of the electrical feed-through and the others were evenly spaced at 45° increments. Thus, a total of 16 measurements were taken to record the state of compression of each of the closure O-ring seals in the ICV and OCV. Because these measurements were taken before and after testing, a grand total of 128 measurements were made. Table 2.10.14-1 gives the copper tubing crushed height measurements in the pre-test and post-test condition for the ICV, and Table 2.10.14-2 is for the OCV. The column labeled "Change" is the difference in space available for the O-ring to occupy brought about by the drop testing. A positive result indicates an increase in space available, that is, a decrease in O-ring compression.

When tightening the closure bolts to crush the tubing, a star pattern (alternating sides of the OCV) was used. For the pre-drop measurements, full nominal closure bolt torques were used. For post-drop measurements, each bolt was carefully tightened in 25% increments to the residual torque value that was measured when the package was disassembled after leakage rate testing.

TABLE 2.10.14-1. ICV Containment O-ring Groove Direct Compression Measurements (in.)

Angular position	Inner groove (1/4 in.)			Outer groove (1/4 in.)		
	Pre-test	Post-test	Change	Pre-test	Post-test	Change
Feed-thru	0.204	0.206	0.001	0.201	0.213	0.012
45	0.204	0.203	-0.001	0.201	0.207	0.006
90	0.204	0.203	-0.001	0.200	0.208	0.008
135	0.203	0.203	0.0	0.200	0.208	0.008
180	0.204	0.206	0.001	0.202	0.210	0.008
225	0.204	0.204	0.0	0.201	0.208	0.007
270	0.204	0.203	-0.001	0.201	0.208	0.007
315	0.204	0.203	-0.001	0.201	0.208	0.007

TABLE 2.10.14-2. OCV Containment O-ring Groove Direct Compression Measurements (in.) Base.

Angular position	Inner groove (5/16 in.)			Outer groove (1/4 in.)		
	Pre-test	Post-test	Change	Pre-test	Post-test	Change
Feed-thru	0.282	0.287	0.005	0.207	0.213	0.006
45	0.282	0.283	0.001	0.207	0.207	0.0
90	0.282	0.282	0.0	0.207	0.208	0.001
135	0.282	0.283	0.001	0.207	0.208	0.001
180	0.282	0.284	0.002	0.207	0.210	0.003
225	0.282	0.282	0.0	0.207	0.208	0.001
270	0.282	0.283	0.001	0.207	0.208	0.001
315	0.282	0.283	0.001	0.207	0.208	0.001

The negative change values (a decrease in space available) in the tables above do not exceed -0.001, and can be attributed to measurement error.

From Table 2.10.14-1, the maximum change in compression of the containment O-ring seal (the inner location) is a reduction of 0.001 in. for the ICV. From Table 2.10.14-2, the corresponding value for the OCV is a reduction of 0.005 in. This data is used further in Section 4.3.2.

2.10.15 Summary of Damage from Certification Testing

2.10.15.1 Introduction. This section provides detailed information regarding the Certification Testing of the RTG Transportation System Package. Two full-scale prototypes of the package were used during the drop test program. The first certification test article (CTA-1) experienced two failures during the first drop test series. The package design was subsequently modified and a second certification test article (CTA-2) was fabricated. All of the 4-ft and 30-ft free drop tests that were performed on CTA-1 were repeated for CTA-2. During the first drop test series, CTA-1 was subjected to nine puncture tests. For the second drop test series, four of these puncture tests were repeated and two additional puncture tests were performed on CTA-2.

The first drop test series is described in Test Plan WHC-SD-RTG-TP-008 and the second drop test series is described in Test Plan WHC-SD-RTG-TP-018. The first drop test series was performed in accordance with Test Procedure WHC-SD-RTG-TP-003 and the second drop test series was performed using Test Procedure WHC-SD-RTG-TP-015. The drop testing was performed to the requirements of 10 CFR 71. The HAC fire was evaluated by analysis as shown in Chapter 3.0.

The CTA-2 unit was fabricated in accordance with the drawings contained in Section 1.3.2, with any differences noted in Section 2.10.15.2.1 below. The differences between CTA-1 and CTA-2 are listed below in Section 2.10.15.2.2. The RTG payload mass, center of gravity, and potential for inflicting damage on the interior of the ICV was simulated in the drop testing as described in Section 2.10.15.2.3. The test pad puncture bars are described in Section 2.10.15.3. It is noted that only CTA-1 had accelerometer instrumentation attached during the drop testing.

The test data included for CTA-1 consists of accelerometer output for the NCT and HAC free drops and damage results from puncture tests CTA-1 Test No. 12, No. 13, No. 15, No. 18 and No. 19. The accelerometer data is included for information only. The results of the above listed CTA-1 puncture tests are included because these tests were not repeated during the second drop test series.

The test data included in this appendix consists of helium leakage rate results, closure bolt torques, accelerometer output (CTA-1 only), completed test data sheets, impact deformations, and a written and photographic record of damage. Seal area measurements are presented in Appendix 2.10.14. A brief explanation of the data is included where needed. A complete summary and discussion of the data is given in Section 2.7.6. Results that are pertinent to NCT are summarized in Section 2.6.7.

2.10.15.2 Test Article. Two full-sized prototypes of the package were fabricated for use as CTAs. This section identifies any differences between CTA-1 and CTA-2, and between CTA-2 and the General Arrangement drawings provided in Section 1.3.2. Unless a specific exception is stated herein, CTA-2 fully complied with the General Arrangement drawings of Section 1.3.2.

2.10.15.2.1 Itemized Differences Between CTA-2 and General Arrangement Drawings. Differences between CTA-2 and the drawings presented in Section 1.3.2 fall into two broad categories:

- Items related specifically to certification testing, such as special vent ports
- Items that were not needed for certification testing, such as paint or coolant.

Each difference is detailed below. In each case, it is demonstrated that the difference had no material effect on the outcome of the certification tests.

1. **Measurement Tool Mounting Tabs.** Small, 1-in. square, 1/4-in.-thick tabs made of 304L stainless steel were welded to the CTA-2 coolant jacket outer surface in each of four quadrants. One quadrant was located at the electrical feed-through, and the others were at 90° intervals. Three tabs were used in each quadrant to assist in temporarily fastening a measurement reference tool to CTA-2. The tool was used to obtain measurements of impact limiter deformation after each drop test. The tabs did not significantly alter the weight or c.g. of CTA-2 and were not directly involved in any free drop or puncture drop events.
2. **Impact Limiter Shell Hole.** A single, 5/16-in.-diameter hole was drilled into the center of the bottom plate of the CTA-2 impact limiter. The hole was used in conjunction with a measuring rod, used to determine impact limiter deformations. The hole had no influence on any CTA-2 response.
3. **Adjustment of Foam Density in Impact Limiter.** The density of the nominally 12 lb/in.³ foam was adjusted upward to approximately 15.5 lb/in.³ to simulate cold (-20 °F) conditions. This adjustment was made to allow ambient temperature certification testing and is fully described in Section 2.7.1.3.
4. **Added Leak Test Ports.** One seal test port was added to both the ICV and OCV to aid in establishing the dwell time for helium leakage rate testing. The construction of each port is fully prototypical, i.e., is identical to the standard seal test ports shown in the General Arrangement drawings. The location of each added seal test port is 180° opposite the standard seal test port for each vessel.
5. **Added Vent Ports.** Three port holes, sealed by 1/4-in. NPT pipe plugs, were added to CTA-2: two on the OCV and one on the ICV. The purpose of the ports was to allow the introduction of helium into the vessels (and its subsequent removal) during the certification test leakage rate testing procedure, without the necessity of disturbing the prototypic vent port seals. The ICV port was located in the 2-in. thick lifting block at the top of the bell, and the OCV ports were located just above the top of the coolant jacket. The added ports were not directly involved in any free drop or puncture drop events.
6. **Striping.** CTA-2 featured tape and paint stripes to aid in drop testing.
7. **Nameplate.** A nameplate was not present on CTA-2. This omission had no effect on any CTA-2 response.
8. **Tamper-Indicating Seal.** An impact limiter bolt tamper-indicating seal was not present on CTA-2. This omission had no effect on any CTA-2 response.
9. **Paint.** Paint was not present on CTA-2. This included the black paint normally used for interior bell surfaces and the white paint normally used for exterior surfaces. This omission had no effect on any CTA-2 response.
10. **Electrical Feed-through, Spring-loaded Electrical Pins.** The spring-loaded pins that complete the electrical connection between the ICV and OCV for the electrical feed-through were not present on CTA-2. When compressed, they exert only a few ounces of force and have no structural significance. This omission had no effect on any CTA-2 response.
11. **Coolant.** Coolant was not present in the CTA-2 coolant passages. The passages were essentially dry and contained air. The normal quantity of coolant weighs approximately 180 lb, and therefore its absence had a negligible effect on CTA-2 mass and c.g. The structural significance of coolant is also small. The absence of coolant would cause slightly greater (more conservative) deformations of the OCV vessel wall from puncture events.

12. **Personnel Barrier.** The personnel barrier was in place for all of the CTA-2 free drops. After the 30-ft top-down drop (CTA-2 Test No. 13), the thin expanded metal screen on top of the personnel barrier was removed. In puncture drop No. 15, the distance to the puncture pin was conservatively measured as though the personnel barrier was undamaged and the screen was present. This amounted to a top-down puncture drop distance of approximately 45 in. instead of 40 in. and is therefore conservative.
13. **Electrical Feed-through Receptacle-to-Sheave Weld.** This weld was an electron beam (EB) weld on CTA-2, but will be a Gas Tungsten Arc Weld (GTAW) for production units. The GTAW will be stronger and less subject to microfractures than the EB weld, and therefore the use of the EB weld in the certification tests was conservative. Further information on this weld is provided in Reference 6 of Chapter 4.
14. **Instrumentation Cables.** Cables were connected to each electrical feed-through, which terminated in the respective bracket-mounted connectors. Wiring was not used, however, from the ICV connector to the simulated payload, or from the OCV connector to external instrumentation. The absence of these secondary wires had no effect on any CTA-2 response.
15. **Small holes,** which penetrated approximately 2 in. into the foam, were placed in the four plastic melt-out plugs in the impact limiter, to facilitate temperature measurement of the foam. There was no effect on any CTA-2 response.
16. **OCV coolant jacket and thermal shield weld inspections.** The CTA-2 OCV coolant jacket and thermal shield welds were not dye-penetrant inspected. Also, the CTA-2 OCV coolant jacket channels were not pressure tested. These welds are not part of the OCV containment boundary and the inspections were considered to be unnecessary for drop testing. The elimination of these requirements had no effect on any CTA-2 response.
17. The CTA-2 unit used cadmium-plated ICV closure bolt washers for certification drop tests Nos. 1 through 9. The remaining drop tests (Nos. 10 through 16) used the non-cadmium-plated washers. See Section 2.10.15.4.8.
18. The impact limiter guide tubes were not welded to the top of the OCV flange for the CTA-2 unit. The tubes were only welded to the OCV flange thermal shield.
19. The CTA-2 impact limiter attachment holes did not use the bottom cap.

In summary, several minor differences existed between CTA-2 and the General Arrangement drawings. None of these differences, however, had any significant effect on the response of CTA-2 to drop or puncture events.

2.10.15.2.2 Itemized Differences Between CTA-1 and CTA-2. As mentioned in Section 2.10.15.1, CTA-1 experienced two failures and a new certification test article (CTA-2) was fabricated. The main differences between the two test articles were the hardware changes that were made to CTA-2 to correct the failures experienced by CTA-1. The differences between CTA-1 and CTA-2 are listed below.

1. **Accelerometer Mounting Blocks and Protective Covers.** Mounting blocks for active and passive accelerometers were added to the outside of CTA-1. There were three active accelerometer mounting blocks and one mounting plate used to attach a bank of three passive accelerometers. The mounting blocks were made of 304L stainless steel, and had threaded holes for mounting of the accelerometers. The mounting blocks were welded to the coolant

jacket ribs with at least four 1/8-in. fillet welds to provide a rigid connection to CTA-1. To obtain access to the ribs, a short (approx. 6-in.-long) section of the outer coolant jacket shell was removed in each case. Two mounting blocks were located at the approximate axial location of the CTA-1 center of gravity, one at 90° and the other at 270° CCW from the location of the electrical feed-through. The third was located 30 in. above the center of gravity, at 270° CCW of the electrical feed-through. The mounting plate for the bank of positive accelerometers was located approximately 280° CCW from the electrical feed-through at the c.g., and was welded firmly to the outer exposed edges of the coolant jacket ribs. Protective covers, made of 304L, were fastened using 1/4-in. cap screws to small mounting plates welded to the coolant jacket ribs. There were a total of three covers. These items did not significantly alter the weight or c.g. of CTA-1. Further, they were located in areas of CTA-1 not subject to either free drop or puncture drop damage, and did not impart or alter package stresses.

2. **Added vent ports.** One additional hole, sealed by a 1/4-in. NPT pipe plug, was added to the CTA-2 OCV. The purpose of the port was to allow the introduction of helium into the vessels (and its subsequent removal) during the certification test leakage rate testing procedure, without the necessity of disturbing the prototype vent port seals. The additional OCV port was located just above the top of the coolant jacket and 180° from the other port that is in the same location as the CTA-1 OCV port. The added port was not directly involved in any free drop or puncture drop events.
3. **Personnel Barrier.** The screen (expanded metal) that forms the sides of the barrier was placed outside the barrier framework, not inside as on CTA-1. This difference had no effect on any CTA-2 response.
4. **Wear Pads.** The wear pads mounted in the CTA-1 OCV flange were made of Kevlar[®]/Nylon, instead of Vespel[®], as was used on CTA-2. The purpose of the pads is to protect the black heat transfer paint on the vessel bells when installing the OCV bell, and they play no structural role. Therefore, this substitution had no effect on any CTA-2 response.
5. **Impact Limiter Alignment Pins.** The CTA-1 impact limiter contained two extra threaded mounting holes for the alignment pins (because of initial mislocation of the holes). CTA-2 did not contain these extra holes.
6. **Payload Shipping Rack Underside Insulation.** During normal use of the package, small tufts of Kaowool insulation (located beneath the payload shipping rack) could become loose and hamper helium leak testing. To prevent this, a 16-gauge-thick sheet of 304 stainless steel was used to enclose it on CTA-2, as shown on drawing H-9-5005 in Appendix 1.3.2. This 16-gauge sheet was not used on CTA-1.
7. **ICV Bolting System.** The redesign consists of an increase in bolt quantity from 12 for CTA-1 to 24 for CTA-2; a change in bolt material to ASTM A540 Class 1; the use of hardened steel thread inserts (identical in material and design to those used in the CTA-1 OCV); the use of hardened steel washers under the bolt heads; and an increase in bolt installation torque, from 100 ft-lb to 250 ft-lb.

The 24 bolt holes used in the CTA-2 ICV are equally spaced, and the design details of the flange hole and counterbore are identical to the CTA-1 ICV 12-bolt design. The hardened thread inserts are mounted from beneath the ICV baseplate. The bolt diameter remains the same, but bolt length increased by 1/8 in. to account for the added washer thickness. The bottoms of the bolt, insert, and baseplate are approximately flush.

8. **Impact Limiter Corner Joints.** The original CTA-1 design consisted of a simple corner joint,

joined by a fillet weld and reinforced by angle shapes. The new CTA-2 design consists of a single angle-shape corner piece, full-penetration butt welded on the ends of its legs to the limiter shells. The thickness of the new corner material is equal to the sum of the thicknesses of the CTA-1 impact limiter shell material and reinforcing angle shape.

9. **Impact Limiter Attachment Bolts.** The diameter of the impact limiter attachment bolts was increased from 3/4 in. (CTA-1) to 1 in. (CTA-2). The bolt length was increased from 7.5 to 8.0 in. The diameter of the central length of the CTA-2 impact limiter attachment bolts is 0.805 in. versus 0.55 in. for CTA-1. For CTA-2, the bolt material was changed to ASTM 9637, Alloy NO7760 Type 3. The bolt access tube size for CTA-2 was changed to 2.00-in. diameter by 0.083-in. wall. Bolt torque was increased to 200 from 100 ft-lb. The thread size and depth of engagement in the CTA-2 impact limiter holding ring were increased to accommodate the larger bolts and Hell-coil thread inserts were installed. The CTA-1 impact limiter bolt ring did not have through holes or caps.
10. **OCV Coolant Jacket and Thermal Shield Weld Inspections.** The CTA-2 OCV coolant jacket and thermal shield welds were not dye-penetrant inspected. Also, the CTA-2 OCV coolant jacket was not pressure tested. These welds are not a part of the OCV containment boundary and the inspections were considered to be unnecessary for drop testing. The inspection and pressure tests were performed on CTA-1.

2.10.15.2.3 Payload Representation. Simulated payload weight and c.g. location was designed to simulate a maximum weight, maximum c.g. height payload including a maximum weight payload shipping rack. The combined weight and c.g. of the simulated payload with shipping rack was 785 pounds and 24.6 in. above the ICV base plate, respectively. The simulated payload alone weighed 570 pounds and had a c.g. 26.9 in. above its lower mounting surface. The height of the simulated payload c.g. corresponded to within about 1 in. of the height of the c.g. of the maximum weight payload. Fin position relative to payload c.g. was also closely simulated as further discussed below. The total weight of the minimum weight payload and shipping rack is approximately 425 pounds. Because the difference was only 370 pounds, or 3.9% of the total RTG Transportation Package weight, any difference in behavior due to a minimum weight payload can be neglected. The CTA-2 c.g. was also negligibly affected.

The simulated payload consisted of a cylindrical, reinforced steel container, mounted on a 14-in. diameter, 1/2-in. wall thickness steel pipe, which was in turn mounted on a 1/2-in.-thick bolting plate. To simulate the fins present on the actual payloads, eight 1/4-in.-thick steel fins were located radially around the steel container. The top corners of the fins were located 39.4 in. above the top of the shipping rack barrier plate, which corresponded to the position of the top corners of the fins of the heaviest payload. The simulated fins were stronger and had sharper corners than the actual RTG fins, which are made from aluminum, have generally lower buckling strengths, and have chamfered corners. The simulated fins and the open end design of the 14-in. pipe conservatively modeled any damage that could accrue from interaction with an actual payload in a drop. Figure 2.10.9.1-1 shows the simulated payload mounted within the ICV. Section 2.10.9.1 contains more information on the simulated payload. The simulated payload was mounted to the ICV baseplate in a manner identical to an actual payload.

It can be concluded that the simulated payload conservatively models the action of an actual payload in NCT and HAC drop and puncture events.

2.10.15.2.4 Initial Conditions.

CTA-1 Configuration

The first certification test article (CTA-1) was tested in July, 1984 and was similar to the second

certification test article (CTA-2) as previously discussed in Section 2.10.15.2.2. The CTA-1 unit experienced two failures that led to a subsequent redesign of the package and fabrication of a second certification test article (CTA-2). The same prototypical shipping rack and simulated payload were used in both CTA-1 and CTA-2.

CTA-2 Configuration

The CTA-2 consisted of a prototypical package, constructed according to the General Arrangement drawings (see Section 1.3.2), with exceptions and differences as outlined in Section 2.10.15.2.1 above. A prototypical payload shipping rack and a simulated payload were installed as discussed in Section 2.10.15.2.2 above. Before testing, the package containment seals and containment boundaries were subjected to helium leakage rate testing in accordance with the procedure described in document WHC-SD-RTG-TC-015.

Temperature

The CTA-2 impact limiter foam strength was selected to simulate the strength of the production foam at a temperature of -20 °F, assuming the temperature at the time of the certification tests would be approximately 75 °F. A permissible variation in CTA-2 foam temperature of ±15 °F was selected to ensure that cold conditions were adequately simulated. At the time of each drop test, foam temperatures were measured by a thermometer inserted through a hole in the plastic burn out plugs, approximately 2 in. deep into the foam.

Weight

The weight of the completely assembled CTA-2, including impact limiter and simulated payload, was 9,360 pounds. This is only 2.3% below the value of 9,600 pounds used in calculations and had no significant effect on any CTA-2 response. The weight of the completely assembled CTA-1 was 9,350 pounds.

2.10.15.3 Test Facilities. The test pad is located in the 300 Area of the Hanford Site. It is constructed of ASTM C 150, Type II cemented aggregate, having dimensions of 13 ft 6 in. by 18 ft 6 in. by 70 in. thick. The concrete foundation monolith is encased with #6 steel reinforcing bar on 6-in. centers and was poured on soil compacted to 95% of maximum density. It is topped by a steel plate 125 in. by 70 in. by 8-1/2 in. thick. The weight of the impact test pad, including the steel plate, is estimated at 110 short tons. This weight is far in excess of the minimum factor of ten times the dropped weight of approximately 5 tons.

The puncture bars were designed to be in compliance with the requirements of 10 CFR 71.73(c)(2). A short (24-in.) bar was used for all puncture drop tests except CTA-1 tests Nos. 17 through 19 and CTA-2 test No. 3, where a long (80-in.) puncture bar was used. The puncture bars were firmly welded at the lower end to a 2-in.-thick mounting plate, and fastened to a 2-in.-thick mounting pad using 1-3/4-in.-diameter bolts. The mounting pad was firmly welded to the test pad. Figures 2.10.15.3-1 and 2.10.15.3-2 show photographs of the puncture bars.

2.10.15.4 Test Results. The following sections provide details of the results of free drop and puncture testing. The tests using CTA-1 were conducted from July 25 to 27, 1994, in the 300 Area of the Hanford Site. The tests using CTA-2 were conducted in November, 1995 at the same location.

2.10.15.4.1 Drop Test Sequence. The second certification test series, which used CTA-2, consisted of a series of four sets of tests as described in document WHC-SD-RTG-TP-018. Each set of tests included as a minimum a 4-ft free drop, a 30-ft free drop and a 40-in. puncture test. The first set consisted of CTA-2 tests Nos. 1, 2 and 3; the second set consisted of CTA-2 tests Nos. 4, 5 and 6; the third set consisted of CTA-2 tests Nos. 7, 8 and 9; and the fourth set consisted of CTA-2 tests Nos. 10 through 16. Damage caused by each of these tests is described in Section 2.10.16.4.3.

After the first test set was completed, the OCV containment O-ring seal was leakage rate tested, the OCV closure bolt removal torques were recorded, and the OCV was removed. The ICV containment O-ring seal was leakage rate tested and the ICV closure bolt retention torques were checked. The OCV was then reinstalled and the O-ring seal was leakage rate tested. This series of inspections was also performed after the second test set.

At the conclusion of the third test set, the OCV containment seal O-ring was leakage rate tested, the OCV closure bolt removal torques were measured, and the ICV containment seal O-ring was leakage rate tested. The ICV closure bolt removal torques were measured and the ICV was disassembled. All interaction between the simulated payload and ICV was noted. The CTA-2 unit was then reassembled and during the assembly process the ICV and OCV O-ring seals and the ICV and OCV entire containment boundaries were leakage rate tested.

At the conclusion of the fourth and final set of tests, all closure bolt removal torques were checked and the OCV and ICV O-ring seals and containment boundaries were leakage rate tested. All test data recorded for the second certification test series is included on the data sheets at the end of this appendix.

The first certification test series, using CTA-1, consisted of one sequential and continuous set of 19 drops. This test series included five 4-ft free drops followed by five 30-ft free drops, which were in turn followed by nine 40-in. puncture tests. During the testing, the impact limiter corner weld failed, exposing an unacceptable amount of foam. Also, at the conclusion of the testing, the ICV bolts were found to be loose. Both of these anomalies were considered to be failures. The package design was subsequently modified and a second certification test article (CTA-2) was fabricated. All of the 4-ft and 30-ft free drops from the first certification drop test series were repeated for the second certification drop test series. Four of the nine puncture tests performed during the first drop test series were repeated during the second drop test series and two new puncture tests were added. The five puncture tests that were not repeated are included in this appendix for completeness. The location of those puncture tests and resultant damage to the package are independent of the design changes that occurred between CTA-1 and CTA-2. Also included for completeness is the accelerometer data that was obtained during the first test series.

2.10.15-4.2 Helium Leakage Rate Test Results. After completing the first and second sets of free drop and puncture tests, CTA-2 was leakage rate tested in accordance with the procedure outlined in document WHC-SD-RTG-TC-017, Rev. 1. After completing the third set of free drop and puncture tests, CTA-2 was leakage rate tested in accordance with the procedures outlined in documents WHC-SD-RTG-TC-016, Rev. 1 and WHC-SD-RTG-TC-017, Rev. 1. After completing the fourth and final set of free drop and puncture tests, CTA-2 was leakage rate tested in accordance with procedure WHC-SD-RTG-016, Rev. 1.

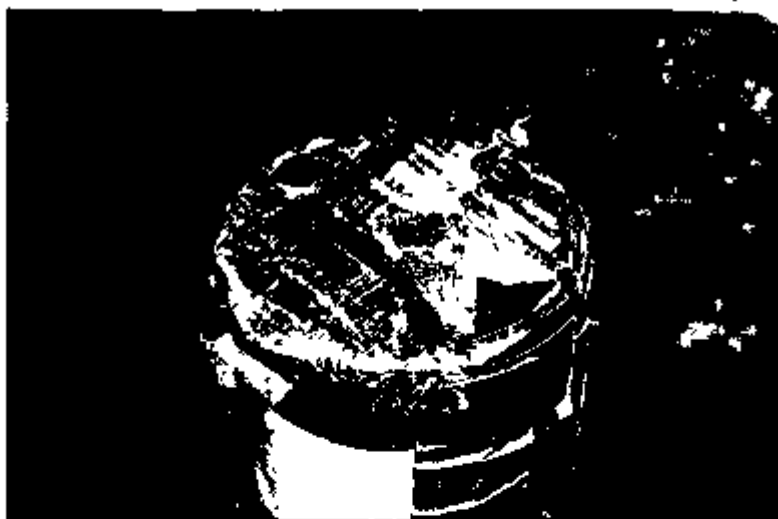


FIGURE 2.10.15.3-1. Short (24-in.) Puncture Bar.

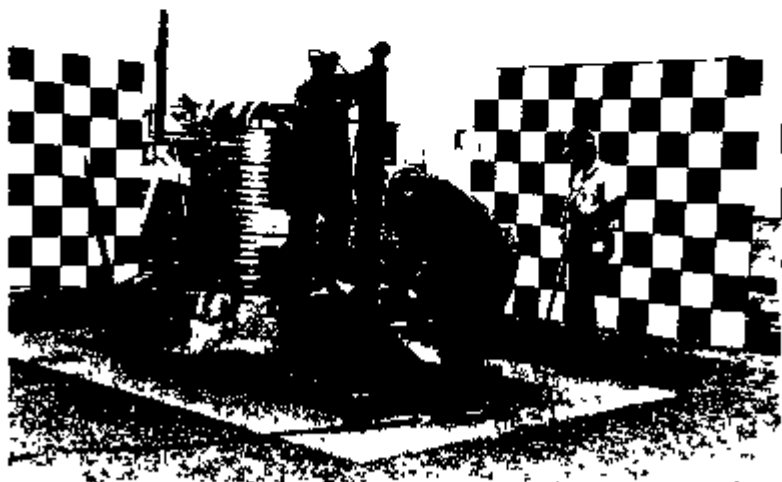


FIGURE 2.10.15.3-2. Long (80-in.) Puncture Bar.

Measured leakage rates (as air) for each set of drop tests are given in Tables 2.10.15.4.2-1 through 2.10.15.4.2-4 below. Note that the original leakage rate test data is for helium, the medium used in the testing. The rate for air is calculated by dividing the rate for helium by a factor of 2.6. The Westinghouse NDE Leak Test Procedure and Test Reports are attached to the end of this section.

**TABLE 2.10.15.4.2-1. Containment Vessel Leakage Rate Test Results,
After First Set of Drop Tests.**

Test location	Leakage rate, scc/sec (Air)	
	OCV	ICV
Primary closure O-ring seal	No detectable rate	No detectable rate
Containment boundary	Not applicable	Not applicable
Primary vent port	No detectable rate	No detectable rate
Secondary vent port	Not applicable	No detectable rate
Total vessel	Not applicable	Not applicable

**TABLE 2.10.15.4.2-2. Containment Vessel Leakage Rate Test Results,
After Second Set of Drop Tests.**

Test location	Leakage rate, scc/sec (Air)	
	OCV	ICV
Primary closure O-ring seal	No detectable rate	No detectable rate
Containment boundary	Not applicable	Not applicable
Primary vent port	No detectable rate	No detectable rate
Secondary vent port	Not applicable	No detectable rate
Total vessel	Not applicable	Not applicable

**TABLE 2.10.15.4.2-3. Containment Vessel Leakage Rate Test Results,
After Third Set of Drop Tests.**

Test location	Leakage rate, scc/sec (Air)	
	OCV	ICV
Primary closure O-ring seal	No detectable rate	No detectable rate
Containment boundary	5.5(10 ⁻⁶)	7.5(10 ⁻⁶)
Primary vent port	3.9(10 ⁻¹⁰)	No detectable rate
Secondary vent port	Not applicable	No detectable rate
Total vessel	5.5(10 ⁻⁶)	7.5(10 ⁻⁶)

TABLE 2.10.15.4.2-4. Containment Vessel Leakage Rate Test Results, After Fourth Set of Drop Tests.

Test location	Leakage rate, soc/sec (Air)	
	OCV	ICV
Primary closure O-ring seal	No detectable rate	No detectable rate
Containment boundary	4.35(10 ⁻⁶)	8.3(10 ⁻⁶)
Primary vent port	No detectable rate	No detectable rate
Secondary vent port	Not applicable	No detectable rate
Total vessel	4.35(10 ⁻⁶)	8.3(10 ⁻⁶)

The criterion for a leaktight condition is a leakage rate of 1.0(10⁻⁷) soc/sec of air. Thus, both levels of containment are leaktight, in satisfaction of the requirements of 10 CFR 71.

2.10.15.4.3 Localized Deformation Results and Photographs. Descriptions of the damage sustained by CTA-2 caused by each free drop and puncture event, including photographs, are given below. Actual data sheets used at the drop site to record damage are given in Section 2.10.15.5. Descriptions and photographs of the damage sustained by CTA-1 from the puncture events is also included. Drop orientations are fully described in Appendix 2.10.9.

CTA-2 first set of drop tests.

CTA-2 Test No. 1. The CTA-2 was oriented bottom-down at 10° from the vertical and the drop height was 4 ft. A small amount of damage to the impact limiter was caused by this drop. The most notable damage was a very slight bulge on the side of the impact limiter. See Figures 2.10.15.4.3-1 and 2.10.15.4.3-2.

CTA-2 Test No. 2. The CTA-2 was oriented bottom-down at 10° from the vertical and the drop height was 30 ft. As with the 4-ft version of this drop, the initial point of impact was located at 75° clockwise (CW) (when viewed from above) from the electrical feed-through. The damage to the impact limiter was similar to that incurred during the 4-ft drop, but of a greater magnitude. See Figures 2.10.15.4.3-3 and 2.10.15.4.3-4.

CTA-2 Test No. 3. This was a 40-in. puncture test with the CTA-2 oriented top-down and the point of impact was located on the outer top surface of the impact limiter. The impact circumferential location was next to the loosest impact limiter bolt (Bolt #7), which was 75° CW (when viewed from above) from the electrical feed-through location. The long (80-in.) puncture bar was used. The resulting dent was 5/16 in. deep and there was no evidence of any movement of the impact limiter relative to the test article. See Figure 2.10.15.4.3-5.

At the conclusion of the first set of drop tests using the CTA-2 unit, the following inspections/leakage rate tests were performed.

- Impact limiter bolt removal torques and lengths
- OCV containment O-ring seal leakage rate test
- OCV closure bolt removal torques and lengths
- ICV containment O-ring seal leakage rate test

ICV closure bolt retention torques.

The data sheets for each of these operations are included at the end of this appendix. In summary, one impact limiter bolt stretched approximately 0.023 in., the OCV closure bolts did not lose any torque and did not stretch, the OCV and ICV containment O-rings were leaktight, and the ICV closure bolt torque values were higher than the retention check torque of 78 ft-lb.

Once these inspections were completed, the ICV closure bolts were retorqued to their original pre-test values, the ICV containment O-ring seal was leakage rate tested, the OCV was reassembled, the OCV containment O-ring seal was leakage rate tested, and the impact limiter was reinstalled using new attachment bolts. It was noted that the torque wrench did not move when the pre-test torque was applied to the ICV closure bolts. This was a good indication that the bolts had retained all of their pre-test torque values.

CTA-2 second set of drop tests.

CTA-2 Test No. 4. This was a bottom-down, c.p.-over-corner, 4-ft free drop. The CTA-2 was oriented so that the impact was directed at the electrical feed-through. This drop produced an oval-shaped damaged area that was approximately 2 ft long. No cracking of the impact limiter corner joints was observed. See Figures 2.10.15.4.3-6 and 2.10.15.4.3-7.

CTA-2 Test No. 5. This was a repeat of CTA-2 Test No. 4 except the drop height was 30 ft. The eye-shaped damage area was 42 in. long and 18 in. wide and caused a total crush depth of 5.6 in. The impact limiter corner joint welds remained intact and did not crack. See Figures 2.10.15.4.3-8 and 2.10.15.4.3-9.

CTA-2 Test No. 6. This was a 40-in. puncture test directed at the damage created by the c.p.-over-bottom impact limiter corner free drops (CTA-2 Tests No. 4 and No. 5). The impact with the puncture bar caused a localized 10-in.-wide-by-1.7-in.-deep indentation on the bottom surface of the impact limiter. No welds were cracked and the impact limiter outer shell material was not ruptured. See Figures 2.10.15.4.3-10 and 2.10.15.4.3-11.

At the conclusion of the second set of drop tests using the CTA-2 unit, the inspection/leakage rate tests that were performed after the first set of CTA-2 drop tests were repeated. The data sheets for these operations are included at the end of this appendix. In summary, no impact limiter bolts broke, no significant movement of the impact limiter relative to the OCV base occurred, the OCV closure bolts did not lose any torque and did not stretch, the OCV and ICV containment O-rings were leaktight, and the ICV closure bolt torque values were higher than the retention check torque of 78 ft-lb.

Once the inspections were completed, the same reassembly procedure as performed after the first set of tests was completed. New impact limiter attachment bolts were installed.

CTA-2 third set of drop tests.

CTA-2 Test No. 7. This was a 4-ft, bottom-down, flat-on-end free drop. This drop caused only slight changes to the previous damage done to the impact limiter. See Figure 2.10.15.4.3-12.

CTA-2 Test No. 8. This was a repeat of CTA-2 Test No. 7 except the drop height was 30 ft. This drop caused a flattening of the previous deformations that protruded from the bottom of the impact limiter. See Figures 2.10.15.4.3-13 and 2.10.15.4.3-14.

CTA-2 Test No. 9. This was a 40-in. puncture test with the edge of the puncture bar directed at the weld between the impact limiter side shell and the lower corner joint. The point of impact was located 75° CW (when viewed from above) from the electrical feed-through and was directed through the CTA-2 c.g. The resulting localized deformation was approximately 3.5 in. deep. There were no indications of cracking or any other weld failure. Also, the impact limiter sidewall was not breached. See Figures 2.10.15.4.3-15.

At the conclusion of the third set of drop tests on the CTA-2 unit, the entire test article was disassembled and inspected. The OCV and ICV closure bolt removal torques and lengths were recorded, the OCV and ICV containment O-ring seals were leakage rate tested, and the OCV and ICV entire containment boundaries were leakage rate tested. The data obtained from these operations is included at the end of this appendix. In summary, no impact limiter bolts broke, no significant movement of the impact limiter relevant to the OCV base occurred, the OCV and ICV closure bolts retained all of their pre-test torque, and the OCV and ICV O-ring seals were leaktight. The OCV and ICV structural (non-O-ring) containment boundaries were also leaktight (6.6 x 10⁻⁶ /cc/sec, air and 7.6 x 10⁻⁶ /cc/sec, air respectively).

It was noted that the majority of the ICV closure bolt washers were fractured. The fractured washers did not cause the ICV closure bolts to loosen. The significance of the fractured washers is discussed in Section 2.10.15.4.7. New ICV closure bolt washers were installed prior to the last set of drop tests. New ICV and OCV containment O-ring seals were also installed.

CTA-2 fourth set of drop tests. The fourth and final set of drop tests using the CTA-2 unit consisted of seven separate tests as listed below.

CTA-2 Test No. 10. This was a 4-ft. side-slip-down free drop. The point of impact was 80° CCW from the electrical feed-through when viewed from above the CTA-2. The CTA-2 axis was oriented at 18° from the horizontal and the fins contacted the drop pad first. Three fins were distorted but there was no other contact with the top of the test article. The side of the impact limiter was flattened slightly. No impact limiter welds cracked or showed any other sign of failure. See Figures 2.10.15.4.3-16 and 2.10.15.4.3-17.

CTA-2 Test No. 11. This was a 4-ft. top-end-down, flat-on-end free drop. This drop resulted in a uniform flattening of the CTA-2 fins. The personnel shield was only slightly damaged and still intact. See Figure 2.10.15.4.3-18.

CTA-2 Test No. 12. This was a repeat of CTA-2 Test No. 10, except the drop height was 30 ft. As with the 4-ft version of this drop, the primary impact was at the top of the test article. The impact caused minor cracking of the fin and upper coolant jacket welds that were directly beneath the point of impact. The damage to the impact limiter was a flat area 32 in. long at the top that tapered to negligible damage at the bottom. The depth of crush was 4.0 in. radially inward at the top of the impact limiter and a negligible amount at the bottom. See Figures 2.10.15.4.3-19 and 2.10.15.4.3-20.

CTA-2 Test No. 13. This was a 30-ft. top-end-down, flat-on-end free drop. The fins and personnel barrier collapsed until the OCV head contacted the drop test pad. See Figures 2.10.15.4.3-21 and 2.10.15.4.3-22. The top cover screen on the personnel barrier was removed after this test.

CTA-2 Test No. 14. This was a 40-in. puncture test with the puncture bar normal to the OCV sidewall through the CTA-2 c.g. The test article was oriented with the electrical feed-through down. The resulting dent depth in the coolant jacket was slightly under 1 in. The ICV sidewall had a dent 3/8 in. in depth. See Figures 2.10.15.4.3-23 and 2.10.15.4.3-24.

CTA-2 Test No. 15. The CTA-2 was oriented top-down at 9° from vertical so that the puncture bar would contact the unreinforced area of the OCV head. The drop height between the puncture bar and the OCV head was 45 in. to simulate conservatively a 40-in. puncture drop onto the personnel barrier screen. The OCV head dent depth was approximately 1-1/4 in. See Figure 2.10.15.4.3-25.

CTA-2 Test No. 16. This was a 40-in. puncture test that was directed at the center line of one of the impact limiter plastic melt plugs. The puncture bar was directed through the CTA-2 c.g. and 120° CW from the electrical feed-through location. The impact caused the upper weld around the plastic melt plug holder to fail, which in turn allowed the sidewall of the impact limiter to rip open a small amount. The opening in the impact limiter sidewall was approximately 8-3/4 in. long and varied in width from 0 to 1-1/4 in. The total amount of exposed impact limiter foam was estimated to be 12.7 in³. See Figure 2.10.15.4.3-26. This small amount of exposed foam has no effect on the package's ability to withstand the HAC fire (see Section 3.5).

CTA-1 puncture tests. As noted in Section 2.10.15.1, five of the nine puncture tests performed on the CTA-1 unit were not repeated during the second certification test series, which used the CTA-2 unit. For completeness, the results of these five CTA-1 puncture tests are included below.

CTA-1 Test No. 12. The 40-in. puncture was performed on the bottom of the impact limiter, through the CTA-1 c.p., and located on the low-density foam next to the joint with the high-density foam. The initial impact was 20 in. from the impact limiter center, with the corner of the puncture bar contacting first. The resulting dent was 2-1/2 in. deep, with a surrounding damage area 15 in. in diameter. The puncture bar did not penetrate the impact limiter shell, and there were no signs of impending rupture in the damaged area. There was also a smaller, secondary impact. See Figures 2.10.15.4.3-27 and 2.10.15.4.3-28.

CTA-1 Test No. 13. This 40-in. puncture was directed through the CTA-1 c.g. onto the impact limiter side shell, in line with the OCV vent port. The resulting dent was 3 in. deep, with a surrounding damage area 15 in. in diameter. The puncture bar did not penetrate the impact limiter shell, and there were no signs of impending rupture in the damaged area. Further, the OCV vent port was leaktight after testing. See Figures 2.10.15.4.3-29 and 2.10.15.4.3-30.

CTA-1 Test No. 15. This 40-in. puncture using CTA-1 was similar to CTA-2 Test No. 14, except with the puncture bar at an oblique (45°) angle to the OCV surface. The puncture bar contacted the coolant jacket at 45° CCW from the electrical feed-through, directed through the CTA-1 c.p. The maximum dent depth was 1-1/2 in. The ICV sidewall had a dent 0.22 in. in depth. The coolant jacket ribs were heavily damaged, but no damage (other than inward deformation) occurred to the OCV sidewall. See Figures 2.10.15.4.3-31 and 2.10.15.4.3-32.

CTA-1 Test No. 18. This 40-in. puncture was directed at the thermal shield of the OCV. The 80-in.-long puncture bar was used, and contacted the top of the thermal shield 1 in. inboard from its outside edge and 30° CCW from the electrical feed-through. The CTA-1 was oriented at 30° from the vertical. The resulting dent was 1-1/4 in. deep at its center and of lesser depth elsewhere. The surrounding damaged area in the thermal shield was 7 in. wide. Some damage was inflicted on the adjacent portion of the coolant jacket. Also, the upper relief valve nipple was crushed by secondary impact with the puncture bar. See Figures 2.10.15.4.3-33 and 2.10.15.4.3-34.

CTA-1 Test No. 19. The last puncture using CTA-1 was directed at an impact limiter bolt

access tube. The CTA-1 was oriented vertically, and the puncture bar contacted the bolt access tube located 330° CCW from the electrical feed-through. The 80-in.-long puncture bar was used. Portions of two adjacent OCV closure bolt access tubes were also impacted. The closure bolt access tubes buckled from the impact. The maximum deformation of the thermal shield was 3/4 in. Also, one of the coolant jacket nipples was crushed by secondary impact with the puncture bar. See Figures 2.10.15.4.3-35 and 2.10.15.4.3-36.

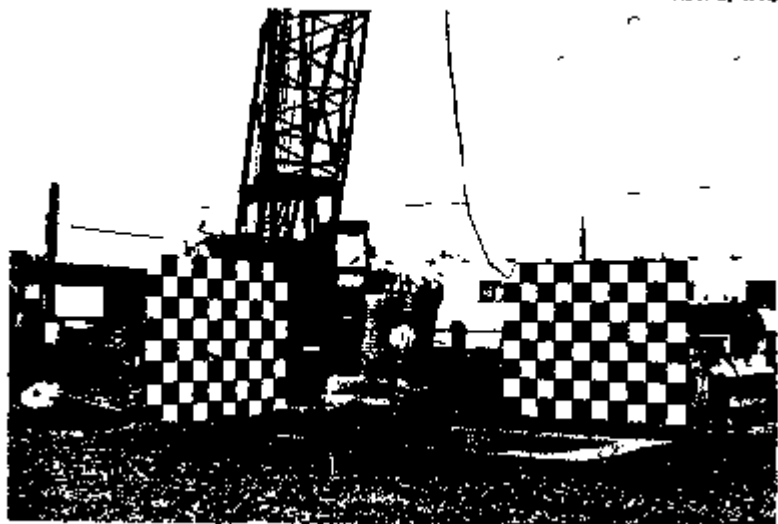


FIGURE 2.10.15.4.3-1. CTA-2 Drop No. 1, 4-ft, 10° from Vertical.



FIGURE 2.10.16.4.3-2. CTA-2 Drop No. 1, 4-ft, 10° from Vertical). Side View of Drop Damage.

BEST COPY AVAILABLE

2.10.15-15

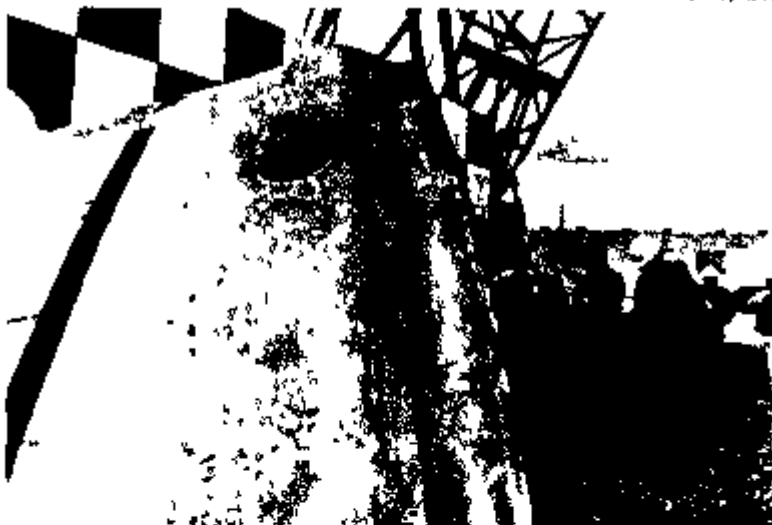


FIGURE 2 10 15 4 3-3 CTA-2 Drop No. 2, 30-ft, 10° from Vertical

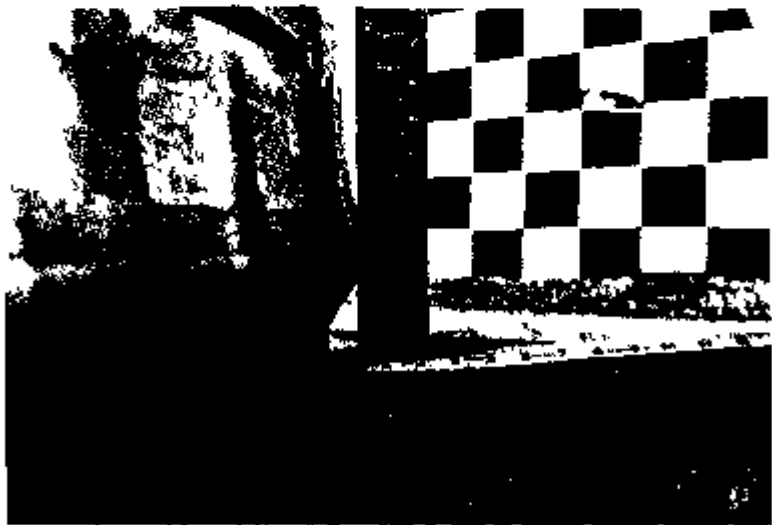


FIGURE 2 10 15 4 3-4 CTA-2 Drop No. 2, 30-ft, 10° from Vertical



FIGURE 2.10.15.4.3-6. CTA-2 Drop No. 3, 40-in. Puncture, Tap-down on Impact Limiter Edge.



FIGURE 2.10.15.4.3-6. CTA-2 Drop No. 4, 4-ft. C.G. over Impact Limiter Bottom Corner.

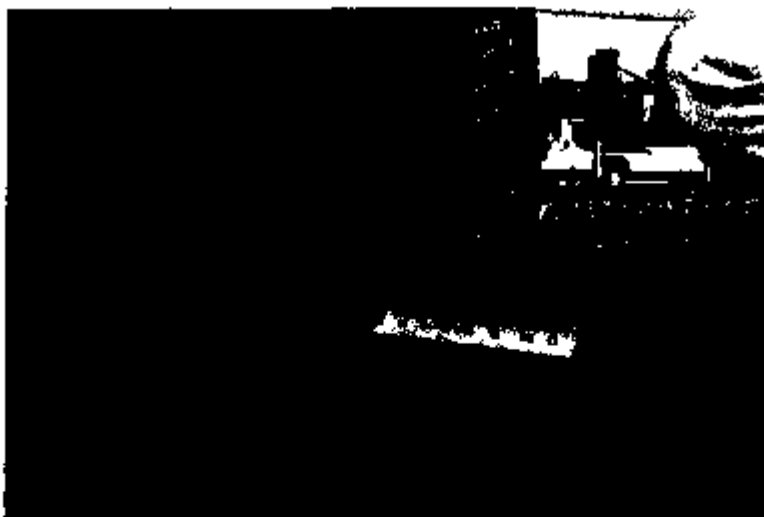


FIGURE 2.10.15.4.3-7. CTA-2 Drop No. 4, 4-ft. C.G. over Impact Limiter Bottom Corner.



FIGURE 2.10.15.4.3-8. CTA-2 Drop No. 6, 30-ft. C.G. over Impact Limiter Bottom Corner.



FIGURE 2 10 15 4 3-8 CTA-2 Drop No. 5, 30-ft, C G over Impact Limiter Bottom Corner



FIGURE 2 10 15 4 3 10 CTA 2 Drop No. 8, 40-in Puncture on Previous
C G over corner Damage

BEST COPY AVAILABLE



FIGURE 2.10.15.4.3-11. CTA-2 Drop No. 6, 40-in. Puncture on Previous C.O.-over-corner Damage.

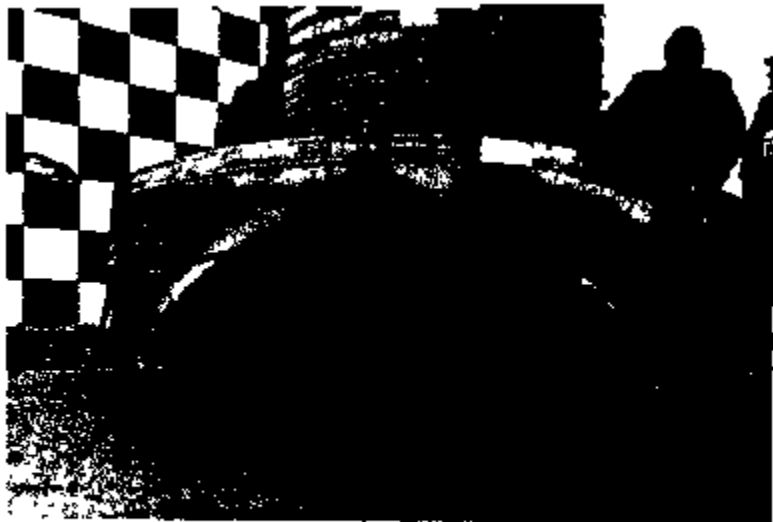


FIGURE 2.10.15.4.3-12. CTA-2 Drop No. 7, 4-ft, Bottom End Down.

BEST COPY AVAILABLE

2.10.15-20

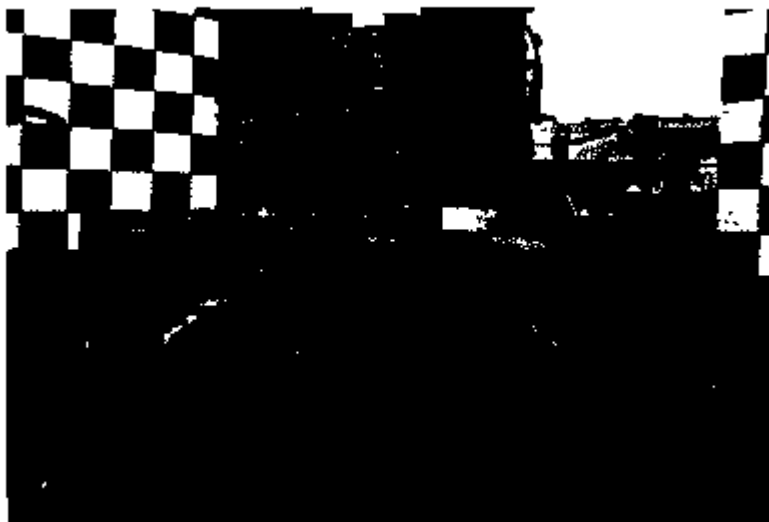


FIGURE 2 10.15.4.3-13. CTA-2 Drop No. 8, 30-ft Bottom End Drop.



FIGURE 2 10.15.4.3-14. CTA-2 Drop No. 8, 30-ft, Bottom End Drop.



FIGURE 2 10 16 4 3 15 CTA-2 Drop No. 9, 40-in. Puncture at Impact Limiter Lower Corner Weld



FIGURE 2 10 16 4 3 16 CTA-2 Drop No. 10, 4-ft. Side Slakedown, Showing View of Primary Impact

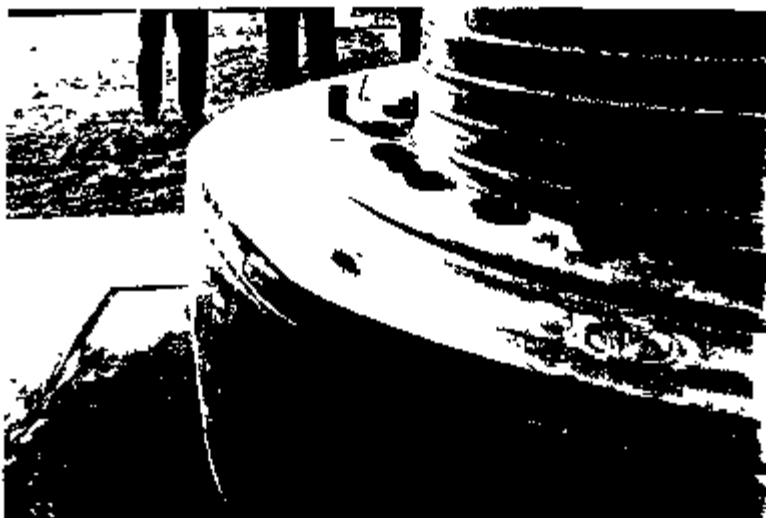


FIGURE 2.10 15.4 3-17. CTA-2 Drop No. 10, 4-ft. Side Slatdown, Showing View of Secondary Impact.



FIGURE 2 10.16.4.3-18 CTA-2 Drop No. 11, 4-ft. Top End Down.



FIGURE 2.10.15.4.3-19. CTA-2 Drop No. 12, 30-ft, Side Stepdown, Showing View of Primary Impact.



FIGURE 2.10.15.4.3-20. CTA-2 Drop No. 12, 30-ft, Side Stepdown, Showing View of Secondary Impact.



FIGURE 2 10 15 4 3-21 CTA-2 Test No. 13, 30-ft. Top End Down



FIGURE 2 10 15 4 3-22 CTA 2 Test No. 13, 30-ft. Top End Down

BEST COPY AVAILABLE ^{2 10 15 25}



FIGURE 2.10.15.4.3-23. CTA-2 Test No. 14, 40-in. Puncture on Side of Package Through C.G.



FIGURE 2.10.15.4.3-24. CTA-2 Test No. 14, 40-in. Puncture Showing Closeup of Damage.



FIGURE 2.10.16.4.3-26. CTA-2 Test No. 18, 40-in. Puncture, Top End Down.



FIGURE 2.10.16.4.3-26. CTA-2 Test No. 18, 40-in. Puncture Directed at Impact Liner Melt Plug.

BEST COPY AVAILABLE

2 10.15-27

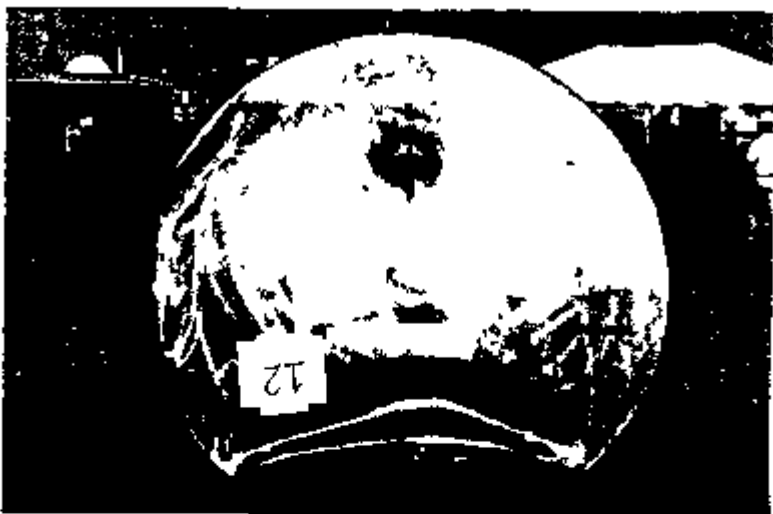


FIGURE 2 10 15 4 3-27 CTA-1 Test No. 12, 40-in Puncture, C G over Foam Transition



FIGURE 2 10 15 4 3-28 CTA-1 Test No. 12, 40 in Puncture Showing Closeup of Damage

2 10 15-28

BEST COPY AVAILABLE



FIGURE 2.10.15.4.3-29. CTA-1 Test No. 13, 40-in. Puncture on Side of Liner, C.G. over Beal Test Port.

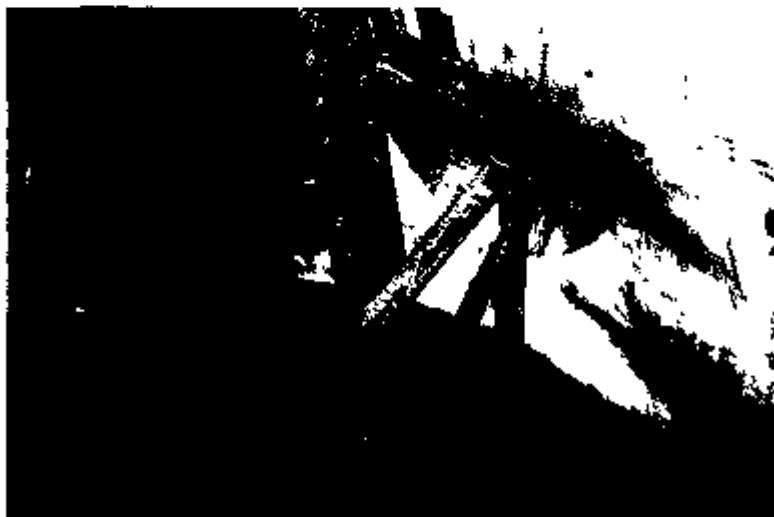


FIGURE 2.10.15.4.3-30. CTA-1 Test No. 13, 40-in. Puncture Showing Closeup of Damage.



FIGURE 2.10.15.4.3-31. CTA-1 Test No. 15, 40-in. Puncture Oblique to Package Side Through C.G.



FIGURE 2.10.15.4.3-32. CTA-1 Test No. 15, 40-in. Puncture Showing Closeup of Damage.
Note: Picture was rotated CCW.

BEST COPY AVAILABLE

2.10.15-30



FIGURE 2 10 15 4 3 33 CTA 1 Test No. 18, 40-m Puncture, Top End Down, Oblique on Top of Thermal Shield



FIGURE 2 10 15 4 3 34 CTA-1 Test No. 18, 40-m Puncture, Showing Closeup of Damage

BEST COPY AVAILABLE

2 10 15 31



FIGURE 2.10.15.4.3-35. CTA-1 Test No. 19, 40-in. Puncture, Top End Down, Vertical on Impact Limiter Bolt Tube.



FIGURE 2.10.15.4.3-36. CTA-1 Test No. 19, 40-in. Puncture Showing Closeup of Damage.

2.10.15-32

BEST COPY AVAILABLE

2.10.15.4.4 Accelerometer Results. During the first certification drop test series, CTA-1 was instrumented with active and passive accelerometers. (CTA-1 was not instrumented for the puncture drops.) Accelerometer instrumentation was not used during the second certification test series, which used CTA-2. For completeness, the instrumentation set-up, filtering, and data reduction from the first certification test series are given in the sections below.

2.10.15.4.4.1 System Configuration and Data Acquisition. Because of the compact shape of the RTG package, the rigid body impact at the center of gravity of the package was the parameter of primary interest. For this reason, most of the transducers (and passive indicators) were located at or near the c.g. of CTA-1. A triaxial set of accelerometers was also located at 30 in. above the c.g. to measure package rotations.

Active accelerometers were mounted as shown in Figure 2.10.15.4.4.1-1. There were nine channels of data from three triaxial sets. The axes of measurement, relative to CTA-1, were axial, radial, and circumferential. Set "a" was located at the height of the c.g. (25.2 in. from the bottom of the impact limiter) and 270° CCW (viewed from above) from the electrical feed-through. Set "c" was mounted 30 in. directly above set "a". Set "b" was located at the height of the c.g., at 90° CCW from the electrical feed-through. Each set was secured to a mounting block using four 1/4-in.-diameter cap screws. Each mounting block consisted of a solid piece of 304L stainless steel, welded to two coolant jacket ribs using at least four 1/8-in. fillet welds, as shown in Figure 2.10.15.4.4.1-2 and -5. Signals from "a" and "c" were fed to a common junction block, from which they were carried by a single cable to the data acquisition equipment. Signals from "b" were carried by a separate cable. Transducers were protected from secondary damage or falling rigging with 3/16-in.-thick steel covers.

The transducers were made by Endevco[®], and were of the piezoresistive type with ± 750 g capacity, including dc capability. The flat portion of the response is 0 - 2000 Hz, ± 100 Hz, with a resonance of 25 kHz and 0.5% of critical damping. Accuracy was 1% of full scale, or 7.5 g.

Passive accelerometers (Impact-o-graph[®]**, manufactured by Chatsworth Data Corporation) were mounted as shown in Figures 2.10.15.4.4.1-3 and 2.10.15.4.4.1-6. They consisted of trip-level indicators of ball-and-spring construction. A bank of three passive accelerometers having trip levels of 200, 300, and 400 g was mounted at approximately 260° CCW of the electrical feed-through, with the middle (300 g) passive accelerometer at the c.g. height, in close proximity to active accelerometer set "a".

Active accelerometer signals were carried to signal conditioning equipment, and recorded on analog tape using a tape recorder having a frequency response well in excess of 2 kHz. Subsequent to the drop event, the data was filtered using a Cauer Elliptic analog filter. Then the data was digitized in a Tektronix 2630 analyzer using a sampling frequency of 2.50 times the filter cutoff frequency, and downloaded to a laptop PC running Tektronix software for display. Figure 2.10.15.4.4.1-4 shows the schematic of the instrumentation, indicating an option to input raw data to the Tektronix 2630.

[®]Endevco is a registered trademark of Meggitt Aerospace/Endevco Corporation Division.

^{**}Impact-o-graph is a registered trademark of the Chatsworth Data Corporation.

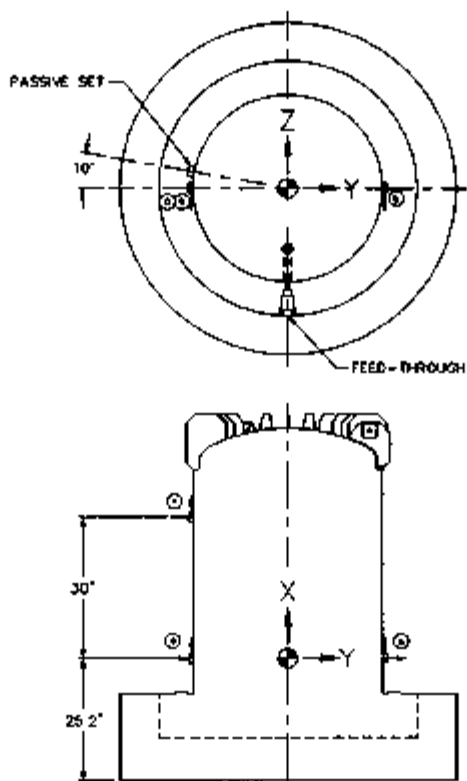


FIGURE 2.10.15.4.4.1-1. Accelerometer Mounting.

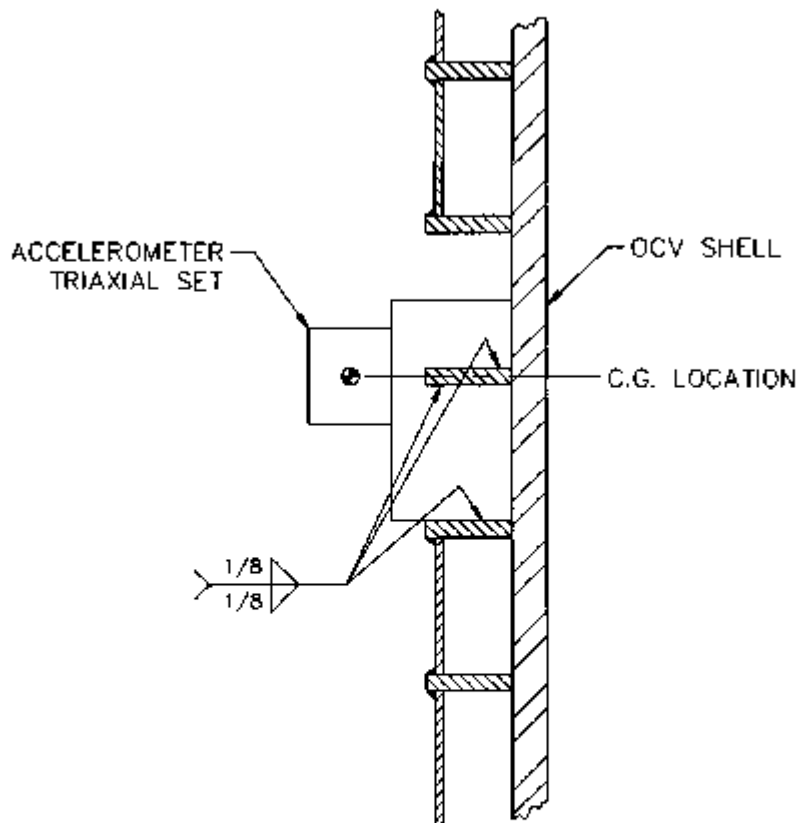


FIGURE 2.10.15.4.1-2. Active Accelerometer Mounting Block Details.

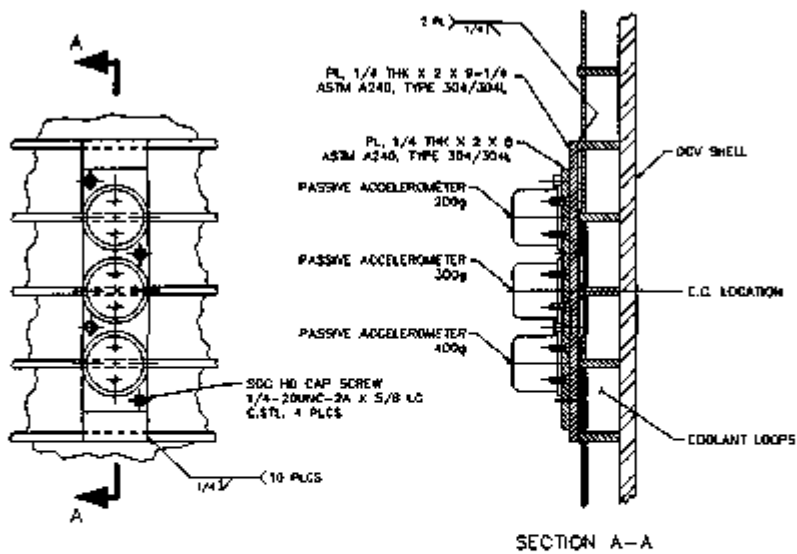


FIGURE 2.10.15.4.4.1-3. Passive Accelerometer Mounting Details.

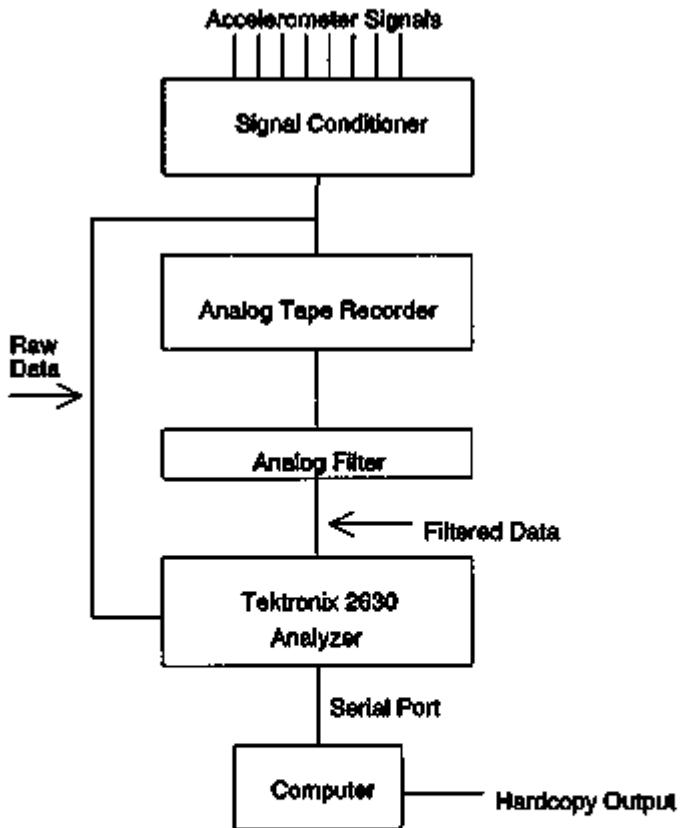


FIGURE 2.10.15.4.4.1-4. Data Acquisition System Schematic.

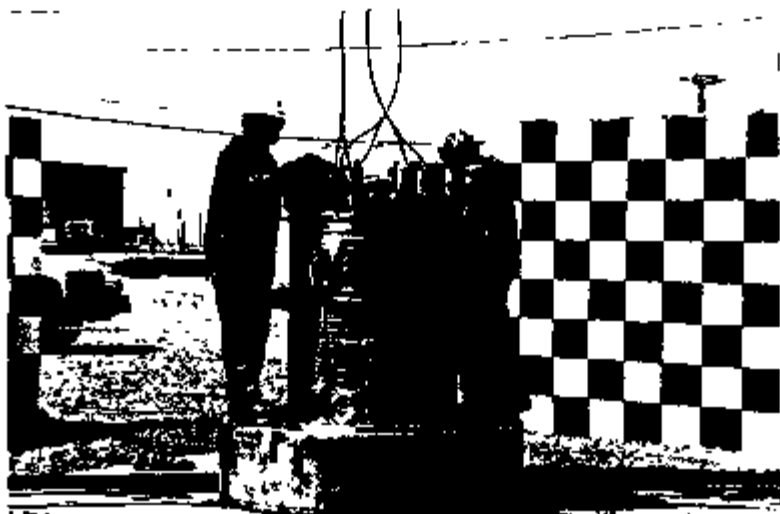


FIGURE 2.10.15.4.4.1-5. Package Before Testing. Shows Accelerometer Locations "a" (lower) and "c" (upper).

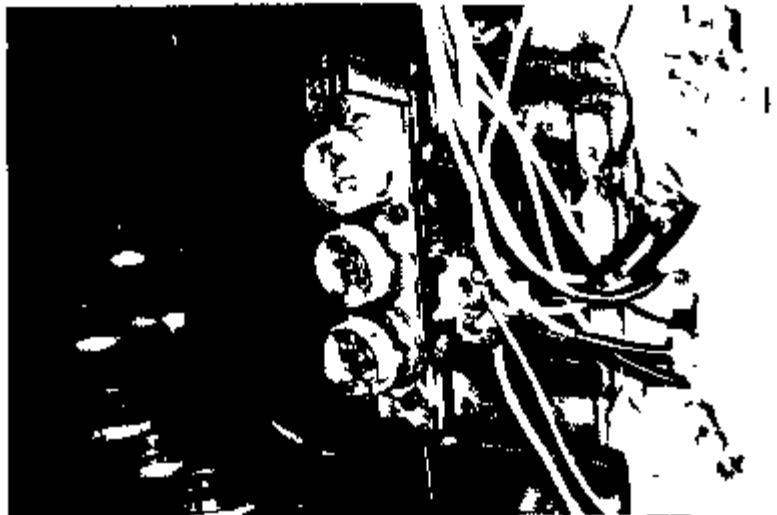


FIGURE 2.10.15.4.4.1-6. Accelerometer Mounting. Showing the Three Passive Accelerometers on the Left and Active Accelerometer Position "a" to the Right.

2.10.15.4.4.2 Filtering. The data was filtered using a low pass filter with a cutoff frequency of 300 Hz. This cutoff frequency was chosen to eliminate vibratory responses from the transducer signals, while preserving the entire value of the rigid-body impact. The pulse length of the impacts were approximately 20 ms and greater, and therefore the maximum equivalent pulse "frequency" would be $1/(2 \times 0.02) = 25$ Hz or less. This was far below the filter frequency of 300 Hz and demonstrates that there was no risk of loss of the rigid body signal. Inspection of the filtered time histories shows that the use of even lower cutoff frequencies could be justified. A study was done to evaluate the effect of filter frequency on peak impact level. The location "a"-axial signal from the second 30-ft free drop (CTA-1 test No. 7, 30-ft. c.g. over corner) was filtered at various levels, with the results as shown in Table 2.10.15.4.4.2-1 below. The results change little for cutoff frequencies in the range of 100 to 200 Hz.

TABLE 2.10.15.4.4.2-1 Effect of Cutoff Frequency.

Cutoff Freq., Hz	Peak Impact, g
Unfiltered	180
500	95
300	77
200	67
100	61

Before performing the free drop tests, modal testing was performed by striking the CTA with a small weight in numerous locations. The results were post-processed to form frequency response spectra of CTA-1. The lowest response of significance was approximately 850 Hz.

2.10.15.4.4.3 Accelerometer Reduced Data. For each free drop in the NCT and HAC test series, a filtered time history of each accelerometer signal was prepared. From the time history, a peak value was extracted and entered into Table 2.10.15.4.4.3-1 (NCT) and Table 2.10.15.4.4.3-2 (HAC). Calculations are shown in the tables to determine resultant impacts in cases where the drop axis was not parallel to an accelerometer axis. It was found that in most cases in which the accelerometer axis was normal to the impact of CTA-1, the resultant signal was dominated by ringing, which appears as oscillation at approximately the filter frequency, with an essentially zero or insignificant average value. These cases are not needed to determine c.g. impacts and are indicated in the tables as dominated by ringing (DR). In other cases, no data exists because of transducer failure, and these cases are indicated in the tables as no data (ND). The maximum value for the drop is indicated by bold type. The data is identified by location and direction, as shown in the matrix below. Passive accelerometer results for CTA-1 are given in Table 2.10.15.4.3-3.

	Loc. a	Loc. b	Loc. c
Axial	a_x	b_x	c_x
Radial	a_y	b_y	c_y
Circumf	a_z	b_z	c_z

Figures 2.10.15.4.4.3-1 to 2.10.15.4.4.3-14 show the time histories for the important signals listed in Table 2.10.15.4.4.3-2, filtered at 300 Hz (the HAC results).

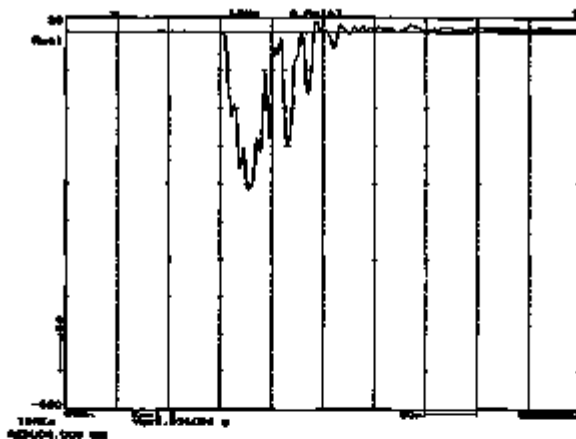


Figure 2.10.15.4.4.3-1. Test No. 6, 30-ft. Bottom Down, Near Vertical, A-Axial Accelerometer Time History.

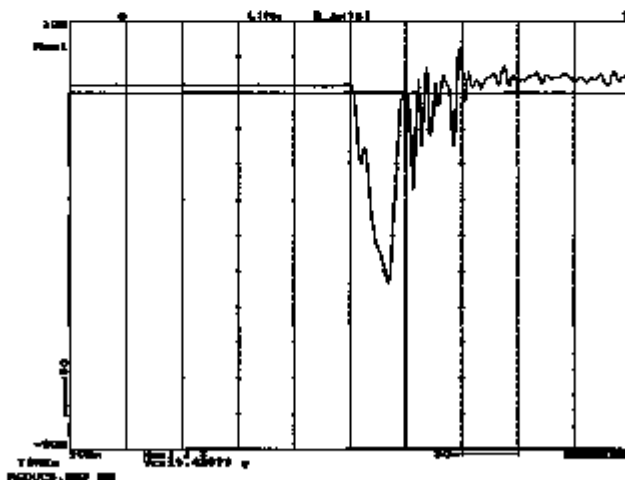


Figure 2.10.15.4.4.3-2. Test No. 6, 30-ft. Bottom Down, Near Vertical, B-Axial Accelerometer Time History.

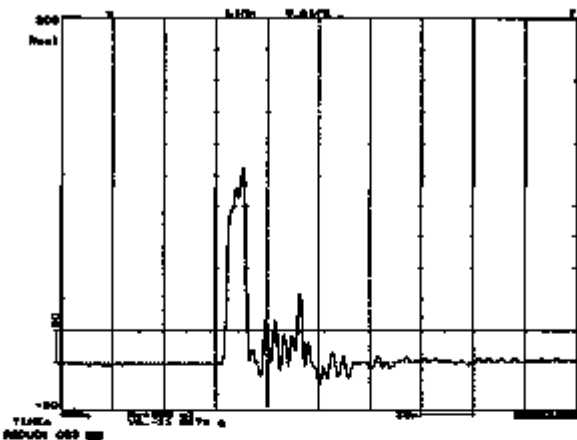


Figure 2 10 15 4 4 3 3 Test No. 6, 30-ft, Bottom Down, Near Vertical, C Circumferential Accelerometer Time History

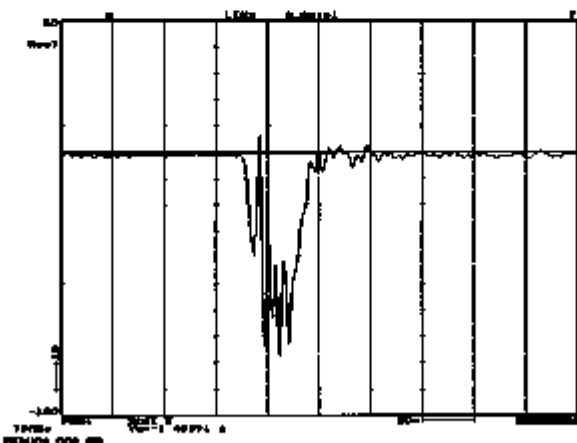


Figure 2 10 15 4 4 3-4 Test No. 7, 30-ft, C.G. over Corner, A-Axial Accelerometer Time History

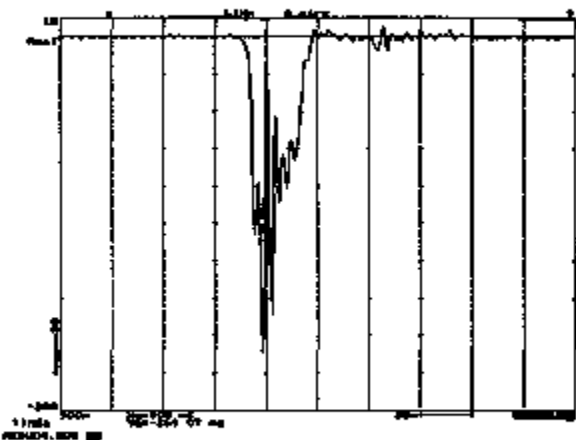


Figure 2.10.15.4.4.3-5 Test No. 7, 30-ft, C.G. over Corner.
A-Circumferential Accelerometer Time History.

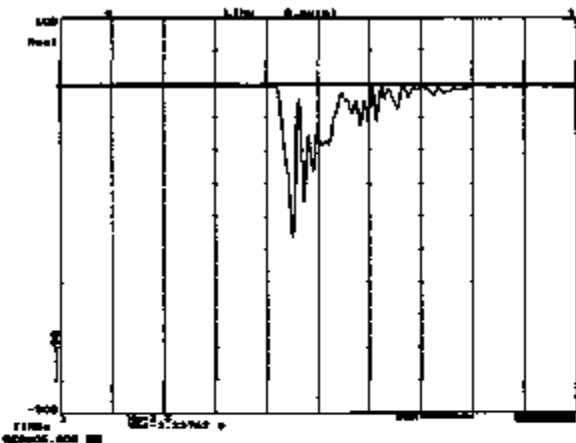


Figure 2.10.15.4.4.3-6 Test No. 7, 30-ft, C.G. over Corner.
B-Axial Accelerometer Time History.

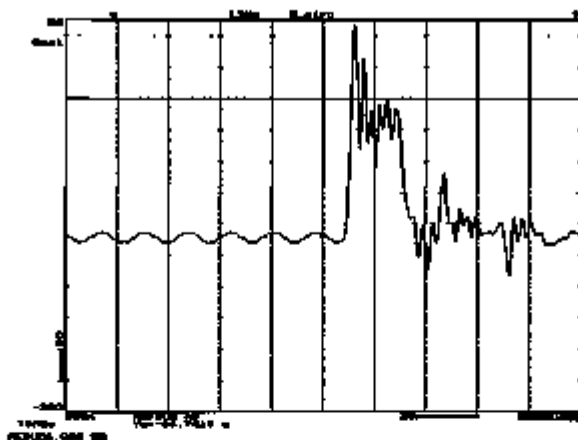


Figure 2.10.15.4.4.3-7. Test No. 7, 30-ft, C.G. over Corner,
B-Circumferential Accelerometer Time History.

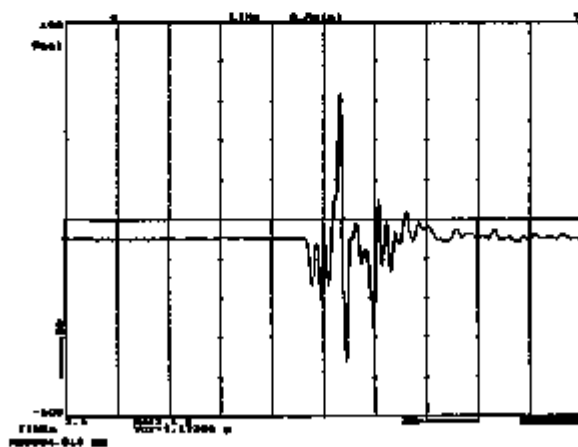


Figure 2.10.15.4.4.3-8. Test No. 8, 30-ft, Side Stepdown,
A-Axial Accelerometer Time History.

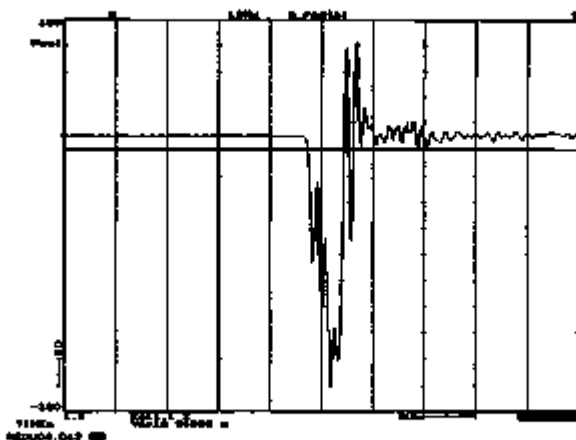


Figure 2.10.15.4.4.3-9. Test No. 8, 30-ft. Side Slapdown,
A-Radial Accelerometer Time History.

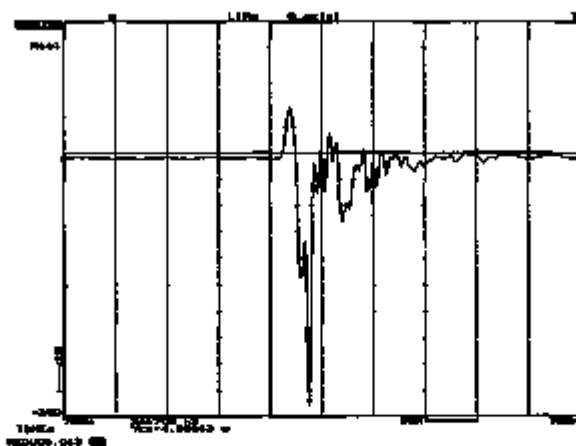


Figure 2.10.15.4.4.3-10. Test No. 8, 30-ft. Side Slapdown,
B-Axial Accelerometer Time History.

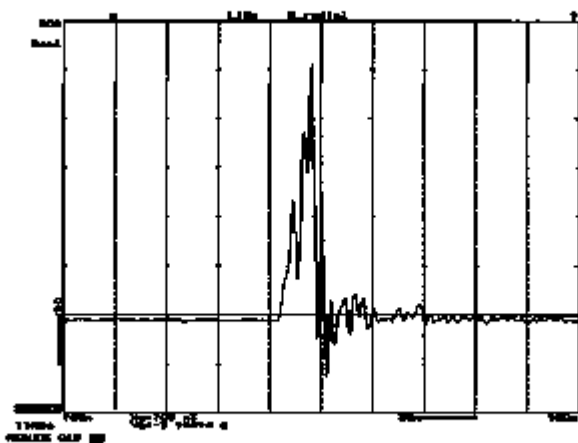


Figure 2 10 15 4 4 3-11 Test No. 8, 30-ft, Side Slapdown,
B-Radial Accelerometer Time History

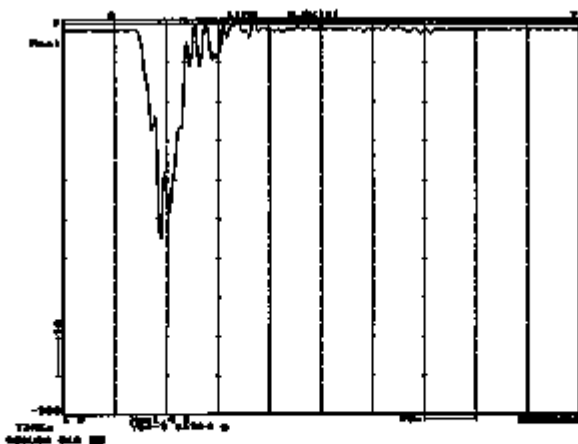


Figure 2 10 15 4 4 3-12 Test No. 8, 30-ft, Flat on Bottom,
A-Axial Accelerometer Time History

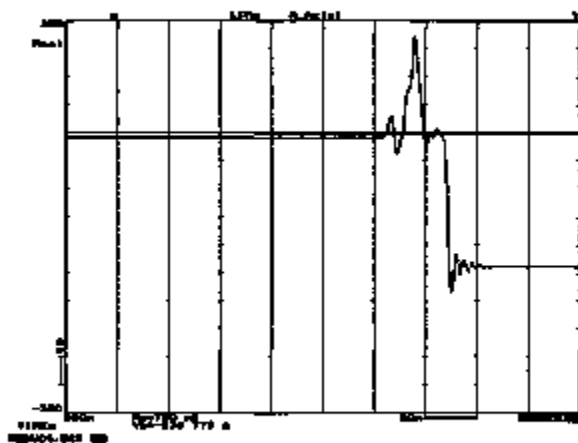


Figure 2.10.15.4.3-13 Test No. 10, 30-ft, Flat on Bottom,
A-Axial Accelerometer Time History.

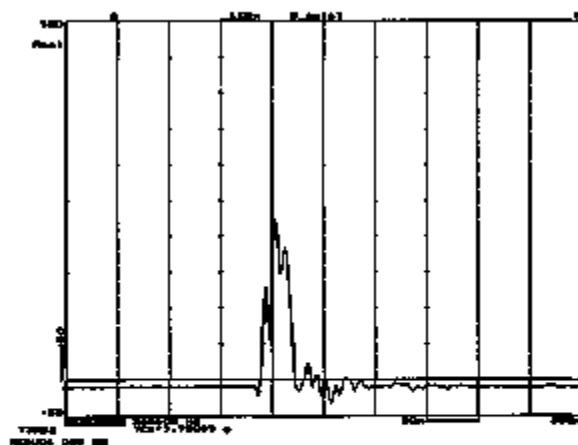


Figure 2.10.15.4.3-14 Test No. 10, 30-ft, Flat on Bottom,
C-Axial Accelerometer Time History.

TABLE 2.10.15.4.4.3-1. NCT Accelerometer Results (CTA-1).

Test	a_x	a_y	a_z	b_x	b_y	b_z	c_x	c_y	c_z
1	data:	50 g	DR ¹	16 g	53 g	DR	ND ²	ND	ND
		c.g accel.		c.g accel.			angular		
		$(a_x^2 + a_z^2)^{.5} = 52 \text{ g}$		$(b_x^2 + b_z^2)^{.5} = 53 \text{ g}$			$(a_z - c_z)/30 = \text{ND}$		
2	data:	28 g	DR	63 g	23 g	DR	16 g	52 g	27 g
		c.g accel.		c.g accel.					
		$(a_x^2 + a_z^2)^{.5} = 69 \text{ g}$		$(b_x^2 + b_z^2)^{.5} = 28 \text{ g}$					
3	data:	20 g	42 g	DR	28 g	61 g	DR	17 g	33 g
		axial net = AN = $(a_x + b_x)/2 = 24 \text{ g}$							
		c.g accel.		c.g accel.			angular		
		$(AN^2 + a_y^2)^{.5} = 48 \text{ g}$		$(AN^2 + b_y^2)^{.5} = 60 \text{ g}$			$(a_y - c_y)/30 = 0.3 \text{ rad/sec}^2$		
4	data:	130 g	DR	20 g	170 g	DR	DR	138 g	DR
		c.g accel.		c.g accel.					
		$a_x = 130 \text{ g}$		$b_x = 170 \text{ g}$					
5	data:	80 g	DR	17 g	88 g	DR	102 g	61 g	DR
		c.g accel.		c.g accel.					
		$a_x = 80 \text{ g}$		$b_x = 88 \text{ g}$					

¹ Dominated by ringing.² No Data.

TABLE 2.10.15.4.4.3-2. HAC Accelerometer Results(CTA-1).

Test	a _x	a _y	a _z	b _x	b _y	b _z	c _x	c _y	c _z
data:	210 g	DR ³	ND ⁴	275 g	DR	ND	ND	DR	125 g
8	c.g accel.			c.g accel.			angular		
Note 1	$(a_x^2 + a_z^2)^{1/2} = 210$ g			$(b_x^2 + b_z^2)^{1/2} = 275$ g			$c_x/(25.2 + 30) = 2.26$ rad/sec ²		
data:	77 g	DR	168 g	230 g	121 g	140 g	102 g	ND	84 g
7	c.g accel.			c.g accel.					
	$(a_x^2 + a_z^2)^{1/2} = 185$ g			$(b_x^2 + b_z^2)^{1/2} = 269$ g					
data:	73 g	181 g	48 g	188 g	265 g	DR	DR	ND	DR
8	axial net = AN = $(a_x + b_x)/2 = 131$ g								
Note 2	c.g accel.			c.g accel.			angular		
	$(AN^2 + a_y^2)^{1/2} = 232$ g			$(AN^2 + b_y^2)^{1/2} = 236$ g			$(a_x - b_x)/41.4 = 2.78$ rad/sec ²		
data:	260 g	ND	131 g	ND	ND	DR	ND	DR	DR
8	c.g accel.			c.g accel.					
	a _x = 260 g			b _y = ND					
data:	180 g	ND	75 g	ND	ND	ND	240 g	ND	49 g
10	c.g accel.			c.g accel.			c.g accel.		
	a _x = 180 g			b _y = ND			c _x = 240 g		

Notes:

1. No circumferential (z-direction) readings were available from either location "a" or "b". However, since the package impact angle was only 10° from the vertical, the contribution of the missing directions is small. Further, the angular acceleration is found from the circumferential reading at "c" and the distance from "c" to the pivot point on the impact pad.
2. The angular acceleration is found from the difference between the axial signals at "a" and "b" divided by the distance between them, or 41.4 in. (For the side-slapdown drop, "a" is located on the top of CTA-1, and "b" is located on the bottom.)
3. Dominated by ringing.
4. No data.

TABLE 2.10.15.4.4.3-3. Passive Accelerometer Results (CTA-1).

Test No.	200 g	300 g	400 g
1	No trip	No trip	No trip
2	No trip	No trip	No trip
3	No trip	No trip	No trip
4	Trip	No trip	No trip
5	No trip	No trip	No trip
6	Trip	Trip	Trip
7	Trip	No trip	No trip
8	Trip	Trip	Trip
9	Trip	Trip	Trip
10	Trip	Trip	No trip

2.10.15.4.5 Bolt Residual Torque and Length Measurements. As described in Section 2.10.15.4.1, CTA-2 was subjected to four sets of drop tests. At the end of both the first and second set, the OCV closure bolt removal torques and ICV closure bolt retention check torques were recorded. These torque measurements are listed in Tables 2.10.15.4.5-1 to -4. The lengths of the OCV closure bolts are also included. At the end of both the third and fourth set of drop tests, the OCV closure bolt removal torques and ICV closure bolt removal torques were recorded. The pre- and post-test lengths of all of these bolts were also measured. These torque values and length measurements are included in Tables 2.10.15.4.5-5 to -9.

A study done prior to drop testing showed that bolt removal torque can be as low as 50% of tightening torque. From reviewing data in the tables, it can be concluded that the OCV and ICV closure bolts did not experience any significant loss of torque. The OCV and ICV closure bolt length measurements indicated that no permanent deformation occurred.

Most of the impact limiter attachment bolts were bent during the drop testing and accurate post-test length measurements were difficult to obtain. The impact limiter attachment bolt measurements are given in Tables 2.10.15.4.5-2 and -10.

TABLE 2.10.15.4.5-1. ICV Closure Bolt Removal Torque and Length Measurements
After First Set of Drop Tests.

Bolt No.	Removal torque, ft-lb	Pre-test len., in.	Post-test len., in.	Change, in.	Bolt No.	Removal torque, ft-lb	Pre-test len., in.	Post-test len., in.	Change, in.
1	210	5.9730	5.9731	+0.0001	13	235	5.9604	5.9605	+0.0001
2	220	5.9564	5.9566	+0.0002	14	238	5.9703	5.9703	0.0
3	222	5.9654	5.9654	0.0	15	220	5.9698	5.9702	+0.0004
4	188	5.9740	5.9742	+0.0002	16	230	5.9631	5.9633	+0.0002
5	220	5.9618	5.9623	+0.0004	17	235	5.9674	5.9676	+0.0002
6	220	5.9780	5.9784	+0.0004	18	240	5.9681	5.9659	-0.0002
7	230	5.9803	5.9803	0.0	19	260	5.9578	5.9581	+0.0003
8	210	6.0336	6.0336	0.0	20	245	5.9685	5.9661	-0.0004
9	206	5.9762	5.9762	0.0	21	260	5.9547	5.9548	+0.0001
10	190	5.9682	5.9682	0.0	22	230	5.9539	5.9540	+0.0001
11	175	5.9666	5.9667	+0.0001	23	240	5.9730	5.9727	-0.0003
12	180	5.9749	5.9740	-0.0009	24	200	5.9692	5.9691	-0.0001

TABLE 2.10.15.4.5-2. ICV Closure Bolt Retention Torque Check
After First Set of Drop Tests.

Bolt #	Torque, ft-lb	Bolt #	Torque, ft-lb
1	>78	13	>78
2	>78	14	>78
3	>78	15	>78
4	>78	16	>78
5	>78	17	>78
6	>78	18	>78
7	>78	19	>78
8	>78	20	>78
9	>78	21	>78
10	>78	22	>78
11	>78	23	>78
12	>78	24	>78

TABLE 2.10.15.4.6-3. OCY Closure Bolt Retention Torque Check
After Second Set of Drop Tests.

Bolt No.	Removal torque, ft-lb	Pre-test len., in.	Post-test len., in.	Change, in.	Bolt No.	Removal torque, ft-lb	Pre-test len., in.	Post-test len., in.	Change, in.
1	160	5.8730	6.8728	-0.0002	13	230	5.9804	5.9803	-0.0001
2	190	5.9564	6.9566	+0.0002	14	226	5.9703	6.9700	-0.0003
3	200	5.9854	5.9850	-0.0004	15	230	5.9898	5.9894	-0.0004
4	200	5.9740	5.9738	-0.0002	16	250	5.9631	6.9631	0.0
5	230	5.9619	5.9619	0.0	17	276	5.9674	5.9671	-0.0003
6	300	5.9760	6.9761	+0.0001	18	320	5.9661	6.9668	-0.0003
7	280	5.9803	5.9801	-0.0002	19	330	5.9578	5.9581	+0.0003
8	270	5.0336	6.0337	+0.0001	20	340	5.9686	6.9682	-0.0003
9	225	5.9762	5.9766	-0.0006	21	285	5.9547	5.9549	+0.0002
10	225	5.9682	6.9682	0.0	22	240	5.9639	6.9639	0.0
11	195	5.9666	5.9663	-0.0003	23	280	5.9730	5.9722	-0.0008
12	220	5.9749	6.9746	-0.0003	24	230	5.9692	6.9691	-0.0001

TABLE 2.10.15.4.5-4. ICY Closure Bolt Retention Torque Check
After Second Set of Drop Tests.

Bolt #	Torque, ft-lb	Bolt #	Torque, ft-lb
1	>78	13	>78
2	>78	14	>78
3	>78	15	>78
4	>78	16	>78
5	>78	17	>78
6	>78	18	>78
7	>78	19	>78
8	>78	20	>78
9	>78	21	>78
10	>78	22	>78
11	>78	23	>78
12	>78	24	>78

TABLE 2.10.15.4.5-5. OCY Closure Bolt Removal Torque and Length Measurement
After Third Set of Drop Tests.

Bolt No.	Removal torque, ft-lb	Pre-test len., in.	Post-test len., in.	Change, in.	Bolt No.	Removal torque, ft-lb	Pre-test len., in.	Post-test len., in.	Change, in.
1	180	5.9730	5.9731	+0.0001	13	280	5.9604	5.9604	0.0
2	230	5.9664	5.9667	+0.0003	14	276	5.9703	5.9702	-0.0001
3	310	5.9654	5.9653	-0.0001	15	270	5.9698	5.9700	+0.0002
4	300	5.9740	5.9739	-0.0001	16	280	5.9631	5.9633	+0.0002
5	290	5.9619	5.9621	+0.0002	17	280	5.9674	5.9677	+0.0003
6	265	5.9760	5.9763	+0.0003	18	280	5.9661	5.9661	0.0
7	235	5.9803	5.9806	+0.0003	19	270	5.9678	5.9679	+0.0001
8	240	6.0338	6.0338	0.0	20	230	5.9665	5.9664	-0.0001
9	250	5.9762	5.9761	-0.0001	21	270	5.9647	5.9649	+0.0002
10	265	5.9682	5.9681	-0.0001	22	260	5.9539	5.9536	-0.0003
11	210	5.9666	5.9666	0.0	23	200	5.9730	5.9723	-0.0007
12	240	5.9749	5.9747	-0.0002	24	200	5.9692	5.9690	-0.0002

TABLE 2.10.15.4.5-6. ICY Closure Bolt Removal Torque and Length Measurements
After Third Set of Drop Tests.

Bolt No.	Removal torque, ft-lb	Pre-test len., in.	Post-test len., in.	Change, in.	Bolt No.	Removal torque, ft-lb	Pre-test len., in.	Post-test len., in.	Change, in.
1	180	1.9580	1.9582	+0.0002	13	185	1.9490	1.9492	+0.0002
2	136	1.9624	1.9626	+0.0002	14	175	1.9686	1.9699	+0.0001
3	190	1.9675	1.9674	-0.0001	15	185	1.9554	1.9555	+0.0001
4	180	1.9711	1.9711	0.0	16	170	1.9644	1.9646	+0.0002
5	150	1.9687	1.9687	0.0	17	180	1.9594	1.9595	+0.0001
6	190	1.9870	1.9869	-0.0001	18	180	1.9802	1.9802	0.0
7	185	1.9694	1.9883	-0.0001	19	180	1.9692	1.9690	-0.0002
8	190	1.9561	1.9559	-0.0002	20	180	1.9887	1.9887	0.0
9	175	1.9643	1.9643	0.0	21	180	1.9580	1.9560	0.0
10	190	1.9728	1.9729	+0.0001	22	186	1.9641	1.9639	-0.0002
11	190	1.9614	1.9616	+0.0002	23	187	1.9616	1.9616	0.0
12	165	1.9667	1.9557	-0.0001	24	170	1.9595	1.9592	-0.0003

TABLE 2.10.15.4.5-7. OCV Closure Bolt Removal Torque and Length Measurements
After Fourth Set of Drop Tests.

Bolt No.	Removal torque, ft-lb	Pre-test len., in.	Post-test len., in.	Change, in.	Bolt No.	Removal torque, ft-lb	Pre-test len., in.	Post-test len., in.	Change, in.
1	225	5.9730	5.9734	+0.0004	13	250	5.9604	5.9610	+0.0006
2	240	5.9564	5.9568	+0.0004	14	260	5.9703	5.9708	+0.0005
3	250	5.9654	5.9658	+0.0004	15	230	5.9698	5.9701	+0.0003
4	240	5.9740	5.9741	+0.0001	16	280	5.9631	5.9636	+0.0005
5	285	5.9618	5.9622	+0.0003	17	280	5.9674	5.9678	+0.0004
6	260	5.9780	5.9784	+0.0004	18	265	5.9561	5.9565	+0.0004
7	255	5.9803	5.9802	-0.0001	19	280	5.9578	5.9580	+0.0002
8	265	6.0336	6.0338	+0.0003	20	240	5.9665	5.9666	0.0
9	240	5.9762	5.9764	+0.0002	21	260	5.9547	5.9550	+0.0003
10	280	5.9662	5.9663	+0.0001	22	265	5.9538	5.9540	+0.0001
11	260	5.9668	5.9667	+0.0001	23	260	5.9730	5.9727	-0.0003
12	210	5.9748	5.9754	+0.0006	24	215	5.9692	5.9692	0.0

TABLE 2.10.15.4.5-8. ICV Closure Bolt Removal Torque and Length Measurements
After Fourth Set of Drop Tests.

Bolt No.	Removal torque, ft-lb	Pre-test len., in.	Post-test len., in.	Change, in.	Bolt No.	Removal torque, ft-lb	Pre-test len., in.	Post-test len., in.	Change, in.
1	215	1.9580	1.9586	+0.0006	13	230	1.9490	1.9491	+0.0001
2	210	1.9624	1.9626	+0.0002	14	220	1.9698	1.9699	+0.0001
3	210	1.9675	1.9672	-0.0003	15	200	1.9554	1.9552	-0.0002
4	220	1.9711	1.9714	+0.0003	16	215	1.9644	1.9644	0.0
5	230	1.9687	1.9685	-0.0002	17	220	1.9694	1.9698	+0.0004
6	226	1.9670	1.9668	-0.0001	18	210	1.9602	1.9601	-0.0001
7	220	1.9694	1.9690	-0.0004	19	220	1.9692	1.9691	-0.0001
8	200	1.9661	1.9667	+0.0006	20	200	1.9687	1.9688	+0.0001
9	200	1.9643	1.9646	+0.0003	21	175	1.9680	1.9682	+0.0002
10	190	1.9726	1.9728	+0.0003	22	200	1.9641	1.9641	0.0
11	215	1.9614	1.9616	+0.0002	23	175	1.9616	1.9616	0.0
12	190	1.9557	1.9555	-0.0002	24	200	1.9596	1.9601	+0.0006

TABLE 2.10.15.4.5-9. Impact Limiter Attachment Bolt Length Measurements After First and Second Sets of Drop Tests.

Bolt #	Pre-test len., in.	Post-test len., in.	Bolt #	Pre-test len., in.	Post-test len., in.
1	9.00	8.9997	9	8.9911	8.9904
2	9.00	8.0065	10	8.9910	8.9954
3	9.00	9.0231	11	8.9950	8.9888
4	9.00	8.9959	12	8.9953	9.0004
5	9.00	8.9795	13	8.9884	8.9839*
6	9.00	9.0053	14	8.9835	8.9832
7	9.00	8.0140	15	8.9848	8.9878
8	9.00	8.9967	16	8.9914	8.9933

* Bolt severely bent, precluding accurate post-test measurement.

The first set of drop tests used bolts 1 through 8. The second set of drops used new bolts numbered 9 through 16.

TABLE 2.10.15.4.6-10. Impact Limiter Attachment Bolt Length Measurements After Third and Fourth Sets of Drop Tests.

Bolt #	Pre-test len., in.	Post-test len., in.	Bolt #	Pre-test len., in.	Post-test len., in.
17	8.9920	8.9931	17	8.9931	9.0039
18	8.9841	8.9878	18	8.9878	9.0085
19	8.9914	8.9895	19	8.9895	8.9895
20	8.9805	8.9804	20	8.9804	9.0035
21	8.9944	8.9951	21	8.9951	9.0102
22	8.9868	8.9895	22	8.9895	8.9868
23	8.9891	8.9901	23	8.9901	8.9941
24	8.9913	8.9924	24	8.9924	8.9982

The same impact limiter bolts were used for all of these drop tests.

2.10.15.4.6 Payload Interaction and Shipping Rack Condition. During the drop test series, the simulated payload interacted structurally with the ICV and the shipping rack assembly. The simulated payload broke free in that all four payload attaching bolt heads pulled through the payload base. This allowed the payload to strike the inside of the ICV wall and head. Two payload fins were struck direct-on and buckled up to the sturdy payload body. Three other payload fins were involved to a lesser extent (see Figure 2.10.15.4.6-1). Further, interaction with the ICV lifting block also occurred, in that the end of the 14-in. o.d., 1/2-in.-thick wall pipe of the simulated payload impacted the lifting block. As shown in Figure 2.10.15.4.6-2, the impact produced a dent

in the end of the pipe approximately 4.5 in. long and 0.6 in. deep. Figures 2.10.15.4.8-1 and -2 show the damage to the simulated payload that occurred during the first drop test series, which used CTA-1. The damage to the simulated payload during the second drop test series was very similar.

Damage to the shipping rack assembly was negligible. The shipping rack assembly top plate (the barrier plate) was deformed approximately 1/16 in. by contact with the loose payload. All four of the shipping rack assembly attachment bolts were still tight. There was no observable damage to the shipping rack assembly attachment bolts and the shipping rack remained substantially in its initial position. The simulated payload attachment bolts demonstrated some deformation, consistent with separation of the payload. The underside insulation was in place.



FIGURE 2 10 15 4 8-1 Simulated Payload Damage to Fins
Note: Picture was rotated CCW

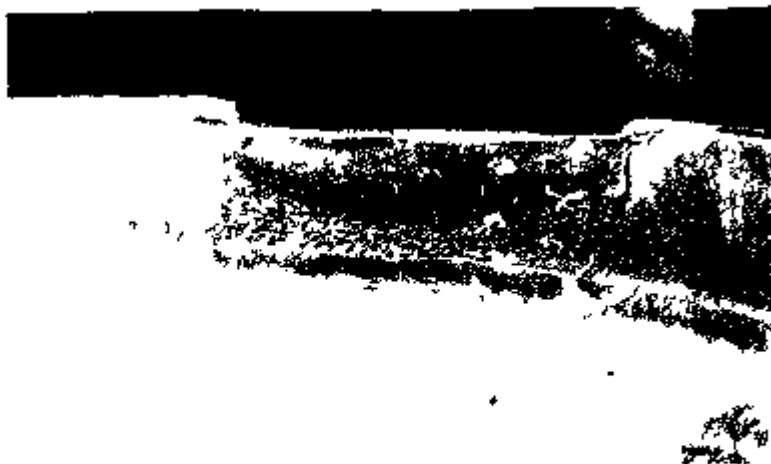


FIGURE 2 10 15 4 8-2 Simulated Payload Top End Damage

2 10 15 65

BEST COPY AVAILABLE

2.10.15.4.7 Anomalies. The following test anomaly was noted.

As indicated in Section 2.10.15.4.1, the ICV closure bolts were not removed until after the third set of drop tests (CTA-2 Test Nos. 4 through 8) was completed. After removal of the ICV closure bolts, it was noted that most of the ICV closure bolt washers were fractured. The fracturing can best be described as fine, hairline cracks that extend radially through the washers in one or more locations. In general, the washers remained intact and were not broken into small pieces. Only one washer fell into two parts during disassembly of the ICV. From the data sheets, it is noted that the fractured washers did not result in any loss of torque in the ICV closure bolts. Further, even if broken, the washers are effectively trapped by the ICV bell flange closure bolt counterbore. The washers are high-strength flat washers that meet the requirements of ASTM F438. The washers are purchased from a commercial vendor and then the OD is machined down to drawing specifications. After machining, the washers are cadmium plated. During the search for possible causes for the fracturing, it was determined the washers were not baked out after the cadmium plating process. This could result in a potential for hydrogen embrittlement and subsequent fracturing of the washers.

Prior to performing the last set of drop tests (CTA-2 Test Nos. 10 through 16), new washers were fabricated and installed. These washers were not cadmium plated. After completion of the drop testing, the ICV was disassembled and the ICV closure bolt washers were inspected and found to be free of any fractures. For the production packagings, the washers will be properly baked-out to ensure there is no potential for hydrogen embrittlement.

2.10.15.5 Certification Test Data Sheets.

Test Set 1: Drop Test Nos. 1, 2, and 3

Data Sheet A from WHC-SD-RTG-TC-016, Rev. 1
Data Sheets, B, C, D, and E1 from WHC-SD-RTG-TC-017, Rev. 1
NDE Leak Test Procedure and Test Report

DATA SHEET A

Impact Limiter Measurements — Pretest Reference Only

Obtain all measurements (in) in four quadrants, with quadrant No. 1 centered on feed-through (quadrants measured CCW looking down on package top).

Quadrant	X (±0.13)	Y (±0.13)	Z (±0.13)	H (±0.13)	D (±0.13)	G (±0.06)	S (±0.06)
1	4	3 7/8	4	17 15/16	9	1/4	- 3/16
2	4 1/4	3 7/8	3 7/8	17 15/16	9	1/4	- 3/16
3	3 3/4	3 3/8	4	17 1/2	8 1/2	3/8	- 19/32
4	3 1/2	3 3/4	3 3/4	17 7/8	9	3/8	- 7/16

Thickness near center using 5/16" hole (T, ±0.13): 8 5/8 in.

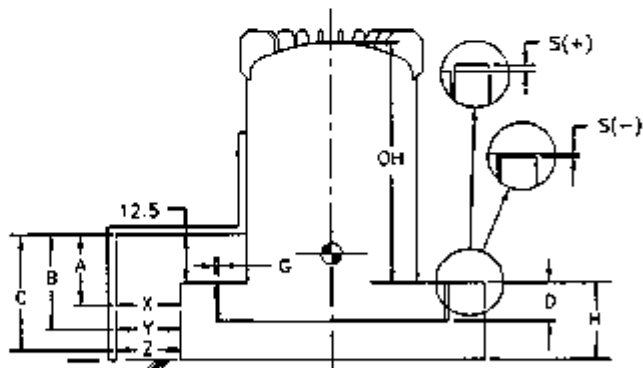
Height (OH) of OCV from top of thermal shield to top of OCV head, excluding fins (±0.25): 56 1/16

The 12.5 dimension shown below is a reference dimension to the top of the OCV flange thermal shield.

A = 14.5 ±0.25 in.

B = 21.5 ±0.25 in.

C = 28.5 ±0.25 in.



[Signature]
Test Engineer

11/1/96
Date

[Signature]
QA Representative

11/1/96
Date

DATA SHEET A

Drop Test No. 1, NCT 4-ft Drop, Near Vertical

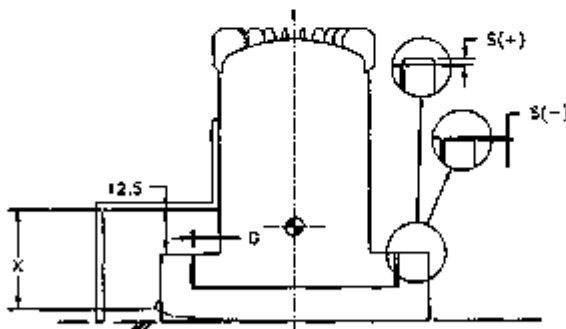
Ambient Temperature: 18°C Impact Limiter Foam Temperature: 22°C

Damage Measurements: (See sketch below)

Quadrant	X (±0.13)	G (±0.06)	S (±0.06)
1			
2			
3			
4			

Due to high winds these measurements were not taken

The 12.5 dimension shown below is a reference dimension to the top of the DCV Flange thermal shield.



J. L. Carter
Test Engineer

11/08/95
Date

[Signature]
QA Representative

11/08/95
Date

DATA SHEET A

Drop Test No. 1, MCT 4-ft Drop, Near Vertical

Sketch of Damage and Notes:

Torque checking impact limiter bolts

# 1	85 ft lb	brake loose
2	80 + ft lb	
3	60 ft lb	
4	75 ft lb	
5	Ø ft lb	<u>loose</u>
6	30 ft lb	
7	88 ft lb	tight (reached max)
8	Ø ft lb	<u>loose</u>

J. S. [Signature]
Test Engineer

11/18/95
Date

M. S. [Signature]
QA Representative

11/21/95
Date

DATA SHEET A

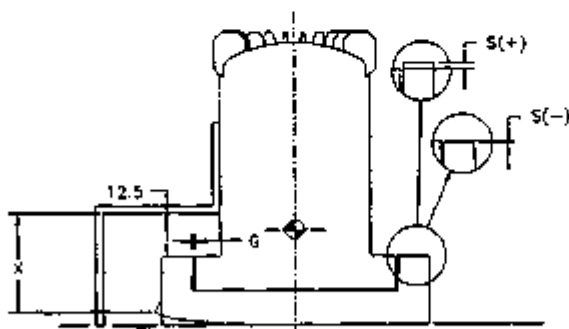
Drop Test No. 2, HAC 30-ft Drop, Near Vertical

Ambient Temperature: 18 °C Impact Limiter Foam Temperature: 22 °C

Damage Measurements: (See sketch below)

Quadrant	X (±0.13)	G (±0.06)	S (±0.06)
1	30 3/4	9/32	-18/32
2	30 3/4	8/32	-12/32
3	29 3/8	7/32	-17/32
4	30 1/4	12/32	-22/32

The 12.5 dimension shown below is a reference dimension to the top of the OCY flange thermal shield.



J.A. Quatro
Test Engineer

11/08/95
Date

M.E. [Signature]
QA Representative

11/8/95
Date

DATA SHEET A

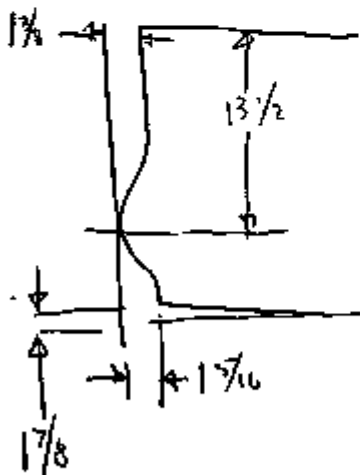
Drop Test No. 2, NAC 30-ft Drop, Near Vertical

Sketch of Damage and Notes:

Torque checking

Impact Limiter Bolts

#1	88 Ft-lb (reached max)
2	50 Ft-lb
3	37 Ft-lb
4	65 Ft-lb
5	88 Ft-lb (reached max)
6	30 Ft-lb
7	Ø Ft-lb (Loose)
8	15 Ft-lb



At impact point

J. L. Carter
Test Engineer

11/28/95
Date

M. S. [Signature]
QA Representative

11/28/95
Date

DATA SHEET A

Drop Test No. 3, HAC Puncture

VIEW LOOKING
FROM TOP

Drop on #7 bolt

Sc distance at point of impact = $27/32$

(see page 58)

Impact limiter bolt residual torque
(remove ocv/cr from impact limiter)

Bolt #	Residual Torque
1	200 ft-lb
2	70
3	50
4	65
5	190
6	0
7	0
8	0

W.L. Quade
Test Engineer

11/05/96
Date

B.L. Allen
QA Representative

11/05/96
Date

DATA SHEET B

Record of OCY closure residual bolt torque performed after completion of interim drop tests. Bolts are numbered CCW, viewed from the top of the Test Article, starting with the first bolt CCW from the feed-through.



OCY Bolts:

Loosen each bolt in turn just sufficient to establish the residual preload, followed by retorquing to the torque level equal to the installation torque, starting with Bolt No. 1, crossing the bell to Bolt No. 13, proceeding to Bolt No. 2 and across to Bolt No. 14, proceed to Bolt No. 4 and across to Bolt No. 12. The balance of the pattern is: 3-15, 23-11, 4-16, 22-10, 5-17, 21-9, 6-18, 20-8, 7-19.

OCY Closure Bolts			
Residual Preload			
Bolt #	Torque, ft-lb	Bolt #	Torque, ft-lb
1	210	13	235
2	220	14	238
3	222	15	220
4	198	16	230
5	220	17	235
6	220	18	240
7	230	19	280
8	210	20	245
9	205	21	260
10	190	22	230
11	175	23	240
12	190	24	200

TORQUE WARRANT
 S/N 584-88-01-00
 CAL STD 9/29/96

473-9123

 Test Engineer Date QA Representative Date

OFFICIAL COPY

DATA SHEET 0

Record of ICV retention bolt torque performed after completion of interim drop tests and after removal of DCV bell. Bolts are numbered CCW, viewed from the top of the Test Article, starting with the first bolt CCW from the electrical feed-through. Apply loosening torque of one-half the average residual torque established in assembly (see MHC 1995a), starting with Bolt No. 1, crossing the bell to Bolt No. 13, proceeding to Bolt No. 2 and across to Bolt No. 14, proceed to Bolt No. 24 and across to Bolt No. 12. The balance of the pattern is: 3-15, 23-11, 4-16, 22-10, 5-17, 21-9, 6-18, 20-8, 7-19. If bolt loosens below this torque, record the loosening torque and proceed to the next bolt.

Average residual torque from initial assembly 156 ft-lb. ($\frac{1}{2} \Rightarrow 78 \text{ ft-lb}$)

(Check in loosening direction to 1/2 this value)

ICV Closure Bolts			
Retention Torque Check*			
Bolt #	Torque, ft-lb	Bolt #	Torque, ft-lb
1	OK	13	OK
2		14	
3		15	
4		16	
5		17	
6		18	
7		19	
8		20	
9		21	
10		22	
11		23	
12	OK	24	OK

TORQUE WRENCH
S/N 950-88-01-06
CAL EXP 10/20/96

*Record OK if half the initial assembly torque is met; record loosening torque if bolt loosens.

[Signature]
Test Engineer

[Signature]
Date

[Signature]
QA Representative

11/8/95
Date

OFFICIAL COPY

DATA SHEET E1

Record of RTG Certification Test Article OCY and Impact limiter bolt length performed after interim drop tests. Bolts are numbered CCW, viewed from the top of the Test Article, starting with the first bolt CCW from the electrical feed-through.

OCY Closure Bolts			
Bolt no.	Length (in.)	Bolt no.	Length (in.)
1	5.9731	13	5.9605
2	5.9566	14	5.9703
3	5.9654	15	5.9702
4	5.9742	16	5.9633
5	5.9623	17	5.9676
6	5.9764	18	5.9659
7	5.9583	19	5.9581
8	6.0336	20	5.9661
9	5.9762	21	5.9548
10	5.9682	22	5.9540
11	5.9667	23	5.9727
12	5.9740	24	5.9671

Impact Limiter Bolts	
Bolt no.	Length (in.)
1	8.9897
2	9.0068
3	9.0231
4	8.9999
5	8.9796
6	9.0053
7	9.0140
8	8.9967

J. L. [Signature]
Test Engineer

[Signature]
Date

[Signature] 11-15-85
QA Representative Date

OFFICIAL COPY

Westinghouse Hanford Company		NDE LEAK TEST PROCEDURE AND TEST REPORT				MHC-SD-RTG-SARP-001 Rev. 09/15/96	
Requestor Larry S. Averette		Company PacTec		Project/System/Work Package/Transfer No. Helium Leak Test of Radioisotope Thermoelectric Generator (RTG) After Drop Tests #1-#3 on Certification Test Article NCTA-2, per MHC-SD-RTG-TC-017, Rev. 1			
MEPR 62-02	Mag NO-916	Area 1100	Date <input type="checkbox"/> MA <input type="checkbox"/> NA H-4-302118		WDR <input checked="" type="checkbox"/> MA <input type="checkbox"/> NA Alcohol		Case No. 89-1596
Acceptance Std Leakage Rate < 2.6 x 10⁻⁷ atm.cm³/sec Helium		Section Para		Date <input type="checkbox"/> MA <input type="checkbox"/> NA H-4-112301		WDR <input checked="" type="checkbox"/> MA <input type="checkbox"/> NA Alcohol	
TEST CONDITIONS		TEST EQUIPMENT				WDR PROCEDURE NO.	
Temperature Amb. Device ID <input checked="" type="checkbox"/> NA	Manufacturer L/H "UL-100+", #2		<input type="checkbox"/> MA		<input checked="" type="checkbox"/> NDTLT 6000 Rev 3		
Barometric Pressure <input checked="" type="checkbox"/> NA	Mfg. No. S/p896-38 (MC8869)		<input type="checkbox"/> NA		Appendix A Rev 2		
Test Pressure = 1 Atm. (14.7 psia) <input type="checkbox"/> NA	Flow Range 1.0 x 10⁻¹¹ Atm(cc)/Div		<input type="checkbox"/> MA		<input type="checkbox"/> Special Tech. No. _____		
Gas UHP Helium <input type="checkbox"/> NA	Std. No. 586-40-03 018		<input type="checkbox"/> NA		WORK PRTY <input checked="" type="checkbox"/> NA		
Concentration >90% <input type="checkbox"/> NA	Std. Leak 1.6 x 10⁻⁸ Atm(cc)		<input type="checkbox"/> NA		<input type="checkbox"/> NDTLT-601 Rev _____		
GTUR <input checked="" type="checkbox"/> NA	Cald. Exp. July 7, 1996		<input type="checkbox"/> NA		<input type="checkbox"/> Other _____		
Bubble Solution <input checked="" type="checkbox"/> NA	Flow Range 1.0 x 10⁻¹¹ Atm(cc)/Div		<input type="checkbox"/> MA		SYSTEM SENSITIVITY		
Bech. No. _____	Std. No. 586-40-03 006		<input type="checkbox"/> NA		<input type="checkbox"/> Same as WGLD Cald. of		
Gage # 198 31-06-007 <input type="checkbox"/> NA	Std. Leak 1.3 x 10⁻⁷ Atm(cc)		<input type="checkbox"/> NA		First Range 1.0 x 10⁻¹¹ Atm(cc)/Div		
Range 0 to 50 psia	Cald. Exp. July 7, 1996		<input type="checkbox"/> NA		Mid Range x 10⁻ Atm(cc)/Div		
Cald. Exp. March 9, 1996	Flow Range x 10⁻ Atm(cc)/Div		<input checked="" type="checkbox"/> MA		Gross Range x 10⁻ Atm(cc)/Div		
Gage # 586 31 06 <input checked="" type="checkbox"/> NA	Std. No. 586-40-03		<input type="checkbox"/> NA		TEST TIME		
Range _____	Std. Leak x 10⁻ Atm(cc)		<input type="checkbox"/> NA		STEP-DOWN SCALE - AN-WAY OPERATED		
Exp. _____	Cald. Exp. _____		<input type="checkbox"/> NA		RESPONSE TIME - 3 MINUTES <input type="checkbox"/> NA		
Reset Value <input checked="" type="checkbox"/> NA			<input type="checkbox"/> NA		No. of Drops - TEST DROPS ONLY <input type="checkbox"/> NA		
			<input type="checkbox"/> NA		Sensitivity - 1.0 x 10⁻¹¹ atm <input type="checkbox"/> NA		
Test No.	Part No. or Serial No.	Acc.	Ret.	No. Rat. Ind.	Comments		
					OUTER CONTAINMENT VESSEL (OCV) LEAK RATE TESTS:		
"V" Port Stat.-O-Seal	X	X	X		No Detectable Leakage (Per Step #5.2)		
"T" Port Prim.-O-Ring	X	X	X		No Detectable Leakage (Per Step #5.3)		
					INNER CONTAINMENT VESSEL (ICV) LEAK RATE TESTS:		
"P" Port Stat.-O-Seal	X	X	X		No Detectable Leakage (Per Step #6.2)		
"S" Port Stat.-O-Seal	X	X	X		No Detectable Leakage (Per Step #6.3)		
"T" Port Prim.-O-Ring	X	X	X		No Detectable Leakage (Per Step #6.4)		
					OUTER CONTAINMENT VESSEL (OCV) LEAK RATE TESTS: ASSEMBLY		
"V" Port Stat.-O-Seal	X	X	X		No Detectable Leakage (Per Step #7.2)		
"T" Port Prim.-O-Ring	X	X	X		No Detectable Leakage (Per Step #7.3)		
Technician's Approval		LT Level/Dates		OFFICIAL COPY			
W.H. Nelson B.J. Stewart Date of Examination Nov. 8, 1995		Interpreted by B.J. Stewart Date Nov. 8, 1995		LT Level/N II		Date of Test 11-14-95 2.10.15-69	

Test Set 2: Drop Test Nos. 4, 5, and 6

**Data Sheet A from WHC-SD-RTG-TC-015, Rev. 1
Data Sheets B, C, D, and E1 from WHC-SD-RTG-TC-017, Rev. 1
NDE Leak Test Procedure and Test Report**

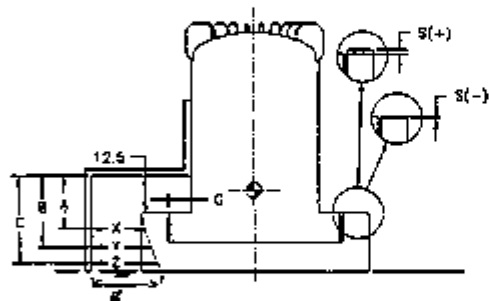
DATA SHEET A

Drop Test No. 4, MCT 4-ft Drop, c.g. Over Bottom Corner

Ambient Temperature: 10°C Impact Limiter Foam Temperature: 26°C

The 12.5 dimension shown below is a reference dimension to the top of the OCY flange thermal shield.

Damage Measurements: (See sketch below)



Quadrant	S (± 0.06)	S (± 0.06)
1	$8/32$	$6/32$
2	$13/32$	$3/32$
3	$20/32$	$12/32$
4	$25/32$	$14/32$

Z₁ = ~~20~~
12.5"

A (± 0.25)	B (± 0.25)	C (± 0.25)	X (± 0.25)	Y (± 0.25)	Z (± 0.25)
22	27	30	3 1/8	3 5/8	5 3/8

J. L. [Signature]
Test Engineer

11/9/95
Date

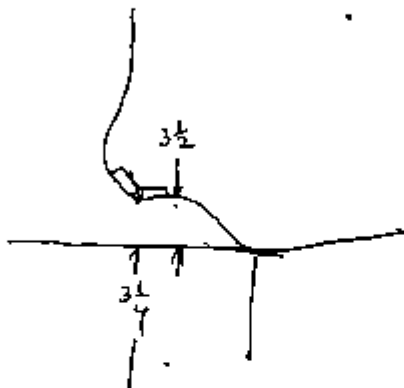
[Signature]
QA Representative

11/9/95
Date

DATA SHEET A

Drop Test No. 4, MCT 4-ft Drop, c.g. Over Bottom Corner

Sketch of Damage and Notes:



J. L. Austin
Test Engineer

11/9/95
Date

M. E. R. S.
QA Representative

11/9/95
Date

DATA SHEET A

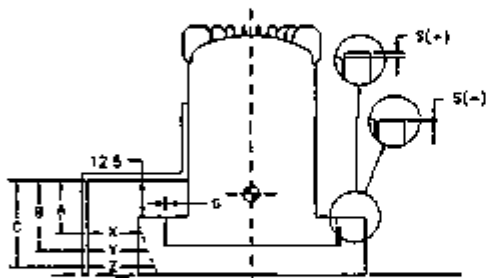
Drop Test No. 5, HAC 30-ft Drop, c.g. Over Bottom Corner

Ambient Temperature: 10°C Impact Limiter Foam Temperature: 22°C

The 12.5 dimension shown below is a reference dimension to the top of the OCY flange thermal shield.

Damage Measurements: (See sketch below)

Quadrant	5 (±0.06)	6 (±0.06)
1	- 14/32	2/32
2	- 12/32	4/32
3	- 20/32	1/2
4	- 2 1/32	12/32



A (±0.25)	B (±0.25)	C (±0.25)	X (±0.25)	Y (±0.25)	Z (±0.25)
22 3/4	26 3/4	30 1/4	6.0	8.3	10.5

John R. ...
 Test Engineer

6/23/95
 Date

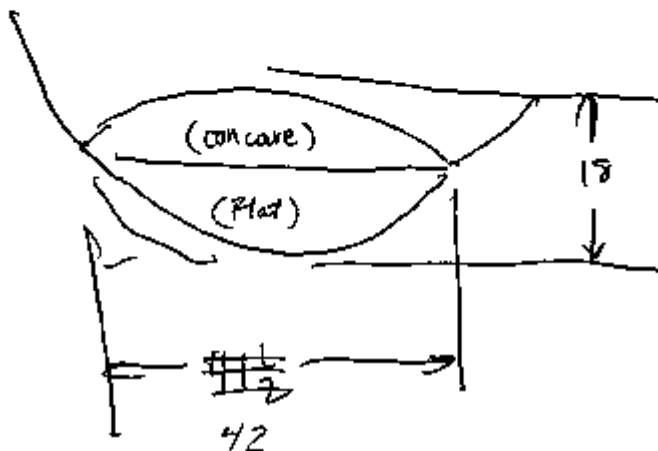
[Signature]
 QA Representative

11/9/95
 Date

DATA SHEET A

Drop Test No. 5, HAC 30-7t Drop, c.g. Over Bottom Corner

Sketch of Damage and Notes:



J. S. Smith
Test Engineer

11/19/86
Date

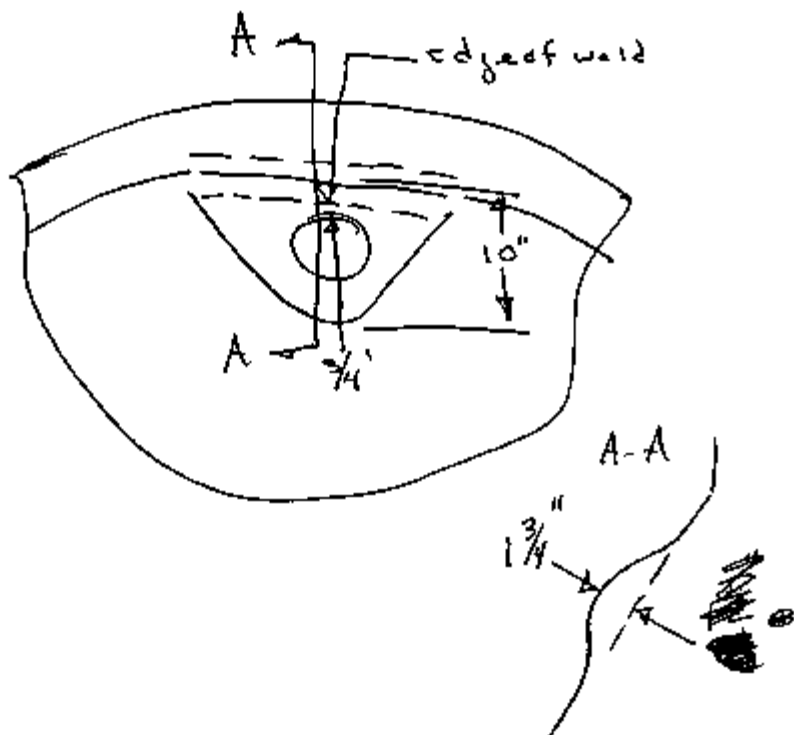
M. R. D.
QA Representative

11/19/86
Date

DATA SHEET A

Drop Test No. 6, HAC Puncture

Impact Counter From Temp. = 20°C	} <u>Post Test</u>	
Ambient Temp. = 10°C		18°C - Counter
		10°C - Ambient



J.S. Q. D.
Test Engineer

1/28/95
Date

M.E. P.
QA Representative

1/10/95
Date

DATA SHEET B

Record of OCY closure residual bolt torque performed after completion of interim drop tests. Bolts are numbered CCW, viewed from the top of the Test Article, starting with the first bolt CCW from the feed-through.

OCY Bolts:

Loosen each bolt in turn just sufficient to establish the residual preload, followed by retorquing to the torque level equal to the installation torque, starting with Bolt No. 1, crossing the bell to Bolt No. 13, proceeding to Bolt No. 2 and across to Bolt No. 14, proceed to Bolt No. 23 and across to Bolt No. 12. The balance of the pattern is: ~~4-15, 23-11, 4-16, 22-10, 5-17, 21-9, 6-18, 20-8, 7-19.~~

OCY Closure Bolts			
Residual Preload			
Bolt #	Torque, ft-lb	Bolt #	Torque, ft-lb
1	150	13	230
2	190	14	225
3	200	15	230
4	200	16	250
5	230	17	275
6	300	18	(300)
7	280	19	(330)
8	270	20	(340)
9	225	21	265
10	225	22	240
11	195	23	260
12	220	24	230

300 (max)

300 (max)

300 (max)

AVERAGE → 241

H. L. Quate 11/09/95
Test Engineer Date

B. L. King 11/09/95
QA Representative Date

OFFICIAL COPY

DATA SHEET C

Record of ICV closure bolt relative position in relation to the ICV flange after removal of DCV bell. Bolts are numbered CCW, viewed from the top of the Test Article, starting with the first bolt CCW from the electrical feed-through.

ICV Closure Bolts			
Relative Angular Position			
Bolt #	Position	Bolt #	Position
1	✓OK	13	✓OK
2	↓	14	
3		15	
4		16	
5		17	
6		18	
7		19	
8		20	
9		21	
10		22	
11		23	
12	✓OK	24	✓OK

H. S. Runko 11/09/95
Test Engineer Date

B. D. [Signature] 11/09/95
QA Representative Date

OFFICIAL COPY

DATA SHEET D

Record of ICV retention bolt torque performed after completion of interim drop tests and after removal of OCV bell. Bolts are numbered CCW, viewed from the top of the Test Article, starting with the first bolt CCW from the electrical feed-through. Apply loosening torque of one-half the average residual torque established in assembly (see WNC 1995a), starting with Bolt No. 1, crossing the bell to Bolt No. 13, proceeding to Bolt No. 2 and across to Bolt No. 14, proceed to Bolt No. 24 and across to Bolt No. 12. The balance of the pattern is: 3-15, 23-11, 4-16, 22-10, 5-17, 21-9, 6-18, 20-8, 7-19. If bolt loosens below this torque, record the loosening torque and proceed to the next bolt.

Average residual torque from initial assembly 156 ft-lb. ($\frac{1}{2} \Rightarrow 78 \text{ ft-lb}$)
 (Check in loosening direction to 1/2 this value)

ICV Closure Bolts			
Retention Torque Check*			
Bolt #	Torque, ft-lb	Bolt #	Torque, ft-lb
1	✓OK	13	✓OK
2	✓OK	14	✓OK
3	✓OK	15	✓OK
4	✓OK	16	✓OK
5	✓OK	17	✓OK
6	✓OK	18	✓OK
7	✓OK	19	✓OK
8	✓OK	20	✓OK
9	✓OK	21	✓OK
10	✓OK	22	✓OK
11	✓OK	23	✓OK
12	✓OK	24	✓OK

*Record ✓OK if half the initial assembly torque is met; record loosening torque if bolt loosens.

J.L. Kuntler 11/09/95
 Test Engineer Date

B.J. Hany 11/09/95
 QA Representative Date

OFFICIAL COPY

DATA SHEET E1

Record of RTG Certification Test Article OCV and impact limiter bolt length performed after interim drop tests. Bolts are numbered CCW, viewed from the top of the Test Article, starting with the first bolt CCW from the electrical feed-through.

OCV Closure Bolts			
Bolt no.	Length (in.)	Bolt no.	Length (in.)
1	5.9728	13	5.9603
2	5.9566	14	5.9700
3	5.9650	15	5.9694
4	5.9738	16	5.9631
5	5.9619	17	5.9671
6	5.9761	18	5.9658
7	5.9801	19	5.9581
8	6.0337	20	5.9662
9	5.9756	21	5.9549
10	5.9682	22	5.9539
11	5.9663	23	5.9722
12	5.9746	24	5.9691

Impact Limiter Bolts	
Bolt no.	Length (in.)
9	8.9915 8.9904
10	8.9910 8.9959
11	8.9950 8.9889
12	8.9963 8.9904
13	8.9889 8.9931
14	8.9835 8.9932
15	8.9848 8.9878
16	8.9914 8.9933

BEFORE TEST	AFTER TEST
-------------	------------

*SEVERELY BENT

Impact Limiter Before
 Test Engineer: *J.L. Quilley* 11/10/95
 Date: 11/07/95
 OCV after impact limiter after test to

QA Representative: *Randy Salyer* 10/01/95
 Date: 10/01/95
 M+TZ QC 11083

OFFICIAL COPY

Westinghouse Hanford Company		NDE LEAK TEST PROCEDURE AND TEST REPORT UL-100				NON DESTRUCTIVE EXAMINATION 306 BLDG 300 AREA TEL 378-5401		JOB NO 95-8		
Requester A. AVERITE		Company FACTEC		Project/System/Work Package/Traveler No INTERIM DISASSEMBLY & REASSEMBLY OF THE RADIOISOTOPIC THERMOELECTRIC GENERATOR, SECOND CERTIFICATION, TEST ARTICLE CTA-2. DROP TEST 4,5,6 PER WMC-SO-RTG-TC-017 R/1						
MS&I	Spec	Area	TEST CONDITIONS						Draw No	
G2-02	NO-916	3100	LEAK RATE= <2.6 X 10 ⁻⁷ Atm cc/sec. H ₂ LIN						H-4-302118 H-4-112301	
Accepted By	Batch	Date	TEST EQUIPMENT						NA	
			Manufacturer: <u>L/M UL 100 PLUS</u>						MCR	
			Ident No: <u>WC48896</u>						NA	
			Mach Ser: <u>1 X 10-11</u> Almic/Sec/Dr						NA	
			Std No: <u>584 40 03 018</u>						WMC PROCEDURE NO	
			Std Leg: <u>1.6 X 10⁻⁸</u> Almic/Sec						NA	
			Cable Exp: <u>7-7-96</u>						NOV LT 0000 Rev 3	
			SYSTEM SENSITIVITY						Appendix <u>A</u> Rev <u>2</u>	
			<input type="checkbox"/> Same as M&I&B Cable or						Special Tech No	
			Sensitivity: <u>2.3 X 10⁻¹¹</u> Almic/Sec/Dr						Work Test	
			Std No: <u>584-40-03-006</u>						TEST TIME	
			Std Leak: <u>1.3 X 10⁻⁷</u> Almic/Sec						No Response Time <u>IMMEDIATE</u> NA	
			Cable Exp: <u>7-7-96</u>						No Accum Time <u>NA</u> NA	
			ADDITIONAL STD						Soak Time <u>NA</u> NA	
			Sensitivity: <u>NA</u> Almic/Sec/Dr						Additional Times	
			Std No: <u>NA</u>						TEST TIME 2 MIN NA	
			Std Leak: <u>NA</u> Almic/Sec							
			Cable Exp: <u>NA</u>							
Weld No	Part No or Serial No	App	Rel	No Rat Ind	Comments					
					OUTER CONTAINMENT VESSEL (OVC) LEAK RATE TESTS					
"V"	PORT STAT-O-SEAL	X	X	X	NO DETECTABLE LEAKS (PER STEP #7.2)					
"T"	PORT PRIM.O-RING	X	X	X	NO DETECTABLE LEAKS (PER STEP #7.3)					
					INNER CONTAINMENT VESSEL (IVC) LEAK RATE TESTS					
"P"	PORT STAT-O-SEAL	X	X	X	NO DETECTABLE LEAKS (PER STEP #6.2)					
"S"	PORT STAT-O-SEAL	X	X	X	NO DETECTABLE LEAKS (PER STEP #6.3)					
"T"	PORT PRIM.O-RING	X	X	X	NO DETECTABLE LEAKS (PER STEP #6.4)					
Technique Pre Approved				LT Level/Dir		OFFICIAL COPY				
Name				Level						
W. NELSON		I		Intercepted by		LT Level #		Reviewed by		
<i>W. Nelson</i>				B. L. HOPKINS		<i>B. Hopkins</i>		<i>John K. ...</i>		
Date of Examination		Date		Date		Date		Date		
11-09-95		11-09-95		11-09-95		11-13-95		2.10.15-80		

Westinghouse Nuclear Company		NDE LEAK TEST PROCEDURE AND TEST REPORT UL-100				MHC-SD-RTG-SARP-001 Rev. 0 8/15/95	
Requestor ary S. Averette		Company PacTec		Project/Stream/Node Package/Transfer No Helium Leak Test of Radioisotope Thermoelectric Generator (RTG) After Drop Tests #4-#6 on Certification Test Article NCTA-2, per MHC-SD-RTG-TC-017, Rev.1			
MSW G2-02	ORG MO-916	Area 1100	Para 4.0		Date 10/95	Dwg No H-4-302118 H-4-112301	
Acceptance Std MHC-SD-RTG-TC-017 (Rev.1)		Section Leakage Rate < 2.6 x 10⁻⁷ atm.cc3/sec Helium		Date 10/95		Dwg No H-4-302118 H-4-112301	
TEST CONDITIONS		TEST EQUIPMENT				MCA	
Temperature <u>Atm.</u> Device ID <input checked="" type="checkbox"/> NA		Manufacturer <u>L/H "UL-100+", #2</u>				Cleaning <input type="checkbox"/> NA	
Resonance Pressure <input checked="" type="checkbox"/> NA		Ident No <u>5/n996-38 (WC48869)</u>				Alcohol	
Test Pressure <u>1 Atm. (14.7 psia)</u> <input type="checkbox"/> NA		Mesh Size <u>9.47 x 10⁻¹² Alumina/Su/Dev</u>				MHC PROCEDURE NO <input type="checkbox"/> NA	
Gas <u>UHP Helium</u> <input type="checkbox"/> NA		Std No <u>504 40-02 01B</u>				MHT LT 8000 Rev. <u>3</u>	
Concentration <u>>90%</u> <input type="checkbox"/> NA		Std Leak <u>1.6 x 10⁻⁸ Atm/cc3/sec</u>				Appendix <u>A</u> Rev. <u>2</u>	
Other <input checked="" type="checkbox"/> NA		Calb Exp <u>July 7, 1996</u>				Special Tech No <input type="checkbox"/> NA	
Bubble Solution <input checked="" type="checkbox"/> NA		SYSTEM SENSITIVITY <input type="checkbox"/> NA				Work Inst <input type="checkbox"/> NA	
Beach No <input type="checkbox"/> NA		Sensitivity <u>1.70 x 10⁻¹¹ Atm/cc3/Dev</u>				TEST TIME	
Gate 1 <u>504 33-04 007</u> <input type="checkbox"/> NA		Std No <u>504 40-03-006</u>				STAT-O-SEAL + PRIMARY O-RING	
Range <u>0 to 50 psia</u>		Std Leak <u>1.3 x 10⁻⁷ Atm/cc3/sec</u>				No Response Time: <u>IMMEDIATE</u> <input type="checkbox"/> NA	
Calb Exp <u>March 9, 1996</u>		Calb Exp <u>July 7, 1996</u>				No Acquit Time <input checked="" type="checkbox"/> NA	
Gate 2 <u>504 21 04</u> <input checked="" type="checkbox"/> NA		ADDITIONAL STD <input checked="" type="checkbox"/> NA				Soak Time <input checked="" type="checkbox"/> NA	
Range <input type="checkbox"/> NA		Sensitivity <input type="checkbox"/> NA				Additional Times: <u>TEST DURATION</u>	
Calb Exp <input type="checkbox"/> NA		Std No <input type="checkbox"/> NA				STAT-O-SEAL = <u>3 min</u> <input type="checkbox"/> NA	
Related Value <input checked="" type="checkbox"/> NA		Std Leak <input type="checkbox"/> NA				PRIMARY O-RING = <u>10 min</u>	
Calb Exp <input type="checkbox"/> NA		Calb Exp <input type="checkbox"/> NA					
Weld No	Part No. or Serial No	Acc	Rep	No. Fail and	Comments		
					OUTER CONTAINMENT VESSEL (OCV) LEAK RATE TESTS:		
"Y" Port Stat-O-Seal	X	X	X		No Detectable Leakage (Per Step #5.2)		
"Y" Port Prim.O-Ring	X	X	X		No Detectable Leakage (Per Step #5.3)		
Note: For results of the remaining leak tests, Steps #6.2, 6.3, 6.4, 7.2 and 7.3, see B.L.Hopkins report dated November 10, 1995.							
Technique Pre Approval <input checked="" type="checkbox"/> NA				LT (Date/Data)			
W.H. Nelson B.J. Sewart				Level I II			
Date of Examination Nov. 9, 1995				Date Nov. 9, 1995			
Approved by <i>[Signature]</i>				Reviewed by <i>[Signature]</i>			
Date 11-14-95				Date 2.10.15-81			

Test Set 3: Drop Test Nos. 7, 8, and 9

**Data Sheet A from WHC-SD-RTG-TC-015, Rev. 1
Data Sheets A, B, C1, and C2 from WHC-SD-RTG-TC-018, Rev. 1
NDE Leak Test Procedure and Test Report**

DATA SHEET A

Drop Test No. 7, MCT 4-Ft Drop, Bottom End

Ambient Temperature: 0°C Impact Limiter Foam Temperature: 24°C

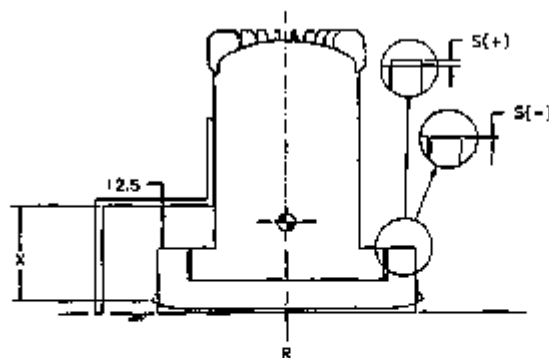
The 12.5 dimension shown below is a reference dimension to the top of the OCY flange thermal shield.

Damage Measurements: (See sketch below)

Quadrant	X (±0.13)	S (±0.08)
1		
2		
3		
4		

R = _____ ±0.13

These Dimension Data
were not taken ~~USA~~ 11/10/95



B.Q. King 11/10/95

Test Engineer

Date

QA Representative

Date

DATA SHEET A

Drop Test No. 7, MCT 4-ft Drop, Bottom End

Sketch of Damage and Notes:

Insufficient damage to record
See 30 ft drop test (Drop Test No. 8)


Test Engineer


Date


QA Representative


Date

DATA SHEET A

Drop Test No. 8, HAC 30-ft Drop, Bottom End

Ambient Temperature: 2°C Impact Limiter Foam Temperature: 20°C

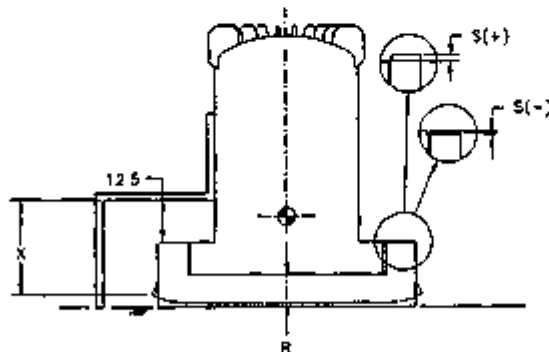
The 12.5 dimension shown below is a reference dimension to the top of the OCY flange thermal shield.

Damage Measurements: (See sketch below)

Quadrant	X (± 0.13)	S (± 0.06)
1	28 1/8	- 7/16
2	30 1/8	- 3/8
3	29 1/4	- 1/2
4	29 1/8	- 1/2

$$R = \text{---} \pm 0.13$$

X1 - distance taken at corner of angle
(previously indented due to other drops)



* NOT TAKEN DUE TO
DISTORTION OF
LOWER PLATE
APPROXIMATE
DEPTH OF FOAM
~ 8"

J.L. Smith
Test Engineer

11/10/95
Date

[Signature]
QA Representative

11/10/95
Date

DATA SHEET A

Drop Test No. 8, HAC 30-ft Drop, Bottom End

Sketch of Damage and Notes:

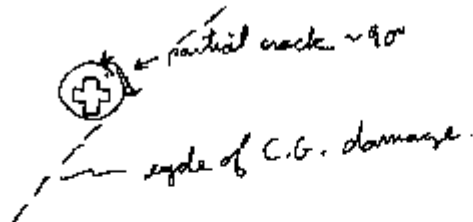
1. Small bulge or pooch most of the way around
the package



2. C.G. over corner damage ~~to~~ now looks like it did after
C.G. 4-ft drop:



3. Small crack in weld around the melt out plug



J.L. Quetta
Phil D...
Test Engineer

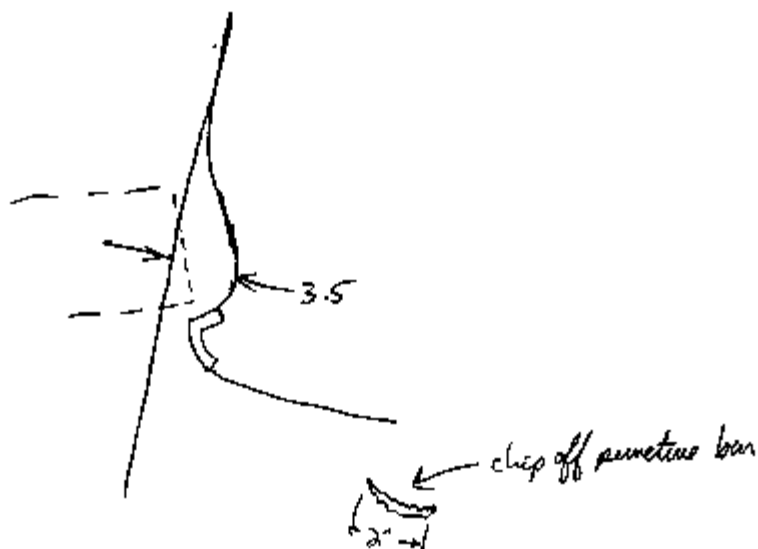
11/10/95
11/10/95
Date

M. R. B.
QA Representative

11/10/95
Date

DATA SHEET A

Drop Test No. 9, HAC Puncture

No weld distress.

Phil Alan
 Test Engineer

11/1/85
 11/1/85
 Date

[Signature]
 QA Representative

11/1/85
 Date

DATA SHEET A

Record of residual OCY closure and Impact Limiter pre-load bolt torque performed after completion of drop tests. Bolts are numbered CCW, viewed from the top of the Test Article, starting with the first bolt CCW from the feed-through.

OCY Bolts:

Loosen each bolt in turn just sufficient to establish the residual preload, followed by retorquing to the torque level equal to the installation torque multiplied by the ratio of the disassembly residual preload to the assembly residual preload (See WMC-SD-TC-014, Data Sheet A) or the disassembly preload torque, whichever is less, starting with Bolt 1, crossing the bell to Bolt 13, proceeding to Bolt 2 and across to Bolt 14, proceed to Bolt 24 and across to Bolt 12. The balance of the pattern is: 3-15, 23-11, 4-16, 22-10, 5-17, 21-9, 6-18, 20-8, 7-19.

Impact Limiter Bolts:

In a similar manner, loosen each bolt, starting with Bolt 1, crossing the bell to Bolt 5, proceeding to Bolt 2 and across to Bolt 6, proceed to Bolt 8 and across to Bolt 4, then to Bolt 3 and to Bolt 7.

OCY Closure Bolts			
Residual Preload			
Bolt #	Torque, ft-lb	Bolt #	Torque, ft-lb
1	180	13	260
2	230	14	275
3	(310)	15	270
4	300	16	280
5	290	17	280
6	255	18	260
7	235	19	270
8	240	20	230
9	250	21	270
10	255	22	250
11	210	23	260
12	240	24	200

Impact Limiter Bolts	
Residual Preload	
Bolt #	Torque, ft-lb
1	85
2	90
3	165
4	50
5	30
6	35
7	loose
8	20

Test Engineer

Date

QA Representative

Date

OFFICIAL COPY

2.10.15-88

DATA SHEET 8

Record of ICV residual pre-load bolt torque performed after completion of drop tests and after removal of OCY bell. Bolts are numbered CCW, viewed from the top of the Test Article, starting with the first bolt CCW from the electrical feed-through. Loosen each bolt in turn just sufficient to establish the residual preload, followed by retorquing to the torque level equal to the installation torque multiplied by the ratio of the disassembly residual preload to the assembly residual preload (See MHC-SD-TC-014, Data Sheet 8) or the disassembly preload torque, whichever is less, starting with Bolt 1, crossing the bell to Bolt 13, proceeding to Bolt 2 and across to Bolt 14, proceed to Bolt 24 and across to Bolt 12. The balance of the pattern is: 3-15, 23-11, 4-16, 22-10, 5-17, 21-9, 6-18, 20-8, 7-19.

ICV Closure Bolts			
Residual Preload			
Bolt #	Torque, ft-lb	Bolt #	Torque, ft-lb
1	180	13	185
2	135	14	175
3	190	15	185
4	180	16	170
5	150	17	180
6	190	18	180
7	185	19	180
8	190	20	180
9	175	21	180
10	190	22	185
11	190	23	187
12	165	24	170

76-6-2-9-20-8-20-7-21
 200-0-9-20-8-20-7-21

AKC = 170 FT-LB

J. L. Curtis 11/15/85
 Test Engineer Date

[Signature] 11/10/85
 QA Representative Date

OFFICIAL COPY

DATA SHEET C1

Record of RTG Certification Test Article bolt length performed after drop tests. Bolts are numbered CCW, viewed from the top of the Test Article, starting with the first bolt CCW from the electrical feed-through.

OCY Closure Bolts			
Bolt #	Length (in.)	Bolt #	Length (in.)
1	5.9731	13	5.9604
2	5.9567	14	5.9702
3	5.9653	15	5.9700
4	5.9739	16	5.9633
5	5.9621	17	5.9677
6	5.9763	18	5.9661
7	5.9805	19	5.9579
8	6.0336	20	5.9664
9	5.9761	21	5.9549
10	5.9681	22	5.9536
11	5.9666	23	5.9723
12	5.9747	24	5.9690

Note: these measurements apply to "before tests" for tests 10-49

NEW BOLTS TEST 7, 8, 9

Impact Limiter Bolts	
Bolt #	Length (in.)
X17	8.9928
X18	8.9841
X19	8.9914
X20	8.9905
X21	8.9944
X22	8.9868
X23	8.9891
X24	8.9913

Bolt #	Before Test	After Test
A		

Note: the "other" measurement apply to "before testing" for tests 10-49

Impact
Limiters
before test

J. L. Quitt
Test Engineer

11/15/95
Date

Randy J. [Signature]
QA/Representative

11-15-95
Date

J. L. Quitt
11/15/95

OFFICIAL COPY

DATA SHEET 02

ICV Closure Bolts			
Bolt #	Length (in.)	Bolt #	Length (in.)
1	1.9582	13	1.9492
2	1.9626	14	1.9699
3	1.9674	15	1.9555
4	1.9711	16	1.9646
5	1.9687	17	1.9595
6	1.9669	18	1.9602
7	1.9693	19	1.9690
8	1.9559	20	1.9687
9	1.9643	21	1.9580
10	1.9729	22	1.9639
11	1.9615	23	1.9616
12	1.9557	24	1.9592

Note: These measurements apply to "before test" for tests 10-19

J.L. [Signature] / 11/15/95
Test Engineer Date

[Signature] 11-15-95
QA Representative Date

OFFICIAL COPY

2.10.15-91

Westinghouse Hanford Company		NDE LEAK TEST PROCEDURE AND TEST REPORT UL-100				JOB No.	
MNC-SD-RTG-SARP-001		NON DESTRUCTIVE EXAMINATION 300 BLDG 300 AREA TEL 378-8401				95-8	
Requester: A. AVERETTE		Company: PACKED					
Spec: NO-916		Area: 1100		Paper/Envelope/Work Package/Transfer Kit			
Acceptance Std: NO-916		Section: 1100		INTERIM DISASSEMBLY & REASSEMBLY OF THE RADIOISOTOPIC THERMOELECTRIC GENERATOR, SECOND CERTIFICATION, TEST ARTICLE CIA-2, DROP TEST 7,8,9 PER MNC-SD-RTG-TC-017 R/1			
LEAK RATE = 2.6×10^{-7} ATM CC/SEC. HELIUM		Date: <input type="checkbox"/> NA		Drop No. <input type="checkbox"/> NA		E-4-302118 E-4-112301	
TEST CONDITIONS				TEST EQUIPMENT <input type="checkbox"/> NA			
Temperature: AMB. Device ID: <input checked="" type="checkbox"/> NA		Manufacture: L/H UL 100 PLUS		NCR: <input checked="" type="checkbox"/> NA		Cleaning: <input checked="" type="checkbox"/> NA	
Operating Pressure: AMB. <input type="checkbox"/> NA		Name: WC48896		WMC PROCEDURE NO: <input type="checkbox"/> NA		APPENDIX A Rev 2	
Test Pressure: 1 ATM. <input type="checkbox"/> NA		Spec: 1 X 10-11 atm(cc)/sec		Sensitivity: 1.6 X 10-11 atm(cc)/sec		Special Tech No: <input type="checkbox"/> NA	
Gas: HELIUM <input type="checkbox"/> NA		Std No: 504-40-03 016		Std Leak: 1.6 X 10-8 atm(cc)/sec		Work Int: <input type="checkbox"/> NA	
Detection: APPROX. 100% <input type="checkbox"/> NA		Std Exp: 7-7-96		Sensitivity: 1.6 X 10-11 atm(cc)/sec		TEST TIME	
Other: <input checked="" type="checkbox"/> NA		Sensitivity: 1.6 X 10-11 atm(cc)/sec		Std Leak: 1.3 X 10-7 atm(cc)/sec		No Response Time: IMMEDIATE <input type="checkbox"/> NA	
Seal Solution: <input checked="" type="checkbox"/> NA		Sensitivity: 1.6 X 10-11 atm(cc)/sec		Cable Exp: 7-7-96		He Accum Time: <input checked="" type="checkbox"/> NA	
Check No: <input type="checkbox"/> NA		Sensitivity: 1.6 X 10-11 atm(cc)/sec		ADDITIONAL STD: <input checked="" type="checkbox"/> NA		Soak Time: <input checked="" type="checkbox"/> NA	
Step 1: 007 <input type="checkbox"/> NA		Sensitivity: 1.6 X 10-11 atm(cc)/sec		Sensitivity: 1.6 X 10-11 atm(cc)/sec		Additional Tests	
Range: 0 TO 50 PSIA		Sensitivity: 1.6 X 10-11 atm(cc)/sec		Std Leak: 1.3 X 10-7 atm(cc)/sec		TEST TIME 2 MIN. <input type="checkbox"/> NA	
Cable Exp: 3-9-96		Sensitivity: 1.6 X 10-11 atm(cc)/sec		Cable Exp: 7-7-96			
Step 2: <input checked="" type="checkbox"/> NA		Sensitivity: 1.6 X 10-11 atm(cc)/sec		ADDITIONAL STD: <input checked="" type="checkbox"/> NA			
Range: <input type="checkbox"/> NA		Sensitivity: 1.6 X 10-11 atm(cc)/sec		Sensitivity: 1.6 X 10-11 atm(cc)/sec			
Cable Exp: <input type="checkbox"/> NA		Sensitivity: 1.6 X 10-11 atm(cc)/sec		Std Leak: <input type="checkbox"/> NA			
Rated Value: <input checked="" type="checkbox"/> NA		Sensitivity: 1.6 X 10-11 atm(cc)/sec		Cable Exp: <input type="checkbox"/> NA			
Test No	Part No	in Serial No	App	Req	No Def Ind	Comments	
						OUTER CONTAINMENT VESSEL (OVC) LEAK RATE TESTS	
"W" PORT STAT-O-SEAL	X					LEAK RATE = 1.0×10^{-9} ATM CC/SEC. (PER STEP #6.6)	
"I" PORT PRIM.O-RING	X		X			NO DETECTABLE LEAKS (PER STEP #6.5)	
						INNER CONTAINMENT VESSEL (IVC) LEAK RATE TESTS	
"B" PORT STAT-O-SEAL	X		X			NO DETECTABLE LEAKS (PER STEP #7.2)	
"S" PORT STAT-O-SEAL	X		X			NO DETECTABLE LEAKS (PER STEP #7.3)	
"I" PORT PRIM.O-RING	X		X			NO DETECTABLE LEAKS (PER STEP #7.4)	
Technician Per Approval: W.H. NELSON		LT Level/Date					
Level: I		Interpreted by: B. L. HOPKINS II		Requested by: RE Layner			
Date of Examination: 11-10-95		Date: 11-10-95		Date: 11/21/95		2 10.15-92	

Westinghouse Hanford Company		NDE LEAK TEST PROCEDURE AND TEST REPORT UL-100				Rev 0	
Company		Prep/Exam/Work Package/Transfer No				95-8	
Company		Pack/EC				Generator (RTG) After Drop Tests #7-#9 on Certification	
Part No		Area		Test Article #CTA-2, per WNC-SD-RTG-TC-016, Rev.1			
62-02		MO-916		1100			
Appearance Std		Section		Para		Date	
WNC-SD-RTG-TC-016, Rev.1		Para. 5.0		10/95		10/95	
Leakage Rate < 2.6×10^{-7} atm.cm ³ /sec Helium						H-4-302118 H-4-112301	
TEST CONDITIONS				TEST EQUIPMENT			
Temperature <u>Amb</u> Devs ID <input checked="" type="checkbox"/> NA		<input checked="" type="checkbox"/> NA		Manufacturer <u>L/H "UL-100+", #2</u>		<input checked="" type="checkbox"/> NA	
Electrical Pressure <input checked="" type="checkbox"/> NA		<input checked="" type="checkbox"/> NA		Mater No <u>S/NB95-38 (MC48869)</u>		<input checked="" type="checkbox"/> NA	
Test Pressure <u>-1 Atm. (14.7psia)</u> <input checked="" type="checkbox"/> NA		<input checked="" type="checkbox"/> NA		Mesh Size <u>1.07 x 10⁻¹¹</u> <input checked="" type="checkbox"/> NA		WNC PROCEDURE NO	
Gas <u>UHP Helium</u> <input checked="" type="checkbox"/> NA		<input checked="" type="checkbox"/> NA		Std No <u>504-45-09 018</u>		<input checked="" type="checkbox"/> NA	
Concentration <u>> 90%</u> <input checked="" type="checkbox"/> NA		<input checked="" type="checkbox"/> NA		Std Leak <u>1.6 x 10⁻⁸</u> <input checked="" type="checkbox"/> NA		Appendix <u>A</u> Rev <u>2</u>	
Gauge <input checked="" type="checkbox"/> NA		<input checked="" type="checkbox"/> NA		Cals Exp <u>July 7, 1996</u>		<input checked="" type="checkbox"/> NA	
System Isolation <input checked="" type="checkbox"/> NA		<input checked="" type="checkbox"/> NA		SYSTEM SENSITIVITY		<input checked="" type="checkbox"/> NA	
Blank No <input checked="" type="checkbox"/> NA		<input checked="" type="checkbox"/> NA		<input type="checkbox"/> SENS OF MS&D Cals or		<input checked="" type="checkbox"/> NA	
Step 1 <u>504-21-04-007</u> <input checked="" type="checkbox"/> NA		<input checked="" type="checkbox"/> NA		Sensitivity <u>2.36 x 10⁻¹⁰</u> <input checked="" type="checkbox"/> NA		<input checked="" type="checkbox"/> NA	
Step <u>0 to 50 psia</u> <input checked="" type="checkbox"/> NA		<input checked="" type="checkbox"/> NA		Std No <u>588-40-03-006</u>		TEST TIME	
Cals Exp <u>March 9, 1996</u> <input checked="" type="checkbox"/> NA		<input checked="" type="checkbox"/> NA		Std Leak <u>1.3 x 10⁻⁷</u> <input checked="" type="checkbox"/> NA		<u>ICV STRUCTURE TEST</u>	
Step 2 <u>504-31-04</u> <input checked="" type="checkbox"/> NA		<input checked="" type="checkbox"/> NA		Cals Exp <u>July 7, 1996</u>		No Response Time = <u>3 min.</u> <input checked="" type="checkbox"/> NA	
Step <input checked="" type="checkbox"/> NA		<input checked="" type="checkbox"/> NA		ADDITIONAL STD		No Leak Time <input checked="" type="checkbox"/> NA	
Cals Exp <input checked="" type="checkbox"/> NA		<input checked="" type="checkbox"/> NA		Sensitivity <input checked="" type="checkbox"/> NA		Soak Time <input checked="" type="checkbox"/> NA	
Std Valve <input checked="" type="checkbox"/> NA		<input checked="" type="checkbox"/> NA		Std No <input checked="" type="checkbox"/> NA		Additional Times	
				Std Leak <input checked="" type="checkbox"/> NA		<u>TEST DURATION = 30 min</u> <input checked="" type="checkbox"/> NA	
				Cals Exp <input checked="" type="checkbox"/> NA			
Work No	Part No	or Serial No	Acc	Req	No Ret Use	Comments	
						INNER CONTAINMENT VESSEL (ICV) LEAK RATE TESTS:	
			X			Leak Rate- 1.96×10^{-7} atm.cm ³ /sec Helium (Per Step #7.6)	
						Note: For results of the remaining leak tests, Steps	
						#6.2, 6.4, 6.5, 7.2, 7.3 and 7.4, see B.L.Hopkins report	
						dated November 10, 1995.	
Technician For Approval			LT Level/Date				
W.M. Nelson			II				
B.J. Stewart			II				
Date of Examination			Date				
Nov. 13, 1995			Nov. 13, 1995				
Reviewed by			Date				
John K. R...			11-14-95				
2.10.15-93			8-2051 482 (11/94)				

OFFICIAL COPY

Westinghouse Hanford Company		NDE LEAK TEST PROCEDURE AND TEST REPORT UL-100				Job No.
		NON DESTRUCTIVE EXAMINATION 300 BLDG. 300 AREA TEL 279-8401				95-B
Requestor try S. Averette		Company PacTec	Project/System/Work Package/Invoice No. Helium Leak Test of Radioisotope Thermoelectric Generator (RTG) After Drop Tests #7-#9 on Certification Test Article #CTA-2, per NHC-SD-RTG-TC-014, Rev.1			
MSN G2-02	SN# MO-916	Area 1100				
Acceptance Std WHC-SD-RTG-TC-014, Rev.1	Section Para. 5.0	Para 10/95	Draw <input type="checkbox"/> NA	Dog No H-4-302118 H-4-1123D1		
TEST CONDITIONS		TEST EQUIPMENT		NCR		
Temperature Amb. Device ID <input checked="" type="checkbox"/> NA	Manufacturer L/H "UL-100", #2		<input checked="" type="checkbox"/> NA			Clearing <input type="checkbox"/> NA
Barometric Pressure <input checked="" type="checkbox"/> NA	Model No 5/nB96-38 (WC48869)					Alcohol
Test Pressure A = 1 Atm. (14.7psia) <input type="checkbox"/> NA	Mach Fan 9.47 x 10⁻¹² atm/cm²/sec		WMC PROCEDURE NO <input type="checkbox"/> NA			
Gas UHP Helium <input type="checkbox"/> NA	Std No 584-40-DJ D18		<input checked="" type="checkbox"/> NDT LET 8000 Rev. 3			
Concentration >90% <input type="checkbox"/> NA	Std Leak 1.6 x 10⁻⁸ atm/cm²/sec		Appendix A Part 2			
Order <input checked="" type="checkbox"/> NA	Cable Exp July 7, 1996		<input type="checkbox"/> Special Test No _____			
Bubble Solution <input checked="" type="checkbox"/> NA	SYSTEM SENSITIVITY <input type="checkbox"/> NA		<input type="checkbox"/> Work Inct _____			
Batch No _____	<input type="checkbox"/> Same as MSD Cable or					
Gate 1 SB4 01 04 007 <input type="checkbox"/> NA	Sensitivity 1.28 x 10⁻¹¹ atm/cm²/sec/Div					
Range 0 to 50 psia	Std No 584-40-03-006					
Cable Exp March 9, 1996	Std Leak 1.3 x 10⁻⁷ atm/cm²/sec					
Gate 2 SB4 01 04 <input checked="" type="checkbox"/> NA	Cable Exp July 7, 1996					
Range _____	ADDITIONAL STD <input checked="" type="checkbox"/> NA					
Cable Exp _____	Sensitivity _____					
Reset Valve <input checked="" type="checkbox"/> NA	Std No _____					
	Std Leak _____					
	Cable Exp _____					
Weld No	Part No. or Serial No.	Acc	Req	No Def Ind	Comments	
					INNER CONTAINMENT VESSEL (ICV) LEAK RATE TESTS:	
"P" Port Stat-O-Seal	X	X	X	No Detectable Leakage	(Per Step #6.4)	
"S" Port Stat-O-Seal	X	X	X	No Detectable Leakage	(Per Step #6.5)	
"T" Port Prim-O-Ring	X	X	X	No Detectable Leakage	(Per Step #6.6)	
					OUTER CONTAINMENT VESSEL (OCV) LEAK RATE TESTS:	
"V" Port Stat-O-Seal	X	X	X	No Detectable Leakage	(Per Step #7.4)	
"T" Port Prim-O-Ring	X	X	X	No Detectable Leakage	(Per Step #7.5)	
Technique Per Approval <input checked="" type="checkbox"/> NA		LT Level/Dose				
Inspector W. N. Melson	Level 1	Interpreted by B. J. Sewar		LT Level 11	Reviewed by John T. Ken	
Date of Examination Nov. 14, 1995		Date Nov. 14, 1995			11-15-95 2.10.15-94	

Westinghouse Hanford Company		NOE LEAK TEST PROCEDURE AND TEST REPORT UL-100 NON DESTRUCTIVE EXAMINATION 308 BLDG., 300 AREA - TEL 376-3401				Job No 95-8
Inspector S. A. Verette		Company PacTec		Project/System/Work Package/Transfer No Helium Leak Test of Radioisotope Thermoelectric Generator (RTG) After Drop Tests #7-#9 on Certification		
MSR# G2-02	Doc# MO-916	Area 1100	Test Article #CTA-2, per NHC-SD-RTG-TC-016, Rev.1			
Acceptance S/N NHC-SD-RTG-TC-016 (Rev.1)	Section Leakage Rate < 2.6×10^{-7} atm.cm ³ /sec. Helium	Para 5.0	Date 10/95	<input type="checkbox"/> NA	Dwg No H-4-302118 H-4-112301	<input type="checkbox"/> NA
TEST CONDITIONS		TEST EQUIPMENT		NCR		<input type="checkbox"/> NA
Temperature <u>Amb.</u> Device ID <input checked="" type="checkbox"/> NA	Barometric Pressure <input checked="" type="checkbox"/> NA	Manufacturer <u>L/H "UL-100+", #2</u>	Model No <u>5/n896-3B (WC40869)</u>	<input checked="" type="checkbox"/> NA		Clearing <input type="checkbox"/> NA
Test Pressure <u>= 1 Atm. (14.7psia)</u> <input type="checkbox"/> NA	Gas <u>UHP Helium</u> <input type="checkbox"/> NA	Mach Gen <u>9.47×10^{-12} Am/Sec/Sec/Dir</u>	End No <u>684 40-09 019</u>	WMC PROCEDURE NO <input type="checkbox"/> NA		Alcohol <input type="checkbox"/> NA
Concentration <u>>90%</u> <input type="checkbox"/> NA	Other <input checked="" type="checkbox"/> NA	Std Leak <u>1.6×10^{-8} Am/Sec/Sec</u>	Date Exp <u>July 7, 1996</u>	<input checked="" type="checkbox"/> WOT LT-0000 Rev 3		Appendix <u>A</u> Rev <u>2</u>
Bubble Detector <input checked="" type="checkbox"/> NA	Beach No _____	SYSTEM SENSITIVITY <input type="checkbox"/> NA	<input type="checkbox"/> Same as MSLO Code or	<input type="checkbox"/> Special Tech No _____		<input type="checkbox"/> Work Incc _____
Gage 1 <u>584 01 04 007</u> <input type="checkbox"/> NA	Range <u>0 to 50 psia</u>	Sensitivity <u>8.13×10^{-11} Am/Sec/Sec/Dir</u>	End No <u>584-40-03-006</u>	TEST TIME		<input type="checkbox"/> NA
Date Exp <u>March 9, 1996</u>	<input checked="" type="checkbox"/> 2 584-01-04 <input checked="" type="checkbox"/> NA	Std Leak <u>1.3×10^{-7} Am/Sec/Sec</u>	Date Exp <u>July 7, 1996</u>	OCV STRUCTURE		<input type="checkbox"/> NA
Range _____	Calb Exp _____	ADDITIONAL DTG <input checked="" type="checkbox"/> NA	Calb Exp _____	No Response Time = <u>4 minutes</u>		<input type="checkbox"/> NA
Retest Value _____	Calb Exp _____	Std No _____	Std Leak _____	No Assum Time _____		<input checked="" type="checkbox"/> NA
		Std Leak _____	Calb Exp _____	Seal Time _____		<input checked="" type="checkbox"/> NA
				Additional Times "TEST DURATION"		<input type="checkbox"/> NA
				OCV STRUCTURE = <u>30 minutes</u>		<input type="checkbox"/> NA
Used No	Part No. or Serial No	Acc	Qty	Comments		
				OUTER CONTAINMENT VESSEL (OCV) LEAK RATE TESTS:		
		X		Leak Rate- 1.42×10^{-7} atm.cm ³ /sec.Helium (Per Step #6.2)		
				Note: This is the last OCV Structure leak rate test done prior to reassembly of package per NHC-SD-RTG-TC-014.		
Technician No	Approved	CF Level	Date			
W.H. Nelson		I		Interpreted by	ET Level	Reviewed by
B.J. Swart		II		B.J. Swart	II	
Date of Examination				Date		
Nov. 14, 1995				11/15/95		11-15-95 2.10.15-95

Test Set 4: Drop Test Nos. 10, 11, 12, 13, 14, 15, and 16

Data Sheet A from WHC-SD-RTG-TC-015, Rev. 1
Data Sheets A, B, C1, and C2 from WHC-SD-RTG-TC-018, Rev. 1
NDE Leak Test Procedure and Test Report

DATA SHEET A

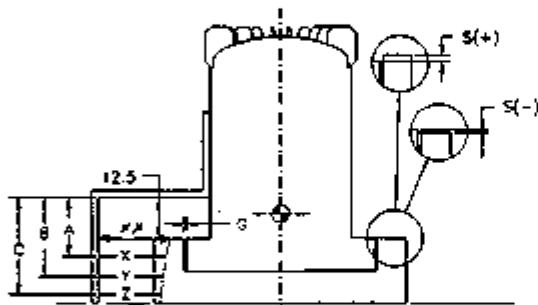
Drop Test No. 10, MCT 4-ft Drop, Side Slapdown

Ambient Temperature: 4°C Impact Limiter Foam Temperature: 28°C

The 12.5 dimension shown below is a reference dimension to the top of the OCY flange thermal shield.

Damage Measurements: (See sketch below)

Quadrant	S (±0.06)	G (±0.06)
1	- ⁶ / ₁₀	¹² / ₃₂
2	- ¹¹ / ₃₂	¹ / ₁₆
3	- ¹⁷ / ₃₂	⁶ / ₃₂
4	- ¹⁹ / ₃₂	¹² / ₃₂



xx = 5 9/8

A (±0.25)	B (±0.25)	C (±0.25)	X (±0.25)	Y (±0.25)	Z (±0.25)
14 3/8	22.0	30 1/8	5 1/4	4 1/2	4 1/4

[Signature]
 Test Engineer

11/20/95
 Date

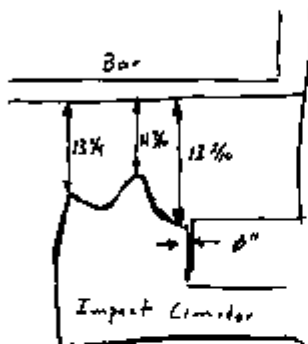
[Signature]
 QA Representative

11/20/95
 Date

DATA SHEET A

Drop Test No. 10, NET 4-ft Drop, Side Slapdown

Sketch of Damage and Notes:



J. A. Grant
Test Engineer

1/1/98
Date

M. S. P. D.
QA Representative

1/1/98
Date

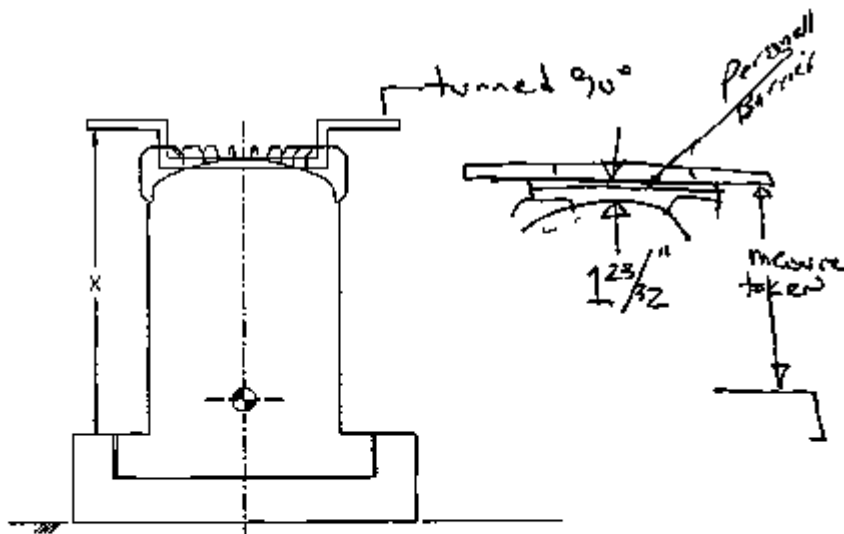
DATA SHEET A

Drop Test No. 11, NCT 4-ft Drop, Top End

Ambient Temperature: 70 Impact Limiter Foam Temperature: N/A

Damage Measurements: (See sketch below)

Quadrant	X (± 0.13)
1	57 ³ / ₄
2	57 ¹ / ₂
3	58 ¹ / ₂
4	58



J.P. Pinto
Test Engineer

W.P.
Date

W.P.
QA Representative

W.P.
Data

DATA SHEET A

Drop Test No. 11, NCT 4-ft Drop, Top End

Sketch of Damage and Notes:

SEE PHOTOS OF DENT
EVEN FLATTENING OF FINS

J. S. Quisto
Test Engineer

11/20/95
Date

MC RST
QA Representative

11/20/95
Date

DATA SHEET A

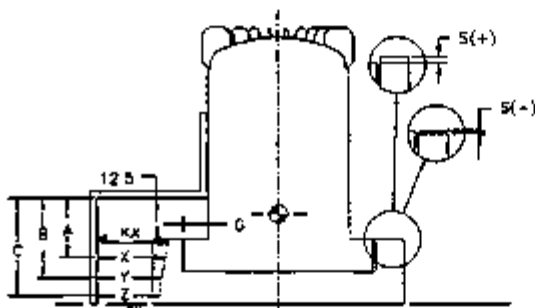
Drop Test No. 12, HAC 30-ft Drop, Side Slapdown

Ambient Temperature: 11°C Impact Limiter Foam Temperature: 28°C

The 12.5 dimension shown below is a reference dimension to the top of the OCV flange thermal shield.

Damage Measurements: (See sketch below)

Quadrant	S (± 0.06)	G (± 0.06)
1	-18/32	11/32
2	-16/32	1/16
3	-21/32	12/32
4	-14/32	10/32



$$XX = 7 \frac{8}{10}''$$

A (± 0.25)	B (± 0.25)	C (± 0.25)	X (± 0.25)	Y (± 0.25)	Z (± 0.25)
14 ³ / ₈ "	22.0"	30 ¹ / ₈ "	7 ³ / ₄	5 ³ / ₄	4 ³ / ₈

D. S. Smith
Test Engineer

11/20/95
Date

MEI
QA Representative

11/20/95
Date

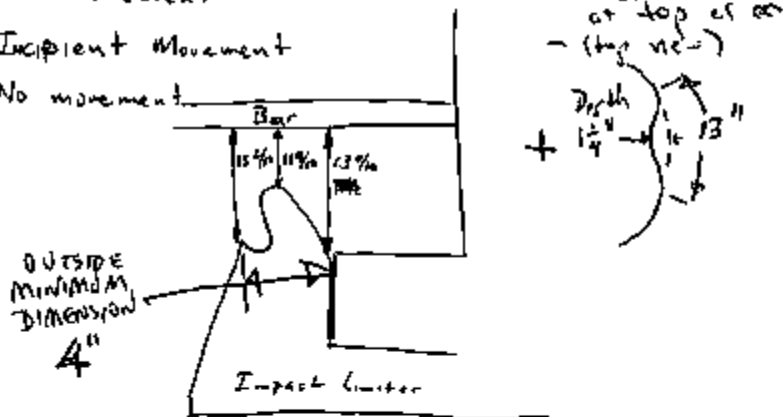
DATA SHEET A

Drop Test No. 12, HAC 30-ft Drop, Side Slapdown

Sketch of Damage and Notes:

Impact Limiter BoltsTORQUE WRENCH
#4 - 58A-88-01-02
CAL EXP 9/29/86

- 1 - No movement
- 2 - Incipient Movement
- 3 - Loose
- 4 - Loose
- 5 - No Movement
- 6 - No Movement
- 7 - Incipient Movement
- 8 - No movement



J. S. Peltz
Test Engineer

4/20/85
Date

NERP
QA Representative

4/20/85
Date

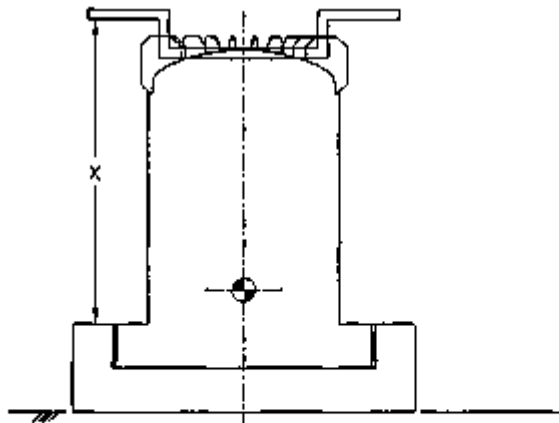
DATA SHEET A

Drop Test No. 13, HAC 30-ft Drop, Top End

Ambient Temperature: 19°C Impact Limiter Foam Temperature: M/A ^{25°C}

Damage Measurements: (See sketch below)

Quadrant	X (±0.13)
1	60 3/4
2	60 3/8 58 7/8
3	60 3/16
4	61 7/16



[Signature]
Test Engineer

11/20/95
Date

[Signature]
QA Representative

11/20/95
Date

DATA SHEET A

Drop Test No. 13, HAC 30-ft Drop, Top End

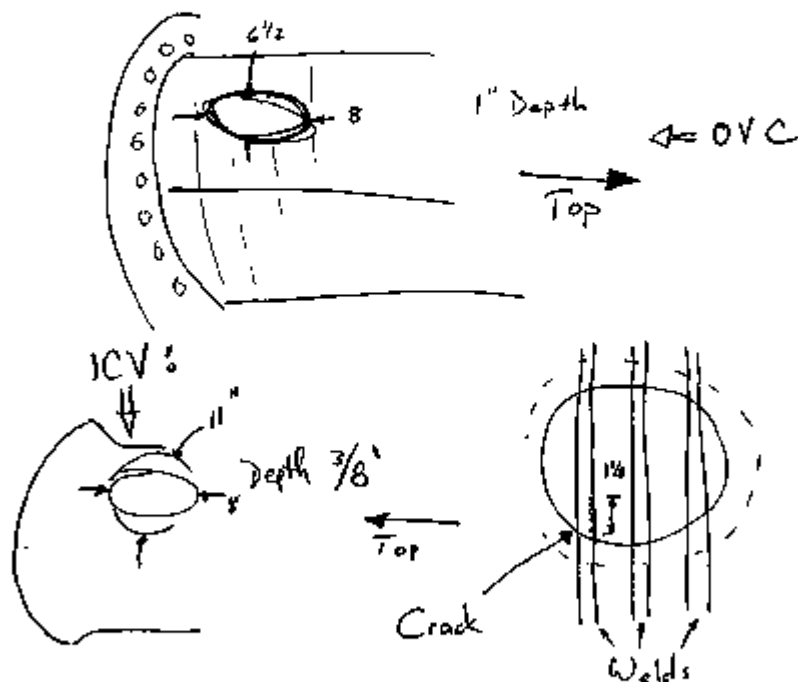
Sketch of Damage and Notes:

See Photos
J. A. Pank
Test Engineer*11/24/75*
Date*M. E. Pank*
QA Representative*11/24/75*
Date

DATA SHEET A

Drop Test No. 14, MAC Puncture

AMBIENT TEMP 10°C
 FOUR HOURS AFTER
 TEST 23°C



J. L. [Signature]
 Test Engineer

11/10/95
 Date

[Signature]
 QA Representative

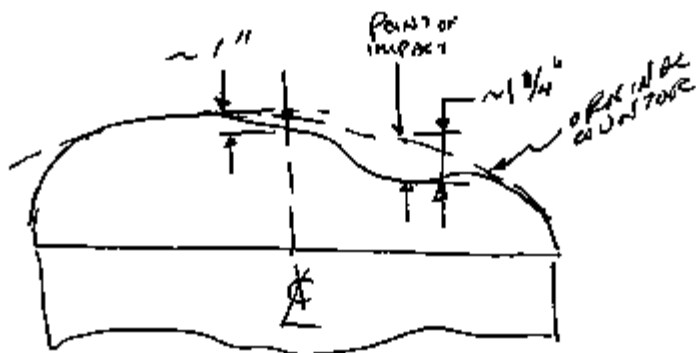
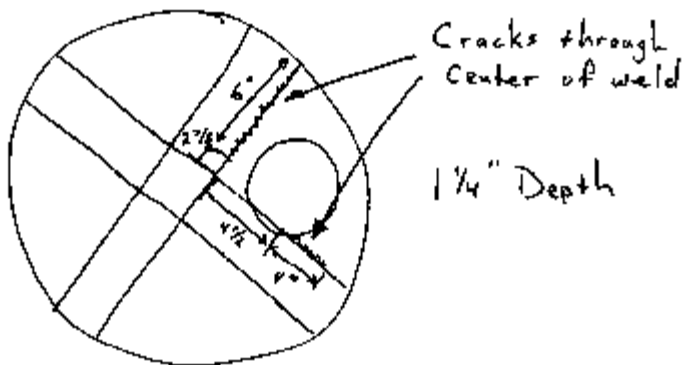
11/20/95
 Date

DATA SHEET A

Drop Test No. 15, HAC Puncture

Impact Limiter From Temp = 25°C

Ambient Temp = ~~10°C~~
8°C 15:15
~~10°C~~



J. L. Pinto
Test Engineer

11/15/56
Date

M. S. [Signature]
QA Representative

11/15/56
Date

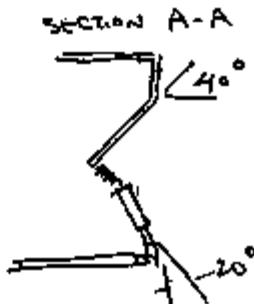
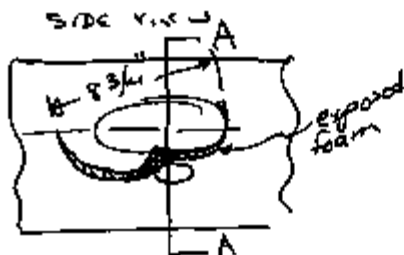
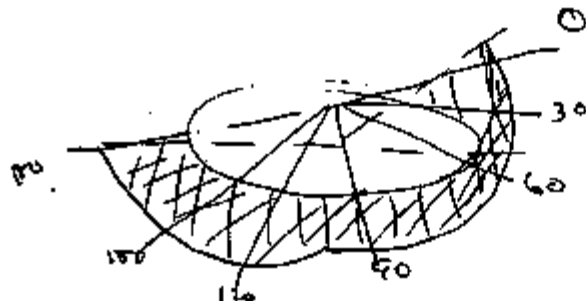
DATA SHEET A

Drop Test No. 16, HAC Puncture

Impact Limiter Foam Temp = 20°C

Ambient Temp = 8°C

SIDE WALL OF IMPACT LIMITER CRACKED.

exposed foam
(projected dimension)

FOAM EXP. IN

0	0
30	7/8"
60	1"
90	1 1/4"
120	1"
150	3/4"
180	0

J. L. Auto
Test Engineer

11/2/88
Date

W. P. R. O.
QA Representative

11/2/88
Date

DATA SHEET A

Record of residual OCY closure and Impact Limiter pre-load bolt torque performed after completion of drop tests. Bolts are numbered CCW, viewed from the top of the Test Article, starting with the first bolt CCW from the feed-through.

OCY Bolts:

Loosen each bolt in turn just sufficient to establish the residual preload, followed by retorquing to the torque level equal to the installation torque multiplied by the ratio of the disassembly residual preload to the assembly residual preload (See WMC-SD-TC-014, Data Sheet A) or the disassembly preload torque, whichever is less, starting with Bolt 1, crossing the ball to Bolt 13, proceeding to Bolt 2 and across to Bolt 14, proceed to Bolt 24 and across to Bolt 12. The balance of the pattern is: 3-15, 23-11, 4-16, 22-10, 5-17, 21-9, 6-18, 20-8, 7-19.

Impact Limiter Bolts:

In a similar manner, loosen each bolt, starting with Bolt 1, crossing the ball to Bolt 5, proceeding to Bolt 2 and across to Bolt 6, proceed to Bolt 8 and across to Bolt 4, then to Bolt 3 and to Bolt 7.

TORQUE WIPERCH 9/21/96
950-88-01-068
CAL EXP 10-20-96

OCY Closure Bolts			
Residual Preload			
Bolt #	Torque, ft-lb	Bolt #	Torque, ft-lb
1	225	13	250
2	240	14	260
3	250	15	230
4	240	16	250
5	265	17	260
6	260	18	265
7	255	19	280
8	265	20	240
9	240	21	260
10	280	22	265
11	260	23	280
12	210	24	215

Impact Limiter Bolts	
Residual Preload	
Bolt #	Torque, ft-lb
1	112
2	LOOSE
3	LOOSE
4	LOOSE
5	80
6	82
7	35
8	62

Average = 252 ft-lb

M. A. Smith
 Test Engineer Date

M. R. D.
 QA Representative Date

OFFICIAL COPY

DATA SHEET B

Record of ICV residual pre-load bolt torque performed after completion of drop tests and after removal of OCY bell. Bolts are numbered CCM, viewed from the top of the Test Article, starting with the first bolt CCM from the electrical feed-through. Loosen each bolt in turn just sufficient to establish the residual preload, followed by retorquing to the torque level equal to the installation torque multiplied by the ratio of the disassembly residual preload to the assembly residual preload (See MHC-SD-TC-014, Data Sheet B) or the disassembly preload torque, whichever is less, starting with Bolt 1, crossing the bell to Bolt 13, proceeding to Bolt 2 and across to Bolt 14, proceed to Bolt 24 and across to Bolt 12. The balance of the pattern is: 3-15, 23-11, 4-16, 22-10, 5-17, 21-9, 6-18, 20-8, 7-19.

ICV Closure Bolts			
Residual Preload			
Bolt #	Torque, ft-lb	Bolt #	Torque, ft-lb
1	215	13	230
2	210	14	220
3	210	15	200
4	220	16	215
5	230	17	220
6	225	18	210
7	220	19	220
8	200	20	200
9	200	21	175
10	190	22	200
11	215	23	175
12	190	24	200

lines on bolts were engaging in line with lines on ICV counter-bore

TORQUE WRENCH
584-88-01-002
CAL EXP 9/29/96

AVERAGE = 208 FT-LB

[Signature] 11/29/95
Test Engineer Date

[Signature] 11/29/95
QA Representative Date

OFFICIAL COPY

DATA SHEET C1

Record of RTG Certification Test Article bolt length performed after drop tests. Bolts are numbered CCW, viewed from the top of the Test Article, starting with the first bolt CCW from the electrical feed-through.

OCV Closure Bolts			
Bolt #	Length (in.)	Bolt #	Length (in.)
1	5.9734	13	5.9610
2	5.9588	14	5.9706
3	5.9658	15	5.9701
4	5.9741	16	5.9636
5	5.9622	17	5.9678
6	5.9764	18	5.9665
7	5.9802 5.9682	19	5.9580
8	6.0338	20	5.9665
9	5.9764	21	5.9550
10	5.9683	22	5.9540
11	5.9667	23	5.9727
12	5.9754	24	5.9692

Impact Limiter Bolts	
Bolt #	Length (in.)
1	9.0039
2	9.0065
3	8.9996
4	9.0085
5	9.0102
6	8.9969
7	8.9941
8	8.9982

F. L. Smith *1/2/96*
Test Engineer Date

Paul L. Lally *12/24/95*
QA Representative Date

M. Q. TE QL11083

OFFICIAL COPY

DATA SHEET 02

ICV Closure Bolts			
Bolt #	Length (in.)	Bolt #	Length (in.)
1	1.9586	13	1.9491
2	1.9626	14	1.9699
3	1.9672	15	1.9552
4	1.9714	16	1.9644
5	1.9685	17	1.9599
6	1.9669	18	1.9601
7	1.9690	19	1.9691
8	1.9567	20	1.9689
9	1.9646	21	1.9582
10	1.9729	22	1.9641
11	1.9616	23	1.9616
12	1.9555	24	1.9601

H. J. Smith *reforges*
 Test Engineer Date

James L. Kelly 1204-98
 QA Representative Date
 MATE QC 11083

Westinghouse Manford Company		NDE LEAK TEST PROCEDURE AND TEST REPORT UL-100 NON DESTRUCTIVE EXAMINATION 300 BLDG., 300 AREA - TEL. 376-8403				Job No. 95-8
Requester Jerry S. Averette		Company PacTec		Project/System/Work Package/Traveler No. Helium Leak Test of Radioisotope Thermoelectric		
MSR GZ-02		MSR MO-916		Generator (RTG) After Drop Test #10-#16 on Certification		
Acceptance Std. WHC-SD-RTG-TC-016, Rev.1		Section Para. 5.0		Test Article NCTA-2, per WHC-SD-RTG-TC-016, Rev.1		
Date 10/95		Date 10/95		Date No. <input type="checkbox"/> NA M-4-30211B M-4-112301		
TEST CONDITIONS		TEST EQUIPMENT		WHC PROCEDURE NO.		
Temperature Amb. Device ID <input checked="" type="checkbox"/> NA		Manufacturer L/H "UL-100", #2		<input type="checkbox"/> NA		
Calibration Pressure <input checked="" type="checkbox"/> NA		Ident No. s/n895-38 (WC40869)		<input checked="" type="checkbox"/> NA		
Test Pressure A=1 Atm. (14.7 psia) <input type="checkbox"/> NA		Mach Sen. 1.04 x 10⁻¹¹ Abn/Inch/Dir		<input type="checkbox"/> NA		
Gas UMP Helium <input type="checkbox"/> NA		Std No. 584-40-03 018		<input checked="" type="checkbox"/> NOT LT 0000 Rev. 3		
Concentration >90% <input type="checkbox"/> NA		Std Leak 1.5 x 10⁻⁸ Abn/Inch/Sec		Appendix A Rev. 2		
Orbit <input checked="" type="checkbox"/> NA		Calc Exp. July 7, 1996		<input type="checkbox"/> Special Tech No. _____		
Bubble Solution <input checked="" type="checkbox"/> NA		CALIBRATION SENSITIVITY		<input type="checkbox"/> Work Int. _____		
Batch No. _____		<input type="checkbox"/> Same as NSLD Calc. or		TEST TIME		
Step 1 Std. 31-02-007 <input type="checkbox"/> NA		Sensitivity 1.48 x 10⁻¹¹ Abn/Inch/Dir		Std. No. 584-40-03-006		
Range 0 to 50 psia		Std Leak 1.3 x 10⁻⁷ Abn/Inch/Sec		No Accum. Time <input checked="" type="checkbox"/> NA		
Calc Exp. March 9, 1996		Calc Exp. July 7, 1996		Soak Time <input checked="" type="checkbox"/> NA		
Step 2 Std. 31-02- <input checked="" type="checkbox"/> NA		ADDITIONAL STD		Additional Tests - "TEST CURRENTLY" <input type="checkbox"/> NA		
Range _____		Sensitivity _____ Abn/Inch/Dir		GRAT-OR-SERIAL 3-VALUES <input type="checkbox"/> NA		
Calc Exp. _____		Std No. _____		Preliminary Results - <input type="checkbox"/> NA		
Releak Valve <input checked="" type="checkbox"/> NA		Std Leak _____ Abn/Inch/Sec		STRUCTURES - 23-11111111		
Calc Exp. _____		Calc Exp. _____				
Weld No.	Part No. or Serial No.	Area	Qty	No. Per Ind.	Comments	
					OUTER CONTAINMENT VESSEL (OCV) LEAK RATE TESTS:	
					Leak Rate = 1.13×10^{-8} atm.cm ³ /sec. (Per Step #6.2)	
OCV Structure	X				No Detectable Leakage (Per Step #6.4)	
"V" Port Stat-O-Seal	X		X		No Detectable Leakage (Per Step #6.5)	
"T" Port Prim.O-Ring	X		X		Sum of 6.2, 6.4, and 6.5 = 1.13×10^{-8} atm.cm ³ /sec.	
Total OCV Leak Rate:	X					
Technician For Approval		LT Level/Date				
<input checked="" type="checkbox"/> NA						
non	Level	Interpreted by	LT Level	Reviewed by		
W.H. Nelson	I	B.J. Stewart	II	11-28-95		
B.J. Stewart	II			2.10.15-112		
Date of Examination		Date				
Nov. 21, 1995		Nov. 21, 1995				

Westinghouse Hanford Company		NDE LEAK TEST PROCEDURE AND TEST REPORT UL-100 NON DESTRUCTIVE EXAMINATION 300 BLDG 300 AREA, TEL. 378-6401			300 No 95-8	
Requestor J. S. Averette		Company PacTec		Project/Item/Work Package/Transfer No. Helium Leak Test of Radioisotope Thermoelectric Generator (RTG) After Drop Test #10-#16 on Certification		
Material G2-02	Design NO-916	Area 1100	Test Article # CTA-2, per WMC-SD-RTG-TC-016, Rev. 1			
Appearance Std WMC-SD-RTG-TC-016, Rev. 1		Section Para. 5.0	Date 10/95	<input type="checkbox"/> NA	Draw No H-4-302118 H-4-112301	<input type="checkbox"/> NA
Leakage Rate < 2.5×10^{-7} atm.cc3/sec Helium				<input type="checkbox"/> NA	Draw No	<input type="checkbox"/> NA
TEST CONDITIONS		TEST EQUIPMENT		<input type="checkbox"/> NA	WMC	<input checked="" type="checkbox"/> NA
Temperature Amb. Device ID <input checked="" type="checkbox"/> NA	Manufacturer L/M "UL-100+", #2	Material No s/n896-38 (WC48869)	Match Svc 1.13×10^{-11} atm/cc/sec/Div	Std No 504 40 03-017	Std Leak 1.8×10^{-8} atm/cc/sec	Calib Exp July 7, 1996
Barometric Pressure <input checked="" type="checkbox"/> NA	System Sensitivity <input checked="" type="checkbox"/> NA	<input type="checkbox"/> Same as MSLD Calib or Sensitivity 1.67×10^{-11} atm/cc/sec/Div		Std No 584-40-03-006	Std Leak 1.3×10^{-7} atm/cc/sec	Calib Exp July 7, 1996
Test Pressure $\Delta = 1$ Atm. (14.7 psia) <input type="checkbox"/> NA	Gas UHP Helium <input type="checkbox"/> NA	Concentration >90% <input type="checkbox"/> NA	Other <input checked="" type="checkbox"/> NA	Bubble Solution <input checked="" type="checkbox"/> NA	Batch No	Range 1 Sdr 31 04- 007 <input type="checkbox"/> NA
Range 0 to 50 psia	Case Exp March 9, 1996	Range 2 Sdr 31 04- <input checked="" type="checkbox"/> NA	Code Exp	Range	Code Exp	Refut Value <input checked="" type="checkbox"/> NA
Additional STD	Sensitivity	Std No	Std Leak	Calib Exp	TEST TIME STAND-O-SEAL - PRIMARY O-RING No Response Time = IMMEDIATE <input type="checkbox"/> NA No Accum Time <input checked="" type="checkbox"/> NA Soak Time <input checked="" type="checkbox"/> NA Additional Time: "TEST DURATION" STAND-O-SEAL = 3min. PRIMARY O-RING = 5min <input type="checkbox"/> NA	
Weld Rep. Plan No. or Serial No.	Acc	Proj	No Fail Ind	Comments		
				Inner Containment Vessel (ICY) Leak Rate Tests:		
"P" Port Stat.-O-Seal	X	X		No Detectable Leakage (Per Step #7.2)		
"S" Port Stat.-O-Seal	X	X		No Detectable Leakage (Per Step #7.3)		
"I" Port Prim.-O-Ring	X	X		No Detectable Leakage (Per Step #7.4)		
Technician Pts Approval		CT Level/Data				
<input checked="" type="checkbox"/> NA						
W.M. Nelson	Level I	Interpreted by	CT Level II	Reviewed by		
B.J. Stewart	II	B.J. Stewart	II	Date		
Nov. 29, 1995		Nov. 29, 1995		12-14-95 2.10.15-113		

Data Sheets from Copper Tube Test
(Seal Area Measurement Data Sheets)

Seal Area Measurement Data Sheet

CTA-2

Direct Compression Method, Section 4.1. (Method #1, primary)

Measurement (circle one): Pre-Test Post-Test

TUBING MEASUREMENTS (inch)								
Angular Position	ICV				OCV ¹⁶			
	INNER (1/4-inch)		OUTER (1/4-inch)		INNER 3/16 (2/8-inch)		OUTER (1/4-inch)	
	Before Comp.	After Comp.	Before Comp.	After Comp.	Before Comp.	After Comp.	Before Comp.	After Comp.
Feed-through	.253	.204	.253	.201	.316	.282	.250	.207
45°	.252	.204 ¹⁶	.253	.201	.316	.282	.250	.207
90°	.253	.204	.253	.200	.316	.282	.250	.207
135°	.252	.203	.252	.200	.316	.282	.250	.207
180°	.253	.204	.252	.202	.316	.282	.250	.207
225°	.253	.204	.252	.201	.316	.282	.250	.207
270°	.252	.204	.253	.201	.316	.282	.250	.207
315°	.253	.204	.253	.201	.316	.282	.250	.207

Comments: * NOTE: OCV BASE FROM CTA-1 UNIT WAS REUSED FOR CTA-2 UNIT. THESE MEASUREMENTS ARE PRIOR TO REFURBISHMENT OF BASE PLATE.

Accepted ^{DATE} 9-20-95
 Data by Phil Noss

Date 9/20/95

Seal Area Measurement Data Sheet (con't)

CTA-2

Direct Compression Method, Section 4.1. (Method #1, primary)

Measurement (circle one): Pre-Test Post-TestClosure Bolt Torque Values Utilized

(Bolt #1 is first bolt CCW from feed-through location)

ICV	
Bolt #	Torque ft-lb
1	250
2	
3	
4	
5	
6	
7	
8	
9	
10	
11	
12	↓

OCV			
Bolt #	Torque ft-lb	Bolt #	Torque ft-lb
1	300	13	300
2		14	
3		15	
4		16	
5		17	
6		18	
7		19	
8		20	
9		21	
10		22	
11		23	
12	↓	24	↓

Phil Nover 9-20-95

Data by Phil NoverDate 9/20/95

Seal Area Measurement Data Sheet

Direct Compression Method, Section 4.1. (Method #1, primary)

CTA-2

AFTER I.C. BOLT
RE-MACHININGMeasurement (circle one): Pre-Test Post-Test

TUBING MEASUREMENTS (inch)								
	ICV				OCV*			
	INNER ($\frac{1}{4}$ -inch)		OUTER ($\frac{1}{2}$ -inch)		INNER ($\frac{5}{16}$ IN) ($\frac{3}{8}$ -inch)		OUTER ($\frac{1}{2}$ -inch)	
Angular Position	Before Comp.	After Comp.	Before Comp.	After Comp.	Before Comp.	After Comp.	Before Comp.	After Comp.
Feed-through					.315	.282	.250	.208
45°					.316	.282	.249	.207
90°					.315	.282	.250	.208
135°					.316	.283	.251	.208
180°					.316	.283	.250	.208
225°					.316	.282	.251	.207
270°					.316	.282	.250	.208
315°					.316	.282	.251	.207

Comments:

MEASURED CCW FROM FEED-THROUGH

* THESE MEASUREMENTS ARE AFTER REFINISHMENT
OF CTA-1 BASE PLATE FOR USE AS CTA-2 BASE PLATE.

COPY

Data by Richard P. JonesDate 10/27/95

Seal Area Measurement Data Sheet

Direct Compression Method, Section 4.1. (Method #1, primary)

Measurement (circle one): Pre-Test Post-Test

TUBING MEASUREMENTS (inch)								
	ICV				OCV			
	INNER (1/4-inch)		OUTER (1/2-inch)		INNER (3/8-inch)		OUTER (3/4-inch)	
Angular Position	Before Comp.	After Comp.	Before Comp.	After Comp.	Before Comp.	After Comp.	Before Comp.	After Comp.
Feed-through	.253	.205	.252	.202	.314	.287	.252	.213
45°	.252	.203	.252	.201	.314	.283	.251	.207
90°	.253	.203	.251	.201	.314	.282	.251	.208
135°	.253	.203	.251	.201	.314	.283	.251	.208
180°	.253	.205	.251	.202	.314	.284	.250	.210
225°	.253	.204	.251	.2015	.313	.282	.252	.208
270°	.253	.203	.251	.201	.313	.283	.252	.208
315°	.253	.203	.251	.201	.313	.283	.252	.208

Comments:

OCV VARIANCE: INNER .005
OUTER .006ICV VARIANCE: INNER .002
OUTER .001 (NO)

Data by



Date

OCV: 11/22/95
ICV 12/05/95

TP-004, Rev. 1

Seal Area Measurement Data Sheet (cont)

Direct Compression Method, Section 4.1. (Method #1, primary)

Measurement (circle one): Pre-Test Post-TestClosure Bolt Torque Values Utilized

(Bolt #1 is first bolt CCW from feed-through location)

ICV	
Bolt #	Torque ft-lb
1	215
2	240
3	250
4	240
5	265
6	260
7	255
8	265
9	240
10	280
11	260
12	210

40-24

OCV			
Bolt #	Torque ft-lb	Bolt #	Torque ft-lb
1	225	13	250
2	240	14	260
3	250	15	230
4	240	16	250
5	265	17	260
6	260	18	265
7	255	19	280
8	265	20	240
9	240	21	260
10	280	22	265
11	260	23	280
12	210	24	215

Data by

J. L. Smith

Date

11/22/95

RMIS View/Print Document Cover Sheet

This document was retrieved from the Documentation and Records Management (DRM) ISEARCH System. It is intended for Information only and may not be the most recent or updated version. Contact a Document Service Center (see Hanford Info for locations) if you need additional retrieval information.

Accession #: D196080883

Document #: SD-RTG-SARP-001

Title/Desc:

RTG TRANSPORTATION SYSTEM SARP DOCKET NO 94-6-9904
[VOL II] [SEC 3 OF 4]

Pages: 289

This document was too large to scan as a whole document, therefore it required breaking into smaller sections.

Document number: SD-RIG-SARP-001

Section 3 of 4

Title: RADIOISOTOPE THERMOELECTRIC GENERATOR
TRANSPORTATION SYSTEM SAFETY ANALYSIS REPORT
FOR PACKAGING

Date: 4/18/96 Revision: 0

Originator: FERRELL PC

Co: WHC

Recipient: _____

Co: _____

References: EDT-613639

Radioisotope Thermoelectric Generator Transportation System Safety Analysis Report for Packaging

Docket No. 94-6-9904

Prepared for the U.S. Department of Energy
Office of Environmental Restoration and
Waste Management



Westinghouse
Hanford Company Richland, Washington

Management and Operations Contractor for the
U.S. Department of Energy under Contract DE-AC06-87RL10880

Approved for Public Release

3.0 THERMAL EVALUATION

This chapter describes the principal thermal aspects and performance of the Radioisotope Thermoelectric Generator (RTG) Transportation System Package. The following evaluation demonstrates the compliance per 10 CFR 71 (Reference 1). See Section 1.0 for a detailed description of the RTG Transportation System Package and its key features.

3.1 DISCUSSION

The RTG Transportation System Package is designed to safely transport a variety of RTG payloads. The maximum decay heat load of 4,500 W occurs with a payload consisting of one General Purpose Heat Source (GPHS) RTG. The results for the GPHS RTG will thermally encompass all other potential payloads. The minimum thermal decay heat is assumed to be zero.

Each RTG is a functioning device with an extremely high replacement cost. As such, while the primary purpose of the package design is to provide a Type B packaging meeting the 10 CFR 71 regulatory requirements for safety, the package design must also maintain the RTGs below their thermal limits during the normal operational conditions for load, unload, and transportation. To accomplish this dual purpose, an active cooling system is used to control the boundary conditions on the package's external surface and, thereby, maintain the various RTGs within their respective thermal limits. The cooling system is not required to be active for the RTG Transportation System Package to successfully comply with 10 CFR 71.

The RTG Transportation System Package consists of a double-containment packaging and payload. The remote chillers, interconnecting hoses, associated controls, and power systems needed to provide the active cooling are not considered part of the RTG Transportation System Package and, thus, are not addressed by this Safety Analysis Report for Packaging (SARP). The packaging consists of two separate containment vessels: an inner containment vessel (ICV) and an outer containment vessel (OCV). Each containment vessel consists of a bell assembly and a heavy base. The bell assembly is made of a cylindrical shell with an integral standard American Society of Mechanical Engineers (ASME) torispherical head at the top and a bolt flange at the bottom. The bell assembly is attached to the base with high-strength alloy steel closure bolts. The containment structures are fabricated from AISI Type 304L stainless steel.

The OCV bell assembly incorporates an integral cooling jacket on its outer surface. The cooling jacket provides two equal and independent cooling loops that can be used separately or together to provide the required cooling. The loops are formed by spiral wrapping 0.25 by 1.25 in. Type 304L stainless steel bar stock on 2.25-in. centers around the OCV bell and then welding a 10 gauge (0.136-in.) Type 304L stainless steel cover sheet between the bars to form 1 by 2 in. coolant flow channels. Full length welds at all joints will not only provide a leak-tight environment, but also maximizes the heat transfer through the jacket if coolant fluid is lost. Conversely, the relatively thin shell of the coolant jacket acts as a radiation shield, reducing OCV heating during the hypothetical accident condition (HAC) fire transient from that which would occur with a bare OCV bell.

The bolt flange is protected from pin puncture damage and the HAC fire ambient temperature by a 3/8-in. thick thermal shield. The cavity within the thermal shield is filled with 2.4 lb/ft³ fiberglass insulation to limit conduction, convection, and radiation heat transfer within the cavity. Plugs or caps for the OCV bolt access tubes are not used for reasons of convenience and because the thermal analysis shows they are unnecessary.

A water/propylene glycol solution is used as the cooling medium. The choice of coolant

fluid is based on the possibility of ambient temperatures below the freezing point of water during operation or storage of the package and the desire for a nontoxic solution. In the absence of freezing temperatures, pure water can also be used. The 70%/30%, by volume, mixture of water and propylene glycol provides burst protection down to -80 °F.

The removable impact limiter is fabricated of two densities of fire resistant, polyurethane foam encased in a 0.25 in. or thicker Type 304 stainless steel shell. The center section (41 in.) of the limiter uses a solid block of 3 lb/ft³ FR-3700 polyurethane foam. The remaining portion of the limiter uses 12 lb/ft³ poured-in-place FR-3700 polyurethane foam. A sheetmetal thermal shield is incorporated in the center section of the impact limiter, adjacent to the bottom of the OCV base. This thermal shield provides backup thermal protection over the area of the OCV base plate covered by the low density foam. Plastic melt-out plugs provide pressure relief if foam overgassing occurs during the HAC fire event. The relatively thick steel shell of the limiter prevents the puncture pin from tearing the shell and penetrating the foam.

Most of the design aspects of the RTG Transportation System Packaging are set by nonthermal considerations. A combination of shielding, structural, weight, and operational considerations set the overall size of the packaging, the wall thicknesses for the ICV and OCV, and all the stainless steel construction. Even the thickness of the fluid passages in the cooling jacket is set by neutron absorption considerations and not by thermal requirements. Despite this, many of these design aspects work to the thermal advantage of the package. The heavy base plates, OCV flange thickness, and ICV/OCV bell thickness provide a significant thermal mass to absorb the heat fluxes generated during the HAC fire. The relatively low thermal conductivity of Type 304L stainless steel restricts the axial flow of heat to the seal areas of the package. The thin outer shell of the cooling jacket and the air gap created by the flow passages act as a thermal radiation shield and insulator during the HAC fire.

The design features specifically added to enhance the thermal performance of the package under both normal operation and regulatory normal conditions of transport (NCT) are as follows:

- An external cooling jacket
- High emissivity surface treatments
- Control of the gap dimension between the ICV and OCV
- Use of a helium blanket gas within the ICV and OCV cavities
- RTG payload shipping rack assembly with integral barrier plates
- Seal area insulation.

Although the OCV external cooling jacket was specifically added for normal operation conditions, its desirable effects for regulatory conditions have already been addressed. A high temperature coating (Carboline 4674 black paint) yielding a normal emittance of 0.875 is used on the inner and outer surfaces of the ICV and on the inner surfaces of the OCV. The coatings enhance the heat transfer performance of the package, especially between the RTG and ICV. The coating is purposely omitted from the lower 7 in. of the ICV inner wall, the ICV/OCV base plates, and the shipping rack to minimize the heat transfer to the seal region of the package. An emittance of 0.48 is assumed for these areas.

The interior surfaces of the cooling jacket are also not coated because these enclosed surfaces cannot be maintained once the package is assembled, and analysis shows enhanced emittance is not required in this area. The exterior surface of the OCV and impact limiter are coated with a two-part white epoxy paint. This surface treatment provides a long wave radiation emittance of 0.80 or greater, while limiting solar radiation absorptivity to 0.25 or less.

The third special design feature used to enhance thermal performance is dimensional control of the ICV-to-OCV gap. By manufacturing the ICV and OCV bells as a nested pair, the inter-vessel

gap is controlled to 1/4 in. maximum at the sides and 1/2 in. maximum between the torispherical heads. These controlled dimensions provide a definitive basis for determining the temperature rise between the bells.

Using helium as the blanket gas within the ICV and OCV cavities increases the convective heat transfer rates within the package over that possible with other inert blanket gases. Although the thermal analysis assumes a pure helium gas, analytical calculations showed no significant temperature sensitivity for gas mixtures down to 95% helium and 5% air. Development and operational tests have shown helium gas purity of 95% or greater is easily achievable using the proposed operating procedures. The target pressure for helium gas within the ICV and ICV/OCV cavities is 19 ± 1 psia. This pressure will be established when the payload is loaded into the packaging. Once the packaging is loaded there is no active control of the cavity pressures, instead the pressure will vary according to the ideal gas law. For analysis purposes, the ambient condition at the time of RTG loading is assumed to be 70 °F with no solar insolation.

Each RTG payload has its own shipping rack assembly that is attached to the ICV base plate. The shipping rack assemblies incorporate a stainless steel barrier plate structure; its purpose is to maintain a positive separation between the RTG heat sources and the ICV/OCV seal areas under all circumstances. The 0.5-in. radial gap between the shipping rack assembly O.D. and the ICV I.D. is less than the smallest portion of a HAC impact reconfigured RTG heat source. The rectangular GPHS aeroshell is the smallest size heat-producing fragment that could potentially arise from the breakup of an RTG under a HAC impact. The smallest dimension of the aeroshell is 2.09 in. Consequently, even if an accident during transportation results in severe RTG damage and subsequent spilling of the heat sources within ICV cavity, no heat generating material will be permitted to reach the seal area.

The final design feature added to the package to enhance its thermal performance is thermal insulation at critical locations. These locations are the underside of the shipping rack assembly, the electrical feed-through connector on the ICV base, the OCV base plate, and the OCV seal flange. Heat transfer via radiation and convection between the ICV base plate/seal area and the underside of the shipping rack assembly is restricted by using a 2-in.-thick blanket of "Kao wool"™ ceramic fiber insulation. Kao wool™ insulation is also used to isolate the electrical feed-through connector housing on the ICV base plate from the hot gas in the ICV cavity.

Additional lower end insulation in the form of an impact limiter protects the ICV/OCV seats from the high external temperatures that arise during the HAC fire. The impact limiter is filled with a combination of 3 and 12 lb/ft³ rigid polyurethane foam. The structural attachments for the impact limiter prevent it from being torn from the package during the pre-HAC free drops and puncture bar drops. Additional information regarding the performance of the impact limiter in the free drops and HAC fire transient is presented in Appendices 2-10, 11 and 3-6.3.

The bolt flange on the OCV is protected from direct exposure to high external temperatures by a thermal shield enclosure fabricated of 0.375-in.-thick stainless steel and filled with fiberglass insulation. The wall thickness prevents a puncture bar impact from penetrating the shield and/or collapsing the shield onto the bolt flange. The thermal shield is shown on Drawing H-9-5002, sheet 3, Appendix 1.3.2. This drawing illustrates the 3/8-inch plate material used for the top and outer plates that enclose approximately 2.5 inches of fiberglass insulation.

The thermal evaluation of the RTG Transportation System Package is conducted using a variety of two- and three-dimensional (2-D and 3-D, respectively) analysis and full-scale test models. Data from the test models confirm that the package design will maintain the various RTGs

™Kao wool is a registered trademark of the Babcock & Wilcox Company.

within their temperature limits during the normal operational conditions (i.e., with the chillers operating) for load, unload, and transportation. In addition to thermally qualifying the package for the nonregulatory aspects transportation, the test data validates the analytical thermal models of the package and its inherent heat transfer mechanisms.

Qualification of the package for regulatory aspects of transportation is accomplished analytically. The following sections, appendices, and references detail the basis for the analytical models, tests used to validate the models, and the analysis results for regulatory conditions. The analysis uses conservative assumptions for such nondefinitive parameters as RTG reconfiguration, impact limiter damage, and foam properties during the HAC fire. The results of the analyses demonstrate that the package meets all of the 10 CFR 71 requirements for Type B packaging.

3.2 SUMMARY OF THERMAL PROPERTIES OF MATERIALS

The RTG Transportation System Package is fabricated primarily of Type 304L and Type 304 stainless steel, rigid polyurethane foam, and minor amounts of miscellaneous materials. The shell of the GPHS RTG, the maximum heat payload, is fabricated primarily of 2219 aluminum. Each of the 18 GPHS modules used in the RTG are fabricated of four PuD₂ fuel pellets within iridium shells which, in turn, are mounted within a carbon-carbon composite housing called an "aeroshell." Of the total heat source module weight, 55% is in the fueled capsules and 45% is in the aeroshell. The individual components of the heat source modules are not modeled. Instead, a composite thermal mass of 14.2 Btu/°F is used for all 18 heat source modules, based on data provided by the manufacturer of the GPHS RTG.

The void spaces within the package are filled with helium gas to a purity of 95% or greater and to a pressure of 18 ± 1 psia at the time of package assembly. Air surrounds and fills all package voids outside the OCV containment boundary. The coolant passages are assumed to be drained, dried, and filled with air for all regulatory conditions. For normal operational conditions, with the chillers operating, the coolant passages are assumed to be filled with a coolant mixture of 30% propylene glycol and 70% water, by volume.

The thermal properties of the principal materials used in the fabrication of the packaging and GPHS RTG payload are listed in Tables 3.2-1 through 3.2-5. Where significant, the properties are presented as a function of temperature.

TABLE 3.2-1. Thermal Conductivity Curve Fts.

$k = C_0 + C_1 T + C_2 T^2$; $\text{Btu-In/Ah-Ft}^2\text{-F}$, $T = \text{Temperature (}^\circ\text{F)}$				
Material	C_0	C_1	C_2	Notes and remarks
Type 304 and 304L stainless steel	81.346	7.1489E-2	-3.9267E-8	Reference 4 and 6
ASTM A320 bolts	303.50	-4.5162E-2	-9.2082E-6	Reference 27
2219-T6 aluminum	804.70	0.5831	-2.2703E-4	Reference 4; same for -T67
Polyurethane foam • 12 lb/ft ³ • 3 lb/ft ³	0.276 0.181	0 0	0 0	Reference 10
30% propylene glycol /70% water solution	2.7818	5.6033E-3	-1.2853E-6	Reference 16
Helium	0.8412	1.2381E-3	-6.1711E-8	Reference 8
Air	0.1674	2.6264E-4	-3.2429E-8	Reference 2 and 3
Fiberglass insulation	0.2217	1.6604E-4	8.9412E-7	References 26 and 28
Kaowool [®] ceramic insulation	0.1893	3.6879E-4	2.5800E-7	Reference 26

TABLE 3.2-2. Material Density.

Material	Density, Lbm/in. ³	Notes and remarks
Type 304 and 304L stainless steel	0.29	Reference 20
ASTM A320 bolts	0.283	Reference 20
2219-T6 aluminum	0.103	Reference 20; same for -T67
30% propylene glycol and 70% water solution	0.0374 at 40 °F	Reference 16; computed as a function of temperature
Kaowool [®] ceramic insulation	0.00463	Reference 26
Fiberglass insulation	0.00139	Reference 26
Helium	4.8322E-6 at 200 °F and 14.7 psia	Reference 3; computed from ideal gas law
Air	4.1087E-6 at 100 °F and 14.7 psia	Reference 3; computed from ideal gas law

TABLE 3.2-3. Specific Heat Curve Fits.

$$C_p = C_0 + C_1 \cdot T + C_2 \cdot T^2; \text{ Btu/Lbm} \cdot \text{F}; T = \text{Temperature (}^\circ\text{F)}$$

Material	C_0	C_1	C_2	Notes and remarks
Type 304 & 304L stainless steel	0.1155	3.3284E-5	1.1252E-9	Reference 9
ASTM A320 bolts	0.1118	1.3018E-5	3.8778E-9	Reference 27
2219-T6 aluminum	0.1988	8.08729E-5	-2.1837E-9	Reference 4; same for -T87
FR-3700 polyurethane foam				Reference 10
• 12 lb/ft ³	0.30	0	0	
• 3 lb/ft ³	0.30	0	0	
30% propylene glycol and 70% water solution	0.8958	3.6607E-4	-1.7342E-8	Reference 16
Helium	1.2404	0	0	Reference 7
Air	0.2362	2.7871E-5	-2.2871E-9	Reference 2 and 3
Fiberglass insulation	0.20	0	0	Reference 28
Kaowool [®] ceramic insulation	0.20	0	0	Reference 28
Fuel source modules (18)	14.2 Btu/°F	--	--	Reference 21

TABLE 3.2-4. Viscosity Curve Fits.

$$\mu = C_0 + C_1 \cdot T + C_2 \cdot T^2; \text{ Lbm/ft} \cdot \text{ft}; T = \text{Temperature (}^\circ\text{F)}$$

Material	C_0	C_1	C_2	Notes and remarks
30% Propylene Glycol / 70% Water Solution	1.5601	-1.1492E-2	2.1454E-5	Reference 16; fit on \log_{10} of viscosity value
Helium	4.4557E-2	5.3443E-5	-4.2091E-9	Reference 9
Air	4.0234E-2	5.8418E-5	-8.5246E-9	Reference 2 and 3

TABLE 3.2-5. Surface Emittance.

Surface/Surface Treatment	Surface Emittance	Solar Absorptivity	Remarks
OCV dome & shell interior - as rolled 304L, abrasive blasted, heat-resistant coating	0.875, 0.54 w/o coating	N/A	See Note 1
OCV flange, bottom surface - 304L machined to 32 μ in/in	0.3	N/A	See Note 2
OCV dome exterior & jacket exterior - as rolled 304L, brush-off blast, acid etch, Thermec [™] epoxy paint	0.8	0.25	See Note 3
OCV shell exterior below coolant jacket - as rolled 304L	0.3	N/A	See Note 4
ICV dome & shell interior above 7" point & exterior above 3" point - as rolled 304L, abrasive blasted, heat-resistant coating	0.875, 0.54 w/o coating	N/A	See Note 1
ICV shell interior below 7" point, exterior below 3" point, & flange - machine finished 304L	0.30	N/A	See Note 2
ICV base & OCV base - machine finished 304L	0.30	N/A	See Note 2
Shipping rack barrier plate - machine finished 304	0.30	N/A	See Note 2
Shipping rack barrier plate, upper ring - as rolled 304	0.48	N/A	See Note 5
Shipping rack support legs - as rolled 304	0.48	N/A	See Note 5
Shipping rack barrier plate, lower ring - as rolled 304	0.48	N/A	See Note 5
Coolant jacket 1/4"x1" bars - as rolled 304L	0.48	N/A	See Note 5
Coolant jacket cover interior - as rolled 304L	0.48	N/A	See Note 5
Impact limiter shell exterior - as rolled 304, Thermec [®] epoxy paint	0.8	0.25	See Note 3
2219-T6 aluminum with coating	0.91	N/A	See Note 6
Heat source aeroshell (graphite)	0.5	N/A	See Note 7

**Thermec is a registered trademark of the Thermec Company, Incorporated.

- Notes: (1) References 22 and 32 indicate an emissivity range of 0.83 to 0.80 for the Carboline[™] 4674, C800 black heat-resistant coating. Reference 34 emissivity testing on 18 samples of Type 304 stainless steel indicates an emissivity value of 0.54 for the 'white metal blast' surface treatment that exists prior to the application of the Carboline[®] coating. Figure 360, Reference 24 indicates an emissivity of 0.6 to 0.8 for grit-blasted Type 310 stainless steel. Conclusion is to use an emissivity of 0.875 when the Carboline[®] coating is present and 0.54 when the coating is not present.
- (2) Figure 361, Curves 126 and 132, Reference 24 indicates an emissivity of 0.136 to 0.175 at 1000 °F for mechanically finished Type 304 stainless steel, measured in helium gas. The average value of 0.15 for this condition was doubled to 0.30 to account for long-term oxidation, etc.
- (3) Page 8, Reference 15 gives emissivity values of 0.89 or greater for white paints. Similar values are presented in Table 347, Reference 35. During the HAC event, the Tnemec Series 66 epoxy paint is expected to 'craze', flake off, and expose the underlying stainless steel surfaces. While the brush-off blast treatment of the stainless steel used in preparation for the epoxy paint is expected to yield an emissivity of 0.40 (per Reference 34 for 'commercial sand blast' condition), a minimum emissivity of 0.80 is to be used for all HAC conditions in accordance with the Reference 1 requirements. Therefore, a value of 0.80 provides a conservative estimate for NCT conditions and meets the Reference 1 requirements for HAC conditions.
- (4) Reference 34 emissivity testing on 18 samples of Type 304 stainless steel indicates an emissivity value of 0.26 to 0.28 for the 'as-received' condition. Table 148, Reference 35 provides values of 0.44 at 420 °F and 0.36 at 914 °F for a light silvery, rough surface. An emissivity value of 0.30 provides an accurate representation of the actual conditions for the OCY shell surface.
- (5) Same references as Note 4; however, since these surfaces are light silvery in color and rough, an emissivity value of 0.48 is used.
- (6) Emissivity set by manufacturer of GPHS RTG. See Reference 21.
- (7) Reference 18 provides emissivity values of 0.49 at 500 °F and 0.54 at 2500 °F. Table 78, Reference 35 provides emissivity values of 0.49 at 500 °F, 0.54 at 1000 °F, and 0.64 at 2000 °F. A value of 0.50 is used since it provides a conservative estimate of the temperature of the heat source aeroshells and the package temperatures in the vicinity of the aeroshells.

The solar absorptivity value of 0.25 used for the Tnemec[®] Series 66 white epoxy paint is appropriate, given the referenced measured values, the fact the package will be shipped in a vented, enclosed trailer, and because the International Atomic Energy Agency (IAEA) guidelines recognize the validity of using coatings to reduce the heat flux caused by insolation.

[™] Carboline is a registered trademark of the Carboline Company.

3.3 TECHNICAL SPECIFICATIONS OF COMPONENTS

The materials used in the RTG Transportation System Package that are considered temperature sensitive are the Butyl O-ring seals, the polyurethane foam used in the impact limiter, the pressure relief valves used in the coolant jacket, the instrumentation electrical feed-through connector assemblies, and the Carbolina[®] and Tnemec[®] coatings.

The Butyl O-ring seals (Rainier rubber compound No. RR-0405-70) have a working temperature range of -40 to 350 °F. Exposure to temperatures in excess of 350 °F is allowable for limited time periods. Developmental test data (see Appendix 2.10.6) has shown that the Butyl seals have a peak temperature rating of 400 °F for time periods of eight hours or less. Seal temperatures between 400 and 350 °F are allowed for time periods that vary as a function of temperature. See SARP Section 4.1.3.1.2 for the time versus temperature capability of the Butyl seals.

The rigid polyurethane foam used in the impact limiter has a working temperature range of -40 to 300 °F. While the foam's compressive strength diminishes rapidly with increasing temperature, temperature excursions within this range will not permanently degrade its properties. The foam begins to break down and outgas at temperatures above 400 °F. This thermal breakdown and outgassing accelerates at temperatures between 500 and 750 °F, levels off between 750 and 1000 °F, and then accelerates again until 1500 °F. The foam will have been reduced to a relatively stable char at temperatures beyond 1500 °F. No definitive high temperature data exists for the foam. For this reason, a conservative approach based on fire test results was used to simulate the foam's response to the HAC fire. Further discussion of the thermal properties of the foam under fire transient conditions is provided in Section 3.5.1, Appendix 3.6.3, and Reference 10.

Outgassing from the polyurethane foam during a HAC fire could produce relatively large volumes of gas within the impact limiter. To prevent an excessive buildup of pressure within its shell, the impact limiter is fitted with four PVC plugs located at 90° intervals around the outer circumference of the shell. During any potential HAC fire, the plugs will burn/melt before any significant charring of the foam. Because the center 3 lb/ft³ foam disk is not directly poured in the impact limiter shell, it does not bond with the shell walls. Hence, adequate gas communication paths will exist to the PVC plugs.

The cooling jacket on the OCV of the package is protected from overpressurization by relief valves on each coolant channel. The valves prevent a pressure buildup within the coolant channels if a coolant system malfunction occurs. The 1/2-in. valves are fabricated of 300 series stainless steel and have a pre-set cracking pressure of 50 psi. The relief valves have a temperature rating of 375 °F. These performance limits affect the operational mode only. Failure of the relief valves from either impact damage or the HAC fire will not affect the containment boundaries of the package. The valves will not puncture the OCV if struck during impact.

The temperature-sensitive components of the electrical feed-through assembly is the D.G. O'Brien Series 107 connectors. The temperature rating for the electrical feed-through connector assembly is 475 °F. The basis for the temperature rating is provided in Appendix 4.5.2.

The Carbolina[®] high emissivity coating has a continuous temperature rating of 750 °F and a noncontinuous rating of 1000 °F. The required inspection and maintenance of the coating before individual shipments is addressed in Chapter 8 of the SARP. These O&M procedures require corrective action whenever damaged coating exceeds 5% of any one-square-foot area or 2% of the total area. Since the total loss of the heat-resistant coating over 5% of any given one-square-foot area is equivalent to a reduction in the average emittance over the one-square-foot area of 2%, no impact on package temperatures will occur before the heat-resistant coating is repaired.

The heat-resistant coating is protected from wear and tear during normal transport operations (i.e., loading and unloading procedures) by eight Vespel[®] wear pads mounted near the OCV flange. These wear pads are illustrated in the Section B-B detail on Sheet 2 of Drawing H-8-5001. The wear pads maintain the alignment between the ICV and the OCV shells during package assembly and disassembly, thereby preventing inadvertent hard contact between the ICV and the OCV. During the Reference 14 qualification tests, the package was assembled and disassembled approximately 40 times. Throughout the tests, the coating remained in excellent condition with only a slight dulling of the finish on the outer surface of the ICV shell where these pads had made contact.

The Tnemec[®] Series 95 epoxy coating has a continuous temperature rating of 250 °F and a maximum rating of 275 °F. During the HAC fire, the Tnemec[®] coating is expected to craze and flake off.

The remaining materials used in the fabrication of the packaging have significantly higher temperature capabilities. The Type 304L stainless steel used in the ICV and OCV containment vessels and bases has a melting point of 2800 °F. The Type 304 stainless steel used for shipping racks and the shell of the impact limiter has a similar melting point. The Kwoool[®] and fiberglass insulations have maximum temperature ratings of 2300 °F and 1000 °F, respectively.

The 1000 °F rating for mineral fiber insulation is set primarily by the loss of structural strength within the individual fibers. The material (Owens Corning TIW type II) will begin to soften at 1200 °F and becomes liquidus at a temperature of 1700 °F. Since the surfaces surrounding the fiberglass insulation do not exceed 1250 °F during the HAC fire event and only exceed 1000 °F for less than an hour, the thermal capability of the fiberglass insulation is consistent with its use in this application.

The shell and fins of the GPHS RTG payload is constructed of 2219-T8 and 2219-T87 aluminum. These materials have a melting point of approximately 1100 °F. The graphite, PuO₂, and the other materials used in the fabrication of the RTG and have a temperature capability between 1100 °F and 6000 °F.

3.4 THERMAL EVALUATION FOR NORMAL CONDITIONS OF TRANSPORT

This section presents the thermal analyses for the normal conditions of transport (NCT). Because of the dual requirements of the package to provide regulatory safety and to protect the RTGs from excessive operational temperatures, the evaluation of thermal performance for NCT is divided into two categories. The first category covers the regulatory NCT as defined in 10 CFR 71, while the second category involves the normal operational conditions expected in day-to-day operation and transport of the package with the cooling system active. The objectives and ground rules are different for each category.

Evaluation of the thermal performance for compliance with the 10 CFR 71.43(g) and 71.71 is conducted to ensure the safety of the packaging for the transportation of radioactive materials. The health and functionality of the RTGs is immaterial for the purposes of compliance with 10 CFR 71. Instead, the temperature distribution within the RTG is important only in establishing the heat flux on the various ICV surfaces. Load cases 1 and 2 evaluate the maximum package temperatures and NCT differential thermal expansions, respectively. Load cases 4 and 5 provide steady-state package temperatures used as pre-accident conditions for the HAC fire presented in Section 3.5.

In contrast, evaluation for normal operational conditions (i.e., with active cooling) ensures that the package design will maintain the RTG payloads within their respective thermal limits, as

well as meeting all regulatory requirements. Although the evaluation covered the full range of expected conditions to be imposed by the load, unload, and transport procedures for the GPMS RTG, only three cases (i.e., cases 3, 6, and 7) are presented in this section. The resultant package temperatures encompass those seen by the other conditions and payloads.

Load case 3 represents the normal operational condition assuming the maximum heat load payload, 100 °F ambient temperature, regulatory solar loading, and active cooling. The conditions for active cooling is assumed to be a flowrate of 4.5 gal/minute in each cooling channel and a coolant inlet temperature of 40 °F. The expected coolant temperature rise will be 5 °F or less. Because the package will be shaded by its transport trailer, the resultant temperatures encompass those expected with the package loaded in an enclosed and vented trailer. Load case 6 evaluates compliance of the package per 10 CFR 71.43(g). Load case 7 illustrates package temperatures and pressures when the GPMS RTG is loaded into the packaging within a climate-controlled facility.

In addition to these seven NCT load cases, a loading/unloading transient case was evaluated to determine the maximum differential thermal expansion in the package during these procedures. Section 2.6.1 provides the results of this evaluation. This information helps establish the entire range of stress in the package. Thermal analysis output for when the KCV sidewall reaches its maximum temperature during the load transient is presented in Section 3.6.4.

TABLE 3.4-1. Table of Normal Conditions of Transport Load Combinations.

Load combination/condition	Solar	Ambient temp. (°F)	Payload	Cooling status
Case 1	Yes	100	GPMS	No active cooling*
Case 2	No	-40	GPMS	No active cooling
Case 3	Yes	100	GPMS	Active cooling*
Case 4	No	100	GPMS	No active cooling
Case 5	No	-20	GPMS	No active cooling
Case 6	No	100	GPMS	Active cooling
Case 7	No	70	GPMS	Active cooling

*"No Active Cooling" defined as coolant channels drained and filled with air.

**"Active Cooling" defined as coolant flowrate of 4.5 gal/minute per channel with an inlet temperature of 40 °F.

3.4.1 Thermal Model

Evaluation of the thermal performance for the package under NCT is accomplished using an analytical model. The results of physical model testing confirm the validity of the analytical model. The analytical model is described in Section 3.4.1.1; the test models are described in Section 3.4.1.2.

3.4.1.1 Analytical Model. Four categories of analytical thermal models were developed to analyze the performance of the RTG Transportation System Package for the NCT events. These models are (1) those used to represent the thermal characteristics of the RTG payload, (2) the thermal model of the basic packaging, (3) thermal models of the interface between the undamaged RTG payload

and the packaging, and (4) models used to analyze package configurations for regulatory conditions. All of the analytical thermal models developed used the SINDA '85/Fluitt thermal analysis program²⁰. SINDA is a finite differencing program developed by NASA's Johnson Space Center.

3.4.1.1.1 RTG Thermal Models. As stated previously, the GPHS RTG is used as the basis for the analysis presented herein. The analytical thermal model developed for the GPHS RTG payload is defined in a separate configuration controlled document. This model has been approved by the manufacturer of the RTG as being a valid thermal model of the undamaged RTG. Model changes can only be made via formal change procedures.

For the sake of brevity, the details of the model are not discussed in this document. Instead, the reader is directed to the Reference 21 payload model document for these details.

Figures 3.4.1-1a and 3.4.1-1b present the layout of the 57 nodes used to thermally model the GPHS RTG. The model provides a 2-D model of the RTG heat source modules and a quasi 3-D model of the outer shell and fins. Symmetry conditions are used to account for other sections of the RTG not specifically modeled. The level of model resolution is set by the need for operational temperature predictions and not by regulatory analysis. Full details of the model are provided in Reference 21.

3.4.1.1.2 Packaging Thermal Model. The thermal analysis of the undamaged RTG Transportation System Packaging is conducted with a 2-D, axisymmetric model. The model uses 124 nodes along 15 axial stations to represent components or portions of components for the packaging. The thermal properties (i.e., specific heat, thermal conductivity, and convective and radiative heat transfer coefficients) are computed as a function of the associated temperatures.

Figure 3.4.1-2 illustrates the distribution of the thermal model nodes for the packaging. See Appendix 3.6.2.1 for specific details about the model. Nodes 200 to 266 represent the inner vessel bell, seal area, and base plate. Nodes 300 to 369 represent similar components in the OCV. The independent loops in the cooling jacket are modeled separately using 16 nodes at three axial stations (i.e., nodes 311, 312, 313, 315, 316, ... 321, ... 335, 336). Detail A illustrates the typical node placement for the thermal model of the coolant jacket. Nodes 311, 312, 321, 322, 331, and 332 represent the coolant fluid in the channels. The odd coolant node numbers represent one coolant loop and the even node numbers represent the second coolant loop. This approach permits simulating the failure of one or both of the cooling loops. The coolant fluid is assumed to be a 70% water/30% propylene glycol mixture by volume. For the regulatory analysis, which assumes the coolant channels to be drained, the thermal properties of the coolant nodes are replaced by those appropriate for air. The coolant is assumed to enter the coolant channels at 40 °F and at a flow rate of 4.5 gallons per minute per channel. The temperature rise is less than 5 °F, assuming both coolant loops are operating.

Details B and C of Figure 3.4.1-2 illustrate node placement at the OCV closure bolts and impact limiter attachment bolts, respectively. The only difference is the node placement and numbering for the two types of attachment bolts.

Detail D of Figure 3.4.1-2 illustrates six of the seven nodes used to model heat transfer within the electrical feed-through connector assembly that extends above the ICV base plate. The seventh node that is not shown is an arithmetic node that represents the mean gas temperature in the electrical feed-through connector cavity. Because of their recessed placement, the thermal mass of the surrounding material, and the limited heat flux in these regions, no specific modeling is made of the electrical feed-through connector assemblies in the ICV and OCV base plates. Instead, the temperatures for these components are assumed to be encompassed by the temperatures of the surrounding base plate material (i.e., node 264 for the ICV electrical feed-through and node

368 for the OCV electrical feed-through).

The temperature of the OCV electrical feed-through connector is assumed to be equivalent to that of node No. 367.

The impact limiter is simulated with a 2-D thermal model using 33 nodes (node 401, the thermal barrier, is not shown). This quantity provides resolution of the temperature through the foam for both structural and thermal calculations. The impact limiter is assumed to rest on an adiabatic surface. This assumption provides a conservative estimate of the package temperatures for NCT events.

The RTG shipping rack assembly is modeled with 21 nodes. Figure 3.4.1-2 illustrates the location of the eight primary shipping rack assembly nodes. The remaining 13 nodes are arithmetic nodes that ease the calculation of the heat transfer in and around this geometrically complex assembly. Heat transfer via conduction, convection, and radiation are addressed for the interfaces between the shipping rack assembly and the various RTG/ICV surfaces.

Based on the O&M requirements presented in Chapter 8 for the heat-resistant coating, the results from the Reference 14 tests that showed little or no degradation of the coating despite the package being assembled and disassembled approximately 40 times, and analysis showing that no surface exceeded 750 °F for NCT, it is concluded that no loss of the Carbolins heat-resistant coating will occur for any NCT event.

The basis for the calculation of thermal capacitance at each node and for heat transfer via conduction, convection, and radiation between the model nodes is presented in Appendix 3.6.2.

3.4.1.1.3 RTG-to-ICV Thermal Interface Model. The heat transfer between the GPHS RTG and the ICV occurs by a combination of radiation, convection, and conduction. The complexity of the heat transfer modes depended on the geometries involved, the interaction of the shipping rack assembly, and the heat paths internal to the RTG. Therefore, a third category of thermal model was developed to define the thermal relationship between the nodes used in the RTG model and the nodes used in the packaging model.

The following paragraphs provide a brief overview of the modeling approach used for the GPHS RTG. Further details of the GPHS RTG-to-ICV thermal interface model are provided in Appendix 3.6.2.

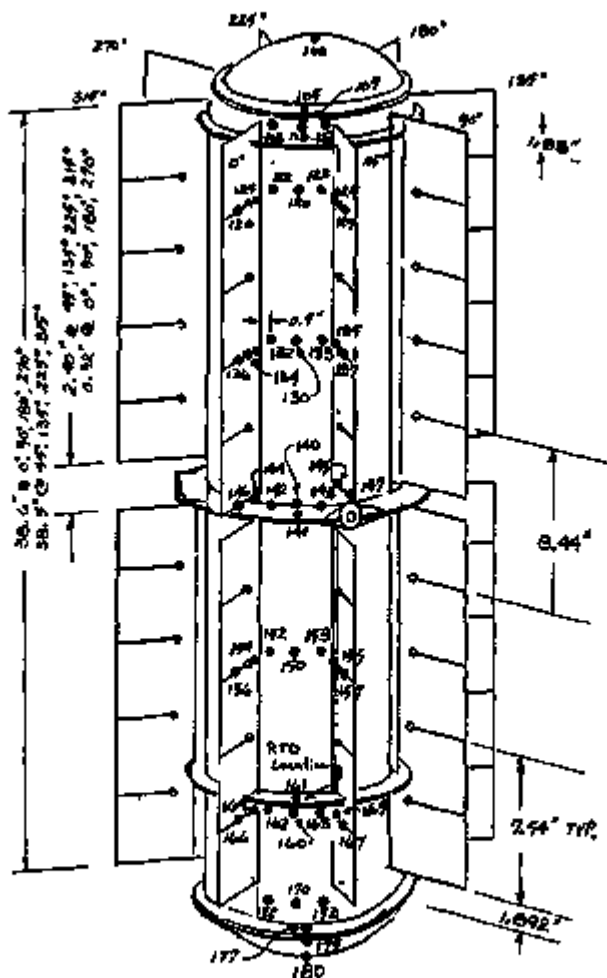


FIGURE 3.4.1-1a. GPHS RTG Thermal Model Nodes (Exterior Shell Nodes).

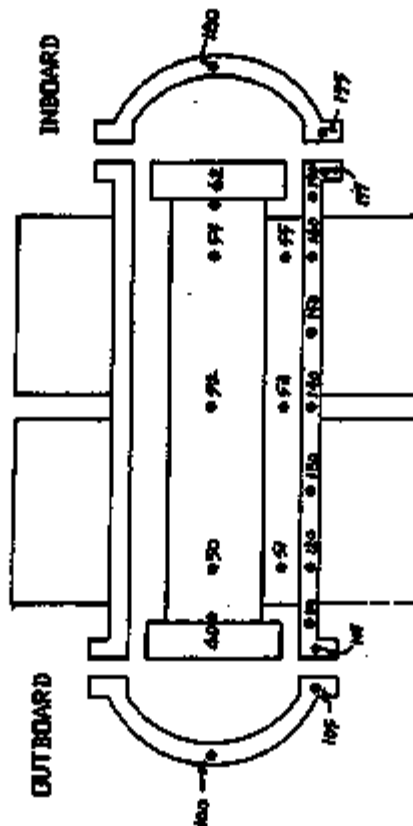


FIGURE 3.4.1-1b. GPHS RTG Thermal Model Nodes (Interior Nodes).

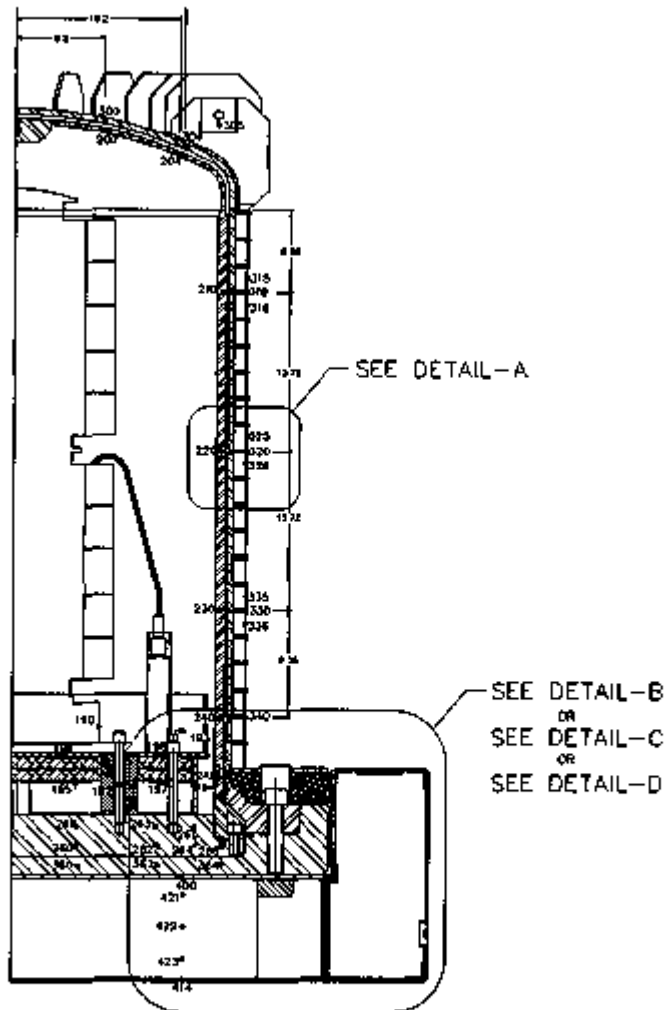
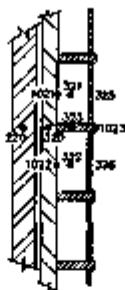
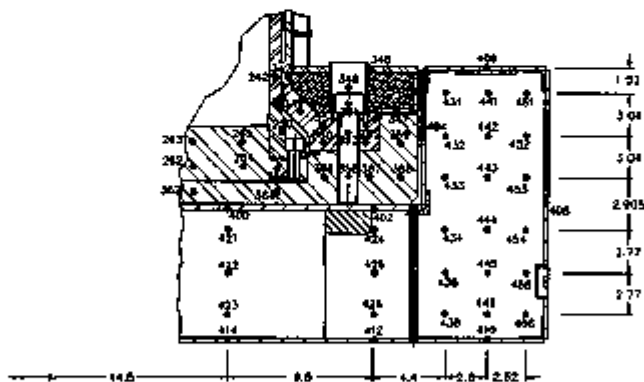


FIGURE 3.4.1-2. RTG Transportation System Package Thermal Model (details).



DETAIL-A



DETAIL-B

CLOSURE BOLTS ATTACHMENT

FIGURE 3.4.1-2. RTG Transportation System Package Thermal Model (details).

The convection coefficients for the GPHS RTG-to-ICV heat transfer are computed using equation 22 from Khan and Kumar¹¹. This correlation was developed for the case of convective heat transfer across a vertical annulus with a constant heat flux on the inner wall. The area of the inner and outer annular walls is not explicitly entered, but are implied by a characteristic length parameter that is a combination of the ratio of diameters and gap dimension. As such, the coefficients predicted by the correlation require adjustment to account for the fact that the GPHS RTG is a finned cylinder. The general applicability of the Khan and Kumar correlation to the specific geometry of the GPHS RTG and the method used to adjust the correlation was the subject of a thermal development test using a simulator of the GPHS RTG. The test results show that the Khan and Kumar correlation is applicable to the GPHS RTG/ICV geometry and that it can provide an accurate prediction of the convective coefficients. The Reference 12 test report presents a detailed discussion of the test setup, results, and the adjustment procedure used to apply the correlation to this payload. The validity of the adjusted correlation developed under the Reference 12 report was confirmed by qualification testing documented in the Reference 14 report.

Because a significant fraction of the heat transfer between the GPHS RTG and the ICV is via radiation, the shape factors between the various surfaces were determined by computer analysis using the University of Washington's VIEW⁹¹ program. The computed shape factors were validated using results from the GPHS development tests (see Section 3.4.1.2).

3.4.1.1.4 Package Models For Regulatory Conditions. The final category of thermal model developed for this analysis is that used to predict the package response under the regulatory normal conditions of transport specified 10 CFR 71. These models were similar to those used for the normal operational conditions. The primary model modifications involved the assumptions that the chillers are inoperative and that the coolant fluid has been drained or boiled out. As such, the forced fluid conductors in the cooling jacket are replaced with radiation and convection across a dry coolant channel. This modification is appropriate because analysis shows that the steady-state coolant temperatures will exceed the boiling point for the regulatory, inoperative chiller conditions. The package's cooling jacket incorporates pressure relief valves that will relieve pressure should the coolant system malfunction.

Package damage resulting from the NCT free drop tests was minor and would not affect the thermal performance of the package.

3.4.1.2 Test Model. In addition to the analytical models, developmental and qualification test models of the packaging were built to qualify the package design as capable of maintaining the RTGs within their temperature limits and to validate the analytical models. The developmental tests examined the basic heat transfer mechanisms that occur within the ICV cavity during the transport of an undamaged RTG. Included were steady-state results for radiative heat transfer only (i.e., with the ICV cavity evacuated of all gases), combined radiation/convection heat transfer with an air-filled ICV cavity, and combined radiation/convection heat transfer with a helium-filled ICV cavity. The effects on convective heat transfer caused by increasing the helium gas pressure and tilting the package were also examined.

The developmental test model consisted of an ICV bell and base plate, support stand assembly, and a simulator of the GPHS RTG. The ICV bell and base plate and the impact limiter were not modeled for this test. Instead, a cooling jacket was placed directly on the ICV bell, and the coolant temperatures adjusted to simulate the temperature rise across the ICV-OCV gap. Carbon steel was used for the ICV bell and base plate, while the GPHS RTG simulator was fabricated of 6061-T6 aluminum. The various differences in geometry and material were accounted for in the analytical model used to analyze the test results. The thermal

developmental test model was designed to replicate only the geometry of the ICV/RTG interface

used in the calculation of the radiation view-factors and the convective heat transfer coefficients. The developmental test did not address the heat transfer modes between the ICV and OCV or between the OCV and the external environment because these heat transfer modes are well defined and could be modeled analytically using established equations.

The development test results validated the procedures used to calculate the radiation and convection heat transfer conductances between the various nodes on the RTG thermal model and the nodes on the package thermal model. Reference 12 describes the test setup, procedures, conditions, results, and data analysis.

The thermal qualification tests built on the validation of the analytical modeling approach begun by the development tests by removing the majority of the hardware differences between the test and actual articles. The test article was a full-scale representation of the RTG Transportation System Package. The ICV and OCV bells were built to the production drawings. The RTGs were simulated with electrically heated hardware (ETG) built to production drawings and specifications. The shipping rack assembly was built to specifications with two main exceptions. First, the shipping rack included a center hole to allow instrumentation and power cables to pass through. Second, the electrical feed-through instrumentation hardware (see Figure 3.4.1-2, Detail D) was not present.

Only the base plates and impact limiter were built as simplified replicas of the actual articles. This approach was taken for a combination of fabrication ease, cost savings, and the need for numerous instrumentation leads to pass through the base plate.

Instead of separate stainless steel base plates for the ICV and OCV, the test article for the thermal qualification tests used a single carbon steel base plate with integral seal flange areas for both vessels. The impact limiter was simulated using 9 lb/ft³ polyethylene foam instead of the 12 lb/ft³ polyurethane foam. The simulated impact limiter was dimensionally correct, but did not have a stainless steel shell. Both test component designs had a negligible effect on the test results because of their similarity to the actual components and the low heat flux to the lower end of the package under normal operational conditions. Polyethylene foam has a thermal conductivity of 0.40 Btu-in/ft²·°F·hr at 70°F, versus 0.28 Btu-in/ft²·°F·hr for polyurethane foam at the same temperature.

The thermal qualification tests covered prototypic procedures for loading, unloading, and transporting the RTGs. A limited number of off-design operational conditions were also covered by the tests. No regulatory conditions were tested because of potential damage to the ETG test hardware that these conditions could cause. However, results from the thermal qualification tests further validated the analytical models used to simulate the RTG payload within the package under both operational and regulatory conditions.

Reference 13 defines the test hardware, test procedures, and test conditions used in the thermal qualification tests. Reference 14 documents the test data reduction and correlation with analytic predictions. Figures 3.4.1-3 and 3.4.1-4 present typical benchmark results between the thermal model used for the SARP and the thermal qualification test data. Figure 3.4.1-3 illustrates the comparison between test data and analytical model predictions for package steady-state temperatures under simulated normal operational conditions (i.e., cooling system active) with a GPHS RTG payload. The figure shows an excellent agreement between test and predicted temperatures for all but thermocouple locations TC-10, TC-182, and TC-180.

Thermocouple TC-10 was located at the center of the ICV torispherical head. The closest thermal model node to TC-10 is 200, but the temperature at this node represents the mean temperature of a 26-in. diameter section of the dome. Because of the high temperature gradients in this region, the predicted temperature at node 200 would be lower than that measured by

TC-10. This fact is borne out by the good agreement with TC-8, which is located close to the geometric mean point on the ICV dome area represented by node 200. The mismatch at TC-180 and TC-182 locations occurs at a section of test hardware (i.e., electric power inlet spool piece) that was not directly modeled by the RTG thermal model and does not exist on the real article. The suspected cause is an underestimation of the heat leakage through the interior ETG insulation where the power cables enter the body of the ETG test article. No adjustment was made to the SARP thermal model for the mismatch at the TC-180 and TC-182 locations because the spool piece is not present on the actual RTG.

Figure 3.4.1-4 presents a comparison between model predictions and test data for the prototypic loading of the GPHS RTG into the packaging. The illustrated transient temperatures represent key thermocouple locations on the GPHS ETG and the packaging. Similar results were seen for the other thermocouple locations. The analytical model provides a close, but conservative estimate of the resulting package and RTG transient temperatures. In conclusion, the thermal qualification tests validate the thermal model for both steady-state and transient calculations of an undamaged packaging and payload.

3.4.2 Maximum Temperatures

NCT thermal load case No. 1 evaluated the maximum temperatures in the package under the 10 CFR 71.71(c) conditions for heat. According to the referenced regulatory condition, the analysis assumes an ambient air temperature of 100 °F and insolation. The total insolation over a 12-hour period on the package is given in Table 3.4.2-1. The hourly average of the table data is the appropriate insolation value to use because the high thermal mass of the package ensures that it will not respond to short-term variations in insolation. A precise modeling of the data in Table 3.4.2-1 calls for a cyclic step function of insolation for 12 hours (daylight) followed by 12 hours of no insolation (nightsime) until steady periodic behavior is established. However, this analysis used the simple, but more conservative approach of assuming a uniform heat flux equal to the hourly average (based on 12 hours) of the table values in a steady-state analysis.

TABLE 3.4.2-1. Insolation Data.

Form and location of surface	Total insolation for a 12-hour period (g cal/cm ²)
Flat surfaces transported horizontally:	
• Base	None
• Other surfaces	500
Flat surfaces not transported horizontally	200
Curved surfaces	400

The amount of solar energy absorbed by the package is calculated as the product of the hourly insolation value times the solar absorption factor for the package surface in question. Because the entire exterior surface of the package is coated with a white, two-part epoxy paint, the appropriate solar absorption factor is 0.26. With the exception of the base of the impact limiter, the full-surface area is used to determine the total solar insolation heat flux on the package's individual surfaces. Shading of one package surface on another surface is assumed to not occur.

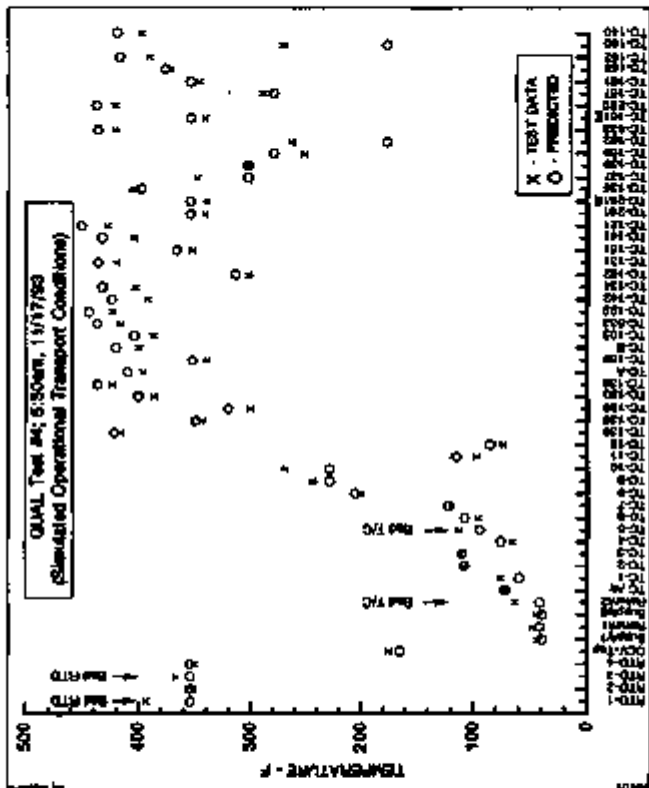


FIGURE 3.4.1-3. Thermal Model Benchmark With Steady-State Test Data.

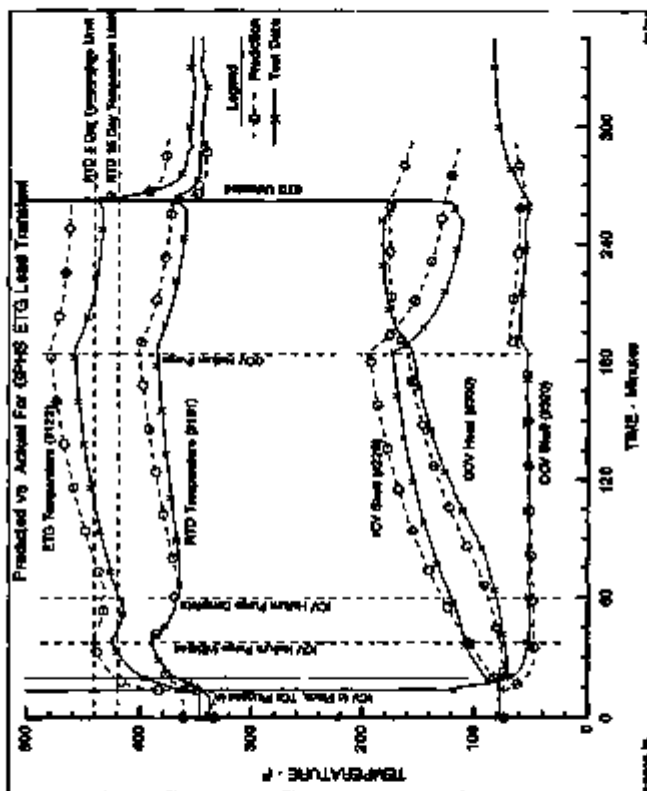


FIGURE 3 4 1-4 Thermal Model Benchmark With Transient Test Data

Additional assumptions for NCT thermal load case No. 1 include an undamaged payload and packaging, a maximum decay heat load of 4,500 W, and an inactive cooling system with the cooling jacket drained.

Figure 3.4.2-1 presents the maximum package temperatures expected under regulatory NCT. All temperatures are within component allowables.

Figure 3.4.2-2 illustrates the package temperature distribution for the same conditions as above, except without solar insolation. This load case is used as one of the pre-accident conditions for the HAC fire transients presented in Section 3.5.

3.4.3 Minimum Temperature

The package minimum temperatures are evaluated for two categories of regulatory NCT: worst case differential thermal expansion and minimum component temperatures.

The NCT thermal load case No. 2 helped determine the maximum differential thermal expansion in the seal areas. This load case assumes an undamaged payload and packaging, the maximum decay heat payload of 4,500 W, and that the cooling system is inactive and the cooling jacket is drained. The environmental conditions are those of the 10 CFR 71.71(c) conditions for cold: -40 °F still air and no solar loading.

Figure 3.4.2-3 presents the package temperature distribution for NCT load case No. 2. All temperatures are within component allowables.

Figure 3.4.2-4 illustrates the temperature distribution in the package for NCT load case No. 5. This temperature is used as one of the two pre-accident conditions for the HAC fire presented in Section 3.5.

Package component compatibility with the minimum temperatures expected was determined assuming no solar loading, no active cooling, minimum heat load payload, and either -20 °F (dynamic conditions) or -40 °F (static conditions) ambient temperature. No specific analysis was made for these conditions. Instead, it is assumed that the package temperature distribution will be uniform and equal to the ambient temperature. All package components are capable of operating at temperatures down to -40 °F.

3.4.4 Maximum Internal Pressures

Table 3.4.4-1 presents the gas temperatures and pressures within the ICV and OCV. The gas pressures are estimated using the ideal gas law. The base pressures and temperatures used in the calculations are set by the steady-state condition for NCT load case 7 (see Table 3.4-1). The analysis assumes worst case initial pressures at the time of RTG loading into the packaging (i.e., 19 psia base pressure + 1 psi tolerance = 20 psia). Other sources of pressure rise within the ICV/OCV, and their contribution to the final pressure level are addressed in Section 2.6.1.

TABLE 3.4.4-1. Maximum ICV/OCV Pressures and Temperatures For Normal Conditions of Transport.

Load case/condition	ICV pressure (psia)	ICV gas temp. (°F)	OCV pressure (psia)	OCV gas temp. (°F)
Case 1	24.4	354	20.3	285
Case 2	21.5	256	22.1	166
Case 3	20.2	213	20.3	115
Case 4	24.1	342	25.8	271
Case 5	21.8	269	22.5	181
Case 6	20.1	210	20.1	111
Case 7	20.0	207	20.0	107

3.4.5 Maximum Thermal Stresses

The results from finite element analyses of the ICV and OCV for NCT load cases 1, 2, and 3 are presented in Section 2.6.1. These are the governing cases for stresses because they result in the worst case combination of temperatures and temperature gradients. All margins of safety are positive and the design criteria of Regulatory Guide 7.6 are satisfied. See Section 2.6.1.3 for specific details and further discussion.

3.4.6 Temperatures For Operational Conditions

The NCT thermal load case No. 3 evaluated the package temperature distributions with the mechanical cooling system active, regulatory solar insolation, and the maximum heat payload. The resultant temperatures encompass those seen by a shielded package loaded in a vented trailer that is exposed to 100 °F ambient temperature and regulatory solar insolation.

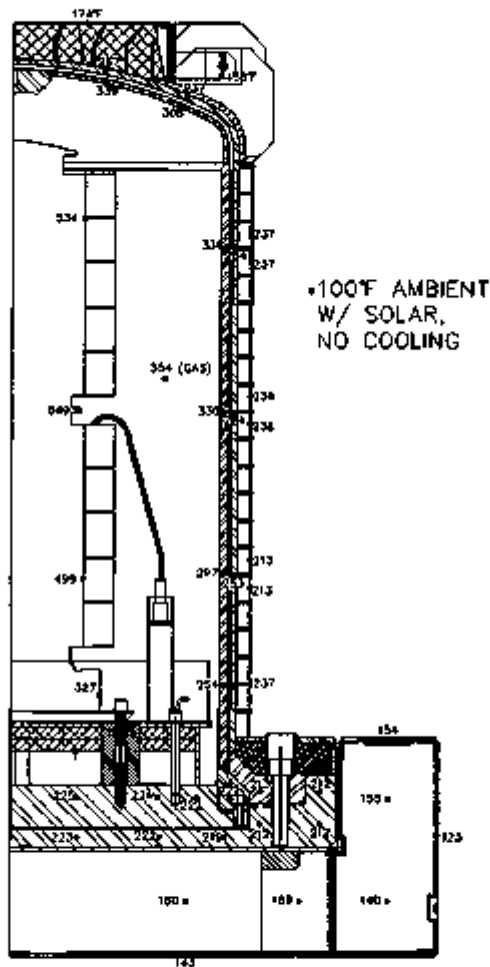


FIGURE 3.4.2-1. Maximum RTG Transportation System Package Temperatures
For NCT Load Case No. 1

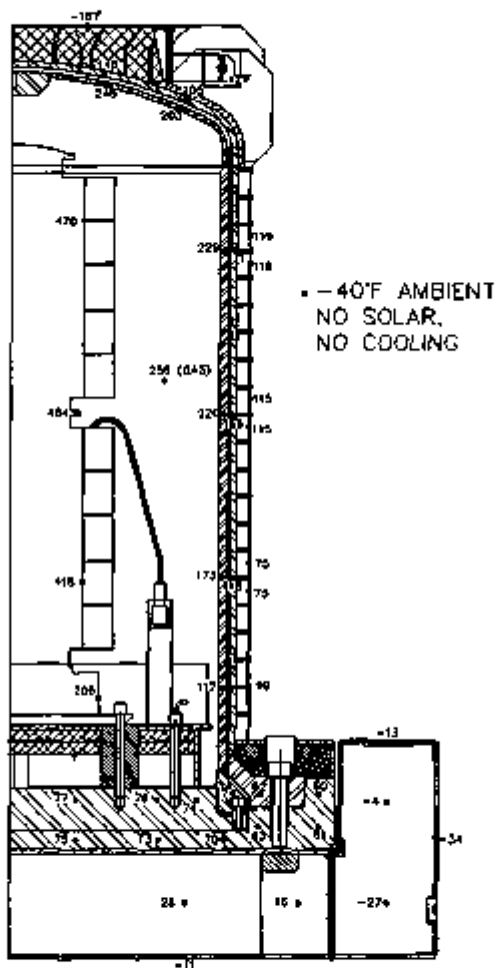


FIGURE 3.4.2-3. Minimum RTG Transportation System Package Temperature For NCT Load Case No. 2.

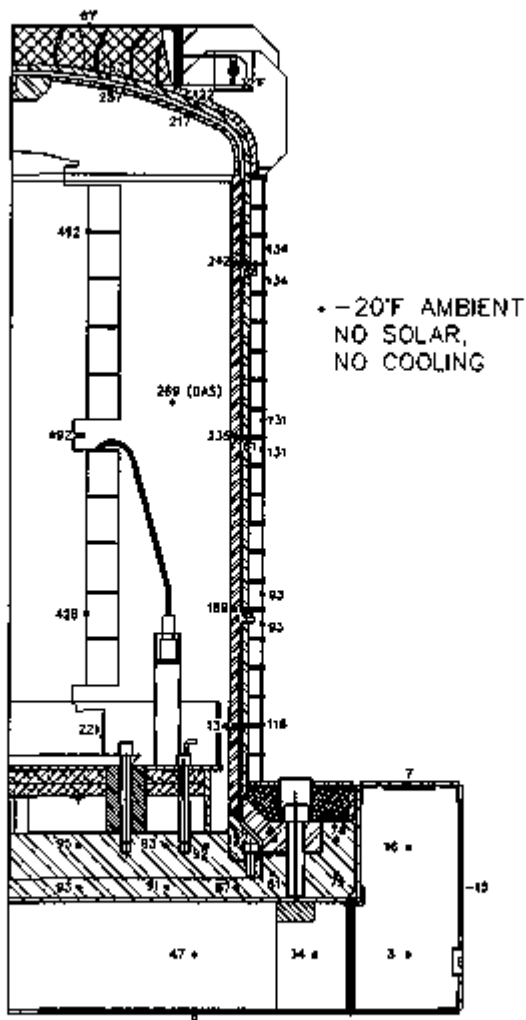


FIGURE 3.4.2-4. RTG Transportation System: Package Temperature Distribution for NCT Load Case No. 5.

This load case illustrates the maximum package temperatures seen with active cooling. These temperature levels are the maximums expected during package transport, except in the remote possibility where multiple and independent failures deactivate the cooling system. As such, this load case also illustrates the additional thermal conservatism imposed by the regulatory requirement of starting the package at steady-state under NCT before imposing the HAC fire.

Figure 3.4.6-1 illustrates the temperature distribution for NCT load case No. 3. In general, the ICV sidewall temperatures run 180 °F cooler with active cooling than without cooling for the same ambient temperatures. Package base plate and seal temperatures are approximately 130 °F cooler, while head temperatures are 80 °F cooler.

Figures 3.4.6-2 and 3.4.6-3 illustrate package temperatures without solar for 100 and 70 °F ambient air conditions, respectively (i.e., NCT load cases 5 and 7). Figure 3.4.6-2 confirms compliance with the 10 CFR 71.43(g) requirement that no accessible surface exceed 180 °F. Figure 3.4.6-3 illustrates the temperature distribution after loading the RTG in the packaging. All subsequent calculation of internal ICV and OCV gas pressures are keyed to this temperature distribution.

3.4.7 Evaluation of Package Performance for Normal Conditions of Transport

Through analysis and physical testing, the RTG Transportation System Package is shown to meet the thermal requirements of 10 CFR 71.71. Based on Sections 3.4.2 and 3.3, all components will remain within their working temperature range. The maximum temperature reached in the OCV is 268 °F, while the ICV reaches a maximum temperature of 338 °F. The ICV and OCV seal temperatures are 222 °F and 213 °F, respectively. The electrical feed-through connector remains below 226 °F for NCT, while a maximum temperature of 206 °F is reached in the impact foam adjacent to the OCV base plate. The RTG payload shell remains below 550 °F.

The minimum temperature from Section 3.4.3 for any package component is taken as -40 °F for static conditions and -20 °F for dynamic conditions.

3.5 HYPOTHETICAL ACCIDENT THERMAL EVALUATION

This section presents the thermal analysis of the RTG Transportation System Package for the HAC fire specified in 10 CFR 71.73(c)(3). The thermal performance of the package is evaluated analytically using a 3-D thermal model. The thermal model is based on the NCT model with modifications made to simulate the damage sustained from the HAC 30-ft free drops and the HAC 40-in. puncture drops. The results from a series of drop tests conducted on the Certification Test Article are presented in Sections 2.7.6 and 2.10.15. Analysis of the expected thermal impact associated with the package damage noted after each of the drop tests is presented in Section 3.6.2.4. The initial temperature distribution in the package before the HAC fire is taken from the steady-state conditions with the worst case ambient temperature, no insulation, and no active cooling.

To determine the effect of the HAC fire, the package is exposed to a convective and radiative heat flux based on still, ambient air at 1475 °F and with an emissivity of 0.80. The HAC fire is assumed to last for 30 minutes, after which time the thermal boundary is returned to the original ambient temperature. The thermal transient analysis is continued for a sufficient time to determine the maximum values for all package components, concluding with a post-HAC fire steady-state analysis.

3.5.1 Thermal Model

3.5.1.1 Analytical Model. The analytical model for the regulatory NCT is used as the basis for the HAC fire model. The primary modification made for HAC fire evaluation was to create a 3-D model to permit simulation of asymmetric damage caused by the HAC fire drop. The 3-D model was created using a SINDA program feature that allows a series of thermal submodels to be combined into one large thermal model. Each of these submodels can be independently scaled and modified as necessary to represent their contribution to the overall thermal model. For this application, the 2-D package models described for the undamaged case were used to represent axial and radial heat transfer within the individual subsegments making up the 3-D model of the package. Circumferential conductors are used to complete the 3-D model by providing thermal communication between the various 2-D model subsegments.

In general, heat transfer within each 2-D submodel is modeled using the same axisymmetric regulatory model data for thermal capacitance, conductance, and radiation as defined in Sections 3.4.1.1 and 3.6.2. Each value for conductance and capacitance is scaled according to the subtended angle represented by the associated submodel. Where appropriate, the individual 2-D submodels are modified to simulate changes in heat transfer modes and/or values because of damage and package orientation caused by the regulatory drops. The specific model changes are described in Appendix 3.6.2.4.

The 3-D HAC fire thermal model uses four 2-D submodels to represent one-half of the package. Symmetry conditions are assumed for the temperatures in the other half of the package. One of the submodel segments represents the damaged section of the package, while the other three segments provide circumferential temperature resolution within the package components. Sections 3.5.2 and 3.6.2.4 describe the type and extent of package damage assumed.

Additional model modifications for the HAC fire included the 10 CFR 71.73(c)(3) requirements for a package external surface absorptivity of 0.8 or greater and exposure of the entire package (including the impact limiter bottom) to the HAC fire.

3.5.1.2 Test Model. No thermal testing for the HAC fire was performed for the RTG Transportation System Package as an entire assembly. However, performance tests were conducted for the polyurethane foam used in the impact limiter, the Butyl seals, and the electrical feed-through connectors. The test results are documented in Appendix 3.6.3, 2.10.6, and 4.6.2, respectively. Briefly, these tests demonstrated the following major findings:

Polyurethane Foam

- Below 400 °F, the variation in foam thermal properties with temperature are slight and reversible. As such, fixed values for specific heat and thermal conductivity are appropriate.
- Irreversible thermal degradation of the foam begins at temperatures above 400 °F. The degradation is accompanied by vigorous outgassing that removes a significant amount of heat through mass transport processes.

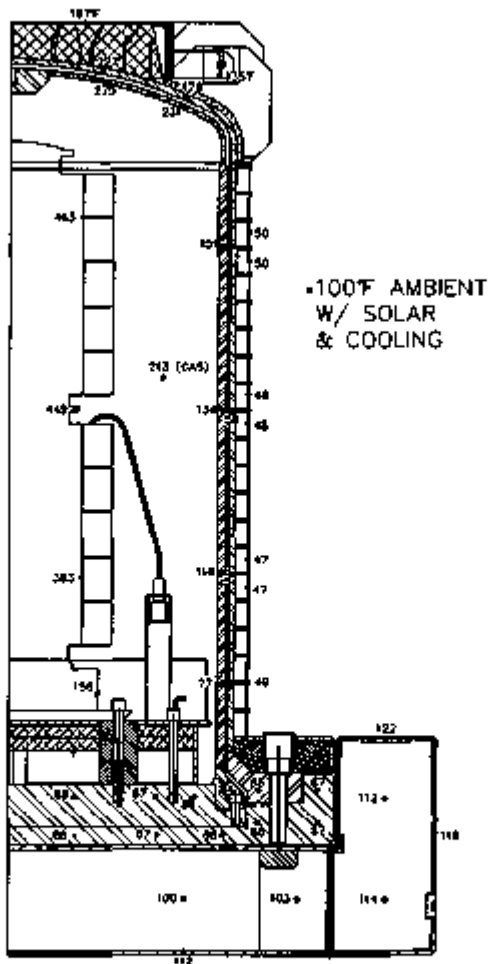


FIGURE 3.4.8-1. RTG Transportation System Package Temperature Distribution For NCT Load Case No. 3.

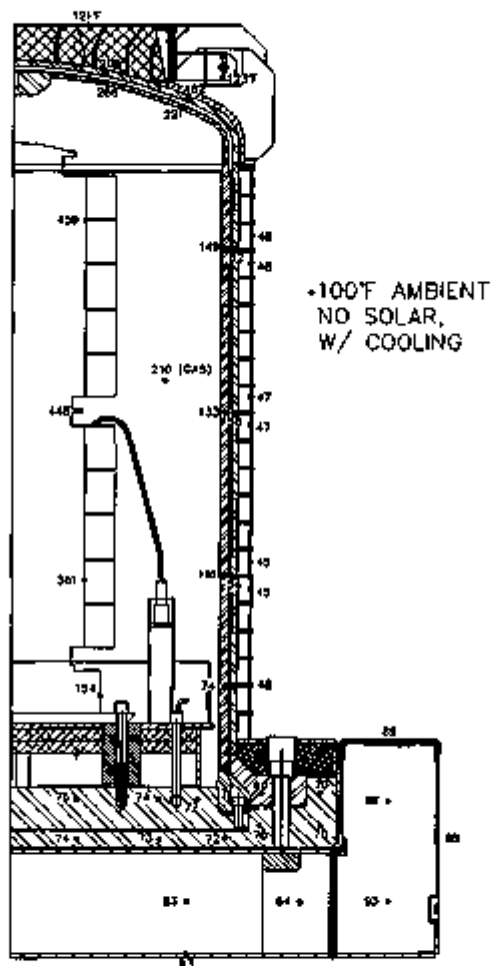


FIGURE 3.4.6-2. RTG Transportation System Package Temperature Distribution For NCT Load Case No. 8.

- A rigid char layer is formed as the thermal degradation continues. In the absence of direct exposure to the flame, the char layer will be the same or slightly thicker than the original foam depth. This char layer provides radiative shielding to the underlying foam material.
- Where a layer of undisturbed 12 lb/ft³ foam in excess of 3 in. or a layer of 3 lb/ft³ foam in excess of 8.5 in. exists before the initiation of the fire, little or no thermal response will be seen on the backside of the foam because of the fire event.

O-ring Seal Tests

The butyl O-ring containment seals have successfully demonstrated leaktight behavior at a temperature as high as 380 °F over short durations (24 hours) and 350 °F over extended periods (6 days). The complete details of the time-temperature testing of the O-ring seals is provided in Appendix 2.10.6. Butyl O-ring containment seals exhibiting time-history characteristics below those identified in Appendix 2.10.6 are considered satisfactory for maintenance of leaktight containment in the package.

3.5.2 Package Conditions and Environment

Several combinations of HAC free and puncture drops were evaluated to determine the worst case thermal damage to the package. Details of the analysis and the tests used to support the damage evaluations are presented in Sections 2.7 and 2.10.15. Section 3.6.2.4 summarizes the thermal analysis associated with the damaged package.

Briefly, the finding of these analyses and tests is that the most thermally sensitive post-impact package reconfiguration will result from either (1) a bottom-down c.g. over corner impact orientation, or (2) a side slapdown impact, defined for the package as the near-simultaneous impact of the top-end fins and the bottom-end impact limiter. The impact limiter damage for each of these impact scenarios is illustrated in Figures 3.5.2-1 and 3.5.2-2, respectively. Thermal evaluation of the above potential package reconfigurations showed that the side slapdown impact poses the most conservative case for the thermally sensitive package seals. As such, this drop orientation serves as the basis for all of the HAC fire transients. In addition, the center of the side slap down impact damage is assumed to be aligned with the electrical feed-through.

Based on drop tests and analysis (see Sections 2.7 and 3.6.2.4), the side slapdown impact will crush the top of the impact limiter to about 25% of its original side thickness at the centerline of the damage. The lower end of the impact limiter will sustain essentially no damage. The circumferential extent of the damage to the top of the impact limiter will extend over a 67° arc. Figures 3.5.2-2 and 3.6.2-3 illustrate how the impact limiter damage is modeled analytically. Segment A of the 3-D model assumes the foam thickness to be reduced by 50% over the full height and subtended angle of the segment. Impact limiter damage beyond the angle subtended by segment A is assumed to be encompassed by the conservative assumption that the first 2.5 in. of foam ablates away at the initiation of the HAC fire (see Appendix 3.6.3 for more discussion of this assumption).

In addition to damaging the impact limiter, the side slapdown impact will cause localized damage to the impact fins at the OCV torispherical head and the top 4 in. of the coolant jacket. The damage will consist of buckling and/or bending of two or three fins onto the OCV head and potential contact between the ICV and OCV shells over a 2-in. high by 13-in. wide area. The fin damage will tend to lower the heat transfer with the exterior environment, while the possible ICV/OCV contact will tend to raise the local ICV temperature during the fire and lower the ICV temperatures after the fire. The nature and extent of the damage will not have a significant effect

on the heat transfer characteristics in this area and was not specifically addressed by the analytical thermal model for the HAC fire event.

Beyond the damage described above, no significant damage will occur to the package because of the HAC free drop. Puncture bar damage will be limited and highly localized. The structural strength of the impact limiter shell is sufficient to limit puncture bar damage to relatively minor indentations of the shell. Tearing of the shell, with subsequent penetration and gouging of the underlying foam will not occur. Puncture bar impact to the OCV head will produce localized indentation with associated contact between the ICV and DCV heads over a 7-in. diameter area. Puncture bar impact to the cooling jacket will produce localized collapsing of the cooling jacket thickness and, possibly, localized indentation of the OCV and ICV shells. Any subsequent contact between the ICV and OCV will tend to raise the local peak temperature for the ICV during the fire, but lower the local ICV temperature following the fire.

Finally, puncture bar impact to the OCV thermal shield at the bolt flange will result in only minor damage. Because of the location of the surface and the package center of gravity, the impact will be a glancing blow. Damage will be limited to crescent-shaped indentation of the OCV thermal shield, but no penetration. At its greatest depth, the OCV thermal shield will be collapsed to 1/2 its original height above the bolt flange.

Of the various potential puncture bar damage described above, only the potential for damage to the OCV bolt flange thermal shield is considered significant enough to warrant modeling. The potential damage is conservatively modeled by locating the damaged area adjacent to the impact limiter damage (i.e., Segment A, Figure 3.5.2-3) and by assuming the shield to be collapsed to 1/2 its original height over a 6-in. diameter area (the puncture bar). The density and conductance of the fiberglass insulation underlying the damaged area is increased to account for the collapse of the OCV thermal shield.

The damage analysis indicates that a side slapdown impact will cause the GPHS RTG payload to break away from its shipping rack mounts. For conservatism, it is also assumed that the shell of the GPHS RTG payload is ruptured in the impact and that all 18 GPHS heat-source modules (aeroshells) spill out. The aeroshells, which are the outer housing of each heat source module, measure 92.4 by 97.2 by 53.1 mm. The aeroshells are the smallest heat-producing fragment of the RTG that will occur because of the HAC free drop.

Following the side slapdown impact, the package is envisioned as coming to rest in one of only two credible orientations: upright (resting on the impact limiter's bottom) or on its side. In the first post-HAC orientation, the 18 aeroshells are assumed to be distributed uniformly around the outer circumference of the package shipping rack assembly (i.e., nearest the ICV containment seal). The shell of the GPHS RTG payload is assumed to have broken off from its stand and to be canted at an angle within the ICV. Figure 3.5.2-4 illustrates the configuration for this HAC case.

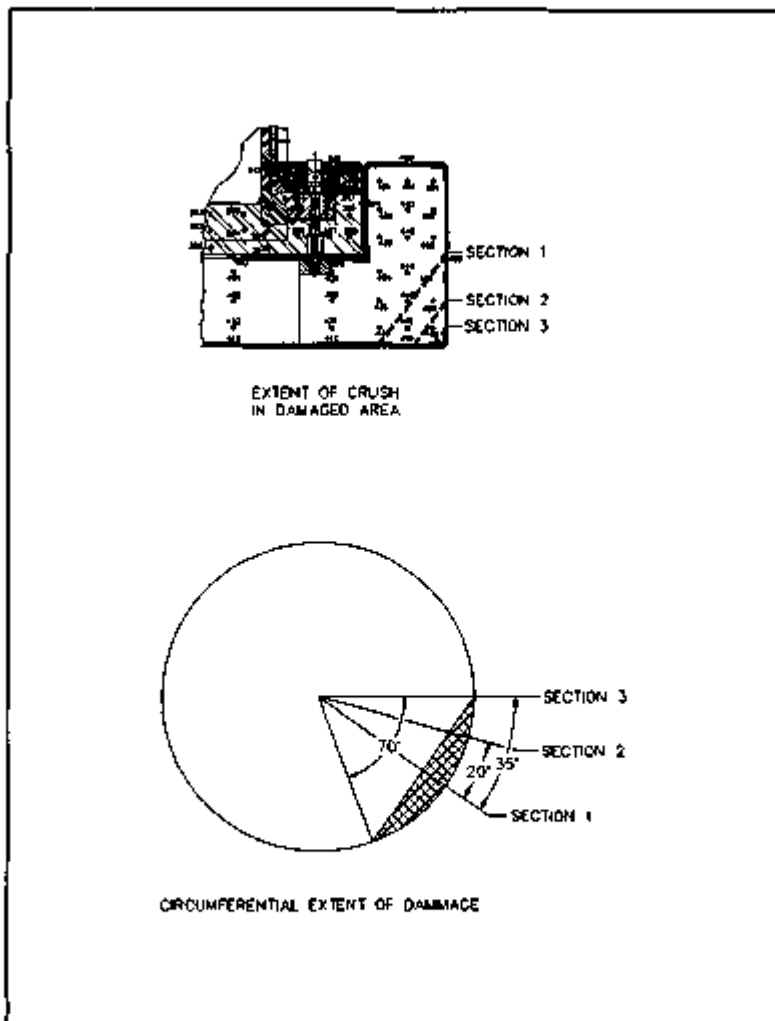


FIGURE 3.5.2-1. Impact Limiter Damage With C.G.-Over-Corner Drop.

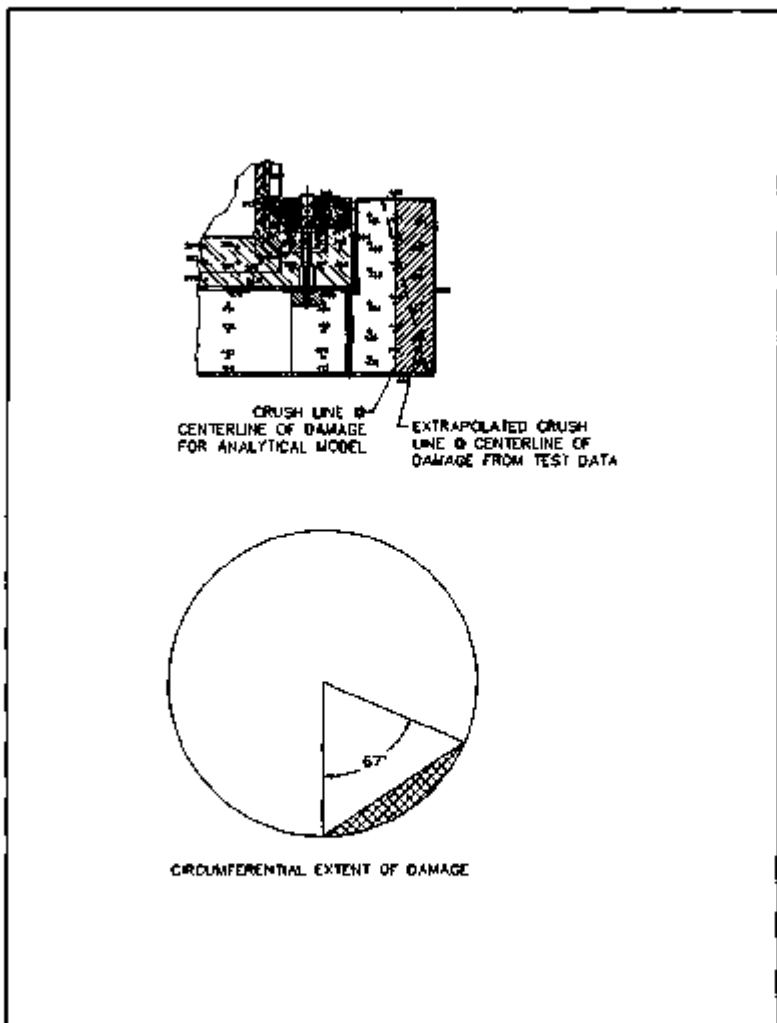


FIGURE 3.5.2-2. Impact Limiter Damage With Side Slapdown Drop.

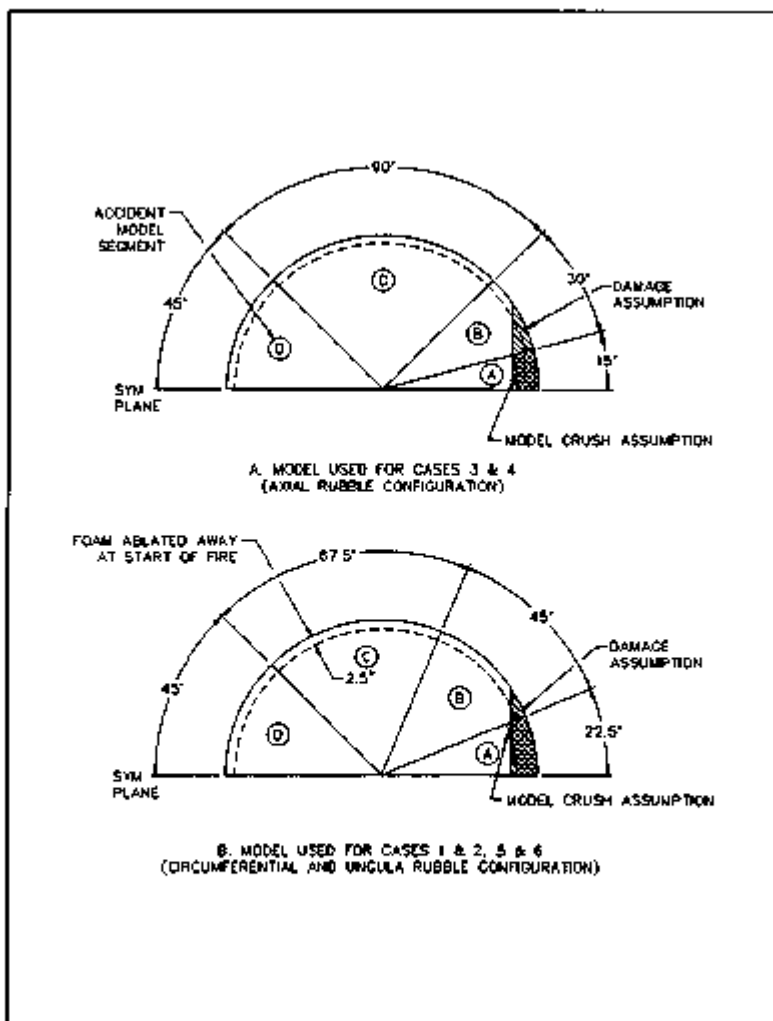


FIGURE 3.5.2-3. Impact Linker Modeling Assumptions.

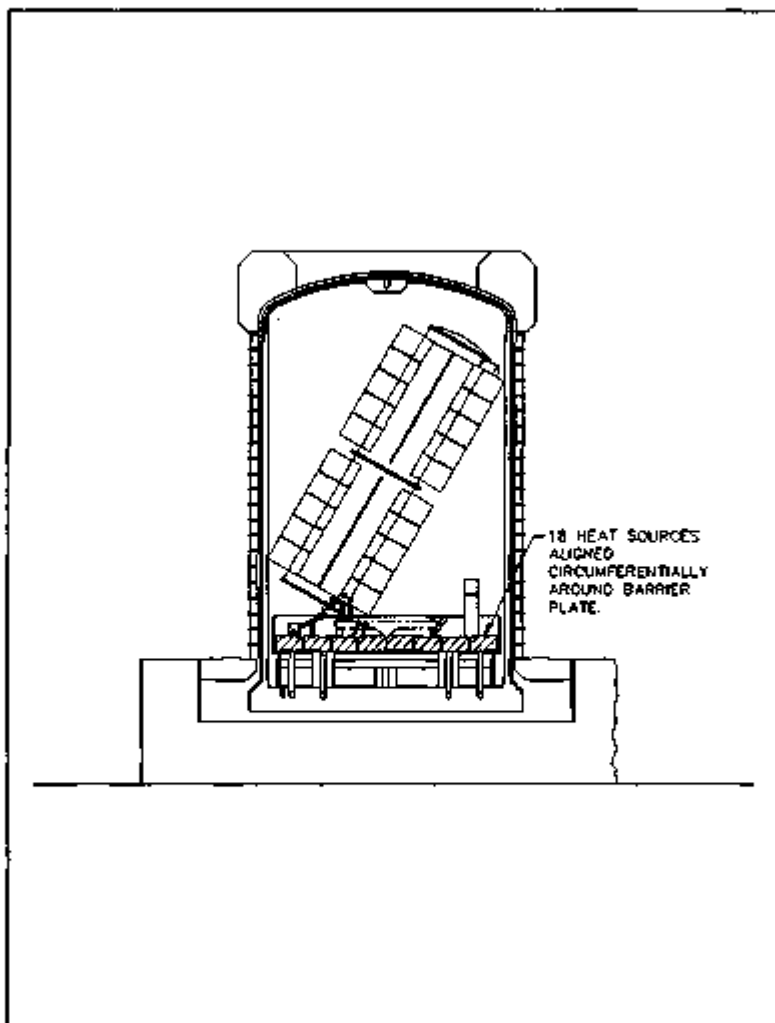


FIGURE 3.6.2-4. Post-HAC Free Drop Package Orientation For Circumferential Heat Source Alignment.

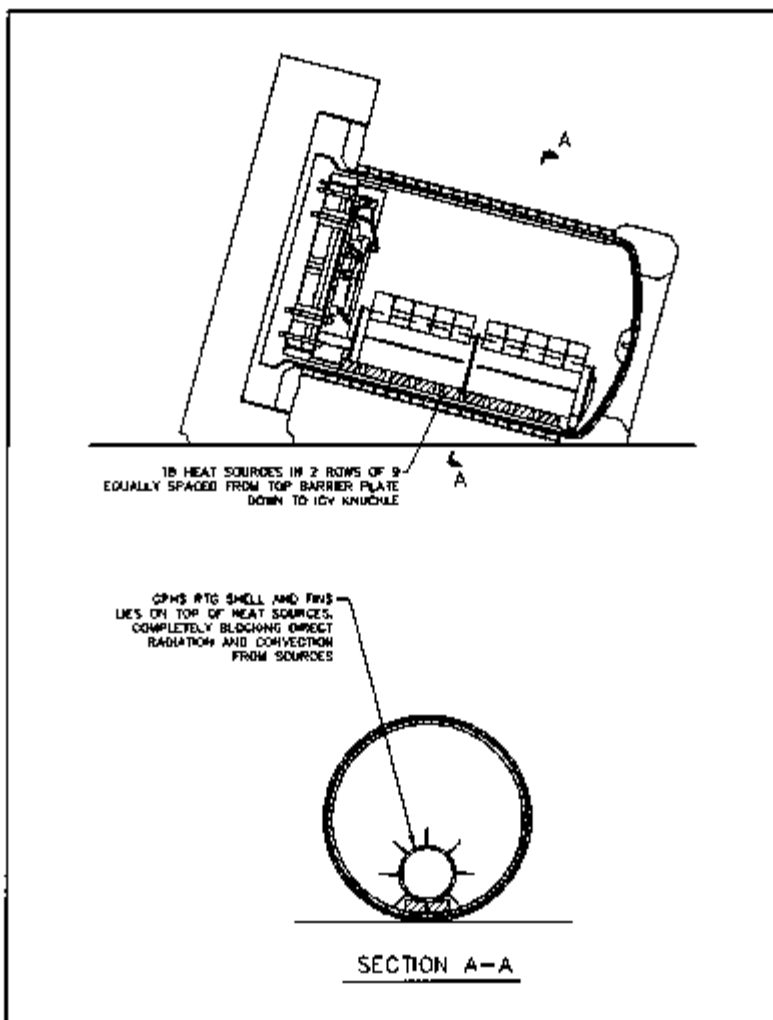


FIGURE 3.5.2-5. Post-MAC Free Drop Package Orientation For Axial Heat Source Alignment.

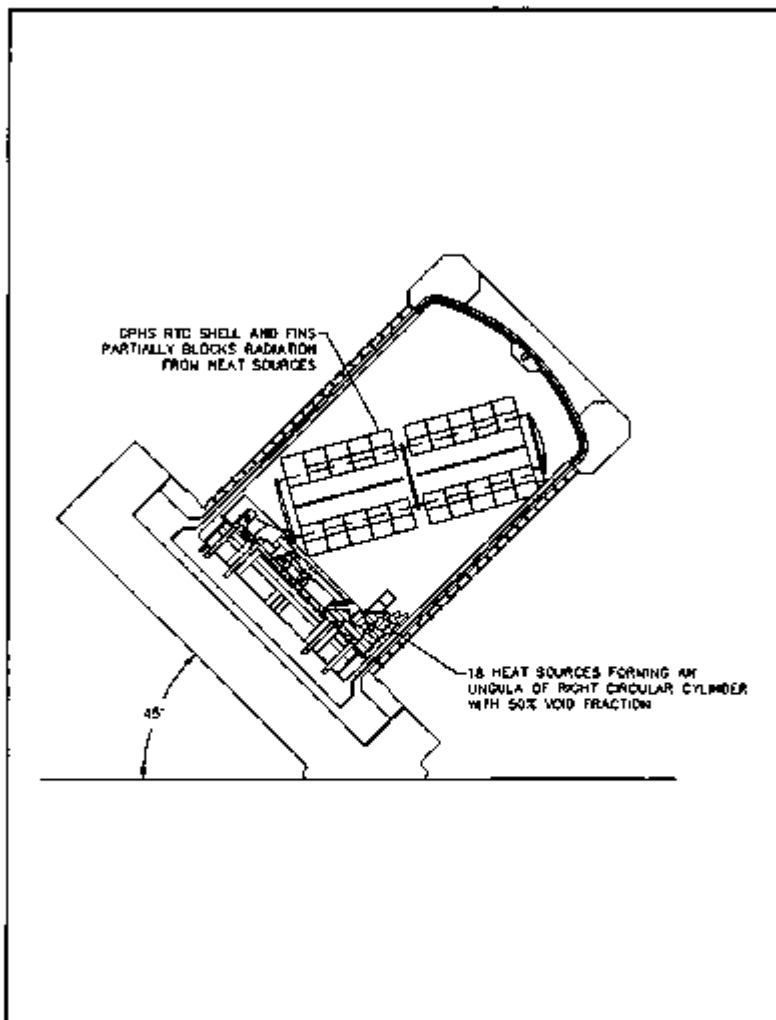


FIGURE 3.5.2-6. Post-HAC Free Drop Package Orientation For Ungula Heat Source Alignment.

For conservatism, the RTG shell is canted in the direction of the impact limiter damage, where it shields the underlying aeroshells from direct radiation interchange with the inside surfaces of the ICV. Convection from the aeroshells is not significantly affected by the position of the RTG shell.

In the second post-HAC package orientation, the 18 GPHS aeroshells are assumed to come to rest in an axial alignment on the ICV wall. The assumed alignment has two modules arranged side by side, starting at the top of the shipping rack assembly and extending to the ICV torispherical head. For conservatism, the centerline of the aeroshells and the package side drop damage are assumed to be aligned. The shell of the GPHS RTG is assumed to end up lying directly on top of the aeroshells, blocking direct convection and radiation interchange between the aeroshells and the interior of the ICV cavity. Figure 3.5.2-5 illustrates the assumed alignment of the package, RTG shell, and aeroshells for this post-HAC free drop condition.

In addition to these credible post-HAC package/payload configurations, an extremely conservative configuration is evaluated wherein the package somehow ends up on its bottom corner, at a 45° orientation relative to the flat, unyielding regulatory impact surface. In this statically unstable post-HAC drop orientation, the 18 aeroshells are assumed to come to rest in an ungula-shaped rubble pile. For further conservatism, the rubble pile is assumed to be on the side of the shipping rack assembly barrier plate adjacent to side drop damage area of the package. Based on analysis and simple experiments, the rubble pile is assumed to have a 50% void fraction and to subtend a 135° arc. The RTG shell is assumed to have come to rest canted at an angle across the rubble pile. This orientation of the RTG shell is assumed to block the underlying aeroshells from direct radiation interchange with the inside surfaces of the ICV. Convection from the aeroshells is assumed to not be significantly affected by the position of the RTG shell. Figure 3.5.2-6 illustrates the assumed alignment of the package, RTG shell, and aeroshells for this post-drop condition.

All of the HAC fire transients begin with the undamaged package at steady-state with the chillers inoperative and the cooling jacket drained, no solar insulation, and an ambient temperature of either 100 or -20 °F. The temperature of the various package components, the shell of the RTG, and the aeroshells are initialized at the temperatures established by the NCT model. Specifically, the convective and radiation heat transfer links for the undamaged payload are used to determine the temperature of each modeled component just prior to the HAC accident sequence occurring. By this means the temperatures presented for NCT load case 4 (i.e., 100 °F, no solar, no active cooling) or NCT load case 5 (i.e., -20 °F, no solar, no active cooling) are used to initialize the equivalent components of the re-configured payload and the packaging prior to beginning the HAC transient. Since the HAC impact/puncture damage and payload reconfiguration is assumed to occur immediately before the start of the HAC fire event, the initial temperatures will be the same as for the associated NCT condition. Following the HAC damage and payload reconfiguration, the HAC model with its revised method of calculating the convective and radiative heat transfer is used to determine the subsequent changes in component temperatures.

Although portions of the ICV/OCV surfaces coated with the Carboline high emissivity coating will briefly exceed the coating's peak temperature rating of 1000 °F, it is assumed to remain intact throughout the HAC fire. This assumption maximizes the heat input to the package during the HAC fire. The Tremac epoxy paint and primer used on the package exterior will lose its adhesion to the package surfaces during the HAC fire, flake off, and expose the stainless steel surfaces to the HAC fire environment. Although this action will tend to reduce the package surface absorptivity from 0.8 to 0.48, the regulatory value of 0.8 is used to account for soot.

Six HAC fire load cases are used in the evaluation of the damaged package/payload configurations. Table 3.5.2-3 summarizes the pre- and post-HAC state assumed for each HAC load case. Section 2.7.3.1.1.2 provides additional details and background discussion on each HAC load case. The results of each analysis is presented in the following sections.

TABLE 3.5.2-1. Load Cases For The Hypothetical Accident Condition Analysis.

Load case	Pre-accident conditions	Post-accident conditions
1	<ul style="list-style-type: none"> a. Undamaged payload, 4,500 W maximum decay heat load b. Undamaged package; upright position, adiabatic bottom conditions c. Cooling jacket drained d. Steady-state conditions with 100 °F still air; no solar 	<ul style="list-style-type: none"> a. Circumferential distribution of heat source modules on banner plate, 4,600 W total. b. Side drop impact limiter damage; package upright, all surfaces exposed to ambient. c. Cooling jacket drained. d. 1475 °F fire for 30 minutes, followed by ambient air at 100 °F; no solar during and after fire.
2	Same as load case No. 1 except: <ul style="list-style-type: none"> d. Steady-state conditions with -20 °F still air; no solar 	Same as load case No. 1 except: <ul style="list-style-type: none"> d. 1475 °F fire for 30 minutes, followed by ambient air at -20 °F; no solar during and after fire.
3	Same as load case No. 1	Same as load case No. 1 except: <ul style="list-style-type: none"> a. Axial distribution of heat source modules along ICV wall above rubble dam; 4,500 W total. b. Side drop impact limiter damage; package on its side, all surfaces exposed.
4	Same as load case No. 2	Same as load case No. 3 except: <ul style="list-style-type: none"> d. 1475 °F fire for 30 minutes, followed by ambient air at -20 °F; no solar during and after fire.
5	Same as load case No. 1	Same as load case No. 1 except: <ul style="list-style-type: none"> a. Ungula shaped rubble pile of heat source modules on shipping rack; 4,500 W total. b. Side drop impact limiter damage; package at 45° angle of repose, all surfaces exposed.
6	Same as load case No. 2	Same as load case No. 5 except: <ul style="list-style-type: none"> d. 1475 °F fire for 30 minutes, followed by ambient air at -20 °F; no solar during and after fire.

3.5.3 Package Temperatures

The HAC load case Nos. 1 and 2 evaluate the transient thermal response of the first post-HAC package configuration per 10 CFR 71.73(c)(3). Steady-state package temperature distributions with 100 and -20 °F ambient air, respectively, are used as the initial starting conditions for the HAC fire.

Figures 3.5.3-1 and 3.5.3-2 illustrate the transient temperature response for the circumferential heat source distribution thermal load cases. The plotted package temperatures are taken from the 3-D model segment centered on the area of the side drop damage (i.e., model segment A, Figure 3.5.2-3). Temperatures at the other circumferential locations are equal to or less than those shown in the figures. The peak ICV and OCV temperatures occur at or just after the end of the HAC fire. The figures provide the peak ICV/OCV temperatures noted during the HAC fire. The maximum temperature of the helium gas internal to the OCV and ICV noted during the HAC fire are 848 and 836 °F, respectively. Thermal protection within the package and temperature stratification within the ICV cavity prevents these relatively hot gas temperatures from affecting the package containment seals.

All of the predicted package temperatures for HAC load case Nos. 1 and 2 remain within the thermal limits of the associated component. The containment seal temperatures reach maximums (see Figures 3.5.3-1 and 3.5.3-2) that are below the temperature limits of the Butyl elastomer material. The peak electrical feed-through connector temperature of 332 °F is substantially less than its 475 °F temperature rating.

The HAC load case Nos. 3 and 4 evaluate the thermal response for the second post-HAC package configuration per 10 CFR 71.73(c)(3). Figure 3.5.3-3 illustrates the transient temperature response for the HAC load case No. 3 damage configuration (i.e., axial heat source distribution and the package on its side) with initial package steady-state temperatures for 100 °F ambient and no solar loading. Figure 3.5.3-4 illustrates the same configuration except with an initial steady-state for -20 °F. Again, the representative package temperatures illustrated are taken from the 3-D model segment A.

Representative peak ICV/OCV temperatures reached during the HAC fire are noted on the figures. The maximum helium gas temperatures internal to the OCV and ICV during the HAC fire are 851 and 747 °F, respectively. The elevated temperatures seen for the ICV and OCV walls for model segment A are because the aeroshells lying directly on the ICV wall under this damage configuration. However, all package component temperatures will remain within their associated working limits. The peak Butyl O-ring seal and electrical feed-through connector temperatures of 326 and 314 °F, respectively, are within the limits of both components.

The HAC load case Nos. 5 and 6 evaluate the worst case post-HAC configuration for the package containment seal temperatures. Figures 3.5.3-5 and 3.5.3-6 illustrate the transient temperature responses for these conservative damage configurations (i.e., the aeroshells piled into a single unguale-shaped rubble pile and the package at a 45° angle). The conservatism of these load cases is increased by the basic analysis criteria applied to all HAC load cases; that is, that the package has suffered a double failure in the active cooling system, and the failure has existed long enough for the package to reach steady-state temperatures. If either of these conditions do not exist, the subsequent peak package temperatures reached during the HAC fire will be less than those shown in the figures. Again, the plotted package temperatures are taken from the 3-D model segment A which is centered on the rubble pile and the HAC side drop damage area.

As expected, the transient results for HAC load case No. 5 produces the worst case containment seal temperatures. Although the peak ICV containment seal temperature of 360 °F exceeds the steady-state capability for Butyl, the seal temperature returns to below 350 °F within

15 hours. As such, the time duration versus temperature curve is below the tested temperature capability of the Buryl seal material. The peak electrical feed-through connector temperature of 377 °F is nearly 100 °F below its temperature capability. Likewise, all other predicted package temperatures remain within the associated thermal limits.

The maximum helium gas temperatures internal to the OCV and ICV during either the HAC load case Nos. 5 and 6 HAC fire are 652 and 840 °F, respectively.

Because the Carboline® heat-resistant coating has a continuous rating of 750 °F and a non-continuous rating of 1000 °F and because the temperature of some portions of the OCV and ICV is predicted to exceed 1000 °F during portions of each HAC fire event, it is possible that the coating may fail in these areas. The exact nature of any coating failure that may occur is uncertain since those portions of the ICV and OCV that exceed the non-continuous temperature limit for the coating do so for less than 30 minutes (except for HAC load cases 3 and 4 in which the heat source modules are aligned on the ICV sidewall) and the peak temperature seen will be less than 1250 °F. It is possible that, given the brief period involved and the limited temperature excursion above the non-continuous temperature limit, the coating would remain essentially intact. Assuming a complete loss of the coating, however, the surface emittance would revert to that of the underlying stainless steel. Based on the near-white surface blast preparation used for the application of the heat resistant coating, the appropriate surface emittance is set at 0.54.

A review of the results for the six HAC load cases showed that each case resulted in temperatures at the OCV and ICV dish heads that exceed 1000 °F. With the exception of HAC load cases 3 and 4, all other ICV and OCV surfaces that are treated with the Carboline coating remain below 1000 °F. With HAC load cases 3 and 4, the ICV sidewall at thermal model segment 'A' reaches temperatures of 1200 °F during the HAC event and steady-state temperatures of 950 + °F after the fire. The OCV sidewall temperatures at the same location run about 100 °F cooler.

These elevated temperatures occur because these load cases assume that the re-configured heat source modules end up axially aligned on the ICV sidewall. The ICV and OCV sidewall temperatures at locations a short distance from the heat source modules do not exceed the 1000 °F non-continuous temperature limit of the coating and are well below the coating's 750 °F continuous temperature limit by the time the package reaches steady-state after the HAC fire.

The potential effect on the thermal response of the package due to the loss of the Carboline® coating was investigated using HAC load case 5. The load case was selected for this analysis because it had resulted in the highest ICV/OCV seal temperatures. The re-analysis of HAC load case 5 was conducted under the assumption that the heat-resistant coating fails for any surface that exceed 1000 °F during the fire. Based on the temperatures seen under the original analysis, only the heads of the ICV and OCV are expected to experience a loss of coating due to excessive temperature. The re-analysis shows that the peak temperature at the OCV head would increase by less than 26 °F, while the peak ICV head temperature would be reduced by approximately 80 °F. This occurs because of the reduction in radiative heat transfer between the ICV and OCV heads during the HAC fire event. The coating failure did not increase the peak ICV seal temperatures, but is predicted to increase the steady-state ICV seal temperature following the HAC fire event by 5 °F. No change to the OCV seal temperature is noted.

The loss of coating on both the ICV and OCV domes simultaneously with the loss of coating below the heat source modules (i.e., HAC load cases 3 and 4) was considered but not specifically analyzed. Instead, the results for this scenario would be encompassed by those for HAC load case 5 because both would experience similar temperature variations at the domes, because HAC load cases 3 and 4 yield lower seal temperatures, and because the extent of the loss of coating on the ICV sidewall would be linked to the immediate vicinity of the heat sources. The general effect of a

loss of coating below the heat source module will be to increase the heat source temperature, causing an increased heat transfer to the rest of the ICV cavity and a slight decrease in the temperature of the ICV wall directly below the heat sources. Metal temperatures would still remain within their allowables, with little to no change in the predicted differential expansion.

3.5.4 Maximum Internal Pressures

Table 3.5.4-1 presents the maximum gas temperatures and pressures within the ICV and OCV for the HAC fire. The gas pressures are estimated using the ideal gas law and the computed temperatures of the various ICV/OCV thermal model nodes. The pressure calculation does not include the contribution to pressure rise from material outgassing. Outgassing was neglected for these calculations because the timing of material outgassing is difficult to determine and because the effect of the outgas constituents on the thermal conductivity of the blanket gas will be negligible. The sources of and contribution to pressure rise by material outgassing within the ICV/OCV are addressed in Section 2.7.3.1.2.

The base pressures and temperatures used in the calculations are set by the steady-state condition for NCT load case No. 7 (see Table 3.4-1). The analysis assumes the worst case initial pressure at the time of RTG loading into the packaging (i.e., 18 psia base pressure + 1 psi tolerance = 20 psia). Estimates of the maximum ICV/OCV internal pressure are provided for the six HAC fire load cases. See Table 3.5.2-1 for a definition of each load case.

TABLE 3.5.4-1. Maximum ICV/OCV Gas Pressures and Temperatures For HAC.

Load case/condition	ICV pressure	ICV gas temp. (°F)	OCV pressure	OCV gas temp. (°F)
Case 1	38.9 psia	836	46.2 psia	849
Case 2	37.2 psia	779	44.3 psia	786
Case 3	38.2 psia	747	46.2 psia	851
Case 4	34.3 psia	684	44.4 psia	798
Case 5	39.0 psia	840	46.3 psia	852
Case 6	37.3 psia	782	44.4 psia	789

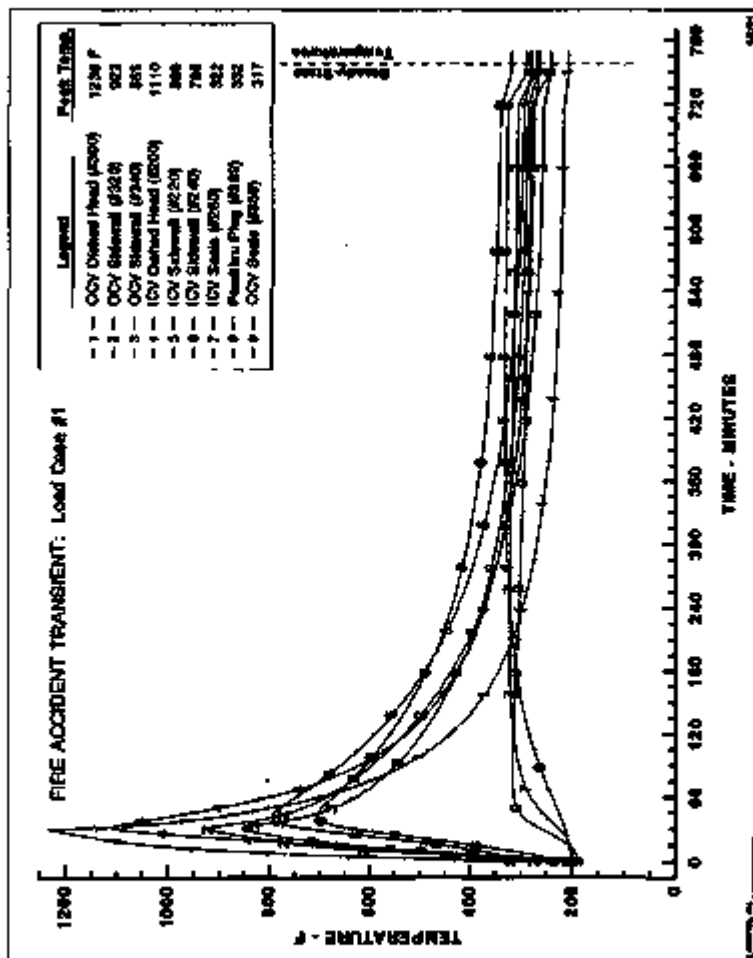


FIGURE 3.5.3-1. HAC Fire Transient For Load Case No. 1.

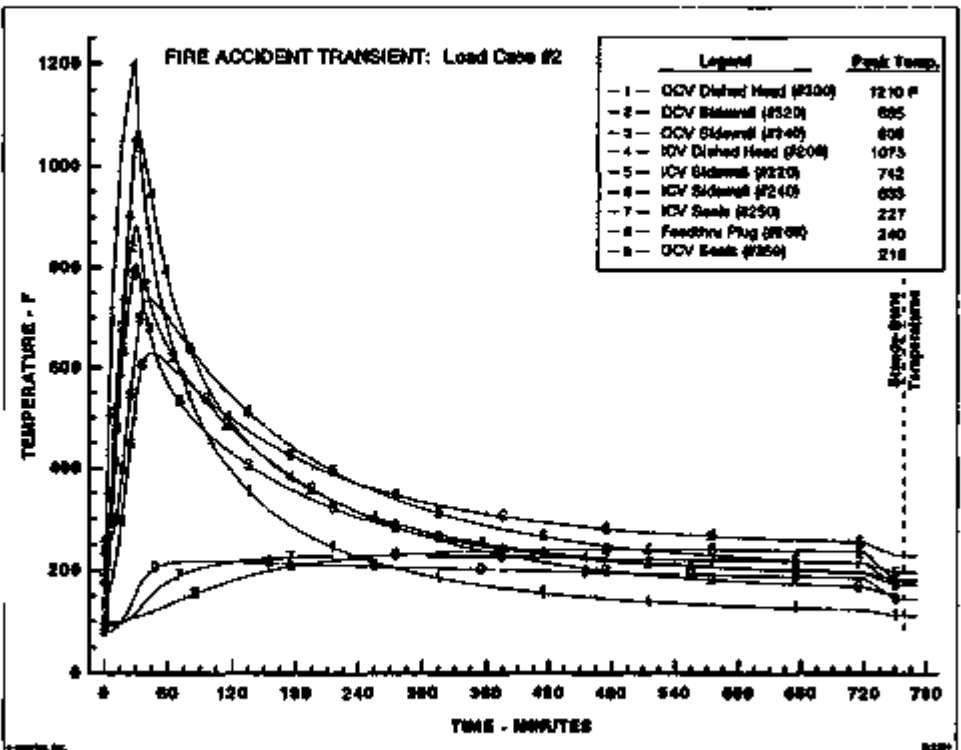


FIGURE 3.5.3-2. HAC Fire Transient For Load Case No. 2.

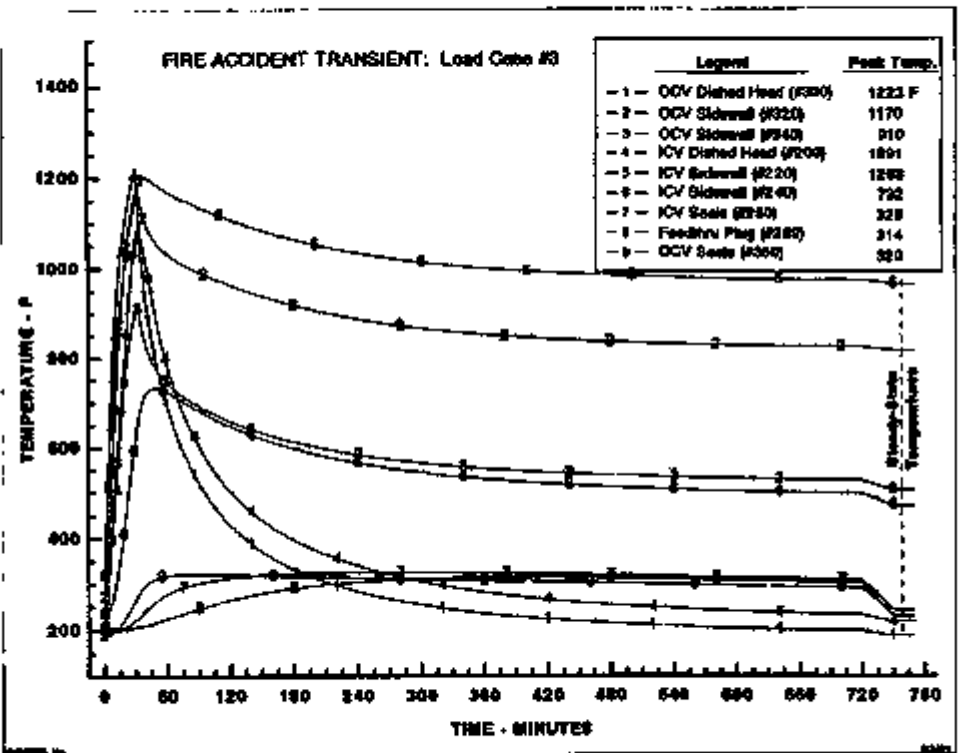


FIGURE 3.5.3.3. HAC Fire Transient For Load Case No. 3.

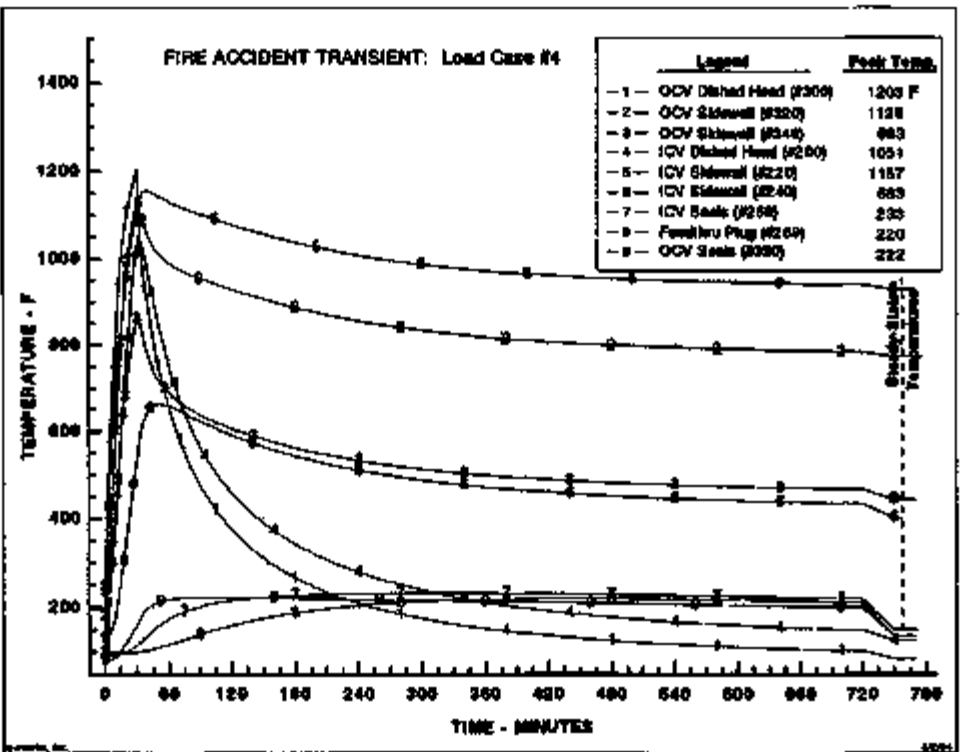


FIGURE 3 5 3-4 HAC Fire Transient For Load Case No. 4

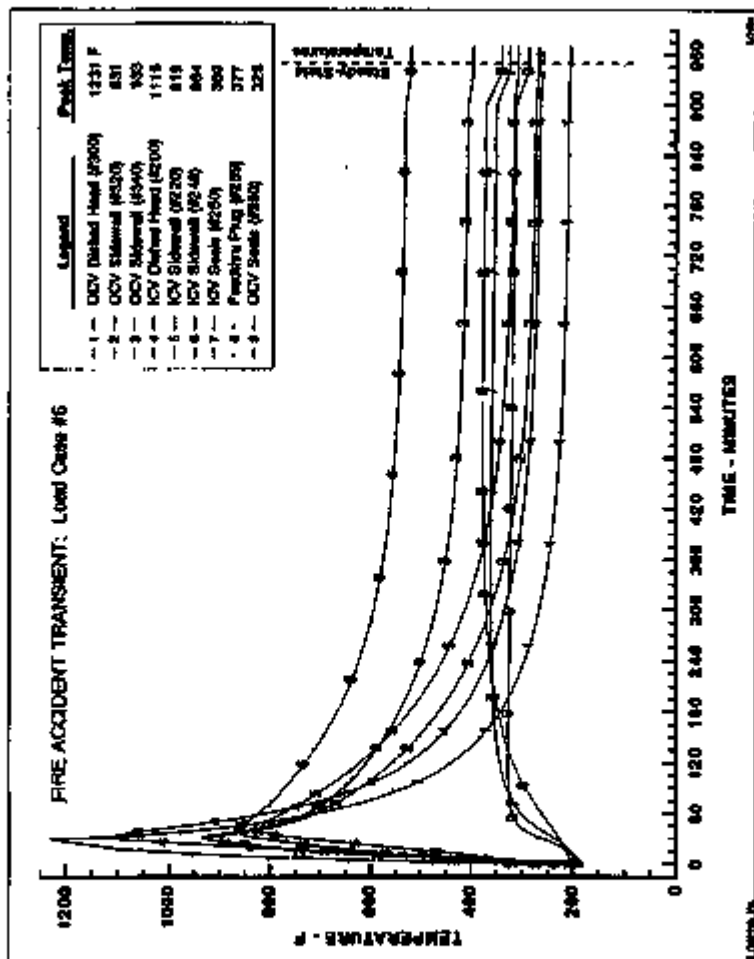


FIGURE 3.5.3-5. HAC Fire Transient For Load Case No. 5.

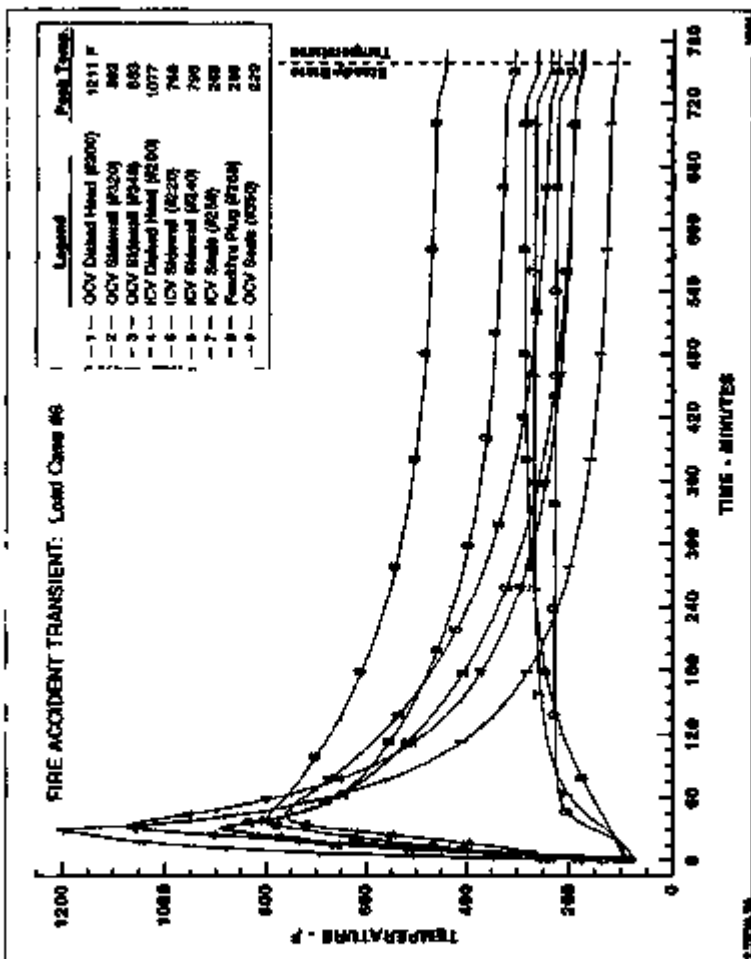


FIGURE 3.5.3-6. HAC Fire Transient For Load Case No. 6

3.6.6 Maximum Thermal Stresses

The results from finite element analyses of the ICV and DCV are presented in Section 2.7.3.3. The analysis shows that all margins of safety are positive and that the design criteria of Regulatory Guide 7.6 are satisfied.

3.6.6 Evaluation of Package Performance for the Thermal Hypothetical Accident Conditions

Analysis is used to evaluate the thermal performance of the RTG Transportation System Package for the HAC fire event. The analysis is backed up by test data, which validates the basic heat transfer modeling of the package, and conservative assumptions that suppose the worst case combination of parameters. Results of the analysis shows that the package design meets the requirements of 10 CFR 71 regulatory conditions for transport.

The peak containment seal temperatures seen for all six HAC load cases are below the time versus temperature operating curve for the Butyl elastomer O-ring seal material. In fact, the 350 °F steady-state temperature limit for Butyl is exceeded in only one of the six HAC load cases evaluated. The peak seal temperature of 360 °F seen for HAC load case No. 5 is 40 °F below the maximum temperature rating for Butyl, while the transient temperature response is well within the time versus temperature limits of the Butyl.

The electrical feed-through connector remains 100 °F or more below its 475 °F temperature rating for all six HAC load cases. Although the analysis assumes large portions of the impact limiter foam are lost because of outgassing/ablation during the HAC fire, the impact limiter is expected to survive the HAC fire essentially intact.

All other package materials remain within their respective temperature limits.

3.6 APPENDIX

The following is a list of appendices contained within this section:

- 3.6.1 References
- 3.6.2 Thermal Modeling Details
- 3.6.3 Performance of Rigid Polyurethane Foam Under Fire Accident Conditions
- 3.6.4 SINDA Output for Normal Conditions of Transport
- 3.6.5 SINDA Output for Hypothetical Accident Conditions
- 3.6.6 Miscellaneous Calculations
- 3.6.7 Listing of 2-D Computer Model

3.6.1 References

1. 10 CFR 71, 1983, "Packaging and Transportation of Radioactive Material," *Code of Federal Regulations*, Washington, D.C.
2. *Handbook of Heat Transfer Fundamentals*, 2nd Edition, Rohsenow, Hartnett, & Ganic, McGraw-Hill Publishers.
3. Kreith, F., *Principles of Heat Transfer*, 3rd Edition, Frank Kreith, Harper & Row Publishers.
4. *Metallic Materials and Elements for Aerospace Vehicle Structures*, 1986, Military Handbook, Vol. 1, MIL-HDBK-5E.
5. *Specific Heat-Metallic Elements and Alloys*, TPRC Data Series, Vol. 3, Purdue University.
6. *Thermal Conductivity-Metallic Elements and Alloys*, TPRC Data Series, Vol. 1, Purdue University.
7. *Specific Heat-Nonmetallic Liquids and Gases*, TPRC Data Series, Vol. 6, Purdue University.
8. *Thermal Conductivity-Nonmetallic Liquids and Gases*, TPRC Data Series, Vol. 3, Purdue University.
9. *Viscosity*, TPRC Data Series, Vol. 11, Purdue University.
10. *LAST-A-FOAM FR-3700 for Crash & Fire Protection of Nuclear Material Shipping Containers*, General Plastics Manufacturing Company, P.O. Box 8097, Tacoma, Washington.
11. Khan, J. and Kumar, R., 1989, *Natural Convection in Vertical Annuli: A Numerical Study For Constant Heat Flux On The Inner Wall*, ASME'S Journal of Heat Transfer, pp. 909-915, Washington, D.C.
12. *RTG/DIPS/LWRHU Package Transportation System Thermal Design Development Test*, 1992, Rev. 0; prepared for Westinghouse Hanford Company by Packaging Technology, Inc.
13. *Thermal Qualification Test Plan*, 1992, Rev. 2, Packaging Technology, Inc., Document ED-92-005, Tacoma, Washington.
14. *Thermal Qualification Test Report*, 1984, Rev. 1, Packaging Technology, Inc., Document ED-84-008, Tacoma, Washington.
15. *General Electric Heat Transfer Data Book*, 1961, Section 516.5, Properties of Solids: Emissivity, pp. 515.5-8; Eased solar absorptivity values for white paint varies from 0.12 to 0.26; emissivity at 750 °F varies from 0.53 to 0.84; emissivity values at 125 °F varies from 0.90 to 0.95.
16. *Engineering and Operating Guide For DOWFROST Heat Transfer Fluids*, The Dow Chemical Company, Midland, Michigan.
17. SARP, 1987, *Safety Analysis Report for Packaging*, Vol. 1, TES-32130-056, Teledyne Energy Systems, pp. 3-4.
18. *General Electric Heat Transfer Data Book—Section 515.5, Properties of Solids: Emissivity*, 1961.

19. Guyer, E. C., 1989, *Handbook of Applied Thermal Design*, McGraw-Hill Publishers.
20. *Materials Engineering*, Penton Publishing, Inc. Cleveland, Ohio.
21. *GPMS RTG Thermal Model*, 1982, Rev. 2, Packaging Technology, Inc., Document ED-91-001, Bellevue, Washington.
22. *Carbofine 4674 Product Structure*, The Carbolins Company, St. Louis, Missouri.
23. Siegel, R., and Howell, J., 1982, *Thermal Radiation Heat Transfer*, Hemisphere Publishing Co., Washington, D.C.
24. *Thermal Radiative Properties—Metallic Elements and Alloys*, TPRC Data Series, Vol. 7, Purdue University.
25. Song, S., Yovanovich, M., and Nho, K., 1992, *Thermal Gap Conductance: Effects of Gas Pressure and Mechanical Load*, *AIAA's Journal of Thermophysics and Heat Transfer*, January-March pp. 62-68, New York, New York.
26. *Kaowool Blanket Product Literature*, Morgan Thermal Ceramics Company.
27. Brandes, E. A., 1983, *Smithells Metals Reference Book*, 6th Edition, Butterworths Publishing Co., London.
28. *Thermal and Water Vapor Transmission Data*, 1993, Table 13, Chapter 22, American "Handbook of Fundamentals," Society of Heating, Refrigerating and Air-Conditioning Engineers, Inc.
29. *Fiberglass Insulation Blanket Product Literature*, McMaster-Carr Company.
30. SINDA '85/FLUENT, 1987, *Systems Improved Numerical Differencing Analyzer and Fluid Integrator*, Version 2.1, Prepared for NASA, Johnson Spacecraft Center, Contract NAS8-17448. Prepared by Martin Marietta Corporation, Denver Aerospace.
31. Emery, A., 1991, VIEW—A Radiation Viewfactor Calculation Program, 1991, Version 5.6.9, NASA Grant NAG-1-41, University of Washington, Seattle, Washington.
32. WNC, 1994, *Radioisotope Thermoelectric Generator Transportation System—Carbofine 4674-C900 Point Emissivity Test Report*, WNC-SD-RTG-TRP-006, Westinghouse Hanford Company, Richland, Washington.
33. Lage, J., Lim, J., and Bejan, A., 1992, *Natural Convection With Radiation in a Cavity With Open Top End*, in "ASME's Journal of Heat Transfer," Vol. 114, pp. 479-486, Washington, D.C.
34. Coordination Sheet R. C. Frank and W. L. Pagenmann to S. Goetsch, *Emissivity Testing of Metal Specimens*, testing accomplished by Boeing Analytical Engineering for Nuclear Packaging, Inc.
35. Gubareff, G. G., Jensen, J. E., and Torborg, R. H., 1980, *Thermal Radiation Properties Survey*, Honeywell Research Center, Minneapolis, Minnesota.

3.6.2 Thermal Modeling Details

3.6.2.1 Undamaged Package Thermal Model With Operating Chillers. The undamaged RTG Transportation System Package is modeled using a 2-D, axisymmetric thermal model. The model uses 124 nodes along 15 axial stations to represent components or portions of components for the package. The thermal properties (i.e., specific heat, thermal conductivity, and convective and radiative heat transfer coefficients) are computed as a function of the associated temperatures whenever the variation with temperature is significant.

The thermal capacitance, conductance, and radiation values associated with each node in the package model are presented in Tables 3.6.2.1-1, 3.6.2.1-2, and 3.6.2.1-3, respectively. Each table was created using Microsoft's EXCEL® spreadsheet program. As such, the value under the heading Specific Heat Multiplier was automatically calculated based on the data presented in the preceding columns. Where appropriate, these table columns describe the element shape, material, material property, and the pertinent dimensional data used to determine the thermal model values at each node in the thermal model. The terms and equations used in each table are defined in the Nomenclature list in Section 3.6.2.5. Tables 3.6.2.1-4 and 3.6.2.1-5 present the thermal capacitance and conductance calculations for the RTG shipping rack assembly.

The thermal capacitance for each node in the GPHS RTG thermal model is presented in Table 3.6.2.1-8. The location of the nodes is shown in Figure 3.4.1-1. See Reference 21 for a full description of the model.

Because the SINDA thermal analyzer program is a finite-differencing program, the calculated temperatures for each model node actually represents the volumetric mean temperature of the particular component (or portion thereof) that the node represents. The reader is advised to study model node layout in Figure 3.4.1-2 and the dimensional data in Table 3.6.2.1-1 to determine the physical location of each node in the model and what portion of the package that it represents.

The following paragraphs describe the assumed heat transfer modes across each boundary of the package. The description is ordered from the outside environment inward.

Heat transfer between the exterior environment and the package outer surface is assumed to occur via convection and radiation. Natural or "free" convection heat transfer coefficients for the vertical surfaces are calculated as a function of Rayleigh number using the flat plate correlations given in equations 39 to 42 from Chapter 6 of Reference 2. Natural convection correlations for horizontal surfaces are obtained from equations 21, 22, and 23 from Chapter 7 of Reference 3. The calculated free convection coefficient for the OCV bolt tubes and the bolt heads contained within were reduced to account for the fact that the recessed nature of these surfaces and the narrow width of the tubes will restrict the convective heat transfer coefficient below that obtained for a "free" surface. As such, the computed "free" convection coefficient for node 349 was reduced by 50%, while those for nodes 361 and 371 were reduced to 25% of the values computed for a "free" surface.

These correction factors were selected to provide a conservative estimate of the peak closure bolt and access tube temperatures. The actual reduction factors will vary from about 20% when the ambient air temperature is below that of the closure bolts or access tubes (i.e., NCT or following the HAC fire event) to almost 100% when the ambient temperature is above that of the bolts or access tubes (i.e., during the HAC fire event). The 20% reduction factor is based on the work presented in Reference 33 for natural convection in a cavity with an open top end as

*Excel is a registered trademark of the Microsoft Corporation.

The 100% reduction factor is based on the fact that with "still" air, as specified by 10 CFR 71, there will be no driving force to transport the warm air above the tubes down and into the relatively cold access tube cavities.

Forced convection coefficients for the coolant flow within the OCV coolant jacket are computed using a combination of correlations taken from Table 4.7 of Reference 19 and equations 7, 43 to 44, and 57 from Chapter 7 of Reference 2. The actual equation used depends on the computed Reynold's number for the flow. The hydraulic diameter of the coolant passages is 1.33 in. Coolant flow within each coolant loop is assumed to be 4.5 g/min. Although the chiller system could provide lower coolant temperatures, a 40 °F coolant inlet temperature is used as the lowest available temperature for design purposes because it provides adequate temperature margin for the GPHS RTG, and it will avoid potential problems with frost buildup on the coolant jacket. Condensate, should it form, is collected, drained away, and retained in a storage tank in the transportation trailer. Although condensation will increase the load on the chiller, it will have a negligible effect on package temperatures assuming the chiller is sufficiently sized to handle the added load that condensation will place on it.

TABLE 3.4.2.1-1 THERMAL CAPACITANCE VALUES FOR RTG TRANSPORT THERMAL MODEL

NODE	ELEMENT	MATERIAL	DENSITY	GEOMETRIC DATA			SPEC HEAT HEAT CAPACITY	REMARKS
				X1	X2	X3		
200	CYLINDER	8 IN 304L	0.29	0	18	0.292	71.66266	RTG Transportation Head - 12.242 Per Flug
201	CYLINDER	8 IN 304L	0.29	18	17.8426	0.292	47.44661	RTG Transportation Head Outer Portion
202	CYLINDER	8 IN 304L	0.29	17.8426	17.6426	1.649	30.42664	RTG Transportation Head, Outer Portion
203	CYLINDER	8 IN 304L	0.29	17	17.74	17.72	226.7762	RTG Head
204	SPECIAL	8	0	0	0	0	0.00000	Arithmetic Node @ 75 Between Above Subtle Item
210	CYLINDER	8 IN 304L	0.29	17	17.74	0	128.72276	RTG Head
212	CYLINDER	8 IN 304L	0.29	17	17.74	0.29	124.64666	RTG Head & Portion of Range Above Base Plate
213	CYLINDER	8 IN 304L	0.29	17	19.078	1.0292	143.97666	RTG Flange, Equivalent Thickness Head
221	CYLINDER	8 IN 304L	0.29	0	10	1.23	164.70266	RTG Base Plate, Inner Portion
222	CYLINDER	8 IN 304L	0.29	10	10	1.23	168.07666	RTG Base Plate
223	CYLINDER	8 IN 304L	0.29	10	10.94	0.72	39.80172	RTG Base Plate @ Edge
224	CYLINDER	8 IN 304L	0.29	0	10	1.70	163.48266	RTG Base Plate, Outer Portion
225	CYLINDER	8 IN 304L	0.29	10	10	1.70	168.26672	RTG Base Plate
226	CYLINDER	8 IN 304L	0.29	10	18.87	1.70	180.41812	RTG Base Plate @ Base
227	CYLINDER	8 IN 304L	0.29	18.87	18.44	1.67	123.02666	RTG Base Plate @ End Flange
228	CYLINDER	8 IN 304L	0.29	1.278	1.892	0.13	3.27226	Head Thin Flange
229	CYLINDER	8 IN 304L	0.29	1.023	1.43	0.44	1.47266	Head Thin Flange
230	SPECIAL	0.00000	0.0	1	1	0	0.00000	Head Thin Flange
1256	SPECIAL	1.25	0	1.25	1.25	0.1	0.00000	Arithmetic Node At Center of Reaction Coordinate
1257	SPECIAL	1.25	0	1.25	1.25	0.1	0.00000	Arithmetic Node At Center of Reaction Coordinate
1258	SPECIAL	1.25	0	0	1.25	0	0.00000	Arithmetic Node At Center of Reaction Coordinate
1199	SPECIAL	1.00	0	1.00	1.00	0.1	0.00000	Arithmetic Node Head Middle Reaction Coordinate
230	CYLINDER	8 IN 304L	0.29	0	18	0.1	58.26672	RTG Transportation Head - 25.824 Per Reaction
231	SPECIAL	8 IN 304L	0.29	0	0	0	18.00000	RTG Head Per Reaction Coordinate Value
204a	CYLINDER	8 IN 304L	0.29	18	17.74	0.1	69.04400	RTG Transportation Head - 19.524 Per Reaction
204b	CYLINDER	8 IN 304L	0.29	17.84	19.44	0.44	40.48266	RTG Transportation Head, Vertical Portion
205	PARALLEL	8 IN 304L	0.29	0.225	0.225	0	118.12618	RTG Head Reaction Coordinate & Transport Level
210a	CYLINDER	8 IN 304L	0.29	17.94	18.44	12.72	227.87666	RTG Head
240	CYLINDER	8 IN 304L	0.29	12.74	18.44	0	89.07666	RTG Head
241	SPECIAL	0	0	0	0	0	0.00000	Arithmetic Node At Join of Thermal Model
242	CYLINDER	8 IN 304L	0.29	12.44	18.44	0.1	70.48192	RTG Head
243	CYLINDER	Reaction Head	0.00125	10	20.25	0.5	1.01672	RTG Head @ RTG For Both Access Tube Connect
244	PARALLEL	8 IN 304L	0.29	1.7	1.3	1.18	70.03261	RTG Range Access Reaction
245	CYLINDER	8 IN 304L	0.29	20.25	20.425	1.425	47.41876	RTG Head Thermal Model

See Nomenclature List For Definition Of Terms & Symbols Used In This Table

Revised: 11/1/94

3080 000076

FILE: RTGTRM01.DT, 01/1

04/20/95

Page 3 of 27

TABLE 3 B 2-1-1 THERMAL CAPACITANCE VALUES FOR RTG TRANSPORT THERMAL MODEL (Continued)

MODE	ELEMENT	MATERIAL	DENSITY	GEOMETRIC DATA			SPEC HEAT	REMARKS
				X1	X2	X3		
345	CYLINDER	3 20 304L	0.29	19.94	20.528	0.978	120.0426	OCV End Thermal Shield
347	CYLINDER	3 20 304L	0.29	19.75	20.59	0.95	121.4708	OCV End Thermal Shield
346a	CYLINDER	3 20 304L	0.29	7.18	1.88	78	20.1204	34 Ammonia Tubes, Super Insulation, Super Insulation
346b	CYLINDER	3 20 304L	0.29	0.78	0.88	35	4.8473	34 Ammonia Tubes, Super Insulation, Super Insulation
350	CYLINDER	3 20 304L	0.29	19.84	22.125	1.13	110.8922	OCV Super Insulation
352	CYLINDER	3 20 304L	0.29	21.125	23.125	1.18	95.2324	OCV Super Insulation
354	CYLINDER	3 20 304L	0.29	19.89	22.125	1.08	104.6279	OCV Super Insulation
348	CYLINDER	3 20 304L	0.29	22.125	24.125	1.08	141.42178	OCV Super Insulation
357	SPECIAL	AL7054 A300	0.28	0	0	0	30.8860	OCV Cap Head Structure @ Top Left, Head Position
359	CYLINDER	AL7054 A300	0.28	0	0.228	2.48	2.2.6764	OCV Cap Head Structure @ Top Left
360	CYLINDER	AL7054 A300	0.28	0	0.426	2.21	23.27184	OCV Cap Head Structure @ Top Left, Thermal Shield
357	SPECIAL	0	0	0	0	0.00000	Asbestos Made Between Nodes 358 & 359	
358	SPECIAL	0	0	0	0	0.00000	Asbestos Made At Base Of OCV End Shield	
358	SPECIAL	0	0	0	0	0.00000	Asbestos Made Between Nodes 358 & 359	
360	CYLINDER	3 20 304L	0.29	0	19	7.8	136.46208	OCV Super Insulation, Super Insulation
362	CYLINDER	3 20 304L	0.29	0	18	1.8	139.62640	OCV Super Insulation
363	CYLINDER	3 20 304L	0.29	15	29.045	1.9	234.62607	OCV Super Insulation, Super Insulation
364	CYLINDER	3 20 304L	0.29	18.545	22.125	2.5	242.81448	OCV Super Insulation, Super Insulation
367	CYLINDER	3 20 304L	0.29	22.125	24.125	2.5	269.40438	OCV Super Insulation, Super Insulation
369	CYLINDER	3 20 304L	0.29	24.125	26.025	2.5	459.22652	OCV Super Insulation, Super Insulation
369	CYLINDER	3 20 304L	0.29	24.125	26.025	2.5	279.21419	OCV Super Insulation, Super Insulation
371	SPECIAL	AL7054 A300	0.28	0.75	0	0	1.7808	OCV Cap Head Structure @ Top Left, Head Position
373	CYLINDER	AL7054 A300	0.28	0	0.20	2.22	1.31145	OCV Cap Head Structure @ Top Left, Head Position
373	CYLINDER	AL7054 A300	0.28	0	0.20	2.5	1.89948	OCV Cap Head Structure @ Top Left, Head Position
377	CYLINDER	AL7054 A300	0.28	0	0.20	1.97	1.23118	OCV Cap Head Structure @ Top Left, Head Position
378	SPECIAL	0	0	0	0	0.00000	Asbestos Made Between Nodes 379 & 380	
311A21	CYLINDER	WATER/ICE	0.92411	19.84	19.84	0.1	26.2190	Overhead Tank to Tank @ Super Insulation Structure
311A22	CYLINDER	WATER/ICE	0.92411	19.84	19.84	0.1	26.2190	Overhead Tank to Tank @ Super Insulation Structure
311A23	CYLINDER	3 20 304L	0.29	18.44	19.7	1.52	94.28459	Overhead Tank to Tank @ Super Insulation Structure
311A24	CYLINDER	3 20 304L	0.29	19.44	19.875	0.3	22.27137	Overhead Tank to Tank @ Super Insulation Structure
311A25	CYLINDER	3 20 304L	0.29	18.44	19.875	0.3	22.27137	Overhead Tank to Tank @ Super Insulation Structure

See Nomenclature List for Definition of Terms & Symbols Used in This Table

Revised 04, 0

WMC 000048

FILE PROPLM 007

112

042284

Page 1 of 23

TABLE 3.6.2.1-1 THERMAL CAPACITANCE VALUES FOR RTG TRANSPORT THERMAL MODEL (Continued)

NODE	ELEMENT	MEDIUM	DENSITY	GEOMETRIC DATA			SPEC HEAT	REMARKS
				X1	X2	X3		
621/601	CYLINDER	Water/Water	0.00411	14.44	19.44	0.74	27.73017	Coolant Flow In Hot Shield Wound Channel
229	CYLINDER	S IN SOL	0.28	14.44	19.7	1.1	26.32119	See 207 14"X11.50"
230/230	CYLINDER	S IN SOL	0.28	15.64	19.976	0.76	41.13158	Cover Shell Over Primary & Secondary Channel
227	SPECIAL	0	0	0	0	0	0.0000	Arbitrarily Made At End Of Node 241 & 242
1013/023	SPECIAL	0	0	0	0	0	0.0000	Arbitrarily Made At End Of Node 213 & 215
1018	SPECIAL	0	0	0	0	0	0.0000	Arbitrarily Made At End Of Node 218
1071/1072	SPECIAL	0	0	0	0	0	0.0000	Arbitrarily Made At End Of Node 219
1081/1082	SPECIAL	0	0	0	0	0	0.0000	Arbitrarily Made At End Of Node 220
1091/1092	SPECIAL	0	0	0	0	0	0.0000	Arbitrarily Made At End Of Node 221
1043/044	SPECIAL	0	0	0	0	0	0.0000	Arbitrarily Made At End Of Node 243
1047/044	SPECIAL	0	0	0	0	0	0.0000	Arbitrarily Made At End Of Node 244
440	CYLINDER	S IN SOL	0.28	0	20.8	0.578	143.87798	Support Shield Base Plate
447	CYLINDER	S IN SOL	0.28	0	20.8	0.0866	21.26248	Support Thermal Shield Support Upriser
452	CYLINDER	S IN SOL	0.28	20.8	23.475	0.379	228.60200	Down Pipe - 121.42 lbs Per Section One
457	SPECIAL	0	0	0	0	0	0.0000	Arbitrarily Made At Support Upriser With Pipe
454	CYLINDER	S IN SOL	0.28	20.876	27.128	0.68	143.92615	Support Upriser Shell - 24.50 lbs Per Single Pipe
456	CYLINDER	S IN SOL	0.28	27.128	24.76	0.25	147.00068	Support Upriser Shell - 24.50 lbs Per Single Pipe
458	CYLINDER	S IN SOL	0.28	24.76	0	17.8	202.09423	Support Upriser Shell - 22.24 lbs Per Single Pipe
419	CYLINDER	S IN SOL	0.28	20.876	24.76	0.2128	128.18724	Support Upriser Shell
412	CYLINDER	S IN SOL	0.28	0	20.876	0.2128	85.86911	Support Upriser Shell
414	CYLINDER	S IN SOL	0.28	0	24.76	0.2128	118.94028	Support Upriser Shell
421/422/423	CYLINDER	BF Foam	0.00478817	0	20.8	2.27	8.24614	BF Support Upriser Base Water Shield
424/425/426	CYLINDER	120 Foam	0.00294444	20.8	27.128	2.27	18.84719	120 Support Upriser Foam
427 to 432	CYLINDER	120 Foam	0.00294444	27.128	24.76	2.04	8.80174	120 Support Upriser Foam
434 to 439	CYLINDER	120 Foam	0.00294444	27.128	23.76	1.77	8.82321	120 Support Upriser Foam
441 to 443	CYLINDER	120 Foam	0.00294444	29.78	22.36	2.04	10.37288	120 Support Upriser Foam
444 to 446	CYLINDER	120 Foam	0.00294444	29.78	23.25	2.27	8.24628	120 Support Upriser Foam
451 to 453	CYLINDER	120 Foam	0.00294444	24.36	24.76	2.04	11.82841	120 Support Upriser Foam
454 to 456	CYLINDER	120 Foam	0.00294444	24.36	24.76	2.27	15.12228	120 Support Upriser Foam
458	CYLINDER	120 Foam	0.00294444	21.28	24.76	2.27	22.00000	Mean Value Used For Weight Difference Only

Notes: Components Not Specifically Identified
See Nomenclature List For Definition Of Terms & Equations Used In This Table

Total Wt. = 6778.881964

FILE: PTPR1,TDI.GDT

DATE:

04/29/98

Page 3 of 24

TABLE 3.3.2.1-2 THERMAL CONDUCTANCE UNITS FOR RTG TRANSPORT SYSTEM MODEL

MODE 1	MODE 2	ELEMENT	GEOMETRIC DATA			CONDUCTOR MULTIPLIER	REMARKS
			MEDIUM	X1	X2		
200	204	CYLINDER	S. 00 204L	5.2	18.1	0.205	0.000000
204	PT. 8	CYLINDER	S. 00 204L	10.1	12.776	0.205	0.260879
PL. 8	PL. 8	CIRCLE	S. 00 204L	17.9478	17.9478	0.205	0.146826
PL. 8	PL. 8	CIRCLE	S. 00 204L	17	17.76	0.205	0.042848
210	206	CIRCLE	S. 00 206L	17	17.76	12.72	0.044463
207	206	CIRCLE	S. 00 206L	17	17.76	12.72	0.044463
208	206	CIRCLE	S. 00 206L	17	17.76	5.11	0.180244
226	210	CIRCLE	S. 00 210L	17	17.76	5.23	0.150266
240	242	CIRCLE	S. 00 240L	17	17.76	5.23	0.150266
241	PL. 0	CIRCLE	S. 00 240L	17	17.76	2.828	0.210006
PL. C	250	CIRCLE	S. 00 240L	17	17.7626	0.810	0.874417
281	243	CYLINDER	S. 00 240L	7	12.76	1.20	0.126997
282	246	CYLINDER	S. 00 240L	16.70	16	1.20	0.290213
280	242	CYLINDER	S. 00 240L	7	12.76	0.76	0.127264
283	244	CYLINDER	S. 00 240L	12.76	16	1.20	0.238286
284	248	CYLINDER	S. 00 240L	16	12.76	1.67	0.407469
281	250	CIRCLE	S. 00 240L	0	70	1.68	1.207442
282	252	CIRCLE	S. 00 240L	10	70	1.70	1.074682
286	254	CIRCLE	S. 00 240L	10	10.67	1.20	0.700000
287	253	CIRCLE	S. 00 240L	1.20	1.20	1.20	0.000220
287	*	CIRCLE	S. 00 240L	1.20	1.20	1.21	0.000000
*	*	CYLINDER	S. 00 240L	1.20	1.275	0.1070	0.000000
*	288	CIRCLE	S. 00 240L	1.070	1.20	1.06	0.007117
287	288	CYLINDER	Medium	1.00	1.270	1.00	0.010000
288	*	CIRCLE	S. 00 240L	1.070	1.20	1.06	0.007117
*	289	CYLINDER	S. 00 240L	0.75	1.070	0.75	0.000000
289	289	CYLINDER	Medium	0.8	1.01	0.99	0.100000
289	289	CYLINDER	200 240L	10	10.00	1.70	0.070000
290	289	CYLINDER	Medium 200	16.07	17	1.70	0.000000
284	289	CYLINDER	200 240L	10	10.00	0.60	0.000000
284	289	CYLINDER	Medium 200	16.07	17	0.60	0.017000
284	289	CIRCLE	S. 00 240L	17	10.070	1.00	1.150777
289	289	SPHERICAL	Center	0.1			0.000000
289	289	CIRCLE	Medium 200	10.00	10.00	0.60	17.000000

001 Homogeneity Unit Per Division Of The Three 6 Elements Used In Three Orientations

FILE: T700A.PC:0001

PAGE

002264

Page 3.3.2-6

TABLE 3.5.2.1-2 THERMAL CONDUCTANCE VALUES FOR RTG TRANSPORT THERMAL MODEL (Continued)

NODE 1	NODE 2	ELEMENT	GEOMETRIC DATA			CONDUCTOR MATERIAL	REMARKS
			INTERNAL	X1	X2		
303	304	CYLINDER	0.00 304	0.7	10.0	0.0	0.00000
304	*	CYLINDER	0.00 304	18.0	10.15	0.0	0.00010
*	310	CIRCLE	0.00 304	17.04	10.44	0.001	0.00000
304	*	RECTANGLE	0.00 304	0.3	0.44	1	0.00000
*	308	RECTANGLE	0.00 304	0	0	3	0.12000
310	310	CIRCLE	0.00 304	17.04	10.44	10.72	0.00000
310	310	CIRCLE	0.00 304	17.04	10.44	10.72	0.00000
310	310	CIRCLE	0.00 304	17.04	10.44	10.72	0.00000
310	310	CIRCLE	0.00 304	17.04	10.44	10.72	0.00000
311	317	CYLINDER	0.00 304	10.10	10.00	0.000	0.00000
317	346	CYLINDER	0.00 304	10.00	10.0	0.000	0.00000
341	342	CIRCLE	0.00 304	17.04	10.44	0.000	0.00000
300	*	CIRCLE	0.00 304	10.00	10.00	1.0	0.00000
*	004	CYLINDER	0.00 304	10.10	10.00	1.0	0.00000
004	004	CYLINDER	0.00 304	10.00	10.00	1.00	0.70000
304	304	CYLINDER	0.00 304	10.00	10.10	1.00	0.00000
300	300	CYLINDER	0.00 304	10.00	10.10	1.10	0.00000
304	304	CIRCLE	0.00 304	10.00	10.10	1.01	0.00000
300	300	CIRCLE	0.00 304	10.10	10.10	1.01	0.00000
300	300	CYLINDER	0.00 304	10.0	10.000	0.000	0.11000
1000	000	CIRCLE	0.00 304	10.00	10.00	1.0	0.00000
000	*	CIRCLE	0.00 304	10.00	10.00	1.000	0.00000
*	317	CYLINDER	0.00 304	10.00	10.00	0.00	0.10010
000	*	CYLINDER	0.00 304	10.00	10.00	0.00	0.00100
*	308	CIRCLE	0.00 304	10.00	10.00	0.0	0.70000
300	*	RECTANGLE	0.00 304	0.100	0.200	0.0	0.00000
*	004	CIRCLE	0.00 304	1.100	1.00	1.000	0.00000
300	300	CIRCLE	0.00 304	1.100	1.00	1.000	0.10000
300	300	SPHERICAL	Carbon	0.0	0.0	0.00000	1.00 0.00 x 0.00 0.00 x 0.00 0.00
300	300	CIRCLE	Carbon	0.7076	1.0	0.000	1.00000
301	300	CIRCLE	Carbon Bond	0	0.000	1.00	0.11000
300	300	CIRCLE	Carbon Bond	0	0.0077	2	0.00000

See Specifications for the Definition of the Terms & Equations Used in These Calculations

FILE: P:\RTG\T.C.000; 04/15/98

Page 3.5.2.6

TABLE B 2 1-2 THERMAL CONDUCTANCE VALUES FOR RTG TRANSPORT NEUTRAL MODEL (Continued)

NODE 1	NODE 2	ELEMENT	MEDIUM	GEOMETRIC DATA			CONDUCTANCE MW/TEMPER	REMARKS
				X1	X2	X3		
363	*	CYLINDER	Air	0.000	0.7675	1.48	1.677918	This conductance to be in series w/ next. Both are multiplied by .50 factor for total conductance
*	367	CYLINDER	S 24 SOL	0.44	0.88	1.48	1.338818	are multiplied by .50 factor for total conductance
364	*	CYLINDER	Air	0.638	0.7675	1.12	0.646689	This conductance to be in series w/ next. Both are multiplied by .50 factor for total conductance
*	368	CYLINDER	S 24 SOL	0.44	0.88	1.12	1.746993	are multiplied by .50 factor for total conductance
367	364/368	CYLINDER	S 24 SOL	0.68	1.36	1.58	1.837389	Multiplied by .12 for 24 holes & .50 each way
368	364/367	CYLINDER	S 24 SOL	0.68	1.36	1.12	1.687771	Multiplied by .12 for 24 holes & .50 each way
369	370	SPRING	Common	14.31		1.07	2.28 260798	Multiplied by .50 for 24 holes
369	*	CYLINDER	Air	0.625	0.88	1.07	1.876904	This conductance to be in series w/ next. Both are multiplied by .50 factor for total conductance
*	375	CYLINDER	S 24 SOL	0.46	0.88	1.07	3.010407	are multiplied by .50 factor for total conductance
376	369/375	CYLINDER	S 24 SOL	0.94	1.76	2.1	1.874744	Multiplied by .12 for 24 holes & .50 each way
371	388	SPRING	Common	12.0			1.640080	0.48 Spgs x 3.0 Spgs/F-Block x F-Block
371	372	CIRCLE	Carbon Steel	0	0.125	1.23	0.007974	Multiplied by 0 factor for total
372	375	CIRCLE	Carbon Steel	0	0.125	0.085	0.004988	Multiplied by 0 factor for total
373	377	CIRCLE	Carbon Steel	0	0.125	2.3	0.003788	Multiplied by 0 factor for total
378	*	CYLINDER	Air	0.278	0.406	1.82	1.276897	This conductance to be in series w/ next. Both are multiplied by 0 factor for total conductance
*	387	CYLINDER	S 24 SOL	0.2	0.81	1.82	0.889132	are multiplied by 0 factor for total conductance
379	*	CYLINDER	Air	0.278	0.406	1.24	1.016811	This conductance to be in series w/ next. Both are multiplied by 0 factor for total conductance
*	388	CYLINDER	S 24 SOL	0.2	0.81	1.18	0.888828	are multiplied by 0 factor for total conductance
375	*	CYLINDER	Air	0.278	0.406	2.1	1.039281	This conductance to be in series w/ next. Both are multiplied by 0 factor for total conductance
*	377	CYLINDER	S 24 SOL	0.2	0.81	2.1	0.884808	are multiplied by 0 factor for total conductance
377	384	SPRING	Thermal Invar	8.1		1.6	3.6 808000	Multiplied by 0 factor for total
380	381	CYLINDER	S 24 SOL	7	13.79	1.6	0.148486	
382	384	CYLINDER	S 24 SOL	1.175	17.6	1.6	0.131681	
384	385	CYLINDER	S 24 SOL	17.8	31.2	1.5	0.287188	
385	387	CYLINDER	S 24 SOL	28.2	33.18	0.6	0.008384	Multiplied by .50 for 24 Hole Alignment
387	389	CYLINDER	S 24 SOL	28.18	36.4	2.6	1.994761	
389	388	CIRCLE	S 24 SOL	34.18	38.825	2.86	0.893274	
388	*	CIRCLE	S 24 SOL	18.845	33.125	1.818	1.018164	This Conductance To Be in Series w/ Next
*	389	SPRING	Common	17.0			670.80	0.12 Spgs x 3.75 Spgs/F-Block x F-Block
387	*	CIRCLE	S 24 SOL	33.125	36.12	2.25	0.758889	This Conductance To Be in Series w/ Next
*	384	SPRING	Common	17.0			678.78	0.12 Spgs x 3.0 Spgs/F-Block x F-Block

See Memorandum Unit For Definition Of The Terms & Conditions Used In These Calculations

FILE: PTP/RTG.DAT. JOB

04/28/94

Page 3 of 27

TABLE 3.6.2.1-2 THERMAL CONDUCTANCE VALUES FOR RTG TRANSPORT THERMAL MODEL (Continued)

NODE 1	NODE 2	ELEMENT	MEDIUM	GEOMETRIC DATA			CONDUCTOR RELATIVES	REMARKS
				X1	X2	X3		
247	1347	CIRCLE	0	24.43	28.428	0.25	0.000000	
400	1347	CYLINDER	0	29.8	29.85	0.8	0.000000	
400	401	CYLINDER	0.00004	14.5	24	0.875	0.000000	
400	401	RECTANGLE	0.00004	3	1.8	4.34	0.000000	
400	+	CYLINDER	0.00004	24	21	0.875	0.000000	
+	404	CIRCLE	0.00004	26.80	27.1	4.8075	0.000000	
404	+	CIRCLE	0.00004	26.80	27.1	0.6975	0.000000	
+	409	CYLINDER	0.00004	27	21	0.20	0.000000	
409	+	CYLINDER	0.00004	27	24.875	0.20	0.000000	
+	400	CIRCLE	0.00004	34.70	30	0.875	0.000000	
400	+	CIRCLE	0.00004	34.70	30	0.875	0.000000	
+	410	CYLINDER	0.00004	31	34.875	0.2100	0.000000	
410	410	CYLINDER	0.00004	28	31	0.2100	0.000000	
412	414	CYLINDER	0.00004	14.5	24	0.2100	0.000000	
100	401	CIRCLE	0	0	20.875	0.0000	1.000000	
101	421	CIRCLE	0	0	20.875	1.0000	0.000000	
401/421	421/401	CIRCLE	0	0	20.875	0.27	0.000000	
401	410	CIRCLE	0	0	20.875	1.0000	0.000000	
401	410	CIRCLE	1.20 Feet	00.000	27.1	1.0000	0.000000	
401/410	410/401	CIRCLE	1.20 Feet	20.875	27.1	0.27	0.000000	
401	412	CIRCLE	1.20 Feet	20.875	27.1	1.0000	0.000000	
412/401	401/412	CYLINDER	1.20 Feet	14.5	24	0.27	0.000000	
401	431	CIRCLE	1.20 Feet	27.1	29.70	1.00	0.000000	
431/401	401/431	CIRCLE	1.20 Feet	27.1	29.70	0.04	1.000000	
431	434	CIRCLE	1.20 Feet	27.1	29.70	0.008	1.000000	
434/431	431/434	CIRCLE	1.20 Feet	27.1	29.70	0.27	1.000000	
431	470	CIRCLE	1.20 Feet	27.1	29.70	1.0000	0.000000	
470	481/401/434	CYLINDER	1.20 Feet	27.1	29.4	0.04	0.000000	
481/401/434	401/481/434	CYLINDER	1.20 Feet	24	29.4	0.27	0.000000	
401	481	CIRCLE	1.20 Feet	29.70	29.8	1.00	0.000000	
481/401	401/481	CIRCLE	1.20 Feet	29.70	29.8	0.04	1.000000	
481	484	CIRCLE	1.20 Feet	29.70	32.00	0.008	1.000000	
484/481	481/484	CIRCLE	1.20 Feet	29.70	32.20	0.27	1.000000	

See Nomenclature List For Definition Of The Terms & Symbols Used In These Callouts

R&C: P748,75,407, 408

040000

Page 262-9

TABLE 3-21-2 THERMAL CONDUCTANCE VALUES FOR RTG TRANSPORT THERMAL MODEL (Continued)

NODE 1	NODE 2	ELEMENT	MEDIUM	GEOMETRIC DATA			CONDUCTOR MULTIPLIER	REFERENCE
				X1	X2	X3		
488	478	CIRCLE	12F Foam	29.75	32.25	1.325	2.441571	
4514822483	4414812484	CYLINDER	12F Foam	26.4	31	1.84	1.914248	
4344824485	4244814486	CYLINDER	12F Foam	26.4	31	1.27	1.270787	
488	481	CIRCLE	12F Foam	31.25	34.75	1.53	2.409744	
481483	482484	CIRCLE	12F Foam	31.25	34.75	1.24	1.262567	
483	484	CIRCLE	12F Foam	32.25	34.75	1.205	1.267828	
484485	485486	CIRCLE	12F Foam	32.25	34.75	1.27	1.313336	
485	474	CIRCLE	12F Foam	32.25	34.75	1.205	2.326472	
4414814482	4414824483	CYLINDER	12F Foam	31	32.52	1.24	1.497284	
4414824483	4414834484	CYLINDER	12F Foam	31	32.52	1.27	1.544435	
4414834484	441	CYLINDER	12F Foam	32.52	34.75	1.04	1.420773	
4414844485	441	CYLINDER	12F Foam	32.52	34.75	1.27	2.323490	
308	300	CIRCLE	Medium	0	1.0	0.6	3.224815	Shield Gas Oxygen Pass (8) by 1/2 Insulation
308	304	CIRCLE	Medium	15	17.9425	0.6	3.092223	Shield Gas Oxygen Pass (4) by 1/2 Insulation
304	306	CYLINDER	Medium	17.9425	19	3.67	4.32288	
2483082489	2483092490	CYLINDER	Medium	17.75	19	1.27	42.10089	Gap Range From 1/8 to 1/4 Insulation
249	240	CYLINDER	Medium	17.75	19	5	15.528223	Gap Range From 1/8 to 1/4 Insulation
240	242	CYLINDER	Medium	17.75	19	4.25	13.242823	Gap Range From 1/8 to 1/4 Insulation
242	244	RECTANGULAR	Medium	1.25	117	0.25	2.221214	
244	3042485	CYLINDER	Medium	79.875	19.04	0.8	3.228789	
300	308	CIRCLE	80% 304	0	19	1.025	1.428811	This Conductor To Be In Series W/ 304
300	308	SPECIAL	Conduct + 80% 304	83.98			83.98	174.2 Ins to 2.1 Ins by 7-4x -in
301	302	CIRCLE	80% 304	10	18	1.045	1.478204	This Conductor To Be In Series W/ 304
301	302	SPECIAL	Conduct + 80% 304	76.54			76.54	162.7 Ins to 2.1 Ins by 7-4x -in
304	304	SPECIAL	80% 304	12	18.87	1.025	2.408237	This Conductor To Be In Series W/ 304
304	304	SPECIAL	Conduct + 80% 304	28.6			88.803	187.8 Ins to 2.1 Ins by 7-4x -in
304	304	CIRCLE	80% 304	14.83	18.89	1.025	1.499202	This Conductor To Be In Series W/ 304
304	304	SPECIAL	Conduct + 80% 304	87.5			87.503	187.8 Ins to 2.1 Ins by 7-4x -in

See Nomenclature List For Definition of The Terms & Equations Used in These Calculations

R&E #12947c 057 gms 04/29/94

Page 2 & 2 of 0

TABLE 3.6.2-13 THERMAL CONDUCTANCE VALUES FOR RTG TRANSPORT THERMAL MODEL (continued)

NODE 1	NODE 2	ELEMENT	MEDIUM	GEOMETRIC DATA			CONDUCTOR MULTIPLIER	REMARKS
				K1	X2	X3		
289	AMBENT	CONNECTIVE	air	890.00	1	26	2.047814	Use half plate correction; reduced by 25%
289	Ambient	CONNECTIVE	air	830	1	0.1	2.048888	Use vertical plate correction
289	Ambient	CONNECTIVE	air	782.00	1	26	1.288640	Use horizontal plate correction
289	Ambient	CONNECTIVE	air	2100	1	12	21.888944	Use vertical plate correction
218/218	Ambient	CONNECTIVE	air	3	276.1	49	1.209750	Use vertical plate correction
228/228	Ambient	CONNECTIVE	air	3	276.1	24	1.209722	Use vertical plate correction
228/228	Ambient	CONNECTIVE	air	3	296.28	21	1.497817	Use vertical plate correction
1042	Ambient	CONNECTIVE	air	0.5	266.28	49	1.209699	Use vertical plate correction
1022	Ambient	CONNECTIVE	air	0.1	266.28	21	2.405008	Use vertical plate correction
1024	Ambient	CONNECTIVE	air	0.5	1070.00	19	2.748982	Use vertical plate correction
246	Ambient	CONNECTIVE	air	805.00	1	26	1.123028	Use horizontal plate correction with 25% reduction
249	Ambient	CONNECTIVE	air	878	1	2	4.268832	Use vertical rectangular column by 25%
281	Ambient	CONNECTIVE	air	28	1	1.292	0.687860	Use horizontal rectangular column by 25%
871	Ambient	CONNECTIVE	air	12	1	1.188	0.698242	Use horizontal rectangular column by 25%
1406	Ambient	CONNECTIVE	air	0.48	187.6	0.6	0.234527	Use vertical plate correction
408	Ambient	CONNECTIVE	air	1241	1	26	26.701288	Use horizontal plate correction
408	Ambient	CONNECTIVE	air	2888	1	19	27.488111	Use vertical plate correction
The Following Corrections Are Used Only For The Res Ambient								
410	Ambient	CONNECTIVE	air	1528	1	28	28.218228	Use vertical plate correction
412	Ambient	CONNECTIVE	air	828	1	28	8.444884	Use vertical plate correction
414	Ambient	CONNECTIVE	air	1258	1	28	8.277728	Use vertical plate correction
The Following Corrections Are Used Only For Ducted Or Zero-Flow Coefficient Jacket Conditions								
1841/1812	21/1812	CYLINDER	AirCooled	18.44	18.84	0.1	0.888888	
Repeat Above Conditions For Stations 409 & 340								
1841/1842	22/1842	CYLINDER	AirCooled	18.44	18.84	1.222	3.822222	
1842/1844	23/1842	CYLINDER	AirCooled	18.44	18.84	0.482	4.784422	
312	311/312	RECTANGLE	AirCooled	1	248.5	1	8.840674	
318/314	311/312	CYLINDER	AirCooled	18.44	18.84	0.1	28.214147	
Repeat Above Conditions For Station 308; Multiply By 7.44 For Station 282								
317	302	RECTANGLE	AirCooled	7	118	1	0.826189	

See Specifications List For Definition Of The Factors & Equations Used In These Calculations

Rev: PTH6.YG.007; gms 04/08/94
Page 3.6.2-12

TABLE 3.2.1-3 RADIATION INTERCHANGE VALUES FOR RTG TRANSPORT THERMAL MODEL COMPONENTS

NODE 1	NODE 2	EMISS 1	EMISS 2	VIEW		RADIATION		REMARKS
				FACTOR	AREA 1	AREA 2	FACTOR	
440	441	0.88	0.18	1	1288.4	1338.4	3.94870	
340	440	0.8	0.78	1	874.8	816.2	0.78883	
240	440	0.8	0.88	1	581.7	331.7	0.61748	
244	440	0.8	0.78	1	488.7	488.7	0.77840	
344	440	0.8	0.88	1	236.8	236.8	0.62876	
348	444	0.8	0.88	1	588.8	588.8	0.82888	
348	444	0.8	0.88	1	404.8	404.8	0.82128	
348	444	0.8	0.88	1	478.1	438.1	1.80888	
240	Arbitary	0.8	1	0.5382	890.88	1	7.78184	
240	241	0.8	0.88	0.1	282.88	318	0.88878	
300	301	0.8	1	0.0488	130.88	3184.8	0.17888	
301	Arbitary	0.88	1	1	318	1	1.04888	
304	Arbitary	0.8	1	0.5877	782.88	1	1.88888	
304	304	0.8	0.8	0.1388	88.88	31.78	0.88877	Multiply By 60 For Total
304	Arbitary	0.8	1	0.47773	3188	1	8.88888	
308	Arbitary	0.8	0.8	0.818787	88.88	17.58	0.88888	Multiply By 60 For Total
318/319	Arbitary	0.8	1	0.88888	788.8	1	4.18888	
218/320	Arbitary	0.8	1	0.888	788.8	1	0.88888	
218/320	Arbitary	0.8	1	0.7888	1077.7	1	4.88888	
340	Arbitary	0.8	1	0.4288	888.88	1	3.88888	Multiply Area Minus Area For Net Area Value
1000	340	0.8	0.8	0.1288	182.88	888.88	0.88888	
218/318	340	0.8	0.8	0.1788	1078.7	888.88	8.88888	
1000	340	0.8	0.8	0.887888	878.13	888.88	2.08888	
218/318	340	0.8	0.8	0.887888	788.7	888.88	8.88888	
1013	340	0.8	0.8	0.888888	878.13	888.88	8.88888	
218/318	340	0.8	0.8	0.888888	788.7	888.88	8.88888	
341	Arbitary	0.8	1	0.88888	88	1	0.88888	240 x 30" Cap Head Section
348	Arbitary	0.8	1	0.18888	878	1	0.71888	54 OCY & 8 Inspec. Liner Section
349	348	0.8	0.8	0.88771	88	814	0.48888	
374	Arbitary	0.8	1	0.88888	12	1	0.88888	140 x 78" Cap Head Section
377	348	0.8	0.8	0.88771	12	724	0.88888	
1348	Arbitary	0.8	1	0.88888	77	1	0.88888	

See Nomenclature List For Definition Of The Terms & Equations Used In These Calculations

FILE: RTGSTR001 v38 Date:04/04

Page 3 of 14

TABLE 3-8-21-3 RADIATION INTERCHANGE VALUES FOR RTG TRANSPORT THERMAL MODEL (Continued)

MODE 1	MODE 2	EMISS 1	EMISS 2	VIEW FACTOR	AREA 1	AREA 2	RADIATION FACTOR	REFERENCE
1044	404	0.8	0.8	0.4834	72	1643	0.33893	
1045	404	0.8	0.8	0.1043	848.24	1643	0.26738	
2362194	404	0.8	0.8	0.1013	8479.7	1643	0.21881	
1023	404	0.8	0.8	0.03894	276.13	1643	0.04363	
2362195	404	0.8	0.8	0.03894	790.3	1643	0.18227	
1019	404	0.8	0.8	0.01328	378.13	1643	0.02844	
2362198	404	0.8	0.8	0.01328	790.3	1643	0.04880	
304	404	0.3	0.48	0.9	78.8	84.43	0.71817	
304	1000-47	0.8	0.8	0.45	44.24	294.8	0.09200	
2002047	404	0.3	0.48	0.8836	324.8	84.43	0.74790	
207	304	0.3	0.8	0.8848	294.8	294.8	0.47724	
304	304	0.3	0.3	1	171.3	171.3	0.31069	
304	304	0.3	0.3	1	187.1	187.1	0.24784	
404	Arbitary	0.8	1	0.2744	1488	1	7.88841	
404	Arbitary	0.8	1	1	2868	1	21.88849	
1043	Arbitary	0.8	1	0.8843	436.13	1	3.88798	
1003	Arbitary	0.8	1	0.952	526.13	1	2.81294	
1003	Arbitary	0.8	1	0.7848	649.04	1	2.41693	
THE FOLLOWING VALUES ARE USED ONLY FOR THE "NO-COOLANT" CONDITION								
1011/1042	1100/11	0.3	0.48	0.41606	704.8	746	0.24570	
1011/1042	314	0.3	0.48	0.28195	704.8	729.9	0.41720	
1011/1001	316/304	0.3	0.48	0.41606	704.8	746	0.24570	
1011/1000	314	0.3	0.48	0.28195	704.8	729.9	0.41720	
1011/1002	316/304	0.3	0.48	0.41606	704.8	746	0.24570	
1011/1003	314	0.3	0.48	0.28195	704.8	729.9	0.41720	
1041/1002	1100/104	0.3	0.48	0.21608	387.2	371.2	0.25500	
1041/1041	314	0.3	0.48	0.26138	387.2	364.2	0.25748	
1000/1041	1100/104	0.3	0.48	0.21608	44.7	44.8	0.07460	
1042/1044	304	0.3	0.48	0.26138	44.7	44.2	0.04370	
314	1100/11	0.3	0.48	0.26138	728.8	708	0.44819	
304	1100/104	0.3	0.48	0.26138	728.8	708	0.44819	
304	1100/104	0.3	0.48	0.26138	1006.2	1071.8	1.26643	

See Dimensions List for Definition of The Terms & Symbols Used in These Calculations

FILE: P706/TRA002 .JOB

DATE: 04/16/00
Page 3 of 2-15

TABLE 3.8.2-1-4 THERMAL CAPACITANCE VALUES FOR SPMS RTG BIRYING RACK

ROOM	ELEMENT	MEDIUM	DENSITY	GEOMETRIC DATA			SPEC. HEAT	REMARKS
				X1	X2	X3		
	BIRYING RACK FOR SPMS RTG							
100	PARALLEL	17-4PH 8.50	0.276	1	0.04	0.5	1.0274	Portion of Handling Bin; Multiplied by 4 for total.
	PARALLEL	17-4PH 8.50	0.176	1	0.4	2	2.0000	
	PARALLEL	17-4PH 8.50	0.176	1	1.00	0.075	2.2611	
	CYLINDER	0001 AL	0.100	2.0	7.25	1	2.2429	Portion of RTG Ring Assembly
	PANNAIR	0001 AL	0.100	0.200	1.07	1.01	1.2000	Portion of Hot Box; Air - circulation allowed
						Total Wt. =	11,649.75	Combined Heats Mass
101	CYLINDER	0001 AL	0.100	7.5	10.00	0.75	1.68700	Converter Support Ring Assembly
102	STUMBER	8.00 804	0.20	0.07	1.5	0.30	42.0000	Support Leg B Only; Multiplied by 4 for total.
103	STUMBER	8.00 804	0.20	10.0000	10.25	0	27.00007	Mobile Dash On Support Plate
104	CYLINDER	8.00 804	0.20	10.125	10.5	0.750	26.41700	Support Plate Under Support
105	CYLINDER	Various	0.00000	0	0	0.750	2.47000	Support Junction Member
107	CYLINDER	Various	0.00000	0	10.125	0.750	10.24000	Dash Junction Member
108	CYLINDER	8.00 804	0.20	0	0	0.250	1.200000	Lower Portion of Support Ring
109	CYLINDER	8.00 804	0.20	0	10.5	0.750	26.71000	Upper Portion of Support Plate
100								Substrate made at top of mobile bin
1001								Substrate made between 100 & 101
1002								Substrate made between 104 & 100
1003								Substrate made at top of support legs
1004								Substrate made at bottom of support legs
1005								Substrate made for support from 102 to 103
1006								Substrate made between 101 & 102
1007								Substrate made between SPMS RTG #170 & 100
1008								Substrate made between 1007 & 100
1009								Substrate made representing total gas volume
1000								Substrate made representing total gas volume

See Memorandum Data For Definition Of Terms & Symbols Used In This Table

Total Wt. = 294,247.8220

Pub: 000796.004 0171 040004

Page 3.8.2-10

TABLE 3.6.2.1-5 CONDUCTANCE VALUES FOR GPHE RTG SHIPPING RACK

NODE 1	NODE 2	ELEMENT	MEDIUM	GEOMETRIC DATA			CONDUCTOR MULTIPLIER	REMARKS
				X1	X2	K2		
174	1487	SPECIAL	Common	11.62			11.020000	4 legs w/ 2 22 Sphs. Total Area = 2.5 Spheres
1007	1488	RECTANGUL	6061 AL	2	0.5	1.7	0.043248	Multiplied by 4 for Four Legs
1008	149	RECTANGUL	6061 AL	1	1	2.04	0.020086	Multiplied by 4 for 4 legs & 2 paths per leg
1009	1420	RECTANGUL	4061 AL	1.5	0.263	2.9	0.015812	Multiplied by 4 for Four legs
1020	151	RECTANGUL	4061 AL	0.78	0.15	2.61	0.020287	Multiplied by 4 for 4 legs & 2 paths per leg
101	150	SPECIAL	Common	270			270.000000	120 Sphs. Total Area = 1.5 Spheres
100	151	CONNECTIVE	Hydro	225	1		1.940000	Hydro. Two paths Use Aerial Connection
101	151	CONNECTIVE	Hydro	225	1		1.940000	Hydro. Two paths Use Aerial Connection
100	1001	CYLINDER	6.04 204	0.21	0	0.373	0.021008	
1001	130	CYLINDER	6.04 204	0	13.41	0.375	0.020523	
100	1002	CYLINDER	6.04 204	11.41	16.2125	0.375	0.017205	
1002	104	CIRCLE	6.04 204	15.225	16.0	0.00	0.000000	
1002	106	CYLINDER	6.04 204	18.2125	18.16625	0.375	0.000000	
100	102	CIRCLE	6.04 204	18.0000	18.25	0.0000	0.000000	
1001	1002	RECTANGUL	6.04 204	0	0.479	2.824	0.017600	Multiplied by 4 for 4 legs & 2 paths per leg
1001/02	1001/02	CIRCLE	6.04 204	0.07	0.0	2.15120	0.077441	Multiplied by 4 for four legs
1009	1000	SPECIAL	Common	70.70			70.700000	4 Legs w/ 20 S Sphs. Total Area = 2.5 Spheres
1000	1000	CIRCLE	6.04 204	0	0.378	1	0.048178	Multiplied by 4 for four legs
1000	1000	RECTANGUL	6.04 204	2	0.0	3.224	0.000000	Multiplied by 4 for 4 legs & 2 paths per leg
1001	1000	CYLINDER	6.04 204	7	0	1.72	0.000007	
1000	100	CYLINDER	6.04 204	0	12.70	1.72	0.018460	
100	100	CIRCLE	Hydro	0	0	1	0.000000	Two one inch legs of 2000 # insulation
100	107	CIRCLE	Hydro	0	18.225	1	2.102707	Two one inch legs of 2000 # insulation
100	200	CYLINDER	Hydro	18.25	17	0	4.630190	
100	100	CONNECTIVE	Hydro	112	0	0	0.704731	Use overall conductance
100	100	CONNECTIVE	Hydro	202.2	1	0	8.154187	Use overall conductance
100	1000	CONNECTIVE	Hydro	112	1	00	0.704722	Use Horizontal Plate Conductance
100	1000	CONNECTIVE	Hydro	217	1	0	1.008344	Use Vertical Plate Conductance
100	1000	CONNECTIVE	Hydro	200.0	1	0	1.000000	Use Vertical Plate Conductance
107	1000	CONNECTIVE	Hydro	400.0	1	00	4.000000	Use Horizontal Plate Conductance
100	101-0	CONNECTIVE	Hydro	400.0	1	0	2.100000	Use Vertical Plate Conductance
1001	1000	CONNECTIVE	Hydro	100.0	1	1	0.400007	Use Horizontal Plate Conductance

Use Horizontal Plate For Definition Of The Term & Equations Used In These Calculations

RLE SHEET 004, 5/12

4/24/88

TABLE 2.3.2.1-8 THERMAL CAPACITANCE VALUES FOR BPHS RTG THERMAL MODEL

20	SPECIAL	HEAT SOURCE	1	2.7180	0	7.84	2.7280	See Note 11 G - 974-976 Wagon
22	SPECIAL	HEAT SOURCE	1	0.4924	0	24.82	0.4924	See Note 21 G - 2741-284 Wagon
24	SPECIAL	HEAT SOURCE	1	3.7390	0	7.84	2.7280	See Note 11 G - 974-976 Wagon
21	SPECIAL	UNCOUPLE	1	1.172	0	7.84	1.1720	See Note 2
23	SPECIAL	UNCOUPLE	1	3.496	0	22.21	3.4960	See Note 2
25	SPECIAL	UNCOUPLE	1	1.172	0	7.84	1.1720	See Note 2
26	SPECIAL	END SUPPORT	1	7.11	0	0	1.7800	From SW's Mode 12
27	SPECIAL	END SUPPORT	1	0.8	0	0	0.8000	From SW's Mode 2
108	SPECIAL	CUTTING EDGE	1	0.072	0	0	0.0720	From SW's Mode 13
109	SPECIAL	FLANGE	1	0.064	0	0	0.0640	From SW's Mode 14
107	SPECIAL	FLANGE	1	0.12	0	0	0.1200	From SW's Mode 15
120	CYLINDER	AL-2210-T8	0.108	4.23	4.23	1.62	0.3477	Multiply By 0.4797 For Effective Area - See Note 4
112 & 113	PANELS	AL-2210-T8	0.703	0.88	0.008	1.62	0.0074	Multiply By 0.88 For Total
78	CYLINDER	AL-2210-T8	0.103	4.23	4.23	1.62	1.1400	Multiply By 0.4797 For Effective Area
122 & 123	PANELS	AL-2210-T8	0.103	0.88	0.008	1.62	0.0074	Multiply By 0.88 For Total
124 & 125	PANELS	AL-2210-T8	0.103	1.07	0.008	1.62	0.0074	Multiply By 4 for the total
126 & 127	PANELS	AL-2210-T8	0.103	3.03	0.008	1.62	0.0074	Multiply By 4 for the total
128	CYLINDER	AL-2210-T8	0.103	4.23	4.23	1.62	1.1400	Multiply By 0.4797 For Effective Area
129 & 130	PANELS	AL-2210-T8	0.103	0.88	0.008	1.62	0.0074	Multiply By 0.88 For Total
131 & 132	PANELS	AL-2210-T8	0.103	1.07	0.008	1.62	0.0074	Multiply By 4 for the total
133 & 137	PANELS	AL-2210-T8	0.103	3.03	0.008	1.62	0.0074	Multiply By 4 for the total
136	CYLINDER	AL-2210-T8	0.103	4.23	4.23	1.62	1.1400	Multiply By 0.4797 For Effective Area
141	CYLINDER	AL-2210-T8	0.103	4.2	0	0.81	1.3100	See Note 21a
142 & 143	PANELS	AL-2210-T8	0.103	0.88	0.008	1.62	0.0074	Multiply By 0.88 For Total
144	PANELS	AL-2210-T8	0.103	1.07	0.008	1.62	0.0074	Multiply By 4 for the total
145	PANELS	AL-2210-T8	0.103	3.03	0.008	1.62	0.0074	Multiply By 4 for the total
146	PANELS	AL-2210-T8	0.103	1.07	0.008	1.62	0.0074	Multiply By 4 for the total
147	PANELS	AL-2210-T8	0.103	1.03	0.008	1.62	0.0074	Multiply By 4 for the total
148	CYLINDER	AL-2210-T8	0.103	4.23	4.23	1.62	1.1400	Multiply By 0.4797 For Effective Area
112 & 113	PANELS	AL-2210-T8	0.103	0.88	0.008	1.62	0.0074	Multiply By 0.88 For Total
149	PANELS	AL-2210-T8	0.103	1.07	0.008	1.62	0.0074	Multiply By 4 for the total

See Nomenclature List For Definition Of Terms & Equations Used In This Table

FILE: 041676A.DWG p1/2 7/22/81

BEST COPY AVAILABLE

2.6.2-20

Radiation heat transfer is calculated assuming standard gray-body equations. The shape factors between the various package components were computed using either pre-defined relationships or the string method for nonstandard geometric configurations.

Heat transfer across the ICV-to-OCV gap (1/4-in. maximum at the sides and 1/2-in. maximum at the heads) is assumed to be via radiation and conduction through the 10 ± 1 psia helium gas medium. The emittance of both surfaces is assumed to be 0.90, based on the use of the Carbolite 4874-C900 high emissivity coating. Subsequent testing²² on three sample coupons with Carbolite coating yielded a measured normal emittance of 0.875 on all three sample coupons. While the measured values are slightly less than the assumed value of 0.90 used in the SARP analysis, the impact on the predicted temperatures is slight. This conclusion is based on the close match between the results for the qualification testing (see Reference 14) and the temperatures predicted by an analytical model that used a surface emittance value of 0.90. In addition, further analysis with an assumed emittance value of 0.70 to simulate possible wear-and-tear of the surface coating showed that the surface temperatures of the RTG increased by 4 °F or less. The temperature of the ICV sidewall increased about 2 °F. Therefore, the temperature levels presented in the SARP analysis herein are considered accurate despite the differences in assumed and measured emittance values for the Carbolite coating. Because of the narrowness of the gap, convection heat transfer across the gap reduces to straight conduction (i.e., $Nu = 1.0$).

Thermal conductance between surfaces in direct contact with each other was determined using the data in Figure 8, page 4-19 of Reference 2. The specific value used depended on the surface materials, surface finish, gap material, and contact pressure. Table 3.6.2.1-2 provides the contact area and heat transfer coefficient assumed for each contact surface pair.

3.6.2.2 RTG-to-ICV Thermal Interface Model. The convection coefficients for the GPHS RTG to ICV heat transfer are computed using equation 22 from the Reference 11 paper by Khan and Kumar. This correlation was developed for the case of convective heat transfer across vertical annuli with a constant heat flux on the inner wall, adiabatic end surfaces, and smooth inner and outer walls. As such, the correlation predicted coefficients needed to be adjusted to account for the fact that the GPHS RTG is a finned cylinder, the end walls are not adiabatic, and the fact that a straight application of the correlation with the GPHS RTG would imply a larger ICV wall area than exists. A comparison of implied annuli areas with the actual geometry indicated that the calculated heat transfer coefficient needed to be multiplied by 0.75 to correct for these factors. Furthermore, because the correlation only provides the average coefficient, a second adjustment based on Figure 3 in the paper was made to account for temperature rise between the top and bottom of the package.

The general applicability of the Khan and Kumar correlation to the GPHS RTG-ICV geometry and the specific modifications made to the correlation were verified in the Reference 12 thermal development test and the Reference 14 thermal qualification tests. The results from both sets of tests showed that the adjusted correlation resulted in an accurate prediction of the convective coefficients and, hence, the RTG temperatures. Because of the good match-up with test results, only modest refinement to the correlation adjustments have been needed to those derived before testing.

For a detailed discussion of the test setup, results, and the adjustment procedure used to apply the correlation to this payload, the reader is directed to the referenced test reports.

Because a significant fraction of the heat transfer between the GPHS RTG and the ICV is via radiation, the shape factors between the various surfaces were determined by computer analysis using the University of Washington's VIEW program. The computed shape factors were validated by results from the GPHS development and qualification tests (References 12 and 14). The interchange factors between individual nodes of the GPHS RTG and other GPHS RTG nodes or the

ICV are not documented herein because of the sheer number of factors involved (more than 800). Instead, these radiation interchange factors may be found in the SINDA listing at the end of this section.

The shipping rack assembly for the GPHS RTG is modeled using 21 nodes. Heat transfer via conduction, convection, and radiation are addressed for the interfaces between the shipping rack assembly and the various RTG/ICV surfaces. Because the existing RTG support structure is used, the direct conduction between the GPHS RTG and the shipping rack assembly is essentially the same as it now exists with the current shipping method.

3.6.2.3 Package Model for Regulatory Normal Conditions of Transport. The package thermal model for the regulatory normal conditions of transport (NCT) used a slightly modified version of the normal operational condition model discussed in Sections 3.6.2.1 and 3.6.2.2. The model modifications assume an inoperative chiller system and that the coolant jacket is drained and dry. The damage from the NCT free drop will cause a negligible effect on the remaining aspects of the package thermal model.

Thermal modeling of an inoperative chiller system simply involved setting the conductors between the boundary node representing the chiller output and fluid nodes in the coolant jacket to zero. Modeling of a drained coolant jacket involved the following modifications:

- ◆ The thermal capacitance at the fluid nodes in the coolant jacket (i.e., nodes 311, 312, 321, etc.) were replaced by the thermal capacitance of an equivalent volume of air
- ◆ The forced convection conductors between the coolant jacket fluid nodes and the various surfaces of the coolant jacket were replaced with conductance across an equivalent air gap
- ◆ Radiation conductors were added to the model of the coolant jacket to simulate radiative interchange between the various coolant jacket surfaces.

All other aspects of the thermal model are the same as those described above for the normal operational conditions.

3.6.2.4 Package Model for Hypothetical Accident Conditions Fire. The thermal performance of the Package under the 10 CFR 71.73 hypothetical accident conditions (HAC) is evaluated analytically. The thermal model is based on the NCT model with modifications made to simulate the damage sustained from the HAC 30-ft free drops and the HAC 40-in. puncture drops. The results from a series of drop tests conducted on the two Certification Test Articles are presented in Sections 2.7.6 and 2.10.15. The following table summarizes the results from both test series and the logic for the selection of the worst case damage to the package that would occur under the HAC.

Test No.	Test description	Thermal impact
CTA-2 No.2	30-ft. free drop, bottom-down, near vertical	No significant damage to Packaging. RTG assumed to be damaged (typical for all MAC drops).
CTA-2 No.5	30-ft free drop, e.g. over corner	No ICV or OCV damage. Extrapolated impact limiter crush of 6.1 in. will leave 4.9 in. of foam at minimum distance.
CTA-2 No.12	30-ft free drop, side-slakedown	Minimal damage to ICV or OCV shells, possible local contact between ICV and OCV shells over 13 wide by 2-in.-long segment near the torispherical heads. Extrapolated 5.9 in. of foam crush at the top of the impact limiter will leave 1.75 in. of foam minimum.
CTA-2 No.8	30-ft free drop, bottom end down	No significant damage to Packaging.
CTA-2 No.13	30-ft free drop, top end down	No damage to the impact limiter. ICV and OCV contact over 15-in. diameter at the torispherical head. Crushing of all fins will reduce convective/radiative heat transfer between ambient and the OCV head.
CTA-2 No.8	40-in. puncture drop, e.g. over corner	The puncture bar increased previous e.g. over corner foam crush by 1.7 in. This left $4.9 - 1.7 = 3.2$ in. of foam at the minimum distance.
CTA-1 No.12	40-in. puncture drop, bottom-down, over low density foam	The local foam crush of 2.6 in. leaves 5.6 in. of foam depth.
CTA-1 No.13	40-in. puncture drop, over OCV vent port	Maximum local foam crush of 3 in., leaving 4.6 in. at minimum distance.
CTA-2 No.14	40-in. puncture drop, normal impact to OCV sidewall	Localized deformation of ICV and OCV sidewalls over a 9-in. diameter area. Possible contact between ICV and OCV shells over 8-in. diameter area.
CTA-1 No.15	40-in. puncture drop, oblique impact to OCV sidewall	Localized deformation of ICV and OCV sidewalls less than CTA-1 test No. 14. No contact assumed between ICV and OCV shells because ICV deformed more than OCV.
CTA-2 No.15	40-in. puncture drop, top end impact	Maximum denting of ICV and OCV torispherical heads was 1.25 in.
CTA-2 No.3	40-in. puncture drop, impact limiter top edge	Denting of impact limiter top surface by 5/16 in. will cause no significant thermal effects.
CTA-1 No.18	40-in. puncture drop, top surface of thermal shield	Thermal shield dented by 1.3 in. at center and less elsewhere over a total diameter of 7 in. The damage reduced the underlying fiberglass to approximately 1/2 of its original thickness.
CTA-1 No.19	40-in. puncture drop, over impact limiter bolt access tube.	Crushing of impact limiter top surface by 3/4 in. will cause no significant thermal effect. The buckling of the access tubes will reduce the convective and radiative heat transfer between the tube and bolt heads with the ambient.
CTA-2 No.9	40-in. puncture drop on side of impact limiter at lower corner weld.	The puncture dent depth was approximately 3.5 in. No evidence of equipment rimping of either impact limiter shell or weld was noted.

Test No.	Test description	Thermal Impact
CTA-2 No.18	40-in. puncture drop on to impact limiter side wall plastic melt plug.	The melt plug holder weld failed and allowed the impact limiter side wall to tear, exposing about 12.7 sq. in. of foam.

Of the various combinations of 30-ft free drops and 40-in. puncture drops, the worst combination of the two events from a thermal point of view is represented by the 30-ft free drop with side-shoulder followed by the 40-in. puncture drop on the thermal shield (i.e., test Nos. 5 and 18). The damage caused by these test events maximizes the Package damage adjacent to the temperature sensitive Guryl O-rings. The amount of foam exposed by the puncture bar in CTA-2 test no. 18 was approximately 12.7 in². This area is quite small relative to the area of the impact limiter, and due to the intumescent behavior of the polyurethane foam material (see Reference 10), the opening will be effectively closed during the fire event.

Other combinations of free drop and puncture events exhibited lesser damage to the impact limiter and damage to the ICV/OCV shells that is more remote from the O-rings. While the top and down drops will cause an increase in the peak ICV temperature due to contact between the ICV and OCV heads, the increase will be less than 200 °F, and the same head contact will result in lower ICV temperatures following the fire because of the reduced thermal resistance between the ICV head and the ambient environment. Localized contact between the ICV and OCV shells due to the free and/or puncture drops will produce a similar effect on the peak and long-term ICV temperature.

A 3-D analytical thermal model is used to evaluate the package performance under the 10 CFR 71.73 HAC fire. This level of modeling permits the simulation of the non-axisymmetric damage caused by the HAC free and puncture drops. The 3-D model is created using a SANDA program feature that permits a thermal model to be broken into submodels. Each submodel can be independently scaled and modified as necessary to represent their contribution to the overall thermal model. Conductors are used to complete the 3-D model by providing thermal communication between the various 2-D circumferential segments of the package. Table 3.6.2.4-1 presents the circumferential conductances used to tie the various 2-D submodels together. The values presented in the table are based on a 15° angle of separation. These conductances were scaled up or down to match the actual angle of separation between the 2-D submodels.

For this application, each circumferential segment of the package is represented by a different 2-D submodel. A total of four 2-D submodels represent one-half of the packaging and its payload about a line of symmetry. The plane of symmetry passes through the vertical axis of the package and the centerline of the HAC side drop damage. Symmetry conditions are assumed for the temperature in the other half of the package. The first submodel (i.e., segment A) simulates the damaged section of the package, while the other three segments (i.e., segments B, C, and D) provide circumferential temperature resolution within the package components. The 3-D models for the circumferential heat source distribution (i.e., HAC thermal load case Nos. 1 and 2) and the ungula rubble pile (i.e., HAC thermal load case Nos. 5 and 6) assumptions use submodel segments with subtended angles of 22.5, 45, 87.5, and 45 degrees for segments A through D, respectively. For the axial alignment of the assemblies (i.e., HAC thermal load case Nos. 3 and 4), the subtended angles used are 15, 30, 90, and 45 degrees, respectively. The subtended angles used for each 3-D model were selected based on extent of the internal and external damage and the requirements of the associated thermal stress model.

Heat transfer within each of the 2-D submodel segments that make up the 3-D model is based on the same data for thermal capacitance, conductance, and radiation as used for the axisymmetric regulatory model for NCT (see Appendix 3.5.1 to 3.6.3). Modifications to this model data were made to reflect the presence of package damage and the payload reconfiguration. Additional general model modifications made for the HAC fire included the 10 CFR 71.73(c)(3) requirements for a package external surface absorptivity of 0.8 or greater and exposure of the entire package including the impact limiter bottom to the HAC fire environment. Although the credible post-accident orientation for thermal load case Nos. 1 and 2 is for the package to be resting on the impact limiter's bottom surface (thus

shedding the bottom); for conservatism the bottom surface was exposed to the fire environment for these load cases as well.

Because all of the HAC scenarios assume breakup of the RTG, the Iken and Kumer relationship for convective heat transfer between the RTG and the ICV is no longer applicable for the damaged configurations and was abandoned for the 3-D models. Instead, the convective heat transfer from each surface was treated as a free surface with a mean ICV gas temperature node serving as the appropriate boundary node. This approach is known to be conservative because it does not account for temperature stratification in the ICV, and the strength of a convective heat transfer flow is stronger in an enclosure for a given delta temperature.

Specific model modifications are made to each submodel of the 3-D model to account for the HAC fire and puncture drop induced damage to the package exterior and the payload. As discussed above, several impact orientations were evaluated to determine the worst case thermal damage to the package. The following paragraphs describe the modifications made for each type of damage.

The impact limiter model for the 2-D segment that encompasses the crush zone of impact limiter damage (i.e., segment A) was modified to reflect a 4-in. inward crush of the exterior shell of the impact limiter. This crush depth represents the maximum crush seen from the side-staple-down drop test. Although extrapolation of the foam structural properties for the warm foam conditions indicates a worst case crush depth of 5.8 in., using a 4-in. crush depth provides sufficient conservatism since it is applied across the entire 2-D segment. Under actual conditions the 5.8 in. of crush will only occur a single radial location and only at the top of the impact limiter. Further analyses of both configurations showed that the use of the 5.9 in. crush depth causes no increase in the predicted O-ring temperatures. This occurs because the conservative foam modeling assumptions used results in all foam in the damaged segment being ablated away at the start of the HAC fire under either crush depth scenario.

Additional conservatism lies in the fact that credit is not taken for the higher equivalent foam density that will result from the impact limiter crush (see Appendix 3.6.3 for the effect of foam density on the fire protection qualities of the foam). The impact limiter thermal model also assumes that the remaining foam in the damaged zone will be ablated away during the fire, exposing the inner shell of the limiter (i.e., thermal model node No. 404) to direct radiation and conduction exposure to the outer shell of the impact limiter (node No. 40B). This is a conservative assumption because prior tests (see Reference 10) have shown that a char layer will form and act as a radiative shield.

The impact limiter at the undamaged sections of the 3-D model assumes the loss of the outer 2.5 in. of the impact limiter foam, because of ablation during the HAC fire, and this foam loss occurs immediately upon the initiation of the HAC fire.

Again, this assumption is conservative because the Reference 10 fire tests showed that the foam will actually expand slightly when exposed to the fire. The presence of an expanded foam will limit, at a greater rate than assumed by the 3-D model, radiative heat transfer to the interior foam nodes. The remaining foam is assumed to remain in place, either as a char layer or as virgin foam according to the modeling rules provided in Appendix 3.6.3.

The payload reconfiguration described in Section 3.5 is modeled as a combination of an empty GPHS RTG shell and 18 GPHS aeroshells. For the circumferential distribution assumption of HAC thermal load cases Nos. 1 and 2, heat transfer between the aeroshells and the shipping rack assembly are modeled by a combination of radiation and conduction. Convection and radiation interchange with the ICV interior is also included.

TABLE 3 B 2.4-1 CONDUCTOR VALUES FOR RTG PACKAGE Based On 16 Degree Separation

NODE 1	NODE 2	ELEMENT	MEDIUM	DIMENSIONS (IN)			CONDUCTOR MULTIPLIER	REMARKS
				K1	K2	K3		
200a	200a200a	RECTANGLE	0.00 00a	0.275	12	3.4000	0.01000	
201a	200a200a	RECTANGLE	0.00 00a	0.275	4.000	4.2072	0.00000	
202a	200a200a	RECTANGLE	0.00 00a	0.275	3.000	4.0400	0.00000	
210a	210a210a	RECTANGLE	0.00 00a	0.25	12.75	4.0000	0.01000	Based On 200 & 210
240a	240a240a	RECTANGLE	0.00 00a	0.25	5	4.5000	0.00000	
245a	245a245a	RECTANGLE	0.00 00a	0.25	8.75	4.6000	0.00000	
250a	250a250a	RECTANGLE	0.00 00a	0.275	1.000	4.7000	0.00000	
260a	260a260a	RECTANGLE	0.00 00a	1.75	10	1.0000	0.00000	
265a	265a265a	RECTANGLE	0.00 00a	1.75	5	3.0000	0.01000	
280a	280a280a	RECTANGLE	0.00 00a	1.75	4.000	4.1000	0.01000	
285a	285a285a	RECTANGLE	0.00 00a	1.75	10	1.0000	0.00000	
290a	290a290a	RECTANGLE	0.00 00a	1.75	5	3.0000	0.01000	
295a	295a295a	RECTANGLE	0.00 00a	1.75	8	3.0000	0.01000	
300a	300a300a	RECTANGLE	0.00 00a	1.75	4.000	4.1000	0.01000	
305a	305a305a	RECTANGLE	0.00 00a	1.47	2.000	4.2000	0.00000	
310a	310a310a	RECTANGLE	0.00 00a	1.47	2.000	4.2000	0.00000	
320a	320a320a	RECTANGLE	0.00 00a	0.0	12	0.0000	0.00000	
330a	330a330a	RECTANGLE	0.00 00a	0.0	4.00	0.0000	0.00000	
340a	340a340a	RECTANGLE	0.00 00a	0.0	3.000	0.0000	0.00000	

Use Multiplication Unit For Redlines In The Tables & Equations Used In These Calculations

P&L PFD&M TO M&P p10 02/11/04

TABLE 3.8.2.4-1 CIRCUMFERENTIAL COMPACTOR VALUES FOR RTG PACKAGE: Based On 15 Degree Segment

NODE 1	NODE 2	ELEMENT	MEDIUM	GEOMETRIC DATA			CORRUPTION MULTIPLIER	REMARKS
				X1	X2	X3		
210a	210a/210a	RECTANGLE	0.20 204	0.8	10.73	4.7811	0.048866	Support For LRM 8.240
242a	242a/242a	RECTANGLE	0.24 204	0.5	5	4.7811	0.088648	
242b	242a/242a	RECTANGLE	0.24 204	0.8	4.83	4.7811	0.088880	
246a	246a/246a	RECTANGLE	0.24 204	1.7	1.2	4.8342	0.082808	
246b	246a/246a	RECTANGLE	0.24 204	0.276	3.628	4.8342	0.088880	
246c	246a/246a	RECTANGLE	0.24 204	4.195	0.278	4.8342	0.088645	
252a	252a/252a	RECTANGLE	0.28 204	2.843	7	4.8884	0.082258	
252b	252a/252a	RECTANGLE	0.28 204	2	7	4.8887	0.082282	
252c	252a/252a	RECTANGLE	0.28 204	2.843	1.88	4.8882	0.088607	
252d	252a/252a	RECTANGLE	0.28 204	2	1.88	4.8887	0.088677	
256a	256a/256a	RECTANGLE	0.28 204	1.5	10	4.8938	0.088641	
256b	256a/256a	RECTANGLE	0.28 204	1.5	8	4.8939	0.088648	
256c	256a/256a	RECTANGLE	0.28 204	1.8	4.988	4.8933	0.088638	
256d	256a/256a	RECTANGLE	0.28 204	2.84	2.8	4.8938	0.081352	
267a	267a/267a	RECTANGLE	0.28 204	2.828	2.8	4.8938	0.088672	
267b	267a/267a	RECTANGLE	0.28 204	2.878	2.8	4.8938	0.088615	
267c	267a/267a	RECTANGLE	0.28 204	2.878	2.8	4.8938	0.088624	
182a	182a/182a	RECTANGLE	0.24 204	10.8	0.278	3.2408	0.088418	
184a	184a/184a	RECTANGLE	0.24 204	8	0.278	1.1758	0.048844	
184b	184a/184a	RECTANGLE	0.24 204	8	0.1878	4.2237	0.088888	

Use Intermediate List For Definition Of The Terms & Quantities Used In These Calculations

FILE: PTP00001.DWG PLOT: 02/01/84

The HAC thermal load case Nos. 3 and 4 model the axial alignment of the aeroshells on the ICV wall by a combination of radiation and conduction. For conservatism, the centerline of the aeroshells is assumed to be aligned with the package HAC side drop damage. The shell of the GPHS RTG is assumed to end up lying directly on top of the aeroshells, thereby blocking direct convection and radiation interchange between the aeroshells and the interior of the ICV cavity. Instead, all decay heat from the aeroshells must first pass into the ICV wall or the GPHS RTG shell of segment A and B, be conducted to the neighboring submodel segments before being convected or radiated to other portions of the 3-D model.

The HAC thermal load case Nos. 5 and 6 rely on radiation and conduction interchange between a lumped rubble pile of aeroshells and the shipping rack assembly. The rubble pile is assumed to be in the shape of an "ungula" with a total subtended angle of 135° arc. As such, the rubble pile is distributed across submodel segments A and B. The RTG shell is assumed to have come to rest at an angle across the rubble pile, providing a partial blockage of radiative heat loss between the rubble pile and the ICV wall. Because of the substantial void fraction of the rubble pile, free convection from within the rubble pile is assumed to be possible. The convection heat transfer rate is based on 50% of the total surface area of the aeroshells being directly exposed to helium gas. Additional details on the modeling of the rubble pile, conduction and radiation between the aeroshells and the shipping rack assembly/ICV wall is provided in Section 3.6.6.

3.6.2.5 Nomenclature Used in Spreadsheets, Tables 3.6.2.1-1 Through -5, and Table 3.6.2.4-1.

Area1: area, in square in., associated with node 1.

Area2: area, in square in., associated with node 2.

Conductor multiplier: the factor to be multiplied by the thermal conductivity of the material (i.e. in terms of BTU-in./ft²in-°F) listed under 'Medium' and the temperature difference between nodes 1 and 2 to yield the heat transferred by conduction between nodes 1 and 2. If the Element type equals 'Special,' this value is in terms of BTU-in-°F (i.e., kA/L); if the Element type is 'Convective,' this value is in terms of square feet since it is to be multiplied by a calculated h_c. For all other Element types, the value listed is in terms of ft²/in. (i.e., A/L).

Density: the mass per unit volume, pounds-mass/in.³. A value of "1" indicates that this variable is unused for this calculation.

Element: geometric shape used to calculate the volume or conduction area for the associated node(s). These shape definitions are as follows:

Circle—a circular conduction element with Conductor Multiplier = $\pi[(X2^2 - X1^2)/X3]/144$.

Convective-surface heat transfer via convection. Conductor Multiplier = $X1^2 X2 / 144$ (i.e., Area1). The h_c from correlation listed in the 'REMARKS' column using X3/12 as the characteristic length.

Cylinder—a right cylinder solid. Volume = $\pi(X2^2 \cdot X1^2) \cdot X3$. Conductor multiplier = $2 \cdot \pi \cdot X3 / 144 \cdot \ln(X2/X1)$.

Parallel—a solid whose surfaces are parallelograms. Volume = $X1 \cdot X2 \cdot X3$.

Rectangle—an element with a rectangular-shaped heat transfer path. Conductor multiplier = $X1 \cdot X2 / X3 / 144$.

Special—indicates an element whose thermal capacitance or conductance is obtained from other sources and is included as a direct input. See the 'Remarks' column for specific details. A node with zero mass is known as an Arithmetic node. A heat balance is performed at the node, but it cannot store thermal energy.

Sphere—a solid of spherical shape. X2 = outer radius, X1 = inner radius, X3 = height of spherical segment. Volume = $\pi * X3 * X2^2 + X2 * X3 / 3$ minus $\pi * (X3 * X2 + X1) * X2^2 * (X1 - X3 - X2 * X1 / 3)$.

- Emiss-1:** Thermal emissivity of the surface area for node 1.
- Emiss-2:** Thermal emissivity of the surface area for node 2.
- Medium:** The material, component, or condition for which the thermal capacitance or conductance is being calculated.
- Node:** Number of the node in the thermal model. See Figures 1 and 2.
- Radiation:** Factor to be multiplied by the Stefan-Boltzmann constant (i.e., 1.71415×10^{-8} Btu/hr-ft²·R⁴) and the difference of ($T_1^4 - T_2^4$) to yield the heat transferred factor by radiation.
- Shape factor:** The fraction of diffusely distributed radiation leaving surface at node 1 that reaches the surface at node 2.
- Specific heat multiplier:** The factor, when multiplied by the specific heat of the material listed under Medium, yields the thermal capacitance, in terms of Btu/°F. If the Element type equals Special, this value is already in terms of Btu/°F and X3 indicates the height/length of the node section involved. Otherwise, the multiplier is equivalent to density times volume, or the weight of the node being modeled. A node with zero weight is known as an Arithmetic node. Heat balances are performed about these nodes, but because heat energy is not stored at these nodes, they have no effect on the transient behavior of the model.
- X1,X2,X3** Geometric lengths (in in.) for the volume or conductor calculation. See 'Element' above.

3.4.3 Performance Of Rigid Polyurethane Foam Under Fire Accident Conditions

The General Plastic's LAST-A-FOAM® FR-3700 (see Reference 10) selected for the impact limiter has been used in a number of similar applications over the last 12 years. A special thermal feature of this proprietary rigid polyurethane foam is that exposure to fire causes the foam to degrade into an intumescent char that swells and tends to fill voids or gaps created by impact on a puncture bar or other damage. The char is structurally strong and will shield the underlying undamaged foam from direct exposure to external high temperatures. In addition, the foam will not support a flame once the external fire is removed.

The mechanisms behind variations in the thermal properties of FR-3700 foam at elevated temperatures are varied and complex. Because only a limited amount of research has been done on the thermal properties of foam during a fire, no definitive analytical model of the foam properties exists. Instead, a combination of empirical data and modeling conservatism is used for this application.

The Reference 10 product brochure describes the setup and results of a series of fire tests conducted on the foam. The test articles consisted of six 5 gallon paint cans filled with FR-3700 foam at densities of 8, 16, and 24 lb/ft³. One end of the test articles (i.e., the "hot face (HF)" surface) was subjected to an open burner flame for 45 minutes. This flame duration is 15 minutes longer than called for by the 10 CFR 71.73 requirements. A thermal shield prevented direct exposure to the flame by any surface of the test article other than the HF. Each test article was instrumented with nine thermocouples: one on the HF of the can and then at distances of 1, 2, 3, 4, 5, 6, 9, and 12 in. in from the HF.

In addition, foam samples were subjected to thermal decomposition testing in a radiant oven. The exposure temperatures for the tests varied from 70 to 1500 °F and were conducted in air and nitrogen atmospheres. A thermogravimetric analysis (TGA) was conducted to evaluate the sample weight loss as a function of temperature.

Test results, together with visual observations during these and the TRUPACT II HAC fire testing, indicate the following steps in the thermal breakdown of the foam during a HAC fire.

- Below 500 °F, the variation in foam thermal properties with temperature are slight and reversible. As such, fixed values for specific heat and thermal conductivity are appropriate.
- Irreversible thermal degradation of the foam begins as the temperature rises above 500 °F. This degradation is accompanied by a vigorous outgassing from the foam and indeterminate amount of internal heat generation. Although the outgassing removes a significant amount of heat through mass transport processes, quantifying this heat removal as a function of temperature and time would require a complex analysis and series of benchmark tests.
- The weight loss due to outgassing not only has direct effect on the heat flux into the remaining virgin foam, but it changes the composition of the resulting foam char because the foam constituents are lost at different rates. This change in composition affects both the specific heat and the thermal conductivity of the foam char layer.
- As the temperature continues to rise, the developing char layer begins to take on the characteristics of a gas-filled cellular structure where radiative interchange from one cell surface to another becomes a significant portion of the overall heat transfer mechanism. This change in the dominant heat transfer mechanism causes the apparent heat conductivity to take on a highly nonlinear relationship with temperature.
- Finally, at temperatures near 1200 °F, the thermal breakdown of the foam is essentially completed. In the absence of direct exposure to the flame, the char layer will be the same or slightly thicker than the original foam depth. This char layer will continue to provide radiative

shielding to the underlying foam material.

Because of this complex variation in thermal properties, and in absence of a community consensus in the modeling approach necessary, a simplified and conservative modeling approach has been taken for this application. The approach used is the same as that in the HAC fire modeling for the 125B rail packaging SARP. The three main elements of the approach are described below.

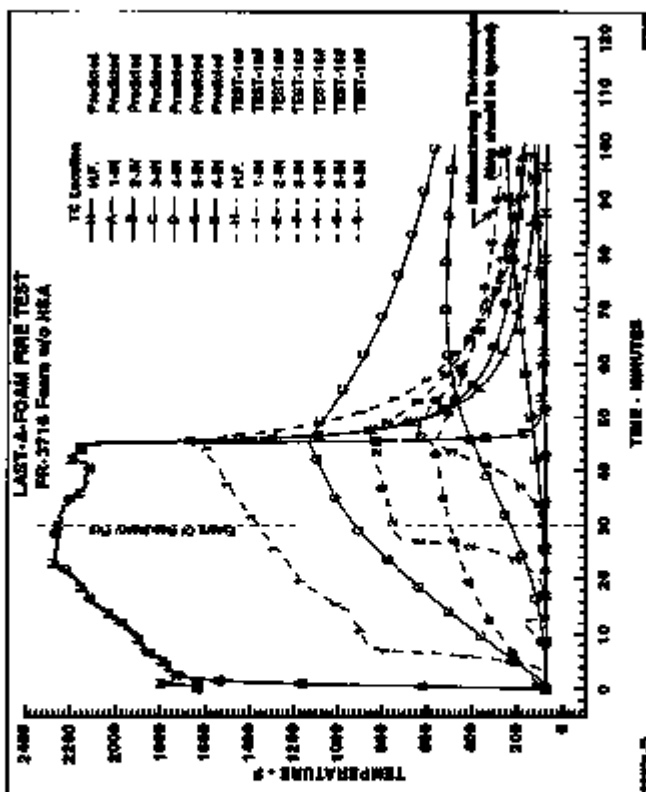
1. For foam temperatures below 400 °F, a fixed specific heat of 0.30 Btu/lbm-°F and a fixed thermal conductivity of 0.278 Btu-in./hr-ft²-°F is used for the 12 lb/ft³ foam. The same fixed specific heat and a fixed thermal conductivity of 0.181 Btu-inch/hr-ft²-°F is used for the 3 lb/ft³ foam.
2. Once the temperature at any foam model node exceeds 400 °F, it is assumed to have been reduced to a char in an instantaneous process. The thermal conductance from the node to the surrounding nodes is replaced by that for an equivalent volume of air. The thermal mass of the node is left unchanged.
3. At the initiation of the HAC fire, the foam nodes adjacent to the exterior surfaces of the impact limiter are assumed to instantaneously ablate away. Heat transfer via conduction across an equivalent air gap and radiation assuming an emissivity of 0.8 is used to compute the heat flux from the impact limiter shell to the next set of interior foam nodes of the impact limiter model.

Figures 3.6.3-1 and 3.6.3-2 illustrate a comparison between the Reference 10 fire test data and the thermal model of the test setup using the above three modeling assumptions. Test data for 8 and 16 lb/ft³ foam is used because it brackets the 12 lb/ft³ foam data used in this application. The HF and the 12-in. T/C temperatures from the test are used as boundary node inputs in the model.

As expected, the simplified modeling assumptions over estimate the foam temperatures near the HF surface for the 8 lb/ft³ foam and at all depths for the 16 lb/ft³ foam. The higher density of the 16 lb/ft³ foam provides a greater amount of material to outgas and, thus, to transport heat away from the underlying foam. In addition, despite flame temperatures up to 700 °F hotter than specified by 10 CFR 71.78, the test data indicates that undisturbed foam depths of 8 in. for 8 lb/ft³ foam or 3 in. for 16 lb/ft³ foam will prevent a rise in the cold face temperature because of the fire accident condition. Direct scaling of these results would yield a requirement for 4 in. of 12 lb/ft³ foam to provide the same level of thermal protection. However, given the significantly lower 10 CFR 71 HAC fire temperatures, as little as 3 in. of 12 lb/ft³ foam is expected to provide thermal protection to the package.

While no equivalent test data exists for the 3 lb/ft³ foam, its performance during the HAC fire can be implied from that seen for the 8, 16, and 24 lb/ft³ foam data. Assuming the required depth varies in proportion with foam thermal conductivity (i.e., greater depth needed for higher conductivity) and inversely with foam density (i.e., less depth needed as more mass is available for outgassing), then a curve fit of the ratio of (density versus the required depth of undisturbed foam can be developed. The resulting relationship indicates a need for 8.7 in. of undisturbed 3 lb/ft³ foam to provide an equivalent level of thermal protection. This conclusion is supported by tests conducted by SANDIA National Laboratory on the SST trailers for Rocky Flats. In these tests, a 1-ft-thick panel of 2 lb/ft³ foam showed no temperature rise on the cold face 30 minutes after HAC fire initiation.

In conclusion, while it does not provide an accurate representation of the thermal properties of the foam, the thermal assumptions used for the foam are shown by Figures 3.6.3-1 and 3.6.3-2 to provide a conservative estimate of the internal foam temperatures. The test data indicates that the 8.3 in. of 3 lb/ft³ foam installed at the bottom of the impact limiter is adequate to protect the center of the OCV base plate against the HAC fire temperatures, while depths of 3 in. or greater in the 12 lb/ft³ foam will provide thermal protection at edges of the OCV base plate.

FIGURE 3.8.3-1. Simplified Foam Model Versus Test Data For 16 lb/ft³ Foam.

3.6.4 SRDA Output For Normal Conditions Of Transport

SYSTEM IMPROVED NUMERICAL DIFFERENCING ANALYZER '85 (Sigma '85)

MODEL = SPY4
STWHLNORMAL TRANSPORT CONDITIONS: 100F AM., FULL SOLAR, SPY4 RTG
SNP Normal Condition Case #1 -- MAX. Temperature For Regulatory Conditions 4/27/94, 10am

SUBMODEL NAME = PTE7

MAX DIFF DELTA T PER ITER	CALCULATED	1963--1.621033E-04	VS.	ALLOWED	2.000000E-03
MAX ARITH DELTA T PER ITER	DALXCC(PTE7	10073--1.831053E-04	VS.	ARLXCC	9.000000E-02
MAX SYSTEM ENERGY BALANCE	ENALXCC	= 0.908099	VS.	ENALBA * EDNTE	= 2.000000E-01
				ENALBA=	1.000000E-04
				ENRMB=	20079.3
ENERGY INTO AND OUT OF SYS	ENRMB		VS.	ENRMB=	20079.3
MAX NORMAL ENERGY BALANCE	ENALXCCPTS7	3663--2.627039E-02	VS.	ENALBA=	1.000000E-03
NUMBER OF ITERATIONS	LODPT	= 1201	VS.	BLDPT=	1200
PROGRAM TIME	TIMER	= 0.	VS.	TIMER=	0.

DIFFUSION NODES IN ASCENDING NODE NUMBER ORDER

T 30=	1293.9	T 51=	1169.4	T 72=	1914.1	T 93=	1250.1	T 114=	1404.3	T 135=	1159.0
T 40=	973.41	T 62=	1210.9	T 83=	664.23	T 104=	481.34	T 125=	489.91	T 146=	484.24
T 112=	485.74	T 133=	483.75	T 154=	334.21	T 175=	368.08	T 196=	548.06	T 217=	513.22
T 225=	815.18	T 246=	435.52	T 267=	438.36	T 288=	566.08	T 309=	562.66	T 330=	562.53
T 354=	326.35	T 375=	525.97	T 396=	446.00	T 417=	445.52	T 438=	548.27	T 459=	549.21
T 482=	561.34	T 503=	563.15	T 524=	327.36	T 545=	326.76	T 566=	643.04	T 587=	642.00
T 615=	536.33	T 636=	332.23	T 657=	333.28	T 678=	315.92	T 699=	514.48	T 720=	435.04
T 753=	424.30	T 774=	300.90	T 795=	498.90	T 816=	516.99	T 837=	514.93	T 858=	481.67
T 891=	468.84	T 912=	397.31	T 933=	395.11	T 954=	392.53	T 975=	393.67	T 996=	393.84
T 1029=	369.75	T 1050=	389.93	T 1071=	387.23	T 1092=	326.07	T 1113=	308.29	T 1134=	251.09
T 1167=	219.80	T 1188=	257.58	T 1209=	248.10	T 1230=	316.12	T 1251=	246.30	T 1272=	507.35
T 1306=	338.33	T 1327=	307.57	T 1348=	338.42	T 1369=	329.47	T 1390=	295.92	T 1411=	251.95
T 1445=	230.44	T 1466=	216.91	T 1487=	221.34	T 1508=	221.84	T 1529=	230.88	T 1550=	228.79
T 1584=	218.37	T 1605=	219.40	T 1626=	216.83	T 1647=	223.53	T 1668=	323.33	T 1689=	322.87
T 1723=	287.45	T 1744=	174.20	T 1765=	226.61	T 1786=	156.19	T 1807=	283.84	T 1828=	262.42
T 1862=	237.06	T 1883=	237.06	T 1904=	284.07	T 1925=	262.78	T 1946=	237.60	T 1967=	237.65
T 2001=	251.28	T 2022=	229.93	T 2043=	211.47	T 2064=	211.47	T 2085=	239.37	T 2106=	220.96
T 2140=	192.55	T 2161=	212.54	T 2182=	189.09	T 2203=	182.85	T 2224=	281.61	T 2245=	190.81
T 2279=	309.80	T 2300=	206.87	T 2321=	209.38	T 2342=	207.99	T 2363=	289.57	T 2384=	210.14
T 2418=	288.59	T 2439=	220.18	T 2460=	210.76	T 2481=	215.78	T 2502=	210.59	T 2523=	289.99
T 2568=	289.21	T 2589=	208.57	T 2610=	204.95	T 2631=	207.85	T 2652=	289.00	T 2673=	289.67
T 2718=	214.85	T 2739=	214.43	T 2760=	309.79	T 2781=	194.98	T 2802=	153.67	T 2823=	122.99
T 2868=	132.28	T 2889=	137.30	T 2910=	142.44	T 2931=	209.28	T 2952=	178.10	T 2973=	154.06
T 3018=	193.87	T 3039=	167.78	T 3060=	146.83	T 3081=	172.44	T 3102=	178.63	T 3123=	175.53
T 3168=	162.09	T 3189=	149.44	T 3210=	138.89	T 3231=	754.18	T 3252=	154.70	T 3273=	151.87
T 3318=	145.15	T 3339=	138.91	T 3360=	133.84	T 3381=	130.45	T 3402=	133.34	T 3423=	131.94

T 454=	150.05	T 495=	128.45	T 454=	128.44			T 199=	279.71	T 238=	276.76
ARITHMETIC NODES IN ASCENDING NODE NUMBER ORDER											
T 158=	494.06	T 199=	491.84	T 168=	499.45	T 169=	502.91	T 199=	279.71	T 238=	276.76
T 311=	260.62	T 512=	260.62	T 321=	261.02	T 322=	261.02	T 331=	228.47	T 332=	228.47
T 337=	213.14	T 341=	279.45	T 357=	308.60	T 358=	307.05	T 399=	209.34	T 379=	210.26
T 483=	299.71	T 1000=	244.23	T 1001=	500.51	T 1002=	279.05	T 1003=	260.38	T 1004=	244.59
T 1005=	263.83	T 1006=	222.37	T 1007=	343.45	T 1008=	327.96	T 1009=	314.27	T 1010=	243.88
T 1011=	283.39	T 1012=	283.39	T 1013=	246.28	T 1021=	283.53	T 1022=	283.55	T 1023=	266.67
T 1031=	250.74	T 1032=	250.74	T 1033=	218.09	T 1041=	225.18	T 1042=	223.18	T 1043=	220.99
T 1044=	226.99	T 1266=	224.79	T 1267=	227.75	T 1268=	225.43	T 1269=	225.52	T 1368=	184.58
T 1347=	284.76										

HEATER NODES IN ASCENDING NODE NUMBER ORDER

NONE

BOUNDARY NODES IN ASCENDING NODE NUMBER ORDER

T 1=	100.00	T 2=	100.00	T 501=	-999.00	T 502=	-999.00
------	--------	------	--------	--------	---------	--------	---------

MEAN (CY GAS TEMP)= 353.6 F MEAN (CY GAS PRESSURE)= 24.41 PSIA

MEAN (CY-CY GAS TEMP)= 284.6 F MEAN (CY-CY GAS PRESSURE)= 24.27 PSIA

SYSTEM IMPROVED NUMERICAL DIFFERENCING ANALYZER (SI CNTRL -MS)

MODEL = QPSS
#DSTLSNORMAL TRANSPORT CONDITIONS: -CDF AND., NO SOLAR, QPSS STD, NO COOLING
SARP Normal Condition Case 02 -- Maximum Temperature Gradients

4/28/96, 4pm

SIMMODEL NAME = PTST

MAX DIFF DELTA T PER ITER	CALCULATED	164)=-1.229703E-04	VS.	ALLOWED	1.000000E-03
MAX WITH DELTA T PER ITER	REL12C(PTST)	168)=-1.229703E-04	VS.	REL12CA	5.000000E-02
MAX SYSTEM ENERGY BALANCE	REL12C(PTST)	=-0.108992	VS.	EMBALA	= EMBALB
	EMBALC			EMBALB	1.000000E-04
				EMBALC	13358.9
				EMBALD	1.000000E-03
EMBALD INTO AND OUT OF STD	EMBALD(PTST)	367)=-2.304650E-02	VS.	EMBALD	1.000000E-03
MAX NORMAL ENERGY BALANCE	LOEPT	= 1291	VS.	RLDPTB	1200
NUMBER OF ITERATIONS	TIMER	= 0.	VS.	TIMEDB	0.
PROBLEM TIME					

DIFFUSION NODES IN ASCENDING NODE NUMBER ORDER																	
T	50=	1727.3	T	91=	1105.1	T	52=	1045.0	T	53=	1168.4	T	54=	1723.3	T	55=	1070.6
T	60=	911.29	T	62=	1125.4	T	100=	406.77	T	105=	420.80	T	107=	628.25	T	110=	422.31
T	112=	425.62	T	113=	425.83	T	120=	470.26	T	122=	484.00	T	125=	484.07	T	126=	447.58
T	125=	447.53	T	126=	361.79	T	127=	361.66	T	130=	481.56	T	132=	497.22	T	133=	497.10
T	134=	459.32	T	135=	458.96	T	136=	378.91	T	137=	379.01	T	140=	482.52	T	143=	486.00
T	142=	495.51	T	143=	497.30	T	144=	459.96	T	145=	458.74	T	146=	369.17	T	147=	344.51
T	150=	465.70	T	152=	481.48	T	153=	482.79	T	154=	443.18	T	155=	442.26	T	156=	352.83
T	157=	339.79	T	160=	417.80	T	161=	417.71	T	162=	431.60	T	163=	631.32	T	164=	395.91
T	165=	382.70	T	166=	290.92	T	167=	293.90	T	170=	288.63	T	172=	299.98	T	173=	289.99
T	175=	268.05	T	177=	273.21	T	180=	281.65	T	190=	205.36	T	191=	184.06	T	192=	114.65
T	193=	168.60	T	194=	123.60	T	195=	103.71	T	196=	189.33	T	197=	190.49	T	198=	183.19
T	200=	244.68	T	204=	203.42	T	210=	228.74	T	220=	229.17	T	230=	172.54	T	240=	116.79
T	242=	89.097	T	250=	73.094	T	260=	75.442	T	261=	76.277	T	262=	73.913	T	263=	74.725
T	264=	71.920	T	265=	73.291	T	266=	70.152	T	267=	79.433	T	268=	78.443	T	269=	77.605
T	300=	147.57	T	301=	-15.935	T	304=	164.81	T	305=	12.075	T	310=	170.76	T	312=	164.94
T	315=	110.48	T	316=	118.46	T	320=	145.30	T	323=	142.23	T	325=	114.73	T	326=	114.73
T	330=	117.43	T	332=	94.005	T	333=	74.430	T	334=	74.450	T	340=	98.262	T	342=	76.850
T	343=	55.294	T	364=	44.665	T	365=	36.295	T	366=	26.399	T	367=	50.443	T	369=	29.705
T	390=	60.819	T	351=	56.913	T	352=	60.183	T	353=	58.378	T	354=	60.511	T	355=	61.312
T	356=	59.221	T	360=	74.322	T	362=	72.506	T	364=	48.676	T	366=	61.669	T	367=	61.118
T	368=	60.230	T	369=	59.493	T	371=	56.809	T	375=	56.073	T	379=	59.601	T	377=	60.642
T	400=	60.881	T	401=	89.280	T	402=	60.846	T	404=	39.732	T	406=	-13.751	T	409=	-34.411
T	410=	-23.433	T	412=	-17.342	T	414=	-11.750	T	421=	54.094	T	422=	27.477	T	423=	1.4094
T	424=	42.564	T	425=	13.210	T	426=	-7.2255	T	431=	12.518	T	432=	21.742	T	433=	20.699
T	434=	7.2220	T	435=	-9.3575	T	436=	-17.394	T	441=	-8.0580	T	442=	-4.2604	T	443=	-5.2707
T	444=	-11.826	T	446=	-17.122	T	446=	-22.043	T	451=	-22.431	T	452=	-26.596	T	453=	-28.488
T	454=	-27.810	T	455=	-28.444	T	456=	-28.099									

ARITHMETIC NODES IN ASCENDING NODE NUMBER ORDER

T 150= 415.78	T 195= 410.40	T 140= 419.26	T 160= 422.66	T 180= 158.05	T 230= 148.32
T 211= 144.99	T 312= 144.99	T 321= 140.36	T 322= 140.36	T 331= 92.385	T 332= 92.385
T 337= 68.337	T 341= 75.005	T 337= 39.947	T 350= 84.842	T 380= 68.480	T 370= 81.447
F 405= 80.705	T 1000= 181.98	F 1001= 173.69	T 1002= 149.11	F 1003= 129.82	T 1004= 186.15
F 1005= 105.24	T 1006= 76.917	F 1007= 225.21	T 1008= 206.20	F 1009= 191.48	T 1010= 185.02
T 1011= 170.32	T 1012= 170.32	T 1013= 128.33	T 1021= 164.88	T 1022= 144.88	T 1023= 124.70
T 1031= 117.89	T 1032= 117.00	T 1033= 81.520	T 1041= 98.145	T 1042= 98.145	T 1043= 76.947
T 1044= 76.947	T 1264= 80.194	T 1267= 98.450	T 1268= 92.143	T 1269= 81.244	T 1346= 29.821
T 1367= 54.581					

HEATER NODES IN ASCENDING NODE NUMBER ORDER

BOME

BOUNDARY NODES IN ASCENDING NODE NUMBER ORDER

T 1= -48.000	T 2= -40.880	T 901= -999.00	T 902= -999.00
--------------	--------------	----------------	----------------

MEAN ICV GAS TEMP= 235.9 F MEAN ICV GAS PRESSURE= 21.43 PSIA

MEAN ICV-OCV GAS TEMP= 165.1 F MEAN ICV-OCV GAS PRESSURE= 22.85 PSIA

SYSTEMS IMPROVED NUMERICAL DIFFERENCING ANALYZER '85 (SINDA '85)

MODEL = OPW6
STRTFLNORMAL TRANSPORT CONDITIONS: 100F AIR, FULL SOLAR, GPRE RTG, ACTIVE COOLING
SARP Normal Condition Case 05 -- Simulated Conditions in Vented Trailer 4/26/96, 10pm

RUNMODEL NAME = P187

MAX DIFF DELTA T PER ITER	CALCULATED	143=	1.83103E-04	VS.	ALLOWED	2.00000E-03
MAX ARITH DELTA T PER ITER	DELTA(COPT)??	1090=	-6.70351E-05	VS.	DELTA(C)	5.00000E-02
MAX SYSTEM ENERGY BALANCE	DELTA(EOPT)??	=	-2.504923E-02	VS.	EMAX(IA)	5.00000E-01
	EMALSC				EMAX(II)	2.00793
					EMAX(III)	1.00000E-04
ENERGY INTO AND OUT OF SYS	EMIN(IE)		30079.5		EMAX(IV)	20079.3
NAT NORMAL ENERGY BALANCE	EMALSC(OPT)??	330=	-4.953709E-02	VS.	EMAX(V)	1.00000E-03
NUMBER OF ITERATIONS	LOOPCT		1281	VS.	EMAX(VI)	1280
PROBLEM TIME	TIMER		0.	VS.	TIMEEND	0.

		DIFFUSION		NODES IN PROGRESS		NODE ORDER											
T	50=	1716.6	T	51=	1094.9	T	52=	1833.0	T	53=	1134.3	T	54=	1688.5	T	55=	1842.0
T	60=	907.89	T	62=	1067.4	T	100=	690.06	T	105=	623.68	T	107=	629.32	T	110=	621.67
T	112=	623.18	T	113=	623.18	T	120=	662.68	T	122=	676.31	T	123=	676.30	T	124=	680.66
T	125=	629.40	T	126=	633.93	T	127=	633.75	T	130=	646.16	T	132=	644.71	T	132=	644.62
T	134=	625.78	T	135=	625.48	T	136=	631.53	T	137=	631.08	T	140=	647.36	T	141=	649.28
T	142=	666.34	T	143=	662.25	T	144=	625.54	T	145=	622.89	T	146=	626.95	T	147=	621.28
T	150=	628.73	T	152=	644.58	T	153=	645.99	T	154=	605.88	T	155=	606.53	T	156=	608.60
T	157=	604.08	T	160=	682.33	T	161=	682.99	T	162=	694.82	T	163=	696.61	T	164=	668.67
T	165=	647.61	T	166=	668.61	T	167=	655.73	T	170=	646.19	T	172=	647.59	T	173=	647.59
T	175=	616.09	T	177=	629.64	T	180=	639.68	T	190=	156.36	T	191=	157.52	T	192=	106.43
T	193=	121.61	T	194=	906.68	T	195=	90.882	T	196=	941.89	T	197=	102.52	T	198=	136.89
T	200=	676.80	T	204=	696.97	T	210=	698.93	T	220=	694.32	T	230=	117.85	T	260=	77.762
T	242=	76.929	T	250=	83.473	T	260=	87.321	T	261=	87.423	T	262=	86.323	T	263=	86.514
T	264=	85.332	T	265=	85.388	T	266=	84.770	T	267=	87.577	T	268=	87.576	T	269=	87.326
T	300=	222.44	T	301=	167.43	T	304=	177.88	T	305=	135.36	T	310=	64.166	T	311=	44.660
T	312=	64.669	T	313=	51.890	T	315=	49.894	T	316=	49.894	T	320=	58.601	T	321=	42.925
T	322=	42.929	T	323=	48.418	T	325=	48.075	T	326=	48.075	T	330=	54.685	T	331=	41.648
T	332=	41.640	T	333=	46.137	T	333=	46.779	T	336=	46.779	T	340=	49.230	T	342=	61.982
T	343=	95.132	T	344=	79.513	T	345=	92.439	T	346=	96.169	T	347=	88.919	T	349=	101.29
T	350=	84.744	T	351=	86.361	T	352=	85.139	T	353=	86.026	T	354=	84.125	T	355=	85.531
T	356=	85.149	T	360=	86.901	T	362=	86.175	T	364=	85.408	T	366=	85.434	T	367=	85.567
T	368=	85.905	T	369=	86.078	T	371=	86.609	T	373=	86.307	T	378=	85.932	T	377=	85.864
T	400=	86.189	T	401=	86.370	T	402=	85.853	T	404=	95.096	T	406=	122.86	T	408=	119.25
T	410=	115.85	T	412=	113.99	T	414=	112.74	T	421=	98.844	T	422=	99.602	T	423=	98.05
T	426=	92.989	T	425=	102.43	T	426=	110.39	T	431=	106.02	T	432=	102.12	T	433=	101.39
T	434=	105.50	T	435=	109.72	T	436=	113.75	T	441=	116.22	T	442=	119.33	T	443=	110.38
T	444=	111.73	T	445=	113.63	T	446=	115.32	T	451=	119.13	T	452=	117.86	T	453=	116.60

T 434= 114.90	T 435= 117.33	T 436= 117.84	ARITHMETIC NODES IN ASCENDING NODE NUMBER ORDER					
T 156= 379.78	T 159= 375.61	T 168= 384.37	T 169= 387.88	T 199= 117.98	T 256= 109.38			
T 337= 34.396	T 341= 38.892	T 337= 38.892	T 338= 84.373	T 339= 84.944	T 370= 85.308			
T 408= 85.842	T 1000= 98.637	T 1001= 132.84	T 1002= 117.75	T 1003= 109.76	T 1004= 108.82			
T 1005= 100.21	T 1006= 87.613	T 1007= 182.47	T 1008= 160.95	T 1009= 144.79	T 1010= 91.860			
T 1011= 58.790	T 1012= 58.790	T 1013= 51.070	T 1021= 54.511	T 1022= 54.511	T 1023= 48.956			
T 1031= 50.948	T 1032= 58.948	T 1033= 47.275	T 1041= 47.143	T 1042= 47.143	T 1043= 56.424			
T 1044= 56.424	T 1266= 89.091	T 1267= 93.193	T 1268= 91.608	T 1269= 88.388	T 1348= 94.223			
T 1347= 87.235								

HEATER NODES IN ASCENDING NODE NUMBER ORDER

==NODE==

BOUNDARY NODES IN ASCENDING NODE NUMBER ORDER

T 1= 100.00 F 2= 100.00 F 901= 48.000 T 902= 40.000

MEAN ICV GAS TEMP= 212.8 F MEAN ICV GAS PRESSURE= 28.15 PSIA

MEAN ICV-DCV GAS TEMP= 115.1 F MEAN ICV-DCV GAS PRESSURE= 20.27 PSIA

SYSTEMS IMPROVED NUMERICAL DIFFERENCING ANALYZER '86 (SIBMA '86)

MODEL = CPW64
STEELNORMAL TRANSPORT CONDITIONS: 100F AM, NO DELAY, SPED RTG, NO COOLING
SARP Normal Condition Case 34 -- Pre-RAC Steady-State Condition

4/27/94, 11m

SUBMODEL NAME = P187

MAX DIFF DELTA T PER ITER	CALCULATED		ALLOWED
MAX ARITH DELTA T PER ITER	DLNDC(P187)	26814	DLNDCA= 2,800000E-03
MAX SYSTEM ENERGY BALANCE	ARLNDC(P187)	3321	ARLNCA= 5,800000E-02
	ERLALC	*-2.956650E-02	ERLACA = 8.0001E
			* 1.52585
ENERGY INTO AND OUT OF SYS	ERLALB	= 15358.5	ERLALB= 1,800000E-04
MAX NORMAL ENERGY BALANCE	ERLALB(P187)	3261	ERLALB= 13399.2
NUMBER OF ITERATIONS	LDOPCT	= 1201	ERLALB= 1,800000E-03
PROBLER TIME	TIME1	= 0.	VS. ELSP01= 1200
			VS. TIME01= 0.

DIFFUSION NODES IN ASCENDING NODE NUMBER ORDER	
T	S
T 50= 1794.1	T 51= 1761.6
T 60= 963.66	T 62= 1203.9
T 112= 477.96	T 113= 477.07
T 121= 505.17	T 126= 426.33
T 134= 518.63	T 125= 518.25
T 142= 353.75	T 143= 393.57
T 150= 920.30	T 152= 566.90
T 157= 616.54	T 160= 491.06
T 165= 458.54	T 166= 385.75
T 175= 356.51	T 177= 367.96
T 199= 274.73	T 194= 239.00
T 200= 326.59	T 204= 294.26
T 242= 211.22	T 250= 199.13
T 264= 197.41	T 265= 196.54
T 300= 232.66	T 301= 138.68
T 315= 225.23	T 316= 225.23
T 330= 225.34	T 333= 213.80
T 343= 186.88	T 344= 191.16
T 350= 187.94	T 351= 184.48
T 356= 186.37	T 360= 199.36
T 368= 187.60	T 369= 186.71
T 400= 195.76	T 401= 195.33
T 410= 113.04	T 412= 117.97
T 424= 171.82	T 425= 147.36
T 434= 161.35	T 435= 129.62
T 444= 125.07	T 445= 119.23
T 454= 118.65	T 455= 109.19
	T 464= 108.27
	T 470= 1006.2
	T 484= 484.48
	T 120= 526.41
	T 127= 436.39
	T 136= 437.36
	T 144= 319.77
	T 153= 545.07
	T 161= 408.42
	T 167= 381.28
	T 180= 374.45
	T 195= 221.17
	T 210= 319.47
	T 200= 388.58
	T 266= 195.77
	T 384= 219.55
	T 320= 271.83
	T 335= 195.49
	T 345= 167.59
	T 352= 167.39
	T 362= 197.79
	T 371= 184.66
	T 402= 188.83
	T 434= 123.96
	T 428= 127.17
	T 436= 118.61
	T 446= 114.48
	T 454= 116.48
	T 50= 1228.3
	T 105= 475.64
	T 122= 548.27
	T 130= 539.37
	T 137= 634.88
	T 143= 318.91
	T 154= 567.49
	T 162= 505.02
	T 170= 389.03
	T 190= 311.58
	T 196= 380.87
	T 220= 317.83
	T 201= 281.12
	T 267= 202.97
	T 305= 143.52
	T 323= 250.54
	T 336= 195.49
	T 346= 157.83
	T 353= 185.80
	T 364= 196.58
	T 373= 185.56
	T 404= 172.19
	T 421= 182.44
	T 431= 148.90
	T 441= 139.78
	T 451= 116.48
	T 54= 1794.8
	T 107= 482.18
	T 123= 540.27
	T 132= 335.11
	T 140= 340.69
	T 148= 437.19
	T 155= 306.86
	T 163= 304.59
	T 172= 381.37
	T 191= 283.15
	T 197= 227.71
	T 230= 281.23
	T 262= 199.22
	T 269= 202.97
	T 310= 272.10
	T 325= 225.39
	T 340= 218.19
	T 347= 179.40
	T 354= 187.66
	T 366= 188.86
	T 375= 187.00
	T 406= 127.92
	T 422= 157.84
	T 432= 156.11
	T 442= 132.49
	T 452= 113.43
	T 55= 1160.2
	T 110= 476.43
	T 124= 305.22
	T 133= 354.99
	T 141= 341.68
	T 147= 423.87
	T 156= 425.33
	T 164= 471.61
	T 175= 381.37
	T 182= 232.37
	T 198= 292.62
	T 240= 235.01
	T 263= 199.97
	T 269= 202.25
	T 313= 250.66
	T 326= 225.39
	T 342= 201.28
	T 349= 162.29
	T 355= 186.38
	T 367= 188.21
	T 377= 187.88
	T 488= 183.95
	T 423= 134.39
	T 433= 134.61
	T 443= 120.85
	T 432= 112.28

ARITHMETIC NODES IN ASCENDING NODE NUMBER ORDER

T 150=	485.30	T 159=	482.14	T 168=	490.07	T 169=	493.31	T 199=	263.19	I 230=	261.10
T 311=	248.88	T 312=	248.88	T 321=	248.78	T 322=	248.78	T 331=	212.30	F 332=	212.30
T 337=	192.49	T 341=	199.68	T 357=	196.10	T 358=	194.52	T 359=	187.65	T 370=	168.50
T 488=	187.92	T 1000=	225.33	T 1001=	204.82	T 1002=	242.45	T 1003=	242.42	T 1004=	225.60
T 1005=	224.80	T 1006=	201.69	T 1007=	329.68	T 1008=	313.81	T 1009=	299.38	F 1010=	234.57
T 1011=	271.57	T 1012=	271.57	T 1013=	234.41	T 1021=	271.30	T 1022=	271.30	F 1023=	234.43
T 1031=	234.91	T 1032=	234.91	T 1033=	202.07	T 1041=	218.41	T 1042=	218.41	F 1043=	201.37
T 1044=	201.37	T 1266=	204.34	T 1267=	218.87	T 1268=	213.96	T 1269=	209.15	T 1346=	162.88
T 1347=	182.70										

READER NODES IN ASCENDING NODE NUMBER ORDER

--NONE--

BOUNDARY NODES IN ASCENDING NODE NUMBER ORDER

T 1= 100.00 T 2= 100.00 T 981= -999.00 T 992= -999.00

MEAN IDV GAS TEMP= 342.3 F MEAN IDV GAS PRESSURE= 24.07 PSIA

MEAN IDV-DEV GAS TEMP= 270.7 F MEAN IDV-DEV GAS PRESSURE= 25.78 PSIA

SYSTEM IMPROVED NUMERICAL DIFFERENTIAL ANALYSIS '95 (SIMBA '95)

MODEL = 0P934
ST00TLNORMAL TRANSPORT CONDITIONS: 200F AMB., NO SOLAR, 0000 RTG, NO COOLING
SARP Normal Condition Case 45 -- Alternative Pre-RAC Steady-State Condition 4/28/94, 3pm

SUBMODEL NAME = P187

MAX DIFF DELTA 1 PER ITER	ALLOWED	2491= 4.182514E-08	VS. DR1XCA= 2.000000E-08
MAX ARITH DELTA 1 PER ITER	DR1XCA= 1.226702E-04	9810= 1.226702E-04	VS. AR1XCA= 5.000000E-02
MAX SYSTEM ENERGY BALANCE	DR1XCA= 1.226702E-04	a=0.184330	VS. DR1XCA= 5.000000E-02
	ERUNIS		VS. ERUNIS = 1.000000E-04 * 1.E25E8
ENERGY INTO AND OUT OF SVT	ERUNIS= 15355.5		VS. ERUNIS= 15355.5
MAX NORMAL ENERGY BALANCE	ERUNIS= 3.368978E-02	3791= 3.368978E-02	VS. ERUNIS= 1.000000E-05
NUMBER OF ITERATIONS	LOOPCT	n = 1201	VS. LOOPCT= 1200
PROBLEM TIME	TIME	n = 0.	VS. TIME= 0.

		DIFFUSION NODES IN ASCENDING		NODE NUMBER ORDER				
T	50=	1113.1	1	50=	1054.5	1	53=	
T	50=	1735.3		50=	1054.5		53=	1177.0
T	60=	916.88		100=	411.94		105=	428.12
T	60=	916.88		100=	411.94		105=	428.12
T	110=	431.36		120=	478.79		120=	492.08
T	110=	431.36		120=	478.79		120=	492.08
T	125=	433.47		127=	370.81		130=	489.81
T	125=	433.47		127=	370.81		130=	489.81
T	134=	447.78		134=	388.08		137=	379.59
T	134=	447.78		134=	388.08		137=	379.59
T	142=	503.83		144=	448.48		143=	447.53
T	142=	503.83		144=	448.48		143=	447.53
T	150=	474.77		158=	491.74		154=	458.43
T	150=	474.77		158=	491.74		154=	458.43
T	157=	330.41		161=	437.59		163=	443.71
T	157=	330.41		161=	437.59		163=	443.71
T	165=	302.85		167=	384.82		170=	348.11
T	165=	302.85		167=	384.82		170=	348.11
T	175=	274.34		180=	295.23		190=	221.93
T	175=	274.34		180=	295.23		190=	221.93
T	193=	177.89		194=	140.98		196=	206.17
T	193=	177.89		194=	140.98		196=	206.17
T	200=	256.50		210=	242.08		220=	234.68
T	200=	256.50		210=	242.08		220=	234.68
T	242=	107.21		250=	91.611		261=	94.762
T	242=	107.21		250=	91.611		261=	94.762
T	264=	90.510		265=	89.737		267=	90.679
T	264=	90.510		265=	89.737		267=	90.679
T	300=	163.24		301=	5.6498		305=	31.927
T	300=	163.24		301=	5.6498		305=	31.927
T	313=	134.34		314=	134.34		320=	151.16
T	313=	134.34		314=	134.34		320=	151.16
T	330=	134.89		333=	111.84		336=	92.434
T	330=	134.89		333=	111.84		336=	92.434
T	343=	54.821		344=	83.413		345=	44.195
T	343=	54.821		344=	83.413		345=	44.195
T	350=	79.666		351=	75.887		352=	77.259
T	350=	79.666		351=	75.887		352=	77.259
T	354=	78.083		360=	62.833		364=	87.317
T	354=	78.083		360=	62.833		364=	87.317
T	368=	79.854		369=	78.521		371=	78.793
T	368=	79.854		369=	78.521		371=	78.793
T	400=	86.521		401=	87.946		402=	79.674
T	400=	86.521		401=	87.946		402=	79.674
T	410=	-3.8082		412=	2.1189		414=	8.2887
T	410=	-3.8082		412=	2.1189		414=	8.2887
T	424=	61.376		425=	34.441		428=	12.198
T	424=	61.376		425=	34.441		428=	12.198
T	434=	24.746		435=	13.987		438=	2.2809
T	434=	24.746		435=	13.987		438=	2.2809
T	444=	8.6613		445=	8.9501		446=	-2.6088
T	444=	8.6613		445=	8.9501		446=	-2.6088
T	454=	-7.2080		455=	-8.6772		456=	-8.3575
T	454=	-7.2080		455=	-8.6772		456=	-8.3575

ARITHMETIC NODES IN ASCENDING NODE NUMBER ORDER

T 156=	424.18	T 159=	421.00	T 168=	429.35	T 169=	432.78	T 199=	166.90	T 238=	165.05
T 111=	160.38	T 312=	160.38	T 321=	156.52	T 322=	156.52	T 331=	110.24	T 332=	110.24
T 237=	85.877	T 541=	93.526	T 352=	75.011	T 398=	75.754	T 389=	79.322	T 379=	80.269
T 483=	79.536	T 1008=	125.73	T 1001=	198.22	T 1002=	169.99	T 1003=	143.34	T 1904=	123.88
T 1005=	122.99	T 1006=	95.394	T 1007=	243.22	T 1008=	223.88	T 1009=	207.50	T 1010=	122.61
T 1011=	185.30	T 1012=	183.38	T 1013=	144.59	T 1021=	188.73	T 1022=	180.73	T 1023=	141.87
T 1031=	134.64	T 1032=	134.64	T 1033=	99.467	T 1041=	116.09	T 1042=	116.09	T 1043=	95.445
T 1064=	95.445	T 1266=	98.584	T 1267=	118.27	T 1268=	118.27	T 1269=	89.597	T 1266=	49.434
T 1347=	73.680										

HEATER NODES IN ASCENDING NODE NUMBER ORDER

NONE

BOUNDARY NODES IN ASCENDING NODE NUMBER ORDER

T 1=	-20.000	T 2=	-20.000	T 901=	-999.00	T 982=	-999.00
------	---------	------	---------	--------	---------	--------	---------

MEAN ICY GAS TEMP= 246.6 F MEAN ICY GAS PRESSURE= 21.06 PSIA

MEAN ICY-OCY GAS TEMP= 180.7 F MEAN ICY-OCY GAS PRESSURE= 22.60 PSIA

SYSTEMS IMPROVED NUMERICAL DIFFERENCING ANALYZER '85 (SINBA '85)

MODEL = GPNDA
STD61LNORMAL TRANSPORT CONDITIONS: 100% NH₃, NO SOLAR, GPM RTG, ACTIVE ECOLINE
SARP Normal Condition Case 96 -- Compliance w/ 10 EPR 71.43c) 4/27/94, 10m

RUNMODEL NAME = P157

MAX DIFF DELTA T PER ITER	CALCULATED DELTA(CP)ST	197)=-1.220780E-04	VS. ALLOWED	2.000000E-03	
MAX ARITH DELTA T PER ITER	ARLX(CD)PTK7	199)=-1.831455E-06	VS. ALLOWED	5.000000E-02	
MAX SYSTEM ENERGY BALANCE	EBAL3C	=-0.102929	VS. EBAL3L	0.000000E+00	= 1.76592
			VS. EBAL3R	1.000000E-06	
ENERGY INTO AND OUT OF SYS	EBAL3L	= 17659.2	VS. EBAL3D	17659.6	
MAX NORMAL ENERGY BALANCE	EBALX(CP)T07	379)=-3.663809E-02	VS. EBAL3M	1.000000E-05	
NUMBER OF ITERATIONS	LOOPT7	= 1291	VS. MLOOPT	1200	
PROBLET TIME	TIME97	= 0.	VS. TIME10	0.	

DIFFUSION MODES IN ACCORDING MODE NUMBER ORDER

T 50= 1711.1	T 91= 1091.1	T 82= 1811.0	T 85= 1132.6	T 54= 1686.6	T 53= 1840.1
T 48= 905.69	T 48= 1085.3	T 90= 409.32	T 105= 418.17	T 90= 425.00	T 110= 417.29
T 112= 418.88	T 113= 418.88	T 120= 458.62	T 122= 472.34	T 125= 472.33	T 126= 485.41
T 125= 435.35	T 126= 369.24	T 127= 349.86	T 130= 447.88	T 132= 462.67	T 133= 462.39
T 134= 423.66	T 135= 423.29	T 134= 329.16	T 137= 328.69	T 140= 443.62	T 141= 447.36
T 142= 458.61	T 143= 460.52	T 144= 421.79	T 145= 420.31	T 146= 324.94	T 147= 319.19
T 150= 427.11	T 152= 442.86	T 153= 444.35	T 154= 403.62	T 155= 402.89	T 156= 306.75
T 157= 292.17	T 160= 580.64	T 161= 381.16	T 163= 394.92	T 163= 394.72	T 164= 358.71
T 165= 345.65	T 166= 258.38	T 167= 253.37	T 170= 244.04	T 172= 245.44	T 173= 245.44
T 175= 213.79	T 177= 227.38	T 180= 237.44	T 190= 153.05	T 191= 134.60	T 192= 95.665
T 193= 117.84	T 194= 97.840	T 195= 89.304	T 196= 138.78	T 197= 92.950	T 198= 133.92
T 200= 265.59	T 204= 228.57	T 210= 148.99	T 220= 135.18	T 230= 116.23	T 240= 74.444
T 242= 89.333	T 250= 71.349	T 260= 75.780	T 261= 75.832	T 262= 73.721	T 263= 74.013
T 264= 72.577	T 265= 72.814	T 266= 71.810	T 267= 75.592	T 268= 75.533	T 269= 75.197
T 300= 288.38	T 301= 121.12	T 304= 162.13	T 305= 122.71	T 310= 65.139	T 311= 44.807
T 312= 44.807	T 313= 58.192	T 315= 46.397	T 316= 48.337	T 320= 37.067	T 321= 43.568
T 322= 42.582	T 325= 47.714	T 326= 44.655	T 328= 44.688	T 330= 53.791	T 331= 41.391
T 332= 41.391	T 333= 45.315	T 338= 45.226	T 336= 45.226	T 340= 48.054	T 342= 55.811
T 343= 71.741	T 344= 66.881	T 345= 72.147	T 346= 71.430	T 347= 70.853	T 349= 73.874
T 350= 69.973	T 351= 70.309	T 352= 70.160	T 353= 70.489	T 354= 69.388	T 355= 70.748
T 356= 69.944	T 360= 75.280	T 362= 75.341	T 364= 72.044	T 366= 70.784	T 367= 70.754
T 368= 70.685	T 369= 70.890	T 371= 70.256	T 373= 70.339	T 375= 70.688	T 377= 70.941
T 400= 72.981	T 401= 73.119	T 402= 70.995	T 404= 75.376	T 406= 88.721	T 408= 98.461
T 410= 95.665	T 412= 94.161	T 414= 92.719	T 421= 76.443	T 422= 83.887	T 423= 80.568
T 424= 76.473	T 425= 84.342	T 426= 91.176	T 431= 82.699	T 432= 80.775	T 433= 81.466
T 434= 86.149	T 435= 90.214	T 436= 93.828	T 441= 88.525	T 442= 88.571	T 443= 89.342
T 444= 91.468	T 445= 93.497	T 446= 93.141	T 451= 93.528	T 452= 95.184	T 453= 95.433

T 454=	96.237	T 455=	96.762	T 456=	96.795						
ARITHMETIC NODES IN ASCENDING NODE NUMBER ORDER											
T 758=	376.91	T 190=	373.76	T 100=	392.54	T 109=	395.82	T 199=	113.02	T 238=	98.039
T 337=	50.732	T 341=	53.331	T 397=	69.795	T 398=	70.289	T 399=	70.069	T 379=	70.763
T 403=	70.957	T 1000=	89.781	T 1001=	128.88	T 1002=	112.72	T 1003=	181.93	T 1004=	91.074
T 1005=	90.587	T 1006=	75.290	T 1007=	188.05	T 1009=	158.43	T 1009=	141.98	T 1010=	83.541
T 1011=	57.916	T 1012=	57.916	T 1013=	45.621	T 1021=	53.779	T 1022=	53.770	T 1023=	47.618
T 1031=	50.390	T 1032=	50.390	T 1033=	45.887	T 1041=	44.287	T 1042=	44.287	T 1043=	51.866
T 1044=	51.866	T 1266=	74.296	T 1267=	83.787	T 1268=	81.436	T 1269=	76.720	T 1346=	72.951
T 1347=	78.966										

HEATER NODES IN ASCENDING NODE NUMBER ORDER

NONE

BOUNDARY NODES IN ASCENDING NODE NUMBER ORDER

T 1=	100.00	T 2=	100.00	T 901=	40.800	T 902=	40.800
------	--------	------	--------	--------	--------	--------	--------

MEAN ICV GAS TEMP= 209.6 F MEAN ICV GAS PRESSURE= 20.18 PSIA

MEAN ICV-OXY GAS TEMP= 111.4 F MEAN ICV-OXY GAS PRESSURE= 20.16 PSIA

SYSTEMS IMPROVED NUMERICAL DIFFERENCING ANALYZER '85 (SINUM '85)

MODEL = SP44
STRTLNORMAL OPERATIONAL CONDITIONS, AMB. TEMP= 70F, NO SOLAR, 6PH RTG, ACTIVE COOLING
SARP Normal Condition Case #7 -- Simulated Conditions At Facility 4/27/98, Yes

SUBJECT NAME = PR37

MAX DIFF DELTA T PER ITER	CALCULATED		ALLOWED
MAX XDIRT DELTA Y PER ITER	EMALXZ(PTR)?	128)= 1.220780E-06	VS. EMALXZ= 2.000000E-03
MAX SYSTEM ENERGY BALANCE	EMALXZ(PTR)?	1003)= 6.163516E-05	VS. EMALXZ= 5.000000E-02
	EMALXZ	= 6.303866E-02	VS. EMALXZ = 1.000000E-06
			= 1.34235
ENERGY INTO AND OUT OF SYS	ESINUS	= 25432.8	VS. ESINUS= 15434.7
MAX MINOR ENERGY BALANCE	EMALXZ(PTR)?	132)= 3.484325E-02	VS. EMALXZ= 1.000000E-05
NUMBER OF ITERATIONS	LOOPCT	= 1291	VS. LOOPCT= 1200
PROBLEM TIME	TIMEH	= 0.	VS. TIMEH= 0.

DIFFUSION NODES IN ASCENDING NODS NUMBER ORDER																	
T	50=	1707.0	T	51=	1066.8	T	52=	1808.8	T	53=	1130.5	T	54=	1086.5	T	55=	1030.1
T	60=	808.97	T	62=	1085.4	T	100=	399.98	T	105=	613.08	T	107=	428.07	T	110=	412.32
T	112=	413.83	T	113=	413.86	T	120=	654.08	T	122=	467.81	T	123=	467.80	T	126=	430.78
T	128=	430.72	T	129=	343.88	T	127=	343.78	T	130=	644.69	T	132=	460.29	T	133=	440.17
T	134=	421.26	T	135=	420.87	T	136=	326.43	T	137=	325.96	T	140=	443.68	T	141=	445.60
T	142=	456.63	T	143=	458.54	T	144=	419.78	T	145=	418.28	T	146=	322.65	T	147=	316.88
T	150=	425.30	T	152=	441.86	T	153=	442.54	T	154=	401.58	T	155=	601.08	T	156=	386.69
T	157=	298.05	T	160=	378.79	T	161=	379.27	T	162=	392.97	T	163=	392.78	T	164=	356.78
T	165=	343.64	T	166=	295.05	T	167=	296.96	T	170=	262.12	T	172=	243.52	T	173=	243.52
T	175=	211.83	T	177=	225.43	T	180=	235.54	T	190=	351.96	T	191=	132.51	T	192=	90.221
T	195=	115.11	T	196=	93.445	T	199=	85.642	T	194=	136.17	T	197=	57.424	T	198=	131.61
T	200=	225.04	T	204=	208.71	T	210=	146.72	T	220=	131.82	T	230=	114.79	T	240=	72.194
T	243=	64.875	T	250=	64.084	T	260=	67.226	T	261=	67.550	T	262=	66.136	T	263=	66.488
T	264=	66.929	T	265=	65.381	T	266=	64.848	T	267=	68.280	T	268=	68.282	T	269=	67.871
T	300=	191.87	T	301=	92.096	T	304=	163.86	T	305=	97.247	T	310=	61.853	T	311=	43.616
T	312=	63.416	T	313=	48.951	T	315=	46.898	T	316=	46.016	T	320=	37.217	T	321=	42.184
T	322=	62.366	T	323=	46.743	T	325=	44.520	T	326=	44.920	T	330=	53.108	T	331=	41.125
T	332=	61.725	T	333=	46.410	T	339=	43.209	T	336=	43.209	T	340=	47.089	T	342=	52.887
T	343=	59.375	T	344=	59.141	T	345=	59.996	T	348=	57.818	T	347=	60.681	T	349=	60.180
T	350=	61.371	T	351=	61.087	T	352=	61.336	T	353=	61.300	T	354=	60.761	T	359=	61.757
T	356=	61.636	T	360=	64.889	T	362=	65.615	T	364=	66.625	T	366=	62.862	T	367=	61.932
T	368=	61.904	T	369=	61.808	T	371=	68.964	T	373=	61.205	T	375=	61.688	T	377=	62.811
T	400=	64.959	T	401=	64.977	T	402=	62.088	T	404=	62.698	T	406=	65.221	T	408=	69.318
T	410=	68.686	T	412=	68.349	T	414=	68.092	T	421=	65.397	T	422=	66.635	T	423=	67.561
T	426=	65.615	T	428=	68.839	T	429=	67.565	T	431=	66.209	T	432=	66.080	T	433=	66.595
T	434=	65.950	T	435=	67.162	T	436=	66.783	T	441=	65.721	T	442=	66.226	T	443=	66.660
T	444=	67.382	T	445=	66.616	T	446=	68.515	T	491=	67.469	T	492=	68.256	T	493=	68.696

SYSTEMS IMPROVED NUMERICAL DIFFERENTIATION ANALYZER '86 (SIMDA '86)

PAGE 1/1

MODEL = QMSA
RDSCKLOAD TRANSPORT W/ QMSA STD, Worst Case Load Procedure Timing Head
Normal Condition Case 40 -- Peak ICY Sidewall Temperature

SUBMODEL NAME = PT37

MAX DIFF DELTA 1 PER ITER	CALCULATED	0)=	0.	VS. ALLOWED	2.800000E-03
MAX ARITH DELTA 1 PER ITER	DELTA(C)	1004)=	2.543477E-03	VS. ABSNCA=	3.800000E-02
MAX DIFF DEL 2 PER TIME STEP	DELTA(CP1ST)	62)=	3.295908E-03	VS. DTMPCA=	20.0000
MAX ARITH DEL 2 PER TIME STEP	DELTA(CP2ST)	1004)=	2.563477E-03	VS. ATMPCA=	50.0000
MIN STABILITY CRITERIA	CRMIN(CP1ST)	161)=	1.582954E-02		
MIN STABILITY CRITERIA	CRMIN(CP2ST)	434)=	4.81424		
NUMBER OF ITERATIONS	LOOPCT	=	1	VS. MLOOPCT=	800
PROBLEM TIME	TIMER	=	8.50008	VS. TIMER=	8.50000
TIME STEP USED	DTIME	=	8.258888E-04	VS. DTIME1=	8.

		DIFFUSION NODES IN ASCENDING NODE NUMBER ORDER						
		50=	51=	52=	53=	54=	55=	
T	50=	173.5	T	51=	1125.9	T	52=	1855.8
T	53=	1179.7	T	54=	1735.7	T	55=	1091.6
T	60=	929.47	T	62=	1137.9	T	180=	428.60
T	185=	444.83	T	190=	428.60	T	195=	112.15
T	112=	446.82	T	113=	446.83	T	120=	492.24
T	122=	545.96	T	123=	505.97	T	124=	478.10
T	125=	470.05	T	126=	388.01	T	127=	387.85
T	130=	499.44	T	132=	511.04	T	133=	510.71
T	134=	473.53	T	135=	473.14	T	136=	386.75
T	137=	386.75	T	138=	472.85	T	139=	471.77
T	142=	508.07	T	143=	589.04	T	144=	384.14
T	146=	495.11	T	148=	495.11	T	149=	495.71
T	150=	478.95	T	152=	496.60	T	153=	495.84
T	154=	454.73	T	155=	454.73	T	156=	449.55
T	157=	383.70	T	160=	433.60	T	161=	434.63
T	162=	449.55	T	163=	449.23	T	164=	414.75
T	165=	401.74	T	166=	322.20	T	167=	317.51
T	170=	310.99	T	172=	312.25	T	173=	312.33
T	175=	263.61	T	177=	296.34	T	180=	303.94
T	190=	251.91	T	191=	218.98	T	192=	127.67
T	195=	179.85	T	196=	154.04	T	197=	129.91
T	198=	210.94	T	200=	250.44	T	210=	246.43
T	220=	234.14	T	221=	246.43	T	222=	234.14
T	242=	94.285	T	250=	77.074	T	260=	77.180
T	261=	77.683	T	262=	78.444	T	263=	77.400
T	264=	75.594	T	265=	76.503	T	266=	74.424
T	267=	81.261	T	268=	81.214	T	269=	89.262
T	300=	172.32	T	301=	85.003	T	304=	138.69
T	305=	94.166	T	310=	61.969	T	311=	63.337
T	312=	63.337	T	313=	48.927	T	316=	63.951
T	320=	58.236	T	321=	62.074	T	322=	62.074
T	325=	44.378	T	326=	44.378	T	327=	44.378
T	330=	52.897	T	331=	41.091	T	332=	41.091
T	335=	41.091	T	336=	43.155	T	337=	43.155
T	340=	47.382	T	341=	47.382	T	342=	54.284
T	343=	63.286	T	344=	63.286	T	345=	64.381
T	346=	60.424	T	347=	66.360	T	348=	64.029
T	350=	60.069	T	351=	67.379	T	352=	67.379
T	354=	67.245	T	355=	67.245	T	356=	67.379
T	358=	67.533	T	360=	74.199	T	362=	73.645
T	364=	73.645	T	365=	73.645	T	366=	73.645
T	368=	68.812	T	369=	68.548	T	371=	67.248
T	375=	67.675	T	376=	67.675	T	377=	69.049
T	400=	73.847	T	401=	73.721	T	402=	69.186
T	404=	67.959	T	406=	66.388	T	408=	69.664
T	410=	69.912	T	412=	69.972	T	414=	70.880
T	421=	72.130	T	422=	70.790	T	423=	70.184
T	424=	69.383	T	425=	69.822	T	426=	69.986
T	431=	68.039	T	432=	68.918	T	433=	69.136
T	434=	69.790	T	435=	69.970	T	436=	70.880
T	441=	67.986	T	442=	69.263	T	443=	69.604
T	444=	69.814	T	445=	69.926	T	446=	69.949
T	451=	68.529	T	452=	69.504	T	453=	69.694
T	454=	69.785	T	455=	69.866	T	456=	69.842

ARITHMETIC NODES IN ASCENDING NODE NUMBER ORDER

T 150=	430.98	T 199=	427.82	T 148=	436.17	T 149=	430.41	T 199=	178.86	T 208=	164.10
T 238=	149.49	T 337=	68.597	T 341=	51.658	T 357=	67.344	T 358=	67.188	T 359=	68.966
T 379=	69.194	T 405=	69.182	T 1009=	127.97	T 1001=	198.28	T 1002=	177.41	T 1003=	160.97
T 1004=	114.88	T 1005=	115.52	T 1006=	79.825	T 1007=	253.88	T 1008=	234.34	T 1009=	218.49
T 1010=	128.53	T 1011=	56.884	T 1012=	56.884	T 1013=	47.481	T 1021=	52.359	T 1022=	52.359
T 1023=	45.441	T 1031=	49.078	T 1032=	49.078	T 1033=	43.858	T 1041=	45.453	T 1042=	45.453
T 1043=	40.649	T 1044=	50.649	T 1264=	83.385	T 1267=	104.83	T 1268=	98.137	T 1269=	83.631
T 1346=	43.375	T 1347=	67.397								

WEATHER MODES IN ASCENDING MODE NUMBER ORDER

++NONE++

BOUNDARY MODES IN ASCENDING MODE NUMBER ORDER

T 1=	78.000	T 2=	70.800	T 901=	40.800	T 902=	40.800
------	--------	------	--------	--------	--------	--------	--------

MEAN ICV GAS TEMP= F MEAN ICV GAS PRESSURE= 20.08 PSIA

MEAN ICV-GCV GAS TEMP= 143.3 F MEAN ICV-GCV GAS PRESSURE= 14.79 PSIA

3.6.5 SINDA Output For Hypothetical Accident Conditions Of Transport

The following pages present output from the SINDA computer program for the six HAC load cases (see Table 3.5-1 for a description of each). Because a transient analysis is used to evaluate each HAC load case, it is impractical to present the entire output in this document. Instead, the following pages present output at three significant time points in the HAC fire for each load case. These time points are: (1) time of maximum OCV sidewall temperature (typically at the end of the HAC fire), (2) time of maximum ICV sidewall temperature (typically 40 to 50 minutes into the HAC fire), and (3) the final steady-state package temperatures following the HAC fire.

The printouts are arranged in order of the HAC load case number. Within each HAC load case grouping, printouts are arranged by time point within the HAC fire. Finally, within the printout for each time point, four pages of output are used to present the thermal model node temperatures for each of the four submodel segments (A through D). As such, a total of 12 pages of output are presented for each HAC load case.

Temperatures on each printout are arranged by thermal model node number. All temperatures are in terms of °F, time is listed in hours, and energy is presented as of Btu/hour.

SYSTEM IMPROVED NUMERICAL DIFFERENCING ANALYZER (SIS (ELMAN '88))

PAGE 1/4

MODEL = DAMAGE1
PUBDCHAC LOAD CASE NO. 1 CONDITIONS - Circumferential Distribution, 900F
Peak OCY Sidewall Temperature Time Point

5/2/96

SUBMODEL NAME = MAIN
PROBLEM TIME

TIMEN = 0.100000 VS. TIMEIN = 0.900000

DIFFUSION NODES IN ASCENDING NODE NUMBER ORDER

T 257=	210.65	T 260=	210.45	T 269=	214.38
T 201=	780.84	T 1264=	229.11	T 1267=	231.06
				T 1268=	209.78
				T 1269=	225.85

ARITHMETIC NODES IN ASCENDING NODE NUMBER ORDER

HEATER NODES IN ASCENDING NODE NUMBER ORDER

++NODE++

BOUNDARY NODES IN ASCENDING NODE NUMBER ORDER

--NODE--

MEAN ICV GAS TEMP= 780.8 F MEAN ICV GAS PRESSURE= 37.19 PSIA
MEAN ICV-OCV GAS TEMP= 241.3 F MEAN ICV-OCV GAS PRESSURE= 45.69 PSIA

SUBMODEL NAME = P73A

MAX DIFF DELTA T PER ITER	CALCULATED	RELXIC(P73A	161)=	1.75781E-02	VS.	RELXIC=	5.00000E-02
MAX ARITH DELTA T PER ITER	ANLYICL(P73A	1004)=	2.32813E-02	VS.	ANLYICL=	0.200000	
MAX DIFF DEL T PER TIME STEP	DTMPC(P73A	1005)=	3.01950	VS.	DTMPC=	10.0000	
MAX ARITH DEL T PER TIME STEP	ATMPC(P73A	238)=	3.24358	VS.	ATMPC=	100.000	
MIN STABILITY CRITERIA	CSMIN(P73A	431)=	3.004479E-03				
MAX STABILITY CRITERIA	CSMAX(P73A	424)=	1.95463				
NUMBER OF ITERATIONS	LEXPOT	=	5	VS.	MLEXPOT=	600	
PROBLEM TIME	TIMEN	=	0.100000	VS.	TIMENO=	0.500000	
MEAN PROBLEM TIME	TIMEN	=	0.468798				
AVERAGE TIME STEP USED	DTIMEU	=	9.257960E-04	VS.	DTIMEI=	0.	

DIFFUSION NODES IN ASCENDING NODE NUMBER ORDER

T 51=	700.54	T 93=	720.78	T 95=	762.31	T 98=	858.68	T 42=	1809.3	T 100=	1016.4
T 180=	913.91	T 107=	868.37	T 110=	825.95	T 112=	825.48	T 113=	826.34	T 120=	716.97
T 182=	714.16	T 123=	721.82	T 124=	711.41	T 125=	716.62	T 126=	709.05	T 127=	710.23
T 130=	696.84	T 132=	695.32	T 133=	699.39	T 134=	694.25	T 135=	697.07	T 136=	694.83
T 137=	695.33	T 140=	684.19	T 141=	682.53	T 142=	684.55	T 143=	686.83	T 144=	684.19
T 143=	684.01	T 144=	684.43	T 147=	687.54	T 150=	695.28	T 152=	695.50	T 153=	696.44
T 134=	694.90	T 159=	695.34	T 154=	695.39	T 157=	695.42	T 160=	709.28	T 161=	704.40
T 162=	718.57	T 163=	709.67	T 164=	709.25	T 165=	708.47	T 166=	709.27	T 167=	709.77
T 170=	698.63	T 172=	690.27	T 173=	690.08	T 175=	682.67	T 177=	682.66	T 180=	670.64
T 190=	677.41	T 191=	708.61	T 192=	294.95	T 193=	705.75	T 194=	287.74	T 196=	594.39
T 190=	794.12	T 200=	1093.5	T 204=	1115.4	T 210=	725.48	T 220=	710.08	T 220=	672.49
T 240=	622.90	T 242=	378.75	T 250=	324.77	T 260=	282.96	T 261=	205.17	T 262=	204.86
T 263=	210.08	T 264=	284.80	T 265=	289.90	T 266=	286.25	T 300=	1229.0	T 304=	1238.3
T 305=	1376.7	T 316=	654.12	T 313=	1166.8	T 315=	1281.3	T 316=	1281.3	T 320=	921.23
T 323=	1097.8	T 325=	1274.7	T 326=	1874.7	T 330=	880.12	T 333=	1053.4	T 339=	1267.3
T 350=	1247.2	T 348=	854.77	T 342=	579.37	T 343=	1835.5	T 344=	332.33	T 345=	965.43
T 346=	1260.0	T 347=	543.98	T 349=	1044.0	T 350=	258.87	T 351=	425.43	T 352=	263.11
T 353=	341.74	T 354=	296.08	T 353=	224.81	T 356=	346.40	T 360=	208.33	T 362=	208.01
T 364=	200.28	T 360=	217.19	T 367=	222.86	T 366=	246.23	T 369=	267.71	T 371=	435.40
T 373=	347.02	T 373=	258.26	T 377=	223.43	T 400=	199.77	T 401=	209.85	T 402=	221.70
T 404=	1202.2	T 406=	1371.8	T 408=	1363.1	T 410=	1611.5	T 412=	1611.8	T 414=	1619.3
T 421=	471.47	T 422=	1414.7	T 423=	1417.9	T 424=	264.28	T 425=	1401.7	T 426=	1404.3

T 431=	1361.6	T 432=	1361.6	T 433=	1368.6	T 434=	1347.3	T 435=	1382.1	T 436=	1363.6
T 916=	983.86										
ARITHMETIC NODES IN ASCENDING NODE NUMBER ORDER											
T 50=	723.30	T 52=	723.72	T 54=	779.89	T 158=	701.95	T 159=	704.99	T 166=	704.91
T 169=	705.18	T 195=	388.14	T 197=	348.89	T 199=	544.37	T 238=	658.87	T 311=	1123.1
T 312=	1123.1	T 321=	1113.8	T 322=	1113.8	T 331=	1866.0	T 332=	908.8	T 337=	756.73
T 341=	683.78	T 357=	327.06	T 358=	487.31	T 359=	261.54	T 379=	221.16	T 403=	224.20
T 1000=	333.38	T 1081=	669.84	T 1002=	563.31	T 1083=	379.86	T 1004=	275.89	T 1005=	273.64
T 1806=	219.12	T 1087=	700.42	T 1008=	718.60	T 1089=	764.75	T 1018=	359.26	T 1011=	956.37
T 1012=	956.37	T 1013=	1238.4	T 1021=	943.65	T 1022=	943.65	T 1023=	1283.6	T 1031=	901.96
T 1032=	901.96	T 1033=	1191.1	T 1041=	878.37	T 1042=	878.37	T 1043=	620.18	T 1044=	620.18
T 1346=	1135.8	T 1347=	448.87								
HEATED NODES IN DESCENDING NODE NUMBER ORDER											
==NONE==											
BOUNDARY NODES IN ASCENDING NODE NUMBER ORDER											
T 1=	1475.9	T 2=	1628.7								

SYSTEMS IMPROVED NUMERICAL DIFFERENCING ANALYZER '85 (SINDA '85)

PAGE 2/4

MODEL = BARKUE1
FLDBCKEAC LOAD CASE NO. 1 CONDITIONS - Circumferential Distribution, 100F
Peak CVR Radwell Temperature Time Point

5/2/94

SUMMEL LINE = PTM

MAX DIFF DELTA T PER ITER	CALCULATED	161)=	2.441400E-03	VS.	ALLOWED	5.000000E-02
MAX ARITH DELTA T PER ITER	DELROCP100	166)=	7.348359E-05	VS.	ARLROCA	0.500000
MAX DIFF DEL T PER TIME STEP	DTMPCDPT00	167)=	2.99057	VS.	DTMPCAL	10.0000
MAX ARITH DEL T PER TIME STEP	ATMPCCP100	168)=	2.25630	VS.	ATMPCAL	100.0000
MIN STABILITY CRITERIA	CSRODMPT00	169)=	3.086579E-05			
MAX STABILITY CRITERIA	CSROKCP100	170)=	3.26347			
NUMBER OF ITERATIONS	LSMPC		5	VS.	MLCPT	500
PROBLEM TIME	TIMEH		0.340500	VS.	TIMEAL	0.500000
REAL PROBLEM TIME	TIMEH		0.498750			
AVERAGE TIME STEP USED	DTMSEU		0.259240E-04	VS.	DTMSEI	0.

T		51=		719.72		T		53=		721.05		T		55=		725.56		T		60=		868.04		T		62=		1027.9		T		100=		1079.4																																																																																																																																																																																																																																																																																																																																																																																																																																		
T	105=	991.45	T	107=	977.87	T	110=	935.48	T	113=	832.67	T	113=	844.43	T	130=	739.23	T	122=	727.75	T	123=	759.06	T	124=	722.99	T	125=	743.54	T	126=	717.04	T	137=	722.72	T	130=	707.88	T	132=	702.91	T	133=	719.38	T	134=	701.33	T	135=	711.06	T	136=	701.06	T	137=	703.37	T	140=	690.20	T	141=	685.45	T	142=	689.17	T	143=	694.94	T	144=	688.89	T	145=	692.14	T	146=	691.25	T	147=	692.94	T	150=	696.73	T	152=	697.14	T	153=	697.19	T	154=	696.91	T	155=	696.36	T	156=	696.99	T	157=	696.62	T	160=	707.83	T	161=	705.09	T	162=	705.52	T	163=	704.92	T	164=	709.05	T	165=	706.38	T	166=	710.86	T	167=	710.82	T	170=	689.87	T	172=	689.85	T	173=	688.09	T	175=	682.62	T	177=	681.82	T	180=	669.44	T	190=	678.59	T	191=	704.23	T	192=	291.58	T	193=	707.14	T	194=	364.09	T	196=	589.44	T	198=	802.12	T	200=	1092.4	T	204=	1195.5	T	210=	725.94	T	220=	718.81	T	230=	679.34	T	240=	623.33	T	242=	372.44	T	250=	224.82	T	260=	202.59	T	261=	284.93	T	262=	292.75	T	263=	385.93	T	264=	203.58	T	265=	206.39	T	266=	205.31	T	300=	1229.0	T	304=	1230.3	T	305=	1376.7	T	310=	934.12	T	313=	1906.7	T	315=	1201.1	T	316=	1281.1	T	320=	920.99	T	323=	1097.3	T	324=	1274.2	T	326=	1274.2	T	330=	881.42	T	333=	1052.8	T	335=	1245.9	T	336=	1243.9	T	340=	854.10	T	342=	578.23	T	343=	903.7	T	344=	328.47	T	345=	804.62	T	346=	1234.9	T	347=	468.44	T	349=	9040.6	T	350=	252.46	T	351=	418.29	T	352=	253.52	T	353=	336.21	T	354=	284.99	T	356=	217.58	T	356=	292.32	T	360=	260.18	T	362=	199.32	T	364=	199.27	T	366=	211.33	T	367=	215.85	T	368=	219.98	T	368=	229.85	T	371=	427.73	T	373=	341.63	T	375=	252.76	T	377=	214.24	T	400=	199.32	T	401=	286.80	T	402=	211.29	T	404=	934.27	T	406=	1548.3	T	408=	1388.3	T	410=	1486.3	T	412=	1610.4	T	414=	1619.2	T	421=	471.36	T	422=	1414.7	T	423=	1417.3	T	424=	245.79	T	425=	1600.9	T	426=	1406.3	T	431=	1250.3	T	432=	1323.1	T	433=	246.10	T	436=	222.10	T	439=	1306.4	T	436=	1396.6	T	441=	1379.9	T	442=	1378.0	T	443=	1375.2	T	444=	1375.2	T	445=	1391.4	T	446=	1386.9	T	451=	1372.2	T	452=	1380.6	T	453=	1376.5	T	454=	1381.2	T	455=	1405.8	T	456=	1201.9	T	950=	908.53	T	90=	792.23	T	50=	726.29	T	54=	776.34	T	150=	704.21	T	150=	703.34	T	160=	703.47

† 169= 708.58	† 195= 291.75	† 197= 350.35	† 199= 587.91	† 238= 634.94	† 311= 1123.0
† 312= 1123.0	† 321= 1113.4	† 322= 1113.4	† 331= 1067.3	† 332= 1067.5	† 337= 795.18
† 341= 482.50	† 357= 316.94	† 358= 396.82	† 359= 253.56	† 379= 213.47	† 483= 214.48
† 1000= 317.91	† 1001= 672.92	† 1002= 581.01	† 1003= 348.92	† 1004= 272.98	† 1005= 270.76
† 1006= 208.02	† 1007= 702.12	† 1008= 713.42	† 1009= 770.89	† 1010= 379.72	† 1011= 956.36
† 1012= 956.34	† 1013= 1220.3	† 1021= 943.37	† 1022= 943.37	† 1023= 1223.1	† 1031= 983.08
† 1032= 903.88	† 1033= 1189.9	† 1041= 877.64	† 1042= 877.64	† 1043= 618.91	† 1044= 618.91
† 1346= 1057.4	† 1347= 381.55	HEATER NODES IN ASCENDING NODE NUMBER ORDER			
		***NONE**			
		BOUNDARY NODES IN ASCENDING NODE NUMBER ORDER			
† 1= 1475.0	† 2= 1424.7				

SYSTEMS IMPROVED NUMERICAL DIFFERENCING ANALYZER '85 (SINDA '85)

PAGE 3/6

MODEL = DAMA01
PBLCCMAX LOAD CASE NO. 1 CONDITIONS - Circumferential Distribution, 1000
**** Peak OCY sidewall Temperature Time Point ****

5/2/96

RUMMODEL NAME = PTSC

MAX DIFF DELTA T PER ITER	CALCULATED	ALLOWED
MAX ANGLE DELTA T PER ITER	ARLHCC(P18C	VR. ARLHCA= 5.80000E-02
MAX DIFF DEL T PER TIME STEP	ARLHCC(P18C	VR. ARLHCA= 5.80000E-02
MAX ANGLE DEL T PER TIME STEP	ATMPC(P18C	VR. ATMPCA= 10.0000
MIN STABILITY CRITERIA	CSMNH(P18C	VR. CSMNHA= 3.00E-05
MIN STABILITY CRITERIA	CSMNH(P18C	VR. CSMNHA= 3.2655E-05
NUMBER OF ITERATIONS	LOOPCT	VR. MLOOPF= 600
PROBLEM TIME	TIMEH	VR. TIMEH= 0.500000
MEAN PROBLEM TIME	TIMEH	VR. TIMEH= 0.498792
AVERAGE TIME STEP USED	DTIMEH	VR. DTIMEH= 0.

DIFFUSED NODES IN ASCENDING NODE NUMBER ORDER

T 51= 755.27	T 53= 720.64	T 55= 733.48	T 60= 766.26	T 62= 1025.4	T 100= 1001.4
T 105= 993.45	T 107= 928.07	T 110= 911.37	T 112= 906.03	T 113= 913.26	T 120= 830.01
T 122= 815.18	T 125= 834.80	T 126= 838.48	T 129= 843.34	T 126= 857.08	T 127= 859.27
T 130= 751.43	T 132= 734.28	T 133= 753.04	T 134= 751.90	T 135= 758.38	T 136= 784.20
T 137= 767.35	T 140= 799.70	T 141= 799.85	T 142= 797.67	T 143= 791.18	T 144= 798.68
T 145= 713.31	T 146= 719.51	T 147= 728.97	T 150= 696.18	T 152= 697.08	T 153= 696.84
T 154= 697.12	T 155= 696.40	T 156= 699.82	T 157= 699.13	T 160= 693.11	T 161= 694.59
T 162= 696.28	T 163= 693.27	T 164= 696.44	T 165= 691.95	T 166= 694.08	T 167= 693.64
T 170= 678.18	T 172= 678.95	T 173= 677.78	T 175= 679.11	T 177= 676.76	T 180= 681.65
T 190= 672.65	T 191= 795.67	T 192= 291.93	T 193= 799.13	T 194= 294.58	T 196= 284.38
T 198= 601.89	T 200= 1074.2	T 204= 1062.4	T 210= 719.62	T 220= 714.26	T 230= 654.19
T 240= 621.29	T 242= 372.06	T 250= 223.96	T 260= 202.92	T 261= 204.48	T 262= 202.66
T 263= 205.01	T 264= 203.52	T 265= 206.31	T 266= 205.27	T 300= 1295.2	T 304= 1299.6
T 305= 1375.5	T 310= 937.95	T 313= 1108.6	T 315= 1281.8	T 316= 1281.8	T 320= 922.24
T 323= 1008.8	T 325= 1274.5	T 326= 1274.5	T 330= 871.39	T 333= 1648.3	T 335= 1244.1
T 336= 1244.1	T 340= 851.75	T 342= 577.04	T 343= 1053.4	T 344= 328.14	T 345= 823.75
T 346= 1256.4	T 347= 448.32	T 349= 1040.4	T 350= 253.25	T 351= 418.17	T 352= 253.48
T 353= 336.15	T 354= 286.44	T 355= 217.96	T 356= 293.37	T 360= 288.14	T 362= 199.28
T 364= 199.25	T 366= 211.28	T 367= 212.95	T 368= 219.78	T 369= 229.37	T 371= 427.68
T 373= 341.37	T 375= 252.74	T 377= 256.21	T 400= 199.31	T 401= 208.79	T 402= 211.26
T 404= 936.19	T 405= 1360.1	T 406= 1368.3	T 410= 9406.3	T 412= 1610.4	T 414= 1410.2
T 421= 671.36	T 422= 9414.7	T 423= 9417.3	T 424= 265.79	T 425= 1400.0	T 426= 1406.5
T 431= 1250.3	T 432= 1322.9	T 433= 246.10	T 434= 222.10	T 435= 1326.4	T 436= 1326.6
T 441= 1379.0	T 442= 1369.9	T 443= 1375.2	T 444= 1375.2	T 445= 1391.4	T 446= 1328.0
T 451= 1372.2	T 452= 1368.5	T 453= 1376.5	T 454= 1381.2	T 455= 1405.8	T 456= 1391.9
T 950= 908.84					
	ARITHMETIC NODES IN ASCENDING NODE NUMBER ORDER				
T 50= 760.80	T 52= 724.31	T 54= 756.23	T 158= 694.67	T 159= 694.04	T 168= 694.42

T 169=	694.70	T 195=	291.32	T 197=	250.38	T 199=	588.31	T 225=	639.81	T 311=	1124.8
T 312=	1124.8	T 321=	1114.1	T 322=	1114.1	T 331=	1043.1	T 332=	1063.1	T 337=	793.98
T 341=	681.14	T 357=	316.88	T 358=	390.68	T 359=	253.43	T 379=	213.39	T 405=	214.57
T 9088=	218.85	T 1001=	671.67	T 1002=	381.39	T 1003=	348.62	T 1004=	272.93	T 1005=	270.71
T 1084=	287.92	T 1087=	698.33	T 1008=	709.35	T 1009=	768.26	T 1018=	379.78	T 1011=	959.66
T 1012=	939.66	T 1013=	1231.6	T 1021=	944.68	T 1023=	945.68	T 1023=	1223.5	T 1031=	893.43
T 1032=	893.43	T 1033=	1187.3	T 1041=	874.60	T 1042=	875.60	T 1043=	617.45	T 1044=	617.45
T 1346=	1056.7	T 1347=	381.26								
HEATER NODES IN ASCENDING NODE NUMBER ORDER											
++NODE++											
BOUNDARY NODES IN ASCENDING NODE NUMBER ORDER											
T 1=	1673.0	T 2=	1424.7								

SYSTEMS IMPROVED NUMERICAL DIFFERENCE ANALYZER '85 (SINGA '85)

PAGE 4/4

MODEL = BANGAL1
FACORZNAC LOAD CASE NO. 1 CONDITIONS = Circumferential Distribution, 100F
Peak OCY Side-wall Temperature Time Point

5/2/96

SUBMODEL NAME = P180

MAX DIFF DELTA T PER ITER	CALCULATED	141)= -2.529648E-03	VI. DELTICA=	5.000000E-02
MAX ARITH DELTA T PER ITER	ARLMOCC(P180	1004)= -6.486597E-03	VI. ARLICA=	0.500000
MAX DIFF DEL T PER TIME STEP	DTMOC(P180	1081)= 2.77323	VI. DTMCA=	10.0000
MAX ARITH DEL T PER TIME STEP	ATMOC(P180	2381)= 3.26043	VI. ATMCA=	100.000
NIN STABILITY CRITERIA	CLGMIN(P180	444)= 5.088726E-08		
NIN STABILITY CRITERIA	ESDMAX(P180	434)= 3.24657		
NUMBER OF ITERATIONS	LOOPCT	= 5	VI. WLOOP=	600
PROBLEM TIME	TINEN	= 0.508000	VI. TIMEN=	0.500000
MEAN PROBLEM TIME	TINEM	= 0.498793		
AVERAGE TIME STEP USED	DTINEM	= 9.259260E-04	VI. DTINEM=	0.

DIFFUSION NODES IN ASCENDING NODE NUMBER ORDER

T 51=	763.23	T 53=	720.66	T 55=	726.89	T 60=	867.25	T 62=	904.2	T 100=	904.0
T 105=	961.12	T 107=	935.79	T 110=	919.76	T 113=	919.41	T 115=	926.86	T 120=	845.16
T 122=	842.07	T 123=	844.29	T 124=	849.80	T 125=	851.09	T 126=	864.08	T 127=	864.01
T 130=	795.89	T 132=	796.17	T 133=	799.40	T 134=	793.91	T 135=	783.10	T 136=	771.25
T 137=	771.25	T 140=	714.34	T 143=	714.27	T 142=	714.15	T 143=	714.78	T 144=	713.96
T 145=	716.78	T 146=	723.16	T 147=	724.16	T 150=	698.12	T 152=	698.51	T 153=	698.64
T 154=	699.16	T 155=	698.79	T 156=	702.99	T 157=	702.59	T 160=	692.15	T 161=	694.32
T 162=	693.22	T 163=	693.02	T 164=	693.14	T 165=	693.02	T 166=	695.20	T 167=	696.34
T 170=	676.75	T 172=	676.67	T 173=	676.44	T 175=	676.92	T 177=	672.65	T 180=	679.44
T 190=	670.80	T 191=	792.22	T 192=	291.08	T 195=	706.38	T 196=	393.54	T 198=	583.16
T 199=	796.36	T 200=	1076.4	T 204=	1063.8	T 210=	736.38	T 220=	714.78	T 230=	666.77
T 240=	622.70	T 242=	372.27	T 250=	223.97	T 260=	202.58	T 261=	204.43	T 262=	208.43
T 263=	205.77	T 264=	203.51	T 265=	208.29	T 266=	205.27	T 300=	1223.3	T 304=	1229.7
T 305=	1371.5	T 310=	997.73	T 313=	1108.7	T 315=	1281.9	T 316=	1281.0	T 320=	922.41
T 323=	1096.1	T 325=	1274.3	T 326=	1274.3	T 330=	876.24	T 332=	1060.5	T 338=	1244.9
T 336=	1244.9	T 340=	852.70	T 342=	577.42	T 343=	1023.5	T 344=	928.27	T 345=	823.61
T 346=	1256.6	T 347=	468.34	T 349=	1048.6	T 350=	252.37	T 351=	148.28	T 382=	253.42
T 383=	336.15	T 354=	288.48	T 355=	217.50	T 356=	293.39	T 360=	200.14	T 362=	199.27
T 364=	199.25	T 366=	211.26	T 367=	212.96	T 368=	219.78	T 369=	229.57	T 371=	427.64
T 373=	361.39	T 375=	252.74	T 377=	216.21	T 680=	199.31	T 681=	208.79	T 682=	211.86
T 684=	936.20	T 686=	1369.2	T 689=	1369.5	T 610=	1486.3	T 612=	1470.4	T 616=	1419.2
T 621=	471.36	T 622=	1414.7	T 623=	1417.5	T 624=	245.79	T 625=	1400.9	T 626=	1406.3
T 631=	1250.4	T 632=	1323.0	T 633=	246.10	T 634=	222.10	T 635=	1386.4	T 636=	1394.6
T 641=	1379.9	T 642=	1370.0	T 643=	1373.2	T 644=	1373.2	T 645=	1391.6	T 646=	1388.9
T 651=	1372.2	T 652=	1360.6	T 653=	1376.5	T 654=	1381.2	T 655=	1405.8	T 656=	1391.9
T 950=	905.99										

ARITHMETIC NODES IN ASCENDING NODE NUMBER ORDER

T 50=	764.93	T 52=	724.45	T 54=	751.81	T 150=	694.34	T 159=	694.18	T 168=	693.96
-------	--------	-------	--------	-------	--------	--------	--------	--------	--------	--------	--------

1	169=	894.11	T	195=	291.07	F	197=	349.51	T	199=	587.00	T	238=	447.54	T	311=	1124.9
1	212=	1184.9	T	321=	1114.2	T	322=	1114.2	T	331=	1063.3	T	332=	1063.3	T	337=	794.48
T	341=	681.81	T	357=	316.83	T	358=	398.72	T	359=	253.46	T	379=	213.99	T	483=	234.58
T	1000=	217.41	T	1001=	659.36	T	1002=	579.69	T	1003=	367.73	T	1004=	272.59	T	1005=	270.34
T	1006=	207.87	T	1007=	696.18	T	1008=	707.89	T	1009=	744.17	T	1010=	379.29	T	1011=	959.85
T	1012=	959.85	T	1013=	1231.4	T	1021=	944.74	T	1022=	944.74	T	1023=	1233.5	T	1031=	898.10
T	1032=	898.10	T	1033=	1108.6	T	1041=	876.18	T	1042=	876.18	T	1043=	818.14	T	1044=	818.14
T	1346=	1054.8	T	1347=	387.27												

HEATER NODES IN ASCENDING NODE NUMBER ORDER

NONE

BOUNDARY NODES IN ASCENDING NODE NUMBER ORDER

T	1=	1475.0	F	2=	1426.7
---	----	--------	---	----	--------

RESTART RECORD NUMBER SAYS WRITTEN FOR TITER = 0.500000

SYSTEM IMPROVED NUMERICAL DIFFERENCING ANALYSIS (65 (RIMGA 'MS)

PAGE 1/4

MODEL = DAMAGED
SUBMODHAC LOAD CASE NO. 1 CONDITIONE - Circumferential Distribution, 100F
**** Peak ICV Elbow Wall Temperature (Flow Point) ****

5/2/94

SUBMODEL NAME = MATH

PROBLEM TIME

TIMEN = 0.700000 VS. TIMENB = 12.0000

T 237=	228.80	T 268=	228.57	T 269=	229.25	DIFFUSION NODES IN ASCENDING NODE NUMBER ORDER	
T 201=	829.47	T 1264=	241.81	T 1267=	378.34	T 1268=	327.34
ARITHMETIC NODES IN ASCENDING NODE NUMBER ORDER							
HEATER NODES IN ASCENDING NODE NUMBER ORDER							
--NONE--							
BOUNDARY NODES IN ASCENDING NODE NUMBER ORDER							
--NONE--							

MEAN ICV GAS TEMP= 835.5 F MEAN ICV GAS PRESSURE= 38.88 PSIA
MEAN ICV-OOV GAS TEMP= 790.8 F MEAN ICV-OOV GAS PRESSURE= 44.11 PSIA

SUBMODEL NAME = PISA

MAX DIFF DELTA T PER ITER	DELCCOPTSA	161)=	2.797266E-02	VS.	DELICR=	5.000000E-02
MAX ARITH DELTA T PER ITER	ARLCCOPTSA	337)=	0.321562	VS.	ARLICR=	0.340000
MAX DIFF DEL T PER TIME STEP	DTMCCOPTSA	423)=	-3.65091	VS.	DTMPCR=	10.0000
MAX ARITH DEL T PER TIME STEP	ATMCCOPTSA	1246)=	-1.75336	VS.	ATMPCR=	100.000
RUN STABILITY CRITERIA	CRSNOOPTSA	431)=	1.479725E-04			
MAX STABILITY CRITERIA	CRSNOOPTSA	424)=	2.06472			
NUMBER OF ITERATIONS	LDOPCT	=	3	VS.	BLDOPCT=	600
PROBLEM TIME	TIMEN	=	0.700000	VS.	TIMENB=	12.0000
MEAN PROBLEM TIME	TIMEN	=	0.699196			
AVERAGE TIME STEP USED	BTIMED	=	0.771932E-04	VS.	BTIMEN=	0.

DIFFUSION NODES IN ASCENDING NODE NUMBER ORDER																	
T	51=	751.58	T	53=	737.60	T	55=	765.44	T	80=	860.20	T	62=	978.56	T	100=	966.60
T	905=	910.62	T	107=	895.74	T	110=	869.10	T	112=	869.15	T	113=	870.65	T	120=	881.07
T	122=	790.34	T	123=	882.95	T	124=	796.42	T	125=	801.44	T	126=	798.39	T	127=	799.15
T	130=	782.12	T	132=	790.29	T	133=	783.25	T	134=	781.82	T	135=	783.74	T	136=	784.85
T	137=	785.89	T	140=	773.08	T	141=	773.09	T	142=	771.88	T	143=	774.81	T	144=	772.94
T	145=	776.58	T	146=	775.87	T	147=	776.54	T	150=	772.33	T	152=	771.10	T	153=	772.76
T	154=	772.34	T	155=	773.78	T	156=	775.61	T	157=	776.88	T	160=	776.42	T	161=	775.28
T	162=	775.98	T	163=	776.74	T	164=	776.98	T	165=	777.73	T	166=	779.78	T	167=	780.38
T	170=	761.11	T	172=	760.58	T	173=	761.85	T	175=	752.87	T	177=	753.67	T	180=	763.65
T	190=	752.61	T	191=	824.23	T	192=	321.39	T	193=	776.86	T	194=	431.07	T	196=	897.37
T	198=	829.20	T	208=	997.75	T	206=	992.32	T	210=	812.97	T	220=	793.93	T	238=	765.23
T	260=	703.60	T	242=	679.85	T	250=	251.76	T	260=	305.39	T	261=	298.39	T	262=	210.61
T	263=	217.68	T	266=	275.84	T	265=	222.96	T	266=	222.67	T	300=	897.33	T	304=	982.07
T	305=	622.74	T	318=	602.65	T	315=	732.43	T	315=	620.24	T	316=	620.26	T	320=	788.38
T	323=	723.03	T	325=	675.00	T	326=	675.88	T	330=	746.69	T	333=	794.38	T	333=	623.92
T	336=	623.92	T	340=	730.71	T	342=	562.65	T	343=	664.88	T	344=	368.67	T	343=	321.36
T	346=	735.62	T	347=	562.89	T	349=	573.86	T	350=	256.89	T	351=	337.34	T	382=	301.43
T	353=	329.21	T	354=	328.84	T	355=	254.86	T	356=	334.89	T	360=	202.06	T	362=	200.73
T	364=	216.91	T	368=	247.65	T	367=	255.19	T	368=	279.33	T	369=	307.66	T	371=	361.36
T	373=	334.87	T	375=	280.23	T	377=	250.21	T	400=	305.93	T	401=	218.15	T	402=	264.66
T	404=	348.82	T	406=	716.35	T	408=	746.83	T	410=	733.81	T	412=	783.09	T	414=	723.83

T 421=	494.30	T 422=	754.86	T 423=	744.72	T 424=	304.83	T 425=	891.13	T 426=	821.27
T 431=	750.19	T 432=	843.12	T 433=	921.76	T 434=	919.88	T 435=	851.12	T 436=	748.54
T 950=	934.81										
ARITHMETIC NODES IN ASCENDING NODE NUMBER ORDER											
T 50=	759.30	T 52=	748.75	T 54=	708.27	T 150=	775.33	T 159=	773.79	T 160=	775.36
T 168=	775.34	T 195=	325.43	T 197=	379.88	T 199=	469.87	T 230=	738.38	T 217=	714.51
T 312=	714.51	T 321=	785.86	T 322=	789.26	T 331=	488.91	T 332=	486.91	T 337=	612.15
T 341=	584.42	T 357=	338.29	T 358=	358.32	T 359=	299.37	T 379=	251.04	T 408=	248.95
T 1000=	363.62	T 1081=	728.21	T 1002=	466.62	T 1083=	402.38	T 1084=	297.04	T 1805=	295.12
F 1006=	215.88	F 1887=	705.90	T 1888=	773.66	T 1889=	880.71	T 9018=	605.66	T 1017=	796.90
F 1012=	796.98	F 1813=	657.21	T 1821=	783.24	T 1822=	783.24	T 1023=	657.84	T 1037=	761.33
F 1032=	761.33	F 1033=	649.37	T 1841=	727.94	F 1042=	727.94	T 1843=	547.17	T 9044=	547.17
T 1346=	758.18	F 1347=	468.48								
HEATER NODES IN ASCENDING NODE NUMBER ORDER											
--(H)M--											
BOUNDARY NODES IN ASCENDING NODE NUMBER ORDER											
F 1=	100.00	F 2=	180.00								

SYSTEMS IMPROVED NUMERICAL DIFFERENCING ANALYZER '85 (SIMBA '85)

PAGE 2/4

MODEL = DAKANE1
PWRXKNAC LONG CASE NO. 1 CONDITIONS = Circumferential Distribution, 100W
Peak 1CV (100W) Temperature Time Point

5/2/94

SUBMODEL NAME = PTSS

MAX DIFF DELTA T PER ITER	CALCULATED	161)= 2.124823E-02	VL	ARLXCA= 5.000000E-02
MAX ARITH DELTA T PER ITER	ARLXCA(PTSS)	137)= 0.128361	VL	ARLXCA= 0.500000
MAX DIFF DEL T PER TIME STEP	BTMPC(PTSS)	423)= -2.65889	VL	BTMPCA= 10.0000
MAX ARITH DEL T PER TIME STEP	ATMPC(PTSS)	1344)= -1.48927	VL	ATMPCA= 100.0000
MIN STABILITY CRITERIA	CSMCR(PTSS)	493)= 1.701530E-04		
MIN STABILITY CRITERIA	CSMPC(PTSS)	434)= 3.35291		
NUMBER OF ITERATIONS	LODPT	= 3	VL	MLODPT= 600
PROBLEM TIME	TIMEB	= 0.708800	VL	TIMEB= 12.0000
MEAN PROBLEM TIME	TIMEH	= 0.599196		
AVERAGE TIME STEP USED	BTIME)	= 8.771930E-04	VL	BTIME= 0.

DIFFUSION MODES IN ASCENDING MODE NUMBER ORDER

T 51= 766.95	T 23= 761.58	T 95= 762.74	T 60= 862.98	T 62= 970.91	T 100= 967.85
T 105= 922.72	T 107= 900.95	T 110= 875.38	T 112= 874.87	T 113= 879.76	T 120= 815.21
T 122= 804.38	T 123= 825.61	T 124= 805.28	T 125= 816.88	T 126= 805.39	T 127= 805.93
T 130= 798.60	T 132= 788.56	T 133= 795.20	T 134= 786.96	T 135= 795.39	T 136= 789.58
T 137= 798.73	T 140= 778.76	T 141= 778.83	T 142= 776.34	T 143= 781.27	T 144= 777.33
T 145= 781.08	T 146= 788.56	T 147= 781.62	T 150= 775.81	T 152= 774.89	T 153= 776.30
T 154= 773.99	T 155= 777.67	T 156= 779.82	T 157= 788.61	T 160= 777.49	T 161= 778.99
T 162= 777.37	T 163= 778.00	T 164= 779.31	T 165= 779.17	T 166= 783.43	T 167= 783.83
T 170= 762.95	T 172= 762.40	T 173= 761.95	T 175= 756.73	T 177= 755.37	T 180= 763.43
T 180= 755.58	T 181= 833.75	T 182= 316.60	T 185= 781.95	T 186= 430.38	T 186= 662.69
T 198= 839.18	T 200= 996.85	T 204= 992.13	T 210= 813.98	T 220= 795.44	T 230= 778.59
T 240= 795.41	T 242= 444.47	T 250= 290.58	T 260= 284.71	T 281= 207.28	T 282= 286.98
T 283= 211.21	T 284= 213.95	T 285= 220.22	T 286= 219.98	T 300= 896.88	T 304= 981.87
T 305= 622.69	T 310= 802.95	T 313= 732.83	T 315= 680.45	T 316= 628.65	T 328= 789.07
T 325= 723.64	T 325= 616.61	T 328= 616.61	T 330= 748.39	T 333= 706.14	T 338= 625.71
T 336= 625.71	T 340= 751.64	T 342= 341.83	T 343= 660.88	T 344= 348.53	T 345= 737.02
T 346= 729.54	T 347= 502.77	T 349= 367.84	T 350= 283.74	T 351= 344.06	T 352= 286.98
T 353= 316.85	T 354= 314.78	T 355= 239.97	T 356= 317.36	T 360= 881.72	T 362= 802.85
T 364= 288.16	T 366= 235.87	T 367= 238.57	T 368= 846.62	T 369= 265.39	T 371= 347.78
T 373= 323.00	T 375= 369.17	T 377= 236.73	T 408= 206.95	T 401= 217.43	T 402= 232.23
T 404= 793.80	T 406= 766.80	T 408= 688.12	T 418= 785.83	T 419= 784.33	T 414= 723.88
T 421= 494.09	T 422= 754.88	T 423= 744.88	T 424= 277.90	T 425= 881.88	T 426= 829.24
T 431= 794.88	T 432= 952.46	T 433= 392.39	T 434= 256.48	T 435= 905.14	T 436= 817.34
T 441= 691.85	T 442= 775.21	T 443= 796.39	T 444= 796.17	T 445= 785.91	T 446= 683.36
T 451= 713.95	T 452= 739.71	T 453= 734.47	T 454= 737.73	T 455= 763.66	T 456= 727.66
T 920= 956.32					

ARITHMETIC MODES IN ASCENDING MODE NUMBER ORDER

T 90= 721.37	T 50= 766.84	T 54= 776.33	T 150= 777.45	T 159= 777.54	T 168= 777.82
--------------	--------------	--------------	---------------	---------------	---------------

T 169=	776.86	F 195=	315.31	T 199=	326.89	T 199=	637.63	T 236=	742.21	T 311=	714.94
F 312=	714.94	F 321=	705.95	T 322=	705.95	T 331=	688.77	T 332=	688.77	T 337=	610.23
T 341=	583.67	F 357=	322.71	T 358=	344.12	T 359=	284.57	T 379=	237.56	F 409=	235.22
T 1000=	344.53	T 1001=	724.48	T 1002=	627.78	T 1003=	399.66	T 1004=	293.33	T 1805=	290.55
T 1006=	212.34	T 1007=	789.54	T 1008=	773.11	T 1009=	814.75	T 1010=	630.99	T 1811=	797.48
T 1012=	797.60	T 1013=	657.61	F 1021=	783.92	T 1022=	783.92	T 1023=	651.75	T 1831=	763.96
T 1032=	763.96	T 1033=	651.16	F 1041=	728.98	T 1042=	728.98	T 1043=	546.65	T 1864=	546.65
T 1346=	783.69	T 1347=	410.32	HEATER NODES IN ASCENDING NODE NUMBER ORDER							
++NONE++											
BOUNDARY NODES IN ASCENDING NODE NUMBER ORDER											
T 1=	100.00	T 2=	100.00								

SYSTEMS IMPROVED NUMERICAL DIFFERENCE ANALYZER '85 (SINR '85)

PAGE 3/4

MODEL = BMMGET
PDDCKNAC LONG CASE NO. 1 CONDITIONS - Circumferential Distribution, 100°
***** Peak ICY Sidewall Temperature Time Point *****

5/2/94

SUBMODEL NAME = PTSC

		CALCULATED		ALLOWED
MAX DIFF DELTA T PER ITER		DELXCC/PTSC	561)= 1.625328E-02	VS. DELXCA= 5.000000E-02
MAX ARITH DELTA T PER ITER		ARLXCC/PTSC	352)= 0.121460	VS. ARLXCA= 0.500000
MAX DIFF DEL T PER TIME STEP		DTMPC/PTSC	425)= -2.65817	VS. OTHPCA= 10.0000
MAX ARITH DEL T PER TIME STEP		ATMPC/PTSC	1364)= -1.41000	VS. ATMPCA= 100.000
MIN STABILITY CRITERIA		CSMIN/PTSC	455)= 1.791548E-04	
MIN STABILITY CRITERIA		CSMAX/PTSC	424)= 3.518254	
NUMBER OF ITERATIONS		LOOPCT	= 3	VS. NLOOPC= 600
PROBLEM TIME		TIMER	= 0.700000	VS. TTIMEID= 12.0000
MEAN PROBLEM TIME		TIMER	= 0.699196	
AVERAGE TIME STEP USED		DTIME	= 0.771520E-04	VS. GTIMEI= 0.

DIFFUSION NODES IN ASCENDING NODE NUMBER ORDER																	
T	51=	811.50	T	53=	751.47	T	55=	751.00	T	60=	873.77	T	82=	974.89	T	108=	140.30
T	105=	934.02	T	107=	922.86	T	110=	989.80	T	112=	987.54	T	113=	911.11	T	120=	859.31
T	122=	851.18	T	123=	851.63	T	124=	857.77	T	125=	864.71	T	126=	847.65	T	127=	846.95
T	130=	816.49	T	132=	810.97	T	133=	817.07	T	134=	816.59	T	135=	820.60	T	136=	825.66
T	137=	826.12	T	140=	794.63	T	141=	795.50	T	142=	791.70	T	143=	794.71	T	144=	794.55
T	145=	794.80	T	146=	800.44	T	147=	801.22	T	150=	779.64	T	152=	778.40	T	153=	779.50
T	154=	780.32	T	153=	780.94	T	154=	784.22	T	157=	784.23	T	160=	771.68	T	161=	774.73
T	162=	772.16	T	163=	771.27	T	164=	773.08	T	165=	773.91	T	166=	773.84	T	167=	773.17
T	170=	750.85	T	172=	756.13	T	173=	757.72	T	179=	784.65	T	177=	753.39	T	180=	753.67
T	190=	750.63	T	191=	832.63	T	192=	816.66	T	193=	780.37	T	194=	839.31	T	196=	888.49
T	198=	837.88	T	200=	975.48	T	204=	956.74	T	210=	823.63	T	220=	796.50	T	230=	733.17
T	240=	781.73	T	242=	445.30	T	250=	290.13	T	260=	204.33	T	261=	207.09	T	262=	206.77
T	243=	218.96	T	264=	213.17	T	265=	220.81	T	266=	219.86	T	300=	885.09	T	304=	852.96
T	305=	616.67	T	310=	806.66	T	313=	737.63	T	315=	623.48	T	316=	623.48	T	320=	790.98
T	323=	725.05	T	325=	617.80	T	380=	617.80	T	330=	757.92	T	333=	699.45	T	335=	621.11
T	336=	621.11	T	340=	727.11	T	342=	540.80	T	343=	660.26	T	344=	359.87	T	345=	735.89
T	348=	729.87	T	347=	902.16	T	349=	567.21	T	350=	283.40	T	351=	543.76	T	352=	284.68
T	353=	316.38	T	354=	314.29	T	355=	239.71	T	356=	316.97	T	360=	201.63	T	362=	202.14
T	364=	206.05	T	366=	234.82	T	367=	238.27	T	368=	247.94	T	369=	264.75	T	371=	347.44
T	373=	322.70	T	375=	849.04	T	377=	236.60	T	400=	284.98	T	401=	217.41	T	402=	232.10
T	406=	793.63	T	408=	748.67	T	409=	688.00	T	410=	765.85	T	412=	784.33	T	414=	723.82
T	421=	694.80	T	422=	754.88	T	423=	764.88	T	424=	277.60	T	425=	801.88	T	426=	829.24
T	431=	796.60	T	432=	932.39	T	433=	292.38	T	434=	258.48	T	435=	965.14	T	436=	817.33
T	441=	891.81	T	442=	775.08	T	443=	796.37	T	444=	796.15	T	445=	785.89	T	446=	493.33
T	451=	713.00	T	452=	739.40	T	453=	734.41	T	454=	737.70	T	455=	763.63	T	456=	727.44
T	950=	937.73															
ARITHMETIC NODES IN ASCENDING NODE NUMBER ORDER																	
T	50=	809.34	T	52=	753.29	T	54=	779.54	T	58=	774.60	T	159=	774.61	T	160=	774.44

T 149=	774.57	T 195=	214.87	T 197=	376.58	T 199=	636.79	T 238=	720.74	T 311=	719.18
T 152=	775.18	T 221=	707.38	T 322=	707.38	T 331=	682.14	T 332=	682.14	T 337=	608.34
T 341=	581.37	T 397=	332.32	T 398=	343.75	T 399=	284.23	T 379=	237.87	T 403=	225.10
T 1000=	344.25	T 1001=	722.44	T 1002=	627.01	T 1003=	399.13	T 1004=	293.18	T 1005=	298.40
T 1006=	212.33	T 1007=	747.35	T 1008=	775.04	T 1009=	814.89	T 1010=	430.43	T 1011=	502.97
T 1012=	880.97	T 1013=	880.92	T 1021=	785.77	T 1022=	785.77	T 1023=	652.89	T 1031=	753.67
T 1032=	753.47	T 1033=	645.85	T 1041=	724.34	T 1042=	726.34	T 1043=	544.64	T 1044=	544.64
T 1344=	782.72	T 1347=	409.72								
HEATER NODES IN ASCENDING PIPE NUMBER ORDER											
++NONE++											
BOUNDARY NODES IN ASCENDING PIPE NUMBER ORDER											
T 1=	100.00	T 2=	100.00								

BYTORG IMPROVED NUMERICAL DIFFERENCE ANALYZER V05 (MINDA '95)

PAGE 4/4

MODEL = BANGSET
FUDGEMAC LOAD CASE NO. & CONDITIONS = Circumferential distribution, 100F
***** Peak ICV Sidewall Temperature Time Point *****

572/94

SUMMODEL NAME = P130

MAX DIFF DELTA T PER ITER	CALCULATED	161=	1.570000E-02	VS.	ALLOWED	61=	5.000000E-02
MAX ARITH DELTA T PER ITER	ARLXCC(PT0)	187=	-0.128605	VS.	ARLXCA=	65=	0.500000
MAX DIFF DEL T PER TIME STEP	DYNACC(PT0)	423=	-2.63820	VS.	DYNPCA=	10=	0.0000
MAX ARITH DEL T PER TIME STEP	ATMPOCC(PT0)	1344=	-1.60030	VS.	ATMPCA=	100=	0.00
MIN STABILITY CRITERIA	CGMIN(PT0)	403=	1.701647E-04				
MIN STABILITY CRITERIA	CBMINAX(PT0)	434=	3.35083				
NUMBER OF ITERATIONS	LOOPCT	=	3	VS.	WLOOPCT=	600	
PROBLEM TIME	TIMEH	=	0.700000	VS.	TIMEAB=	12.0000	
MEAN PROBLEM TIME	TIMEH	=	0.699956				
AVERAGE TIME STEP UMDS	DTIMEU	=	0.771050E-04	VS.	DTIMEI=	0.	

DIFFUSION NODS (IN ASCENDING NODE NUMBER ORDER)

T	51=	821.90	T	53=	754.68	T	55=	749.28	T	60=	875.78	T	62=	972.77	T	100=	962.14
T	105=	938.53	T	107=	927.25	T	110=	914.91	T	112=	914.83	T	113=	913.35	T	120=	866.28
T	122=	866.14	T	123=	867.76	T	124=	868.82	T	125=	869.83	T	126=	872.22	T	127=	872.30
T	130=	822.48	T	132=	826.17	T	133=	821.26	T	134=	822.61	T	135=	824.44	T	136=	829.32
T	143=	829.34	T	144=	799.35	T	145=	800.20	T	146=	797.84	T	143=	796.57	T	144=	799.83
T	145=	800.51	T	144=	804.11	T	147=	804.55	T	150=	783.10	T	152=	781.95	T	153=	782.62
T	154=	783.90	T	153=	786.33	T	154=	788.86	T	157=	788.11	T	160=	773.27	T	161=	776.68
T	162=	772.94	T	163=	773.80	T	164=	774.90	T	165=	772.54	T	166=	778.95	T	167=	779.33
T	170=	759.04	T	172=	758.67	T	173=	758.74	T	175=	754.87	T	177=	754.18	T	180=	753.94
T	190=	730.92	T	191=	631.47	T	192=	513.97	T	198=	780.80	T	194=	438.62	T	195=	689.90
T	198=	836.94	T	200=	979.44	T	204=	957.57	T	210=	823.04	T	220=	799.71	T	230=	762.33
T	240=	708.65	T	242=	445.86	T	250=	238.21	T	260=	204.52	T	281=	207.05	T	282=	206.74
T	283=	210.99	T	284=	213.16	T	285=	219.09	T	286=	219.85	T	280=	206.89	T	304=	883.28
T	308=	616.77	T	310=	889.39	T	313=	737.53	T	315=	483.81	T	318=	623.81	T	320=	791.89
T	323=	725.48	T	325=	617.88	T	326=	617.88	T	330=	768.20	T	333=	702.87	T	335=	623.45
T	336=	623.45	T	348=	729.42	T	342=	348.80	T	343=	640.44	T	344=	348.18	T	345=	733.97
T	366=	729.85	T	347=	502.21	T	349=	567.38	T	350=	383.45	T	351=	343.80	T	352=	284.45
T	353=	316.62	T	384=	314.37	T	385=	239.72	T	354=	317.01	T	360=	281.82	T	362=	282.13
T	364=	308.85	T	366=	234.83	T	367=	234.27	T	368=	247.94	T	369=	284.74	T	371=	347.31
T	373=	322.82	T	375=	369.06	T	377=	234.61	T	400=	204.92	T	681=	217.41	T	402=	232.90
T	484=	779.45	T	406=	760.65	T	408=	688.18	T	410=	783.83	T	412=	786.33	T	414=	723.82
T	421=	484.88	T	422=	734.88	T	423=	744.28	T	424=	227.80	T	425=	891.88	T	426=	829.24
T	431=	794.68	T	432=	992.38	T	433=	292.38	T	434=	258.48	T	435=	965.14	T	436=	817.33
T	441=	691.82	T	442=	775.15	T	443=	706.37	T	444=	706.16	T	445=	788.90	T	446=	698.34
T	451=	713.88	T	452=	739.57	T	453=	734.44	T	454=	737.71	T	455=	768.63	T	456=	727.43
T	950=	926.34															
ARITHMETIC NODS (IN ASCENDING NODE NUMBER ORDER)																	
T	50=	818.88	T	52=	758.43	T	54=	769.45	T	150=	776.32	T	150=	776.39	T	160=	776.37

T	169=	776.21	T	165=	314.57	T	197=	376.13	T	199=	634.46	T	238=	736.87	T	311=	719.78
T	312=	719.70	T	321=	707.82	T	328=	707.82	T	331=	685.55	T	332=	685.55	T	337=	680.26
F	341=	582.40	F	357=	522.58	T	358=	543.83	F	359=	284.27	T	379=	237.30	T	483=	235.18
T	1000=	543.92	T	1001=	721.85	T	1002=	426.52	T	1003=	378.59	T	1004=	292.92	T	1005=	278.14
F	1006=	212.27	F	1007=	767.57	T	1008=	774.94	F	1009=	814.48	T	1010=	438.37	T	1011=	883.68
T	1012=	803.48	F	1013=	641.52	T	1021=	786.38	F	1022=	786.38	T	1023=	653.22	T	1031=	758.91
F	1032=	758.91	F	1033=	648.55	T	1041=	726.67	T	1042=	726.67	T	1043=	545.62	T	1044=	545.62
T	1346=	702.89	T	1347=	489.75												
HEATER NOSES (IN ASCENDING NOME NUMBER ORDER																	
NOME																	
BOUNDARY NOSES (IN ASCENDING NOME NUMBER ORDER																	
T	1=	100.00	F	2=	180.00												

T 421=	214.04	T 422=	115.39	T 423=	110.38	T 424=	104.01	T 425=	113.13	T 426=	109.47
T 431=	126.86	T 432=	127.34	T 433=	124.14	T 434=	117.30	T 435=	110.48	T 436=	112.90
T 950=	797.82										
ARITHMETIC MODES IN ASCENDING NODE NUMBER ORDER											
T 50=	312.93	T 52=	358.11	T 54=	429.30	T 156=	430.37	T 199=	437.94	T 148=	434.01
T 169=	437.76	T 195=	328.34	T 197=	344.97	T 199=	448.48	T 238=	218.58	T 311=	214.81
T 319=	216.81	T 321=	224.83	T 322=	224.82	T 331=	244.08	T 332=	244.05	T 337=	242.57
T 341=	253.96	T 357=	249.75	T 358=	237.37	T 395=	243.21	T 379=	245.43	T 403=	243.67
T 1000=	343.28	T 1001=	531.01	T 1002=	437.34	T 1003=	400.28	T 1004=	350.37	T 1005=	548.27
T 1006=	288.17	T 1007=	327.49	T 1008=	337.95	T 1009=	378.04	T 1010=	352.19	T 1011=	256.19
T 1012=	234.15	T 1013=	208.34	T 1021=	242.95	T 1022=	242.95	T 1023=	212.83	T 1031=	263.44
T 1032=	268.44	T 1033=	258.33	T 1041=	267.29	T 1042=	267.29	T 1043=	258.68	T 1044=	258.68
T 1344=	195.39	T 1347=	232.83								
HEATER MODES IN ASCENDING NODE NUMBER ORDER											
--NONE--											
BOUNDARY MODES IN ASCENDING NODE NUMBER ORDER											
T 1=	100.00	T 2=	100.00								

SYSTEMS IMPROVED NUMERICAL DIFFERENCING ANALYZER '85 (SINBA '85)

PAGE 2/4

MODEL = DANADE1
STDDELNAC LOAD CASE NO. 1 CONDITIONS - Circumferential Distribution, 100F
*** Steady-state Conditions After The Fire ***

5/2/94 Dan

SUBMODEL NAME = FT08

MAX DIFF DELTA 1 PER ITER	CALCULATED			ALLOWED
MAX AP1TH DELTA 3 PER ITER	DALNCC(PT08)	4851= -1.35334		VS. DALNCA= 5.00000E-02
MAX SYSTEM ENERGY BALANCE	ARLNCC(PT08)	12463= -1.28237E+02		VS. ARLNCA= 5.00000E-02
	BR4,SC	= 1.00000E+30		VS. BR4,SA = 0.00000E+00
ENERGY INTO AND OUT BY EYE	ERLNIS	= 0.		ERLNIS= 0.
MAX NODAL ENERGY BALANCE	BRALNCC	D= 0.		VS. BRALNCA= 1.00000E-03
NUMBER OF ITERATIONS	LOOPTC	= 1001		VS. LLOOPTD= 1000
PROBLEM TIME	TIMED	= 999.008		VS. TIMED= 999.000

DIFFUSION NODES IN ASCENDING NODE NUMBER ORDER

T 51= 304.95	T 53= 350.25	T 55= 429.74	T 60= 275.95	T 62= 495.75	T 700= 284.48
T 105= 267.35	T 107= 286.80	T 110= 290.75	T 112= 290.44	T 113= 289.73	T 120= 299.18
T 123= 300.18	T 123= 297.93	T 124= 299.51	T 125= 297.99	T 126= 299.05	T 127= 298.63
T 130= 323.54	T 132= 329.94	T 133= 321.31	T 134= 324.88	T 135= 321.87	T 136= 322.02
T 137= 320.95	T 140= 344.88	T 141= 343.09	T 142= 347.09	T 143= 344.28	T 144= 348.01
T 145= 343.58	T 146= 350.78	T 147= 348.90	T 150= 380.87	T 152= 384.48	T 153= 373.09
T 154= 388.44	T 155= 380.48	T 156= 395.37	T 157= 394.70	T 160= 439.12	T 161= 429.88
T 162= 442.66	T 163= 431.25	T 164= 444.73	T 165= 437.78	T 166= 447.91	T 167= 443.03
T 170= 492.44	T 172= 493.34	T 173= 490.36	T 175= 511.89	T 177= 502.74	T 180= 505.47
T 190= 533.88	T 191= 602.83	T 193= 372.88	T 193= 460.70	T 194= 387.42	T 196= 474.53
T 198= 606.30	T 200= 244.89	T 204= 256.51	T 210= 272.12	T 220= 288.94	T 230= 314.99
T 240= 320.62	T 242= 290.62	T 250= 268.14	T 260= 280.85	T 261= 288.63	T 262= 276.47
T 263= 279.82	T 264= 289.62	T 268= 273.84	T 266= 283.86	T 300= 209.88	T 304= 195.94
T 305= 156.35	T 310= 234.68	T 313= 218.33	T 315= 199.00	T 316= 199.00	T 320= 263.72
T 323= 226.29	T 325= 205.72	T 326= 206.72	T 330= 289.20	T 333= 248.05	T 335= 223.61
T 336= 223.61	T 340= 269.63	T 342= 258.86	T 343= 204.91	T 344= 247.47	T 345= 284.55
T 346= 187.72	T 347= 225.80	T 349= 197.57	T 350= 243.28	T 351= 234.77	T 352= 242.14
T 353= 239.59	T 354= 242.33	T 355= 244.50	T 356= 248.64	T 360= 278.99	T 362= 271.88
T 364= 261.51	T 366= 249.88	T 367= 244.81	T 368= 261.58	T 369= 250.71	T 371= 236.67
T 373= 238.79	T 375= 241.56	T 377= 243.80	T 400= 264.86	T 401= 262.70	T 402= 243.38
T 406= 196.40	T 406= 133.28	T 408= 112.65	T 410= 104.96	T 412= 185.73	T 416= 156.78
T 421= 213.14	T 422= 115.38	T 423= 119.29	T 424= 198.85	T 425= 113.32	T 426= 108.83
T 431= 117.28	T 432= 143.48	T 433= 199.61	T 434= 138.14	T 435= 188.20	T 436= 108.12
T 441= 118.27	T 443= 122.91	T 443= 114.69	T 444= 114.38	T 445= 189.26	T 446= 111.29
T 451= 121.56	T 452= 128.56	T 453= 116.56	T 454= 112.84	T 455= 186.96	T 456= 189.28
T 950= 712.61					

ARITHMETIC NODES IN ASCENDING NODE NUMBER ORDER

T 50= 318.87	T 52= 751.75	T 54= 621.18	T 190= 431.23	T 195= 429.29	T 198= 429.73
T 169= 429.25	T 195= 331.36	T 197= 361.96	T 199= 662.33	T 220= 317.44	T 311= 216.95

T 312=	216.95	T 321=	224.84	T 322=	224.84	T 331=	266.30	T 332=	266.30	T 337=	262.62
T 341=	264.04	T 357=	248.30	T 358=	234.83	T 359=	262.70	T 376=	266.84	T 443=	263.18
T 1800=	350.12	T 1801=	534.92	T 1802=	448.51	T 1803=	404.56	T 1804=	353.77	T 1805=	350.78
T 1006=	204.78	T 1807=	532.64	T 1808=	544.59	T 1809=	588.09	T 1810=	338.58	T 1811=	234.31
T 1012=	234.31	T 1813=	208.98	T 1821=	263.32	T 1822=	263.32	T 1823=	213.12	T 1831=	266.69
T 1032=	266.69	T 1033=	232.37	T 1841=	269.11	T 1043=	269.11	T 1063=	258.51	T 1844=	256.51
T 1344=	195.43	T 1347=	232.32								
HEATER NODES IN ASCENDING NODE NUMBER ORDER											
--NONE--											
BOUNDARY NODES IN ASCENDING NODE NUMBER ORDER											
T 1=	100.00	F 2=	100.00								

SYSTEMS IMPROVED NUMERICAL DIFFERENCING ANALYZER '85 (SINBA '85)

PAGE 3/4

MODEL = DANABE1
87647LHAC LIMB CASE NO. 1 CONDITIONS - Differential Distribution, 1000
*** Steady-state Conditions After The Fire ***

9/2/94 Sun

SUBMODEL NAME = PTSC

MAX DIFF DELTA T PER ITER	CALCULATED	651)= 0.240091	VS. ALLOWED	\$,000000E-02	
MAX ARITH DELTA T PER ITER	DELTA(DPTSC	1004)= 3.833936E-02	VS. ALLOWED	\$,000000E-02	
MAX SYSTEM ENERGY BALANCE	ADJUT(DPTSC	= 3.77577	VS. EBALSA =	EBALMS	= 2.87972
	EBALSC		VS. EBALSA =	EBALMS	= 1.000000E-05
ENERGY INTO AND OUT OF SYS	EBALMS	= 2879.72	ZCALMS=	2857.42	
MAX NORMAL ENERGY BALANCE	EBALMS(DPTSC	367)= 1.02500	VS. EBALMS=	1.000000E-05	
NUMBER OF ITERATIONS	LOCPCT	= 1001	VS. BLRCPB=	1000	
PROGRAM TIME	TIMER	= 999.999	VS. TFLRND=	999.900	

DIFFERENTIAL MODES IN ASCENDING MODE NUMBER ORDER

T 51= 290.38	T 53= 332.25	T 55= 401.62	T 60= 291.34	T 62= 448.37	T 98= 262.88
T 105= 284.74	T 107= 285.70	T 110= 286.70	T 112= 287.05	T 113= 284.57	T 120= 294.05
T 123= 294.97	T 123= 293.42	T 124= 293.82	T 125= 292.52	T 126= 291.97	T 127= 291.24
T 130= 312.45	T 132= 314.83	T 133= 311.55	T 134= 312.28	T 135= 309.55	T 136= 307.49
T 137= 305.90	T 140= 326.89	T 141= 327.17	T 142= 329.38	T 143= 328.55	T 144= 326.78
T 143= 323.49	T 144= 321.48	T 147= 320.59	T 150= 321.11	T 152= 325.44	T 153= 327.72
T 154= 325.12	T 125= 327.09	T 156= 327.85	T 157= 324.21	T 160= 328.77	T 161= 327.72
T 162= 411.41	T 163= 400.27	T 164= 406.42	T 165= 399.57	T 166= 399.97	T 167= 396.21
T 170= 475.41	T 172= 475.39	T 173= 472.94	T 175= 484.21	T 177= 498.23	T 180= 508.22
T 194= 518.88	T 191= 604.27	T 192= 372.49	T 193= 477.14	T 194= 368.92	T 196= 474.93
T 198= 608.87	T 200= 267.13	T 204= 262.79	T 210= 274.74	T 220= 282.97	T 230= 296.57
T 240= 329.88	T 242= 289.52	T 250= 266.71	T 260= 279.99	T 261= 281.79	T 262= 275.12
T 263= 277.69	T 264= 260.18	T 265= 271.43	T 266= 262.39	T 300= 210.36	T 304= 197.84
T 305= 137.18	T 310= 236.71	T 313= 229.09	T 315= 208.43	T 316= 200.43	T 320= 244.99
T 323= 227.39	T 325= 204.61	T 326= 204.61	T 330= 259.38	T 333= 241.08	T 335= 217.96
T 336= 217.98	T 340= 285.13	T 342= 254.11	T 343= 285.21	T 344= 248.59	T 345= 205.11
T 346= 186.07	T 347= 225.24	T 349= 196.12	T 350= 241.84	T 351= 225.13	T 352= 240.59
T 353= 257.75	T 354= 240.64	T 355= 242.99	T 356= 239.80	T 360= 275.45	T 362= 270.21
T 364= 260.05	T 366= 244.20	T 367= 242.42	T 368= 240.04	T 369= 238.10	T 371= 235.83
T 373= 237.15	T 375= 239.84	T 377= 241.46	T 400= 263.21	T 401= 261.57	T 402= 261.79
T 404= 195.22	T 406= 133.32	T 408= 112.81	T 410= 184.90	T 412= 165.67	T 414= 166.72
T 427= 212.21	T 422= 115.17	T 423= 118.20	T 424= 195.01	T 425= 113.88	T 426= 108.74
T 431= 156.76	T 432= 163.28	T 433= 198.98	T 434= 137.72	T 435= 108.18	T 436= 108.02
T 441= 118.10	T 442= 122.83	T 443= 116.52	T 444= 116.21	T 445= 109.15	T 446= 111.13
T 451= 121.44	T 452= 128.55	T 453= 116.43	T 454= 112.51	T 455= 108.88	T 456= 109.17
T 950= 714.95					

ARITHMETIC MODES IN ASCENDING MODE NUMBER ORDER

T 90= 202.42	T 92= 333.97	T 94= 399.95	T 150= 397.83	T 156= 306.41	T 168= 397.41
T 169= 397.71	T 198= 331.23	T 197= 342.20	T 199= 447.68	T 250= 308.68	T 311= 218.49

1	312=	214.69	1	321=	225.95	1	328=	225.95	1	331=	239.47	1	332=	239.47	1	337=	239.99
1	341=	251.17	1	357=	258.64	1	358=	255.19	1	359=	261.06	1	379=	283.26	1	403=	261.58
1	900=	334.36	1	9001=	338.88	1	9002=	472.39	1	9003=	464.62	1	9004=	362.59	1	9005=	356.11
1	9006=	285.18	1	9007=	327.93	1	9008=	541.34	1	9009=	545.16	1	9010=	338.78	1	9913=	296.33
1	1012=	236.33	1	1013=	207.34	1	1021=	264.59	1	1022=	264.59	1	1023=	214.89	1	1031=	258.09
1	1032=	258.93	1	1033=	226.26	1	1041=	264.58	1	1042=	264.58	1	1063=	255.72	1	1064=	255.72
1	1346=	194.01	1	1347=	239.79												
HEATER NODES IN ASCENDING NODE NUMBER ORDER																	
==MEME==																	
BOUNDARY NODES IN ASCENDING NODE NUMBER ORDER																	
1	1=	100.00	1	2=	100.00												

SYSTEMS IMPROVED NUMERICAL DIFFERENCING ANALYZER '89 (SINBA '89)

PAGE 6/4

MODEL + MANAGE1
STRETLRAC LOAD CASE NO. 1 CONDITION - Circumferential distribution, 100P
Steady-state Conditions After The Fire ***

5/2/94 9am

SUBMODEL NAME = P130

MAX DIFF DELTA T PER ITER	CALCULATED	406) = -1.34836	VS. ALLOWED	
MAX AXIUM DELTA T PER ITER	DELTA(C) (P130)	TS46) = -1.326463E-02	VS. DRALCA = 3.800000E-02	
MAX SYSTEM ENERGY BALANCE	ALALCC (PTNG)	= 1.600000E+30	VS. ARALCA = 3.800000E-02	
	ENR:AC		VS. EALCA = * EWRMS	= 0.
ENERGY INTO AND OUT OF STE	NUMBER	= 0.	VS. EALBA = 1.000000E-03	
MAX LOCAL ENERGY BALANCE	EBALCC	= 0.	VS. EALBA = 1.000000E-05	
NUMBER OF ITERATIONS	LOOPCT	= 1001	VS. EALDOPS = 1000	
PROBLEM TIME	T:MEM	= 999,000	VS. T:MEMD = 999,000	

DIFFUSION		NODES IN ASCENDING		NODE NUMBER ORDER	
T	51= 295.60	T	53= 325.54	T	60= 389.29
T	105= 283.30	T	107= 284.10	T	110= 285.14
T	123= 292.23	T	123= 291.70	T	124= 291.39
T	130= 306.90	T	132= 309.17	T	133= 308.11
T	137= 308.61	T	140= 320.67	T	141= 320.92
T	145= 319.36	T	146= 317.27	T	147= 317.37
T	154= 343.11	T	155= 341.37	T	156= 341.75
T	162= 367.85	T	163= 395.88	T	164= 395.31
T	170= 466.88	T	172= 444.94	T	173= 444.37
T	198= 511.90	T	191= 392.85	T	192= 370.02
T	198= 597.31	T	200= 244.95	T	204= 242.33
T	240= 322.10	T	242= 289.78	T	250= 264.68
T	243= 277.12	T	244= 267.94	T	265= 271.13
T	305= 137.10	T	310= 236.34	T	313= 219.77
T	323= 227.20	T	325= 206.66	T	326= 206.44
T	334= 220.95	T	340= 267.98	T	342= 257.31
T	344= 186.78	T	347= 225.48	T	349= 196.63
T	353= 238.14	T	354= 241.85	T	355= 243.31
T	364= 259.97	T	364= 244.49	T	367= 242.73
T	373= 237.35	T	375= 240.30	T	377= 241.80
T	404= 195.41	T	404= 132.17	T	408= 132.51
T	421= 212.08	T	422= 115.18	T	423= 118.19
T	431= 156.67	T	432= 142.56	T	433= 150.82
T	441= 118.05	T	442= 122.37	T	443= 116.11
T	451= 121.22	T	452= 127.69	T	453= 118.29
T	450= 707.97				
		ARITHMETIC		NODE NUMBER ORDER	
T	50= 299.25	T	52= 327.24	T	54= 386.67
T	169= 388.15	T	195= 329.65	T	197= 330.43
T		T		T	199= 442.67
T		T		T	238= 313.61
T		T		T	313= 210.37
T		T		T	319= 287.74
T		T		T	340= 242.61
T		T		T	341= 242.61
T		T		T	342= 242.61
T		T		T	343= 242.61
T		T		T	344= 242.61
T		T		T	345= 242.61
T		T		T	346= 242.61
T		T		T	347= 242.61
T		T		T	348= 242.61
T		T		T	349= 242.61
T		T		T	350= 242.61
T		T		T	351= 242.61
T		T		T	352= 242.61
T		T		T	353= 242.61
T		T		T	354= 242.61
T		T		T	355= 242.61
T		T		T	356= 242.61
T		T		T	357= 242.61
T		T		T	358= 242.61
T		T		T	359= 242.61
T		T		T	360= 242.61
T		T		T	361= 242.61
T		T		T	362= 242.61
T		T		T	363= 242.61
T		T		T	364= 242.61
T		T		T	365= 242.61
T		T		T	366= 242.61
T		T		T	367= 242.61
T		T		T	368= 242.61
T		T		T	369= 242.61
T		T		T	370= 242.61
T		T		T	371= 242.61
T		T		T	372= 242.61
T		T		T	373= 242.61
T		T		T	374= 242.61
T		T		T	375= 242.61
T		T		T	376= 242.61
T		T		T	377= 242.61
T		T		T	378= 242.61
T		T		T	379= 242.61
T		T		T	380= 242.61
T		T		T	381= 242.61
T		T		T	382= 242.61
T		T		T	383= 242.61
T		T		T	384= 242.61
T		T		T	385= 242.61
T		T		T	386= 242.61
T		T		T	387= 242.61
T		T		T	388= 242.61
T		T		T	389= 242.61
T		T		T	390= 242.61
T		T		T	391= 242.61
T		T		T	392= 242.61
T		T		T	393= 242.61
T		T		T	394= 242.61
T		T		T	395= 242.61
T		T		T	396= 242.61
T		T		T	397= 242.61
T		T		T	398= 242.61
T		T		T	399= 242.61
T		T		T	400= 242.61
T		T		T	401= 242.61
T		T		T	402= 242.61
T		T		T	403= 242.61
T		T		T	404= 242.61
T		T		T	405= 242.61
T		T		T	406= 242.61
T		T		T	407= 242.61
T		T		T	408= 242.61
T		T		T	409= 242.61
T		T		T	410= 242.61
T		T		T	411= 242.61
T		T		T	412= 242.61
T		T		T	413= 242.61
T		T		T	414= 242.61
T		T		T	415= 242.61
T		T		T	416= 242.61
T		T		T	417= 242.61
T		T		T	418= 242.61
T		T		T	419= 242.61
T		T		T	420= 242.61
T		T		T	421= 242.61
T		T		T	422= 242.61
T		T		T	423= 242.61
T		T		T	424= 242.61
T		T		T	425= 242.61
T		T		T	426= 242.61
T		T		T	427= 242.61
T		T		T	428= 242.61
T		T		T	429= 242.61
T		T		T	430= 242.61
T		T		T	431= 242.61
T		T		T	432= 242.61
T		T		T	433= 242.61
T		T		T	434= 242.61
T		T		T	435= 242.61
T		T		T	436= 242.61
T		T		T	437= 242.61
T		T		T	438= 242.61
T		T		T	439= 242.61
T		T		T	440= 242.61
T		T		T	441= 242.61
T		T		T	442= 242.61
T		T		T	443= 242.61
T		T		T	444= 242.61
T		T		T	445= 242.61
T		T		T	446= 242.61
T		T		T	447= 242.61
T		T		T	448= 242.61
T		T		T	449= 242.61
T		T		T	450= 242.61
T		T		T	451= 242.61
T		T		T	452= 242.61
T		T		T	453= 242.61
T		T		T	454= 242.61
T		T		T	455= 242.61
T		T		T	456= 242.61
T		T		T	457= 242.61
T		T		T	458= 242.61
T		T		T	459= 242.61
T		T		T	460= 242.61
T		T		T	461= 242.61
T		T		T	462= 242.61
T		T		T	463= 242.61
T		T		T	464= 242.61
T		T		T	465= 242.61
T		T		T	466= 242.61
T		T		T	467= 242.61
T		T		T	468= 242.61
T		T		T	469= 242.61
T		T		T	470= 242.61
T		T		T	471= 242.61
T		T		T	472= 242.61
T		T		T	473= 242.61
T		T		T	474= 242.61
T		T		T	475= 242.61
T		T		T	476= 242.61
T		T		T	477= 242.61
T		T		T	478= 242.61
T		T		T	479= 242.61
T		T		T	480= 242.61
T		T		T	481= 242.61
T		T		T	482= 242.61
T		T		T	483= 242.61
T		T		T	484= 242.61
T		T		T	485= 242.61
T		T		T	486= 242.61
T		T		T	487= 242.61
T		T		T	488= 242.61
T		T		T	489= 242.61
T		T		T	490= 242.61
T		T		T	491= 242.61
T		T		T	492= 242.61
T		T		T	493= 242.61
T		T		T	494= 242.61
T		T		T	495= 242.61
T		T		T	496= 242.61
T		T		T	497= 242.61
T		T		T	498= 242.61
T		T		T	499= 242.61
T		T		T	500= 242.61

T 312=	218.37	T 321=	225.74	T 322=	225.74	T 331=	243.09	T 332=	243.09	T 337=	261.38
T 345=	251.53	T 357=	239.05	T 358=	235.60	T 359=	261.43	T 379=	263.34	T 483=	261.98
T 1000=	348.12	T 1001=	530.53	T 1002=	446.91	T 1003=	600.99	T 1004=	250.56	T 1005=	248.12
T 1006=	280.46	T 1007=	580.11	T 1008=	533.50	T 1009=	573.47	T 1010=	337.32	T 1011=	233.96
T 1012=	235.96	T 1013=	297.25	T 1021=	244.37	T 1022=	244.37	T 1023=	213.92	T 1031=	263.99
T 1032=	263.99	T 1033=	229.50	T 1041=	267.34	T 1042=	267.34	T 1043=	256.95	T 1044=	256.95
T 1344=	104.51	T 1347=	231.14								
HEAVY WOODS (IN ASCENDING WOOD NUMBER ORDER +-----+)											
T 1=	100.00	T 2=	100.00	BOUNDARY WOODS (IN ASCENDING WOOD NUMBER ORDER)							

SYSTEMS IMPROVED NUMERICAL DIFFERENCE ANALYZER '85 (SINDA '85)

PAGE 1/4

MODEL = CUNAGE2
FUBKELGAS LOAD CASE NO. 2 CONDITIONS - Circumferential Distribution, -2M
Peak Dev Sidewall Temperature Time Point

5/2/84

RUNNING NAME = PA1B

MEAN PROBLEM TIME = 0.580000

T 267= 113.15		T 268= 113.01		T 269= 188.77			
T 201= 713.93		T 1266= 124.44		T 1857= 253.35		T 1348= 198.28	
						T 1250= 131.59	

DIFFUSION NODES IN ASCENDING NODE NUMBER ORDER
 ARITHMETIC NODES IN ASCENDING NODE NUMBER ORDER
 HEATER NODES IN ASCENDING NODE NUMBER ORDER
 BOUNDARY NODES IN ASCENDING NODE NUMBER ORDER

MEAN IGV GAS TEMP= 715.5 F MEAN IGV GAS PRESSURE= 35.82 PSIA
 MEAN IGV-OCV GAS TEMP= 706.9 F MEAN IGV-OCV GAS PRESSURE= 43.94 PSIA

SUBMODEL NAME = PTBA

MAX DIFF DELTA T PER ITER	DR1DCC(PTBA	165)= 3.64280E-04	VS. DR1DCA= 8.00000E-02
MAX ARITH DELTA T PER ITER	AR1DCC(PTBA	1348)= 0.122803	VS. AR1DCA= 0.500000
MAX DIFF DEL T PER TIME STEP	DTMPC(PTBA	165)= 3.94285E-04	VS. DTMPCA= 10.0000
MAX ARITH DEL T PER TIME STEP	ATMPC(PTBA	1348)= 0.122772	VS. ATMPCA= 100.000
RUN STABILITY CRITERIA	CRDM(PTBA	431)= 3.841521E-05	
MAX STABILITY CRITERIA	CRDMAX(PTBA	424)= 1.96051	
NUMBER OF ITERATIONS	IGDCT	= 1	VS. HIGDPT= 608
MEAN PROBLEM TIME	TIMER	= 0.580000	VS. TIMED= 0.500000
AVERAGE TIME STEP USED	DTIME1	= 1.666667E-02	VS. DTIME2= 8.

DIFFUSION NODES IN ASCENDING NODE NUMBER ORDER

T 31= 648.69	T 33= 658.69	T 35= 696.20	T 40= 807.36	T 42= 961.21	T 100= 963.85
T 105= 805.87	T 107= 809.90	T 110= 764.89	T 112= 764.18	T 113= 767.31	T 120= 649.83
T 122= 646.92	T 123= 634.73	T 124= 642.07	T 128= 648.44	T 129= 637.72	T 127= 639.69
T 150= 625.00	T 132= 625.08	T 133= 628.09	T 134= 621.15	T 135= 624.55	T 136= 620.28
T 137= 620.08	T 140= 610.08	T 141= 608.39	T 142= 618.59	T 143= 613.26	T 144= 609.39
T 145= 611.51	T 146= 610.08	T 147= 611.48	T 150= 622.46	T 152= 623.81	T 153= 623.91
T 154= 621.06	T 155= 622.08	T 156= 620.89	T 157= 621.03	T 160= 636.87	T 161= 632.85
T 162= 639.38	T 163= 638.73	T 164= 637.99	T 165= 636.92	T 166= 637.56	T 167= 638.04
T 170= 628.09	T 172= 619.81	T 173= 619.56	T 175= 613.73	T 177= 612.98	T 180= 681.47
T 188= 607.85	T 191= 736.72	T 193= 197.27	T 195= 630.17	T 194= 298.17	T 196= 583.18
T 198= 732.41	T 200= 1032.4	T 204= 1075.4	T 210= 637.01	T 220= 637.32	T 230= 588.79
T 240= 538.67	T 242= 266.63	T 250= 197.67	T 260= 97.248	T 261= 89.661	T 262= 95.303
T 263= 105.36	T 264= 97.661	T 265= 102.97	T 266= 98.919	T 300= 1210.1	T 384= 1218.2
T 205= 1372.4	T 310= 899.89	T 313= 1085.5	T 315= 1272.5	T 316= 1272.5	T 320= 883.49
T 323= 1874.9	T 325= 1385.2	T 328= 1265.2	T 338= 856.80	T 335= 1024.4	T 338= 1294.5
T 336= 1234.5	T 340= 807.28	T 342= 518.69	T 343= 1811.9	T 344= 233.74	T 348= 906.03
T 346= 1266.1	T 347= 635.36	T 349= 1018.3	T 350= 152.36	T 351= 390.25	T 352= 156.13
T 353= 242.36	T 354= 192.93	T 355= 116.57	T 356= 282.90	T 360= 94.402	T 362= 93.449
T 364= 98.889	T 366= 908.35	T 367= 113.25	T 368= 136.12	T 369= 153.39	T 371= 343.30
T 373= 248.17	T 378= 154.80	T 377= 118.00	T 400= 92.753	T 481= 100.71	T 402= 113.17
T 404= 1185.5	T 446= 1387.5	T 448= 1357.4	T 410= 1489.8	T 412= 1408.6	T 414= 1418.6

T	421=	395.60	T	432=	943.7	T	433=	946.6	T	434=	139.20	T	425=	1397.7	T	436=	1460.9
T	431=	1356.0	T	435=	1355.9	T	437=	1339.2	T	438=	1337.7	T	435=	1377.5	T	434=	1356.0
T	950=	849.23															
ARITHMETIC INDEX IN ASCENDING HOME NUMBER ORDER																	
T	50=	643.86	T	52=	661.85	T	54=	714.13	T	158=	633.52	T	159=	633.28	T	160=	633.30
T	169=	633.39	T	195=	212.20	T	197=	209.41	T	199=	492.70	T	238=	563.48	T	311=	1182.7
T	312=	1102.7	T	321=	1091.3	T	322=	1091.9	T	331=	1040.1	T	332=	1040.1	T	337=	747.70
T	341=	624.62	T	357=	226.85	T	358=	215.04	T	359=	134.83	T	379=	112.28	T	408=	194.47
T	1008=	337.92	T	1001=	397.09	T	1002=	489.32	T	1003=	279.14	T	1004=	174.64	T	1005=	174.32
T	1006=	104.37	T	1007=	632.62	T	1008=	643.44	T	1009=	701.29	T	1010=	262.68	T	1011=	522.38
T	1012=	922.36	T	1013=	1217.8	T	1021=	907.25	T	1022=	907.25	T	1023=	1210.0	T	1031=	357.80
T	1032=	357.80	T	1033=	1173.3	T	1041=	832.89	T	1042=	832.89	T	1043=	352.89	T	1044=	352.89
T	1346=	1099.1	T	1347=	356.95												
HEATER INDEX IN ASCENDING HOME NUMBER ORDER																	
==HOME==																	
BOUNDARY INDEX IN ASCENDING HOME NUMBER ORDER																	
T	1=	9475.8	T	2=	1424.7												

T 189=	631.43	T 195=	262.64	T 197=	262.42	T 199=	516.85	T 239=	589.48	T 311=	1982.7
T 312=	1102.7	T 321=	1992.0	T 322=	1992.0	T 337=	1841.1	T 332=	1041.1	T 337=	746.89
T 341=	626.15	T 357=	217.23	T 358=	287.37	T 359=	147.72	T 379=	905.31	T 403=	907.30
T 1000=	221.24	T 1001=	699.00	T 1002=	365.11	T 1003=	276.56	T 1004=	172.89	T 1005=	179.63
T 1806=	102.29	T 1807=	434.38	T 1808=	446.11	T 1809=	787.71	T 1810=	282.19	T 1811=	922.51
T 1012=	923.51	T 1813=	1217.9	T 1821=	907.42	T 1822=	907.42	T 1823=	1218.0	T 1831=	860.57
T 1032=	860.57	T 1833=	1173.7	T 1841=	832.78	T 1842=	832.78	T 1843=	552.63	T 1844=	552.63
T 134=	1022.3	T 1347=	288.60								
HEATER MODES IN ASCENDING MODE NUMBER ORDER											
<--MODE-->											
BOUNDARY MODES IN ASCENDING MODE NUMBER ORDER											
T 1=	1475.0	T 2=	1426.7								

SYSTEMS IMPROVED NUMERICAL DIFFERENCING ANALYZER '88 (SINDA '85)

PAGE 3/4

MODEL = NANGZ2
RNDCENAC LOAD CASE NO. 2 CONDITIONS - Circumferential distribution, -20F
Peak OCY Rimwall Temperature Time Point

5/2/96

MINI-MODEL NAME = P14C

MAX DIFF DELTA T PER ITER	CALCULATED	320)= 2.441406E-04	VS.	ALLOWED	5.000000E-02
MAX ARITH DELTA T PER ITER	ARLACC(PTSC	1344)= 0.139404	VS.	ARLNCA=	0.350000
MAX DIFF DEL T PER TIME STEP	DTMPC(PTSC	320)= 2.746582E-04	VS.	DTMPCA=	18.0000
MAX ARITH DEL T PER TIME STEP	ATMPC(PTSC	1344)= 0.139374	VS.	ATMPCA=	180.000
MIN STABILITY CRITERIA	CSMIN(PTSC	440)= 3.012900E-05			
MAX STABILITY CRITERIA	CSMAX(PTSC	424)= 3.0594E			
NUMBER OF ITERATIONS	LOOPCT	= 1	VS.	MAXLOOP=	608
PROBLEM TIME	TIMEM	= 0.580000	VS.	TIMEMAX=	8.000000
MEAN PROBLEM TIME	TIMEM	= 0.580000			
AVERAGE TIME STEP USED	DTIME	= 1.666667E-02	VS.	DTIME1=	8.

DIFFUSION NODES IN ASCENDING NODE NUMBER ORDER

T 51= 695.00	T 53= 699.45	T 55= 666.48	T 60= 814.71	T 62= 957.55	T 100= 972.29
T 105= 982.30	T 107= 874.83	T 110= 856.92	T 113= 851.17	T 115= 858.84	T 120= 770.86
T 122= 754.46	T 125= 775.59	T 126= 770.82	T 128= 785.80	T 129= 800.43	T 127= 805.13
T 130= 684.38	T 132= 676.66	T 133= 687.27	T 134= 684.54	T 135= 691.74	T 136= 700.86
T 137= 781.89	T 140= 637.81	T 141= 637.60	T 142= 635.84	T 143= 637.68	T 144= 638.42
T 145= 641.36	T 146= 647.47	T 147= 649.20	T 150= 625.84	T 152= 624.23	T 153= 625.86
T 154= 629.65	T 155= 622.70	T 156= 625.25	T 157= 624.24	T 160= 619.68	T 161= 620.91
T 162= 623.23	T 163= 619.76	T 164= 629.69	T 165= 617.56	T 166= 619.08	T 167= 618.61
T 170= 606.44	T 172= 687.38	T 173= 685.99	T 175= 689.31	T 177= 604.27	T 180= 611.31
T 190= 603.00	T 191= 733.97	T 192= 192.97	T 193= 634.86	T 194= 303.41	T 196= 692.58
T 198= 740.18	T 200= 1036.3	T 204= 1644.4	T 210= 666.93	T 220= 641.72	T 230= 567.31
T 240= 328.51	T 242= 287.28	T 250= 718.96	T 260= 98.754	T 261= 98.864	T 262= 96.076
T 263= 99.182	T 264= 96.416	T 265= 181.55	T 266= 98.007	T 300= 1206.2	T 306= 1218.8
T 308= 1379.5	T 310= 902.18	T 313= 1087.2	T 315= 1273.1	T 316= 1273.1	T 320= 884.95
T 323= 1075.5	T 325= 1265.4	T 326= 1265.4	T 330= 886.87	T 333= 1028.6	T 335= 1232.7
T 336= 1232.7	T 340= 884.55	T 342= 308.90	T 343= 899.84	T 344= 232.18	T 345= 762.68
T 346= 1243.4	T 347= 380.27	T 349= 1013.3	T 350= 146.64	T 351= 323.77	T 352= 147.39
T 353= 237.32	T 354= 186.07	T 333= 109.84	T 356= 189.67	T 344= 94.137	T 362= 92.684
T 364= 92.043	T 366= 183.15	T 367= 104.24	T 368= 108.42	T 369= 116.47	T 371= 234.29
T 373= 344.13	T 375= 149.68	T 377= 169.20	T 400= 92.041	T 401= 100.89	T 402= 103.10
T 404= 888.75	T 406= 1365.2	T 408= 1379.8	T 410= 1413.8	T 412= 1408.8	T 414= 1418.4
T 421= 398.35	T 422= 1419.7	T 423= 1416.7	T 424= 148.67	T 425= 1397.8	T 426= 1464.7
T 433= 1224.0	T 432= 1380.0	T 433= 264.44	T 434= 213.27	T 435= 1405.6	T 436= 1466.6
T 441= 1379.2	T 442= 1372.3	T 443= 1372.3	T 444= 1372.5	T 445= 1394.6	T 446= 1380.2
T 451= 1373.8	T 452= 1366.5	T 453= 1376.5	T 454= 1381.5	T 455= 1412.4	T 456= 1394.5
T 950= 883.84					
ARITHMETIC NODES IN ASCENDING NODE NUMBER ORDER					
T 50= 701.72	T 52= 643.04	T 54= 690.73	T 130= 620.99	T 139= 628.19	T 160= 629.78

T 169=	621.13	T 195=	802.25	T 197=	862.24	T 199=	914.17	T 239=	550.37	T 319=	1104.4	
T 312=	1104.4	T 321=	1092.6	T 322=	1092.6	T 331=	1030.3	T 332=	1036.5	T 337=	765.36	
T 341=	622.61	T 357=	217.09	T 358=	347.24	T 359=	147.03	T 379=	105.24	T 403=	987.20	
T 1000=	221.25	T 1001=	508.38	T 1002=	505.62	T 1003=	276.13	T 1004=	172.00	T 1009=	178.54	
T 1006=	102.18	T 1007=	430.31	T 1008=	442.22	T 1009=	705.95	T 1010=	281.98	T 1011=	925.43	
T 1012=	925.43	T 1013=	1218.3	T 1021=	988.45	T 1022=	988.45	T 1023=	1210.3	T 1031=	858.14	
T 1032=	850.16	T 1033=	1170.9	T 1041=	829.28	T 1042=	829.28	T 1043=	551.00	T 1044=	551.00	
T 1366=	1021.7	T 1367=	280.34									
NEAREST NODES IN ASCENDING NODE NUMBER ORDER												
NONE												
BOUNDARY NODES IN ASCENDING NODE NUMBER ORDER												
T 1=	1475.8	T 2=	1624.7									

SYSTEM IMPROVED NUMERICAL DIFFERENCING ANALYZER '85 (EMMA '85)

PAGE 4/4

MODEL = DAMAGE
PINDEXMAC LOAD CASE NO. 3 CONDITIONS = Circumferential Distribution, -20F
***** Peak QCV SideWall Temperature Time Point *****

5/2/94

SUBMODEL NAME = DT20

MAX DIFF DELTA T PER ITER	CALCULATED	345>= 2.441480E-04	ALLOWED	5.000000E-02
MAX ARITH DELTA T PER ITER	DELTA(CP1SD)	1346>= 0.159526	VS. DELTCA=	0.500000
MAX DIFF DEL T PER TIME STEP	DELTA(CP1SD)	345>= 2.746580E-04	VS. ATNPCA=	10.0000
MAX ARITH DEL T PER TIME STEP	ATNPCA(P1SD)	1346>= 0.139496	VS. ATNPCA=	100.000
REF STABILITY CRITERIA	CRMLN(P1SD)	446>= 3.072940E-05		
MAX STABILITY CRITERIA	CRMLN(P1SD)	424>= 1.05948		
NUMBER OF ITERATIONS	LOOPCT	= 1	VS. MLCOPT=	600
PROBLEM TIME	TIMEH	= 0.500000	VS. TIMEH=	0.500000
NEAR PROBLEM TIME	TIMEH	= 0.500000		
AVERAGE TIME STEP USED	DTMAG	= 1.644444E-02	VS. DTTIME=	0.

		DIFFUSION NODES IN ASCENDING NODE NUMBER ORDER									
		1	2	3	4	5	6	7	8	9	10
T	51= 704.20	T	33= 669.63	T	35= 660.77	T	40= 875.72	T	42= 954.11	T	100= 973.13
T	102= 908.50	T	107= 881.03	T	110= 866.27	T	112= 868.79	T	112= 866.50	T	120= 787.03
T	122= 785.80	T	123= 784.30	T	124= 792.24	T	125= 793.74	T	126= 884.50	T	127= 886.52
T	130= 693.83	T	132= 692.13	T	133= 693.51	T	134= 694.56	T	133= 697.39	T	136= 786.08
T	137= 704.00	T	140= 643.03	T	141= 642.79	T	142= 643.03	T	143= 643.78	T	144= 644.59
T	148= 645.81	T	146= 651.69	T	147= 652.86	T	150= 629.04	T	132= 629.70	T	133= 629.87
T	154= 625.60	T	155= 625.29	T	154= 628.78	T	157= 628.18	T	140= 618.22	T	141= 620.12
T	162= 619.37	T	143= 619.23	T	144= 619.00	T	143= 618.53	T	146= 621.27	T	147= 623.57
T	170= 606.52	T	172= 604.56	T	173= 604.30	T	174= 604.81	T	177= 601.66	T	180= 608.43
T	190= 600.90	T	191= 720.06	T	192= 102.44	T	193= 633.56	T	194= 302.56	T	196= 490.95
T	198= 736.33	T	200= 1036.5	T	204= 1045.0	T	210= 667.66	T	220= 642.32	T	230= 583.31
T	240= 530.37	T	242= 367.50	T	250= 116.98	T	260= 96.736	T	261= 96.866	T	262= 96.054
T	263= 99.160	T	264= 96.484	T	265= 101.53	T	266= 96.980	T	300= 1206.3	T	304= 1210.9
T	308= 1371.9	T	310= 902.33	T	313= 1087.3	T	315= 1475.2	T	316= 1873.2	T	320= 885.11
T	325= 1679.6	T	325= 1265.4	T	326= 1265.4	T	328= 832.50	T	333= 1023.0	T	333= 1233.6
T	336= 1233.6	T	340= 806.26	T	342= 589.54	T	343= 1000.0	T	344= 283.34	T	343= 762.73
T	346= 1263.7	T	347= 308.29	T	340= 1418.4	T	350= 144.66	T	351= 323.81	T	352= 147.41
T	353= 237.34	T	354= 180.11	T	355= 189.87	T	356= 189.69	T	360= 94.158	T	362= 92.688
T	364= 92.041	T	364= 103.15	T	367= 194.24	T	368= 188.62	T	360= 116.47	T	371= 334.36
T	373= 264.15	T	373= 149.69	T	377= 109.20	T	400= 92.030	T	401= 100.09	T	402= 105.10
T	404= 886.76	T	404= 1362.5	T	408= 1379.8	T	410= 1415.0	T	412= 1408.5	T	614= 1418.6
T	421= 393.39	T	422= 1413.7	T	423= 1516.7	T	424= 148.07	T	425= 1397.0	T	426= 1404.7
T	431= 1224.1	T	432= 1356.1	T	433= 244.45	T	434= 213.27	T	435= 1405.6	T	436= 1404.6
T	441= 1379.2	T	442= 1372.3	T	443= 1372.3	T	444= 1372.5	T	445= 1384.6	T	446= 1388.2
T	451= 1373.8	T	452= 1345.6	T	453= 1376.5	T	454= 1381.5	T	455= 1412.4	T	456= 1854.3
T	950= 869.61										
		ARITHMETIC NODES IN ASCENDING NODE NUMBER ORDER									
T	50= 786.33	T	52= 663.31	T	34= 686.18	T	150= 628.14	T	150= 620.01	T	188= 620.00

T 160=	420.21	T 195=	201.66	T 197=	261.20	T 199=	512.60	T 238=	560.20	T 311=	1186.5
T 312=	1186.5	T 321=	902.7	T 322=	902.7	T 331=	902.8	T 332=	1090.8	T 337=	766.20
T 361=	623.36	T 357=	217.12	T 358=	287.28	T 359=	147.44	T 379=	905.24	T 403=	907.28
T 1000=	220.23	T 1001=	395.52	T 1002=	305.44	T 1003=	275.08	T 1004=	172.37	T 1008=	170.13
F 1006=	182.12	F 1007=	627.39	T 1008=	637.49	T 1009=	792.34	T 1010=	281.47	T 1011=	925.59
F 1013=	925.59	T 1013=	1218.8	T 1021=	908.62	T 1022=	908.62	T 1023=	1290.4	T 1031=	895.36
T 1032=	855.34	F 1033=	1172.3	T 1041=	831.03	T 1042=	831.03	T 1043=	331.79	T 1044=	351.79

T 1347= 268.36

HEATER NODES IN ASCENDING NODE NUMBER ORDER

=*****

BOUNDARY NODES IN ASCENDING NODE NUMBER ORDER

T 1= 1475.0

F 2= 1424.7

SYSTEMS IMPROVED NUMERICAL DIFFERENCING ANALYZER '85 (SINDA '85)

PAGE 1/4

MODEL = DAMAGE2 MAC LOAD CASE NO. 2 CONDITION = Circumferential Distribution, -200 5/2/94
 PABOCC ***** Peak ICV Sidewall Temperature Time Point *****

SUBMODEL NAME = MAIN

PROBLEM TIME

TIMEIN = 0.744666 VS. TIMEEND = 12.0000

DIFFUSION NODES IN ASCENDING NODE NUMBER ORDER

1 267+ 136.52 T 268+ 136.49 T 269+ 137.62
 1 281+ 776.77 T 1266+ 141.98 T 1267+ 284.47 T 1268+ 234.04 T 1269+ 130.30

ARITHMETIC NODES IN ASCENDING NODE NUMBER ORDER

HEATER NODES IN ASCENDING NODE NUMBER ORDER

BOUNDARY NODES IN ASCENDING NODE NUMBER ORDER

MEAN ICV GAS TEMP= 776.8 F MEAN ICV GAS PRESSURE= 37.12 PSIA
 MEAN ICV-OCV GAS TEMP= 713.6 F MEAN ICV-OCV GAS PRESSURE= 41.43 PSIA

SUBMODEL NAME = PTAB

	CALCULATED	ALLOWED
MAX DIFF DELTA T PER ITER	DELTDIFF(PTAB 761)= 5.1269528E-03	VS. DELTDIFF= 5.000000E-02
MAX ARITH DELTA T PER ITER	ARLNDCC(PTAB 537)= 8.4516130E-02	VS. ARLNDCC= 0.500000
MAX DIFF DEL T PER TIME STEP	DYNDIFF(PTAB 425)= -9.27973	VS. DYNDC= 10.0000
MAX ARITH DEL T PER TIME STEP	ATMDC(PTAB 1244)= -0.252617	VS. ATMDC= 100.000
MIN STABILITY CRITERIA	CSQMIN(PTAB 431)= 2.095422E-04	
MAX STABILITY CRITERIA	CSQMAX(PTAB 424)= 2.15480	
NUMBER OF ITERATIONS	LOOPCT = 3	VS. MLOOPCT= 400
PROBLEM TIME	TIMEIN = 0.744666	VS. TIMEEND = 12.0000
MEAN PROBLEM TIME	TIMEIN = 0.744672	
AVERAGE TIME STEP USED	DYTIME = 7.074100E-04	VS. BYTIME= 0.

DIFFUSION NODES IN ASCENDING NODE NUMBER ORDER

T 51+ 704.31	T 53+ 682.10	T 55+ 704.48	T 60+ 806.24	T 62+ 896.88	T 100+ 888.30
T 105+ 847.24	T 107+ 828.97	T 110+ 886.31	T 112+ 886.42	T 115+ 907.85	T 120+ 744.58
T 122+ 742.27	T 123+ 756.54	T 124+ 761.76	T 125+ 744.76	T 126+ 740.86	T 127+ 741.69
T 130+ 723.80	T 132+ 721.99	T 133+ 729.87	T 134+ 723.30	T 135+ 725.32	T 136+ 725.86
T 137+ 726.79	T 140+ 715.00	T 141+ 715.29	T 142+ 715.81	T 143+ 716.11	T 144+ 714.49
T 145+ 716.24	T 146+ 716.00	T 147+ 717.38	T 150+ 716.51	T 152+ 713.27	T 153+ 715.88
T 154+ 714.54	T 155+ 715.84	T 156+ 717.24	T 157+ 717.76	T 160+ 719.83	T 161+ 718.66
T 162+ 719.20	T 163+ 720.06	T 164+ 720.20	T 165+ 721.18	T 166+ 723.21	T 167+ 723.84
T 170+ 708.63	T 172+ 708.16	T 173+ 708.71	T 175+ 702.57	T 177+ 702.78	T 180+ 692.32
T 190+ 703.51	T 191+ 773.83	T 192+ 234.97	T 193+ 719.59	T 194+ 357.33	T 196+ 640.30
T 198+ 778.60	T 200+ 919.42	T 204+ 982.74	T 210+ 756.48	T 230+ 734.57	T 230+ 701.24
T 250+ 839.94	T 242+ 356.52	T 250+ 153.99	T 260+ 109.56	T 261+ 108.97	T 268+ 105.71
T 283+ 112.98	T 264+ 112.43	T 265+ 120.20	T 266+ 121.81	T 300+ 813.55	T 304+ 804.48
T 309+ 505.98	T 310+ 730.15	T 313+ 654.51	T 315+ 543.37	T 316+ 343.97	T 320+ 711.13
T 325+ 642.24	T 325+ 536.59	T 326+ 536.59	T 330+ 481.88	T 333+ 418.43	T 335+ 311.51
T 334+ 311.51	T 340+ 642.17	T 342+ 454.17	T 343+ 558.05	T 344+ 478.11	T 345+ 790.44
T 344+ 646.41	T 347+ 444.49	T 348+ 454.34	T 350+ 200.83	T 351+ 292.86	T 352+ 204.99
T 353+ 224.21	T 354+ 232.78	T 355+ 134.48	T 356+ 237.39	T 340+ 96.77%	T 362+ 98.59%
T 364+ 107.72	T 366+ 148.27	T 367+ 135.31	T 368+ 175.24	T 369+ 202.25	T 371+ 257.12
T 373+ 231.32	T 375+ 180.03	T 377+ 158.10	T 400+ 181.12	T 481+ 195.89	T 402+ 144.08
T 404+ 745.84	T 406+ 803.05	T 408+ 648.91	T 410+ 628.50	T 412+ 673.44	T 434+ 608.33

T 421= 416.18	T 422= 441.06	T 423= 529.49	T 424= 212.77	T 425= 788.42	T 426= 719.28
T 431= 645.09	T 432= 742.51	T 433= 819.98	T 434= 817.82	T 435= 765.19	T 436= 442.83
T 950= 886.15					
ARITHMETIC NODES IN ASCENDING NODE NUMBER ORDER					
T 50= 718.62	T 52= 685.26	T 54= 718.28	T 150= 718.84	T 159= 719.12	T 168= 718.70
T 189= 718.67	T 195= 249.10	T 197= 381.26	T 199= 551.42	T 238= 670.24	T 317= 698.98
T 312= 638.98	T 321= 626.95	T 322= 626.95	T 331= 597.94	T 332= 897.94	T 337= 515.83
T 341= 495.28	T 357= 248.95	T 358= 256.73	T 359= 262.83	T 379= 932.46	T 403= 140.87
T 1800= 278.36	T 1881= 445.31	T 1882= 545.41	T 1883= 523.08	T 1804= 207.69	T 1005= 204.59
T 1808= 112.07	T 1887= 716.87	T 1888= 723.83	T 1889= 756.36	T 1810= 325.85	T 1011= 723.21
T 1012= 725.21	T 1813= 581.81	T 1821= 786.89	T 1822= 786.99	T 1823= 872.11	T 1081= 677.91
T 1832= 677.91	T 1833= 558.30	T 1841= 439.78	T 1842= 439.78	T 1843= 458.87	T 1044= 458.87
T 1346= 648.79	T 1347= 366.53				
HEATER NODES IN ASCENDING NODE NUMBER ORDER					
==NONE==					
BOUNDARY NODES IN ASCENDING NODE NUMBER ORDER					
T 1= -20.000	T 2= -20.000				

SYSTEMS IMPROVED NUMERICAL DIFFERENCING ANALYZER '85 (SINCE '85)

PAGE 2/4

MODEL = DAMAGED
FIXDCKMAC LONG CASE NO. 2 CONDITION = Circumferential Distribution, -20P
***** Peak ICY Sidewall Temperature Time Point *****

8/2/84

SUBMODEL NAME = P788

	CALCULATED	ALLOWED
MAX DIFF DELTA 1 PER ITER	DELK00CP788	1681P 4.862812E-03 VS. DELK00P= 5.000000E-02
MAX ARITH DELTA 1 PER ITER	ARLK00CP788	337P -4.408388E-08 VS. ARLK00P= 0.500000
MAX DIFF DEL. 1 PER TIME STEP	GTWPC0CP788	432P -1.25936 VS. DTWPC0P= 10.0000
MAX ARITH DEL. 1 PER TIME STEP	ATWPC0CP788	1244P -0.785627 VS. ATWPC0P= 100.000
MIN STABILITY CRITERIA	CRMINCP788	455P 2.659042E-04
MAX STABILITY CRITERIA	CRMAXCP788	421P 2.22717
NUMBER OF ITERATIONS	LOOPCT	= 3 VS. MLOOPP= 400
PROBLEM TIME	TIMER	= 0.766664 VS. TIME0P= 12.0000
MEAN PROBLEM TIME	TIMER	= 0.764772
AVERAGE TIME STEP USED	DTIMER	= 7.958909E-04 VS. DTIMEP= 0.

DIFFUSION NODES IN ASCENDING NODE NUMBER ORDER																	
T	51=	719.43	T	53=	687.23	T	55=	782.58	T	60=	811.51	T	62=	895.36	T	100=	889.70
T	705=	851.09	T	107=	833.78	T	110=	812.23	T	113=	811.05	T	115=	815.81	T	120=	755.88
T	122=	749.81	T	125=	764.37	T	124=	746.49	T	125=	758.69	T	126=	746.04	T	127=	748.53
T	130=	751.69	T	131=	727.45	T	133=	736.47	T	134=	728.71	T	135=	734.88	T	136=	731.06
T	137=	732.29	T	140=	720.96	T	141=	721.27	T	142=	718.56	T	143=	723.33	T	144=	719.49
T	145=	723.01	T	146=	721.94	T	147=	723.06	T	150=	718.90	T	152=	716.49	T	153=	718.27
T	154=	718.52	T	155=	719.68	T	156=	721.99	T	157=	722.63	T	160=	720.76	T	161=	720.85
T	162=	720.68	T	163=	716.89	T	164=	722.61	T	168=	722.50	T	169=	727.22	T	167=	727.95
T	170=	770.71	T	172=	710.24	T	173=	789.67	T	175=	784.98	T	177=	704.88	T	180=	685.18
T	190=	707.25	T	191=	784.41	T	192=	728.47	T	193=	723.28	T	194=	565.62	T	196=	635.18
T	198=	789.95	T	200=	918.39	T	204=	902.54	T	210=	757.88	T	220=	736.52	T	230=	718.16
T	240=	632.89	T	242=	363.45	T	250=	152.61	T	260=	99.789	T	281=	302.89	T	282=	981.68
T	263=	304.39	T	264=	110.03	T	265=	117.99	T	266=	110.87	T	300=	616.71	T	386=	886.24
T	305=	503.92	T	310=	728.81	T	313=	659.62	T	315=	543.95	T	316=	545.95	T	320=	712.24
T	323=	643.18	T	325=	537.24	T	326=	537.26	T	330=	686.36	T	333=	615.89	T	335=	533.95
T	336=	533.15	T	340=	644.50	T	342=	633.62	T	343=	546.63	T	344=	269.43	T	345=	637.49
T	346=	609.66	T	347=	612.52	T	349=	447.46	T	350=	186.83	T	351=	237.90	T	352=	187.53
T	353=	210.78	T	354=	218.78	T	355=	139.90	T	356=	220.51	T	360=	96.337	T	362=	96.038
T	364=	304.53	T	366=	134.95	T	367=	135.01	T	368=	144.98	T	369=	161.06	T	371=	242.78
T	373=	218.62	T	375=	187.92	T	377=	136.36	T	400=	99.788	T	401=	114.82	T	482=	131.40
T	404=	704.72	T	406=	688.34	T	480=	575.67	T	490=	630.98	T	412=	676.28	T	414=	688.38
T	421=	495.69	T	422=	661.18	T	423=	689.68	T	424=	104.77	T	425=	783.69	T	426=	715.66
T	431=	662.35	T	432=	736.68	T	433=	348.36	T	434=	294.54	T	435=	747.25	T	436=	663.41
T	441=	579.45	T	442=	658.41	T	443=	688.46	T	444=	688.15	T	445=	667.08	T	446=	588.75
T	451=	585.62	T	482=	608.89	T	453=	618.91	T	454=	622.60	T	433=	620.23	T	456=	686.67
T	590=	803.17															
ARITHMETIC NODES IN ASCENDING NODE NUMBER ORDER																	
T	50=	723.42	T	52=	690.47	T	54=	717.25	T	150=	720.78	T	159=	720.82	T	168=	728.33

T 169=	720.13	T 195=	237.08	T 197=	279.73	T 199=	578.48	T 238=	675.44	T 311=	639.51
T 312=	639.51	T 321=	627.81	T 322=	627.81	T 331=	600.34	T 332=	600.34	T 337=	513.90
T 341=	442.45	T 357=	226.89	T 358=	241.98	T 359=	167.33	T 379=	137.25	T 403=	134.64
T 1000=	258.04	T 1001=	648.17	T 1002=	545.84	T 1003=	319.08	T 1004=	201.83	T 1005=	196.81
T 1006=	188.51	T 1007=	729.45	T 1008=	729.35	T 1009=	767.99	T 1010=	349.73	T 1011=	723.88
T 1012=	723.88	T 1013=	361.44	T 1021=	707.68	T 1022=	707.68	T 1023=	572.84	T 1031=	481.79
T 1032=	481.79	T 1033=	545.22	T 1041=	441.68	T 1042=	441.68	T 1043=	457.62	T 1044=	457.62
T 1346=	398.97	T 1347=	318.70								

ENTER NODES IN ASCENDING NODE NUMBER ORDER

++BOME++

BOUNDARY NODES IN ASCENDING NODE NUMBER ORDER

T 1=	-20.000	T 2=	-20.000
------	---------	------	---------

SYSTEM: IMPROVED NUMERICAL DIFFERENCING ANALYZER '88 (SIMO '85)

PAGE 3/4

MODEL = BAWOZ2
PUBCKMC LOAD CASE NO. 3 CONDITIONS - Circumferential Distribution, -20F
Initial Peak ICV Sidewall Temperature Time Point

5/2/79

SUBMODEL NAME = P76C

MAX DIFF DELTA T PER ITER	CALCULATED	120)= -4.514402E-05	VS.	ALLOWED	5.000000E-02
MAX ABNTH DELTA T PER ITER	DELTAOC(P76C	337)= -5.496347E-02	VS.	DELHCA=	8.500000
MAX DIFF DEL T PER TIME STEP	ARLACC(P76C	435)= -1.2942E	VS.	DTMPCA=	10.0000
MAX ABNTH DEL T PER TIME STEP	DTMPC(P76C	134)= -0.701279	VS.	ATMPCA=	100.0000
MIN STABILITY CRITERIA	CSGHI(P76C	455)= 2.441064E-04			
MIN STABILITY CRITERIA	CRSMC(P76C	424)= 2.22717			
NUMBER OF ITERATIONS	LOOPCT	= 3	VS.	MLCOPF=	500
PROBLEM TIME	TIMEH	= 0.756564	VS.	TIMEWA=	12.0000
NEAR PROBLEM TIME	TIMEH	= 0.756572			
AVERAGE TIME STEP USED	OTIMEU	= 7.956699E-04	VS.	OTIMEI=	0.

DIFFUSION NODES IN ASCENDING NODE NUMBER ORDER																	
T	51=	74.98	T	53=	499.50	T	55=	495.00	T	58=	825.74	T	62=	892.46	T	100=	843.29
T	109=	840.97	T	107=	851.41	T	110=	839.84	T	112=	837.90	T	115=	840.88	T	120=	794.88
T	122=	786.91	T	123=	797.33	T	124=	793.17	T	125=	799.42	T	126=	800.89	T	127=	802.23
T	130=	793.43	T	132=	750.68	T	133=	756.34	T	134=	753.99	T	135=	759.43	T	136=	763.66
T	137=	764.42	T	140=	735.89	T	141=	736.31	T	142=	733.00	T	143=	739.91	T	144=	739.61
T	145=	737.60	T	146=	748.42	T	147=	741.23	T	148=	728.84	T	152=	719.88	T	153=	720.92
T	154=	721.29	T	155=	721.79	T	156=	726.28	T	157=	726.21	T	160=	713.44	T	163=	716.33
T	162=	714.31	T	163=	712.95	T	164=	714.63	T	165=	714.23	T	166=	716.58	T	167=	716.57
T	170=	704.68	T	172=	704.90	T	173=	706.60	T	175=	704.07	T	177=	702.14	T	180=	702.40
T	190=	702.11	T	191=	702.63	T	192=	828.16	T	193=	722.68	T	194=	365.89	T	196=	638.05
T	198=	787.82	T	200=	897.78	T	204=	870.06	T	210=	766.53	T	220=	738.91	T	230=	688.20
T	240=	827.49	T	262=	341.92	T	250=	158.25	T	260=	98.560	T	281=	102.56	T	282=	901.63
T	263=	106.08	T	264=	109.81	T	265=	117.32	T	284=	117.87	T	300=	802.51	T	304=	785.33
T	305=	497.09	T	310=	734.41	T	313=	689.34	T	315=	547.08	T	316=	547.02	T	320=	713.88
T	325=	644.38	T	325=	538.21	T	326=	538.21	T	330=	673.17	T	333=	687.62	T	335=	527.21
T	336=	527.21	T	340=	638.12	T	342=	451.19	T	343=	948.97	T	344=	268.57	T	345=	636.29
T	346=	608.97	T	347=	411.64	T	349=	446.91	T	350=	186.42	T	351=	237.51	T	352=	187.12
T	353=	210.39	T	354=	218.28	T	355=	139.19	T	356=	228.04	T	360=	96.218	T	362=	94.496
T	364=	104.41	T	366=	136.65	T	367=	137.67	T	368=	144.43	T	369=	140.34	T	371=	242.37
T	373=	218.33	T	378=	167.75	T	379=	136.01	T	400=	99.733	T	401=	114.80	T	402=	131.24
T	404=	704.54	T	406=	408.42	T	408=	375.63	T	410=	630.58	T	412=	674.20	T	414=	608.38
T	421=	415.68	T	422=	441.90	T	423=	629.60	T	424=	184.16	T	425=	783.69	T	426=	715.63
T	427=	662.11	T	432=	736.43	T	433=	348.83	T	434=	294.54	T	435=	747.28	T	436=	663.40
T	441=	579.40	T	442=	658.45	T	443=	688.64	T	444=	688.13	T	445=	687.06	T	446=	580.72
T	451=	599.43	T	452=	686.30	T	453=	619.33	T	454=	682.37	T	455=	629.23	T	456=	604.65
T	950=	892.99															
ARITHMETIC NODES IN ASCENDING NODE NUMBER ORDER																	
T	50=	761.78	T	52=	703.12	T	54=	711.33	T	150=	716.17	T	159=	716.18	T	168=	716.04

T 149=	716.88	T 195=	236.38	T 197=	299.87	T 199=	577.80	T 238=	667.85	T 319=	643.83
T 312=	643.83	T 321=	629.18	T 322=	629.18	T 331=	592.18	T 332=	592.18	T 332=	511.60
T 341=	489.66	T 357=	224.42	T 358=	241.47	T 359=	186.92	T 379=	136.91	T 408=	134.49
T 1008=	257.61	T 1009=	605.89	T 1002=	508.53	T 1003=	378.32	T 1004=	201.34	T 1005=	198.52
T 1006=	703.24	T 1007=	777.87	T 1008=	725.84	T 1009=	718.27	T 1010=	344.73	T 1011=	729.56
T 1012=	729.56	T 1013=	584.95	T 1021=	789.29	T 1022=	789.29	T 1023=	173.91	T 1024=	669.37
T 1032=	669.37	T 1033=	553.47	T 1041=	635.68	T 1042=	635.68	T 1043=	454.98	T 1044=	454.98
T 1346=	597.90	T 1347=	316.84								
GREATER NODES IN ASCENDING NODE NUMBER ORDER											
←←NODE←←											
SMALLER NODES IN ASCENDING NODE NUMBER ORDER											
T 1=	-20.000	T 2=	-20.000								

SYSTEMS IMPROVED NUMERICAL DIFFERENTIATION ANALYZER '85 (SINGA '85)

PAGE 4/4

MODEL = BUNAGE2
FIXEDMIL LOAD CASE NO. 2 CONDITION = Circumferential Distribution, -20F
**** Peak ICV Sidewall Temperature Time Profile ****

5/2/94

SUBMODEL NAME = PTM

MAX DIFF DELTA T PER ITER	CALCULATED	128)= -6.39453E-03	ALLOWED
MAX ARITH DELTA T PER ITER	DRUNCC(PTM)	337)= -6.39468E-02	VS. BRUNCA= 5.00000E-02
MAX DIFF DEL T PER TIME STEP	ARUNCC(PTM)	439)= -1.29625	VS. ARUNCA= 0.50000
MAX ARITH DEL T PER TIME STEP	ATMPC(PTM)	1346)= -0.70053	VS. ATMPCA= 10.0000
MIN STABILITY CRITERIA	CBMIN(PTM)	495)= 2.66107E-04	VS. CBMINA= 100.000
MAX STABILITY CRITERIA	CBMAX(PTM)	426)= 2.82717	
NUMBER OF ITERATIONS	LOOPT	= 3	VS. MLOOPT= 600
PROBLEM TIME	TIMD	= 8.74466	VS. TIMEMD= 12.0000
NEAR PROBLEM TIME	TIMER	= 8.766172	
AVERAGE TIME STEP USED	DTIME	= 7.936500E-04	VS. DTIMEA= 0.

DIFFUSION NODES IN ASCENDING NODE NUMBER ORDER																	
T	51=	775.98	T	53=	743.63	T	55=	692.10	T	60=	468.19	T	62=	891.38	T	100=	684.99
T	105=	864.45	T	107=	855.57	T	110=	864.59	T	112=	864.46	T	113=	844.97	T	120=	803.37
T	122=	801.70	T	125=	883.32	T	126=	883.44	T	125=	806.51	T	126=	805.48	T	137=	805.75
T	130=	761.65	T	132=	759.52	T	133=	760.68	T	134=	762.74	T	135=	763.45	T	136=	767.74
T	137=	767.82	T	140=	740.66	T	161=	741.54	T	162=	739.23	T	163=	740.85	T	164=	740.90
T	145=	741.62	T	166=	764.46	T	167=	744.91	T	150=	726.52	T	152=	723.68	T	153=	726.26
T	154=	725.15	T	155=	725.54	T	156=	728.94	T	137=	728.98	T	160=	715.88	T	161=	718.39
T	162=	714.33	T	163=	714.82	T	164=	716.14	T	165=	717.15	T	166=	720.18	T	167=	720.57
T	170=	705.88	T	172=	705.91	T	173=	705.61	T	175=	704.44	T	177=	702.68	T	180=	702.14
T	190=	702.68	T	191=	701.90	T	192=	727.62	T	193=	723.58	T	194=	766.64	T	196=	629.54
T	199=	707.13	T	200=	697.68	T	204=	670.91	T	210=	768.04	T	220=	768.36	T	230=	699.38
T	240=	638.18	T	262=	362.57	T	290=	152.35	T	260=	99.518	T	261=	182.51	T	262=	181.59
T	263=	106.82	T	264=	109.80	T	268=	117.31	T	266=	117.69	T	300=	862.25	T	304=	785.67
T	305=	497.21	T	318=	735.27	T	319=	669.94	T	315=	547.45	T	316=	547.45	T	320=	714.72
T	323=	644.99	T	325=	538.62	T	326=	538.68	T	330=	679.97	T	333=	611.96	T	335=	530.33
T	326=	538.33	T	360=	641.16	T	362=	452.36	T	543=	546.23	T	364=	288.85	T	365=	636.48
T	366=	689.06	T	367=	419.78	T	369=	447.13	T	390=	186.48	T	351=	257.59	T	352=	187.16
T	353=	218.44	T	354=	218.38	T	375=	139.21	T	376=	320.18	T	380=	98.187	T	382=	96.677
T	364=	104.61	T	366=	134.67	T	367=	137.68	T	368=	144.43	T	369=	168.35	T	371=	262.63
T	373=	218.30	T	375=	167.77	T	377=	156.82	T	400=	90.728	T	401=	114.78	T	402=	131.23
T	404=	706.57	T	406=	608.85	T	408=	373.64	T	410=	630.38	T	412=	674.20	T	414=	608.38
T	421=	415.88	T	422=	641.18	T	423=	629.88	T	424=	184.16	T	425=	783.69	T	428=	713.45
T	431=	662.32	T	432=	736.57	T	433=	348.94	T	434=	264.54	T	435=	747.28	T	436=	663.41
T	441=	379.42	T	442=	658.53	T	443=	688.85	T	444=	688.13	T	445=	667.07	T	446=	580.73
T	451=	593.35	T	452=	608.72	T	453=	619.87	T	454=	622.38	T	455=	629.23	T	456=	604.64
T	910=	890.95															
ARITHMETIC NODES IN ASCENDING NODE NUMBER ORDER																	
T	50=	771.15	T	52=	707.29	T	54=	711.83	T	150=	738.19	T	155=	718.46	T	160=	718.09

T 169=	717.94	T 195=	236.05	T 197=	296.64	T 199=	576.82	T 230=	669.18	T 311=	644.47
T 312=	644.47	T 321=	629.72	T 322=	629.72	T 351=	996.49	T 332=	996.49	T 337=	512.62
T 347=	491.82	T 357=	224.59	T 358=	241.56	T 399=	186.97	T 379=	136.92	T 485=	134.58
T 900=	257.18	T 1001=	663.17	T 1002=	588.21	T 1005=	317.76	T 1006=	281.22	T 1005=	196.21
T 906=	108.18	T 1007=	718.34	T 1008=	736.01	T 1009=	764.82	T 1010=	348.76	T 1011=	750.28
T 9012=	730.28	T 1013=	585.45	T 1001=	790.12	T 1022=	790.12	T 1023=	574.39	T 1031=	676.83
T 1032=	676.83	T 1033=	557.02	T 1041=	638.74	T 1042=	638.74	T 1043=	656.27	T 1044=	656.27
T 1346=	598.18	T 1347=	516.88								
HEATER MODES IN ASCENDING MODE NUMBER ORDER											
++BENE++											
BOUNDARY MODES IN ASCENDING MODE NUMBER ORDER											
T 1=	-20.880	T 2=	-20.880								

T 429= 110.73	T 430= 0.44304	T 431= -7.3431	T 432= 86.074	T 433= 1.4922	T 434= -8.5987
T 431= 21.232	T 432= 20.090	T 433= 19.082	T 434= 2.9044	T 435= -8.9075	T 436= -8.8851
T 450= 453.54	ARITHMETIC NODES IN ASCENDING NODE NUMBER ORDER				
T 50= 335.12	T 52= 332.08	T 54= 333.58	T 58= 337.35	T 59= 346.90	T 60= 347.83
T 169= 366.77	T 195= 343.69	T 197= 350.95	T 199= 379.48	T 238= 226.55	T 311= 125.44
T 312= 125.46	T 321= 130.54	T 322= 130.54	T 331= 146.90	T 332= 146.90	T 337= 142.83
T 361= 154.67	T 357= 141.92	T 358= 137.93	T 399= 144.54	T 379= 147.08	T 483= 145.37
T 908= 253.96	T 1001= 468.53	T 1008= 387.33	T 903= 322.58	T 1004= 288.89	T 1005= 267.13
T 908= 309.18	T 1007= 469.01	T 1008= 600.18	T 909= 319.94	T 1010= 242.59	T 1011= 142.72
T 1012= 142.72	T 1013= 111.27	T 1021= 154.77	T 902= 154.77	T 1023= 117.71	T 1031= 170.15
T 1032= 170.15	T 1023= 152.43	T 1061= 171.31	T 904= 171.31	T 1043= 159.86	T 1064= 159.86
T 1364= 90.917	T 1347= 133.98	HEATER NODES IN ASCENDING NODE NUMBER ORDER			

T 1= -20.000	T 2= -20.000	BOUNDARY NODES IN ASCENDING NODE NUMBER ORDER			

SYSTEMS IMPROVED NUMERICAL DIFFERENCING ANALYZER '85 (SIRDA '85)

PAGE 2/4

MODEL # MANAGE
STDBLMC LOAD CASE NO. 2 CONDITIONS - Circumferential Distribution, -20
*** Steady-state Conditions After The Fire ***

5/2/94 10am

SUBMODEL NAME # P158

MAX DIFF DELTA 1 PER ITER	CALCULATED DRUNCCPTIM	194)=-3.66823E+02	VS. ALLOWED DRUNCA= 3.00000E-02
MAX ARITH DELTA 1 PER ITER	ARUNCCPTIM	197)=-0.189563	VS. ARALCA= 6.50000E-02
MAX SYSTEM ENERGY BALANCE	EBALBC	= 1.76287	VS. EBALCA = EBUNIS = 1.91921
	EBUNIS	= 1919.21	EBALCA= 1.80000E-02
ENERGY INTO AND OUT OF SYS	EBALNCPTIM	347)=-0.349181	VS. EBALCA= 1.00000E-02
MAX NODAL ENERGY BALANCE	LOOPCT	= 340	VS. NLOOP# = 1288
NUMBER OF ITERATIONS	TIMER	= 999.908	VS. TITER# = 999.999
PROBLEM TIME			

DISPERION		MONEY		IN ASCENDING		NODE		NUMBER		ORDER	
T 51=	226.68	T 53=	274.15	T 55=	359.91	T 60=	218.38	T 62=	590.49	T 100=	207.30
T 108=	209.08	T 107=	211.06	T 110=	212.27	T 112=	212.34	T 113=	271.93	T 120=	221.08
T 122=	221.82	T 123=	219.95	T 124=	221.34	T 125=	219.73	T 126=	220.78	T 127=	279.75
T 130=	247.05	T 132=	249.36	T 133=	245.01	T 134=	245.74	T 135=	246.45	T 136=	249.82
T 137=	263.68	T 140=	268.11	T 141=	268.28	T 142=	270.25	T 143=	264.67	T 144=	271.08
T 145=	266.66	T 144=	273.05	T 147=	271.59	T 150=	305.01	T 152=	308.59	T 182=	297.47
T 154=	312.88	T 155=	304.78	T 156=	329.29	T 157=	318.74	T 160=	349.32	T 161=	359.06
T 162=	372.78	T 163=	341.58	T 164=	374.34	T 165=	347.74	T 166=	378.23	T 167=	374.81
T 170=	431.85	T 172=	432.43	T 173=	429.69	T 175=	434.08	T 177=	443.83	T 180=	448.00
T 190=	468.74	T 191=	546.74	T 192=	296.45	T 198=	392.35	T 194=	373.86	T 196=	414.65
T 198=	930.29	T 200=	182.88	T 204=	175.22	T 210=	188.71	T 220=	166.10	T 230=	229.94
T 240=	252.49	T 242=	200.33	T 250=	174.55	T 260=	186.85	T 261=	188.84	T 262=	182.70
T 282=	184.75	T 284=	173.32	T 283=	178.74	T 286=	169.68	T 300=	112.84	T 304=	95.888
T 305=	22.181	T 310=	143.44	T 313=	123.29	T 315=	102.72	T 316=	145.72	T 320=	154.81
T 323=	132.74	T 325=	118.06	T 326=	118.06	T 330=	175.72	T 333=	152.83	T 335=	128.64
T 334=	124.64	T 340=	175.09	T 342=	163.01	T 343=	102.01	T 344=	151.71	T 345=	106.63
T 346=	81.863	T 347=	129.59	T 348=	92.972	T 350=	167.85	T 351=	148.69	T 352=	146.76
T 353=	143.51	T 354=	146.99	T 355=	149.66	T 356=	144.69	T 360=	142.81	T 362=	777.43
T 364=	167.11	T 366=	180.89	T 367=	149.19	T 368=	147.27	T 369=	145.83	T 371=	148.40
T 373=	142.86	T 375=	144.27	T 377=	148.33	T 400=	170.65	T 401=	188.68	T 402=	148.76
T 404=	170.98	T 406=	17.606	T 408=	-12.453	T 410=	-13.287	T 412=	-12.538	T 414=	-12.156
T 421=	112.84	T 422=	8.72698	T 423=	-7.3447	T 424=	94.051	T 425=	3.8869	T 426=	-5.9913
T 431=	36.762	T 432=	40.788	T 433=	56.308	T 434=	23.701	T 435=	-8.3984	T 436=	-11.349
T 441=	1.1814	T 442=	4.7527	T 443=	-1.8142	T 444=	-6.9082	T 445=	-12.854	T 446=	-12.804
T 451=	1.4443	T 452=	8.2599	T 453=	-4.9319	T 454=	-9.7364	T 455=	-13.794	T 456=	-13.494
T 950=	699.54										
ARITHMETIC		NODES		IN ASCENDING		NODE		NUMBER		ORDER	
T 50=	232.49	T 52=	275.84	T 54=	359.68	T 158=	340.39	T 159=	358.41	T 160=	358.90
T 160=	358.43	T 195=	252.49	T 197=	265.65	T 199=	326.37	T 230=	236.93	T 311=	123.78

T 312=	123.78	T 321=	131.17	T 322=	131.17	T 331=	150.98	T 332=	130.08	T 337=	144.56
T 341=	157.53	T 357=	144.39	T 358=	140.36	T 399=	147.28	T 379=	149.95	T 403=	148.47
T 1008=	268.58	T 1007=	476.94	T 1002=	402.28	T 1003=	321.58	T 1004=	273.01	T 1005=	270.22
T 1006=	190.89	T 1007=	476.34	T 1008=	489.26	T 1009=	529.25	T 1010=	255.86	T 1011=	143.89
T 1012=	143.89	T 1013=	111.36	T 1021=	151.48	T 1022=	151.48	T 1023=	118.88	T 1021=	175.34
T 1032=	175.30	T 1033=	136.18	T 1041=	174.59	T 1042=	174.59	T 1043=	162.76	T 1044=	162.74
T 1344=	93.279	T 1347=	136.80								
HEATER NODES IN ASCENDING NODE NUMBER ORDER											
←←NODE→→											
BOUNDARY NODES IN ASCENDING NODE NUMBER ORDER											
T 1=	-20.000	T 2=	-20.000								

SYSTEMS IMPROVED NUMERICAL DIFFERENCING ANALYZER *85 (SINGA *85)

PAGE 3/4

MODEL = DAMAGED
STBST1MAX LOAD CASE NO. 3 CONDITIONS = Circumferential Distribution, *28
*** Steady-state Conditions After The Fire ***

5/2/94 1000

SUBMODEL NAME = PTSC

MAX DIFF DELTA T PER ITER	CALCULATED	250>	4.962158E-02	VS.	ALLOWED	5.000000E-02
MAX ARITH DELTA T PER ITER	ANALYZED(PTSC)	1044>	3.637493E-02	VS.	ANALYZED	0.500000
MAX SYSTEM ENERGY BALANCE	REALSC		+ 25.1190	VS.	REALSC	+ 25.1190
ENERGY INTO AND OUT OF ITS	ERRDIS		+ 2879.72	VS.	ERRDIS	2887.14
MAX LOCAL ENERGY BALANCE	ERRALC(PTSC)	367>	3.11621	VS.	ERRALC	1.00000E-02
NUMBER OF ITERATIONS	LEXPCT		= 140	VS.	LEXPCT	1200
PROBLEM TIME	TIMEN		= 999.000	VS.	TIMEN	999.000

DISPUSION NODES IN ASCENDING NODE NUMBER ORDER		DISPUSION NODES IN ASCENDING NODE NUMBER ORDER		DISPUSION NODES IN ASCENDING NODE NUMBER ORDER	
I	51=	I	53=	I	55=
	221.16		257.09		294.19
I	103=	I	105=	I	107=
	307.42		308.20		309.59
I	122=	I	123=	I	124=
	217.43		216.08		216.20
I	138=	I	132=	I	134=
	256.87		239.11		236.01
I	137=	I	140=	I	141=
	229.06		251.32		261.64
I	145=	I	146=	I	147=
	248.86		245.68		244.57
I	154=	I	195=	I	156=
	278.83		272.20		273.08
I	162=	I	163=	I	164=
	362.35		354.24		337.39
I	170=	I	172=	I	173=
	413.58		415.68		415.86
I	190=	I	191=	I	192=
	446.38		547.71		296.90
I	198=	I	200=	I	204=
	551.49		384.80		179.18
I	240=	I	242=	I	260=
	238.54		198.61		173.48
I	263=	I	266=	I	268=
	184.38		174.68		178.11
I	306=	I	310=	I	312=
	22.893		145.33		126.99
I	323=	I	325=	I	326=
	153.29		110.51		110.51
I	336=	I	340=	I	342=
	118.35		167.66		159.87
I	346=	I	367=	I	368=
	79.851		127.96		91.267
I	383=	I	354=	I	355=
	141.91		168.87		168.22
I	366=	I	366=	I	367=
	166.24		149.69		167.76
I	373=	I	373=	I	377=
	161.24		144.77		146.91
I	406=	I	406=	I	410=
	189.59		16.658		-12.640
I	421=	I	422=	I	423=
	111.60		0.85468		-7.3983
I	431=	I	432=	I	433=
	95.889		39.887		57.658
I	441=	I	442=	I	443=
	0.20661		4.2047		-1.8882
I	451=	I	452=	I	453=
	1.1726		7.5487		-9.2288
I	950=				
	661.60				
I	50=	I	52=	I	54=
	225.57		258.92		326.17
I	160=	I	195=	I	197=
	327.70		282.92		286.24
I	150=	I	150=	I	150=
	323.48		327.57		327.57
I	140=	I	140=	I	140=
	327.65		327.65		327.65
I	230=	I	230=	I	230=
	217.89		217.89		217.89
I	210=	I	210=	I	210=
	129.47		129.47		129.47

T 312=	125.47	T 321=	131.72	T 322=	131.72	T 331=	141.07	T 332=	141.07	T 337=	148.67
T 341=	138.51	T 337=	142.71	T 358=	138.70	T 359=	145.68	T 379=	148.53	T 483=	147.06
T 1000=	270.23	T 1001=	478.00	T 1002=	488.75	T 1003=	332.13	T 1004=	273.46	T 1005=	278.64
T 1006=	190.73	T 1007=	471.47	T 1008=	488.94	T 1009=	538.92	T 1010=	253.78	T 1011=	143.03
T 1012=	148.63	T 1013=	113.08	T 1014=	132.32	T 1025=	152.32	T 1023=	118.77	T 1031=	161.66
T 1032=	161.46	T 1033=	127.95	T 1041=	167.23	T 1042=	167.23	T 1043=	158.76	T 1044=	158.76
T 1344=	91.628	T 1347=	129.31								
HEATER MODES IN ASCENDING MODE NUMBER ORDER											
+-----+											
BOUNDARY MODES IN ASCENDING MODE NUMBER ORDER											
T 1=	-20.000	T 2=	-20.000								

T 312=	125.19	F 321=	132.01	F 322=	132.01	T 331=	146.66	F 332=	146.66	T 337=	142.07
F 341=	155.82	T 387=	143.78	F 356=	139.74	T 359=	146.73	F 379=	149.48	T 482=	148.01
F 1006=	368.24	T 1001=	449.41	F 1002=	399.55	T 1003=	328.16	F 1004=	271.38	T 1005=	288.65
T 1006=	191.90	F 1007=	442.43	T 1008=	676.58	F 1009=	517.70	T 1010=	264.68	T 1011=	144.71
T 1012=	144.71	F 1013=	112.83	T 1021=	152.46	F 1022=	152.46	F 1023=	119.83	T 1031=	149.26
F 1032=	169.36	T 1033=	132.20	F 1041=	171.69	F 1042=	171.69	F 1043=	161.12	T 1044=	161.12
T 1346=	92.636	T 1347=	136.31								
HEATER NODES IN ASCENDING NODE NUMBER ORDER											
--<NODE--											
BRIGHTLY NODES IN ASCENDING NODE NUMBER ORDER											
T 1=	-20.000	T 2=	-20.000								

SYSTEM IMPROVED NUMERICAL DIFFERENCING ANALYZER '85 (SIBMA '85)

PAGE 1/4

MODEL = DAMAGED
FUBCZLOAD CASE NO. 3 CONDITIONS = Axial Distribution, 100%
Peak OCY Sidewall Temperature Time Point

5/2/76

SUBMODEL NAME = MAIN
PROBLEM TIME

TIMER = 0.500000 VS. TIME0 = 0.500000

T 267= 207.98 T 268= 207.85 T 269= 206.93
 DIFFUSION NODES IN ASCENDING NODE NUMBER ORDER
 T 207= 895.88 T 1266= 213.32 T 1267= 269.96 T 1268= 265.54 T 1269= 219.11
 ARITHMETIC NODES IN ASCENDING NODE NUMBER ORDER
 BEATER NODES IN ASCENDING NODE NUMBER ORDER
 --NONE--
 BOUNDARY NODES IN ASCENDING NODE NUMBER ORDER
 --NONE--

MEAN OCY GAS TEMP= 875.9 F MEAN OCY GAS PRESSURE= 34.46 PSIA
 MEAN ICY-OCY GAS TEMP= 856.1 F MEAN ICY-OCY GAS PRESSURE= 45.67 PSIA

SUBMODEL NAME = PTSA

	CALCULATED	ALLOWED
MAX DIFF DELTA T PER ITER	MRUCO(PTSA 161)= 4.05191E-02	VS. MRUCO= 5.00000E-02
MAX NBITU DELTA T PER ITER	MRUCO(PTSA 168)= 3.49121E-02	VS. MRUCO= 0.500000
MAX DIFF DEL T PER TIME STEP	BTMPC(PTSA 200)= 7.76336	VS. BTMPC= 10.0000
MAX NBITU DEL T PER TIME STEP	ATMPC(PTSA 258)= 9.17447	VS. ATMPC= 100.000
NIR STABILITY CRITERIA	CSGRH(PTSA 431)= 3.00166E-05	
MAX STABILITY CRITERIA	CSGRH(PTSA 424)= 1.95861	
NUMBER OF ITERATIONS	LOOPCT = 11	VS. MLOOP= 500
PROBLEM TIME	TIMER = 0.500000	VS. TIME0 = 0.500000
MEAN PROBLEM TIME	TIMEN = 0.499871	
AVERAGE TIME STEP USED	DTMEN = 5.99555E-03	VS. DTMEL= 0.

DIFFUSION NODES IN ASCENDING NODE NUMBER ORDER

T 51= 995.11	T 53= 965.76	T 55= 940.87	T 60= 925.22	T 62= 1044.3	T 100= 971.05
T 105= 919.51	T 107= 925.78	T 110= 946.69	T 112= 945.54	T 113= 951.97	T 120= 1057.3
T 122= 1095.1	T 123= 967.75	T 124= 1071.7	T 125= 962.63	T 126= 1085.2	T 127= 952.25
T 130= 1034.3	T 132= 1081.1	T 133= 954.29	T 134= 1078.6	T 135= 920.01	T 136= 1075.7
T 137= 911.41	T 140= 984.50	T 141= 967.45	T 142= 1019.0	T 143= 895.16	T 144= 1076.4
T 145= 889.37	T 146= 1018.9	T 147= 881.34	T 150= 1000.0	T 152= 1053.4	T 153= 875.73
T 154= 1049.6	T 155= 872.18	T 156= 1048.5	T 157= 863.79	T 160= 934.78	T 161= 822.45
T 162= 983.92	T 163= 819.81	T 164= 979.26	T 165= 823.02	T 166= 975.65	T 167= 818.34
T 170= 979.36	T 172= 588.01	T 173= 958.50	T 175= 488.93	T 177= 523.83	T 180= 589.15
T 190= 365.03	T 191= 357.90	T 192= 235.84	T 193= 448.69	T 194= 264.64	T 196= 329.23
T 198= 359.36	T 200= 1076.1	T 204= 1129.0	T 210= 1166.6	T 220= 1155.6	T 230= 1090.3
T 240= 626.11	T 242= 357.80	T 250= 222.54	T 260= 201.14	T 261= 208.13	T 262= 201.52
T 268= 204.96	T 269= 302.33	T 265= 265.28	T 266= 265.56	T 300= 1222.4	T 304= 1268.6
T 308= 1380.3	T 310= 1177.4	T 313= 1253.4	T 315= 1363.1	T 316= 1343.1	T 320= 1169.3
T 323= 1247.8	T 325= 1338.9	T 326= 1338.9	T 330= 1889.0	T 333= 1158.2	T 335= 1287.9
T 336= 1287.9	T 340= 908.95	T 342= 682.20	T 343= 1888.6	T 344= 344.88	T 345= 971.87
T 346= 1277.3	T 347= 951.95	T 349= 1879.2	T 350= 267.63	T 351= 465.21	T 352= 271.69
T 353= 308.36	T 354= 308.73	T 355= 229.94	T 356= 318.79	T 360= 199.74	T 362= 199.86
T 364= 200.23	T 366= 229.19	T 367= 225.71	T 368= 249.34	T 369= 246.90	T 371= 461.65
T 373= 365.32	T 373= 246.37	T 377= 227.96	T 400= 199.65	T 401= 209.81	T 403= 223.25
T 404= 1203.3	T 406= 1380.2	T 406= 1261.7	T 410= 1411.6	T 412= 1411.0	T 414= 1419.3

T	421=	471.48	T	422=	5414.7	T	423=	5417.5	T	424=	264.34	T	425=	1461.7	T	426=	1464.3
T	431=	1342.5	T	432=	1345.5	T	433=	1349.2	T	434=	1347.9	T	435=	1382.4	T	436=	1384.2
T	950=	1478.9	T	952=	1487.4	T	954=	1443.5									
ARITHMETIC MODES IN ASCENDING MODE NUMBER ORDER																	
T	50=	986.00	T	52=	984.23	T	54=	954.75	T	56=	942.74	T	159=	896.83	T	160=	896.71
T	169=	928.56	T	193=	256.86	T	197=	258.49	T	199=	347.22	T	238=	897.84	T	219=	1245.6
T	312=	1269.6	T	321=	1259.7	T	322=	1259.7	T	331=	1161.3	T	332=	1161.3	T	337=	821.99
T	343=	790.27	T	337=	342.69	T	338=	432.13	T	339=	270.25	T	379=	224.37	T	403=	226.40
T	1000=	252.34	T	1001=	332.35	T	1002=	332.01	T	1003=	254.28	T	1004=	228.64	T	1005=	227.43
T	1006=	204.02	T	1007=	422.10	T	1008=	382.72	T	1009=	368.21	T	1010=	288.31	T	1011=	1189.7
T	1012=	1189.7	T	1013=	1317.8	T	1021=	1182.8	T	1022=	1182.8	T	1023=	1313.3	T	1031=	1181.2
T	1032=	1401.2	T	1033=	1248.6	T	1041=	935.43	T	1042=	935.43	T	1043=	449.61	T	1044=	449.61
T	1346=	1143.4	T	1347=	453.43												
HEATER MODES IN ASCENDING MODE NUMBER ORDER																	
***MODE**																	
BOUNDARY MODES IN ASCENDING MODE NUMBER ORDER																	
T	7=	1473.8	T	2=	1424.7												

SYSTEMS IMPROVED NUMERICAL DIFFERENCING ANALYZER '85 (FINDA '85)

PAGE 2/4

MODEL = DAMAGES
PUBCKLOAD CASE NO. 3 CONDITION - Axial distribution, IMOF
Peak OCY Sidwell Temperature Time Pulse

5/27/94

RUNMODEL NAME = P108

MAX DIFF DELTA T PER ITER	MILNCC(P108)	1321= 3.209473E-02	VS.	ALLOWED	5.000000E-02
MAX ARITH DELTA T PER ITER	ARLNCC(P108)	1481= 1.110840E-02	VS.	ARLNCA=	0.500000
MAX DIFF DEL T PER FINE STEP	DYNCC(P108)	1901= 7.19913	VS.	DYNCA=	10.0000
MAX ARITH DEL T PER FINE STEP	ATNCC(P108)	2381= 4.23135	VS.	ATNCA=	100.000
MIN STABILITY CRITERIA	CSQMIN(P108)	4461= 3.048285E-09			
MAX STABILITY CRITERIA	CSQMAX(P108)	4341= 3.26635			
NUMBER OF ITERATIONS	LOOPCT	= 11	VS.	NLOOP=	600
PROBLEM TIME	TIMER	= 8.500000	VS.	TINDAP=	0.500000
MEAN PROBLEM TIME	TIMER	= 0.496871			
AVERAGE FINE STEP USED	DTIMEJ	= 3.355502E-03	VS.	OTIME1=	0.

DIFFUSION MODES IN ASCENDING MODE NUMBER ORDER

T 51=	831.24	T 53=	808.91	T 55=	799.89	T 60=	788.57	T 62=	7005.2	T 100=	1005.4
T 109=	955.02	T 107=	953.49	T 910=	923.21	T 112=	920.73	T 113=	918.19	T 121=	889.27
T 122=	931.01	T 125=	861.22	T 126=	912.89	T 125=	866.62	T 126=	863.59	T 127=	875.11
T 130=	828.20	T 132=	879.42	T 133=	799.26	T 134=	853.65	T 135=	795.48	T 136=	816.95
T 137=	798.76	T 140=	789.40	T 141=	789.54	T 142=	838.75	T 143=	796.85	T 144=	813.08
T 148=	796.95	T 146=	767.02	T 147=	793.62	T 150=	799.31	T 152=	825.17	T 193=	717.83
T 154=	789.27	T 155=	716.22	T 156=	733.20	T 157=	775.44	T 160=	782.73	T 161=	787.44
T 162=	765.42	T 163=	664.16	T 164=	733.59	T 165=	663.38	T 166=	688.34	T 167=	481.23
T 170=	529.76	T 172=	539.89	T 173=	519.26	T 175=	454.81	T 177=	485.47	T 180=	448.32
T 190=	369.36	T 191=	573.21	T 192=	234.59	T 193=	471.69	T 194=	268.46	T 196=	343.41
T 198=	376.60	T 200=	1058.5	T 204=	1072.8	T 210=	762.59	T 220=	745.33	T 230=	673.14
T 240=	553.61	T 242=	347.90	T 250=	820.73	T 260=	200.90	T 261=	281.73	T 262=	288.23
T 263=	201.38	T 264=	201.41	T 265=	204.39	T 266=	204.44	T 200=	1218.7	T 284=	1227.5
T 280=	1375.2	T 310=	951.75	T 315=	1116.3	T 315=	1284.9	T 316=	1284.9	T 320=	937.36
T 323=	1106.2	T 325=	1277.7	T 326=	1277.7	T 330=	870.77	T 330=	1049.2	T 335=	1244.4
T 336=	1244.4	T 340=	856.87	T 342=	573.42	T 343=	1839.6	T 344=	334.11	T 345=	650.78
T 346=	1262.3	T 347=	476.32	T 349=	1067.8	T 350=	248.03	T 351=	430.22	T 352=	261.23
T 353=	361.79	T 354=	298.81	T 355=	221.67	T 356=	343.34	T 360=	199.68	T 362=	790.63
T 364=	199.39	T 366=	214.28	T 367=	215.99	T 368=	221.71	T 369=	231.85	T 371=	451.84
T 373=	334.51	T 373=	260.71	T 377=	218.72	T 400=	199.30	T 401=	280.78	T 402=	212.85
T 404=	933.43	T 408=	1361.3	T 408=	1380.7	T 430=	1406.4	T 412=	1410.4	T 414=	1419.2
T 421=	471.36	T 422=	1414.7	T 428=	1417.5	T 434=	248.83	T 425=	1400.9	T 426=	1406.5
T 431=	1291.7	T 432=	1323.1	T 433=	246.42	T 434=	222.11	T 435=	1386.4	T 436=	1396.7
T 441=	1380.1	T 442=	1370.6	T 443=	1371.3	T 444=	1371.3	T 443=	1391.3	T 444=	1381.0
T 451=	1372.7	T 452=	1361.7	T 433=	1376.7	T 454=	1381.4	T 455=	1405.9	T 456=	1392.0
ARITHMETIC MODES IN ASCENDING MODE NUMBER ORDER											
T 50=	531.51	T 52=	897.25	T 54=	763.62	T 138=	717.98	T 150=	697.29	T 160=	708.38
T 160=	711.89	T 195=	225.44	T 197=	241.60	T 199=	359.90	T 230=	421.61	T 211=	1132.7

T 312=	1132.7	T 321=	1122.4	T 322=	1122.4	F 331=	1064.1	F 332=	1064.1	T 337=	792.05
F 341=	477.12	F 337=	330.97	T 338=	421.99	T 339=	261.33	T 379=	216.69	T 443=	216.78
F 1000=	227.24	T 1001=	343.99	T 1002=	343.42	T 1005=	293.82	T 1006=	227.39	T 1009=	226.56
T 1004=	252.68	T 1007=	414.16	F 1008=	390.28	T 1009=	376.48	T 1010=	381.02	T 1011=	973.33
F 1012=	973.33	F 1013=	1239.6	T 1021=	959.15	T 1022=	959.15	F 1023=	1228.2	T 1031=	901.33
T 1032=	901.33	F 1033=	1187.8	T 1041=	860.62	F 1042=	860.62	F 1043=	614.13	T 1044=	614.13
T 1344=	9042.3	T 1347=	366.93	HEATER WORDS IN ASCENDING WORD NUMBER ORDER							
				←NONE←							
				BOUNDARY WORDS IN ASCENDING WORD NUMBER ORDER							
T 1=	1479.0	T 2=	1426.7								

SYSTEM IMPROVED NUMERICAL DIFFERENCING ANALYZER '85 (Edna '85)

PAGE 3/4

MODEL = CHANGES
PUBCKLOAD CASE NO. 3 CONDITIONS - Axial Distribution, Y08F
Peak OCv (Sidewall) Temperature Time Point

5/2/84

SUBMODEL NAME = PTSC

MAX DIFF DELTA T PER ITER	CALCULATED	ALLOWED
MAX ALITH DELTA T PER ITER	ORLDCOPTSC	VS. ORLDC= 9.00000E-02
MAX DIFF DEL T PER TIME STEP	WRLDCOPTSC	VS. WRLDC= 0.50000E+00
MAX ANITS DEL T PER TIME STEP	BTWPCOPTSC	VS. BTWPCA= 10.0000
MIN STABILITY CRITERIA	ATWPCOPTSC	VS. ATWPCA= 100.000
MAX STABILITY CRITERIA	CSGNHOPTSC	
NUMBER OF ITERATIONS	CRWAOPTSC	
PROBING TIME	LOOPCT	n 11 VS. BLKPT= 400
HEAT PROBLEM TIME	TIMER	= 0.500000 VS. TIMED= 0.500000
AVERAGE TIME STEP USED	TIMER	= 0.456871
	DTIMEJ	= 3.535552E-03 VS. BTIMEJ= 0.

DIFFUSION MODES IN ASCENDING MODE NUMBER ORDER																	
T	51=	732.69	T	53=	703.66	T	55=	663.70	T	60=	660.81	T	63=	687.74	T	100=	689.26
T	105=	699.66	T	107=	666.69	T	110=	663.75	T	112=	694.35	T	113=	692.43	T	120=	625.19
T	122=	638.79	T	123=	621.78	T	124=	631.80	T	125=	626.02	T	126=	627.69	T	127=	636.58
T	130=	741.88	T	132=	766.76	T	133=	737.90	T	134=	746.03	T	135=	739.23	T	136=	765.67
T	137=	766.03	T	140=	692.82	T	141=	691.67	T	142=	699.83	T	143=	699.71	T	144=	695.76
T	145=	689.31	T	146=	692.65	T	147=	691.65	T	150=	687.54	T	152=	666.33	T	153=	654.63
T	156=	668.48	T	155=	651.48	T	156=	653.53	T	157=	690.64	T	160=	683.26	T	161=	618.96
T	162=	632.66	T	163=	601.67	T	164=	608.32	T	165=	609.89	T	166=	606.08	T	167=	601.62
T	170=	688.75	T	172=	689.96	T	173=	687.29	T	175=	663.60	T	177=	639.32	T	180=	646.23
T	190=	687.53	T	191=	356.28	T	192=	325.63	T	193=	486.11	T	194=	270.15	T	196=	603.16
T	198=	600.58	T	200=	1045.8	T	204=	1035.6	T	210=	712.81	T	220=	668.07	T	230=	620.26
T	240=	566.10	T	243=	346.38	T	250=	220.49	T	260=	200.92	T	261=	201.69	T	262=	300.89
T	265=	281.21	T	264=	201.49	T	263=	206.16	T	266=	206.36	T	300=	1234.3	T	304=	1321.3
T	305=	1376.1	T	310=	927.68	T	313=	1182.9	T	315=	1279.5	T	316=	1279.3	T	320=	911.32
T	325=	1091.7	T	325=	1271.9	T	326=	1271.9	T	330=	858.04	T	333=	1039.8	T	335=	1268.7
T	336=	1260.7	T	340=	828.55	T	342=	570.63	T	343=	1638.9	T	346=	333.29	T	349=	628.86
T	346=	1251.1	T	347=	675.61	T	349=	1067.6	T	350=	259.76	T	351=	635.95	T	352=	260.99
T	353=	361.62	T	354=	298.63	T	355=	221.00	T	356=	362.96	T	360=	199.65	T	362=	988.56
T	364=	199.33	T	364=	214.12	T	367=	215.77	T	368=	221.29	T	369=	231.22	T	370=	651.34
T	373=	336.38	T	375=	268.85	T	377=	218.87	T	400=	199.29	T	401=	208.77	T	402=	212.79
T	484=	933.45	T	480=	1360.7	T	480=	1360.7	T	410=	1086.4	T	412=	1410.6	T	414=	1419.2
T	621=	671.37	T	620=	1614.7	T	623=	1617.5	T	626=	265.84	T	625=	1408.9	T	606=	1606.3
T	631=	1251.3	T	632=	1326.8	T	633=	246.42	T	634=	232.12	T	635=	1386.4	T	636=	1399.7
T	641=	1380.0	T	642=	1378.3	T	643=	1373.3	T	644=	1373.3	T	645=	1391.4	T	646=	1381.0
T	651=	1372.5	T	652=	1361.1	T	653=	1376.7	T	654=	1381.3	T	655=	1405.9	T	656=	1382.0
ARITHMETIC MODES IN ASCENDING MODE NUMBER ORDER																	
T	50=	753.33	T	52=	704.95	T	54=	695.67	T	150=	612.88	T	150=	610.38	T	160=	611.30
T	160=	612.90	T	165=	239.73	T	177=	246.34	T	199=	371.20	T	230=	588.03	T	311=	1119.3

T 312=	1119.3	T 321=	1107.9	T 322=	1107.9	T 331=	1054.7	T 332=	1084.7	T 337=	789.10
T 341=	673.72	T 357=	330.21	T 358=	421.26	T 359=	261.85	T 379=	216.50	T 483=	216.72
T 1000=	229.48	T 1001=	375.12	T 1002=	374.67	T 1003=	242.48	T 1004=	228.18	T 1005=	227.32
T 1006=	202.51	T 1007=	422.14	T 1008=	409.92	T 1009=	490.44	T 1010=	301.61	T 1013=	950.16
T 1012=	950.36	T 1013=	1228.8	T 1021=	954.85	T 1022=	954.85	T 1023=	1219.7	T 1033=	580.50
T 1032=	880.90	T 1033=	1182.3	T 1041=	652.99	T 1042=	652.99	T 1043=	690.41	T 1044=	690.41
T 1346=	1860.8	T 1347=	366.29	HEATER NODES IN ASCENDING NODE NUMBER ORDER --BOWE--							
T 1=	475.0	T 2=	1424.7	BOUNDARY NODES IN ASCENDING NODE NUMBER ORDER							

SYSTEM IMPROVED NUMERICAL DIFFERENCING ANALYZER '85 (SINBA '85)

PAGE 4/4

MODEL = DAMAGE3
FINNOCLOAD CASE NO. 3 CONDITIONS = Axial Distribution, 100F
Peak DCV Stowell Temperature Time Point

1/2/94

SUBMODEL NAME = P130

	CALCULATED	ALLIED
MAX DIFF DELTA T PER ITER	BRNDCOPT10	1610= 1.709904E-03 VS. BRNDCR= 5.000000E-02
MAX ARITH DELTA T PER ITER	BRNDCOPT10	9491= 1.448844E-03 VS. BRNDCR= 0.300000
MAX DIFF DEL T PER TIME STEP	ATMPCOPT10	1001= 7.26185 VS. ATMPCR= 10.0000
MAX ARITH DEL T PER TIME STEP	ATMPCOPT10	2581= 5.89102 VS. ATMPCR= 100.000
MIN STABILITY CRITERIA	CONMINOPT10	4441= 3.008498E-05
MAX STABILITY CRITERIA	CONMINOPT10	4541= 5.21601
NUMBER OF ITERATIONS	LOOPCT	= 11 VS. BRDOPT= 400
PROBLEM TIME	TIMER	= 0.508800 VS. TIMRAB= 0.500000
MEAN PROBLEM TIME	TIMM	= 0.494871
AVERAGE TIME STEP USED	DTDELU	= 5.535532E-03 VS. DTTIME= 0.

DIFFUSION NODES IN ASCENDING NODE NUMBER ORDER

T 51= 764.30	T 53= 690.71	T 55= 652.06	T 60= 658.03	T 63= 985.73	T 100= 988.43
T 105= 928.07	T 107= 904.45	T 110= 890.04	T 112= 890.54	T 113= 899.07	T 120= 818.77
T 122= 818.59	T 123= 817.02	T 124= 824.16	T 125= 823.91	T 130= 834.48	T 127= 833.99
T 130= 791.07	T 132= 791.80	T 133= 729.56	T 134= 734.43	T 135= 732.76	T 136= 740.00
T 137= 739.32	T 140= 678.07	T 141= 678.28	T 142= 681.12	T 143= 678.80	T 144= 681.38
T 143= 688.02	T 144= 684.06	T 147= 688.19	T 150= 644.66	T 152= 647.69	T 133= 644.81
T 154= 645.42	T 155= 642.97	T 156= 643.60	T 157= 644.66	T 160= 590.26	T 161= 598.64
T 162= 594.07	T 163= 591.36	T 164= 593.82	T 165= 591.30	T 166= 595.91	T 167= 595.32
T 170= 681.90	T 172= 481.79	T 173= 488.90	T 173= 438.86	T 177= 453.65	T 180= 443.47
T 190= 405.42	T 191= 395.35	T 192= 239.62	T 193= 403.56	T 194= 260.06	T 196= 407.70
T 198= 399.80	T 200= 1045.0	T 204= 1054.8	T 210= 711.19	T 220= 686.13	T 230= 620.36
T 240= 345.72	T 242= 346.19	T 250= 228.49	T 260= 200.92	T 261= 201.69	T 262= 201.80
T 263= 201.20	T 264= 201.49	T 265= 206.16	T 266= 206.55	T 300= 1214.8	T 304= 1221.0
T 305= 1276.0	T 310= 927.08	T 313= 1102.4	T 315= 1279.4	T 316= 1279.4	T 320= 910.50
T 323= 1091.3	T 325= 1271.7	T 326= 1271.7	T 330= 888.08	T 333= 9099.8	T 335= 1340.7
T 336= 1240.7	T 340= 828.46	T 342= 578.41	T 343= 1036.9	T 344= 833.23	T 346= 828.84
T 346= 1261.1	T 347= 475.61	T 349= 1067.4	T 350= 259.76	T 351= 455.93	T 352= 260.95
T 353= 361.62	T 354= 298.43	T 355= 221.90	T 356= 302.99	T 360= 199.65	T 362= 198.56
T 364= 199.33	T 366= 214.72	T 367= 215.77	T 368= 221.25	T 369= 251.22	T 371= 451.34
T 373= 358.36	T 375= 260.65	T 377= 218.67	T 400= 199.29	T 481= 208.77	T 602= 212.79
T 404= 925.48	T 406= 1360.7	T 408= 1300.7	T 410= 1406.4	T 412= 1410.4	T 414= 1419.2
T 421= 471.37	T 422= 1494.7	T 423= 1417.5	T 424= 245.04	T 425= 1480.9	T 426= 1486.5
T 431= 1281.3	T 432= 1234.4	T 433= 246.42	T 434= 222.18	T 435= 1386.4	T 436= 1396.7
T 441= 1380.8	T 442= 1370.3	T 443= 1379.3	T 444= 1379.3	T 445= 1391.4	T 446= 1381.8
T 451= 1372.5	T 452= 1361.1	T 453= 1376.7	T 454= 1361.3	T 455= 1405.9	T 456= 1392.8
ARITHMETIC NODES IN ASCENDING NODE NUMBER ORDER					
T 50= 747.27	T 52= 678.24	T 54= 665.04	T 158= 399.83	T 159= 399.18	T 168= 398.06
T 169= 399.30	T 195= 231.03	T 197= 243.95	T 199= 370.11	T 230= 567.93	T 311= 1118.9

T 312=	1118.0	T 321=	1107.5	T 332=	1107.5	T 333=	1054.7	T 332=	1054.7	T 337=	789.88
T 341=	673.78	T 357=	530.21	T 358=	421.26	T 359=	261.85	T 379=	214.58	T 408=	214.72
T 1008=	228.45	T 1001=	575.76	T 1002=	353.79	T 1003=	262.68	T 1004=	228.17	T 1005=	227.31
T 1006=	202.61	T 1007=	419.32	T 1008=	407.83	T 1009=	599.16	T 1010=	301.61	T 1011=	949.54
T 1012=	949.54	T 1013=	1227.6	T 1014=	853.54	T 1022=	933.34	T 1023=	1217.5	T 1051=	800.48
T 1052=	889.48	T 1053=	1402.3	T 1041=	852.98	T 1042=	852.98	T 1043=	610.59	T 1044=	610.59
T 1346=	9048.8	T 1347=	386.29								
HEATER MODES IN ASCENDING MODE NUMBER ORDER											
MODE											
BOUNDARY MODES IN ASCENDING MODE NUMBER ORDER											
T 1=	1475.0	T 2=	1424.7								

SYSTEMS IMPROVED NUMERICAL DIFFERENTIATION ANALYZER '85 (31MDA '85)

PAGE 1/4

MODEL = BARRELS
PUBCKLOW CASE NO. 3 CONDITIONS = Axial Distribution, 180F
Peak JOY Sidewall Temperature Time Point

5/2/94

SUBMODEL NAME = PA1H

MEAN PROBLEM TIME TMIN = 0.232405
 DIFFUSION NODES IN ASCENDING NODE NUMBER ORDER
 † 367= 220.25 † 349= 220.18 † 346= 217.49
 ARITHMETIC NODES IN ASCENDING NODE NUMBER ORDER
 † 281= 726.76 † 1266= 229.76 † 1267= 224.68 † 1268= 283.13 † 1269= 239.07
 HEATER NODES IN ASCENDING NODE NUMBER ORDER
 →NONE→
 DELTA NODES IN ASCENDING NODE NUMBER ORDER
 →NONE→
 PEAK JOY GAS TEMP= 728.0 F PEAK JOY GAS PRESSURE= 35.80 PSIA
 MEAN JOY-OCV GAS TEMP= 746.5 F MEAN JOY-OCV GAS PRESSURE= 42.51 PSIA

SUBMODEL NAME = P1HA

ALLOWED
 MAX DIFF DELTA T PER ITER CALCULATED 1233= -4.852734E-02 VS. ORLSDA= 5.000000E-02
 MAX ARITH DELTA T PER ITER CALCULATED 10873= 9.338379E-02 VS. ARLSDA= 0.300000
 MAX DIFF DEL T PER TIME STEP CALCULATED 4253= -1.85397 VS. OTMPCA= 30.0000
 MAX ARITH DEL T PER TIME STEP CALCULATED 13463= -1.43378 VS. ATMPCA= 900.000
 MAX STABILITY CRITERIA CALCULATED 4313= 2.399240E-04
 MAX STABILITY CRITERIA CALCULATED 4263= 2.20953
 NUMBER OF ITERATIONS = 3 VS. KLOOPT= 600
 PROBLEM TIME TMIN = 0.833333 VS. TMINEM= 12.0000
 MEAN PROBLEM TIME TMIN = 0.832405
 AVERAGE TIME STEP USED DTMIN = 0.232405 VS. DTTIME= 0.

DIFFUSION NODES IN ASCENDING NODE NUMBER ORDER

† 51= 1055.2	† 53= 914.5	† 55= 961.06	† 60= 963.57	† 62= 972.38	† 100= 968.90
† 103= 967.44	† 107= 966.07	† 110= 969.79	† 112= 981.43	† 113= 954.41	† 120= 1000.7
† 122= 1125.4	† 123= 977.67	† 124= 1126.1	† 125= 979.03	† 126= 1127.4	† 127= 981.70
† 130= 1080.4	† 132= 1127.5	† 133= 969.82	† 134= 1127.6	† 135= 970.28	† 136= 1128.0
† 137= 971.49	† 140= 983.0	† 141= 1038.2	† 142= 1066.2	† 143= 962.11	† 144= 1066.2
† 145= 962.42	† 146= 1066.1	† 147= 962.97	† 150= 1067.3	† 152= 1117.8	† 153= 967.52
† 154= 1136.0	† 155= 968.02	† 156= 1115.4	† 157= 968.09	† 160= 1066.1	† 161= 996.26
† 162= 1051.4	† 188= 896.78	† 164= 1066.4	† 168= 903.38	† 166= 1067.4	† 167= 982.96
† 170= 665.63	† 172= 672.22	† 173= 651.97	† 174= 971.03	† 177= 609.34	† 180= 585.51
† 190= 638.08	† 191= 454.59	† 192= 252.31	† 193= 663.31	† 194= 339.23	† 196= 419.62
† 198= 656.85	† 200= 877.60	† 204= 886.90	† 210= 1190.0	† 220= 1145.1	† 230= 1118.9
† 260= 731.60	† 262= 667.99	† 258= 266.23	† 260= 283.29	† 261= 305.85	† 268= 209.22
† 263= 214.14	† 264= 220.38	† 265= 225.24	† 266= 233.32	† 300= 781.94	† 284= 781.88
† 305= 305.32	† 310= 1058.0	† 313= 923.74	† 315= 787.60	† 316= 793.60	† 320= 1089.2
† 325= 982.91	† 325= 758.40	† 326= 758.40	† 330= 866.98	† 333= 804.37	† 335= 683.28
† 336= 683.39	† 340= 771.77	† 342= 567.86	† 343= 546.54	† 344= 381.90	† 345= 699.36
† 346= 620.08	† 347= 516.56	† 349= 448.60	† 380= 313.20	† 351= 342.43	† 352= 316.08
† 383= 323.27	† 384= 339.79	† 355= 271.64	† 386= 343.18	† 360= 301.88	† 362= 304.87
† 364= 219.72	† 366= 266.41	† 367= 273.25	† 368= 290.53	† 369= 316.34	† 371= 348.41
† 373= 330.84	† 375= 289.35	† 377= 265.88	† 400= 210.28	† 401= 221.46	† 402= 368.02
† 404= 698.51	† 406= 599.18	† 408= 601.29	† 410= 374.01	† 412= 622.34	† 414= 599.64

T 421=	472.14	T 422=	388.80	T 423=	378.00	T 424=	318.03	T 425=	722.45	T 426=	656.53
T 431=	406.24	T 432=	497.92	T 433=	762.13	T 434=	740.34	T 435=	689.14	T 436=	682.72
T 950=	1517.5	T 952=	1507.1	T 954=	1475.8						
ARITHMETIC NODES IN ASCENDING NODE NUMBER ORDER											
T 90=	1024.4	T 92=	1012.8	T 94=	968.67	T 95=	1015.8	T 150=	971.47	T 160=	999.93
T 169=	975.85	T 195=	263.68	T 197=	306.75	T 199=	654.19	T 230=	956.45	T 311=	985.04
T 312=	908.84	T 321=	907.61	T 322=	907.61	T 331=	791.65	T 332=	791.08	T 337=	590.91
T 341=	583.62	T 357=	343.04	T 358=	348.58	T 359=	314.72	T 379=	270.28	T 483=	264.67
T 1080=	293.37	T 1001=	615.24	T 1002=	429.57	T 1003=	383.87	T 1004=	262.79	T 1005=	261.64
T 1086=	218.29	T 1007=	503.62	T 1008=	464.11	T 1009=	487.49	T 1010=	353.24	T 1011=	1844.8
T 1012=	964.8	T 1013=	811.66	T 1021=	9042.2	T 1022=	9042.2	T 1023=	812.83	T 1031=	957.81
T 1032=	957.01	T 1033=	724.17	T 1041=	770.72	T 1042=	770.72	T 1043=	356.48	T 1044=	356.48
T 1346=	646.45	T 1347=	434.68								
BETTER NODES IN ASCENDING NODE NUMBER ORDER											
NONE											
REDUNDANT NODES IF ASCENDING NODE NUMBER ORDER											
T 1=	100.00	T 2=	100.00								

F 312=	696.56	T 321=	684.72	F 322=	684.72	F 331=	633.45	F 332=	633.45	F 337=	561.27
F 341=	530.34	T 357=	325.77	F 358=	329.91	F 359=	296.88	F 379=	254.33	T 403=	249.79
F 1000=	252.30	F 1001=	439.66	F 1002=	443.95	F 1003=	284.49	F 1004=	237.79	F 1005=	236.75
F 1006=	296.97	T 1007=	519.78	T 1008=	496.30	T 1009=	488.87	F 1010=	375.07	F 1011=	785.66
T 1013=	783.64	T 1013=	653.37	T 1021=	769.64	F 1022=	769.66	T 1023=	636.58	F 1031=	721.81
T 1032=	721.81	T 1033=	593.06	T 1041=	657.95	F 1042=	657.95	T 1043=	595.92	F 1044=	595.92
T 1346=	606.62	T 1347=	597.72								
HEATER NODES IN ASCENDING NODE NUMBER ORDER											
--HOME--											
BOUNDARY NODES IN ASCENDING NODE NUMBER ORDER											
T	1=	100.00	T	2=	100.00						

SYSTEM APPROXIMATED NUMERICAL DIFFERENTIATION ANALYZER '85 (SINBA '85)

PAGE 3/4

MODEL = BARRAGE
FUDGELOAD CASE NO. 3 CONDITIONS = Anal Distribution, 100F
Peak 1CV Small Temperature Time Point

5/2/94

SUBMODEL NAME = PTAC

MAX DIFF DELTA T PER ITER	CALCULATED	120)= -2.319536E-02	ALLOWED	5.000000E-02
MAX ARITH DELTA T PER ITER	RELDCO(PTAC	1807)= 8.125408	VS. RELDCO=	0.500000
MAX DIFF DEL T PER TIME STEP	OTMPCO(PTAC	485)= -1.50427	VS. OTMPCO=	10.0000
MAX ARITH DEL T PER TIME STEP	ATMPCO(PTAC	1346)= -1.24252	VS. ATMPCO=	100.000
MIN STABILITY CRITERIA	CMARK(PTAC	482)= 2.891408E-04		
MIN STABILITY CRITERIA	CMARK(PTAC	434)= 3.8984E		
NUMBER OF ITERATIONS	LOOPCT	= 2	VS. NLOOP=	600
PROBLEM TIME	TIMED	= 0.833333	VS. TIMED=	12.0000
MEAN PROBLEM TIME	TIMED	= 0.833485		
AVERAGE TIME STEP USED	DTIMEJ	= 9.259240E-04	VS. DTIMEJ=	0.

WITHESSION NODES IN ASCENDING NODE NUMBER ORDER

T	51=	812.82	T	53=	747.71	T	55=	697.74	T	60=	663.15	T	62=	604.86	T	108=	844.38
T	105=	837.35	T	107=	834.07	T	110=	827.38	T	112=	829.48	T	113=	828.06	T	128=	887.94
T	122=	813.63	T	123=	805.60	T	124=	809.33	T	125=	803.91	T	126=	808.60	T	127=	799.68
T	138=	782.68	T	132=	788.48	T	133=	778.78	T	134=	785.49	T	135=	778.88	T	136=	779.58
T	137=	778.11	T	140=	766.78	T	141=	767.28	T	142=	772.63	T	143=	763.84	T	144=	768.57
T	149=	762.38	T	146=	760.31	T	147=	758.91	T	150=	740.98	T	132=	748.36	T	133=	737.69
T	154=	743.21	T	155=	735.54	T	156=	734.84	T	157=	732.76	T	160=	699.80	T	161=	706.86
T	168=	708.61	T	163=	697.86	T	164=	703.63	T	165=	697.16	T	166=	699.18	T	167=	697.68
T	170=	695.20	T	172=	625.32	T	173=	634.14	T	175=	589.71	T	177=	604.38	T	180=	585.28
T	190=	547.11	T	191=	549.39	T	192=	552.87	T	193=	627.34	T	194=	544.93	T	196=	544.99
T	198=	551.59	T	208=	650.69	T	204=	619.85	T	210=	786.11	T	220=	780.00	T	230=	708.21
T	240=	627.33	T	242=	629.29	T	250=	637.34	T	258=	682.53	T	261=	608.85	T	262=	605.33
T	263=	287.90	T	264=	218.89	T	265=	321.42	T	266=	228.86	T	308=	744.18	T	304=	733.67
T	305=	681.84	T	318=	742.67	T	313=	670.74	T	315=	569.26	T	316=	569.26	T	320=	722.84
T	323=	656.29	T	321=	561.23	T	328=	561.29	T	330=	681.63	T	332=	617.44	T	335=	546.91
T	336=	546.91	T	340=	638.47	T	342=	493.44	T	343=	523.48	T	344=	257.19	T	345=	647.19
T	346=	585.43	T	347=	476.10	T	349=	429.30	T	358=	294.97	T	351=	325.32	T	352=	296.01
T	363=	305.53	T	354=	319.54	T	355=	254.88	T	360=	321.26	T	360=	281.39	T	362=	283.04
T	364=	295.37	T	368=	258.89	T	367=	254.77	T	368=	263.98	T	369=	280.13	T	371=	328.76
T	373=	212.99	T	375=	274.33	T	377=	258.30	T	400=	288.80	T	481=	220.32	T	402=	247.18
T	406=	685.86	T	406=	608.89	T	408=	540.98	T	410=	607.86	T	412=	626.91	T	416=	539.78
T	421=	671.82	T	422=	588.95	T	423=	378.21	T	434=	288.95	T	425=	723.92	T	426=	664.03
T	431=	688.92	T	432=	793.36	T	439=	310.24	T	434=	271.29	T	439=	793.84	T	436=	632.92
T	441=	546.81	T	442=	624.85	T	443=	628.68	T	444=	623.24	T	445=	627.40	T	446=	546.69
T	451=	569.78	T	432=	601.34	T	433=	582.34	T	454=	588.29	T	435=	605.22	T	454=	574.31
T	50=	808.69	T	52=	749.37	T	54=	720.63	T	158=	707.38	T	159=	785.43	T	160=	786.34
T	149=	708.67	T	195=	255.68	T	197=	292.33	T	199=	484.21	T	238=	675.73	T	311=	658.09

T 312=	658.09	T 321=	644.05	T 322=	644.05	T 331=	685.75	T 332=	605.15	T 337=	532.19	
T 341=	589.29	T 357=	322.25	T 359=	520.43	T 359=	295.56	T 379=	293.33	T 403=	249.25	
T 1000=	253.05	T 1001=	503.05	T 1002=	445.05	T 1003=	382.47	T 1004=	262.40	T 1005=	241.20	
T 1006=	206.94	T 1007=	576.27	T 1008=	545.47	T 1009=	554.30	T 1010=	375.36	T 1011=	737.62	
T 1012=	757.62	T 1013=	603.75	T 1021=	718.45	T 1022=	718.45	T 1023=	505.35	T 1031=	677.70	
T 1032=	677.70	T 1033=	570.25	T 1041=	636.50	T 1042=	636.50	T 1043=	490.48	T 1044=	490.48	
T 1544=	605.75	T 1547=	505.02									
HEATER NODES IN ASCENDING NODE NUMBER ORDER												
+-----+												
BOUNDARY NODES IN ASCENDING NODE NUMBER ORDER												
T 1=	100.00	T 2=	180.00									

SYSTEM IMPROVED NUMERICAL DIFFERENCING ANALYSIS '95 (SIMA '95)

PAGE 4/4

MODEL = DAMAGED
PBRSCLOAD CASE NO. 3 CONDITION - Axial Distribution, 100%
Peak ICV Sidewall Temperature Time Point

5/2/96

SUBMODEL NAME = PT30

MAX DIFF DELTA T PER ITER	CALCULATED	120>= 2.233807E-02	VS.	ALLOWED	3.000000E-02
MAX ARITH DELTA T PER ITER	ACCEPTED	1007>= 0.125411	VS.	ALLOWED	4.500000
MAX DIFF DEL T PER TIME STEP	BTMPC(P130)	435>= -1.98427	VS.	BTMPC=	18.0000
MAX ARITH DEL T PER TIME STEP	ATMPC(P130)	1544>= -1.24283	VS.	ATMPC=	180.000
MIN STABILITY CRITERIA	CONV(CPT30)	455>= 2.891499E-04			
MAX STABILITY CRITERIA	CONV(UPT30)	434>= 3.89642			
NUMBER OF ITERATIONS	LOOPY	= 5	VS.	BL00PT=	400
PROBLEM TIME	TIMEH	= 0.453333	VS.	TIMEHD=	12.0000
MEAN PROBLEM TIME	TIMEH	= 0.453205			
AVERAGE TIME STEP USED	BTIMDU	= 9.256262E-04	VS.	BTMEL=	0.

DIFFUSION NODES IN ASCENDING NODE NUMBER ORDER																				
T	51>	846.70	T	53>	735.85	T	55>	636.32	T	57>	536.38	T	59>	438.39	T	61>	344.25	T	63>	254.11
T	65>	164.06	T	67>	167.01	T	69>	823.01	T	71>	823.31	T	73>	823.36	T	75>	796.31	T	77>	796.24
T	79>	801.22	T	81>	799.01	T	83>	799.09	T	85>	799.04	T	87>	796.31	T	89>	796.31	T	91>	779.75
T	93>	772.40	T	95>	773.16	T	97>	771.40	T	99>	775.71	T	101>	775.61	T	103>	754.49	T	105>	754.25
T	107>	773.44	T	109>	755.06	T	111>	755.64	T	113>	756.01	T	115>	734.85	T	117>	731.30	T	119>	729.21
T	121>	729.90	T	123>	728.21	T	125>	728.06	T	127>	727.33	T	129>	689.30	T	131>	686.89	T	133>	686.89
T	135>	698.83	T	137>	688.99	T	139>	691.40	T	141>	690.43	T	143>	692.04	T	145>	692.81	T	147>	692.81
T	149>	621.53	T	151>	621.21	T	153>	620.79	T	155>	588.29	T	157>	601.77	T	159>	584.13	T	161>	584.13
T	163>	565.04	T	165>	548.01	T	167>	553.89	T	169>	625.89	T	171>	544.49	T	173>	558.72	T	175>	558.72
T	177>	551.07	T	179>	549.43	T	181>	517.03	T	183>	784.79	T	185>	757.40	T	187>	707.91	T	189>	707.91
T	191>	626.74	T	193>	629.06	T	195>	627.29	T	197>	602.32	T	199>	609.85	T	201>	609.31	T	203>	609.31
T	205>	607.44	T	207>	616.87	T	209>	621.39	T	211>	620.04	T	213>	745.33	T	215>	752.99	T	217>	752.99
T	219>	641.39	T	221>	741.47	T	223>	649.79	T	225>	548.54	T	227>	548.54	T	229>	721.00	T	231>	721.00
T	233>	654.28	T	235>	548.19	T	237>	548.19	T	239>	689.72	T	241>	617.03	T	243>	644.64	T	245>	644.64
T	247>	546.64	T	249>	637.99	T	251>	693.26	T	253>	525.43	T	255>	597.14	T	257>	647.17	T	259>	647.17
T	261>	505.38	T	263>	674.00	T	265>	629.37	T	267>	294.96	T	269>	325.31	T	271>	294.08	T	273>	294.08
T	275>	305.32	T	277>	319.52	T	279>	254.79	T	281>	321.23	T	283>	281.36	T	285>	283.04	T	287>	283.04
T	289>	293.34	T	291>	258.98	T	293>	254.77	T	295>	263.09	T	297>	288.12	T	299>	328.79	T	301>	328.79
T	303>	312.59	T	305>	274.32	T	307>	258.30	T	309>	296.79	T	311>	228.32	T	313>	347.38	T	315>	347.38
T	317>	445.86	T	319>	605.85	T	321>	540.58	T	323>	607.84	T	325>	636.91	T	327>	599.20	T	329>	599.20
T	331>	471.82	T	333>	548.95	T	335>	578.21	T	337>	286.35	T	339>	723.92	T	341>	604.03	T	343>	604.03
T	345>	638.89	T	347>	798.39	T	349>	310.23	T	351>	371.29	T	353>	793.84	T	355>	692.92	T	357>	692.92
T	359>	546.01	T	361>	624.84	T	363>	638.67	T	365>	695.24	T	367>	627.18	T	369>	548.09	T	371>	548.09
T	373>	566.74	T	375>	601.31	T	377>	589.33	T	379>	589.29	T	381>	609.22	T	383>	574.31	T	385>	574.31
ARITHMETIC NODES IN ASCENDING NODE NUMBER ORDER																				
T	387>	800.34	T	389>	737.74	T	391>	709.04	T	393>	894.09	T	395>	666.37	T	397>	666.34	T	399>	666.34
T	401>	696.26	T	403>	257.12	T	405>	289.77	T	407>	483.24	T	409>	672.66	T	411>	657.34	T	413>	657.34

T 312=	487.16	T 321=	442.63	T 322=	442.63	T 331=	406.71	T 332=	404.71	T 337=	532.02	
T 341=	328.88	T 347=	322.22	T 356=	328.44	T 359=	295.58	T 376=	251.32	T 483=	269.25	
T 1008=	253.62	T 1007=	507.18	T 1002=	444.89	T 1003=	303.21	T 1004=	242.69	T 1005=	241.48	
T 1006=	264.95	T 1007=	572.78	T 1008=	563.94	T 1009=	583.42	T 1010=	379.04	T 1011=	736.64	
T 1012=	736.64	T 1013=	602.94	T 1021=	716.64	T 1022=	716.64	T 1023=	592.20	T 1031=	677.08	
T 1032=	677.08	T 1033=	569.95	T 1041=	636.63	T 1042=	636.63	T 1043=	486.38	T 1044=	496.38	
T 1344=	603.72	T 1347=	596.81									
GREATER INDEX IN ASCENDING INDEX NUMBER ORDER												
==NONE==												
SECONDARY INDEX IN ASCENDING INDEX NUMBER ORDER												
T 1=	100.00	T 2=	100.00									

SYSTEM IMPROVED NUMERICAL DIFFERENCING ANALYZER '85 (EIMBA '85)

PAGE 1/4

MODEL = DMWGES
STARTLLOAD CASE NO. 3 CONDITIONS = Axial Distribution, 100F
*** Steady-state Conditions After The Fire ***

5/2/94 Tim

SUBMODEL NAME = MAIN

PROBLEM TIME TIME = 999.990 VS. TIME= 999.990
 T 257= 230.87 T 256= 230.91 T 26= 229.87
 T 201= 238.58 T 1266= 233.72 T 1267= 243.76 T 1268= 232.01 T 1269= 236.97

DIFFUSION NODES IN ASCENDING NODE NUMBER ORDER
 ARITHMETIC NODES IN ASCENDING NODE NUMBER ORDER
 HEATER NODES IN ASCENDING NODE NUMBER ORDER
 --MORE--
 BOUNDARY NODES IN ASCENDING NODE NUMBER ORDER
 --MORE--

MEAN ICV GAS TEMP= 258.4 F MEAN ICV GAS PRESSURE= 20.96 PSIA
 MEAN ICV-OCV GAS TEMP= 267.8 F MEAN ICV-OCV GAS PRESSURE= 24.91 PSIA

SUBMODEL NAME = P13A

MAX DIFF DELTA T PER ITER	CALCULATED		ALLOWED
MAX ARITH DELTA T PER ITER	DELTA(CP)SA	261)= -3.34075	VS. DELTA= 5.00000E-02
MAX SYSTEM ENERGY BALANCE	ARLHC(CP)SA	1044)= -0.628784	VS. ARLHCA= 0.300000
	EBALSC	= -2.95444	VS. EBALSA = ESUMI
			EBALBA = 1.00000E-03
ENERGY INTO AND OUT OF SYS	ESUMI	= 7879.25	ESUMOB= 3394.01
NUM MODAL ENERGY BALANCE	EBAL(CP)SA	338)= -0.266734	VS. EBALMA= 1.80000E-02
NUMBER OF ITERATIONS	LOOPCT	= 156	VS. NLOOPB= 9000
PROBLEM TIME	TIME	= 999.000	VS. TIMEB= 999.000

DIFFUSION NODES IN ASCENDING NODE NUMBER ORDER			
T	51=	53=	55=
T	51= 686.15	T 53= 714.88	T 55= 684.16
T	59= 535.19	T 107= 834.37	T 110= 541.59
T	123= 786.08	T 123= 986.90	T 124= 788.07
T	130= 760.82	T 132= 823.30	T 133= 815.10
T	137= 615.10	T 140= 739.86	T 141= 720.88
T	145= 621.63	T 146= 703.46	T 147= 621.63
T	154= 836.60	T 155= 625.74	T 156= 836.60
T	162= 785.35	T 163= 594.88	T 164= 781.88
T	170= 447.12	T 172= 439.27	T 173= 412.86
T	190= 326.12	T 191= 287.33	T 192= 344.93
T	198= 285.77	T 200= 217.27	T 204= 336.43
T	240= 609.42	T 262= 319.93	T 258= 243.23
T	263= 223.12	T 264= 325.43	T 263= 327.82
T	305= 176.92	T 318= 798.30	T 313= 492.77
T	323= 714.49	T 325= 594.70	T 326= 594.70
T	336= 470.40	T 340= 594.48	T 342= 351.06
T	346= 233.15	T 347= 228.39	T 349= 214.73
T	383= 227.78	T 384= 236.09	T 383= 225.75
T	384= 222.80	T 386= 223.34	T 387= 226.66
T	373= 229.19	T 373= 226.11	T 377= 223.95
T	404= 197.66	T 408= 209.94	T 408= 121.83
T			T 410= 186.11
T			T 62= 563.85
T			T 100= 837.66
T			T 113= 486.39
T			T 120= 727.21
T			T 127= 846.92
T			T 136= 823.80
T			T 144= 783.46
T			T 153= 624.71
T			T 161= 712.83
T			T 167= 602.31
T			T 180= 396.35
T			T 186= 254.24
T			T 196= 868.24
T			T 262= 239.19
T			T 306= 366.27
T			T 316= 575.68
T			T 326= 678.40
T			T 335= 225.23
T			T 352= 229.50
T			T 362= 816.40
T			T 376= 229.74
T			T 402= 823.54
T			T 414= 905.18

T 421=	179.61	T 428=	111.19	F 425=	107.76	T 424=	181.96	F 425=	112.36	T 426=	110.12
T 431=	140.45	T 432=	168.26	T 433=	122.33	T 434=	124.18	T 435=	115.56	T 436=	119.72
T 950=	1233.5	T 952=	1389.4	F 954=	1298.7						
ARITHMETIC NODES IN ASCENDING NODE NUMBER ORDER											
T 50=	681.48	T 32=	713.33	T 34=	679.33	T 168=	799.97	T 159=	682.02	T 160=	717.33
T 169=	709.88	T 198=	233.91	F 197=	237.90	F 199=	307.97	T 238=	782.62	T 311=	688.26
T 312=	684.26	T 321=	785.66	F 322=	709.66	F 331=	546.07	F 332=	546.07	T 337=	343.42
T 341=	563.46	F 357=	233.04	T 358=	230.43	F 359=	250.39	F 379=	225.04	T 403=	223.88
T 1008=	251.97	T 1001=	271.82	T 1002=	249.78	T 1003=	249.96	F 1804=	237.25	T 1005=	237.11
T 1004=	215.32	T 1007=	348.53	T 1008=	324.11	T 1009=	298.61	T 1010=	261.25	T 1011=	263.93
T 1012=	783.95	T 1013=	646.45	T 1021=	807.94	T 1022=	807.94	T 1023=	635.65	T 1031=	627.89
T 1032=	677.89	T 1033=	499.81	T 1041=	504.98	T 1042=	504.98	T 1043=	355.87	T 1044=	355.87
T 1346=	227.72	T 1347=	234.85	HEATER NODES IN ASCENDING NODE NUMBER ORDER							
--NONE--											
BOUNDARY NODES IN ASCENDING NODE NUMBER ORDER											
T 1=	108.88	T 2=	100.00								

T 341=	245.76	T 357=	285.54	T 358=	282.47	T 359=	286.16	T 379=	205.33	T 403=	206.08
T 1000=	222.81	T 1001=	243.74	T 1002=	267.29	T 1003=	234.33	T 1004=	222.68	T 1005=	222.07
T 1006=	286.50	T 1007=	309.41	T 1008=	299.47	T 1009=	284.39	T 1010=	247.05	T 1011=	332.62
T 1012=	332.62	T 1013=	298.48	T 1021=	348.58	T 1022=	348.58	T 1023=	311.39	T 1031=	318.37
T 1032=	318.27	T 1033=	264.85	T 1041=	268.38	T 1042=	268.38	T 1043=	246.13	T 1044=	246.15
T 1246=	182.00	T 1247=	199.90	HEATER MODES IN ASCENDING MODE NUMBER ORDER --NONE--							
T 1=	100.00	T 2=	100.00	BOUNDARY MODES IN ASCENDING MODE NUMBER ORDER							

SYSTEMS IMPROVED NUMERICAL DIFFERENCING ANALYZER '88 (SINDA '85)

PAGE 3/4

MODEL = BARRAGE
STDTLLOAD CASE NO. 3 CONDITIONS - Axial Distribution, 100F
*** Steady-state Conditions After The Fire ***

5/2/84 11am

SUBMODEL NAME = P19C

MAX DIFF DELTA T PER ITER	CALCULATED	1751e-2.876750E-02	VS. ALLOWED	5.000000E-02
MAX ARITH DELTA T PER ITER	DRUIDC(PTSC	1084)e-2.905273E-02	VS. ARITHMO=	0.300000
MAX SYSTEM ENERGY BALANCE	ARLHCC(PTSC	= -23.1527	VS. ETRAL3=	ESLHNS
	REAL BC		REAL3A=	1.000000E-02
ENERGY INTO AND OUT OF STA	EBURIS	=	VS. ETRAL3=	1.000000E-02
MAX INHDL ENERGY BALANCE	DRUIDC(PTSC	367)e-2.94931	VS. ETRAL3=	1.000000E-02
NUMBER OF ITERATIONS	LOOPCT	=	VS. N.LOOPS=	1000
PROBLEM TIME	TIMEN	=	VS. TIMENO=	599.000

DIFFUSION NODES IN ASCENDING NODE NUMBER ORDER																	
T	31=	271.82	T	33=	288.73	T	35=	277.25	T	40=	253.72	T	42=	262.14	T	100=	239.27
T	105=	246.07	T	107=	248.67	T	110=	251.63	T	112=	258.00	T	113=	248.05	T	120=	249.04
T	123=	283.94	T	123=	259.10	T	126=	274.48	T	125=	253.89	T	126=	252.92	T	127=	241.76
T	130=	281.34	T	132=	297.65	T	133=	270.75	T	134=	287.26	T	135=	244.99	T	136=	263.88
T	137=	291.90	T	140=	290.24	T	141=	290.58	T	142=	306.01	T	143=	282.29	T	144=	293.05
T	145=	275.47	T	146=	299.43	T	147=	299.47	T	150=	283.60	T	133=	299.75	T	153=	273.19
T	154=	289.33	T	155=	267.24	T	156=	266.22	T	157=	252.28	T	160=	274.85	T	161=	276.77
T	160=	289.17	T	163=	266.07	T	164=	250.21	T	165=	260.12	T	166=	260.61	T	167=	269.94
T	170=	248.95	T	170=	253.94	T	173=	246.74	T	175=	240.48	T	177=	244.11	T	180=	239.82
T	190=	231.04	T	191=	223.98	T	192=	196.87	T	195=	212.13	T	194=	280.06	T	196=	231.13
T	190=	225.60	T	200=	187.86	T	204=	185.85	T	210=	199.72	T	220=	205.62	T	220=	198.60
T	210=	186.05	T	312=	178.46	T	250=	176.32	T	260=	185.42	T	261=	185.74	T	262=	181.40
T	263=	181.84	T	264=	178.40	T	265=	179.26	T	266=	175.85	T	300=	139.04	T	304=	131.95
T	305=	119.94	T	310=	180.23	T	313=	171.40	T	313=	168.99	T	316=	160.99	T	320=	185.80
T	323=	176.51	T	325=	163.67	T	326=	163.67	T	330=	178.24	T	333=	168.68	T	335=	159.12
T	336=	159.12	T	340=	173.75	T	342=	169.86	T	343=	167.66	T	344=	167.98	T	345=	169.63
T	346=	161.35	T	347=	159.63	T	349=	162.60	T	350=	167.21	T	351=	163.18	T	352=	166.80
T	353=	164.85	T	354=	164.66	T	355=	168.17	T	356=	165.78	T	360=	164.19	T	360=	180.27
T	364=	175.52	T	366=	168.70	T	367=	168.00	T	368=	167.15	T	369=	166.37	T	371=	163.50
T	373=	164.75	T	375=	166.67	T	377=	167.48	T	400=	177.34	T	401=	176.18	T	402=	167.64
T	404=	163.36	T	408=	115.92	T	409=	165.82	T	410=	182.38	T	412=	192.88	T	414=	185.34
T	421=	182.87	T	422=	187.63	T	423=	185.03	T	424=	163.34	T	425=	166.41	T	426=	164.29
T	431=	187.11	T	432=	120.95	T	433=	128.07	T	434=	118.00	T	435=	103.91	T	436=	103.84
T	443=	188.63	T	442=	118.80	T	443=	187.81	T	444=	186.88	T	445=	104.38	T	446=	105.20
T	451=	190.16	T	452=	113.46	T	453=	107.75	T	454=	102.87	T	455=	183.25	T	456=	184.31
ARITHMETIC NODES IN ASCENDING NODE NUMBER ORDER																	
T	50=	272.27	T	52=	281.55	T	54=	277.05	T	158=	278.83	T	159=	270.84	T	160=	273.86
T	169=	275.78	T	195=	192.40	T	197=	198.84	T	199=	210.01	T	238=	193.10	T	311=	178.64
T	312=	170.64	T	321=	175.72	T	322=	175.72	T	331=	167.87	T	332=	167.87	T	337=	143.26

T 341= 147.86	T 357= 145.49	T 358= 163.48	T 359= 166.99	T 379= 148.30	T 403= 147.53
T 1008= 190.98	T 1001= 222.34	T 1002= 210.19	T 1003= 201.64	T 1004= 196.27	T 1005= 195.95
T 1006= 184.53	T 1007= 234.72	T 1008= 231.13	T 1009= 227.55	T 1010= 189.60	T 1011= 180.06
T 1012= 180.86	T 1013= 164.76	T 1021= 185.71	T 1022= 185.71	T 1023= 149.44	T 1031= 178.06
T 1032= 178.86	T 1033= 162.54	T 1041= 173.63	T 1042= 173.63	T 1043= 149.81	T 1044= 149.81
T 1346= 145.42	T 1347= 162.51				
GREATER NODES IN ASCENDING NODE NUMBER ORDER					
==NONE==					
BOUNDARY NODES IN ASCENDING NODE NUMBER ORDER					
T 1= 188.00	T 2= 108.50				

SYSTEMS IMPROVED NUMERICAL DIFFERENCING ANALYZER *88 (RHM1 08)

PAGE 4/6

MODEL # 848623
87037LLOAD CASE NO. 3 CONDITIONS - Axial Distribution, 100F
*** Steady-state Conditions after the Fire ***

5/2/94 11am

**MODEL NAME - P100

MAX DIFF DELTA T PER ITER	CALCULATED	Y06)=-4.418949E-02	VS.	ALLOWED	DELTA= 5.000000E-02	
MAX ANITH DELTA T PER ITER	DELTA(C)P100	X033)=-2.380377E-02	VS.	ANLKA= 0.500000		
MAX SYSTEM ENERGY BALANCE	ANLNC(PT00)	= 3.52679	VS.	EBALBA * EXINTE		0.
	EDALSC			EBALBA= 1.000000E-03		
EMERG INTO AND OUT OF STE	ESUMIE	= 0.		EXUMD= 731.116		
MAX NODAL ENERGY BALANCE	EDALNC(PT00)	367)= 1.37906	VS.	EBALBA= 1.000000E-02		
NUMBER OF ITERATIONS	LOOPT	= 156	VS.	BLSEPS= 1000		
PROBLEM TIME	TIMEH	= 999.900	VS.	TIME00= 999.000		

DIFFUSION NODES IN ASCENDING NODE NUMBER ORDER																	
T	51=	232.39	T	53=	243.82	T	55=	258.25	T	58=	252.90	T	62=	251.72	T	100=	213.46
T	100=	217.19	T	107=	218.61	T	110=	220.32	T	112=	222.82	T	113=	218.68	T	120=	230.56
T	122=	234.30	T	123=	227.51	T	124=	231.44	T	125=	224.89	T	126=	220.64	T	127=	216.36
T	130=	239.99	T	132=	245.67	T	133=	236.10	T	134=	248.38	T	135=	252.38	T	136=	228.49
T	137=	228.78	T	140=	245.75	T	141=	245.91	T	142=	251.19	T	143=	243.45	T	144=	245.88
T	145=	239.34	T	146=	233.04	T	147=	229.22	T	150=	241.91	T	152=	247.70	T	153=	238.29
T	154=	242.44	T	155=	234.33	T	156=	238.82	T	157=	226.69	T	160=	250.98	T	161=	250.81
T	162=	242.38	T	163=	234.36	T	164=	237.97	T	165=	230.37	T	166=	227.92	T	167=	224.77
T	170=	225.51	T	172=	227.39	T	173=	225.01	T	175=	222.15	T	177=	223.59	T	180=	222.08
T	190=	218.25	T	191=	215.65	T	192=	185.43	T	193=	201.59	T	194=	188.88	T	196=	228.68
T	198=	215.64	T	200=	180.74	T	204=	177.64	T	210=	187.63	T	220=	191.17	T	230=	186.84
T	240=	175.35	T	242=	165.87	T	250=	163.08	T	260=	175.31	T	261=	175.64	T	262=	169.39
T	263=	169.62	T	264=	165.85	T	268=	166.71	T	269=	163.21	T	300=	155.43	T	306=	163.68
T	305=	117.90	T	310=	168.83	T	313=	161.35	T	315=	152.53	T	316=	152.53	T	320=	172.47
T	323=	164.67	T	325=	155.49	T	326=	155.49	T	330=	167.83	T	333=	158.64	T	335=	150.68
T	336=	150.68	T	340=	162.38	T	342=	158.86	T	343=	139.21	T	344=	135.50	T	348=	140.63
T	346=	134.26	T	347=	148.68	T	349=	125.13	T	350=	154.73	T	391=	131.98	T	392=	134.37
T	353=	132.85	T	354=	154.15	T	355=	155.97	T	356=	153.95	T	360=	173.85	T	362=	168.33
T	364=	163.04	T	366=	156.89	T	367=	153.61	T	368=	154.64	T	369=	155.99	T	371=	151.75
T	373=	152.78	T	375=	154.25	T	377=	155.89	T	400=	165.68	T	401=	166.67	T	402=	155.21
T	404=	134.80	T	406=	113.26	T	408=	106.77	T	410=	101.86	T	412=	102.33	T	414=	102.85
T	421=	145.02	T	422=	106.32	T	423=	104.28	T	424=	137.18	T	425=	105.29	T	426=	103.56
T	431=	122.21	T	432=	117.33	T	433=	122.93	T	434=	114.72	T	435=	108.22	T	436=	103.16
T	441=	107.09	T	442=	108.95	T	443=	108.61	T	444=	105.48	T	445=	103.53	T	446=	104.26
T	451=	105.41	T	452=	111.19	T	453=	106.37	T	454=	104.82	T	455=	102.71	T	456=	103.54
ARITHMETIC ORDER IN ASCENDING NODE NUMBER ORDER																	
T	50=	232.82	T	52=	242.29	T	54=	239.23	T	150=	237.36	T	150=	235.13	T	160=	236.99
T	160=	237.31	T	191=	181.66	T	197=	182.23	T	199=	199.22	T	238=	180.94	T	311=	160.71
T	312=	160.71	T	321=	164.01	T	322=	164.01	T	331=	157.99	T	332=	157.99	T	333=	152.66

3.8.5-72

T 341=	156.55	T 357=	153.35	F 368=	181.76	T 359=	156.85	F 379=	159.70	T 403=	155.15
T 909=	170.78	T 1001=	211.84	T 1009=	199.37	T 1005=	190.38	F 1004=	182.41	T 908=	182.52
T 906=	173.68	T 1007=	219.70	F 1008=	218.15	T 1006=	216.41	F 1010=	177.58	T 9011=	166.49
T 9012=	968.69	T 1013=	199.75	T 1021=	172.32	T 1022=	172.32	F 1023=	156.81	T 9031=	166.88
T 9052=	966.88	T 1003=	153.95	F 1041=	162.38	T 1042=	162.38	F 1043=	156.05	T 9044=	156.05
T 1346=	137.33	T 1347=	150.98	HEATER MODES IN ASCENDING MODE NUMBER ORDER +-+MODE+-+							
T 1=	16	108.99	T 2=	100.88	REDUNDANT MODES IN ASCENDING MODE NUMBER ORDER						

SYSTEMS IMPROVED AMERICAN DIFFERENTIAL ANALYZER '85 (SINCE '83)

PAGE 1/4

MODEL = 844064
PUBDCMAC LOAD CASE NO. 4 CONDITIONS - Axial Distribution, -30F
***** Peak GCY Sidwall Temperature Time Point *****

3/2/94

RUNMODEL NAME = MAIN

PROBLEM TIME TIME = 0.580000 VS. TIME= 0.500000
 DIFFUSION NODES IN ASCENDING NODE NUMBER ORDER
 T 267= 100.60 T 268= 100.66 T 269= 99.476
 ARITHMETIC NODES IN ASCENDING NODE NUMBER ORDER
 T 281= 620.52 T 1260= 108.89 T 1287= 161.78 T 1269= 137.59 T 1290= 111.78
 HEATER NODES IN ASCENDING NODE NUMBER ORDER

 BOUNDARY NODES IN ASCENDING NODE NUMBER ORDER

MEAN GCY GAS TEMP= 620.5 F MEAN GCY GAS PRESSURE= 32.43 PSIA
 MEAN LCY-GCY GAS TEMP= 786.1 F MEAN LCY-GCY GAS PRESSURE= 43.95 PSIA

RUNMODEL NAME = PTBA

	CALCULATED	ALLOWED
MIN DIFF DELTA T PER ITER	DRLOCC(P)TA	384)= 2.441604E-04 VS. DRLOCC= 1.000000E-02
MAX ARITH DELTA T PER ITER	ARLXCC(P)TA	1346)= -0.269775 VS. ARLXCC= 0.500000
MIN DIFF DEL T PER TIME STEP	STMPCC(P)TA	384)= 2.746822E-04 VS. STMPCC= 10.0000
MAX ARITH DEL T PER TIME STEP	ATMPCC(P)TA	1346)= -0.269745 VS. ATMPCC= 10.0000
MIN STABILITY CRITERIA	CRSMIN(P)TA	431)= 3.857513E-05
MAX STABILITY CRITERIA	CRSMAX(P)TA	424)= 1.96759
NUMBER OF ITERATIONS	LOOPCT	= 1 VS. BLOOPF= 600
PROBLEM TIME	TIME#	= 0.500000 VS. TIME#0= 0.500000
MEAN PROBLEM TIME	TIME#	= 0.500000
AVERAGE TIME STEP USED	DTIME#	= 1.056667E-02 VS. DTIME# = 0.

DIFFUSION NODES IN ASCENDING NODE NUMBER ORDER

T 51= 941.30	T 53= 934.14	T 55= 885.93	T 60= 874.54	T 62= 976.45	T 100= 884.80
T 105= 863.00	T 107= 860.23	T 110= 884.44	T 112= 889.48	T 113= 876.27	T 120= 1003.9
T 122= 1042.1	T 125= 915.54	T 126= 9038.6	T 129= 908.88	T 136= 1031.8	T 127= 897.16
T 130= 979.59	T 132= 1027.4	T 133= 867.61	T 134= 1024.9	T 135= 863.25	T 136= 1080.1
T 137= 854.60	T 140= 928.11	T 141= 910.86	T 142= 963.57	T 143= 834.39	T 144= 961.86
T 149= 830.68	T 146= 955.82	T 147= 823.09	T 150= 944.12	T 152= 998.91	T 153= 816.96
T 154= 995.15	T 155= 813.53	T 156= 991.38	T 157= 889.89	T 160= 875.47	T 163= 863.96
T 162= 928.92	T 163= 757.68	T 164= 921.57	T 165= 781.37	T 166= 918.88	T 167= 756.94
T 170= 803.99	T 172= 912.41	T 173= 488.66	T 175= 488.35	T 177= 444.58	T 180= 429.49
T 190= 278.54	T 191= 268.74	T 192= 134.50	T 193= 363.72	T 194= 163.68	T 196= 832.07
T 198= 271.20	T 200= 900.4	T 204= 1087.9	T 210= 1114.3	T 220= 1983.7	T 230= 1029.4
T 240= 535.26	T 242= 253.99	T 250= 113.54	T 280= 95.303	T 261= 96.446	T 262= 94.806
T 263= 97.046	T 264= 95.316	T 265= 98.193	T 266= 98.231	T 268= 1262.5	T 304= 1229.1
T 305= 1375.8	T 310= 1136.4	T 313= 1226.7	T 315= 1331.1	T 316= 1331.1	T 320= 1106.2
T 323= 1249.2	T 325= 1325.9	T 328= 1325.9	T 330= 1840.1	T 332= 1118.2	T 335= 1273.2
T 336= 1273.2	T 340= 861.27	T 362= 534.47	T 363= 1036.7	T 344= 244.64	T 348= 912.83
T 346= 1263.4	T 347= 464.82	T 349= 1002.8	T 350= 162.36	T 351= 375.26	T 382= 145.98
T 393= 272.47	T 394= 207.31	T 395= 121.99	T 364= 217.09	T 340= 95.786	T 362= 92.437
T 344= 95.982	T 366= 111.83	T 367= 116.57	T 368= 137.44	T 349= 164.79	T 373= 371.27
T 373= 270.33	T 375= 166.60	T 377= 121.02	T 400= 92.709	T 481= 109.68	T 402= 116.96
T 404= 1186.7	T 406= 1375.4	T 408= 1358.0	T 410= 1489.9	T 412= 1488.4	T 414= 1418.6

T 42*	392.41	T 422*	1413.7	T 423*	1416.4	T 424*	150.27	T 425*	1507.7	T 426*	1401.0
T 43*	1354.7	T 432*	1359.2	T 433*	1320.8	T 434*	1358.3	T 435*	1377.8	T 436*	1954.3
T 450*	1437.8	T 452*	1426.4	T 454*	1403.1						
ARITHMETIC NODES IN ASCENDING NODE NUMBER ORDER											
T 50*	934.45	T 52*	932.38	T 54*	897.96	T 150*	804.33	T 154*	836.52	T 160*	867.86
T 169*	861.58	T 195*	134.27	T 197*	154.21	T 199*	258.25	T 230*	825.71	T 311*	1244.3
T 312*	1848.3	T 321*	1232.8	T 328*	1232.8	T 331*	1158.5	T 338*	1130.8	T 337*	772.92
T 341*	451.77	T 357*	244.43	T 358*	343.41	T 359*	144.81	T 370*	115.95	T 408*	150.10
T 1080*	144.60	T 1001*	239.82	T 1002*	235.32	T 1003*	154.86	T 1004*	126.22	T 1005*	125.33
T 1085*	97.962	T 1007*	358.88	T 1008*	294.84	T 1009*	277.34	T 1010*	183.18	T 1011*	1750.5
T 1012*	1158.5	T 1015*	1301.5	T 1021*	1148.5	T 1022*	1148.5	T 1023*	1295.9	T 1081*	1054.1
T 1032*	1894.1	T 1035*	1228.7	T 1041*	888.79	T 1042*	888.79	T 1043*	582.91	T 1044*	582.91
T 1344*	1198.0	T 1347*	363.95								
HEATER NODES IN ASCENDING NODE NUMBER ORDER											
←→											
BOUNDARY NODES IN ASCENDING NODE NUMBER ORDER											
T 1*	1475.6	T 2*	1434.7								

SYSTEM IMPROVED NUMERICAL DIFFERENCE ANALYZER (S (SINMA) (S))

PAGE 2/4

MODEL = BROWNS
FIXEDBIC LOAD CASE NO. 4 CONDITIONS - Axial Distribution, -20P
Peak DCV Sidewall Temperature Time Point

3/2/84

SUBMODEL NAME = PTM

CALCULATED		ALLOWED	
MAX DIFF DELTA T PER ITER	DRLECC(PTSS	404)= 2.441400E-04	VR. DRLECC= 5.800000E-02
MAX ARITH DELTA T PER ITER	ARLCCOPTSS	1348)= 0.304993	VR. ARLCC= 0.340000
MAX DIFF DEL T PER TIME STEP	DTMPC(PTSS	404)= 2.346588E-04	VR. ATRMPC= 18.8000
MAX ARITH DEL T PER TIME STEP	ATMPC(PTSS	1348)= 0.304991	VR. ATRMPC= 100.000
MIN STABILITY CRITERIA	CSMIN(PTSS	4467)= 3.012875E-05	
MAX STABILITY CRITERIA	CSMAX(PTSS	4247)= 2.05956	
NUMBER OF ITERATIONS	LEDCPT	=	VR. MLCOPT= 600
PROBLEM TIME	TIMEN	= 0.500000	VR. TIMEN= 0.500000
NEAR PROBLEM TIME	TIMEN	= 0.500000	
AVERAGE TIME STEP USED	DTMNU	= 1.666667E-02	VR. DTMNU= 0.

DIFFUSION NODES IN ASCENDING NODE NUMBER ORDER		DIFFUSION NODES IN ASCENDING NODE NUMBER ORDER	
T 51= 276.45	T 53= 260.34	T 55= 699.47	T 60= 829.89
T 109= 900.27	T 107= 878.67	T 100= 868.29	T 112= 873.49
T 132= 876.50	T 123= 803.91	T 124= 858.33	T 125= 809.24
T 138= 768.34	T 132= 821.88	T 133= 727.97	T 134= 795.28
T 127= 734.59	T 148= 727.16	T 141= 727.36	T 142= 778.77
T 145= 691.41	T 144= 702.76	T 147= 687.77	T 150= 695.93
T 154= 727.74	T 135= 648.23	T 154= 666.76	T 157= 644.59
T 162= 781.83	T 143= 594.26	T 164= 649.02	T 163= 592.19
T 170= 647.69	T 172= 459.77	T 175= 457.16	T 173= 372.89
T 190= 299.63	T 191= 383.13	T 192= 133.51	T 193= 369.86
T 196= 286.11	T 200= 1013.4	T 204= 1032.2	T 210= 693.37
T 240= 661.89	T 262= 263.54	T 238= 113.94	T 268= 95.240
T 263= 95.082	T 264= 94.829	T 265= 97.634	T 266= 97.344
T 309= 1371.2	T 310= 915.99	T 313= 1090.2	T 315= 1275.8
T 323= 1082.9	T 325= 1268.2	T 328= 1268.2	T 330= 838.20
T 336= 1233.4	T 340= 792.25	T 342= 507.06	T 343= 1018.2
T 346= 1250.3	T 347= 289.68	T 349= 1048.5	T 380= 155.87
T 353= 266.79	T 334= 198.18	T 335= 114.88	T 386= 202.42
T 366= 92.278	T 366= 186.62	T 367= 107.89	T 388= 190.46
T 375= 284.17	T 379= 159.36	T 377= 112.39	T 400= 92.044
T 406= 898.54	T 406= 1366.2	T 408= 1379.9	T 410= 1418.8
T 421= 303.34	T 422= 1413.7	T 428= 1436.7	T 426= 160.73
T 431= 1225.1	T 632= 1351.1	T 633= 263.22	T 484= 213.32
T 441= 1379.5	T 442= 1372.8	T 443= 1372.7	T 444= 1372.6
T 451= 1376.5	T 452= 1366.4	T 453= 1376.7	T 454= 1381.4
T 50= 777.87	T 52= 746.84	T 54= 725.96	T 150= 652.38
T 109= 645.89	T 193= 124.98	T 197= 189.91	T 199= 262.79
			T 250= 534.97
			T 311= 1111.8

T 312=	1111.5	T 321=	1100.1	T 322=	1100.1	T 331=	1030.2	T 332=	1030.2	T 337=	745.37
T 341=	620.41	T 357=	233.12	T 358=	233.76	T 359=	156.76	T 370=	109.06	T 405=	109.90
T 900=	123.66	T 901=	252.87	T 902=	244.37	T 903=	154.13	T 904=	125.91	T 905=	124.22
T 906=	94.938	T 907=	328.19	T 908=	301.40	T 909=	288.82	T 910=	106.07	T 911=	597.96
T 1012=	937.96	T 1013=	1222.8	T 1021=	921.00	T 1022=	921.00	T 1023=	1214.5	T 1031=	858.97
T 1032=	858.97	T 1033=	1171.9	T 1041=	817.88	T 1042=	817.88	T 1043=	340.40	T 1044=	340.40
T 1346=	1827.9	T 1347=	295.89								
GREATER NODES IN ASCENDING NODE NUMBER ORDER											
++BONE++											
BOUNDARY NODES IN ASCENDING NODE NUMBER ORDER											
T 1=	1475.0	T 2=	1424.7								

SYSTEMS IMPROVED NUMERICAL DIFFERENTIATION ANALYZER '80 (X)MDA '85)

PAGE 3/4

NORTEL = SANAGSA
RODCKNAC LOAD CASE NO. 4 CONDITIONS - Axial Distribution, -20F
Peak OCY sidewall Temperature Time Point

5/2/79

ELEMENT NAME = FTCL

MAX DIFF DELTA T PER ITER	CALCULATED	127)= 2.441406E-04	VS.	ALLOWED	5.000000E-02
MAX ANITH DELTA T PER ITER	ARLACC(P1SC	1344)= -0.383467	VS.	ARLWCA=	0.500000
MAX DIFF DEL T PER TIME STEP	DTMPCG(P1SC	127)= 2.746582E-04	VS.	DTMPCA=	10.0000
MAX ANITH DEL T PER TIME STEP	ATMPCG(P1SC	1344)= -0.288436	VS.	ATMPCA=	100.0000
MIN STABILITY CRITERIA	CSMNTV(P1SC	444)= 3.812212E-05			
MAX STABILITY CRITERIA	CSMNOI(P1SC	424)= 2.887648			
NUMBER OF ITERATIONS	LIMPTCT	=	1	VS.	MLOOPT= 600
PROBLEM TIME	TIMER	=	0.580000	VS.	TINDM= 0.500000
NEAR PROBLEM TIME	TIMER	=	0.500000		
AVERAGE TIME STEP USED	DTMTR	=	1.846647E-02	VS.	DTMTR= 0.

DIFFUSION NODES IN ASCENDING NODE NUMBER ORDER																	
T	51=	493.73	T	53=	443.26	T	55=	359.86	T	60=	488.62	T	62=	919.21	T	100=	936.00
T	105=	873.03	T	107=	850.79	T	110=	834.81	T	112=	828.41	T	113=	836.37	T	120=	766.23
T	122=	779.36	T	123=	762.67	T	124=	773.34	T	125=	768.23	T	126=	780.36	T	127=	778.96
T	130=	675.77	T	132=	682.34	T	133=	671.66	T	134=	681.06	T	135=	673.69	T	136=	688.06
T	137=	676.02	T	140=	623.34	T	141=	622.32	T	142=	630.84	T	143=	628.71	T	144=	626.88
T	145=	619.61	T	146=	621.96	T	147=	628.55	T	150=	586.73	T	152=	596.45	T	153=	583.59
T	154=	589.32	T	155=	579.34	T	156=	588.34	T	157=	576.43	T	160=	528.60	T	161=	536.85
T	162=	538.59	T	163=	526.44	T	164=	533.68	T	165=	523.83	T	166=	527.39	T	167=	526.25
T	170=	602.34	T	172=	604.34	T	173=	601.03	T	175=	393.21	T	177=	371.00	T	180=	560.94
T	190=	313.68	T	191=	303.36	T	192=	134.25	T	195=	392.33	T	194=	369.77	T	196=	384.47
T	198=	309.38	T	200=	1800.4	T	204=	1615.7	T	210=	642.68	T	220=	614.88	T	230=	537.03
T	240=	434.18	T	242=	242.30	T	250=	113.75	T	260=	95.195	T	261=	96.896	T	262=	93.793
T	263=	96.900	T	264=	94.788	T	265=	97.336	T	266=	97.271	T	300=	1185.4	T	304=	1282.8
T	305=	1370.2	T	310=	892.64	T	313=	1681.8	T	315=	1271.0	T	316=	1271.8	T	320=	876.62
T	323=	1069.7	T	325=	1262.9	T	326=	1262.9	T	330=	816.24	T	333=	1813.6	T	335=	1250.1
T	336=	1230.1	T	340=	785.67	T	342=	594.35	T	343=	1017.6	T	344=	238.82	T	345=	769.05
T	346=	1249.2	T	347=	389.04	T	349=	1845.2	T	350=	159.34	T	391=	386.88	T	392=	156.21
T	393=	288.45	T	394=	187.85	T	395=	114.54	T	356=	202.12	T	360=	93.678	T	363=	92.057
T	364=	92.226	T	366=	186.68	T	367=	187.51	T	368=	110.07	T	369=	116.27	T	371=	360.05
T	375=	266.45	T	375=	159.15	T	377=	112.15	T	400=	92.037	T	404=	100.30	T	400=	106.86
T	406=	880.63	T	406=	1368.7	T	408=	1379.9	T	410=	1433.8	T	430=	1608.5	T	414=	1618.6
T	421=	393.35	T	422=	1613.7	T	423=	1436.7	T	426=	140.73	T	425=	1397.8	T	428=	1604.7
T	421=	1224.8	T	432=	1350.6	T	433=	269.21	T	434=	213.82	T	438=	1485.6	T	436=	1604.7
T	441=	1379.3	T	442=	1372.5	T	443=	1372.6	T	444=	1372.6	T	445=	1394.7	T	448=	1380.3
T	451=	1376.9	T	452=	1365.9	T	453=	1376.6	T	454=	1381.6	T	455=	1612.4	T	456=	1394.6
ARITHMETIC NODES IN ASCENDING NODE NUMBER ORDER																	
T	50=	807.11	T	52=	645.36	T	54=	632.37	T	150=	328.88	T	180=	535.90	T	168=	537.18
T	160=	536.86	T	195=	129.97	T	197=	140.36	T	199=	275.88	T	230=	581.23	T	311=	1899.1

T 318=	1099.1	T 321=	1086.8	T 322=	1086.8	T 331=	1029.7	T 332=	1029.7	T 337=	742.72
T 361=	417.34	T 367=	252.82	T 368=	355.48	T 389=	156.53	T 379=	108.86	T 403=	109.56
T 1880=	125.15	T 1081=	270.33	T 1082=	258.40	T 1803=	162.32	T 1084=	125.83	T 1085=	124.92
T 1886=	84.906	T 1087=	351.39	T 1088=	317.38	T 1809=	307.57	T 1818=	199.10	T 1011=	916.21
T 1812=	916.21	T 1813=	1213.4	T 1821=	898.47	T 1822=	898.47	T 1823=	1206.8	T 1831=	899.79
T 1832=	899.79	T 1833=	1166.9	T 1841=	811.00	T 1842=	811.00	T 1863=	348.20	T 1864=	348.20
T 1346=	296.53	T 1347=	296.53								
NEATER NODES IN ASCENDING NODE NUMBER ORDER											
-->NODE-->											
BOUNDARY NODES IN ASCENDING NODE NUMBER ORDER											
T 1=	1675.0	T 2=	1425.7								

SYSTEMS IMPROVED NUMERICAL DIFFERENCING ANALYZER '85 (SIMA '85)

PAGE 4/4

MODEL = OMMBKS
FINRCENAC LOAD CASE NO. & CONDITIONS = Axial Distribution, -20P
***** Peak DCV SimaML Temperature Time Point *****

3/2/94

SUBMODEL NAME = PT30

	UNACCEPTED	107) = 2.443406E-04	VS. UNACCU= 9.000000E-02
MAX DIFF DELTA T PER ITER	ACCEPTED	1346) = 8.303467	VS. UNACCU= 0.500000
MAX ARITH DELTA T PER ITER	BTMPCOPTSD	107) = 7.764582E-04	VS. BTMPCA= 10.0000
MAX DIFF DEL T PER TIME STEP	ATMPCOPTSD	1346) = 0.303436	VS. ATMPCA= 100.000
MAX ARITH DEL T PER TIME STEP	CGRNHOPTSD	444) = 3.012212E-05	
MIN STABILITY CRITERIA	CBMHOPTSD	426) = 2.059948	
MAX STABILITY CRITERIA	LDPCPT	= 1	VS. BKLOPT= 400
NUMBER OF ITERATIONS	TIMER	= 0.500000	VS. TIMESP= 8.500000
PROBLEM TIME	TIMER	= 0.500000	
NEAR PROBLEM TIME	BTIME)	= 1.666667E-02	VS. BTIME)= 0.
AVERAGE TIME STEP USED			

DIFFUSION NODES IN ASCENDING		NODE NUMBER ORDER									
T	51= 684.35	T	53= 625.94	T	33= 588.11	T	40= 806.58	T	62= 914.99	T	100= 935.62
T	105= 872.78	T	107= 848.05	T	110= 833.99	T	112= 824.84	T	113= 823.51	T	120= 758.98
T	120= 759.85	T	123= 757.22	T	124= 765.10	T	125= 763.44	T	126= 776.60	T	127= 776.12
T	130= 666.47	T	130= 665.58	T	133= 663.02	T	134= 668.80	T	135= 666.03	T	136= 673.47
T	137= 672.86	T	140= 608.10	T	141= 607.62	T	142= 610.82	T	143= 608.26	T	144= 610.47
T	145= 608.85	T	146= 613.01	T	147= 613.28	T	150= 571.99	T	152= 573.98	T	153= 572.26
T	154= 572.59	T	159= 569.44	T	156= 570.94	T	157= 569.53	T	160= 513.31	T	161= 522.62
T	162= 517.93	T	163= 514.80	T	164= 516.72	T	168= 513.92	T	166= 517.71	T	167= 516.27
T	170= 394.79	T	172= 394.91	T	173= 394.08	T	175= 350.47	T	177= 343.71	T	180= 337.43
T	190= 311.49	T	191= 342.35	T	192= 134.25	T	193= 340.49	T	194= 169.48	T	196= 304.08
T	198= 304.52	T	200= 1602.5	T	204= 1014.0	T	210= 641.83	T	220= 612.71	T	230= 587.62
T	240= 454.28	T	242= 242.04	T	250= 113.74	T	260= 95.191	T	263= 96.094	T	262= 95.789
T	263= 94.973	T	264= 94.753	T	265= 97.329	T	266= 97.279	T	300= 1195.1	T	304= 1802.4
T	305= 1370.1	T	310= 892.03	T	313= 1081.3	T	315= 1279.9	T	316= 1270.9	T	320= 873.97
T	323= 1069.3	T	325= 1262.8	T	326= 1362.8	T	330= 816.37	T	333= 1013.9	T	335= 1230.1
T	336= 1230.1	T	340= 783.44	T	343= 504.23	T	343= 1017.6	T	344= 230.83	T	345= 769.85
T	346= 1249.2	T	347= 509.87	T	349= 1045.2	T	350= 155.35	T	351= 366.67	T	352= 694.22
T	353= 266.65	T	374= 197.85	T	393= 114.54	T	354= 282.13	T	360= 93.476	T	362= 92.856
T	364= 92.228	T	374= 104.48	T	367= 107.51	T	368= 118.87	T	369= 118.27	T	371= 362.85
T	373= 264.04	T	385= 159.11	T	377= 112.15	T	400= 92.837	T	401= 100.98	T	402= 104.86
T	404= 899.43	T	406= 1843.6	T	409= 1379.9	T	418= 1413.0	T	412= 1408.5	T	434= 1418.6
T	421= 393.33	T	422= 1413.7	T	423= 1416.7	T	424= 148.73	T	425= 1397.8	T	426= 1404.7
T	431= 1226.8	T	432= 1350.4	T	433= 345.21	T	434= 213.32	T	435= 1405.4	T	436= 1404.7
T	441= 1379.3	T	442= 1372.3	T	443= 1372.6	T	444= 1372.6	T	445= 1394.7	T	446= 1380.3
T	451= 1374.0	T	452= 1365.9	T	453= 1376.6	T	454= 1381.6	T	455= 1412.4	T	456= 1394.6
		ARITHMETIC NODES IN ASCENDING		NODE NUMBER ORDER							
T	50= 667.83	T	52= 632.32	T	54= 620.32	T	50= 523.75	T	106= 522.94	T	108= 522.84
T	109= 523.44	T	105= 130.25	T	107= 130.04	T	109= 274.67	T	108= 501.45	T	110= 1098.7

T 312=	1098.7	T 321=	1098.6	T 322=	1098.4	T 331=	1029.8	T 332=	1029.8	T 337=	742.72	
T 341=	617.36	T 357=	232.82	T 358=	232.68	T 359=	164.93	T 379=	108.88	T 403=	149.86	
F 1008=	125.10	T 1081=	279.97	T 1082=	257.50	T 1083=	142.63	T 1084=	125.83	T 1085=	124.92	
T 1086=	96.901	T 1087=	328.43	T 1088=	315.15	T 1089=	306.26	T 1018=	198.98	T 1011=	915.63	
T 1012=	915.63	T 1013=	1215.5	T 1021=	897.84	T 1022=	897.84	T 1023=	1206.6	T 1031=	539.91	
T 1032=	839.91	T 1033=	1167.8	T 1041=	818.98	T 1042=	818.98	T 1043=	546.21	T 1044=	546.21	
F 1346=	1026.6	F 1347=	296.53									
NEATER NODES IN ASCENDING NODE NUMBER ORDER												
++NODE++												
BOUNDARY NODES IN ASCENDING NODE NUMBER ORDER												
T 1=	1475.8	F 2=	1424.7									

T 421=	486.66	T 422=	565.57	T 423=	585.28	T 424=	219.61	T 425=	704.87	T 426=	635.71
T 431=	579.50	T 432=	679.77	T 433=	748.00	T 434=	745.86	T 435=	672.22	T 436=	575.74
T 950=	1482.4	T 952=	1478.7	T 954=	1434.7						
ARITHMETIC NODES IN ASCENDING NODE NUMBER ORDER											
T 50=	975.59	T 52=	960.96	T 54=	911.51	T 150=	942.42	T 159=	918.39	T 160=	947.21
T 169=	941.07	T 195=	160.23	T 197=	284.31	T 199=	347.98	T 238=	902.29	T 311=	870.32
T 312=	879.32	T 321=	868.39	T 322=	868.39	T 331=	744.34	T 332=	744.34	T 337=	830.92
T 341=	819.97	T 357=	246.15	T 318=	252.56	T 329=	215.46	T 379=	167.99	T 443=	158.76
T 1000=	189.40	T 1001=	326.70	T 1002=	340.89	T 1003=	184.83	T 1004=	159.91	T 1005=	128.74
T 1006=	103.67	T 1007=	423.81	T 1008=	392.55	T 1009=	375.95	T 1010=	253.89	T 1011=	1805.7
T 1012=	1005.7	T 1013=	775.18	T 1021=	1001.1	T 1022=	1001.1	T 1023=	774.90	T 1024=	910.85
T 1022=	910.05	T 1033=	679.53	T 1041=	717.73	T 1042=	717.73	T 1043=	487.95	T 1044=	487.95
T 1344=	601.83	T 1347=	322.43								
HEATER NODES IN ASCENDING NODE NUMBER ORDER											
--HOME--											
PRIMARY NODES IN ASCENDING NODE NUMBER ORDER											
T 1=	-20.000	T 2=	-20.000								

SYSTEMS IMPROVED NUMERICAL DIFFERENCING ANALYZER '85 (FINDA '85)

PAGE 2/4

MODEL = BANA024
PDSCK***+*** MAC LOAD CASE NO. 4 CONDITIONS = Axis Distribution -2RF
Peak ICY Stowell Temperature Time Point ***+***

5/2/84

NUMERICAL NAME = P165

MAX DIFF DELTA T PER ITER	CALCULATED	110)= -2.625547E-03	VS.	ALLOWED	5.800000E-02
MAX ARITH DELTA T PER ITER	ARITH(COPTS)	337)= -3.826704E-02	VS.	ARITHC=	0.500000
MAX DIFF DEL T PER TIME STEP	DTMPC(OPTS)	435)= -0.207489	VS.	DTMPC=	10.0000
MAX ARITH DEL T PER TIME STEP	ATMPC(OPTS)	136)= -0.139433	VS.	ATMPC=	180.000
MIN STABILITY CRITERIA	COORD(OPTS)	495)= 1.487195E-04			
MAX STABILITY CRITERIA	COORD(OPTS)	426)= 2.20143			
NUMBER OF ITERATIONS	LOOPCT	= 2	VS.	BL0OPT=	600
PROBLEM TIME	TIMER	= 0.253333	VS.	TIMERB=	12.0000
MEAN PROBLEM TIME	TIMER	= 0.253333			
AVERAGE TIME STEP USED	DTMNU	= 2.427562E-04	VS.	DTMNU=	0.

DIFFUSION NODES IN ASCENDING NODE NUMBER ORDER																	
T	51=	833.70	T	53=	709.37	T	55=	729.34	T	60=	842.04	T	63=	844.16	T	100=	837.57
T	105=	837.02	T	107=	838.45	T	110=	836.61	T	112=	854.03	T	113=	827.04	T	120=	841.63
T	122=	891.29	T	125=	808.02	T	126=	844.76	T	125=	808.97	T	126=	817.65	T	127=	804.67
T	130=	825.81	T	132=	877.61	T	133=	786.01	T	134=	858.72	T	135=	789.15	T	136=	804.57
T	137=	792.35	T	140=	812.18	T	141=	812.75	T	142=	839.99	T	143=	780.13	T	144=	834.95
T	143=	779.80	T	146=	788.35	T	147=	776.18	T	150=	786.37	T	152=	847.02	T	153=	743.23
T	154=	815.34	T	155=	744.22	T	156=	761.76	T	157=	744.27	T	160=	731.73	T	161=	736.91
T	162=	789.85	T	163=	694.21	T	164=	761.53	T	165=	897.29	T	166=	713.16	T	167=	698.83
T	170=	561.34	T	172=	568.86	T	173=	595.07	T	175=	489.43	T	177=	515.66	T	180=	464.58
T	190=	394.50	T	191=	461.67	T	192=	344.93	T	193=	338.73	T	194=	236.68	T	196=	344.64
T	198=	484.58	T	200=	836.93	T	204=	808.13	T	210=	795.86	T	220=	774.08	T	230=	717.74
T	240=	573.96	T	242=	342.37	T	250=	153.61	T	260=	94.781	T	261=	98.196	T	262=	98.814
T	263=	100.89	T	264=	118.34	T	265=	116.86	T	266=	121.58	T	300=	744.15	T	301=	712.38
T	305=	432.76	T	310=	745.38	T	313=	844.72	T	315=	953.66	T	316=	953.66	T	320=	728.72
T	323=	682.42	T	325=	546.96	T	326=	546.96	T	330=	674.39	T	333=	595.80	T	335=	517.68
T	336=	517.68	T	340=	684.36	T	342=	631.74	T	343=	677.21	T	344=	278.15	T	345=	598.06
T	346=	548.37	T	347=	480.91	T	349=	238.88	T	350=	195.45	T	351=	226.82	T	352=	194.18
T	353=	206.12	T	354=	223.94	T	355=	149.44	T	356=	225.23	T	360=	95.341	T	362=	94.449
T	364=	108.90	T	366=	145.49	T	367=	148.88	T	368=	193.21	T	369=	171.49	T	371=	233.54
T	373=	214.97	T	375=	172.49	T	377=	143.34	T	400=	101.85	T	401=	116.39	T	402=	141.19
T	404=	854.38	T	406=	954.32	T	408=	907.38	T	410=	333.76	T	412=	688.88	T	414=	533.04
T	421=	484.00	T	422=	545.63	T	423=	553.46	T	424=	189.08	T	425=	787.20	T	426=	439.48
T	431=	604.56	T	432=	673.32	T	433=	561.86	T	434=	303.88	T	435=	669.69	T	436=	587.85
T	441=	512.44	T	442=	592.78	T	443=	616.47	T	444=	619.75	T	445=	593.77	T	446=	512.76
T	451=	530.49	T	452=	553.09	T	453=	551.26	T	454=	391.39	T	455=	534.23	T	456=	533.11
ARITHMETIC NODES IN ASCENDING NODE NUMBER ORDER																	
T	50=	832.44	T	52=	789.41	T	54=	747.04	T	150=	246.90	T	159=	727.86	T	160=	737.70
T	169=	260.88	T	195=	146.48	T	197=	180.17	T	199=	380.94	T	218=	655.85	T	311=	431.31

T 312= 651.91	T 321= 640.09	T 322= 640.09	T 331= 582.25	T 332= 582.25	T 337= 479.95
T 341= 666.56	T 357= 226.78	T 388= 223.83	T 399= 195.85	T 379= 167.76	T 608= 143.87
T 1000= 147.99	T 1001= 349.77	T 1008= 354.57	T 1003= 185.15	T 1004= 134.97	T 1009= 123.89
T 1006= 100.24	T 1007= 436.20	T 1008= 410.29	T 1009= 606.30	T 1010= 278.98	T 1011= 740.86
T 1012= 740.86	T 1013= 591.62	T 1021= 725.60	T 1022= 725.60	T 1023= 562.86	T 1051= 670.16
T 1032= 670.16	T 1033= 543.51	T 1041= 602.72	T 1042= 602.72	T 1043= 435.70	T 1044= 435.70
T 1344= 395.73	T 1347= 311.92	HEATER MODES IN ASCENDING MODE NUMBER ORDER ++NONE++			
BOUNDARY MODES IN ASCENDING MODE NUMBER ORDER					
T 1= -20.000	T 2= -20.000				

SYSTEMS IMPROVED NUMERICAL DIFFERENCING ANALYZER '85 (IBINA '85)

PAGE 3/4

MODEL = CANADA
FM900CNAC LOAD CASE NO. & CONDITIONS - Aural Distribution, ~20F
Peak (CV sidem) Temperature Time Point

5/2/79

SUBMODEL NAME = P13C

CALCULATED		ALLOWED	
MAX DIFF DELTA T PER ITER	ANLJCC(PTSC	198)= 3.175282E-05	VS. DELTCA= 5.000000E-02
MAX ARITH DELTA T PER ITER	ANLJCC(PTSC	337)= 6.1522980E-02	VS. DELTCA= 8.500000
MAX DIFF DEL T PER TIME STEP	DTMPC(PTSC	425)= 0.207489	VS. ATMPC= 10.0000
MAX ARITH DEL T PER TIME STEP	ATMPC(PTSC	1346)= 0.140843	VS. ATMPC= 100.000
MIN STABILITY CRITERIA	CSM(H)OPTSC	425)= 3.487509E-04	
MAX STABILITY CRITERIA	CSM(H)OPTSC	426)= 2.28137	
NUMBER OF ITERATIONS	LOOPCT	= 2	VS. NLOOP= 600
MINIMUM TIME	TIMEP	= 0.833333	VS. TIMEHD= 12.0000
MEAN MINIMUM TIME	TIMEH	= 0.833334	
AVERAGE TIME STEP USED	DTIMEU	= 2.687502E-04	VS. DTIME= 0.

DIFFUSION NODES IN ASCENDING NODE NUMBER ORDER

T 51= 761.20	T 53= 688.81	T 55= 621.85	T 60= 812.88	T 62= 616.44	T 100= 611.36
T 105= 799.66	T 107= 795.30	T 110= 787.77	T 112= 790.85	T 113= 787.34	T 120= 769.60
T 122= 769.32	T 123= 760.94	T 124= 765.29	T 125= 799.53	T 126= 796.74	T 127= 795.58
T 130= 732.69	T 132= 735.67	T 128= 728.42	T 134= 736.81	T 129= 728.98	T 136= 730.35
T 137= 728.73	T 140= 714.00	T 141= 714.46	T 142= 720.08	T 143= 718.76	T 164= 716.17
T 145= 709.49	T 146= 707.98	T 147= 706.32	T 150= 685.16	T 132= 692.98	T 153= 681.46
T 154= 687.78	T 155= 679.35	T 156= 679.21	T 157= 676.74	T 160= 636.97	T 161= 644.68
T 162= 644.10	T 163= 639.89	T 164= 641.73	T 163= 634.73	T 166= 638.08	T 167= 636.21
T 170= 545.78	T 172= 543.94	T 173= 544.68	T 175= 504.79	T 177= 520.92	T 180= 699.22
T 190= 675.32	T 191= 661.89	T 192= 190.66	T 193= 954.43	T 194= 264.74	T 196= 430.87
T 198= 666.41	T 200= 520.14	T 204= 785.59	T 210= 757.48	T 220= 708.04	T 230= 650.11
T 260= 557.50	T 262= 537.71	T 250= 152.54	T 268= 96.649	T 263= 96.137	T 262= 96.553
T 263= 108.69	T 264= 109.73	T 265= 114.46	T 266= 120.95	T 300= 734.06	T 304= 698.99
T 305= 627.60	T 310= 608.74	T 313= 628.49	T 315= 527.09	T 316= 527.89	T 320= 676.85
T 323= 612.29	T 325= 517.58	T 326= 517.58	T 330= 638.16	T 332= 567.61	T 335= 608.12
T 336= 498.12	T 340= 585.91	T 342= 625.31	T 343= 475.10	T 344= 367.25	T 345= 395.29
T 346= 544.49	T 347= 569.28	T 349= 357.12	T 350= 194.21	T 351= 325.65	T 352= 194.90
T 353= 285.18	T 354= 222.42	T 355= 148.59	T 356= 225.87	T 360= 95.219	T 362= 96.252
T 364= 188.13	T 366= 144.64	T 367= 147.99	T 368= 153.86	T 369= 189.78	T 371= 232.32
T 373= 214.10	T 375= 171.99	T 377= 144.68	T 400= 181.78	T 401= 174.34	T 402= 160.70
T 404= 653.79	T 406= 392.22	T 408= 507.24	T 418= 555.74	T 412= 600.84	T 414= 533.82
T 421= 504.09	T 422= 546.62	T 423= 553.45	T 424= 189.97	T 425= 707.39	T 426= 630.39
T 431= 683.56	T 432= 671.00	T 433= 341.79	T 434= 303.08	T 435= 669.67	T 436= 567.81
T 441= 512.23	T 442= 502.82	T 443= 616.37	T 444= 615.64	T 445= 593.78	T 446= 512.83
T 451= 529.57	T 452= 521.13	T 453= 598.88	T 454= 591.25	T 455= 594.58	T 456= 333.82
ARITHMETIC NODES IN ASCENDING NODE NUMBER ORDER					
T 50= 756.21	T 52= 698.43	T 56= 654.83	T 158= 646.18	T 159= 644.87	T 160= 644.82
T 169= 645.27	T 195= 158.54	T 197= 182.80	T 199= 398.40	T 238= 609.97	T 311= 615.44

1	312=	615.44	T	321=	599.60	1	322=	599.60	1	331=	554.55	1	332=	554.55	T	337=	671.30
1	341=	464.94	T	357=	325.28	T	358=	232.48	1	359=	194.63	1	379=	146.84	T	403=	143.40
1	1086=	152.56	T	1001=	413.81	T	1002=	376.56	1	1003=	302.89	1	1004=	199.44	T	1005=	138.12
1	1084=	100.91	1	1007=	486.67	1	1008=	476.17	1	1009=	466.25	1	1019=	278.53	T	1011=	694.33
1	1012=	694.33	1	1013=	561.68	1	1021=	672.89	1	1022=	672.89	1	1023=	549.67	T	1031=	626.91
1	1032=	626.91	T	1033=	321.13	1	1041=	582.31	1	1042=	582.31	1	1043=	426.65	T	1044=	426.65
1	1246=	552.86	1	1367=	310.25												
SEATER MODES IN ASCENDING MODE NUMBER ORDER																	
NONE																	
REARSEAT MODES IN ASCENDING MODE NUMBER ORDER																	
1	1=	-20.000	1	2=	-20.000												

T 312=	616.95	T 321=	998.24	T 322=	598.34	T 331=	584.28	F 332=	564.28	T 337=	471.18
T 341=	454.80	T 357=	325.27	T 358=	252.48	T 389=	194.62	F 379=	146.84	T 403=	143.68
F 1800=	132.65	T 1801=	416.42	T 1802=	375.74	F 1009=	203.76	T 1084=	139.59	T 1885=	138.36
T 1806=	180.91	T 1007=	486.68	T 9080=	476.34	T 1009=	465.24	F 1810=	278.23	T 1811=	892.24
F 1012=	893.24	T 1815=	548.94	T 1821=	471.18	F 1022=	471.18	F 1023=	548.57	T 1831=	688.45
T 1832=	428.45	T 1833=	528.94	T 1841=	581.99	T 1042=	581.99	T 1843=	428.54	T 1844=	428.54
T 1344=	332.84	T 3347=	318.29								
HEATER NODES IN ASCENDING NODE NUMBER ORDER											
--NONE--											
BOUNDARY NODES IN ASCENDING NODE NUMBER ORDER											
T 1=	-28.000	T 2=	-28.000								

T 429= 78.901	T 432= 0.90166	T 435= -5.9585	T 438= 80.248	T 441= 1.7430	T 426= -6.3260
T 437= 36.914	T 433= 34.843	T 433= 24.943	T 434= 10.323	T 435=-0.84778	T 436= 1.9962
T 950= 1330.4	T 952= 1331.0	T 954= 1371.8			
ARITHMETIC NODES IN ASCENDING NODE NUMBER ORDER					
T 90= 632.82	T 92= 668.84	T 94= 677.99	T 98= 687.18	T 99= 631.71	T 108= 668.80
T 96= 660.26	T 96= 164.75	T 97= 168.87	T 99= 222.84	T 238= 651.39	T 311= 641.26
T 99= 641.26	T 329= 664.86	T 322= 664.86	T 351= 489.96	T 332= 489.96	T 337= 263.78
T 341= 285.47	T 357= 137.78	T 358= 134.01	T 359= 133.17	T 378= 128.31	T 403= 127.98
T 980= 158.92	T 9001= 184.87	T 9002= 214.08	T 9003= 158.83	T 9094= 144.93	T 9005= 144.06
T 986= 117.80	T 9007= 278.46	T 9008= 343.31	T 9899= 215.11	T 9018= 193.28	T 9019= 761.18
T 9912= 741.48	T 9013= 373.34	T 9021= 767.40	T 9022= 767.40	T 9023= 594.71	T 9031= 625.12
T 9832= 625.12	T 9033= 643.49	T 9041= 444.18	T 9042= 444.18	T 9043= 277.88	T 986= 277.80
T 9346= 127.84	T 9347= 128.57				
WATER NODES IN ASCENDING NODE NUMBER ORDER					
--NONE--					
BOUNDARY NODES IN ASCENDING NODE NUMBER ORDER					
T 1= -28.000	T 2= -20.000				

SYSTEMS (IMPROVED NUMERICAL DIFFERENCING ANALYZER) *25 (3100) *05)

PAGE 2/4

MODEL = DANDE4
STDTLMAX LOAD CASE NO. 4 CONDITIONS = Initial Distribution, *200
*** Steady-state Conditions After the Fire ***

5/26/96 9am

SUMMEL NAME = P100

MAX DIFF DELTA T PER ITER	CALCULATED	263)=-0.185835	VS. ALLOWED	1.000000E-02
MAX ARITH DELTA T PER ITER	ERROR(P100)	1000)=-9.716777E-02	VS. ALLOWED	0.500000
MAX SYSTEM ENERGY BALANCE	ERROR(P100)	=-0.250077	VS. ENERGY	1.000000E-03
	ERROR(P100)	= 0.	VS. ENERGY	1000.00
ENERGY INFO AND OUT OF BYE	ERROR(P100)	260) = 0.299775	VS. ENERGY	1.000000E-02
MAX LOCAL ENERGY BALANCE	LOOPCT	= 302	VS. MAXLOOPS	800
NUMBER OF ITERATIONS	TIME	= 999.000	VS. TIMEEND	999.000
PROBLEM TIME				

DIFFUSION NODES IN ASCENDING NODE NUMBER ORDER																	
T	51*	391.40	T	53*	420.91	T	55*	394.02	T	60*	337.59	T	62*	332.01	T	180*	382.73
T	185*	307.77	T	107*	316.12	T	110*	327.07	T	112*	361.71	T	112*	301.13	T	120*	380.42
T	122*	473.82	T	123*	312.95	T	124*	439.80	T	125*	310.33	T	126*	362.51	T	127*	302.84
T	130*	411.80	T	128*	502.22	T	133*	334.33	T	134*	407.05	T	135*	334.36	T	136*	388.58
T	137*	351.01	T	140*	424.34	T	141*	429.32	T	142*	498.68	T	143*	302.57	T	144*	467.98
T	145*	358.56	T	146*	393.92	T	147*	343.95	T	130*	416.34	T	150*	388.01	T	153*	338.06
T	154*	479.52	T	199*	338.12	T	156*	390.18	T	137*	329.69	T	140*	308.24	T	161*	379.79
T	142*	474.00	T	143*	249.38	T	164*	439.34	T	145*	320.52	T	166*	365.10	T	167*	308.53
T	170*	381.18	T	172*	343.32	T	173*	261.48	T	175*	248.58	T	179*	262.00	T	180*	344.03
T	160*	228.00	T	191*	191.74	T	192*	128.13	T	193*	205.77	T	194*	163.73	T	196*	166.43
T	198*	198.60	T	200*	124.32	T	204*	166.68	T	210*	319.76	T	220*	337.12	T	230*	280.54
T	240*	216.51	T	242*	167.66	T	290*	123.43	T	260*	103.42	T	267*	103.99	T	268*	172.38
T	283*	113.17	T	264*	115.38	T	265*	116.78	T	266*	116.27	T	300*	76.425	T	304*	100.28
T	305*	25.600	T	310*	201.18	T	313*	243.71	T	315*	209.96	T	316*	209.96	T	320*	299.53
T	322*	263.36	T	325*	224.33	T	326*	224.33	T	330*	239.97	T	333*	201.73	T	335*	171.25
T	336*	171.33	T	340*	206.58	T	342*	153.43	T	343*	32.429	T	344*	121.39	T	345*	85.114
T	346*	78.630	T	347*	99.281	T	349*	67.864	T	390*	109.79	T	351*	103.09	T	352*	108.65
T	353*	104.99	T	354*	118.79	T	355*	108.27	T	356*	108.19	T	360*	102.68	T	362*	118.26
T	364*	112.19	T	366*	108.83	T	367*	108.87	T	380*	106.68	T	360*	108.25	T	371*	104.26
T	373*	105.44	T	375*	106.46	T	377*	106.94	T	400*	107.20	T	481*	103.17	T	402*	107.01
T	404*	72.257	T	409*	23.291	T	408*	-7.6417	T	410*	-14.447	T	412*	-11.628	T	416*	-12.761
T	421*	89.736	T	422*	-0.92031	T	423*	-7.3216	T	426*	87.853	T	425*	-1.7798	T	426*	-8.3124
T	431*	41.098	T	432*	33.801	T	433*	46.182	T	434*	17.979	T	435*	-9.0433	T	436*	-10.548
T	441*	3.3084	T	442*	0.6180	T	443*	-0.13501	T	444*	-4.3262	T	445*	-10.212	T	446*	-9.2725
T	451*	6.0781	T	452*	13.436	T	453*	-1.2695	T	454*	-8.3633	T	455*	-11.684	T	456*	-14.530
ARITHMETIC NODES IN ASCENDING NODE NUMBER ORDER																	
T	50*	309.35	T	52*	418.00	T	54*	392.60	T	158*	486.77	T	159*	371.34	T	160*	391.29
T	160*	395.27	T	195*	124.44	T	197*	136.34	T	199*	163.28	T	230*	257.89	T	311*	266.03
T	312*	246.83	T	321*	262.46	T	322*	262.46	T	331*	199.04	T	332*	199.06	T	337*	142.38

T 341=	155.34	T 357=	166.24	T 365=	164.28	T 385=	169.28	T 379=	188.60	T 483=	186.96
T 1800=	129.61	T 1801=	175.53	T 1802=	180.11	T 1805=	142.75	T 1804=	129.21	T 9893=	128.57
T 1006=	106.74	T 1007=	228.05	T 1008=	218.57	T 9089=	199.34	T 1010=	117.37	T 1011=	280.50
T 1012=	280.38	T 1013=	224.98	T 1011=	298.68	T 9022=	298.68	T 1023=	239.09	T 1031=	239.22
T 9032=	239.22	T 1033=	182.34	T 1041=	206.35	T 9042=	206.35	T 1043=	155.92	T 1044=	155.92
T 1344=	79.078	T 1347=	101.86								
HEATER MODES IN ASCENDING MODE NUMBER ORDER											
++MODE++											
SECONDARY MODES IN ASCENDING MODE NUMBER ORDER											
T 1=	-20.000	T 2=	-20.000								

T 341=	66.354	T 352=	62.603	T 358=	59.857	F 359=	44.369	F 379=	45.960	T 403=	65.063
T 1800=	94.492	T 1801=	134.46	T 1802=	120.39	F 1003=	107.76	T 1804=	97.979	T 1805=	97.591
T 1806=	85.499	T 1807=	151.67	T 1808=	146.03	F 1009=	141.80	T 1810=	93.968	T 1811=	84.669
F 1012=	84.668	F 1815=	67.319	T 1821=	91.305	F 1022=	91.305	T 1023=	73.126	F 1831=	80.489
F 1832=	80.425	T 1833=	62.862	T 1841=	74.886	F 1042=	74.886	T 1043=	68.722	T 1844=	68.722
T 1344=	37.784	T 1347=	59.074	HEATER WORES IN ASCENDING WORE NUMBER ORDER							
				BOME							
				BOUNDARY WORES IN ASCENDING WORE NUMBER ORDER							
T 1=	-20.000	T 2=	-20.000								

SYSTEM IMPROVED NUMERICAL DIFFERENCING ANALYZER '85 (SIMA '85)

PAGE 4/4

MODEL = DANUSA
STD01MC LOAD CASE NO. 4 CONDITIONS = axial dispersion, -20P
*** Steady-state Conditions After The Fire ***

5/9/86 9am

SCHEMEL NAME = P180

MAX DIFF DELTA T PER ITER	CALCULATED	351)=-4.53794E-02 VS.	ALLOWED	
MAX ARITH DELTA T PER ITER	ARITHOCPTIM	350)=-3.33623E-02 VS.	ARITHOC= 5.00000E-02	
MAX SYSTEM ENERGY BALANCE	ARLMOCPY80	= -6.77978	VS.	ARLMO= 0.300000
	EBALAC		VS.	EBALSA= 0.00000E+00
			VS.	EBALSA= 1.00000E-02
ENERGY INTO AND OUT OF SYS	EBRINIS	= 0.	VS.	EBRINIS= 787.950
MAX NORMAL ENERGY BALANCE	EBRINOCPTIM	350)=-1.09441	VS.	EBRINOC= 1.00000E-02
NUMBER OF ITERATIONS	LOOPCT	= 343	VS.	ALOSPC= 800
PROBLEIN TIME	TIMEN	= 999.880	VS.	TIMEN= 999.000

		DIFFUSION NODES IN ASCENDING NODE NUMBER ORDER									
T	51=	T	53=	T	55=	T	60=	T	62=	T	100=
T	51= 161.18	T	53= 175.38	T	55= 184.88	T	60= 190.87	T	62= 194.86	T	100= 140.40
T	106= 144.49	T	107= 146.01	T	110= 147.92	T	112= 150.78	T	113= 167.20	T	120= 199.32
T	122= 165.40	T	123= 158.88	T	124= 160.24	T	125= 151.84	T	126= 167.94	T	127= 142.49
T	130= 160.71	T	132= 176.56	T	133= 165.99	T	134= 170.80	T	135= 161.61	T	136= 157.43
T	137= 151.47	T	160= 177.07	T	141= 177.29	T	142= 182.99	T	143= 174.47	T	144= 177.22
T	145= 169.56	T	146= 162.80	T	147= 197.89	T	150= 171.37	T	152= 176.99	T	153= 167.74
T	154= 172.40	T	155= 163.15	T	156= 159.31	T	157= 151.44	T	160= 168.34	T	161= 163.79
T	162= 169.27	T	163= 160.43	T	164= 164.60	T	165= 156.95	T	166= 153.54	T	167= 148.84
T	170= 145.32	T	172= 147.33	T	175= 144.77	T	175= 139.85	T	177= 142.09	T	180= 139.82
T	190= 133.86	T	191= 129.37	T	192= 90.417	T	193= 112.74	T	194= 96.574	T	196= 134.55
T	198= 129.31	T	200= 88.348	T	204= 84.324	T	210= 96.434	T	220= 100.60	T	230= 94.472
T	240= 76.716	T	242= 66.763	T	250= 63.246	T	260= 75.079	T	261= 75.273	T	262= 69.259
T	265= 49.782	T	264= 49.296	T	265= 46.351	T	266= 62.394	T	300= 58.353	T	304= 30.239
T	280= 2.5289	T	300= 72.574	T	315= 43.993	T	315= 53.813	T	316= 53.813	T	320= 77.800
T	325= 68.953	T	324= 37.457	T	324= 37.457	T	330= 46.946	T	333= 59.073	T	335= 40.866
T	336= 49.866	T	340= 43.143	T	342= 56.750	T	343= 31.413	T	344= 53.939	T	345= 34.250
T	344= 25.202	T	347= 44.434	T	349= 25.344	T	350= 52.563	T	351= 48.380	T	352= 52.122
T	353= 30.089	T	354= 51.795	T	355= 53.313	T	356= 51.050	T	360= 74.344	T	362= 60.049
T	364= 42.043	T	366= 54.186	T	367= 53.346	T	368= 52.528	T	369= 51.814	T	371= 40.708
T	373= 49.966	T	375= 51.748	T	377= 52.854	T	400= 44.583	T	401= 43.218	T	402= 53.857
T	404= 30.429	T	404= -2.6155	T	408= -16.004	T	410= -16.972	T	412= -16.832	T	414= -15.895
T	421= 39.342	T	422= -7.1129	T	423= -11.433	T	424= 30.334	T	425= -9.1542	T	426= -13.854
T	431= 11.425	T	432= 8.1744	T	433= 12.397	T	434= 0.86423	T	435= -13.991	T	436= -14.804
T	441= -0.8477	T	442= -7.6067	T	443= -10.044	T	444= -12.024	T	445= -19.834	T	446= -14.475
T	451= -0.7108	T	452= -6.3098	T	453= -11.320	T	461= -13.322	T	435= -15.795	T	456= -15.299
		ARITHMETIC NODES IN ASCENDING NODE NUMBER ORDER									
T	50=	T	52=	T	54=	T	150=	T	150=	T	160=
T	50= 161.79	T	52= 172.41	T	54= 165.02	T	150= 164.42	T	150= 161.89	T	160= 143.96
T	160= 164.31	T	195= 85.324	T	197= 86.709	T	199= 109.72	T	238= 86.704	T	311= 63.250
T	312= 63.250	T	321= 67.295	T	322= 67.295	T	327= 58.314	T	332= 58.314	T	337= 49.690

T 341=	54.803	F 357=	50.753	T 355=	48.568	F 391=	53.329	T 379=	53.872	F 408=	52.916
F 1000=	48.620	T 1001=	124.28	F 1002=	109.67	T 1003=	96.777	T 1004=	86.747	F 1005=	86.356
T 1006=	74.112	T 1007=	136.09	T 1008=	133.43	T 1009=	130.81	F 1010=	81.790	F 1011=	72.434
F 1012=	72.456	F 1013=	57.328	T 1021=	78.873	T 1022=	78.873	T 1023=	61.312	F 1031=	48.828
F 1032=	68.828	F 1033=	53.215	T 1041=	63.073	F 1042=	63.073	T 1043=	56.745	F 1044=	56.745
T 1346=	20.786	F 1347=	47.730								
GREATER MODES IN ASCENDING MODE NUMBER ORDER											
+-----+											
BOUNDARY MODES IN ASCENDING MODE NUMBER ORDER											
T	1=	-20.000	T	2=	-20.000						

SYSTEMS IMPROVED NUMERICAL DIFFERENTIAL ANALYZER +05 (R)MBA +05)

PAGE 1/2

MODEL = BARRAGES
SUBJECTHAC LONG CASE NO. 5 -- Input Distribution, 100F
Peak COV Sidewall Temperature Time Points

4/30/96

SUBMODEL NAME = MAIN

MEAN PROBLEM TIME

TIMIN = 0.300000

DIFFUSION NODES IN ASCENDING NODE NUMBER ORDER

1	267=	233.32	1	268=	233.07	1	269=	226.43	
1	291=	782.68	1	1264=	249.50	1	1267=	488.35	
							1	1268=	326.43
							1	1269=	259.89

ARITHMETIC NODES IN ASCENDING NODE NUMBER ORDER

MEAN NODES IN ASCENDING NODE NUMBER ORDER

BOUNDARY NODES IN ASCENDING NODE NUMBER ORDER

MEAN COV GAS TEMP= 782.7 F MEAN COV GAS PRESSURE= 37.39 PSIA
 MEAN COV-COV GAS TEMP= 845.2 F MEAN COV-COV GAS PRESSURE= 46.03 PSIA

SUBMODEL NAME = PISA

MAX DIFF DELTA T PER ITER	CALCULATED	264)=-1.831055E-06	VS.	ALLOWED	5.000000E-02
MAX ARITH DELTA T PER ITER	ALLOWED(PISA)	1346)=5.347792E-02	VS.	ALLOWED	0.500000
MAX DIFF DEL T PER TIME STEP	BTMPCO(PISA)	264)=1.831055E-06	VS.	BTMPCO	10.0000
MAX ARITH DEL T PER TIME STEP	ATMPCO(PISA)	1346)=3.854748E-02	VS.	ATMPCO	100.0000
MIN STABILITY CRITERIA	CONMIN(PISA)	4213)=3.002835E-05			
MIN STABILITY CRITERIA	CONMAX(PISA)	424)=1.09834			
NUMBER OF ITERATIONS	LOOPCT	= 1	VS.	ALLOWED	600
PROBLEM TIME	TIMIN	= 0.300000	VS.	TIMEND	0.300000
MEAN PROBLEM TIME	TIMIN	= 0.300000			
AVERAGE TIME STEP USED	BTIMSU	= 1.644447E-02	VS.	BTIMEI	0.

DIFFUSION NODES IN ASCENDING NODE NUMBER ORDER

1	31=	751.24	1	53=	859.75	1	55=	1099.2	1	60=	120.61	1	62=	1144.8	1	180=	1025.1
1	109=	920.38	1	107=	886.45	1	110=	843.84	1	112=	844.08	1	113=	844.34	1	120=	753.32
1	122=	753.16	1	123=	752.61	1	124=	752.12	1	125=	751.67	1	126=	752.38	1	127=	752.10
1	130=	777.59	1	132=	783.34	1	133=	770.09	1	134=	782.97	1	135=	773.64	1	136=	782.93
1	137=	720.50	1	140=	824.31	1	141=	824.72	1	142=	830.40	1	143=	806.15	1	144=	835.00
1	145=	831.58	1	146=	847.77	1	147=	844.54	1	150=	915.54	1	152=	904.36	1	153=	864.13
1	154=	952.92	1	153=	911.49	1	154=	945.01	1	157=	945.24	1	160=	981.60	1	149=	968.76
1	162=	993.43	1	163=	944.32	1	164=	900.2	1	165=	980.11	1	166=	1011.4	1	167=	1007.8
1	170=	958.65	1	172=	962.37	1	173=	932.48	1	175=	926.85	1	177=	937.85	1	180=	877.66
1	190=	950.82	1	191=	1071.8	1	192=	348.92	1	193=	962.51	1	194=	494.17	1	196=	707.73
1	198=	1074.2	1	200=	1007.3	1	204=	1119.8	1	210=	732.95	1	220=	732.91	1	250=	779.58
1	248=	817.12	1	242=	431.79	1	250=	235.13	1	260=	204.96	1	261=	208.51	1	262=	209.96
1	263=	218.92	1	264=	209.04	1	266=	217.66	1	268=	210.81	1	300=	1230.7	1	384=	1239.4
1	305=	1376.9	1	310=	937.22	1	313=	1308.6	1	315=	1282.0	1	316=	1282.8	1	320=	931.09
1	323=	1403.4	1	325=	1277.1	1	326=	1277.1	1	330=	931.38	1	333=	1066.9	1	335=	1260.9
1	336=	1260.9	1	340=	933.00	1	342=	609.86	1	343=	1439.0	1	344=	340.31	1	345=	966.54
1	346=	1265.0	1	347=	844.61	1	349=	1046.9	1	350=	259.90	1	351=	426.74	1	352=	263.83
1	353=	342.52	1	354=	298.15	1	355=	225.13	1	356=	307.43	1	360=	201.07	1	362=	297.62
1	364=	261.31	1	366=	217.61	1	367=	223.10	1	368=	248.31	1	369=	267.79	1	373=	436.06
1	373=	347.83	1	375=	258.52	1	377=	225.35	1	400=	199.97	1	401=	209.20	1	402=	221.81
1	404=	1282.3	1	406=	1373.5	1	408=	1363.2	1	410=	1411.5	1	412=	1411.8	1	414=	1419.3

T 421=	471.58	T 422=	1414.7	T 423=	1417.3	T 424=	264.28	T 425=	1401.7	T 426=	1404.2
T 431=	1362.8	T 432=	1362.4	T 433=	1340.7	T 434=	1347.4	T 435=	1362.1	T 436=	1363.7
T 950=	1064.1	T 952=	1104.8	ARITHMETIC NODES IN ASCENDING NODE NUMBER ORDER							
T 50=	777.34	T 52=	871.08	T 54=	1007.8	T 158=	974.34	T 190=	948.58	T 168=	968.97
T 160=	964.44	T 195=	348.43	T 197=	430.17	T 199=	733.96	T 228=	978.44	T 317=	1124.8
T 312=	1124.8	T 321=	1199.4	T 322=	1199.4	T 331=	1108.5	T 332=	1100.5	T 337=	824.05
T 341=	717.20	T 357=	828.39	T 358=	408.78	T 359=	262.47	T 379=	321.46	T 483=	226.31
T 1080=	485.01	T 1001=	870.86	T 1002=	738.49	T 1003=	459.17	T 1084=	319.78	T 1085=	316.22
T 1086=	217.48	T 1007=	860.68	T 1008=	988.90	T 1089=	1043.2	T 1010=	438.29	T 1011=	959.25
T 1012=	959.38	T 1013=	1231.5	T 1021=	933.13	T 1022=	933.13	T 1023=	1227.0	T 1031=	951.74
T 1032=	951.74	T 1033=	1210.8	T 1041=	934.06	T 1042=	934.06	T 1043=	850.58	T 1044=	850.58
T 1346=	1137.0	T 1347=	648.55	WEATHER NODES IN ASCENDING NODE NUMBER ORDER							
				--NONE--							
				BOUNDARY NODES IN ASCENDING NODE NUMBER ORDER							
T 1=	1475.0	T 2=	1426.7								

SYSTEM IMPROVED NUMERICAL DIFFERENCE ANALYZER *S5 (RTMBA *S5)

PAGE 2/4

MODEL # BUNDES
RNDXK*** HAC LOAD CASE NO. 3 -- Ingress Distribution, 100F ***
Peak OCY Sidwell Temperature Time Point

4/30/96

SUMMERY NAME # PTIM

MAX DIFF DELTA 1 PER ITER	CALCULATED	433)=-1.22078E-04	VS.	ALLOWED	5.00000E-02
MAX ARITH DELTA 1 PER ITER	ARLXCC(P)100	1346)=6.93399E-02	VS.	ARLXCA=	0.500000
MAX DIFF DEL T FOR TIME STEP	OTMPC(P)100	443)=1.52587E-04	VS.	OTMPCA=	10.0000
MAX ARITH DEL T FOR TIME STEP	ATMPC(P)100	1346)=6.93054E-02	VS.	ATMPCA=	100.000
MIN STABILITY CRITERIA	CRMIN(P)100	448)=3.80614E-05			
MIN STABILITY CRITERIA	CRMAX(P)100	434)=3.36878			
NUMBER OF ITERATIONS	LOOPT	= 1	VS.	ALLOPT=	680
PROBLEM TIME	TIMER	= 0.300000	VS.	TIMER=	0.500000
NEAR PROBLEM TIME	TIMER	= 0.500000			
AVERAGE TIME STEP USED	OTIMEJ	= 1.66666E-02	VS.	OTIME=	D.

DIFFUSION NODES IN ASCENDING NODE NUMBER ORDER

1	51=	746.24	1	53=	816.05	1	55=	917.30	1	60=	867.71	1	62=	1082.4	1	100=	1025.3
1	103=	950.59	1	107=	868.22	1	110=	846.66	1	112=	845.22	1	113=	854.02	1	120=	799.08
1	122=	792.25	1	123=	774.42	1	126=	766.52	1	128=	761.99	1	129=	730.33	1	127=	742.12
1	130=	783.84	1	132=	759.48	1	133=	754.23	1	134=	754.23	1	135=	769.92	1	136=	745.74
1	137=	764.22	1	140=	771.71	1	141=	771.45	1	142=	764.23	1	143=	768.48	1	144=	780.77
1	145=	764.71	1	146=	777.06	1	147=	775.60	1	150=	825.04	1	152=	849.60	1	153=	793.37
1	156=	845.44	1	155=	810.83	1	156=	829.57	1	157=	825.81	1	160=	881.11	1	161=	856.44
1	162=	898.47	1	163=	820.83	1	164=	821.48	1	165=	851.25	1	166=	856.22	1	167=	878.87
1	170=	833.85	1	172=	851.49	1	173=	802.71	1	175=	807.78	1	177=	816.43	1	180=	776.64
1	190=	813.63	1	191=	908.44	1	192=	813.95	1	193=	821.20	1	194=	843.44	1	196=	835.82
1	198=	912.05	1	200=	1036.7	1	204=	1119.5	1	210=	729.91	1	220=	722.14	1	220=	713.69
1	240=	697.62	1	242=	396.48	1	250=	327.93	1	260=	283.39	1	261=	205.87	1	262=	204.29
1	263=	208.43	1	264=	205.18	1	265=	211.87	1	266=	286.45	1	300=	1230.4	1	304=	1239.3
1	305=	1376.8	1	310=	935.79	1	313=	1107.7	1	316=	1281.3	1	316=	1281.5	1	320=	925.91
1	323=	1100.2	1	325=	1278.4	1	326=	1278.4	1	330=	898.28	1	333=	1066.8	1	335=	1259.4
1	336=	1250.4	1	340=	881.94	1	342=	589.06	1	343=	1426.9	1	346=	331.37	1	349=	825.86
1	346=	1258.6	1	347=	468.87	1	349=	1041.3	1	350=	252.86	1	351=	418.76	1	352=	253.78
1	353=	336.49	1	354=	289.32	1	355=	217.69	1	356=	292.28	1	360=	280.45	1	362=	199.81
1	366=	199.47	1	366=	211.48	1	367=	213.13	1	368=	220.00	1	369=	229.87	1	371=	428.25
1	373=	341.74	1	373=	252.86	1	377=	216.28	1	400=	199.41	1	481=	208.84	1	408=	211.32
1	406=	934.33	1	406=	1360.8	1	408=	1380.6	1	410=	1406.3	1	412=	1410.4	1	414=	1419.2
1	421=	671.38	1	422=	1414.7	1	423=	1417.5	1	424=	243.78	1	425=	1408.9	1	426=	1408.5
1	431=	1830.8	1	432=	3323.6	1	433=	246.30	1	434=	222.30	1	435=	1386.4	1	436=	1396.6
1	441=	1380.0	1	442=	1370.3	1	443=	1373.2	1	444=	1373.2	1	445=	1391.4	1	446=	1380.0
1	451=	1322.5	1	452=	1361.2	1	453=	1376.4	1	454=	1381.3	1	455=	1405.8	1	456=	1391.0
1	456=	965.57															

ARITHMETIC NODES IN ASCENDING NODE NUMBER ORDER

1	50=	766.14	1	52=	818.68	1	54=	918.41	1	158=	864.61	1	159=	852.86	1	160=	856.74
---	-----	--------	---	-----	--------	---	-----	--------	---	------	--------	---	------	--------	---	------	--------

T 189=	855.75	T 195=	311.66	T 197=	398.28	F 199=	666.98	F 209=	742.74	T 211=	1123.9
T 319=	1123.9	T 321=	1116.2	T 322=	1116.2	T 33=	1078.4	F 332=	1078.4	T 337=	804.26
T 341=	694.51	T 357=	317.69	T 358=	399.34	F 36=	253.89	F 37=	213.59	T 483=	214.44
T 100=	547.13	T 1001=	755.21	T 1002=	458.59	F 1003=	404.48	F 1004=	399.88	T 1005=	205.11
F 1006=	210.54	T 1007=	628.29	T 1008=	840.22	F 1009=	887.68	F 1010=	415.35	F 1011=	957.94
F 1012=	957.96	T 1013=	1230.9	T 1024=	948.12	F 1022=	948.12	F 1023=	1226.3	F 1031=	919.47
F 1032=	919.47	T 1033=	1196.5	T 1041=	904.28	F 1042=	904.28	T 1043=	629.93	F 1044=	629.93
F 1346=	1058.0	F 1347=	381.74								
WEATER NODES IN ASCENDING NODE NUMBER ORDER											
NODE											
BOUNDARY NODES IN ASCENDING NODE NUMBER ORDER											
T 1=	1475.0	F 2=	1424.7								

SYSTEM IMPROVED NUMERICAL DIFFERENCING ANALYZER '85 (SIMBA '85)

PAGE 3/4

MODEL = DRANGES
PUBLOC**** MAC LOAD CASE NO. 5 -- Ungula Distribution, 100T ****
Peak Dev Sidwall Temperature Time Point ****

4/30/94

SUBMODEL NAME = FTSC

MAX DIFF DELTA T PER ITER	CALCULATED	4563= 1.226703E-04	VS.	ALLOWED	5.00000E-02
MAX ARITH DELTA T PER ITER	ARLCCOPTSC	13641= 6.894973E-02	VS.	ARLNCA=	0.500000
MAX DIFF DEL T PER TIME STEP	DTMPCOPTSC	4563= 1.325679E-04	VS.	DTMPCA=	10.0000
MAX ARITH DEL T PER TIME STEP	ATMPCOPTSC	13643= 6.893921E-02	VS.	ATMPCA=	100.000
MIN STABILITY CRITERIA	CRMINOPTSC	4443= 3.005506E-05			
MAX STABILITY CRITERIA	CRMAXOPTSC	4343= 3.34679			
NUMBER OF ITERATIONS	LOOPCT	=	1	VS.	ML00PT= 600
PROBLEM TIME	TIMER	=	0.508800	VS.	TIMEND= 0.500000
NEAR PROBLEM TIME	TIMER	=	0.508800		
AVERAGE TIME STEP USED	DTIME	=	1.066567E-02	VS.	DTIMEI= 0.

DIFFUSION MODES IN ASCENDING MODE NUMBER ORDER

T	91=	759.92	T	53=	734.97	T	35=	724.51	T	48=	667.22	T	62=	1006.7	T	100=	1019.2
T	105=	953.76	T	107=	926.74	T	110=	910.51	T	112=	906.06	T	113=	913.01	T	120=	851.30
T	122=	819.37	T	123=	834.77	T	124=	832.64	T	125=	842.75	T	126=	849.89	T	127=	857.61
T	130=	757.77	T	132=	756.99	T	133=	757.15	T	134=	748.17	T	135=	760.85	T	136=	764.80
T	137=	766.54	T	140=	719.48	T	141=	719.10	T	142=	728.80	T	143=	714.77	T	144=	722.98
T	145=	716.06	T	146=	710.93	T	147=	718.06	T	150=	701.95	T	152=	721.74	T	153=	693.10
T	154=	709.08	T	155=	687.96	T	156=	689.52	T	157=	683.14	T	160=	674.29	T	161=	675.74
T	162=	705.17	T	163=	661.31	T	164=	666.37	T	165=	653.88	T	166=	666.26	T	167=	667.45
T	170=	559.21	T	172=	578.65	T	173=	551.35	T	175=	581.88	T	177=	585.90	T	180=	580.68
T	180=	648.99	T	191=	635.36	T	192=	642.42	T	193=	550.14	T	194=	586.46	T	196=	670.12
T	198=	639.12	T	200=	1675.5	T	204=	1678.9	T	210=	735.15	T	220=	711.62	T	230=	633.83
T	240=	563.54	T	242=	346.85	T	250=	220.17	T	260=	201.14	T	261=	202.09	T	262=	200.27
T	263=	201.56	T	264=	201.90	T	268=	204.53	T	266=	203.87	T	300=	1224.2	T	304=	1228.6
T	305=	1375.3	T	310=	957.66	T	318=	1108.6	T	315=	1281.8	T	316=	1281.8	T	320=	921.64
T	323=	1007.6	T	325=	1274.3	T	326=	1274.3	T	330=	843.87	T	333=	1042.5	T	335=	1241.8
T	336=	1241.8	T	340=	833.74	T	342=	840.38	T	343=	1022.9	T	344=	326.15	T	345=	823.67
T	346=	1235.6	T	347=	668.19	T	349=	1060.1	T	350=	252.87	T	361=	617.92	T	350=	253.25
T	353=	325.98	T	354=	287.95	T	355=	217.64	T	356=	259.13	T	360=	199.73	T	368=	196.95
T	364=	198.79	T	366=	211.12	T	367=	212.88	T	368=	219.75	T	369=	229.55	T	371=	427.33
T	373=	341.23	T	375=	251.48	T	379=	216.18	T	400=	199.28	T	401=	208.72	T	402=	211.22
T	406=	894.18	T	408=	1339.8	T	408=	1380.3	T	410=	1404.3	T	412=	1410.4	T	414=	1419.2
T	421=	471.37	T	422=	1414.7	T	423=	1417.5	T	424=	1405.78	T	425=	1400.9	T	428=	1406.5
T	431=	1258.2	T	432=	1322.7	T	433=	144.88	T	434=	222.18	T	435=	1586.4	T	438=	1396.6
T	441=	1379.9	T	442=	1340.8	T	443=	1373.2	T	444=	1373.2	T	445=	1391.4	T	446=	1380.8
T	451=	1372.1	T	452=	1340.2	T	453=	1376.4	T	454=	1301.2	T	455=	1405.8	T	456=	1391.9
T	50=	764.34	T	52=	739.33	T	54=	759.83	T	150=	680.02	T	150=	670.04	T	168=	676.35
T	169=	678.21	T	195=	245.75	T	197=	261.33	T	199=	405.17	T	238=	462.73	T	313=	1124.8

T 312=	1126.8	T 321=	1113.6	T 322=	1113.6	T 331=	1057.2	T 332=	1057.2	T 337=	787.38	
T 341=	872.92	T 357=	316.45	T 358=	396.37	T 359=	253.22	T 379=	213.28	T 483=	214.54	
T 1000=	250.52	T 1001=	416.09	T 1002=	385.13	T 1003=	276.15	T 1004=	233.53	T 1005=	232.51	
T 1006=	208.18	T 1007=	471.24	T 1008=	453.41	T 1009=	440.87	T 1010=	315.14	T 1011=	999.56	
T 1012=	959.36	T 1013=	1231.2	T 1021=	943.80	T 1022=	943.80	T 1023=	1223.2	T 1031=	695.32	
T 1032=	869.52	T 1033=	1185.9	T 1041=	857.97	T 1042=	857.97	T 1043=	609.70	T 1044=	609.70	
T 1344=	1056.4	T 1347=	281.21									
NEAREST NODES IN ASCENDING NODE NUMBER ORDER												
NODE												
BOUNDARY NODES IN ASCENDING NODE NUMBER ORDER												
T 1=	1475.0	T 2=	1424.7									

SYSTEM IMPROVER NUMERICAL DIFFERENCING ANALYZER *85 (SIMA *85)

PAGE 4/4

MODEL = DMWGD5
PUBXC***** SAC LOAD CASE NO. 5 -- Ungate Distribution, 100%
Peak DCV Sidwell Temperature Time Point *****

4/58/98

SUBMODEL NAME = PTSD

MAX DIFF DELTA T PER ITER	CALCULATED	454)=-1.228709E-04	VS. ALLIRED	5.000000E-02
MAX ARITH DELTA T PER ITER	MAX(DIFF)PTSD	1346)=-6.884766E-02	VS. APLUCA	0.500000
MAX DIFF DEL T PER TIME STEP	BTMPCDPTSD	453)= 1.525879E-04	VS. BTMPCA	10.0000
MAX ARITH DEL T PER TIME STEP	ATMPCDPTSD	1346)=-6.881714E-02	VS. ATMPCA	100.000
MIN STABILITY CRITERIA	CSMINHPTSD	446)= 3.098499E-05		
MAX STABILITY CRITERIA	CSMAXHPTSD	454)= 3.26379		
NUMBER OF ITERATIONS	LOOPCT	= 1	VS. MLDOPF	400
PROBLEM TIME	TIMR	= 0.598000	VS. TIMEIN	0.500000
MEAN PROBLEM TIME	TIMR	= 0.598000		
AVERAGE TIME STEP USED	BTMTRU	= 1.844667E-02	VS. BTMTRU	0.

DIFFERENCING NODES IN ASCENDING NODE NUMBER ORDER

1	51=	791.32	1	53=	715.79	1	55=	685.05	1	60=	844.51	1	82=	991.22	1	100=	1028.2
1	105=	957.26	1	107=	931.35	1	109=	916.12	1	112=	915.09	1	115=	916.25	1	120=	841.68
1	125=	839.31	1	129=	840.56	1	134=	846.43	1	135=	847.88	1	136=	859.62	1	127=	880.49
1	138=	755.23	1	133=	755.10	1	133=	754.02	1	134=	758.27	1	139=	757.35	1	130=	768.01
1	157=	704.67	1	140=	705.33	1	141=	704.75	1	142=	707.61	1	143=	708.18	1	144=	707.56
1	145=	708.86	1	144=	710.90	1	147=	711.60	1	150=	674.77	1	182=	679.58	1	193=	675.96
1	154=	676.28	1	155=	671.68	1	156=	674.38	1	157=	672.84	1	160=	629.33	1	161=	633.75
1	162=	637.34	1	163=	628.61	1	164=	633.97	1	165=	627.16	1	166=	632.33	1	167=	631.17
1	170=	515.88	1	172=	518.32	1	173=	514.18	1	173=	666.34	1	177=	486.50	1	109=	667.66
1	190=	429.34	1	191=	412.20	1	192=	348.00	1	193=	541.54	1	194=	280.14	1	196=	421.32
1	198=	415.68	1	200=	1072.9	1	204=	1079.5	1	210=	734.03	1	220=	707.95	1	230=	641.22
1	240=	560.91	1	242=	367.75	1	250=	219.97	1	260=	200.91	1	281=	201.69	1	262=	280.18
1	283=	281.29	1	264=	281.35	1	265=	286.27	1	266=	203.78	1	300=	1226.8	1	304=	1228.4
1	305=	1275.3	1	310=	936.91	1	313=	1186.2	1	315=	1281.7	1	316=	1281.7	1	320=	919.89
1	323=	1098.7	1	325=	1274.0	1	326=	1274.0	1	330=	865.98	1	333=	1043.7	1	335=	1282.2
1	336=	1242.2	1	340=	833.72	1	342=	569.24	1	343=	1023.9	1	344=	326.19	1	345=	825.89
1	346=	1255.7	1	347=	448.20	1	349=	1040.2	1	350=	252.04	1	351=	417.93	1	352=	253.22
1	353=	335.98	1	354=	287.94	1	355=	217.40	1	356=	292.13	1	360=	199.63	1	362=	198.49
1	364=	198.76	1	366=	211.12	1	367=	212.88	1	368=	219.79	1	369=	229.33	1	371=	427.34
1	373=	341.23	1	375=	252.68	1	377=	216.18	1	400=	199.90	1	401=	280.71	1	402=	211.22
1	404=	934.10	1	406=	1339.9	1	408=	1280.5	1	410=	1406.3	1	412=	1418.4	1	416=	1419.2
1	421=	673.37	1	422=	1414.7	1	423=	1417.5	1	424=	243.78	1	425=	1468.9	1	426=	1406.5
1	431=	1230.2	1	432=	1322.8	1	433=	246.08	1	434=	222.98	1	435=	1386.4	1	436=	1396.6
1	441=	1379.9	1	442=	1369.8	1	443=	1373.2	1	444=	1373.2	1	443=	1391.4	1	446=	1380.0
1	431=	1372.1	1	432=	1360.3	1	453=	1376.4	1	454=	1381.2	1	455=	1465.8	1	456=	1391.0
1	50=	764.29	1	52=	716.34	1	54=	715.34	1	55=	637.41	1	150=	635.52	1	160=	636.04
1	160=	636.78	1	195=	240.62	1	197=	286.95	1	199=	398.08	1	220=	604.33	1	311=	1126.5

ARITHMETIC NODES IN ASCENDING NODE NUMBER ORDER

T 312=	1124.5	T 321=	1112.8	T 322=	1112.8	F 331=	1058.4	T 332=	1058.4	T 337=	787.38
T 341=	672.90	T 357=	316.45	T 358=	398.38	T 359=	253.22	F 379=	213.28	T 485=	214.54
T 1800=	247.94	T 1801=	389.32	T 1802=	374.08	F 1803=	264.91	F 1804=	231.67	T 1805=	230.78
F 1806=	282.80	T 1807=	443.95	T 1808=	430.24	F 1809=	417.71	T 1810=	318.27	T 1811=	959.43
F 1812=	959.03	T 1813=	1251.1	T 1821=	942.31	F 1822=	942.31	T 1823=	1222.7	F 1831=	888.11
F 1832=	888.71	T 1833=	5184.6	T 1841=	858.05	F 1842=	858.05	T 1843=	489.73	F 1844=	489.73
T 1346=	1054.6	T 1347=	381.22								
NEATER NODES IN ASCENDING NODE NUMBER ORDER											
==NONE==											
BOUNDARY NODES IN ASCENDING NODE NUMBER ORDER											
T 1=	1475.8	T 2=	1424.7								

SYSTEMS IMPROVED NUMERICAL DIFFERENCING ANALYZER '85 (RTMA '85)

PAGE 1/4

WORK = MANAGES
PUNCHHAC LOAD CASE NO. 5 -- Inghra Distribution, (DOF
Peak ICV 810mell Temperature Time Point

4/30/96

SUBMODEL NAME = MAIN

```

MEAN PROBLEM TIME          TIMEN          = 0.632697
DIFFUSION NODES IN ASCENDING NODE NUMBER ORDER
T 267= 242.77   T 268= 243.32   T 269= 239.88
ARITHMETIC NODES IN ASCENDING NODE NUMBER ORDER
T 201= 256.93   T 1266= 260.64   T 1267= 429.31   T 1268= 377.23   T 1269= 271.65
WEATER NODES IN ASCENDING NODE NUMBER ORDER
++NODE++
BOUNDARY NODES IN ASCENDING NODE NUMBER ORDER
++NODE++
MEAN ICV GAS TEMP= 456.9 F   MEAN ICV GAS PRESSURE= 38.92 PSIA
MEAN ICV-OCV GAS TEMP= 816.3 F   MEAN ICV-OCV GAS PRESSURE= 45.98 PSIA

```

SUBMODEL NAME = PISA

```

CALCULATOR          ALLOWED
MAX DIFF DELTA T PER ITER   DELTAD(CP)IA   1611= 7.35210E-04   VS. BILCOA= 3.00000E-02
MAX ARITH DELTA T PER ITER  ARITH(CP)IA   1894= 2.97816E-02   VS. ARLXEA= 0.500000
MAX DIFF DEL T PER TIME STEP  DTMP(CP)IA    423= -3.04379      VS. BTRNCA= 10.0000
MAX ARITH DEL T PER TIME STEP  ATMP(CP)IA    1346= -1.59128     VS. ATNPCA= 100.000
MIN STABILITY CRITERIA       STAB(CP)IA    431= 1.06172E-04
MIN STABILITY CRITERIA       STAB(CP)IA    624= 1.98628
NUMBER OF ITERATIONS         LOOPCT          = 5          VS. WLOOPT= 640
PROBLEM TIME                 TIMEN           = 0.633336   VS. TIMDID= 6.00000
MEAN PROBLEM TIME           TIMEN           = 0.632697
AVERAGE TIME STEP USED      DTIMED          = 0.130062E-04   VS. OTIME1= 0.

```

```

DIFFUSION NODES IN ASCENDING NODE NUMBER ORDER
T 51= 779.33   T 53= 868.97   T 55= 1900.6   T 60= 874.32   T 62= 1095.4   T 100= 1022.7
T 105= 966.23  T 107= 934.89  T 110= 901.60  T 112= 902.05  T 113= 981.37  T 120= 628.08
T 122= 827.44  T 123= 825.31  T 126= 828.60  T 128= 827.12  T 129= 838.91  T 127= 838.47
T 130= 844.35  T 132= 848.51  T 133= 836.03  T 136= 850.32  T 138= 841.83  T 136= 852.08
T 137= 850.92  T 140= 860.81  T 141= 861.73  T 142= 885.05  T 143= 865.18  T 144= 898.85
T 145= 878.32  T 146= 962.48  T 147= 879.85  T 150= 950.39  T 152= 887.19  T 153= 821.16
T 154= 965.90  T 155= 947.18  T 158= 978.22  T 157= 978.79  T 168= 1062.5  T 161= 992.88
T 162= 1012.6  T 163= 967.67  T 164= 1020.0  T 165= 1002.3  T 166= 1031.9  T 167= 1029.1
T 170= 960.32  T 172= 983.60  T 173= 955.74  T 175= 968.28  T 177= 959.45  T 180= 902.88
T 198= 976.38  T 191= 1671.4  T 193= 373.94  T 195= 956.06  T 196= 923.20  T 196= 750.69
T 198= 1075.7  T 200= 1088.5  T 204= 1068.4  T 190= 816.62  T 220= 813.00  T 230= 800.82
T 240= 863.72  T 242= 689.24  T 250= 256.91  T 260= 207.38  T 267= 211.48  T 262= 213.42
T 263= 136.14  T 264= 217.85  T 265= 228.34  T 266= 222.31  T 300= 968.54  T 304= 990.03
T 303= 730.47  T 310= 848.64  T 313= 790.45  T 316= 675.32  T 346= 679.32  T 320= 843.02
T 323= 788.25  T 325= 676.26  T 326= 676.26  T 330= 864.75  T 333= 889.13  T 338= 717.89
T 336= 717.80  T 340= 858.95  T 342= 598.82  T 343= 754.51  T 344= 376.85  T 345= 893.74
T 346= 854.43  T 347= 562.51  T 349= 663.71  T 350= 289.71  T 351= 372.59  T 352= 294.18
T 353= 336.85  T 384= 325.33  T 335= 245.85  T 356= 333.71  T 360= 202.90  T 362= 204.83
T 364= 208.73  T 366= 238.50  T 367= 246.89  T 368= 272.72  T 369= 306.14  T 371= 376.48
T 373= 343.32  T 375= 277.88  T 377= 243.24  T 400= 204.21  T 407= 216.13  T 482= 256.01
T 404= 953.51  T 406= 837.66  T 408= 856.18  T 410= 858.86  T 412= 983.83  T 414= 833.53

```


T 421=	499.85	T 422=	885.91	T 423=	876.43	T 424=	294.83	F 425=	1017.4	T 426=	964.25
F 431=	859.04	T 432=	878.37	T 433=	1038.2	F 434=	1036.5	T 435=	975.06	T 436=	858.94
T 950=	1067.0	T 952=	1111.8								
ARITHMETIC MODES IN ASCENDING MODE NUMBER ORDER											
F 30=	799.60	T 52=	871.58	T 54=	991.54	F 75=	998.01	T 180=	992.77	F 189=	992.71
F 189=	990.39	T 195=	363.14	T 197=	430.68	F 199=	732.33	T 236=	1813.9	F 311=	764.37
F 312=	766.37	F 321=	764.41	T 322=	764.41	F 331=	786.69	T 332=	786.69	F 337=	692.78
T 341=	656.27	T 357=	339.14	T 358=	349.73	T 359=	292.84	F 379=	263.46	T 445=	241.82
F 1000=	426.34	T 1001=	895.28	T 1002=	756.07	F 1003=	481.53	T 1004=	360.69	T 1005=	336.57
T 1006=	222.96	T 1007=	879.90	T 1008=	999.03	T 1009=	1049.1	T 1010=	479.96	T 1011=	863.85
F 1012=	863.05	T 1013=	711.72	T 1021=	838.54	F 1022=	838.54	T 1023=	711.64	T 1031=	859.58
F 1032=	859.58	F 1033=	745.97	T 1041=	853.72	T 1042=	853.72	T 1043=	486.22	F 1044=	606.22
F 1346=	838.73	F 1347=	474.59								
HEATER MODES IN ASCENDING MODE NUMBER ORDER											
---NONE---											
BOUNDARY MODES IN ASCENDING MODE NUMBER ORDER											
F 1=	100.00	F 2=	100.00								

T 160=	800.24	T 195=	326.12	T 197=	402.12	T 199=	492.20	T 236=	886.94	T 311=	748.15
T 312=	788.15	T 321=	759.88	T 322=	750.88	T 331=	757.54	T 332=	757.54	T 337=	440.71
T 341=	430.14	T 357=	322.99	T 358=	395.27	T 359=	278.88	T 379=	230.04	T 449=	228.95
T 1000=	364.52	T 1001=	774.25	T 1002=	882.44	T 1003=	423.85	T 1004=	386.45	T 1009=	305.45
T 1006=	213.99	T 1007=	853.59	T 1008=	864.08	T 1009=	902.11	T 1010=	451.74	T 1011=	641.39
T 1012=	841.39	T 1013=	719.43	T 1021=	832.38	T 1022=	832.38	T 1023=	796.24	T 1031=	824.15
T 1032=	824.15	T 1023=	723.39	T 1041=	807.25	T 1042=	801.25	T 1043=	382.54	T 1044=	382.54
T 1346=	747.72	T 1347=	413.87	HEATER MODES IN ASCENDING MODE NUMBER ORDER							
---MODE---											
BOUNDARY MODES IN ASCENDING MODE NUMBER ORDER											
T 1=	100.00	T 2=	100.00								

SYSTEM IMPROVED NUMERICAL DIFFERENCING ANALYZER '85 (SINDA '85)

PAGE 3/4

MODEL # DAMAGED
RABOXBMC LOAD CASE NO. 5 -- Upright Distribution, 100P
Peak ICV Stowell Temperature Time Point

4/30/94

SUBMODEL NAME = P13C

	CALCULATED	ALLOWED
MAX DIFF DELTA T PER ITER	MAXDIFF(P13C) 175= 1.055125E-03	VS. BRMCA= 5.000000E-02
MAX ARITH DELTA T PER ITER	MAXARDC(P13C) 199= 2.673340E-02	VS. ARMCA= 0.300000
MAX DIFF DEL T PER TIME STEP	DIFFDC(P13C) 425= -5.84345	VS. DTMC= 10.0000
MAX ARITH DEL T PER TIME STEP	ARITHDC(P13C) 1033= -1.52632	VS. ATMC= 100.000
MIN STABILITY CRITERIA	MINSTAB(P13C) 455= 1.183402E-06	
MAX STABILITY CRITERIA	MAXSTAB(P13C) 434= 3.68055	
NUMBER OF ITERATIONS	LEDPCT = 5	VS. MAXOPT= 600
PROBLEM TIME	TIMEN = 0.633354	VS. TIME= 6.00000
MEAN PROBLEM TIME	TIMEN = 0.632877	
AVERAGE TIME STEP USED	DTIMEN = 0.130002E-04	VS. DTIME= 0.

		DIFFUSION NODES IN ASCENDING NODE NUMBER ORDER									
T	51= 261.22	T	53= 251.87	T	55= 237.69	T	60= 272.89	T	62= 264.08	T	100= 1066.0
T	105= 971.19	T	107= 954.01	T	110= 938.33	T	112= 938.20	T	113= 939.35	T	120= 873.64
T	122= 865.27	T	125= 875.26	T	126= 873.30	T	128= 879.08	T	129= 885.59	T	127= 886.68
T	130= 819.68	T	132= 818.50	T	133= 817.76	T	136= 821.88	T	135= 821.31	T	134= 827.29
T	137= 827.05	T	140= 798.45	T	141= 798.75	T	142= 795.28	T	143= 787.20	T	144= 793.38
T	145= 787.99	T	146= 791.22	T	147= 798.57	T	150= 767.83	T	152= 782.81	T	153= 768.02
T	154= 774.36	T	155= 758.03	T	158= 761.54	T	157= 757.38	T	160= 754.38	T	161= 758.05
T	162= 759.18	T	163= 723.01	T	164= 748.54	T	166= 719.99	T	168= 725.00	T	167= 719.81
T	170= 626.43	T	172= 642.75	T	175= 619.59	T	175= 568.22	T	177= 591.67	T	180= 562.59
T	190= 520.37	T	191= 501.99	T	192= 250.31	T	193= 635.71	T	194= 315.69	T	195= 543.18
T	198= 905.96	T	200= 1027.0	T	204= 1018.4	T	210= 818.73	T	220= 789.99	T	230= 778.60
T	240= 640.33	T	242= 602.35	T	250= 236.15	T	260= 803.78	T	261= 202.87	T	282= 201.74
T	263= 203.47	T	264= 206.43	T	265= 210.44	T	266= 232.13	T	300= 983.25	T	304= 968.27
T	305= 724.73	T	310= 869.33	T	315= 790.90	T	315= 675.58	T	316= 675.58	T	320= 851.15
T	323= 779.27	T	325= 670.45	T	326= 670.45	T	330= 705.36	T	333= 748.02	T	335= 678.74
T	336= 678.74	T	340= 748.33	T	342= 549.86	T	343= 750.42	T	344= 353.71	T	345= 780.84
T	346= 848.19	T	347= 908.68	T	349= 654.54	T	350= 275.56	T	351= 258.01	T	352= 377.89
T	353= 325.71	T	354= 308.96	T	355= 332.47	T	356= 312.77	T	360= 200.88	T	362= 199.71
T	364= 263.72	T	366= 224.79	T	367= 230.83	T	368= 239.92	T	369= 255.34	T	371= 361.26
T	373= 331.80	T	375= 264.87	T	377= 258.38	T	400= 282.63	T	401= 215.85	T	402= 325.23
T	406= 857.43	T	408= 853.48	T	408= 885.95	T	410= 884.89	T	412= 904.28	T	414= 853.53
T	421= 499.12	T	422= 685.82	T	423= 874.57	T	426= 269.94	T	425= 1077.6	T	428= 952.99
T	431= 806.06	T	432= 5067.1	T	433= 280.28	T	434= 249.31	T	435= 1008.9	T	436= 939.88
T	441= 808.74	T	442= 866.11	T	443= 923.90	T	444= 923.75	T	445= 908.22	T	446= 810.33
T	451= 638.99	T	452= 853.81	T	453= 856.34	T	454= 868.19	T	455= 884.34	T	464= 847.19
ARITHMETIC NODES IN ASCENDING NODE NUMBER ORDER											
T	50= 801.05	T	52= 753.90	T	54= 759.06	T	150= 761.70	T	159= 754.71	T	168= 730.43
T	169= 739.79	T	195= 250.81	T	197= 281.56	T	199= 462.48	T	238= 684.59	T	311= 766.84

T 318=	766.84	T 321=	793.24	T 322=	755.24	T 331=	725.09	T 332=	725.89	T 337=	466.58	
T 341=	682.57	T 357=	321.90	T 358=	333.81	T 389=	276.64	T 379=	229.37	T 443=	226.67	
T 180=	247.67	T 1801=	475.77	T 1802=	436.43	T 1803=	294.45	T 1804=	239.82	T 1805=	238.63	
T 100a=	204.67	T 1007=	539.23	T 1008=	512.33	T 1009=	508.28	T 1010=	283.40	T 1011=	843.75	
T 1012=	843.75	T 1013=	712.06	T 1021=	826.18	T 1022=	826.18	T 1023=	704.74	T 1031=	792.80	
T 1032=	782.80	T 1033=	698.91	T 1041=	716.73	T 1042=	716.73	T 1043=	936.93	T 1044=	556.53	
T 1346=	745.34	T 1347=	412.88	HEATER NODES IN ASCENDING NODE NUMBER ORDER								
				↑=NONE↑↑								
				BOUNDARY NODES IN ASCENDING NODE NUMBER ORDER								
T 1=	100.00	T 2=	160.00									

SYSTEMS IMPROVED NUMERICAL DIFFERENCING ANALYZER '85 (SINDA '85)

PAGE 4/4

MODEL = BARREDS
RUBBER***** SAC LOAD CASE NO. 5 -- Upright Blast-Buffer, 1000
Peak TCV Sidewall Temperature Time Profile *****

4/28/86

SUBMODEL NAME = PT30

	CALCULATED	ALLOWED
MAX DIFF DELTA T PER ITER	DELHCC(PT30) 175=-7.01904E-03	VS. DELHCA= 5.00000E-02
MAX ARITH DELTA T PER ITER	ARLHCC(PT30) 7077=-3.19824E-02	VS. ARLHCA= 8.50000E-02
MAX DIFF DEL T PER TIME STEP	DYHCC(PT30) 423=-3.84343	VS. DYHCA= 10.0000
MAX ARITH DEL T PER TIME STEP	ATYHCC(PT30) 7033=-1.58449	VS. ATYHCA= 100.000
MIN STABILITY CRITERIA	CSMINI(PT30) 435= 1.98186E-04	
MAX STABILITY CRITERIA	CSMAXI(PT30) 434= 3.40005	
NUMBER OF ITERATIONS	LNDCPT = 5	VS. LNDCOPT= 600
PROBLEM TIME	TINER = 0.633334	VS. TIMEPR= 6.00000
NEAR PROBLEM TIME	TINER = 0.632697	
AVERAGE TIME STEP USED	DTIMEU = 0.130048E-04	VS. DTIMEI= 0.

DIFFUSION NODES IN ASCENDING NODE NUMBER ORDER																	
T	51=	805.04	T	53=	731.60	T	55=	491.74	T	60=	872.32	T	62=	947.40	T	100=	1086.4
T	705=	973.81	T	107=	987.04	T	190=	941.95	T	112=	942.09	T	110=	943.48	T	120=	889.38
T	122=	878.18	T	123=	879.18	T	124=	882.18	T	125=	882.78	T	126=	887.74	T	127=	887.78
T	130=	817.16	T	132=	815.82	T	133=	815.86	T	134=	819.60	T	135=	818.99	T	136=	825.38
T	137=	825.36	T	140=	779.99	T	141=	780.25	T	142=	780.45	T	143=	778.61	T	144=	781.73
T	145=	788.69	T	146=	785.36	T	147=	785.04	T	150=	767.39	T	152=	749.79	T	153=	745.88
T	134=	769.34	T	155=	766.02	T	156=	758.43	T	157=	749.88	T	160=	698.66	T	161=	788.76
T	162=	783.85	T	163=	697.18	T	164=	783.76	T	165=	699.75	T	166=	707.12	T	167=	786.39
T	170=	580.80	T	172=	598.44	T	173=	586.95	T	175=	534.04	T	177=	555.43	T	180=	530.60
T	190=	499.50	T	191=	478.87	T	192=	366.75	T	193=	427.93	T	194=	318.41	T	196=	495.18
T	198=	481.98	T	200=	1826.2	T	204=	1818.1	T	210=	817.94	T	220=	785.68	T	230=	726.58
T	240=	837.71	T	242=	480.60	T	250=	235.80	T	250=	281.32	T	261=	202.29	T	262=	281.44
T	263=	288.04	T	264=	286.16	T	285=	218.32	T	286=	211.96	T	300=	952.74	T	304=	968.08
T	305=	726.66	T	310=	848.81	T	313=	790.48	T	315=	675.29	T	316=	673.29	T	320=	829.29
T	323=	777.92	T	325=	669.53	T	326=	669.95	T	330=	788.29	T	338=	749.51	T	335=	679.71
T	336=	679.71	T	340=	768.15	T	342=	569.64	T	343=	756.48	T	344=	953.65	T	345=	788.87
T	346=	840.31	T	367=	588.60	T	369=	656.88	T	370=	375.54	T	351=	358.01	T	352=	277.88
T	353=	325.71	T	354=	389.99	T	361=	232.44	T	356=	312.76	T	360=	209.08	T	362=	169.89
T	364=	208.65	T	366=	226.77	T	367=	230.02	T	368=	230.02	T	369=	231.34	T	371=	361.26
T	373=	331.36	T	379=	266.86	T	377=	238.28	T	400=	202.61	T	401=	215.83	T	402=	225.22
T	406=	857.44	T	406=	853.54	T	408=	802.95	T	490=	886.09	T	412=	984.26	T	416=	853.53
T	421=	489.32	T	422=	885.92	T	423=	878.57	T	424=	269.94	T	425=	1817.6	T	426=	952.99
T	431=	804.11	T	432=	1067.5	T	433=	280.28	T	434=	249.31	T	435=	1882.9	T	436=	939.88
T	441=	808.73	T	442=	896.13	T	443=	923.98	T	444=	923.76	T	445=	989.22	T	446=	810.34
T	449=	830.62	T	482=	813.04	T	435=	856.39	T	454=	860.19	T	455=	886.36	T	456=	847.15

ARITHMETIC NODES IN ASCENDING NODE NUMBER ORDER																	
T	30=	807.43	T	52=	734.47	T	54=	719.18	T	93=	708.21	T	159=	787.09	T	160=	786.85
T	169=	707.19	T	195=	254.12	T	197=	278.91	T	199=	481.89	T	238=	686.88	T	311=	766.43

T 312=	766.43	T 321=	793.87	F 322=	798.87	T 331=	728.96	F 332=	728.56	T 337=	666.46
F 343=	608.38	F 357=	321.08	F 358=	333.51	F 360=	278.64	F 379=	229.36	T 483=	228.64
F 1000=	263.97	F 1801=	448.62	F 1802=	426.89	F 1003=	266.28	T 1604=	237.17	T 988=	228.05
F 1004=	204.84	T 1007=	512.89	T 1008=	498.87	T 9089=	484.42	T 1010=	349.94	F 1011=	843.20
F 1012=	843.28	T 1013=	711.73	F 1021=	824.29	T 1022=	824.29	T 1023=	703.69	F 1031=	784.86
F 1032=	784.86	T 1033=	789.06	F 1041=	716.62	T 9042=	716.62	T 1043=	556.37	F 1044=	556.37
T 1346=	763.39	T 1347=	612.09								
HEATER MODES IN ASCENDING MODE NUMBER ORDER											
--MODE--											
SUMMARY MODES IN ASCENDING MODE NUMBER ORDER											
T	1=	100.00	T	2=	100.00						

EVERETT IMPROVED NUMERICAL DIFFERENCING ANALYZER '88 (SINBA '85)

PAGE 1/4

MODEL = CARRAGE
STDSTLMIX LOAD CASE NO. 9 -- Ungula Distribution, NOF
Steady-state Conditions After The Fire ***

4/30/94 Pan

SUBMODEL NAME = MAIN

PROBLEM TIME		TIMEN		% OFY,NOF		VS. TIMEN0*		% OFY,000	
DIFFUSION NODES IN ASCENDING NODE NUMBER ORDER									
T 267=	342.07	T 268=	342.38	T 269=	333.82				
ARITHMETIC NODES IN ASCENDING NODE NUMBER ORDER									
T 201=	309.92	T 1266=	347.61	T 1267=	412.88	T 1268=	387.18	T 1269=	332.24
HEATED NODES IN ASCENDING NODE NUMBER ORDER									
***NONE**									
BOUNDARY NODES IN ASCENDING NODE NUMBER ORDER									
***NONE**									
NEAR ICV GAS TEMP= 30P.5 F NEAR ICV GAS PRESSURE= 25.50 PSIA									
NEAR ICV-DEV GAS TEMP= 263.6 F NEAR ICV-DEV GAS PRESSURE= 25.50 PSIA									

SUBMODEL NAME = PTSM

MAX DIFF DELTA T PER ITER		CALCULATED		ALLOWED	
MAX ARITH DELTA T PER ITER	ARLHCC(PTSM	375)=	-0.785322	VS. DRLNCA=	5.00000E-02
MAX SYSTEM ENERGY BALANCE	ARLHCC(PTSM	1000)=	-0.409822	VS. ARLMCA=	0.500000
	ERALBC		= -6.56009	VS. ERALBA * HURMIS	= 6.07869
				ERALBA=	1.00000E-05
ENERGY INTO AND OUT OF STS	ERLWIT		= 4076.89	ERLWDE=	1331.31
MAX MODAL ENERGY BALANCE	ERLWCC(PTSM	367)=	-0.778349	VS. ERALMA=	1.00000E-02
NUMBER OF ITERATIONS	LEADPT		= 133	VS. HLDOPB=	1000
PROBLEM TIME	TIMEN		= 999.000	VS. TIMEN0=	999.000

DIFFUSION NODES IN ASCENDING NODE NUMBER ORDER											
T 51=	345.10	T 97=	504.24	T 95=	679.82	T 68=	342.22	T 42=	446.73	T 100=	310.87
T 105=	318.49	T 107=	321.77	T 110=	324.58	T 112=	325.50	T 113=	321.94	T 120=	349.09
T 122=	352.44	T 123=	343.24	T 124=	353.74	T 125=	344.28	T 126=	356.77	T 137=	352.95
T 138=	423.70	T 132=	431.63	T 133=	413.82	T 134=	431.91	T 135=	417.88	T 136=	431.00
T 157=	424.87	T 146=	500.11	T 141=	501.93	T 142=	506.25	T 143=	483.62	T 144=	514.19
T 143=	497.84	T 144=	331.11	T 147=	324.60	T 150=	414.27	T 152=	432.21	T 153=	345.77
T 156=	636.84	T 137=	615.24	T 139=	619.73	T 157=	468.04	T 160=	707.86	T 161=	694.74
T 162=	717.70	T 163=	676.86	T 164=	728.14	T 165=	718.76	T 166=	745.57	T 167=	739.21
T 176=	728.94	T 172=	742.62	T 173=	719.77	T 175=	747.80	T 177=	741.85	T 180=	727.25
T 198=	788.87	T 191=	842.70	T 192=	467.87	T 193=	733.27	T 194=	503.54	T 196=	656.40
T 199=	644.87	T 208=	299.84	T 204=	253.86	T 210=	279.30	T 228=	307.33	T 230=	422.55
T 246=	518.35	T 243=	391.87	T 258=	333.32	T 260=	394.74	T 261=	307.72	T 262=	328.85
T 263=	327.95	T 264=	319.88	T 265=	322.32	T 266=	318.88	T 268=	205.12	T 304=	993.34
T 305=	135.84	T 310=	240.91	T 313=	223.41	T 318=	283.15	T 316=	203.13	T 320=	346.23
T 323=	243.82	T 325=	221.70	T 326=	221.70	T 330=	340.93	T 335=	335.22	T 336=	295.74
T 336=	293.74	T 340=	394.79	T 342=	348.90	T 343=	244.12	T 344=	300.63	T 345=	238.90
T 346=	224.13	T 347=	244.28	T 349=	231.99	T 350=	286.17	T 351=	278.94	T 352=	284.66
T 353=	281.44	T 354=	287.13	T 355=	285.85	T 356=	283.40	T 360=	299.71	T 362=	318.13
T 364=	303.42	T 366=	287.32	T 367=	284.99	T 368=	281.21	T 369=	278.72	T 371=	279.05
T 373=	288.68	T 375=	282.22	T 377=	283.73	T 400=	369.82	T 401=	298.33	T 402=	283.82
T 406=	221.90	T 408=	144.83	T 409=	118.95	T 410=	185.82	T 412=	107.89	T 414=	108.79

F 421=	237.49	F 422=	118.48	F 423=	112.46	F 424=	220.98	F 425=	716.59	F 426=	712.08
F 431=	137.68	F 432=	137.52	F 433=	131.78	F 434=	122.90	F 435=	115.07	F 436=	117.33
T 950=	798.84	T 952=	868.04	ARITHMETIC NODES IN ASCENDING NODE NUMBER ORDER				T 159=	694.59	T 168=	694.19
F 90=	332.25	F 92=	549.29	F 94=	635.15	F 98=	695.90	F 238=	671.54	F 311=	221.95
T 169=	691.62	T 195=	398.30	T 197=	443.38	T 199=	625.41	F 332=	332.23	F 337=	318.32
F 312=	221.95	T 321=	244.12	T 328=	244.12	T 331=	332.23	F 379=	286.70	T 403=	283.76
F 341=	337.76	T 387=	283.88	F 398=	279.43	T 399=	325.42	T 1004=	435.85	F 1003=	431.60
T 1000=	437.55	T 1007=	733.43	T 1008=	634.15	T 1009=	528.78	T 1890=	438.49	T 1811=	240.12
T 1006=	321.37	F 1007=	779.34	F 1008=	797.59	T 1009=	838.90	T 1093=	230.37	F 1021=	265.73
T 1012=	240.12	T 1013=	210.44	T 1021=	265.73	T 1022=	305.73	T 1042=	395.14	T 1043=	340.43
T 1032=	562.69	F 1033=	386.53	F 1041=	391.14	T 1042=	395.14				
T 1346=	271.39	T 1347=	271.39	HEATER NODES IN ASCENDING NODE NUMBER ORDER							
←NODE→											
BOUNDARY NODES IN ASCENDING NODE NUMBER ORDER											
T 1=	100.00	T 2=	100.00								

SYSTEMS IMPROVED NUMERICAL DIFFERENCING ANALYZER '85 (SINCE '83)

PAGE 2/4

MODEL = BARRAGE
SD47L*** WHC LOAD CASE NO. 5 -- Angular Distribution, 100F
Steady-state Conditions After The Firm ***

4/30/86 9am

RUMODEL NAME = PTIB

MAX DIFF DELTA T PER ITER	CALCULATED		ALLOWED
MAX ARITH DELTA T PER ITER	ERLACC(PTIB)	353)= 0.382705	VS. DALDCA= 5.000000E-02
MAX SYSTEM ENERGY BALANCE	ARLACC(PTIB)	1004)= 0.269817	VS. ARLDCA= 0.500000
	ERLACC	= -1.02327	VS. ERALDA = 0.0001E
			ERLACC= 1.000000E-03 = 3.40088
ENERGY INTO AND OUT OF BYE	EPUNIS	= 3600.58	ERLACC= 2234.74
WHC MODAL ENERGY BALANCE	ERLACC(PTIB)	330)= -0.586719	VS. ERALDA= 1.000000E-02
NUMBER OF ITERATIONS	LOOPCT	= 133	VS. ALDOPD= 1000
PROBLEM TIME	TIMER	= 999.000	VS. TIMEID= 999.000

DIFFUSION MILES IN ASCENDING NODE NUMBER ORDER							
T	51=	53=	55=	60=	62=	149=	
T	105=	107=	110=	112=	113=	120=	
T	132=	133=	136=	139=	126=	127=	
T	130=	132=	133=	134=	139=	136=	
T	137=	140=	141=	142=	143=	144=	
T	145=	146=	147=	150=	139=	133=	
T	154=	155=	156=	157=	160=	161=	
T	162=	163=	164=	168=	166=	167=	
T	170=	172=	173=	175=	177=	180=	
T	190=	191=	192=	193=	194=	196=	
T	199=	200=	204=	210=	220=	230=	
T	240=	242=	250=	260=	261=	262=	
T	263=	264=	265=	266=	300=	304=	
T	305=	310=	313=	315=	316=	320=	
T	323=	325=	326=	330=	333=	335=	
T	336=	340=	342=	343=	344=	345=	
T	346=	347=	349=	350=	351=	352=	
T	353=	354=	355=	356=	360=	362=	
T	364=	366=	367=	368=	369=	371=	
T	373=	375=	377=	400=	401=	402=	
T	404=	406=	408=	410=	412=	416=	
T	421=	423=	425=	426=	429=	426=	
T	431=	432=	433=	434=	435=	436=	
T	441=	442=	443=	444=	445=	446=	
T	451=	452=	453=	454=	455=	456=	
T	954=						
ARITHMETIC MILES IN ASCENDING NODE NUMBER ORDER							
T	50=	52=	54=	150=	159=	160=	
T	160=	195=	197=	199=	230=	311=	

T 312=	279.15	T 329=	233.68	T 320=	233.68	T 331=	263.99	T 332=	283.59	T 337=	279.27
T 341=	204.32	T 337=	263.22	T 358=	259.17	T 359=	266.36	T 379=	256.77	T 489=	364.78
T 1000=	399.74	T 1001=	444.44	T 1002=	570.54	T 1003=	468.18	T 1004=	398.25	T 1005=	394.76
T 1006=	302.51	T 1007=	480.82	T 1008=	494.69	T 1009=	717.36	T 1010=	396.48	T 1011=	256.87
T 1012=	256.87	T 1013=	207.94	T 1014=	253.61	T 1020=	253.61	T 1023=	221.09	T 1031=	307.78
T 1032=	307.78	T 1033=	265.66	T 1041=	325.97	T 1042=	325.97	T 1043=	298.47	T 1044=	298.47
T 1346=	212.37	T 1347=	233.12								
HEATER MODES IN ASCENDING MODE NUMBER ORDER											
←-NONE--											
BOUNDARY MODES IN ASCENDING MODE NUMBER ORDER											
T 1=	108.88	T 2=	100.88								

SYSTEM IMPROVED NUMERICAL DIFFERENCING ANALYZER '85 (SINBA '85)

PAGE 3/4

MODEL = DAMAGED
STARTWAC LOW CASE NO. 3 -- Ungula Distribution, 100%
Steady-state Conditions After the Fire

4/30/96 9m

SUMMEL WIRE = P13C

NUM DIFF DELTA T PER ITER	CALCULATED	ALLOWED
NUM ARITH DELTA T PER ITER	ORLXCC/P13C	VS. ORLXCA= 5.00000E-02
NUM SYSTEM ENERGY BALANCE	ARLXCC/P13C	VS. ARLXCA= 0.500000
	ERALBC	VS. ERALBA= 1.00000E-02
		VS. ERALBA= 1.00000E-02
ENERGY INFO AND OUT OF SYS	ERUNIS	VS. ERUNIS= 2530.85
NUM MODAL ENERGY BALANCE	ERALAC/P13C	VS. ERALBA= 1.00000E-02
NUMBER OF ITERATIONS	LOOPCT	VS. ILGOPS= 9000
PROBLEM TIME	TIMCN	VS. TIMECN= 999.800

0.

DIFFUSION NODES IN ASCENDING WIRE NUMBER ORDER											
1	2	3	4	5	6	7	8	9	10		
1	31= 389.97	1	33= 354.34	1	35= 446.47	1	37= 298.44	1	39= 392.66	1	41= 380.39
1	105= 288.59	1	107= 299.34	1	110= 292.02	1	112= 293.82	1	113= 291.11	1	120= 383.28
1	122= 387.91	1	123= 299.84	1	124= 364.36	1	125= 297.77	1	126= 297.13	1	127= 293.81
1	130= 331.17	1	132= 341.45	1	133= 324.87	1	134= 334.95	1	135= 328.67	1	136= 318.91
1	137= 312.28	1	140= 353.02	1	141= 353.19	1	142= 345.81	1	143= 343.49	1	144= 356.38
1	145= 339.71	1	146= 334.97	1	147= 347.48	1	150= 376.62	1	152= 481.80	1	153= 346.62
1	154= 387.18	1	155= 353.43	1	156= 355.21	1	157= 337.35	1	160= 448.50	1	161= 480.07
1	162= 441.83	1	163= 386.51	1	164= 420.41	1	165= 376.96	1	166= 379.14	1	167= 339.72
1	170= 391.95	1	172= 412.27	1	173= 364.34	1	175= 381.47	1	177= 387.12	1	180= 385.01
1	190= 346.35	1	191= 358.54	1	192= 299.48	1	193= 325.01	1	194= 290.76	1	196= 412.47
1	198= 354.23	1	200= 262.30	1	204= 258.92	1	210= 273.34	1	220= 277.23	1	230= 262.16
1	240= 254.81	1	242= 246.43	1	250= 244.12	1	260= 246.89	1	269= 246.94	1	282= 259.99
1	283= 256.98	1	284= 248.84	1	285= 250.64	1	286= 243.17	1	300= 297.08	1	304= 195.54
1	305= 136.35	1	310= 235.56	1	313= 219.12	1	315= 199.64	1	316= 199.66	1	320= 234.86
1	323= 222.93	1	325= 282.94	1	326= 282.94	1	330= 228.97	1	333= 213.07	1	335= 195.16
1	336= 195.16	1	340= 236.73	1	342= 226.37	1	343= 189.67	1	344= 225.99	1	345= 190.65
1	346= 173.59	1	347= 210.67	1	349= 183.92	1	350= 225.49	1	351= 219.56	1	352= 226.70
1	353= 222.13	1	354= 234.81	1	355= 227.62	1	356= 222.85	1	360= 252.61	1	362= 253.61
1	364= 242.80	1	366= 228.43	1	367= 226.96	1	368= 225.88	1	369= 223.67	1	371= 219.40
1	373= 221.69	1	375= 224.44	1	377= 224.11	1	400= 247.74	1	409= 243.75	1	400= 226.40
1	404= 184.53	1	406= 128.65	1	408= 118.98	1	410= 104.34	1	412= 105.89	1	414= 106.11
1	421= 201.33	1	422= 113.77	1	423= 109.26	1	424= 184.77	1	425= 111.72	1	426= 107.82
1	431= 158.12	1	432= 137.85	1	433= 152.27	1	434= 133.51	1	435= 107.18	1	436= 107.10
1	441= 115.87	1	442= 119.75	1	443= 114.52	1	444= 112.38	1	445= 108.04	1	446= 109.77
1	451= 118.60	1	452= 124.34	1	453= 114.33	1	454= 118.97	1	455= 106.07	1	456= 108.85
ARITHMETIC NODES IN ASCENDING WIRE NUMBER ORDER											
1	2	3	4	5	6	7	8	9	10		
1	50= 314.50	1	52= 334.34	1	54= 298.66	1	150= 404.33	1	159= 392.14	1	160= 600.59
1	169= 481.95	1	193= 284.26	1	197= 284.49	1	199= 317.13	1	238= 259.81	1	311= 217.72
1	312= 217.72	1	321= 221.51	1	322= 221.51	1	331= 211.83	1	332= 211.83	1	337= 213.49

T 347=	221.85	T 357=	222.48	T 358=	219.48	T 359=	225.07	T 379=	227.83	T 405=	226.21
T 1000=	221.73	T 1001=	261.81	T 1002=	217.50	T 1003=	206.02	T 1004=	208.25	T 1005=	207.40
T 1006=	263.84	T 1007=	278.06	T 1008=	263.21	T 1009=	259.97	T 1010=	268.79	T 1011=	235.79
T 1012=	235.19	T 1013=	205.69	T 1021=	239.47	T 1022=	239.47	T 1023=	214.12	T 1031=	208.62
T 1032=	229.68	T 1033=	201.59	T 1041=	225.42	T 1042=	225.42	T 1043=	226.86	T 1044=	225.06
T 1346=	182.36	T 1347=	218.20								
HEATER NODES IN ASCENDING NODE NUMBER ORDER +-+NODE+-+											
BOUNDARY NODES IN ASCENDING NODE NUMBER ORDER											
T 1=	100.00	T 2=	100.00								

SYSTEMS IMPROVED NUMERICAL DIFFERENCING ANALYZER '85 (SIMMA '85)

PAGE 4/4

MODEL = DAMAGES
STEP1BAC LOAD CASE NO. 5 -- Ungula Distribution, 100F
*** Steady-state Conditions After The Fire ***

4/30/86 0m

SUBMODEL NAME = FTSD

MAX DIFF DELTA T PER ITER	CALCULATED	62)=-0.125122	VS. ALLOWED
MAX ABSIM DELTA T PER ITER	DELTA(C/PTSD)	64)=-9.34795E-02	VS. DELTA= 5.80000E-02
MAX BYTEN ENERGY BALANCE	DELTA(C/PSD)	= -0.51625	VS. DELTA= 0.500000
	EBALBC		VS. DELTA = EBUM I
			EBALBC = 1.80000E-03
ENERGY INTO AND OUT OF SYS	EBUM I	= 0.	VS. EBUM I = 1608.57
MAX NODAL CURRENT BALANCE	EBALBC(PTSD)	347)=-1.56887	VS. EBALBC = 1.00000E-02
NUMBER OF ITERATIONS	LEPCT	= 133	VS. LEOPR = 5000
PROBLER TIME	TIME	= 999.000	VS. TIMEPR = 999.000

= 0.

		DIFFERENTIAL		NODES IN ASCENDING		NODE NUMBER		ORDER			
T	51= 294.22	T	55= 318.29	T	59= 340.36	T	60= 364.77	T	62= 334.79	T	108= 278.22
T	105= 288.06	T	107= 281.07	T	110= 285.20	T	112= 284.91	T	115= 283.62	T	120= 291.28
T	122= 295.15	T	123= 290.28	T	124= 291.18	T	125= 288.73	T	126= 287.30	T	127= 286.07
T	130= 307.49	T	132= 311.50	T	133= 305.79	T	134= 307.75	T	135= 308.01	T	136= 308.54
T	137= 297.85	T	140= 318.20	T	141= 318.24	T	143= 322.78	T	143= 316.45	T	144= 316.17
T	145= 312.97	T	144= 308.19	T	147= 306.19	T	150= 325.51	T	152= 332.05	T	155= 321.68
T	154= 327.20	T	155= 317.79	T	156= 315.29	T	157= 309.58	T	160= 341.27	T	161= 337.19
T	162= 351.02	T	163= 336.77	T	164= 343.54	T	165= 338.79	T	166= 338.81	T	167= 335.61
T	170= 335.49	T	172= 338.23	T	173= 332.32	T	175= 339.25	T	177= 331.87	T	180= 331.50
T	190= 323.34	T	191= 321.24	T	192= 278.36	T	193= 308.03	T	194= 268.57	T	196= 349.63
T	198= 328.84	T	200= 260.77	T	204= 256.50	T	210= 269.79	T	220= 269.64	T	230= 265.77
T	240= 264.19	T	242= 238.54	T	250= 226.95	T	260= 249.00	T	261= 249.67	T	262= 237.60
T	263= 238.41	T	264= 239.91	T	265= 232.47	T	266= 225.96	T	268= 204.28	T	304= 194.03
T	305= 128.78	T	310= 232.60	T	312= 216.52	T	315= 197.58	T	316= 197.50	T	320= 223.92
T	323= 217.76	T	325= 198.70	T	326= 198.70	T	333= 226.13	T	333= 209.08	T	335= 191.88
T	336= 191.80	T	340= 219.15	T	342= 216.16	T	343= 180.16	T	344= 211.66	T	345= 180.71
T	346= 166.64	T	347= 197.92	T	349= 175.02	T	350= 210.66	T	351= 205.68	T	352= 208.96
T	353= 207.82	T	384= 209.53	T	355= 212.17	T	356= 208.44	T	360= 216.13	T	362= 235.53
T	364= 225.78	T	366= 213.07	T	367= 211.76	T	368= 210.07	T	369= 208.69	T	371= 209.52
T	373= 207.29	T	375= 209.78	T	377= 211.98	T	400= 230.88	T	401= 229.07	T	402= 211.51
T	404= 174.59	T	406= 128.32	T	408= 109.72	T	410= 108.87	T	412= 104.13	T	414= 101.45
T	421= 189.78	T	422= 112.27	T	423= 108.26	T	424= 174.70	T	425= 110.39	T	426= 166.95
T	431= 164.64	T	432= 134.27	T	433= 146.29	T	434= 129.63	T	435= 106.38	T	436= 106.51
T	441= 114.25	T	442= 117.05	T	443= 112.03	T	444= 111.18	T	445= 107.14	T	446= 108.68
T	451= 116.87	T	452= 122.64	T	453= 112.86	T	454= 109.77	T	455= 105.60	T	456= 107.16
			ARITHMETIC		NODES IN		ASCENDING		NODE NUMBER		ORDER
T	50= 296.74	T	52= 318.15	T	54= 334.94	T	58= 338.19	T	150= 334.62	T	160= 337.48
T	169= 337.96	T	195= 263.32	T	197= 262.12	T	199= 292.58	T	230= 255.20	T	311= 215.16
T	312= 215.16	T	321= 216.42	T	322= 216.42	T	331= 207.80	T	332= 207.80	T	337= 209.06

F 321=	210.44	T 337=	208.14	F 338=	205.58	T 339=	218.29	F 379=	212.35	T 403=	211.32
T 1000=	240.25	T 1001=	319.93	T 1002=	291.44	T 1003=	279.69	F 1004=	264.71	T 1005=	264.86
T 1006=	245.79	T 1007=	325.34	T 1008=	323.84	T 1009=	323.04	F 1010=	249.32	T 1011=	232.24
T 1012=	251.24	T 1013=	246.38	T 1021=	233.95	F 1022=	233.95	T 1023=	205.56	T 1031=	223.77
T 1032=	229.77	T 1033=	195.00	T 1041=	216.90	F 1042=	216.90	T 1043=	213.96	T 1044=	213.98
T 1346=	173.51	T 1347=	202.14								
HEATER NODES IN ASCENDING NODE NUMBER ORDER											
--NONE--											
BOUNDARY NODES IN ASCENDING NODE NUMBER ORDER											
T 1=	900.00	T 2=	180.00								

SYSTEMS IMPROVED NUMERICAL DIFFERENCING ANALYZER '85 (VINDA '85)

PAGE 1/4

MODEL = BARRAGE
RDBCKLOAD CASE NO. 4 CONDITIONS - Uprate Distributions, -20F
PEAK OCY SIDEWALL TEMPERATURE TIME POINT

4/30/94

SUBMODEL NAME = MAIN

MEAN PROBLEM TIME

TIMEN = 0.500000

DIFFUSION MODES IN ASCENDING MODE NUMBER ORDER

F 257=	127.15	F 258=	125.94	T 259=	120.10
T 261=	714.43	T 266=	144.05	F 267=	308.34
				F 268=	228.70
				T 269=	185.44

HEATER MODES IN ASCENDING MODE NUMBER ORDER

BOUNDARY MODES IN ASCENDING MODE NUMBER ORDER

+-----+

MEAN ICY GAS TEMP= 74.6 F	MEAN ICY GAS PRESSURE= 35.24 PSIA
MEAN ICY-OCY GAS TEMP= 79.2 F	MEAN ICY-OCY GAS PRESSURE= 44.04 PSIA

SUBMODEL NAME = FTA

MAX DIFF DELTA T PER ITER	CALCULATED	ALLOWED	
MAX ARITH DELTA T PER ITER	DELTAOC(PTBA	2401= 2.441406E-04	VS. DELTA= 5.000000E-02
MAX DIFF DEL T PER TIME STEP	ARLHOC(PTBA	1344= -0.148002	VS. ARLH= 0.200000
MAX ARITH DEL T PER TIME STEP	DTMPC(PTBA	240= 2.746552E-04	VS. OTHPCA= 10.0000
MIN STABILITY CRITERIA	ATMPC(PTBA	1344= -0.108002	VS. ATMPCA= 100.0000
MIN STABILITY CRITERIA	CGMPC(PTBA	4317= 3.840860E-05	
NUMBER OF ITERATIONS	CGMARC(PTBA	424= 1.96090	
PROBLEM TIME	LOOPCT	P = 7	VS. NLOOPT= 600
MEAN PROBLEM TIME	TIMEN	= 0.500000	VS. TIMED= 0.900000
AVERAGE TIME STEP USED	DTIME	= 0.500000	
		= 1.666667E-02	VS. OTIME= 8.

DIFFUSION MODES IN ASCENDING MODE NUMBER ORDER

T 51=	491.41	T 53=	810.51	T 55=	959.38	T 57=	819.13	T 62=	1048.4	T 108=	971.54
T 105=	871.05	T 107=	827.62	T 110=	784.89	T 112=	784.17	T 113=	784.91	T 120=	685.18
F 132=	684.77	F 133=	685.48	T 134=	682.71	T 135=	685.15	T 136=	681.25	T 137=	681.21
T 130=	767.29	T 132=	715.73	T 133=	761.09	T 134=	712.70	T 135=	705.48	T 136=	711.56
T 137=	708.80	F 140=	733.04	T 141=	755.42	T 142=	761.47	T 143=	739.44	T 144=	765.78
F 145=	752.35	T 146=	779.06	T 147=	775.50	T 150=	880.76	T 152=	840.13	T 153=	819.44
F 154=	849.29	T 155=	866.94	T 156=	862.29	T 157=	883.11	T 160=	919.43	T 161=	905.85
T 162=	932.07	F 168=	882.25	T 169=	939.63	T 165=	918.78	T 166=	952.68	T 167=	948.31
T 170=	895.81	T 172=	899.79	T 173=	849.22	T 175=	866.63	T 177=	876.32	T 180=	836.80
T 190=	889.41	F 191=	1017.7	T 192=	253.65	F 193=	902.11	T 194=	412.58	T 195=	418.98
T 198=	1021.1	F 200=	1056.0	T 204=	1079.4	T 210=	663.62	T 220=	658.93	T 230=	694.88
T 248=	757.83	T 242=	329.90	T 250=	127.94	T 260=	99.199	F 281=	183.83	T 282=	182.48
T 263=	113.28	F 284=	101.57	T 285=	110.12	T 266=	102.33	F 300=	1210.9	T 304=	1219.1
T 305=	1372.4	T 310=	901.58	T 313=	1087.8	T 315=	1273.1	F 316=	1273.1	T 320=	892.16
T 323=	1079.7	T 325=	1267.2	T 326=	1267.2	T 330=	883.76	F 333=	1859.3	T 335=	1246.9
T 336=	1266.8	F 340=	862.35	T 342=	838.16	T 343=	1015.8	F 344=	743.17	F 345=	907.05
T 346=	1250.5	T 347=	453.98	F 349=	1020.1	T 250=	153.33	T 351=	331.40	T 352=	156.76
T 353=	262.93	F 354=	196.77	T 355=	116.65	F 356=	203.81	T 360=	95.881	T 362=	94.837
T 364=	93.893	T 366=	106.71	T 367=	113.45	T 368=	136.18	T 369=	153.43	F 371=	362.56
T 373=	249.87	F 375=	155.03	F 377=	118.18	F 400=	99.955	F 401=	186.83	T 402=	113.27
T 404=	1185.7	T 406=	1369.8	T 408=	1757.4	T 410=	1409.8	T 412=	1486.4	T 414=	1438.4

T 421=	395.61	T 422=	1413.7	T 423=	1416.4	T 424=	359.20	T 425=	1397.7	T 426=	1488.9
T 431=	1356.1	T 432=	1356.2	T 433=	1339.3	T 434=	1337.8	T 435=	1377.5	T 436=	1358.0
T 950=	1005.2	T 952=	1853.2								
ALL PARAMETRIC MODES IN ASCENDING NODE NUMBER ORDER											
T 90=	718.31	T 92=	812.70	T 94=	947.55	T 96=	912.87	T 98=	905.88	T 100=	905.96
T 169=	904.47	T 191=	267.91	T 197=	349.07	T 199=	674.21	T 238=	907.01	T 311=	1104.7
T 312=	1104.1	T 321=	1896.7	T 322=	1896.7	T 331=	1070.3	T 332=	1478.3	T 337=	772.85
T 341=	635.77	T 337=	227.91	T 338=	314.53	T 339=	153.44	T 379=	112.47	T 403=	116.57
T 1000=	314.12	T 1001=	813.02	T 1002=	679.08	T 1003=	371.44	T 1004=	222.48	T 1005=	218.84
T 1006=	111.48	T 1007=	901.80	T 1008=	922.61	T 1009=	988.38	T 1010=	346.79	T 1011=	926.87
T 1012=	926.87	T 1013=	1218.7	T 1014=	915.45	T 1022=	915.45	T 1023=	1212.8	T 1031=	984.45
T 1032=	984.45	T 1033=	1191.4	T 1041=	904.28	T 1042=	904.28	T 1043=	581.29	T 1044=	581.29
T 1346=	1368.9	T 1347=	356.97								
HEATER MODES IN ASCENDING NODE NUMBER ORDER											
++4000++											
BOUNDARY MODES IN ASCENDING NODE NUMBER ORDER											
T 1=	1475.8	T 2=	1424.7								

SYSTEMS IMPROVED NUMERICAL DIFFERENCING ANALYZER '85 (SINCL '85)

PAGE 2/4

MODEL = DRUMS
PARMEXLOAD CASE NO. & CONDITIONS - Single Distribution, -20F
PEAK DCN BIREMALL TEMPERATURE TIME POINT

4/30/76

SUMMODEL NAME = PTSP

MAX DIFF DELTA T PER ITER	CALCULATED	2001= 2.441606E-04	VS. DELTA= 5.000000E-02
MAX ARITH DELTA T PER ITER	DELTA(CPTSS	13461= 0.122803	VS. ARITH= 0.500000
MAX DIFF DEL T PER TIME STEP	DTMPC(CPTSS	2001= 2.746842E-04	VS. DTMPC= 10.0000
MAX ARITH DEL T PER TIME STEP	ATMPC(CPTSS	13461= 0.122772	VS. ATMPC= 100.000
MIN STABILITY CRITERIA	CSMIN(CPTSS	4461= 3.012734E-05	
MAX STABILITY CRITERIA	CSMAX(CPTSS	4261= 2.05948	
NUMBER OF ITERATIONS	LOOPCT	= 1	VS. NLOOP= 600
PROBLEM TIME	TIMEN	= 0.500000	VS. TIMEIN= 0.500000
MEAN PROBLEM TIME	TIMEN	= 0.500000	
AVERAGE TIME STEP USED	DTIMEU	= 1.406667E-02	VS. DTIME= 0.

DIFFUSION NODES IN ASCENDING NODE NUMBER ORDER

1	51=	487.30	T	95=	737.82	T	53=	857.71	T	88=	418.33	T	62=	1016.0	T	90=	972.72
T	102=	473.99	T	107=	830.88	T	110=	700.72	T	112=	786.91	T	113=	796.50	T	180=	694.05
T	120=	468.22	T	123=	711.31	T	126=	679.30	T	125=	697.15	T	126=	666.94	T	127=	675.87
T	130=	481.93	T	132=	601.84	T	133=	687.22	T	134=	688.26	T	135=	681.88	T	136=	675.21
T	137=	473.68	T	140=	703.47	T	141=	703.34	T	142=	716.19	T	143=	662.50	T	144=	712.45
T	145=	486.04	T	146=	708.07	T	147=	704.12	T	150=	760.02	T	152=	785.37	T	153=	727.71
T	154=	781.84	T	155=	745.17	T	156=	775.16	T	157=	771.55	T	160=	862.17	T	161=	793.47
T	162=	836.46	T	163=	756.55	T	164=	831.49	T	165=	787.96	T	166=	826.43	T	167=	814.78
T	170=	769.06	T	172=	787.46	T	173=	736.83	T	175=	744.88	T	177=	752.63	T	180=	711.54
T	190=	750.16	T	191=	852.64	T	192=	216.56	T	193=	737.00	T	194=	356.01	T	196=	543.26
T	198=	854.30	T	200=	1035.6	T	204=	1079.4	T	210=	661.23	T	220=	649.23	T	230=	432.32
T	240=	410.28	T	242=	192.41	T	240=	128.92	T	240=	97.629	T	261=	100.36	T	262=	97.538
T	263=	181.66	T	264=	98.095	T	265=	104.21	T	266=	99.312	T	300=	1219.6	T	304=	1219.0
T	306=	1372.5	T	310=	908.56	T	313=	1086.4	T	318=	1273.8	T	316=	1272.6	T	320=	888.15
T	329=	1877.4	T	328=	1266.2	T	326=	1266.2	T	330=	813.03	T	333=	1833.3	T	333=	1238.4
T	336=	1838.6	T	340=	833.79	T	342=	520.02	T	343=	1801.2	T	344=	235.10	T	346=	763.87
T	348=	1245.5	T	347=	380.75	T	349=	1816.1	T	350=	147.90	T	351=	324.28	T	352=	167.71
T	353=	237.62	T	354=	185.86	T	355=	110.02	T	356=	190.11	T	360=	94.471	T	362=	93.176
T	364=	92.431	T	366=	185.83	T	367=	184.38	T	368=	108.60	T	369=	116.71	T	371=	334.65
T	373=	244.44	T	379=	149.78	T	377=	189.25	T	400=	92.117	T	401=	180.14	T	402=	103.15
T	404=	888.85	T	406=	1368.9	T	408=	1379.8	T	410=	1413.8	T	412=	1408.5	T	416=	1618.6
T	421=	309.35	T	422=	1413.7	T	423=	1416.7	T	424=	140.67	T	425=	1397.8	T	426=	1404.7
T	431=	1324.4	T	432=	1350.7	T	433=	264.45	T	434=	213.27	T	435=	1408.6	T	436=	1406.6
T	441=	1379.2	T	442=	1372.6	T	443=	1372.5	T	444=	1372.5	T	445=	1394.6	T	446=	1380.2
T	451=	1874.1	T	452=	1366.2	T	453=	1376.8	T	454=	1381.5	T	455=	1412.4	T	456=	1394.5
T	954=	891.43															

ARITHMETIC NODES IN ASCENDING NODE NUMBER ORDER

T	50=	707.89	T	52=	760.10	T	54=	858.24	T	58=	802.88	T	159=	789.68	T	160=	795.71
T	160=	792.78	T	195=	225.64	T	197=	301.86	T	199=	599.37	T	200=	661.51	T	311=	1105.3

T 312=	1109.5	T 321=	1096.4	T 322=	1096.4	F 331=	1051.0	F 332=	1051.0	T 337=	798.72
T 341=	835.07	F 357=	217.70	T 358=	307.82	F 359=	148.08	T 379=	185.40	T 408=	187.33
T 1000=	252.76	T 1001=	686.27	T 1008=	588.96	T 1009=	314.06	T 1004=	191.61	T 1005=	185.31
T 1006=	194.81	T 1007=	766.57	T 1008=	779.07	T 1009=	830.11	F 1010=	319.83	T 1011=	923.87
T 1012=	923.87	T 1013=	1218.3	T 1021=	911.95	T 1022=	911.95	T 1023=	1211.4	T 1031=	873.54
F 1032=	879.90	F 1033=	1179.4	T 1041=	857.55	F 1042=	857.55	T 1043=	562.62	T 1044=	562.62
F 1346=	1022.9	T 1347=	288.72	HEATER WORES IN ASCENDING NODE NUMBER ORDER							
				--NONE--							
				BOUNDARY WORES IN ASCENDING NODE NUMBER ORDER							
T 1=	1475.0	F 2=	1426.7								

SYSTEM IMPROVED NUMERICAL DIFFERENCING ANALYZER (SINDA '85)

PAGE 3/6

MODEL = DAMAGED
PUBDCLOAD CASE NO. & CONDITIONS = Single Distributions, -2DF
PEAK OCY SIDEWALL TEMPERATURE TIME POINT

4/30/86

RUNMODEL NAME = FTWC

MAX DIFF DELTA T PER ITER	CALCULATED	4083= 2.441406E-04	ALLOWED	5.000000E-02
MAX ARITH DELTA T PER ITER	DELTA(T)PASC	13461= 0.322637	VS. DELTA(T)	0.380000
MAX DIFF DEL T PER TIME STEP	DTMPDCOPTSC	4081= 2.714542E-04	VS. DTMPDC	10.0000
MAX ARITH DEL T PER TIME STEP	ATMPDCOPTSC	13461= 0.322626	VS. ATMPDC	106.000
MIN STABILITY CRITERIA	CGMIN(P)PASC	4461= 3.013940E-05		
MAX STABILITY CRITERIA	CSGMAN(P)PASC	4241= 2.05948		
NUMBER OF ITERATIONS	LOOPCT	= 1	VS. NLOOPTE	600
PROBLEM TIME	TIMIN	= 0.500000	VS. TIMEMAX	8.500000
MEAN PROBLEM TIME	TIMIN	= 0.500000		
AVERAGE TIME STEP USED	DTIMDU	= 1.444447E-02	VS. DTMPCT	0.

DIFFUSION NODES IN ASCENDING NODE NUMBER ORDER

1	51=	701.59	T	53=	679.27	T	55=	676.27	T	60=	815.91	T	62=	954.99	T	100=	970.28
1	105=	900.95	T	107=	879.25	T	110=	856.59	T	112=	831.73	T	113=	824.15	T	120=	772.28
1	120=	759.48	T	123=	776.36	T	124=	773.77	T	125=	785.11	T	126=	799.93	T	127=	802.10
1	130=	692.85	T	132=	691.82	T	133=	692.63	T	134=	695.13	T	135=	698.45	T	136=	702.61
1	137=	702.22	T	140=	651.83	T	141=	651.38	T	142=	659.34	T	143=	649.21	T	144=	695.15
1	145=	647.96	T	146=	650.18	T	147=	649.18	T	150=	634.62	T	152=	629.22	T	193=	625.27
T	154=	641.70	T	155=	619.00	T	156=	619.70	T	157=	611.75	T	160=	606.88	T	161=	607.72
T	162=	636.39	T	163=	592.09	T	164=	618.77	T	165=	562.70	T	166=	585.69	T	167=	576.92
T	170=	677.88	T	172=	699.10	T	173=	649.68	T	175=	616.68	T	177=	641.18	T	180=	617.15
T	190=	553.78	T	191=	542.93	T	192=	141.44	T	195=	683.82	T	196=	186.64	T	198=	370.89
T	198=	346.40	T	200=	1033.9	T	204=	1042.3	T	210=	666.77	T	220=	648.04	T	250=	548.93
T	240=	671.85	T	242=	244.58	T	210=	113.37	T	260=	95.390	T	261=	96.386	T	262=	93.622
T	263=	95.258	T	264=	94.742	T	265=	97.695	T	266=	95.721	T	300=	1285.4	T	304=	1240.0
T	306=	1371.4	T	310=	962.21	T	313=	1867.3	T	315=	1273.2	T	316=	1273.2	T	320=	884.55
T	325=	1078.4	T	329=	1263.3	T	336=	1265.3	T	390=	820.48	T	333=	1016.0	T	335=	1230.9
T	336=	1230.9	T	340=	789.90	T	342=	382.44	T	343=	996.68	T	344=	238.49	T	345=	782.59
T	346=	1242.8	T	347=	380.36	T	348=	1015.1	T	350=	146.43	T	381=	323.97	T	382=	147.23
T	353=	237.20	T	354=	185.66	T	355=	189.78	T	356=	189.47	T	360=	93.741	T	362=	92.031
T	364=	91.621	T	366=	183.03	T	367=	184.38	T	368=	108.29	T	369=	116.44	T	371=	334.88
T	373=	244.91	T	375=	169.64	T	377=	189.17	T	400=	91.947	T	401=	108.04	T	402=	103.66
T	404=	888.78	T	406=	1365.0	T	408=	1379.7	T	410=	1418.8	T	412=	1688.5	T	414=	1418.6
T	421=	395.35	T	422=	1473.7	T	423=	1436.7	T	424=	140.67	T	425=	1597.8	T	426=	1404.7
T	431=	1225.0	T	432=	1349.8	T	433=	244.42	T	434=	813.27	T	435=	1605.6	T	436=	1604.6
T	441=	1379.2	T	442=	1373.3	T	443=	1372.5	T	444=	1372.5	T	445=	1396.6	T	446=	1380.2
T	451=	1375.7	T	452=	1365.3	T	453=	1376.4	T	454=	1381.5	T	455=	1612.4	T	456=	1396.5

ARITHMETIC NODES IN ASCENDING NODE NUMBER ORDER

T	50=	708.46	T	52=	681.69	T	54=	699.29	T	158=	612.34	T	159=	602.30	T	160=	608.32
T	160=	610.22	T	195=	148.32	T	197=	171.17	T	199=	313.88	T	250=	515.48	T	311=	1104.4

T 319= 1104.4	T 321= 1092.4	T 322= 1092.4	T 331= 1031.9	T 332= 1031.9	T 337= 760.13
T 341= 819.78	T 337= 218.81	T 358= 307.89	T 359= 147.44	T 379= 108.19	T 400= 107.25
T 300= 347.34	T 1007= 380.39	T 1002= 291.38	T 1003= 176.37	T 1004= 131.35	T 1009= 136.47
T 3006= 97.421	T 1007= 342.26	T 1008= 341.83	T 1009= 345.72	T 1010= 210.77	T 1011= 929.46
T 1012= 925.46	T 1013= 1218.8	T 1021= 908.86	T 1022= 908.86	T 1023= 1210.2	T 1031= 845.89
T 1032= 843.89	T 1033= 1148.3	T 1041= 815.28	T 1042= 815.28	T 1043= 344.57	T 1044= 544.37
T 1346= 1021.3	T 1347= 268.26				
WEATER INDEX IN ASCENDING INDEX NUMBER ORDER ↔BONE↔					
T 1= 1475.0	T 2= 1426.7				
BOUNDARY INDEX IN ASCENDING INDEX NUMBER ORDER					

SYSTEMS IMPROVED NUMERICAL DIFFERENCING ANALYZER -05 (SIMD 125)

PAGE 4/4

MODEL = DWAGDS
SUBCODE

LONG CASE NO. & CONDITIONS - UngAu Distributions, -209
PEAK ODV SIDEWALL TEMPERATURE TIME POINT

4/30/96

SUBMODEL NAME = PTSD

	CALCULATED	ALLOWED
MAX DIFF DELTA T PER ITER	ORL=CCPT00 127= 2.44146E-04	VS. MAXDEL= 5.00000E-02
MAX ARITH DELTA T PER ITER	ARL=CCPT00 1346= 0.122316	VS. MAXDEL= 0.300000
MAX DIFF DEL T PER TIME STEP	ORW=CCPT00 127= 2.26458E-04	VS. BTHPC= 10.0000
MAX ARITH DEL T FOR TIME STEP	ARW=CCPT00 1346= 0.122286	VS. BTHPC= 100.000
MIN STABILITY CRITERIA	CRMIN=CCPT00 4469= 3.03522E-05	
MAX STABILITY CRITERIA	CRMAX=CCPT00 424= 2.05948	
NUMBER OF ITERATIONS	LOOPCT = 1	VS. MLDOP= 500
PROBLEM TIME	FINEM = 0.500000	VS. TIMEM= 0.300000
MEAN PROBLEM TIME	FINEM = 0.500000	
AVERAGE TIME STEP USED	BTIMEU = 1.666667E-02	VS. BTIME= 0.

DIFFUSION MODEL IN ASCENDING MODE NUMBER ORDER

† 51= 705.19	† 53= 855.25	† 55= 823.18	† 60= 875.23	† 62= 926.90	† 106= 971.76
† 105= 905.16	† 107= 876.67	† 110= 863.17	† 112= 862.90	† 113= 863.53	† 120= 784.28
† 122= 781.79	† 125= 785.58	† 128= 769.61	† 125= 790.42	† 126= 806.72	† 127= 804.63
† 130= 690.78	† 132= 690.51	† 133= 689.74	† 134= 688.93	† 135= 693.00	† 136= 791.03
† 137= 700.45	† 140= 636.85	† 141= 636.19	† 142= 639.51	† 143= 636.80	† 144= 638.98
† 145= 637.32	† 146= 641.62	† 147= 642.13	† 150= 605.85	† 152= 619.46	† 153= 604.30
† 154= 606.30	† 155= 601.81	† 156= 602.49	† 157= 608.61	† 160= 556.48	† 161= 563.69
† 162= 565.75	† 163= 585.93	† 164= 561.66	† 165= 553.63	† 166= 558.61	† 167= 536.88
† 170= 639.01	† 172= 432.86	† 173= 428.33	† 175= 377.99	† 177= 397.04	† 180= 381.83
† 190= 334.06	† 191= 317.98	† 192= 139.87	† 193= 457.11	† 196= 180.03	† 196= 318.21
† 198= 329.66	† 200= 1033.5	† 204= 1041.9	† 210= 665.73	† 220= 636.63	† 230= 560.66
† 260= 649.91	† 242= 243.57	† 250= 113.18	† 260= 95.151	† 263= 95.045	† 262= 95.767
† 263= 95.801	† 264= 94.682	† 265= 87.652	† 266= 96.664	† 300= 1205.2	† 304= 1209.8
† 302= 1271.3	† 310= 891.76	† 313= 1087.8	† 315= 1273.8	† 316= 1273.8	† 320= 863.26
† 323= 1074.6	† 320= 1265.8	† 324= 1265.8	† 330= 826.19	† 333= 1017.4	† 335= 1231.5
† 336= 1251.3	† 340= 790.28	† 362= 502.54	† 363= 999.57	† 364= 230.58	† 365= 762.63
† 366= 1263.0	† 367= 588.17	† 369= 9015.2	† 350= 944.43	† 351= 323.59	† 352= 147.25
† 353= 237.21	† 354= 105.67	† 355= 100.78	† 356= 189.48	† 360= 93.649	† 362= 91.978
† 364= 91.593	† 366= 103.83	† 367= 104.17	† 368= 108.39	† 369= 116.44	† 371= 334.10
† 373= 244.08	† 375= 149.66	† 377= 109.17	† 400= 91.928	† 401= 100.84	† 402= 103.86
† 406= 888.70	† 406= 1365.1	† 408= 1379.7	† 410= 1413.0	† 412= 1408.3	† 414= 1418.6
† 421= 393.33	† 422= 1413.7	† 423= 1416.7	† 424= 148.67	† 425= 1397.8	† 426= 1404.7
† 431= 1223.9	† 432= 1349.9	† 433= 244.42	† 434= 213.27	† 435= 1405.6	† 436= 1406.6
† 441= 1379.2	† 442= 1378.2	† 443= 1372.5	† 444= 1372.5	† 445= 1391.6	† 446= 1380.2
† 451= 1373.7	† 452= 1385.4	† 453= 1376.3	† 454= 1381.5	† 455= 1412.4	† 456= 1394.5
		ARITHMETIC MODEL IN ASCENDING MODE NUMBER ORDER			
† 50= 786.67	† 52= 657.64	† 54= 652.58	† 150= 365.39	† 159= 563.19	† 160= 563.96
† 160= 564.81	† 195= 142.22	† 197= 157.32	† 199= 302.61	† 230= 521.35	† 311= 1104.3

T 312= 1904.1	T 321= 1001.7	T 322= 1091.7	T 331= 1053.4	T 332= 1093.4	T 337= 748.27
T 341= 495.02	T 357= 298.01	T 358= 307.01	T 359= 347.44	T 379= 105.15	T 403= 907.25
T 9089= 145.77	T 1001= 291.46	T 1002= 279.28	T 1003= 168.80	T 1006= 129.81	T 1008= 128.58
T 9084= 97.046	T 1007= 251.95	T 1008= 234.57	T 1009= 323.32	T 1018= 207.74	T 10114= 925.00
T 1012= 925.00	T 1013= 1218.7	T 1021= 906.82	T 1022= 906.82	T 1023= 1209.8	T 10314= 847.45
T 1032= 847.48	T 1033= 1149.2	T 1041= 815.71	T 1042= 815.71	T 1043= 544.77	T 1044= 544.77
T 1346= 1021.3	T 1347= 208.27				
NEAREST NODES IN ASCENDING NODE NUMBER ORDER					
--HOME--					
BOUNDARY NODES IN ASCENDING NODE NUMBER ORDER					
T 1= 1475.0	T 2= 1424.7				

SYSTEMS IMPROVED NUMERICAL DIFFERENCING ANALYZER '85 (RMDA '85)

PAGE 1/4

MODEL = DMM465
FIDUCYLONG CASE NO. & CONDITIONS - Ungula Distribution, -28F
PEAK ICY TIP/SMALL TEMPERATURE TIME POINT

4/30/96

SUBMODEL NAME = M214

MEAN PROBLEM TIME TIMON = 0.566118
 DIFFUSION NODES IN ASCENDING NODE NUMBER ORDER
 1 267= 139.85 T 266= 138.92 T 269= 131.80
 ARITHMETIC NODES IN ASCENDING NODE NUMBER ORDER
 1 201= 788.29 T 1266= 758.95 T 1267= 743.01 T 1268= 724.94 T 1269= 170.75
 HEATER NODES IN ASCENDING NODE NUMBER ORDER
 NONE
 NEUMANN NODES IN ASCENDING NODE NUMBER ORDER
 NONE
 MEAN ICY BAS TEMP= 788.3 F MEAN ICY BAS PRESSURE= 37.82 PSIA
 MEAN ICY-OCV GAS TEMP= 754.3 F MEAN ICY-OCV GAS PRESSURE= 42.80 PSIA

SUBMODEL NAME = P21A

CALCULATED		ALLOWED	
MAX DIFF DELTA T PER ITER	DELTDIFF(P21A)	1613= 0.17871E-03	VS. DELTDIFF= 3.00000E-02
MAX ARITH DELTA T PER ITER	ARLDDIFF(P21A)	327= 9.08285E-02	VS. ARLDDIFF= 0.200000
MAX DIFF DEL T PER TIME STEP	DTMDDIFF(P21A)	423= 2.28376	VS. BTIMECA= 10.0000
MAX ARITH DEL T PER TIME STEP	ATMDDIFF(P21A)	1344= 1.25779	VS. ATMPCAL= 100.000
MAX STABILITY CRITERIA	CRNINCP21A	433= 1.35724E-04	
MAX STABILITY CRITERIA	CRNAXCP21A	4245= 2.02348	
NUMBER OF ITERATIONS	LOOPCI	= 3	VS. MLOOP1= 400
PROBLEM TIME	TIMON	= 0.566118	VS. TIMONS= 4.00000
MEAN PROBLEM TIME	TIMED	= 0.684118	
AVERAGE TIME STEP SIZES	DTIMEJ	= 0.259248E-04	VS. BTIME1= 0.

DIFFUSION NODES IN ASCENDING NODE NUMBER ORDER																	
T	51=	726.56	T	52=	809.55	T	554=	837.85	T	60=	823.35	T	62=	825.6	T	100=	964.56
T	105=	988.33	T	107=	881.29	T	118=	849.65	T	112=	850.01	T	113=	849.73	T	120=	774.33
T	122=	773.71	T	123=	772.19	T	1264=	776.61	T	125=	773.53	T	126=	776.61	T	127=	778.06
T	130=	788.17	T	132=	791.98	T	133=	788.09	T	134=	793.84	T	135=	785.56	T	136=	796.41
T	137=	794.36	T	140=	823.55	T	141=	824.38	T	142=	827.54	T	143=	808.26	T	144=	833.61
T	145=	821.91	T	146=	845.74	T	147=	842.98	T	150=	899.33	T	152=	908.27	T	153=	864.51
T	154=	906.74	T	155=	890.60	T	156=	923.41	T	157=	923.92	T	160=	946.00	T	161=	936.88
T	162=	956.50	T	163=	911.31	T	164=	944.63	T	165=	946.68	T	166=	978.41	T	167=	975.12
T	170=	923.68	T	172=	927.73	T	173=	898.94	T	175=	894.38	T	177=	946.00	T	180=	867.48
T	190=	923.91	T	191=	1019.9	T	192=	286.68	T	193=	931.32	T	194=	458.82	T	196=	679.04
T	198=	1824.5	T	200=	9082.9	T	206=	1004.9	T	210=	785.00	T	220=	796.71	T	230=	788.00
T	240=	795.93	T	242=	406.66	T	250=	135.88	T	260=	182.08	T	281=	788.79	T	282=	189.13
T	283=	119.85	T	286=	112.37	T	285=	123.46	T	286=	117.68	T	300=	998.20	T	304=	919.35
T	305=	433.71	T	310=	785.25	T	313=	721.97	T	315=	687.01	T	316=	687.81	T	320=	777.46
T	323=	717.30	T	325=	606.89	T	326=	605.09	T	330=	793.63	T	333=	732.22	T	335=	648.41
T	336=	448.41	T	340=	783.63	T	342=	528.73	T	343=	678.63	T	344=	285.32	T	345=	814.85
T	346=	764.80	T	347=	581.65	T	349=	545.37	T	350=	190.84	T	351=	268.29	T	352=	94.88
T	353=	233.61	T	354=	228.83	T	355=	142.38	T	356=	236.58	T	360=	96.683	T	362=	98.742
T	364=	183.22	T	366=	135.16	T	367=	142.23	T	368=	164.04	T	369=	192.76	T	371=	273.36
T	373=	241.42	T	375=	176.25	T	377=	140.09	T	400=	96.037	T	401=	112.49	T	402=	136.87
T	404=	883.18	T	406=	731.85	T	408=	779.26	T	610=	774.19	T	612=	824.69	T	614=	767.42

T 421=	427.58	T 422=	880.48	T 423=	790.35	T 424=	199.01	T 425=	939.95	T 426=	865.44
T 431=	782.44	T 432=	892.32	T 433=	965.89	T 434=	963.72	T 435=	897.04	T 436=	781.34
T 450=	1075.9	T 452=	1862.0								
ARITHMETIC MODES IN ASCENDING MODE NUMBER ORDER											
T 50=	744.14	T 52=	812.28	T 54=	928.72	T 150=	942.14	T 159=	936.83	T 160=	958.80
T 169=	934.31	T 195=	290.54	T 197=	374.44	T 199=	467.33	T 236=	933.21	T 311=	700.36
T 312=	708.36	T 321=	695.95	T 322=	695.95	T 331=	711.58	T 332=	711.58	T 337=	611.81
T 341=	577.19	T 357=	241.53	T 358=	269.71	T 359=	195.13	T 370=	139.61	T 408=	138.33
T 1000=	541.60	T 1001=	832.44	T 1002=	667.77	T 1003=	461.83	T 1004=	249.74	T 1005=	245.63
T 1006=	118.28	T 1007=	927.12	T 1008=	946.79	T 1009=	997.42	T 1010=	368.93	T 1011=	780.87
T 1012=	786.07	T 1013=	644.34	T 1021=	772.53	T 1022=	772.53	T 1023=	642.12	T 1031=	788.82
T 1032=	788.82	T 1033=	640.13	T 1041=	779.31	T 1042=	779.31	T 1043=	536.66	T 1044=	524.46
T 1346=	738.13	T 1347=	547.12								
HEATER MODES IN ASCENDING MODE NUMBER ORDER											
4=NONE=											
BOUNDARY MODES IN ASCENDING MODE NUMBER ORDER											
T 1=	-20.000	T 2=	-20.000								

SYSTEM IMPROVED NUMERICAL DIFFERENCING ANALYZER '85 (CIRDA '85)

PAGE 2/4

MODEL = DANABEA
PURBCKLOAD CASE NO. 5 CONDITIONS = Ungula Distribution, -20F
***** PEAK ICY SIDEWALL TEMPERATURE TIME POINT *****

4/30/94

BIBMODEL NAME = PT80

MAX DIFF DELTA T PER ITER	CALCULATED	161) = 1.025391E-02	ALLOWED	5.000000E-02
MAX ARITH DELTA T PER ITER	DELXDD(PT80)	337) = 9.466734E-02	VS. DELXDA =	0.500000
MAX DIFF DEL T PER TIME STEP	ARLXDD(PT80)	433) = -2.22834	VS. ARLXCA =	10.0000
MAX ARITH DEL T PER TIME STEP	BIMPC(PT80)	1344) = -1.04271	VS. BIMPCA =	100.000
MIN STABILITY CRITERIA	ATMPC(PT80)	435) = 1.58945E-04	VS. ATMPCA =	
MAX STABILITY CRITERIA	CDGNR(PT80)	434) = 2.12530		
NUMBER OF ITERATIONS	CONMAX(PT80)			
PROBLEM TIME	LOOPCT	= 3	VS. NLSOPT =	600
NEAR PROBLEM TIME	TIMER	= 0.466667	VS. TIMENP =	6.00000
AVERAGE TIME STEP LOAD	TIMIN	= 0.466670		
	BIMBV	= 9.259200E-04	VS. DTIMER =	0.

DIFFUSION NODES IN ASCENDING NODE NUMBER ORDER

1	51=	725.83	T	93=	760.50	T	95=	840.84	T	101=	920.89	T	107=	963.36	T	113=	963.58	T	119=	963.58	T	125=	963.58	T	131=	963.58	T	137=	963.58	T	143=	963.58	T	149=	963.58	T	155=	963.58	T	161=	963.58	T	167=	963.58	T	173=	963.58	T	179=	963.58	T	185=	963.58	T	191=	963.58	T	197=	963.58	T	203=	963.58	T	209=	963.58	T	215=	963.58	T	221=	963.58	T	227=	963.58	T	233=	963.58	T	239=	963.58	T	245=	963.58	T	251=	963.58	T	257=	963.58	T	263=	963.58	T	269=	963.58	T	275=	963.58	T	281=	963.58	T	287=	963.58	T	293=	963.58	T	299=	963.58	T	305=	963.58	T	311=	963.58	T	317=	963.58	T	323=	963.58	T	329=	963.58	T	335=	963.58	T	341=	963.58	T	347=	963.58	T	353=	963.58	T	359=	963.58	T	365=	963.58	T	371=	963.58	T	377=	963.58	T	383=	963.58	T	389=	963.58	T	395=	963.58	T	401=	963.58	T	407=	963.58	T	413=	963.58	T	419=	963.58	T	425=	963.58	T	431=	963.58	T	437=	963.58	T	443=	963.58	T	449=	963.58	T	455=	963.58	T	461=	963.58	T	467=	963.58	T	473=	963.58	T	479=	963.58	T	485=	963.58	T	491=	963.58	T	497=	963.58	T	503=	963.58	T	509=	963.58	T	515=	963.58	T	521=	963.58	T	527=	963.58	T	533=	963.58	T	539=	963.58	T	545=	963.58	T	551=	963.58	T	557=	963.58	T	563=	963.58	T	569=	963.58	T	575=	963.58	T	581=	963.58	T	587=	963.58	T	593=	963.58	T	599=	963.58	T	605=	963.58	T	611=	963.58	T	617=	963.58	T	623=	963.58	T	629=	963.58	T	635=	963.58	T	641=	963.58	T	647=	963.58	T	653=	963.58	T	659=	963.58	T	665=	963.58	T	671=	963.58	T	677=	963.58	T	683=	963.58	T	689=	963.58	T	695=	963.58	T	701=	963.58	T	707=	963.58	T	713=	963.58	T	719=	963.58	T	725=	963.58	T	731=	963.58	T	737=	963.58	T	743=	963.58	T	749=	963.58	T	755=	963.58	T	761=	963.58	T	767=	963.58	T	773=	963.58	T	779=	963.58	T	785=	963.58	T	791=	963.58	T	797=	963.58	T	803=	963.58	T	809=	963.58	T	815=	963.58	T	821=	963.58	T	827=	963.58	T	833=	963.58	T	839=	963.58	T	845=	963.58	T	851=	963.58	T	857=	963.58	T	863=	963.58	T	869=	963.58	T	875=	963.58	T	881=	963.58	T	887=	963.58	T	893=	963.58	T	899=	963.58	T	905=	963.58	T	911=	963.58	T	917=	963.58	T	923=	963.58	T	929=	963.58	T	935=	963.58	T	941=	963.58	T	947=	963.58	T	953=	963.58	T	959=	963.58	T	965=	963.58	T	971=	963.58	T	977=	963.58	T	983=	963.58	T	989=	963.58	T	995=	963.58	T	1001=	963.58	T	1007=	963.58	T	1013=	963.58	T	1019=	963.58	T	1025=	963.58	T	1031=	963.58	T	1037=	963.58	T	1043=	963.58	T	1049=	963.58	T	1055=	963.58	T	1061=	963.58	T	1067=	963.58	T	1073=	963.58	T	1079=	963.58	T	1085=	963.58	T	1091=	963.58	T	1097=	963.58	T	1103=	963.58	T	1109=	963.58	T	1115=	963.58	T	1121=	963.58	T	1127=	963.58	T	1133=	963.58	T	1139=	963.58	T	1145=	963.58	T	1151=	963.58	T	1157=	963.58	T	1163=	963.58	T	1169=	963.58	T	1175=	963.58	T	1181=	963.58	T	1187=	963.58	T	1193=	963.58	T	1199=	963.58	T	1205=	963.58	T	1211=	963.58	T	1217=	963.58	T	1223=	963.58	T	1229=	963.58	T	1235=	963.58	T	1241=	963.58	T	1247=	963.58	T	1253=	963.58	T	1259=	963.58	T	1265=	963.58	T	1271=	963.58	T	1277=	963.58	T	1283=	963.58	T	1289=	963.58	T	1295=	963.58	T	1301=	963.58	T	1307=	963.58	T	1313=	963.58	T	1319=	963.58	T	1325=	963.58	T	1331=	963.58	T	1337=	963.58	T	1343=	963.58	T	1349=	963.58	T	1355=	963.58	T	1361=	963.58	T	1367=	963.58	T	1373=	963.58	T	1379=	963.58	T	1385=	963.58	T	1391=	963.58	T	1397=	963.58	T	1403=	963.58	T	1409=	963.58	T	1415=	963.58	T	1421=	963.58	T	1427=	963.58	T	1433=	963.58	T	1439=	963.58	T	1445=	963.58	T	1451=	963.58	T	1457=	963.58	T	1463=	963.58	T	1469=	963.58	T	1475=	963.58	T	1481=	963.58	T	1487=	963.58	T	1493=	963.58	T	1499=	963.58	T	1505=	963.58	T	1511=	963.58	T	1517=	963.58	T	1523=	963.58	T	1529=	963.58	T	1535=	963.58	T	1541=	963.58	T	1547=	963.58	T	1553=	963.58	T	1559=	963.58	T	1565=	963.58	T	1571=	963.58	T	1577=	963.58	T	1583=	963.58	T	1589=	963.58	T	1595=	963.58	T	1601=	963.58	T	1607=	963.58	T	1613=	963.58	T	1619=	963.58	T	1625=	963.58	T	1631=	963.58	T	1637=	963.58	T	1643=	963.58	T	1649=	963.58	T	1655=	963.58	T	1661=	963.58	T	1667=	963.58	T	1673=	963.58	T	1679=	963.58	T	1685=	963.58	T	1691=	963.58	T	1697=	963.58	T	1703=	963.58	T	1709=	963.58	T	1715=	963.58	T	1721=	963.58	T	1727=	963.58	T	1733=	963.58	T	1739=	963.58	T	1745=	963.58	T	1751=	963.58	T	1757=	963.58	T	1763=	963.58	T	1769=	963.58	T	1775=	963.58	T	1781=	963.58	T	1787=	963.58	T	1793=	963.58	T	1799=	963.58	T	1805=	963.58	T	1811=	963.58	T	1817=	963.58	T	1823=	963.58	T	1829=	963.58	T	1835=	963.58	T	1841=	963.58	T	1847=	963.58	T	1853=	963.58	T	1859=	963.58	T	1865=	963.58	T	1871=	963.58	T	1877=	963.58	T	1883=	963.58	T	1889=	963.58	T	1895=	963.58	T	1901=	963.58	T	1907=	963.58	T	1913=	963.58	T	1919=	963.58	T	1925=	963.58	T	1931=	963.58	T	1937=	963.58	T	1943=	963.58	T	1949=	963.58	T	1955=	963.58	T	1961=	963.58	T	1967=	963.58	T	1973=	963.58	T	1979=	963.58	T	1985=	963.58	T	1991=	963.58	T	1997=	963.58	T	2003=	963.58	T	2009=	963.58	T	2015=	963.58	T	2021=	963.58	T	2027=	963.58	T	2033=	963.58	T	2039=	963.58	T	2045=	963.58	T	2051=	963.58	T	2057=	963.58	T	2063=	963.58	T	2069=	963.58	T	2075=	963.58	T	2081=	963.58	T	2087=	963.58	T	2093=	963.58	T	2099=	963.58	T	2105=	963.58	T	2111=	963.58	T	2117=	963.58	T	2123=	963.58	T	2129=	963.58	T	2135=	963.58	T	2141=	963.58	T	2147=	963.58	T	2153=	963.58	T	2159=	963.58	T	2165=	963.58	T	2171=	963.58	T	2177=	963.58	T	2183=	963.58	T	2189=	963.58	T	2195=	963.58	T	2201=	963.58	T	2207=	963.58	T	2213=	963.58	T	2219=	963.58	T	2225=	963.58	T	2231=	963.58	T	2237=	963.58	T	2243=	963.58	T	2249=	963.58	T	2255=	963.58	T	2261=	963.58	T	2267=	963.58	T	2273=	963.58	T	2279=	963.58	T	2285=	963.58	T	2291=	963.58	T	2297=	963.58	T	2303=	963.58	T	2309=	963.58	T	2315=	963.58	T	2321=	963.58	T	2327=	963.58	T	2333=	963.58	T	2339=	963.58	T	2345=	963.58	T	2351=	963.58	T	2357=	963.58	T	2363=	963.58	T	2369=	963.58	T	2375=	963.58	T	2381=	963.58	T	2387=	963.58	T	2393=	963.58	T	2399=	963.58	T	2405=	963.58	T	2411=	963.58	T	2417=	963.58	T	2423=	963.58	T	2429=	963.58	T	2435=	963.58	T	2441=	963.58	T	2447=	963.58	T	2453=	963.58	T	2459=	963.58	T	2465=	963.58	T	2471=	963.58	T	2477=	963.58	T	2483=	963.58	T	2489=	963.58	T	2495=	963.58	T	2501=	963.58	T	2507=	963.58	T	2513=	963.58	T	2519=	963.58	T	2525=	963.58	T	2531=	963.58	T	2537=	963.58	T	2543=	963.58	T	2549=	963.58	T	2555=	963.58	T	2561=	963.58	T	2567=	963.58	T	2573=	963.58	T	2579=	963.58	T	2585=	963.58	T	2591=	963.58	T	2597=	963.58	T	2603=	963.58	T	2609=	963.58	T	2615=	963.58	T	2621=	963.58	T	2627=	963.58	T	2633=	963.58	T	2639=	963.58	T	2645=	963.58	T	2651=	963.58	T	2657=	963.58	T	2663=	963.58	T	2669=	963.58	T	2675=	963.58	T	2681=	963.58	T	2687=	963.58</
---	-----	--------	---	-----	--------	---	-----	--------	---	------	--------	---	------	--------	---	------	--------	---	------	--------	---	------	--------	---	------	--------	---	------	--------	---	------	--------	---	------	--------	---	------	--------	---	------	--------	---	------	--------	---	------	--------	---	------	--------	---	------	--------	---	------	--------	---	------	--------	---	------	--------	---	------	--------	---	------	--------	---	------	--------	---	------	--------	---	------	--------	---	------	--------	---	------	--------	---	------	--------	---	------	--------	---	------	--------	---	------	--------	---	------	--------	---	------	--------	---	------	--------	---	------	--------	---	------	--------	---	------	--------	---	------	--------	---	------	--------	---	------	--------	---	------	--------	---	------	--------	---	------	--------	---	------	--------	---	------	--------	---	------	--------	---	------	--------	---	------	--------	---	------	--------	---	------	--------	---	------	--------	---	------	--------	---	------	--------	---	------	--------	---	------	--------	---	------	--------	---	------	--------	---	------	--------	---	------	--------	---	------	--------	---	------	--------	---	------	--------	---	------	--------	---	------	--------	---	------	--------	---	------	--------	---	------	--------	---	------	--------	---	------	--------	---	------	--------	---	------	--------	---	------	--------	---	------	--------	---	------	--------	---	------	--------	---	------	--------	---	------	--------	---	------	--------	---	------	--------	---	------	--------	---	------	--------	---	------	--------	---	------	--------	---	------	--------	---	------	--------	---	------	--------	---	------	--------	---	------	--------	---	------	--------	---	------	--------	---	------	--------	---	------	--------	---	------	--------	---	------	--------	---	------	--------	---	------	--------	---	------	--------	---	------	--------	---	------	--------	---	------	--------	---	------	--------	---	------	--------	---	------	--------	---	------	--------	---	------	--------	---	------	--------	---	------	--------	---	------	--------	---	------	--------	---	------	--------	---	------	--------	---	------	--------	---	------	--------	---	------	--------	---	------	--------	---	------	--------	---	------	--------	---	------	--------	---	------	--------	---	------	--------	---	------	--------	---	------	--------	---	------	--------	---	------	--------	---	------	--------	---	------	--------	---	------	--------	---	------	--------	---	------	--------	---	------	--------	---	------	--------	---	------	--------	---	------	--------	---	------	--------	---	------	--------	---	------	--------	---	------	--------	---	------	--------	---	------	--------	---	------	--------	---	------	--------	---	------	--------	---	------	--------	---	------	--------	---	------	--------	---	------	--------	---	------	--------	---	------	--------	---	------	--------	---	------	--------	---	------	--------	---	------	--------	---	-------	--------	---	-------	--------	---	-------	--------	---	-------	--------	---	-------	--------	---	-------	--------	---	-------	--------	---	-------	--------	---	-------	--------	---	-------	--------	---	-------	--------	---	-------	--------	---	-------	--------	---	-------	--------	---	-------	--------	---	-------	--------	---	-------	--------	---	-------	--------	---	-------	--------	---	-------	--------	---	-------	--------	---	-------	--------	---	-------	--------	---	-------	--------	---	-------	--------	---	-------	--------	---	-------	--------	---	-------	--------	---	-------	--------	---	-------	--------	---	-------	--------	---	-------	--------	---	-------	--------	---	-------	--------	---	-------	--------	---	-------	--------	---	-------	--------	---	-------	--------	---	-------	--------	---	-------	--------	---	-------	--------	---	-------	--------	---	-------	--------	---	-------	--------	---	-------	--------	---	-------	--------	---	-------	--------	---	-------	--------	---	-------	--------	---	-------	--------	---	-------	--------	---	-------	--------	---	-------	--------	---	-------	--------	---	-------	--------	---	-------	--------	---	-------	--------	---	-------	--------	---	-------	--------	---	-------	--------	---	-------	--------	---	-------	--------	---	-------	--------	---	-------	--------	---	-------	--------	---	-------	--------	---	-------	--------	---	-------	--------	---	-------	--------	---	-------	--------	---	-------	--------	---	-------	--------	---	-------	--------	---	-------	--------	---	-------	--------	---	-------	--------	---	-------	--------	---	-------	--------	---	-------	--------	---	-------	--------	---	-------	--------	---	-------	--------	---	-------	--------	---	-------	--------	---	-------	--------	---	-------	--------	---	-------	--------	---	-------	--------	---	-------	--------	---	-------	--------	---	-------	--------	---	-------	--------	---	-------	--------	---	-------	--------	---	-------	--------	---	-------	--------	---	-------	--------	---	-------	--------	---	-------	--------	---	-------	--------	---	-------	--------	---	-------	--------	---	-------	--------	---	-------	--------	---	-------	--------	---	-------	--------	---	-------	--------	---	-------	--------	---	-------	--------	---	-------	--------	---	-------	--------	---	-------	--------	---	-------	--------	---	-------	--------	---	-------	--------	---	-------	--------	---	-------	--------	---	-------	--------	---	-------	--------	---	-------	--------	---	-------	--------	---	-------	--------	---	-------	--------	---	-------	--------	---	-------	--------	---	-------	--------	---	-------	--------	---	-------	--------	---	-------	--------	---	-------	--------	---	-------	--------	---	-------	--------	---	-------	--------	---	-------	--------	---	-------	--------	---	-------	--------	---	-------	--------	---	-------	--------	---	-------	--------	---	-------	--------	---	-------	--------	---	-------	--------	---	-------	--------	---	-------	--------	---	-------	--------	---	-------	--------	---	-------	--------	---	-------	--------	---	-------	--------	---	-------	--------	---	-------	--------	---	-------	--------	---	-------	--------	---	-------	--------	---	-------	--------	---	-------	--------	---	-------	--------	---	-------	--------	---	-------	--------	---	-------	--------	---	-------	--------	---	-------	--------	---	-------	--------	---	-------	--------	---	-------	--------	---	-------	--------	---	-------	--------	---	-------	--------	---	-------	--------	---	-------	--------	---	-------	--------	---	-------	--------	---	-------	--------	---	-------	--------	---	-------	--------	---	-------	--------	---	-------	--------	---	-------	--------	---	-------	--------	---	-------	--------	---	-------	--------	---	-------	--------	---	-------	--------	---	-------	--------	---	-------	--------	---	-------	--------	---	-------	--------	---	-------	--------	---	-------	--------	---	-------	--------	---	-------	--------	---	-------	--------	---	-------	--------	---	-------	--------	---	-------	--------	---	-------	--------	---	-------	--------	---	-------	--------	---	-------	--------	---	-------	--------	---	-------	--------	---	-------	--------	---	-------	--------	---	-------	--------	---	-------	--------	---	-------	--------	---	-------	--------	---	-------	--------	---	-------	--------	---	-------	--------	---	-------	--------	---	-------	--------	---	-------	--------	---	-------	--------	---	-------	--------	---	-------	--------	---	-------	--------	---	-------	--------	---	-------	--------	---	-------	--------	---	-------	--------	---	-------	--------	---	-------	--------	---	-------	--------	---	-------	--------	---	-------	--------	---	-------	--------	---	-------	--------	---	-------	--------	---	-------	--------	---	-------	--------	---	-------	--------	---	-------	--------	---	-------	--------	---	-------	--------	---	-------	--------	---	-------	--------	---	-------	--------	---	-------	--------	---	-------	--------	---	-------	--------	---	-------	--------	---	-------	--------	---	-------	--------	---	-------	--------	---	-------	--------	---	-------	--------	---	-------	--------	---	-------	--------	---	-------	--------	---	-------	--------	---	-------	--------	---	-------	--------	---	-------	--------	---	-------	--------	---	-------	--------	---	-------	--------	---	-------	--------	---	-------	--------	---	-------	--------	---	-------	--------	---	-------	--------	---	-------	--------	---	-------	--------	---	-------	--------	---	-------	--------	---	-------	--------	---	-------	--------	---	-------	--------	---	-------	--------	---	-------	--------	---	-------	--------	---	-------	--------	---	-------	--------	---	-------	--------	---	-------	--------	---	-------	--------	---	-------	--------	---	-------	--------	---	-------	--------	---	-------	--------	---	-------	----------

T 160= 834.47	T 195= 248.47	F 197= 322.74	T 199= 431.72	F 238= 745.34	T 311= 409.34
F 312= 699.54	T 321= 691.85	T 322= 691.85	F 331= 482.47	F 332= 482.47	T 337= 588.77
T 341= 311.19	T 337= 229.08	T 358= 254.96	T 359= 176.51	T 379= 126.12	T 403= 125.37
T 1000= 375.57	T 1001= 713.74	T 1002= 419.71	T 1003= 339.66	T 1004= 212.92	T 1005= 209.16
T 1006= 109.13	T 1007= 798.89	T 1008= 509.87	T 1009= 549.88	T 1010= 367.67	T 1011= 778.72
T 1012= 778.72	T 1013= 643.56	T 1019= 767.11	T 1022= 767.11	T 1023= 636.97	F 1037= 754.49
T 1032= 754.49	T 1033= 846.36	T 1041= 727.31	T 1042= 727.31	T 1043= 503.15	T 1044= 503.15
T 1346= 487.27	T 1347= 325.86	GREATER MODES IN ASCENDING MODE NUMBER ORDER			
		---BENE---			
		BOUNDARY MODES IN ASCENDING MODE NUMBER ORDER			
T 1= -20.800	T 2= -20.800				

I 312=	701.21	T 321=	687.52	F 322=	687.52	T 331=	649.45	T 332=	649.45	F 337=	566.88
I 341=	524.16	T 357=	223.28	T 398=	293.22	T 399=	177.16	T 379=	125.43	F 409=	125.88
I 900=	169.63	I 1001=	394.55	F 1002=	358.14	I 1003=	199.33	I 1004=	139.35	F 1005=	138.88
I 906=	99.825	I 1007=	664.38	T 1008=	645.93	I 1009=	431.86	T 1010=	261.65	F 1011=	701.26
I 9012=	701.26	I 1015=	644.98	T 1021=	761.32	T 1022=	761.32	I 1023=	635.65	T 1031=	762.82
I 1032=	712.82	I 1033=	620.92	T 1041=	673.39	T 1042=	673.39	I 1043=	477.67	T 1044=	477.67
I 1346=	686.87	T 1347=	324.85	HEATER MODES IN ASCENDING MODE NUMBER ORDER **NONE**							
REDUNDANT MODES IF ASCENDING MODE NUMBER ORDER											
I 14	-20.900	I 2=	-20.900								

SYSTEMS IMPROVED NUMERICAL DIFFERENCING ANALYZER '85 (S)ND4 '89;

PAGE 4/4

MODEL = DAMAGED
RIBBEXLOAD CASE NO. & CONDITIONS = Ungula Distribution, -30F
PEAK ICV SIDEWALL TEMPERATURE TIME POINT

4/30/94

SUBMODEL NAME = PTSD

		CALCULATED		ALLOWED	
MAX DIFF DELTA T PER ITER	DRUNDCPTSD	1613 = 1.354998E-02	VS. DELTMAX = 5.000000E-02		
MAX ARITH DELTA T PER ITER	ARUNDCPTSD	10873 = 0.116882	VS. ARITHMAX = 0.300000		
MAX DIFF DEL T PER TIME STEP	DTMPCPTSD	4251 = -2.22534	VS. DTMPMAX = 10.0000		
MAX ARITH DEL T PER TIME STEP	ATMPCPTSD	10331 = -1.11667	VS. ATHPMAX = 100.000		
MIN STABILITY CRITERIA	CRMIN(CPTSD	4551 = 1.509508E-04			
MAX STABILITY CRITERIA	CRMAX(CPTSD	4243 = 2.12508			
NUMBER OF ITERATIONS	LOOPCT	= 3	VS. MLOOP = 500		
PROBLEM TIME	TDRW	= 0.666467	VS. TIMDND = 4.00000		
MEAN PROBLEM TIME	TMRN	= 0.666118			
AVERAGE TIME STEP USED	DTIME	= 0.259248E-04	VS. DTIME = 0.		

DIFFUSION NODES IN ASCENDING NODE NUMBER ORDER

T 51= 756.15	T 53= 677.34	T 55= 638.09	T 60= 523.18	T 62= 506.25	T 180= 949.77
T 105= 916.36	T 107= 902.99	T 110= 886.15	T 112= 880.17	T 113= 880.55	T 120= 826.45
T 122= 824.49	T 123= 820.63	T 124= 820.22	T 125= 820.92	T 126= 823.47	T 127= 833.98
T 130= 763.02	T 132= 761.65	T 133= 760.92	T 134= 765.48	T 135= 764.91	T 136= 771.76
T 137= 771.53	T 140= 782.78	T 141= 782.09	T 142= 782.22	T 143= 784.36	T 144= 727.69
T 145= 726.42	T 146= 730.09	T 147= 731.23	T 150= 691.75	T 152= 694.26	T 153= 690.13
T 154= 693.47	T 155= 690.22	T 156= 694.48	T 157= 693.79	T 160= 639.18	T 161= 648.25
T 162= 644.74	T 163= 637.58	T 164= 644.89	T 165= 640.53	T 166= 648.53	T 167= 647.83
T 170= 517.22	T 172= 519.17	T 175= 519.34	T 175= 460.25	T 177= 481.54	T 180= 656.06
T 190= 419.16	T 191= 399.13	T 192= 147.42	T 193= 565.21	T 194= 217.92	T 196= 608.74
T 198= 402.74	T 200= 970.70	T 204= 957.24	T 210= 767.07	T 220= 732.67	T 230= 664.90
T 240= 966.46	T 242= 511.17	T 250= 123.67	T 260= 95.424	T 261= 96.759	T 262= 95.379
T 263= 97.079	T 264= 100.58	T 265= 105.04	T 266= 906.04	T 300= 890.29	T 304= 896.89
T 305= 629.37	T 310= 706.08	T 315= 722.47	T 315= 607.26	T 316= 607.26	T 320= 764.32
T 323= 707.91	T 325= 399.69	T 326= 999.69	T 330= 719.41	T 335= 475.02	T 335= 606.81
T 336= 600.81	T 340= 675.32	T 342= 471.06	T 343= 669.06	T 344= 264.23	T 346= 705.21
T 346= 750.48	T 347= 428.38	T 349= 354.32	T 350= 174.31	T 351= 295.31	T 352= 177.43
T 353= 228.77	T 354= 212.16	T 356= 128.58	T 356= 213.33	T 360= 94.166	T 362= 95.347
T 364= 97.837	T 366= 122.97	T 367= 125.79	T 368= 133.12	T 369= 147.67	T 371= 257.63
T 373= 228.63	T 375= 165.64	T 377= 126.99	T 400= 94.137	T 401= 111.13	T 402= 128.98
T 404= 793.99	T 406= 756.20	T 408= 721.88	T 410= 787.09	T 412= 825.46	T 414= 767.44
T 421= 427.14	T 422= 800.79	T 423= 796.67	T 424= 172.80	T 425= 950.83	T 426= 871.51
T 431= 793.80	T 432= 891.14	T 433= 323.23	T 434= 275.68	T 435= 909.34	T 436= 822.02
T 441= 724.46	T 442= 810.89	T 443= 843.08	T 444= 842.76	T 445= 821.93	T 446= 726.24
T 451= 741.20	T 452= 756.41	T 453= 778.95	T 454= 776.40	T 455= 785.79	T 456= 756.34
ARITHMETIC NODES IN ASCENDING NODE NUMBER ORDER					
T 50= 753.53	T 52= 628.06	T 54= 656.92	T 150= 649.77	T 159= 648.55	T 160= 648.28
T 169= 648.65	T 195= 160.87	T 197= 182.33	T 199= 373.99	T 230= 622.39	T 311= 709.86

T 312=	780.86	T 321=	686.27	T 322=	686.27	T 331=	651.66	T 332=	651.66	T 337=	566.17
T 341=	924.21	T 357=	225.20	T 358=	253.25	T 359=	177.15	T 379=	125.42	T 403=	125.07
F 1800=	165.72	T 1801=	344.73	T 1802=	343.95	T 1803=	190.22	T 1804=	136.42	T 1805=	139.22
F 1806=	95.567	T 1807=	434.75	T 1808=	419.86	F 1809=	405.46	T 1810=	257.93	T 1811=	780.28
T 1812=	700.80	F 1813=	644.69	T 1821=	759.78	F 1822=	759.78	F 1823=	634.66	T 1831=	716.05
T 1852=	716.05	F 1833=	422.68	T 1841=	673.82	T 1842=	673.82	T 1843=	477.75	T 1844=	477.75
F 1345=	684.94	T 1347=	326.86								
BEATER ORDER IN ASCENDING NODE NUMBER ORDER											
++HOME++											
SUMMARY ORDER IN ASCENDING HOME NUMBER ORDER											
T 1=	-20.000	F 2=	-20.000								

T 421= 142.87	T 422= 12.658	T 423= 1.4431	T 424= 122.60	T 425= 8.7826	T 426= -1.1861
T 431= 33.137	T 432= 27.524	T 433= 24.827	T 434= 9.5292	T 435= -2.9236	T 436= -0.91998
T 950= 738.82	T 952= 817.84				
ARITHMETIC NODES IN ASCENDING NODE NUMBER ORDER					
T 50= 389.64	T 52= 446.69	T 54= 501.38	T 150= 636.29	T 159= 630.84	T 160= 630.50
T 169= 628.08	T 196= 536.80	T 197= 578.03	T 199= 575.48	T 230= 509.83	T 311= 128.50
T 312= 128.50	T 321= 156.69	T 322= 156.69	T 331= 243.02	T 332= 243.02	T 337= 225.45
T 341= 246.83	T 357= 191.89	T 358= 183.97	T 359= 193.33	T 379= 196.36	T 443= 191.83
T 1800= 368.34	T 1901= 679.23	T 1803= 581.33	T 1005= 656.44	T 1004= 265.81	T 1005= 361.83
T 1006= 256.78	T 1007= 726.34	T 1008= 743.93	T 1009= 777.82	T 1090= 268.30	T 1811= 168.51
T 1012= 148.51	T 1013= 113.83	T 1029= 173.89	T 1022= 173.89	T 1023= 138.71	T 1831= 274.49
T 1032= 274.49	T 1033= 218.58	T 1041= 305.44	T 1042= 305.44	T 1043= 250.49	T 1844= 250.49
T 1344= 125.05	T 1347= 177.96				
HEATER NODES IN ASCENDING NODE NUMBER ORDER					
NONE					
BOUNDARY NODES IN ASCENDING NODE NUMBER ORDER					
T 1= -20.000	T 2= -20.000				

SYSTEMS IMPROVED NUMERICAL DIFFERENCING ANALYZER *R5 (SINGL *R5)

PAGE 2/4

MODEL = BARRAGE
RTSS1)LOAD CASE NO. 6 CONDITIONS = Inplane Distributions, -20F
*** Steady-state Conditions After The Fire ***

5/2/94 1pm

SUBMODEL NAME = PTDF

MAX DIFF DELTA T PER ITER	CALCULATED	351)=+1.798242E-02	VI.	ALICOR	5.000000E-02
MAX ARITH DELTA T PER ITER	DELTA(COPTF)	352)=+2.654829E-02	VI.	ARLXCA	0.580000
MAX SYSTEM ENERGY BALANCE	DELTA(CPTF)	= -11.3250	VI.	EMALM	* ESUM I
	EMALC	= 3409.55		EMALM	= 3.60058
ENERGY INTO AND OUT OF SYS	ESUMIS	= 3679.77	VI.	ESUMO	2221.32
MAX BEAM ENERGY BALANCE	EMALC(PTF)	= 125	VI.	EMALM	1.000000E-02
NUMBER OF ITERATIONS	LOOPCT	= 125	VI.	RELOCP	1000
PROBLEM TIME	TIMER	= 999.000	VI.	TJMCN	999.000

		DIFFUSION NODES IN ASCENDING NODE NUMBER ORDER									
		1	53=	54=	55=	56=	57=	58=	59=	60=	61=
T	51=	170.31	T	53=	384.53	T	55=	323.85	T	58=	253.11
T	100=	234.72	T	107=	236.99	T	110=	129.07	T	112=	241.22
T	122=	263.19	T	125=	349.77	T	124=	262.16	T	125=	250.96
T	130=	316.33	T	132=	331.98	T	133=	304.41	T	134=	328.80
T	137=	389.97	T	140=	377.67	T	141=	378.74	T	142=	392.33
T	143=	367.81	T	146=	409.25	T	147=	385.56	T	150=	484.40
T	156=	496.39	T	153=	452.08	T	156=	511.05	T	157=	502.35
T	162=	578.59	T	163=	499.48	T	166=	502.52	T	165=	537.87
T	170=	587.40	T	172=	602.85	T	173=	396.38	T	175=	601.38
T	180=	635.75	T	191=	675.19	T	192=	355.52	T	193=	575.31
T	186=	676.89	T	200=	177.71	T	206=	170.62	T	210=	191.78
T	240=	336.86	T	242=	297.89	T	250=	287.50	T	260=	204.17
T	263=	212.43	T	266=	285.46	T	265=	286.29	T	266=	198.27
T	305=	21.458	T	310=	146.02	T	313=	127.59	T	315=	105.65
T	323=	142.09	T	325=	117.86	T	326=	117.86	T	330=	217.78
T	336=	160.43	T	340=	236.11	T	342=	206.83	T	343=	123.28
T	366=	301.86	T	347=	152.32	T	349=	112.80	T	350=	173.54
T	353=	160.60	T	354=	172.97	T	353=	175.50	T	356=	178.08
T	364=	193.80	T	366=	175.78	T	367=	173.58	T	368=	178.64
T	373=	167.76	T	375=	170.71	T	377=	172.32	T	400=	192.60
T	404=	114.25	T	406=	23.895	T	408=	-3.9888	T	410=	-12.648
T	421=	129.50	T	422=	10.348	T	423=	0.15268	T	426=	111.86
T	431=	61.572	T	432=	45.027	T	435=	64.812	T	434=	34.497
T	441=	8.2619	T	442=	11.348	T	443=	5.4431	T	444=	0.76790
T	451=	8.7225	T	452=	14.790	T	453=	2.4964	T	454=	-2.5789
T	934=	699.99									
		ARITHMETIC NODES IN ASCENDING NODE NUMBER ORDER									
		1	52=	54=	54=	153=	153=	153=	153=	153=	153=
T	50=	286.10	T	52=	382.58	T	54=	304.37	T	153=	346.00
T	160=	534.43	T	195=	297.46	T	197=	345.87	T	199=	312.90
T			T			T			T	230=	340.44
T			T			T			T	250=	340.44
T			T			T			T	319=	326.06

T 312=	126.06	T 321=	148.62	T 322=	148.42	F 331=	191.51	F 332=	191.51	T 337=	164.38
T 361=	291.47	T 357=	178.88	T 356=	165.43	F 350=	172.72	T 379=	176.56	T 463=	172.41
T 1800=	325.62	T 1881=	587.44	T 1882=	512.90	F 1008=	400.98	T 1886=	326.69	T 1885=	320.48
T 1806=	214.17	T 1887=	627.10	T 1808=	641.66	T 1009=	665.02	T 1810=	322.22	T 1811=	145.78
F 1012=	145.78	T 1813=	113.63	T 1081=	163.09	F 1022=	162.09	T 1033=	126.64	T 1831=	217.26
F 1032=	217.26	F 1883=	172.48	T 1041=	253.38	T 1042=	253.38	T 1043=	286.47	F 1844=	286.47
T 1346=	111.26	F 1347=	159.27								
HEATER NUMBER IS ASCENDING MODE NUMBER ORDER											
NONE											
BOUNDARY MODES IS ASCENDING MODE NUMBER ORDER											
T	1=	-20.000	T	2=	-20.000						

F 341= 121.56	F 337= 124.12	T 358= 120.58	F 359= 127.14	F 379= 128.21	T 483= 128.62
T 1000= 195.28	T 1001= 290.11	F 1002= 238.04	T 1003= 226.88	F 1004= 202.01	T 1005= 201.87
T 1006= 171.18	F 1007= 341.34	F 1008= 298.52	T 1009= 289.09	T 1010= 180.51	T 1011= 144.54
T 1012= 144.54	T 1013= 112.68	T 1021= 148.06	T 1022= 148.06	T 1023= 113.95	F 1031= 151.33
T 1032= 131.35	T 1033= 181.52	T 1041= 128.81	T 1042= 128.81	T 1043= 127.95	T 1044= 127.95
T 1046= 77.355	T 1047= 117.33	HEATER HOSES IN ASCENDING HOSE NUMBER ORDER			
		++NOTE++			
		BULKHEAD HOSES IN ASCENDING HOSE NUMBER ORDER			
F 1= -20.000	T 2= -20.000				

SYSTEMS IMPROVED NUMERICAL DIFFERENCING ANALYZER '85 (SINDA '85)

PAGE 4/4

MODEL = BUNLGE
SDSTLLOAD CASE NO. 6 CONDITIONS = Unipolar Distribution, -20P
*** Steady-state Conditions After The Fire ***

5/2/94 Jpn

SUBMODEL NAME = P740

MAX DIFF DELTA T PER ITER	CALCULATED		ALLOWED	
MAX ARITH DELTA T PER ITER	DELTA(COPTED	351)=-1.953125E-02	VS.	DELTA(C= 5.00000E-02
MAX CRSTEN ENERGY BALANCE	ARX(COPTED	197)=-2.361270E-02	VS.	ARX(C= 8.50000E
	EBALSC	= -7.97927	VS.	EBAL(C= 1.00000E-03
				= 0.
ENERGY INTO AND OUT OF SVS	ESUM(S	= 0.	VS.	ESUM(C= 1633.44
MAX NODAL ENERGY BALANCE	EBAL(C(PTED	367)=-1.01213	VS.	EBAL(C= 1.00000E-02
NUMBER OF ITERATIONS	LOOPCT	= 128	VS.	NLOOP(C= 1000
PROBLEM TIME	TIME	= 999.000	VS.	TIME(C= 999.800

DIFFUSION NODES IN ASCENDING NODE NUMBER ORDER

T 51= 221.52	T 53= 269.81	T 55= 274.11	T 60= 213.58	T 62= 265.95	T 100= 204.34
F 105= 267.07	F 107= 298.13	F 110= 299.49	F 112= 210.25	F 113= 209.20	F 120= 216.11
T 122= 220.02	T 123= 217.02	T 124= 217.73	T 125= 215.23	T 126= 215.41	T 127= 211.91
T 130= 237.78	T 132= 261.98	T 133= 235.92	T 134= 237.92	T 135= 232.77	T 136= 229.60
T 137= 226.93	T 140= 258.04	T 141= 258.10	T 142= 254.78	T 143= 248.44	T 144= 249.89
T 145= 264.25	T 146= 238.84	T 147= 236.29	T 150= 238.30	T 152= 265.90	T 153= 253.94
T 134= 259.96	T 155= 269.68	T 156= 246.92	T 137= 239.25	T 160= 275.56	T 161= 271.21
T 162= 285.91	T 163= 278.62	T 164= 278.06	T 165= 264.01	T 166= 261.92	T 167= 256.75
F 170= 263.56	F 172= 288.66	F 173= 262.25	F 175= 258.40	F 177= 268.85	T 180= 259.45
T 190= 249.89	T 191= 265.96	T 192= 186.76	T 193= 230.01	T 194= 183.72	T 196= 280.60
T 198= 245.54	T 200= 179.50	T 204= 173.76	T 210= 187.65	T 220= 186.84	T 230= 178.09
T 240= 153.23	T 242= 136.94	T 250= 131.53	T 260= 155.68	T 261= 156.38	T 282= 162.95
F 263= 143.87	F 264= 135.58	T 265= 137.41	F 266= 130.16	F 300= 118.67	F 304= 94.868
T 305= 21.817	F 310= 142.30	T 313= 124.32	F 315= 102.91	F 316= 102.91	F 320= 163.42
F 323= 128.36	F 325= 103.90	F 326= 103.90	F 330= 131.89	F 333= 112.60	F 335= 93.233
T 336= 93.233	T 340= 123.34	T 342= 116.57	F 343= 75.486	F 344= 113.95	F 345= 77.216
T 346= 59.442	F 347= 97.478	T 349= 66.868	F 350= 112.51	F 351= 106.69	F 352= 111.73
T 353= 109.19	F 354= 111.34	T 383= 114.34	T 356= 109.91	F 360= 132.57	F 362= 160.73
F 364= 129.72	F 366= 115.37	T 367= 113.95	F 368= 112.29	F 369= 118.86	F 371= 106.56
T 373= 106.55	F 375= 111.40	T 377= 113.30	F 400= 135.07	T 401= 132.69	F 482= 113.42
T 404= 72.024	F 406= 8.8451	T 408= -9.3798	F 410= -16.864	T 412= -13.195	T 414= -11.586
F 421= 88.870	F 422= 2.6016	F 423= -5.1375	F 426= 71.638	T 425= -0.95108	T 426= -7.6722
T 431= 33.991	T 432= 25.091	T 433= 38.095	F 434= 17.605	F 435= -9.4630	T 436= -11.908
T 441=-8.75407	F 442= 1.0695	F 443=-2.5211	T 444=-5.9183	T 445=-11.302	T 446=-10.688
T 451=-8.76688	T 452= 3.0514	F 453=-4.9045	T 454=-8.2768	T 455=-12.584	T 456=-11.456

ARITHMETIC NODES IN ASCENDING NODE NUMBER ORDER

T 50= 224.36	T 52= 249.57	F 54= 270.17	T 150= 272.29	F 159= 268.38	F 168= 271.45
T 169= 272.82	T 195= 176.49	F 197= 176.18	T 199= 232.35	F 230= 167.22	F 311= 122.83
T 512= 122.85	F 381= 123.88	F 382= 123.88	T 231= 111.18	F 332= 111.48	F 337= 103.35

T 341= 112.48	T 337= 109.56	T 358= 106.46	T 359= 112.10	F 379= 114.99	T 402= 112.21
F 1000= 172.23	T 1001= 244.56	T 1002= 219.94	F 1003= 186.05	F 1004= 177.48	T 1005= 176.62
F 1006= 152.24	F 1007= 253.36	T 1008= 250.95	F 1009= 247.22	F 1010= 160.06	T 1011= 161.99
F 1012= 141.99	F 1013= 110.78	T 1021= 143.11	T 1022= 143.11	T 1023= 111.68	F 1024= 131.59
T 1025= 131.59	T 1033= 100.34	T 1041= 123.14	T 1042= 123.14	T 1043= 116.45	F 1044= 116.45
T 1346= 60.486	T 1347= 103.38	HEATER NODES IN ASCENDING NODE NUMBER ORDER			
		NONE			
		BOUNDARY NODES IN ASCENDING NODE NUMBER ORDER			
T 1= -20.000	F 2= -20.000				

3.6.6 Miscellaneous Calculations

The following pages present miscellaneous hand calculations that support various parameters used in the package thermal model.

"Ungula" Rubble Pile Thermal Data

Objective: Determine heat transfer parameters for an ungula-shaped pile of GPHS heat source modules (aeroshells).

Basis of**Analysis:**

- 1) Conservatively assume that all 18 aeroshells escape from the RTG shell.
- 2) Worst case package orientation would be a 45° tip angle with aeroshells grouped in a ungula shaped pile.
- 3) Model testing and analytical calculations indicate the pile would be 60% void space and substand at a 135° angle.

Analysis:

Use three 45° model segments to simulate the rubble pile (ungula-shaped pile of aeroshells).

Per analytical calculations, the various dimensions of the rubble pile are as follows:



	Total	Side 45°	Middle 45°	Side 45°
Bottom area (in. ²)	241.2	72.1	97.0	72.1
Side area (in. ²)	277.2	70.5	136.2	70.5
Volume (in. ³)	1048.9	245.9	557.1	245.9

Side Area of Shipping

$$\begin{aligned}
 \text{Rock Assembly Barrier Plate} &= \frac{45^\circ}{360^\circ} \times 2\pi \times 16.0625 \text{ in.} \times 5 \text{ in.} \\
 &= 63.08 \text{ in.}^2 \text{ per } 45^\circ \text{ segment}
 \end{aligned}$$

$$\text{Bottom Area of Barrier Plate} = \frac{45^\circ}{360^\circ} \times \pi \times 16.0625^2$$

$$= 101.318 \text{ in}^2 \text{ per } 45^\circ \text{ segment}$$

Because side area of barrier plate is less than side area of ungula pile, some of the pile will extend above the edge of the barrier plate and lie against the ICV wall.

Because the bottom area of the ungula pile at each 45° segment is less than the bottom area of the barrier plate, the rubble pile will not extend past the centerline of the barrier plate. Therefore, the appropriate distribution of rubble pile area and model nodes is:

	Side 45°	Middle 45°	Side 45°
ICV wall at #238	7.42 in. ²	73.2 in. ²	7.42 in. ²
Barrier plate at #193	83.08	83.08	83.08
Barrier plate at #198	72.1	87.2	72.1
Barrier plate at #193	0	8.6	0

Combine area with that at #198 under the assumption that RTG support legs will keep aeroshells from center.

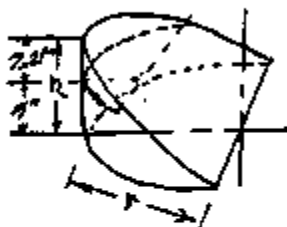
Model rubble pile as homogenous mass with one node representing side segment pile and two at center segment, one for portion of pile above barrier plate vertical wall and one for portion below the barrier plate vertical wall.

This approach is valid because pile will be a porous and open assembly of aeroshells. Therefore, radiation and convection can and will occur from deep within the pile. Using the bulk average temperatures will be appropriate given the conservative assumption that all 18 aeroshells spill out during an accident.

Peak height, h , and average depth, r , of pile is:

$$r = 11.35 \text{ in.}$$

$$h = 12.21 \text{ in.}$$



\therefore peak height above barrier plate is

$$12.21 \text{ in.} - 5 \text{ in.} = 7.21 \text{ in.} = h'$$

Depth of pile above barrier plate is

$$\begin{aligned} r' &= 73.2 \text{ in.}^2 + 2 + 7.21 \text{ in.} \\ &= 5.08 \text{ in.} \end{aligned}$$

Now volume of pile above barrier plate is

$$\begin{aligned} V' &= \frac{2}{3} r'^2 \times h' \\ &= \frac{2}{3} \times (5.08)^2 \times 7.21 \\ &= 124.0 \text{ in.}^3 \end{aligned}$$

Surface Area of pile above barrier plate is

$$\begin{aligned} A' &= \frac{\pi}{2} \times 5.08 \text{ in.} \sqrt{5.08^2 + 7.21^2} \\ &= 70.4 \text{ in.}^2 \end{aligned}$$

Surface area of aeroshells is:

$$\begin{aligned} A_{\text{aeroshell}} &= 18 \times [(3.83 \text{ in.} \times 3.64 \text{ in.} \times 2) + \\ &\quad (3.64 \text{ in.} \times 2.09 \text{ in.} \times 2) + (2.09 \text{ in.} \times 3.83 \text{ in.} \times 2)] \\ &= 1063.93 \text{ in.}^2 \end{aligned}$$

Assume 50% of surface area of each aeroshell is sufficiently exposed to participate in convective heat transfer.

Radiation from the pile will be based on the plane area of the rubble pile. Radiation from rubble pile will be to the RTG shell only, because of assumed blockage by shell and for reasons of conservatism.

Therefore, a summary of thermal properties assumed for each model node is as follows:

	Node #954 side segment	Center segment top #950	Center segment bottom #952
Rubble volume	245.8 in. ³	124.0 in. ³	433.1 in. ³
Thermal mass	3.33 Btu/°F	1.68 Btu/°F	5.56 Btu/°F
Heat dissipation	1054.96 W	531.39 W	1558.09 W
File surface area	75.6 in. ²	70.4 in. ²	75.6 in. ²
Convection area	124.7 in. ²	82.9 in. ²	219.7 in. ²

Further Assumptions

- Existivity of graphite aeroshells approximately 0.5
- Nominal gap between aeroshells and ICV/barrier plate walls is approximately 0.25 in.; assume full area contact
- Nominal gap between aeroshells and barrier plate bottom is assumed to be 0.05 in.; use full area contact

$$\begin{aligned} \text{Gap/Ends from 954 to 100} &= \frac{63.08 \text{ in.}^2/144 \text{ in.}^2}{\left(\frac{1}{0.5} - 1\right) + \frac{1}{1} + \left(\frac{1}{0.48} - 1\right)} \\ &= 0.324 \times \frac{63.08}{144} \text{ in.}^2 \end{aligned}$$

$$\begin{aligned} 954 \text{ to } 228 &= \frac{7.42 \text{ in.}^2/144 \text{ in.}^2}{\left(\frac{1}{0.5} - 1\right) + \frac{1}{1} + \left(\frac{1}{0.9} - 1\right)} \\ &= 0.474 \times \frac{7.42}{144} \text{ in.}^2 \end{aligned}$$

$$\begin{aligned} 954 \text{ to } 190 &= \frac{72.1/144 \text{ in.}^2}{\left(\frac{1}{0.5} - 1\right) + \frac{1}{1} + \left(\frac{1}{0.48} - 1\right)} \\ &= 0.324 \times \frac{72.1}{144} \text{ in.}^2 \end{aligned}$$

$$950 \text{ to } 238 = 0.474 \times \frac{73.2}{2} / 144 \times e$$

$$= \frac{1}{2} \text{ factor for symmetry condition}$$

$$952 \text{ to } 193 = 0.324 \times \frac{83.08}{2} / 144 \times e$$

$$952 \text{ to } 198 = 0.324 \times \frac{97.0}{2} / 144 \times e$$

Conduction

$$954 \text{ to } 193 = \frac{83.08/144}{0.26 \text{ in. gap}} \times K_{ins}$$

$$= 1.7522 \pi K_{ins}$$

$$954 \text{ to } 238 = \frac{7.42/144}{0.26 \text{ in.}} \times K_{ins}$$

$$= 0.2081 \pi K_{ins}$$

$$954 \text{ to } 198 = \frac{72.1/144}{0.05 \text{ in.}} \times K_{ins}$$

$$= 10.0139 \pi K_{ins}$$

$$950 \text{ to } 238 = \frac{73.2/144}{0.26 \text{ in.}} \times K_{ins} \times \frac{1}{2}$$

$$= 1.0167 \pi K_{ins}$$

$$952 \text{ to } 193 = \frac{83.08/144}{0.26 \text{ in.}} \times K_{ins} \times \frac{1}{2}$$

$$= 0.8761 \pi K_{ins}$$

$$962 \text{ to } 198 = \frac{87.0144}{0.25 \text{ in.}} \times K_{\text{iso}} \times \frac{1}{2}$$

$$= 0.7381 \times K_{\text{iso}}$$

Radiation View Factors

Objective: Determine miscellaneous view factors for RTG transport package.

Analysis:

OCV Box Tubes →



Tube diameter = 2.26 in.

Tube Length = 34 in.

$$F_{2-\infty} = 2H(1+H^2)^{-\frac{1}{2}} - H \quad H = \frac{\text{length}}{\text{diameter}}$$

Reference: Table B.2, Item O, Handbook of Applied Thermal Design, Eric C. Guyer

$$H = \frac{34}{2.26}$$

$$= 1.49806$$

$$\therefore F_{2-\infty} = 0.90171$$

$$F_{1-\infty} = 1.0 - F_{2-\infty}$$

$$= 1.0 - 0.90171$$

$$= 0.09829$$

$$F_{\text{tube, } \infty} = A_1 \times F_{1-\infty} / A_{\text{tube}}$$

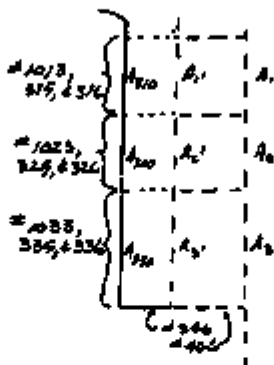
$$= \left(\frac{\pi}{4} \times 2.26^2 \times 0.90171\right) / (\pi \times 2.26 \times 34)$$

$$= 0.15676$$

Impact Limber Tubes → tube diameter = 1.51 in.

$$F_{2-\infty} = 0.96117 \text{ with } H = 2.15232$$

$$F_{\text{tot}, -e} = \left(\frac{\pi}{8} \times 1.51^2 \times 0.95117\right)(\pi \times 1.51 \times 3.25) \\ = 0.11048$$

OCV Cooling Jacket and Impact Limiter

Computer shape factor via equations for configuration #5, page 14-41, Handbook of Heat Transfer Fundamentals, Rohsenow, et al.

$$F_{\text{coolant} - \text{air}} = A_1 = (A_1 \times F_{A_1 - \text{coolant}}) / (A_{\text{coolant}}) \\ = \frac{2\pi \times 26.625 \text{ in} \times 19.75 \text{ in} \times 0.644300}{2\pi \times 19.575 \text{ in} \times 19.75 \text{ in}} \\ = 0.74045 \\ \therefore F_{\text{tot} - \text{tot}} = \frac{1}{2}(1.0 - 0.74045) \\ = 0.129775$$

$$\begin{aligned}
 F_{\text{top} - \text{top}} &= A_b \times F_{A_b - \text{top}/A_{\text{top}/\text{top}}} \\
 &= \frac{2\pi \times 95 \text{ ft} \times 19.75 \text{ ft} \times 0.300818}{2\pi \times 19.575 \times 19.75 \text{ ft}} \\
 &= 0.53798
 \end{aligned}$$

$$\begin{aligned}
 F_{\text{top} - \text{side}} &= \frac{1}{3} \times (1.0 - 0.53798) \\
 &= 0.23107
 \end{aligned}$$

$$\begin{aligned}
 F_{\text{top} - \text{bot}} &= F_{\text{top} - \text{side}} - F_{\text{top} - \text{bot}} \\
 &= 0.23107 - 0.129776 \\
 &= 0.101295
 \end{aligned}$$

$$\begin{aligned}
 F_{\text{top} - \dots} &= 0.53798 + 0.23107 \\
 &= 0.76905
 \end{aligned}$$

$$\begin{aligned}
 F_{\text{side} - \text{side}} &= A_{\text{side}} \times \frac{F_{A_{\text{side}} - \text{side}}/A_{\text{side}/\text{side}}}{A_{\text{side}/\text{side}}} \\
 &= \frac{2\pi \times 26.625 \text{ ft} \times 33.48 \text{ ft} \times 0.617842}{2\pi \times 19.575 \text{ ft} \times 33.48 \text{ ft}} \\
 &= 0.84036
 \end{aligned}$$

$$\begin{aligned}
 \dots F_{\text{side} - \text{side}} &= \frac{1}{3} (1.0 - 0.84036) \\
 &= 0.0798
 \end{aligned}$$

$$\begin{aligned}
 A_{\text{top}} F_{\text{top} - \text{bot}} &= A_{\text{side}} F_{\text{side} - \text{bot}} - A_{\text{top}} F_{\text{top} - \text{side}} \\
 2\pi \times 19.575 \text{ ft} \times 19.75 \text{ ft} \times F_{\text{top} - \text{bot}} &= (2\pi \times 19.575 \text{ ft} \times 33.48 \text{ ft} \times 0.0798 \text{ ft}) - \\
 &\quad (2\pi \times 19.575 \text{ ft} \times 19.75 \text{ ft} \times 0.129776) \\
 F_{\text{top} - \text{bot}} &= 0.007624
 \end{aligned}$$

$$\begin{aligned}
 F_{200000-400} - A_{200} &= A_{200} \times F_{A_{200} - 200000} / A_{200000} \\
 &= \frac{95 \text{ ft}}{19.575 \text{ ft}} \times 0.000012 \\
 &= 0.001616
 \end{aligned}$$

$$\begin{aligned}
 F_{200000-40000} &= \frac{1}{2}(1.0 - 0.001616) \\
 &= 0.154191
 \end{aligned}$$

$$\begin{aligned}
 F_{200000-400} &= F_{200000-200000} - F_{200000-400} \\
 &= 0.154191 - 0.0708 \\
 &= 0.07439
 \end{aligned}$$

$$\begin{aligned}
 A_{200} F_{200-400} &= A_{200000} F_{200000-400} - A_{200} F_{200-400} \\
 2\pi \times 19.575 \text{ ft} \times 19.72 \text{ ft} \times F_{200-400} &= (2\pi \times 19.575 \text{ ft} \times 33.48 \text{ ft} \times 0.07439) - \\
 &\quad (2\pi \times 19.575 \text{ ft} \times 19.76 \text{ ft} \times 0.101295) \\
 F_{200-400} &= 0.058841 \\
 F_{200-400} &= 1.0 - F_{200-400} - F_{200-400} \\
 &= 0.957098
 \end{aligned}$$

$$\begin{aligned}
 F_{210000000} - A_{210} &= \frac{A_{210} \times F_{A_{210} - 210000000}}{A_{210000000}} \\
 &= \frac{2\pi \times 26.825 \text{ ft} \times 47.2 \text{ ft} \times 0.660983}{2\pi \times 19.575 \text{ ft} \times 47.2 \text{ ft}} \\
 &= 0.88540
 \end{aligned}$$

$$\begin{aligned}
 F_{210000000-600} &= \frac{1}{2}(1.0 - 0.88540) \\
 &= 0.0573
 \end{aligned}$$

$$A_{910} F_{910 - 920} = (A_{100000000} \times F_{100000000 - 920}) -$$

$$(A_{900000} \times F_{900000 - 920})$$

$$13.72 \text{ in.} \times F_{910 - 920} = (47.2 \text{ in.} \times 0.0573) - (33.48 \text{ in.} \times 0.0799)$$

$$F_{910 - 920} = 0.002396$$

$$F_{100000000 - 920} = A_{920} = \frac{A_{910} \times F_{910 - 920000000}}{A_{900000000}}$$

$$= \frac{2\pi \times 35 \text{ in.} \times 47.2 \text{ in.} \times 0.431549}{2\pi \times 19.676 \text{ in.} \times 47.2 \text{ in.}}$$

$$= 0.77214$$

$$F_{100000000 - 900000} = \frac{1}{2} (1.0 - 0.77214)$$

$$= 0.11393$$

$$F_{100000000 - 920} = F_{100000000 - 900000} + F_{100000000 - 910}$$

$$= 0.11393 + 0.0573$$

$$= 0.05663$$

$$A_{910} \times F_{910 - 920} = A_{100000000} \times F_{100000000 - 920}$$

$$- A_{900000} \times F_{900000 - 920}$$

$$13.72 \text{ in.} \times F_{910 - 920} = (47.2 \text{ in.} \times 0.05663) - (33.48 \text{ in.} \times 0.07439)$$

$$F_{910 - 920} = 0.01329$$

$$F_{910 - 900} = (1.0 - F_{910 - 920}) - F_{910 - 920}$$

$$= (1.0 - 0.002396) - 0.01329$$

$$= 0.984316$$

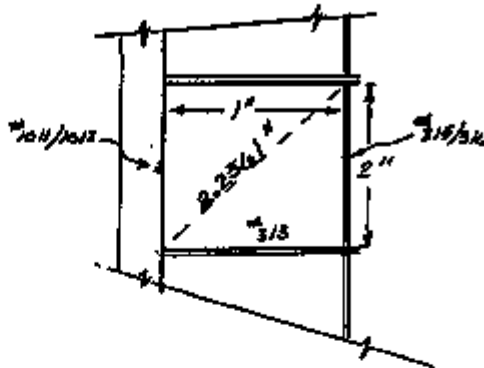
$$\begin{aligned}
 F_{\text{air - storage}} &= \frac{A_{\text{storage}} \times F_{\text{storage}} - \text{air}}{A_{\text{tot}}} \\
 &= \frac{2\pi \times 19.575 \text{ ft} \times 47.2 \text{ ft} \times 0.06663}{\pi (35^2 - 19.575^2) \text{ ft}^2} \\
 &= 0.124599 \\
 \therefore F_{\text{air - }} &= 1.0 - 0.124599 \\
 &= 0.8754
 \end{aligned}$$

$$\begin{aligned}
 F_{\text{soil - storage}} &= \frac{A_{\text{storage}} \times F_{\text{storage}} - \text{soil}}{A_{\text{tot}}} \\
 &= \frac{2\pi \times 19.575 \text{ ft} \times 47.2 \text{ ft} \times 0.0673}{\pi (20.025^2 - 19.575^2) \text{ ft}^2} \\
 &= 0.32509
 \end{aligned}$$

$$\begin{aligned}
 F_{\text{soil - }} &= 1.0 - F_{\text{soil - storage}} \\
 &= 1.0 - 0.32509 \\
 &= 0.6749
 \end{aligned}$$

Coolant Channels:

- ignore curvature of shell
- use string method



$$F_{1011-010} = 2 \times \frac{(2 \text{ ft} + 1 \text{ ft}) - (2.2361 \text{ ft} + 0 \text{ ft})}{2 \times 2 \text{ ft}}$$

$$= 0.38195$$

$$F_{1011-010} = \frac{(2.2361 \text{ ft} + 2.2361 \text{ ft}) - (1 \text{ ft} + 1 \text{ ft})}{2 \times 2 \text{ ft}}$$

$$= 0.61805$$

$$F_{010-010} = \frac{(1 \text{ ft} + 2 \text{ ft}) - (2.2361 \text{ ft} + 0 \text{ ft})}{2 \times 1 \text{ ft}}$$

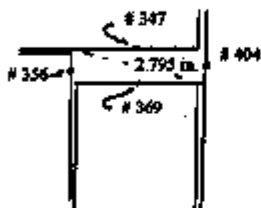
$$= 0.38195$$

$$F_{1000} - 400 = \frac{35 \text{ in.} \times 0.024836}{26.825 \text{ in.}} + \frac{1}{8} \times \left[1 - \frac{35 \text{ in.} \times 0.024836}{26.825 \text{ in.}} \right]$$

$$= 0.5164$$

$$F_{1000} - 400 = \frac{1}{8} \left[1 - \frac{35 \text{ in.} \times 0.024836}{26.825 \text{ in.}} \right]$$

$$= 0.4836$$



$$F_{1000} - 400 = \frac{(2 \times 2.795 \text{ in.}) - (2 \times 2.750 \text{ in.})}{2 \times 0.50 \text{ in.}}$$

$$= 0.09$$

$$F_{1000} - 400 = \frac{0.50 \text{ in.} - 2.5 \text{ in.} - 2.55 \text{ in.}}{2 \times 0.60 \text{ in.}}$$

$$= 0.45$$

$$F_{1000} - 400 = \frac{0.50 \text{ in.} + 2.750 \text{ in.} - 2.795 \text{ in.}}{2 \times 2.750 \text{ in.}}$$

$$= 0.0627$$

3.6.7 Listing of 2-D Computer Model

The following pages list the input file for the SINDA 2-D model of the RTG Transportation System Package and its GPHS RTG payload. The model is valid for the Normal Conditions of Transport (NCT) load case No. 1 (i.e., an undamaged Package, 100 °F, regulatory solar).

READER OPTIONS DATA

TITLE NORMAL COMBUSTION OF TRANSPORT - CASE 1: 100P,
MOLAR, GPMR RTG

MODEL = GPMR4

OUTPUT = p100p4.nc7.sa

PPSWT = ALL1

USERID = p100p4.007.dat

MSR12 = rd case 1.00a

READER NODE DATA, P107

E INCLUDE GPMR4.002

C *** RTG OXIDND ***

C GPMR FUEL SOURCE

50, 1779.4, 2.7738

52, 1915.3, 0.6524

54, 1809.4, 2.7738

C GPMR THERMOPILE

51, 1156.2, 1.172

53, 1237.8, 3.456

55, 1409.8, 1.172

60, 94.8, 1.11

62, 1210., 0.0

C GPMR OUTER SHELL AND FINS

100, 428.1, 0.073

105, 449.3, 0.004

107, 499.0, 0.128

SPV 110, 455., A6, 0.24777 * 4.797

SPV 112, 457., A6, 0.00974 * 8.

SPV 113, 457., A6, 0.08974 * 8.

SPV 120, 520., A6, 1.16533 * 4.797

SPV 122, 534., A6, 0.06493 * 8.

SPV 123, 534., A6, 0.06493 * 8.

SPV 124, 2.1, 498., N6, 0.04370 * 4.

SPV 126, 2.1, 422., A6, 0.08171 * 4.

SPV 130, 547., A6, 1.16263 * 4.797

SPV 132, 562., A6, 0.06493 * 8.

SPV 133, 562., A6, 0.06493 * 8.

SPV 134, 2.1, 584., N6, 0.04570 * 4.

SPV 136, 2.1, 441., A6, 0.08171 * 4.

SPV 140, 549., A6, 1.27002 * 4.797

SPV 141, 547., A6, 1.33130

SPV 142, 562., A6, 0.05029 * 8.

SPV 143, 564., A6, 0.05029 * 8.

SPV 144, 587., A6, 0.04558 * 4.

SPV 145, 528., A6, 0.03661 * 4.

SPV 146, 443., A6, 0.08214 * 4.

SPV 147, 445., A6, 0.04510 * 4.

SPV 150, 545., A6, 1.14263 * 4.797

SPV 152, 560., A6, 0.04493 * 8.

SPV 153, 561., A6, 0.04493 * 8.

SPV 154, 523., A6, 0.04370 * 4.

SPV 159, 521., A6, 0.05348 * 4.

SPV 156, 430., A6, 0.06171 * 4.

SPV 157, 429., A6, 0.07085 * 4.

SPV 160, 509., A6, 1.14263 * 4.797

SPV 161, 505., A6, 0.34544

SPV 162, 524., A6, 0.04493 * 8.

SPV 163, 523., A6, 0.04493 * 8.

SPV 164, 490., A6, 0.04570 * 4.

SPV 165, 478., A6, 0.06034 * 4.

SPV 166, 418., A6, 0.08171 * 4.

SPV 167, 408., A6, 0.04241 * 4.

SPV 170, 384., A6, 0.24959 * 4.797

SPV 172, 387., A6, 0.00981 * 8.

SPV 173, 387., A6, 0.00981 * 8.

177, 370.2, 0.0

175, 355.2, 0.177

180, 361.8, 0.00

C ARITHMETIC MODES

190, 581., -1.0

199, 479., -1.0

198, 306., -1.0

197, 509., -1.0

C INCLUDE Icvtm.007

C INNER-CONTAINMENT SHELL - SARP MODEL, 2/28/84

SPV 209, 276., A2, 71.06295

SPV 206, 283., A2, 78.06855

SPV 210, 317., A2, 325.77525

SPV 220, 375., A2, 325.77525

SPV 230, 312., A2, 325.77525

SPV 240, 236., A2, 118.72275

SPV 242, 213., A2, 124.65289

SPV 250, 201., A2, 143.97989

SPV 260, 204., A2, 159.43945

SPV 281, 204., A2, 158.70284

SPV 283, 201., A2, 177.29478

SPV 287, 219., A2, 189.41312

SPV 285, 200., A2, 96.40275

SPV 286, 198., A2, 122.52831

SPV 287, 281., A2, 5.57233 Speed Thru

SPV 288, 281., A2, 1.07168 Speed Thru

SPV 289, 281., A2, 0.58000 Speed Thru

238, 274., -1. 3 Arithmetic Mode

Between #230 & #240

1268, 157., -1. 3 Metal Housing II Inside

Of Feedthru Insulation

1267, 157., -1. 3 Metal Housing II

Outside Of Feedthru Insulation

1268, 157., -1. 3 Arith. Mode 3

Underside Of Barrier Insulation

1267, 157., -1. 3 Arith. Ops Both w/

Feedthru Convty

C INCLUDE Svcrtm.027

C OUTER-CONTAINMENT SHELL w/ Drained Coolant Jacket -

SARP MODEL, 4/28/84

SPV 300, 252., A2, 95.26475

SPV 301, 131., A2, 29.20000

SPV 304, 220., A2, 129.99777

SPV 305, 146., A2, 118.17610

SPV 310, 272., A2, 227.37080

SPV 320, 273., A2, 227.37080

SPV 330, 250., A2, 227.37080

SPV 340, 280., A2, 82.88108

SPV 342, 283., A2, 78.43792

SPV 343, 170., 3.30147 * 0.20

SPV 344, 195., A2, 79.62581

SPV 345, 171., A2, 47.41978

SPV 346, 162., A2, 128.01954

SPV 347, 162., A2, 128.47048

SPV 348, 165., A2, 26.95726

SPV 350, 190., A2, 110.07622

SPV 352, 190., A2, 95.22874

SPV 354, 190., A2, 164.62726

SPV 354, 180., A2, 142.43175

SPV 351, 187., A70, 20.88888 3 OCY Cap Head

SPV 353, 188., A70, 22.97584 3 OCY Cap Head

Screen - Shunt Partition

SPV 355, 190., A70, 26.37139 3 OCY Cap Head

Screen - Thread End

SPV 360, 281..	A2,	136.45925	
SPV 362, 288..	A2,	170.82610	
SPV 364, 197..	A2,	214.34487	
SPV 366, 191..	A2,	342.81445	
SPV 367, 190..	A2,	298.80466	
SPV 368, 189..	A2,	408.72003	
SPV 369, 189..	A2,	278.21419	
SPV 371, 187..	A7B,	1.74000	3 Cap Head
Screw - Impact Liner			
SPV 372, 188..	A7B,	1.61948	3 Cap Head
Screw - Shank Portion			
SPV 375, 189..	A7B,	1.99906	3 Cap Head
Screw - Shank Portion			
SPV 377, 190..	A7D,	1.22390	3 Cap Head
Screw - Thread End			
C			
SIM 311, 2, 1,	40.,	A20,	26.21300
C			
SNW 321, 2, 1,	40.,	A20,	26.21363
GEN 311, 2, 1,	249.,	-1,	
GEN 321, 2, 1,	249.,	-1,	
SPV 313,	251.,	A2,	66.54918
SPV 323,	251.,	A2,	86.54918
SPW 315, 2, 1,	225.,	A2,	29.27137
SPW 325, 2, 1,	224.,	A2,	29.27137
C			
SIM 331, 2, 1,	40.,	A20,	37.72557
GEN 331, 2, 1,	214.,	-1,	
SPV 333,	215.,	A2,	36.32118
SPW 333, 2, 1,	197.,	A2,	42.13158
C			
ARITHMETIC NODES			
337, 195..	-1,	3	Arithmetic Node On Bolt
Shield Ring			
341, 201..	-1,	3	Arithmetic Node At Joint
w/ Thermal Shield			
337, 186..	-1,	3	Arithmetic Node/ Ribway
Between #354 & #336			
358, 187..	-1,	3	Arithmetic Node/ B Base
of OCV Bolt Heads			
359, 190..	-1,	3	Arithmetic Node/ Ribway
Between #350 & #352			
370, 191..	-1,	3	Arithmetic Node/ Ribway
Between #366 & #347			
1031, 272..	-1.0	3	Outer Surface Of OCV
Wall B 314; Channel #1			
1012, 272..	-1.0	3	Outer Surface Of OCV
Wall B 318; "			
1013, 255..	-1.0	3	End Of Coolant Jacket
Bar B 310			
1021, 272..	-1.0	3	Outer Surface Of OCV
Wall B 328; Channel #1			
1022, 272..	-1.0	3	Outer Surface Of OCV
Wall B 320; "			
1023, 255..	-1.0	3	End Of Coolant Jacket
Bar B 328			
1031, 256..	-1.0	3	Outer Surface Of OCV
Wall B 330; Channel #1			
1032, 236..	-1.0	3	Outer Surface Of OCV
Wall B 330; "			
1033, 203..	-1.0	3	End Of Coolant Jacket
Bar B 338			
1041, 219..	-1.0	3	Outer Surface Of OCV
Wall B 340; Channel #1			
1042, 219..	-1.0	3	Outer Surface Of OCV
Wall B 340; "			
1043, 203..	-1.0	3	Outer Surface Of OCV
Wall B 342; Channel #1			
1044, 203..	-1.0	3	Outer Surface Of OCV
Wall B 342; "			
1346, 146..	-1.0	3	Junction Between 346 &
345			
1347, 185..	-1.0	3	Air Gap Between 347 &
349			
C			
** SUPPORT STAND FOR CPMS ETC **			
C			
GE'S CPMS RTG ADAPTOR RING & QUICK CONNECT ASSEMBLY			
SPV 190, 312..	A6,	11.64571	
SPV 191, 294..	A6,	13.87586	
C			
RTG SUPPORT STAND			
SPV 192, 234..	A2,	42.05393	
SPV 193, 276..	A2,	27.59677	3 ROSSLE BAR
SPV 194, 261..	A2,	49.43756	3 OUTER PLATE
SUPPORT			
SPV 196, 301..	A2,	10.29934	3 INNER BAR/PIECE
PLATE			
SPV 198, 293..	A2,	80.71438	3 OUTER BAR/PIECE
PLATE			
C			
195, 223..	-1,	3	INNER INSULATION
C			
197, 229..	-1,	3	OUTER INSULATION
195, 223..	2.47428	40.28	3 TUBES
INSULATION			
197, 229..	13.24834	40.20	3 OUTER
INSULATION			
199, 264..	-1,	3	NODE AT BASE OF
RIVS			
1000, 227..	-1,	3	INNER GAS VOLUME
1030, 226..	-1,	3	OUTER GAS VOLUME
1001, 236..	-1,	3	NODE BETWEEN 196 &
198			
1002, 243..	-1,	3	NODE BETWEEN 194 &
198			
1003, 244..	-1,	3	NODE BETWEEN 192 &
1001			
1004, 227..	-1,	3	NODE BETWEEN 192 &
1005			
1005, 226..	-1,	3	NODE AT JOY BASE
1006, 203..	-1,	3	NODE BETWEEN 241 &
263			
1007, 330..	-1,	3	NODE BETWEEN 175 &
1008			
1008, 314..	-1,	3	NODE BETWEEN 1007
B 190			
1009, 300..	-1,	3	NODE BETWEEN 190 &
191			
C			
INCLUDE POINTS:007			
E			
IMPACT LINER MODEL NODES - SARP Model, 4/28/90			
SPV 480, 196..	A2,	143.57766	
SPV 401, 192..	A2,	22.89788	
SPV 402, 188..	A2,	284.68309	
SPV 486, 172..	A2,	142.60818	
SPV 486, 128..	A2,	147.38904	
SPV 408, 196..	A2,	300.35432	
SPV 410, 113..	A2,	158.16734	
SPV 412, 118..	A2,	85.08591	
SPV 414, 123..	A2,	179.64800	
421,	182.,	6.36916*	.3
422,	196.,	6.34914*	.3
423,	134.,	6.36916*	.3
424,	172.,	19.86724*	.3
425,	147.,	19.86724*	.3
426,	127.,	19.86724*	.3
431,	149.,	9.98174*	3#2.1
432,	134.,	9.98174*	3#2.1
433,	195.,	9.98174*	3#2.1
434,	143.,	9.82231*	3#2.1
435,	128.,	9.82231*	3#2.1
436,	110.,	9.82231*	3#2.1
441,	131.,	10.27998*	.3
442,	133.,	10.27998*	.3
443,	131.,	10.27998*	.3
444,	129.,	9.36686*	.3
445,	110.,	9.36686*	.3
446,	115.,	9.36686*	.3
451,	117.,	11.18901*	.3
452,	113.,	11.18901*	.3

WY 171, 2.1, 162.1, 172.1, AS, 0.000867 * B.
 WY 173, 170, 172, AS, 0.006535 * B.
 WY 173.1, 170, 173, AS, 0.000836 * B.
 WY 174, 170, 177, AS, 0.012407 * 4797
 WY 175, 2.1, 172.1, 177.0, AS, 0.000448 * B.

-126230, 126, 230, 0.01478
 -126198, 126, 198, 0.00382
 -126196, 126, 196, 0.00367
 -127700, 127, 200, 0.10497
 -127204, 127, 204, 0.17131
 -127210, 127, 210, 0.37696

C
 C
 C
 C
 RADIATION BETWEEN RTG & ICY SURFACES w/ ICY = B.90
 #193/#67196 @ B.48, & #190 @ 0.20

-100800, 100, 200, 0.3061 B Hand

Calculator: -109200, 109, 204, 0.008125 B Hand

Calculator: -107210, 107, 210, 0.01684

-107200, 107, 200, 0.00740

-107230, 107, 230, 0.00272

-107193, 107, 193, 0.00034

-107198, 107, 198, 0.00119

-107190, 107, 190, 0.00011

-190200, 190, 200, 0.01288

-190204, 190, 204, 0.03083

-190210, 190, 210, 0.04873

-190220, 190, 220, 0.03663

-190230, 190, 230, 0.00055

-112200, 112, 200, 0.00791

-112204, 112, 204, 0.02156

-112210, 112, 210, 0.02456

-112220, 112, 220, 0.00333

-112230, 112, 230, 0.00028

-112193, 112, 193, 0.00005

-112200, 112, 200, 0.00007

-112204, 112, 204, 0.02135

-112210, 112, 210, 0.02484

-112220, 112, 220, 0.00333

-112230, 112, 230, 0.00028

-112193, 112, 193, 0.00005

-112200, 120, 200, 0.04121

-120204, 120, 204, 0.09990

-120210, 120, 210, 0.22520

-120220, 120, 220, 0.05770

-120230, 120, 230, 0.00791

-120193, 120, 193, 0.00091

-120198, 120, 198, 0.00171

-122200, 122, 200, 0.04634

-122204, 122, 204, 0.04049

-122210, 122, 210, 0.09406

-122220, 122, 220, 0.05429

-122230, 122, 230, 0.00348

-122193, 122, 193, 0.00049

-122198, 122, 198, 0.00071

-122200, 122, 200, 0.01433

-122204, 122, 204, 0.04055

-122210, 122, 210, 0.09544

-122220, 122, 220, 0.05452

-122230, 122, 230, 0.00339

-122193, 122, 193, 0.00049

-122198, 122, 198, 0.00079

-124200, 124, 200, 0.02186

-124204, 124, 204, 0.04018

-124210, 124, 210, 0.07888

-124220, 124, 220, 0.02242

-124230, 124, 230, 0.00334

-124193, 124, 193, 0.00046

-124198, 124, 198, 0.00080

-126200, 126, 200, 0.02181

-126204, 126, 204, 0.03908

-126210, 126, 210, 0.08138

-126220, 126, 220, 0.03370

-126230, 126, 230, 0.00330

-126193, 126, 193, 0.00045

-126198, 126, 198, 0.00073

-126200, 126, 200, 0.10543

-126204, 126, 204, 0.17223

-126210, 126, 210, 0.34443

-126220, 126, 220, 0.10236

-130200, 130, 200, 0.03798

-130204, 130, 204, 0.03798

-130210, 130, 210, 0.30613

-130220, 130, 220, 0.16796

-130230, 130, 230, 0.00701

-130193, 130, 193, 0.00021

-130198, 130, 198, 0.00057

-132200, 132, 200, 0.00425

-132204, 132, 204, 0.01526

-132210, 132, 210, 0.06498

-132220, 132, 220, 0.00992

-132230, 132, 230, 0.01449

-132193, 132, 193, 0.00102

-132198, 132, 198, 0.00108

-133200, 133, 200, 0.00425

-133204, 133, 204, 0.01530

-133210, 133, 210, 0.06513

-133220, 133, 220, 0.01150

-133230, 133, 230, 0.00996

-133193, 133, 193, 0.00104

-133198, 133, 198, 0.00108

-134200, 134, 200, 0.00517

-134204, 134, 204, 0.01420

-134210, 134, 210, 0.07078

-134220, 134, 220, 0.00500

-134230, 134, 230, 0.01182

-134193, 134, 193, 0.00107

-134198, 134, 198, 0.00140

-135200, 135, 200, 0.00529

-135204, 135, 204, 0.01406

-135210, 135, 210, 0.07070

-135220, 135, 220, 0.00519

-135230, 135, 230, 0.01006

-135193, 135, 193, 0.00102

-135198, 135, 198, 0.00111

-136200, 136, 200, 0.02107

-136204, 136, 204, 0.05886

-136210, 136, 210, 0.31903

-136220, 136, 220, 0.24133

-136230, 136, 230, 0.04195

-136193, 136, 193, 0.00044

-136198, 136, 198, 0.00079

-137200, 137, 200, 0.02100

-137204, 137, 204, 0.05795

-137210, 137, 210, 0.31899

-137220, 137, 220, 0.26065

-137230, 137, 230, 0.04099

-137193, 137, 193, 0.00140

-137198, 137, 198, 0.00075

-140200, 140, 200, 0.00967

-140204, 140, 204, 0.00657

-140210, 140, 210, 0.00579

-140220, 140, 220, 0.37825

-140230, 140, 230, 0.00088

-140193, 140, 193, 0.00032

-140198, 140, 198, 0.00076

-140200, 140, 200, 0.00049

-141200, 141, 200, 0.01616

-141204, 141, 204, 0.02250

-141210, 141, 210, 0.05648

-141220, 141, 220, 0.05418

-141230, 141, 230, 0.00599

-141193, 141, 193, 0.00094

-141198, 141, 198, 0.00152

-141196, 141, 196, 0.00062

-141190, 141, 190, 0.00344

-142260,	142,200,	0.00130	-154230,	154,230,	0.00408
-142284,	142,204,	0.00441	-154193,	154,193,	0.00522
-142210,	142,210,	0.00454	-154156,	154,156,	0.00574
-142220,	142,220,	0.11532	-154190,	154,190,	0.00131
-142250,	142,250,	0.00387	-154200,	154,200,	0.00031
-142193,	142,193,	0.00226	-154206,	154,206,	0.00804
-142198,	142,198,	0.00198	-154210,	154,210,	0.01378
-142180,	142,180,	0.00025	-154220,	154,220,	0.07600
-142200,	142,200,	0.00134	-154210,	154,210,	0.00900
-143284,	143,304,	0.00480	-153193,	153,193,	0.01204
-143210,	143,210,	0.03709	-153198,	153,198,	0.00794
-143220,	143,220,	0.12377	-153190,	153,190,	0.00178
-143230,	143,230,	0.03618	-154200,	154,200,	0.00272
-143193,	143,193,	0.00232	-154204,	154,204,	0.01167
-143198,	143,198,	0.00218	-154210,	154,210,	0.04282
-143190,	143,190,	0.00026	-154220,	154,220,	0.26584
-144200,	144,200,	0.00118	-154230,	154,230,	0.24528
-144204,	144,204,	0.00364	-154193,	154,193,	0.03332
-144210,	144,210,	0.02869	-154198,	154,198,	0.02677
-144220,	144,220,	0.09161	-154194,	154,194,	0.00116
-144230,	144,230,	0.02833	-154190,	154,190,	0.00482
-144193,	144,193,	0.00185	-154200,	154,200,	0.00274
-144198,	144,198,	0.00182	-154204,	154,204,	0.00037
-144190,	144,190,	0.00030	-154210,	154,210,	0.03937
-145200,	145,200,	0.00097	-154220,	154,220,	0.24599
-145204,	145,204,	0.00299	-154230,	154,230,	0.28802
-145210,	145,210,	0.02366	-154193,	154,193,	0.03195
-145220,	145,220,	0.00872	-154198,	154,198,	0.02494
-145230,	145,230,	0.02436	-154190,	154,190,	0.00115
-145193,	145,193,	0.00158	-154200,	154,200,	0.00556
-145198,	145,198,	0.00140	-154204,	154,204,	0.00144
-145190,	145,190,	0.00024	-154210,	154,210,	0.00681
-146200,	146,200,	0.00018	-154220,	146,220,	0.00338
-146204,	146,204,	0.02139	-154230,	146,230,	0.22821
-146210,	146,210,	0.12902	-160193,	160,193,	0.00309
-146220,	146,220,	0.34497	-160198,	160,198,	0.03367
-146230,	146,230,	0.12406	-160190,	160,190,	0.01787
-146193,	146,193,	0.01610	-161200,	161,200,	0.00225
-146198,	146,198,	0.01861	-161204,	161,204,	0.00435
-146190,	146,190,	0.00133	-161210,	161,210,	0.00749
-147200,	147,200,	0.00521	-161220,	161,220,	0.02496
-147204,	147,204,	0.01768	-161230,	161,230,	0.02626
-147210,	147,210,	0.10758	-161193,	161,193,	0.01221
-147220,	147,220,	0.30347	-161198,	161,198,	0.01512
-147230,	147,230,	0.10444	-161194,	161,194,	0.00474
-147193,	147,193,	0.00890	-161190,	161,190,	0.00073
-147198,	147,198,	0.00906	-162200,	162,200,	0.00059
-147190,	147,190,	0.00128	-162210,	162,210,	0.00271
-150200,	150,200,	0.00035	-162220,	162,220,	0.00778
-150204,	150,204,	0.00251	-162230,	162,230,	0.00528
-150210,	150,210,	0.03433	-162193,	162,193,	0.00148
-150220,	150,220,	0.17062	-162198,	162,198,	0.01388
-150230,	150,230,	0.20394	-162190,	162,190,	0.00498
-150193,	150,193,	0.02214	-163204,	163,204,	0.00029
-150198,	150,198,	0.01584	-163210,	163,210,	0.00068
-150190,	150,190,	0.00238	-163220,	163,220,	0.02189
-152200,	152,200,	0.00022	-163230,	163,230,	0.09532
-152204,	152,204,	0.00228	-163193,	163,193,	0.02599
-152210,	152,210,	0.31184	-163198,	163,198,	0.01373
-152220,	152,220,	0.07138	-163190,	163,190,	0.00788
-152230,	152,230,	0.08484	-164204,	164,204,	0.00087
-152193,	152,193,	0.00064	-164210,	164,210,	0.00266
-152198,	152,198,	0.00658	-164220,	164,220,	0.00129
-152190,	152,190,	0.00094	-164230,	164,230,	0.01151
-153200,	153,200,	0.00020	-164193,	164,193,	0.00260
-153204,	153,204,	0.00223	-164198,	164,198,	0.01265
-153210,	153,210,	0.01180	-164190,	164,190,	0.00054
-153220,	153,220,	0.07129	-164194,	164,194,	0.00088
-153230,	153,230,	0.00309	-165200,	165,200,	0.00043
-153193,	153,193,	0.00943	-165204,	165,204,	0.00148
-153198,	153,198,	0.00434	-165210,	165,210,	0.00914
-153190,	153,190,	0.00094	-165220,	165,220,	0.02687
-154200,	154,200,	0.00022	-165230,	165,230,	0.13351
-154204,	154,204,	0.00279	-165193,	165,193,	0.04631
-154210,	154,210,	0.01169	-165198,	165,198,	0.02471
-154220,	154,220,	0.05926	-165194,	165,194,	0.00144

-165198	165, 198	0.01762		-112126	112, 126	0.00269	
-166200	166, 200	0.00136		-112127	112, 127	0.00044	
-166204	166, 204	0.00605		-113125	113, 125	0.00582	
-166210	166, 210	0.00495		-113126	113, 126	0.00044	
-166220	166, 220	0.00148		-113127	113, 127	0.00561	
-166230	166, 230	0.00289		-120124	120, 124	0.01065	
-166193	166, 193	0.00213		-120125	120, 125	0.01049	
-166198	166, 198	0.00548		-120126	120, 126	0.00532	
-166196	166, 196	0.00577		-120127	120, 127	0.00532	
-167190	167, 190	0.03726		-120134	120, 134	0.00059	
-167192	167, 192	0.00122		-120137	120, 137	0.00059	
-167204	167, 204	0.00455		-120136	120, 136	0.01029	
-167210	167, 210	0.01275		-120137	120, 137	0.01025	
-167220	167, 220	0.00609		-122124	122, 124	0.00698	
-167230	167, 230	0.01247		-122126	122, 126	0.00442	
-167193	167, 193	0.00382		-122127	122, 127	0.00832	
-167198	167, 198	0.00259		-122134	122, 134	0.00134	
-167196	167, 196	0.00768		-122136	122, 136	0.00641	
-167190	167, 190	0.03013		-122137	122, 137	0.00099	
-170204	170, 204	0.00036		-123125	123, 125	0.00645	
-170210	170, 210	0.00098		-123126	123, 126	0.00933	
-170220	170, 220	0.00467		-123127	123, 127	0.00605	
-170230	170, 230	0.00857		-123135	123, 135	0.00112	
-170193	170, 193	0.02795		-123136	123, 136	0.00097	
-170198	170, 198	0.00699		-123137	123, 137	0.00041	
-170196	170, 196	0.01035		-124125	124, 125	0.01377	
-172204	172, 204	0.00020		-124127	124, 127	0.00094	
-172210	172, 210	0.00061		-124136	124, 136	0.00094	
-172220	172, 220	0.00336		-124137	124, 137	0.00114	
-172230	172, 230	0.02499		-124135	124, 135	0.00321	
-172193	172, 193	0.01372		-124137	124, 137	0.01328	
-172198	172, 198	0.00344		-124141	124, 141	0.00036	
-172196	172, 196	0.00804		-124147	124, 147	0.00072	
-172190	172, 190	0.00576		-125126	125, 126	0.00396	
-173204	173, 204	0.00015		-125130	125, 130	0.00093	
-173210	173, 210	0.00061		-125133	125, 133	0.00114	
-173220	173, 220	0.00337		-125134	125, 134	0.00321	
-173230	173, 230	0.02533		-125136	125, 136	0.01121	
-173193	173, 193	0.01343		-125141	125, 141	0.00037	
-173198	173, 198	0.00334		-125146	125, 146	0.00094	
-173196	173, 196	0.00094		-126127	126, 127	0.01768	
-173190	173, 190	0.00259		-126130	126, 130	0.01804	
-177200	177, 200	0.00183		-126132	126, 132	0.00361	
-177204	177, 204	0.00205		-126133	126, 133	0.00103	
-177206	177, 206	0.00253		-126135	126, 135	0.01661	
-177210	177, 210	0.00253		-126137	126, 137	0.00021	
-177220	177, 220	0.00719		-126141	126, 141	0.00129	
-177230	177, 230	0.01591		-126143	126, 143	0.00064	
-175194	175, 194	0.00831	B Hand	-127147	127, 147	0.00326	
Calculations	180, 190	0.004525	S Hand	-127150	127, 150	0.01067	
Calculations	180, 196	0.00505	S Hand	-127152	127, 152	0.00184	
Calculations	180, 198	0.006525	B Hand	-127153	127, 153	0.00361	
Calculations				-127154	127, 154	0.01436	
				-127156	127, 156	0.04266	
				-127161	127, 161	0.00128	
				-127164	127, 164	0.00072	
				-127166	127, 166	0.00377	
				-130136	130, 136	0.01199	
				-130138	130, 138	0.01169	
				-130139	130, 139	0.00981	
				-130137	130, 137	0.00513	
				-130141	130, 141	0.00581	
				-130144	130, 144	0.00093	
				-130145	130, 145	0.00089	
				-130146	130, 146	0.00069	
				-130147	130, 147	0.00092	
				-132134	132, 134	0.00445	
				-132136	132, 136	0.00905	
				-132137	132, 137	0.00375	
				-132141	132, 141	0.00096	
				-132144	132, 144	0.00151	
				-132146	132, 146	0.00219	
				-132147	132, 147	0.00094	
				-133135	133, 135	0.00445	
				-133136	133, 136	0.00576	
				-133137	133, 137	0.00905	

-133141	133, 141	0.00095	-144167	144, 167	0.00068
-133145	133, 142	0.00150	-143146	143, 146	0.00117
-133146	133, 144	0.00093	-143159	143, 159	0.00099
-133147	133, 147	0.00326	-143153	143, 153	0.00140
-134123	134, 121	0.01797	-143154	143, 154	0.00239
-134137	134, 137	0.06052	-143156	143, 156	0.00080
-134140	134, 140	0.00095	-143166	143, 166	0.00063
-134141	134, 141	0.00039	-144147	144, 147	0.11238
-134142	134, 142	0.00145	-144150	144, 150	0.00094
-134143	134, 143	0.00259	-144152	144, 152	0.00316
-134147	134, 147	0.01132	-144153	144, 153	0.00093
-135134	135, 134	0.09754	-144155	144, 155	0.01173
-135140	135, 140	0.00093	-144157	144, 157	0.04256
-135141	135, 141	0.00039	-144161	144, 161	0.00076
-135143	135, 143	0.00145	-144165	144, 165	0.00097
-135144	135, 144	0.00230	-144167	144, 167	0.00328
-135149	135, 146	0.00953	-147150	147, 150	0.00090
-136127	136, 127	0.17394	-147152	147, 152	0.00040
-136140	136, 140	0.00932	-147153	147, 153	0.00326
-136141	136, 141	0.00930	-147154	147, 154	0.01173
-136142	136, 142	0.00337	-147156	147, 156	0.03764
-136143	136, 143	0.00023	-147161	147, 161	0.00065
-136148	136, 145	0.01088	-147166	147, 166	0.00324
-136147	136, 147	0.03993	-190154	190, 154	0.01199
-136157	136, 157	0.00242	-190155	190, 155	0.02144
-137140	137, 140	0.00995	-190156	190, 156	0.07190
-137141	137, 141	0.00990	-190157	190, 157	0.06344
-137142	137, 142	0.00085	-190161	190, 161	0.00250
-137143	137, 143	0.00337	-190164	190, 164	0.00070
-137144	137, 144	0.01200	-190165	190, 165	0.00216
-137148	137, 144	0.03725	-190166	190, 166	0.01033
-137150	137, 150	0.00244	-190167	190, 167	0.00084
-140141	140, 141	0.10044	-192154	192, 154	0.10645
-140164	140, 164	0.01062	-192156	192, 156	0.05904
-140163	140, 165	0.00878	-192157	192, 157	0.00465
-140166	140, 166	0.00907	-192161	192, 161	0.00037
-140167	140, 167	0.00323	-192162	192, 162	0.00106
-140154	140, 154	0.00990	-192165	192, 165	0.00642
-140155	140, 155	0.00152	-192167	192, 167	0.00110
-140156	140, 156	0.01008	-193155	193, 155	0.11592
-140157	140, 157	0.00952	-193156	193, 156	0.00876
-141142	141, 142	0.04094	-193157	193, 157	0.02962
-141143	141, 143	0.04103	-193161	193, 161	0.00047
-141144	141, 144	0.04274	-193165	193, 165	0.00182
-141145	141, 145	0.02488	-193166	193, 166	0.00162
-141146	141, 146	0.06250	-193167	193, 167	0.00270
-141147	141, 147	0.04382	-194155	194, 155	0.02281
-141150	141, 150	0.00012	-194157	194, 157	0.05340
-141152	141, 152	0.00097	-194160	194, 160	0.00075
-141153	141, 153	0.00097	-194161	194, 161	0.00936
-141154	141, 154	0.00849	-194162	194, 162	0.00005
-141155	141, 155	0.00430	-194163	194, 163	0.01172
-141156	141, 156	0.00951	-194164	194, 164	0.00566
-141157	141, 157	0.00078	-194165	194, 165	0.00037
-141161	141, 161	0.00204	-194169	194, 169	0.00057
-141165	141, 165	0.00040	-194161	194, 161	0.00475
-141186	141, 186	0.00032	-199163	199, 163	0.00147
-141167	141, 167	0.00907	-199164	199, 164	0.00804
-142144	142, 144	0.10468	-199166	199, 166	0.01435
-142146	142, 146	0.03496	-194157	194, 157	0.18448
-142147	142, 147	0.00230	-194160	194, 160	0.00084
-142154	142, 154	0.00150	-194161	194, 161	0.00790
-142156	142, 156	0.00953	-194162	194, 162	0.00981
-142157	142, 157	0.00094	-194163	194, 163	0.00063
-143143	143, 143	0.08449	-194165	194, 165	0.01794
-143146	143, 146	0.00291	-196167	196, 167	0.04224
-143147	143, 147	0.02896	-197160	197, 160	0.00706
-143155	143, 155	0.00188	-197161	197, 161	0.00682
-143156	143, 156	0.00088	-197162	197, 162	0.00079
-143157	143, 157	0.00526	-197163	197, 163	0.00027
-144148	144, 148	0.01930	-197164	197, 164	0.00023
-144147	144, 147	0.00344	-197165	197, 165	0.04334
-144150	144, 150	0.00099	-140161	140, 161	0.00053
-144152	144, 152	0.00150	-140164	140, 164	0.01004
-144153	144, 153	0.00097	-140165	140, 165	0.00716
-144157	144, 157	0.01967	-140166	140, 166	0.04338

SPV 5, 263, 259, AT, 0.180640
 C 1CV BASE TO 1CV #LAW8
 SPV 4, 265, 250, AT, 0.370885, AT,
 42.490320
 SPV 7, 264, 250, AT, 0.092853, AT,
 6.917099
 SPV 8, 264, 250, AT, 0.420856, 2.75, 115,
 SPV 9, 266, 250, AT, 0.721917, AT,
 17.334881
 -25068, 250, 265, 0.23237
 -25068, 259, 264, 0.03662
 -25068, 250, 268, 0.70773
 -268262, 263, 262, 0.97977

C INCLUDE acvte.na7
 C CONDUCTANCE WITHIN OUTER-CONTAINMENT SHELL BY
 BOUNDED CYLINDRICAL JACKET
 C GCY BOLT NUTS ARE INCLUDED - Version 007, -
 SARP Model, 4/28/94
 C This file separates the Convexion Conductances from
 The Remaining Conductors

C CONDUCTANCE WITHIN OUTER-CONTAINMENT SHELL

SPV 30, 300, 304, AT, 0.056988
 SPV 31, 304, 318, AT, 0.238513, AT, 0.063567
 SPV 32, 304, 305, AT, 0.906667, AT, 0.125000
 SPV 33, 319, 318, 10, 320, 10, AT, 0.028925
 SPV 35, 330, 340, AT, 0.042398
 SPV 36, 340, 344, AT, 0.099211
 SPV 37, 341, 337, AT, 0.440970
 SPV 38, 337, 346, AT, 0.086181
 SPV 39, 341, 342, AT, 0.634961
 SPV 40, 342, 344, AT, 0.264589, AT,
 1.626189
 SPV 41, 344, 354, AT, 0.799954
 SPV 42, 354, 356, AT, 0.428709
 SPV 43, 350, 352, AT, 0.286452
 SPV 44, 354, 350, AT, 1.654381
 SPV 45, 354, 352, AT, 1.431252
 SPV 46, 346, 346, AT, 0.113908
 SPV 47, 344, 345, AT, 0.268388
 SPV 48, 343, 347, AT, 0.384280, AT,
 0.195115
 SPV 49, 347, 356, AT, 0.211778, AT,
 0.783333
 SPV 70, 346, 349, AT, 0.156388
 SPV 71, 349, 358, AT, 0.127543
 72, 351, 358, 96.4 8 CONTACT

RESISTANCE

SPV 73, 358, 357, AT, 1.645375
 SPV 74, 351, 353, AG, 0.116211
 SPV 75, 353, 355, AG, 0.852954
 SPV 76, 353, 357, AT, 12.877918, AT, 2.232818
 SPV 77, 353, 350, AT, 0.844089, AT, 1.764393
 SPV 771, 357, 354, AT, 2.327259
 SPV 772, 357, 356, AT, 2.327259
 SPV 773, 359, 358, AT, 1.685771
 SPV 774, 359, 352, AT, 1.685771
 78, 359, 370, 336.84
 SPV 79, 359, 379, AT, 19.792404, AT, 2.970837
 SPV 92, 379, 368, AT, 5.221414
 SPV 93, 379, 367, AT, 5.221414
 94, 371, 368, 12.99
 SPV 95, 371, 375, AG, 0.007476
 SPV 96, 373, 375, AG, 0.004365
 SPV 97, 375, 377, AG, 0.009389
 SPV 98, 373, 357, AT, 1.370997, AT, 0.358112
 SPV 982, 373, 359, AT, 1.048931, AT, 0.266225
 SPV 983, 375, 370, AT, 1.589251, AT, 0.424480
 99, 377, 403, 24.80

SPV 80, 368, 362, AT, 0.189152
 SPV 81, 342, 344, AT, 0.218491
 SPV 82, 364, 366, AT, 0.357105
 SPV 83, 368, 367, AT, 0.892604
 SPV 84, 367, 368, AT, 1.456161
 SPV 85, 368, 369, AT, 0.929374
 SPV 86, 368, 350, AT, 1.813164, 263.8, 2.75
 SPV 87, 367, 352, AT, 0.894566, 209.8, 2.88
 SPV 88, 354, 349, AT, 0.604358, AT,
 54.766248
 SPV 89, 352, 349, AT, 0.512708, AT,
 47.624508

C *** COOLANT JACKET - BOTH LOOPS ACTIVE ***

C 31101, 311, 1011, 321, 1021, 331, 1031, 1. 8
 BUNNY VALUE
 C 31201, 312, 1012, 322, 1022, 332, 1032, 1. 8
 BUNNY VALUE
 C 33101, 331, 1041, 1. 8
 BUNNY VALUE
 C 33202, 332, 1042, 1. 8
 BUNNY VALUE
 C 33103, 331, 1043, 1. 8
 BUNNY VALUE
 C 33204, 332, 1044, 1. 8
 BUNNY VALUE
 C 31115, 311, 319, 321, 325, 1. 8 BUNNY
 VALUE
 C 31216, 312, 316, 322, 326, 1. 8 BUNNY
 VALUE
 C 31113, 311, 313, 321, 323, 1. 8 BUNNY
 VALUE
 C 31213, 312, 313, 322, 323, 1. 8 BUNNY
 VALUE
 C 33133, 331, 333, 1. 8 BUNNY
 VALUE
 C 33233, 332, 333, 1. 8 BUNNY
 VALUE
 C 33135, 331, 335, 1. 8 BUNNY
 VALUE
 C 33236, 332, 336, 1. 8 BUNNY
 VALUE
 C 33732, 337, 331, 337, 332, 1. 8 BUNNY
 VALUE
 C 328, -991, 321, -331, 321, -321, 311, -311, 901,
 37.4464, 43*0.911
 C 381, -992, 332, -332, 332, -328, 312, -312, 902,
 37.4464, 43*0.911

C BEGIN MODIFICATIONS FOR BUNNY CYLINDRICAL JACKET

SIMULATION
 SPV 31101, 311, 311, 10, 1011, 10, AT, 9.948509
 SPV 31201, 311, 312, 10, 1012, 10, AT, 9.948509
 SPV 33101, 331, 1041, AT, 3.423888
 SPV 33202, 332, 1042, AT, 3.423888
 SPV 33103, 331, 1043, AT, 0.734482
 SPV 33204, 332, 1044, AT, 0.734482
 SPV 31113, 311, 311, 10, 319, 10, AT, 5.040972
 SPV 31216, 311, 312, 10, 316, 10, AT, 5.040972
 SPV 31115, 311, 311, 10, 313, 10, AT, 10.214747
 SPV 31213, 311, 312, 10, 313, 10, AT, 10.214747
 SPV 33133, 331, 333, AT, 10.214747
 SPV 33233, 332, 333, AT, 10.214747
 SPV 33135, 331, 335, AT, 10.214747
 SPV 33236, 332, 336, AT, 10.214747
 SPV 33732, 337, 331, 337, 332, AT, 10.214747
 SPV 328, 2, 1, 337, 0, 331, 1, AT, 0.626389*0.3

C DRAINAGE COOLANT JACKET RADIATION - w/ m = 0.3 @ 0.5V

Shell & m = 0.48 @ Jacket				
-101115	1011,315	1012,316	0.68879	
-101113	1011,313	1012,313	0.81720	
-102125	1021,325	1022,326	0.98679	
-102123	1021,323	1022,323	0.81720	
-103135	1031,335	1032,336	0.98579	
-103133	1031,333	1032,333	0.81720	
-104135	1041,335	1042,336	0.93886	
-104133	1041,333	1042,333	0.29768	
-104335	1043,335	1044,336	0.87690	
-104333	1043,333	1044,333	0.86210	

-513315	313,315	313,316	0.80916	
-323325	323,325	323,326	0.83916	
-333335	333,335	333,336	1.20842	

C DRAINAGE COOLANT JACKET RADIATION - w/ m = 0.5

-901115	9011,315	1012,316	1.37615	
-901113	9011,313	1012,313	1.86893	
-902125	9021,325	1022,326	1.37615	
-902123	9021,323	1022,323	1.06893	
-903135	9031,335	1032,336	1.37615	
-903133	9031,333	1032,333	1.06893	
-904135	9041,335	1042,336	0.50096	
-904133	9041,333	1042,333	0.28911	
-904335	9043,335	1044,336	0.10439	
-904333	9043,333	1044,333	0.06323	

-313315	313,315	313,316	1.09745	
-323325	323,325	323,326	1.08765	
-333335	333,335	333,336	1.38042	

C DRAINAGE COOLANT JACKET RADIATION - w/ m = 0.1

-101115	1011,315	1012,316	0.79516	
-101113	1011,313	1012,313	0.67950	
-102125	1021,325	1022,326	0.79616	
-102123	1021,323	1022,323	0.67950	
-103135	1031,335	1032,336	0.79616	
-103133	1031,333	1032,333	0.67950	
-104135	1041,335	1042,336	0.28983	
-104133	1041,333	1042,333	0.26735	
-104335	1043,335	1044,336	0.60049	
-104333	1043,333	1044,333	0.49164	

C END OF NET COOLANT JACKET RADIATION REVISIONS

SPW 31011	2.1, 310.0, 1011.1	AT	3.525433	
SPW 32011	2.1, 320.0, 1021.1	AT	3.525455	
SPW 33011	2.1, 330.0, 1031.1	AT	3.525433	
SPW 34011	2.1, 340.0, 1041.1	AT		

3.525435 @ 0.364

SPW 34211, 2.1, 342.0, 1043.1, AT,

1.325433 @ 0.878

SPW 31013, 3.1, 310.10, 313.10, AT, 1.378570

SPW 34013, 340, 333, AT,

1.378570 @ 0.364

SPW 34213, 342, 333, AT,

1.378570 @ 0.878

SPW 31315, 2.1, 303.0, 315.1, AT, 1.264129

SPW 31325, 2.1, 303.0, 325.1, AT, 1.264121

SPW 31313, 303.0, 313.1, AT, 1.833801

SPW 31323, 303.0, 323.1, AT, 1.833801

SPW 33315, 2.1, 303.0, 333.1, AT,

1.264121 @ 1.44

SPW 33313, 303.0, 333.0, AT,

1.833801 @ 1.44

C FIBERGLASS INSULATION WITHIN BOLT CIRCLE CAVITY

SPW 401, 342, 343, AAS, 0.526760

SPW 402, 346, 343, AAS, 5.772259
SPW 403, 348, 343, AAS, 0.768888
SPW 404, 354, 343, AAS, 1.772278
SPW 405, 356, 343, AAS, 1.537552
SPW 407, 349, 343, AAS, 7.786219
DPV 90, 349, 1347, AT, 2.284711, AT,
0.752088
SPW 91, 356, 1347, AT, 1.787473, AT,
0.293598
SPW 911, 347, 1347, AT, 10.966613
SPW 912, 404, 1347, AT, 0.422506

C INCLUDE STANDOFFS

E

C CONDUCTION FROM RTD TO SUPPORT STAND & ICV BASE

E

C

175187, 175, 1007, 11.62
SPV 187103, 1007, 1808, AS, 0.516340
SPV 188100, 1008, 190, AS, 0.020884
SPV 188100, 1008, 1809, AS, 0.015913
SPV 189101, 1009, 191, AS, 0.026257
191198, 191, 198, 270,

SPV 196101, 198, 1801, AT, 0.821808
SPV 198101, 198, 1801, AT, 0.658929
SPV 198102, 198, 1802, AT, 0.877285
SPV 196102, 198, 1803, AT, 0.898825
SPV 199102, 199, 1802, AT, 0.386556
SPV 199103, 199, 179, AT, 0.849123
SPV 101103, 1009, 1003, AT, 0.817625
SPV 182103, 192, 1003, AT, 0.877404
SPV 902106, 192, 9004, AT, 0.877481
184105, 1084, 9085, 78.78 @ CONTACT

SPV 905104, 1084, 9085, AT, 0.012272
SPV 905106, 1005, 9004, AT, 0.023980
SPV 905261, 261, 9006, AT, 0.303836
SPV 904253, 1086, 343, AT, 0.719227
SPV 990195, 196, 995, A64, 0.392689
SPV 998197, 198, 997, A64, 2.902747

SPV 993260, 193, 244, A64, 4.83796
195100, 195, 1800, 1.0
192100, 192, 1800, 1.0
194100, 194, 1800, 1.0
197100, 197, 1800, 1.0
194110, 194, 1810, 1.0
182110, 1802, 1810, 1.0
242110, 242, 1810, 1.0
261100, 261, 1800, 1.0
263100, 263, 1800, 1.0
265110, 265, 1090, 1.0

-19924, 199, 242, 0.20178

-19926, 199, 240, 1.63179

-19424, 194, 242, 0.73438

-19423, 194, 263, 0.22678

-19499, 194, 199, 0.23384

-19463, 194, 263, 0.34950

-19497, 194, 197, 0.48880

-19261, 192, 264, 0.18362

-19263, 192, 263, 0.18997

-19285, 192, 195, 0.11237

-19297, 192, 197, 0.11372

-19294, 192, 196, 0.13883

-19541, 195, 261, 0.35501

-19763, 197, 263, 0.80672

C RADIATION BETWEEN ICV & RTD STAND SURFACES

C

-200193, 200, 199, 0.01239

-200198, 200, 199, 0.04436

-200196	200, 196	0.81605	4307, 422, 423	0.239853 * 0.278
-200198	200, 190	0.81054	4308, 423, 424	0.239853 * 0.278
-204193	204, 193	0.81433		
-204198	204, 196	0.80412	4381, 406, 431	2.162321 * 0.278
-204199	204, 194	0.81539	4302, 431, 432	1.061168 * 0.278
-204199	204, 190	0.81488	4303, 432, 433	1.061168 * 0.278
-198193	216, 193	0.80895	4304, 430, 434	1.031486 * 0.278
-198199	216, 196	0.82025	4309, 433, 435	1.060564 * 0.278
-198199	216, 190	0.81737	4304, 433, 434	1.060564 * 0.278
-218198	218, 190	0.81529	4307, 434, 430	2.373089 * 0.278
-228193	228, 193	0.83505		
-228198	228, 198	0.81957	4306, 446, 431	2.090643 * 0.278
-228198	228, 196	0.85379	4309, 484, 432	2.090643 * 0.278
-228199	228, 190	0.86585	4310, 484, 433	2.438963 * 0.278
-230193	230, 193	0.83374		
-230198	230, 198	0.82518	6208, 624, 634	0.717996 * 0.278
-230198	230, 196	0.81887	4209, 423, 433	0.717996 * 0.278
-230199	230, 198	0.85487	4290, 426, 434	0.717996 * 0.278
-193198	193, 198	0.73948		
-193199	193, 196	0.81430	4401, 406, 441	2.244721 * 0.278
-193199	193, 190	0.86321	4402, 441, 442	1.112300 * 0.278
			4403, 442, 443	1.102350 * 0.278
			4404, 443, 444	1.104854 * 0.278
			4405, 444, 445	1.088780 * 0.278
			4406, 445, 446	1.228705 * 0.278
			4407, 446, 448	2.441571 * 0.278
			4488, 441, 431	1.531170 * 0.278
			4489, 442, 432	1.531170 * 0.278
			4418, 443, 433	1.531170 * 0.278
			4411, 444, 434	1.395178 * 0.278
			4412, 445, 435	1.395178 * 0.278
			4413, 444, 436	1.395178 * 0.278
			4581, 406, 451	2.484134 * 0.278
			4582, 451, 452	1.280067 * 0.278
			4583, 452, 453	1.202067 * 0.278
			4584, 453, 454	1.357929 * 0.278
			4585, 454, 455	1.319234 * 0.278
			4586, 455, 456	1.319234 * 0.278
			4587, 454, 430	2.636472 * 0.278
			4508, 441, 451	1.697283 * 0.278
			4309, 442, 452	1.697283 * 0.278
			4510, 443, 453	1.697283 * 0.278
			4511, 444, 454	1.546445 * 0.278
			4512, 443, 455	1.644445 * 0.278
			4513, 444, 456	1.546445 * 0.278
			4608, 488, 451	3.688771 * 0.278
			4609, 488, 452	3.688771 * 0.278
			4610, 488, 453	3.688771 * 0.278
			4611, 488, 454	3.352960 * 0.278
			4612, 488, 455	3.352960 * 0.278
			4613, 488, 456	3.352960 * 0.278

344	190, 230	1.		
344	191, 230	1.		
347	196, 230	1.		
348	198, 230	1.		

C FEEDTHRU PILEUP

SPV 2268	267, 1266	AP, 0.994472		
SPV 2267	1266, 1267	AP, 0.422958		
SPV 1008	198, 1268	AP, 0.076899		
SPV 2266	1268, 1266	AP, 0.004712		
SPV 2267	1268, 1267	AP, 0.007334		

267108	1267, 1000	1.0	8 BUNNY VALVE	
267118	1267, 1010	1.0		
268269	1268, 1369	1.0	8 BUNNY VALVE	
268269	1369, 268	1.0		
268269	1267, 268	1.0		
268269	1266, 1369	1.0		

108100	198, 1088	1.0		
-26763	1267, 263	0.03118		
-26762	1267, 262	0.02859		
-26797	1267, 197	0.04801		

C INCLUDE Feascc.087

C FROM IMPACT LIMITER CONDUCTORS - Version 087 - B&B Model, 3/29/94

C CONDUCTANCE WITHIN IMPACT LIMITER SHELL

SPV 921	480, 482	AP, 0.032471		
SPV 922	488, 482	AP, 0.115207		
SPV 923	402, 484	AP, 0.136529	AP, 0.042774	
SPV 921	488, 486	AP, 0.803774	AP, 0.073660	
SPV 923	486, 488	AP, 0.892634	AP, 0.042861	
SPV 924	488, 418	AP, 0.042861	AP, 0.115747	
SPV 971	418, 412	AP, 0.053777		
SPV 981	412, 414	AP, 0.027059		

C MODEL BORN AT NON-DAMAGED SECTIONS

SPV 4180	400, 401	AP, 148.489348		
4109	401, 421	0.780783	* 0.181	
4103	421, 422	3.350391	* 0.181	
4104	422, 423	3.350391	* 0.181	
4105	421, 414	4.700783	* 0.181	
4200	402, 424	4.867895	* 0.278	
4201	424, 425	2.433847	* 0.278	
4202	425, 426	2.433847	* 0.278	
4203	426, 412	4.867895	* 0.278	
4106	421, 424	0.239853	* 0.278	

C RADIATION WITHIN IMPACT LIMITER

- 4101, 490, 501, 2.396788

C INCLUDE Inventory

C CONDUCTORS BETWEEN CONTAINMENT SHELLS - Version 087, 3/28/94

C ICV TO OCV Conductance w/ Maximum Gaps

SPV 200, 200, 300, AP, 7.374816 \$ w/

Maximum 1/2" Gap

SPV 201, 304, 304, AP, 10.412879 \$ w/

Maximum 1/2" Gap At Top &

C

Gap At Side

SPV 202, 1, 7, 210, 30, 310, 30, AP, 42.80261 \$

w/ Maximum 1/4" Gap

SPV 206, 240, 348, AP, 15.398826 \$ w/

Maximum 1/4" Gap

SPV 207, 242, 342, AP, 15.258032 \$ w/

Maximum 1/4" Gap

C ICV TO OCV Conductance w/ Barical Gaps

C	BPV 298, 208, 300, AP, 11.798426	6 W
C	Minimum 3/16" Gap	
C	BPV 291, 204, 304, AP, 16.776072	6 W
C	Minimum 3/16" Gap At Top &	
C		3/16"
C	Gap At Side	
C	BPV 292, 3, 1, 210, 10, 310, 10, AP, 56.978004	9
C	w/ Minimum 1/8" Gap	
C	BPV 226, 250, 348, AP, 20.761955	6 W
C	Minimum 3/16" Gap	
C	BPV 207, 242, 342, AP, 17.647662	6 W
C	Minimum 3/16" Gap	
C	ICV to OCV Conductance w/ Minimum Gaps	
C	BPV 200, 200, 308, AP, 20.498804	6 W
C	Minimum 1/8" Gap	
C	BPV 281, 204, 384, AP, 31.672483	6 W
C	Minimum 1/8" Gap At Top &	
C		1/16"
C	Gap At Side	
C	BPV 262, 3, 1, 210, 10, 310, 10, AP, 179.315662	6 W
C	w/ Minimum 1/16" Gap	
C	BPV 296, 240, 340, AP, 62.068208	6 W
C	Minimum 1/16" Gap	
C	BPV 287, 342, 342, AP, 52.737976	6 W
C	Minimum 1/16" Gap	

BPV 208, 250, 344, AP, 5.222124	
BPV 200, 250, 350, AP, 2.295739	
BPV 210, 250, 366, AP, 2.295739	
BPV 211, 266, 360, AI, 1.342561, 334.2, 0.2	
OPV 212, 262, 362, AI, 1.678201, 392.7, 0.2	
BPV 213, 264, 364, AI, 0.848101, 192.8, 0.2	
OPV 214, 266, 364, AI, 1.223529, 286.3, 0.2	
BPV 218, 268, 368, AI, 0.473071, AP	

30.457365

BPV 216, 368, 400, AI, 2.908882, AP	
43.633251	
BPV 217, 362, 400, AI, 3.636903, AP	
54.549239	
BPV 218, 364, 400, AI, 4.589903, AP	
68.849538	
BPV 219, 366, 402, AI, 1.330599, 202., 0.8	
BPV 220, 367, 402, AI, 1.168219, 234., 0.8	
BPV 221, 368, 402, AI, 1.566690, AP	
54.833044	
BPV 222, 368, 404, AI, 3.242285, AP	
10.147681	
BPV 223, 369, 404, AI, 2.223281, AP	
12.444126	
BPV 224, 343, 406, AP, 0.099998	

-2090, 208, 308, 3.01948	
-2094, 204, 306, 4.11381	
-2111, 210, 318, 8.798236	
-2271, 228, 328, 8.798236	
-2311, 250, 338, 8.798236	
-2421, 240, 348, 5.17141	
-3452, 242, 342, 2.499589	
-3433, 250, 344, 0.53078	
-2454, 250, 350, 0.122776	
-2435, 250, 366, 0.874889	
-3636, 266, 346, 0.228282	
-4020, 400, 340, 0.49608	
-4032, 400, 342, 0.61743	
-4034, 400, 344, 0.779610	
-4238, 402, 348, 0.62075	
-4438, 404, 348, 0.92600	
-4439, 404, 350, 0.63129	
-4434, 404, 343, 1.34688	

C INCLUDE extec.087		C EXTERIOR CONDUCTORS - Braided Package, Upright		Position - Ver. 087, 4/28/76	
300,	300,	1,	1.0	6 DUBBY VALUE	
301,	301,	1,	1.0	6 DUBBY VALUE	
304,	306,	1,	1.0	6 DUBBY VALUE	
309,	309,	1,	1.0	6 DUBBY VALUE	
319,	319,	1,	1.0	6 DUBBY VALUE	
316,	316,	1,	1.0	6 DUBBY VALUE	
323,	323,	1,	1.0	6 DUBBY VALUE	
324,	324,	1,	1.0	6 DUBBY VALUE	
335,	335,	1,	1.0	6 DUBBY VALUE	
334,	334,	1,	1.0	6 DUBBY VALUE	
1013,	1013,	1,	1.0	6 DUBBY VALUE	
1023,	1023,	1,	1.0	6 DUBBY VALUE	
1033,	1033,	1,	1.0	6 DUBBY VALUE	
346,	346,	1,	1.0	6 DUBBY VALUE	
349,	349,	1,	1.0	6 DUBBY VALUE	
351,	351,	1,	1.0	6 DUBBY VALUE	
371,	371,	1,	1.0	6 DUBBY VALUE	
1346,	1346,	1,	1.0	6 DUBBY VALUE	
406,	406,	1,	1.0	6 DUBBY VALUE	
408,	408,	1,	1.0	6 DUBBY VALUE	

E EXTERIOR ENVIATION

-303,	308,	2,	1.79184	
-3031,	304, 301,	0.860990		
-3035,	304, 305,	0.17056		
-3015,	301,	2,	1.06333	
-3041,	304,	2,	2.84936	
-3045,	305, 306,	0.85370 = 48.		
-3051,	305,	2,	0.59153	
-3058	305, 315, 340, 346,	0.00488 = 48.		
-3752,	371, 2, 316, 2,	4.11333		
-3752,	371, 2, 336, 2,	4.02655		
-3752,	371, 2, 336, 2,	4.03561		
-3462,	344, 2,	3.35293		
-3433,	344, 1033,	0.46794		
-3433,	344, 325,	346, 334,	0.00787	
-3433,	344, 1033,	0.00333		
-3432,	344, 113,	344, 324,	0.04841	
-34613,	344, 1013,	0.00623		
-34313,	344, 113,	344, 314,	0.01264	
-3512,	351, 2,	0.06585		
-3492,	349, 2,	0.71024		
-3519,	351, 349,	0.48978		
-3712,	371, 2,	0.00799		
-3719,	371, 349,	0.04825		
-1348,	1346, 2,	0.27895		
-1347,	1346, 406,	0.25413		
-1336,	1033, 406,	0.36736		
-3336,	335, 406,	356, 406,	0.72851	
-1236,	1023, 406,	0.09183		
-3256,	325, 406,	356, 406,	0.18327	
-1136,	1013, 406,	0.03648		
-3156,	315, 406,	346, 404,	0.04890	
-35604,	356, 404,	0.11917		
-35647,	356, 347, 356, 348,	0.06206		
-36906,	369, 404,	347, 404,	0.16150	
-34789,	347, 349,	0.67134		
-33260,	332, 349,	0.21008		
-25660,	256, 349,	0.24164		
-4063,	406, 2,	7.89541		
-4082,	408, 2,	21.90899		
-1014,	1013, 2,	2.05783		
-1024,	1023, 2,	2.01544		

T2 = 1424.7
END IF

IF(TIMER .LE. 0.75) THEN
OUTPUT = 1./60.
ELSE IF(TIMER .GT. .75) THEN
OUTPUT = 5./60.
ELSE IF(TIMER .GT. 5.9991) THEN
OUTPUT = 28./60.
ELSE IF(TIMER .GT. 10.901) THEN
OUTPUT = 1.
ELSE IF(TIMER .GT. 25.901) THEN
OUTPUT = 5.
END IF

C INCLUDE behavior.act

C VARIABLE BLOCK FOR OCV EXTERIOR CONDITIONS -
Brazed Jacket = SARP Model, 4/20/94
C SUBROUTINE FRCV(M,ST,AREA,CL,D,G,CP,K,U,
C * RNO, PRESS, E)
C SUBROUTINE FRCV(M,ST,AREA,CL,D,G,CP,K,U,
C * RNO, PRESS, E)
C SUBROUTINE FRCV(M,SCH,STI,STZ,AREA,CL,C,G,
C * CP,K,
C * U,RNO,PRESS,R,M,G,BADY,HAI)
C SUBROUTINE FRCV(M,ST,AREA,CL,D,G,CP,K,U,
C * RNO, PRESS, E)
C SUBROUTINE
FRCV(M,ST,AREA,CL,D,VEL,CP,K,U,
C * RNO, PRESS, E)

XG6 = 0.5*(T304 + T1)
IF(TIMER .GT. 0. .OR. TIMER .LE. 0.5) XG6 = T1
CALL FRCV(M304, T304, XG6, 3.687, 3.240,
+ XG10, 0., A15, A14, A16, 0., 14.69, 53.35)
G304 = G304*0.25
XG6 = 0.20*(T301 + 0.80*T1
IF(TIMER .GT. 0. .OR. TIMER .LE. 0.5) XG6 = T1
CALL FRCV(M301, T301, XG6, 2.4866, 0.1,
+ XG10, 0., A15, A14, A16, 0., 14.69, 53.35)

CALL FRCV(M304, T304, T1, 9.2985, 3.240,
+ XG10, 0., A15, A14, A16, 0., 14.69, 53.35)
G304 = G304 * 0.75
CALL FRCV(M304, T304, T1, 22.007, 1.0,
+ XG10, 0., A15, A14, A16, 0., 14.69, 53.35)

CALL FRCV(M315, T315, T1, 5.20972, 4.00,
+ XG10, 0., A15, A14, A16, 0., 14.69, 53.35)
CALL FRCV(M316, T316, T1, 5.20972, 4.00,
+ XG10, 0., A15, A14, A16, 0., 14.69, 53.35)
CALL FRCV(M325, T325, T1, 5.20972, 3.00,
+ XG10, 0., A15, A14, A16, 0., 14.69, 53.35)
CALL FRCV(M326, T326, T1, 5.20972, 3.00,
+ XG10, 0., A15, A14, A16, 0., 14.69, 53.35)
CALL FRCV(M335, T335, T1, 7.46979, 1.75,
+ XG10, 0., A15, A14, A16, 0., 14.69, 53.35)
CALL FRCV(M334, T334, T1, 7.46979, 1.75,
+ XG10, 0., A15, A14, A16, 0., 14.69, 53.35)

CALL FRCV(M1013, T1013, T1, 2.6051, 4.00,
+ XG10, 0., A15, A14, A16, 0., 14.69, 53.35)
CALL FRCV(M1023, T1023, T1, 2.6051, 2.67,
+ XG10, 0., A15, A14, A16, 0., 14.69, 53.35)
CALL FRCV(M1033, T1033, T1, 3.7496, 1.33,
+ XG10, 0., A15, A14, A16, 0., 14.69, 53.35)

CALL FRCV(M1346, T346, T1, 6.1526, 3.0000,
+ XG10, 0., A15, A14, A16, 0., 14.69, 53.35)

C CONNECTION AT HOAT TUBES
CALL FRCV(M349, T349, T1, 4.70333, 0.14,
+ XG10, 0., A15, A14, A16, 0., 14.69, 53.35)
G349 = G349*.5
CALL FRCV(M351, T351, T1, 0.4873, 0.156,
+ XG10, 0., A15, A14, A16, 0., 14.69, 53.35)
G351 = G351*.25

CALL FRCV(M1371, T371, T1, 0.0853, 0.094,
+ XG10, 0., A15, A14, A16, 0., 14.69, 53.35)
G371 = G371*.25

CALL FRCV(M1346, T346, T1, 0.5344, 0.04,
+ XG10, 0., A15, A14, A16, 0., 14.69, 53.35)
CALL FRCV(M1406, T406, T1, 16.701, 3.0000,
+ XG10, 0., A15, A14, A16, 0., 14.69, 53.35)
CALL FRCV(M1406, T406, T1, 27.486, 1.33,
+ XG10, 0., A15, A14, A16, 0., 14.69, 53.35)

C INCLUDE standover.006
C COMPUTE CONVECTIVE HEAT TRANSFER W/ FALSE FLOOR
SECTION
C BELOW SUPPORT RACK
C

CALL FRCV(M1095100, T100, T1000, 0.7847, 3.58,
+ XG10, 0., A12, A11, A13, 0., XG11, 384.04)
CALL FRCV(M1092100, T102, T1000, 1.6349, 0.25,
+ XG10, 0., A12, A11, A13, 0., XG11, 384.04)
CALL FRCV(M1094100, T104, T1000, 1.8431, 0.23,
+ XG10, 0., A12, A11, A13, 0., XG11, 384.04)
G109700 = G1095100*4.2056/0.7847
CALL FRCV(M104110, T104, T1010, 3.1058, 0.5,
+ XG10, 0., A12, A11, A13, 0., XG11, 384.04)
CALL FRCV(M102110, T102, T1010, 0.6979, 0.08,
+ XG10, 0., A12, A11, A13, 0., XG11, 384.04)
CALL FRCV(M242110, T242, T1010, 5.7083,
0.41667,
+ XG10, 0., A12, A11, A13, 0., XG11, 384.04)
CALL FRCV(M243110, T243, T1000, 3.7271, 2.58,
+ XG10, 0., A12, A11, A13, 0., XG11, 384.04)
G241100 = G243110 = 2.1813/2.7271
CALL FRCV(M249110, T249, T1010, 0.8792, 0.08,
+ XG10, 0., A12, A11, A13, 0., XG11, 384.04)

C CONVECTION FROM FEED FIRM PLUG ASSEMBLY
CALL FRCV(M267100, T1267, T1000, 0.2667,
0.323,
+ XG10, 0., A12, A11, A13, 0., XG11, 384.04)
CALL FRCV(M267110, T1267, T1010, 0.2667,
0.323,
+ XG10, 0., A12, A11, A13, 0., XG11, 384.04)

CALL FRCV(M268240, T1248, T1240, 0.0621,
0.323,
+ XG10, 0., A12, A11, A13, 0., XG11, 384.04)
CALL FRCV(M269240, T248, T1240, 0.1149,
0.2083,
+ XG10, 0., A12, A11, A13, 0., XG11, 384.04)
CALL FRCV(M269240, T249, T1240, 0.0830,
0.1647,
+ XG10, 0., A12, A11, A13, 0., XG11, 384.04)
CALL FRCV(M268240, T1244, T1240, 0.0640,
0.063,
+ XG10, 0., A12, A11, A13, 0., XG11, 384.04)

CALL FRCV(M109100, T100, T1000, 0.803,
0.1667,
+ XG10, 0., A12, A11, A13, 0., XG11, 384.04)

C INCLUDE behavior.004
C

C Updated RTG-TCV Convection Linkage Based on
OASIS DUAL TUBE RESULTS
C COMPUTE VARIABLE CONVECTION BETWEEN THE RTG &
PACKAGE

M2 = ((T120 + T130 + T140 + T150 + T160
+ T170 + T180 + T190 + T200 + T210 + T220 + T230 + T240 + T250 + T260 + T270 + T280 + T290 + T300 + T310 + T320 + T330 + T340 + T350 + T360 + T370 + T380 + T390 + T400 + T410 + T420 + T430 + T440 + T450 + T460 + T470 + T480 + T490 + T500 + T510 + T520 + T530 + T540 + T550 + T560 + T570 + T580 + T590 + T600 + T610 + T620 + T630 + T640 + T650 + T660 + T670 + T680 + T690 + T700 + T710 + T720 + T730 + T740 + T750 + T760 + T770 + T780 + T790 + T800 + T810 + T820 + T830 + T840 + T850 + T860 + T870 + T880 + T890 + T900 + T910 + T920 + T930 + T940 + T950 + T960 + T970 + T980 + T990 + T1000 + T1010 + T1020 + T1030 + T1040 + T1050 + T1060 + T1070 + T1080 + T1090 + T1100 + T1110 + T1120 + T1130 + T1140 + T1150 + T1160 + T1170 + T1180 + T1190 + T1200 + T1210 + T1220 + T1230 + T1240 + T1250 + T1260 + T1270 + T1280 + T1290 + T1300 + T1310 + T1320 + T1330 + T1340 + T1350 + T1360 + T1370 + T1380 + T1390 + T1400 + T1410 + T1420 + T1430 + T1440 + T1450 + T1460 + T1470 + T1480 + T1490 + T1500 + T1510 + T1520 + T1530 + T1540 + T1550 + T1560 + T1570 + T1580 + T1590 + T1600 + T1610 + T1620 + T1630 + T1640 + T1650 + T1660 + T1670 + T1680 + T1690 + T1700 + T1710 + T1720 + T1730 + T1740 + T1750 + T1760 + T1770 + T1780 + T1790 + T1800 + T1810 + T1820 + T1830 + T1840 + T1850 + T1860 + T1870 + T1880 + T1890 + T1900 + T1910 + T1920 + T1930 + T1940 + T1950 + T1960 + T1970 + T1980 + T1990 + T2000 + T2010 + T2020 + T2030 + T2040 + T2050 + T2060 + T2070 + T2080 + T2090 + T2100 + T2110 + T2120 + T2130 + T2140 + T2150 + T2160 + T2170 + T2180 + T2190 + T2200 + T2210 + T2220 + T2230 + T2240 + T2250 + T2260 + T2270 + T2280 + T2290 + T2300 + T2310 + T2320 + T2330 + T2340 + T2350 + T2360 + T2370 + T2380 + T2390 + T2400 + T2410 + T2420 + T2430 + T2440 + T2450 + T2460 + T2470 + T2480 + T2490 + T2500 + T2510 + T2520 + T2530 + T2540 + T2550 + T2560 + T2570 + T2580 + T2590 + T2600 + T2610 + T2620 + T2630 + T2640 + T2650 + T2660 + T2670 + T2680 + T2690 + T2700 + T2710 + T2720 + T2730 + T2740 + T2750 + T2760 + T2770 + T2780 + T2790 + T2800 + T2810 + T2820 + T2830 + T2840 + T2850 + T2860 + T2870 + T2880 + T2890 + T2900 + T2910 + T2920 + T2930 + T2940 + T2950 + T2960 + T2970 + T2980 + T2990 + T3000 + T3010 + T3020 + T3030 + T3040 + T3050 + T3060 + T3070 + T3080 + T3090 + T3100 + T3110 + T3120 + T3130 + T3140 + T3150 + T3160 + T3170 + T3180 + T3190 + T3200 + T3210 + T3220 + T3230 + T3240 + T3250 + T3260 + T3270 + T3280 + T3290 + T3300 + T3310 + T3320 + T3330 + T3340 + T3350 + T3360 + T3370 + T3380 + T3390 + T3400 + T3410 + T3420 + T3430 + T3440 + T3450 + T3460 + T3470 + T3480 + T3490 + T3500 + T3510 + T3520 + T3530 + T3540 + T3550 + T3560 + T3570 + T3580 + T3590 + T3600 + T3610 + T3620 + T3630 + T3640 + T3650 + T3660 + T3670 + T3680 + T3690 + T3700 + T3710 + T3720 + T3730 + T3740 + T3750 + T3760 + T3770 + T3780 + T3790 + T3800 + T3810 + T3820 + T3830 + T3840 + T3850 + T3860 + T3870 + T3880 + T3890 + T3900 + T3910 + T3920 + T3930 + T3940 + T3950 + T3960 + T3970 + T3980 + T3990 + T4000 + T4010 + T4020 + T4030 + T4040 + T4050 + T4060 + T4070 + T4080 + T4090 + T4100 + T4110 + T4120 + T4130 + T4140 + T4150 + T4160 + T4170 + T4180 + T4190 + T4200 + T4210 + T4220 + T4230 + T4240 + T4250 + T4260 + T4270 + T4280 + T4290 + T4300 + T4310 + T4320 + T4330 + T4340 + T4350 + T4360 + T4370 + T4380 + T4390 + T4400 + T4410 + T4420 + T4430 + T4440 + T4450 + T4460 + T4470 + T4480 + T4490 + T4500 + T4510 + T4520 + T4530 + T4540 + T4550 + T4560 + T4570 + T4580 + T4590 + T4600 + T4610 + T4620 + T4630 + T4640 + T4650 + T4660 + T4670 + T4680 + T4690 + T4700 + T4710 + T4720 + T4730 + T4740 + T4750 + T4760 + T4770 + T4780 + T4790 + T4800 + T4810 + T4820 + T4830 + T4840 + T4850 + T4860 + T4870 + T4880 + T4890 + T4900 + T4910 + T4920 + T4930 + T4940 + T4950 + T4960 + T4970 + T4980 + T4990 + T5000 + T5010 + T5020 + T5030 + T5040 + T5050 + T5060 + T5070 + T5080 + T5090 + T5100 + T5110 + T5120 + T5130 + T5140 + T5150 + T5160 + T5170 + T5180 + T5190 + T5200 + T5210 + T5220 + T5230 + T5240 + T5250 + T5260 + T5270 + T5280 + T5290 + T5300 + T5310 + T5320 + T5330 + T5340 + T5350 + T5360 + T5370 + T5380 + T5390 + T5400 + T5410 + T5420 + T5430 + T5440 + T5450 + T5460 + T5470 + T5480 + T5490 + T5500 + T5510 + T5520 + T5530 + T5540 + T5550 + T5560 + T5570 + T5580 + T5590 + T5600 + T5610 + T5620 + T5630 + T5640 + T5650 + T5660 + T5670 + T5680 + T5690 + T5700 + T5710 + T5720 + T5730 + T5740 + T5750 + T5760 + T5770 + T5780 + T5790 + T5800 + T5810 + T5820 + T5830 + T5840 + T5850 + T5860 + T5870 + T5880 + T5890 + T5900 + T5910 + T5920 + T5930 + T5940 + T5950 + T5960 + T5970 + T5980 + T5990 + T6000 + T6010 + T6020 + T6030 + T6040 + T6050 + T6060 + T6070 + T6080 + T6090 + T6100 + T6110 + T6120 + T6130 + T6140 + T6150 + T6160 + T6170 + T6180 + T6190 + T6200 + T6210 + T6220 + T6230 + T6240 + T6250 + T6260 + T6270 + T6280 + T6290 + T6300 + T6310 + T6320 + T6330 + T6340 + T6350 + T6360 + T6370 + T6380 + T6390 + T6400 + T6410 + T6420 + T6430 + T6440 + T6450 + T6460 + T6470 + T6480 + T6490 + T6500 + T6510 + T6520 + T6530 + T6540 + T6550 + T6560 + T6570 + T6580 + T6590 + T6600 + T6610 + T6620 + T6630 + T6640 + T6650 + T6660 + T6670 + T6680 + T6690 + T6700 + T6710 + T6720 + T6730 + T6740 + T6750 + T6760 + T6770 + T6780 + T6790 + T6800 + T6810 + T6820 + T6830 + T6840 + T6850 + T6860 + T6870 + T6880 + T6890 + T6900 + T6910 + T6920 + T6930 + T6940 + T6950 + T6960 + T6970 + T6980 + T6990 + T7000 + T7010 + T7020 + T7030 + T7040 + T7050 + T7060 + T7070 + T7080 + T7090 + T7100 + T7110 + T7120 + T7130 + T7140 + T7150 + T7160 + T7170 + T7180 + T7190 + T7200 + T7210 + T7220 + T7230 + T7240 + T7250 + T7260 + T7270 + T7280 + T7290 + T7300 + T7310 + T7320 + T7330 + T7340 + T7350 + T7360 + T7370 + T7380 + T7390 + T7400 + T7410 + T7420 + T7430 + T7440 + T7450 + T7460 + T7470 + T7480 + T7490 + T7500 + T7510 + T7520 + T7530 + T7540 + T7550 + T7560 + T7570 + T7580 + T7590 + T7600 + T7610 + T7620 + T7630 + T7640 + T7650 + T7660 + T7670 + T7680 + T7690 + T7700 + T7710 + T7720 + T7730 + T7740 + T7750 + T7760 + T7770 + T7780 + T7790 + T7800 + T7810 + T7820 + T7830 + T7840 + T7850 + T7860 + T7870 + T7880 + T7890 + T7900 + T7910 + T7920 + T7930 + T7940 + T7950 + T7960 + T7970 + T7980 + T7990 + T8000 + T8010 + T8020 + T8030 + T8040 + T8050 + T8060 + T8070 + T8080 + T8090 + T8100 + T8110 + T8120 + T8130 + T8140 + T8150 + T8160 + T8170 + T8180 + T8190 + T8200 + T8210 + T8220 + T8230 + T8240 + T8250 + T8260 + T8270 + T8280 + T8290 + T8300 + T8310 + T8320 + T8330 + T8340 + T8350 + T8360 + T8370 + T8380 + T8390 + T8400 + T8410 + T8420 + T8430 + T8440 + T8450 + T8460 + T8470 + T8480 + T8490 + T8500 + T8510 + T8520 + T8530 + T8540 + T8550 + T8560 + T8570 + T8580 + T8590 + T8600 + T8610 + T8620 + T8630 + T8640 + T8650 + T8660 + T8670 + T8680 + T8690 + T8700 + T8710 + T8720 + T8730 + T8740 + T8750 + T8760 + T8770 + T8780 + T8790 + T8800 + T8810 + T8820 + T8830 + T8840 + T8850 + T8860 + T8870 + T8880 + T8890 + T8900 + T8910 + T8920 + T8930 + T8940 + T8950 + T8960 + T8970 + T8980 + T8990 + T9000 + T9010 + T9020 + T9030 + T9040 + T9050 + T9060 + T9070 + T9080 + T9090 + T9100 + T9110 + T9120 + T9130 + T9140 + T9150 + T9160 + T9170 + T9180 + T9190 + T9200 + T9210 + T9220 + T9230 + T9240 + T9250 + T9260 + T9270 + T9280 + T9290 + T9300 + T9310 + T9320 + T9330 + T9340 + T9350 + T9360 + T9370 + T9380 + T9390 + T9400 + T9410 + T9420 + T9430 + T9440 + T9450 + T9460 + T9470 + T9480 + T9490 + T9500 + T9510 + T9520 + T9530 + T9540 + T9550 + T9560 + T9570 + T9580 + T9590 + T9600 + T9610 + T9620 + T9630 + T9640 + T9650 + T9660 + T9670 + T9680 + T9690 + T9700 + T9710 + T9720 + T9730 + T9740 + T9750 + T9760 + T9770 + T9780 + T9790 + T9800 + T9810 + T9820 + T9830 + T9840 + T9850 + T9860 + T9870 + T9880 + T9890 + T9900 + T9910 + T9920 + T9930 + T9940 + T9950 + T9960 + T9970 + T9980 + T9990 + T10000 + T10010 + T10020 + T10030 + T10040 + T10050 + T10060 + T10070 + T10080 + T10090 + T10100 + T10110 + T10120 + T10130 + T10140 + T10150 + T10160 + T10170 + T10180 + T10190 + T10200 + T10210 + T10220 + T10230 + T10240 + T10250 + T10260 + T10270 + T10280 + T10290 + T10300 + T10310 + T10320 + T10330 + T10340 + T10350 + T10360 + T10370 + T10380 + T10390 + T10400 + T10410 + T10420 + T10430 + T10440 + T10450 + T10460 + T10470 + T10480 + T10490 + T10500 + T10510 + T10520 + T10530 + T10540 + T10550 + T10560 + T10570 + T10580 + T10590 + T10600 + T10610 + T10620 + T10630 + T10640 + T10650 + T10660 + T10670 + T10680 + T10690 + T10700 + T10710 + T10720 + T10730 + T10740 + T10750 + T10760 + T10770 + T10780 + T10790 + T10800 + T10810 + T10820 + T10830 + T10840 + T10850 + T10860 + T10870 + T10880 + T10890 + T10900 + T10910 + T10920 + T10930 + T10940 + T10950 + T10960 + T10970 + T10980 + T10990 + T11000 + T11010 + T11020 + T11030 + T11040 + T11050 + T11060 + T11070 + T11080 + T11090 + T11100 + T11110 + T11120 + T11130 + T11140 + T11150 + T11160 + T11170 + T11180 + T11190 + T11200 + T11210 + T11220 + T11230 + T11240 + T11250 + T11260 + T11270 + T11280 + T11290 + T11300 + T11310 + T11320 + T11330 + T11340 + T11350 + T11360 + T11370 + T11380 + T11390 + T11400 + T11410 + T11420 + T11430 + T11440 + T11450 + T11460 + T11470 + T11480 + T11490 + T11500 + T11510 + T11520 + T11530 + T11540 + T11550 + T11560 + T11570 + T11580 + T11590 + T11600 + T11610 + T11620 + T11630 + T11640 + T11650 + T11660 + T11670 + T11680 + T11690 + T11700 + T11710 + T11720 + T11730 + T11740 + T11750 + T11760 + T11770 + T11780 + T11790 + T11800 + T11810 + T11820 + T11830 + T11840 + T11850 + T11860 + T11870 + T11880 + T11890 + T11900 + T11910 + T11920 + T11930 + T11940 + T11950 + T11960 + T11970 + T11980 + T11990 + T12000 + T12010 + T12020 + T12030 + T12040 + T12050 + T12060 + T12070 + T12080 + T12090 + T12100 + T12110 + T12120 + T12130 + T12140 + T12150 + T12160 + T12170 + T12180 + T12190 + T12200 + T12210 + T12220 + T12230 + T12240 + T12250 + T12260 + T12270 + T12280 + T12290 + T12300 + T12310 + T12320 + T12330 + T12340 + T12350 + T12360 + T12370 + T12380 + T12390 + T12400 + T12410 + T12420 + T12430 + T12440 + T12450 + T12460 + T12470 + T12480 + T12490 + T12500 + T12510 + T12520 + T12530 + T12540 + T12550 + T12560 + T12570 + T12580 + T12590 + T12600 + T12610 + T12620 + T12630 + T12640 + T12650 + T12660 + T12670 + T12680 + T12690 + T12700 + T12710 + T12720 + T12730 + T12740 + T12750 + T12760 + T12770 + T12780 + T12790 + T12800 + T12810 + T12820 + T12830 + T12840 + T12850 + T12860 + T12870 + T12880 + T12890 + T12900 + T12910 + T12920 + T12930 + T12940 + T12950 + T12960 + T12970 + T12980 + T12990 + T13000 + T13010 + T13020 + T13030 + T13040 + T13050 + T13060 + T13070 + T13080 + T13090 + T13100 + T13110 + T13120 + T13130 + T13140 + T13150 + T13160 + T13170 + T13180 + T13190 + T13200 + T13210 + T13220 + T13230 + T13240 + T13250 + T13260 + T13270 + T13280 + T13290 + T13300 + T13310 +

```

* T156 + T157 + T166 + T167 )*(B1.315 +
+ ( T122 + T123 + T124 + T125 + T142 + T143 +
+ T152 + T153 + T162 + T163 )*(S2.086)/2850.3
XK2 = (T200*0.371 + T204*0.431 + T210 + T228 +
+ T230 + T240)*0.444/4.426

C COMPUTE IGV GAS TEMPERATURE & PRESSURE
XG2 = LXG2*2820.5 + XG3*4891.45/RTG7.0
XK11 = 20. * (XG2 + 446.)/666.6

C
C SURROTIME FROM/CM,ST,1,STZ, ANGA, N, DR,
EL,
C E, N, CP, K, U, RND, PRESS, R)
CALL FRO/CM(GS18, XK2, XK3, 0.7570, 3.5000,
3.985,
+ 1.01, XK10, D., A12, A11, A13, R., XK11,
304.04)
GS18 = GS18 + D.75
GS20 = GS18 + 58.31/109.001
XK5 = ( T126 + T127 + T136 + T137 + T146 +
1147
+ T156 + T157 + T166 + T167 )/W.
CALL FRO/CM(GS22, XK5, XK3, 1.219, 3.5000,
1.669,
+ 0.548, XK10, D., A12, A11, A13, W., XK11,
304.04)
GS22 = GS22 + 0.75
GS43 = GS18 + 0.70 + 21.158/109.001
GS44 = GS18 + 0.70 + 11.2615/109.001
GS45 = GS18 + 0.75 + 97.378/109.001
GS46 = GS18 + 0.75 + 52.926/109.001
GS10 = GS22 + 0.95 + 181.315/175.498
GS12 = GS18 + 0.95 + 97.378/109.001
GS14 = GS18 + 0.95 + 52.926/109.001
GS16 = GS22 + 0.95 + 181.315/175.498
GS24 = GS18 + 1.10 + 97.378/109.001
GS26 = GS18 + 1.10 + 52.926/109.001
GS28 = GS22 + 1.10 + 181.315/175.498
GS30 = GS18 + 1.10 + 97.378/109.001
E GS31 = GS18 + 1.10 + 0.75 + 58.336/109.001
C GS33 = GS18 + 1.10 + 59.336/109.001 *.25
GS32 = GS18 + 1.10 + 52.924/109.001
GS34 = GS22 + 1.05 + 181.315/175.498
GS36 = GS18 + 1.10 + 21.271/109.001
GS38 = GS18 + 1.10 + 11.264/109.001

C
C
F TAVE = .5*(BT + AT)
F TDIFF = ABS(BT - AT)
F IF(TDIFF .GT. 0.) TDIFF = 1.0E-10

C COMPUTE FLUID TEMPERATURE
F TAVE = .5*(BT + AT)
F TDIFF = ABS(BT - AT)
F IF(TDIFF .GT. 0.) TDIFF = 1.0E-10

C COMPUTE FLUID DENSITY FROM TABLE LOOKUP OR IDEAL
GAS TABLES
F IF(ORND .GT. 0.) THEN
F RHOX = PRESS*144./((R*(TAVE+459.67))
F ELSE
F CALL D10EGT(TAVE, RND, RHOX)
F END IF

C COMPUTE HELEDOF NUMBER
F IF(ORND .GT. 0.) THEN
F HANE = 1./((TAVE+459.67)
F ELSE
F CALL D10EGT(TAVE, R, HANE)
F END IF
F CALL D10EGT(TAVE, W, HANE)
F OR = RND**2 + G*(3600.**2) *HANE *TDIFF
FOL=3/HANE**2

C COMPUTE PRANDTL NUMBER
F CALL D10EGT(TAVE, E, HANE)
F CALL D10EGT(TAVE, CP, SPANE)
F PE = CP*W + HANE*HANE

```

```

C COMPUTE CONVECTION HEAT TRANSFER COEFF. USING
C EQUATIONS 7-21, 7-22, & 7-23; FROM PRINCIPLES OF
HEAT TRANSFER, 3RD EDITION, FRANK INCITIS
C
C NA = PR * GR
F IF(ST .GE. AT .AND. NA .LT. 1E+09) THEN
C
C NOT SURFACE FACING DOWN ; LAMINAR FLOW
C
C NA = AREA * 0.27 * KAVE * (GR**PR)**-.25/CL
F ELSE IF(ST .GE. AT .AND. NA .GT. 1E+09) THEN
C
C NOT SURFACE FACING DOWN ; TURBULENT FLOW
C
C NA = AREA * 0.37 * KAVE * (GR**PR)**-.33/CL
F ELSE IF(ST .LT. AT .AND. NA .LT. 1E+09) THEN
C
C COLD SURFACE FACING DOWN ; LAMINAR FLOW
C
C NA = AREA * 0.54 * KAVE * (GR**PR)**-.25/CL
F ELSE IF(ST .LT. AT .AND. NA .GT. 1E+09) THEN
C
C COLD SURFACE FACING DOWN ; TURBULENT FLOW
C
C NA = AREA * 0.34 * KAVE * (GR**PR)**-.33/CL
F
F END IF
F RETURN
F END
C INCLUDE FROM/F
C SUBROUTINE FLOW/NA,ST,AT,AREA,CL,G,R,CP,K,U,
+ RHO, PRESS, R)
C
C NA = FREE CONVECTION HEAT TRANSFER CONDUCTANCE
FROM
C
C A HEATED PLATE FACING UP OR A COOLED PLATE
C FACING DOWN - BTU/HR-F
C ST = SURFACE TEMP - F
C AT = AMBIENT TEMP - F
C AREA= SURFACE AREA - SQ.-FT.
C CL = CHARACTERISTIC LENGTH - FEET
C G = GRAVITATIONAL CONSTANT - FT/SEC**2
C R = COEFF. OF THERMAL EXPANSION ARRAY - 1/F
C CP = SPECIFIC HEAT VS. TEMPERATURE ARRAY -
BTU/LB-F
C K = THERMAL CONDUCTANCE VS. TEMPERATURE ARRAY -
BTU/FT-HR
C U = ABSOLUTE VISCOSITY VS. TEMPERATURE ARRAY
C RHO = FLUID DENSITY ARRAY OR G. FOR IDEAL GAS
C PRESS = FLUID PRESSURE - LBS/SG.-INCH
C R = GAS CONSTANT
C
C REAL NA, ST, AT, AREA, CL, G, RHO, PRESS, R, GR,
+ PR, KAVE, WAVE, TRIFF, KAVE, CPAVE, RHOX
C
C COMPUTE MEAN FLUID TEMPERATURE
C
C TAVE = .5*(ST + AT)
F TDIFF = ABS(ST - AT)
F IF(TDIFF .EQ. 0.) TDIFF = 1.0E-10
C
C COMPUTE FLUID DENSITY FROM TABLE LOOKUP OR IDEAL
C GAS EQUATIONS
C
F IF(RHO .EQ. 0.) THEN
F RHOX = PRESS*144./((TAVE+459.67))
F ELSE
F CALL DINDEX(TAVE, RHO, RHOX)
F END IF
C
C COMPUTE GRASHOF NUMBER
C
F IF(RHO .EQ. 0.) THEN
F KAVE = 1./((TAVE+459.67))
F ELSE
F CALL DINDEX(TAVE, K, KAVE)
F END IF

```

```

F END IF
F CALL DINDEX(TAVE, U, UAVE)
GR = RHOX**2 *R*(5660.**2)* WAVE *10/IF
+KAVE**3/NAVE**2
C
C COMPUTE PRANDTL NUMBER
C
C CALL DINDEX(TAVE, K, KAVE)
C CALL DINDEX(TAVE, CP, CPAVE)
C PR = CPAVE * WAVE/KAVE
C
C COMPUTE CONVECTION HEAT TRANSFER COEFF. USING
C EQUATIONS 7-21, 7-22, & 7-23; FROM PRINCIPLES OF
HEAT TRANSFER, 3RD EDITION, FRANK INCITIS
C
C NA = PR * GR
F IF(ST .GE. AT .AND. NA .LT. 1E+09) THEN
C
C NOT SURFACE FACING UPWARD; LAMINAR FLOW
C
C NA = AREA * 0.54 * KAVE * (GR**PR)**-.25/CL
F ELSE IF(ST .GE. AT .AND. NA .GT. 1E+09) THEN
C
C NOT SURFACE FACING UPWARD; TURBULENT FLOW
C
C NA = AREA * 0.34 * KAVE * (GR**PR)**-.33/CL
F ELSE IF(ST .LT. AT .AND. NA .LT. 1E+09) THEN
C
C COLD SURFACE FACING UPWARD; LAMINAR FLOW
C
C NA = AREA * 0.27 * KAVE * (GR**PR)**-.25/CL
F ELSE IF(ST .LT. AT .AND. NA .GT. 1E+09) THEN
C
C COLD SURFACE FACING UPWARD; TURBULENT FLOW
C
C NA = AREA * 0.37 * KAVE * (GR**PR)**-.33/CL
F
F END IF
F RETURN
F END
C INCLUDE FROM/F
C SUBROUTINE FLOW/NA,ST,AT,AREA,CL,G,R,CP,K,U,
+ RHO, PRESS, R)
C
C NA = FREE CONVECTION HEAT TRANSFER CONDUCTANCE
FROM
C
C A VERTICAL FLAT PLATE - BTU/HR-F
C ST = SURFACE TEMP - F
C AT = AMBIENT TEMP - F
C AREA= SURFACE AREA - FT**2
C CL = CHARACTERISTIC LENGTH - FT
C G = GRAVITATIONAL CONSTANT - FT/SEC**2
C R = COEFF. OF THERMAL EXPANSION ARRAY - 1/F
C CP = SPECIFIC HEAT VS. TEMPERATURE ARRAY -
BTU/LB-F
C K = THERMAL CONDUCTANCE VS. TEMPERATURE ARRAY
- BTU/FT-HR
C U = ABSOLUTE VISCOSITY VS. TEMPERATURE ARRAY -
LB/FT-HR
C RHO = FLUID DENSITY ARRAY OR G. FOR IDEAL GAS
C PRESS = FLUID PRESSURE - LBS/SG.-INCH
C R = GAS CONSTANT
C
F REAL NA, ST, AT, AREA, CL, G, RHO, PRESS, R, GR,
+ PR, WAVE, KAVE, TRIFF, KAVE, CPAVE, RHOX, RR,
+ MUT
C
C COMPUTE MEAN FLUID TEMPERATURE
C
C TAVE = .5*(ST + AT)
F TDIFF = ABS(ST - AT)
F IF(TDIFF .EQ. 0.) TRIFF = 1.0E-10
C
C COMPUTE FLUID DENSITY FROM TABLE LOOKUP OR IDEAL
C GAS EQUATIONS

```



```

F      1F(IND .EQ. 0.) THEN
F      RHO = PRES**146./((TAVE+459.67)**3)
F      ELSE
F      CALL D1DESI(TAVE, RHO, RHOX)
F      END IF
C      COMPUTE GRASSHOP NUMBER
C      IF(IND .EQ. 0.) THEN
F      BAVE = 1./((TAVE+459.67)**3)
F      ELSE
F      CALL D1DESI(TAVE, B, BAVE)
F      END IF
F      CALL D1DESI(TAVE, U, UAVE)
F      GE = RHO**2
F      *D*(3600.**2)**BAVE**D1DIFF**CL**3/UAVE**3
C      COMPUTE PRANDTL NUMBER
F      CALL D1DESI(TAVE, K, KAVE)
F      CALL D1DESI(TAVE, CP, CPAVE)
F      PR = CPAVE * UAVE/KAVE
C      COMPUTE CONVECTION HEAT TRANSFER COEFF. USING
C      EQUATIONS 6-39 TO 6-42; HANDBOOK OF HEAT TRANSFER
C      FUNDAMENTALS, 2ND EDITION, ROSENHOW, SERFHETT, &
C      JAGNER
F      NA = PR * GE
C      CLAM = 1.3333**503/(1. +
F      (0.492/PR)**0.3625)**0.44444444
F      CLMB = 0.13**PR**0.22/(1. + 0.61**PR**0.81)**0.42
C      NUT = CLAM * NA**0.25
F      NUA = 2.8/(LOG(1. + 2.8/NUT))
F      NUF = CLMB * NA**.3333333
F      NU = (NUA**8. + NUF**8.)**.8. 1.444444444
C      NA = AREA * BAVE * NUT/EL
C      RETURN
F      END
F      INCLUDE SPYHALL.F
F      SUBROUTINE PRCHURKHA,ST1,ST2,AREA,H,K,HA,
F      CT,H,B,EP,K,U,
F      * RHO, PRESB, R)
C      HA = FREE CONVECTION HEAT TRANSFER COEFFICIENTANCE
C      WITHIN
C      A VERTICAL ENCLOSURE WITH ONE SIDE HEATED,
C      ONE
C      COOLED, AND THE TOP/BOTTOM ADIABATIC
C      BTU/HR-F
C      ST1= FIRST SURFACE TEMP - F
C      ST2= SECOND SURFACE TEMP - F
C      AREA= SURFACE AREA - SQ. FT.
C      H = CAVITY HEIGHT - FEET
C      DR = RATIO OF CAVITY TO INNER DIAMETERS
C      CL = CHARACTERISTIC LENGTH (GAP) - FT
C      G = GRAVITATIONAL CONSTANT - FT/SEC**2
C      B = COEFF. OF THERMAL EXPANSION ARRAY - 1/F
C      CP = SPECIFIC HEAT VS. TEMPERATURE ARRAY
C      BTU/LB-H-F
C      K = THERMAL CONDUCTANCE VS. TEMPERATURE ARRAY
C      WTRM/F-SF
C      U = ABSOLUTE VISCOSITY VS. TEMPERATURE ARRAY
C      RHO = FLUID DENSITY ARRAY OR D. FOR IDEAL GAS
C      PRESB = FLUID PRESSURE - LBS/SQ.-INCH
C      A = GAS CONSTANT
C      REAL HA, ST1, ST2, AREA, H, CL, G, RHO, PRESB,
F      B, CP,
F      * PR, BAVE, UAVE, D1DIFF, KAVE, CPAVE, RHOX
F      REAL NU, NUCKIT, NUA, NUT

```

```

C      COMPUTE MEAN FLUID TEMPERATURE
C      TAVE = .5*(ST1 + ST2)
C      D1DIFF = ABS(ST1 - ST2)
C      IF(D1DIFF .EQ. 0.) D1DIFF = (.001-10)
C      COMPUTE FLUID DENSITY FROM TABLE LOOKUP OR IDEAL
C      GAS EQUATIONS
F      IF(IND .EQ. 0.) THEN
F      RHO = PRES**146./((TAVE+459.67)**3)
F      ELSE
F      CALL D1DESI(TAVE, RHO, RHOX)
F      END IF
C      IF(IND .EQ. 0.) THEN
F      BAVE = 1./((TAVE+459.67)**3)
F      ELSE
F      CALL D1DESI(TAVE, B, BAVE)
F      END IF
C      COMPUTE GRASSHOP, PRANDTL, & RAYLEIGH NUMBERS
F      CALL D1DESI(TAVE, K, KAVE)
F      CALL D1DESI(TAVE, CP, CPAVE)
F      PR = CPAVE * UAVE/KAVE
F      NA = RHO**2 *D*(3600.**2)** BAVE *TDIFF
F      *CL**3/UAVE**2
C      NA = PR * GE
C      NUCKIT = 62.3*OH + 750
F      IFCBA .LE. 1,1*NUCKIT) GO TO 99
C      COMPUTE CONVECTION HEAT TRANSFER COEFF. USING
C      EQUATIONS 22 FROM "NATURAL CONVECTION IN VERTICAL
C      CHANNEL", JOURNAL OF HEAT TRANSFER, NOV. 1969,
C      PAGES 909
C      TO 915. NOTE: THE EQN. AS PUBLISHED CONTAINS
C      ERRORS.
C      SET THE EQN. FORMAT BELOW FOR CORRECT EXPONENTS.
C      ASPECT = H/CL
F      X1 = DR**((0.39087/DR) + 0.40764)
C      NUA = 0.158*(G**0.25)*X1/(RNUCKIT**0.0445)
C      NA = AREA * NUA * KAVE/EL
C      RETURN
F      99 CONTINUE
F      NUA = 1.
F      NA = AREA * NUA * KAVE/EL
F      RETURN
F      END
END OF DATA

```

RMIS View/Print Document Cover Sheet

This document was retrieved from the Documentation and Records Management (DRM) ISEARCH System. It is intended for Information only and may not be the most recent or updated version. Contact a Document Service Center (see Hanford Info for locations) if you need additional retrieval information.

Accession #: D196080893

Document #: SD-RTG-SARP-001

Title/Desc:

RTG TRANSPORTATION SYSTEM SARP DOCKET NO 94-6-9904
[VOL II] [SEC 4 OF 4]

Pages: 194

This document was too large to scan as a whole document, therefore it required breaking into smaller sections.

Document number: SD-RTG-SARP-001

Section 4 of 4

Title: RADIOISOTOPE THERMOELECTRIC GENERATOR
TRANSPORTATION SYSTEM SAFETY ANALYSIS REPORT
FOR PACKAGING

Date: 4/18/96 Revision: 0

Originator: FERRELL PC

Co: WHC

Recipient: _____

Co: _____

References: EDT-613639

4.0 CONTAINMENT

The Radioisotope Thermoelectric Generator (RTG) Transportation System Package possesses two levels of leaktight containment: the inner containment vessel (ICV), which acts as the secondary containment boundary, and the outer containment vessel (OCV), which acts as the primary containment boundary. Two levels of containment are required per 10 CFR 71.83¹ for packages transporting quantities of plutonium greater than 20 curies (Ci). Both the OCV and ICV containment boundaries are leaktight per the requirements of Paragraph 5.4 of ANSI standards N14.5².

Although the entire containment boundary is addressed herein, this section will concentrate on the butyl rubber elastomer O-ring seals used for maintaining closure between metallic components. The use of circular cross-section elastomer O-rings has been proven as a reliable method of sealing the containment system(s) of transportation packages subject to the requirements of 10 CFR 71. Of particular concern are the maximum temperature and minimum compression experienced by the containment O-ring seals over the course of the normal conditions of transport (NCT) and hypothetical accident condition (HAC) test requirements. This section will demonstrate that temperature and compression limits are met under all NCT and HAC events for both containment vessels of the RTG Transportation System Package.

4.1 CONTAINMENT BOUNDARY

Each of the two packaging vessels is an independent containment boundary, which consists of a bell, a base, two elastomer O-ring seals (one of which is the containment seal), an electrical feed-through connector, and one (for the OCV) or two (for the ICV) vent port plugs with elastomer O-ring seals. Both vessels are sealed between their flange and base by a pair of face-type O-rings, of which the inner O-ring is the containment seal and the outer O-ring is used for leakage rate testing purposes.

4.1.1 Containment Vessel

As described in Section 2.1.1.1, the OCV consists of a stainless steel base, to which a stainless steel bell is attached by 24, 1-1/4-in. diameter, high-strength steel alloy closure bolts. The bell is made of a cylindrical shell, welded to an American Society of Mechanical Engineers (ASME) torispherical head and a bolting flange. The bell flange fits within a counterbore in the base, which limits radial motion in an accident such that the closure bolts cannot be loaded in direct shear. The seal between the bell flange and the base is effected by two concentrically arranged butyl rubber O-ring face seals. The inner containment seal has a nominal diameter of 0.393 in., and the outer test seal has a nominal diameter of 0.275 in. Figure 4.1.1-1 illustrates an exploded view of the OCV containment boundary components.

As described in Section 2.1.1.2, the ICV consists of a stainless steel base to which a stainless steel bell is attached by 24, 3/4-in. diameter, high-strength steel alloy closure bolts. The bell is made of a cylindrical shell welded to an ASME torispherical head and a bolting flange. The bell fits closely over the base, which limits radial motion in an accident such that the closure bolts cannot be loaded in direct shear. The seal between the bell flange and the base is effected by two concentrically arranged butyl rubber O-ring face seals. Both the inner containment seal and the outer test seal have a nominal diameter of 0.276 in. Figure 4.1.1-2 illustrates an exploded view of the ICV containment boundary components.

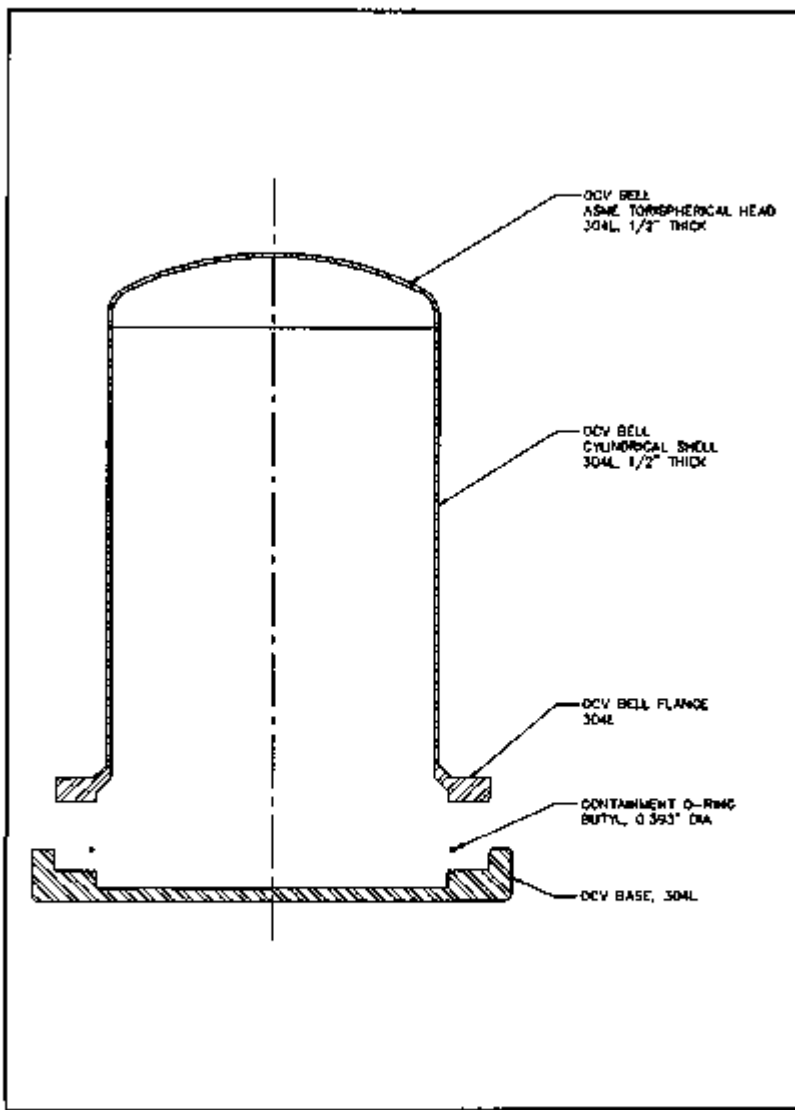


FIGURE 4.1.1-1. Exploded View of DCV Containment Boundary Components.

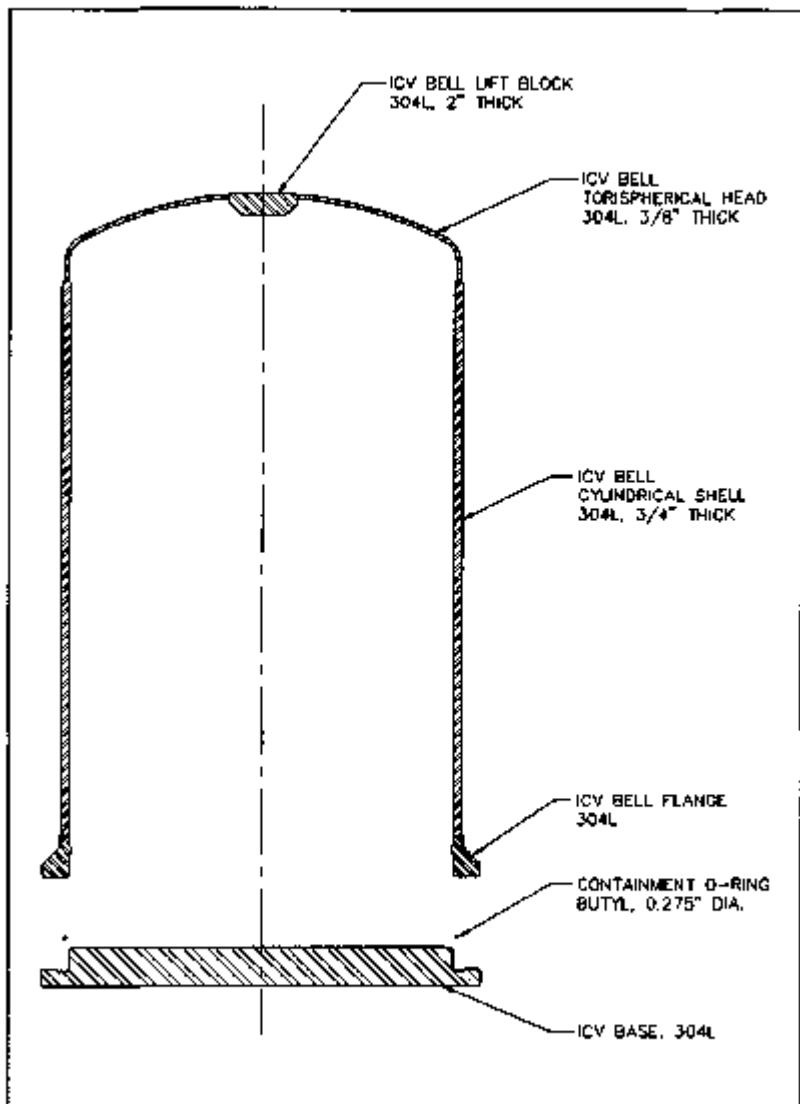


FIGURE 4.1.1-2. Exploded View of ICV Containment Boundary Components.

Two additional design features are used to help protect the integrity of the ICV containment boundary. The GPHS RTG payload requires a specific shipping rack assembly that has an integral barrier plate. The shipping rack assembly is securely fastened to the ICV base, and is designed to remain in place during a HAC drop to prevent heat generating payload debris from reaching the proximity of the ICV O-ring seal area. To further protect the ICV O-ring seals from smaller, nonheat generating debris, a stainless steel debris shield is located at the internal junction of the ICV ball and base.

Demonstration of containment vessel integrity under NCT and HAC free drops and HAC puncture drops has been primarily demonstrated by an extensive certification test program (see Appendices 2.10.9 and 2.10.10, and Section 2.7.8 for details).

4.1.2 Containment Penetrations

The containment vessels include two types of penetrations: (1) those that are periodically made and broken through the life of the package, and (2) those that are permanently installed during initial fabrication. The only OCV containment make-and-break type of boundary penetration is one vent port, through which air is evacuated from the annulus between the ICV and OCV, and through which helium is backfilled. One seal test port is also provided, but does not penetrate the OCV containment boundary because the port only accesses a region outboard of the containment O-ring. Vent and test port plugs are made of brass and sealed using butyl Parker Stat-O-Seals[®]. Each plug is protected by a brass cap sealed with a Teflon[™] weather gasket. An exploded view of the OCV vent port and cover design is shown in Figure 4.1.2-1.

A primary and secondary vent port, which are used during the helium purge process, are the only ICV make-and-break type of containment penetrations. One seal test port is also provided, but does not penetrate the ICV containment boundary because the port accesses a region outboard of the containment O-ring. Vent and test port plugs are made of brass and sealed using butyl Parker Stat-O-Seals[®]. An exploded view of the ICV vent port and cover design is shown in Figure 4.1.2-2.

One permanently installed electrical feed-through connector is installed in each containment boundary base plate. The electrical feed-through connector consists of an AISI Type 316L stainless steel body and sleeve, electrical conductor pins, and a glass sealing material between the body and the pins. Each electrical feed-through connector assembly fits closely within its surrounding base plate, and is sealed to the base plate material with a 3/16-in. fillet weld. Inside the ICV containment and outside the OCV containment, removable connectors are used to connect the electrical feed-through devices to the RTG-mounted thermocouples and to the recording devices, respectively. Permanent wire connections are used in conjunction with a spring-loaded pin contact assembly to complete the electrical feed-through circuit between the two vessels. See Figure 4.1.2-3 for a schematic of the electrical feed-through components. Details of the electrical feed-through components are shown in the drawings in Section 1.3.2. The containment boundary portions of the ICV and OCV electrical feed-through penetrations are shown in Figures 4.1.2-4 and 4.1.2-5, respectively.

The electrical feed-through assemblies are manufactured by D. G. O'Brien, part No. 1070019-112 (receptacle, containing the sealed pins). The connector used inside the ICV and outside the OCV is part No. 1071003-110 (straight plug). This design was tested by Teledyne Energy Systems to determine the peak temperature at which a leaktight seal can be assured. Two reports, HPG5-DST-238 and HPG3-DST-1000 (see Appendix 4.5.2,) conclude that an electrical feed-through device of this design can withstand temperatures of at least 475 °F before degradation of the seal can be expected. As shown in Section 2.10.7, the peak temperature of

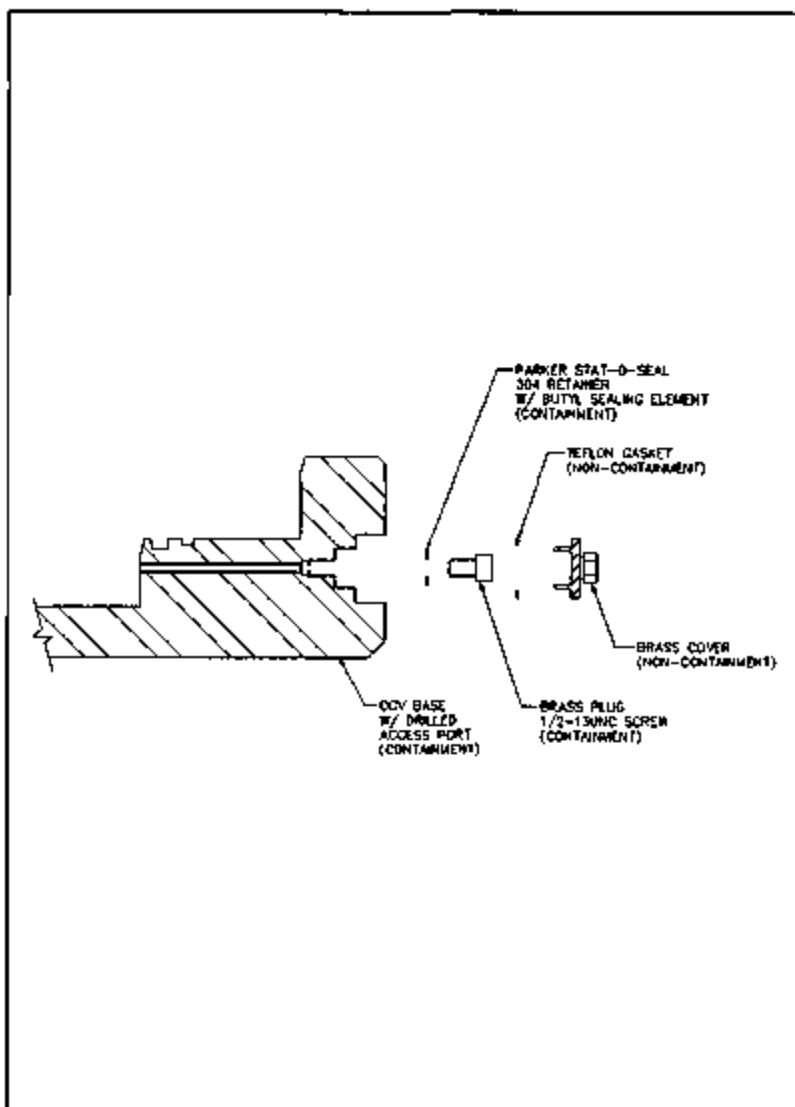


FIGURE 4.1.2-1. Exploded View of OCV Vent Port and Cover Design.

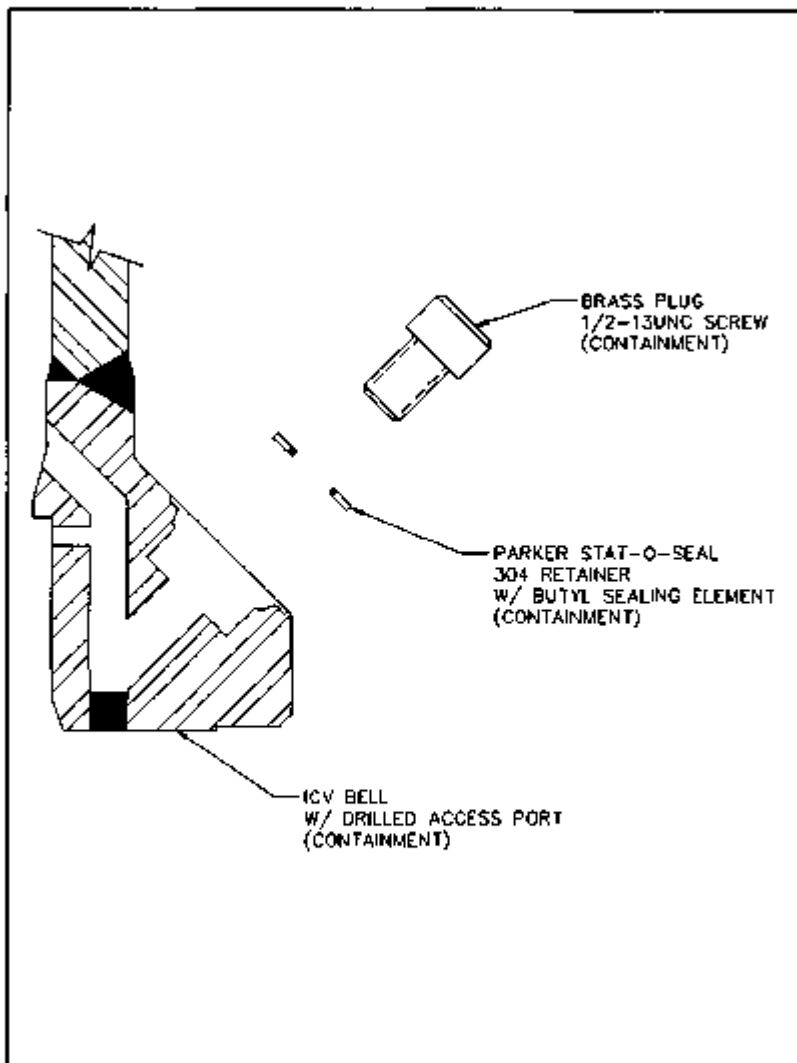


FIGURE 4.1.2-2. Exploded View of ICV Vent Port Design. (Primary and secondary vent ports are identical except for noncontainment primary vent port inner tube.)

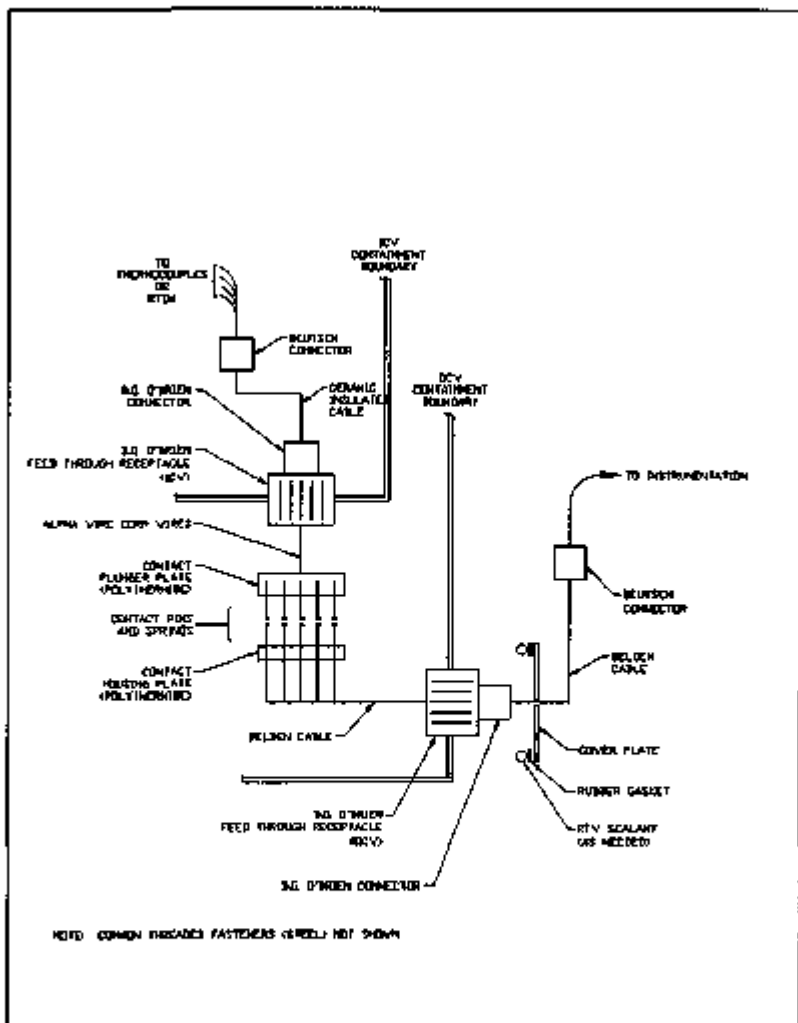


FIGURE 4.1.2-3. Feed-through Meterkite Schematic.

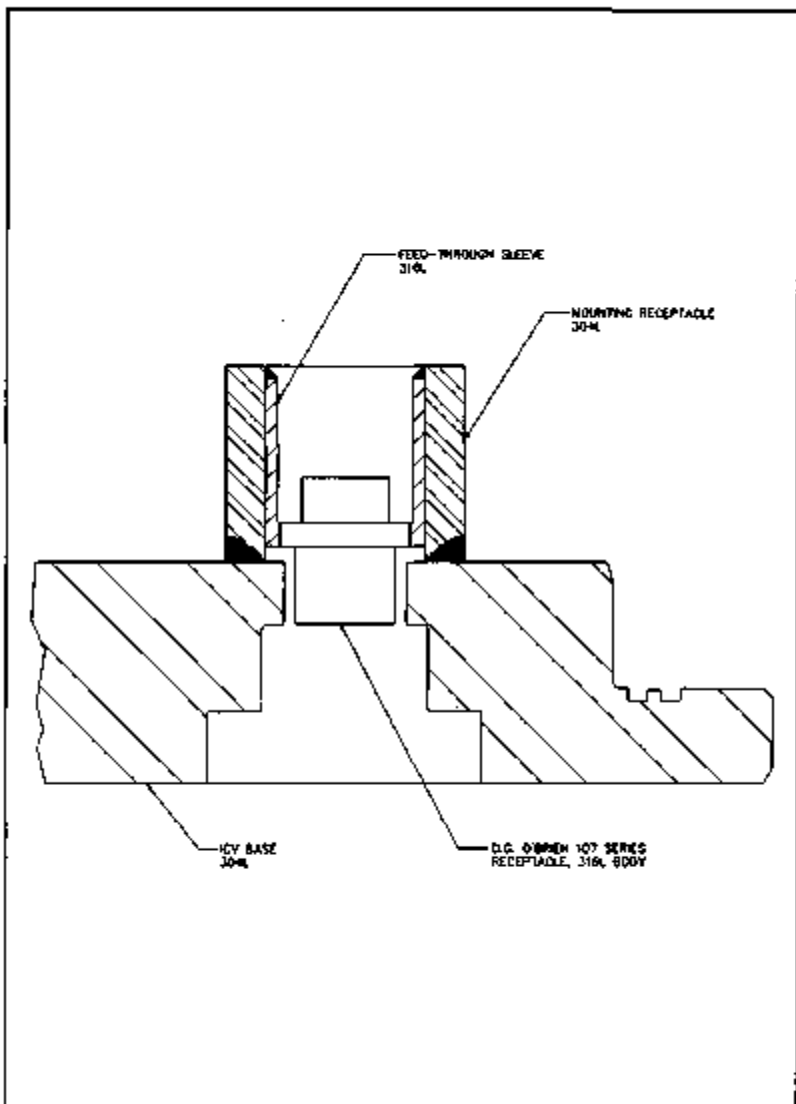


FIGURE 4.1.2-4. ICV Feed-through Containment Boundary Components and Welds.

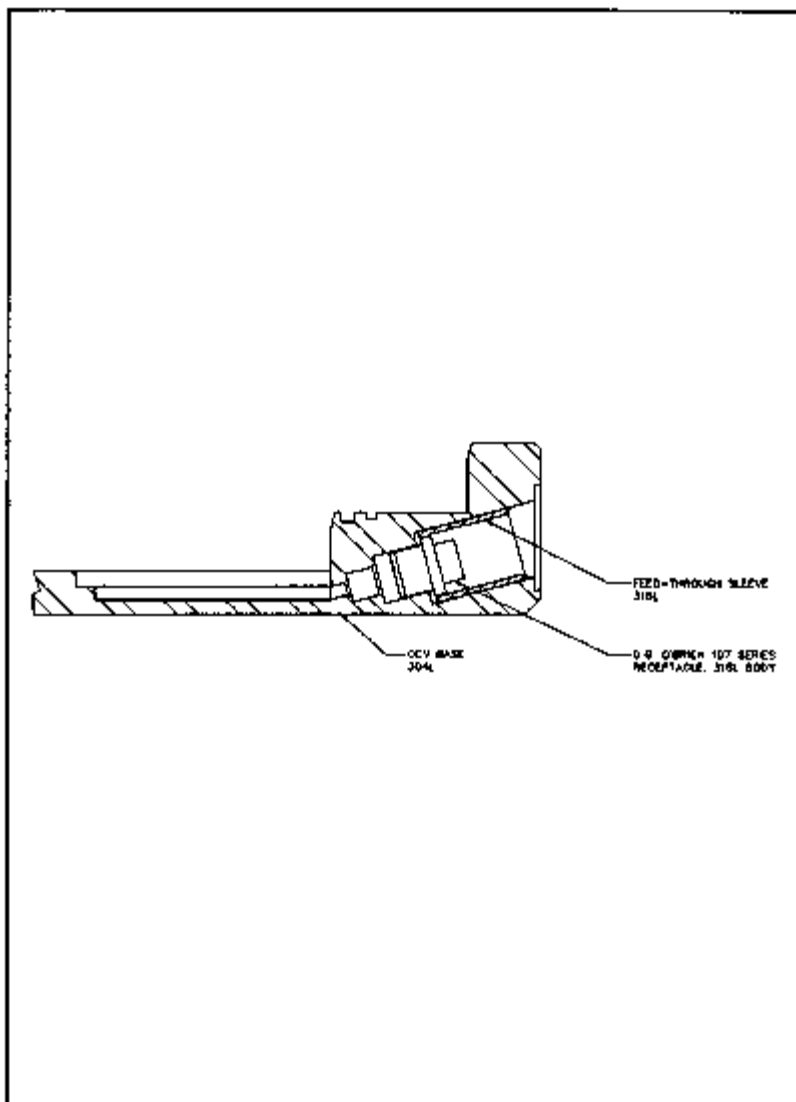


FIGURE 4.1,2-5. OCV Feed-through Containment Boundary Components and Welds.

thermal model node 269 (the ICV electrical feed-through) or node 368 (the OCV electrical feed-through) in the worst-case HAC event is 377 °F (for HAC load case No. 5). Thus, worst-case HAC electrical feed-through temperatures are well below those for which a leaktight seal has been demonstrated. The electrical feed-through connectors were also subjected to the full series of regulatory drop tests without loss of leaktight condition (see Section 2.7.6.).

4.1.3 Seals and Welds

4.1.3.1 Seals. The containment O-ring seals must possess the ability to maintain a leaktight seal (a leakage rate of less than 1×10^{-7} cc/sec air) when subjected to the compressions and temperatures associated with MCT and HAC events as defined by 10 CFR 71. Extreme conditions are addressed in the following sections. Emphasis is placed on the primary containment seals, because the vent and fill port seals do not experience any worst-case temperature or any loss of compression for the following reasons:

- The ICV vent port plugs, because of proximity to the main ICV seals, have virtually the same temperature as the main seals.
- The OCV vent port is located on the side of the base, in a position that is somewhat cooler than the primary OCV seals.
- The OCV and ICV vent ports are well protected within the impact limiter from frag drop or puncture bar impacts. Consequently, once sealed, no change of seal compression is experienced by the vent and fill port seals.

The compound chosen for the primary containment O-ring seals is butyl, Rainier Rubber compound No. RR-0405-70. Butyl rubber has excellent impermeability under helium pressure, thus enhancing leakage rate test operations. Further, this particular compound has also been approved by the Nuclear Regulatory Commission (NRC) for the TRUPACT-II Package.

Section 2.10.6 contains a report of leakage rate testing of seals fabricated from this compound. The material was made into O-rings and leakage rate tested in a fixture at various low temperatures and after high temperature soaks. The test fixture simulated a face-type seal, and the O-ring compression values were controlled by shims and O-ring groove depth. The test commenced with a leakage rate test at a seal temperature of -40 °F followed by a soak for a specified time at high temperature and another leakage rate test. Subsequent to the high temperature soak, the fixture was returned to -20 °F and leakage rate tested again. Permanent results are summarized in the following sections.

4.1.3.1.1 Cold Tests. Butyl rubber remained leaktight at -40 °F (before the high-temperature soak) and at -20 °F (subsequent to high temperature soak). The minimum compression in the test fixture was at least as low as 10%, as calculated in Section 2.10.6.

4.1.3.1.2 Elevated Temperature Tests. Elevated temperature tests were performed on the butyl rubber O-rings with compressions as low as 10%. The time/temperature test parameters were 380 °F for 24 hours followed by 350 °F for 144 hours for a total of 168 hours (1 week). At these high temperatures, rapid helium permeability of the O-rings occurs and helium leakage rate detection is not feasible. Therefore, after each of the high-temperature soak periods, a hard vacuum, less than 0.2 mbar, was pulled on the test O-rings. This indicated there were no leaks. At the end of the test sequence, the O-rings were stabilized at -20 °F and helium leakage rate tested. The O-rings were leaktight and showed no permanent degradation.

The data collected in the testing covers NCT cold and HAC fire temperatures. Normal regulatory warm conditions, however, are assumed to be experienced for up to 60 days. The test data can be conservatively extrapolated to 60 days as follows.

The high temperature capability of elastomer materials is commonly plotted on semilog scales, with temperature plotted on a linear ordinate and time on a logarithmic abscissa (see Figure A3-6 from the Parker O-ring Handbook³). Because of the direction of curvature of the elastomer time/temperature limit curves, the linear extrapolation from one time to a greater time is conservative, because it would result in a lower temperature limit than the one actually indicated by the curve itself. Therefore, linear extrapolation of time/temperature data to longer times is conservative, using a logarithmic scale for time. Linearly extrapolating the segment between the 380 °F/24-hour point and the 350 °F/144-hour point leads to

$$\frac{(380^{\circ} - 350^{\circ})}{\ln 144 \text{ hr} - \ln 24 \text{ hr}} = \frac{x}{\ln 1,440 \text{ hr} - \ln 144 \text{ hr}}$$

where x is the reduction in temperature limit below 350 °F because of the extension of soak time from 144 hours to 1,440 hours (60 days). Solving the above equation yields $x = 39$ °F. The conservative limit at 60 days is therefore 350 °F - 39 °F = 311 °F. The full range of acceptable temperature/time results for the butyl material is shown in Table 4.1.3.1.2-1.

TABLE 4.1.3.1.2-1. Performance Capability of Rainier Rubber RR-0405-70 Butyl Rubber (compressed at 10%).

Seal temperature (°F)	Time at temperature	Leaktight	Related conditions
-40	Steady state	Yes	NCT cold
311	Steady state (60 days)	Yes	NCT warm
350	Steady state (144 hours)	Yes*	HAC post fire
380	24 hours	Yes*	HAC peak fire

*The O-rings were subjected to a hard vacuum (less than 0.2 mbar). This was used to infer they were leaktight.

4.1.3.1.3 Impermeability and Helium Retention. Heat rejection by the payload depends, in part, upon the convection currents within the ICV. For this purpose, a nominal charge of 19 psia of helium gas is used during shipment of the payloads. Butyl rubber has excellent helium gas retention capability, as is demonstrated in the following calculations.

The Parker O-Ring Handbook³, page A2-4, gives this relation for permeation through an O-ring seal:

$$L = (0.7) FDPO (1 - S)^2$$

111

where: L = approximate permeation rate, scc/sec
 F = permeability rate, scc-cm/cm²-sec-bar
 D = O-ring inside diameter, in.
 P = differential pressure across seal, psid
 Q = permeability factor (Parker Table A2-2)
 S = percent compression, expressed in decimal form

From Figure A2-2 of Reference 3, conservatively assume Q is equal to 1.82 for a dry O-ring. Then, using Table A2-4, F at temperature is as shown in Table 4.1.3.1.3-1.

Table 4.1.3.1.3-1. Permeability Rate Versus Temperature for Butyl Elastomer.

Temperature (°F)	F cc-cm/cm ² -sec-bar
178	52(10) ⁸
302	240(10) ⁸

Linearly interpolating for the maximum NCT seal temperature of approximately 220 °F, a value for F of 117.65(10)⁸ results. Assuming a conservatively large diameter for the seals of 40 in., and a conservatively low value of minimum squeeze, S, of 0.15 (15%), the permeation rate as a function of internal pressure will then be the following:

$$L = 3.618(10)^8 (P) \text{ scc/sec} \quad (2)$$

The loss of pressure over time within the ICV will be what is known as a first order fall, that is, exponential. It can be determined by considering the perfect gas law given below:

$$PV = nRT \quad (3)$$

where: P = pressure, psia
 V = void volume of ICV, 22.25 ft³ (see Section 2.5.1.1.1)
 n = the number of lb-moles
 R = the gas constant, 10.74 psia-ft³/lb-mole-°R (Handbook of Chemistry and Physics)
 T = temperature, 460 + 220 = 680 °R

Differentiating this equation with respect to time, yields the following:

$$\frac{dP}{dt} = \left(\frac{RT}{V} \right) \frac{dn}{dt} \quad (4)$$

Because there are $3.53(10)^3$ standard cubic feet in a standard cubic centimeter and 352 ft³ in one lb-mole of any gas¹, the permeation rate, L , is converted into lb-moles per second, which is identical to the quantity dn/dt above:

$$\frac{dn}{dt} = -3.26(10)^{-12} (P) \text{ lb-moles/sec}$$

where the minus sign signifies a decreasing quantity of moles in the ICV. Substituting this into Equation 4, along with values for R , T , and V , and rearranging, yields the following:

$$\frac{dP}{P} = -1.07(10)^{-4} dt$$

This differential equation is solved to yield the following:

$$\ln P = -1.07(10)^{-4} (t) + C \quad [5]$$

The constant of integration is evaluated by noting that, from Section 2.6.1.1, the ICV internal pressure differential is 10 psid. Taking $t = 0$, the constant C is determined to be 2.303. Substituting this value and performing the exponential on Equation 5, the pressure differential with respect to time is given below:

$$P = \exp [-1.07(10)^{-4} (t) + 2.303] \text{ psid} \quad [6]$$

Using Equation 6 with 86,400 seconds/day, the remaining differential pressure after 60 days (maximum assumed transport duration) is 9.949 psid, where $60 \times 86,400$ has been used for t . This is a drop of $10.0 - 9.949 = 0.051$ psid, or the following:

$$\left(\frac{0.051}{10.0} \right) \times 100 = 0.51\%$$

In one year (i.e., $3.1536(10)^7$ seconds), the pressure differential will fall to 9.872 psid, a decrease of 0.328 psid, or 3.28%.

¹Obtainable from the perfect gas law for ambient pressure and 77 °F, which is the standard leak test temperature used in ANSI N14.5.

4.1.3.1.4 Temperature Conditions. 10 CFR 71 requires the package containment seals to successfully operate under the following conditions:

1. Ambient temperature of -40 °F, no insulation, internal heat load, or dynamic conditions
2. Ambient temperature of -20 °F, no insulation or internal heat load, with HAC free drop and puncture events
3. Ambient temperature of 100 °F, maximum insulation and internal heat load with and without active cooling
4. Ambient temperature of 100 °F, maximum insulation and internal heat load, with HAC free drop and puncture events
5. Ambient temperature of 1476 °F for 30 minutes, maximum internal heat load, subsequent to HAC free drop and puncture events.

To determine the temperature conditions and exposure times experienced by the O-ring seals, detailed thermal analyses were made for each of the above conditions. Two aspects of package configuration were taken into account to determine these relationships.

1. The redundant active cooling systems are assumed to be inoperative when maximum temperatures are calculated per 10 CFR 71.51(b).
2. For HAC, the possibility of payload structural failure and reconfiguration has been considered. Analysis of the GPHS RTG by its manufacturer (General Electric) established that the smallest heat-producing elements that could be released from the GPHS RTG would be the 18 heat source modules, which are brick-like rectangular aeroshells designed to survive atmospheric re-entry conditions. A worst-case configuration of the aeroshells was considered in the HAC thermal analyses.

The temperatures and times corresponding to the above five conditions are listed in Table 4.1.3.1.4-1. Maximums for either OCV or ICV containment seals are presented. Comparison with Table 4.1.3.1.2-1 indicates that seals will remain leaktight for all conditions.

TABLE 4.1.3.1.4-1. Package O-ring Seal Environments.

Seal temperature (°F)	Time at temperature	Condition (as defined in 4.1.3.1.4 above)	Case No. (from Secs. 2.6.1 and 2.7.3)
-40*	Steady state	(1) NCT cold	-
-20*	Steady state	(2) Initial cold condition for HAC free drop and puncture	-
53	Steady state	(3a) Normal operating steady state (with cooling)	NCT case 3
219	80 days (1,440 hours)	(3b) NCT regulatory steady state (without cooling)	NCT case 1
323*	1 week (168 hours)	(4) Post-HAC steady state with reconfigured payload	HAC case 5
360*	Instantaneous peak	(5) Reconfigured payload plus HAC fire	HAC case 5

*Because the minimum payloads heat load is assumed to be zero, the minimum temperatures are taken as identical to prescribed ambient.

*A post-HAC recovery time of 168 hours (1 week) is used, consistent with 10 CFR 71.51(a)(2).

*This is the maximum temperature that could result from a reconfigured payload plus 10 CFR 71 HAC fire conditions. The temperature duration above 350 °F is about 15 hours.

4.1.3.2 Welds. All containment welds, except the ICV vent port plug welds and those associated with the electrical feed-through connector, are full penetration, radiograph inspected, and in full accordance with NUREG/CR-3019⁸. The electrical feed-through weld (GTAW) and vent port plug welds are classified as nonstructural, seal-type welds. Per Subsection NB-6271, Section III of the ASME Boiler and Pressure Code, liquid penetrant inspection of this type of weld is sufficient to qualify the weld integrity. Containment weld integrity under NCT and HAC free drops and HAC puncture drops has been demonstrated by the certification test program (see Section 2.7.6.)

4.1.4 Closure

The OCV closure is effected by 24, 1-1/4-in. diameter bolts, torqued to 300 ± 30 ft-lb. The ICV closure is via 24, 3/4-in. diameter bolts, torqued to 260 ± 25 ft-lb. The OCV closure bolt material is ASTM-A320, Grade L43 and the ICV closure bolt material is ASTM-A540, Grade B23. All closure bolts are cadmium plated.

4.2 REQUIREMENTS FOR NORMAL CONDITIONS OF TRANSPORT

4.2.1 Containment of Radioactive Material

The release rate limits of 10 CFR 71.51 are satisfied by the leaktight sealing criterion (a leakage rate of less than 1×10^3 acc/sec air) imposed on the RTG Transportation System Package. All elastomeric sealing components are sized and dimensioned so that minimum seal compression during the NCT test sequence is never less than that demonstrated to be adequate for leaktight

sealing (see Section 4.1.3.1). Additionally, the maximum O-ring seal temperature for NCT is maintained below the allowable limit. This limit, as listed in Table 4.1.3.1.2-1, is 311 °F for 60 days. The maximum calculated seal temperature for NCT, from Table 4.1.3.1.4-1 is 219 °F. The structural and leaktight integrity of the remaining containment boundary is demonstrated by reference to Section 2.6.1.3 and the successful leakage rate testing of both ICV and QCV vessels at the end of the structural certification testing. Consequently, containment is maintained for the RTG Transportation System Package under NCT.

4.2.2 Pressurization of Containment Vessel

The maximum normal operational pressure (MNOP) for the ICV is 30 psia. This includes the nominal operational installed pressure of 19 psia, as well as a conservative allowance for thermal increase and gas pressure buildup, as detailed in Section 2.6.1.1.1. The analyses in Section 2.6.1 demonstrate that this pressure has negligible consequences on the ICV operation.

The MNOP for the QCV is also 30 psia. This value results from conservative upward adjustment of the nominal operational installed pressure of 19 psia to account for thermal increase. Again, as shown in Section 2.6.1, the consequences of this internal pressure have been shown to be insignificant.

4.2.3 Containment Criterion

Package containment for NCT is ensured by initially accepting packaging hardware that has been demonstrated to be leaktight, by maintaining O-rings and electrical feed-through connectors below their respective time-temperature limits, and by the maintenance of the minimum O-ring compression. A combination of certification testing and analysis helps establish minimum residual O-ring compression and maximum O-ring temperature for NCT. Electrical feed-through connector temperature limits are established by test as detailed in Appendix 4.5.2. All main containment seals and vent port plug seals are leakage rate tested at the time of package assembly.

Maximum O-ring seal temperatures for NCT are maintained below the temperature limit established for the 60-day maximum shipping period. The NCT seal area distortion does not control the minimum residual compression requirement. This is because temperatures and temperature gradients, as well as impact-induced seal area deformations, are worse for the HAC events, as detailed below. Similarly, maximum electrical feed-through temperatures are controlled by HAC.

4.3 CONTAINMENT REQUIREMENTS FOR HYPOTHETICAL ACCIDENT CONDITIONS

4.3.1 Fission Gas Products

As detailed in Section 2.6.1.1.1, the gas product developed by the GPMS RTG payload is a maximum of 2.08(10)⁷ acf/acc of helium. The resulting pressure increase is insignificant, and is accounted for (in Section 2.6.1.1.1) by conservatively increasing the calculated ICV normal operating pressure.

4.3.2 Containment of Radioactive Materials

The release rate limits of 10 CFR 71.51 are satisfied by the leaktight sealing criterion imposed on the RTG Transportation System Package. Leak tightness is determined by the containment criteria set out below. These criteria depend in part on maintenance of a minimum residual containment O-ring seal compression during and after the HAC test sequence, including the fire event. An important aspect of the containment capability of the containment vessels is the maximum amount of relative differential thermal expansion between seal flange and base plate exhibited during and following the HAC fire event. Additionally, maximum allowable O-ring seal temperatures and times at temperature are imposed per Section 4.1.3.1.2, and all O-ring seal temperatures must be maintained below the allowable limits. Maximum electrical feed-through connector temperature is imposed per Section 4.1.2.

Thermal distortion values were determined from the ANSYS finite element models presented in Appendices 2.10.12 and 2.10.8. The ICV deflections were determined with a three-dimensional (3-D) finite element model. An axisymmetric model was used to evaluate OCV thermal expansions, because it exhibits much more uniform circumferential temperature distributions. This is because the OCV does not have concentrated heat sources (aerohulls) applied directly to its interior, and the HAC fire is applied uniformly to the OCV exterior. Temperatures used for both ICV and OCV models were derived from the 3-D SINDA thermal analysis code (see Section 3.4.1). The temperatures used for the axisymmetric OCV model are conservatively assumed to be those of the warmest segment of the 3-D thermal model. Appendix 2.10.13 demonstrates the conservatism of this approach.

The HAC load cases evaluated are detailed in Section 2.7.3.1.1.3. All HAC load cases combine maximum HAC free drop and puncture damage with the HAC fire. The thermal load cases evaluated comply with the load combination requirements of 10 CFR 71 and Regulatory Guide 7.8 by imposing minimum and maximum ambient temperature conditions (-20 and 100 °F, respectively) with package temperatures arising from minimum and maximum payload heat generation. The maximum heat is generated by the GPHS RTG payload. Minimum payload heat generation and minimum ambient temperature result in essentially uniform package component temperatures. The structural and containment effects of this load case are insignificant and are not included in the summary table. In addition to the regulatory load combinations, the nonregulatory combination of minimum ambient temperature and maximum payload heat generation is conservatively imposed. This latter load case is evaluated because of its greater potential for inducing maximum differential thermal expansions in the package components.

Relative differential thermal expansion results at the containment seal location for both vessels are summarized in Tables 4.3.2-1 and 4.3.2-2. The HAC load cases are defined in Section 2.7.3.1.1.3. The effect of thermal distortion of the vessel flanges is a rotation of the flange, which causes a slight separation of the flange and base in the area of the O-rings. The amount of rotation at the location of the containment O-ring seal can be converted directly into compression reduction, as shown below. To the thermal separation must also be added the separation resulting from distortions related to the free drop and puncture events. The measurements of the seal area taken after the full series of NCT free drops and HAC free drops and puncture events are given in Section 2.10.14. The conservative assumption is made that the maximum seal area separation from drop events is circumferentially coincident with the maximum thermal distortion separation.

For the OCV containment seal, the minimum O-ring diameter is 0.388 in. The maximum seal area groove depth is 0.285 in. From Table 4.3.2-1, the maximum thermally-induced separation for HAC load case 6 is 0.0263 in., and from Table 2.10.14-2, the HAC free drop event-induced separation is 0.005 in., for a total compression reduction of 0.0313 in. Minimum O-ring percent compression is given below.

$$\left[\frac{0.388 - 0.285 - 0.0313}{0.388} \right] \times 100 = 18.1\% \quad (9)$$

For the ICV containment seal, the minimum O-ring diameter is 0.270 in. The maximum seal area groove depth is 0.203 in. From Table 4.3.2-2, the maximum thermally-induced separation for HAC load case B is 0.0098 in., and from Table 2.10.14-1, the HAC free drop event-induced separation is 0.0107 in., for a total compression reduction of 0.0108 in. Minimum O-ring percent compression is given below:

$$\left[\frac{0.270 - 0.203 - 0.0108}{0.270} \right] \times 100 = 20.8\%$$

Of the two containment vessels, the OCY possesses the least containment O-ring seal compression in the worst case HAC fire, having a value of 18.1%. This value results from the worst case tolerances on the O-ring and the O-ring mounting groove, as well as (1) measured distortions caused by the free drop and puncture events and (2) calculated thermal distortions resulting from worst case HAC fire and payload reconfiguration assumptions. In Appendix 2.10.5, Table 3 shows that the butyl material used for the RTG packaging containment seals was capable of maintaining a leaktight seal under conditions of 10% compression, while subjected to temperature conditions that were more severe than those predicted for the containment seals both during and after the HAC fire. Therefore, containment will be maintained in the HAC fire event.

TABLE 4.3.2-1. Maximum Seal Area Distortion and Residual Compression for the OCY.

HAC load case No.	Case 1	Case 2	Case 3	Case 4	Case 5	Case 6
Maximum thermal axial separation (in.)	0.0213	0.0255	0.0218	0.0260	0.0222	0.0263
Maximum permanent axial separation (in.)	0.006	0.006	0.006	0.006	0.006	0.006
Sum (in.)	0.0273	0.0316	0.0278	0.0320	0.0282	0.0323
Minimum residual O-ring compression (%)	19.1	18.0	19.0	17.9	18.9	17.8

TABLE 4.3.2-2. Maximum Seal Area Distortion and Residual Compression for the ICV.

HAC load case no.	Case 1	Case 2	Case 3	Case 4	Case 5	Case 6
Maximum thermal axial separation (in.)	0.0088	0.0091	0.0091	0.0084	0.0086	0.0089
Maximum permanent axial separation (in.)	0.001	0.001	0.001	0.001	0.001	0.001
Sum (in.)	0.0098	0.0101	0.0101	0.0104	0.0106	0.0109
Minimum residual O-ring compression (%)	21.2	21.1	21.1	21.0	20.9	20.8

According to reference 23, the preload force may vary by up to $\pm 30\%$ for a given applied torque value. The low end of this range (i.e., 70% of nominal preload force) could allow a greater thermal axial separation to occur. Therefore, the cases for each vessel having the largest thermal axial separation were run using a pre-stretch in the elements representing the bolts of 70% of the nominal preload force. For both vessels, the worst case is HAC load case 5. The results are given in Table 4.3.2-3. Minimum residual O-ring compression is calculated using the equations previously presented for each vessel. As shown, the minimum compression (again for the OCV) is well above the limit established by testing and discussed in Section 2.10.6.

TABLE 4.3.2-3. Maximum Seal Area Distortion for Low-limit Bolt Preload (70% of Nominal).

Vessel and HAC load case no.	ICV (Case 4)	OCV (Case 8)
Maximum thermal axial separation (in.)	0.0100	0.0303
Maximum permanent axial separation (in.)	0.001	0.006
Sum (in.)	0.0110	0.353
Minimum residual O-ring compression (%)	20.7	17.0

A summary of containment O-ring seal and electrical feed-through connector maximum HAC temperatures is summarized in Table 4.3.2-4. Time at temperature can be evaluated from Figures 3.5.3-1 to 3.5.3-6. As discussed in Sections 3.4.2 and 3.5.3, the OCV electrical feed-through connector temperatures are in each case lower than the ICV electrical feed-through temperatures, and are therefore not listed.

TABLE 4.3.2-4. Summary of Maximum O-ring Seal and Electrical Feed-through HAC Temperatures.

HAC load case No.	Case 1	Case 2	Case 3	Case 4	Case 5	Case 6
OCV peak seal temperature ($^{\circ}$ F)	317	218	320	222	325	229
ICV peak seal temperature ($^{\circ}$ F)	322	227	325	233	360	289
ICV peak feed-through ($^{\circ}$ F)	332	240	314	220	377	288

4.3.3 Containment Criterion

Package containment for HAC is ensured by maintaining O-rings and electrical feed-through connectors below their respective time-temperature limits, and by the maintenance of the minimum required O-ring compression. A combination of (1) certification testing and (2) analysis determines

minimum resultant O-ring compression and maximum O-ring temperature for HAC events. O-ring and electrical feed-through connector temperature limits are established by test as detailed in Section 2.10.6 and Appendix 4.6.2, respectively.

1. Certification testing has determined what seal area deformations may arise from the HAC free drop and puncture events, as well as to determine worst-case deformations of the thermally-insulating impact limiter. Seal area measurements are detailed in Section 2.10.14.
2. Worst-case temperatures are established by analysis, and are evaluated against the limits for temperature sensitive components such as containment O-ring seals and electrical feed-through connectors. Analytically derived temperatures are then used with structural analysis to establish maximum sealing surface deformations. Worst-case payload heat redistribution is assumed, and worst-case impact limiter deformations (extrapolated to maximum temperatures using certification test unit deformations) are used. Additionally, closure bolt stresses are limited to the yield strength of the bolting material to ensure that there will be no additional reduction in containment seal compression.

For a detailed summary of HAC thermal load cases used in evaluating seal area differential thermal expansions, see Sections 2.7.3.1.1.1 and 2.7.3.1.1.2. The load cases evaluated for the HAC fire event are given below.

1. Package in upright position, GPHS RTG aeroshells situated symmetrically around the perimeter of the payload shipping rack barrier plate in positions nearest the ICV containment seal.
2. Package lying on its side, GPHS RTG aeroshells situated linearly along the length of the ICV, from the payload shipping rack barrier plate to the ICV torispherical head.
3. Package conservatively balanced in an unstable position at a 45° angle. GPHS RTG aeroshells piled up in one corner (at the intersection of the shipping rack barrier plate and the ICV wall) in random orientations.

Summaries of relative differential thermal expansion values (relative expansion between seal flanges and base sealing surfaces) for all HAC load cases are presented in Tables 4.3.2-1 and 4.3.2-2. The worst-case impact limiter deformation was used for all HAC load cases, as discussed in Section 2.7.3.1.1.3.

Leak tightness for both vessels comprising the RTG Transportation System Package following the full-scale structural certification testing has been demonstrated (see Section 2.7.2.3). It has also been shown that the containment seals meet the temperature and residual compression requirements under the combined effects of the following:

- Maximum combinations of seal area deformations arising from the NCT and HAC free drops and HAC puncture tests
- Maximum seal area relative thermal differential expansion arising from worst-case assumptions regarding post-HAC impact package and payload reconfiguration.

Summaries of minimum residual O-ring seal compressions for the various HAC load cases are given in Tables 4.3.2-1 and 4.3.2-2. Maximum HAC O-ring seal temperatures are summarized in Table 4.3.2-4. The butyl O-ring material capabilities are given in Appendix 2.10.6. No loss of containment or leaktight capability is suffered by the package in any NCT or HAC event.

4.4 SPECIAL REQUIREMENTS

The special requirements of 10 CFR 71.63 apply to the RTG Transportation System Package. As detailed above, the secondary containment of the package consists of an ICV. This vessel and the primary containment, the OCV, both feature leaktight sealing capability, ensuring compliance with the regulatory release rate limits.

4.5 APPENDIX

The following is a list of appendices contained within this section:

4.5.1 References

4.5.2 Teledyne Test Reports

4.6.1 References

1. 10 CFR 71, 1983, "Packaging and Transportation of Radioactive Materials," Code of Federal Regulations, as amended.
2. ANSI 1987, *American National Standard for Radioactive Materials--Leakage Tests on Packages for Shipment*. ANSI Standard N14.5, American National Standards Institute, New York, New York.
3. *Parker O-Ring Handbook*. ORD 5700, Parker Seal O-Ring Division, Lexington, Kentucky.
4. *Handbook of Chemistry and Physics*, 66th Edition, Chemical Rubber Co., Boca Raton, Florida.
5. NUREG/CR-3019 1985, *Recommended Welding Criteria For Use in the Fabrication of Shipping Containers for Radioactive Materials*.

4.5.2 Teledyne Test Reports HPG5-DST-238 and HP03-DST-1000

MEMORANDUM**TELEDYNE
ENERGY SYSTEMS**

20 February 1982

Refer to: HPG5-DST-236

To: T. Christenbury, W. Brittain, O. Anderson, M. McKittrick, T. Hammett, A. Lieberman,
C. Heuser, E. Chayrszyn, K. Campbell

From: D. Trimmer

Subject: Results of Five-Watt High Pressure Receptacle Thermal Margin Tests

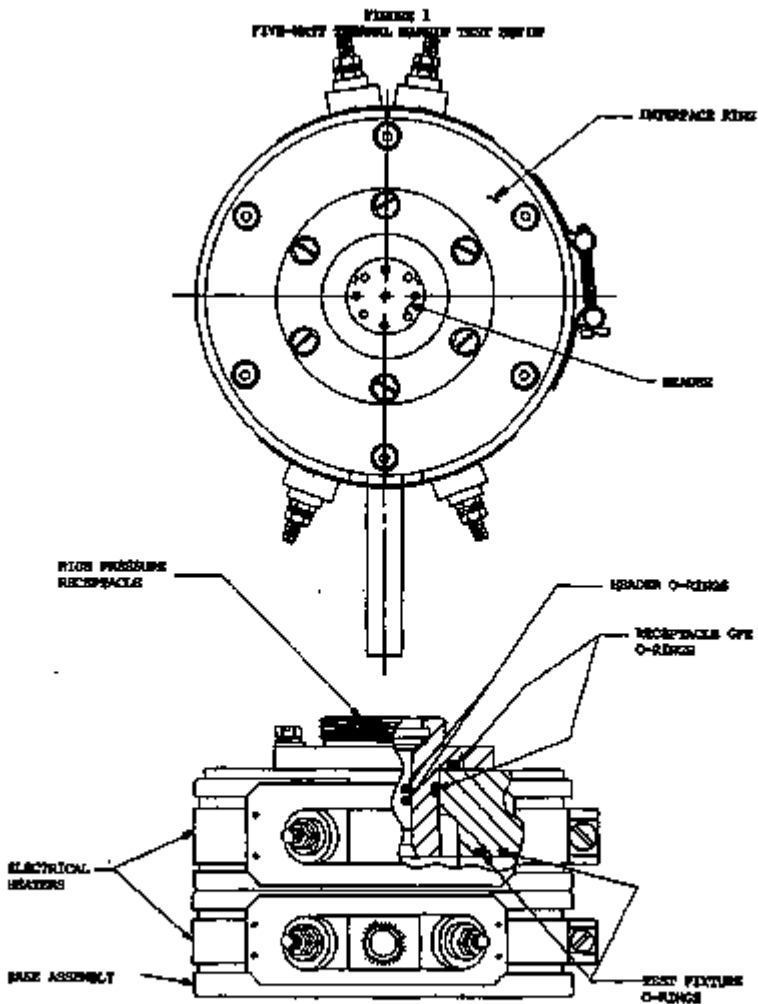
Introduction

Two Five-Watt high pressure receptacles were selected to undergo thermal margin testing in accordance with the HPG MOD 3/Five-Watt RTG High Pressure Electrical Receptacle Elevated Temperature Qualification Test Procedure, HPGA3040303. Figure 1 shows the receptacle mounted in the test fixture. Receptacles S/N 5291AD and S/N 5296AD were chosen for the tests. Both receptacles underwent identical inspection, thermal testing and evaluation procedures. The part numbers of the two receptacles differed because the receptacle headers were fabricated using different materials. Receptacle S/N 5291AD had a monel header and the part number was C12C0072GQ1. Receptacle S/N 5296AD had a stainless steel header and the part number was C12C0072GQ6.

The thermal margin test is divided into two phases. The first is a thirty day soak of the receptacle at 400 °F followed by a test of the header only which basically consists of quickly heating the high pressure receptacle headers one at a time to a temperature high enough to cause a failure in the glass-to-metal hermetic seals. Ideally, the heating rate is sufficiently high that the glass-to-metal hermetic seal failure occurs before any failure can occur of O-rings used in the test configuration. Failure is indicated by a rapid increase in the measured helium leak rate for a small temperature increase. At failure, the measured leak rate typically increases 2 or 3 orders of magnitude with very little temperature increase.

Initial Inspection of Receptacles

The O-rings and O-ring grooves of both receptacles were inspected and measured. In addition, the headers were removed from their receptacle bodies and the header O-rings were discarded. The solder cups of all the pins for each header were filled with solder using the Five-Watt standard procedure to simulate attachment of wires. Eutectic lead-tin solder and Kester's type 1644 flux were used. The soldered pins were cleaned using the standard Five-Watt procedure.



A new set of header O-rings and the O-ring grooves were inspected and measured. After installing the new O-rings, the headers were inserted into the receptacle bodies. The percent fill for each of the O-rings (header and receptacle) in its O-ring groove was calculated and is recorded in Table 1. As noted in the table, each of the four O-rings had an approximate 70% fill in their respective O-ring groove.

TABLE 1

PERCENT FILL AND COMPRESSION SET

FOR O-RINGS USED IN FIVE-WATT THERMAL MARGIN TEST

O-Ring ¹	Location	Receptacle S/N 5291AD		Receptacle S/N 5298AD	
		% Fill	Compression Set (%) ²	% Fill	Compression Set (%)
-224	Receptacle Flange	69.7	65.0	70.0	63.1
-21B	Receptacle Gland	68.3	34.6	68.2	42.7
-118	Header #1	69.3	19.5	68.8	0
-118	Header #2	69.3	0	69.0	5.0
Predicted Compression Set for Thermal History Experienced			64		68

1. All O-rings are Viton™ per M8324871.
2. Measured after 30-day soak at 400 °F.

¹ Viton is a registered trademark of the E.I. duPont de Nemours Company.

A helium leak test of the receptacle before and after soldering the pins was used to confirm that the thermal cycle of the soldering operation did not cause damage to the glass-to-metal hermetic seals.

Thermal Margin Test - Receptacle S/N E291AD

High pressure receptacle S/N E291AD was installed into the thermal margin test fixture first. Prior to beginning the test, an insulation resistance test and a dielectric strength test were conducted between the pins and the receptacle body in accordance with the test procedure. The results of both tests were negative, indicating no shoring problems existed.

The thermal margin test began by heating the receptacle in temperature increments to 400 °F. At each step, two helium leak tests were conducted, one on the "pins plus header O-rings" and another on the "total" receptacle (pins plus header O-rings plus receptacle O-rings). The "pins only" leak rate cannot be measured in this test fixture (except as an initial test conducted quickly after helium is introduced and before the helium has permeated the header O-ring seals). The measured leak rates for the two O-ring configurations were very similar with the "total" being generally higher than the "pins + header O-ring" measurements as expected (see Figure 2). The receptacle was maintained at 400 °F for 30 days and then the temperature was reduced to room temperature in the same increments used during the heat-up. The "total" leak rate versus temperature for the heat up and cooldown portion of this test is shown in Figure 3 and is representative of test results measured on other Five-Watt receptacles. These leak rates are representative of the permeation of helium through the O-rings and the fact that the leak rates during cooldown are essentially the same as those measured during heat-up indicates that the glass-to-metal and O-ring hermetic seals were unaffected by the operation at 400 °F. It was observed that the conformal coating in the receptacle header began to form cracks in its surface above 300 °F and some flaking of the coating occurred. No change in color was observed in the conformal coating as a result of the 400 °F operation. Solder had melted and dripped from the solder cups as expected because of the 400 °F operating temperature. The solder cups were still tinned with relatively clean looking solder. The insulation resistance and dielectric strength tests were repeated on the pins of the receptacle with the results again being negative.

The header O-rings were removed and compression set was measured on these as well as on the receptacle O-rings. The results are presented in Table 1. The predicted compression set of 64% is in fair agreement with the value measured on the receptacle flange (55%) but the comparison is poor with the values measured on the other three O-rings.

All of the O-rings were replaced and the header was installed in the Two-Watt thermal margin test fixture, STA4040007-008 as shown in Figure 4, and thermal margin testing was continued in accordance with the High Pressure Receptacle Header Qualification Test Procedure, STA4040400. With the receptacle header in this test fixture, the "pins only" leak rate measurement can be obtained at all operating temperatures. The "pins only" leak rate measurement was monitored as the receptacle header was heated rapidly from room temperature to 750 °F. The measured leak rate remained at the lowest detectable level (2×10^{-10} acCHa/sec) until the temperature reached 511 °F in which time the leak rate increased to 2.9×10^{-9} acCHa/sec indicating a failure of the glass-to-metal hermetic seal. The measured leak rate continued to increase as the temperature was increased from 511 °F to 750 °F. The temperature was then cooled rapidly to room temperature. Figure 5 presents the "pins only" helium leak rate measurement for the thermal cycle to 750 °F.

FIVE-WATT HIGH PRESSURE RECEPTACLE THERMAL MARGIN TEST

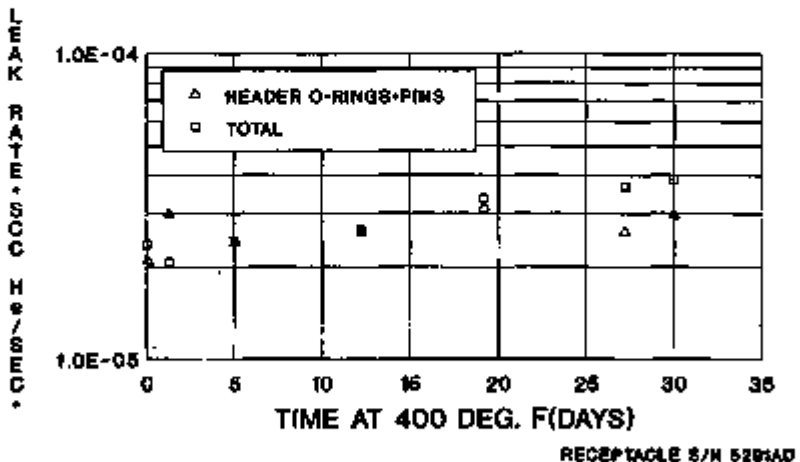
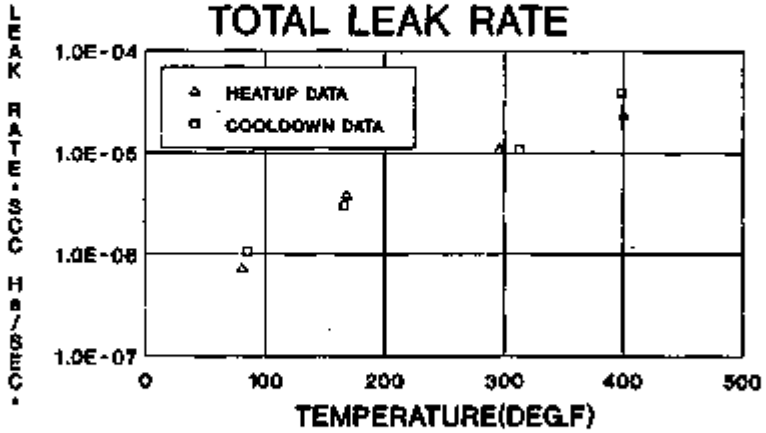


FIGURE 2

FIVE-WATT HIGH PRESSURE RECEPTACLE THERMAL MARGIN TEST TOTAL LEAK RATE



RECEPTACLE S/N 8291AD

FIGURE 3

To assure that the failure was in the hermetic seal and not in the header O-rings, the header O-rings were replaced and a final "pins only" room temperature leak rate measurement was made. This final leak rate measurement was in good agreement with the initial value measured at 511 °F confirming that the failure was in the glass-to-metal hermetic seal and not the viton O-rings. This test also confirmed that the leak in the glass-to-metal seal did not reoccur after returning to room temperature. All of the helium leak rate measurements are presented in Appendix A.

Thermal Margin Test - Receptacle S/N 5286AD

The thermal margin test with high pressure receptacle, S/N 5198AD, was performed using the same procedure as with the first receptacle. Before the thermal margin test was begun, insulation resistance and dielectric strength tests were conducted on the pins of this receptacle and the results were negative.

The "pins plus header O-rings" and "total" helium leak rate measurements were obtained as the receptacle was heated from room temperature to 400 °F. The receptacle was maintained at 400 °F for 30 days (see Figure 6 for test data) and then the temperature was reduced to room temperature. The "total" helium leak rate was always greater than the "pins plus header O-rings" leak rate as expected. Figure 7 shows the "total" leak rate measurements versus temperature for this receptacle for the heatup and cooldown portion of the 400 °F thermal cycle. The results agree well with those of receptacle S/N 5291AD and also of other Five-Watt receptacles previously tested in this manner. The results again confirm that the glass-to-metal hermetic seal of this receptacle has maintained its integrity during this 400 °F thermal cycle and that the helium leak rate measurements are representative of normal helium permeation through the viton O-rings.

The conformal coating in the receptacle header was also observed to have formed cracks as a result of operation at 400 °F and some flaking of the coating occurred. No change in color was observed. The solder cups on the back of the pins were still coated with clean solder but most of the solder had melted and dripped from the cups as expected. Insulation resistance and dielectric strength measurements were repeated on the pins of the receptacle with the results again being negative.

FIVE WATT HIGH PRESSURE RECEPTACLE THERMAL MARGIN TEST

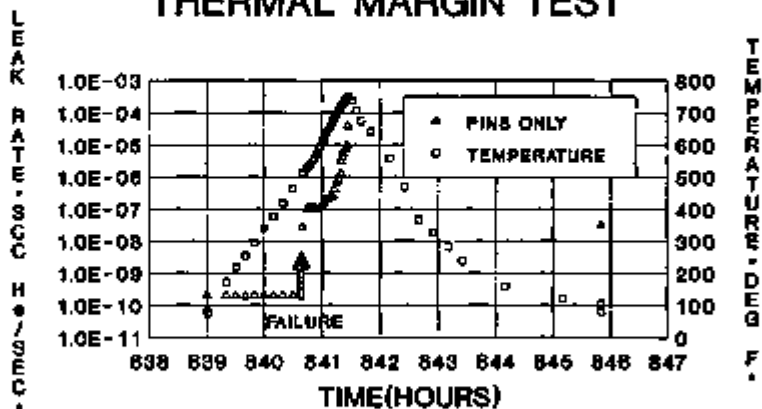
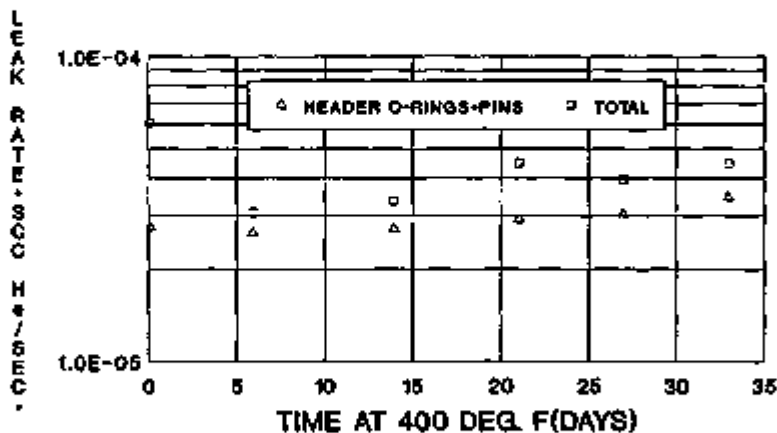


FIGURE 5

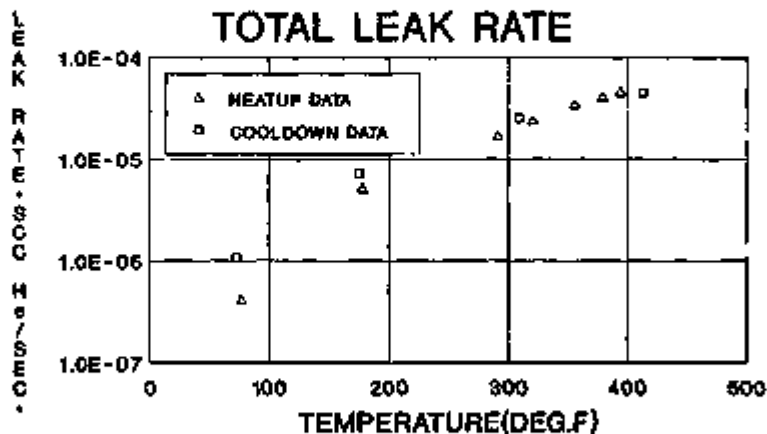
FIVE-WATT HIGH PRESSURE RECEPTACLE THERMAL MARGIN TEST



RECEPTACLE S/N 5296AD

FIGURE 6

FIVE-WATT HIGH PRESSURE RECEPTACLE THERMAL MARGIN TEST TOTAL LEAK RATE



RECEPTACLE S/N 5288AD

FIGURE 7

The header O-rings were removed to measure the compression set. The compression set measurements of these O-rings and those of the receptacle O-rings also are presented in Table 1. For this receptacle, the predicted compression set is 65% which is in fair agreement with the measurements on the receptacle O-rings (especially the receptacle flange O-ring) but does not agree with measurements made on the header O-rings.

All of the O-rings were replaced and the receptacle header was assembled again into the Two-Watt thermal margin test fixture. Using the Two-Watt test procedure previously mentioned, the receptacle header was rapidly heated from room temperature to 718 °F while monitoring the "pins only" helium leak rate. At a temperature of 487 °F, the leak rate measurement changed from the lowest detectable level 12×10^{-12} scCH₄/sec to 2.89×10^{-8} scCH₄/sec. This abrupt change indicates a failure of the glass-to-metal hermetic seal. As the temperature was increased above 487 °F the measured leak rate increased significantly as expected. The receptacle header temperature was then reduced to room temperature. Figure 8 presents the "pins only" leak rate measurement for the thermal cycle to 718 °F. At room temperature the "pins only" leak rate measurement was 1.71×10^{-4} scCH₄/sec which would indicate a failure through the O-rings due to excessive compression set or a further deterioration of the hermetic seal. In order to confirm the hermetic seal failure, the header O-rings were replaced with new O-rings and the "pins only" room temperature helium leak rate measurement was repeated. This time the measure leak rate was nearly the same value as measured at 487 °F when the failure was first observed. This result indicates that the glass-to-metal hermetic seal failure did not change since it was first observed and the very large leak rate measured when the receptacle header was at room temperature was indeed a result of a failure of the header viton O-rings. The helium leak rate measurements for receptacle S/N 5296AD are presented in Appendix B.

Disassembly and Final Inspection

After completion of the thermal margin test, each header was removed from the Two-Watt test fixture and carefully inspected. More cracking was observed in the conformal coating than had initially been observed during the thermal soak at 400 °F. Small pieces of the coating continued to flake off the surface. But there was still no noticeable change in color of the conformal coating. The header O-rings were still compliant. Compression set measurements of the header O-rings were not made after the 700 °F thermal cycle, but visual observations indicated that permanent deformation was significant; approaching 100% compression set as expected.

The remaining solder coating the solder cups appeared very oxidized and burnt as expected from the very high operating temperature of 700 °F compared to the solder melting point of 381 °F. The headers of both receptacles only exhibited a slight amount of oxidation of their metallic surfaces. The monel header of receptacle S/N 5291AD had less oxidation of its surface than the stainless steel header of receptacle S/N 5288AD but the difference in amount of oxidation was small and may not be statistically significant. Therefore, the limiting consideration for elevated temperature operation should be the O-ring seals.

FIVE WATT HIGH PRESSURE RECEPTACLE THERMAL MARGIN TEST

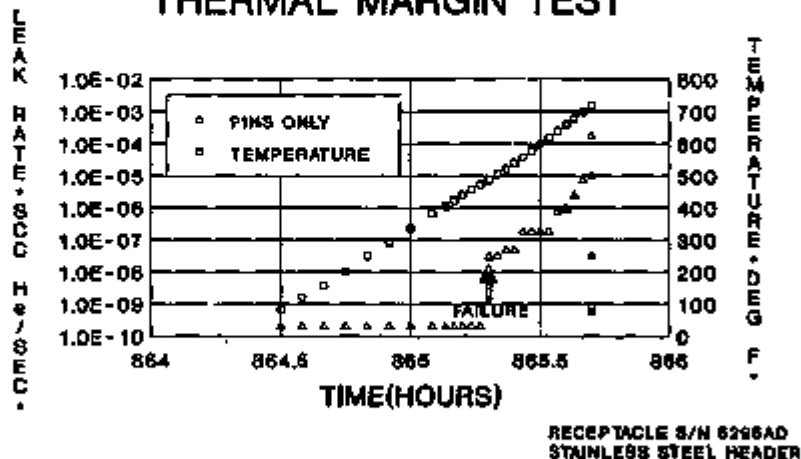


FIGURE 8

Conclusions

The glass-to-metal hermetic seal of receptacle S/N 5281AD failed at 511 °F and failure of receptacle S/N 5286AD occurred at 487 °F. It can therefore be concluded that failure of the Five-Watt receptacle headers will occur at 500 ± 25 °F. There appears to be no noticeable advantage for either of the two header body materials (monel vs stainless steel) tested. The test results obtained and observations made were similar for both headers in all instances.

Two (2) Two-Watt receptacle headers were tested to failure in the same thermal margin test fixture in 1988. The criteria for determining failure was different for these headers. Therefore conclusions drawn in the earlier test must be reevaluated using the same failure criteria as used in this test. Using the present Five-Watt failure criteria (sudden large changes in "pin only" helium leak rate), the failure of the Two-Watt headers occurred 80 °F to 100 °F higher than the Five-Watt headers which is reasonable agreement when compared to the qualification temperature of 300 °F. However, a direct comparison of the hermetic seal failure temperatures for the two types of headers is questionable because of differences in the test programs and hermetic seal configurations. The Two-Watt headers were not exposed to a 400 °F thermal soak prior to the thermal margin test and they have eight pins compared to nine pins in the Five-Watt header design.

The receptacle and header O-ring seals survived the 400 °F thermal test although the compression set experienced by the receptacle O-rings was significant for the relatively short duration of the test. The compression set on the face seal O-rings was comparable to expectations. The compression set for the gland O-rings was much less than expected. Perhaps this is related to the geometry of the gland O-ring configuration. Compression set is probably related to the amount of squeeze or O-ring deformation. The TES data base is based on face type seals. None of the O-rings survived the 700 °F thermal cycle without excessive compression set. However, the O-rings were not expected to withstand these high temperatures for very long. They were only required to survive until the glass-to-metal hermetic seals failed which they did. Under normal operation of the receptacles, the temperature is not expected to exceed 300 °F which is within the normal range of operation for viton O-rings.

The conformal coating cracked and more pronounced flaking of the coating occurred for both receptacles at temperatures above 400 °F. The possibility of flaking at the expected maximum operating temperature of 300 °F is being investigated as a part of the 300 °F soak tests being conducted concurrently with this thermal margin test. It is not desirable to have the conformal coating experience any flaking during normal operation as it may interfere with proper mating/demating operations and could cause poor electrical contact between mated pins and sockets. The conformal coating of both receptacles showed no evidence of a color change as a result of the 700 °F temperature extreme.

The insulation resistance and dielectric strength measurements all demonstrated good isolation between the receptacle pins and the receptacle body at the end of the 400 °F thermal soak test. This confirms that the conformal coating is not changing its insulating properties as a result of the 400 °F operating temperature.

APPENDIX A

**RECEPTACLE S/N 5291AD HELIUM LEAK RATE
MEASUREMENTS DURING THERMAL MARGIN TEST**

HPG5-DST-236

20 February 1992

APPENDIX A
RTG RATE INFORMATION THROUGH APRIL 1985

UNITS: \$/hr
COSTS: \$/hr

TRUCK CLASS	TRUCK CLASS	APPROXIMATE TRUCK #	LOAD RATE INFORMATION			PARAMETER	RATED RATE
			"TRUCK SIZE" (sq ft)	"TRUCK 0-20000-0100" (sq ft)	"TRUCK" (sq ft)		
572591	18100	88	2,000-7	2,000-7	2,000-7	8	
572601	18100	112		1,500-4		9	
572611	18100	140			2,000-1	10	
572621	18100	170				11	
572631	18100	200		1,000-2		12	
572641	18100	230			1,000-1	13	
572651	18100	260			1,500-1	14	
572661	18100	290		0,000-0		15	
572671	18100	320		2,000-0	1,000-1	16	
572681	18100	350			1,500-1	17	
572691	18100	380				18	
572701	18100	410				19	
572711	18100	440				20	
572721	18100	470				21	
572731	18100	500				22	
572741	18100	530				23	
572751	18100	560				24	
572761	18100	590				25	
572771	18100	620				26	
572781	18100	650				27	
572791	18100	680				28	
572801	18100	710				29	
572811	18100	740				30	
572821	18100	770				31	
572831	18100	800				32	
572841	18100	830				33	
572851	18100	860				34	
572861	18100	890				35	
572871	18100	920				36	
572881	18100	950				37	
572891	18100	980				38	
572901	18100	1010				39	
572911	18100	1040				40	
572921	18100	1070				41	
572931	18100	1100				42	
572941	18100	1130				43	
572951	18100	1160				44	
572961	18100	1190				45	
572971	18100	1220				46	
572981	18100	1250				47	
572991	18100	1280				48	
573001	18100	1310				49	
573011	18100	1340				50	
573021	18100	1370				51	
573031	18100	1400				52	
573041	18100	1430				53	
573051	18100	1460				54	
573061	18100	1490				55	
573071	18100	1520				56	
573081	18100	1550				57	
573091	18100	1580				58	
573101	18100	1610				59	
573111	18100	1640				60	
573121	18100	1670				61	
573131	18100	1700				62	
573141	18100	1730				63	
573151	18100	1760				64	
573161	18100	1790				65	
573171	18100	1820				66	
573181	18100	1850				67	
573191	18100	1880				68	
573201	18100	1910				69	
573211	18100	1940				70	
573221	18100	1970				71	
573231	18100	2000				72	
573241	18100	2030				73	
573251	18100	2060				74	
573261	18100	2090				75	
573271	18100	2120				76	
573281	18100	2150				77	
573291	18100	2180				78	
573301	18100	2210				79	
573311	18100	2240				80	
573321	18100	2270				81	
573331	18100	2300				82	
573341	18100	2330				83	
573351	18100	2360				84	
573361	18100	2390				85	
573371	18100	2420				86	
573381	18100	2450				87	
573391	18100	2480				88	
573401	18100	2510				89	
573411	18100	2540				90	
573421	18100	2570				91	
573431	18100	2600				92	
573441	18100	2630				93	
573451	18100	2660				94	
573461	18100	2690				95	
573471	18100	2720				96	
573481	18100	2750				97	
573491	18100	2780				98	
573501	18100	2810				99	
573511	18100	2840				100	
573521	18100	2870				101	
573531	18100	2900				102	
573541	18100	2930				103	
573551	18100	2960				104	
573561	18100	2990				105	
573571	18100	3020				106	
573581	18100	3050				107	
573591	18100	3080				108	
573601	18100	3110				109	
573611	18100	3140				110	
573621	18100	3170				111	
573631	18100	3200				112	
573641	18100	3230				113	
573651	18100	3260				114	
573661	18100	3290				115	
573671	18100	3320				116	
573681	18100	3350				117	
573691	18100	3380				118	
573701	18100	3410				119	
573711	18100	3440				120	
573721	18100	3470				121	
573731	18100	3500				122	
573741	18100	3530				123	
573751	18100	3560				124	
573761	18100	3590				125	
573771	18100	3620				126	
573781	18100	3650				127	
573791	18100	3680				128	
573801	18100	3710				129	
573811	18100	3740				130	
573821	18100	3770				131	
573831	18100	3800				132	
573841	18100	3830				133	
573851	18100	3860				134	
573861	18100	3890				135	
573871	18100	3920				136	
573881	18100	3950				137	
573891	18100	3980				138	
573901	18100	4010				139	
573911	18100	4040				140	
573921	18100	4070				141	
573931	18100	4100				142	
573941	18100	4130				143	
573951	18100	4160				144	
573961	18100	4190				145	
573971	18100	4220				146	
573981	18100	4250				147	
573991	18100	4280				148	
574001	18100	4310				149	
574011	18100	4340				150	
574021	18100	4370				151	
574031	18100	4400				152	
574041	18100	4430				153	
574051	18100	4460				154	
574061	18100	4490				155	
574071	18100	4520				156	
574081	18100	4550				157	
574091	18100	4580				158	
574101	18100	4610				159	
574111	18100	4640				160	
574121	18100	4670				161	
574131	18100	4700				162	
574141	18100	4730				163	
574151	18100	4760				164	
574161	18100	4790				165	
574171	18100	4820				166	
574181	18100	4850				167	
574191	18100	4880				168	
574201	18100	4910				169	
574211	18100	4940				170	
574221	18100	4970				171	
574231	18100	5000				172	
574241	18100	5030				173	
574251	18100	5060				174	
574261	18100	5090				175	
574271	18100	5120				176	
574281	18100	5150				177	
574291	18100	5180				178	
574301	18100	5210				179	
574311	18100	5240				180	
574321	18100	5270				181	
574331	18100	5300				182	
574341	18100	5330				183	
574351	18100	5360				184	
574361	18100	5390				185	
574371	18100	5420				186	
574381	18100	5450				187	
574391	18100	5480				188	
574401	18100	5510				189	
574411	18100	5540				190	
574421	18100	5570				191	
574431	18100	5600				192	
574441	18100	5630				193	
574451	18100	5660				194	
574461	18100	5690				195	
574471	18100	5720				196	
574481	18100	5750				197	
574491	18100	5780				198	
574501	18100	5810				199	
574511	18100	5840				200	
574521	18100	5870				201	
574531	18100	5900				202	
574541	18100	5930				203	
574551	18100	5960				204	
574561	18100	5990				205	
574571	18100	6020				206	
574581	18100	6050				207	
574591	18100	6080				208	
574601	18100	6110				209	
574611	18100	6140				210	
574621	18100	6170				211	
574631	18100	6200				212	
574641	18100	6230				213	
574651	18100	6260				214	
574661	18100	6290				215	
574671	18100	6320				216	
574681	18100	6350				217	
574691	18100	6380				218	
574701	18100	6410				219	
574711	18100	6440				220	
574721	18100	6470				221	
574731	18100	6500				222	
574741	18100	6530				223	
574751	18100	6560				224	
574761	18100	6590				225	
574							

APPENDIX B
RTG WMT FARE/TICKET SCHEDULE (SARP) SummaryOPERATOR'S USE ONLY
SCHEDULE NO. 001

Line Item Description						
LINE	DATE	DESCRIPTION	FROM	TO	FARE	CLASS
NO.			STATION	STATION	AMOUNT	
1734701	08/07	047			3.100-7	100
1734701	08/09	050			3.500-7	100
1734701	08/21	070			3.600-7	101
1734701	08/29	080			3.700-7	102
1734701	08/29	080			3.800-7	101
1734701	08/27	090			3.900-7	102
1734701	08/28	100			3.900-6	101
1734701	08/28	100			4.000-6	101
1734701	08/25	107			4.000-5	100
1734701	08/02	111			4.000-6	102
1734701	08/03	120			4.000-6	101
1734701	08/04	130			4.100-6	101
1734701	08/06	140			4.100-6	101
1734701	08/07	150			4.200-5	101
1734701	08/08	160			4.200-5	101
1734701	08/09	170				100
1734701	08/09	180				100
1734701	08/09	190				100
1734701	08/09	200				100
1734701	08/09	210				100
1734701	08/09	220				100
1734701	08/09	230				100
1734701	08/09	240				100
1734701	08/09	250				100
1734701	08/09	260				100
1734701	08/09	270				100
1734701	08/09	280				100
1734701	08/09	290				100
1734701	08/09	300				100
1734701	08/09	310				100
1734701	08/09	320				100
1734701	08/09	330				100
1734701	08/09	340				100
1734701	08/09	350				100
1734701	08/09	360				100
1734701	08/09	370				100
1734701	08/09	380				100
1734701	08/09	390				100
1734701	08/09	400				100
1734701	08/09	410				100
1734701	08/09	420				100
1734701	08/09	430				100
1734701	08/09	440				100
1734701	08/09	450				100
1734701	08/09	460				100
1734701	08/09	470				100
1734701	08/09	480				100
1734701	08/09	490				100
1734701	08/09	500				100
1734701	08/09	510				100
1734701	08/09	520				100
1734701	08/09	530				100
1734701	08/09	540				100
1734701	08/09	550				100
1734701	08/09	560				100
1734701	08/09	570				100
1734701	08/09	580				100
1734701	08/09	590				100
1734701	08/09	600				100
1734701	08/09	610				100
1734701	08/09	620				100
1734701	08/09	630				100
1734701	08/09	640				100
1734701	08/09	650				100
1734701	08/09	660				100
1734701	08/09	670				100
1734701	08/09	680				100
1734701	08/09	690				100
1734701	08/09	700				100
1734701	08/09	710				100
1734701	08/09	720				100
1734701	08/09	730				100
1734701	08/09	740				100
1734701	08/09	750				100
1734701	08/09	760				100
1734701	08/09	770				100
1734701	08/09	780				100
1734701	08/09	790				100
1734701	08/09	800				100
1734701	08/09	810				100
1734701	08/09	820				100
1734701	08/09	830				100
1734701	08/09	840				100
1734701	08/09	850				100
1734701	08/09	860				100
1734701	08/09	870				100
1734701	08/09	880				100
1734701	08/09	890				100
1734701	08/09	900				100
1734701	08/09	910				100
1734701	08/09	920				100
1734701	08/09	930				100
1734701	08/09	940				100
1734701	08/09	950				100
1734701	08/09	960				100
1734701	08/09	970				100
1734701	08/09	980				100
1734701	08/09	990				100
1734701	08/09	1000				100

- 00000000

APPENDIX B

**RECEPTACLE S/N 5296AD HELIUM LEAK RATE
MEASUREMENTS DURING THERMAL MARGIN TEST**

HPGS-DST-238

20 February 1992

APPENDIX B
FIVE YEAR ACCEPTABLE THERMAL HISTORY TEST DATA

RECORDING P/N C100419996
 RECORDING S/N 529648

TEST DATE	TEST TIME	SPECIMEN TWP. (F)	LEAD RATE MEASUREMENT			COMMENTS	FLANGED BORE
			"FINE ONLY" (per Hr/Sec)	"SHARP 0-2700-0100" (per Hr/Sec)	"SMOOTH" (per Hr/Sec)		
7/29/91	10:04	76	2,000-10	3,370-7	4,040-7		9
7/31/91	12:04	179		3,320-6	5,600-8		29
8/1/91	12:04	251		1,100-5	1,470-8		49
8/1/91	12:18	329			2,300-5		49
8/1/91	12:30	394			2,170-5		49
8/1/91	12:38	379			4,620-9		50
8/1/91	12:48	354			4,820-5		50
8/1/91	12:50	359			2,520-9		50
8/1/91	13:00	443			6,520-5		51
8/1/91	13:38	404			2,570-8		52
8/1/91	14:08	492		2,750-3	4,020-3		53
8/7/91	10:00	286		2,640-5	2,500-3		193
8/13/91	10:00	384		2,720-5	2,970-5		194
8/22/91	12:38	461		2,920-5	4,400-5		199
8/26/91	10:10	497		2,420-3	1,620-8		197
9/2/91	12:00	413		2,480-3	4,470-8		211
9/9/91	14:30	266		1,620-5	2,820-5		245
9/14/91	10:30	173		2,420-4	7,120-6		245
9/14/91	10:00	72		4,720-7	1,070-6	POSTING IS MISSING INSIDE GUIDANCE	
						ARMED TIME	
10/21/91	04:00	83	2,800-10			SPD 2.2.4 *	249
10/21/91	04:05	112	2,000-10			SPD 2.2.2 *	249
10/21/91	04:10	130	2,000-10				249
10/21/91	04:15	263	2,000-10				249
10/21/91	04:20	249	2,000-10				249
10/21/91	04:25	283	2,800-10				249
10/21/91	04:30	214	2,000-10				249
10/21/91	04:35	361	2,000-10				249
10/21/91	04:39	484	2,800-10				249
10/21/91	04:46	423	2,600-10				249
10/21/91	04:47	420	2,000-10				249
10/21/91	04:44	454	2,000-10				249
10/21/91	04:45	473	2,000-10				249
10/21/91	04:46	487	2,800-8				249
10/21/91	04:50	504	2,100-8			FAILURE	249
10/21/91	04:55	539	4,420-8				249
10/21/91	04:54	551	4,250-8				249
10/21/91	04:54	550	1,400-3				249
10/21/91	04:54	511	1,800-3				249
10/21/91	04:58	570	1,900-3				249
10/21/91	04:57	610	1,700-7				249
10/21/91	04:54	430	2,300-7				249

APPENDIX B
RTG TUBE INSPECTION RECORDSINSPECTION #/N 01200972000
INSPECTION #/N 321600

TEST DATE	TEST TIME	SPEAKER TEMP. (F)	LEAK RATE MEASUREMENT			CORRECTION	ELI/Probe COUNT
			PIPE GELT (see N/000)	*TUBING 0-01000-01000* (see N/000)	*TUBING* (see N/000)		
10/21/91	00:00	600	0.000-7				000
10/21/91	00:00	570	1.000-6				000
10/21/91	00:10	600	1.200-6				000
10/21/91	00:10	710	1.000-5				000
10/28/91	10:00	80	1.700-4	1.700-4			000
10/29/91	10:10	70	1.100-0			STED 0.1.7 *	000

MEMORANDUM

13 December 1991

Refer to: HPG3-DST-1000

To: T. Christenbury, W. Brittain, D. Anderson, M. McKittrick, T. Hammel, A. Lieberman, C. Heusler

From: D. Tréner

Subject: Results of HPG MOD 3 High Pressure Receptacle Thermal Margin Tests

Introduction

Two HPG MOD 3 high pressure receptacles (P/N NCM242174-200M) were selected to undergo thermal margin testing in accordance with the HPG MOD 3/Five-Watt RTG High Pressure Electrical Receptacle Elevated Temperature Qualification Test Procedure, HPGA3040303. Figure 1 shows the receptacle mounted in the test fixture. The thermal margin test basically consists of quickly heating the high pressure receptacles one at a time to a temperature high enough to cause a failure in the hermetic seals. Receptacles S/N 813 and S/N 814 were chosen for the tests.

Initial Inspection of Receptacles

Both receptacles were inspected and measurements were taken of the O-rings and O-ring grooves so that the percentage fill of the grooves could be determined. Table 1 lists the percent fill for the O-rings associated with each receptacle. Then the pins of each receptacle were soldered using the HPG MOD 3 standard procedure to simulate attachment of wires. The solder used was eutectic lead-tin solder and in the case of the thermocouple pins, type 817 flux was used to wet the pins with the solder. All pins were then cleaned by the HPG MOD 3 standard process depending on the type of flux used. A helium leak test of the hermetic seals before and after soldering the pins was used to confirm that the thermal cycle of the soldering operation did not cause damage to the hermetic seals.

Thermal Margin Test-Receptacle S/N 813

High pressure receptacle S/N 813 was installed into the thermal margin test fixture first. Prior to beginning the test, an insulation resistance test and a dielectric strength test were conducted between the pins and the receptacle body in accordance with the test procedure. The results of both tests were negative, indicating no shorting problems existed. The actual thermal test began by quickly heating the receptacle (S/N 813) in small temperature increments. At each step, two helium leak tests were conducted, one on the hermetic seals (pins only) and another on the entire receptacle (pins plus receptacle O-rings). The "pins only" helium leak rate measurement is the most

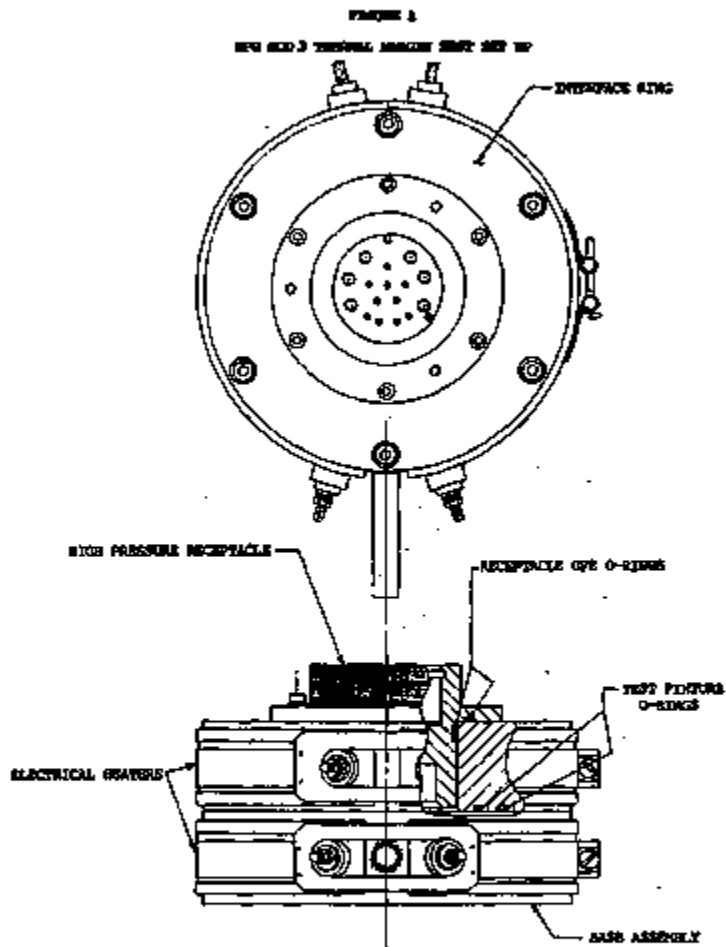


TABLE 1

PERCENT FILL AND COMPRESSION SETFOR O-RINGS USED IN HPG MOD 3 THERMAL MARGIN TEST

O-Ring ¹	Location	Receptacle S/N B13		Receptacle S/N B14	
		% Fill	Compression Set (%) ²	% Fill	Compression Set (%) ²
-234	Receptacle Flange	89.3	68.9	70.0	NA
-230	Receptacle Gland	70.3	59.5	70.3	NA
-348	Interface Ring	NA	62.0	NA	NA
-340	Interface Ring	NA	56.5	NA	NA

1. All O-rings are Viton per MS9248/1.
2. Measured at completion of test.
3. O-rings destroyed by high temperature operation.

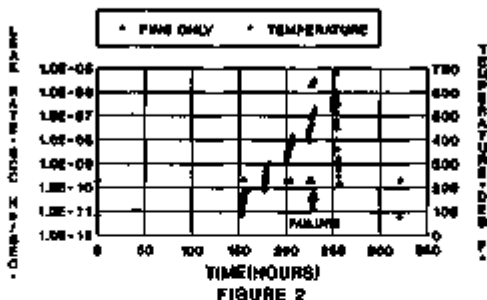
reliable determination of the integrity of the receptacle glass-to-metal hermetic seals since this measurement should remain very small until a leak appears. Essentially, no helium should be detected greater than the sensitivity of the equipment as long as the hermetic seal is intact. This minimum measured leak rate is approximately 2×10^{-10} scCH₄/sec. Figures 2 and 3 show the test data for the "pins only" and "total" helium leak rates respectively. As the temperature was increased on receptacle S/N 813, the helium leak rate remained very low until a temperature of 487 °F was reached at which point the "pins only" leak rate increased to 1.9×10^{-9} scCH₄/sec. This leak rate implied a failure of the hermetic seal. The total leak rate measurements indicated that the initial O-ring seal leakage increased as expected due to increased helium permeation through the O-rings. Figure 4 shows this increasing permeation of helium through the O-rings for the first 225 hours of the test. The temperature continued to be increased until it reached 500 °F without failure of the receptacle O-ring seals. In fact, the measured total leak rate decreased as the temperature was further increased. This effect has been observed before with other O-ring seals and has been attributed to formation of a metal-to-metal seal. Then the receptacle was cooled to room temperature. A final room temperature "pins only" helium leak check indicated that the leak had resealed; see Figure 2 at about 320 hours. This type behavior has been observed by TES on other receptacle O-ring designs. Also as seen in Figure 3 at the same time, the "total" leak rate returned to a value near the initial measurement. At the completion of the thermal margin test, the insulation resistance and dielectric strength tests were repeated with the results again being negative. The helium leak test results for this thermal margin test are presented in Appendix A.

Thermal Margin Test-Receptacle S/N 814

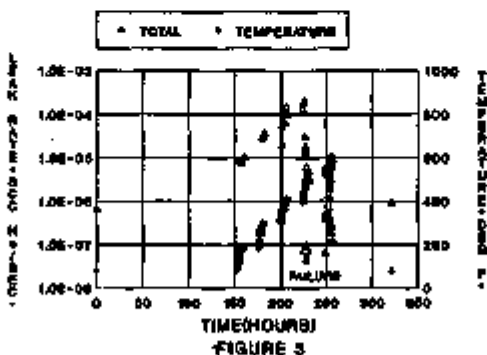
The thermal margin test with high pressure receptacle, S/N 814, was performed essentially the same as with the first receptacle except that Engineering Work Order HPGM3-718 was written to allow the thermal cycle to be repeated a second time. Before the thermal margin test was begun, the insulation resistance and dielectric strength tests were conducted on the pins of this receptacle and the results were negative.

The thermal margin test was begun by heating the receptacle in small temperature increments. Two helium leak tests were performed at each temperature step ("pins only" and "total"). Figures 5 and 6 show the results for each of the leak rate tests. The receptacle was heated in this manner to a temperature of 700 °F without observing any increase in the "pins only" helium leak rate measurement above the background value. At 700 °F, the insulation resistance and dielectric strength tests were repeated and the results were negative (no low impedance paths). The receptacle was then cooled to room temperature. The "total" helium leak rate measured during this temperature cycle showed normal expected variations with temperature during the heat-up until a metal-to-metal seal began appearing above a temperature of 450 °F. The initial heat-up of the receptacle is shown in Figure 7 and the results are very much like those seen in Figure 4 for receptacle S/N 813. At temperatures above 450 °F the leak rate of receptacle S/N 814 became unreliable, sometimes decreasing as the temperature was increasing and finally increasing as the temperature was being reduced. These changes can be explained by a combination of effects: first a metal-to-metal seal behavior at high temperature resulting in a decreased leak rate and second an O-ring failure as the receptacle was being cooled down from 700 °F due to excessive compression set of the O-rings. This type behavior has been observed on other O-ring seal configurations.

HPG MOD 3
HIGH PRESSURE RECEPTACLE
THERMAL MARGIN TEST

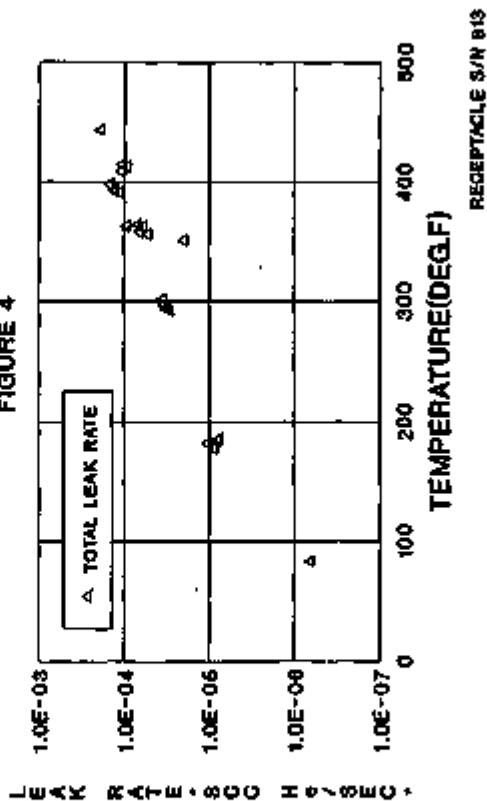


RECEPTACLE S/N 013

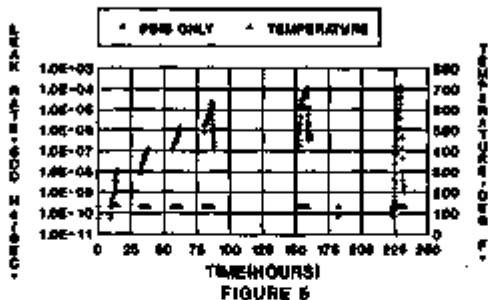


HPG MOD 3 HIGH PRESSURE RECEPTACLE THERMAL MARGIN TEST

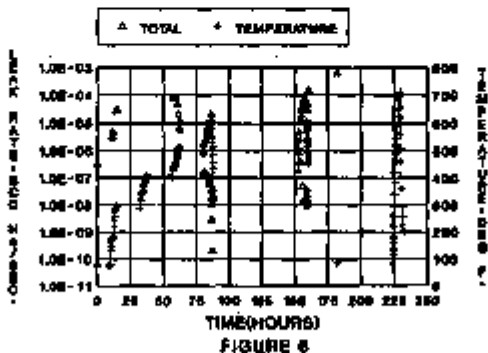
FIGURE 4



HPG MOD 3 HIGH PRESSURE RECEPTACLE THERMAL MARGIN TEST



RECEPTACLE S/N 614



The receptacle was then reheated as specified in the Engineering Work Order. This time the receptacle temperature reached 711 °F and the "pine only" helium leak rate measurements still indicated no failure of the hermetic seals. Insulation resistance and dielectric strength tests were conducted again at the high temperature and again the results were negative. The receptacle was then cooled to room temperature. The insulation resistance and dielectric strength measurements were repeated with the results being negative. All of the helium leak test results taken on receptacle S/N 814 are presented in Appendix B.

Disassembly And Final Inspection

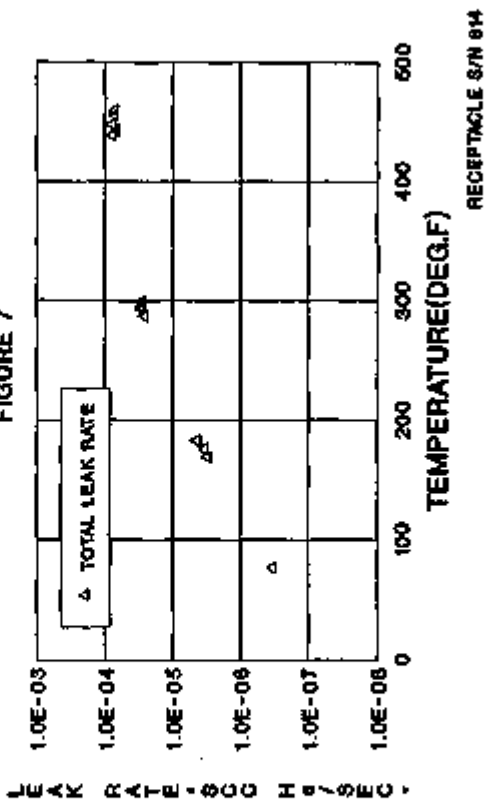
After completion of the thermal margin test, each receptacle was removed from the test fixture and inspected carefully. The bolts used to hold the receptacle to the interface ring were checked and it was confirmed that all bolts for each receptacle had maintained the original torque values. Three 8-32 screws placed in the tapped holes of the receptacle mounting flange were used to carefully force the receptacles from the interface ring.

The conformal coating in the hermetic seal area of each receptacle was very dark and much of the surface appeared as though it had melted, formed bubbles, and chips and flakes appeared when it was cooled. Comparing the coatings of both receptacles, the bubbling and melting was more extensive with receptacle S/N 814 than for receptacle S/N 813. This difference in appearance is likely the result of the higher maximum temperature of S/N 814 compared to S/N 813 rather than an indication of receptacle conformal coating variability. During heat up several observations were made concerning changes to the conformal coating. A small flake of conformal coating from receptacle S/N 813 had chipped off at a temperature of about 415 °F. The initial color change to brown began at about 300 °F for both receptacles. The color continued to darken at higher temperatures. At about 500 °F the coating began to melt and bubbles began forming.

The O-rings from receptacle S/N 813 appeared to have some permanent deformation. The flange O-ring was sticking to the flange but was easy to remove. Both O-rings were still quite pliable. The majority of the solder in the solder cups of the receptacle had dripped down to the bottom of the interface ring. This is expected because the test temperature of 600 °F exceeds the solder melting temperature of 361 °F. The solder remaining on the pins appeared oxidized and burned. The thermocouple pins were checked for residual acid flux using the HPG MOD 3 standard test but none was found. As expected, the receptacle body was noticeably oxidized. The interface ring was also removed to examine the O-rings sealing it to the rest of the fixture (see Figure 1). These O-rings also had some compression set but were quite pliable. All four O-rings (receptacle and interface ring) were measured to determine their compression set. Table 1 presents the results of these measurements. In all cases, the O-rings experienced a compression set of 57% or more.

HPG MOD 3 HIGH PRESSURE RECEPTACLE THERMAL MARGIN TEST

FIGURE 7



As expected, the O-rings from receptacle S/N B14 were destroyed by the 700 °F temperature. They fell apart as the receptacle was being removed. The O-rings were very hard and brittle; somewhat like graphite. This was also true of the O-rings in the interface ring. Therefore, no compression set measurements could be obtained for these O-rings as indicated in Table 1. The solder had dripped out of the solder cups in each receptacle pin and large drops had collected in the bottom of the interface ring. The solder remaining on the pins again appeared very oxidized and burned. This was undoubtedly due to the very high temperature of operation compared to the normal operating temperature of the solder (melting point of 381 °F). The thermocouple pins were checked for residual Acid flux and none was detected. The surfaces of the receptacle shell were darkened from oxidation due to the high temperature operation.

Conclusions

The glass-to-metal hermetic seals of receptacle S/N B13 failed at a temperature of 487 °F whereas for receptacle S/N B14, the hermetic seals did not fail when cycled twice to 700 °F. It may have been that the conformal coating on receptacle S/N B14 masked a failure of this receptacle's hermetic seals. However, the conclusion must still be that temperatures in the range of 450-500 °F are sufficient to cause failure of the glass-to-metal hermetic seals of the HPG MOD 3 high pressure receptacles.

The receptacle-to-housing O-ring seals of receptacle S/N B13 survived the 600 °F thermal cycle although the measured compression set of 60% or more after about 300 hours of operation indicates that Viton O-rings would be unsatisfactory for long term use at these temperatures. Similar O-rings on receptacle S/N B14 were completely destroyed by the short term operation at temperatures up to 700 °F. However, none of these O-rings were expected to survive the 600-700 °F temperature extremes for very long. The thermal margin tests are short term high temperature tests where the temperature limit of the glass-to-metal hermetic seals is expected to be exceeded before the O-rings fail. During normal operation, the maximum service temperature of the receptacles is intended to be about 300 °F which is within the normal range of operation for these viton O-rings.

The conformal coating began to change color at about 300 °F and showed signs of melting at about 600 °F. The manufacturer of the high pressure receptacles has indicated that there are other coating materials which will maintain their original color to higher temperatures. If the coating material is changed, then further tests should be performed to assure the compatibility of the new coating at the expected operating temperature of the receptacles.

Insulation resistance and dielectric strength measurements all indicated good isolation of the receptacle pins for each other and the receptacle body at elevated temperatures as well as at room temperature after completing the thermal test.

APPENDIX A

**RECEPTACLE 6/N 813 HELIUM LEAK RATE
MEASUREMENTS DURING THERMAL MARGIN TEST**

APPENDIX B
BRIEF DESCRIPTION OF THE TRANSPORTATION SYSTEMS

Worksheet: B-1
Worksheet Path: \\wnc\sd\rtg\B-1

LINE NO.	LINE NO.	SECTION	SECTION		SECTION	SECTION
			NO.	NO.		
1790701	0000	701	1,000-00			200
1790701	0000	702	1,000-00			200
1790701	0000	703	1,000-00			200
1790701	0000	704	1,000-00			200
1790701	0000	705	1,000-00			200
1790701	0000	706	1,000-00			200
1790701	0000	707	1,000-00			200
1790701	0000	708	1,000-00			200
1790701	0000	709	1,000-00			200
1790701	0000	710	1,000-00			200
1790701	0000	711	1,000-00			200
1790701	0000	712	1,000-00			200
1790701	0000	713	1,000-00			200
1790701	0000	714	1,000-00			200
1790701	0000	715	1,000-00			200
1790701	0000	716	1,000-00			200
1790701	0000	717	1,000-00			200
1790701	0000	718	1,000-00			200
1790701	0000	719	1,000-00			200
1790701	0000	720	1,000-00			200
1790701	0000	721	1,000-00			200
1790701	0000	722	1,000-00			200
1790701	0000	723	1,000-00			200
1790701	0000	724	1,000-00			200
1790701	0000	725	1,000-00			200
1790701	0000	726	1,000-00			200
1790701	0000	727	1,000-00			200
1790701	0000	728	1,000-00			200
1790701	0000	729	1,000-00			200
1790701	0000	730	1,000-00			200
1790701	0000	731	1,000-00			200
1790701	0000	732	1,000-00			200
1790701	0000	733	1,000-00			200
1790701	0000	734	1,000-00			200
1790701	0000	735	1,000-00			200
1790701	0000	736	1,000-00			200
1790701	0000	737	1,000-00			200
1790701	0000	738	1,000-00			200
1790701	0000	739	1,000-00			200
1790701	0000	740	1,000-00			200
1790701	0000	741	1,000-00			200
1790701	0000	742	1,000-00			200
1790701	0000	743	1,000-00			200
1790701	0000	744	1,000-00			200
1790701	0000	745	1,000-00			200
1790701	0000	746	1,000-00			200
1790701	0000	747	1,000-00			200
1790701	0000	748	1,000-00			200
1790701	0000	749	1,000-00			200
1790701	0000	750	1,000-00			200
1790701	0000	751	1,000-00			200
1790701	0000	752	1,000-00			200
1790701	0000	753	1,000-00			200
1790701	0000	754	1,000-00			200
1790701	0000	755	1,000-00			200
1790701	0000	756	1,000-00			200
1790701	0000	757	1,000-00			200
1790701	0000	758	1,000-00			200
1790701	0000	759	1,000-00			200
1790701	0000	760	1,000-00			200
1790701	0000	761	1,000-00			200
1790701	0000	762	1,000-00			200
1790701	0000	763	1,000-00			200
1790701	0000	764	1,000-00			200
1790701	0000	765	1,000-00			200
1790701	0000	766	1,000-00			200
1790701	0000	767	1,000-00			200
1790701	0000	768	1,000-00			200
1790701	0000	769	1,000-00			200
1790701	0000	770	1,000-00			200
1790701	0000	771	1,000-00			200
1790701	0000	772	1,000-00			200
1790701	0000	773	1,000-00			200
1790701	0000	774	1,000-00			200
1790701	0000	775	1,000-00			200
1790701	0000	776	1,000-00			200
1790701	0000	777	1,000-00			200
1790701	0000	778	1,000-00			200
1790701	0000	779	1,000-00			200
1790701	0000	780	1,000-00			200
1790701	0000	781	1,000-00			200
1790701	0000	782	1,000-00			200
1790701	0000	783	1,000-00			200
1790701	0000	784	1,000-00			200
1790701	0000	785	1,000-00			200
1790701	0000	786	1,000-00			200
1790701	0000	787	1,000-00			200
1790701	0000	788	1,000-00			200
1790701	0000	789	1,000-00			200
1790701	0000	790	1,000-00			200
1790701	0000	791	1,000-00			200
1790701	0000	792	1,000-00			200
1790701	0000	793	1,000-00			200
1790701	0000	794	1,000-00			200
1790701	0000	795	1,000-00			200
1790701	0000	796	1,000-00			200
1790701	0000	797	1,000-00			200
1790701	0000	798	1,000-00			200
1790701	0000	799	1,000-00			200
1790701	0000	800	1,000-00			200

BEST COPY AVAILABLE

APPENDIX B
 THE 1988 B BIDDING SYSTEM, SPECIAL BIDDING DATA

SECTION 210 B/B BIDDING SYSTEM
 SECTION 210 B/B B/B

BIDDING ITEM	UNIT TYPE	QUANTITY REQ'D (P)	UNIT PRICE ADJUSTMENT		APPROXIMATE QUANTITY	ESTIMATED BIDDING
			"FORM B" (P) (per B/B)	"FORM B" (P) (per B/B)		
210100	1130	800	2,000-0			1600
210101	1130	800	2,100-0			1680
210102	1131	800		1,000-0		1600
210103	1131	800		1,100-0		1760
210104	1132	800		1,200-0		1920
210105	1133	800		1,300-0		2080
210106	1134	800		1,400-0		2240
210107	1135	800		1,500-0		2400
210108	1136	800		1,600-0		2560
210109	1137	800		1,700-0		2720
210110	1138	800		1,800-0		2880
210111	1139	800		1,900-0		3040
210112	1140	800		2,000-0		3200
210113	1141	800		2,100-0		3360
210114	1142	800		2,200-0		3520
210115	1143	800		2,300-0		3680
210116	1144	800		2,400-0		3840
210117	1145	800		2,500-0		4000
210118	1146	800		2,600-0		4160
210119	1147	800		2,700-0		4320
210120	1148	800		2,800-0		4480
210121	1149	800		2,900-0		4640
210122	1150	800		3,000-0		4800
210123	1151	800		3,100-0		4960
210124	1152	800		3,200-0		5120
210125	1153	800		3,300-0		5280
210126	1154	800		3,400-0		5440
210127	1155	800		3,500-0		5600
210128	1156	800		3,600-0		5760
210129	1157	800		3,700-0		5920
210130	1158	800		3,800-0		6080
210131	1159	800		3,900-0		6240
210132	1160	800		4,000-0		6400
210133	1161	800		4,100-0		6560
210134	1162	800		4,200-0		6720
210135	1163	800		4,300-0		6880
210136	1164	800		4,400-0		7040
210137	1165	800		4,500-0		7200
210138	1166	800		4,600-0		7360
210139	1167	800		4,700-0		7520
210140	1168	800		4,800-0		7680
210141	1169	800		4,900-0		7840
210142	1170	800		5,000-0		8000
210143	1171	800		5,100-0		8160
210144	1172	800		5,200-0		8320
210145	1173	800		5,300-0		8480
210146	1174	800		5,400-0		8640
210147	1175	800		5,500-0		8800
210148	1176	800		5,600-0		8960
210149	1177	800		5,700-0		9120
210150	1178	800		5,800-0		9280
210151	1179	800		5,900-0		9440
210152	1180	800		6,000-0		9600
210153	1181	800		6,100-0		9760
210154	1182	800		6,200-0		9920
210155	1183	800		6,300-0		10080
210156	1184	800		6,400-0		10240
210157	1185	800		6,500-0		10400
210158	1186	800		6,600-0		10560
210159	1187	800		6,700-0		10720
210160	1188	800		6,800-0		10880
210161	1189	800		6,900-0		11040
210162	1190	800		7,000-0		11200
210163	1191	800		7,100-0		11360
210164	1192	800		7,200-0		11520
210165	1193	800		7,300-0		11680
210166	1194	800		7,400-0		11840
210167	1195	800		7,500-0		12000
210168	1196	800		7,600-0		12160
210169	1197	800		7,700-0		12320
210170	1198	800		7,800-0		12480
210171	1199	800		7,900-0		12640
210172	1200	800		8,000-0		12800
210173	1201	800		8,100-0		12960
210174	1202	800		8,200-0		13120
210175	1203	800		8,300-0		13280
210176	1204	800		8,400-0		13440
210177	1205	800		8,500-0		13600
210178	1206	800		8,600-0		13760
210179	1207	800		8,700-0		13920
210180	1208	800		8,800-0		14080
210181	1209	800		8,900-0		14240
210182	1210	800		9,000-0		14400
210183	1211	800		9,100-0		14560
210184	1212	800		9,200-0		14720
210185	1213	800		9,300-0		14880
210186	1214	800		9,400-0		15040
210187	1215	800		9,500-0		15200
210188	1216	800		9,600-0		15360
210189	1217	800		9,700-0		15520
210190	1218	800		9,800-0		15680
210191	1219	800		9,900-0		15840
210192	1220	800		10,000-0		16000
210193	1221	800		10,100-0		16160
210194	1222	800		10,200-0		16320
210195	1223	800		10,300-0		16480
210196	1224	800		10,400-0		16640
210197	1225	800		10,500-0		16800
210198	1226	800		10,600-0		16960
210199	1227	800		10,700-0		17120
210200	1228	800		10,800-0		17280
210201	1229	800		10,900-0		17440
210202	1230	800		11,000-0		17600
210203	1231	800		11,100-0		17760
210204	1232	800		11,200-0		17920
210205	1233	800		11,300-0		18080
210206	1234	800		11,400-0		18240
210207	1235	800		11,500-0		18400
210208	1236	800		11,600-0		18560
210209	1237	800		11,700-0		18720
210210	1238	800		11,800-0		18880
210211	1239	800		11,900-0		19040
210212	1240	800		12,000-0		19200
210213	1241	800		12,100-0		19360
210214	1242	800		12,200-0		19520
210215	1243	800		12,300-0		19680
210216	1244	800		12,400-0		19840
210217	1245	800		12,500-0		20000
210218	1246	800		12,600-0		20160
210219	1247	800		12,700-0		20320
210220	1248	800		12,800-0		20480
210221	1249	800		12,900-0		20640
210222	1250	800		13,000-0		20800
210223	1251	800		13,100-0		20960
210224	1252	800		13,200-0		21120
210225	1253	800		13,300-0		21280
210226	1254	800		13,400-0		21440
210227	1255	800		13,500-0		21600
210228	1256	800		13,600-0		21760
210229	1257	800		13,700-0		21920
210230	1258	800		13,800-0		22080
210231	1259	800		13,900-0		22240
210232	1260	800		14,000-0		22400
210233	1261	800		14,100-0		22560
210234	1262	800		14,200-0		22720
210235	1263	800		14,300-0		22880
210236	1264	800		14,400-0		23040
210237	1265	800		14,500-0		23200
210238	1266	800		14,600-0		23360
210239	1267	800		14,700-0		23520
210240	1268	800		14,800-0		23680
210241	1269	800		14,900-0		23840
210242	1270	800		15,000-0		24000
210243	1271	800		15,100-0		24160
210244	1272	800		15,200-0		24320
210245	1273	800		15,300-0		24480
210246	1274	800		15,400-0		24640
210247	1275	800		15,500-0		24800
210248	1276	800		15,600-0		24960
210249	1277	800		15,700-0		25120
210250	1278	800		15,800-0		25280
210251	1279	800		15,900-0		25440
210252	1280	800		16,000-0		25600
210253	1281	800		16,100-0		25760
210254	1282	800		16,200-0		25920
210255	1283	800		16,300-0		26080
210256	1284	800		16,400-0		26240
210257	1285	800		16,500-0		26400
210258	1286	800		16,600-0		26560
210259	1287	800		16,700-0		26720
210260	1288	800		16,800-0		26880
210261	1289	800		16,900-0		27040
210262	1290	800		17,000-0		27200
210263	1291	800		17,100-0		27360
210264	1292	800		17,200-0		27520
210265	1293	800		17,300-0		27680
210266	1294	800		17,400-0		27840
210267	1295	800		17,500-0		28000
210268	1296	800		17,600-0		28160
210269	1297	800		17,700-0		28320
210270	1298	800		17,800-0		28480
210271	1299	800		17,900-0		28640
210272	1300	800		18,000-0		28800
210273	1301	800		18,100-0		28960
210274	1302	800		18,200-0		29120
210275	1303	800		18,300-0		29280
210276	1304	800		18,400-0		29440
210277	1305	800		18,500-0		29600
210278	1306	800		18,600-0		29760
210279	1307	800		18,700-0		29920
210280	1308	800		18,800-0		30080
210281	1309	800		18,900-0		30240
210282	1310	800		19,000-0		30400
210283	1311	800		19,100-0		30560
210284	1312	800		19,200-0		30720
210285	1313	800		19,300-0		30880
210286	1314	800		19,400-0		31040
210287	1315	800		19,500-0		31200
210288	1316	800		19,600-0		31360

APPENDIX B
RTG SD-RTG TRANSPORTATION SYSTEM COST DATAAPPENDIX B-1 JUNE 1974-1996
APPENDIX B-1-1

FISCAL YEAR	TOTAL COST (\$M)	TOTAL COST (\$M)	TOTAL COST (\$M)		TOTAL COST (\$M)	TOTAL COST (\$M)
			1974-1975	1975-1976		
1974/75	1700	200		1,500-1		170
1975/76	1225	215		1,010-1		215
1976/77	1520	307	2,225-2	1,918-2		325
1977/78	1500	210		1,290-2		210
1978/79	1575	150		1,425-2		250
1979/80	1000	200		800-2		150
1980/81	1010	210		800-2		200
1981/82	975	75	2,000-10	2,075-1		90

APPENDIX B

**RECEPTACLE S/N 814 HELIUM LEAK RATE
MEASUREMENTS DURING THERMAL MARGIN TEST**

APPENDIX B
RTG SD-3 OPERABLE THERMAL SHIELD TEST DATAOPERABLE 6/1 000213/1-2420
OPERABLE 6/1 011

TEST DATE	TEMP CLASS	OPERABLE TIME (H)	LINE SHIELD CHARACTERISTICS		REMARKS	STATUS
			"LINE SHIELD" (mm 20/100)	"FIELD" (mm 20/100)		
6/2/91		36	1,000-10	1,000-7		0
6/2/91	0000	70	1,000-10			7
6/2/91	0000	70	1,000-10			7
6/2/91	1000	80	1,000-10			10
6/2/91	1000	100	1,000-10			10
6/2/91	1000	120	1,000-10			10
6/2/91	1000	140	1,000-10			10
6/2/91	1000	160	1,000-10			10
6/2/91	1000	180	1,000-10			10
6/2/91	1000	200	1,000-10			10
6/2/91	1000	220	1,000-10			10
6/2/91	1000	240	1,000-10			10
6/2/91	1000	260	1,000-10			10
6/2/91	1000	280	1,000-10			10
6/2/91	1000	300	1,000-10			10
6/2/91	1000	320	1,000-10			10
6/2/91	1000	340	1,000-10			10
6/2/91	1000	360	1,000-10			10
6/2/91	1000	380	1,000-10			10
6/2/91	1000	400	1,000-10			10
6/2/91	1000	420	1,000-10			10
6/2/91	1000	440	1,000-10			10
6/2/91	1000	460	1,000-10			10
6/2/91	1000	480	1,000-10			10
6/2/91	1000	500	1,000-10			10
6/2/91	1000	520	1,000-10			10
6/2/91	1000	540	1,000-10			10
6/2/91	1000	560	1,000-10			10
6/2/91	1000	580	1,000-10			10
6/2/91	1000	600	1,000-10			10
6/2/91	1000	620	1,000-10			10
6/2/91	1000	640	1,000-10			10
6/2/91	1000	660	1,000-10			10
6/2/91	1000	680	1,000-10			10
6/2/91	1000	700	1,000-10			10
6/2/91	1000	720	1,000-10			10
6/2/91	1000	740	1,000-10			10
6/2/91	1000	760	1,000-10			10
6/2/91	1000	780	1,000-10			10
6/2/91	1000	800	1,000-10			10
6/2/91	1000	820	1,000-10			10
6/2/91	1000	840	1,000-10			10
6/2/91	1000	860	1,000-10			10
6/2/91	1000	880	1,000-10			10
6/2/91	1000	900	1,000-10			10
6/2/91	1000	920	1,000-10			10
6/2/91	1000	940	1,000-10			10
6/2/91	1000	960	1,000-10			10
6/2/91	1000	980	1,000-10			10
6/2/91	1000	1000	1,000-10			10

APPENDIX B
 THE AIR TRANSPORTATION SYSTEM (ATS) DATA

APPENDIX B-1: WHC-SD-RTG-001
 APPENDIX B-2: 001

DATE	TIME	AIRPORT	AIR TRAFFIC		STATUS	REMARKS
			ARRIVAL	DEPARTURE		
01/01/88	1100	101		1,000-0		00
01/02/88	1100	101	1,000-00	1,000-0		00
01/03/88	1100	101	1,000-00	1,000-0		00
01/04/88	1100	101	1,000-00	1,000-0		00
01/05/88	1100	101	1,000-00	1,000-0		00
01/06/88	1100	101	1,000-00	1,000-0		00
01/07/88	1100	101	1,000-00	1,000-0		00
01/08/88	1100	101	1,000-00	1,000-0		00
01/09/88	1100	101	1,000-00	1,000-0		00
01/10/88	1100	101	1,000-00	1,000-0		00
01/11/88	1100	101	1,000-00	1,000-0		00
01/12/88	1100	101	1,000-00	1,000-0		00
01/13/88	1100	101	1,000-00	1,000-0		00
01/14/88	1100	101	1,000-00	1,000-0		00
01/15/88	1100	101	1,000-00	1,000-0		00
01/16/88	1100	101	1,000-00	1,000-0		00
01/17/88	1100	101	1,000-00	1,000-0		00
01/18/88	1100	101	1,000-00	1,000-0		00
01/19/88	1100	101	1,000-00	1,000-0		00
01/20/88	1100	101	1,000-00	1,000-0		00
01/21/88	1100	101	1,000-00	1,000-0		00
01/22/88	1100	101	1,000-00	1,000-0		00
01/23/88	1100	101	1,000-00	1,000-0		00
01/24/88	1100	101	1,000-00	1,000-0		00
01/25/88	1100	101	1,000-00	1,000-0		00
01/26/88	1100	101	1,000-00	1,000-0		00
01/27/88	1100	101	1,000-00	1,000-0		00
01/28/88	1100	101	1,000-00	1,000-0		00
01/29/88	1100	101	1,000-00	1,000-0		00
01/30/88	1100	101	1,000-00	1,000-0		00
01/31/88	1100	101	1,000-00	1,000-0		00
02/01/88	1100	101	1,000-00	1,000-0		00
02/02/88	1100	101	1,000-00	1,000-0		00
02/03/88	1100	101	1,000-00	1,000-0		00
02/04/88	1100	101	1,000-00	1,000-0		00
02/05/88	1100	101	1,000-00	1,000-0		00
02/06/88	1100	101	1,000-00	1,000-0		00
02/07/88	1100	101	1,000-00	1,000-0		00
02/08/88	1100	101	1,000-00	1,000-0		00
02/09/88	1100	101	1,000-00	1,000-0		00
02/10/88	1100	101	1,000-00	1,000-0		00
02/11/88	1100	101	1,000-00	1,000-0		00
02/12/88	1100	101	1,000-00	1,000-0		00
02/13/88	1100	101	1,000-00	1,000-0		00
02/14/88	1100	101	1,000-00	1,000-0		00
02/15/88	1100	101	1,000-00	1,000-0		00
02/16/88	1100	101	1,000-00	1,000-0		00
02/17/88	1100	101	1,000-00	1,000-0		00
02/18/88	1100	101	1,000-00	1,000-0		00
02/19/88	1100	101	1,000-00	1,000-0		00
02/20/88	1100	101	1,000-00	1,000-0		00
02/21/88	1100	101	1,000-00	1,000-0		00
02/22/88	1100	101	1,000-00	1,000-0		00
02/23/88	1100	101	1,000-00	1,000-0		00
02/24/88	1100	101	1,000-00	1,000-0		00
02/25/88	1100	101	1,000-00	1,000-0		00
02/26/88	1100	101	1,000-00	1,000-0		00
02/27/88	1100	101	1,000-00	1,000-0		00
02/28/88	1100	101	1,000-00	1,000-0		00
02/29/88	1100	101	1,000-00	1,000-0		00
02/30/88	1100	101	1,000-00	1,000-0		00

APPENDIX B
 RTG TRIP & THROUGHPUT PERIOD, TRAVEL TIME PERIOD

Multi-Period RTG Multi-Period
 Multi-Period RTG RTG

TRIP NO.	TRIP NO.	TRIP NO.	(TRIP PERIOD)		TRIP NO.	TRIP NO.
			TRIP NO.	TRIP NO.		
1/1/79	001	01	1,000-00			100
1/1/79	001	02	1,000-00			100
1/1/79	001	03	1,000-00			100
1/1/79	001	04	1,000-00			100
1/1/79	001	05	1,000-00			100
1/1/79	001	06	1,000-00			100
1/1/79	001	07	1,000-00			100
1/1/79	001	08	1,000-00			100
1/1/79	001	09	1,000-00			100
1/1/79	001	10	1,000-00			100
1/1/79	001	11	1,000-00			100
1/1/79	001	12	1,000-00			100
1/1/79	001	13	1,000-00			100
1/1/79	001	14	1,000-00			100
1/1/79	001	15	1,000-00			100
1/1/79	001	16	1,000-00			100
1/1/79	001	17	1,000-00			100
1/1/79	001	18	1,000-00			100
1/1/79	001	19	1,000-00			100
1/1/79	001	20	1,000-00			100
1/1/79	001	21	1,000-00			100
1/1/79	001	22	1,000-00			100
1/1/79	001	23	1,000-00			100
1/1/79	001	24	1,000-00			100
1/1/79	001	25	1,000-00			100
1/1/79	001	26	1,000-00			100
1/1/79	001	27	1,000-00			100
1/1/79	001	28	1,000-00			100
1/1/79	001	29	1,000-00			100
1/1/79	001	30	1,000-00			100
1/1/79	001	31	1,000-00			100
1/1/79	001	32	1,000-00			100
1/1/79	001	33	1,000-00			100
1/1/79	001	34	1,000-00			100
1/1/79	001	35	1,000-00			100
1/1/79	001	36	1,000-00			100
1/1/79	001	37	1,000-00			100
1/1/79	001	38	1,000-00			100
1/1/79	001	39	1,000-00			100
1/1/79	001	40	1,000-00			100
1/1/79	001	41	1,000-00			100
1/1/79	001	42	1,000-00			100
1/1/79	001	43	1,000-00			100
1/1/79	001	44	1,000-00			100
1/1/79	001	45	1,000-00			100
1/1/79	001	46	1,000-00			100
1/1/79	001	47	1,000-00			100
1/1/79	001	48	1,000-00			100
1/1/79	001	49	1,000-00			100
1/1/79	001	50	1,000-00			100
1/1/79	001	51	1,000-00			100
1/1/79	001	52	1,000-00			100
1/1/79	001	53	1,000-00			100
1/1/79	001	54	1,000-00			100
1/1/79	001	55	1,000-00			100
1/1/79	001	56	1,000-00			100
1/1/79	001	57	1,000-00			100
1/1/79	001	58	1,000-00			100
1/1/79	001	59	1,000-00			100
1/1/79	001	60	1,000-00			100
1/1/79	001	61	1,000-00			100
1/1/79	001	62	1,000-00			100
1/1/79	001	63	1,000-00			100
1/1/79	001	64	1,000-00			100
1/1/79	001	65	1,000-00			100
1/1/79	001	66	1,000-00			100
1/1/79	001	67	1,000-00			100
1/1/79	001	68	1,000-00			100
1/1/79	001	69	1,000-00			100
1/1/79	001	70	1,000-00			100
1/1/79	001	71	1,000-00			100
1/1/79	001	72	1,000-00			100
1/1/79	001	73	1,000-00			100
1/1/79	001	74	1,000-00			100
1/1/79	001	75	1,000-00			100
1/1/79	001	76	1,000-00			100
1/1/79	001	77	1,000-00			100
1/1/79	001	78	1,000-00			100
1/1/79	001	79	1,000-00			100
1/1/79	001	80	1,000-00			100
1/1/79	001	81	1,000-00			100
1/1/79	001	82	1,000-00			100
1/1/79	001	83	1,000-00			100
1/1/79	001	84	1,000-00			100
1/1/79	001	85	1,000-00			100
1/1/79	001	86	1,000-00			100
1/1/79	001	87	1,000-00			100
1/1/79	001	88	1,000-00			100
1/1/79	001	89	1,000-00			100
1/1/79	001	90	1,000-00			100
1/1/79	001	91	1,000-00			100
1/1/79	001	92	1,000-00			100
1/1/79	001	93	1,000-00			100
1/1/79	001	94	1,000-00			100
1/1/79	001	95	1,000-00			100
1/1/79	001	96	1,000-00			100
1/1/79	001	97	1,000-00			100
1/1/79	001	98	1,000-00			100
1/1/79	001	99	1,000-00			100
1/1/79	001	100	1,000-00			100

APPENDIX B
RTG AND 2 MONTHLY VEHICLE TRAVEL TRUCK DATA

APPENDIX B.P.01 0002411/1-0-0000
MICROSOFT EXCEL 5.0A

YEAR MM/DD	TRUCK COUNT	OPERATING HOURS (FH)	TRUCK MILES TRAVELLED		MILES PER TRUCK (MPH)	MILES PER HOUR (MPH)
			"TOTAL" (Miles)	"NET" (Miles)		
01/1/91	1002	690	2,000-10			200
02/1/91	1000	700	2,000-10			200
03/1/91	1000	677	2,000-10			200
04/1/91	1000	660	2,000-10			200
05/1/91	1000	660	2,000-10			200
06/1/91	1000	660	2,000-10			200
07/1/91	1000	660	2,000-10			200
08/1/91	1000	660	2,000-10			200
09/1/91	1000	660	2,000-10			200
10/1/91	1000	660	2,000-10			200
11/1/91	1000	660	2,000-10			200
12/1/91	1000	660	2,000-10			200
01/1/92	1000	660	2,000-10			200
02/1/92	1000	660	2,000-10			200
03/1/92	1000	660	2,000-10			200
04/1/92	1000	660	2,000-10			200
05/1/92	1000	660	2,000-10			200
06/1/92	1000	660	2,000-10			200
07/1/92	1000	660	2,000-10			200
08/1/92	1000	660	2,000-10			200
09/1/92	1000	660	2,000-10			200
10/1/92	1000	660	2,000-10			200
11/1/92	1000	660	2,000-10			200
12/1/92	1000	660	2,000-10			200
01/1/93	1000	660	2,000-10			200
02/1/93	1000	660	2,000-10			200

5.0 SHIELDING EVALUATION

Adequate shielding in the Radioisotope Thermoelectric Generator (RTG) Transportation System Package ensures that the most radioactive payload will not cause external dose rates to exceed the requirements of 71.47 and 71.51 of 10 CFR 71.

5.1 DISCUSSION AND RESULTS

The primary payload configuration to be transported inside a single RTG Transportation System Package is a general purpose heat source (GP-HS) RTG. Because of a 5,000-W thermal limit inside the semitrailer, only one GP-HS RTG can be shipped in the RTG exclusive-use transportation system trailer.

Primary shielding for the payload is provided by self-shielding of the plutonium fuel, the RTG body, the inner containment vessel (ICV), the outer containment vessel (OCV), and, out the side of the package by the external coolant jacket. While the semitrailer provides little significance in the way of shielding, it defines the physical boundary for determining external dose rates by regulatory normal conditions of transport (NCT). Regulatory hypothetical accident condition (HAC) dose rates are determined relative to the package surface.

Regulatory NCT and HAC shielding requirements for the package are determined by the following criteria:

NCT: per the requirements of 10 CFR 71.47, maximum dose rates of 1,000 mrem/hr at any point in contact with the secured package within the closed transport vehicle; 200 mrem/hr at any point on the outer surface of the vehicle; 10 mrem/hr at any lateral point 2 m from the outer surface of the vehicle; and 2 mrem/hr in the normally occupied positions of the vehicle.

HAC: per the requirement of 10 CFR 71.51(a)(2), a maximum dose rate of 1,000 mrem/hr at any point 1 m from the package.

Tables 5-1 and 5-1a summarize the results of the radiation shielding analyses for the regulatory NCT and HAC events. The 2nd entry in the "Gamma" column of Tables 5-1 and 5-1a is the contribution from gamma rays produced by neutrons, the 3rd entry is the contribution from the gamma source and the 1st entry is the total contribution from gammas (sum of 2nd and 3rd entry). Adequate shielding is available to meet all regulatory requirements in all cases. Also, the dose rates for NCT are verified before releasing the package for shipment. The calculations summarized in Table 5-1 were made with coolant in the coolant jacket. To compensate for the presence of coolant, new dose rate limits were calculated to ensure the limits of 10 CFR 71.47 would be met if the coolant water was lost. These operational control dose limits are listed in Table 5-1 and are used when coolant is present in the package. For completeness, the shielding results without coolant in the package coolant jacket are listed in Table 5-1a. However, it is noted that water is included in the coolant jacket for the NCT model described in Section 5.3.1 and the NCT model input files listed in Appendices 5.5.2 and 5.5.3.

Even though the generic payload definition (see Chapter 1) allows a PuO_2 content per trailer that is higher than that for a single GP-HS RTG, the potential increase in dose rates due to the larger total PuO_2 mass is offset by geometry effects. Specifically, the minimum required separation distance of 9.5 feet between package centerlines when shipping more than a single package is sufficient to ensure reduced dose rates for two-package shipments. The shielding analysis for two packages per trailer is documented in the RTG Transportation System SARP Addendum.

WHC-SD-RTG-SARP-002.

5.2 SOURCE SPECIFICATION

The GPHS RTG is comprised of 18 GPHS modules consisting of a graphite aeroshell which, in turn, houses two graphite impact shells. Each graphite impact shell contains two iridium-cladded fuel pellets. Each of the 72 fuel pellets contain a maximum of 157 g of plutonia for a maximum total fuel mass of 11,304 g. Figure 5-1 illustrates the GPHS RTG and internal subcomponents and Figure 5-2 depicts a GPHS fuel module.

Tables 5-2 and 5-3 delineate the fuel pellet and initial fuel properties for the GPHS RTG. Tables 5-4 and 5-6 present the gamma¹ and neutron² spectra respectively for a single 15T-g fueled clad. The values in Tables 5-4 and 5-6 are multiplied by 72 in the shielding analyses to reflect the total number of fueled clads in a GPHS RTG. Further, the gamma spectrum used in Table 5-4 is for a fuel age of 17.5 years, at which time the maximum gamma flux occurs. The neutron spectrum used in Table 5-5 conservatively ignores flux reduction because of plutonium decay ($T_{1/2}$ for ²³⁸Pu is 87.74 years) and is based on a maximum neutron emission rate of 8000 n/s-g ²³⁸Pu for a GPHS fueled clad. The alpha-n source was determined by subtracting the spontaneous fission source from the maximum neutron emission rate of 8000 n/s-g ²³⁸Pu. The neutron spectrum from the Monte Carlo Neutron Photon (MCNP)¹⁴ calculation includes all subcritical multiplication from fissions of ²³⁸Pu and ²³⁹Pu. Additional source term data are provided in Tables 5-6 and 5-7.

TABLE 5-1. Summary of Maximum Dose Rates With Coolant in the Jacket (mrem/hr).

Normal conditions of transport location	Gamma	Neutron	Total	Regulatory Limit	Operational Control Limit*
Side, surface of package	68.32 (.16%) ^a 2.09 (.47%) 66.23 (.14%)	116.5 (.33%)	183.8 (.22%)	1,000	590
Side, surface of semitrailer	11.64 (.32%) 0.262 (.8%) 11.28 (.31%)	21.69 (.48%)	33.22 (.34%)	200	120
Two meters from side surface of semitrailer	1.83 (.17%) 0.041 (.35%) 1.79 (.15%)	3.93 (.24%)	5.76 (.18%)	10	6.4
Top surface of package	53.68 (.82%) 0.78 (2.6%) 52.90 (.76%)	156.1 (1.2%)	209.7 (.92%)	1,000	1,000
Top surface of semitrailer	12.97 (.52%) 0.184 (1.6%) 12.78 (.56%)	34.90 (.8%)	47.87 (.81%)	200	200
Bottom surface of semitrailer	1.025 (1.3%) 0.052 (2.8%) 0.973 (1.2%)	13.32 (0.8%)	14.35 (.75%)	200	190
Tractor cab (operator's seat)	0.31 (.18%) 0.0088 (.39%) 0.284 (.15%)	0.705 (.26%)	1.01 (.18%)	2	1.2
Hypothetical accident conditions	Gamma	Neutron	Total	Regulatory Limit	
One meter from the top surface of the package ^b	20.64 (.36%) 0.40 (1.2%) 20.24 (.32%)	112.60 (1.0%)	133.1 (.85%)	1,000	

^a) - One standard deviation statistical uncertainties.

^bFor the HAC analyses, the plutonic fuel is conservatively reconfigured as a sphere located at the package top where shielding is a minimum (see Section 5.3.2).

*Operational control limit used when coolant is present in package. This applies only to NCT.

TABLE 5-1a. Summary of Maximum Dose Rates Without Coolant in the Jacket (transport).

Normal conditions of transport location	Gamma	Neutron	Total	Regulatory Limit
Side, surface of package	74.92 (1.16%) ^a 0.57 (1.95%) 74.35 (1.14%)	230.2 (1.40%)	305.1 (1.51%)	1,000
Side, surface of semitrailer	12.64 (1.32%) 0.087 (2.2%) (2.55 (3.1%))	39.46 (1.67%)	52.10 (1.52%)	200
Two meters from side surface of semitrailer	2.01 (1.18%) 0.014 (1.71%) 1.99 (1.69%)	6.99 (1.30%)	8.00 (1.24%)	10
Top surface of package	53.65 (1.80%) 0.39 (4.4%) 53.26 (1.74%)	147.73 (1.8%)	201.4 (1.4%)	1,000
Top surface of semitrailer	12.66 (1.64%) 0.090 (2.6%) 12.79 (1.59%)	33.33 (1.1%)	46.21 (1.62%)	200
Bottom surface of semitrailer	1.14 (1.3%) 0.023 (4.1%) 1.120 (1.2%)	13.82 (1.2%)	14.96 (1.1%)	200
Tractor cab (operator's seat)	0.332 (1.14%) 0.0025 (1.74%) 0.329 (1.17%)	1.26 (1.33%)	1.59 (1.26%)	2
Hypothetical accident conditions	Gamma	Neutron	Total	Regulatory Limit
One meter from the top surface of the package ^b	20.64 (1.36%) 0.40 (1.2%) 20.24 (1.32%)	112.50 (1.0%)	133.1 (1.85%)	1,000

^a) = One standard deviation statistical uncertainties.

^bFor the HAC analysis, the plutonia fuel is conservatively reconfigured as a sphere located at the package top where shielding is a minimum (see Section 5.3.2).

TABLE 6-2. GPHS RTG Fuel Physical, Thermal, and Radiological Properties.

Fuel pellet property (excluding cladding)	GPHS fuel pellet
Diameter (cm)	2.7534 (± 0.0254)
Length (cm)	2.7559 (± 0.0381)
Volume (cm ³)	18.409
Density (g/cm ³)	9.8
Weight (g)	187
Thermal power (W)	62.5
Power density (W/cm ³)	3.81
Activity (Ci)	1,930
Specific activity (Ci/g)	12.6

TABLE 6-3. Plutonium-239 Initial Fuel Properties.

²³⁹ Pu content	80 to 88 mol-% of total plutonium
²⁴⁰ Pu content	<0.0001 mol-% of total plutonium
Sum of actinide impurities	<1.0 mol-% of total plutonium
Individual actinide impurities	<0.6 mol-% of total plutonium
¹⁸ O contained in PuO ₂ (a)	>99.98 mol-% of total oxygen in PuO ₂
Sum of nonactinide cationic impurities	<0.2250 wt-% of fuel
Individual nonactinide cationic impurities	<0.0800 wt-% of fuel
Specific thermal power at time of manufacture	0.40 W per gram PuO ₂ fuel
Approximate reduction of thermal power	0.8% per year
Maximum neutron emission rate for GPHS fueled (d)	8000 n/s-g ²³⁹ Pu

(a) Atoms of oxygen are exchanged until the oxygen in PuO₂ is 99.98 mol-% ¹⁸O. See Reference 5.1.

TABLE 5-4. Total Gamma Ray Source from One 157-g Pellet*
(17% -year plutonia fuel).

E_{min} (MeV)	E_{max} (MeV)	E_{avg} (MeV)	$\Gamma_{ppm}^{239}Pu$ Source (ph/sec)
0.15	0.20	0.25	6.82E+08
0.25	0.30	0.35	4.96E+07
0.35	0.40	0.45	4.03E+06
0.45	0.50	0.55	9.25E+08
0.55	0.60	0.65	7.33E+06
0.65	0.70	0.75	1.76E+07
0.75	0.80	0.85	5.79E+06
0.85	0.90	0.95	6.72E+06
0.95	1.00	1.05	1.37E+06
1.05	1.10	1.15	5.30E+05
1.15	1.20	1.25	1.87E+05
1.25	1.30	1.35	1.00E+05
1.35	1.40	1.45	2.20E+04
1.45	1.50	1.55	3.31E+05
1.55	1.60	1.65	1.42E+06
1.65	1.70	1.75	8.22E+04
1.75	1.80	1.85	1.17E+05
1.85	1.90	1.95	1.31E+04
1.95	2.00	2.05	1.11E+04
2.05	2.10	2.15	1.00E+04

TABLE 5-4. Total Gamma Ray Source from One 187-g
 Pellet¹ (17½-year plutonia fuel). (Cont.)

E_{min} (MeV)	E_{max} (MeV)	E_{center} (MeV)	100m ²³⁹ Pu Source (ph/sec)
2.15	2.20	2.25	8.95E+03
2.25	2.30	2.36	7.86E+03
2.35	2.40	2.45	7.08E+03
2.45	2.50	2.55	6.25E+03
2.65	2.60	2.66	3.33E+07
2.65	2.70	2.76	4.89E+03
2.75	2.80	2.85	4.50E+03
2.85	2.90	2.95	4.03E+03
2.95	3.00	3.06	3.84E+03
3.05	3.10	3.16	3.27E+03
3.15	3.20	3.25	2.98E+03
3.25	3.30	3.35	2.67E+03
3.35	3.40	3.46	2.42E+03
3.45	3.50	3.56	2.21E+03
3.55	3.60	3.66	2.01E+03
3.65	3.70	3.76	1.83E+03
3.75	3.80	3.85	1.66E+03
3.85	3.90	3.95	1.54E+03
3.95	4.00	4.05	1.42E+03
4.05	4.10	4.16	1.28E+03

TABLE 5-4. Total Gamma Ray Source from One 157-g
PuBe² (17 1/2-year plutonia fuel). (Cont.)

E_{min} (MeV)	E_w (MeV)	E_{max} (MeV)	1ppm ²³⁸ Pu Source (ph/sec)
4.15	4.20	4.25	1.20E+03
4.25	4.30	4.35	1.11E+03
4.35	4.40	4.45	1.01E+03
4.45	4.40	4.55	8.33E+02
4.55	4.50	4.65	6.68E+02
4.65	4.60	4.75	7.92E+02
4.75	4.70	4.85	7.37E+02
4.85	4.80	4.95	6.78E+02
4.95	5.00	5.05	6.34E+02
5.05	5.10	5.15	5.74E+02
5.15	5.20	5.25	6.25E+02
5.25	5.30	5.35	4.87E+02
5.35	5.40	5.45	4.53E+02
5.45	5.50	5.55	4.16E+02
5.55	5.60	5.65	3.83E+02
5.65	5.70	5.75	3.54E+02
5.75	5.80	5.85	3.22E+02
5.85	5.90	5.85	2.97E+02
5.95	6.00	6.05	2.72E+02
6.05	6.10	6.15	2.48E+02

TABLE E-4. Total Gamma Ray Source from One 157-g
Pellet¹ (17%-year plutonia fuel). (Cont.)

E_{min} (MeV)	E_{max} (MeV)	E_{center} (MeV)	1ppm ²³⁹ Pu Source (ph/sec)
6.15	6.20	6.25	2.30E+02
6.26	6.30	6.35	2.10E+02
6.35	6.40	6.45	1.92E+02
6.45	6.50	6.55	1.70E+02
6.55	6.60	6.65	1.50E+02
6.65	6.70	6.75	1.40E+02
6.75	6.80	6.85	1.26E+02
6.85	6.90	6.95	1.12E+02
6.95	7.00	7.05	1.02E+02
7.05	7.10	7.15	8.92E+01
7.15	7.20	7.25	7.68E+01
7.25	7.30	7.35	6.68E+01
7.35	7.40	7.45	5.70E+01
7.45	7.50	7.55	4.74E+01
7.55	7.60	7.65	3.76E+01
	Total		8.21E+08

TABLE 5-5. Neutron Spectrum for a Single Fueled Clad¹ (157 g maximum, new plutonia fuel).

Energy (MeV)	n/pellet-sec for (o,n)	n/pellet-sec for s.f.	n/pellet-sec total	Fraction of flux at E
0.1	4.89x10 ⁸	5.80x10 ⁸	1.02x10 ⁹	1.43x10 ⁻²
0.2	5.17x10 ⁸	7.42x10 ⁸	1.26x10 ⁹	1.78x10 ⁻²
0.3	6.03x10 ⁸	8.61x10 ⁸	1.36x10 ⁹	1.90x10 ⁻²
0.4	5.98x10 ⁸	9.14x10 ⁸	1.51x10 ⁹	2.12x10 ⁻²
0.5	8.16x10 ⁸	9.56x10 ⁸	1.77x10 ⁹	2.48x10 ⁻²
0.6	9.19x10 ⁸	9.78x10 ⁸	1.90x10 ⁹	2.68x10 ⁻²
0.7	1.01x10 ⁹	8.86x10 ⁸	2.00x10 ⁹	2.79x10 ⁻²
0.8	1.10x10 ⁹	8.82x10 ⁸	2.08x10 ⁹	2.82x10 ⁻²
0.9	1.06x10 ⁹	9.74x10 ⁸	2.03x10 ⁹	2.84x10 ⁻²
1.0	8.70x10 ⁸	8.55x10 ⁸	1.83x10 ⁹	2.56x10 ⁻²
1.1	8.11x10 ⁸	8.34x10 ⁸	1.84x10 ⁹	2.58x10 ⁻²
1.2	8.86x10 ⁸	9.06x10 ⁸	1.89x10 ⁹	2.65x10 ⁻²
1.3	1.11x10 ⁹	8.81x10 ⁸	1.99x10 ⁹	2.73x10 ⁻²
1.4	1.20x10 ⁹	8.52x10 ⁸	2.05x10 ⁹	2.87x10 ⁻²
1.5	1.22x10 ⁹	8.20x10 ⁸	2.04x10 ⁹	2.87x10 ⁻²
1.6	1.28x10 ⁹	7.87x10 ⁸	2.07x10 ⁹	2.91x10 ⁻²
1.7	1.40x10 ⁹	7.54x10 ⁸	2.15x10 ⁹	3.01x10 ⁻²
1.8	1.56x10 ⁹	7.21x10 ⁸	2.27x10 ⁹	3.19x10 ⁻²
1.9	1.61x10 ⁹	6.80x10 ⁸	2.30x10 ⁹	3.23x10 ⁻²
2.0	1.89x10 ⁹	6.57x10 ⁸	2.36x10 ⁹	3.30x10 ⁻²
2.1	1.70x10 ⁹	6.28x10 ⁸	2.33x10 ⁹	3.28x10 ⁻²

TABLE 5-5. Neutron Spectrum for a Single Fueled Clad^a (157 g maximum, new plutonia fuel). (Cont.)

Energy (MeV)	n/pellet-sec for (0,n)	n/pellet-sec for α,f	n/pellet-sec total	Fraction of flux at E _i
2.2	1.78x10 ⁴	5.88x10 ³	2.38x10 ⁴	3.33x10 ⁻⁴
2.3	1.81x10 ⁴	5.88x10 ³	2.38x10 ⁴	3.32x10 ⁻⁴
2.4	1.72x10 ⁴	5.39x10 ³	2.26x10 ⁴	3.18x10 ⁻⁴
2.5	1.66x10 ⁴	5.10x10 ³	2.16x10 ⁴	3.03x10 ⁻⁴
2.6	1.59x10 ⁴	4.82x10 ³	2.07x10 ⁴	2.91x10 ⁻⁴
2.7	1.52x10 ⁴	4.58x10 ³	1.98x10 ⁴	2.77x10 ⁻⁴
2.8	1.40x10 ⁴	4.33x10 ³	1.83x10 ⁴	2.70x10 ⁻⁴
2.9	1.36x10 ⁴	4.08x10 ³	1.77x10 ⁴	2.48x10 ⁻⁴
3.0	1.28x10 ⁴	3.84x10 ³	1.66x10 ⁴	2.33x10 ⁻⁴
3.1	1.13x10 ⁴	3.63x10 ³	1.49x10 ⁴	2.09x10 ⁻⁴
3.2	1.08x10 ⁴	3.44x10 ³	1.40x10 ⁴	1.7x10 ⁻⁴
3.3	9.11x10 ³	3.42x10 ³	1.24x10 ⁴	1.73x10 ⁻⁴
3.4	7.41x10 ³	3.04x10 ³	1.04x10 ⁴	1.47x10 ⁻⁴
3.5	6.26x10 ³	2.84x10 ³	9.10x10 ³	1.28x10 ⁻⁴
3.6	5.37x10 ³	2.69x10 ³	8.06x10 ³	1.13x10 ⁻⁴
3.7	4.35x10 ³	2.63x10 ³	6.88x10 ³	9.66x10 ⁻⁵
3.8	3.74x10 ³	2.38x10 ³	6.12x10 ³	8.55x10 ⁻⁵
3.9	3.26x10 ³	2.23x10 ³	5.49x10 ³	7.70x10 ⁻⁵
4.0	2.65x10 ³	2.07x10 ³	4.72x10 ³	6.62x10 ⁻⁵
4.1	2.38x10 ³	1.86x10 ³	4.34x10 ³	6.08x10 ⁻⁵
4.2	1.66x10 ³	1.84x10 ³	3.40x10 ³	4.77x10 ⁻⁵

TABLE 5-5. Neutron Spectrum for a Single Fueled Clad² (1157 g maximum, new plutonia fuel). (Cont.)

Energy (MeV)	n/pellet-sec for (α,n)	n/pellet-sec for s.f.	n/pellet-sec total	Fraction of flux at E _i
4.3	1.22x10 ⁹	1.72x10 ⁹	2.94x10 ⁹	4.13x10 ⁻²
4.4	7.48x10 ⁸	1.61x10 ⁹	2.36x10 ⁹	3.30x10 ⁻²
4.5	4.78x10 ⁸	4.47x10 ⁸	4.95x10 ⁸	6.84x10 ⁻³
5.0		5.20x10 ⁸	5.20x10 ⁸	7.48x10 ⁻³
5.5		3.79x10 ⁸	3.79x10 ⁸	5.30x10 ⁻³
6.0		2.66x10 ⁸	2.66x10 ⁸	3.72x10 ⁻³
6.5		1.85x10 ⁸	1.85x10 ⁸	2.60x10 ⁻³
7.0		1.29x10 ⁸	1.29x10 ⁸	1.81x10 ⁻³
7.5		8.92x10 ⁷	8.92x10 ⁷	1.25x10 ⁻³
8.0		6.13x10 ⁷	6.13x10 ⁷	8.60x10 ⁻⁴
8.5		4.21x10 ⁷	4.21x10 ⁷	5.80x10 ⁻⁴
9.0		2.67x10 ⁷	2.67x10 ⁷	4.03x10 ⁻⁴
9.5		1.97x10 ⁷	1.97x10 ⁷	2.76x10 ⁻⁴
10.0		1.86x10 ⁷	1.86x10 ⁷	2.78x10 ⁻⁴
11.0		1.21x10 ⁷	1.21x10 ⁷	1.70x10 ⁻⁴
12.0		5.53x10 ⁶	5.53x10 ⁶	7.75x10 ⁻⁵
13.0		2.48x10 ⁶	2.48x10 ⁶	3.48x10 ⁻⁵
14.0		1.11x10 ⁶	1.11x10 ⁶	1.55x10 ⁻⁵
15.0		4.90x10 ⁵	4.90x10 ⁵	6.88x10 ⁻⁶
Total	4.38x10 ⁹	2.77x10 ⁹	7.13x10 ⁹	

TABLE 5-6. Concentrations of Plutonium Isotopes and Actinide Impurities
Used in Developing Tables 5-4 and 5-5.

Isotope	Wt-% Pu	Wt Fraction of PuO ₂
²³⁹ Pu	1 x 10 ⁻⁴	8.81 x 10 ²
²⁴⁰ Pu	86	7.58 x 10 ¹
²⁴¹ Pu	11.5	1.01 x 10 ¹
²⁴² Pu	2.0	1.76 x 10 ²
²⁴³ Pu	0.4	3.52 x 10 ²
²⁴⁴ Pu	0.1	8.81 x 10 ⁴
²⁴¹ Am		2.6 x 10 ⁻⁴
²⁴³ Am		6.0 x 10 ⁻⁴
²³² Th		2.0 x 10 ⁻⁴
²³⁷ Np		2.0 x 10 ⁻⁴

TABLE 5-7. Limits on Impurities and Quantity of Oxygen
and Their Contribution to the Neutron Spectrum.

Element	Max. concentration in fuelled clad (wt%)	n/sec per fuel clad	% of total
B	1 x 10 ⁻⁶	1.55 x 10 ²	0.22
Mg	5 x 10 ⁻⁶	4.94 x 10 ²	0.69
Na	2.5 x 10 ⁻⁶	4.07 x 10 ²	5.70
Si	2 x 10 ⁻⁶	1.72 x 10 ²	0.24
O*	1.19 x 10 ⁻¹	8.88 x 10 ²	54.34
(α,n) Total		4.36 x 10 ²	81.20
Total neutrons		7.13 x 10 ⁴	100.00

* Not an impurity; O is present as the oxide in PuO₂.

GPHS - RTG

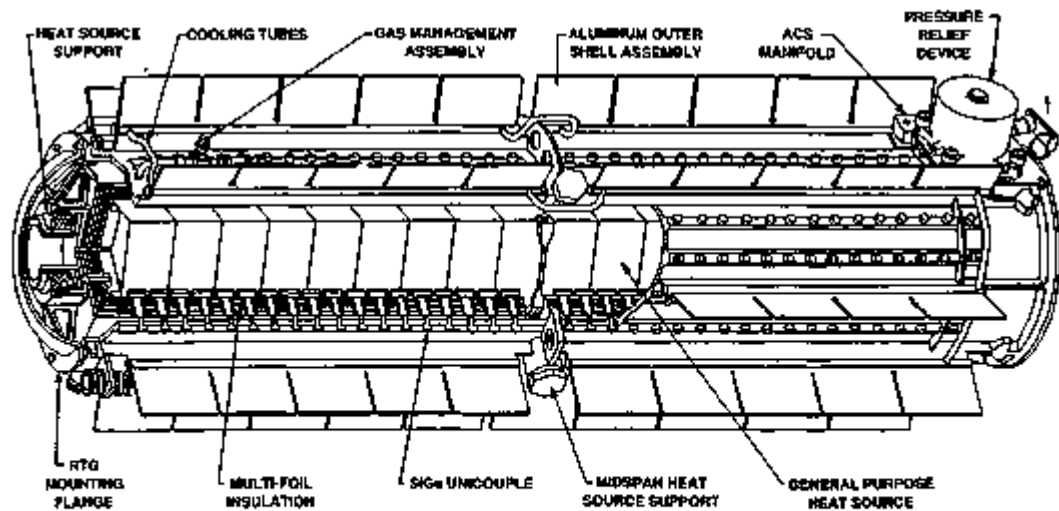


FIGURE 5-1. GPHS RTG Assembly Detail.

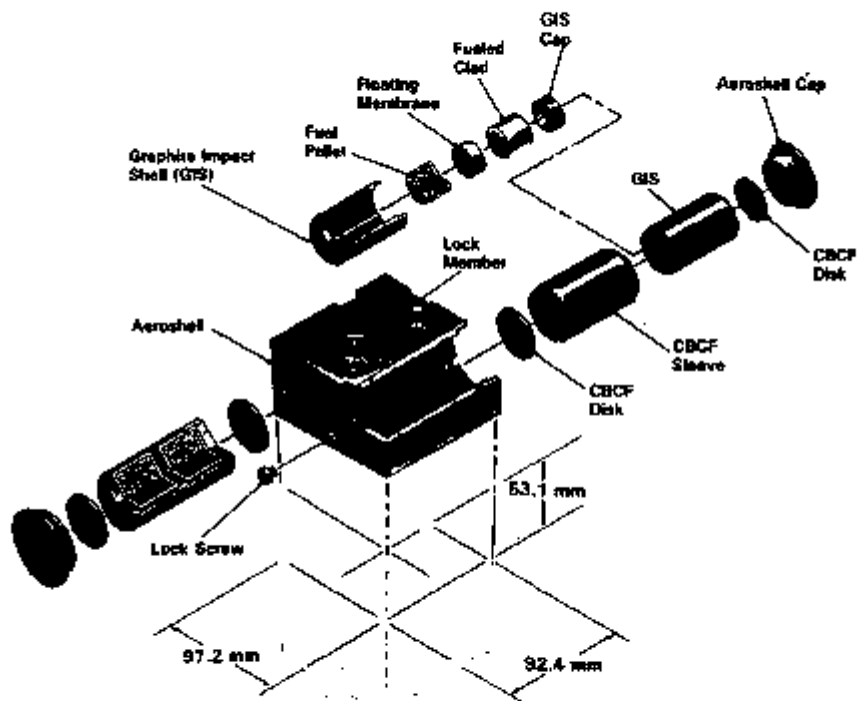


FIGURE 5-2. General Purpose Heat Source (GPHS) Assembly Detail.

6.3 MODEL SPECIFICATION

Two calculational models determine NCT and HAC dose rates. All gamma and neutron analyses are based on these two calculational models.

6.3.1 Regulatory Normal Conditions of Transport Model

Figure 5-3 shows an elevation view of the calculational model used for the NCT analyses. The NCT calculational model is comprised of a GPHS RTG payload model and RTG packaging model. The dimensions in Figure 5-3 are in centimeters. The central portion of the GPHS RTG payload model is identical to the central portion (without water reflector) of the calculational model for the criticality assessment (Chapter 6.0). The astroquartz insulation and thermopile and outer aluminum shell have been included beyond this central portion as shown in Figure 5-3.

Table 5-8 delineates the material compositions and densities used in this shielding calculational model. The neutron and gamma-ray sources are within the 72 small cylindrical cells of plutonia fuel.

Figure 6-4 shows an elevation view of the calculational model including the minimum width and height boundaries of the RTG Transportation System exclusive-use semitrailer. These boundaries were the locations for determining dose rates at the surfaces of the semitrailer.

The ground was treated in these calculations as Hanford soil. Only 11% of the neutron dose rate given in Table 6-1 at a distance of two meters from the side surface of the semitrailer was from scattering off the ground. Changing from Hanford soil to pure carbon for the ground reduces this dose rate from 0.43 (.50%) to 0.39 (.53%) $\mu\text{rads/hr}$; hence, the use of Hanford soil is conservative. The percentage contribution to the gamma ray portion of the dose rate is less than 2% from gamma rays scattering off the ground.

6.3.2 Regulatory Hypothetical Accident Condition Model

As shown in Figure 5-5, the HAC calculational model is conservatively configured into a spherical mass of homogenized plutonia fuel adjacent to the top center of the package model. The radius of this sphere is simply the radius to contain the 11,304 grams of plutonium oxide at a density of 9.60 g/cm^3 , or $r = 6.8508 \text{ cm}$. This spherical zone is summarized in Table 5-8, where the ICV and OCY are not changed for this HAC calculational model.

6.4 SHIELDING EVALUATION

This section discusses the basic methods used to determine the dose rates presented in the summary table for the NCT and HAC.

In all cases, NCT dose rates out the side of the package are determined at (1) $r = 50.38 \text{ cm}$, which corresponds to the outside surface of the package, (2) 127.0 cm , which corresponds to the outside of a minimum width semitrailer (i.e., the semitrailer minimum width is 100 in.; thus, the trailer centerline-to-edge distance is 50 in.), (3) 327.0 cm , which corresponds to a distance 2 m from the side of the semitrailer, and (4) 847.69 cm , which corresponds to the tractor cab (estimated to be a minimum of 27.8 ft from the package centerline). All side detector distances are with reference to the source radial centerline.

TABLE 5-8. Summary of Material Compositions for the Normal Conditions of Transport Analysis Model.

Material description	Element name	Atomic No. (Z)	Partial density (g/cc)
RTG (3 different materials) 11,304 g Plutonium and Oxide 3370 g Clad 6732 g Carbon*	Plutonium	94	8.483
	Oxygen	8	1.137
	Iridium	77	22.60
	Carbon	6	1.950
Outer shell (0.1624 cm thick)	Aluminum	13	2.8523
ICV and OCV, Steel of Cooling Jacket; All Type 304L stainless steel*	Chromium	24	1.809
	Iron	26	8.509
	Nickel	28	0.852
	Manganese	25	0.169
	Carbon	6	0.0008
Cooling jacket coolant (water)	Hydrogen	1	0.1110
	Oxygen	8	0.8881
Dry air at 1.0 atmosphere	Nitrogen	7	0.0002333
	Oxygen	8	0.0002887

* The partial densities for the listed elements of Type 304L stainless steel are taken from the reference 4 data sets.

TABLE 5-9. Summary of the RTG Composition for the Hypothetical Accident Condition Analysis Model.

Material description	Element name	Atomic number (Z)	Partial density (g/cc)
RTG (11,304 g plutonia in sphere)	Plutonium	94	8.483
	Oxygen	8	1.137

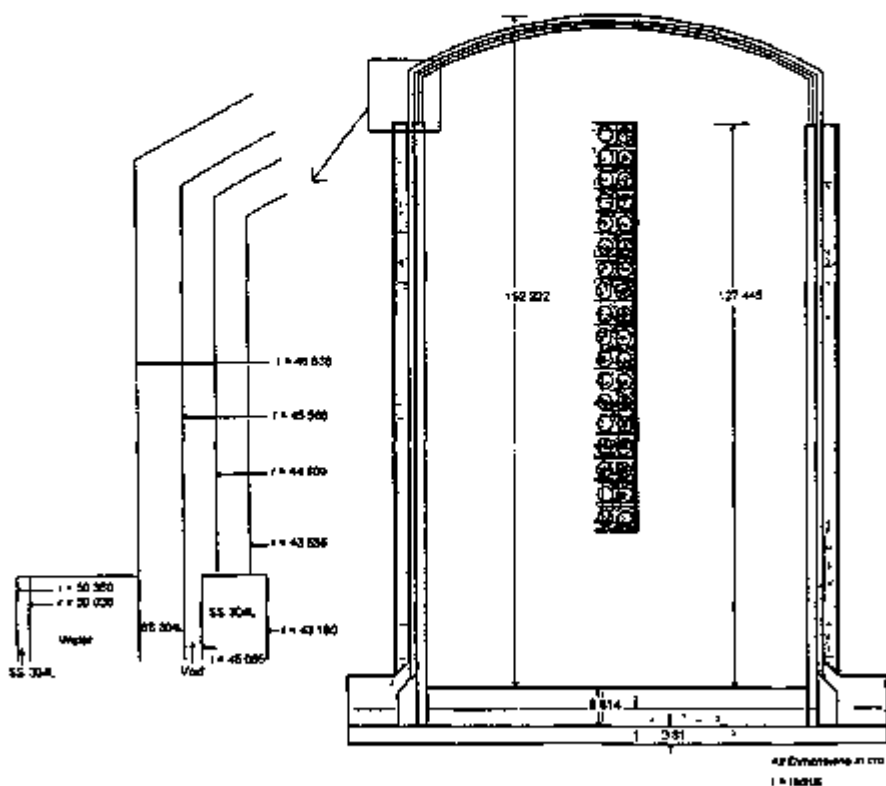


FIGURE 5-3 Elevation View of NCT Calculational Model Geometry Showing Dimensions

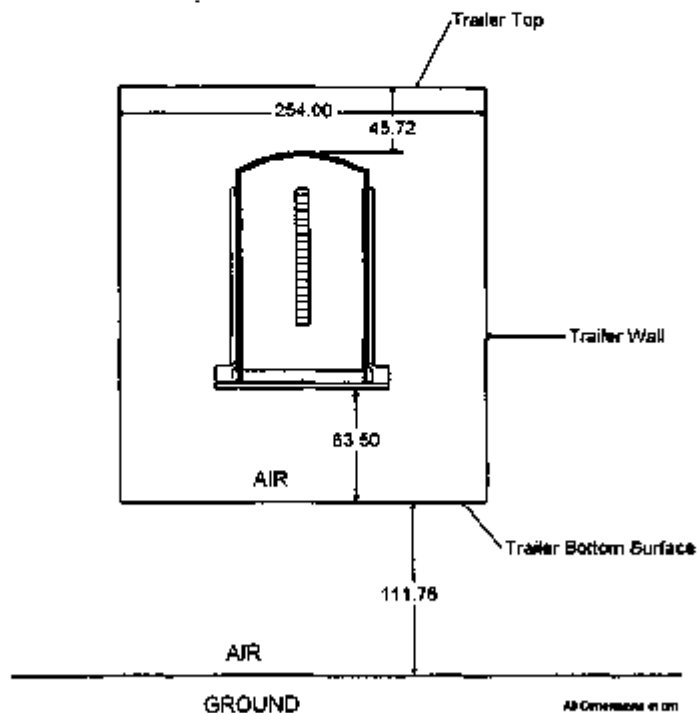


FIGURE 5-4. Elevation View of NCT Calculational Model Geometry Showing Outline of Semitrailer.

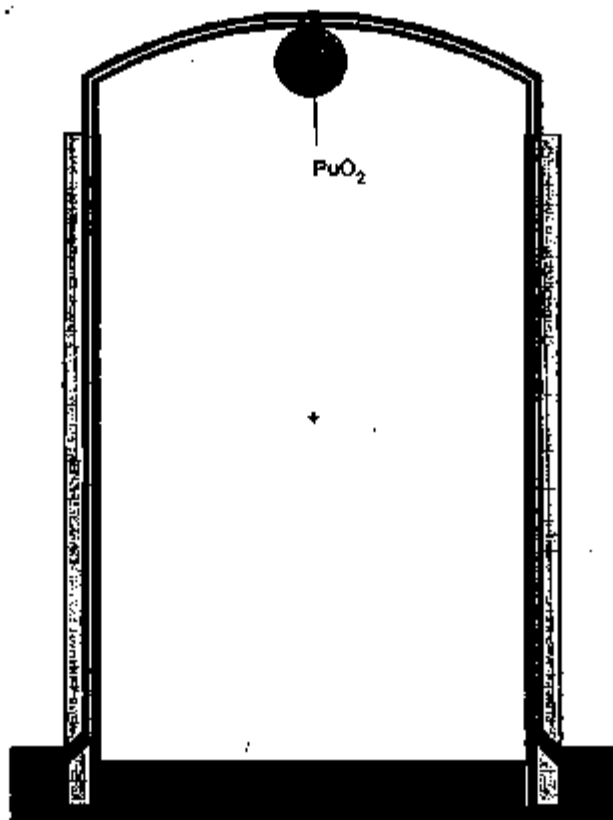


FIGURE B-6. HAC Computational Model Geometry.

Regulatory NCT dose rates out the package top are determined on the outer OCV surface, which corresponds to the outside surface of the package, and on the top of the hemisphere - 45.75 cm (18 inches) above the top of the outer OCV surface.

Regulatory HAC dose rates are only determined out the package top where the minimum amount of gamma and neutron shielding exists. The HAC dose rates are determined at a distance of 1 m from the package top.

5.4.1 Gamma Shielding Analyses

All gamma shielding analyses are performed using the computer code MCNP[®]. There are two components to the gamma-rays, one from the gamma source in the RTG and the other from the gamma rays produced at neutron collisions. These latter gamma rays are included in the dose rate summary given in Table 5-1, but their contribution is typically only about one percent of that due to the gamma rays from the gamma source in the RTG. The MCNP analysis included Bremsstrahlung from the electrons produced during the photon transport, and the gamma source term included Bremsstrahlung from the electrons of the source. Gamma fluence-to-dose-rate (mrem/hr) conversion factors are based on ANSI/ANS 6.1.1⁶. The two MCNP input files for the NCT and HAC gamma shielding analysis are listed in Appendix 5.5.2.

5.4.2 Neutron Shielding Analyses

The neutron shielding analyses were also performed using the computer code MCNP[®]. The neutron input file was identical to that used for the gamma analysis except the neutron source of Table 5-5 was used rather than the gamma source of Table 5-4 and neutron tables of dose rates were included. These analyses automatically included subcritical neutron multiplication.

Neutron fluence-to-dose-rate (mrem/hr) conversion factors, which include standard neutron quality factors, are based on ANSI/ANS 6.1.1⁶.

The two MCNP input files for the NCT and HAC neutron shielding analysis are listed in Appendix 5.5.3.

5.4.3 Uncertainties in the Shielding Analysis Models

Components of uncertainties include sources, geometry description with the calculational models, attenuation (cross sections), and statistical in the Monte Carlo calculations. Because substantial detail has been included in the three-dimensional geometry calculational models, the uncertainty because of this is negligible compared to the other components of uncertainty. Similarly, neutron and photon cross sections are reasonably well known, especially for the rather small attenuations here, so their uncertainty is also assumed to be small. The statistical uncertainties shown in Table 5-1 are small - a maximum of about 1.7% for the neutron portion of the dose rates, and about 1.4% for the gamma portion of the dose rates. Hence, the source is the dominant uncertainty. The neutron and gamma sources used in these calculations are conservative so that the dose rates given in Table 5-1 are really upper limit.

5.5 APPENDIX

The following is a list of appendices contained within this section:

5.5.1 References

5.5.2 Gamma Shielding Analyses MCNP Input Files

5.5.3 Neutron Shielding Analyses MCNP Input Files

5.5.1 References

1. Goldberg, H. J., 1985, *Neutron and Photon Spectrum and Abundances for an RTG Fuel Pellet and Comparison with Mound Document* (internal memo 8M730-HJG-85-020 to P. C. Farrell, October 3, Table 2, Total Gamma Ray Source from one 157 g Pellet), Westinghouse Hanford Company, Richland, Washington.
2. Goldberg, H. J., 1985, *Neutron and Photon Spectrum and Abundances for an RTG Fuel Pellet and Comparison with Mound Document* (internal memo 8M730-HJG-85-020 to P. C. Farrell, October 3, Table 1, Neutron Spectrum and Abundance), Westinghouse Hanford Company, Richland, Washington.
3. Braemelester, J.F., 1983, Editor, "MCNP - A General Monte Carlo Code N-Particle Transport Code, Version 4A," LA-12828, Los Alamos National Laboratory, Los Alamos, New Mexico.
4. Carter, L.L., 1984, "Certification of MCNP Version 4A for WHC Computer Platforms," ECN 186710, Westinghouse Hanford Company, Richland, Washington.
5. ANSUANS-1977 (N866), *Neutron and Gamma Ray Flux-to-Dose Rate Factors*, American Nuclear Society, and DOE 5480.11, *Radiation Protection for Occupational Workers*, 12-21-88.
6. General Electric, 1991, *Acceptance Specification for Fine Weave Pierced Fabric (FWPF) Graphite*, NS0080-01-20, Rev. C, 12/91, General Electric Astro Space Division.

6.5.2 Gamma Shielding Analyses MCNP Input Files

NCT GAMMA SHIELDING MCNP INPUT FILE

```

SHLD. CALC., GPHS-RTG, GAMMA, water, no q, p.det., rev mar 96 igdq
1 0 -5 6 -1 3 -4 2 trc=1 fill=1
2 0 -7 8 u=1 lat=1
   fill=0:17 0:0 0:0 2 17r
3 1 -1.9500 -9 (12 :-11 :20 )(14 :-13 :20 ) u=2
4 1 -1.9500 -10 (12 :-11 :22 )(14 :-13 :22 ) u=2
5 1 -1.9500 9 10 u=2
6 2 -22.5 -12 11 -20 (-15 :16 :19 ) u=2
7 2 -22.5 -14 13 -20 (-17 :18 :19 ) u=2
8 3 -9.6000 -16 15 -19 u=2
9 3 -9.6000 -18 17 -19 u=2
10 2 -22.5 -12 11 -22 (-15 :16 :21 ) u=2
11 2 -22.5 -14 13 -22 (-17 :18 :21 ) u=2
12 3 -9.6000 -16 15 -21 u=2
13 3 -9.6000 -18 17 -21 u=2
c Astroquartz insulation and thermopile and Al shell
14 231 -.00122 -121 134 -135 #1
15 0 -122 133 -136 (121:-134:135)
16 231 -.00122 -123 132 -137 (122:-133:136)
17 12 -2.85 -124 131 -138 (123:-132:137)
c inner containment
21 231 -.00122 ((6 -52 -31 ):(52 -33 -53 )) (124:-131:138)
22 201 -8.0300 51 -52 31 -32
23 201 -8.0300 (52 -34 -54 )(33 :53 )
24 201 -8.0300 51 -6 -31
c outer containment
41 231 -.00122 51 35 -64 -39
42 231 -.00122 ((51 -35 -62 )(52 :32 ))(-52 :34 :54 )
43 201 -8.0300 (-36 64 -63 )(62 :36 )
44 237 -1.0 -52 65 36 -37
45 201 -8.0300 -52 65 37 -38
46 201 -8.0300 ((64 -65 36 51 -40 ):(-64 39 51 )):(65 38 -66 -40 )
47 201 -8.0300 61 -51 -40
c beyond outer containment and inside truck boundary
71 231 -.00122 (((-52 :36 :63 ))(52 :38 :-66 ))(66 :40 :-61 )
   71 -72 73 -74 75 -76
c beyond truck and inside large sphere, above ground
72 231 -.00122 (-71:72:-73:74:-75:76) 77 -111
c ground
73 221 -1.67 -77 -111
c outside world
74 0 111

1 py 4.659
2 px -4.859
3 py -4.659
4 px 4.859
5 pz 95.544
6 p2 0.0000

```

7	pz	5.30801		
8	pz	-0.00001		
9	c/y	-2.184	2.654	1.831
10	c/y	2.184	2.654	1.831
11	py	-3.1618		
12	py	-0.2941		
13	py	0.2941		
14	py	3.1618		
15	py	-3.1059		
16	py	-0.350		
17	py	0.350		
18	py	3.1059		
19	c/y	-2.1840	2.6540	1.3767
20	c/y	-2.1840	2.6540	1.4326
21	c/y	2.1840	2.6540	1.3767
22	c/y	2.1840	2.6540	1.4326
c	radial surfaces for inner and outer containment			
31	cz	43.1800		
32	cz	45.0850		
33	cz	43.6562		
34	cz	44.6088		
35	cz	45.5676		
36	cz	46.8376		
37	cz	50.0380		
38	cz	50.3796		
39	cz	49.6443		
40	cz	61.3410		
c	inner containment			
51	pz	-8.8138		
52	pz	127.4450		
53	sz	60.3377	88.9000	
54	sz	60.3377	89.8525	
c	outer containment			
61	pz	-12.6238		
62	sz	60.1472	90.8050	
63	sz	60.1472	92.0750	
64	kz	48.7807	1.0000	-1.0000
65	kz	53.0733	1.0000	-1.0000
66	pz	2.6940		
c	truck outside boundary			
71	px	-615.95		
72	px	603.25		
73	py	-127.00		
74	py	127.00		
75	pz	-72.3138		
76	pz	198.0		
77	pz	-184.0738		
c	tally fs surfaces on outside of truck			
81	px	-90.0		
82	px	-30.0		
83	px	90.0		
84	px	90.0		
85	py	-90.0		
86	py	-30.0		

```

87   py   30.0
88   py   90.0
89   pz  -11.0
90   pz   49.0
91   pz  109.0
92   pz  169.0
93   pz   63.76
94   pz   94.24
95   cz   15.24
c    outside world.
111      so 5000.0000
121   cz   7.1265
122   cz   8.8945
123   cz  10.6426
124   cz  10.7950
131   pz  23.348
132   pz  23.5004
133   pz  29.6725
134   pz  31.4505
135   pz  127.0055
136   pz  128.7835
137   pz  134.9556
138   pz  135.108

*tr1 0 0 31.4560
mode  p
m1   6000.01p -1.950000
m2   77000.01p -22.500000
m3   94000.01p -8.463      8000.01p -1.137
m11  8000.01p -.9631 14000.01p -.8452 42000.01p -.3391 $ ins.+therm.
m12  13000.01p -1.
m201 26000.01p 67.970001 24000.01p 20.000000 28000.01p 10.000000
      25000.01p 2.000000 6000.01p 0.030000
m221 8000.01p -0.511000 14000.01p -0.278200 20000.01p -0.071700
      26000.01p -0.109100 13000.01p -0.083260 12000.01p -0.031420
      19000.01p -0.011550 11000.01p -0.020220 22000.01p -0.016550
      25000.01p -0.001751 15000.01p -0.002400
m231 7000.01p -0.765000 8000.01p -0.235000
m236 1000.01p 0.666700 8000.01p 0.333300
imp:p  l      16r      4      3r      16      $ 1, 41
      8r 8      0      $ 42, 73
print 10 30 40 50 60 100 110 120 126 170
c      phys:p  j  l
cut:p  j j 0, 0.
sdef   cal d3  axs 0 1 0  rad d4  ext d5  org-d9
      pos fcal d6  wgt=5.9118e10
c      source uniformly in all 72 lattice cells
sil 1  1:2(0 0 0):8  1:2(0 0 0):9  1:2(0 0 0):12  1:2(0 0 0):13
      1:2(1 0 0):8  1:2(1 0 0):9  1:2(1 0 0):12  1:2(1 0 0):13
      1:2(2 0 0):8  1:2(2 0 0):9  1:2(2 0 0):12  1:2(2 0 0):13
      1:2(3 0 0):8  1:2(3 0 0):9  1:2(3 0 0):12  1:2(3 0 0):13
      1:2(4 0 0):8  1:2(4 0 0):9  1:2(4 0 0):12  1:2(4 0 0):13
      1:2(5 0 0):8  1:2(5 0 0):9  1:2(5 0 0):12  1:2(5 0 0):13
      1:2(6 0 0):8  1:2(6 0 0):9  1:2(6 0 0):12  1:2(6 0 0):13

```


h	d	d
0.1500	0.0000E+00	0.0000E+00
0.2500	0.6820E+09	0.1066E+08
0.3500	0.4960E+08	0.2127E+07
0.4500	0.4030E+07	0.3672E+06
0.5500	0.9250E+07	0.3773E+07
0.6500	0.7330E+07	0.3841E+07
0.7500	0.1780E+08	0.1156E+08
0.8500	0.5760E+07	0.5298E+07
0.9500	0.6720E+07	0.6222E+07
1.0500	0.1370E+07	0.1474E+07
1.1500	0.5300E+06	0.6536E+06
1.2500	0.1970E+06	0.2753E+06
1.3500	0.1000E+06	0.1569E+06
1.4500	0.2200E+05	0.3841E+05
1.5500	0.3310E+06	0.6387E+06
1.6500	0.1420E+07	0.3010E+07
1.7500	0.8220E+05	0.1903E+06
1.8500	0.1170E+06	0.2944E+06
1.9500	0.1310E+05	0.3567E+05
2.0500	0.1110E+05	0.3258E+05
2.1500	0.1600E+05	0.3153E+05
2.2500	0.8950E+04	0.3021E+05
2.3500	0.7950E+04	0.2864E+05
2.4500	0.7080E+04	0.2715E+05
2.5500	0.6250E+04	0.2545E+05
2.6500	0.3330E+08	0.1437E+09
2.7500	0.4990E+04	0.2276E+05
2.8500	0.4500E+04	0.2165E+05
2.9500	0.4030E+04	0.2042E+05
3.0500	0.3640E+04	0.1939E+05
3.1500	0.3270E+04	0.1828E+05
3.2500	0.2980E+04	0.1746E+05
3.3500	0.2670E+04	0.1637E+05
3.4500	0.2420E+04	0.1551E+05
3.5500	0.2210E+04	0.1478E+05
3.6500	0.2030E+04	0.1402E+05
3.7500	0.1830E+04	0.1329E+05
3.8500	0.1660E+04	0.1254E+05
3.9500	0.1540E+04	0.1209E+05
4.0500	0.1420E+04	0.1157E+05
4.1500	0.1290E+04	0.1091E+05
4.2500	0.1200E+04	0.1051E+05
4.3500	0.1110E+04	0.1007E+05
4.4500	0.1010E+04	0.9481E+04
4.5500	0.9330E+03	0.9055E+04
4.6500	0.8590E+03	0.8613E+04
4.7500	0.7920E+03	0.8199E+04
4.8500	0.7370E+03	0.7872E+04
4.9500	0.6790E+03	0.7478E+04
5.0500	0.6340E+03	0.7195E+04
5.1500	0.5740E+03	0.6708E+04
5.2500	0.5250E+03	0.6315E+04
5.3500	0.4870E+03	0.6026E+04

	5.4500	0.4530E+03	0.5764E+04
	5.5500	0.4160E+03	0.5439E+04
	5.6500	0.3830E+03	0.5144E+04
	5.7500	0.3540E+03	0.4881E+04
	5.8500	0.3220E+03	0.4556E+04
	5.9500	0.2970E+03	0.4311E+04
	6.0500	0.2720E+03	0.4048E+04
	6.1500	0.2490E+03	0.3798E+04
	6.2500	0.2300E+03	0.3594E+04
	6.3500	0.2100E+03	0.3360E+04
	6.4500	0.1920E+03	0.3145E+04
	6.5500	0.1700E+03	0.2850E+04
	6.6500	0.1560E+03	0.2675E+04
	6.7500	0.1400E+03	0.2485E+04
	6.8500	0.1260E+03	0.2259E+04
	6.9500	0.1120E+03	0.2052E+04
	7.0500	0.1020E+03	0.1909E+04
	7.1500	0.8920E+02	0.1705E+04
	7.2500	0.7680E+02	0.1499E+04
	7.3500	0.6680E+02	0.1331E+04
	7.4500	0.5700E+02	0.1159E+04
	7.5500	0.4740E+02	0.9833E+03
	7.6500	0.3760E+02	0.7956E+03
c	total =	0.82108E+09	
c	total =	0.2108E+08 x 72 =	5.9118E+10
ctma	2400		
nps	5446924		
c	nps	619115	
pramp	j -960 l		
e0	.2 .6 .8 2. 20.		
fc2	p dose rates (mrem/hr) on sides of truck, 7th entry = nearest		
f2:p	73 74		
fs2	-81 84 -82 83 -89 -90 -91 -92 t		
sd2	142172 138738 16219 16219 3679 3600 2r 1740 329567		
	142172 138738 16219 16219 3679 3600 2r 1740 329567		
c	ansi/ans-6.1.1-1977 fluence-to-dose, photons(mrem/hr)/(p/cm**2/s)		
de2	0.01 0.03 0.05 0.07 0.10 0.15 0.20 0.25 0.30		
	0.35 0.40 0.45 0.50 0.55 0.60 0.65 0.70 0.80		
	1.00 1.40 1.80 2.20 2.60 2.80 3.25 3.75 4.25		
	4.75 5.00 5.25 5.75 6.25 6.75 7.50 9.00 11.0		
	13.0 15.0		
df2	3.96-3 5.82-4 2.90-4 2.58-4 2.83-4 3.79-4 5.01-4 6.31-4 7.59-4		
	8.78-4 9.85-4 1.08-3 1.17-3 1.27-3 1.36-3 1.44-3 1.52-3 1.58-3		
	1.98-3 2.51-3 2.99-3 3.42-3 3.82-3 4.01-3 4.41-3 4.83-3 5.23-3		
	5.60-3 5.80-3 6.01-3 6.37-3 6.74-3 7.11-3 7.66-3 8.77-3 1.03-2		
	1.18-2 1.33-2		
fc12	p dose rates (mrem/hr) on ends of truck, 7th entry = nearest		
fl2:p	71 72		
fs12	-85 88 -86 87 -89 -90 -91 -92 t		
sd12	10002 10002 16219 16219 3679 3600 2r 1740 68660		
	10002 10002 16219 16219 3679 3600 2r 1740 68660		
c	ansi/ans-6.1.1-1977 fluence-to-dose, photons(mrem/hr)/(p/cm**2/s)		
de12	0.01 0.03 0.05 0.07 0.10 0.15 0.20 0.25 0.30		
	0.35 0.40 0.45 0.50 0.55 0.60 0.65 0.70 0.80		

	1.00	1.40	1.80	2.20	2.60	2.80	3.25	3.75	4.25
	4.75	5.00	5.25	5.75	6.25	6.75	7.50	9.00	11.0
	13.0	15.0							
df12	3.96-3	5.82-4	2.90-4	2.58-4	2.83-4	3.79-4	5.01-4	6.31-4	7.59-4
	8.78-4	9.85-4	1.08-3	1.17-3	1.27-3	1.36-3	1.44-3	1.52-3	1.68-3
	1.98-3	2.51-3	2.99-3	3.42-3	3.82-3	4.01-3	4.41-3	4.83-3	5.23-3
	5.60-3	5.80-3	6.01-3	6.37-3	6.74-3	7.11-3	7.66-3	8.77-3	1.03-2
	1.18-2	1.33-2							
fc22	p dose rates (mrem/hr) on bottom and top, 7th entry - nearest								
f22:p	75 76								
fs22	-81 84 -82 83 -85 -86 -87 -88 t								
sd22	133591 130366 15240 15240 2220 3600 2r 2220 309677								
	133591 130366 15240 15240 2220 3600 2r 2220 309677								
c	ansi/ans-6.1.1-1977 fluence-to-dose, photons(mrem/hr)/(p/cm**2/s)								
de22	0.01	0.03	0.05	0.07	0.10	0.15	0.20	0.25	0.30
	0.35	0.40	0.45	0.50	0.55	0.60	0.65	0.70	0.80
	1.00	1.40	1.80	2.20	2.60	2.80	3.25	3.75	4.25
	4.75	5.00	5.25	5.75	6.25	6.75	7.50	9.00	11.0
	13.0	15.0							
df22	3.96-3	5.82-4	2.90-4	2.58-4	2.83-4	3.79-4	5.01-4	6.31-4	7.59-4
	8.78-4	9.85-4	1.08-3	1.17-3	1.27-3	1.36-3	1.44-3	1.52-3	1.68-3
	1.98-3	2.51-3	2.99-3	3.42-3	3.82-3	4.01-3	4.41-3	4.83-3	5.23-3
	5.60-3	5.80-3	6.01-3	6.37-3	6.74-3	7.11-3	7.66-3	8.77-3	1.03-2
	1.18-2	1.33-2							
fc102	p dose rates (mrem/hr) on side of package, 2nd entry								
f102:p	38								
fs102	-132 -90 -93 -94 -91 -138 t								
sd102	1 53 1 1								
c	ansi/ans-6.1.1-1977 fluence-to-dose, photons(mrem/hr)/(p/cm**2/s)								
de102	0.01	0.03	0.05	0.07	0.10	0.15	0.20	0.25	0.30
	0.35	0.40	0.45	0.50	0.55	0.60	0.65	0.70	0.80
	1.00	1.40	1.80	2.20	2.60	2.80	3.25	3.75	4.25
	4.75	5.00	5.25	5.75	6.25	6.75	7.50	9.00	11.0
	13.0	15.0							
df102	3.96-3	5.82-4	2.90-4	2.58-4	2.83-4	3.79-4	5.01-4	6.31-4	7.59-4
	8.78-4	9.85-4	1.08-3	1.17-3	1.27-3	1.36-3	1.44-3	1.52-3	1.68-3
	1.98-3	2.51-3	2.99-3	3.42-3	3.82-3	4.01-3	4.41-3	4.83-3	5.23-3
	5.60-3	5.80-3	6.01-3	6.37-3	6.74-3	7.11-3	7.66-3	8.77-3	1.03-2
	1.18-2	1.33-2							
fc122	p dose rates (mrem/hr) on top of package, 1st entry								
f122:p	63								
fs122	-95 t								
c	ansi/ans-6.1.1-1977 fluence-to-dose, photons(mrem/hr)/(p/cm**2/s)								
de122	0.01	0.03	0.05	0.07	0.10	0.15	0.20	0.25	0.30
	0.35	0.40	0.45	0.50	0.55	0.60	0.65	0.70	0.80
	1.00	1.40	1.80	2.20	2.60	2.80	3.25	3.75	4.25
	4.75	5.00	5.25	5.75	6.25	6.75	7.50	9.00	11.0
	13.0	15.0							
df122	3.96-3	5.82-4	2.90-4	2.58-4	2.83-4	3.79-4	5.01-4	6.31-4	7.59-4
	8.78-4	9.85-4	1.08-3	1.17-3	1.27-3	1.36-3	1.44-3	1.52-3	1.68-3
	1.98-3	2.51-3	2.99-3	3.42-3	3.82-3	4.01-3	4.41-3	4.83-3	5.23-3
	5.60-3	5.80-3	6.01-3	6.37-3	6.74-3	7.11-3	7.66-3	8.77-3	1.03-2
	1.18-2	1.33-2							
fc5	p dose rates (mrem/hr) at detectors, 2 m, driver								

```

f5:p  0. 327.00 79. 100.
      847.09 0. 79. 100.
      0. 327.00 0.0 100.
      0. 327.00 -79.0 100.
      0. 327.00 168.0 100.
c
ansi/ans-6.1.1-1977 fluence-to-dose,photons(mrem/hr)/(p/cm**2/s)
de5   0.01  0.03  0.05  0.07  0.10  0.15  0.20  0.25  0.30
      0.35  0.40  0.45  0.50  0.55  0.60  0.65  0.70  0.80
      1.00  1.40  1.80  2.20  2.60  2.80  3.25  3.75  4.25
      4.75  5.00  5.25  5.75  6.25  6.75  7.50  9.00  11.0
      13.0  15.0
df5   3.96-3 5.62-4 2.90-4 2.58-4 2.83-4 3.79-4 5.01-4 6.31-4 7.59-4
      8.78-4 9.65-4 1.08-3 1.17-3 1.27-3 1.36-3 1.44-3 1.52-3 1.68-3
      1.98-3 2.51-3 2.99-3 3.42-3 3.82-3 4.01-3 4.41-3 4.83-3 5.23-3
      5.60-3 5.80-3 6.01-3 6.37-3 6.74-3 7.11-3 7.66-3 8.77-3 1.03-2
      1.18-2 1.33-2
ft5   lcd
fa5   3 4 5 6 7 8 9 10 11 12 13 14 15 16 17 21 22 23 24
      41 42 43 44 45 46 47 71 72 73

```

HAC GAMMA SHIELDING MCNP INPUT FILE

```

SHLD. CALC., GPHS-RTG, GAMMA, , accident igaci
c   sphere of PuO2 for accident condition
1   3 -9.60 -100
c   inner containment
21  231 -.00122 ((6 -52 -31):(52 -33 -53)) 100
22  201 -8.0300 51 -52 31 -32
23  201 -8.0300 (52 -34 -54)(33 :53 )
24  201 -8.0300 51 -6 -31
c   outer containment
41  231 -.00122 51 35 -64 -39
42  231 -.00122 ((51 -35 -62)(52 :32))(-52 :34 :54 )
43  201 -8.0300 (-36 64 -63)(62 :35 )
44  236 -1.0 -52 65 36 -37
45  201 -8.0300 -52 65 37 -38
46  201 -8.0300 ((64 -65 36 51 -40 ):(-64 39 51 )):(65 38 -66 -40 )
47  201 -8.0300 61 -51 -40
c   beyond outer containment and inside truck boundary
71  231 -.00122 (((-52 :36 :63))(52 :38 :-66 ))(66 :40 :-61 )
    71 -72 73 -74 75 -76
c   beyond truck and inside large sphere, above ground
72  231 -.00122 (-71:72:-73:74:-75:76) 77 -111
c   ground
73  221 -1.67 -77 -111
c   outside world
74  0 111

1   py  4.659
2   px -4.859
3   py -4.659
4   px  4.859
5   pz  95.544
6   pz  0.0000
7   pz  5.30601
8   pz -0.00001
9   c/y -2.184 2.654 1.831
10  c/y  2.184 2.654 1.831
11  py -3.1618
12  py -0.2941
13  py  0.2941
14  py  3.1618
15  py -3.1059
16  py -0.350
17  py  0.350
18  py  3.1059
19  c/y -2.1840 2.6540 1.3767
20  c/y -2.1840 2.6540 1.4326
21  c/y  2.1840 2.6540 1.3767
22  c/y  2.1840 2.6540 1.4326
c   radial surfaces for inner and outer containment
31  cz  43.1800
32  cz  45.0850
33  cz  43.6562

```

```

34      cz  44.6088
35      cz  45.5676
36      cx  46.8376
37      cz  50.0380
38      cz  50.3796
39      cz  49.6443
40      cz  61.3410
c  inner containment
51      pz  -8.8138
52      pz  127.4450
53      sz  60.3377 88.9000
54      sz  60.3377 89.8525
c  outer containment
61      pz  -12.6238
62      sz  60.1472 90.8050
63      sz  60.1472 92.0750
64      kz  48.7807 1.0000 -1.0000
65      kz  53.0733 1.0000 -1.0000
66      pz  2.6940
c  truck outside boundary
71      px  -615.95
72      px  603.25
73      py  -127.00
74      py  127.00
75      pz  -72.3138
76      pz  198.0
77      pz  -184.0738
c  tally fs surfaces on outside of truck
81      px  -90.0
82      px  -30.0
83      px  30.0
84      px  90.0
85      py  -90.0
86      py  -30.0
87      py  30.0
88      py  90.0
89      pz  -11.0
90      pz  49.0
91      pz  109.0
92      pz  169.0
93      pz  63.76
94      pz  94.24
95      cz  15.24
100     s   0. 0. 142.6  6.5508
c  outside world.
111     so  5000.0000

*tr1  0 0 31.4560
mode   p
m1     6000.0ip -1.950000
m2     77000.0ip -22.500000
m3     94000.0ip -8.463      8000.0ip -1.137
m201   26000.0ip 67.97000ip 24000.0ip 20.000000 28000.0ip 10.000000
        25000.0ip 2.000000 6000.0ip 0.030000

```

```

m221 8000.01p -0.511000 14000.01p -0.278200 20000.01p -0.071700
      25000.01p -0.109100 13000.01p -0.083250 12000.01p -0.031420
      19000.01p -0.011550 13000.01p -0.020220 22000.01p -0.016550
      25000.01p -0.001781 15000.01p -0.002400
m231 7000.01p -0.785000 8000.01p -0.235000
m236 1000.01p 0.666700 8000.01p 0.333300
imp:p 1 4 3r 16 $ 1, 41
      8r 8 0 $ 42, 73
print 10 30 40 50 60 100 110 120 126 170
phys:p j j
cut:p j j 0. 0.
sdef rad d4 arg-d9
      pos 0. 0. 142.6 wgt=5.9118e10
s14 6.5508
sp4 -21 2
c gamma spectrum from Table 5-4, 157 g fueled clad
# s19 sp9 sb9
  l d d
0.1500 0.0000E+00 0.0000E+00
0.2500 0.6820E+09 0.1066E+08
0.3500 0.4960E+08 0.2127E+07
0.4500 0.4030E+07 0.3672E+06
0.5500 0.9250E+07 0.3773E+07
0.6500 0.7330E+07 0.3841E+07
0.7500 0.1780E+08 0.1156E+08
0.8500 0.6760E+07 0.5298E+07
0.9500 0.6720E+07 0.6222E+07
1.0500 0.1370E+07 0.1474E+07
1.1500 0.5300E+06 0.6536E+06
1.2500 0.1970E+06 0.2753E+06
1.3500 0.1000E+06 0.1569E+06
1.4500 0.2200E+05 0.3841E+05
1.5500 0.3310E+06 0.6387E+06
1.6500 0.1420E+07 0.3010E+07
1.7500 0.8220E+05 0.1903E+06
1.8500 0.1170E+06 0.2944E+06
1.9500 0.1310E+05 0.3567E+05
2.0500 0.1110E+05 0.3258E+05
2.1500 0.1000E+05 0.3153E+05
2.2500 0.8950E+04 0.3021E+05
2.3500 0.7950E+04 0.2864E+05
2.4500 0.7080E+04 0.2715E+05
2.5500 0.6250E+04 0.2545E+05
2.6500 0.3330E+08 0.1437E+09
2.7500 0.4990E+04 0.2276E+05
2.8500 0.4500E+04 0.2165E+05
2.9500 0.4030E+04 0.2042E+05
3.0500 0.3640E+04 0.1939E+05
3.1500 0.3270E+04 0.1828E+05
3.2500 0.2980E+04 0.1746E+05
3.3500 0.2670E+04 0.1637E+05
3.4500 0.2420E+04 0.1551E+05
3.5500 0.2210E+04 0.1478E+05
3.6500 0.2010E+04 0.1402E+05

```

3.7500	0.1830E+04	0.1129E+05
3.8500	0.1660E+04	0.1254E+05
3.9500	0.1540E+04	0.1209E+05
4.0500	0.1420E+04	0.1157E+05
4.1500	0.1290E+04	0.1091E+05
4.2500	0.1200E+04	0.1051E+05
4.3500	0.1110E+04	0.1007E+05
4.4500	0.1010E+04	0.9481E+04
4.5500	0.9330E+03	0.9055E+04
4.6500	0.8590E+03	0.8613E+04
4.7500	0.7920E+03	0.8199E+04
4.8500	0.7370E+03	0.7672E+04
4.9500	0.6790E+03	0.7478E+04
5.0500	0.6340E+03	0.7195E+04
5.1500	0.5740E+03	0.6708E+04
5.2500	0.5250E+03	0.6315E+04
5.3500	0.4870E+03	0.6026E+04
5.4500	0.4530E+03	0.5764E+04
5.5500	0.4160E+03	0.5439E+04
5.6500	0.3830E+03	0.5144E+04
5.7500	0.3540E+03	0.4881E+04
5.8500	0.3220E+03	0.4556E+04
5.9500	0.2970E+03	0.4311E+04
6.0500	0.2720E+03	0.4048E+04
6.1500	0.2490E+03	0.3798E+04
6.2500	0.2300E+03	0.3594E+04
6.3500	0.2100E+03	0.3360E+04
6.4500	0.1920E+03	0.3145E+04
6.5500	0.1700E+03	0.2850E+04
6.6500	0.1560E+03	0.2675E+04
6.7500	0.1400E+03	0.2455E+04
6.8500	0.1260E+03	0.2259E+04
6.9500	0.1120E+03	0.2052E+04
7.0500	0.1020E+03	0.1909E+04
7.1500	0.8920E+02	0.1705E+04
7.2500	0.7680E+02	0.1499E+04
7.3500	0.6680E+02	0.1331E+04
7.4500	0.5700E+02	0.1159E+04
7.5500	0.4740E+02	0.9833E+03
7.6500	0.3780E+02	0.7954E+03
c	total =	0.82108E+09
c	total =	.82108+9 * 72 = 6.9118+10
ctme	120	
nps	1654422	
prdep	j -950	
e0	.2 .6 .8 2. 20.	
fc2	p	dosa rates (mrem/hr) on sides of truck, 7th entry = nearest
fz:p	73 74	
fs2	-8) 84 -82 83 -89 -90 -91 -92 t	
sd2	142172 138738 16219 16219 3679 3600 2r 1740 329567	
	142172 138738 16219 16219 3679 3600 2r 1740 329567	
c	ans1/ans-6.1.1-1977	Fluence-to-dose, photons(mrem/hr)/(p/cm**2/s)
de2	0.01 0.03 0.05 0.07 0.10 0.15 0.20 0.25 0.30	
	0.35 0.40 0.45 0.50 0.55 0.60 0.65 0.70 0.80	

	1.00	1.40	1.80	2.20	2.60	2.80	3.25	3.75	4.25
	4.75	5.00	5.25	5.75	6.25	6.75	7.50	9.00	11.0
	13.0	15.0							
df2	3.96-3	5.82-4	2.90-4	2.58-4	2.83-4	3.79-4	5.01-4	6.31-4	7.59-4
	8.78-4	9.85-4	1.08-3	1.17-3	1.27-3	1.36-3	1.44-3	1.52-3	1.68-3
	1.98-3	2.51-3	2.99-3	3.42-3	3.82-3	4.01-3	4.41-3	4.83-3	5.23-3
	5.60-3	5.80-3	6.01-3	6.37-3	6.74-3	7.11-3	7.66-3	8.77-3	1.03-2
	1.18-2	1.33-2							
fc12	p dose rates (mrem/hr) on ends of truck, 7th entry = nearest								
f12:p	71 72								
fs12	-85 88 -86 87 -89 -90 -91 -92 t								
sd12	10002 10002 16219 16219 3679 3600 2r 1740 68660								
	10002 10002 16219 16219 3679 3600 2r 1740 68660								
c	ansi/ans-6.1.1-1977 fluence-to-dose, photons(mrem/hr)/(p/cm**2/s)								
de12	0.01	0.03	0.05	0.07	0.10	0.15	0.20	0.25	0.30
	0.35	0.40	0.45	0.50	0.55	0.60	0.65	0.70	0.80
	1.00	1.40	1.80	2.20	2.60	2.80	3.25	3.75	4.25
	4.75	5.00	5.25	5.75	6.25	6.75	7.50	9.00	11.0
	13.0	15.0							
df12	3.96-3	5.82-4	2.90-4	2.58-4	2.83-4	3.79-4	5.01-4	6.31-4	7.59-4
	8.78-4	9.85-4	1.08-3	1.17-3	1.27-3	1.36-3	1.44-3	1.52-3	1.68-3
	1.98-3	2.51-3	2.99-3	3.42-3	3.82-3	4.01-3	4.41-3	4.83-3	5.23-3
	5.60-3	5.80-3	6.01-3	6.37-3	6.74-3	7.11-3	7.66-3	8.77-3	1.03-2
	1.18-2	1.33-2							
fc22	p dose rates (mrem/hr) on bottom and top, 7th entry = nearest								
f22:p	75 76								
fs22	-81 84 -82 83 -85 -86 -87 -88 t								
sd22	133591 130366 15240 15240 2220 3600 2r 2220 309677								
	133591 130366 15240 15240 2220 3600 2r 2220 309677								
c	ansi/ans-6.1.1-1977 fluence-to-dose, photons(mrem/hr)/(p/cm**2/s)								
de22	0.01	0.03	0.05	0.07	0.10	0.15	0.20	0.25	0.30
	0.35	0.40	0.45	0.50	0.55	0.60	0.65	0.70	0.80
	1.00	1.40	1.80	2.20	2.60	2.80	3.25	3.75	4.25
	4.75	5.00	5.25	5.75	6.25	6.75	7.50	9.00	11.0
	13.0	15.0							
df22	3.96-3	5.82-4	2.90-4	2.58-4	2.83-4	3.79-4	5.01-4	6.31-4	7.59-4
	8.78-4	9.85-4	1.08-3	1.17-3	1.27-3	1.36-3	1.44-3	1.52-3	1.68-3
	1.98-3	2.51-3	2.99-3	3.42-3	3.82-3	4.01-3	4.41-3	4.83-3	5.23-3
	5.60-3	5.80-3	6.01-3	6.37-3	6.74-3	7.11-3	7.66-3	8.77-3	1.03-2
	1.18-2	1.33-2							
fc102	p dose rates (mrem/hr) on side of package, 2nd entry								
f102:p	38								
fs102	-93 -94 t								
c	ansi/ans-6.1.1-1977 fluence-to-dose, photons(mrem/hr)/(p/cm**2/s)								
de102	0.01	0.03	0.05	0.07	0.10	0.15	0.20	0.25	0.30
	0.35	0.40	0.45	0.50	0.55	0.60	0.65	0.70	0.80
	1.00	1.40	1.80	2.20	2.60	2.80	3.25	3.75	4.25
	4.75	5.00	5.25	5.75	6.25	6.75	7.50	9.00	11.0
	13.0	15.0							
df102	3.96-3	5.82-4	2.90-4	2.58-4	2.83-4	3.79-4	5.01-4	6.31-4	7.59-4
	8.78-4	9.85-4	1.08-3	1.17-3	1.27-3	1.36-3	1.44-3	1.52-3	1.68-3
	1.98-3	2.51-3	2.99-3	3.42-3	3.82-3	4.01-3	4.41-3	4.83-3	5.23-3
	5.60-3	5.80-3	6.01-3	6.37-3	6.74-3	7.11-3	7.66-3	8.77-3	1.03-2
	1.18-2	1.33-2							

```

fc122  p dose rates (mrem/hr) on top of package, 1st entry
f122:p  63
fs122  -95 t
c      ans1/ans-6.1.1-1977 fluence-to-dose,photons(mrem/hr)/(p/cm**2/s)
del122 0.01 0.03 0.05 0.07 0.10 0.15 0.20 0.25 0.30
      0.35 0.40 0.45 0.50 0.55 0.60 0.65 0.70 0.80
      1.00 1.40 1.80 2.20 2.60 2.80 3.25 3.75 4.25
      4.75 5.00 5.25 5.75 6.25 6.75 7.50 9.00 11.0
      13.0 15.0
df122  3.96-3 5.82-4 2.90-4 2.58-4 2.83-4 3.79-4 5.01-4 6.31-4 7.59-4
      8.78-4 9.85-4 1.08-3 1.17-3 1.27-3 1.36-3 1.44-3 1.52-3 1.68-3
      1.98-3 2.51-3 2.99-3 3.42-3 3.82-3 4.01-3 4.41-3 4.83-3 5.23-3
      5.60-3 5.80-3 6.01-3 6.37-3 6.74-3 7.11-3 7.66-3 8.77-3 1.03-2
      1.18-2 1.33-2
fc5     p dose rates (mrem/hr) at detectors, 1 m above top s
f5:p   0. 0. 252.22 50.
c      ans1/ans-6.1.1-1977 fluence-to-dose,photons(mrem/hr)/(p/cm**2/s)
de5    0.01 0.03 0.05 0.07 0.10 0.15 0.20 0.25 0.30
      0.35 0.40 0.45 0.50 0.55 0.60 0.65 0.70 0.80
      1.00 1.40 1.80 2.20 2.60 2.80 3.25 3.75 4.25
      4.75 5.00 5.25 5.75 6.25 6.75 7.50 9.00 11.0
      13.0 15.0
df5    3.96-3 5.82-4 2.90-4 2.58-4 2.83-4 3.79-4 5.01-4 6.31-4 7.59-4
      8.78-4 9.85-4 1.08-3 1.17-3 1.27-3 1.36-3 1.44-3 1.52-3 1.68-3
      1.98-3 2.51-3 2.99-3 3.42-3 3.82-3 4.01-3 4.41-3 4.83-3 5.23-3
      5.60-3 5.80-3 6.01-3 6.37-3 6.74-3 7.11-3 7.66-3 8.77-3 1.03-2
      1.18-2 1.33-2

```


5.5.3 Neutron Shielding Analyses MCNP Input Files

NCT NEUTRON SHIELDING MCNP INPUT FILE

SHLD. CALC., SPMS-RTG, N-GAMMA, water, no q, p.det., rev Mar 96 ingdq

```

1 0 -5 6 -1 3 -4 2 trcl=1 fill=1
2 0 -7 8 u=1 lat=1
   fill=0:17 0:0 0:0 2 17r
3 1 -1.9500 -9 (12 :-11 :20 )(14 :-13 :20 ) u=2
4 1 -1.9500 -10 (12 :-11 :22 )(14 :-13 :22 ) u=2
5 1 -1.9500 9 10 u=2
6 2 -22.5 -12 11 -20 (-15 :16 :19 ) u=2
7 2 -22.5 -14 13 -20 (-17 :18 :19 ) u=2
8 3 -9.6000 -16 15 -19 u=2
9 3 -9.6000 -18 17 -19 u=2
10 2 -22.5 -12 11 -22 (-15 :16 :21 ) u=2
11 2 -22.5 -14 13 -22 (-17 :18 :21 ) u=2
12 3 -9.6000 -16 15 -21 u=2
13 3 -9.6000 -18 17 -21 u=2
c Astroquartz insulation and thermopile and Al shell
14 231 -.00122 -121 134 -135 #1
15 0 -122 133 -136 (121:-134:135)
16 231 -.00122 -123 132 -137 (122:-133:136)
17 12 -2.85 -124 131 -138 (123:-132:137)
c inner containment
21 231 -.00122 ((6 -52 -31 ):(52 -33 -53 )) (124:-131:138)
22 201 -8.0300 51 -52 31 -32
23 201 -8.0300 (52 -34 -54 )(33 :53 )
24 201 -8.0300 51 -5 -31
c outer containment
41 231 -.00122 51 35 -64 -39
42 231 -.00122 ((51 -35 -62 )(52 :32 ))(-52 :34 :54 )
43 201 -8.0300 (-36 64 -63 )(62 :35 )
44 236 -1.0 -52 65 36 -37
45 201 -8.0300 -52 65 37 -38
46 201 -8.0300 ((64 -65 36 51 -40 ):(-64 39 51 )):(65 38 -66 -40 )
47 201 -8.0300 61 -51 -40
c beyond outer containment and inside truck boundary
71 231 -.00122 (((-52 :36 :63 ))(52 :38 :-66 ))(66 :40 :-61 )
   71 -72 73 -74 75 -76
c beyond truck and inside large sphere, above ground
72 231 -.00122 (-71:72:-73:74:-75:76) 77 -111
c ground
73 221 -1.67 -77 -111
c outside world
74 0 111

1 py 4.659
2 px -4.859
3 py -4.659
4 px 4.859
5 pz 95.544
6 pz 0.0000

```

7	pz	5.30801			
8	pz	-0.00001			
9	c/y	-2.184	2.654	1.831	
10	c/y	2.184	2.654	1.831	
11	py	-3.1618			
12	py	-0.2941			
13	py	0.2941			
14	py	3.1618			
15	py	-3.1059			
16	py	-0.350			
17	py	0.350			
18	py	3.1059			
19	c/y	-2.1840	2.6540	1.3767	
20	c/y	-2.1840	2.6540	1.4326	
21	c/y	2.1840	2.6540	1.3767	
22	c/y	2.1840	2.6540	1.4326	
c	radial surfaces for inner and outer containment				
31	cz	43.1800			
32	cz	45.0850			
33	cz	43.6562			
34	cz	44.6088			
35	cz	45.5676			
36	cz	46.8376			
37	cz	50.0380			
38	cz	50.3796			
39	cz	49.6443			
40	cz	61.3410			
c	inner containment				
51	pz	-8.8138			
52	pz	127.4450			
53	sz	60.3377	88.9000		
54	sz	60.3377	89.8526		
c	outer containment				
61	pz	-12.6238			
62	sz	60.1472	90.8050		
63	sz	60.1472	92.0750		
64	kz	48.7807	1.0000	-1.0000	
65	kz	53.0733	1.0000	-1.0000	
66	pz	2.6940			
c	truck outside boundary				
71	px	-615.95			
72	px	603.25			
73	py	-127.00			
74	py	127.00			
75	pz	-72.3138			
76	pz	198.0			
77	pz	-184.0738			
c	tally fs surfaces on outside of truck				
81	px	-90.0			
82	px	-30.0			
83	px	30.0			
84	px	90.0			
85	py	-90.0			

```

86 py -30.0
87 py 30.0
88 py 90.0
89 pz -11.0
90 pz 49.0
91 pz 109.0
92 pz 169.0
93 pz 63.76
94 pz 94.24
95 cz 15.24
c outside world.
111 so 5000.0000
121 cz 7.1165
122 cz 8.8945
123 cz 10.6426
124 cz 10.7950
131 pz 23.348
132 pz 23.5004
133 pz 29.6725
134 pz 31.4505
135 pz 127.0055
136 pz 128.7835
137 pz 134.9556
138 pz 135.108

*tr1 0 0 31.4560
mode n p
m1 6000.50 -1.950000
m2 77000.55 -22.500000
m3 94238.50 -6.765000 94239.55 -1.698000 8016.50 -1.137000
ml1 8016.50c -.9631 14000.50c -.8452 42000.50c -.3391 $ ins.+therm.
ml2 13027.50c -1.
m201 26000.55c 67.970001 24000.50c 20.000000 28000.50c 10.000000
25055.50c 2.000000 6000.50c 0.030000
c Hanford hwpv soil
m221 8016.50c -0.511000 14000.50c -0.278200 20000.50c -0.071700
26000.55c -0.109100 13027.50c -0.083260 12000.50c -0.031420
19000.50c -0.011550 11023.50c -0.020220 22000.50c -0.016550
25055.50c -0.001781 15031.50c -0.002400
m231 7014.50c -0.765000 8016.50c -0.235000
m236 1001.50c 0.666700 8016.50c 0.333300
imp:n 1 16r 4 3r 16 $ 1, 41
8r 0 0 $ 42, 73
imp:p 1 16r 4 3r 16 $ 1, 41
8r 0 0 $ 42, 73
print 10 30 40 50 60 100 110 120 126 170
c phys:p j 1
cut:p j j 0. 0.
cut:n j j 0. 0.
sdef cel dl axs 0 1 0 rad d4 ext d5 erg-d9
pos fce? d6 wgt=5.13252e7
c source uniformly in all 72 lattice cells
sll 1 1:2(0 0 0):8 1:2(0 0 0):9 1:2(0 0 0):12 1:2(0 0 0):13

```


2.184 -3.1059 2.654 2.184 .35 2.654
 -2.184 -3.1059 2.654 -2.184 .35 2.654
 2.184 -3.1059 2.654 2.184 .35 2.654
 -2.184 -3.1059 2.654 -2.184 .35 2.654
 2.184 -3.1059 2.654 2.184 .35 2.654

c Harvey's new neutron spectrum , 157 g fueled clad
 f

h	d
0.00	0.0000E+00
0.10000	0.1020E+05
0.20000	0.1260E+05
0.30000	0.1350E+05
0.40000	0.1510E+05
0.50000	0.1770E+05
0.60000	0.1900E+05
0.70000	0.2000E+05
0.80000	0.2080E+05
0.90000	0.2030E+05
1.00000	0.1830E+05
1.10000	0.1840E+05
1.20000	0.1890E+05
1.30000	0.1990E+05
1.40000	0.2050E+05
1.50000	0.2040E+05
1.60000	0.2070E+05
1.70000	0.2150E+05
1.80000	0.2270E+05
1.90000	0.2300E+05
2.00000	0.2350E+05
2.10000	0.2330E+05
2.20000	0.2380E+05
2.30000	0.2380E+05
2.40000	0.2260E+05
2.50000	0.2160E+05
2.60000	0.2070E+05
2.70000	0.1980E+05
2.80000	0.1830E+05
2.90000	0.1770E+05
3.00000	0.1660E+05
3.10000	0.1490E+05
3.20000	0.1400E+05
3.30000	0.1240E+05
3.40000	0.1040E+05
3.50000	0.9100E+04
3.60000	0.8060E+04
3.70000	0.6880E+04
3.80000	0.6120E+04
3.90000	0.5490E+04
4.00000	0.4720E+04
4.10000	0.4340E+04
4.20000	0.3400E+04
4.30000	0.2940E+04
4.40000	0.2360E+04

	4.50000	0.4950E+04
	5.00000	0.5200E+04
	5.50000	0.3700E+04
	6.00000	0.2660E+04
	6.50000	0.1850E+04
	7.00000	0.1290E+04
	7.50000	0.8920E+03
	8.00000	0.6130E+03
	8.50000	0.4210E+03
	9.00000	0.2570E+03
	9.50000	0.1970E+03
	10.00000	0.1900E+03
	11.00000	0.1210E+03
	12.00000	0.5530E+02
	13.00000	0.2400E+02
	14.00000	0.1110E+02
	15.00000	0.4900E+01
c	total =	0.71285E+06 x 72 = 5.13252E+07
ctme	1200	
nps	161911	
prdm	j -960	
e0	.2 .6 .8 2. 20.	
fc2	p dose rates (mrem/hr) on sides of truck, 7th entry = nearest	
f2:p	73 74	
fs2	-81 84 -82 83 -89 -90 -91 -92 t	
sd2	142172 138738 16219 16219 3679 3600 2r 1740 329567	
	142172 138738 16219 16219 3679 3600 2r 1740 329567	
c	ansi/ans-6.1.1-1977 fluence-to-dose, photons(mrem/hr)/(p/cm ² /s)	
de2	0.01 0.03 0.05 0.07 0.10 0.15 0.20 0.25 0.30	
	0.35 0.40 0.45 0.50 0.55 0.60 0.65 0.70 0.80	
	1.00 1.40 1.80 2.20 2.60 2.80 3.25 3.75 4.25	
	4.75 5.00 5.25 5.75 6.25 6.75 7.50 9.00 11.0	
	13.0 15.0	
df2	3.96-3 5.82-4 2.90-4 2.58-4 2.83-4 3.79-4 5.01-4 6.31-4 7.59-4	
	8.78-4 9.85-4 1.08-3 1.17-3 1.27-3 1.36-3 1.44-3 1.52-3 1.68-3	
	1.98-3 2.51-3 2.99-3 3.42-3 3.82-3 4.01-3 4.41-3 4.83-3 5.23-3	
	5.60-3 5.80-3 6.01-3 6.37-3 6.74-3 7.11-3 7.66-3 8.77-3 1.03-2	
	1.18-2 1.33-2	
fc12	p dose rates (mrem/hr) on ends of truck, 7th entry = nearest	
f12:p	71 72	
fs12	-85 88 -86 87 -89 -90 -91 -92 t	
sd12	10002 10002 16219 16219 3679 3600 2r 1740 68660	
	10002 10002 16219 16219 3679 3600 2r 1740 68660	
c	ansi/ans-6.1.1-1977 fluence-to-dose, photons(mrem/hr)/(p/cm ² /s)	
de12	0.01 0.03 0.05 0.07 0.10 0.15 0.20 0.25 0.30	
	0.35 0.40 0.45 0.50 0.55 0.60 0.65 0.70 0.80	
	1.00 1.40 1.80 2.20 2.60 2.80 3.25 3.75 4.25	
	4.75 5.00 5.25 5.75 6.25 6.75 7.50 9.00 11.0	
	13.0 15.0	
df12	3.96-3 5.82-4 2.90-4 2.58-4 2.83-4 3.79-4 5.01-4 6.31-4 7.59-4	
	8.78-4 9.85-4 1.08-3 1.17-3 1.27-3 1.36-3 1.44-3 1.52-3 1.68-3	
	1.98-3 2.51-3 2.99-3 3.42-3 3.82-3 4.01-3 4.41-3 4.83-3 5.23-3	
	5.60-3 5.80-3 6.01-3 6.37-3 6.74-3 7.11-3 7.66-3 8.77-3 1.03-2	

1.1E-2 1.33-2

fc22 p dose rates (mrem/hr) on bottom and top, 7th entry - nearest
 f22:p 75 76
 fs22 -81 84 -82 83 -85 -86 -87 -88 t
 sd22 133591 130366 15240 15240 2220 2220 3600 2r 2220 309677
 133591 130366 15240 15240 2220 2220 3600 2r 2220 309677

c ansi/ans-6.1.1-1977 fluence-to-dose,photons(mrem/hr)/(p/cm**2/s)
 de22 0.01 0.03 0.05 0.07 0.10 0.15 0.20 0.25 0.30
 0.35 0.40 0.45 0.50 0.55 0.60 0.65 0.70 0.80
 1.00 1.40 1.80 2.20 2.60 2.80 3.25 3.75 4.25
 4.75 5.00 5.25 5.75 6.25 6.75 7.50 9.00 11.0
 13.0 15.0

df22 3.96-3 5.82-4 2.90-4 2.58-4 2.83-4 3.79-4 5.01-4 6.31-4 7.59-4
 8.78-4 9.85-4 1.08-3 1.17-3 1.27-3 1.36-3 1.44-3 1.52-3 1.68-3
 1.98-3 2.51-3 2.99-3 3.42-3 3.82-3 4.01-3 4.41-3 4.83-3 5.23-3
 5.60-3 5.80-3 6.01-3 6.37-3 6.74-3 7.11-3 7.66-3 8.77-3 1.03-2
 1.1E-2 1.33-2

fc102 p dose rates (mrem/hr) on side of package, 2nd entry
 f102:p 38
 fs102 -132 -90 -93 -94 -91 -138 t
 sd102 1 5j 1 1

c ansi/ans-6.1.1-1977 fluence-to-dose,photons(mrem/hr)/(p/cm**2/s)
 de102 0.01 0.03 0.05 0.07 0.10 0.15 0.20 0.25 0.30
 0.35 0.40 0.45 0.50 0.55 0.60 0.65 0.70 0.80
 1.00 1.40 1.80 2.20 2.60 2.80 3.25 3.75 4.25
 4.75 5.00 5.25 5.75 6.25 6.75 7.50 9.00 11.0
 13.0 15.0

df102 3.96-3 5.82-4 2.90-4 2.58-4 2.83-4 3.79-4 5.01-4 6.31-4 7.59-4
 8.78-4 9.85-4 1.08-3 1.17-3 1.27-3 1.36-3 1.44-3 1.52-3 1.68-3
 1.98-3 2.51-3 2.99-3 3.42-3 3.82-3 4.01-3 4.41-3 4.83-3 5.23-3
 5.60-3 5.80-3 6.01-3 6.37-3 6.74-3 7.11-3 7.66-3 8.77-3 1.03-2
 1.1E-2 1.33-2

fc122 p dose rates (mrem/hr) on top of package, 1st entry
 f122:p 63
 fs122 -95 t

c ansi/ans-6.1.1-1977 fluence-to-dose,photons(mrem/hr)/(p/cm**2/s)
 de122 0.01 0.03 0.05 0.07 0.10 0.15 0.20 0.25 0.30
 0.35 0.40 0.45 0.50 0.55 0.60 0.65 0.70 0.80
 1.00 1.40 1.80 2.20 2.60 2.80 3.25 3.75 4.25
 4.75 5.00 5.25 5.75 6.25 6.75 7.50 9.00 11.0
 13.0 15.0

df122 3.96-3 5.82-4 2.90-4 2.58-4 2.83-4 3.79-4 5.01-4 6.31-4 7.59-4
 8.78-4 9.85-4 1.08-3 1.17-3 1.27-3 1.36-3 1.44-3 1.52-3 1.68-3
 1.98-3 2.51-3 2.99-3 3.42-3 3.82-3 4.01-3 4.41-3 4.83-3 5.23-3
 5.60-3 5.80-3 6.01-3 6.37-3 6.74-3 7.11-3 7.66-3 8.77-3 1.03-2
 1.1E-2 1.33-2

fc32 n dose rates (mrem/hr) on sides of truck, 7th entry - nearest
 f32:n 73 74
 fs32 -81 84 -82 83 -89 -90 -91 -92 t
 sd32 142172 138738 16219 16219 3679 3600 2r 1740 329567
 142172 138738 16219 16219 3679 3600 2r 1740 329567

c ansi/ans-6.1.1-1977 fluence-to-dose,neutrons(mrem/hr)/(n/cm**2/s)
 de32 log 2.5e-08 1.0e-07 1.0e-06 1.0e-05 1.0e-04

```

      .001   .01   .1   .5   1.0
      2.5   5.0   7.0  10.0  14.0  20.0
df32  log  3.67e-3 3.67e-3 4.46e-3 4.54e-3 4.18e-3
      3.76e-3 3.56e-3 2.17e-2 9.26e-2 .132
      .125 .156 .147 .147 .208 .227
fc42  n dose rates (mrem/hr) on ends of truck, 7th entry = nearest
f42:n  71 72
fs42  -85 88 -86 87 -89 -90 -91 -92 t
sd42  10002 10002 16219 16219 3679 3600 2r 1740 68660
      10002 10002 16219 16219 3679 3600 2r 1740 68660
c      ansi/ans-6.1.1-1977 fluence-to-dose,neutrons(mrem/hr)/(n/cm**2/s)
de42  log  2.5e-08 1.0e-07 1.0e-06 1.0e-05 1.0e-04
      .001   .01   .1   .5   1.0
      2.5   5.0   7.0  10.0  14.0  20.0
df42  log  3.67e-3 3.67e-3 4.46e-3 4.54e-3 4.18e-3
      3.76e-3 3.56e-3 2.17e-2 9.26e-2 .132
      .125 .156 .147 .147 .208 .227
fc52  n dose rates (mrem/hr) on bottom and top, 7th entry = nearest
fs2:n  75 76
fs52  -81 84 -82 83 -85 -86 -87 -88 t
sd52  133591 130366 15240 15240 2220 3600 2r 2220 309677
      133591 130366 15240 15240 2220 3600 2r 2220 309677
c      ansi/ans-6.1.1-1977 fluence-to-dose,neutrons(mrem/hr)/(n/cm**2/s)
de52  log  2.5e-08 1.0e-07 1.0e-06 1.0e-05 1.0e-04
      .001   .01   .1   .5   1.0
      2.5   5.0   7.0  10.0  14.0  20.0
df52  log  3.67e-3 3.67e-3 4.46e-3 4.54e-3 4.18e-3
      3.76e-3 3.56e-3 2.17e-2 9.26e-2 .132
      .125 .156 .147 .147 .208 .227
fc132 n dose rates (mrem/hr) on side of package, 2nd entry
f132:n  38
fs132  -132 -90 -93 -94 -91 -138 t
sd132  1 5j 1 1
c      ansi/ans-6.1.1-1977 Fluence-to-dose,neutrons(mrem/hr)/(n/cm**2/s)
de132 log  2.5e-08 1.0e-07 1.0e-06 1.0e-05 1.0e-04
      .001   .01   .1   .5   1.0
      2.5   5.0   7.0  10.0  14.0  20.0
df132 log  3.67e-3 3.67e-3 4.46e-3 4.54e-3 4.18e-3
      3.76e-3 3.56e-3 2.17e-2 9.26e-2 .132
      .125 .156 .147 .147 .208 .227
fc152 n dose rates (mrem/hr) on top of package, 1st entry
f152:n  63
fs152  -95 t
c      ansi/ans-6.1.1-1977 fluence-to-dose,neutrons(mrem/hr)/(n/cm**2/s)
de152 log  2.5e-08 1.0e-07 1.0e-06 1.0e-05 1.0e-04
      .001   .01   .1   .5   1.0
      2.5   5.0   7.0  10.0  14.0  20.0
df152 log  3.67e-3 3.67e-3 4.46e-3 4.54e-3 4.18e-3
      3.76e-3 3.56e-3 2.17e-2 9.26e-2 .132
      .125 .156 .147 .147 .208 .227
fc5   p dose rates (mrem/hr) at detectors, 2 m, Driver
f5:p   0. 327.00 79. 100.
      847.09 0. 79. 100.

```



```

0. 327.00 0.0 100.
0. 327.00 -79.0 100.
0. 327.00 158.0 100.
c      ansi/ans-6.1.1-1977 fluence-to-dose, photons(mrem/hr/(p/cm**2/s))
de5   0.01 0.03 0.05 0.07 0.10 0.15 0.20 0.25 0.30
      0.35 0.40 0.45 0.50 0.55 0.60 0.65 0.70 0.80
      1.00 1.40 1.80 2.20 2.60 2.80 3.25 3.75 4.25
      4.75 5.00 5.25 5.75 6.25 6.75 7.50 9.00 11.0
      13.0 15.0
df5   3.96-3 5.82-4 2.90-4 2.58-4 2.83-4 3.79-4 5.01-4 6.31-4 7.59-4
      8.78-4 9.85-4 1.08-3 1.17-3 1.27-3 1.36-3 1.44-3 1.52-3 1.68-3
      1.98-3 2.51-3 2.99-3 3.42-3 3.82-3 4.01-3 4.41-3 4.83-3 5.23-3
      5.60-3 5.80-3 6.01-3 6.37-3 6.74-3 7.11-3 7.66-3 8.77-3 1.03-2
      1.18-2 1.33-2
ft5   fcd
fu5   3 4 5 6 7 8 9 10 11 12 13 14 15 16 17 21 22 23 24
      41 42 43 44 45 46 47 71 72 73
fc15  n dose rates (mrem/hr) at detectors, 2 m, driver
f15:n 0. 327.00 79. 100.
      847.09 0. 79. 100.
      0. 327.00 0.0 100.
      0. 327.00 -79.0 100.
      0. 327.00 158.0 100.
c      ansi/ans-6.1.1-1977 fluence-to-dose, neutrons(mrem/hr/(n/cm**2/s))
de15  log 2.5e-08 1.0e-07 1.0e-06 1.0e-05 1.0e-04
      .001 .01 .1 .5 1.0
      2.5 5.0 7.0 10.0 14.0 20.0
df15  log 3.67e-3 3.67e-3 4.46e-3 4.54e-3 4.18e-3
      3.76e-3 3.56e-3 2.17e-2 9.26e-2 .132
      .125 .156 .147 .147 .208 .227
ft15  fcd
fu15  3 4 5 6 7 8 9 10 11 12 13 14 15 16 17 21 22 23 24
      41 42 43 44 45 46 47 71 72 73

```

HAC GAMMA SHIELDING MCNP INPUT FILE

```

SHLD. CALC., GPMS-RTG, NEUTRON-GAMMA, , accident intact
c   sphere of PuO2 for accident condition
1   3 -9.60 -100
c   inner containment
21  231 -.00122 ((6 -52 -31):(52 -33 -53)) 100
22  201 -8.0300 51 -52 31 -32
23  201 -8.0300 (52 -34 -54)(33 :53 )
24  201 -8.0300 51 -6 -31
c   outer containment
41  231 -.00122 51 35 -64 -39
42  231 -.00122 ((51 -35 -62)(52 :32))(-52 :34 :64 )
43  201 -8.0300 (-35 64 -63)(62 :35 )
44  236 -1.0 -52 65 36 -37
45  201 -8.0300 -52 65 37 -38
46  201 -8.0300 ((64 -65 36 51 -40):(-64 39 51)):(65 38 -66 -40 )
47  201 -8.0300 61 -51 -40
c   beyond outer containment and inside truck boundary
71  231 -.00122 (((-52 :36 :63))(52 :38 :-66))(66 :40 :-61 )
    71 -72 73 -74 75 -76
c   beyond truck and inside large sphere, above ground
72  231 -.00122 (-71:72:-73:74:-75:76) 77 -111
c   ground
73  221 -1.67 -77 -111
c   outside world
74  0 111

1   py 4.659
2   px -4.859
3   py -4.659
4   px 4.859
5   pz 95.544
6   pz 0.0000
7   pz 5.30801
8   pz -0.00001
9   c/y -2.184 2.654 1.831
10  c/y 2.184 2.654 1.831
11  py -3.1618
12  py -0.2941
13  py 0.2941
14  py 3.1618
15  py -3.1059
16  py -0.350
17  py 0.350
18  py 3.1059
19  c/y -2.1840 2.6540 1.3767
20  c/y -2.1840 2.6540 1.4326
21  c/y 2.1840 2.6540 1.3767
22  c/y 2.1840 2.6540 1.4326
c   radial surfaces for inner and outer containment
31  cz 43.1800
32  cz 45.0050

```

```

33      cz  43.6582
34      cz  44.6088
35      cz  45.5676
36      cz  46.8376
37      cz  50.0380
38      cz  50.3796
39      cz  49.6443
40      cz  61.3410
c  inner containment
51      pz  -8.8138
52      pz  127.4450
53      sz  60.3377 88.9000
54      sz  60.3377 89.8525
c  outer containment
61      pz  -12.6238
62      sz  60.1472 90.8050
63      sz  60.1472 92.0750
64      kz  48.7807 1.0000 -1.0000
65      kz  53.0733 1.0000 -1.0000
66      pz  2.6940
c  truck outside boundary
71      px  -615.95
72      px  603.25
73      py  -127.00
74      py  127.00
75      pz  -72.3138
76      pz  198.0
77      pz  -184.0738
c  tally fs surfaces on outside of truck
81      px  -90.0
82      px  -30.0
83      px  30.0
84      px  90.0
85      py  -90.0
86      py  -30.0
87      py  30.0
88      py  90.0
89      pz  -11.0
90      pz  49.0
91      pz  109.0
92      pz  189.0
93      pz  83.76
94      pz  94.24
95      cz  15.24
100     s   0. 0. 142.6  6.5608
c  outside world.
111     sc  5000.0000

*tr1  0 0 31.4560
mode  n p
m1    6000.50 -1.950000
m2    75187.50 -22.500000
m3    94238.50 -6.765000 94239.55 -1.698000 8016.50 -1.137000

```

```

m20j 25000.55c 67.97000j 24000.50c 20.000000 28000.50c 10.000000
      25055.50c 2.000000 6000.50c 0.030000
c      Hanford hwpv soil
m22j 8016.50c -0.511000 14000.50c -0.278200 20000.50c -0.071700
      26000.55c -0.109100 13027.50c -0.083260 12000.50c -0.031420
      19000.50c -0.011550 11023.50c -0.020220 22000.50c -0.016550
      25055.50c -0.001781 15031.50c -0.002400
m23j 7014.50c -0.765000 8016.50c -0.235000
m236 1001.50c 0.666700 8016.50c 0.333300
imp:n 1 4 3r 16 $ 1. 4j
      8r 8 0 $ 42. 73
imp:p 1 4 3r 16 $ 1. 4j
      8r 8 0 $ 42. 73
print 10 30 40 50 60 100 110 120 126 170
phys:p j 1
cut:p j j 0. 0.
cut:n j j 0. 0.
sdef rad d4 erg-d9
      pos 0. 0. 142.6 wgt=5.13252e7
s14 6.5508
sp4 -2j 2
c neutron spectrum from Harvey 10-3-95, 157 g fueled clad
# s19 sp9
      h d
      0.00 0.0000E+00
      0.10000 0.1020E+05
      0.20000 0.1260E+05
      0.30000 0.1350E+05
      0.40000 0.1510E+05
      0.50000 0.1770E+05
      0.60000 0.1900E+05
      0.70000 0.2000E+05
      0.80000 0.2080E+05
      0.90000 0.2030E+05
      1.00000 0.1830E+05
      1.10000 0.1840E+05
      1.20000 0.1890E+05
      1.30000 0.1990E+05
      1.40000 0.2050E+05
      1.50000 0.2040E+05
      1.60000 0.2070E+05
      1.70000 0.2150E+05
      1.80000 0.2270E+05
      1.90000 0.2300E+05
      2.00000 0.2350E+05
      2.10000 0.2330E+05
      2.20000 0.2380E+05
      2.30000 0.2380E+05
      2.40000 0.2260E+05
      2.50000 0.2160E+05
      2.60000 0.2070E+05
      2.70000 0.1980E+05
      2.80000 0.1830E+05

```

	2.90000	0.1770E+05
	3.00000	0.1660E+05
	3.10000	0.1490E+05
	3.20000	0.1400E+05
	3.30000	0.1240E+05
	3.40000	0.1040E+05
	3.50000	0.9100E+04
	3.60000	0.8060E+04
	3.70000	0.6880E+04
	3.80000	0.6120E+04
	3.90000	0.5490E+04
	4.00000	0.4720E+04
	4.10000	0.4340E+04
	4.20000	0.3400E+04
	4.30000	0.2940E+04
	4.40000	0.2360E+04
	4.50000	0.4950E+04
	5.00000	0.5200E+04
	5.50000	0.3790E+04
	6.00000	0.2660E+04
	6.50000	0.1850E+04
	7.00000	0.1290E+04
	7.50000	0.8920E+03
	8.00000	0.6130E+03
	8.50000	0.4210E+03
	9.00000	0.2570E+03
	9.50000	0.1970E+03
	10.00000	0.1980E+03
	11.00000	0.1210E+03
	12.00000	0.5530E+02
	13.00000	0.2480E+02
	14.00000	0.1110E+02
	15.00000	0.4900E+01
c	total =	0.71285E+06 x 72 = 5.13252E+07
ctme	200	
nps	60000	
prdap	j -960	
e0	.2 .6 .8 2. 20.	
fc2	p dose rates (mrem/hr) on sides of truck, 7th entry = nearest	
f2:p	73 74	
fs2	-81 84 -82 83 -89 -90 -91 -92 t	
sd2	142172 138738 16219 16219 3679 3600 2r 1740 329567	
	142172 138738 16219 16219 3679 3600 2r 1740 329567	
c	ans1/ans-6.1.1-1977 fluence-to-dose, photons(mrem/hr)/(p/cm**2/s)	
de2	0.01 0.03 0.05 0.07 0.10 0.15 0.20 0.25 0.30	
	0.35 0.40 0.45 0.50 0.55 0.60 0.65 0.70 0.80	
	1.00 1.40 1.80 2.20 2.60 2.80 3.25 3.75 4.25	
	4.75 5.00 5.25 5.75 6.25 6.75 7.50 9.00 11.0	
	13.0 15.0	
df2	3.96-3 5.82-4 2.90-4 2.58-4 2.83-4 3.79-4 5.01-4 6.31-4 7.59-4	
	8.78-4 9.85-4 1.08-3 1.17-3 1.27-3 1.36-3 1.44-3 1.52-3 1.68-3	
	1.98-3 2.51-3 2.99-3 3.42-3 3.82-3 4.01-3 4.41-3 4.83-3 5.23-3	
	5.60-3 5.80-3 6.01-3 6.37-3 6.74-3 7.11-3 7.66-3 8.77-3 1.03-2	

1.18-2 1.33-2
 fc12 p dose rates (mrem/hr) on ends of truck, 7th entry = nearest
 f12:p 71 72
 fs12 -85 88 -86 87 -89 -90 -91 -92 t
 sd12 10002 10002 16219 16219 3679 3600 2r 1740 68660
 10002 10002 16219 16219 3679 3600 2r 1740 68660
 c ansi/ans-6.1.1-1977 fluence-to-dose, photons(mrem/hr)/(p/cm**2/s)
 de12 0.01 0.03 0.05 0.07 0.10 0.15 0.20 0.25 0.30
 0.35 0.40 0.45 0.50 0.55 0.60 0.65 0.70 0.80
 1.00 1.40 1.80 2.20 2.60 2.80 3.25 3.75 4.25
 4.75 5.00 5.25 5.75 6.25 6.75 7.50 9.00 11.0
 13.0 15.0
 df12 3.96-3 5.82-4 2.90-4 2.58-4 2.83-4 3.79-4 5.01-4 6.31-4 7.59-4
 8.78-4 9.85-4 1.08-3 1.17-3 1.27-3 1.36-3 1.44-3 1.52-3 1.68-3
 1.98-3 2.51-3 2.99-3 3.42-3 3.82-3 4.01-3 4.41-3 4.83-3 5.23-3
 5.60-3 5.80-3 6.01-3 6.37-3 6.74-3 7.11-3 7.66-3 8.77-3 1.03-2
 1.18-2 1.33-2
 fc22 p dose rates (mrem/hr) on bottom and top, 7th entry = nearest
 f22:p 75 76
 fs22 -81 84 -82 83 -85 -86 -87 -88 t
 sd22 133591 130366 15240 15240 2220 3600 2r 2220 309677
 133591 130366 15240 15240 2220 3600 2r 2220 309677
 c ansi/ans-6.1.1-1977 fluence-to-dose, photons(mrem/hr)/(p/cm**2/s)
 de22 0.01 0.03 0.05 0.07 0.10 0.15 0.20 0.25 0.30
 0.35 0.40 0.45 0.50 0.55 0.60 0.65 0.70 0.80
 1.00 1.40 1.80 2.20 2.60 2.80 3.25 3.75 4.25
 4.75 5.00 5.25 5.75 6.25 6.75 7.50 9.00 11.0
 13.0 15.0
 df22 3.96-3 5.82-4 2.90-4 2.58-4 2.83-4 3.79-4 5.01-4 6.31-4 7.59-4
 8.78-4 9.85-4 1.08-3 1.17-3 1.27-3 1.36-3 1.44-3 1.52-3 1.68-3
 1.98-3 2.51-3 2.99-3 3.42-3 3.82-3 4.01-3 4.41-3 4.83-3 5.23-3
 5.60-3 5.80-3 6.01-3 6.37-3 6.74-3 7.11-3 7.66-3 8.77-3 1.03-2
 1.18-2 1.33-2
 fc32 n dose rates (mrem/hr) on sides of truck, 7th entry = nearest
 f32:n 73 74
 fs32 -81 84 -82 83 -89 -90 -91 -92 t
 sd32 142172 138738 16219 16219 3679 3600 2r 1740 329567
 142172 138738 16219 16219 3679 3600 2r 1740 329567
 c ansi/ans-6.1.1-1977 fluence-to-dose, neutrons(mrem/hr)/(n/cm**2/s)
 de32 log 2.5e-08 1.0e-07 1.0e-06 1.0e-05 1.0e-04
 .001 .01 .1 .6 1.0
 2.5 5.0 7.0 10.0 14.0 20.0
 df32 log 3.67e-3 3.67e-3 4.46e-3 4.54e-3 4.18e-3
 3.76e-3 3.56e-3 2.17e-2 9.26e-2 .132
 .125 .156 .147 .147 .208 .227
 fc42 n dose rates (mrem/hr) on ends of truck, 7th entry = nearest
 f42:n 71 72
 fs42 -85 88 -86 87 -89 -90 -91 -92 t
 sd42 10002 10002 16219 16219 3679 3600 2r 1740 68660
 10002 10002 16219 16219 3679 3600 2r 1740 68660
 c ansi/ans-6.1.1-1977 fluence-to-dose, neutrons(mrem/hr)/(n/cm**2/s)
 de42 log 2.5e-08 1.0e-07 1.0e-06 1.0e-05 1.0e-04
 .001 .01 .1 .5 1.0

```

      2.5    5.0    7.0    10.0   14.0   20.0
df42  log  3.67e-3 3.67e-3 4.46e-3 4.54e-3 4.18e-3
      3.76e-3 3.56e-3 2.17e-2 9.26e-2 .132
      .125 .156 .147 .147 .208 .227
fc52  n dose rates (mrem/hr) on bottom and top, 7th entry - nearest
fs2:n 75 76
fs52  -81 84 -82 83 -85 -86 -87 -88 t
sd52  133591 130366 15240 15240 2220 3600 2r 2220 309677
      133591 130366 15240 15240 2220 3600 2r 2220 309677
c      ansi/ans-6.1.1-1977 Fluence-to-dose,neutrons(mrem/hr/(n/cm**2/s)
de52  log  2.5e-08 1.0e-07 1.0e-06 1.0e-05 1.0e-04
      .001 .01 .1 .5 1.0
      2.5    5.0    7.0    10.0   14.0   20.0
df52  log  3.67e-3 3.67e-3 4.46e-3 4.54e-3 4.18e-3
      3.76e-3 3.56e-3 2.17e-2 9.26e-2 .132
      .125 .156 .147 .147 .208 .227
fc102 p dose rates (mrem/hr) on side of package, 2nd entry
f102:p 38
fs102 -93 -94 t
c      ansi/ans-6.1.1-1977 Fluence-to-dose,photons(mrem/hr/(p/cm**2/s)
de102 0.01 0.03 0.05 0.07 0.10 0.15 0.20 0.25 0.30
      0.35 0.40 0.45 0.50 0.55 0.60 0.65 0.70 0.80
      1.00 1.40 1.80 2.20 2.60 2.80 3.25 3.75 4.25
      4.75 5.00 5.25 5.75 6.25 6.75 7.50 9.00 11.0
      13.0 15.0
df102 3.96-3 5.82-4 2.90-4 2.58-4 2.83-4 3.79-4 5.01-4 6.31-4 7.59-4
      8.78-4 9.85-4 1.08-3 1.17-3 1.27-3 1.36-3 1.44-3 1.52-3 1.68-3
      1.98-3 2.51-3 2.99-3 3.42-3 3.82-3 4.01-3 4.41-3 4.83-3 5.23-3
      5.60-3 5.80-3 6.01-3 6.37-3 6.74-3 7.11-3 7.66-3 8.77-3 1.03-2
      1.18-2 1.33-2
fc122 p dose rates (mrem/hr) on top of package, 1st entry
f122:p 63
fs122 -95 t
c      ansi/ans-6.1.1-1977 Fluence-to-dose,photons(mrem/hr/(p/cm**2/s)
de122 0.01 0.03 0.05 0.07 0.10 0.15 0.20 0.25 0.30
      0.35 0.40 0.45 0.50 0.55 0.60 0.65 0.70 0.80
      1.00 1.40 1.80 2.20 2.60 2.80 3.25 3.75 4.25
      4.75 5.00 5.25 5.75 6.25 6.75 7.50 9.00 11.0
      13.0 15.0
df122 3.96-3 5.82-4 2.90-4 2.58-4 2.83-4 3.79-4 5.01-4 6.31-4 7.59-4
      8.78-4 9.85-4 1.08-3 1.17-3 1.27-3 1.36-3 1.44-3 1.52-3 1.68-3
      1.98-3 2.51-3 2.99-3 3.42-3 3.82-3 4.01-3 4.41-3 4.83-3 5.23-3
      5.60-3 5.80-3 6.01-3 6.37-3 6.74-3 7.11-3 7.66-3 8.77-3 1.03-2
      1.18-2 1.33-2
fc132 n dose rates (mrem/hr) on side of package, 2nd entry
f132:n 38
fs132 -93 -94 t
c      ansi/ans-6.1.1-1977 Fluence-to-dose,neutrons(mrem/hr/(n/cm**2/s)
de132  log  2.5e-08 1.0e-07 1.0e-06 1.0e-05 1.0e-04
      .001 .01 .1 .5 1.0
      2.5    5.0    7.0    10.0   14.0   20.0
df132  log  3.67e-3 3.57e-3 4.46e-3 4.54e-3 4.18e-3
      3.76e-3 3.56e-3 2.17e-2 9.26e-2 .132

```

```

      .125 .156 .147 .147 .208 .227
fc152 n dose rates (mrem/hr) on top of package, 1st entry
f152:n 63
fs152 -95 t
c ansi/ans-6.1.1-1977 fluence-to-dose,neutrons(mrem/hr)/(n/cm**2/s)
de152 log 2.5e-08 1.0e-07 1.0e-06 1.0e-05 1.0e-04
      .001 .01 .1 .5 1.0
      2.5 5.0 7.0 10.0 14.0 20.0
df152 log 3.67e-3 3.67e-3 4.46e-3 4.54e-3 4.18e-3
      3.76e-3 3.56e-3 2.17e-2 9.26e-2 .132
      .125 .156 .147 .147 .208 .227
fc5 p dose rates (mrem/hr) at detectors, 1 m above top s
f5:p 0. 0. 252.22 50.
c ansi/ans-6.1.1-1977 fluence-to-dose,photons(mrem/hr)/(p/cm**2/s)
de5 0.01 0.03 0.05 0.07 0.10 0.15 0.20 0.25 0.30
     0.35 0.40 0.45 0.50 0.55 0.60 0.65 0.70 0.80
     1.00 1.40 1.80 2.20 2.60 2.80 3.25 3.75 4.25
     4.75 5.00 5.25 5.75 6.25 6.75 7.50 9.00 11.0
     13.0 15.0
df5 3.96-3 5.82-4 2.90-4 2.68-4 2.83-4 3.79-4 5.01-4 6.31-4 7.59-4
     8.78-4 9.85-4 1.08-3 1.17-3 1.27-3 1.36-3 1.44-3 1.52-3 1.68-3
     1.98-3 2.51-3 2.99-3 3.42-3 3.82-3 4.01-3 4.41-3 4.83-3 5.23-3
     5.60-3 5.80-3 6.01-3 6.37-3 6.74-3 7.11-3 7.66-3 8.77-3 1.03-2
     1.18-2 1.33-2
fc15 n dose rates (mrem/hr) at detectors, 1 m above top s
f15:n 0. 0. 252.22 50.
c ansi/ans-6.1.1-1977 fluence-to-dose,neutrons(mrem/hr)/(n/cm**2/s)
de15 log 2.5e-08 1.0e-07 1.0e-06 1.0e-05 1.0e-04
      .001 .01 .1 .5 1.0
      2.5 5.0 7.0 10.0 14.0 20.0
df15 log 3.67e-3 3.67e-3 4.46e-3 4.54e-3 4.18e-3
      3.76e-3 3.56e-3 2.17e-2 9.26e-2 .132
      .125 .156 .147 .147 .208 .227

```


6.0 CRITICALITY EVALUATION

This chapter discusses the principal criticality engineering-physics design of the Radioisotope Thermoelectrical Generator (RTG) Transportation System Package and contents important to safety and necessary to comply with 10 CFR 71. A single package will be shipped as a fissile class III shipment. For normal conditions of transport (NCT), a one-package shipment is to remain subcritical when it is in contact with an identical one-package shipment and the two-package array is reflected on all sides by water. The single-package shipment must remain subcritical under hypothetical accident conditions (HAC) with optimum hydrogenous moderation and close reflection by water.

6.1 DISCUSSION AND RESULTS

The RTG Transportation System Package is a Type B(U) packaging system that is used to transport a RTG or similar payload. The primary payload for use in the package is one GPHS RTG. Because of the heat load limits, only one GPHS RTG can be shipped in the exclusive-use RTG Transportation System trailer. The GPHS RTG will be inside the package's two containment vessels when shipped. This will aid in preventing damage to the fueled portion of the RTG during HAC events. However, the main thrust of these analyses was to determine the maximum k_{eff} for the fuel involved in the most reactive configuration, assuming only that the fueled clads stay in their original shape and size.

The GPHS RTG criticality analyses were performed with the Monte Carlo Neutron Photon (MCNP) code for both the actual configuration and the most reactive array of fueled clads. These results are summarized in Table 6-1 and show that the GPHS RTG will remain safely subcritical for all NCT and HAC events.

Although the total fuel quantity for the generic payload per trailer is greater (11.1%) than the GPHS RTG total fuel quantity (12,580 g PuO_2 vs. 11,304 g PuO_2), the maximum fuel quantity per package is only 55.8% of that for the GPHS. Consequently, the resultant k_{eff} value for the larger fuel quantity is slightly higher than the values summarized in Table 6-1. For the larger fuel mass, the k_{eff} for the HAC would increase from the GPHS RTG value of 0.745 to 0.780, which is a 4.7% increase. This result is documented in the RTG Transportation System SARP Addendum (WHC-SD-RTG-SARP-002). The higher value for the larger fuel quantity is still well below the k_{eff} limit of 0.95.

TABLE 6-1. Summary of Criticality Analyses (all cases reflected by 30 cm of water).

Case	Total mass of PuO_2 (kg)	Moderator	$k_{eff} \pm 1\sigma$
GPHS RTGs (NCT)	--	--	--
One RTG	11.3	C	0.404 \pm 0.003
Two RTGs	22.6	C	0.409 \pm 0.002
GPHS RTG (HAC)	--	--	--
One RTG	12.6	H ₂ O	0.745 \pm 0.004

6.2 PACKAGE FUEL LOADING

The maximum fuel loading for both NCT and MAC events is contained in Table 6.2-1.

TABLE 6.2-1. RTG Transportation System Package Payload Descriptions.

Payload description	Number of RTGs per package	Total mass of PuO ₂ (kg)
GPHS-RTG	1	11.3

The material compositions used in the analyses are given in Table 6.2-2. The plutonium composition limits specified in Reference 2 are 80 to 86 molecular percent ²³⁹Pu. Therefore, calculations were performed for both the 80 and 86 percent limits. The remainder of the plutonium was (conservatively) ²⁴⁰Pu in all the calculations. The fuel loading is further defined in Table 6.3.2-1.

TABLE 6.2-2. MCNP Material Compositions Used.

Material	Weight %
PuO ₂ (9.6 g/cm ³) ^a	
Plutonium	86.2
Oxygen	11.8
Graphite (1.96 g/cm ³)	100.0
Iridium (22.5 g/cm ³)	100.0
Water (1.0 g/cm ³ , unless indicated otherwise)	
Oxygen	88.9
Hydrogen	11.1

6.3 MODEL SPECIFICATION

This section describes the computer models used for the analyses.

6.3.1 Description of Computational Model

The design of the GPHS modules (also known as aeroshells) is shown in Figure 6.3.1-1. The MCNP computer geometries used for the GPHS RTG evaluation are shown in Figures 6.3.1-2 through 6.3.1-13. These figures show that the GPHS RTGs were evaluated in their normal fuel arrangement in an RTG. But, additional configurations of fuel were evaluated to be sure that the most reactive conditions were considered. Computer models were made for large spheres of fuel, arrays of GPHS aeroshells (which contain four fueled clads), and arrays of fueled clads. As detailed in Section 1.3.1, Reference 3, Chapter 1.0 of this SARP, the GPHS aeroshell is designed to survive atmospheric reentry and is the smallest size of heat-generating fragment that could arise from

break-up of the GPHS RTG during HAC events. The criticality evaluation is considered conservative because arrays of individual fueled clads are evaluated.

The GPHS RTG contains a vertical stack of 18 GPHS aeroshells; each one contains four fueled clads. Each fueled clad contains about 167 grams of PuO_2 (Reference 2).

All MCNP geometries were reflected by 30 cm of water, and water flooding was assumed for all HAC events.

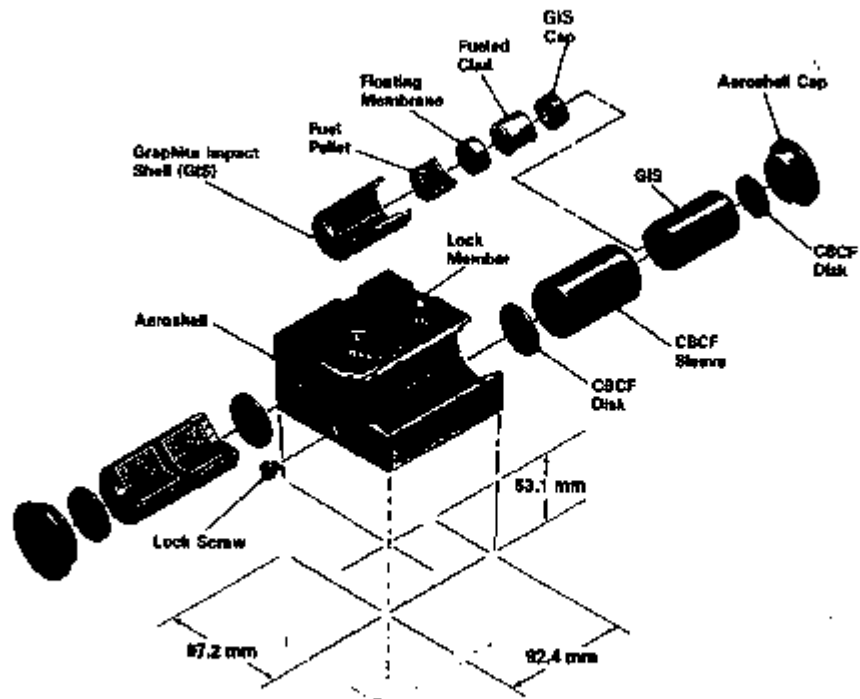


FIGURE 6.3.1-1. An Exploded View of a General Purpose Heat Source Module.

4412-4

11/04/98 08:40:18
DATE, TIME, USER, DEVICE,
REV. 000000
PLOT# = 11/04/98 08:40:18
EPLI =
1. 0.00000, 1.00000, 0.00000
1. 0.00000, 1.00000, 0.00000
1. 0.00000, 1.00000, 0.00000
DATE TIME 11/04/98 08:40:18
EPLI 0.00000 1.00000 0.00000
REV 000000

Material	Densities
	(g/cm ³)
TiO ₂	5.6
C	1.95
Fe	22.5
H ₂ O	1.0

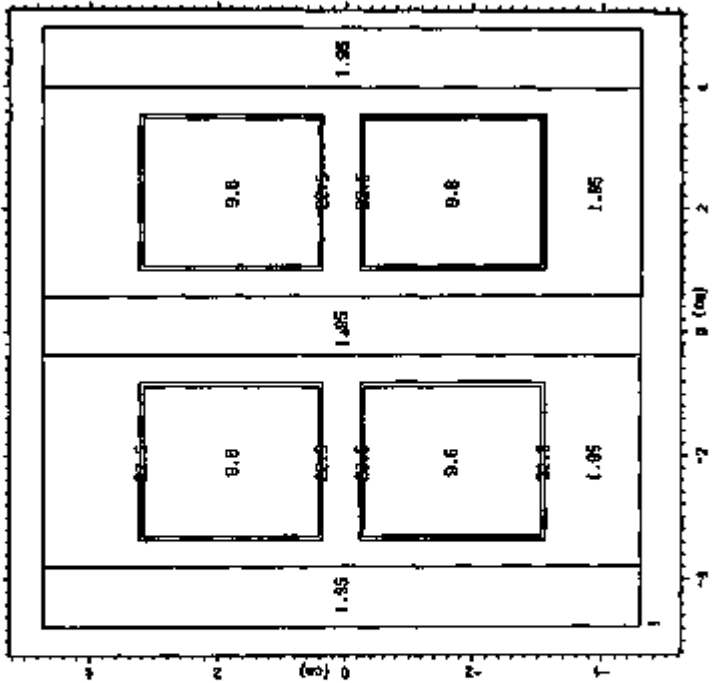


FIGURE B.3.1-8. GPHS RTG with Water Reflector, X-Y Plane.

6.3.2 Package Regional Densities

The material densities used for these analyses are shown in Table 6.3.2-1. There was no change in material densities for the HAC event. The fuel densities and composition are given in Reference 2. This reference calls out a ²³⁹Pu range of 80 to 88%. The remainder of the plutonium used was conservatively ²³⁸Pu. The mass of a GPHS fuel pellet is 157 g.

TABLE 6.3.2-1. Material Densities Used for the GPHS RTG.

Material	Constituents	Mass density (g/cm ³)	Atom density (atoms/b-cm)
PuO ₂ (80%Pu238)	--	9.6	6.4199E-2
--	Pu238	6.765	1.7114E-2
--	Pu239	1.698	4.2776E-3
--	O16	1.137	4.2808E-2
PuO ₂ (88%Pu238)	--	9.6	6.4204E-2
--	Pu238	7.274	1.6402E-2
--	Pu239	1.189	2.8961E-3
--	O16	1.137	4.2807E-2
Graphite	C12	1.96	9.7768E-2
Ir(Ra used)	Re187	22.5	7.2476E-2
Water	--	1.0	9.9666E-2
--	H	0.1111	6.6392E-2
--	O16	0.8889	3.3468E-2

6.4 CRITICALITY CALCULATIONS

This section describes the calculational methods used to determine the reactivity for the maximum fuel loadings of the RTG Transportation System Package.

6.4.1 Calculational Method

The MCNP code (References 1 and 3) was used for the reactivity evaluation of the package. The MCNP code was developed at the Los Alamos National Laboratory (LANL) and is now used extensively both in this country and throughout the world. The MCNP code is a general-purpose, continuous-energy, generalized-geometry neutron and photon transport code that calculates eigenvalues for criticality evaluations.

The MCNP code uses continuous energy cross-sections that are thoroughly documented in Appendix G of Reference 3. These cross-sections are defined with a high-energy resolution. All the cross-sections used in the RTG criticality analyses were generated from either Evaluated Nuclear Data Files (ENDF) or LANL evaluations. Processing this type of data is not required for different moderator-to-fuel ratio conditions.

These analyses help determine the maximum reactivity fueled clad arrays, assuming the fueled clads retained their original size and shape. The actual GPHS RTG geometry was also modeled and evaluated. It was substantially less reactive than equivalent numbers of tightly packed fueled clads.

6.4.2 Fuel/Moderator Loading Optimization

The fuel loadings used are maximum values from Reference 2. Evaluations were made for both the lower and upper limits of ^{239}Pu and ^{240}Pu . Evaluations were also made for maximum moderation even though no room for it existed in some cases. An evaluation was even made for abnormally high water densities (greater than 1 g/cm^3) with a square array of closely packed GPHS fueled clads (Table 6.4.3-1). Therefore, the reactivity increased with increasing water density, thus demonstrating that the square array was undermoderated. This shows that lower density water would decrease the reactivity.

Tighter fueled clad packing could be obtained than that from the square arrays used. But, the evaluation was made for much closer spacing than is possible with the graphite that surrounds the fuel in either NCT or HAC events. The analyses on the GPHS RTG showed that the closely packed fueled clads are more reactive than the larger normal spacing. All the calculations were made with a 30-cm-thick water reflector surrounding the model. All K_{∞} calculations were run to a 1- σ convergence criteria of 0.006 or less. Actual convergence values obtained are specified in Table 6.4.3-7. Continuous cross-sections were used in these evaluations; therefore, no cross-section adjustments were required for various geometric configurations and material compositions.

5.4.3 Criticality Results

The results of the MCNP calculations are contained in Table 5.4.3-1 for the GPHS RTG. It was determined that a sphere of PuO_2 with a mass of 11.3 kg (equivalent mass for one GPHS RTG) would remain safely subcritical. The reactivity increases as fueled clads become more tightly packed. Water moderation also increases reactivity for a tightly packed array of fueled clads. When the array expands, the K_{eff} decreases more from geometric expansion than it increases from increased moderation.

The analyses for the GPHS RTG showed that a single RTG in its normal configuration, except for full water reflection, would have a K_{eff} of 0.404. Two GPHS RTGs could only be brought to within a spacing of about 50 cm center-to-center, even if no credit is taken for the two containment vessels on each package. Two cases were run with this spacing. In the first, the water reflector was around and between both RTGs. In the second, a void channel was left directly between the two RTGs (for maximum neutron communication) with full water reflection around the rest. The maximum K_{eff} from these two calculations (with water reflection between RTGs) was 0.409.

A conservative model was generated for the HAC case. It consisted of a closely packed 4 by 4 array of fueled clads, water moderated, and no iridium cladding. The K_{eff} for this configuration was 0.745.

The remaining calculations reported in Table 5.4.3-1 show that increased spacing between fueled clads reduces the reactivity even with water moderation. The calculations with "normal" high density water show that a tightly packed array of fueled clads with normal water density will be undermoderated.

The cross-sections for iridium (the clad material of the fueled clads) were not available, so rhodium cross-sections were used in their place. This is conservative because the total cross-section for iridium in the thermal range is about five times that of rhodium and the cross sections at higher energies are nearly the same. Therefore, the substitution would be conservative. However, it was still necessary to see the effect of removing the iridium clad for a few MCNP runs. It can be seen in Table 5.4.3-1 that voiding out the iridium regions increased the k_{eff} by about 0.05. Even this unrealistic condition would not alter the conclusion that the package will be critically safe for both NCT and HAC events.

TABLE 6.4.3-1. Results of the MCNP Analyses for GPHS RTGs.

Case	Total mass of PuO_2 (Kgl)	Moderator	$K_{eff} \pm 1\sigma$
Sphere, 80% ^{239}Pu , radius = 6 cm	9.68	None	0.753 \pm 0.005
Sphere, 86% ^{239}Pu , radius = 6 cm	9.68	None	0.743 \pm 0.004
Sphere, 80% ^{239}Pu , radius = 7 cm	13.8	None	0.889 \pm 0.005
Sphere, 86% ^{239}Pu , radius = 7 cm	13.8	None	0.942 \pm 0.005
Sphere, 80% ^{239}Pu , radius = 8 cm	20.6	None	0.954 \pm 0.004
Sphere, 86% ^{239}Pu , radius = 8 cm	20.6	None	0.943 \pm 0.005
Sphere, 80% ^{239}Pu , radius = 9 cm	29.3	None	1.053 \pm 0.004
Sphere, 86% ^{239}Pu , radius = 9 cm	29.3	None	1.031 \pm 0.004
GPHS RTG, 80% ^{239}Pu , norm. config.	11.3	C	0.363 \pm 0.002
GPHS RTG, 80% ^{239}Pu , norm. config. no iridium clad	11.3	C	0.404 \pm 0.003
GPHS RTG, 86% ^{239}Pu , norm. config.	11.3	C	0.350 \pm 0.002
GPHS RTG, 80% ^{239}Pu , norm. config.	11.3	H_2O	0.368 \pm 0.002
GPHS RTG, 86% ^{239}Pu , norm. config.	11.3	H_2O	0.348 \pm 0.002
Two GPHS RTGs, 50 cm center-center spacing, 80% ^{239}Pu , water reflection around and between	22.6	C	0.408 \pm 0.002
Two GPHS RTGs, 50 cm center-center spacing, 80% ^{239}Pu , water reflection around, but void channel between RTGs	22.6	C	0.392 \pm 0.003
2 by 2 by 5 array of GPHSs, 80% ^{239}Pu	12.6	C	0.473 \pm 0.003
2 by 2 by 5 array of GPHSs, 86% ^{239}Pu	12.6	C	0.457 \pm 0.003
2 by 2 by 5 array of GPHSs, 80% ^{239}Pu	12.6	H_2O	0.477 \pm 0.002
2 by 2 by 5 array of GPHSs, 86% ^{239}Pu	12.6	H_2O	0.439 \pm 0.003
4 by 4 by 5 array, close packed fueled clads, 80% ^{239}Pu	12.6	C	0.898 \pm 0.004
4 by 4 by 5 array, close packed fueled clads, 80% ^{239}Pu no iridium clad	12.6	C	0.743 \pm 0.004
4 by 4 by 5 array, close packed fueled clads, 86% ^{239}Pu	12.6	C	0.688 \pm 0.003

TABLE 6.4.3-1. Results of the MCNP Analyses for GPHS RTGs. (Cont.)

Case	Total mass of PuO ₂ (Kg)	Moderator	K _{eff} ± 1σ
4 by 4 by 5 array, close packed fueled clads, 80% ²³⁹ Pu	12.6	H ₂ O	0.686 ± 0.003
4 by 4 by 5 array, close packed fueled clads, 80% ²³⁹ Pu no iridium clad	12.6	H ₂ O	0.745 ± 0.004
4 by 4 by 5 array, close packed fueled clads, 80% ²³⁹ Pu no iridium clad	12.6	Void	0.719 ± 0.004
4 by 4 by 5 array, close packed fueled clads, 86% ²³⁹ Pu	12.6	H ₂ O	0.671 ± 0.003
4 by 4 by 5 array, close packed fueled clads, 80% ²³⁹ Pu	12.6	H ₂ O, 2 g/cm ³	0.700 ± 0.003
4 by 4 by 5 array, close packed fueled clads, 86% ²³⁹ Pu	12.6	H ₂ O, 2 g/cm ³	0.674 ± 0.002
4 by 4 by 5 array, close packed fueled clads, 80% ²³⁹ Pu	12.6	H ₂ O, 4 g/cm ³	0.713 ± 0.003
4 by 4 by 5 array, close packed fueled clads, 80% ²³⁹ Pu, no iridium clad	12.6	H ₂ O, 4 g/cm ³	0.763 ± 0.003
4 by 4 by 5 array, close packed fueled clads, 86% ²³⁹ Pu	12.6	H ₂ O, 4 g/cm ³	0.676 ± 0.003
4 by 4 by 5 array, close packed fueled clads, 80% ²³⁹ Pu	12.6	H ₂ O, 8 g/cm ³	0.667 ± 0.003
4 by 4 by 5 array, close packed fueled clads, 86% ²³⁹ Pu	12.6	H ₂ O, 8 g/cm ³	0.644 ± 0.002
4 by 4 by 5 array, 1 cm between fueled clads, 80% ²³⁹ Pu	12.6	H ₂ O	0.554 ± 0.002
4 by 4 by 5 array, 1 cm between fueled clads, 86% ²³⁹ Pu	12.6	H ₂ O	0.515 ± 0.002
4 by 4 by 5 array, 2 cm between fueled clads, 80% ²³⁹ Pu	12.6	C	0.467 ± 0.003
4 by 4 by 5 array, 2 cm between fueled clads, 86% ²³⁹ Pu	12.6	C	0.448 ± 0.002
4 by 4 by 5 array, 2 cm between fueled clads, 80% ²³⁹ Pu	12.6	H ₂ O	0.478 ± 0.002
4 by 4 by 5 array, 2 cm between fueled clads, 86% ²³⁹ Pu	12.6	H ₂ O	0.440 ± 0.002

Note: All calculations were performed with a 30.48 cm water reflector.

6.5 CRITICAL BENCHMARK EXPERIMENTS

This section justifies the validity of calculational methods and neutron cross-section values used by reporting the results of critical benchmark experiment analyses.

6.5.1 Benchmark Experiments and Applicability

The benchmark analyses were performed with the MCNP code¹ and associated cross-sections that are documented in Appendix G of Reference 3. Analyses were performed for both fast and thermalized benchmark problems (Reference 4).

The MCNP analyses were performed for two metal sphere benchmarks with different ²³⁹Pu enrichments and for one moderated uranium array. A more comprehensive description of the experiments is contained in Section 6.5.2. These benchmarks contained both fast and thermal systems and two of them contained plutonium fuel. However, none of the three used ²³⁹Pu. But, the ²³⁹Pu cross-sections used were obtained from ENDF/B-V files, which are the most reliable sources available.

6.5.2 Details of Benchmark Calculations

The first critical experiment analyzed was Jazabel. It consisted of an unreflected plutonium metal sphere. It was 96.6% ²³⁹Pu enriched. The remaining material was ²⁴⁰Pu. The sphere had a mass of 17.02 kg, a density of 15.61 g/cm³, and a radius of 6.385 cm.

The second critical experiment was also a bare sphere called Jazabel, but it had a ²³⁹Pu enrichment of 80%; the remaining material was ²⁴⁰Pu. It had a mass of 19.46 kg, a density of 15.73 g/cm³, and a radius of 6.660 cm.

The third critical experiment consisted of three unreflected aluminum cylinders containing U(93.2)O₂F₂ water solutions. The inside cylinder diameter and critical height measured 20.3 and 41.4 cm, respectively. The aluminum container had a density of 2.71 g/cm³ and was 0.16 cm thick. The three cylinders were set in an equilateral configuration with a surface separation of 0.38 cm. The MCNP model of this experiment is shown in Figure 6.5.2-1. Benchmark material densities used are contained in Table 6.5.2-1.

TABLE 6.5.2-1. Benchmark Material Densities.

Benchmark and material	Constituents	Mass density (g/cm ³)	Atom density (atoms/b-cm)
Jezabel (95.5% ²³⁹ Pu; 4.5% ²⁴⁰ Pu)	--	15.61	3.9316E-2
--	²³⁹ Pu	14.908	3.7554E-2
--	²⁴⁰ Pu	0.702	1.7821E-3
Jezabel (80% ²³⁹ Pu; 20% ²⁴⁰ Pu)	--	15.73	3.9593E-2
--	²³⁹ Pu	12.584	3.1701E-2
--	²⁴⁰ Pu	3.146	7.8921E-3
U(93.2)O ₂ F ₂ (cylindrical fuel solution)	--	1.131	1.0274E-1
--	²³⁸ U	0.0856	2.1884E-4
--	²³⁵ U	0.0062	1.5411E-5
--	F19	0.0148	4.7066E-4
--	H2	0.1134	6.7736E-2
--	O16	0.9110	3.4296E-2
Aluminum	Al26	2.71	6.0486E-2

03/23/94 09:12:44
 BENCHMARK, 3 (20 MODERATED
 U(93.2)O₂F₂ CYLINDERS IN AIR

probid = 03/23/94 09:10:43
 basis:
 (1.00000, 0.00000, 0.00000)
 (0.00000, 0.00000, 1.00000)
 origin:
 (0.10, 0.10, 0.00)
 extent = (20.20, 24.20)
 cell labels are
 see definition

Material Densities (g/cm ³)	
U(93.2)O ₂ F ₂ Sol.	1.131
aluminum	2.71

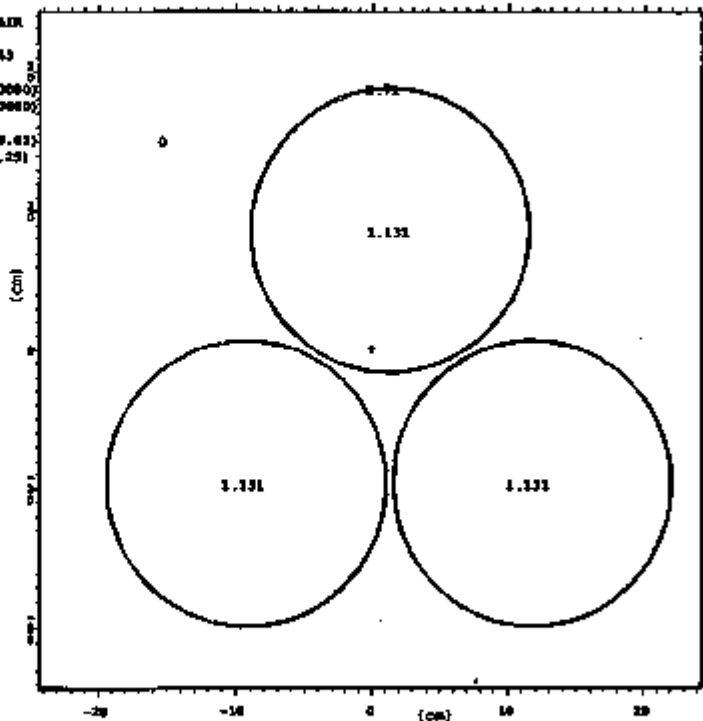


FIGURE B.5.2-1. Benchmark Model U(93.2)O₂F₂ Water Moderated Cylinders.

6.5.3 Results of Benchmark Calculations

The results of these three benchmark calculations are shown in Table 6.6.3-1. The MCNP accurately evaluated all critical experiments. Several other benchmark problems have also been evaluated by LANL personnel with MCNP (Reference 4). The results are shown in Table 6.6.3-2. These benchmark calculations do not produce a significant bias for MCNP.

Since the only experiments involving ^{239}Pu are at very low multiplication, an alternative to comparisons with experiments is to estimate conservative uncertainties in k from uncertainties in the microscopic cross-sections. To accomplish this, a ^{239}Pu -oxide sphere of 8-cm radius and a density of 9.5 g/cm³ will be examined. ^{239}Pu is considered since the RTG fuel is at least 80% ^{239}Pu and has received less cross-section attention than ^{238}Pu . Also, oxide rather than water moderation will be used since water moderation would dramatically reduce k because of the partial fission threshold below an MeV. The 8-cm radius was chosen since this gives a k of 0.823 which is greater than the relevant calculated k values in Chapter 6.

An MCNP calculation was made of the ^{239}Pu -oxide sphere to obtain the following k and one-group cross-sections:

k	= .8237 (.23%)
One-group values:	
total flux	= 0.003213 (.28%)
total cross-section	= 8.154
fission cross-section	= 1.758
ν of fission	= 3.181
capture cross-section	= 0.208
elastic cross-section	= 5.444
$n,2n$ cross-section	= 0.0036
inelastic, by subtraction	= 8.154 - 7.412 = 0.742

It is first observed that these one-group cross-sections are similar in magnitude to values given (H.M. Fisher, "A Nuclear Cross-Section Data Handbook," LA-11711-M, Los Alamos National Laboratory, 1969 (page 234)) at 1 MeV from ENDF/B-V. They are also similar in magnitude to an average of the ENDF/B-V cross-sections over a fission spectrum.

Since

$$k = \nu\phi/(a\phi + L)$$

with ν the number of neutrons per fission, 1 the fission cross-section, a the absorption cross-section, ϕ the total flux, and L the leakage, sensitivities of the one-group cross-sections can be examined. First look at the uncertainty in k due to the uncertainty in the fission cross-section.

$$dk/d1 = \nu\phi/(a\phi + L) \cdot \nu\phi\phi/(a\phi + L)^2 = (k/1) \cdot (k/a)$$

where the absorption (removal) cross-section

$$a = 1 + c + i$$

is used under the assumption that inelastic scattering, i , reduces the neutron energy below the fission threshold of Pu239 most of the time, so k is like an absorption event.

The fission cross-section is measured and has an estimated uncertainty of 0.035 barns, which results in

$$dk = 0.035 * (.8237/1.758) * [1 - (.8237/3.181)] = 0.012$$

i.e., a 1.2% change in k because of the uncertainty in the fission cross-section.

The uncertainty in k due to the uncertainty in the inelastic cross-section is given conservatively (assuming all inelastics reduce the neutron energy below the fission threshold) by

$$dk/di = -\sigma_i \phi / (\sigma_f + I)^2 = k^2 / (i \phi)$$

Comparing the difference in i between the minimum fission spectrum average of four recent evaluations and that of ENDF/B-V gives a di of -0.11 barns; hence

$$dk = 0.11 * 0.8237^2 / (3.181 * 1.758) = 0.014$$

Similarly, for the capture cross-section

$$dk/dc = k^2 / (c \phi)$$

Comparing the difference in c between the minimum fission spectrum average of four recent evaluations and that of ENDF/B-V gives a dc of -0.072 barns; thus

$$dk = 0.072 * 0.8237^2 / (3.181 * 1.758) = 0.009$$

Adding these results in quadrature gives a conservative, one-standard-deviation dk uncertainty of 0.021 or a three-standard-deviation dk uncertainty of 0.063. This is conservative because the largest differences were used to estimate the uncertainty in σ partial and because inelastic scattering was assumed to scatter neutrons below the inelastic threshold of Pu-238.

TABLE 6.6.3-1. Results of MCNP analyses of Critical Experiments.

Critical experiment	Fuel composition and configuration	MCNP calculated K_{eff}
Jezabel (1)	95.5 wt% ^{239}Pu , ~4.5% ^{240}Pu sphere, bare	0.9986 ± 0.0021
Jezabel (2)	80 wt% ^{239}Pu , ~20% ^{240}Pu sphere, bare	1.0080 ± 0.0012
Three uranium cylinders	UN93.2 wt% $^{235}\text{UO}_2\text{F}_6$ water solution, 3 cylinders each at 20.3 cm in diameter and 41.4 cm in height, set in an equilateral triangular configuration with surface separation of 0.38 cm	1.0019 ± 0.0028

TABLE 6.5.3-2. MCNP Calculations of Critical Benchmark Experiments by LANL.

Critical experiment	Fuel composition and configuration	MCNP calculated k_{eff}
Jezabel (1)	95.5 wt% ^{239}Pu , ~ 4.5% ^{240}Pu sphere, bare	0.9886 ± 0.0021
Jezabel (2)	80 wt% ^{239}Pu , ~ 20% ^{240}Pu sphere, bare	1.0075 ± 0.0012
Uranium metal cylinder	10.9 wt% ^{235}U , ~ 89.1% ^{238}U cylinder, bare	1.0024 ± 0.0013
Uranium metal cylinder	14.11 wt% ^{235}U , ~ 86.89% ^{238}U cylinder, bare	1.0003 ± 0.0014
Reflected sphere	83.5 wt% ^{235}U , ~ 8.5% ^{238}U sphere, graphite reflected	0.9981 ± 0.0010
Reflected sphere	87.67 wt% ^{235}U , ~ 2.33% ^{238}U sphere, water reflected	0.9968 ± 0.0022
Three uranium cylinders	U(93.2 wt% ^{235}U) O_2F , water solution, 3 cylinders each at 20.3 cm in diameter and 41.4 cm in height, set in an equilateral triangular configuration with surface separation of 0.38 cm	0.9981 ± 0.0011
3 by 3 by 3 array of Pu fuel rods	Cylindrical cells containing 3 by 3 arrays of Pu (83.666 wt% ^{239}Pu) metal fuel rods, stacked on each other with spacers between	0.991 ± 0.005

6.6 APPENDIX

The following is a list of appendices contained within this section:

6.6.1 References

6.6.2 MCNP Code Input Listings

6.6.1 References

1. Carter, L. L., 1993, "Certification of MCNP Version 4x6 for Westinghouse Hanford Company Computer Platforms," certified with ECN 188708.
2. WMC, 1994, *Specification for RTG Transportation System Package*, WHC-S-4025, Rev. 3, Westinghouse Hanford Company, Richland, Washington.
3. Brassemeister, J., 1993, "MCNP-4A, A General Monte Carlo N-Particle Transport Code," LA-12825.
4. Whalen, D. J., 1991, "MCNP: Neutron Benchmark Problems" LA-12212.
5. Los Alamos National Laboratory, "GPHS 238-Plutonium Dioxide Fuel Pellet Specification," 26Y-318181, Revision B, 11/3/94.

6.6.2 MCNP Code Input Listings

CRIT. CALC., GPHS RTG, GRAPHITE, 80% Pu-238

```

1 0 -5 6 -1 3 -4 2  imp:n=1  fll=1  (0 0 0)
2 0 -7 8             imp:n=1  lat=1  u=1  fll=2
3 1 -1.95 -8 (12:-11:20) (14:-13:20) imp:n=1  u=2
4 1 -1.95 -10 (12:-11:22) (14:-13:22) imp:n=1  u=2
5 1 -1.95   9 10  imp:n=1  u=2
6 2 -22.5 -12 11 -20 (-15:18:19) imp:n=1  u=2
7 2 -22.5 -14 13 -20 (-17:18:19) imp:n=1  u=2
8 3 -9.6 -16 15 -19  imp:n=1  u=2
9 3 -9.6 -18 17 -19  imp:n=1  u=2
10 2 -22.5 -12 11 -22 (-15:18:21) imp:n=1  u=2
11 2 -22.5 -14 13 -22 (-17:18:21) imp:n=1  u=2
12 3 -9.6 -16 15 -21  imp:n=1  u=2
13 3 -9.6 -18 17 -21  imp:n=1  u=2
14 4 -1.0 -24 -23 25 (5:-6:4:-2:1:-3)  imp:n=0.1
15 0      (24:23:25)                   imp:n=0

```

```

1 py 4.859
2 px -4.859
3 py -4.859
4 px 4.859
5 pz 95.544
6 pz 0.0
7 pz 5.30801
8 pz -0.00001
9 c/y -2.184 2.654 1.831
10 c/y 2.184 2.654 1.831
11 py -3.1618
12 py -0.2941
13 py 0.2941
14 py 3.1618
15 py -3.1058
16 py .35
17 py .35
18 py 3.1058
19 c/y -2.184 2.654 1.3767
20 c/y -2.184 2.654 1.4326
21 c/y 2.184 2.654 1.3767
22 c/y 2.184 2.654 1.4326
23 cz 35.0
24 pz 126.
25 pz -30.48

```

```

mode n
m1 6000.50 -1.95 $ carbon
m2 75187.50 -22.5 $ Re for fr
m3 94238.50 -6.765 94238.55 -1.688 8016.50 -1.137 $ 80 molec % Pu-238 fuel
m4 1001.50 -0.11111 8016.50 -0.86888 $ water
kcode 2000 0.4 3 50 $ n/cycle; k guess, skip. # cycles
kacc
-2.184 -1.5 2.654
2.184 1.5 2.654
-2.184 1.5 2.654
2.184 -1.5 2.654
-2.184 -1.5 92.89

```

```
2.184 1.5 92.69
-2.184 1.5 92.69
2.184 -1.5 39.61
-2.184 -1.5 39.61
2.184 1.5 39.61
-2.184 1.5 39.61
2.184 -1.5 39.61
print 10 30 40 50 60 100 110 120 126 170
c      idum 4|1
ctme   50
```


CRIT. CALC., GPHS RTG, H2O replaces GRAPHITE, 80% Pu-238

```

1 0 -5.6 -1.3 -4.2 imp:n=1 ill=1 (0 0 0)
2 0 -7.8 imp:n=1 lat=1 u=1 ill=2
3 4 -1.0 -9 (12:-11:20) (14:-13:20) imp:n=1 u=2
4 4 -1.0 -10 (12:-11:22) (14:-13:22) imp:n=1 u=2
5 4 -1.0 9 10 imp:n=1 u=2
6 2 -22.5 -12 11 -20 (-15:16:19) imp:n=1 u=2
7 2 -22.5 -14 13 -20 (-17:18:19) imp:n=1 u=2
8 3 -9.6 -18 15 -19 imp:n=1 u=2
9 3 -8.6 -18 17 -19 imp:n=1 u=2
10 2 -22.5 -12 11 -22 (-15:16:21) imp:n=1 u=2
11 2 -22.5 -14 13 -22 (-17:18:21) imp:n=1 u=2
12 3 -9.6 -18 15 -21 imp:n=1 u=2
13 3 -9.6 -18 17 -21 imp:n=1 u=2
14 4 -1.0 -24 -23 25 16:-6:4:-2:1:-31 imp:n=0.1
15 0 (24:23:-25) imp:n=0

```

```

1 py 4.658
2 px -4.858
3 py -4.658
4 px 4.858
5 pz 95.544
6 pz 0.0
7 pz 5.30801
8 pz -0.00001
9 c/y -2.184 2.654 1.831
10 c/y 2.184 2.654 1.831
11 py -3.1618
12 py -0.2941
13 py 0.2941
14 py 3.1618
15 py -3.1059
16 py .35
17 py .35
18 py 3.1059
19 c/y -2.184 2.654 1.3767
20 c/y -2.184 2.654 1.4328
21 c/y 2.184 2.654 1.3787
22 c/y 2.184 2.654 1.4328
23 cz 36.0
24 pz 126.
25 pz -30.48

```

```

mode n
m1 8000.50 -1.95 # carbon
m2 75187.50 -22.5 # Re for Ir
m3 94238.50 -8.785 94239.55 -1.698 8018.50 -1.137 # 80 molec % Pu-238 fuel
m4 1001.50 -0.11111 8018.50 -0.68889 # water
kcode 2000 0.4 3 50 # n/cycle; k guess, skip, # cycles
c karc
c -2.184 -1.5 2.654
c 2.184 1.5 2.654
c -2.184 1.5 2.654
c 2.184 -1.5 2.654
c -2.184 -1.5 92.89

```

```
c      2.184  1.5  92.89
c     -2.184  1.5  92.89
c      2.184 -1.5  92.89
c     -2.184 -1.5  92.89
c      2.184  1.5  39.81
c     -2.184  1.5  39.81
c      2.184 -1.5  39.81
print 10 30 40 50 60 100 110 120 128 170
c      idum  4j 1
cmm   50
```

CRIT. CALC., 20 GPHS - 4x6 array, GRAPHTE, 86% Pu-238

```

1 0 -5.6 -1.3 -4.2 imp:n=1 fill=1 (0 0 0)
2 0 27 -29 -28 28 -7.8 imp:n=1 lat=1 u=1
  fill=0:0 0:1 0:4 2 2 2 2 2 2 2 2 2
3 1 -1.95 -9 (12:-11:20) (14:-13:20) imp:n=1 u=2
4 1 -1.95 -10 (12:-11:22) (14:-13:22) imp:n=1 u=2
5 1 -1.95 9 10 imp:n=1 u=2
6 2 -22.5 -12 11 -20 (-15:16:18) imp:n=1 u=2
7 2 -22.5 -14 13 -20 (-17:18:18) imp:n=1 u=2
8 3 -9.6 -16 15 -18 imp:n=1 u=2
9 3 -9.6 -18 17 -18 imp:n=1 u=2
10 2 -22.5 -12 11 -22 (-15:16:21) imp:n=1 u=2
11 2 -22.5 -14 13 -22 (-17:18:21) imp:n=1 u=2
12 3 -9.6 -16 15 -21 imp:n=1 u=2
13 3 -9.6 -18 17 -21 imp:n=1 u=2
14 4 -1.0 -24 -23 25 #1 #18 imp:n=0.1
15 0 (24:23:25) imp:n=0
16 0 -5.6 -1.3 -129 127 imp:n=1 fill=3 (9,719 0 0)
17 0 227 -229 -25 25 -7.8 imp:n=1 lat=t u=3
  fill=0:0 0:1 0:4 4 4 4 4 4 4 4 4
c
  fill=4
103 1 -1.95 -109 (12:-11:120) (14:-13:120) imp:n=1 u=4
104 1 -1.95 -110 (12:-11:122) (14:-13:122) imp:n=1 u=4
105 1 -1.95 109 110 imp:n=1 u=4
106 2 -22.5 -12 11 -120 (-15:16:119) imp:n=1 u=4
107 2 -22.5 -14 13 -120 (-17:18:118) imp:n=1 u=4
108 3 -9.6 -16 15 -119 imp:n=1 u=4
109 3 -9.6 -18 17 -119 imp:n=1 u=4
110 2 -22.5 -12 11 -122 (-15:16:121) imp:n=1 u=4
111 2 -22.5 -14 13 -122 (-17:18:121) imp:n=1 u=4
112 3 -9.6 -16 15 -121 imp:n=1 u=4
113 3 -9.6 -18 17 -121 imp:n=1 u=4

1 py 13.977
2 px -4.859
3 py -4.859
4 px 4.859
5 pz 26.54
6 pz 0.0
7 pz 6.30801
8 pz -0.00001
9 c/y -2.184 2.654 1.831
10 c/y 2.184 2.654 1.831
11 py -3.1618
12 py -0.2941
13 py 0.2941
14 py 3.1618
15 py -3.1059
16 py -.35
17 py .35
18 py 3.1059
19 c/y -2.184 2.654 1.3767
20 c/y -2.184 2.654 1.4326
21 c/y 2.184 2.654 1.3767
22 c/y 2.184 2.654 1.4326

```

23 c/z 4.859 4.859 40.
 24 pz 67.02
 25 pz -30.48
 26 py 4.85901
 27 px -4.85901
 28 py -4.85901
 29 px 4.86901
 109 c/y 7.634 2.654 1.631
 110 c/y 11.903 2.654 1.831
 119 c/y 7.634 2.654 1.3767
 120 c/y 7.634 2.654 1.4326
 121 c/y 11.903 2.654 1.3767
 122 c/y 11.903 2.654 1.4326
 127 px 4.8590002
 129 px 14.577
 227 px 4.859001
 229 px 14.577002

mode n
 m1 6000.50 -1.95 # carbon
 m2 75197.50 -22.5 # Re for Ir
 m3 94238.50 -7.274 94239.55 -1.189 8016.50 -1.137 998 mol% Pu-238 fuel
 m4 1001.50 -0.11111 8015.50 -0.86888 # water
 kcode 2000 0.4 3 80 # n/cycle; k guess, skip, # cycles
 karc
 -2.184 -1.5 2.654
 2.184 1.5 2.654
 -2.184 1.5 2.654
 2.184 -1.5 2.654
 c -2.184 -1.5 92.89
 c 2.184 1.5 92.89
 c -2.184 1.5 92.89
 c 2.184 -1.5 92.89
 c -2.184 -1.5 39.81
 c 2.184 1.5 39.81
 c -2.184 1.5 39.81
 c 2.184 -1.5 39.81
 print 10 30 40 50 60 100 110 120 125 170
 c kum 4j 1
 cema 120

closey packed fuel clade, 4x4x6 array, carbon MOD., 80% Pu-238

```

1 0 -14 13 -18 15 -16 17 imp:n=1 fill=1 {0 0 0}
2 0 -2 1 -4 3 -12 7 imp:n=1 lat=1 u=1 fill=2
3 1 -1.95 {6:-8:11} imp:n=1 u=2
4 2 -22.5 -11 8 -8 {10:-9:5} imp:n=1 u=2
5 3 -8.5 -10 9 -5 imp:n=1 u=2
6 4 -1.0 -22 21 -20 19 -24 23 {14:-13:16:-15:18:-17} imp:n=0.t
7 0 {20:-19:22:-21:24:-23} imp:n=0

```

```

1 px -1.4327
2 px 1.4327
3 pz -1.4327
4 pz 1.4327
5 cy 1.3767
6 cy 1.4326
7 py -1.43386
8 py -1.43385
9 py -1.37795
10 py 1.37795
11 py 1.43385
12 py 1.43386
13 px -1.4326
14 px 10.0282
15 py -10.03895
16 py 1.433855
17 px -1.4326
18 pz 12.6934
19 px -31.9
20 px 40.5
21 py -40.52
22 py 31.92
23 pz -31.92
24 pz 43.37

```

```

mode n
m1 5000.50 -1.95 # carbon
m2 75187.50 -22.5 # Re for Ir
m3 94238.50 -6.766 94238.56 -1.686 8018.60 -1.137 # 80 mole% Pu-238 fuel
m4 1001.50 -0.11111 8016.50 -0.88889 # water
kcode 2000 0.8 3 80 # ncycle; k guess, skip, # cycles
ks/c
0 0 0
print 10 30 40 50 60 80 100 110 120 126 170
c idum 4j 1
ctms 120

```

closely packed fuel clads, 4x4x5 array, 8xden. H2O MOD., 80% Pu-238

```

1 0 -14 13 -16 15 -18 17 imp:n=1 lli=1 j0 0 0
2 0 -2 1 -4 3 -12 7 imp:n=1 lli=1 u=1 NN=2
3 4 -8.0 (0:-8:11) imp:n=1 u=2
4 2 -22.5 -11 8 -6 (10:-9:5) imp:n=1 u=2
5 3 -8.8 -10 9 -5 imp:n=1 u=2
6 4 -1.0 -22 21 -20 19 -24 23 (14:-13:16:-15:18:-17) imp:n=0.1
7 0 (20:-19:22:-21:24:-23) imp:n=0

```

```

1 px -1.4327
2 px 1.4327
3 pz -1.4327
4 pz 1.4327
5 cy 1.3787
6 cy 1.4326
7 py -1.43388
8 py -1.43388
9 py -1.37796
10 py 1.37796
11 py 1.43388
12 py 1.43388
13 px -1.4326
14 px 10.0282
15 py -10.03696
16 py 1.433885
17 pz -1.4326
18 pz 12.8834
19 px -31.9
20 px 40.5
21 py -40.52
22 py 31.92
23 pz -31.92
24 pz 43.37

```

```

mode n
m1 8000.50 -1.95 $ carbon
m2 75187.50 -22.5 $ Re for k
m3 84238.50 -6.785 84239.55 -1.698 8016.50 -1.137 $ 80 mole% Pu-238 fuel
m4 1001.50 -0.11111 8016.50 -0.88889 $ water
kcode 2000 0.0 3 80 $ n/cycle: k guess, skip, # cycles
kerc
0 0 0
print 10 30 40 50 60 100 150 120 128 170
c idum 4j 1
ctme 120

```

BENCHMARK INPUT LISTINGS

BENCHMARK 3 H₂O MODERATED U(S,2)O₂F₂ CYLINDERS IN AIR

```

1 1 -1.131 -1.3 -4 imp:n=1 u=-1
2 2 -2.71 1.314 imp:n=1 u=1
7 0 -2.9 -8 fill=1 imp:n=1
5 0 -7 #7 #8 #9 imp:n=1
6 0 7 imp:n=0
8 like 7 but trcl=t
9 like 7 but trcl=2

1 cy 10.15
2 cy 10.30
3 py 0.0
5 py -15
9 py 41.55
4 py 41.40
7 wa 150.

m1 82235. .000383
   92238. .0000278
   9018. .000621
   1001. .1183
   9016. .05990
m2 13027. 1.0
tr1 20.98 0 0
tr2 10.49 0 18.169
kcode 2000 .7 30 80
sdef axs 0 1 0 pos d1 rad d2 ext d3
sp1 0.33 .33 .34
si1 1 0 20.7 0 20.98 20.7 0 10.49 20.7 18.169
si2 8
si3 15
print

```

JEZEBEL, 95.5% Pu239, 4.5% Pu240, FAST CRITICAL

```

1 1 -15.61 -1 imp:n=1
2 0 1 imp:n=0

1 ad 5.385

m1 94240. -4.5 94239. -95.5
kcode 3000 1.0 80 110
kerc 0. 0. 0.
print

```

JEZEBEL, 80% Pu239, 20% Pu240, FAST CRITICAL

1 1 -15.73 -1 imp:n=1

2 0 1 imp:n=0

1 so 8.880

m1 94240. -20 94239. -80

kcode 3000 1.0 50 150

ksrc 0. 0. 0.

print

7.0 OPERATING PROCEDURES

7.1 PROCEDURES FOR LOADING THE PACKAGE

Loading the Radioisotope Thermoelectric Generator (RTG) Transportation System Package for shipment involves five steps: (1) open the empty packaging, (2) install the RTG payload, (3) close the inner containment vessel (ICV), purging with helium and leakage rate testing, (4) close the outer containment vessel (OCV), purging the OCV with helium and leakage rate testing, and (5) install the impact limiter and prepare for final shipment. The following sections detail the process of loading the RTG Transportation System Package for shipment.

7.1.1 General Information

The following general information establishes the planning, personnel qualifications, equipment, and Quality Assurance (QA) needed to conduct the specific operating procedures of Sections 7.1 through 7.3.

- Written, traceable and approved procedures shall be used throughout the operation.
- All applicable QA requirements of Chapter 9 shall be followed.
- Only trained and qualified (per Chapter 9) packaging and shipping personnel may load the package or direct its loading.
- Quality Assurance personnel shall observe and record the placement of the RTG payload into the packaging.
- Crane and forklift operations shall be performed by trained and qualified operators. A list of qualified operators shall be kept by the manager cognizant of lifting operations.
- Qualified Occupational Health Physics personnel shall survey the payload for measurable contamination before loading the package. Survey results must be recorded and maintained by the Occupational Health Physics personnel.
- The equipment and materials needed for operation of the package includes the following:
 - RTG Transportation System Packaging
 - Payload-specific shipping rack
 - Three-point lifting device (15,000 lb minimum capacity)
 - Vent port/test tool for helium leakage rate testing
 - Helium leakage rate detection system as specified in Chapter 9
 - Miscellaneous tools, including calibrated torque wrenches.
- The RTG Transportation System Packaging must be clean and undamaged before use.
- Personnel entering the equipment compartment of the semitrailer will be exposed to radiation dose rates of up to 267 mrem/hr (dose rate at top surface of package). All personnel entering the semitrailer shall comply with the cognizant facility organization's radiation protection program to minimize radiation exposure and comply with 10 CFR 19.12.

7.1.2 Opening the Empty Package

1. Remove the three 3/4-in. pins that secure the OCV head personnel barrier to the OCV. Remove the personnel barrier.
2. Attach a three-point lifting device to the three lift points (upper fins) on the OCV bell. Remove the eight 1-8 united national coarse (UNC) bolts that secure the impact limiter to the OCV base. Lift and remove the packaging from the impact limiter. Set the packaging down on to the disassembly area surface. Note: The packaging shall be in the upright position with the OCV base resting on the disassembly area surface.
3. Remove the OCV vent port cover. Install a vent/test port tool into the OCV vent port. If desired, plumb a gas sampling line to the vent/test port tool. Rotate the vent/test port tool stem to open the vent port; when the vent port plug is completely unthreaded, withdraw the tool stem to allow free flow of the OCV cavity atmosphere. Remove the vent/test port tool from the OCV vent port after completing any gas sampling operation.
4. Disconnect the feed-through connector from the thermal shield bulkhead connector. Remove the 24, 1X-7 UNC bolts that secure the OCV bell to the OCV base. Lift the OCV bell to install the three spacer blocks. Install and hand tighten two 1X-7 UNC bolts through the OCV bell flange into the top of each spacer block. Install and tighten with a wrench, one 1/2-13 UNC bolt through each spacer block into the ICV bell flange. Lower the OCV bell until it rests on the three spacer blocks. Tighten each of the 1X-7 UNC bolts wrench tight.
5. Install a vent/test port tool into an ICV vent port (i.e., primary or secondary). If desired, plumb a gas sampling line to the vent/test port tool. Rotate the vent/test port tool stem to open the vent port; when the vent port plug is completely unthreaded, withdraw the tool stem to allow free flow of the ICV cavity atmosphere. Remove the vent/test port tool from the ICV vent port after completing any gas sampling operation.
6. Remove the 24, 3/4-10 UNC bolts that secure the ICV bell to the ICV base. Lift and remove the OCV/ICV bell assembly.
7. Alternately, using spacer blocks in steps 4 and 6 may be precluded and vessel bells removed individually. For this option, the lift point at the top center of the ICV bell would be used to remove the ICV bell.

7.1.3 Payload Installation

One general purpose heat source (GPHS) RTG may be installed within the RTG Transportation System Packaging. This section discusses the loading procedure for the payload shipping rack assembly and payload. At the time of payload installation, the ICV base will have been installed within the OCV base and secured with four 1/4-20 UNC bolts tightened to 120 ± 10 in.-lb.

1. Visually inspect the OCV and ICV O-ring seals for nicks, tears, or other damage and replace as necessary. Apply a thin coat of vacuum grease to each O-ring. Install each O-ring in its respective groove in the ICV or OCV base.

2. Install an electrical feed-through plug and cable assembly into the electrical feed-through connector located in the ICV base. With the plug in position, place the ICV electrical feed-through insulation cap over the plug/connector, ensuring that the cable is routed through the cable guide of the cap.
3. Install a GPHS shipping rack assembly onto the ICV base, aligning the eight holes in the shipping rack assembly base with the eight holes in the ICV base. Ensure the vent port tube cutout is aligned with the ICV base. Route the electrical feed-through cable and connector into the connector box located on the shipping rack assembly. Install four 3/4-10 UNC by 5-in.-long bolts through the shipping rack assembly (outermost holes) into the ICV base; tighten each to 75 ± 10 ft-lb torque.
4. Install a GPHS converter support ring onto the top of the GPHS shipping rack assembly, aligning the four holes in the converter support ring with the holes in the barrier plate. Install four 3/4-10 UNC by 8-in.-long bolts through the converter support ring and shipping rack assembly into the ICV base; tighten each bolt to 100 ± 10 ft-lb torque.
5. Lift and suspend the GPHS RTG over the GPHS shipping rack/converter support ring assembly, aligning the four quick-connect/disconnect mechanisms. Engage the four quick-connect devices to secure the GPHS RTG to the shipping rack/converter support ring assembly. Install the GPHS RTG shorting module connector cable, instrumentation connector cable, and the gas connector hose to their respective interface locations. Verify that any excess length of all RTG cables and/or hoses is coiled around the periphery of the shipping rack assembly within the 32.5-in. diameter cylinder and secured to minimize interference with the ICV bell during installation. Finally, connect the electrical feed-through instrumentation cables between the RTG payload and shipping rack assembly and establish temperature monitoring of the RTG payload.

7.1.4 Closure of the Inner Containment Vessel (ICV)

Before ICV closure, the ICV and OCV bells will be in a nested configuration with three spacer blocks installed (Section 7.1.1, Step 4).

1. Lift and install the OCV/ICV bell assembly, aligning the two guide pins in the ICV base with the two guide pin holes in the ICV bell flange. Prevent hitting or scraping against the RTG payload when installing the bell assembly. Install 24 3/4-10 UNC by 2.0-in.-long bolts to secure the ICV bell to the ICV base; tighten each bolt to 250 ± 25 ft-lb torque.
2. Following the guidelines of Section 8.2.2.2, perform the helium purge and leakage rate testing of the main ICV closure seal. Following the guidelines of Sections 8.2.2.3 and 8.2.2.4, perform the leakage rate testing of the primary and secondary ICV vent port plug seats.

7.1.5 Closure of the Outer Containment Vessel (OCV)

1. Remove the two 1 1/2-7 UNC bolts that secure the OCV bell to each of the three spacer blocks. Lift the OCV bell to remove the three spacer blocks. Remove the 1/2-13 UNC bolt securing each spacer block to the ICV bell flange. Remove the three spacer blocks. Lower and install the OCV bell, aligning the two guide pins in the OCV base with the two guide pin holes in the OCV bell flange. Install 24 1 1/2-7 UNC by 8-in.-long bolts to secure the OCV bell to the OCV base; tighten each bolt to 300 ± 30 ft-lb torque.

2. Following the guidelines of Section 8.2.2.5, perform the helium purge and leakage rate testing of the main OCV closure seal. Following the guidelines of Section 8.2.2.6, perform the leakage rate testing of the OCV vent port plug seal.
3. Attach the electrical feed-through cable that protrudes from the OCV base, to the thermal shield bulkhead connector.

7.1.6 Installation of the Impact Limiter and Final Preparations for Shipment

1. Lift and install the package into the impact limiter ensuring the two alignment pins in the limiter mate with the two holes in the OCV base. Install eight 1-8 UNC by 3-in.-long modified bolts to secure the impact limiter to the OCV base; tighten each to 200 ± 20 ft-lb torque. Remove all lifting devices from the lift points on the OCV bell.
2. Install a tamper-indicating device over the top of an impact limiter attachment hole tube, thereby precluding inadvertent removal of the bolt.
3. Install the RTG Transportation System Package into the transport vehicle using the appropriate tie-down devices. Load a maximum of two RTG Transportation System Packages per transport vehicle, as limited by total wattage permitted within a single vehicle.
4. Install the OCV head personnel barrier. Secure the personnel barrier by inserting and securing the three 3/4-in. diameter pins through each of the three OCV lifting holes to preclude their use as a tie-down device.
5. Complete all necessary shipping papers in accordance with 49 CFR 172¹; Subpart C, package marking will be in accordance with 49 CFR 172¹ Subpart D; labeling will be in accordance with 49 CFR 172¹ Subpart E; and placarding will be in accordance with Subpart F of 49 CFR 172¹. Radiation monitor each RTG Transportation System Package per the requirements of Subpart I of 49 CFR 173.441² and determine that surface contamination levels meet the requirements of 49 CFR 173.443². The measured dose rates for the normal conditions of transport shall not exceed the limits specified in Table 7.1.6-1.

TABLE 7.1.6-1. Maximum Dose Rate Limits (mrem/hr).

Normal Conditions of Transport Location	Operational Control Limit(a)
Side, surface of package	590
Side, surface of semitrailer	120
Two meters from side surface of semitrailer	0.4
Top surface of package	1,000
Top surface of semitrailer	200
Bottom surface of semitrailer	190
Tractor cab (operator's seat)	1.2

(a) This limit is used when coolant is present in the package.

7.2 PROCEDURES FOR UNLOADING THE PACKAGE

Unloading the payload from the RTG Transportation System Package involves opening the package and removing the payload. The following sections detail the process of unloading the payload from the RTG Transportation System Package.

7.2.1 Opening the Package

1. Upon receipt, the conveyance and package shall be visually inspected for damage and surveyed for radiation level and smearable contamination. Smearable contamination levels on the external surfaces of each package shall not exceed the maximum permissible limits specified in 49 CFR 173.443. Each package shall be radiation monitored per Subpart I of 49 CFR 173.441.
2. Remove the three 3/4-in. pins that secure the OCV head personnel barrier to the OCV. Remove the personnel barrier.
3. Attach a three-point lifting device to the three lift points (upper ring) on the OCV bell. Remove the tamper indicating device from the top of the impact limiter attachment hole tube. Remove the eight 1-8 UNC bolts securing the impact limiter to the OCV base. Lift and remove the package from the impact limiter. Set the package down on the disassembly area surface. Note: The package will be in the upright position with the OCV base plate resting on the disassembly area surface.
4. Remove the OCV vent port cover. Install a vent/test port tool into the OCV vent port. If desired, plumb a gas sampling line to the vent/test port tool. Rotate the vent/test port tool stem to open the vent port; when vent port plug is completely unthreaded, withdraw the tool stem to allow free flow of the OCV cavity atmosphere. Upon completion of any gas sampling operations, remove the vent/test port tool from the OCV vent port.
5. Disconnect the electrical feed-through connector from the thermal shield bulk head connector. Remove the 24 1 X-7 UNC bolts securing the OCV bell to the OCV base. Lift the OCV bell to install the three spacer blocks. Install and hand tighten two 1 X-7 UNC bolts through the OCV bell flange into the top of each spacer. Install and tighten with a wrench one 1/2-13 UNC bolt through each spacer block into the ICV bell flange. Lower the OCV bell until it rests on the three spacer blocks. Tighten each of the 1 X-7 UNC bolts wrench tight.
6. Install a vent/test port tool into the ICV vent port (i.e., primary or secondary). If desired, plumb a gas sampling line to the vent/test port tool. Rotate the vent/test port tool stem to open the vent port; when the vent port plug is completely unthreaded, withdraw the tool stem to allow free flow of the OCV cavity atmosphere. Upon completion of any gas sampling operations, remove the vent/test port tool from the OCV vent port.
7. Remove the 24, 3/4-10 UNC bolts securing the ICV bell to the ICV base. Lift and remove the OCV/ICV bell assembly.
8. Alternately, using spacer blocks in Steps 5 and 7 may be precluded and vessel bells removed individually. For this option, the lift point at the top center of the ICV bell would be used to remove the ICV bell.

7.2.2 Payload Removal

1. Disconnect the electrical feed-through instrumentation cables between the RTG payload and the shipping rack assembly. Disconnect the GPS RTG shorting module connector cable and gas connector hose from their respective interface locations.
2. Disengage the four quick-connect devices that secure the GPS RTG to the shipping rack/converter support ring assembly. With an overhead crane or other suitable lifting device, lift the GPS RTG from the shipping rack assembly and place it on the site holding stand.
3. The packaging can now be prepared for (1) storage, (2) shipment as an empty package, or (3) readied for shipment of another authorized payload.

7.3 PREPARATION OF AN EMPTY PACKAGE FOR TRANSPORT

Previously used and empty RTG Transportation System Packages shall be handled per Subpart I of 49 CFR 173.427^a.

7.4 REFERENCES

1. 49 CFR 172, "Hazardous Materials Tables and Hazardous Materials Communications Regulations," *Code of Federal Regulations*, as amended.
2. 49 CFR 173, "Shippers--General Requirements for Shipments and Packagings," *Code of Federal Regulations*, as amended.

8.0 ACCEPTANCE TESTS AND MAINTENANCE PROGRAM

8.1 ACCEPTANCE TESTS

This section discusses the tests to be performed before first use of the Radioisotope Thermoelectric Generator (RTG) Transportation System Package.

8.1.1 Visual Inspection

All packaging materials of construction and welds will be examined according to specifications delineated on the packaging drawings found in Appendix 1.3.2. Any items that are not in compliance with the packaging drawings will be identified on a discrepancy report for disposition per Section 9.3.15.

8.1.2 Structural and Pressure Tests

8.1.2.1 Lifting Device Load Testing. The maximum work load of the three outer containment vessel (OCV) lifting devices is 9,600 pounds, or 3,895 pounds per lifting point using a 60° minimum lift angle. However, a conservative value of 3,800 pounds will be used for the structural evaluation (see Section 2.5.1.2.1). Each set of OCV lifting devices will be load tested to at least 150% of their maximum total working load, that is, 6,700 pounds.

The maximum total working load of the inner containment vessel (ICV) bell provision for a lifting device is 1,600 pounds, as delineated in Section 2.5.1.1.1. The ICV provision for a lifting device will be load tested to at least 150% of its maximum total working load, that is, 2,400 pounds.

Per the requirements specified in the drawings in Appendix 1.3.2, accessible base material and welds directly related to the load testing of the lifting devices will be visually inspected for plastic deformation or cracking, and liquid penetrant inspected per Section V, Article 6, and Section III, Division 1, Subsection NB, Article NB-5000¹. Crack indications will be recorded on a discrepancy report for disposition before repair and final acceptance per Section 9.3.15.

8.1.2.2 Containment Vessel Pressure Testing. The OCV and ICV will be pressure tested to at least 150% of the maximum normal operating pressure (MNOP) per the requirements of 10 CFR 71.86(b)² to verify structural integrity. The design pressure for the OCV and ICV is set at 50 psig, which conservatively exceeds the MNOP for either vessel (see Section 2.8.1.1). Thus, both the OCV and ICV will each be pressure tested to 150% of the design pressure, that is, 75 psig.

Per the requirements specified in the drawings in Appendix 1.3.2, accessible welds directly related to the pressure testing of the containment structures will be visually inspected for plastic deformation or cracking, and liquid penetrant inspected per Section V, Article 6, and Section III, Division 1, Subsection NB, Article NB-5000¹. Indications of distortion or cracking will be recorded on a discrepancy report for disposition before repair and final acceptance per Section 9.3.15.

8.1.2.3 OCV Coolant Jacket Pressure Testing. The OCV coolant jacket will be pressure tested to at least 150% of its design pressure. The coolant jacket design pressure is set at 50 psig. Thus, each loop of the coolant jacket will be pressure tested to a minimum of 75 psig.

8.1.3 Leakage Rate Tests

Fabrication Verification Leakage Rate Testing will follow the guidelines of Section 8.3 of ANSI N14.6⁵. Fabrication Verification Leakage Rate Testing shall be performed, after the fitting device and pressure testing described in Section 8.1.2, above, to verify package configuration and performance to design criteria. Each containment vessel shall be thoroughly cleaned and leakage rate tested before installing ancillary components such as the shipping rack assemblies and OCV lead personnel barrier.

Seven separate tests comprise the Fabrication Verification Leakage Rate Testing: four for the ICV and three for the OCV. The seven leakage rate tests are: (1) the main ICV closure seal, (2) the primary ICV vent port plug seal, (3) the secondary ICV vent port plug seal, (4) the ICV structure, (5) the OCV structure, (6) the main OCV closure seal, and (7) the OCV vent port plug seal. Each leakage rate test will meet the acceptance criteria delineated in Section 8.1.3.1.

8.1.3.1 Acceptance Criteria. To constitute acceptance, per Section 5.4(3) of ANSI N14.5-1987, each of the ICV and OCV containment vessels' indicated leakage rates shall be less than or equal to 1×10^{-2} standard cubic centimeters per second (scm/s), air. The sensitivity of the leakage rate test equipment shall be 5×10^{-2} scms, air, or less.

8.1.3.2 Leakage Rate Test of the Main ICV Closure Seal. This test uses helium at atmospheric pressure within the ICV cavity and an evacuated void outside the main ICV O-ring seal, thus following the guidelines of ANSI N14.5-1987, Section A3.10.1.

1. Assemble the RTG Transportation System Package ICV.
2. Install a test/vent port tool into the primary ICV vent port and ensure that the vent port is open.
3. Install a test/vent port tool into the secondary ICV vent port and open the vent port.
4. Install a test/vent port tool into the ICV seal test port and open the seal test port.
5. Establish a vacuum in the ICV seal test port sufficient to operate the helium mass spectrometer leak detector (MSLD) per the manufacturer's recommendations.
6. Plumb in a helium source to the primary vent port and flow helium through the ICV at a minimum flow rate of 5 cubic feet per minute for a minimum of 20 minutes.
7. Following the 20 minute purge, perform the leakage rate test. Record the indicated leakage rate. If the main ICV closure seal leakage rate exceeds the allowable specified in Section 8.1.3.1, disassemble the package, thoroughly clean all components, reassemble the package, and repeat the leakage rate test. If the system cannot pass the test, prepare a discrepancy report for disposition per Section 9.3.15.
8. Close primary and secondary ICV vent ports. Remove all plumbing and the test/vent port tool from the secondary ICV vent port.
9. Close the seal test port. Remove the test equipment, all plumbing, and the test/vent port tool from the ICV seal test port.

8.1.3.3 Leakage Rate Test of the Primary ICV Vent Port Plug Seal. This test uses helium at atmospheric pressure within the ICV cavity and an evacuated void outside the primary ICV vent port plug, thus following the guidelines of ANSI N14.5-1987, Section A3.10.1.

1. Install a test/vent port tool into the primary ICV vent port. Verify that the vent port is closed.
2. Plumb a calibrated helium MSLD to the test/vent port tool in the primary ICV vent port.
3. Establish a vacuum outboard of the closed primary ICV vent port sufficient to operate the MSLD per the manufacturer's recommendations.
4. Record the indicated leakage rate. If the leakage rate exceeds the allowable specified in Section 8.1.3.1, remove the vent port plug, thoroughly clean all components, replace the vent port plug seal (if necessary), replace the vent port plug, and repeat the leakage rate test. If the system cannot pass the test, prepare a discrepancy report for disposition per Section 8.3.15.
5. Remove the test equipment, all plumbing, and the test/vent port tool from the ICV seal test port.

8.1.3.4 Leakage Rate Test of the Secondary ICV Vent Port Plug Seal. This test uses helium at atmospheric pressure within the ICV cavity and an evacuated void outside the secondary ICV vent port plug, thus following the guidelines of ANSI N14.5-1987, Section A3.10.1.

1. Install a test/vent port tool into the secondary ICV vent port. Verify that the vent port is closed.
2. Plumb a calibrated helium MSLD to the test/vent port tool in the secondary ICV vent port.
3. Establish a vacuum outboard of the closed secondary ICV vent port sufficient to operate the MSLD per the manufacturer's recommendations.
4. Record the indicated leakage rate. If the indicated leakage rate exceeds the allowable specified in Section 8.1.3.1, remove the vent port plug, thoroughly clean all components, replace the vent port plug seal (if necessary), replace the vent port plug, and repeat the leakage rate test. If the system cannot pass the test, prepare a discrepancy report for disposition per Section 8.3.15.
5. Remove the test equipment, all plumbing, and the test/vent port tool from the ICV seal test port.

8.1.3.5 Leakage Rate Test of the ICV Structure. This test uses helium at atmospheric pressure within the ICV cavity and an evacuated void outside the ICV structure, thus following the guidelines of ANSI N14.5-1987, Section A3.10.1.

1. Assemble the RTG Transportation System Package ICV within the OCV. The ICV base will be shimmed a minimum of 0.030 in. up from the OCV base and the ICV-to-OCV base bolts (1/4-20 UNC) are not installed (this configuration allows helium to flow between the bases). Remove the ICV seal test port plug.
2. Install a test/vent port tool into the OCV vent port and open the vent port to allow flow into the OCV/ICV annulus.
3. Plumb a calibrated helium MSLD to the test/vent port tool in the OCV vent port.
4. Establish a vacuum in the OCV/ICV annulus sufficient to operate the MSLD per the manufacturer's recommendations.

Note: While evacuating the OCV/ICV annulus to test range, construct a tent of polyethylene plastic around the exterior of the OCV to prepare for Section 8.1.3.B. Use duct tape to seal all tent edges airtight. Seal a helium supply hose at the highest elevation in the tent and a small (1 in. diameter, or less) vent hole at the lowest elevation to ensure a complete helium purge. Ensure that all OCV coolant jacket connections are open and two helium supply hoses are placed into the upper pipe fittings in each of the two coolant loops to purge the coolant channels with helium.

5. Record the indicated leakage rate. If the indicated leakage rate exceeds the allowable specified in Section 8.1.3.1, disassemble the ICV, thoroughly clean all components, reassemble the ICV, and repeat the leakage rate test. If the system cannot pass the test, prepare a discrepancy report for disposition per Section 9.3.15.

8.1.3.6 Leakage Rate Test of the OCV Structure. This test uses helium at atmospheric pressure outside the OCV cavity and an evacuated void inside the OCV structure, thus following the guidelines of ANSI N14.5-1987, Section A3.10.2. This test immediately follows the ICV Structure Test (Section 8.1.3.5) and uses the testhardware configuration existing at the end of that test, except that the OCV seal test port plug is removed.

1. Pressurize the polyethylene tent (see Paragraph 8.1.3.6, Item 4) with sufficient helium flow to cause the tent to bulge, but not burst. Continue to purge for 10 minutes to ensure a high concentration of helium within the tent.

Note: To conservatively account for the less-than-pure concentration of helium within the tent, the measured leakage rate will be multiplied by a factor of two, assuming that the helium concentration inside the tent is 50% minimum.

2. Record the indicated leakage rate. When summed with the OCV vent port seal leakage rate from Section 8.1.3.3, if the total leakage rate exceeds the allowable specified in Section 8.1.3.1, disassemble the OCV, thoroughly clean all components, reassemble the OCV, and repeat the leakage rate test. If the system cannot pass the test, prepare a discrepancy report for disposition per Section 9.3.16.
3. Remove the polyurethane tent from around the OCV structure and the helium supply hoses from the two coolant loops.
4. Close the OCV vent port.

8.1.3.7 Leakage Rate Test of the Main OCV Closure Seal. This test uses helium at atmospheric pressure within the OCV cavity and an evacuated void outside the main OCV O-ring seal, thus following the guidelines of ANSI N14.6-1987, Section A3.10.1.

1. Install a test/vent port tool into the OCV seal test port. Open the seal test port.
2. Plumb a calibrated helium MSLD to the test/vent port tool in the OCV seal test port.
3. Install a test/vent port tool into the OCV vent port.
4. Establish a vacuum in the OCV seal test port sufficient to operate the MSLD per the manufacturer's recommendations.
5. Plumb a vacuum pump and helium gas source into the test/vent port tool in the OCV vent port as shown in Figure 8.1.3.7-1.

8. Open the OCV vent port and evacuate the OCV/ICV annulus to a pressure of 1 psia or less.

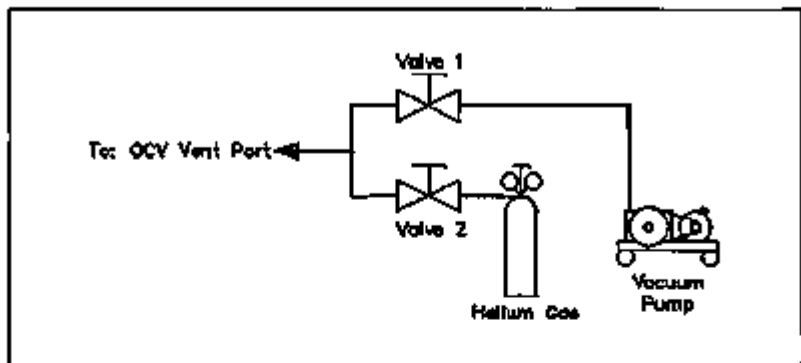


FIGURE B.1.3.7-1.

7. Backfill the OCV/ICV annulus with helium gas to 15 ± 1 psia.
8. Close the OCV vent port. Remove all plumbing and the test/vent part tool from the OCV vent port.
9. Record the indicated leakage rate. If the indicated leakage rate exceeds the allowable specified in Section B.1.3.1, disassemble the package, thoroughly clean all components, reassemble the package, and repeat the leakage rate test. If the system cannot pass the test, prepare a discrepancy report for disposition per Section B.3.16.
10. Close the OCV seal test port. Remove all plumbing and the test/vent port tool from the OCV seal test port.
11. Install the OCV seal test port cover.

B.1.3.8 Leakage Rate Test of the OCV Vent Port Plug Seal. This test uses helium at atmospheric pressure within the OCV cavity and an evacuated void outside the vent port plug, thus following the guidelines of ANSI N14.5-1987, Section A3.10.1.

1. Install a test/vent port tool into the OCV vent port. Verify that the vent port is closed.
2. Plumb a calibrated helium MSLD to the test/vent port tool in the OCV vent port.
3. Establish a vacuum outboard of the closed OCV vent port sufficient to operate the MSLD per the manufacturer's recommendations.
4. Record the indicated leakage rate. When summed with the OCV Structure leakage rate from Section B.1.3.6, if the total leakage rate exceeds the allowable specified in Section B.1.3.1, remove the vent port plug, thoroughly clean all components, replace the vent port plug seal (if necessary), replace the vent port plug, and repeat the leakage rate test. If the system cannot pass the test, prepare a discrepancy report for disposition per

Section 8.3.15.

6. Remove all plumbing and the test/vent port tool from the OCV seal test port.
8. Install the OCV vent port cover.

8.1.4 Component Tests

8.1.4.1 Polyurethane Foam. Before polyurethane foam installation, the impact limiter cavity shall be cleaned of debris, scale, oil, and grease. The impact limiter cavity surfaces shall then be washed with a solvent or cleaner, compatible with the polyurethane foam, and coated with a foam bond release agent.

A cured foam disk with direction of rise parallel to the vertical (axial) axis of the packaging shall be installed into the center of the impact limiter cavity as specified in the drawings in Appendix 1.3.2. The cured foam shall have a density of about 3 pounds per cubic foot (lb/ft³).

The remaining impact limiter cavity shall be foamed in place. Each foam pour shall be controlled to ensure that the liquid components react to form the rigid foam material and rise so that the entire void volume of the single foamed assembly is filled with expanded foam. The resultant foam density is about 12 lb/ft³. The direction of foam rise shall be parallel to the vertical axis of the packaging.

Production records for each foam pouring operation shall be compiled during the operation. As a minimum, the record shall include pour dates, operator name, shell part number and serial number, Quality Assurance buy-off, and material traceability identified by batch number. This record shall be retained for the life of the container.

A certification referencing the production record data and testing data pertaining to each packaging shall be issued by the foam supplier after production. Test data relevant to the pouring operation shall be included with the certification. All Quality Assurance submittals shall be dated and signed by the foam supplier's designated Quality Assurance representative.

Each production pour made into the impact limiter assembly or used to make the low-density center disk, and each sample pour made during each production pour for test purposes shall be recorded. Test sample pours shall be foamed in test containers at the same time as the actual production pour they represent. Test coupons shall be taken from each test sample box prepared during production. If multiple pours into a single foamed assembly occur, test coupons from each pour shall be tested before installation of the next pour, and the level of each batch pour shall be recorded.

The coupons shall be tested for compressive strength per ASTM D1621⁴. Stress-strain plots, similar to that shown in Figure 2.3-2, shall be prepared for both the parallel-to-rise and perpendicular-to-rise orientations for both the 12 lb/ft³ foam and the 3 lb/ft³ foam. A minimum of three samples shall be tested for each pour and each direction of rise. The 3 lb/ft³ foam shall be tested at room temperature (72 to 78 °F). The 12 lb/ft³ foam shall be tested at cold and hot conditions: -20 to -25 °F and 160 to 165 °F. The test data shall be recorded and reviewed to ensure compliance with the foam structural acceptance criteria outlined in Section 2.3.

The coupons shall be tested for fire retardancy per Section 853(a) and Part Hd) of 14 CFR 25⁴. The testing shall satisfy the following criteria.

- The average burn length shall not exceed 6 in.

- The coupons shall self-extinguish in an average time not exceeding 15 seconds.
- After falling, drippings from test specimen shall self-extinguish in an average of 3 seconds.

Polyurethane foam not in compliance with the above requirements shall be documented on a discrepancy report for disposition before repair and final acceptance per Section 9.3.15.

9.1.4.2 O-Ring Seals. The containment O-ring seals and seal material, as appropriate, shall meet the following criteria. Any O-ring that does not satisfy these criteria shall be recorded on a discrepancy report for disposition before repair and final acceptance per Section 9.3.15.

- Compression set shall not exceed 26% after storage for 22 hours at 70 °C when tested per ASTM D395⁶.
- Tensile strength and elongation shall be a minimum of 1,450 psi and 250% respectively, when tested per ASTM D412⁷.
- Hardness shall be a minimum of 80 Durometer and a maximum of 80 Durometer when tested per ASTM D2240⁸.
- All splices shall be subjected to the requirements of Class 3 per ASTM D2527⁹.

9.1.5 Tests for Shielding Integrity

Both the ICV and OCV structures provide shielding for the payloads. Other than the monolithic configuration of these two components, no other materials of construction are singularly designated for shielding. Specific dimensional requirements specified in the drawings in Appendix 1.3.2 shall ensure shielding integrity of the ICV and OCV structures.

9.1.6 Thermal Acceptance Tests

Material properties established in Section 3.2 are consistently conservative for the analyses performed. As such, with the exception of the polyurethane foam fire retardancy test discussed in Section 9.1.4, acceptance tests for material thermal properties are not performed.

9.2 MAINTENANCE PROGRAM

This section describes the maintenance program used to ensure continued performance of the RTG Transportation System Package.

9.2.1 Structural and Pressure Tests

Other than the tests required for first use, no structural or pressure tests are necessary to ensure continued performance of the packaging.

9.2.2 Leakage Rate Tests

Maintenance Verification Leakage Rate Testing shall follow the guidelines of Section 5.4 of

ANSI N14.5-1987. Appropriate sections of the Maintenance Verification Leakage Rate Test shall be performed during routine maintenance to verify package configuration and performance to design criteria. Maintenance Verification Leakage Rate Tests of the main closure seals and vent port plug seals shall be performed upon seal replacement, but all seals need not necessarily be replaced at the same time (i.e., seals are replaced annually or when damaged). Maintenance Verification Leakage Rate Testing shall be used as Assembly Verification Leakage Rate Testing to determine leakage rates before a loaded shipment.

Five separate tests comprise the Maintenance Verification Leakage Rate Testing; two for the OCV and three for the ICV. The five leakage tests are: (1) the main ICV closure seal, (2) the primary ICV vent port plug seal, (3) the secondary ICV vent port plug seal, (4) the main OCV closure seal, and (5) the OCV vent port plug seal. Each leakage rate test shall meet the acceptance criteria delineated in Section 8.2.2.1, below.

8.2.2.1 Acceptance Criteria. To constitute acceptance per Section 5.4(3) of ANSI N14.5-1987, each of the ICV and OCV containment vessels' indicated leakage rates shall be less than or equal to 1×10^{-2} acc/s, air. To demonstrate that a containment vessel is leaktight per Section 7.3.2 of ANSI N14.5-1987, the sensitivity of the leakage rate test equipment shall be 5×10^{-2} acc/s, air, or less.

8.2.2.2 Leakage Rate Test of the Main ICV Closure Seal. This test uses helium at atmospheric pressure or above within the ICV cavity and an evacuated void outside the main ICV O-ring seal, thus following the guidelines of ANSI N14.5-1987, Section A3.10.1.

1. Assemble the RTG Transportation System Package ICV.
2. Install a test/vent port tool into the ICV seal test port and open the seal test port.
3. Plumb a calibrated helium MSLD to the test/vent port tool in the ICV seal test port.
4. Establish a vacuum in the ICV seal test port sufficient to operate the MSLD per the manufacturer's recommendations.
5. Install vent/test port tools into both the primary and secondary ICV vent ports.
6. Connect helium purge lines to the primary ICV vent port (helium purge inlet) and secondary ICV vent port (helium purge outlet). Open each vent port.
7. Flow helium through the ICV cavity at a minimum rate of 5 cubic feet per minute (cfm) for a minimum of 20 minutes.
8. Following the 20-minute purge, record the indicated leakage rate. If the leakage rate exceeds the allowable specified in Section 8.2.2.1, disassemble the package, thoroughly clean all components, reassemble the package, and repeat the leakage rate test. If the system cannot pass the test, prepare a discrepancy report for disposition per Section 8.3.15.
9. Close the seal test port. Remove all plumbing and the test/vent port tool from the ICV seal test port. Torque the seal test port plug to 110 ± 10 in.-lb.
10. Close the secondary ICV vent port. Remove all plumbing and the test/vent port tool from the secondary ICV vent port.
11. Charge the ICV cavity with helium gas to 15 ± 1 psia.

12. Close the primary ICV vent port. Remove all plumbing and the test/vent port tool from the primary ICV vent port. Torque the primary ICV vent port plug to 110 ± 10 in.-lb.

8.2.2.3 Leakage Rate Test of the Primary ICV Vent Port Plug Seal. This test uses helium at atmospheric pressure or above within the ICV cavity and an evacuated void outside the primary ICV vent port plug, thus following the guidelines of ANSI N14.5-1987, Section A3.10.1.

1. Install a test/vent port tool into the primary ICV vent port. Verify that the vent port is closed.
2. Plumb a calibrated helium MSLD to the test/vent port tool in the primary ICV vent port.
3. Establish a vacuum outboard of the closed primary ICV vent port sufficient to operate the MSLD per the manufacturer's recommendations.
4. Record the indicated leakage rate. When summed with the main ICV closure seal leakage rate from Section 8.2.2.2, if the total leakage rate exceeds the allowable specified in Section 8.2.2.1, remove the vent port plug, thoroughly clean all components, replace the vent port plug seal (if necessary), replace the vent port plug, and repeat the leakage rate test. If the system cannot pass the test, prepare a discrepancy report for disposition per Section 9.3.15.
5. Remove all plumbing and the test/vent port tool from the primary ICV vent port.

8.2.2.4 Leakage Rate Test of the Secondary ICV Vent Port Plug Seal. This test uses helium at atmospheric pressure or above within the ICV cavity and an evacuated void outside the secondary ICV vent port plug, thus following the guidelines of ANSI N14.5-1987, Section A3.10.1.

1. Install a test/vent port tool into the secondary ICV vent port. Verify that the port is closed.
2. Plumb a calibrated helium MSLD to the test/vent port tool in the secondary ICV vent port.
3. Establish a vacuum outboard of the closed secondary ICV vent port sufficient to operate the MSLD per the manufacturer's recommendations.
4. Record the indicated leakage rate. When summed with the main ICV closure seal and primary ICV vent port plug seal leakage rates from Sections 8.2.2.2 and 8.2.2.3, if the total leakage rate exceeds the allowable specified in Section 8.2.2.1, remove the vent port plug, thoroughly clean all components, replace the vent port plug seal (if necessary), replace the vent port plug, and repeat the leakage rate test. If the system cannot pass the test, prepare a discrepancy report for disposition per Section 9.3.15.
5. Remove all plumbing and the test/vent port tool from the secondary ICV vent port.

8.2.2.5 Leakage Rate Test of the Main OCV Closure Seal. This test uses helium at atmospheric pressure or above within the OCV cavity and an evacuated void outside the main OCV O-ring seal, thus following the guidelines of ANSI N14.5-1987, Section A3.10.1.

1. Assemble the RTG Transportation System Package OCV.
2. Install a test/vent port tool into the OCV seal test port and open the seal test port.
3. Plumb a calibrated helium MSLD to the test/vent port tool in the OCV seal test port.

4. Establish a vacuum in the OCV seal test port sufficient to operate the MSLD per the manufacturer's recommendations.
5. Install a vent/test port tool into the OCV vent port. Open the vent port.
6. As shown in Figure 8.2.2.5-1, plumb in parallel, with separate isolation valves, a vacuum pump and a source of helium gas to the test/vent port tool in the OCV vent port.

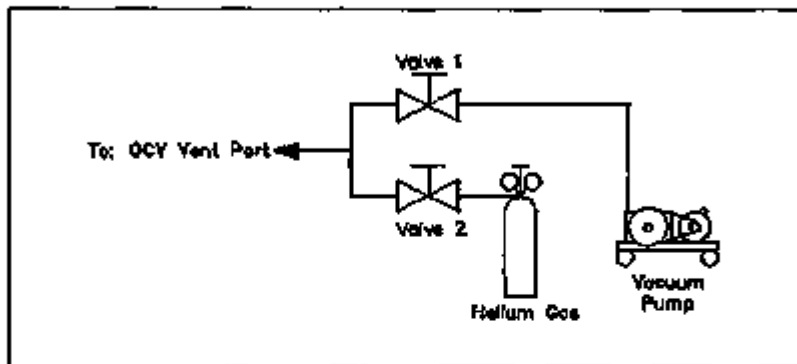


FIGURE 8.2.2.6-1.

7. Close valve 2 and open valve 1; operate the vacuum pump to achieve a vacuum in the OCV annulus equal to or below 25 torr (0.5 psia).
8. Close valve 1 and open valve 2 and pressurize the annulus to 19 ± 1 psia.
9. Record the indicated leakage rate. If the leakage rate exceeds the allowable specified in Section 8.2.2.1, disassemble the package, thoroughly clean all components, reassemble the package, and repeat the leakage rate test. If the system cannot pass the test, prepare a discrepancy report for disposition per Section 9.3.15.
10. Close the seal test port. Remove all plumbing and the test/vent port tool from the OCV seal test port. Torque the seal test port plug to 110 ± 10 in.-lb.
11. Close the OCV vent port. Remove the test/vent port tool from the OCV vent port. Torque the OCV vent port plug to 110 ± 10 in.-lb.
12. Install the OCV seal test port cover.

8.2.2.6 Leakage Rate Test of the OCV Vent Port Plug Seal. This test uses helium at atmospheric pressure or above within the OCV cavity and an evacuated void outside the vent port plug, thus following the guidelines of ANSI N14.5-1987, Section A3.10.1.

1. Install a test/vent port tool into the OCV vent port. Verify that the vent port is closed.
2. Plumb a calibrated helium MSLD to the test/vent port tool in the OCV vent port.

3. Establish a vacuum outboard of the closed OCV vent port plug sufficient to operate the MSLD per the manufacturer's recommendations.
4. Record the indicated leakage rate. When summed with the main OCV closure seal leakage rate from Section 8.2.2.5, if the total leakage rate exceeds the allowable specified in Section 8.2.2.1, remove the vent port plug, thoroughly clean all components, replace the vent port plug seal (if necessary), replace the vent port plug, and repeat the leakage rate test. If the system cannot pass the test, prepare a discrepancy report for disposition per Section 8.3.16.
5. Remove all plumbing and the test/vent port tool from the OCV vent port.
6. Install the OCV vent port cover.

8.2.3 Subsystems Maintenance

8.2.3.1 Fasteners. All threaded fasteners shall be inspected annually and before each use for deformed or stripped threads, or excessive damage to the cadmium-plated coating. Any damaged fasteners shall be replaced before further use. At a minimum, package containment boundary closure fasteners shall be replaced once every 5 years.

Test/vent port plugs and covers, all bolt thread inserts, and all noncontainment fasteners need not be replaced except when damaged.

8.2.3.2 Seal Areas and Grooves. Annually, at the time of seal replacement and before each use, inspect the O-ring seal grooves and mating sealing areas for damage that could impair the sealing capability of the packaging. Using fine emery cloth (e.g., 320 to 600 grid, smooth and polish the damaged areas to a surface finish as specified in the drawing in Appendix 1.3.2.

8.2.3.3 Painted Surfaces. Before each use, inspect the inner and outer surfaces of both the ICV and OCV, including the impact limiter for excessive damage to the coatings. The following criteria help determine if excessive damage is present.

1. **Local damage:** excessive localized damage is defined as bare metal exposure greater than 5% of any one square foot area (i.e., $>7 \text{ in.}^2$) of coated surfaces. The five painted surfaces (ICV inner surface, ICV outer surface, OCV inner surface, OCV outer surface, and impact limiter outer surface) may each be assessed independently to determine local damage. Slight discolorations because of scuffing or rubbing-type abrasions are not considered localized damage unless bare metal is exposed.
2. **Global damage:** excessive global damage is defined as bare metal exposure greater than 2% of a total coated surface area. The five painted surfaces (ICV inner surface, ICV outer surface, OCV inner surface, OCV outer surface, and impact limiter outer surface) may each be assessed independently to determine global damage. Slight discolorations because of scuffing or rubbing-type abrasions are not considered global damage unless bare metal is exposed.

If either of the above criteria are not satisfied, prepare a discrepancy report for disposition per Section 8.3.16. Also inspect the package at the time of shipment to ensure that all external painted white surfaces are clean and free of dirt/debris.

8.2.4 Valves, Rupture Discs, and Gaskets on the Containment Vessel

This section describes the inspection and replacement schedule for these components.

8.2.4.1 Valves. There are no containment boundary valves on the RTG Transportation System Package. The relief valves used on the OCV coolant jacket require no routine maintenance.

8.2.4.2 Rupture Discs. There are no rupture discs on the RTG Transportation System Package.

8.2.4.3 Gaskets. All packaging containment O-ring seats and gaskets shall be replaced annually or when damaged, per the size and material specifications provided in Appendix 1.3.2. During payload loading, all containment seals including the replaced seal(s) shall be leakage rate tested to Section 8.2.2.

8.2.5 Shielding

No shielding inspections or tests are required to ensure continued performance of the RTG Transportation System Package.

8.2.6 Thermal

No thermal tests are required to ensure continued performance of the RTG Transportation System Package. The thermal insulation, located on the bottom of the payload shipping rack assembly and the ICV electrical feed-through insulation sleeve, should be inspected on a minimum of an annual basis for any significant shifting, deterioration, tears, and cuts. The existence of such deterioration shall require replacement of the damaged component.

8.3 REFERENCES

1. American Society of Mechanical Engineers (ASME) Boiler and Pressure Vessel Code.
2. 10 CFR 71, 1993, "Packaging and Transportation of Radioactive Materials," *Code of Federal Regulations*, as amended.
3. ANSI N14.5-1987, American National Standard for Radioactive Materials--Leakage Rate Tests on Packages for Shipment.
4. ASTM D1621, Method of Test for Compressive Properties of Rigid Cellular Plastics.
5. 14 CFR 25, 1986, "Airworthiness Standards; Transport Category Airplanes," *Code of Federal Regulations*, as amended.
6. ASTM D395, Test Methods for Rubber Property--Compression Set.
7. ASTM D412, Standard Test Methods for Rubber Properties in Tension.
8. ASTM D2240, Test Method for Rubber Property--Durometer Hardness.
9. ASTM D2627, Standard Specifications for Rubber Seals--Splice Strength.

8.0 QUALITY ASSURANCE

8.1 INTRODUCTION

The Radioisotope Thermoelectric Generator (RTG) Transportation System Package Quality Assurance Program (QAP) has been established to meet the quality assurance requirements of the U.S. Department of Energy (DOE) Orders, 5700.8C, *Quality Assurance*¹ and 5480.3, *Safety Requirements for the Packaging and Transportation of Hazardous Materials, Hazardous Substances, and Hazardous Wastes*². The QAP defines quality activities necessary to produce shipping containers that comply with 10 CFR 71, Subpart H, *Packaging and Transportation of Radioactive Material, Quality Assurance*³. The program was developed according to the guidance provided by U.S. Nuclear Regulatory Commission Regulatory Guide 7.10, Revision 1, *Establishing Quality Assurance Programs for Packaging Used in the Transport of Radioactive Material*.

The following describes the Westinghouse Hanford Company (WHC) Quality Assurance (QA) Program and its relationship to the RTG Transportation System Program. The RTG Transportation System Program is performed under the requirements of the current DOE-approved WHC QA Program as defined in WHC-CM-4-2, *Quality Assurance Manual*. The requirements in the WHC QA manual apply to all WHC organizations and require that a Quality Assurance Program Plan (QAPP) be developed for each project. In response to this requirement, a QAPP (Document WHC-SD-RTG-QAPP-001) was developed for the RTG Transportation System Program. The QAPP lists the criteria from DOE Order 5700.8C and ASME NQA-1 and the existing implementation procedures that indicate how the criteria are to be met. The criteria listed in ASME NQA-1 not only cover all of the criteria in Title 10 of the Code of Federal Regulations Part 71 (10 CFR 71), Subpart H, but are also more rigorous. Therefore, all of the criteria in 10 CFR 71, Subpart H are met when the criteria of ASME NQA-1 are satisfied. The purpose of the QAPP is to ensure that the RTG Transportation System meets the requirements of the WHC QA manual and that the RTG packaging meets the requirements of 10 CFR 71, Subpart H. The purpose of the QAP described in Chapter 8 of the SARP is to define the quality activities necessary to produce packaging that comply with 10 CFR 71, Subpart H. The WHC QA Program and the RTG Transportation System QAPP comply with DOE Order 5700.8C and Title 10 of the Code of Federal Regulations, Parts 830.120, "Quality Assurance Requirements", and 71, Subpart H, "Quality Assurance".

8.2 SCOPE

The QAP applies to all aspects of packaging, including acquisition, inspection, handling, maintenance, utilization, and control for Type B nuclear shipping packages used for offsite transportation of radioactive material.

The QAP addresses the following quality elements: organization; quality assurance program; design control; procurement document control; instructions, procedures, and drawings; document control; control of purchased items and services; identification and control of items; control of processes; inspection; test control; control of measuring and test equipment; handling, storage, and shipping; inspection, test, and operating status; control of nonconforming items; corrective actions; quality assurance records; and audits. All elements of the QAP apply to subcontractors and sub-tier suppliers.

This QAP is not applicable to the Packaging System operational phase of the RTG Transportation System Package. Upon completion and acceptance of the packaging controlled under the QAP, the Certificate of Conformance holder (DOE) may designate the custodian for the Packaging System. The custodian will operate, maintain, repair, test, and store the RTG

packaging. The custodian will establish a QAP that meets the applicable requirements of DOE Order 5700.6C and 10 CFR 71, Subpart H. The custodian's QAP shall be approved by EH-332 before obtaining custodial control of operating, loading, or unloading the packaging.

9.3 QUALITY ASSURANCE PLAN

9.3.1 Quality Element 1.0. Organization

The Westinghouse Hanford Company (WHC) Quality Assurance manager has delegated the direct responsibility for quality of the RTG Transportation System Package to Engineering Applications and Support Quality Assurance (EA&SQ) and to Engineering Applications Quality Assurance (EAQA). The EA&SQ management hierarchy is independent of management responsible for conduct of the packaging development. The Quality Assurance (QA) personnel are independent from other personnel and organizations as shown in Figure 9.3.1-1.

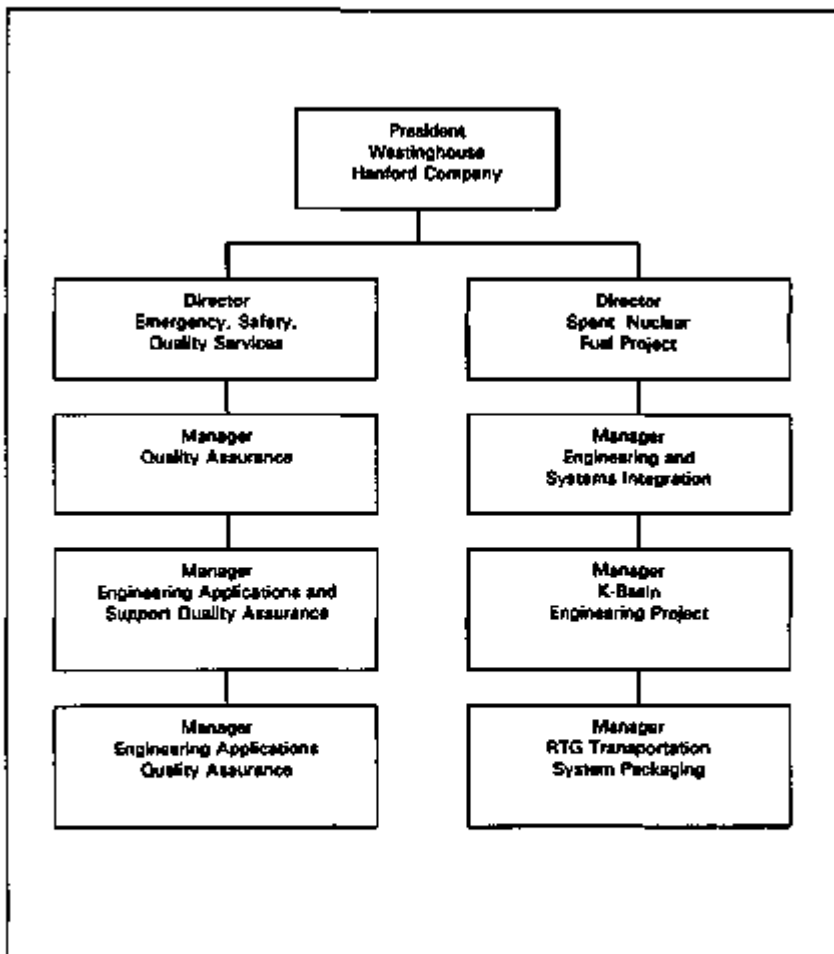


FIGURE 9.3.1-1. Reporting Independence of QA Organization.

9.3.2 Quality Element 2.0, Quality Assurance Program

All departments and service organizations that support the RTG Transportation System Package program shall comply with this QAP. If differences appear between this QAP and other documents, management shall provide resolution for all activities related to the RTG program.

Suppliers of services and equipment that affect the quality of the RTG Transportation System Package shall have a QA program in accordance with the applicable QA of this QAP. Audits of supplier's QA programs shall be per the requirements of this QAP applicable to the goods and services provided. A determination about invoking the contractual clauses that require a QAP, Quality Assurance Plan Index (QAPI), or Forward Surveys shall be made before placing a Request for Quote (RFQ) and shall be approved by QA.

All systems and major equipment designed, fabricated, or procured for the RTG Transportation System Package shall be evaluated and the appropriate documents (procurement specifications) WHC-OM-3-6⁹ shall be used to approve Environmental, Safety, and Quality Affecting Documents.

Quality levels shall be assigned to all RTG Transportation System Packaging components. Quality level assignment shall consider the impact to safety if the component were to fail or perform outside of design parameters. The three levels of QA categories from Appendix A, of NRC Regulatory Guide 7.10⁹, are as follows:

QA Category A (Critical): This level includes those items with a critical impact to safety, such as structures, components, and systems whose failure or malfunction could result directly in a condition adversely affecting public health and safety. This includes such conditions as loss of primary or secondary containment with subsequent release of radioactive material, loss of shielding, or an unsafe geometry compromising criticality control.

QA Category B (Major): This level includes those items with a major impact to safety, such as structures, components, and systems whose failure or malfunction could result indirectly in a condition adversely affecting public health and safety. An unsafe condition could result only if the primary event occurs in conjunction with a secondary event or other failure or environmental occurrence.

QA Category C (Minor): This level includes those items with a minor impact to safety, such as structures, components, and systems whose failure or malfunction would not significantly reduce the packaging effectiveness and would be unlikely to create a condition adversely affecting public health and safety.

Adherence to appropriate design criteria (regulatory guides, safety, performance, maintainability, operability, etc.) shall be the measure of quality and are to be evaluated in reviews of designs and related activities for the scope of this QAP. The graded approach assessment for the RTG Transportation System Package is listed in Table 9.3.2-1.

TABLE B.3.2-1. Quality Assurance Levels for Design and Procurement of RTG Package Components.

Component	Subcomponent	QA level
Outer containment vessel	Bell flange	A
	Bell shell	A
	ASME torispherical head	A
	Fins and lifting doublers	B
	Tiedown doubler straps	B
	Coolant jacket structure	B
	Coolant jacket nipples and couplings	C
	Coolant jacket pressure relief valves	B
	Bell flange thermal shield structure	B
	Bell flange thermal shield insulation	C
	Base	A
	Closure bolts	B
	O-ring seals	B
	Vent and test port plugs	B
	Vent and test port plug seals	B
	Vent and test port covers	C
	Vent and test port cover gaskets	C
	Alignments pins	C
	Internal black paint coating	C
	External white paint coating	C
Inner containment vessel	Bell flange	A
	Bell shell	A
	ASME torispherical head	A
	Lifting plate	A
	Base	A
	Closure bolts	B
	O-ring seals	B
	Vent and test port plugs	B
	Vent and test port plug seals	B
	Alignment pins	C
	Purge tube	C
	Base (OCV-to-ICV) attachment bolts	C
	Debris shield	B
	Black painted coating	C
Electrical feed-through		
• Receptacle	B	
• ICV sleeve	A	
All other components	C	

TABLE 9.3.2-1. Quality Assurance Levels for Design and Procurement of RTG Package Components. (cont.)

Component	Subcomponent	QA level
Impact limiter	Shells and plates	B
	Structural angles	B
	Polyurethane foam	B
	Bolting ring	B
	Thermal shield sheet	B
	Thermal shield wire	C
	Drain tubes	C
	Attachment bolts	B
	Blow-out plug coupling	C
	Blow-out plug	C
	Alignment pins	C
	White external paint coating	C
All other components	C	
GPHS shipping rack	Barrier plate	B
	Cylindrical shells	B
	Legs	C
	Ceramic fiber cloth	C
	Attachment bolts	B
	All other components	C

9.3.3 Quality Element 3.0, Package Design Control

The RTG Transportation System Package design is controlled by the Basic Requirement 3 and Supplement 3S-1 of ASME NQA-1⁷. The design is defined, controlled, and verified. Applicable design inputs are specified on a timely basis and translated into design documents. Design interfaces are identified and controlled. Design adequacy is verified by persons or organizations other than those who designed the item. Design changes, including field changes, are governed by control measures equal to those applied to the original design.

Design inputs consist of WHC-S-4025⁸ specification, applicable DOE orders for the RTG Transportation System Package, national standards, specifications, and drawings. These are controlled by WHC through the Functions and Requirements for the RTG Transportation System Package (Sys. 100). Changes to the design input are formally controlled by a change control process.

9.3.4 Quality Element 4.0, Procurement Document Control

A graded approach shall be implemented for procurement of equipment and services for the RTG Transportation System Package based on safety, performance, and regulatory criteria. Quality Assurance shall ensure that procurement documents are adequate for their intended purpose per the assigned safety quality level described in Section 9.3.2.

Where extensive procurement detail is required, technical requirements and acceptance criteria shall normally be established by approved functions and specifications and/or design

drawings. Where the procurement does not require extensive detail, requirements and criteria may be specified in the body of the purchase order or data sheets referenced by and attached to the purchase order. Certain items, such as "off-the-shelf equipment" and "catalog items," may not require listing of the technical requirements and acceptance criteria and may be specified by model number or equivalent.

Supplier documentation requirements shall be included with the procurement documents identifying which items must be submitted by the supplier. A submittal list shall specify which documents shall be submitted for approval and which documents shall be submitted for information during the contract period. Examples of documents include fabrication and inspection procedures, equipment installation instructions, calibration procedures, operating and maintenance manuals, and spare parts lists.

For procurement involving vendor designs, vendor design control, document control, and change control shall be in accordance with WHC approved methods of document control or equivalent to the requirements of this QAP.

9.3.5 Quality Element 5.0, Instructions, Procedures, and Drawings

All instructions, procedures, and drawings used for the RTG Transportation System Package shall be approved according to the quality level and approval designation assigned by the cognizant design/project engineer and verified by QA as adequate for their intended purpose. Quality Assurance shall ensure that approved and correct documents are employed.

Quality Assurance shall approve witness points and hold points before the procurement, fabrication, or installation documentation approval. Witness and hold points, as a minimum, will be identified in inspection plans prepared per Section 9.3.10. Requirements for instructions, manuals, and equipment data shall be specified in the procurement document.

9.3.6 Quality Element 6.0, Document Control

All documents applicable to and used for the RTG Transportation System Package shall be reviewed and approved per the requirements of the assigned safety quality level, and applicable administrative, engineering, or technical document approval procedures. Changes to documents shall be controlled according to approved change control procedures applicable to each type of document, and are governed by control measures equal to those applied to the original documents.

9.3.7 Quality Element 7.0, Control of Purchased Material, Equipment and Services

This quality element applies to the purchase of items and services that affect quality. Procurement controls provide for source evaluation and selection, evaluation of objective evidence of quality furnished by the supplier, source inspection, audit, and examination of items or services upon delivery or completion.

Procurement activities are performed according to documented procedures to ensure a systematic approach and, as a minimum, address the following:

- Preparation, review, and release of procurement documents
- Selection of procurement sources
- Bid evaluation and award

- ◆ Supplier performance evaluation
- ◆ Control of supplier-generated documents
- ◆ Source end/or receiving inspections
- ◆ Control of changes to procurement documents for items and services
- ◆ Material identification and control
- ◆ Acceptance of items and services.

9.3.8 Quality Element 8.0, Identification and Control of Material, Parts and Components

Material control, where required, shall be specified in procurement documents, fabrication specifications, and construction specifications, so that only correct and accepted items are used and installed. These controls provide identification on items or in documents to ensure traceability. Each participant and subcontractor/supplier are responsible for implementing appropriate portions of the QAP program to identify and control items. The QAP complies with the requirements of DOE 5700.8C.

Items of production (i.e., batch, lot, component, or part) are identified from the initial receipt and fabrication through storage, installation, and use. This relates items to applicable design or other specifying documents.

Physical identification is the preferred method. Where physical identification is insufficient or not practical, control will be established by other approved and appropriate means, such as procedural control and physical separation. Markings, when used, shall be applied using materials and methods that provide clear and legible identification that will not affect the function or service life of the item. Markings will be transferred to each part of an item before subdividing. Caution shall be exercised to prevent obliteration by any surface treatment or coating.

Items that have limited calendar or operating life cycles or shelf life shall be controlled to preclude the use of expired items, and to replace installed items before failure or expiration.

9.3.9 Quality Element 9.0, Control of Special Processes

Processes affecting quality of items and services during fabrication and installation shall be controlled. The process control requirements shall be established in the design documents or in instructions, procedures, or drawings applicable to the process. Procedures that may be prepared to control and ensure the quality of processes shall have detail, based on the level of complexity or unique properties of the process. Stringency of review and approvals of process procedures that may be prepared shall be based on the safety quality level established in Section 9.3.2. Examples of processes that may require procedures are nondestructive examination, chemical analyses, metal finishing and coatings, heat treating, and cleaning. Personnel who perform special processes shall be qualified or certified as required to ensure quality.

All qualification records and support data are retained in the QA data file and maintained in a current status by QA personnel. These documents are controlled as delineated in Section 9.2.6, Document Control.

9.3.10 Quality Element 10.0, Inspection

Inspections shall be required to verify conformance of an item or activity to specified requirements. Inspection requirements shall be identified during the design and in the design documents. Inspection requirements shall be specified in procurement documents.

Inspections shall be performed with approved inspection plans and documented according to approved procedures. Inspectors shall be qualified or certified per the inspection requirements and shall be independent from the activity, process, or product being inspected.

9.3.11 Quality Element 11.0, Test Control

Tests are required when it is necessary to demonstrate that items or processes will perform satisfactorily. Test procedures shall specify the objectives of the tests, testing methods, required documentation, acceptance criteria, and shall be approved per the safety quality level established in Section 9.3.2.

Tests conducted by vendors at vendor plants shall be specified in the procurement documents. The Westinghouse Hanford Company (WHC) test approvals and required test observations shall be specified in test documents of vendor tests.

9.3.12 Quality Element 12.0, Control of Measuring and Test Equipment

All equipment used for measuring or testing shall be calibrated in accordance with the required test or measuring accuracy and repeatability and to approved standards of calibration. Calibrations and calibration records shall be traceable to the required calibration standard and the National Institute of Standards Technology, and the equipment shall be marked with calibration expiration dates.

Measuring and test equipment control shall be required for all suppliers that provide equipment or services that will be used to accept or test equipment or materials for the RTG Transportation System Package. Requirements to be invoked on suppliers in accordance with the QAP shall be specified in procurement documents.

9.3.13 Quality Element 13.0, Handling, Storage, and Shipping Control

All items that are part of the RTG Transportation System Package shall be controlled to prevent damage or loss, to protect against damage or deterioration, and to provide adequate safety of personnel involved in the material handling and storage operations.

Shipment planning with suppliers shall be required for preservation, packaging, shipping, handling, and receiving in accordance with the complexity of equipment and systems for the RTG Transportation System Package. Requirements shall be specified in the procurement document. The planning will be dependent on whether an item will require special or unique handling, storage, or special planning because of vulnerability to damage by the environment or physical damage that could result from normal handling.

Information pertaining to shelf life, environment, packaging, temperature, cleaning, handling, and preservation is included as required to meet design, regulatory package approval, and/or U.S. Department of Transportation (DOT) shipping requirements.

9.3.14 Quality Element 14.0, Inspection, Test, and Operating Status

Work instructions, travelers, and similar documents will help maintain status during procurement and fabrication by the fabricator. In-process inspections, and inspection of incomplete items and activities shall be performed where necessary to verify quality and to ensure required inspections, verifications, and tests are performed.

Planning shall be performed before the turnover of the packaging to WHC upon completion of required assembly by the contractor. This planning will take into account the acceptance testing to be performed by the contractor to verify conformance to the specifications.

9.3.15 Quality Element 15.0, Nonconforming Materials, Parts, or Components

The control of nonconforming items, equipment, or conditions for the RTG Transportation System Package is accomplished by Nonconformance Reports (NCR). The NCR procedure promotes consistency, timeliness of problem resolution, and processing of all necessary documentation. All RTG Transportation System Package participants can initiate an NCR.

Items or practices that do not meet specified requirements, or whose conformance is indeterminate, are documented on NCRs and controlled to prevent inadvertent installation or use. Controls are provided to notify affected organizations and for the identification, documentation, evaluation, segregation, and disposition of the items or conditions. The NCRs are tracked to completion and the verification of corrective action is documented. All personnel associated with the RTG Transportation System Package are responsible for documenting instances of nonconformance and for seeking resolution.

9.3.15.1 Identification. Nonconforming items are identified by marking, tagging, or other methods that do not adversely affect the item. When identification of nonconforming items is not practical, the container or package is marked, or segregated storage is provided.

9.3.15.2 Segregation. Nonconforming items are segregated by placing them in a designated and identified holding area until disposition is complete. When segregation is impossible or not practical because of size, weight, or access limitations, other precautions are used on a case by case basis.

9.3.15.3 Disposition. Documentation to identify, review, and disposition nonconforming items is controlled according to approved procedures that specify responsibilities and authority. Personnel who perform evaluations and approve dispositions must be competent in the specific areas they are evaluating, understand the requirements, and have access to the pertinent background information. Each organization identifies, in writing, the personnel by job title who are authorized to evaluate proposed NCR dispositions.

Control of further processing, delivery, installation, or use of nonconforming items is imposed pending resolution of NCRs.

9.3.16 Quality Element 16.0, Corrective Action

Conditions adverse to quality shall be identified and corrected as soon as practicable. An unsatisfactory condition or nonconformance may be revealed by an audit, an unusual occurrence, a random observation, during inspection, or from trend analyses of other reports. The controls shall

be implemented in accordance with this QAP. Corrective action requirements are described in approved WHC QA procedures.

9.3.17 Quality Element 12.0, Quality Assurance Records

Records that document evidence of quality are specified, prepared, and maintained. The quality records may be either the originals or copies. Copies must be capable of microfilming when used. Microfilm is acceptable, except for radiographs. Records shall be legible, identifiable, and retrievable. Records shall be protected from damage, deterioration, or loss. Lost or damaged records shall be replaced, restored, or substituted to the extent possible.

Requirements and responsibilities for record generation, transmittal, evaluation, distribution, retention, maintenance, and disposition are established and documented in Westinghouse Hanford Company (WHC) QA procedures. Each organization is responsible for generating records that furnish documentary evidence of quality, according to scoping statements appearing in work authorizing documents. The description of controls for records only applies to QA records that have been completed. Incomplete documentary evidence is not subject to the controls described.

Documents are considered valid records only if stamped, initialed, or signed, and dated by authorized personnel or otherwise authenticated.

9.3.17.1 Classification. Records are classified as "lifetime" or "nonpermanent." Lifetime records are required to be maintained by, or for, the owner for the life of the RTG Transportation System Package while it is installed or in service. Lifetime records are those that meet one or more of the following criteria:

- Those specified for lifetime retention by regulatory or contractual requirements
- Those that would be of significant value in demonstrating capability for safe operation
- Those that would be of significant value in maintaining, reworking, repairing, replacing, or modifying an item
- Those that would be of significant value in determining the cause of an accident or malfunction of an item
- Those that provide required baseline data for inservice inspections
- Those that substantiate development or major decisions involving safety and the environment
- Those that evidence conformance to codes and specifications.

Examples of lifetime records are as follows: calculations, drawings, results of design reviews, inspections, tests, and audits. Nonpermanent records are those required to show evidence that an activity was performed according to the applicable requirements, but need not be retained for the life of the item because they do not meet the criteria for lifetime.

9.3.18 Quality Element 18.0, Audits

Quality audits shall be conducted on RTG Transportation System Package activities (internal audits) and on the equipment suppliers (external audits) as required. Audits shall be conducted by qualified auditors and may be performed on a team basis as required by the audit scope.

9.4 REFERENCES

1. DOE, 1991, *Quality Assurance*, DOE Order 5700.6C, U.S. Department of Energy, Washington, D.C.
2. DOE, 1989, *Safety Requirements for the Packaging and Transportation of Hazardous Materials, Hazardous Substances, and Hazardous Wastes*, DOE Order 5480.3, U.S. Department of Energy, Washington, D.C.
3. 10 CFR 71, 1993, "Packaging and Transportation of Radioactive Materials," *Code of Federal Regulations*, as amended.
4. WHC, 1988, *Quality Assurance Manual*, WHC-CM-4-2, Westinghouse Hanford Company, Richland, Washington.
5. WHC, 1994, *Approval of Environmental, Safety, and Quality Effecting Documents*, WHC-CM-3-6, Westinghouse Hanford Company, Richland, Washington.
6. US NRC, 1996, "Establishing Quality Assurance Programs for Packaging Used in the Transport of Radioactive Materials," Regulatory Guide 7.10, Rev. 1.
7. ASME NQA-1, 1988, *Quality Assurance Requirements for Nuclear Facilities*.
8. WHC, 1992, *Specification for RTG Transportation System Package*, WHC-S-4025, Rev. 2, Westinghouse Hanford Company, Richland, Washington.

RTG SARP CONTROLLED DISTRIBUTION

Number of Copies

OFFSITE

2	<u>U S Department of Energy-Headquarters</u> 19901 Germantown Road Germantown, Maryland 20874 A K Kapoor E F Mastal	EM-76 NE-5D
1	<u>Eagle Research Group, Inc.</u> 13241 Executive Park Terrace Germantown, Maryland 20874 R Towell	
2	<u>EG&G Mound Applied Technologies</u> Post Office Box 3000 Miamisburg, Ohio 45343 R G Miller (2)	
7	<u>Lawrence Livermore National Laboratory</u> 7000 East Avenue Building 543 Livermore, California 94551 M Witte	
1	<u>Lockheed Martin</u> Post Office Box 8555 Building B Philadelphia, Pennsylvania 19101 R M Reinstron	
1	<u>Orbital Sciences Corporation</u> 20301 Century Boulevard Germantown, Maryland 20874 R T Carpenter	